AAPS Advances in the Pharmaceutical Sciences Series 10

Margareta Hammarlund-Udenaes
Elizabeth C.M. de Lange
Robert G. Thorne *Editors*

Drug Delivery to the Brain

Physiological Concepts, Methodologies and Approaches

aapspress
Springer

AAPS Advances in the Pharmaceutical Sciences Series

The AAPS Advances in the Pharmaceutical Sciences Series, published in partnership with the American Association of Pharmaceutical Scientists, is designed to deliver well written volumes authored by opinion leaders and authoritarians from around the globe, addressing innovations in drug research and development, and best practice for scientists and industry professionals in the pharma and biotech industries. For more details and to see a list of titles in the Series please visit
http://www.springer.com/series/8825

Margareta Hammarlund-Udenaes
Elizabeth C.M. de Lange • Robert G. Thorne
Editors

Drug Delivery to the Brain

Physiological Concepts, Methodologies and Approaches

aapspress Springer

Editors
Margareta Hammarlund-Udenaes
Department of Pharmaceutical Biosciences
Translational PKPD Research Group
Uppsala University, Uppsala, Sweden

Elizabeth C.M. de Lange
Target Site equilibration Group
LACDR/Pharmacology, Leiden University
Leiden, The Netherlands

Robert G. Thorne
Pharmaceutical Sciences Division
University of Wisconsin-Madison
School of Pharmacy
Madison, WI, USA

ISSN 2210-7371
ISBN 978-1-4614-9104-0
DOI 10.1007/978-1-4614-9105-7
Springer New York Heidelberg Dordrecht London

ISSN 2210-738X (electronic)
ISBN 978-1-4614-9105-7 (eBook)

Library of Congress Control Number: 2013954405

Printed on acid-free paper

Springer is part of Springer Science+Business Media (www.springer.com)

Preface

More than four decades have passed since Reese, Karnovsky, and Brightman used electron microscopy to unequivocally establish that tight junctions between brain endothelial cells form the blood–brain barrier (Brightman and Reese 1969; Reese and Karnovsky 1967). This finding ushered in a new era of research and science investigating precisely what factors determine transport across the blood–brain barrier (BBB), as well as the blood–cerebrospinal fluid barriers (BCSFB) formed by tight junctions between cells of the choroid plexus and arachnoid epithelia. Much interest developed around when and how these barriers to the central nervous system (CNS) form, as well as the interplay between components of the neurovascular unit (principally endothelial cells and their associated astrocytes, pericytes, immune cells, and neurons) that dynamically regulate the BBB. Along with this work, there has been a steady rise in the level of interest and research surrounding drug delivery to the brain. Indeed, there are now more than 10,000 citations in *PubMed* for articles retrieved using the search phrase "drug delivery" along with "brain" or "central nervous system" (Fig. 1). Much of the focus has been on the complex role that influx and efflux transporters play in helping or counteracting small-molecule transport into the brain, but many other research areas have also emerged in recent years.

There are several factors driving the tremendous interest in CNS drug delivery. Most importantly, there is the enormous burden neurological disorders often place on affected individuals and their family members as well as the economic consequences related to the cost of care, lost productivity, and caregiver issues, both for those directly affected as well as the larger society. Neurological disorders affect up to one billion people worldwide and account for more hospitalizations than any other disease group. In the United States alone, neurological illnesses and mental disorders reportedly affect more than 50 million people annually at a cost of more than $650 billion USD.

New CNS drugs have historically suffered from considerably lower success rates during development than those for non-CNS indications, partly due to transporter protection of the brain but also to poor understanding of CNS disease mechanisms. For example, past estimates have suggested only about 7 % of CNS drugs entering clinical development go on to be approved drugs versus about 15 % for

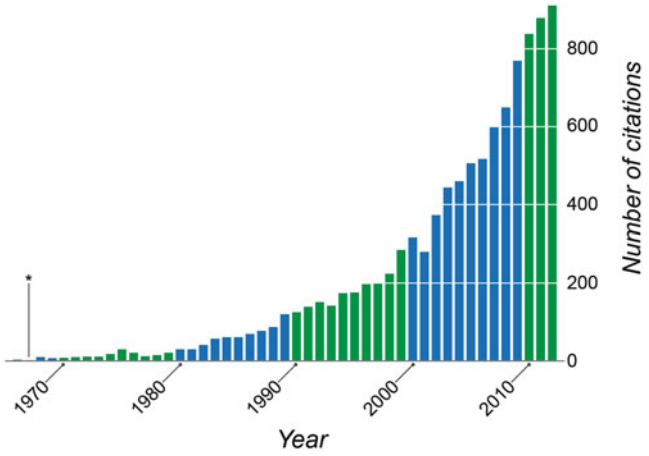

Fig. 1 Increasing number of citations in *PubMed* over time obtained using the search terms "drug delivery"/"delivery of drugs" + "brain"/"central nervous system," shown for the years 1966–2012. The *asterisk* indicates the year in which microvessel endothelial cells were definitively identified as forming the blood–brain barrier (Reese and Karnovsky 1967)

other therapeutic areas (Pangalos et al. 2007). One unfortunate aspect of this added "cost" in developing CNS drugs is that it has likely discouraged larger industry investment in research on CNS disorders. So why do CNS drugs suffer from these low success rates during development? Some of the reasons undoubtedly include: (1) our still incomplete understanding of the brain and its many functions, (2) a propensity for CNS drugs to suffer from off-target side effects, (3) a poor track record for many CNS drugs when it comes to preclinical predictions of clinical challenges, (4) a much larger influence of transporters than in other organs/tissues, (5) a shortage of validated biomarkers for assessing therapeutic efficacy in treating neurological disorders, and (6) a lack of studies integrating more than one aspect of the problem. Drug delivery issues obviously present a key challenge, so it is encouraging that clinical trials have increasingly focused on delivery aspects. As of 2012, approximately one third of the nearly 95,000 clinical trials investigating treatments that were in progress across 179 countries involved the evaluation of a drug delivery technology, system, or device (Ho and Chien 2012); indeed, more than 12 % of these delivery-focused trials related to a device, drug delivery system, formulation, or dosage form were targeted to neurological indications (Fig. 2). It is therefore easy to accept that better ideas, technology, and understanding with respect to CNS delivery are quite likely to translate into better clinical trials and improved clinical success.

Nearly all currently approved CNS drugs are small molecular weight pharmaceuticals. Although lipophilicity has often been emphasized in predicting brain entry, there is increasing awareness that other factors are critical for small molecule drugs to reach their required target site concentrations within the brain. The

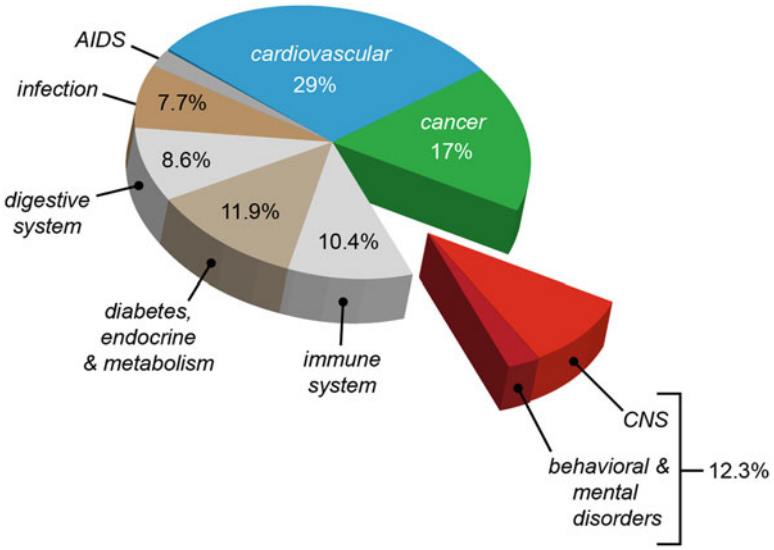

Fig. 2 Distribution of clinical trials associated with drug delivery technologies, systems or devices (Data from Ho and Chien 2012). Clinical trials targeting the central nervous system (including those associated with behavioral and mental disorders) represent the third most common therapeutic area, after cardiovascular- and cancer-directed trials

combination of general BBB diffusion, influx/efflux transport, and carrier-mediated transport, together with plasma and intrabrain distribution, plays an important role in the success or failure of CNS drugs. It is also important to consider the effect that disease conditions may have on these factors.

Biologics (peptides, proteins, oligonucleotides, and gene therapy vectors) are a newer drug class with tremendous potential for treating CNS disorders, but their transport across the CNS barriers from the systemic circulation is most often extremely restricted. Receptor-mediated transcytosis systems may potentially offer certain carefully targeted biologics the opportunity to cross the BBB, but this promising strategy has not yet achieved clinical success despite long interest. There are currently only a handful of biologics approved for clinical use in treating neurological illnesses, but most of these drugs are thought to either act outside the CNS (e.g. type I interferons for treating multiple sclerosis) or cross compromised endothelial barriers associated with some CNS tumors (e.g. the humanized monoclonal antibody bevacizumab for the treatment of recurrent glioblastoma). The ~3 kDa ziconotide peptide, a cone snail toxin, represents one success: it has been administered intrathecally to treat severe, chronic pain in the U.S. since 2004 and in Europe since 2005. Many other biologics have been identified as potential CNS therapeutics based on studies utilizing in vitro systems and animal models; however, it is painfully clear that new drug delivery strategies will be needed to allow these potential drugs to cross or bypass the BBB and/or BCSFB for these studies to translate to the clinic.

The ability to achieve consistent, targeted delivery to the CNS target site has remained a major, largely unmet challenge, but this book attests to the potential we have to address this hurdle in the years ahead. The field has seen a critical mass of dedicated, multidisciplinary scientists from all over the world come together in recent years with shared purpose and commitment to making significant progress in this vitally important research area, as evidenced by joint scholarly output, passionately communicated science at conferences, and rapidly growing national and international societies. This provides perhaps the greatest cause for optimism, because our future success in developing new ideas, technology, and understanding related to CNS barriers/drug delivery will likely require just such cooperation and collegiality.

Lastly, an important reason for producing a book such as this is also to hopefully provide an introduction to the field to promising young scientists who have not yet decided how to direct their careers. We hope this book supports their curiosity and investigation and provides some assistance in identifying CNS barriers and drug delivery science as a field with interesting questions and exceptionally worthy goals.

Book Structure

During the past few decades, great strides have been made in each of the five parts into which this book has been divided. The basic physiology of the BBB and BCSFB has been defined, and the manner in which the brain handles drugs is much better appreciated (Part I). Increasingly elegant in vitro, in vivo, and pharmacokinetic models have been applied to the study of drug transport across the BBB (Part II). Industry experience in developing CNS drugs has deepened, and a better appreciation of the critical factors that lead to development success or failure has been attained (Part III). Many strategies for CNS delivery, mostly focused upon delivering biologics into the brain, have been proposed, developed, and tested with varying degrees of success and optimism for near-term clinical application (Part IV). There have also been major developments in our understanding of barrier changes in disease conditions and how these changes affect CNS drug delivery (Part V).

Each of the 24 chapters contained in this book have been written by experts in the field, carefully chosen so that the book brings diverse, cutting-edge viewpoints and state-of-the-art summaries from scientists representing both academic and industry perspectives. In addition to providing detailed coverage of the different topic areas, chapters also include a description of future challenges and unresolved questions combined with a special concluding section entitled “Points for Discussion.” The “Points for Discussion” section contains further questions and observations intended to stimulate discussion among a group of people in either a classroom or small group setting; these questions may also prove useful as an assignment for a graduate-level survey course. In addition to wide-ranging coverage of physiological concepts relevant to CNS drug delivery, the book also contains a detailed review of brain structure, function, blood supply, and fluids in the Appendix, written as a

concise, detailed “crash course” covering relevant background for the book’s content. We have designed this book to be useful for a wide audience, from graduate or professional students being exposed to this research area for the first time, to established academic and industry scientists looking to learn about the state-of-the-art, to experts already performing CNS drug delivery research or working in related areas. It is our fervent hope that it succeeds in introducing the major questions faced by the field as well as in stimulating new thoughts on how to answer them!

Uppsala, Sweden — Margareta Hammarlund-Udenaes
Leiden, The Netherlands — Elizabeth C.M. de Lange
Madison, WI — Robert G. Thorne

References

Brightman MW, Reese TS (1969) Junctions between intimately apposed cell membranes in the vertebrate brain. J Cell Biol 40(3):648–677

Ho RJ, Chien JY (2012) Drug delivery trends in clinical trials and translational medicine: growth in biologic molecule development and impact on rheumatoid arthritis, Crohn's disease, and colitis. J Pharm Sci 101(8):2668-2674

Pangalos MN, Schechter LE, Hurko O (2007) Drug development for CNS disorders: strategies for balancing risk and reducing attrition. Nat Rev Drug Discov 6(7):521–532

Reese TS, Karnovsky MJ (1967) Fine structural localization of a blood–brain barrier to exogenous peroxidase. J Cell Biol 34:207–217

Acknowledgements

There are many people and experiences to acknowledge in putting such a book together. We are indebted first and foremost to the dynamic and supportive international community of CNS barriers and drug delivery scientists whom we have had the pleasure of interacting with for many years now. Many of our colleagues and collaborators from this community kindly agreed and worked hard to contribute chapters for this book. We also gratefully acknowledge the professionalism, support, and collaborative spirit of our colleagues at Springer throughout the entire process, from project conception to completion.

Finally, we would like to dedicate this book to the research teams we have had the good fortune to work with, to our families, and to the memory of Robert's late father, Ronald G. Thorne (1942–1990), who is among the many who have passed away from CNS disorders and for whom new approaches to deliver drugs into the brain might have made a difference.

Contents

Part I Physiology and Basic Principles for Drug Handling by the Brain

1 Anatomy and Physiology of the Blood–Brain Barriers 3
N. Joan Abbott

2 Recent Progress in Blood–Brain Barrier and Blood–CSF Barrier Transport Research: Pharmaceutical Relevance for Drug Delivery to the Brain 23
Masanori Tachikawa, Yasuo Uchida, Sumio Ohtsuki, and Tetsuya Terasaki

3 Blood–Brain Barrier (BBB) Pharmacoproteomics: A New Research Field Opened Up by Quantitative Targeted Absolute Proteomics (QTAP) 63
Yasuo Uchida, Masanori Tachikawa, Sumio Ohtsuki, and Tetsuya Terasaki

4 Drug Metabolism at the Blood–Brain and Blood–CSF Barriers 101
Xavier Declèves, Nathalie Strazielle, Jean-Michel Scherrmann, and Jean-François Ghersi-Egea

Part II Pharmacokinetic Concepts and Methods for Studying Drug Delivery

5 Pharmacokinetic Concepts in Brain Drug Delivery 127
Margareta Hammarlund-Udenaes

6 In Vitro Models of CNS Barriers 163
N. Joan Abbott, Diana E.M. Dolman, Siti R. Yusof, and Andreas Reichel

7 In Situ and In Vivo Animal Models 199
Quentin R. Smith and Ramakrishna Samala

8 Principles of PET and Its Role in Understanding Drug Delivery to the Brain 213
Stina Syvänen and Roger N. Gunn

9 PKPD Aspects of Brain Drug Delivery in a Translational Perspective 233
Elizabeth C.M. de Lange

Part III Industrial Approaches for Investigation of Potential Central Nervous System Drugs

10 Drug Discovery Methods for Studying Brain Drug Delivery and Distribution 271
Irena Loryan and Margareta Hammarlund-Udenaes

11 Prediction of Drug Exposure in the Brain from the Chemical Structure 317
Markus Fridén

12 Integrated Approach to Optimizing CNS Penetration in Drug Discovery: From the Old to the New Paradigm and Assessment of Drug–Transporter Interactions 339
Andreas Reichel

13 Pharmacoeconomic Considerations in CNS Drug Development 375
David Gray

Part IV Strategies for Improved Central Nervous System Drug Delivery

14 Intranasal Drug Delivery to the Brain 401
Jeffrey J. Lochhead and Robert G. Thorne

15 Blood-to-Brain Drug Delivery Using Nanocarriers 433
Pieter J. Gaillard, Corine C. Visser, Marco de Boer, Chantal C.M. Appeldoorn, and Jaap Rip

16 Development of New Protein Vectors for the Physiologic Delivery of Large Therapeutic Compounds to the CNS 455
Reinhard Gabathuler

17 CNS Gene Therapy Utilizing Intravenously Administered Viral Vectors 485
Adam K. Bevan and Brian K. Kaspar

18 Neurosurgical Approaches: Drug Infusion Directly into the Parenchyma or the Cerebrospinal Fluid 501
Krystof Bankiewicz

19 Osmotic Opening of the BBB for Drug Treatment of Brain Tumors (Focus on Methodological Issues) 519
David Fortin

20 Emerging Engineering Technologies for Opening the BBB 545
Elisa E. Konofagou

Part V Brain Drug Delivery in Disease Conditions

21 Disease Influence on BBB Transport in Inflammatory Disorders 573
Geert J. Schenk, Gijs Kooij, Arie Reijerkerk, and Helga de Vries

22 Disease Influence on BBB Transport in Neurodegenerative Disorders 591
Elizabeth C.M. de Lange

23 Drug Delivery in the Context of Stroke and Brain Trauma 635
Richard F. Keep, Jianming Xiang, Ningna Zhou, and Anuska V. Andjelkovic

24 Which Drug or Drug Delivery Method Can Change Clinical Practice for Brain Tumor Therapy? 657
Tali Siegal

Short Editors' Bios 683

Appendix Primer on Central Nervous System Structure/Function and the Vasculature, Ventricular System, and Fluids of the Brain 685
Robert G. Thorne

Index 709

Contributors

N. Joan Abbott Institute of Pharmaceutical Science, Blood–Brain Barrier Group, King's College London, London, UK

Anuska V. Andjelkovic Department of Neurosurgery, University of Michigan, Ann Arbor, MI, USA

Department of Pathology, University of Michigan, Ann Arbor, MI, USA

Chantal C.M. Appeldoorn to-BBB technologies BV, Leiden, The Netherlands

Krystof Bankiewicz Department of Neurological Surgery, University of California, San Francisco, CA, USA

Adam K. Bevan Department of Gene Therapy, The Research Institute at Nationwide Children's Hospital, The Ohio State University School of Medicine, Columbus, OH, USA

Marco de Boer to-BBB technologies BV, Leiden, The Netherlands

Elizabeth C.M. de Lange Target Site Equilibration Group, Division of Pharmacology, Leiden Academic Center of Drug Research, Leiden, The Netherlands

Division of Pharmacology, Leiden Academic Center for Drug Research, Gorlaeus Laboratories, Leiden University, Leiden, The Netherlands

Helga de Vries Molecular Cell Biology and Immunology, VU University Medical Center, Amsterdam, The Netherlands

Xavier Declèves INSERM, U705, CNRS UMR 8206, Universités Paris Descartes et Didero, Paris, France

Diana E.M. Dolman Blood–Brain Barrier Group, Institute of Pharmaceutical Science, King's College London, London, UK

David Fortin Department of Neurosurgery and Neuro-oncology, Université de Sherbrooke, Sherbrooke, QC, Canada

Markus Fridén Department of Drug Metabolism and Pharmacokinetics, AstraZeneca Research and Development, Respiratory, Inflammation and Autoimmunity Innovative Medicines, Mölndal, Sweden

Reinhard Gabathuler biOasis Technologies Inc., Vancouver, Canada

Pieter J. Gaillard to-BBB technologies BV, Leiden, The Netherlands

Jean-François Ghersi-Egea Inserm U1028, CNRS UMR 5292, Lyon Neuroscience Research Center, Lyon-1 University, Lyon, France

David Gray Pfizer Pharma Therapeutics Research, Cambridge, MA, USA

Roger N. Gunn Department of Medicine, Imperial College London, London, UK

Department of Engineering Science, University of Oxford, Oxford, UK

Imanova, London, UK

Margareta Hammarlund-Udenaes Translational PKPD Research Group, Department of Pharmaceutical Biosciences, Uppsala University, Uppsala, Sweden

Brian K. Kaspar Department of Gene Therapy, The Research Institute at Nationwide Children's Hospital, The Ohio State University School of Medicine, Columbus, OH, USA

Department of Pediatrics, The Ohio State University Medical Center, Columbus, OH, USA

Department of Neuroscience, The Ohio State University Medical Center, Columbus, OH, USA

Richard F. Keep Department of Neurosurgery, University of Michigan, Ann Arbor, MI, USA

Department of Molecular and Integrative Physiology, University of Michigan, Ann Arbor, MI, USA

Elisa E. Konofagou Department of Biomedical Engineering, Columbia University, New York, NY, USA

Department of Radiology, Columbia University, New York, NY, USA

Gijs Kooij Molecular Cell Biology and Immunology, VU University Medical Center, Amsterdam, The Netherlands

Jeffrey J. Lochhead Pharmaceutical Sciences Division, University of Wisconsin – Madison School of Pharmacy, Madison, WI, USA

Irena Loryan Translational PKPD Research Group, Department of Pharmaceutical Biosciences, Uppsala University, Uppsala, Sweden

Sumio Ohtsuki Department of Pharmaceutical Microbiology, Faculty of Life Sciences, Kumamoto University, Kumamoto, Japan

Andreas Reichel Bayer Healthcare Pharmaceuticals, Global Drug Discovery, DMPK, Berlin, Germany

Arie Reijerkerk Molecular Cell Biology and Immunology, VU University Medical Center, Amsterdam, The Netherlands

Jaap Rip to-BBB technologies BV, Leiden, The Netherlands

Ramakrishna Samala Department of Pharmaceutical Sciences, Texas Tech University Health Sciences Center, Amarillo, TX, USA

Geert J. Schenk Department of Anatomy and Neurosciences, VU University Medical Center, Van der Boechorststraat 7, Amsterdam, The Netherlands

Jean-Michel Scherrmann INSERM, U705, CNRS UMR 8206, Universités Paris Descartes et Didero, Paris, France

Tali Siegal Center for Neuro-Oncology, Hadassah Hebrew University Medical Center, Jerusalem, Israel

Quentin R. Smith Department of Pharmaceutical Sciences, Texas Tech University Health Sciences Center, Amarillo, TX, USA

Nathalie Strazielle Brain-i, Lyon, France

Stina Syvänen Department of Public Health and Caring Sciences, Uppsala University, Uppsala, Sweden

Masanori Tachikawa Division of Membrane Transport and Drug Targeting, Graduate School of Pharmaceutical Sciences, Tohoku University, Sendai, Japan

Tetsuya Terasaki Division of Membrane Transport and Drug Targeting, Graduate School of Pharmaceutical Sciences, Tohoku University, Sendai, Japan

Robert G. Thorne Pharmaceutical Sciences Division, University of Wisconsin – Madison School of Pharmacy, Madison, WI, USA

Center for Neuroscience and Neuroscience Training Program, University of Wisconsin – Madison, Madison, WI, USA

Cellular and Molecular Pathology Graduate Training Program, University of Wisconsin – Madison, Madison, WI, USA

Clinical Neuroengineering Training Program, University of Wisconsin – Madison, Madison, WI, USA

Institute for Clinical and Translational Research, University of Wisconsin – Madison, Madison, WI, USA

Yasuo Uchida Division of Membrane Transport and Drug Targeting, Graduate School of Pharmaceutical Sciences, Tohoku University, Sendai, Japan

Corine C. Visser to-BBB technologies BV, Leiden, The Netherlands

Jianming Xiang Department of Neurosurgery, University of Michigan, Ann Arbor, MI, USA

Siti R. Yusof HICoE Centre for Drug Research, Universiti Sains Malaysia, Minden, Penang, Malaysia

Ningna Zhou Department of Neurosurgery, University of Michigan, Ann Arbor, MI, USA

Part I
Physiology and Basic Principles for Drug Handling by the Brain

Chapter 1
Anatomy and Physiology of the Blood–Brain Barriers

N. Joan Abbott

Abstract This chapter covers the three main barrier layers separating blood and the central nervous system (CNS): the endothelium of the brain vasculature, the epithelium of the choroid plexus secreting cerebrospinal fluid (CSF) into the ventricles and the arachnoid epithelium forming the middle layer of the meninges on the brain surface. There are three key barrier features at each site that control the composition of brain fluids and regulate CNS drug permeation: (1) physical barriers result from features of the cell membranes and of the tight junctions restricting the paracellular pathway through intercellular clefts; (2) transport barriers result from membrane transporters mediating solute uptake and efflux, together with vesicular mechanisms mediating transcytosis of larger molecules such as peptides and proteins and (3) enzymatic barriers result from cell surface and intracellular enzymes that can modify molecules in transit. Brain fluids (CSF and brain interstitial fluid) are secreted, flow through particular routes and then drain back into the venous system; this fluid turnover aids central homeostasis and also affects CNS drug concentration. Several CNS pathologies involve changes in the barrier layers and the fluid systems. Many of these aspects of physiology and pathology have implications for drug delivery.

1.1 Neural Signalling and the Importance of CNS Barrier Layers

The brain and spinal cord (central nervous system, CNS) are the control centres of the body, generating central programmes, coordinating sensory input and motor output and integrating many of the activities of peripheral organs and tissues.

N.J. Abbott (✉)
Institute of Pharmaceutical Science, Blood–Brain Barrier Group, King's College London, Franklin Wilkins Building 3.10, 150 Stamford Street, London SE1 9NH, UK
e-mail: joan.abbott@kcl.ac.uk

M. Hammarlund-Udenaes et al. (eds.), *Drug Delivery to the Brain*, AAPS Advances in the Pharmaceutical Sciences Series 10, DOI 10.1007/978-1-4614-9105-7_1,

CNS neurons use chemical and electrical signals for communication, requiring precise ionic movements across their membranes. This is particularly critical at central synapses generating graded synaptic potentials and somewhat less so along axons signalling via all-or-none action potentials. Hence precise control (homeostasis) of the CNS microenvironment is crucial for reliable neural signalling and integration. It has been argued that this was one of the strongest evolutionary pressures driving the development of cellular barriers at the interfaces between the blood and the CNS, since animals with better CNS regulation would have more reliable, efficient and rapid neural signalling, giving selective advantage in finding and remembering food sources, catching prey and avoiding predators (Abbott 1992). These cellular barriers at the interfaces act as key regulatory sites, controlling ion and molecular flux into and out of the CNS, while the resident cells of the CNS including neurons and their associated glial cells, the macroglia (astrocytes, oligodendrocytes) and microglia, contribute to local regulation of the composition of the interstitial (or extracellular) fluid (ISF, ECF) (for review see Abbott et al. 2010). The molecular flux control at CNS barriers includes delivering essential nutrients, removing waste products and severely restricting the entry of potentially toxic or neuroactive agents and pathogens. The barrier layers also act as the interface between the central and peripheral immune systems, exerting strong and selective control over access of leukocytes from the circulation (Engelhardt and Coisne 2011; Greenwood et al. 2011; Ransohoff and Engelhardt 2012).

Three main barrier sites can be identified (Fig. 1.1): the endothelium of the brain microvessels (forming the blood–brain barrier, BBB) (Reese and Karnovsky 1967), the epithelium of the choroid plexus (specialised ependyma) secreting cerebrospinal fluid (CSF) into the cerebral ventricles (Becker et al. 1967) and the epithelium of the arachnoid mater covering the outer brain surface above the layer of subarachnoid CSF (Nabeshima et al. 1975); the choroid plexus and arachnoid form the blood–CSF barrier (BCSFB) (Abbott et al. 2010). The endothelium forms the largest interface (based on surface area) between blood and CNS and hence represents the major site for molecular exchange and the focus for drug delivery; the choroid plexus also plays a critical role, while the properties of the arachnoid membrane suggest that it plays a minor role in exchange. At each of these sites intercellular tight junctions (*zonulae occludentes*) restrict diffusion of polar solutes through the cleft between cells (paracellular pathway), forming the 'physical barrier'. Solute carriers on the apical and basal membranes together with ecto- and endo-enzymes regulate small solute entry and efflux. In brain endothelium, mechanisms of adsorptive and receptor-mediated transcytosis allow restricted and regulated entry of certain large molecules (peptides, proteins) with growth factor and signalling roles within the CNS. Finally the barriers help regulate the innate immune response and the recruitment of leukocytes, contributing to the surveillance and the reactive functions of the central immune cell population. Thus the interface layers work together as physical, transport, enzymatic (metabolic) and immunological barriers (for reviews see Abbott and Friedman 2012; Abbott 2013). The barrier functions are not fixed but dynamic, are able to respond to a variety of regulatory signals from the

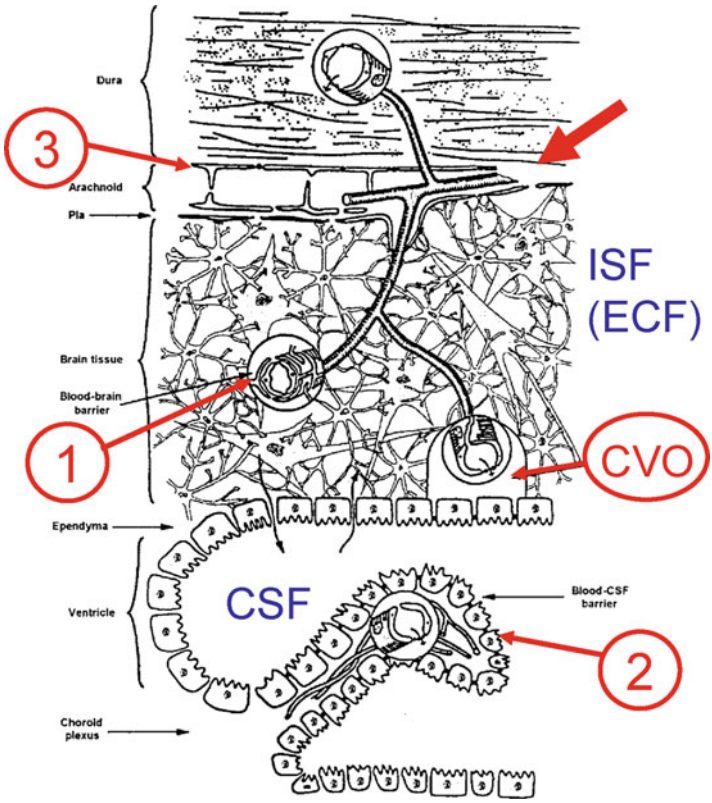

Fig. 1.1 Location of barrier sites in the CNS. Blood enters the brain via surface arteries (*red arrow, top*). Barriers between blood and neural tissue are present at three main sites: (1) the brain endothelium forming the blood–brain barrier (BBB), (2) the choroid plexus epithelium which secretes cerebrospinal fluid (CSF) and (3) the arachnoid epithelium forming the middle layer of the meninges. At each site, the physical barrier results from tight junctions that reduce the permeability of the paracellular pathway (intercellular cleft). In circumventricular organs (CVO), containing neurons specialised for neurosecretion and/or chemosensitivity, the endothelium is leaky. This allows tissue–blood exchange, but as these sites are separated from the rest of the brain by an external glial barrier and from CSF by a barrier at the ependyma, CVOs do not form a leak across the BBB. ISF (ECF): interstitial or extracellular fluid. Figure based on Segal MB and Zlokovic BV 1990 Fig. 1, p2 in 'The Blood–brain Barrier, Amino Acids and Peptides' (Kluwer), modified by A Reichel. Reproduced from Abbott et al. (2003) Lupus 12:908, and with permission of Springer

blood and the brain side and can be significantly disturbed in many CNS and systemic pathologies. This chapter focuses on the physical, transport and enzymatic barrier functions of the BBB and the choroid plexus, as most relevant to CNS drug delivery. As this chapter is meant primarily to provide an overview, references to key reviews are interspersed with those to original findings; if desired, more detailed background may be obtained by consulting sources within the reviews cited.

1.2 The Brain Endothelium and the Neurovascular Unit

The brain capillaries supply blood in close proximity to neurons (maximum diffusion distances typically 8–25 μm); hence, the activities of the BBB are key to brain homeostasis. The brain endothelium of the BBB acts within a cellular complex, the neurovascular unit (NVU) (Fig. 1.2) (Abbott et al. 2010), composed in grey matter of the segment of capillary, its associated pericytes, perivascular astrocytes, basement membranes and microglial cells, the resident immune cells of the CNS (Ransohoff and Perry 2009; Mäe et al. 2011). Together this cellular complex supports a small number of neurons within that NVU module (Iadecola and Nedergaard 2007; Abbott et al. 2010).

Several functions of the BBB can be identified and their roles in CNS homeostasis highlighted (Abbott et al. 2010; Abbott 2013). By regulating ionic and molecular traffic and keeping out toxins the barrier contributes to neuronal longevity and the health and integrity of neural network connectivity. Ionic homeostasis is essential for normal neural signalling. Restricting protein entry limits the innate immune response of the brain and the proliferative potential of the CNS microenvironment. Separating the neurotransmitter pools of the peripheral nervous system (PNS) and CNS minimises interference between signalling networks using the same transmitters while allowing 'non-synaptic' signalling by agents able to move within the protected interstitial fluid (ISF) compartment. Regulating entry of leukocytes allows

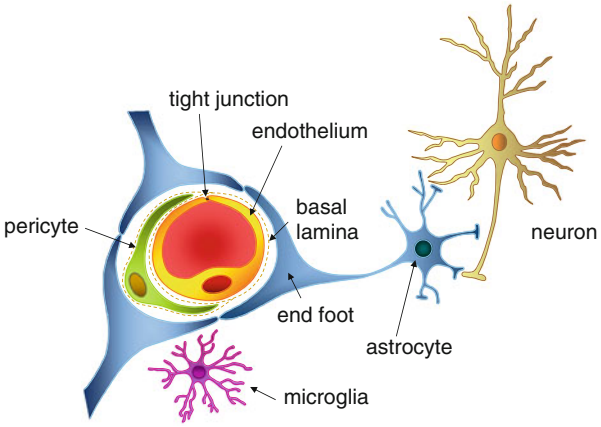

Fig. 1.2 The neurovascular unit (NVU). The NVU is composed of several cell types in close association, working together to maintain an optimal neuronal microenvironment. Cerebral endothelial cells forming the BBB make tight junctions which restrict the paracellular pathway. Pericytes partially envelope the endothelial cells and share a common basal lamina with them. Astrocytes ensheath the microvessel wall. Pericytes and astrocytes are important in barrier induction and maintenance, and astrocytes provide links to neurons. Microglia are CNS-resident immune cells with highly motile cellular processes, some of which can contact the astrocyte basal lamina. By S. Yusof and N.J. Abbott, from Abbott (2013) with permission

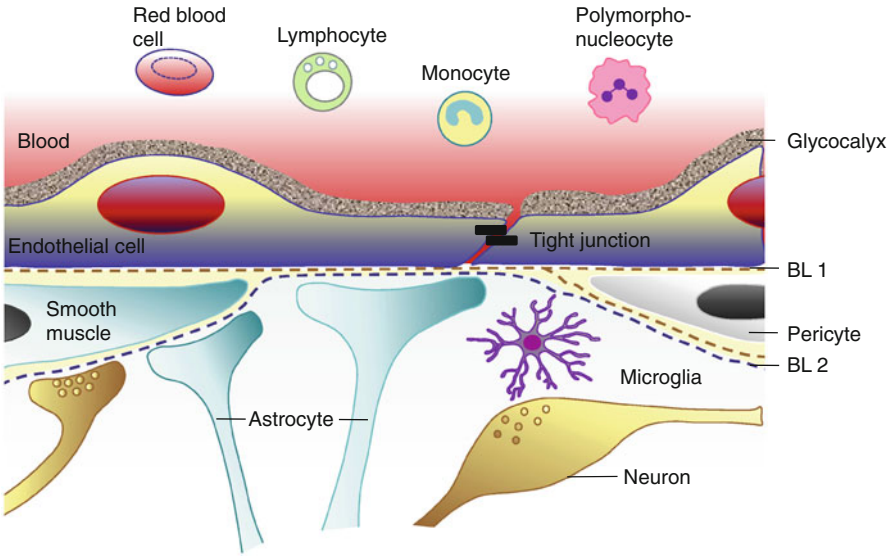

Fig. 1.3 The 'extended' NVU at the level of the microvessel wall, incorporating the glycocalyx and circulating cells. Recent work has highlighted the importance of the glycocalyx on the luminal endothelial surface for endothelial function and the role of circulating leukocytes in monitoring and interacting with this surface. By S. Yusof and N.J. Abbott, modified from Abbott et al. (2010) with permission

immune surveillance with minimal inflammation and cellular damage. Finally, the system is well organised for endogenous protection and 'running repairs' (Liu et al. 2010; Tian et al. 2011; Ransohoff and Brown 2012; Daneman 2012). The other cells of the NVU, especially the astrocytes, pericytes and microglia, together with components of the extracellular matrix (ECM), contribute to these activities.

Given the key role of circulating leukocytes in patrolling, surveillance and repair of the CNS, it has been proposed that these cells, plus the glycocalyx at the endothelial surface (Haqqani et al. 2011), should be included in an 'extended NVU' (Neuwelt et al. 2011) (Fig. 1.3). Current research on the cell:cell interactions involved is revealing further details of the complexity of the NVU and its critical role in maintaining a healthy BBB.

1.3 Nature and Organisation of the Membranes of the Barrier Layers

Many powerful techniques are being applied to increase molecular understanding of barrier function (Redzic 2011; Pottiez et al. 2011; Daneman 2012; Saunders et al. 2013), including biophysical investigation of the lipid membranes, quantitative proteomics, imaging at close to the level of individual molecules and use of genetic mutants and siRNA to test the roles of individual components.

The outer cell membranes (plasmalemma) of the barrier layers, like other mammalian cell membranes, consist of a lipid bilayer with embedded protein, the 'fluid mosaic' model of the membrane. The membrane lipids include glycerophospholipids, sterols and sphingolipids. The hydrophilic polar heads of phospholipids form a continuous layer at the outer and inner leaflets of the membrane, with hydrophobic chains extending into the core of the membrane; the outer leaflet contains mainly zwitterionic phosphatidylcholine (PC) and phosphatidylethanolamine (PE), while the inner leaflet contains mainly negatively charged phosphatidylserine. PC and PE are the main phospholipids in brain endothelium at 20 and 30 %, respectively, with cholesterol at ~20 % (Krämer et al. 2002). Under physiological conditions the lipid bilayer is in a liquid crystalline state. The high percentage of PE and cholesterol in brain endothelium helps to increase its packing density (Gatlik-Landwojtowicz et al. 2006; Seelig 2007) which affects the way molecules partition into and diffuse through the membrane. At the molecular level, there is continual motion of the phospholipid tails within the membrane, creating transient gaps that permit flux of small gaseous molecules (oxygen, CO_2) and small amounts of water (Abbott 2004; Dolman et al. 2005; MacAulay and Zeuthen 2010). Many lipophilic agents including drugs permeate well through the lipid bilayer (Bodor and Buchwald 2003) (Fig. 1.4). However, the tight lipid packing restricts permeation of certain hydrophobic molecules including many drugs and regulates access to particular membrane transport proteins such as the ABC (ATP-binding cassette) efflux transporters, P-glycoprotein (P-gp) (Aänismaa et al. 2008) and breast-cancer resistance protein (BCRP) (Fig. 1.4).

In certain regions of cell membranes, zones enriched in cholesterol and sphingolipids form dynamic microdomains termed 'lipid rafts'; these 10–200 nm heterogeneous structures are associated with a variety of proteins and play roles in cell polarisation, endocytosis, signal transduction, adhesion, migration and links to the cytoskeleton, among others. In brain endothelium, such rafts (Cayrol et al. 2011) have documented functions in leukocyte adhesion and trafficking, junctional molecular architecture and localisation and function of transporters (Dodelet-Devillers et al. 2009). A subset of rafts form caveolae, with high expression of caveolin-1, and can be further classified by function in *scaffolding* for junctional proteins and adhesion to basal lamina, immune cell *adhesion* and recruitment and transendothelial *transport*.

1.4 Tight Junctions in Brain Endothelium and Barrier Epithelia: Structure and Restrictive Properties

The tight junctions of the CNS barrier layers forming the 'physical' barrier (Fig. 1.4) involve a complex 3-D organisation of transmembrane proteins (claudins, occludin), spanning the cleft to create the diffusional restriction and coupling on the cytoplasmic side to an array of adaptor and regulatory proteins linking to the cytoskeleton (Cording et al. 2013). Adherens junctions, while not themselves restricting

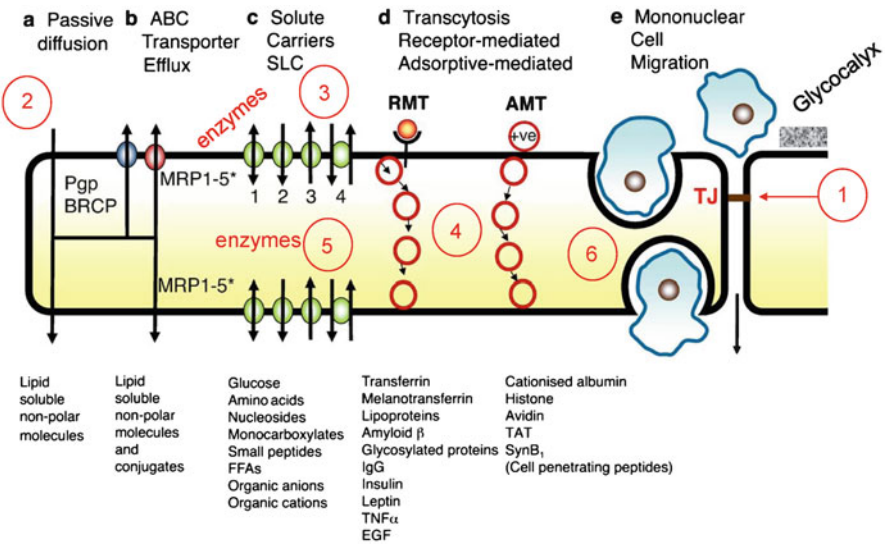

Fig. 1.4 Routes across the brain endothelium. Diagram of brain endothelium showing (*numbered red circles*) the tight junctions (1) and cell membranes (2) forming the 'physical barrier', transporters (3) and vesicular mechanisms (4) (forming the 'transport barrier'), enzymes forming the 'enzymatic barrier' (5) and regulated leukocyte traffic (6) the 'immunologic barrier'. Labels at top of diagram: (**a**) Solutes may passively diffuse through the cell membrane and cross the endothelium; a higher lipid solubility and several other physicochemical factors favour this process. (**b**) Active efflux carriers (ABC transporters) may intercept some of these passively penetrating solutes and pump them out. P-gp and BCRP are strategically placed in the luminal membrane of the BBB endothelium. MRPs 1–5 are inserted into either luminal or abluminal membranes, with some species differences in the polarity and the MRP isoforms expressed. (**c**) Carrier-mediated influx via solute carriers (SLCs) may be passive or primarily or secondarily active and can transport many essential polar molecules such as glucose, amino acids and nucleosides into the CNS. The solute carriers (*black numbers*) may be bidirectional, the direction of net transport being determined by the substrate concentration gradient (1); may be unidirectional either into or out of the cell (2/3) or may involve an exchange of one substrate for another or may be driven by an ion gradient (4). In this last case the direction of transport is also reversible depending on electrochemical gradients. (**d**) RMT requires receptor binding of ligand and can transport a variety of macromolecules such as peptides and proteins across the cerebral endothelium (transcytosis). AMT appears to be induced in a non-specific manner by positively charged macromolecules and can also transport across the endothelium. Both RMT and AMT appear to be vesicular-based systems which carry their macromolecule content across the endothelial cells. (**e**) Leukocyte entry is strictly regulated; under some conditions leukocytes may cross the endothelium by diapedesis either through the endothelial cells or via modified tight junctions. Tight junction modulation can result from signals from cells associated with the NVU or be induced pharmacologically. Modified from Abbott et al. (2010), with permission

paracellular permeability, are important in formation and stabilisation of tight junctions (Paolinelli et al. 2011; Daneman 2012).

The brain endothelial tight junctions are capable of restricting paracellular ionic flux to give high transendothelial electrical resistance (TEER) in vivo of >1,000 Ω. cm^2, while choroid plexus tight junctions are leakier, although the complex

frond-like morphology of the in vivo mammalian plexus makes TEER harder to measure. TEER of ~150 Ω.cm^2 has been recorded across the simpler bullfrog choroid plexus. The brain endothelium shows high expression of the 'barrier-forming' claudin 5, together with claudin 3 and 12, while in choroid plexus the 'pore-forming' claudin 1 dominates, with detectable claudin 2, 3 and 11 (Strazielle and Ghersi-Egea 2013).

For the arachnoid epithelium the situation is less clear; the arachnoid barrier layer is closely apposed to the dura and difficult to isolate intact. It has recently proved possible to culture arachnoid cells in vitro, which express claudin 1 and generate a TEER of ~160 Ω.cm^2 with restriction of larger solute permeation (Lam et al. 2011, 2012; Janson et al. 2011). The perineurium, forming part of the outer sheath of peripheral nerves, is a continuation of the arachnoid layer of the spinal meninges and easier to study than the arachnoid; a TEER of ~480 Ω.cm^2 (Weerasuriya et al. 1984) and expression of claudin 1 have been observed (Hackel et al. 2012). The pattern of barrier properties is consistent with the brain endothelium exerting the most stringent effect on paracellular permeability, while the choroid plexus with a major role in secreting CSF is leakier; the arachnoid epithelium appears to create a barrier of intermediate tightness.

Several junctional proteins, especially occludin and ZO-1, show considerable dynamic activity (half times 100–200 s) (Shen et al. 2008) while maintaining overall junctional integrity and selectivity. Many modulators from both the blood and the brain side can cause junctional opening, some via identified receptor-mediated processes (Abbott et al. 2006; Fraser 2011), possibly aiding repair and removal of debris, but in healthy conditions this is local and transient and does not significantly disturb the homeostatic function of the barrier. Indeed, the presence of endogenous 'protective' molecules and mechanisms able to tighten the barriers is increasingly recognised as important in protection and maintenance at the barrier sites (Bazan et al. 2012; Cristante et al. 2013). Recent studies have highlighted the possible role of microRNAs in barrier protection (Reijerkerk et al. 2013).

1.5 Small Solute Transport at the Barrier Layers

Many BBB solute carriers (SLCs) with relatively tight substrate specificities have been described (Abbott et al. 2010; Redzic 2011; Neuwelt et al. 2011; Parkinson et al. 2011), mediating the entry of major nutrients such as glucose, amino acids, nucleosides, monocarboxylates and organic anions and cations and efflux from the brain of some metabolites (Fig. 1.4). Among the group of ABC (efflux) transporters, P-gp (ABCB1) and/or BCRP (ABCG2) are the dominant players on the apical (blood-facing) membrane, especially P-gp in rodents and BCRP in primates, but the expression levels, localisation and roles of the multidrug resistance-associated proteins (MRPs, ABCC group) are less clear (Shawahna et al. 2011) (Fig. 1.4). ABC transporters have broader substrate specificity than the SLCs, making analysis of their structure–activity relationship (SAR) difficult (Demel et al. 2009).

Synergistic activity between P-gp and BCRP has been observed (Kodaira et al. 2010), and ABC transporters and cytochrome P450 (CYP) enzymes together generate an active metabolic barrier within the NVU (Declèves et al. 2011).

There are many differences between the transporters and enzymes expressed in the different barrier layers, suggesting that they play different but complementary roles in regulation of molecular flux (Strazielle and Ghersi-Egea 2013; Saunders et al. 2013; Yasuda et al. 2013). The transporters present include considerable overlap in function/apparent redundancy at each site, reflecting their evolutionary history (Dean and Annilo 2005) and ensuring maintained function in case of loss or defect of a single transporter.

1.6 Vesicular Transport and Transcytosis

Classification of types of vesicular transport by cells is complex, but it is clear that certain features of endocytosis and transcytosis in the highly polarised brain endothelium are different from those of less polarised endothelia such as that of skeletal muscle. Non-specific fluid-phase endocytosis and transcytosis are downregulated in brain compared with non-brain endothelium. However for certain endogenous peptides and proteins, two main types of vesicle-mediated transfer have been documented in the BBB: receptor-mediated transcytosis (RMT) and adsorptive mediated transcytosis (AMT) (Abbott et al. 2010) (Fig. 1.4). There appears to be some overlap in the function between caveolar and clathrin-mediated vesicular routes and likely involvement of other types of molecular entrapment, engulfment and transendothelial movement that are less well characterised (Mayor and Pagano 2007; Strazielle and Ghersi-Egea 2013). Electron microscopy of the choroid plexus shows a variety of vesicular and tubular profiles, but the epithelium appears to be specialised for secretion rather than transcytosis (Strazielle and Ghersi-Egea 2013).

1.7 Routes for Permeation Across Barrier Layers and Influence on Drug Delivery

Many of these routes for permeation across the brain endothelium (Fig. 1.4) can be used for drug delivery; several classical CNS drugs are sufficiently lipid soluble to diffuse through the endothelial cell membranes to reach the brain ISF (Bodor and Buchwald 2003). However, for less lipophilic agents with slower permeation and hence longer dwell time in the lipid bilayer, activity of ABC efflux transporters can significantly reduce CNS access (Seelig 2007; Aänismaa et al. 2008). As barrier tightness, transporter expression/activity and vesicular mechanisms can be altered in pathology, it is difficult to predict CNS distribution and pharmacokinetics of drugs in individual patients, particularly where barrier dysfunction may change both regionally and in time during the course of pathologies such as epilepsy, stroke and cancer (Stanimirovic and Friedman 2012).

1.8 Development, Induction, Maintenance and Heterogeneity of the BBB

Study of BBB evolution, development and maintenance gives valuable insights into both normal physiology and the changes that can occur in pathology. Studies in invertebrates, and lower vertebrates especially archaic fish, provide strong evidence that the first barrier layers protecting the CNS were formed by specialised glial cells at the vascular-neural interface and that as the intracerebral vasculature became more complete and complex, the barrier was increasingly supported by pericytes and endothelium. Later there was a shift to the dominant modern vertebrate pattern, where the endothelium forms the principal barrier layer (Bundgaard and Abbott 2008). Interestingly, the pericytes and astrocytes still remain closely associated with the brain endothelium, reflecting their evolutionary history and contributing to the NVU.

In development of the mammalian brain, the endothelium of the ingrowing vessel sprouts develops basic restrictive barrier properties under the influence of neural progenitor cells (NPCs) (Liebner et al. 2008; Daneman et al. 2009), with pericytes subsequently refining the phenotype by downregulating features characteristic of non-brain endothelium; later, astrocytes help upregulate the full differentiated BBB phenotype (Daneman et al. 2010; Armulik et al. 2010).

Certain of the signalling mechanisms involved in this induction are known including the Wnt/β-catenin (Liebner et al. 2008) and sonic hedgehog pathways (Alvarez et al. 2011), and some of them may be involved in maintaining barrier integrity in the adult. It is clear that endothelial cells and pericytes are in turn involved in signalling to astrocytes to regulate the expression of ion and water channels, receptors, transporters and enzymes on the astrocyte endfeet so that mutual induction and maintenance are involved in sustaining the critical features of barrier and NVU function (Abbott et al. 2006). This regulation extends to the microanatomy and microenvironment of the perivascular space created by the extracellular matrix/basal laminae components of the endothelial–pericyte–astrocyte complex (Liebner et al. 2011). Microglial cell processes are found among the astrocyte endfeet (Mathiisen et al. 2010), suggesting roles in monitoring and influencing the local cellular organisation and function; indeed, microglial cells have been shown to regulate leukocyte traffic (reviewed in Daneman 2012). Specific perivascular nerve fibres associated with cerebral microvessels are involved in regulation of vascular tone (Hamel 2006). However, less is known about microglial and neuronal induction of barrier properties, and the signalling pathways involved in barrier maintenance on a minute-by-minute basis are relatively unexplored.

The NVU contains several mechanisms for protection of the BBB against minor damage such as local oxidative stress, e.g. by tightening the barrier (Abbott et al. 2006), and presence of detoxifying transporters and enzymes (Strazielle and Ghersi-Egea 2013), but this field is expanding with recognition that some of the 'protectins', protective agents identified in peripheral tissues, are also active in the brain (Bazan et al. 2012). Recently the protein Annexin-A1/lipocortin has been shown to

be involved in the anti-inflammatory and neuroprotective effects of microglia (McArthur et al. 2010) and to act as an endogenous BBB tightening agent (Cristante et al. 2013). Improved understanding of the mechanisms for 'self-repair' within the NVU to correct minor local damage is likely to prove critical in future development of therapies that treat CNS disorders at much earlier phases of the pathology than currently possible, with expected major gains in efficacy.

There are several phenotypic and functional differences between the endothelial cells of different segments of the cerebral microvasculature (reviewed in Ge et al. 2005; Patabendige et al. 2013). Compared with arteriolar or venular endothelium, cerebral capillary endothelium has a more complex pattern of tight junction strands in freeze-fracture images consistent with tighter tight junctions, and higher expression of solute transporters including efflux transporters, and of certain receptors involved in transcytosis. Arteriolar endothelium shows higher expression of certain enzymes, absence of P-gp and, in a few regions, bidirectional transcytosis of tracers such as horseradish peroxidase, creating a local protein 'leak'. The post-capillary venule segment is specialised for regulation of leukocyte traffic and control of local inflammation. Some differences between the vascular beds of different brain regions have been observed at both micro- and macro-levels, but in general their significance is unclear.

1.9 Beyond the Barrier: The Fluid Compartments of the ISF and CSF

The cells of the brain, chiefly neurons and macroglia (astrocytes and oligodendrocytes) but also microglia, the resident immune cells of the brain, are bathed by an ionic medium similar to plasma but containing very low protein and slightly more Mg^{2+} and less K^{+} and Ca^{2+} (Somjen 2004). This extracellular or interstitial fluid (ECF, ISF) occupies around 20 % of the brain volume (Sykova and Nicholson 2008). The ventricles and subarachnoid space contain CSF, secreted by the choroid plexuses of the lateral, third and fourth ventricles and with a daily turnover in humans of 2–4 times per day (Silverberg et al. 2003). The outflow pathways include arachnoid granulations (outpouchings of the arachnoid membrane into veins in the dura), but some CSF also drains along cranial nerves (especially olfactory) and blood vessel sheaths to the lymph nodes of the neck. Species differences have been reported in the relative importance of these drainage routes (Johanson et al. 2008).

The origin and dynamics of the ISF are less well understood. The brain microvessels have the ionic transport mechanisms and channels, and low but sufficient water permeability, to generate ISF as a secretion (Fig. 1.5), and calculations show that a proportion of ISF water may come from glucose metabolism of the brain, aided by aquaporin 4 (AQP4) water channels in the perivascular endfeet membranes of astrocytes (Abbott 2004; Dolman et al. 2005). Within the neuropil, the small blocks of tissue demarcated by the lattice of fine microvessels, in which neural communication occurs, the distances from the vessel to the furthest neuron are small, typically

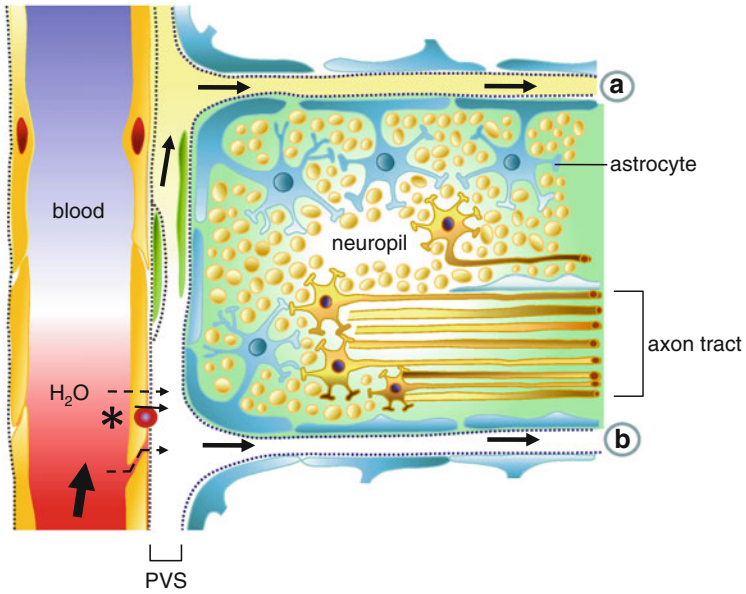

Fig. 1.5 Proposed sites of generation of ISF and routes for ISF flow. A large fraction of ISF is proposed to be formed by brain capillary endothelium, driven by the ionic gradient set up by the abluminal Na, K, ATPase (* *circle + arrow*). Water follows passively either through the endothelial cell membranes or via the tight junctions (*dashed arrows*). Driven by this hydrostatic pressure gradient and with the addition of some CSF from the subarachnoid space, ISF moves by bulk flow through low-resistance pathways formed by perivascular spaces (PVS, predominantly around larger vessels including arterioles and arteries, venules and veins), connecting with (A) glial-lined boundary zones between blocks of neuropil and (B) regions adjacent to axon tracts. The narrow spaces between cells within the neuropil appear to be too narrow to permit significant bulk flow. Not to scale. Modified by S. Yusof from Abbott (2004), with permission

<30 μm, so that diffusion within the neuropil is an effective means of ionic and molecular movement. Indeed many studies in isolated brain slices and in situ confirm the local diffusive behaviour of test molecules injected into the brain (Thorne and Nicholson 2006; Wolak and Thorne 2013). However, superimposed on this local diffusion is the possibility for flow of ISF over longer distances.

There is considerable historical evidence for flowing ISF, capable of clearing waste products including large molecules such as β-amyloid from the interstitium moving via routes offering the least resistance to flow, along axon tracts and blood vessels (Abbott 2004; Weller et al. 2008, 2009). Careful studies of clearance of tracer molecules injected into the parenchyma give a figure for clearance half-time of 2–3 h (Groothuis et al. 2007), around ten times faster than reported earlier (Cserr et al. 1981). Most of this flow can be accounted for by fluid secretion across cerebral capillary endothelium (Abbott 2004) (Fig. 1.5), but recent studies add to a body of earlier evidence showing that a proportion of CSF from the subarachnoid space can flow into the brain along periarterial (Virchow–Robin) spaces, contributing to ISF,

with return out along nerve fibre tracts and blood vessels (Abbott 2004; Iliff et al. 2012; Yang et al. 2013). However, there is some controversy over whether arteries (Weller et al. 2008, 2009) or veins (Iliff et al. 2012) are chiefly responsible for the ISF outflow route from the brain parenchyma. In any event, with the flow largely confined to major extracellular 'highways' in the tissue, the rate of turnover will be similar to that of CSF. Thus ISF and CSF can be regarded as parallel fluids maintaining a continuous flow through the low-resistance pathways of the brain (ISF) and through the ventricles and subarachnoid space (CSF), capable of some mixing and hence with some shared roles, but also many distinct and complementary functions. Between them the CSF and ISF contribute to maintaining tissue buoyancy, waste removal, circulation of secretory products such as vitamins and hormones from choroid plexuses, non-synaptic or 'distance' signalling ('volume transmission') and providing routes for immune surveillance without disturbing neuronal networks (Strazielle and Ghersi-Egea 2013).

1.10 Changes in BBB and BCSFB in Pathology

The BBB is altered in many CNS pathologies including stroke, multiple sclerosis and epilepsy (reviewed in Abbott et al. 2006, 2010; Friedman 2011; Abbott and Friedman 2012; Daneman 2012; Stanimirovic and Friedman 2012; Potschka 2012). Changes can include upregulation of luminal adhesion molecules, increased adhesion and transmigration of leukocytes, increased leakiness of tight junctions, extravasation of plasma proteins via paracellular or transcellular routes and altered expression of drug transporters. Given the importance of the BBB in CNS homeostasis, it is clear that gross barrier dysfunction is likely to be associated with disturbance of neural signalling, in both the short and the long term (Abbott and Friedman 2012). In many pathologies, a combination or a sequence of events may make the barrier vulnerable, including trauma, hypoxia, infection, activation of the clotting system and inflammation; components of the diet, environmental toxins and genetic factors may also contribute (Shlosberg et al. 2010). Inflammation and free radicals are now recognised to play major roles in many or even most of the pathologies with BBB disturbance, but the aetiology and sequence of changes are generally unclear, and in many cases it is not known whether changes occur simultaneously or as part of an inflammatory cascade (Friedman 2011; Kim et al. 2013). Certain brain regions are more often affected, including the hippocampus and cerebral cortex grey matter, but again the reasons are uncertain.

For minor damage, the cells of the NVU aided by recruitment of leukocytes may effect a repair, and short- and long-term changes in protective mechanisms including upregulation of efflux transporters and enzymes may be involved. Certainly several types of altered cell:cell interaction can be detected in pathology, particularly between endothelium and astrocytes, but also with powerful roles played by microglia, changing from a relatively quiescent and static process-bearing morphology to a more amoeboid and migratory form, secreting a different repertoire of

cytokines and chemokines (Saijo and Glass 2011; Smith et al. 2012; Daneman 2012). Agents released from most of the cells of the NVU in pathology can modulate brain endothelial tight junctions, with several inflammatory mediators increasing barrier permeability and a few agents able to counter or reverse this (Abbott et al. 2006). Potentiating effects of several cytokines including IL-1β and TNFα on the 'first line' of inflammatory mediators (e.g. bradykinin) have been documented (Fraser 2011). At the molecular level, a great many signalling pathways can be identified, regulating both the expression and activity of barrier features, particularly well documented for the effects of xenobiotics, neurotransmitters and inflammation on P-gp (Miller 2010). Recent identification of a number of microRNAs (miRNAs) shown to influence angiogenesis (Caporali and Emanueli 2011), vascular functions (Hartmann and Thum 2011) and BBB physiology/pathology (Reijerkerk et al. 2013; Mishra and Singh 2013) adds a further level of complexity. Furthermore, new information on a whole family of secreted and information-carrying extracellular vesicles including exosomes (György et al. 2011; Haqqani et al. 2013) adds to the repertoire of ways in which a cell or a group of cells can influence other cells nearby or further away. Indeed the flow pathways allowing circulation of the brain ISF have suitable properties for this kind of non-neural communication (Abbott 2004) and could also play an important part in the dissemination of CNS pathologies (multiple sclerosis, cancers) that start at a relatively restricted locus.

The choroid plexus and CSF/ISF flow system are also affected by ageing and many pathologies, including tumours, infection, trauma, ischaemia, neurodegenerative disease and hydrocephalus (Johanson et al. 2008; Serot et al. 2012). Many of these affect the anatomy, connectivity and outflow routes of the fluid flow systems, but changes in the physiology of the choroid plexus and the resulting disturbance in generation and composition of CSF are also critical. Ageing is associated with a reduction in CSF production and in secretion of many choroid plexus-derived proteins, particularly important for the zones of neurogenesis close to the ventricular wall.

1.11 Implications for Drug Delivery

The anatomy and physiology of the CNS barriers and fluid systems described here have many implications for drug delivery, whether for agents designed to act in the CNS or for those with peripheral targets where the aim is to minimise CNS side effects. Clearly barrier changes in ageing and pathology will affect distribution and delivery of both CNS and peripheral drugs. Improved experimental methods and models, molecular and pharmacokinetic modelling and new developments in understanding barrier function help in measuring and predicting the concentration of drugs at the active site. The expanding field of 'biologic' therapeutics, large molecules with specific actions in the CNS, poses new challenges but is also giving novel insights into mechanisms and ways to improve CNS drug delivery of complex molecules. Many of these issues will be discussed in further chapters in this volume.

1.12 Points for Discussion

- Why is it important to understand the different properties of the three main barrier layers (Sect. 1.1)? What kinds of technique can be used to establish the relative importance of each in determining CNS distribution of a particular drug?
- Several 'key functions' of the BBB are listed (Sect. 1.2). Is it possible to put these in order of importance for brain function?
- Much of the BBB and choroid plexus literature is devoted to documenting changes in pathology. Why has maintenance of healthy function received less attention?
- What models and techniques would you propose for a new study on cell:cell interaction within the NVU?
- What is the glycocalyx of the brain endothelium, and what properties of the cells is it most likely to influence?
- Why is it important to know about the organisation of the BBB lipid membrane in modelling drug permeation? Why are potential substrates for ABC transporters particularly affected by the membrane composition?
- Why is it difficult to establish how water moves across the BBB and choroid plexus?
- How does knowledge of BBB development help in understanding barrier function?
- What is the significance of heterogeneity in function, e.g. between the capillary and post-capillary venule segments of the cerebral microvasculature?

Acknowledgements I am grateful to Dr Siti R. Yusof for help with artwork and many colleagues for discussions.

References

Aänismaa P, Gatlik-Landwojtowicz E, Seelig A (2008) P-glycoprotein senses its substrates and the lateral membrane packing density: consequences for the catalytic cycle. Biochemistry 47:10197–10207

Abbott NJ (1992) Comparative physiology of the blood–brain barrier. In: Bradbury MWB (ed) Physiology and pharmacology of the blood–brain barrier, vol 103, Handb Exp Pharmacol. Springer, Heidelberg, pp 371–396

Abbott NJ, Mendonça LL, Dolman DE (2003) The blood-brain barrier in systemic lupus erythematosus. Lupus 12:908–915

Abbott NJ (2004) Evidence for bulk flow of brain interstitial fluid: significance for physiology and pathology. Neurochem Int 45:545–552

Abbott NJ (2013) Blood–brain barrier structure and function and the challenges for CNS drug delivery. J Inherit Metab Dis 36:437–449

Abbott NJ, Friedman A (2012) Overview and introduction: the blood–brain barrier in health and disease. Epilepsia 53 (Suppl 6):1–6

Abbott NJ, Rönnbäck L, Hansson E (2006) Astrocyte-endothelial interactions at the blood–brain barrier. Nat Rev Neurosci 7:41–53

Abbott NJ, Patabendige AA, Dolman DE, Yusof SR, Begley DJ (2010) Structure and function of the blood–brain barrier. Neurobiol Dis 37:13–25

Alvarez JI, Dodelet-Devillers A, Kebir H, Ifergan I, Fabre PJ, Terouz S, Sabbagh M, Wosik K, Bourbonnière L, Bernard M, van Horssen J, de Vries HE, Charron F, Prat A (2011) The

Hedgehog pathway promotes blood–brain barrier integrity and CNS immune quiescence. Science 334:1727–1731
Armulik A, Genové G, Mäe M, Nisancioglu MH, Wallgard E, Niaudet C, He L, Norlin J, Lindblom P, Strittmatter K, Johansson BR, Betsholtz C (2010) Pericytes regulate the blood–brain barrier. Nature 468:557–561
Bazan NG, Eady TN, Khoutorova L, Atkins KD, Hong S, Lu Y, Zhang C, Jun B, Obenaus A, Fredman G, Zhu M, Winkler JW, Petasis NA, Serhan CN, Belayev L (2012) Novel aspirin-triggered neuroprotectin D1 attenuates cerebral ischemic injury after experimental stroke. Exp Neurol 236:122–130
Becker NH, Novikoff AB, Zimmerman HM (1967) Fine structure observations of the uptake of intravenously injected peroxidase by the rat choroid plexus. J Histochem Cytochem 15:160–165
Bodor N, Buchwald P (2003) Brain targeted drug delivery; experiences to date. Am J Drug Deliv 1:13–26
Bundgaard M, Abbott NJ (2008) All vertebrates started out with a glial blood–brain barrier 4–500 million years ago. Glia 56:699–708
Caporali A, Emanueli C (2011) MicroRNA regulation in angiogenesis. Vascul Pharmacol 55:79–86
Cayrol R, Haqqani AS, Ifergan I, Dodelet-Devillers A, Prat A (2011) Isolation of human brain endothelial cells and characterization of lipid raft-associated proteins by mass spectroscopy. Methods Mol Biol 686:275–295
Cording J, Berg J, Käding N, Bellmann C, Tscheik C, Westphal JK, Milatz S, Günzel D, Wolburg H, Piontek J, Huber O, Blasig IE (2013) In tight junctions, claudins regulate the interactions between occludin, tricellulin and marvelD3, which, inversely, modulate claudin oligomerization. J Cell Sci 26:554–564
Cristante E, McArthur S, Mauro C, Maggioli E, Romero IA, Wylezinska-Arridge M, Couraud PO, Lopez-Tremoleda J, Christian HC, Weksler BB, Malaspina A, Solito E (2013) Identification of an essential endogenous regulator of blood–brain barrier integrity, and its pathological and therapeutic implications. Proc Natl Acad Sci U S A 110:832–841
Cserr HF, Cooper DN, Suri PK, Patlak CS (1981) Efflux of radiolabeled polyethylene glycols and albumin from rat brain. Am J Physiol 240:F319–F328
Daneman R (2012) The blood–brain barrier in health and disease. Ann Neurol 72:648–672
Daneman R, Agalliu D, Zhou L, Kuhnert F, Kuo CJ, Barres BA (2009) Wnt/beta-catenin signaling is required for CNS, but not non-CNS, angiogenesis. Proc Natl Acad Sci U S A 106:641–646
Daneman R, Zhou L, Kebede AA, Barres BA (2010) Pericytes are required for blood–brain barrier integrity during embryogenesis. Nature 468:562–566
Dean M, Annilo T (2005) Evolution of the ATP-binding cassette (ABC) transporter superfamily in vertebrates. Annu Rev Genomics Hum Genet 6:123–142
Declèves X, Jacob A, Yousif S, Shawahna R, Potin S, Scherrmann JM (2011) Interplay of drug metabolizing CYP450 enzymes and ABC transporters in the blood–brain barrier. Curr Drug Metab 12:732–741
Demel MA, Krämer O, Ettmayer P, Haaksma EE, Ecker GF (2009) Predicting ligand interactions with ABC transporters in ADME. Chem Biodivers 6:1960–1969
Dodelet-Devillers A, Cayrol R, van Horssen J, Haqqani AS, de Vries HE, Engelhardt B, Greenwood J, Prat A (2009) Functions of lipid raft membrane microdomains at the blood–brain barrier. J Mol Med (Berl) 87:765–774
Dolman D, Drndarski S, Abbott NJ, Rattray M (2005) Induction of aquaporin 1 but not aquaporin 4 messenger RNA in rat primary brain microvessel endothelial cells in culture. J Neurochem 93:825–833
Engelhardt B, Coisne C (2011) Fluids and barriers of the CNS establish immune privilege by confining immune surveillance to a two-walled castle moat surrounding the CNS castle. Fluids Barriers CNS 8:4. doi:10.1186/2045-8118-8-4
Fraser PA (2011) The role of free radical generation in increasing cerebrovascular permeability. Free Radic Biol Med 51:967–977

Friedman A (2011) Blood–brain barrier dysfunction, status epilepticus, seizures, and epilepsy: a puzzle of a chicken and egg? Epilepsia 52(Suppl 8):19–20

Gatlik-Landwojtowicz E, Aänismaa P, Seelig A (2006) Quantification and characterization of P-glycoprotein-substrate interactions. Biochemistry 45:3020–3032

Ge S, Song L, Pachter JS (2005) Where is the blood–brain barrier … really? J Neurosci Res 79:421–427

Greenwood J, Heasman SJ, Alvarez JI, Prat A, Lyck R, Engelhardt B (2011) Review: Leucocyte-endothelial cell crosstalk at the blood–brain barrier: a prerequisite for successful immune cell entry to the brain. Neuropathol Appl Neurobiol 37:24–39

Groothuis DR, Vavra MW, Schlageter KE, Kang EW, Itskovich AC, Hertzler S, Allen CV, Lipton HL (2007) Efflux of drugs and solutes from brain: the interactive roles of diffusional transcapillary transport, bulk flow and capillary transporters. J Cereb Blood Flow Metab 27:43–56

György B, Szabó TG, Pásztói M, Pál Z, Misják P, Aradi B, László V, Pállinger E, Pap E, Kittel A, Nagy G, Falus A, Buzás EI (2011) Membrane vesicles, current state-of-the-art: emerging role of extracellular vesicles. Cell Mol Life Sci 68:2667–2688

Hackel D, Krug SM, Sauer RS, Mousa SA, Böcker A, Pflücke D, Wrede EJ, Kistner K, Hoffmann T, Niedermirtl B, Sommer C, Bloch L, Huber O, Blasig IE, Amasheh S, Reeh PW, Fromm M, Brack A, Rittner HL (2012) Transient opening of the perineurial barrier for analgesic drug delivery. Proc Natl Acad Sci U S A 109:E2018–E2027

Hamel E (2006) Perivascular nerves and the regulation of cerebrovascular tone. J Appl Physiol 100:1059–1064

Haqqani AS, Hill JJ, Mullen J, Stanimirovic DB (2011) Methods to study glycoproteins at the blood–brain barrier using mass spectrometry. Methods Mol Biol 686:337–353

Haqqani AS, Delaney CE, Tremblay TL, Sodja C, Sandhu JK, Stanimirovic DB (2013) Method for isolation and molecular characterization of extracellular microvesicles released from brain endothelial cells. Fluids Barriers CNS 10:4. doi:10.1186/2045-8118-10-4

Hartmann D, Thum T (2011) MicroRNAs and vascular (dys)function. Vascul Pharmacol 55:92–105

Iadecola C, Nedergaard M (2007) Glial regulation of the cerebral microvasculature. Nat Neurosci 10:1369–1376

Iliff JJ, Wang M, Liao Y, Plogg BA, Peng W, Gundersen GA, Benveniste H, Vates GE, Deane R, Goldman SA, Nagelhus EA, Nedergaard M (2012) A paravascular pathway facilitates CSF flow through the brain parenchyma and the clearance of interstitial solutes, including amyloid β. Sci Transl Med 4:147ra111. doi:10.1126/scitranslmed.3003748

Janson C, Romanova L, Hansen E, Hubel A, Lam C (2011) Immortalization and functional characterization of rat arachnoid cell lines. Neuroscience 177:23–34

Johanson CE, Duncan JA 3rd, Klinge PM, Brinker T, Stopa EG, Silverberg GD (2008) Multiplicity of cerebrospinal fluid functions: new challenges in health and disease. Cerebrospinal Fluid Res 5:10. doi:10.1186/1743-8454-5-10

Kim SY, Buckwalter M, Soreq H, Vezzani A, Kaufer D (2013) Blood–brain barrier dysfunction-induced inflammatory signaling in brain pathology and epileptogenesis. Epilepsia 53(Suppl 6):37–44

Kodaira H, Kusuhara H, Ushiki J, Fuse E, Sugiyama Y (2010) Kinetic analysis of the cooperation of P-glycoprotein (P-gp/Abcb1) and breast cancer resistance protein (Bcrp/Abcg2) in limiting the brain and testis penetration of erlotinib, flavopiridol, and mitoxantrone. J Pharmacol Exp Ther 333:788–796

Krämer SD, Schütz YB, Wunderli-Allenspach H, Abbott NJ, Begley DJ (2002) Lipids in blood–brain barrier models in vitro II: influence of glial cells on lipid classes and lipid fatty acids. In Vitro Cell Dev Biol 38:566–571

Lam CH, Hansen EA, Hubel A (2011) Arachnoid cells on culture plates and collagen scaffolds: phenotype and transport properties. Tissue Eng Part A 17:1759–1766

Lam CH, Hansen EA, Janson C, Bryan A, Hubel A (2012) The characterization of arachnoid cell transport II: paracellular transport and blood-cerebrospinal fluid barrier formation. Neuroscience 222:228–238

Liebner S, Corada M, Bangsow T, Babbage J, Taddei A, Czupalla CJ, Reis M, Felici A, Wolburg H, Fruttiger M, Taketo MM, von Melchner H, Plate KH, Gerhardt H, Dejana E (2008) Wnt/beta-catenin signaling controls development of the blood–brain barrier. J Cell Biol 183:409–417

Liebner S, Czupalla CJ, Wolburg H (2011) Current concepts of blood–brain barrier development. Int J Dev Biol 55:467–476

Liu DZ, Ander BP, Xu H, Shen Y, Kaur P, Deng W, Sharp FR (2010) Blood–brain barrier breakdown and repair by Src after thrombin-induced injury. Ann Neurol 67:526–533

MacAulay N, Zeuthen T (2010) Water transport between CNS compartments: contributions of aquaporins and cotransporters. Neuroscience 168:941–956

Mäe M, Armulik A, Betsholtz C (2011) Getting to know the cast–cellular interactions and signaling at the neurovascular unit. Curr Pharm Des 17:2750–2754

Mathiisen TM, Lehre KP, Danbolt NC, Ottersen OP (2010) The perivascular astroglial sheath provides a complete covering of the brain microvessels: an electron microscopic 3D reconstruction. Glia 58:1094–1103

Mayor S, Pagano RE (2007) Pathways of clathrin-independent endocytosis. Nat Rev Mol Cell Biol 8:603–612

McArthur S, Cristante E, Paterno M, Christian H, Roncaroli F, Gillies GE, Solito E (2010) Annexin A1: a central player in the anti-inflammatory and neuroprotective role of microglia. J Immunol 185:317–328

Miller DS (2010) Regulation of P-glycoprotein and other ABC drug transporters at the blood brain barrier. Trends Pharmacol Sci 31:246–254

Mishra R, Singh SK (2013) HIV-1 Tat C modulates expression of miRNA-101 to suppress VE-cadherin in human brain microvascular endothelial cells. J Neurosci 33:5992–6000

Nabeshima S, Reese TS, Landis DMD, Brightman MW (1975) Junctions in the meninges and marginal glia. J Comp Neurol 164:127–169

Neuwelt EA, Bauer B, Fahlke C, Fricker G, Iadecola C, Janigro D, Leybaert L, Molnár Z, O'Donnell ME, Povlishock JT, Saunders NR, Sharp F, Stanimirovic D, Watts RJ, Drewes LR (2011) Engaging neuroscience to advance translational research in brain barrier biology. Nat Rev Neurosci 12:169–182

Paolinelli R, Corada M, Orsenigo F, Dejana E (2011) The molecular basis of the blood brain barrier differentiation and maintenance. Is it still a mystery? Pharmacol Res 63:165–171

Parkinson FE, Damaraju VL, Graham K, Yao SY, Baldwin SA, Cass CE, Young JD (2011) Molecular biology of nucleoside transporters and their distributions and functions in the brain. Curr Top Med Chem 11:948–972

Patabendige A, Skinner RA, Morgan L, Abbott NJ (2013) A detailed method for preparation of a functional and flexible blood–brain barrier model using porcine brain endothelial cells. Brain Res 1521:16–30, doi:pii: S0006-8993(13)00519-2. 10.1016/j.brainres.2013.04.006

Potschka H (2012) Role of CNS efflux drug transporters in antiepileptic drug delivery: overcoming CNS efflux drug transport. Adv Drug Deliv Rev 64:943–952

Pottiez G, Duban-Deweer S, Deracinois B, Gosselet F, Camoin L, Hachani J, Couraud PO, Cecchelli R, Dehouck MP, Fenart L, Karamanos Y, Flahaut C (2011) A differential proteomic approach identifies structural and functional components that contribute to the differentiation of brain capillary endothelial cells. J Proteomics 75:628–641

Ransohoff RM, Brown MA (2012) Innate immunity in the central nervous system. J Clin Invest 122:1164–1171

Ransohoff RM, Engelhardt B (2012) The anatomical and cellular basis of immune surveillance in the central nervous system. Nat Rev Immunol 12:623–635

Ransohoff RM, Perry VH (2009) Microglial physiology: unique stimuli, specialized responses. Annu Rev Immunol 27:119–145

Redzic Z (2011) Molecular biology of the blood–brain and the blood-cerebrospinal fluid barriers: similarities and differences. Fluids Barriers CNS 8:3. doi:10.1186/2045-8118-8-3

Reese TS, Karnovsky MJ (1967) Fine structural localization of a blood–brain barrier to exogenous peroxidase. J Cell Biol 34:207–217

Reijerkerk A, Lopez-Ramirez MA, van Het Hof B, Drexhage JA, Kamphuis WW, Kooij G, Vos JB, van der Pouw Kraan TC, van Zonneveld AJ, Horrevoets AJ, Prat A, Romero IA, de Vries HE (2013) MicroRNAs regulate human brain endothelial cell-barrier function in inflammation: implications for Multiple Sclerosis. J Neurosci 33:6857–6863

Saijo K, Glass CK (2011) Microglial cell origin and phenotypes in health and disease. Nat Rev Immunol 11:775–787

Saunders NR, Daneman R, Dziegielewska KM, Liddelow SA (2013) Transporters of the blood–brain and blood-CSF interfaces in development and in the adult. Mol Aspects Med 34: 742–752

Seelig A (2007) The role of size and charge for blood–brain barrier permeation of drugs and fatty acids. J Mol Neurosci 33:32–41

Serot JM, Zmudka J, Jouanny P (2012) A possible role for CSF turnover and choroid plexus in the pathogenesis of late onset alzheimer's disease. J Alzheimers Dis 30:17–26

Shawahna R, Uchida Y, Declèves X, Ohtsuki S, Yousif S, Dauchy S, Jacob A, Chassoux F, Daumas-Duport C, Couraud PO, Terasaki T, Scherrmann JM (2011) Transcriptomic and quantitative proteomic analysis of transporters and drug metabolizing enzymes in freshly isolated human brain microvessels. Mol Pharm 8:1332–1341

Shen L, Weber CR, Turner JR (2008) The tight junction protein complex undergoes rapid and continuous molecular remodeling at steady state. J Cell Biol 181:683–695

Shlosberg D, Benifla M, Kaufer D, Friedman A (2010) Blood–brain barrier breakdown as a therapeutic target in traumatic brain injury. Nat Rev Neurol 6:393–403

Silverberg GD, Mayo M, Saul T, Rubenstein E, McGuire D (2003) Alzheimer's disease, normal-pressure hydrocephalus, and senescent changes in CSF circulatory physiology: a hypothesis. Lancet Neurol 2:506–511

Smith JA, Das A, Ray SK, Banik NL (2012) Role of pro-inflammatory cytokines released from microglia in neurodegenerative diseases. Brain Res Bull 87:10–20

Somjen GG (2004) Ions in the brain: normal function, seizures and stroke. Oxford University Press, Oxford

Stanimirovic DB, Friedman A (2012) Pathophysiology of the neurovascular unit: disease cause or consequence? J Cereb Blood Flow Metab 32:1207–1221

Strazielle N, Ghersi-Egea JF (2013) Physiology of blood–brain interfaces in relation to brain disposition of small compounds and macromolecules. Mol Pharm 10:1473–1491

Sykova E, Nicholson C (2008) Diffusion in brain extracellular space. Physiol Rev 88:1277–1340

Thorne RG, Nicholson C (2006) In vivo diffusion analysis with quantum dots and dextrans predicts the width of brain extracellular space. Proc Natl Acad Sci U S A 103:5567–5572

Tian W, Sawyer A, Kocaoglu FB, Kyriakides TR (2011) Astrocyte-derived thrombospondin-2 is critical for the repair of the blood–brain barrier. Am J Pathol 179:860–868

Weerasuriya A, Spangler RA, Rapoport SI, Taylor RE (1984) AC impedance of the perineurium of the frog sciatic nerve. Biophys J 46:167–174

Weller RO, Subash M, Preston SD, Mazanti I, Carare RO (2008) Perivascular drainage of amyloid-beta peptides from the brain and its failure in cerebral amyloid angiopathy and Alzheimer's disease. Brain Pathol 18:253–266

Weller RO, Djuanda E, Yow HY, Carare RO (2009) Lymphatic drainage of the brain and the pathophysiology of neurological disease. Acta Neuropathol 117:1–14

Wolak DJ, Thorne RG (2013) Diffusion of macromolecules in the brain: implications for drug delivery. Mol Pharm 10:1492–1504

Yang L, Kress BT, Weber HJ, Thiyagarajan M, Wang B, Deane R, Benveniste H, Iliff JJ, Nedergaard M (2013) Evaluating glymphatic pathway function utilizing clinically relevant intrathecal infusion of CSF tracer. J Transl Med 11:107, [Epub ahead of print] PubMed PMID: 23635358

Yasuda K, Cline C, Vogel P, Onciu M, Fatima S, Sorrentino BP, Thirumaran RK, Ekins S, Urade Y, Fujimori K, Schuetz EG (2013) Drug transporters on arachnoid barrier cells contribute to the blood-cerebrospinal fluid barrier. Drug Metab Dispos 41:923–931

Chapter 2
Recent Progress in Blood–Brain Barrier and Blood–CSF Barrier Transport Research: Pharmaceutical Relevance for Drug Delivery to the Brain

Masanori Tachikawa, Yasuo Uchida, Sumio Ohtsuki, and Tetsuya Terasaki

Abstract The blood–brain barrier (BBB) and the blood–CSF barrier (BCSFB) possess multiple transport systems for endogenous and xenobiotic compounds to maintain functional homeostasis in the central nervous system (CNS). Accumulating evidence on the transport systems has provided a basis for the development of rational strategies for drug delivery and targeting to CNS. The blood-to-brain influx transport systems at the BBB have a great potential for CNS-acting drug delivery and targeting to the brain. The brain-to-blood efflux transport systems at the BBB including ATP-binding cassette transporters hinder the drug penetration to the brain. Efflux transport systems at the BBB and BCSFB also play an important role in cerebral clearance of endogenous neurotoxic compounds which are associated with disorders of the CNS. Several drugs influence the endogenous clearance system at the brain barriers. This chapter focuses on the current state of knowledge concerning the roles of transport systems for endogenous and xenobiotic compounds at the BBB and the BCSFB, and the potential implications of these systems for CNS drug delivery.

Abbreviations

ABC	ATP-binding cassette
Aβ	Amyloid-β peptide
AD	Alzheimer's disease

M. Tachikawa • Y. Uchida • T. Terasaki, Ph.D. (✉)
Division of Membrane Transport and Drug Targeting, Graduate School of Pharmaceutical Sciences, Tohoku University, Aramaki, Aoba-ku, Sendai, Japan
e-mail: terasaki.tetsuya@m.tohoku.ac.jp

S. Ohtsuki
Department of Pharmaceutical Microbiology, Faculty of Life Sciences, Kumamoto University, Kumamoto, Japan

M. Hammarlund-Udenaes et al. (eds.), *Drug Delivery to the Brain*, AAPS Advances in the Pharmaceutical Sciences Series 10, DOI 10.1007/978-1-4614-9105-7_2,

α2M	α2-macrogloblin
AMA	Amantadine
ANP	Atrial natriuretic peptide
Apo	Apolipoprotein
Asct	Alanine-serine-cysteine transporter
Ata	Amino acid transporter
$ATB^{0,+}$	Amino acid transporter $B^{0,+}$
BBB	Blood–brain barrier
BCSFB	Blood–cerebrospinal fluid barrier
BCRP	Breast cancer-resistance protein
Cat	Cationic amino acid transporter
Cht	Choline transporter
Cnt	Concentrative nucleoside transporter
CNS	Central nervous system
Crt	Creatine transporter
Ctl	Choline transporter-like protein
DHEAS	Dehydroepiandrosterone sulfate
DPDPE	[D-penicillamine2,5]encephalin
Eaat	Excitatory amino acid transporter
ENT	Equilibrative nucleoside transporter
4F2hc	Heavy chain of the 4F2 cell-surface antigen
GABA	γ-Aminobutyric acid
GAMT	S-Adenosylmethionine:guanidinoacetate N-methyltransferase
Gat	γ-Aminobutyric acid transporter
GLUT	Glucose transporter
GC	Guanidino compound
GlySar	Glycylsarcosine
hCMEC/D3	Human capillary endothelial cell line
HDL	High-density lipoprotein
HVA	Homovanillic acid
IS	Indoxyl sulfate
LAT/Lat	L-type amino acid transporter
LRP	Low-density lipoprotein receptor-related protein
Mate	Multidrug and toxin extrusion transporter
MCT/Mct	Monocarboxylic acid transporter
MDR	Multidrug-resistance protein
6-MP	6-Mercaptopurine
MPP^{+}	1-Methyl-4-phenylpyridinium
MRP/Mrp	Multidrug-resistance-associated protein
mTOR	Mammalian target of rapamycin
Npr-C	Natriuretic peptide receptor C
NSAID	Nonsteroidal anti-inflammatory drug
Oat	Organic anion transporter
OATP/Oatp	Organic anion transporting polypeptide
Oct	Organic cation transporter

Octn	Organic cation/carnitine transporters
PAO	Phenylarsine oxide
Pept	Proton-coupled oligopeptide transporter
PGE_2	Prostaglandin E_2
P-gp	P-glycoprotein
Pmat	Plasma membrane monoamine transporter
RIM	Rimantadine
Taut	Taurine transporter
TCDD	2,3,7,8-Tetrachlorodibenzo-*p*-dioxin
PPx	Pharmacoproteomics
SLC	Solute carrier
6-TG	6-Thioguanine
TR-BBB	Rat conditionally immortalized brain capillary endothelial cell line
TR-CSFB	Conditionally immortalized choroid plexus epithelial cell line

2.1 Introduction

The development of drugs targeting the central nervous system (CNS) is a major challenge in pharmaceutical research. Successful treatment of CNS disorders such as epilepsy, Alzheimer's disease, Parkinson's disease, and brain tumors requires the development of rational strategies not only to identify appropriate targets in the brain but also to deliver drugs at appropriate concentrations to the brain across the blood–brain/CSF interfaces. The development of many CNS-acting drug candidates has had to be discontinued at an early stage due to the lack of molecular features essential for crossing these interfaces (Abbott et al. 2006; Pardridge 2012). It is thus essential to design drugs with the necessary characteristics for effective entry into the brain (Ohtsuki and Terasaki 2007; Terasaki and Tsuji 1994; Pardridge 2001).

The blood–brain and blood–CSF interfaces consist of the blood–brain barrier (BBB) and the blood–cerebrospinal fluid barrier (BCSFB), respectively (Fig. 2.1). The BBB and the BCSFB, which are created by the complex tight junctions of brain capillary endothelial cells and choroid plexus epithelial cells, respectively, possess a variety of transport systems which serve to maintain functional CNS homeostasis, though the molecular components and regulatory mechanisms involved still remain to be fully clarified. Figure 2.2 illustrates two typical BBB or BCSFB transport models in brain capillary endothelial cells and choroid plexus epithelial cells. One is the blood-to-brain/CSF influx transport system that supplies nutrients to the brain/CSF. The other is the brain/CSF-to-blood efflux transport system that acts to eliminate metabolites, neurotoxic compounds, and drugs from brain/CSF. Pharmacokinetic analysis using a distributed model has demonstrated distinct contributions of BBB and BCSFB transport systems to the restricted distribution of antihuman immunodeficiency virus drugs in brain parenchyma and CSF (Takasawa et al. 1997). Specifically, (1) efflux transport across the BBB plays a predominant role in the apparently restricted distribution of these drugs in brain parenchymal tissues, but

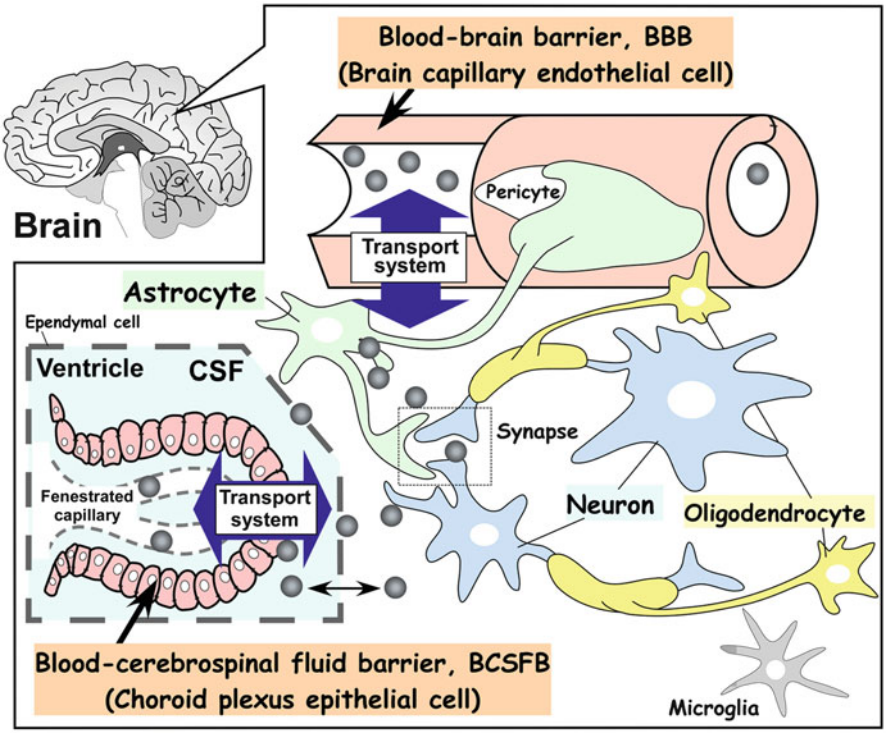

Fig. 2.1 Roles of the blood–brain barrier (BBB) and the blood–cerebrospinal fluid barrier (BCSFB) in drug distribution to brain parenchyma and CSF

not in the CSF, whereas (2) efflux transport across the BCSFB determines the restricted distribution in the CSF, but not in brain parenchymal tissues.

It has become increasingly clear that transporters on the plasma membrane of rate-limiting functional barriers play an integral role in determining the concentrations of their substrates in the brain (Ohtsuki and Terasaki 2007; Spector and Johanson 2010; Ohtsuki et al. 2011; Pardridge 2012). Identification of various transport systems, including families of solute carrier (SLC) transporters and ATP-binding cassette (ABC) transporters, has provided evidence at the molecular level that the BBB and BCSFB have multiple physiological interfaces: (1) supplying essential nutrients, hormones, and mimetic drugs to the brain, (2) eliminating endogenous metabolites produced within the brain, and (3) preventing the entry of circulating drugs and toxic agents into the brain. Furthermore, research on the regulatory mechanisms of transport functions at the brain barriers has recently progressed well. We have established the quantitative protein expression atlas of transporters at the BBB of humans (Uchida et al. 2011b), as well as mice (Kamiie et al. 2008) and monkeys (Ito et al. 2011a), by means of a liquid chromatography–tandem mass spectrometric quantification method. This new technology has made it

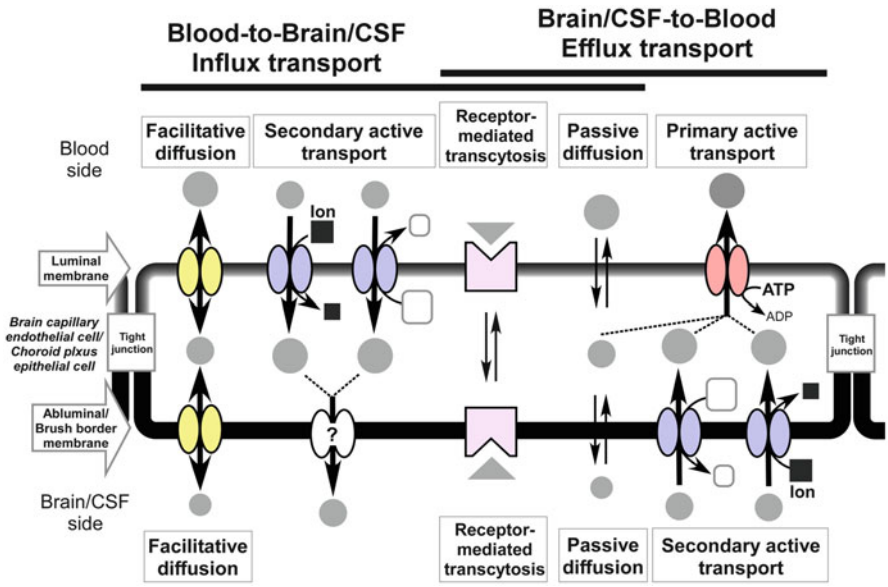

Fig. 2.2 Transport models at the blood–brain barrier (BBB) and blood–cerebrospinal fluid barrier (BCSFB)

possible, for the first time, to measure quantitatively the absolute protein amounts of BBB transporters, including SLC transporters such as Na^+-independent L-type amino acid transporter (LAT1/SLC7A5) and its associated protein (the heavy chain of the 4F2 cell-surface antigen, 4F2hc/CD98/SLC3A2), facilitative glucose transporter 1 (GLUT1/SLC2A1), and monocarboxylic acid transporter 1 (MCT1/SLC16A1), as well as ABC transporters such as the breast cancer-resistance protein (BCRP/ABCG2), P-glycoprotein (P-gp/MDR1/ABCB1), and multidrug-resistance-associated protein 4 (MRP4/ABCC4). However, this work will not be described in detail here, as it is covered in Chap. 3.

It had long been believed that increasing the lipophilicity of a poorly permeable drug tends to increase its BBB permeability (Levin 1980). Indeed, passive diffusion of small molecules across the plasma membrane is dependent on their lipophilicity in general. However, brain distribution of quite highly lipophilic drugs is often restricted, due to the functional barrier formed by BBB efflux transporters. As the concentration of drugs in the brain interstitial fluid would be significantly decreased by active BBB efflux transporter function, an understanding of the molecular mechanisms of both influx and efflux transporters at the BBB is crucial for research on drug delivery and drug targeting to the brain.

In this chapter, we discuss recent progress in research on the molecular mechanisms of the transport systems in the BBB (Table 2.1) and BCSFB (Table 2.2) and their influence on the BBB permeability of drugs.

Table 2.1 Transporters expressed at the BBB

Transporters	Typical substrates	Localization	Direction
Energy transport system			
Glut1 (Slc2a1)	D-Glucose	L, A	In
Mct1 (Slc16a1)	L-Lactate, monocarboxylates	L, A	In
Crt (Slc6a8)	Creatine, guanidino compounds	L, A	In
Amino acid transport system			
Lat1(Slc7a5)/4F2hc(Slc3a2)	Large neutral amino acids	–	In
Cat1 (Slc7a1)	Cationic amino acids	–	In
Eaat1, 2, 3 (Slc1a3, 2, 1)	Anionic amino acids	A	Ef
Asct2 (Slc1a5)	L-Aspartic acid, L-Glutamic acid	A	Ef
Ata2 (Slc38a2)	Small neutral amino acids	–	Ef
xCT(Slc7a11)/4F2hc(Slc3a2)	L-Cystine, L-Glutamic acid	–	In
Taut (Slc6a6)	Taurine, β-alanine	–	In, Ef
$ATB^{0,+}$ (Slc6a14)	Neutral/cationic amino acids	–	–
Neurotransmitter transport system			
Gat2/Bgt1 (Slc6a12)	γ-Aminobutyric acid	–	Ef
Sert (Slc6a4)	Serotonin	L, A	–
Net (Slc6a2)	Norepinephrine	A	–
Organic anion transport system			
Oat3 (Slc22a3)	*para*-Aminohippuric acid, homovanillic acid, indoxyl sulfate	A	Ef
Oatp1a4 (Slco1a4)	Digoxin, organic anions	L, A	In, Ef
Oatp1c1 (Slco1c1)	Thyroid hormone	–	In
Octn2 (Slc22a5)	Carnitine	–	In
Pmat (Slc29a4)	Monoamine neurotransmitters	–	Ef
Nucleoside transport system			
Cnt2 (Slc28a2)	Nucleosides	–	In
ABC transporters			
Abca1	Cholesterol	–	–
Abcb1/Mdr1	Vincristine, cyclosporine A	L	Ef
Abcc4/Mrp4	Topotecan	L	Ef
Abcg2/Bcrp	Mitoxantron, topotecan	L	Ef

Localization: luminal side (L) and abluminal side (A) of brain capillary endothelial cells. Direction: blood-to-brain influx transport (In) and brain-to-blood efflux transport (Ef). –: Not determined. The table is taken from Ohtsuki and Terasaki (2007) with some modifications

Table 2.2 In vivo transport characteristics of cationic drugs at the BBB

Substrate	Influx permeability rate (μl/min/g brain)	Transport characteristics/ compounds that interact with	Species	References
Nicotine	1,080 (In situ)	H^+-coupled antiporter/ Diphenhydramine, MDMA, clonidine (In situ)	Mouse	Cisternino et al. (2013)
Nicotine	272 (IV)	Pyrilamine (BUI)	Rat	Tega et al. (2012)
Clonidine	366 (In situ)	H^+-coupled antiporter/ Diphenhydramine oxycodone, morphine, nicotine (In situ)	Mouse	Andre et al. (2009)

(continued)

Table 2.2 (continued)

Substrate	Influx permeability rate (μl/min/g brain)	Transport characteristics/ compounds that interact with	Species	References
Oxycodone	1,910 (MD)	H^+-coupled antiporter/ Pyrilamine (In situ)	Rat	Boström et al. (2006), Okura et al. (2008)
Pyrilamine	1,620[a] (BUI)	Diphenhydramine, propranolol (BUI)	Rat	Yamazaki et al. (1994b)
Verapamil	131 (IV)	Quinidine, pyrilamine (BUI)	Rat	Kubo et al. (2013)
Naloxone	305 (BUI)	H^+-dependent/Pyrilamine, diphenhydramine, ketotifen, lidocaine, propranolol (BUI)	Rat	Suzuki et al. (2010a, b)
Donepezil	668 (IV)	Choline (IV)	Rat	Kim et al. (2010)
Quinidine	25.5 (IV)	P-gp-mediated efflux/SDZ PSC833 (P-gp inhibitor) (IV)	Rat	Kusuhara et al. (1997)
Fentanyl	1,840 (In situ)	–	Mouse	(Dagenais et al. 2004)
Morphine	10.4 (In situ)	–	Mouse	(Dagenais et al. 2004)
Pentazocine	625 (In situ)	H^+-dependent/Lidocaine, imipramine, propranolol, pyrilamine, diphenhydramine (BUI)	Rat	Suzuki et al. (2002a, b)

IV Intravenous administration, *BUI* brain uptake index method, *In situ* in situ perfusion, *MD* brain microdialysis, *MDMA* N,α-dimethyl-3,4-(methylenedioxy)phenethylamine
[a]Influx permeability rate is shown as maximum influx permeability rate, calculated by dividing Vmax by Km

2.2 Blood-to-Brain Influx Transport Systems at the BBB

2.2.1 Transporters for Nutrients

There is increasing interest in utilizing influx transporters, e.g., Lat1/Slc7a5, Glut1/Slc2a1, and Mct1/Slc16a1, for drug delivery to the brain in the design of CNS-acting drugs, and therefore clarification of the requirements for substrate recognition by influx transporters is essential.

2.2.1.1 LAT1/SLC7A5

Lat1/Slc7a5, which forms a heterodimer with its associated protein, the heavy chain of the 4F2 cell-surface antigen (4F2hc/CD98/Slc3a2), has a high transport capacity (Kanai et al. 1998) and is potentially available as a carrier of drugs that structurally mimic its endogenous substrates. Lat1, which is preferentially localized at the BBB

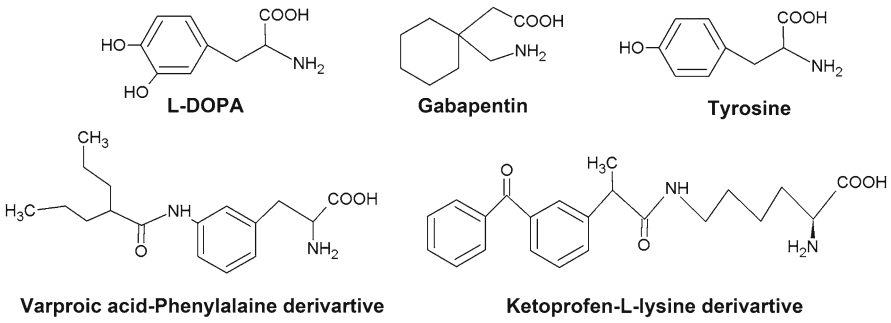

Fig. 2.3 Structures of L-type amino acid transporter (Lat1) substrates

(Boado et al. 1999), transports large neutral L-amino acids with a bulky side chain, e.g., L-phenylalanine, L-tyrosine, L-tryptophan, and L-leucine (Kanai et al. 1998), with high affinity (Km = approximately 10–20 μM for human LAT1 Yanagida et al. 2001). Hence Lat1/4F2hc heterodimer plays a crucial role in the blood-to-brain influx transport of substrate amino acids. The in vivo carrier-mediated influx transport has been studied using an in situ rat brain perfusion technique. In this technique, the influx permeability rate is determined as maximum influx permeability rate, obtained by dividing the maximal influx rate Vmax by the half-saturation concentration Km, because this approach makes it possible to neglect the inhibitory effect of endogenous amino acids in the circulating blood. The maximal influx permeability rates of L-leucine [2,500 μl/(min·g brain)] (Smith et al. 1984) and L-Phenylalanine [3,700 μl/(min·g brain)] (Smith et al. 1987) across the BBB are approximately 20- to 30-fold greater than that of D-glucose [129 μl/(min·g brain)] (Pardridge 1988) in rats. When the plasma concentrations of endogenous amino acids (L-phenylalanine: 80 μM, L-leucine: 180 μM, D-glucose: 5,500 μM) are considered according to Michaelis-Menten kinetics, the influx permeability rates are estimated to be 451 [μl/(min·g brain)] for L-phenylalanine, 311[μl/(min·g brain)] for L-leucine, and 86 [μl/(min·g brain)] for D-glucose (Ohtsuki and Terasaki 2007; Smith et al. 1984, 1987; Pardridge 1988). Lat1 also transports thyroid hormones (T3 and T4), which are essential for brain development, although it was suggested to have only a minimal role in thyroid hormone transport (del Amo et al. 2008).

Several drugs with structures related to Lat1 substrates (Fig. 2.3), including L-DOPA (levodopa; used to treat Parkinson's disease), the alkylating agent melphalan (phenylalanine mustard), the antiepileptic drug gabapentin, and the muscle relaxant baclofen are transported into the brain via Lat1 (Kageyama et al. 2000; Abbott and Romero 1996). Furthermore, a sophisticated pro-drug approach (Rautio et al. 2008) has been developed to transport BBB-nonpermeable drugs into the CNS by conjugating an active drug with a Lat1 substrate-mimicking pro-moiety in a bioreversible manner (Pavan and Dalpiaz 2011). Rautio's group has developed pro-drugs (Fig. 2.3) of ketoprofen, a nonsteroidal anti-inflammatory drug (NSAID)

(L-tyrosine conjugate Gynther et al. 2008) and valproic acid, a broad-spectrum anticonvulsant drug (conjugate with para- and meta-substituted phenylalanine derivatives Peura et al. 2011), which are delivered to the brain via Lat1 at the BBB. It has been reported that the brain uptake of valproic acid is mediated by a transport system for medium-chain fatty acids (Adkison and Shen 1996). On the other hand, the brain-to-blood efflux clearance [508 μl/(min·g brain)] is 2.7-fold greater than the influx clearance [187 μl/(min·g brain)] in rats (Kakee et al. 2002). The predominant brain-to-blood efflux transport at the BBB may explain the restricted distribution of valproic acid to the brain. Although it has been reported that P-gp, Mrp1, and Mrp2 are not involved in the efflux transport of valproic acid at the BBB (Baltes et al. 2007), the molecular identity of the transporter(s) responsible for the BBB active efflux of valproic acid remains to be elucidated. Hence, design of a LAT1-transportable pro-drug of valproic acid would be an intriguing strategy for improving the CNS delivery.

Ylikangas et al. (2012) have established a three-dimensional (3D) pharmacophore for Lat1 substrates through ligand-based molecular modeling of 28 structurally diverse compounds, including endogenous Lat1 substrates (Ylikangas et al. 2012). This 3D pharmacophore features: (1) a hydrogen bond acceptor, (2) an aromatic ring, (3) a negatively charged group, and (4) a hydrogen bond donor. In accordance with this model, it has been reported that the amide conjugate of ketoprofen and L-lysine (Fig. 2.3), both of which are non-Lat1 substrates, exhibits Lat1-mediated brain uptake (Gynther et al. 2010). This 3D pharmacophore for Lat1 has provided new insight for the design and optimization of new Lat1-transportable pro-drugs.

Lat1 is expected to be saturated by endogenous amino acids under physiological conditions, since the values of half-saturation concentration (Km) for Lat1 are smaller than the plasma concentrations of neutral amino acids (del Amo et al. 2008). For example, it has been reported that the Km of rat Lat1-mediated L-DOPA transport is about 34 μM (Uchino et al. 2002), while the typical therapeutic range of L-DOPA concentration in plasma is 1.2–6.5 μM. Further, the total concentration of relevant amino acids in plasma is from 0.4 mM to 2.3 mM, and the average affinity (Ki) of these amino acids for Lat1 is about 70–10 μM (Huang et al. 1998). Calculation based on Michaelis-Menten kinetics indicates that the L-DOPA transport capacity is 99.6–98 % saturated by endogenous amino acids. Therefore, Lat1 substrate drugs are expected to be transported from the blood to the brain at a constant rate. It should be noted that a high-protein diet increased the plasma levels of neutral amino acids and decreased the effect of L-DOPA due to competitive inhibition at the BBB (Pincus and Barry 1988). Thus, it is essential to design new drugs with sufficiently high affinity for Lat1 so that they can compete with endogenous Lat1 substrates for brain uptake.

Although LAT1 is commonly expressed at human and nonprimate BBB, the absolute protein level of LAT1 in human brain capillaries is 19.7 % of that in mouse (Kamiie et al. 2008; Uchida et al. 2011b). Furthermore, there are differences in the amino acid sequence of the transporter (Prasad et al. 1999), implying that there may be species differences in substrate recognition by LAT1. Indeed, the affinity of

rabbit Lat1 for tryptophan and phenylalanine is lower than that of human or rat Lat1, owing to the mutations W234L and G219D (Boado et al. 2003). Most studies have been performed with healthy animals, and some CNS disorders may result in altered expression and function of Lat1. For example, Lat1 mRNA expression in brain capillaries is reduced in a mouse model of Parkinson's disease (Ohtsuki et al. 2010). It is thus important in future studies to clarify fully the substrate specificity of human LAT1, as well as the expression levels of LAT1 at the BBB in patients with CNS disorders.

2.2.1.2 GLUT1/SLC2A1

GLUT1/SLC2A1 is an Na^+-independent facilitative glucose transporter, which plays a major role at the BBB in ensuring a constant supply of D-glucose (the main energy source for the brain) from the circulating blood to the brain. Glut1 is localized on both the luminal and abluminal membranes of brain capillary endothelial cells (Farrell and Pardridge 1991). It is also involved in the blood-to-brain supply of L-dehydroascorbic acid, an oxidized form of L-ascorbic acid that is reduced to L-ascorbic acid in the brain (Agus et al. 1997). Inherited GLUT1-deficiency syndrome involves defective glucose transport at the BBB, leading to persistent hypoglycorrhachia, infantile seizures, and developmental delay (De Vivo et al. 1991). Thus, GLUT1 at the BBB is crucial for CNS development and function. It has been reported that L-serinyl-β-D-glucoside analogs of Met^5-enkephalin exhibit greater BBB permeability than the parent peptide (Polt et al. 1994), implying that Glut1 is a transporter for glycosylated peptides. On the other hand, chemotherapeutic agents coupled with D-glucose (D-glucose-chlorambucil derivatives) inhibit Glut1-mediated transport activity, but are not actually transported by human GLUT1 (Halmos et al. 1996). A recent study on the structure-transport activity relationship of human GLUT1 revealed that Ile287 located at transmembrane 7 (TM7) is a key residue for maintaining high glucose affinity and is located at or near the exofacial glucose-binding site (Kasahara et al. 2009). This raises the possibility that TM7 is involved in the substrate permeation pathway and/or contributes to the dynamic conformational change of GLUT1 caused by substrate binding. Furthermore, Sun et al. (2012) have established the crystal structure of XylE, an *Escherichia coli* homologue of Glut1-4, in the complex with D-glucose (Sun et al. 2012). They identified several amino acid residues that are involved in D-glucose recognition in XylE and are invariant in Glut1-4. Although Glut1-mediated drug transport at the BBB might be feasible, it appears that the substrate specificity of Glut1 is strict and at present Glut1 cannot be considered a target of choice for drug delivery to the CNS. Indeed, the anticonvulsant valproic acid depresses local glucose utilization in humans (Leiderman et al. 1991), and this is at least partly caused by its inhibition of GlutT1 at the BBB (Wong et al. 2005). This result implies that alteration of Glut1 function at the BBB may impair brain energy homeostasis.

2.2.1.3 MCT1/SLC16A1

Mct1/Slc16a1 mediates H^+-coupled blood-to-brain influx transport of monocarboxylates, such as lactate and pyruvate (Kido et al. 2000). Quantitative proteomics has revealed that the expression of Mct1 at the monkey BBB is higher at the neonatal stage and is reduced in the adult (Ito et al. 2011a). Mct1 expression in rodent brain is also induced during the suckling period and by a ketogenic diet (Leino et al. 1999, 2001). This induction enables lactate and ketone bodies derived from milk to be delivered to the brain as alternative energy sources. Considering that Mct1 accepts nicotinate, a monocarboxylate drug, as a transportable substrate, it is likely that Mct1 could be used for drug delivery. However, it should be considered that Mct1 levels change dramatically during brain development and under pathological conditions. For example, MCT1 is deficient in microvessels of human epileptogenic hippocampus (Lauritzen et al. 2011).

2.2.1.4 Others

The BBB has a transport system, i.e., cationic amino acid transporter 1 (Cat1/Slc7a2), for basic amino acids such as L-lysine and L-arginine (Stoll et al. 1993) and a concentrative nucleoside transporter (Cnt1/Slc28a1) which mediates transport of nucleosides (Li et al. 2001). Creatine transporter (Crt/Slc6a8) at the BBB represents a major pathway for supply of creatine, which plays a key role in energy storage in neural cells (Ohtsuki et al. 2002b; Tachikawa et al. 2004). Because creatine supplementation has a neuroprotective effect in neurodegenerative diseases (Beal 2011), the increase and maintenance of brain creatine levels could serve to protect brain function. However, oral administration of 20 g creatine per day for 4 weeks results in only about a 9 % increase in total creatine in the human brain (Dechent et al. 1999). This is probably because Crt at the BBB is almost saturated by endogenous creatine in the circulating blood (Ohtsuki et al. 2002b). Therefore, induction of Crt at the BBB is a possible strategy to increase brain creatine levels. Growth hormone induced myocardial expression of Crt, and coexpression of glucocorticoid-inducible kinase SGK1 and mammalian target of rapamycin (mTOR) stimulated electrogenic creatine transport of Crt in *Xenopus* oocytes (Omerovic et al. 2003; Shojaiefard et al. 2005, 2006). These proteins appear to be targets for induction of Crt at the BBB. Crt may also be a key factor facilitating the blood-to-brain transport of guanidinoacetate (biosynthetic precursor of creatine) in patients deficient in S-adenosylmethionine:guanidinoacetate N-methyltransferase (GAMT), which mediates creatine biosynthesis (Tachikawa et al. 2009). Although Crt at the BBB is almost saturated by endogenous creatine in circulating blood under normal conditions, blood creatine is significantly decreased in GAMT deficiency, and then the Crt-mediated transport system causes an increase of the blood-to-brain influx transport of guanidinoacetate. This may account for the cerebral accumulation of guanidinoacetate in GAMT deficiency, which is associated with mild cognitive impairment (Torremans et al. 2005).

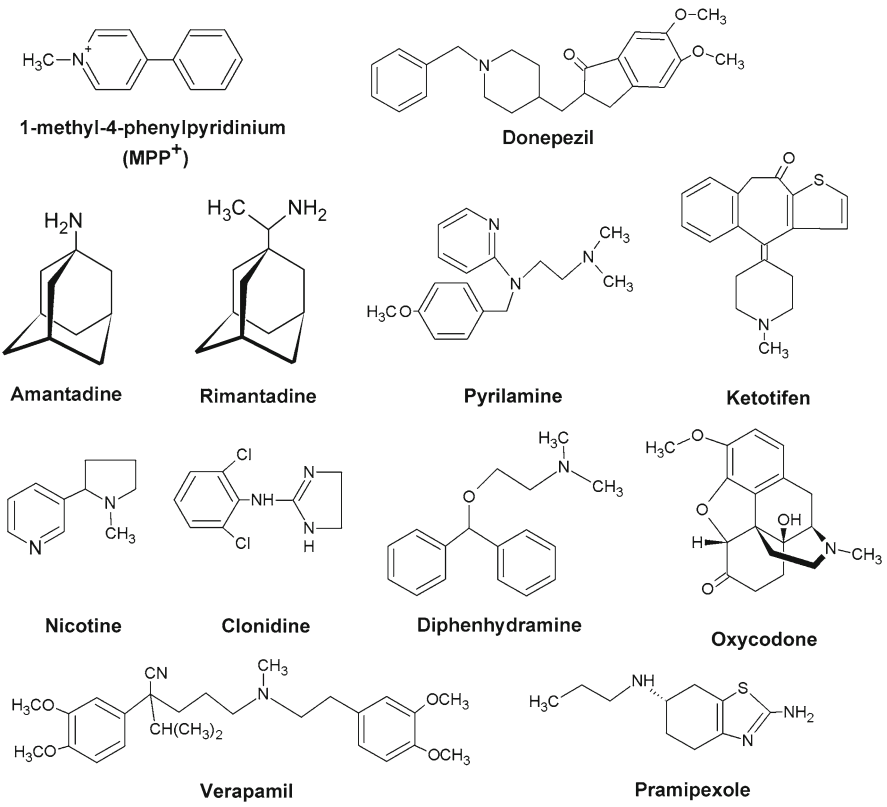

Fig. 2.4 Structures of cationic drugs exhibiting psychotropic efficacy and/or adverse effects in CNS

2.2.2 Transport Systems for Organic Cations

It has been postulated that one of the factors determining the psychotropic efficacy and adverse effects of drugs in the CNS is their BBB permeability. Many psychotropic drugs are cationic at physiological pH (Fig. 2.4). Table 2.2 summarizes the transport characteristics of various cationic compounds at the BBB. The transport systems for cationic compounds include organic cation transporters (Oct1-3/Slc22a1-3), organic cation/carnitine transporters (Octn1-3/Slc22a4-5, 21) (Koepsell et al. 2007), multidrug and toxin extrusion transporters (Mate1-2/Slc47a1-2) (Terada and Inui 2008; Omote et al. 2006), plasma membrane monoamine transporter (Pmat/Slc29a4) (Xia et al. 2007), choline transporter (Cht1/Slc5a7) (Okuda et al. 2000), choline transporter-like protein (Ctl1/Slc44a1) (Traiffort et al. 2005; Zufferey et al. 2004), all of which have been identified at the gene level.

Okura et al. (2011) have reported that Pmat plays a predominant role in brain-to-blood efflux transport of organic cations, such as 1-methyl-4-phenylpyridinium (MPP^+; a cationic neurotoxin), and monoamine neurotransmitters at the BBB.

Indeed, elimination of [^{3}H]MPP$^+$ from the brain was significantly reduced by coperfusion with monoamines such as serotonin and dopamine, although the in vivo brain uptake of [^{3}H]MPP$^+$ did not increase with time. Pmat small interfering RNA (siRNA) significantly suppressed [^{3}H]MPP$^+$ uptake by rat conditionally immortalized brain capillary endothelial cells (TR-BBB13 cells), which express Pmat (Okura et al. 2011). These findings suggest that Pmat functions as a clearance system for monoamine neurotransmitters and neurotoxins produced in the brain.

Acetylcholine esterase inhibitors, such as donepezil and galantamine are clinically useful in the treatment of Alzheimer's disease. It has been reported that rat Octn1, Octn2, and Cht1 mediate the transport of donepezil (Kim et al. 2010). The in vivo brain uptake of donepezil is reduced in rats pretreated with choline, whereas the uptake is unaffected by pretreatment with MPP$^+$ (an Octs substrate), ergothioneine (an Octn1 substrate), or L-carnitine (an Octn2 substrate) (Kim et al. 2010). On the other hand, Lee et al. (2012) reported that the in vivo uptake of [^{3}H]acetyl-l-carnitine is significantly inhibited by donepezil and galantamine (Lee et al. 2012). These results suggest that donepezil transport across the BBB is mediated by choline and/or carnitine transport system(s). The two influenza adamantine compounds amantadine (AMA) and rimantadine (RIM) exhibit the higher rate of in situ RIM transport BBB than that of AMA (Kooijmans et al. 2012). It is suggested that this difference can be explained by the greater uptake of RIM which involves Na^+ and Cl^--dependent neutral and cationic amino acid transporter $B^{0,+}$ ($ATB^{0,+}$/Slc6a14) in human capillary endothelial cell line (hCMEC/D3) (Kooijmans et al. 2012). Taken together, these transport systems of choline, carnitine, and amino acid at the BBB have the potential to be exploited for targeted drug delivery to the brain.

Some classical H_1-antagonists, such as pyrilamine, diphenhydramine, and ketotifen, exhibit a sedative side effect. Since the BBB permeability of H_1-antagonists is an important determinant of this adverse effect (Yanai and Tashiro 2007), the BBB transport process needs to be considered in order to develop H_1-antagonists with little sedative effect. Although it was believed that such cationic drugs were transported by passive diffusion, in vivo and vitro studies have revealed that pyrilamine is transferred across the BBB via a carrier-mediated transport system, as well as by passive diffusion (Yamazaki et al. 1994a, b). The uptake of pyrilamine into primary-cultured bovine brain capillary endothelial cells is inhibited by other H_1-antagonists, such as ketotifen, azelastin, cyproheptadine, and emedastine, indicating that the compounds exhibiting inhibitory effects are recognized by the blood to-brain influx transport system for pyrilamine. Recently, Shimomura et al. (2013) has reported the involvement of an H^+-coupled organic cation antiporter in the transport of pyrilamine and diphenhydramine in hCMEC/D3 cells. In vivo rat microdialysis study revealed that the unbound concentrations of diphenhydramine are 5.5-fold greater in the brain than in the blood, indicating the blood-to-brain active influx transport across the BBB (Sadiq et al. 2011). Therefore, a means to regulate the affinity of H_1-antagonists for the carrier-mediated transport system, i.e., an H^+-coupled antiporter at the BBB is desirable to design drugs without CNS side effects.

Nicotine, the predominant tobacco alkaloid leading to smoking dependence, undergoes rapid influx transport across the BBB after inhalation (Cisternino et al. 2013; Tega et al. 2012). The influx permeability rate of nicotine is greater than that

of glucose (129 μl/min/g brain) (Pardridge 1988) in rats (Table 2.2). At the usual micromolar concentration in plasma, 79 % of the net in vivo influx transport of nicotine occurs via an H^+-coupled antiporter-mediated process, while passive diffusion accounts for 21 %. Knockout of Oct1-3 and two major ABC transporters, P-gp and Bcrp did not reduce nicotine transport to the brain in mice. Substrates/inhibitors of Mate1, Octn, and Pmat also did not inhibit the transport (Cisternino et al. 2013). Clonidine is a selective agonist of the α-2 adrenergic receptor in CNS. The blood-to-brain influx transport of clonidine at the BBB is mediated by an H^+-coupled antiporter, and is saturable (Andre et al. 2009). Secondary or tertiary amines such as oxycodone, morphine, and nicotine inhibit clonidine transport, although tetraethylammonium, a prototypical substrate/inhibitor of Oct, Octn, Mate, and Pmat transporters, did not affect the transport. Oct1-3, P-gp, and Bcrp knockout mice did not exhibit decreased clonidine transport. An H^+ antiporter is also involved in transport of the dopamine agonist for treating early-stage Parkinson's disease pramipexole (Okura et al. 2007), the opioid receptor agonist oxycodone (Boström et al. 2006; Okura et al. 2008), the H_1-antagonist pyrilamine (Okura et al. 2008), and verapamil (Kubo et al. 2013). Furthermore, it has been reported that the pyrilamine uptake by rat brain capillary endothelial cells (TR-BBB) was inhibited by antidepressants such as amitriptyline, imipramine, clomipramine, amoxapine, and fluvoxamine, and antiarrhythmics such as mexiletine, lidocaine, and flecainine, and ketamine (Nakazawa et al. 2010). This implies that those adjuvant analgesics could share the transport system of pyrilamine.

An in vivo microdialysis study revealed that the ratio of unbound oxycodon concentration in brain versus blood at the steady state ($K_{p,uu,brain}$) was 3.0, demonstrating active influx of oxycodone at the BBB against the blood-to-brain concentration gradient (Boström et al. 2006). The potency of oxycodone in postoperative pain treatment is similar to that of morphine (Silvasti et al. 1998), despite the lower affinity of oxycodone for opioid receptors (Peckham and Traynor 2006). Given that the affinity of oxycodone for opioid receptors is lower than that of morphine, a higher concentration of oxycodone would be necessary to produce a similar effect. The action of the active influx transport system for oxycodone could generate a higher concentration of oxycodone in the brain interstitial fluid.

These blood-to-brain influx transport systems seem very promising for cationic drug delivery to the brain, and molecular identification of the proton/amine antiporter is expected to trigger significant progress in the delivery of cationic CNS-acting drugs.

2.3 Brain-to-Blood Efflux Transport Systems at the BBB

2.3.1 P-gp, BCRP, MRP4

Drug efflux transporters, i.e., ATP-binding cassette (ABC) transporters, exist at the luminal membrane of brain capillary endothelial cells. These transporters restrict the brain distribution of drugs by pumping them out of endothelial cells towards the

circulating blood, coupled with the hydrolysis of ATP. Evidence is emerging that many CNS-acting drugs are substrates of unidirectional efflux ABC transporters (Ohtsuki and Terasaki 2007). Quantitative proteomics revealed that P-gp (MDR1/ABCB1), breast cancer-resistance protein (BCRP/ABCG2/MXR/ABCP), and multidrug-resistance-associated protein 4 (MRP4/ABCC4) are the dominantly expressed ABC transporters at the human BBB (Uchida et al. 2011b). These ABC transporters have a distinct, though broad, substrate specificity, and function cooperatively at the BBB, forming an effective functional barrier against drugs with a variety of structures. PET-imaging with P-gp substrates [^{11}C]verapamil, and [^{11}C] desmethyl-loperamide strongly supported the notion that P-gp contributes to the restricted distribution of drugs at the human BBB (Bauer et al. 2012; Mullauer et al. 2012; Kreisl et al. 2010). Consequently, in vitro P-gp substrate screening assay is being introduced at the early stage of drug development. On the other hand, quantitative proteomics has shown that the human BBB abundantly expresses BCRP (8.14 fmol/μg protein), as well as P-gp (6.06 fmol/μg protein) (Uchida et al. 2011b). Considering that BCRP functions as a homodimer, the absolute expression amount of BCRP as a functional transporter is estimated to be 4.1 fmol/μg protein at the BBB. While the expression amount of Bcrp is 16 % of that of P-gp at the mouse BBB (Kamiie et al. 2008), it is 67 % of that of P-gp at the human BBB (Uchida et al. 2011b). Therefore, screening out of BCRP substrates as well as P-gp substrates needs to be considered as a rational strategy for CNS drug development. The absolute expression amount of MRP4 at the human BBB (0.195 fmol/μg protein) is approximately 20- to 30-fold smaller than that of P-gp or BCRP (Uchida et al. 2011b). If the expression of MRP4 is induced at the human BBB under pathological conditions, it is possible that the brain concentration of drugs that are substrates of MRP4 would be significantly reduced. In this case, screening out of MRP4 substrates would also be important for CNS drug development. It is clear that the absolute expression amounts of these ABC transporter subtypes at the human BBB under pathological conditions, as well as the substrate specificities, need to be elucidated to aid in the development of efficient CNS-active drugs. Previously, it has been difficult to reconstruct the in vivo brain distribution of drugs in a quantitative manner due to the lack of the data on absolute expression levels of transporters together with data on intrinsic transporter activity. However, our quantitative targeted absolute proteomics technology has enabled us to predict in vivo BBB transport of drugs that are P-gp substrates from such in vitro data, with the aid of a pharmacokinetic model (Uchida et al. 2011a). This is described in Chap. 3.

2.3.1.1 P-gp

P-gp, a well-known ABC transporter of tumor cells, is localized predominantly on the luminal membrane of human brain capillary endothelial cells (Cordon-Cardo et al. 1989). P-gp lowers not only the brain interstitial fluid-to-plasma concentration ratio of unbound drug but also the permeability rate of its substrates from the circulating blood into the brain (Tsuji et al. 1992). For example, the brain-to-blood efflux transport of [^{3}H]quinidine is reduced by verapamil, a typical inhibitor of P-gp,

whereas the apparent blood-to-brain influx transport of [^{3}H]quinidine is increased by SDZ PSC833, the most potent inhibitor of P-gp (Kusuhara et al. 1997). The impact of P-gp on drug disposition to the brain in vivo was first demonstrated by generating mdr1a gene knockout mice, which lack P-gp (Schinkel et al. 1994). In these mice, the brain-to-plasma concentration ratios of the neurotoxic pesticide ivermectin, the carcinostatic drug vinblastine (Schinkel et al. 1994), and quinidine (Kusuhara et al. 1997) were increased by 27.6-, 26-, and 11-fold compared with those of wild-type mice, respectively. Numerous studies have revealed that P-gp at the BBB plays a very important role in restricting the entry of various drugs, including opioids, antidepressants, antipsychotics, antiepileptics, anticancer drugs, and cardiac drugs, from the circulating blood into the brain (Giacomini et al. 2010; Decleves et al. 2011). It has been demonstrated that folate deficiency disrupts the up-regulation of P-gp function at the BBB by valproic acid and the aryl hydrocarbon receptor ligand 2,3,7,8-tetrachlorodibenzo-*p*-dioxin (TCDD) (Wang et al. 2013). This finding suggests that expression and function of P-gp at the BBB are regulated by external factors. Super-resolution fluorescence microscopy showed that P-gp is distributed in clustered formations in an in vitro human BBB cell model (Huber et al. 2012). In accordance with this, caveolin-1 interacts with P-gp and modulates the P-gp transport activity through the phosphorylation state of caveolin-1 in brain capillary endothelial cells (Barakat et al. 2007). Hence, it is important to take account of the possibility of altered P-gp regulation under pathological conditions, in considering the possible contribution of P-gp to drug distribution to the brain.

2.3.1.2 BCRP

BCRP, which is localized on the luminal membrane of brain capillary endothelial cells (Cooray et al. 2002; Hori et al. 2004; Tachikawa et al. 2005), transports anticancer drugs such as mitoxantrone, topotecan, and methotrexate (Ni et al. 2010) and endogenous anionic compounds such as dehydroepiandrosterone-3-sulfate and estrone 3-sulfate (Suzuki et al. 2003). The impact of Bcrp on the brain distribution of anticancer drugs such as imatinib (Breedveld et al. 2005) and topotecan (de Vries et al. 2007) has been demonstrated by the use of Bcrp knock-out mice. On the other hand, the substrate specificity of Bcrp (hydrophobic and amphiphilic compounds) often overlaps with that of P-gp, suggesting that P-gp and Bcrp may work in a compensatory manner. In support of the notion that P-gp and Bcrp are both major contributors to drug efflux transport, synergistic BBB efflux transport of drugs by P-gp and Bcrp has recently been demonstrated by using mice deficient in both of the transporters. The brain-to-plasma ratio of quinidine, which is a specific substrate of P-gp, exhibited no difference between mdr1a/1b(−/−) and bcrp double-knockout mice and mdr1a/1b(−/−) single-knockout mice (Kodaira et al. 2010). In contrast, mdr1a/1b(−/−) and bcrp double-knockout mice showed a significant increase in the brain-to-plasma ratio of common substrates of both P-gp and Bcrp compared with that in mdr1a/1b(−/−) and bcrp single-knockout mice. Drugs affected include the anticancer drugs topotecan (de Vries et al. 2007), lapatinib (Polli et al. 2009),

dasatinib (Chen et al. 2009), gefitinib (Agarwal et al. 2010), sorafenib (Agarwal et al. 2010), erlotinib, flavopiridol, and mitoxantrone (Kodaira et al. 2010). Based on pharmacokinetic analysis, the synergistic effect of P-gp and Bcrp can be explained in terms of the sum of the independent net effluxes mediated by P-gp and Bcrp, without considering any interaction between P-gp and Bcrp (Kodaira et al. 2010). In accordance with this finding, a quantitative proteomics study revealed that there is no compensatory change of P-gp protein amount per whole cell lysate of brain capillaries in Bcrp-knockout mice, or in Bcrp protein amount per whole cell lysate of brain capillaries in P-gp-knockout mice, compared with the wild type (Agarwal et al. 2012). Since the BBB expressions of other relevant transporters exhibited no significant difference between wild-type mice and P-gp/Bcrp single- or double-knockout mice, the mechanism behind the functional compensation between P-gp and Bcrp at the BBB does not involve compensatory changes in transporter expression (Agarwal et al. 2012). However, we could not exclude the possibilities that transporter protein activity was changed by interaction with associated protein(s) or by modifications such as phosphorylation.

2.3.1.3 MRP4

The luminal membrane localization of MRP4 has been demonstrated in human brain capillary endothelial cells (Nies et al. 2004). Mrp4 knockout mice exhibited increased brain penetration of topotecan compared with that in wild-type mice (Leggas et al. 2004), suggesting that Mrp4 acts as a drug efflux transporter at the BBB. Mrp4 transports cyclic nucleotides (Chen et al. 2001), and it serves to reduce the cytotoxicity of nucleobase analogs, such as azidothymidine, 6-mercaptopurine (6-MP), and 6-thioguanine (6-TG) (Chen et al. 2001; Schuetz et al. 1999). Considering that the BBB possesses an efflux transport system for azidothymidine and 6-MP (Mori et al. 2004; Terasaki and Pardridge 1988), it is conceivable that Mrp4 lowers the distribution of nucleobase analogues into the brain. Since the anti-influenza virus drug oseltamivir has been suspected to have an adverse effect on the CNS, it has been postulated that one possible determinant of the adverse effect is the BBB transport of oseltamivir and/or its pharmacologically active form, Ro 64-0802. While P-gp restricts the brain uptake of oseltamivir (Ose et al. 2008), Mrp4 and organic anion transporter 3 (Oat3/Slc22a8) mediate the efflux transport of Ro 64-0802 at the BBB (Ose et al. 2009). These results suggest that the interplay of P-gp, Mrp4, and Oat3 lowers the brain concentration of oseltamivir and its active form, preventing CNS adverse effects. Therefore, under circumstances where the functional activities of one or more of these transporters are altered, the brain concentrations of oseltamivir and/or Ro 64-0802 might be increased to the point where adverse effects occur. It should be noted that the above data were obtained in rodent studies. A quantitative proteomics study showed that although the absolute expression amount of Oat3 at mouse BBB is 1.97 fmol/μg protein (Kamiie et al. 2008), the amount of OAT3 at human BBB is under the limit of quantification (<0.348 fmol/μg protein) (Uchida et al. 2011b). Therefore, it will be important in future studies to

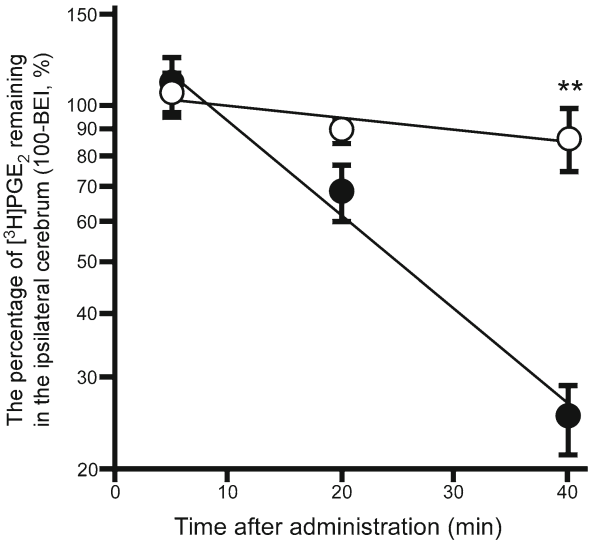

Fig. 2.5 Reduction of the BBB efflux transport of prostaglandin E_2 (PGE2) under inflammatory conditions. Time-course of [^{3}H]PGE_2 in the ipsilateral cerebrum after intracerebral microinjection in LPS-treated mice (*open circles*) and saline-treated mice (*closed circles*). Each point represents the mean ± SEM (n = 4–5). $^{**}p < 0.01$, significantly different from the saline-treated mice. The figure is adapted from Akanuma et al. (2011b)

clarify the mechanisms underlying the transport of Ro 64-0802 at the abluminal membrane of human brain capillary endothelial cells.

Prostaglandin E_2 (PGE_2) acts as a modulator of synaptic signaling and excitability in the brain. PGE_2 (pKa = ~5) exists predominantly in charged form at physiological pH and cannot easily cross the BBB by passive diffusion. PGE_2 undergoes carrier-mediated efflux transport from the rat brain to the blood with a half-life of 16.3 min after cerebral microinjection under normal conditions, since PGE_2 is barely inactivated enzymatically in adult brain (Akanuma et al. 2010). This suggests that brain-to-blood efflux transport functions as a clearance system for PGE_2 produced in the brain, preventing excessive accumulation of PGE_2. It has been found that PGE_2 elimination across the BBB is attenuated in an LPS-induced mouse model of inflammation (Fig. 2.5) (Akanuma et al. 2011b), even though the production of PGE_2 is enhanced under inflammatory conditions (Tachikawa et al. 2012a). Furthermore, β-lactam cephalosporin antibiotics such as cefmetazole, cefazolin, cefotaxime, and ceftriaxone and the nonsteroidal anti-inflammatory drug (NSAID) ketoprofen inhibit MRP4-mediated PGE_2 uptake (Akanuma et al. 2010), and in addition, intravenous administration of cefmetazole dose-dependently reduced [^{3}H]PGE_2 efflux transport across the BBB. Although cephalosporins and NSAIDs are used to treat numerous infectious diseases and to suppress autoimmune responses in fever, such drugs have adverse effects, including inhibitory neuronal signal attenuation and encephalitis (Schliamser et al. 1991; Sunden et al. 2003). Considering that PGE_2 is related to these central nervous system symptoms (Phillis et al. 2006), it is conceivable that reduced MRP4-mediated transport of PGE_2 across the BBB results in alterations of brain function via increased brain levels of PGE_2. In this regard, it is important to know whether these antibiotics are substrates for MRP4-mediated

efflux transport. Measurements of the transport activity of MRP4 for various β-lactam antibiotics indicated that (1) MRP4-mediated transport of cephalosporins occurs at a greater rate than that of penems or monobactams; (2) the transport activity for anionic cephalosporins is greater than that for zwitterionic cephalosporins; and (3) anionic β-lactam antibiotics with higher molecular weight are transported more efficiently than those with lower molecular weight, though no molecular weight dependency is seen in the case of zwitterionic β-lactam antibiotics (Akanuma et al. 2011a). These structure-transport activity relationships should prove useful for understanding MRP4-related adverse effects involving β-lactam antibiotics. It will be necessary to consider drug-PGE_2 interaction as well as drug-drug interaction at MRP4 in evaluating transport function at the BBB.

2.3.2 Transport Systems of Endogenous Peptides and Peptide Drugs

2.3.2.1 β-Amyloid

Cerebral clearance of amyloid-β peptide (Aβ) via brain-to-blood efflux transport at the BBB, as well as via proteolytic degradation, plays a key role in determining the brain levels of Aβ. It has been proposed that reduced Aβ clearance is involved in the development of late-onset alzheimer's disease (AD), which accounts for more than 90 % of AD (Hardy and Selkoe 2002). If this is the case, the BBB clearance system for Aβ would be a promising target for preventive medicine and therapeutic drugs for AD. In support of this notion, the in vivo brain efflux index method has revealed that [^{125}I]human Aβ(1–40) monomer injected into rodent brain undergoes brain-to-blood efflux transport with a half-life of 43–48.8 min via a saturable process (Shiiki et al. 2004; Ito et al. 2006, 2007). The Aβ(1–40) elimination rate was reduced by 30.5 % in 23-month-old rats compared with 7-week-old rats (Shiiki et al. 2004). Aβ(1–42), a more toxic form of Aβ, inhibited [^{125}I]-Aβ(1–40) elimination from the brain, indicating that Aβ(1–40) and Aβ(1–42) share the same elimination process, at least in part (Ito et al. 2006). These results raise the possibility that age-related and Aβ(1–42)-related reduction of the cerebral clearance of Aβ(1–40) results in brain Aβ deposition, which may lead to progression of AD. Therefore, facilitating Aβ clearance across the BBB may lead to decreased cerebral Aβ deposition. It has been found that the active form of vitamin D, 1α,25-dihydroxyvitamin D3, enhances brain-to-blood Aβ(1–40) efflux transport at the BBB, causing a significant reduction of endogenous Aβ(1–40) level in mouse brain (Ito et al. 2011c).

The Aβ elimination mechanism across the BBB remains to be fully established. It has been proposed that the brain-to-blood efflux transport of Aβ involves low-density lipoprotein receptor-related protein-1 (LRP-1; a member of the low-density lipoprotein receptor gene family) (Shibata et al. 2000), P-gp (Cirrito et al. 2005) and Bcrp (Xiong et al. 2009), at least in mice. On the other hand, we have found that (1) preadministration of human receptor-associated protein (RAP), a LRP antagonist,

in rat cerebral cortex reduced the efflux transport of [^{125}I]hAβ(1–40) to the extent of only 20 % (Ito et al. 2006; Shiiki et al. 2004), (2) coadministration of RAP in mouse cerebral cortex did not influence the efflux transport of [^{125}I]hAβ(1–40) (Ito et al. 2010), (3) either [^{125}I]activated α2-macrogloblin (α2M) alone, a typical LRP1 ligand, or activated α2M/[^{125}I]hAβ(1–40) complex was not eliminated from mouse or rat brain, at least up to 90 min (Ito et al. 2007, 2010), and (4) P-gp inhibitors (quinidine and verapamil) do not significantly affect Aβ elimination in rats (Ito et al. 2006). These results strongly suggest that LRP1 and P-gp do not play a major role in the brain-to-blood efflux transport of Aβ(1–40). It is thus intriguing that hAβ(1–40) elimination from rat brain is predominantly mediated by as-yet unidentified molecules. In accordance with these findings, it has been reported that α-tocopherol transfer protein knockout mice exhibit reduced [^{125}I]hAβ(1–40) elimination across the BBB and increased Aβ deposition in the brain, although the protein expression of LRP1 and P-gp in brain capillaries was upregulated in these knockout mice (Nishida et al. 2009). It has been reported that [^{125}I]RAP undergoes efficient blood-to-brain influx transport across the BBB, most likely via LRPs, in mice (Pan et al. 2004), implying that LRP1 is involved in the influx transport of Aβ(1–40) from the circulating blood to the brain. Although great care is needed in evaluating the mechanism(s) behind the BBB efflux transport of Aβ, it will be important to identify the molecule(s) responsible for hAβ(1–40) clearance from the brain.

2.3.2.2 Atrial Natriuretic Peptide

Cerebral atrial natriuretic peptide (ANP), which is generated in the brain, has roles in the regulation of brain water and electrolyte balance, blood pressure and local cerebral blood flow, as well as in neuroendocrine functions. Recently, it has been clarified that [^{125}I]human ANP (hANP) undergoes brain-to-blood efflux transport which involves natriuretic peptide receptor C (Npr-C) as a pathway of cerebral ANP clearance (Ito et al. 2011b). It seems likely that levels of natriuretic peptides in the brain are modulated by 1α,25-dihydroxyvitamin D3 through upregulation of Npr-C expression at the BBB.

2.3.2.3 Peptide Drugs

Although peptide drugs have enormous potential for the treatment of diseases, the BBB generally blocks the entry of peptides, i.e., hydrophilic compounds, into the brain. Peptides that act at opioid receptors in the brain have been designed as analgesics without the side effects of morphine, such as addiction and inhibition of gastric motility (Egleton et al. 1998). Thus, the opioid transport systems at the BBB may be a key determinant of the pharmacological effects of these peptides, such as pain modulation and neuroendocrine regulation. [D-penicillamine2,5]enkephalin (DPDPE), a cyclic opioid pentapeptide, is a δ-opioid receptor agonist and an

enzymatically stable analog of Met-enkephalin. In situ perfusion study demonstrated the blood-to-brain influx transport of DPDPE at a rate of 1.46 μl/(min·g brain), which is approximately fivefold greater than that of impermeable markers, sucrose [0.27 μl/(min·g brain)] and inulin [0.32 μl/(min·g brain)], in rats (Egleton et al. 1998). Since phenylarsine oxide (PAO), an endocytosis inhibitor, inhibited the in vivo uptake of DPDPE in a dose-dependent manner, an energy-dependent transcytotic mechanism was suggested to be involved (Egleton and Davis 1999). Furthermore, uptake studies in *Xenopus laevis* oocytes revealed that human organic anion transporting polypeptide OATP1A2/SLCO1A2 and a rodent homolog of SLCO1A2, rat oatp1a4/Slco1a4, mediate the transport of DPDPE and deltorphin II (Gao et al. 2000). It has been shown that OATP1A2 and oatp1a4 are localized in brain capillary endothelial cells of human and rats, respectively (Gao et al. 1999, 2000). Dagenais et al. (2001) reported that P-gp-deficient mice exhibited a 12-fold increase of DPDPE brain uptake and oatp1a4 substrates, such as digoxin, estradiol-17β-glucuronide, and fexofenadine, inhibited the blood-to-brain transport of DPDPE (Dagenais et al. 2001). This suggests the functional involvements of oapt1a4 as an influx transporter and P-gp as an efflux transporter. Among the oatp transporter family, oatp3/Slco1a5 and oatp14/Slco1c1 are also expressed at the mouse and rat BBB, respectively (Ohtsuki et al. 2004b; Sugiyama et al. 2003). Clarifying their contribution to BBB transport will help increase our understanding of BBB function and the potential for specific delivery of opioids.

The brain uptake of opioids selective for the μ (fentanyl, loperamide, meperidine, methadone, and morphine), δ (DPDPE, deltorphin II, naltrindole, SNC121), and κ (bremazocine and U-69593) receptor subtypes was examined in P-gp-deficient mice (mdr1a−/−) (Dagenais et al. 2004). Although the brain uptake of morphine and phentanyl is increased by 1.24-fold in P-gp-deficient mice, DPDPE, loperamide, and SNC121 showed a more than eightfold-increased brain uptake in the P-gp-deficient mice. This supports the notion that the influence of P-gp on the brain distribution of opioids is one factor modulating pharmacological pain control. Endomorphin 1 and 2 (endogenous opioid tetrapeptides) show the highest affinity and specificity for the μ opioid receptor. It has been demonstrated that there is a saturable brain-to-blood efflux transport system for endomorphin 1 and 2, which is not related to P-gp or the other transport systems for DPDPE and morphine (Somogyvari-Vigh et al. 2004; Kastin et al. 2001, 2002)

2.3.3 Transport Systems of Neurotransmitters and Organic Anions

The brain produces various neurotransmitters, metabolites, and neurotoxic compounds. Because the cerebral accumulation of such compounds may affect neuronal activity, we could postulate the existence of a brain-to-blood efflux transport system to remove neurotransmitters that might be accumulated in the brain interstitial

fluids, in the event of any impairment of the reuptake system by the synaptic cleft (Tachikawa and Hosoya 2011; Terasaki and Hosoya 1999). The BBB has efflux transport systems for neurotransmitters such as γ-aminobutyric acid (GABA) (Kakee et al. 2001), L-glutamic acid, glycine (Takanaga et al. 2002), and L-aspartic acid (Hosoya et al. 1999). It has been reported that GABA transporter 2 (Gat2/Slc6a12; a different subtype from GABA transporter expressed in neurons and astrocytes) (Takanaga et al. 2001), excitatory amino acid transporter 1-3 (Eaat1-3/Slc1a1-3) (O'Kane et al. 1999), alanine-serine-cysteine transporter 2 (Asct2/Slc1a5) (Tetsuka et al. 2003), and amino acid transporter 2 (Ata2/Slc38a2) (Takanaga et al. 2002) are responsible for the efflux transport of GABA, L-glutamic acid, L-aspartic acid, and glycine, respectively .

Organic anion transporter 3 (Oat3/Slc22a8) is localized at the abluminal membrane of brain capillary endothelial cells in mice and rats (Mori et al. 2003; Ohtsuki et al. 2004a). Evidence has accumulated indicating that Oat3 is a multifunctional transport system for organic anions at the BBB, taking up substrates from the brain interstitial fluids into the brain capillary endothelial cells as the first step of brain-to-blood efflux transport. Dehydroepiandrosterone sulfate (DHEAS) is a neuromodulator that interacts with GABA type A receptors and sigma receptors to increase memory and learning ability, and to protect neurons against excitatory amino acid-induced neurotoxicity. DHEAS undergoes brain-to-blood efflux transport from the brain across the BBB (Asaba et al. 2000). The efflux of DHEAS from the brain was significantly decreased in Oat3/Slc22a8-deficient mice compared with that in wild-type mice, although the efflux transport was not altered in oatp1a4-deficient mice, suggesting that Oat3/Slc22a8 plays a major role in the efflux of steroid conjugates across the BBB in mice (Miyajima et al. 2011). Furthermore, we have reported that Oat3 is responsible for the efflux transport of homovanillic acid (HVA; the final metabolite of the monoamine neurotransmitter dopamine), uremic toxins such as indoxyl sulfate (IS), and thiopurine nucleobase analogs such as 6-mercaptopurine (6-MP) and 6-thioguanine (6-TG) (Mori et al. 2003, 2004; Ohtsuki et al. 2002a). Since metabolism is a critical process for efficient dopamine neurotransmission, the oat3-mediated brain-to-blood efflux transport of HVA at the BBB functions as a final clearance process of dopamine from the brain. Therefore, HVA may reflect dopaminergic neuronal activity in the brain, and so its concentration in blood and urine is widely used as a biomarker of dopaminergic neurotransmission. Furthermore, various metabolites of neurotransmitters were found to inhibit Oat3-mediated transport of HVA (Mori et al. 2003), indicating that Oat3 may mediate the BBB efflux transport of various neurotransmitter metabolites. During maintenance chemotherapy for acute lymphoblastic leukemia, CNS relapses often occur due to penetration and proliferation of leukemic cells in the brain (Mori et al. 2004), because of the limited brain distribution of thiopurine nucleobase analogs. Considering that microdialysis studies have shown strong blood-to-brain influx of 6-MP across the BBB (Deguchi et al. 2000), it appears that Oat3 plays a crucial role in limiting the effects of thiopurine nucleobase analogs in the brain.

2.3.4 *Species Differences of Organic Anion Transporters at the BBB*

Quantitative protein expression analysis of transporters at the BBB indicates that there are marked inter-species differences of organic anion transporters, e.g., Oat3 and Oatps. Although Oat3, Oatp1a4, and Oatp1c1 were detected in mouse brain capillaries in amounts of 1.97, 2.11, and 2.41 (fmol/μg protein) (Kamiie et al. 2008), respectively, the potent human homologues OAT3, OATP1A2, and OATP1C1 were under the limit of quantification in human and monkey brain capillaries (Ito et al. 2011a; Uchida et al. 2011b). One possible explanation of this discrepancy is that even small amounts of organic anion transporters could still play a functional role. Another possibility is that human BBB and monkey BBB contain other organic anion transporters. This remains a crucial issue in BBB transporter research, because these transporters are potential pathways for delivering CNS-acting drugs from the circulating blood into the brain.

2.4 Influx and Efflux Transport Systems at the BCSFB

As summarized in Table 2.3, BCSFB transporters play a role in CSF homeostasis by regulating the movement of nutrients and waste products. This section introduces recent progress in BCSFB transporter research, including the significant advances in our understanding of the physiological and therapeutic impact of BCSFB transporters that have resulted from the development of various transporter gene knockout mice.

2.4.1 *Organic Cations*

The plasma membrane monoamine transporter (Pmat/Slc29a4) is a recently found polyspecific organic cation transporter that transports a wide variety of organic cations, including biogenic amines, cationic drugs, and neurotoxins (Xia et al. 2007). Immunofluorescence staining revealed that Pmat is localized at the CSF-facing brush-border membrane of choroid plexus epithelial cells (Duan and Wang 2013). Okura et al. (2011) reported in vivo [^{3}H]1-methyl-4-phenylpyridinium (MPP^+) transport from the CSF to the circulating blood and its inhibition by serotonin and dopamine (Okura et al. 2011). Pmat−/− knockout mice showed reduced uptake of monoamines and the neurotoxin MPP^+ in the choroid plexus (Duan and Wang 2013). Therefore, Pmat appears to be a major choroid plexus uptake transporter for bioactive amines and xenobiotic cations, protecting the brain from cationic neurotoxins and other potentially toxic organic cations.

Table 2.3 Transporters expressed at the BCSFB

Transporters	Substrates	Localization	Direction	References
Energy transport system				
Glut1(Slc2a1)	D-Glucose	BL	–	Hacker et al. (1991)
Crt (Slc6a8)	Guanidinoacetate	BB	Ef	Tachikawa et al. (2008a)
Organic anion transport system				
Oat3 (Slc22a3)	PAH, fluorescein, estrone sulfate, prostaglandin D_2, E_2	BB	Ef	Nagata et al. (2002)
Oatp1a5 (Slco1a5)	Digoxin, organic anions	BB	Ef	Ohtsuki et al. (2004b)
Pgt (Slco2a1)	Prostaglandin D_2	BB	Ef	Tachikawa et al. (2012b)
Organic cation transport system				
Pmat (Slc29a4)	MPP^+, Monoamine neurotransmitters	BB	Ef	Okura et al. (2011), Duan and Wang (2013)
Oct3 (Slc22a3)	Creatinine	BB	Ef	Nakayama et al. (2007), Sweet et al. (2001)
Peptides				
Pept2 (Slc15a2)	Dipeptides	–	Ef	Shen et al. (2004)
ABC transporters				
Abca1	Cholesterol	BB	In	Fujiyoshi et al. (2007)
Abcg1	Cholesterol	BB	In	Fujiyoshi et al. (2007)
Abcb1/Mdr1	–	BB	–	Urquhart and Kim (2009)
Abcc1/Mrp1	Etoposide	BL	Ef	Urquhart and Kim (2009)
Abcc4/Mrp4	Topotecan	BL	Ef	Leiderman et al. (1991)
Abcg2/Bcrp	–	BB	–	Tachikawa et al. (2005)

Localization: brush-border membrane (BB) and basolateral membrane (BL) of choroid plexus epithelial cells. Direction: blood-to-CSF influx transport (In) and CSF-to-blood efflux transport (Ef). –: Not determined. MPP^+: 1-methyl-4-phenylpyridinium

2.4.2 *Organic Anions*

The BCSFB possesses multiple organic anion transporters, including organic anion transporter 3 (Oat3/Slc22a3) (Nagata et al. 2002), prostaglandin transporter (Pgt/Slco2a1) (Kis et al. 2006; Tachikawa et al. 2012b), and organic anion transporting polypeptide 1a5 (Oatp1a5) (Kusuhara et al. 2003; Ohtsuki et al. 2004b). Since Pgt/Slco2a1 (Fig. 2.6) (Tachikawa et al. 2012b), Oat3/Slc22a3 (Nagata et al. 2002), and Oatp1a5/Slco1a5 (Ohtsuki et al. 2004b) were localized on the brush-border membrane of the choroid plexus epithelial cells, it has been well established that these transporters are involved in the uptake of organic anions from the CSF.

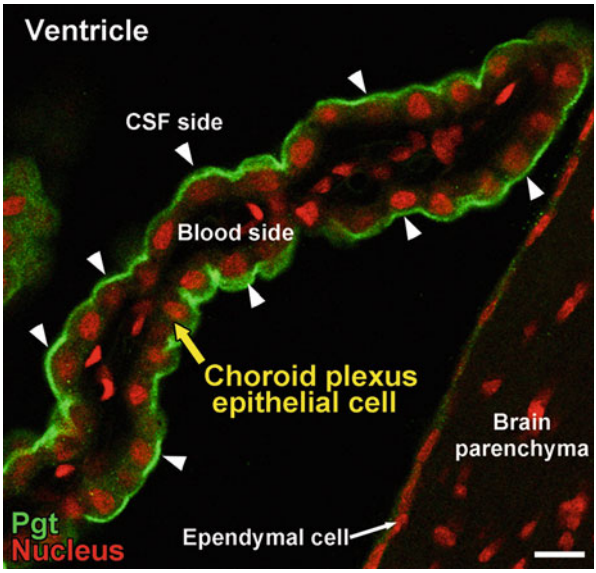

Fig. 2.6 Localization of prostaglandin transporter (Pgt) on the CSF-facing brush-border membrane (*arrowheads*) of the rat choroid plexus epithelial cells. Nuclei were stained by propidium iodide (*red*). Scale bar: 20 μm

Indeed, para-aminohippuric acid and fluorescein uptake by isolated choroid plexus was essentially abolished in Oat3 knockout mice, whereas the uptake of estrone sulfate was only reduced by one-third and taurocholate uptake was not affected (Sweet et al. 2002; Sykes et al. 2004).

Prostaglandin (PG) D_2 is an endogenous sleep-promoting substance, which regulates physiological sleep through D-type prostanoid receptor 1. The system regulating the PGD_2 level in the CSF involves Pgt- and Oat3-mediated PGD_2 uptake by choroid plexus epithelial cells, acting as a pathway for PGD_2 clearance from the CSF via the BCSFB (Tachikawa et al. 2012b). Continuous inhibition of the clearance of PGD_2 from the CSF at the BCSFB may modify the PGD_2 level in the CSF, thus affecting physiological sleep. Some commonly used nonsteroidal anti-inflammatory drugs (NSAIDs), such as indomethacin and diclofenac inhibit Oat3-mediated PGD_2 transport. Thus, the inhibition of Pgt- and Oat3-mediated PGD_2 transport should be taken into consideration in the development of new targets for insomnia. Similarly, a system regulating the CSF level of PGE_2, which appears to be a key determinant of the progression of neuroinflammation, involves Oat3-mediated PGE_2 uptake of locally produced PGE_2 by choroid plexus epithelial cells, acting as a cerebral clearance pathway via the BCSFB (Tachikawa et al. 2012a).

2.4.3 Guanido Compounds

Many guanidino compounds (GCs), such as creatine, phosphocreatine, guanidinoacetic acid, creatinine, methylguanidine, guanidinosuccinic acid, γ-guanidinobutyric

acid, β-guanidinopropionic acid, guanidinoethanesulfonic acid, and aguanidinoglutaric acid, are present in the mammalian brain. Although creatine and phosphocreatine play important roles in energy homeostasis in the brain, accumulation of GCs may induce epileptic discharges and convulsions (Hiramatsu 2003). Transporters for GCs at the BCSFB have emerged as substantial contributors to GCs distribution in the brain. Crt (Tachikawa et al. 2008a), taurine transporter (Taut/Slc6a6) (Tachikawa et al. 2009) and organic cation transporter (Oct3/Slc22a3) (Tachikawa et al. 2008b) expressed at the BCSFB are involved in the uptake of guanidinoacetic acid or creatinine in the CSF-to-epithelial cell direction. Interestingly, the BBB efflux transport of GCs, including guanidinoacetate and creatinine, is negligible (Tachikawa et al. 2008b, 2009), though the BBB has a variety of efflux transport systems for synthetic precursors of GCs, such as amino acids and neurotransmitters (Tachikawa and Hosoya 2011). These findings indicate that the BCSFB functions as a major cerebral clearance system for GCs. Hence, transport of GCs at the BCSFB appears to be the key determinant of the cerebral levels of GCs, and changes in the transport characteristics may cause the abnormal brain distributions of GCs seen in patients with certain neurological disorders.

2.4.4 Peptides

Proton-coupled oligopeptide transporter (Pept2/Slc15a2) is localized at the apical membrane of rat choroid plexus epithelial cells, but is absent at the BBB (Shen et al. 2004). Pept2 knockout mice exhibited a marked increase in the in vivo blood-to-CSF transport of dipeptides such as glycylsarcosine (GlySar), carnosine, cefadroxil, and 5-aminolevulinic acid (Shen et al. 2003; Ocheltree et al. 2004; Teuscher et al. 2004). This suggests that Pept2 is involved in CSF-to-blood efflux transport, serving to block entry of its substrates into the CSF. In accordance with this idea, intracerebroventricular administration of L-kyotorphin (an endogenous analgesic dipeptide) induces greater analgesia in Pept2 knockout mice, probably due to reduced clearance from the CSF to the choroid plexus (Jiang et al. 2009). Although Pept2 dysfunction would affect the brain parenchymal distribution of the drug, autoradiography showed that the brain parenchymal distribution of [^{14}C]GlySar after intraventricular administration was limited to the periventricular zone (Smith et al. 2011). These results are in agreement with the concept that Pept2 at the BCSFB is a determinant of dipeptide concentration in the CSF.

Amyloid-β peptide (Aβ) concentration in CSF is potentially a diagnostic and therapeutic target for Alzheimer's disease (AD). hAβ(1–40) is actively eliminated from CSF and this process is significantly inhibited by human receptor-associated protein (RAP) (Fujiyoshi et al. 2011). The elimination was attenuated in either anti-low-density lipoprotein receptor-related protein 1 (LRP1) antibody-treated or RAP-deficient mice (Fujiyoshi et al. 2011). The amount of LRP1 in rat choroid plexus was determined to be 3.7 fmol/μg protein, whereas the LRP2 content was below the detection limit (Fujiyoshi et al. 2011). Therefore, LRP1-mediated efflux at the BCSFB plays a role in determining the CSF concentration of hAβ(1–40).

2.4.5 Lipophilic Compounds

The release of cholesterol from choroid plexus epithelial cells plays an important role in cholesterol homeostasis in the CSF. Abca1 and Abcg1 proteins were detected in the plasma membrane of a conditionally immortalized choroid plexus epithelial cell line, TR-CSFB3 cells. Apolipoprotein (apo) AI- and high-density lipoprotein (HDL)-mediated cholesterol release to the apical side of TR-CSFB3 cells was facilitated by this treatment, whereas that to the basal side was not affected (Fujiyoshi et al. 2007). These results suggest that Abca1 and Abcg1 are functionally involved in cholesterol release into the CSF from choroid plexus epithelial cells.

2.4.6 Contribution of ATP-Binding Cassette (ABC) Transporters at the BCSFB

Although the roles of P-gp, Bcrp, and Mrp4 at the BBB have been investigated, the functional relevance of these ABC transporters at the BCSFB remains to be established. It has been reported that Mdr1a/1b and Bcrp double-knockout mice exhibit increased blood-to-brain parenchyma penetration, but reduced blood-to-CSF penetration, of the anticancer agent topotecan (Shen et al. 2009). Indeed, P-gp and Bcrp are localized on the CSF-facing brush-border membrane of choroid plexus epithelial cells (Urquhart and Kim 2009; Tachikawa et al. 2005), and thus would be involved in efflux transport in the epithelial cell-to-CSF direction. In contrast, Leggas et al. (2004) found that Mrp4-deficient mice show much greater entry of topotecan into the CSF, which is consistent with the localization in basolateral membrane of choroid plexus epithelial cells (Leiderman et al. 1991). Furthermore, mice with knockout of multidrug-resistance protein 1 (Mrp1), which is also localized on the basolateral membrane (Urquhart and Kim 2009), exhibit tenfold increased levels of etoposide in the CSF (Wijnholds et al. 2000). A western blot analysis showed that the amounts of P-gp in rat and human choroid plexus are less than 0.5 % of those in brain microvessels, whereas the amounts of Mrp1 are much greater in choroid plexus than in brain microvessels (Gazzin et al. 2008). Taking these results into consideration, it is likely that Mrp1 and Mrp4 at the BCSFB are major contributors to the restriction of drug entry from the circulating blood into the CSF at the basolateral membrane of choroid plexus epithelial cells.

2.5 Conclusion and Perspectives

As reviewed in this chapter, recent progress in BBB and BCSFB research has demonstrated the physiological and pharmacological importance of multiple transporters in the brain distribution of endogenous compounds and drugs. The accumulated

data on influx and efflux transport mechanisms at the blood–brain/CSF interfaces will certainly be helpful in the design of optimal drug candidates, as well as for prediction of drug penetration into the brain. On the other hand, we are still far from completely understanding the complexities of the many different transport systems at the brain barriers. Despite advances in molecular biology, genomics, and proteomics, several transport systems, such as H^+-coupled cationic drugs transporter (Sect. 2.2.2) and efflux transporter of β-amyloid peptide (Sect. 2.3.2), remain to be identified at the molecular level.

Further, most of the findings have been obtained in rodents, and the extent to which these findings are applicable to humans remains uncertain. Our strategy of quantitative targeted absolute proteomics has provided a tool to address this issue (Kamiie et al. 2008). The ultimate goal of this strategy is to establish blood–brain barrier pharmacoproteomics (BBB PPx), i.e., to achieve an understanding of the physiological and pharmacological roles of the BBB based on individual protein functions and protein amounts in the BBB in any animal species under any pathophysiological condition. Because the relative impact of drug transporters (e.g., P-gp, BCRP, MRP4, and MRP1) at the BCSFB and BBB on the cerebral distribution of the drugs is likely to depend on the amounts of the transporters, a BCSFB transporter protein atlas is also required. Such data would enable us to reconstruct the in vivo human BBB and/or BCSFB transport activities (Uchida et al. 2011a) and to consider the influence of factors such as disease status, aging (Ito et al. 2011a), and individual differences. The development of BBB pharmacoproteomics is discussed in Chap. 3.

The manipulation of transport systems, e.g., induction of influx transporter expression and inhibition of efflux transporters, may also be a useful approach to improve drug targeting to the brain. Inhibition of efflux transporters is likely to lower the efflux transport rate, leading to increased drug efficacy in the brain by increasing the drug concentration in the brain interstitial fluid. Because these transporters are also expressed in peripheral tissues and inhibition would change the distribution and elimination of drugs, development of brain-selective inhibitors would also be an interesting goal.

In vitro BBB and BCSFB models of human brain capillary endothelial cells and choroid plexus epithelial cells are useful tools for screening candidate drugs and predicting transport rates. We have established conditionally immortalized mouse and rat brain capillary endothelial cell lines (TM-BBB and TR-BBB, respectively) (Hosoya et al. 2000a, b) and a rat choroid plexus epithelial cell line (TR-CSFB) (Kitazawa et al. 2001), and demonstrated that some of their transport functions adequately reflect the in vivo transport function (Terasaki et al. 2003). However, these cell lines have lower expression of multiple transporters than in vivo cells, and lack tight junctions and cell polarity. Weksler et al. (2005) have established an immortalized human brain capillary endothelial cell line (hCMEC/D3) which exhibits a good correlation between in vitro and in vivo BBB permeability (Weksler et al. 2005). Recently, we used our quantitative targeted absolute proteomics technology to show that ABCA2, MDR1, MRP4, BCRP, GLUT1, 4F2hc, MCT1, equilibrative

nucleoside transporter 1 (ENT1), transferrin and insulin receptors, and claudin-5, a tight junction protein, are present in both hCMEC/D3 cells and human brain microvessels (Ohtsuki et al. 2013). The differences in protein expression levels between hCMEC/D3 cells and human brain microvessels were within fourfold for these proteins except for ENT1, transferrin receptor and claudin-5. Lippmann et al. (2012) have shown that endothelial cells derived from human pluripotent stem cells (hPSCs) possesses some of the barrier properties of the BBB, including well-organized tight junctions, appropriate expression of nutrient transporters and polarized efflux transporter activity (Lippmann et al. 2012). Transendothelial electrical resistance reached a maximum of $1{,}450 \pm 140\ \Omega cm^2$ upon astrocyte coculture, and the permeability correlated well with in vivo rodent blood–brain transfer coefficients. These cellular platforms should be useful not only to clarify the molecular mechanisms of the human BBB transport system but also to screen drug candidates for CNS-acting drugs with appropriate brain permeability. A human choroid plexus epithelial cell line has not been established so far. Although numerous challenges remain in the field of BBB and BCSFB research, we believe that integration of the various recently developed strategies and methodologies will trigger substantial progress in CNS drug discovery and delivery in the near future.

2.6 Points for Discussion

1. Why does increasing the lipophilicity of a poorly BBB permeable drug not necessarily increase its BBB permeability?
2. What kinds of transporters and receptors are expressed at the BBB and BCSFB?
3. What are the physiological roles of the BBB and BCSFB transport systems?
4. How can we overcome the problems of the low BBB permeability by utilizing transporters?
5. What kinds of transporters can be utilized for drug delivery to the brain in the design of CNS-acting drugs?
6. What is the impact of the BBB efflux transporters such as P-gp, Bcrp, and Mrp4 on the brain drug distribution?
7. In which cases do we need to consider the drug-endogenous substrate interaction on transporters at the BBB and BCSFB?
8. How can we overcome the problems of species differences in transport systems at the BBB and BCSFB?
9. Why is molecular identification of the H^+-coupled cationic drug transporter expected to make significant progress in the delivery of cationic CNS-acting drugs?
10. What kinds of strategies and methodologies will trigger substantial progress in CNS drug discovery and delivery in the near future?

Acknowledgement We would like to acknowledge the collaboration of Drs. K. Hosoya and S. Akanuma (University of Toyama). This work was supported, in part, by a Grant-in-Aid for Scientific Research from the Japan Society for the Promotion of Science.

References

Abbott NJ, Romero IA (1996) Transporting therapeutics across the blood-brain barrier. Mol Med Today 2:106–113

Abbott NJ, Ronnback L, Hansson E (2006) Astrocyte-endothelial interactions at the blood-brain barrier. Nat Rev Neurosci 7:41–53

Adkison KD, Shen DD (1996) Uptake of valproic acid into rat brain is mediated by a medium-chain fatty acid transporter. J Pharmacol Exp Ther 276:1189–1200

Agarwal S, Sane R, Gallardo JL, Ohlfest JR, Elmquist WF (2010) Distribution of gefitinib to the brain is limited by P-glycoprotein (ABCB1) and breast cancer resistance protein (ABCG2)-mediated active efflux. J Pharmacol Exp Ther 334:147–155

Agarwal S, Uchida Y, Mittapalli RK, Sane R, Terasaki T, Elmquist WF (2012) Quantitative proteomics of transporter expression in brain capillary endothelial cells isolated from P-glycoprotein (P-gp), breast cancer resistance protein (Bcrp), and P-gp/Bcrp knockout mice. Drug Metab Dispos 40:1164–1169

Agus DB, Gambhir SS, Pardridge WM, Spielholz C, Baselga J, Vera JC, Golde DW (1997) Vitamin C crosses the blood-brain barrier in the oxidized form through the glucose transporters. J Clin Invest 100:2842–2848

Akanuma S, Hosoya K, Ito S, Tachikawa M, Terasaki T, Ohtsuki S (2010) Involvement of multidrug resistance-associated protein 4 in efflux transport of prostaglandin E(2) across mouse blood-brain barrier and its inhibition by intravenous administration of cephalosporins. J Pharmacol Exp Ther 333:912–919

Akanuma S, Uchida Y, Ohtsuki S, Kamiie J, Tachikawa M, Terasaki T, Hosoya K (2011a) Molecular-weight-dependent, anionic-substrate-preferential transport of beta-lactam antibiotics via multidrug resistance-associated protein 4. Drug Metab Pharmacokinet 26:602–611

Akanuma S, Uchida Y, Ohtsuki S, Tachikawa M, Terasaki T, Hosoya K (2011b) Attenuation of prostaglandin E2 elimination across the mouse blood-brain barrier in lipopolysaccharide-induced inflammation and additive inhibitory effect of cefmetazole. Fluids Barriers CNS 8:24

Andre P, Debray M, Scherrmann JM, Cisternino S (2009) Clonidine transport at the mouse blood-brain barrier by a new H^+ antiporter that interacts with addictive drugs. J Cereb Blood Flow Metab 29:1293–1304

Asaba H, Hosoya K, Takanaga H, Ohtsuki S, Tamura E, Takizawa T, Terasaki T (2000) Blood-brain barrier is involved in the efflux transport of a neuroactive steroid, dehydroepiandrosterone sulfate, via organic anion transporting polypeptide 2. J Neurochem 75:1907–1916

Baltes S, Fedrowitz M, Tortos CL, Potschka H, Loscher W (2007) Valproic acid is not a substrate for P-glycoprotein or multidrug resistance proteins 1 and 2 in a number of in vitro and in vivo transport assays. J Pharmacol Exp Ther 320:331–343

Barakat S, Demeule M, Pilorget A, Regina A, Gingras D, Baggetto LG, Beliveau R (2007) Modulation of p-glycoprotein function by caveolin-1 phosphorylation. J Neurochem 101:1–8

Bauer M, Zeitlinger M, Karch R, Matzneller P, Stanek J, Jager W, Bohmdorfer M, Wadsak W, Mitterhauser M, Bankstahl JP, Loscher W, Koepp M, Kuntner C, Muller M, Langer O (2012) Pgp-mediated interaction between (R)-[11C]verapamil and tariquidar at the human blood-brain barrier: a comparison with rat data. Clin Pharmacol Ther 91:227–233

Beal MF (2011) Neuroprotective effects of creatine. Amino Acids 40:1305–1313

Boado RJ, Li JY, Nagaya M, Zhang C, Pardridge WM (1999) Selective expression of the large neutral amino acid transporter at the blood-brain barrier. Proc Natl Acad Sci U S A 96: 12079–12084

Boado RJ, Li JY, Pardridge WM (2003) Site-directed mutagenesis of rabbit LAT1 at amino acids 219 and 234. J Neurochem 84:1322–1331

Boström E, Simonsson US, Hammarlund-Udenaes M (2006) In vivo blood-brain barrier transport of oxycodone in the rat: indications for active influx and implications for pharmacokinetics/pharmacodynamics. Drug Metab Dispos 34:1624–1631

Breedveld P, Pluim D, Cipriani G, Wielinga P, van Tellingen O, Schinkel AH, Schellens JH (2005) The effect of Bcrp1 (Abcg2) on the in vivo pharmacokinetics and brain penetration of imatinib

mesylate (Gleevec): implications for the use of breast cancer resistance protein and P-glycoprotein inhibitors to enable the brain penetration of imatinib in patients. Cancer Res 65: 2577–2582

Chen ZS, Lee K, Kruh GD (2001) Transport of cyclic nucleotides and estradiol 17-beta-D-glucuronide by multidrug resistance protein 4. Resistance to 6-mercaptopurine and 6-thioguanine. J Biol Chem 276:33747–33754

Chen Y, Agarwal S, Shaik NM, Chen C, Yang Z, Elmquist WF (2009) P-glycoprotein and breast cancer resistance protein influence brain distribution of dasatinib. J Pharmacol Exp Ther 330: 956–963

Cirrito JR, Deane R, Fagan AM, Spinner ML, Parsadanian M, Finn MB, Jiang H, Prior JL, Sagare A, Bales KR, Paul SM, Zlokovic BV, Piwnica-Worms D, Holtzman DM (2005) P-glycoprotein deficiency at the blood-brain barrier increases amyloid-beta deposition in an Alzheimer disease mouse model. J Clin Invest 115:3285–3290

Cisternino S, Chapy H, Andre P, Smirnova M, Debray M, Scherrmann JM (2013) Coexistence of passive and proton antiporter-mediated processes in nicotine transport at the mouse blood-brain barrier. AAPS J 15:299–307

Cooray HC, Blackmore CG, Maskell L, Barrand MA (2002) Localisation of breast cancer resistance protein in microvessel endothelium of human brain. Neuroreport 13:2059–2063

Cordon-Cardo C, O'Brien JP, Casals D, Rittman-Grauer L, Biedler JL, Melamed MR, Bertino JR (1989) Multidrug-resistance gene (P-glycoprotein) is expressed by endothelial cells at blood-brain barrier sites. Proc Natl Acad Sci U S A 86:695–698

Dagenais C, Ducharme J, Pollack GM (2001) Uptake and efflux of the peptidic delta-opioid receptor agonist. Neurosci Lett 301:155–158

Dagenais C, Graff CL, Pollack GM (2004) Variable modulation of opioid brain uptake by P-glycoprotein in mice. Biochem Pharmacol 67:269–276

De Vivo DC, Trifiletti RR, Jacobson RI, Ronen GM, Behmand RA, Harik SI (1991) Defective glucose transport across the blood-brain barrier as a cause of persistent hypoglycorrhachia, seizures, and developmental delay. N Engl J Med 325:703–709

de Vries NA, Zhao J, Kroon E, Buckle T, Beijnen JH, van Tellingen O (2007) P-glycoprotein and breast cancer resistance protein: two dominant transporters working together in limiting the brain penetration of topotecan. Clin Cancer Res 13:6440–6449

Dechent P, Pouwels PJ, Wilken B, Hanefeld F, Frahm J (1999) Increase of total creatine in human brain after oral supplementation of creatine-monohydrate. Am J Physiol 277:R698–R704

Decleves X, Jacob A, Yousif S, Shawahna R, Potin S, Scherrmann JM (2011) Interplay of drug metabolizing CYP450 enzymes and ABC transporters in the blood-brain barrier. Curr Drug Metab 12:732–741

Deguchi Y, Yokoyama Y, Sakamoto T, Hayashi H, Naito T, Yamada S, Kimura R (2000) Brain distribution of 6-mercaptopurine is regulated by the efflux transport system in the blood-brain barrier. Life Sci 66:649–662

del Amo EM, Urtti A, Yliperttula M (2008) Pharmacokinetic role of L-type amino acid transporters LAT1 and LAT2. Eur J Pharm Sci 35:161–174

Duan H, Wang J (2013) Impaired monoamine and organic cation uptake in choroid plexus in mice with targeted disruption of the plasma membrane monoamine transporter (Slc29a4) gene. J Biol Chem 288:3535–3544

Egleton RD, Davis TP (1999) Transport of the delta-opioid receptor agonist [D-penicillamine2,5] enkephalin across the blood-brain barrier involves transcytosis1. J Pharm Sci 88:392–397

Egleton RD, Abbruscato TJ, Thomas SA, Davis TP (1998) Transport of opioid peptides into the central nervous system. J Pharm Sci 87:1433–1439

Farrell CL, Pardridge WM (1991) Ultrastructural localization of blood-brain barrier-specific antibodies using immunogold-silver enhancement techniques. J Neurosci Methods 37:103–110

Fujiyoshi M, Ohtsuki S, Hori S, Tachikawa M, Terasaki T (2007) 24S-hydroxycholesterol induces cholesterol release from choroid plexus epithelial cells in an apical- and apoE isoform-dependent manner concomitantly with the induction of ABCA1 and ABCG1 expression. J Neurochem 100:968–978

Fujiyoshi M, Tachikawa M, Ohtsuki S, Ito S, Uchida Y, Akanuma S, Kamiie J, Hashimoto T, Hosoya K, Iwatsubo T, Terasaki T (2011) Amyloid-beta peptide(1-40) elimination from cerebrospinal fluid involves low-density lipoprotein receptor-related protein 1 at the blood-cerebrospinal fluid barrier. J Neurochem 118:407–415

Gao B, Stieger B, Noe B, Fritschy JM, Meier PJ (1999) Localization of the organic anion transporting polypeptide 2 (Oatp2) in capillary endothelium and choroid plexus epithelium of rat brain. J Histochem Cytochem 47:1255–1264

Gao B, Hagenbuch B, Kullak-Ublick GA, Benke D, Aguzzi A, Meier PJ (2000) Organic anion-transporting polypeptides mediate transport of opioid peptides across blood-brain barrier. J Pharmacol Exp Ther 294:73–79

Gazzin S, Strazielle N, Schmitt C, Fevre-Montange M, Ostrow JD, Tiribelli C, Ghersi-Egea JF (2008) Differential expression of the multidrug resistance-related proteins ABCb1 and ABCc1 between blood-brain interfaces. J Comp Neurol 510:497–507

Giacomini KM, Huang SM, Tweedie DJ, Benet LZ, Brouwer KL, Chu X, Dahlin A, Evers R, Fischer V, Hillgren KM, Hoffmaster KA, Ishikawa T, Keppler D, Kim RB, Lee CA, Niemi M, Polli JW, Sugiyama Y, Swaan PW, Ware JA, Wright SH, Yee SW, Zamek-Gliszczynski MJ, Zhang L (2010) Membrane transporters in drug development. Nat Rev Drug Discov 9:215–236

Gynther M, Laine K, Ropponen J, Leppanen J, Mannila A, Nevalainen T, Savolainen J, Jarvinen T, Rautio J (2008) Large neutral amino acid transporter enables brain drug delivery via prodrugs. J Med Chem 51:932–936

Gynther M, Jalkanen A, Lehtonen M, Forsberg M, Laine K, Ropponen J, Leppanen J, Knuuti J, Rautio J (2010) Brain uptake of ketoprofen-lysine prodrug in rats. Int J Pharm 399:121–128

Hacker HJ, Thorens B, Grobholz R (1991) Expression of facilitative glucose transporter in rat liver and choroid plexus. A histochemical study in native cryostat sections. Histochemistry 96:435–439

Halmos T, Santarromana M, Antonakis K, Scherman D (1996) Synthesis of glucose-chlorambucil derivatives and their recognition by the human GLUT1 glucose transporter. Eur J Pharmacol 318:477–484

Hardy J, Selkoe DJ (2002) The amyloid hypothesis of Alzheimer's disease: progress and problems on the road to therapeutics. Science 297:353–356

Hiramatsu M (2003) A role for guanidino compounds in the brain. Mol Cell Biochem 244:57–62

Hori S, Ohtsuki S, Tachikawa M, Kimura N, Kondo T, Watanabe M, Nakashima E, Terasaki T (2004) Functional expression of rat ABCG2 on the luminal side of brain capillaries and its enhancement by astrocyte-derived soluble factor(s). J Neurochem 90:526–536

Hosoya K, Sugawara M, Asaba H, Terasaki T (1999) Blood-brain barrier produces significant efflux of L-aspartic acid but not D-aspartic acid: in vivo evidence using the brain efflux index method. J Neurochem 73:1206–1211

Hosoya K, Tetsuka K, Nagase K, Tomi M, Saeki S, Ohtsuki S, Takanaga H, Yanai N, Obinata M, Kikuchi A, Okano T, Terasaki T (2000a) Conditionally immortalized brain capillary endothelial cell lines established from a transgenic mouse harboring temperature-sensitive simian virus 40 large T-antigen gene. AAPS PharmSci 2:E27

Hosoya KI, Takashima T, Tetsuka K, Nagura T, Ohtsuki S, Takanaga H, Ueda M, Yanai N, Obinata M, Terasaki T (2000b) mRNA expression and transport characterization of conditionally immortalized rat brain capillary endothelial cell lines; a new in vitro BBB model for drug targeting. J Drug Target 8:357–370

Huang SC, Stout DB, Yee RE, Satyamurthy N, Barrio JR (1998) Distribution volume of radiolabeled large neutral amino acids in brain tissue. J Cereb Blood Flow Metab 18:1288–1293

Huber O, Brunner A, Maier P, Kaufmann R, Couraud PO, Cremer C, Fricker G (2012) Localization microscopy (SPDM) reveals clustered formations of P-glycoprotein in a human blood-brain barrier model. PLoS One 7:e44776

Ito S, Ohtsuki S, Terasaki T (2006) Functional characterization of the brain-to-blood efflux clearance of human amyloid-beta peptide (1-40) across the rat blood-brain barrier. Neurosci Res 56:246–252

Ito S, Ohtsuki S, Kamiie J, Nezu Y, Terasaki T (2007) Cerebral clearance of human amyloid-beta peptide (1-40) across the blood-brain barrier is reduced by self-aggregation and formation of low-density lipoprotein receptor-related protein-1 ligand complexes. J Neurochem 103:2482–2490

Ito S, Ueno T, Ohtsuki S, Terasaki T (2010) Lack of brain-to-blood efflux transport activity of low-density lipoprotein receptor-related protein-1 (LRP-1) for amyloid-beta peptide(1-40) in mouse: involvement of an LRP-1-independent pathway. J Neurochem 113:1356–1363

Ito K, Uchida Y, Ohtsuki S, Aizawa S, Kawakami H, Katsukura Y, Kamiie J, Terasaki T (2011a) Quantitative membrane protein expression at the blood-brain barrier of adult and younger cynomolgus monkeys. J Pharm Sci 100:3939–3950

Ito S, Ohtsuki S, Katsukura Y, Funaki M, Koitabashi Y, Sugino A, Murata S, Terasaki T (2011b) Atrial natriuretic peptide is eliminated from the brain by natriuretic peptide receptor-C-mediated brain-to-blood efflux transport at the blood-brain barrier. J Cereb Blood Flow Metab 31:457–466

Ito S, Ohtsuki S, Nezu Y, Koitabashi Y, Murata S, Terasaki T (2011c) 1alpha,25-dihydroxyvitamin D3 enhances cerebral clearance of human amyloid-beta peptide(1-40) from mouse brain across the blood-brain barrier. Fluids Barriers CNS 8:20

Jiang H, Hu Y, Keep RF, Smith DE (2009) Enhanced antinociceptive response to intracerebroventricular kyotorphin in Pept2 null mice. J Neurochem 109:1536–1543

Kageyama T, Nakamura M, Matsuo A, Yamasaki Y, Takakura Y, Hashida M, Kanai Y, Naito M, Tsuruo T, Minato N, Shimohama S (2000) The 4F2hc/LAT1 complex transports L-DOPA across the blood-brain barrier. Brain Res 879:115–121

Kakee A, Takanaga H, Terasaki T, Naito M, Tsuruo T, Sugiyama Y (2001) Efflux of a suppressive neurotransmitter, GABA, across the blood-brain barrier. J Neurochem 79:110–118

Kakee A, Takanaga H, Hosoya K, Sugiyama Y, Terasaki T (2002) In vivo evidence for brain-to-blood efflux transport of valproic acid across the blood-brain barrier. Microvasc Res 63: 233–238

Kamiie J, Ohtsuki S, Iwase R, Ohmine K, Katsukura Y, Yanai K, Sekine Y, Uchida Y, Ito S, Terasaki T (2008) Quantitative atlas of membrane transporter proteins: development and application of a highly sensitive simultaneous LC/MS/MS method combined with novel in-silico peptide selection criteria. Pharm Res 25:1469–1483

Kanai Y, Segawa H, Miyamoto K, Uchino H, Takeda E, Endou H (1998) Expression cloning and characterization of a transporter for large neutral amino acids activated by the heavy chain of 4F2 antigen (CD98). J Biol Chem 273:23629–23632

Kasahara T, Maeda M, Boles E, Kasahara M (2009) Identification of a key residue determining substrate affinity in the human glucose transporter GLUT1. Biochim Biophys Acta 1788: 1051–1055

Kastin AJ, Fasold MB, Smith RR, Horner KA, Zadina JE (2001) Saturable brain-to-blood transport of endomorphins. Exp Brain Res 139:70–75

Kastin AJ, Fasold MB, Zadina JE (2002) Endomorphins, met-enkephalin, Tyr-MIF-1, and the P-glycoprotein efflux system. Drug Metab Dispos 30:231–234

Kido Y, Tamai I, Okamoto M, Suzuki F, Tsuji A (2000) Functional clarification of MCT1-mediated transport of monocarboxylic acids at the blood-brain barrier using in vitro cultured cells and in vivo BUI studies. Pharm Res 17:55–62

Kim MH, Maeng HJ, Yu KH, Lee KR, Tsuruo T, Kim DD, Shim CK, Chung SJ (2010) Evidence of carrier-mediated transport in the penetration of donepezil into the rat brain. J Pharm Sci 99:1548–1566

Kis B, Isse T, Snipes JA, Chen L, Yamashita H, Ueta Y, Busija DW (2006) Effects of LPS stimulation on the expression of prostaglandin carriers in the cells of the blood-brain and blood-cerebrospinal fluid barriers. J Appl Physiol 100:1392–1399

Kitazawa T, Hosoya K, Watanabe M, Takashima T, Ohtsuki S, Takanaga H, Ueda M, Yanai N, Obinata M, Terasaki T (2001) Characterization of the amino acid transport of new immortalized choroid plexus epithelial cell lines: a novel in vitro system for investigating transport functions at the blood-cerebrospinal fluid barrier. Pharm Res 18:16–22

Kodaira H, Kusuhara H, Ushiki J, Fuse E, Sugiyama Y (2010) Kinetic analysis of the cooperation of P-glycoprotein (P-gp/Abcb1) and breast cancer resistance protein (Bcrp/Abcg2) in limiting the brain and testis penetration of erlotinib, flavopiridol, and mitoxantrone. J Pharmacol Exp Ther 333:788–796

Koepsell H, Lips K, Volk C (2007) Polyspecific organic cation transporters: structure, function, physiological roles, and biopharmaceutical implications. Pharm Res 24:1227–1251

Kooijmans SA, Senyschyn D, Mezhiselvam MM, Morizzi J, Charman SA, Weksler B, Romero IA, Couraud PO, Nicolazzo JA (2012) The involvement of a Na^+- and Cl^--dependent transporter in the brain uptake of amantadine and rimantadine. Mol Pharm 9:883–893

Kreisl WC, Liow JS, Kimura N, Seneca N, Zoghbi SS, Morse CL, Herscovitch P, Pike VW, Innis RB (2010) P-glycoprotein function at the blood-brain barrier in humans can be quantified with the substrate radiotracer 11C-N-desmethyl-loperamide. J Nucl Med 51:559–566

Kubo Y, Kusagawa Y, Tachikawa M, Akanuma SI, Hosoya KI (2013) Involvement of a novel organic cation transporter in verapamil transport across the inner blood-retinal barrier. Pharm Res 30:847–856

Kusuhara H, Suzuki H, Terasaki T, Kakee A, Lemaire M, Sugiyama Y (1997) P-Glycoprotein mediates the efflux of quinidine across the blood-brain barrier. J Pharmacol Exp Ther 283:574–580

Kusuhara H, He Z, Nagata Y, Nozaki Y, Ito T, Masuda H, Meier PJ, Abe T, Sugiyama Y (2003) Expression and functional involvement of organic anion transporting polypeptide subtype 3 (Slc21a7) in rat choroid plexus. Pharm Res 20:720–727

Lauritzen F, de Lanerolle NC, Lee TS, Spencer DD, Kim JH, Bergersen LH, Eid T (2011) Monocarboxylate transporter 1 is deficient on microvessels in the human epileptogenic hippocampus. Neurobiol Dis 41:577–584

Lee NY, Choi HO, Kang YS (2012) The acetylcholinesterase inhibitors competitively inhibited an acetyl L-carnitine transport through the blood-brain barrier. Neurochem Res 37:1499–1507

Leggas M, Adachi M, Scheffer GL, Sun D, Wielinga P, Du G, Mercer KE, Zhuang Y, Panetta JC, Johnston B, Scheper RJ, Stewart CF, Schuetz JD (2004) Mrp4 confers resistance to topotecan and protects the brain from chemotherapy. Mol Cell Biol 24:7612–7621

Leiderman DB, Balish M, Bromfield EB, Theodore WH (1991) Effect of valproate on human cerebral glucose metabolism. Epilepsia 32:417–422

Leino RL, Gerhart DZ, Drewes LR (1999) Monocarboxylate transporter (MCT1) abundance in brains of suckling and adult rats: a quantitative electron microscopic immunogold study. Brain Res Dev Brain Res 113:47–54

Leino RL, Gerhart DZ, Duelli R, Enerson BE, Drewes LR (2001) Diet-induced ketosis increases monocarboxylate transporter (MCT1) levels in rat brain. Neurochem Int 38:519–527

Levin VA (1980) Relationship of octanol/water partition coefficient and molecular weight to rat brain capillary permeability. J Med Chem 23:682–684

Li JY, Boado RJ, Pardridge WM (2001) Cloned blood-brain barrier adenosine transporter is identical to the rat concentrative Na+ nucleoside cotransporter CNT2. J Cereb Blood Flow Metab 21:929–936

Lippmann ES, Azarin SM, Kay JE, Nessler RA, Wilson HK, Al-Ahmad A, Palecek SP, Shusta EV (2012) Derivation of blood-brain barrier endothelial cells from human pluripotent stem cells. Nat Biotechnol 30:783–791

Miyajima M, Kusuhara H, Fujishima M, Adachi Y, Sugiyama Y (2011) Organic anion transporter 3 mediates the efflux transport of an amphipathic organic anion, dehydroepiandrosterone sulfate, across the blood-brain barrier in mice. Drug Metab Dispos 39:814–819

Mori S, Takanaga H, Ohtsuki S, Deguchi T, Kang YS, Hosoya K, Terasaki T (2003) Rat organic anion transporter 3 (rOAT3) is responsible for brain-to-blood efflux of homovanillic acid at the abluminal membrane of brain capillary endothelial cells. J Cereb Blood Flow Metab 23:432–440

Mori S, Ohtsuki S, Takanaga H, Kikkawa T, Kang YS, Terasaki T (2004) Organic anion transporter 3 is involved in the brain-to-blood efflux transport of thiopurine nucleobase analogs. J Neurochem 90:931–941

Mullauer J, Kuntner C, Bauer M, Bankstahl JP, Muller M, Voskuyl RA, Langer O, Syvanen S (2012) Pharmacokinetic modeling of P-glycoprotein function at the rat and human blood-brain barriers studied with (R)-[11C]verapamil positron emission tomography. EJNMMI Res 2:58

Nagata Y, Kusuhara H, Endou H, Sugiyama Y (2002) Expression and functional characterization of rat organic anion transporter 3 (rOat3) in the choroid plexus. Mol Pharmacol 61:982–988

Nakayama H, Kitaichi K, Ito Y, Hashimoto K, Takagi K, Yokoi T, Ozaki N, Yamamoto T, Hasegawa T (2007) The role of organic cation transporter-3 in methamphetamine disposition and its behavioral response in rats. Brain Res 1184:260–269

Nakazawa Y, Okura T, Shimomura K, Terasaki T, Deguchi Y (2010) Drug-drug interaction between oxycodone and adjuvant analgesics in blood-brain barrier transport and antinociceptive effect. J Pharm Sci 99:467–474

Ni Z, Bikadi Z, Rosenberg MF, Mao Q (2010) Structure and function of the human breast cancer resistance protein (BCRP/ABCG2). Curr Drug Metab 11:603–617

Nies AT, Jedlitschky G, Konig J, Herold-Mende C, Steiner HH, Schmitt HP, Keppler D (2004) Expression and immunolocalization of the multidrug resistance proteins, MRP1-MRP6 (ABCC1-ABCC6), in human brain. Neuroscience 129:349–360

Nishida Y, Ito S, Ohtsuki S, Yamamoto N, Takahashi T, Iwata N, Jishage K, Yamada H, Sasaguri H, Yokota S, Piao W, Tomimitsu H, Saido TC, Yanagisawa K, Terasaki T, Mizusawa H, Yokota T (2009) Depletion of vitamin E increases amyloid beta accumulation by decreasing its clearances from brain and blood in a mouse model of Alzheimer disease. J Biol Chem 284: 33400–33408

O'Kane RL, Martinez-Lopez I, DeJoseph MR, Vina JR, Hawkins RA (1999) Na(+)-dependent glutamate transporters (EAAT1, EAAT2, and EAAT3) of the blood-brain barrier. A mechanism for glutamate removal. J Biol Chem 274:31891–31895

Ocheltree SM, Shen H, Hu Y, Xiang J, Keep RF, Smith DE (2004) Role of PEPT2 in the choroid plexus uptake of glycylsarcosine and 5-aminolevulinic acid: studies in wild-type and null mice. Pharm Res 21:1680–1685

Ohtsuki S, Terasaki T (2007) Contribution of carrier-mediated transport systems to the blood-brain barrier as a supporting and protecting interface for the brain; importance for CNS drug discovery and development. Pharm Res 24:1745–1758

Ohtsuki S, Asaba H, Takanaga H, Deguchi T, Hosoya K, Otagiri M, Terasaki T (2002a) Role of blood-brain barrier organic anion transporter 3 (OAT3) in the efflux of indoxyl sulfate, a uremic toxin: its involvement in neurotransmitter metabolite clearance from the brain. J Neurochem 83:57–66

Ohtsuki S, Tachikawa M, Takanaga H, Shimizu H, Watanabe M, Hosoya K, Terasaki T (2002b) The blood-brain barrier creatine transporter is a major pathway for supplying creatine to the brain. J Cereb Blood Flow Metab 22:1327–1335

Ohtsuki S, Kikkawa T, Mori S, Hori S, Takanaga H, Otagiri M, Terasaki T (2004a) Mouse reduced in osteosclerosis transporter functions as an organic anion transporter 3 and is localized at abluminal membrane of blood-brain barrier. J Pharmacol Exp Ther 309:1273–1281

Ohtsuki S, Takizawa T, Takanaga H, Hori S, Hosoya K, Terasaki T (2004b) Localization of organic anion transporting polypeptide 3 (oatp3) in mouse brain parenchymal and capillary endothelial cells. J Neurochem 90:743–749

Ohtsuki S, Yamaguchi H, Kang YS, Hori S, Terasaki T (2010) Reduction of L-type amino acid transporter 1 mRNA expression in brain capillaries in a mouse model of Parkinson's disease. Biol Pharm Bull 33:1250–1252

Ohtsuki S, Uchida Y, Kubo Y, Terasaki T (2011) Quantitative targeted absolute proteomics-based ADME research as a new path to drug discovery and development: methodology, advantages, strategy, and prospects. J Pharm Sci 100:3547–3559

Ohtsuki S, Ikeda C, Uchida Y, Sakamoto Y, Miller F, Glacial F, Decleves X, Scherrmann JM, Couraud PO, Kubo Y, Tachikawa M, Terasaki T (2013) Quantitative targeted absolute proteomic analysis of transporters, receptors and junction proteins for validation of human cerebral microvascular endothelial cell line hCMEC/D3 as a human blood-brain barrier model. Mol Pharm 10:289–296

Okuda T, Haga T, Kanai Y, Endou H, Ishihara T, Katsura I (2000) Identification and characterization of the high-affinity choline transporter. Nat Neurosci 3:120–125

Okura T, Ito R, Ishiguro N, Tamai I, Deguchi Y (2007) Blood-brain barrier transport of pramipexole, a dopamine D2 agonist. Life Sci 80:1564–1571

Okura T, Hattori A, Takano Y, Sato T, Hammarlund-Udenaes M, Terasaki T, Deguchi Y (2008) Involvement of the pyrilamine transporter, a putative organic cation transporter, in blood-brain barrier transport of oxycodone. Drug Metab Dispos 36:2005–2013

Okura T, Kato S, Takano Y, Sato T, Yamashita A, Morimoto R, Ohtsuki S, Terasaki T, Deguchi Y (2011) Functional characterization of rat plasma membrane monoamine transporter in the blood-brain and blood-cerebrospinal fluid barriers. J Pharm Sci 100:3924–3938

Omerovic E, Bollano E, Lorentzon M, Walser M, Mattsson-Hulten L, Isgaard J (2003) Growth hormone induces myocardial expression of creatine transporter and decreases plasma levels of IL-1beta in rats during early postinfarct cardiac remodeling. Growth Horm IGF Res 13: 239–245

Omote H, Hiasa M, Matsumoto T, Otsuka M, Moriyama Y (2006) The MATE proteins as fundamental transporters of metabolic and xenobiotic organic cations. Trends Pharmacol Sci 27:587–593

Ose A, Kusuhara H, Yamatsugu K, Kanai M, Shibasaki M, Fujita T, Yamamoto A, Sugiyama Y (2008) P-glycoprotein restricts the penetration of oseltamivir across the blood-brain barrier. Drug Metab Dispos 36:427–434

Ose A, Ito M, Kusuhara H, Yamatsugu K, Kanai M, Shibasaki M, Hosokawa M, Schuetz JD, Sugiyama Y (2009) Limited brain distribution of [3R,4R,5S]-4-acetamido-5-amino-3-(1-ethylpropoxy)-1-cyclohexene-1-carboxylate phosphate (Ro 64-0802), a pharmacologically active form of oseltamivir, by active efflux across the blood-brain barrier mediated by organic anion transporter 3 (Oat3/Slc22a8) and multidrug resistance-associated protein 4 (Mrp4/Abcc4). Drug Metab Dispos 37:315–321

Pan W, Kastin AJ, Zankel TC, van Kerkhof P, Terasaki T, Bu G (2004) Efficient transfer of receptor-associated protein (RAP) across the blood-brain barrier. J Cell Sci 117:5071–5078

Pardridge WM (1988) Recent advances in blood-brain barrier transport. Annu Rev Pharmacol Toxicol 28:25–39

Pardridge WM (2001) Brain drug targeting: the future of brain drug development. Cambridge University Press, United Kingdom

Pardridge WM (2012) Drug transport across the blood-brain barrier. J Cereb Blood Flow Metab 32:1959–1972

Pavan B, Dalpiaz A (2011) Prodrugs and endogenous transporters: are they suitable tools for drug targeting into the central nervous system? Curr Pharm Des 17:3560–3576

Peckham EM, Traynor JR (2006) Comparison of the antinociceptive response to morphine and morphine-like compounds in male and female Sprague-Dawley rats. J Pharmacol Exp Ther 316:1195–1201

Peura L, Malmioja K, Laine K, Leppanen J, Gynther M, Isotalo A, Rautio J (2011) Large amino acid transporter 1 (LAT1) prodrugs of valproic acid: new prodrug design ideas for central nervous system delivery. Mol Pharm 8:1857–1866

Phillis JW, Horrocks LA, Farooqui AA (2006) Cyclooxygenases, lipoxygenases, and epoxygenases in CNS: their role and involvement in neurological disorders. Brain Res Rev 52:201–243

Pincus JH, Barry K (1988) Protein redistribution diet restores motor function in patients with DOPA-resistant “off” periods. Neurology 38:481–483

Polli JW, Olson KL, Chism JP, John-Williams LS, Yeager RL, Woodard SM, Otto V, Castellino S, Demby VE (2009) An unexpected synergist role of P-glycoprotein and breast cancer resistance protein on the central nervous system penetration of the tyrosine kinase inhibitor lapatinib (N-{3-chloro-4-[(3-fluorobenzyl)oxy]phenyl}-6-[5-({[2-(methylsulfonyl)ethyl]amino}methyl)-2-furyl]-4-quinazolinamine; GW572016). Drug Metab Dispos 37:439–442

Polt R, Porreca F, Szabo LZ, Bilsky EJ, Davis P, Abbruscato TJ, Davis TP, Harvath R, Yamamura HI, Hruby VJ (1994) Glycopeptide enkephalin analogues produce analgesia in mice: evidence for penetration of the blood-brain barrier. Proc Natl Acad Sci U S A 91:7114–7118

Prasad PD, Wang H, Huang W, Kekuda R, Rajan DP, Leibach FH, Ganapathy V (1999) Human LAT1, a subunit of system L amino acid transporter: molecular cloning and transport function. Biochem Biophys Res Commun 255:283–288

Rautio J, Kumpulainen H, Heimbach T, Oliyai R, Oh D, Jarvinen T, Savolainen J (2008) Prodrugs: design and clinical applications. Nat Rev Drug Discov 7:255–270

Sadiq MW, Borgs A, Okura T, Shimomura K, Kato S, Deguchi Y, Jansson B, Björkman S, Terasaki T, Hammarlund-Udenaes M (2011) Diphenhydramine active uptake at the blood-brain barrier and its interaction with oxycodone in vitro and in vivo. J Pharm Sci 100:3912–3923

Schinkel AH, Smit JJ, van Tellingen O, Beijnen JH, Wagenaar E, van Deemter L, Mol CA, van der Valk MA, Robanus-Maandag EC, te Riele HP et al (1994) Disruption of the mouse mdr1a P-glycoprotein gene leads to a deficiency in the blood-brain barrier and to increased sensitivity to drugs. Cell 77:491–502

Schliamser SE, Cars O, Norrby SR (1991) Neurotoxicity of beta-lactam antibiotics: predisposing factors and pathogenesis. J Antimicrob Chemother 27:405–425

Schuetz JD, Connelly MC, Sun D, Paibir SG, Flynn PM, Srinivas RV, Kumar A, Fridland A (1999) MRP4: A previously unidentified factor in resistance to nucleoside-based antiviral drugs. Nat Med 5:1048–1051

Shen H, Smith DE, Keep RF, Xiang J, Brosius FC 3rd (2003) Targeted disruption of the PEPT2 gene markedly reduces dipeptide uptake in choroid plexus. J Biol Chem 278:4786–4791

Shen H, Smith DE, Keep RF, Brosius FC 3rd (2004) Immunolocalization of the proton-coupled oligopeptide transporter PEPT2 in developing rat brain. Mol Pharm 1:248–256

Shen J, Carcaboso AM, Hubbard KE, Tagen M, Wynn HG, Panetta JC, Waters CM, Elmeliegy MA, Stewart CF (2009) Compartment-specific roles of ATP-binding cassette transporters define differential topotecan distribution in brain parenchyma and cerebrospinal fluid. Cancer Res 69:5885–5892

Shibata M, Yamada S, Kumar SR, Calero M, Bading J, Frangione B, Holtzman DM, Miller CA, Strickland DK, Ghiso J, Zlokovic BV (2000) Clearance of Alzheimer's amyloid-ss(1-40) peptide from brain by LDL receptor-related protein-1 at the blood-brain barrier. J Clin Invest 106:1489–1499

Shiiki T, Ohtsuki S, Kurihara A, Naganuma H, Nishimura K, Tachikawa M, Hosoya K, Terasaki T (2004) Brain insulin impairs amyloid-beta(1-40) clearance from the brain. J Neurosci 24:9632–9637

Shimomura K, Okura T, Kato S, Couraud PO, Schermann JM, Terasaki T, Deguchi Y (2013) Functional expression of a proton-coupled organic cation (H+/OC) antiporter in human brain capillary endothelial cell line hCMEC/D3, a human blood–brain barrier model. Fluids Barriers CNS 10:8

Shojaiefard M, Christie DL, Lang F (2005) Stimulation of the creatine transporter SLC6A8 by the protein kinases SGK1 and SGK3. Biochem Biophys Res Commun 334:742–746

Shojaiefard M, Christie DL, Lang F (2006) Stimulation of the creatine transporter SLC6A8 by the protein kinase mTOR. Biochem Biophys Res Commun 341:945–949

Silvasti M, Rosenberg P, Seppala T, Svartling N, Pitkanen M (1998) Comparison of analgesic efficacy of oxycodone and morphine in postoperative intravenous patient-controlled analgesia. Acta Anaesthesiol Scand 42:576–580

Smith QR, Takasato Y, Rapoport SI (1984) Kinetic analysis of L-leucine transport across the blood-brain barrier. Brain Res 311:167–170

Smith QR, Momma S, Aoyagi M, Rapoport SI (1987) Kinetics of neutral amino acid transport across the blood-brain barrier. J Neurochem 49:1651–1658

Smith DE, Hu Y, Shen H, Nagaraja TN, Fenstermacher JD, Keep RF (2011) Distribution of glycylsarcosine and cefadroxil among cerebrospinal fluid, choroid plexus, and brain parenchyma after intracerebroventricular injection is markedly different between wild-type and Pept2 null mice. J Cereb Blood Flow Metab 31:250–261

Somogyvari-Vigh A, Kastin AJ, Liao J, Zadina JE, Pan W (2004) Endomorphins exit the brain by a saturable efflux system at the basolateral surface of cerebral endothelial cells. Exp Brain Res 156:224–230

Spector R, Johanson CE (2010) Vectorial ligand transport through mammalian choroid plexus. Pharm Res 27:2054–2062

Stoll J, Wadhwani KC, Smith QR (1993) Identification of the cationic amino acid transporter (System y+) of the rat blood-brain barrier. J Neurochem 60:1956–1959

Sugiyama D, Kusuhara H, Taniguchi H, Ishikawa S, Nozaki Y, Aburatani H, Sugiyama Y (2003) Functional characterization of rat brain-specific organic anion transporter (Oatp14) at the blood-brain barrier: high affinity transporter for thyroxine. J Biol Chem 278:43489–43495

Sun L, Zeng X, Yan C, Sun X, Gong X, Rao Y, Yan N (2012) Crystal structure of a bacterial homologue of glucose transporters GLUT1-4. Nature 490:361–366

Sunden Y, Park CH, Matsuda K, Anagawa A, Kimura T, Ochiai K, Kida H, Umemura T (2003) The effects of antipyretics on influenza virus encephalitis in mice and chicks. J Vet Med Sci 65:1185–1188

Suzuki T, Moriki Y, Goto H, Tomono K, Hanano M, Watanabe J (2002a) Investigation on the influx transport mechanism of pentazocine at the blood-brain barrier in rats using the carotid injection technique. Biol Pharm Bull 25:1351–1355

Suzuki T, Oshimi M, Tomono K, Hanano M, Watanabe J (2002b) Investigation of transport mechanism of pentazocine across the blood-brain barrier using the in situ rat brain perfusion technique. J Pharm Sci 91:2346–2353

Suzuki M, Suzuki H, Sugimoto Y, Sugiyama Y (2003) ABCG2 transports sulfated conjugates of steroids and xenobiotics. J Biol Chem 278:22644–22649

Suzuki T, Miyata M, Zaima C, Furuishi T, Fukami T, Kugawa F, Tomono K (2010a) Blood-brain barrier transport of naloxone does not involve P-glycoprotein-mediated efflux. J Pharm Sci 99:413–421

Suzuki T, Ohmuro A, Miyata M, Furuishi T, Hidaka S, Kugawa F, Fukami T, Tomono K (2010b) Involvement of an influx transporter in the blood-brain barrier transport of naloxone. Biopharm Drug Dispos 31:243–252

Sweet DH, Miller DS, Pritchard JB (2001) Ventricular choline transport: a role for organic cation transporter 2 expressed in choroid plexus. J Biol Chem 276:41611–41619

Sweet DH, Miller DS, Pritchard JB, Fujiwara Y, Beier DR, Nigam SK (2002) Impaired organic anion transport in kidney and choroid plexus of organic anion transporter 3 (Oat3 (Slc22a8)) knockout mice. J Biol Chem 277:26934–26943

Sykes D, Sweet DH, Lowes S, Nigam SK, Pritchard JB, Miller DS (2004) Organic anion transport in choroid plexus from wild-type and organic anion transporter 3 (Slc22a8)-null mice. Am J Physiol Renal Physiol 286:F972–F978

Tachikawa M, Hosoya K (2011) Transport characteristics of guanidino compounds at the blood-brain barrier and blood-cerebrospinal fluid barrier: relevance to neural disorders. Fluids Barriers CNS 8:13

Tachikawa M, Fukaya M, Terasaki T, Ohtsuki S, Watanabe M (2004) Distinct cellular expressions of creatine synthetic enzyme GAMT and creatine kinases uCK-Mi and CK-B suggest a novel neuron-glial relationship for brain energy homeostasis. Eur J Neurosci 20:144–160

Tachikawa M, Watanabe M, Hori S, Fukaya M, Ohtsuki S, Asashima T, Terasaki T (2005) Distinct spatio-temporal expression of ABCA and ABCG transporters in the developing and adult mouse brain. J Neurochem 95:294–304

Tachikawa M, Fujinawa J, Takahashi M, Kasai Y, Fukaya M, Sakai K, Yamazaki M, Tomi M, Watanabe M, Sakimura K, Terasaki T, Hosoya K (2008a) Expression and possible role of creatine transporter in the brain and at the blood-cerebrospinal fluid barrier as a transporting protein of guanidinoacetate, an endogenous convulsant. J Neurochem 107:768–778

Tachikawa M, Kasai Y, Takahashi M, Fujinawa J, Kitaichi K, Terasaki T, Hosoya K (2008b) The blood-cerebrospinal fluid barrier is a major pathway of cerebral creatinine clearance: involvement of transporter-mediated process. J Neurochem 107:432–442

Tachikawa M, Kasai Y, Yokoyama R, Fujinawa J, Ganapathy V, Terasaki T, Hosoya K (2009) The blood-brain barrier transport and cerebral distribution of guanidinoacetate in rats: involvement of creatine and taurine transporters. J Neurochem 111:499–509

Tachikawa M, Ozeki G, Higuchi T, Akanuma S, Tsuji K, Hosoya K (2012a) Role of the blood-cerebrospinal fluid barrier transporter as a cerebral clearance system for prostaglandin E(2) produced in the brain. J Neurochem 123:750–760

Tachikawa M, Tsuji K, Yokoyama R, Higuchi T, Ozeki G, Yashiki A, Akanuma S, Hayashi K, Nishiura A, Hosoya K (2012b) A clearance system for prostaglandin D2, a sleep-promoting factor, in cerebrospinal fluid: role of the blood-cerebrospinal barrier transporters. J Pharmacol Exp Ther 343:608–616

Takanaga H, Ohtsuki S, Hosoya K, Terasaki T (2001) GAT2/BGT-1 as a system responsible for the transport of gamma-aminobutyric acid at the mouse blood-brain barrier. J Cereb Blood Flow Metab 21:1232–1239

Takanaga H, Tokuda N, Ohtsuki S, Hosoya K, Terasaki T (2002) ATA2 is predominantly expressed as system A at the blood-brain barrier and acts as brain-to-blood efflux transport for L-proline. Mol Pharmacol 61:1289–1296

Takasawa K, Terasaki T, Suzuki H, Ooie T, Sugiyama Y (1997) Distributed model analysis of 3′-azido-3′-deoxythymidine and 2′,3′-dideoxyinosine distribution in brain tissue and cerebrospinal fluid. J Pharmacol Exp Ther 282:1509–1517

Tega Y, Akanuma SI, Kubo Y, Terasaki T, Hosoya KI (2012) Blood-to-brain influx transport of nicotine at the rat blood-brain barrier: Involvement of a pyrilamine-sensitive organic cation transport process. Neurochem Int 62:173–181

Terada T, Inui K (2008) Physiological and pharmacokinetic roles of H+/organic cation antiporters (MATE/SLC47A). Biochem Pharmacol 75:1689–1696

Terasaki T, Hosoya K (1999) The blood-brain barrier efflux transporters as a detoxifying system for the brain. Adv Drug Deliv Rev 36:195–209

Terasaki T, Pardridge WM (1988) Restricted transport of 3′-azido-3′-deoxythymidine and dideoxynucleosides through the blood-brain barrier. J Infect Dis 158:630–632

Terasaki T, Tsuji A (1994) Drug delivery to the brain utilizing blood-brain barrier transport systems. J Control Release 29:163–169

Terasaki T, Ohtsuki S, Hori S, Takanaga H, Nakashima E, Hosoya K (2003) New approaches to in vitro models of blood-brain barrier drug transport. Drug Discov Today 8:944–954

Tetsuka K, Takanaga H, Ohtsuki S, Hosoya K, Terasaki T (2003) The l-isomer-selective transport of aspartic acid is mediated by ASCT2 at the blood-brain barrier. J Neurochem 87:891–901

Teuscher NS, Shen H, Shu C, Xiang J, Keep RF, Smith DE (2004) Carnosine uptake in rat choroid plexus primary cell cultures and choroid plexus whole tissue from PEPT2 null mice. J Neurochem 89:375–382

Torremans A, Marescau B, Possemiers I, Van Dam D, D'Hooge R, Isbrandt D, De Deyn PP (2005) Biochemical and behavioural phenotyping of a mouse model for GAMT deficiency. J Neurol Sci 231:49–55

Traiffort E, Ruat M, O'Regan S, Meunier FM (2005) Molecular characterization of the family of choline transporter-like proteins and their splice variants. J Neurochem 92:1116–1125

Tsuji A, Terasaki T, Takabatake Y, Tenda Y, Tamai I, Yamashima T, Moritani S, Tsuruo T, Yamashita J (1992) P-glycoprotein as the drug efflux pump in primary cultured bovine brain capillary endothelial cells. Life Sci 51:1427–1437

Uchida Y, Ohtsuki S, Kamiie J, Terasaki T (2011a) Blood-brain barrier (BBB) pharmacoproteomics: reconstruction of in vivo brain distribution of 11 P-glycoprotein substrates based on the BBB transporter protein concentration, in vitro intrinsic transport activity, and unbound fraction in plasma and brain in mice. J Pharmacol Exp Ther 339:579–588

Uchida Y, Ohtsuki S, Katsukura Y, Ikeda C, Suzuki T, Kamiie J, Terasaki T (2011b) Quantitative targeted absolute proteomics of human blood-brain barrier transporters and receptors. J Neurochem 117:333–345

Uchino H, Kanai Y, Kim DK, Wempe MF, Chairoungdua A, Morimoto E, Anders MW, Endou H (2002) Transport of amino acid-related compounds mediated by L-type amino acid transporter 1 (LAT1): insights into the mechanisms of substrate recognition. Mol Pharmacol 61:729–737

Urquhart BL, Kim RB (2009) Blood-brain barrier transporters and response to CNS-active drugs. Eur J Clin Pharmacol 65:1063–1070

Wang X, Cabrera RM, Li Y, Miller DS, Finnell RH (2013) Functional regulation of P-glycoprotein at the blood-brain barrier in proton-coupled folate transporter (PCFT) mutant mice. FASEB J 27:1167–1175

Weksler BB, Subileau EA, Perriere N, Charneau P, Holloway K, Leveque M, Tricoire-Leignel H, Nicotra A, Bourdoulous S, Turowski P, Male DK, Roux F, Greenwood J, Romero IA, Couraud PO (2005) Blood-brain barrier-specific properties of a human adult brain endothelial cell line. FASEB J 19:1872–1874

Wijnholds J, deLange EC, Scheffer GL, van den Berg DJ, Mol CA, van der Valk M, Schinkel AH, Scheper RJ, Breimer DD, Borst P (2000) Multidrug resistance protein 1 protects the choroid plexus epithelium and contributes to the blood-cerebrospinal fluid barrier. J Clin Invest 105: 279–285

Wong HY, Chu TS, Lai JC, Fung KP, Fok TF, Fujii T, Ho YY (2005) Sodium valproate inhibits glucose transport and exacerbates Glut1-deficiency in vitro. J Cell Biochem 96:775–785

Xia L, Engel K, Zhou M, Wang J (2007) Membrane localization and pH-dependent transport of a newly cloned organic cation transporter (PMAT) in kidney cells. Am J Physiol Renal Physiol 292:F682–F690

Xiong H, Callaghan D, Jones A, Bai J, Rasquinha I, Smith C, Pei K, Walker D, Lue LF, Stanimirovic D, Zhang W (2009) ABCG2 is upregulated in Alzheimer's brain with cerebral amyloid angiopathy and may act as a gatekeeper at the blood-brain barrier for Abeta(1-40) peptides. J Neurosci 29:5463–5475

Yamazaki M, Fukuoka H, Nagata O, Kato H, Ito Y, Terasaki T, Tsuji A (1994a) Transport mechanism of an H1-antagonist at the blood-brain barrier: transport mechanism of mepyramine using the carotid injection technique. Biol Pharm Bull 17:676–679

Yamazaki M, Terasaki T, Yoshioka K, Nagata O, Kato H, Ito Y, Tsuji A (1994b) Carrier-mediated transport of H1-antagonist at the blood-brain barrier: a common transport system of H1-antagonists and lipophilic basic drugs. Pharm Res 11:1516–1518

Yanagida O, Kanai Y, Chairoungdua A, Kim DK, Segawa H, Nii T, Cha SH, Matsuo H, Fukushima J, Fukasawa Y, Tani Y, Taketani Y, Uchino H, Kim JY, Inatomi J, Okayasu I, Miyamoto K, Takeda E, Goya T, Endou H (2001) Human L-type amino acid transporter 1 (LAT1): characterization of function and expression in tumor cell lines. Biochim Biophys Acta 1514:291–302

Yanai K, Tashiro M (2007) The physiological and pathophysiological roles of neuronal histamine: an insight from human positron emission tomography studies. Pharmacol Ther 113:1–15

Ylikangas H, Peura L, Malmioja K, Leppanen J, Laine K, Poso A, Lahtela-Kakkonen M, Rautio J (2012) Structure-activity relationship study of compounds binding to large amino acid transporter 1 (LAT1) based on pharmacophore modeling and in situ rat brain perfusion. Eur J Pharm Sci 48:523–531

Zufferey R, Santiago TC, Brachet V, Ben Mamoun C (2004) Reexamining the role of choline transporter-like (Ctlp) proteins in choline transport. Neurochem Res 29:461–467

Chapter 3
Blood–Brain Barrier (BBB) Pharmacoproteomics: A New Research Field Opened Up by Quantitative Targeted Absolute Proteomics (QTAP)

Yasuo Uchida, Masanori Tachikawa, Sumio Ohtsuki, and Tetsuya Terasaki

Abstract The activities of individual functional proteins, such as transporters, receptors, enzymes, and channels, show large variations, including interspecies differences, in vitro/in vivo differences, age-related differences, and normal/disease differences, and these need to be understood in order to guide rational drug discovery and development. To address this issue, we have developed an absolute quantification method of protein expression, called quantitative targeted absolute proteomics (QTAP), by means of liquid chromatography–tandem mass spectrometry (LC-MS/MS) with multiplexed selected/multiple reaction monitoring (SRM/MRM). QTAP has high sensitivity and selectivity, allowing quantification of protein expression over a wide dynamic range (0.1–1,000 fmol/μg protein). Further, its ability to quantify multiple proteins simultaneously enables us to determine the quantitative expression profile of multiple proteins in tissues and cells. In this chapter, we introduce the technical features of QTAP, discuss its advantages and limitations compared with global proteomics, mRNA quantification, and antibody-based protein quantification, and introduce its applications in blood–brain barrier (BBB) research. Species differences (human/monkey/mouse), interindividual differences, and age-related differences in the activities of transporters at the BBB are discussed based on their protein levels, with reference to recently reported data. QTAP also allows us to reconstruct/predict in vivo activities of transporters at the BBB, as well as drug distribution in the brain, from the results of in vitro experiments with the aid of pharmacokinetic modeling. QTAP methodology is expected to open up a new research field, BBB pharmacoproteomics.

Y. Uchida • M. Tachikawa • T. Terasaki, Ph.D. (✉)
Division of Membrane Transport and Drug Targeting, Graduate School of Pharmaceutical Sciences, Tohoku University, Aoba-ku, Sendai, Japan
e-mail: terasaki.tetsuya@m.tohoku.ac.jp

S. Ohtsuki
Department of Pharmaceutical Microbiology, Faculty of Life Sciences, Kumamoto University, Kumamoto, Japan

M. Hammarlund-Udenaes et al. (eds.), *Drug Delivery to the Brain*, AAPS Advances in the Pharmaceutical Sciences Series 10, DOI 10.1007/978-1-4614-9105-7_3,

Abbreviations

BBB	Blood–brain barrier
CNS	Central nervous system
HR-SRM/MRM	High-resolution selected/multiple reaction monitoring
$K_{p,brain}$	Brain-to-plasma concentration ratio
$K_{p,uu,brain}$	Unbound brain-to-plasma concentration ratio
LC-MS/MS	Liquid chromatography–tandem mass spectrometry
MDR1	Multidrug-resistance protein 1
mdr1a	Multidrug-resistance protein 1a
PET	Positron emission tomography
P-gp	P-Glycoprotein
PPx	Pharmacoproteomics
QTAP	Quantitative targeted absolute proteomics
SPECT	Single photon emission computed tomography
SRM/MRM	Selected/multiple reaction monitoring
Triple Q MS	Triple quadrupole mass spectrometer
ULQ	Under the limit of quantification

3.1 Introduction

Among drug candidates that progress to clinical trials, the proportion of compounds finally approved as new drugs is very small. Kola and Landis (2004) found that the proportion was only 5 % for anticancer drugs and 8 % for central nervous system (CNS) drugs during 1991–2000, and the success rate was not higher during 2000–2008 (Yagi and Ohkubo 2010). The major reasons for the high rate of discontinuation of clinical development have been reported to be insufficient efficacy and excessive toxicity in humans (Frank and Hargreaves 2003). Furthermore, more than 98 % of candidate CNS drugs do not cross the blood–brain barrier (BBB) and so cannot provide a pharmacologically effective concentration in the brain (Pardridge 2002). Thus, unfavorable distribution into target tissues in humans can also be a factor in discontinuation of drug development. It is clear from these considerations that the efficacy, toxicity, and distribution of drug candidates in humans are often different from those predicted on the basis of in vitro and animal experiments in preclinical studies. The efficacy, toxicity, and distribution of drugs are regulated by the activities of many individual functional molecules that interact with the drug, including receptors, channels, transporters, and enzymes. Therefore, it is essential to clarify quantitatively the differences in the patterns of activity of functional molecules between in vitro and in vivo, or between experimental animals and humans, in order to increase the success rate in clinical trials. Furthermore, quantitative evaluation of functional changes of individual molecules in various diseases is also

useful for developing more effective drugs, so this is one of the important issues in drug discovery and development.

Imaging technologies such as positron emission tomography (PET) and single photon emission computed tomography (SPECT) have been introduced to evaluate in vivo activities of functional molecules in humans, and to examine interspecies, in vitro/in vivo, and regional differences in the activities of functional molecules. However, the number of available tracers is restricted due to difficulties in the synthesis, use, and disposal of suitable radiolabeled compounds. Specificities for substrates, inhibitors, ligands, agonists, antagonists, etc., are often similar among distinct functional molecules, and it is hard to rule out the possibility that tracers interact with other functionally unknown molecules. Therefore accurate evaluation of the activities of target molecules with these methods remains problematic.

Protein expression levels have been shown to correlate well with activity for a variety of functional proteins, including P-glycoprotein (P-gp/MDR1), Na⁺/glucose cotransporter 1, cytochrome P450 2D6 (CYP2D6), and β-secretase (Dyer et al. 1997; Hoffmeyer et al. 2000; Fukumoto et al. 2002; Shirasaka et al. 2008; Langenfeld et al. 2009; Tachibana et al. 2010). Thus, we considered that in vitro/in vivo and interspecies differences in functional activities might be effectively evaluated in terms of protein expression levels, and so we developed novel methodology for protein quantification based on liquid chromatography-linked tandem mass spectrometry (LC-MS/MS) with selected/multiple reaction monitoring (SRM/MRM) (Kamiie et al. 2008). Because our aim was to determine the absolute protein expression levels of preselected target molecules, we called the new method "quantitative targeted absolute proteomics (QTAP)." In this method, the protein expression of a target molecule is selectively quantified by using a specific peptide probe. We have established in-silico selection criteria that make it possible to select appropriate peptide probes for any target molecule whose amino acid sequence is known, and therefore QTAP is a comprehensive methodology for protein quantification. Given that protein expression is generally well correlated to activity, as mentioned above, we anticipated that it would be possible to predict the in vivo activities of target molecules in humans by integrating the activities measured in in vitro or animal experiments with in vitro/in vivo or interspecies differences in protein expression levels determined by QTAP. Therefore, QTAP is expected to overcome the major limitations of in vivo functional analysis using imaging technologies and to open up the new research field of pharmacoproteomics (PPx).

In this chapter, we introduce the technical features of QTAP as a protein quantification methodology, as well as recent advances, and we summarize its advantages and limitations compared with global proteomics, classical protein quantification with antibodies and mRNA quantification. Furthermore, we introduce some applications of QTAP to illustrate its value in understanding interspecies, interindividual, age-related, and in vitro/in vivo differences in the activities of transporters at the BBB.

3.2 Principles and Methodology of Quantitative Targeted Absolute Proteomics

3.2.1 Protein Quantification by Multiplexed Selected/Multiple Reaction Monitoring (SRM/MRM) Using LC-MS/MS

LC-MS/MS has been widely used for quantification of nonlabeled small-molecular compounds. Recent advances in LC-MS/MS technology allow us to simultaneously quantify multiple compounds with a sensitivity comparable to that of radio-isotope methods, so that LC-MS/MS has become a powerful tool for many purposes, including functional analysis of transporters, enzymes, and receptors. Indeed, we have developed a comprehensive substrate/nonsubstrate screening method for ABC transporters by means of LC-MS/MS, named the LC-MS/MS Cocktail Method, and have used it to identify 18 MRP4 substrates from a mixture of 50 compounds (Uchida et al. 2007).

Therefore, we considered in principle that a similar quantification strategy would be available for proteins. However, proteins are too large to separate by reverse-phase HPLC and their mass lies above the range of the mass filter in MS for quantification (mass-to-charge ratio $(m/z) < 1{,}250$ in API5000 and QTRAP5500). Therefore, proteins must first be digested with a protease, such as trypsin, and then peptide(s) specific for the target protein can be quantified by LC-MS/MS. Trypsin digestion is an important process especially for quantification of membrane proteins, which generally exhibit low solubility and high aggregability due to the presence of hydrophobic regions. From various regions of target protein, trypsin digestion produces some specific peptides for the target protein, and appropriate peptide(s) can be selected for LC-MS/MS-based quantification.

To achieve highly selective quantification, the chosen peptide is quantified by selected/multiple reaction monitoring (SRM/MRM) using triple quadrupole (Triple Q) MS (Fig. 3.1). Triple Q MS employs three chambers, of which the 1st Q (Q1) and 3rd Q (Q3) are mass filters that pass the peptide ion having the target mass. In the 2nd Q (Q2), the peptide ion is fragmented by collision with N_2 gas. The use of two mass filters provides high selectivity and a high S/N ratio. The combination of Q1 and Q3 mass filters is called the transition, which can be changed every 10 ms, and up to 300 different peptide ions can be simultaneously quantified in a single analysis.

An internal standard is important for accurate quantification (Fig. 3.2). A stable isotope-labeled peptide having the same amino acid sequence as the target peptide is used as the internal standard and can be distinguished from the target peptide by MS due to the difference in mass. The labeled internal standard peptide is eluted at the same retention time as the target peptide, thereby making it possible to recognize the peak of the target peptide based on the retention time of the corresponding internal standard peptide. Furthermore, internal standard peptide is also essential to correct for changes of sensitivity between analyses, e.g., between a real protein

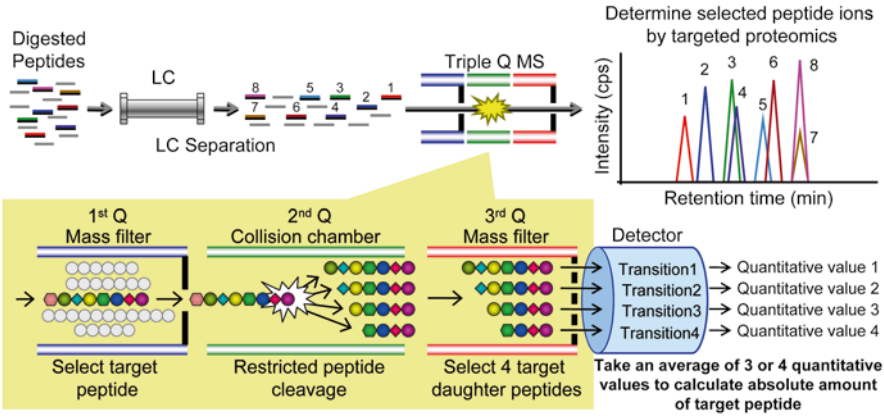

Fig. 3.1 Simultaneous quantification of several target peptides and simultaneous monitoring of four daughter peptides for each target peptide by multiplexed SRM/MRM analysis using a triple quadrupole tandem mass spectrometer (Triple Q MS)

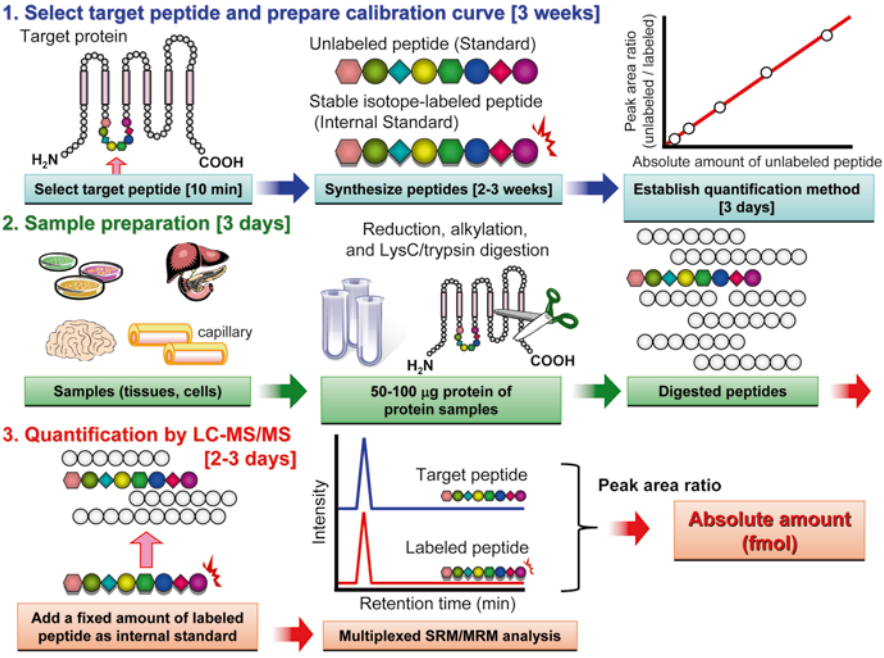

Fig. 3.2 Experimental procedure for quantitative targeted absolute proteomics. Taken from Ohtsuki et al. (2011) and modified

sample and a standard sample for preparing the calibration curve. As regards sensitivity, the target peptide and internal standard peptide have the same amino acid sequence. Therefore, any change of sensitivity can be corrected by taking the peak area ratio of target peptide to internal standard peptide. Because real samples such as tissues and cells suffer significant ion suppression compared to standard samples not including matrix, the correction of sensitivity by using an internal standard peptide is very important to accurately quantify the absolute amount of the target peptide.

Each target peptide is quantified by measuring four different SRM/MRM transitions which consist of a parent ion (Q1) and four different daughter ions (Q3) (Fig. 3.1; Kamiie et al. 2008). This allows us to increase the selectivity for the target peptide by monitoring the chromatographic coelution of eight transitions of the target and internal standard peptides, thereby ensuring reliable identification of signal peaks. Furthermore, this SRM/MRM analysis also increases the accuracy of quantification. By comparing the 4 quantitative values, it can be understood whether noise peaks overlap with the target peptide peak, and when necessary, SRM/MRM transitions can be changed to appropriate ones not affected by noise peaks.

Eight SRM/MRM transitions (4 transitions for the target peptide and 4 corresponding transitions for the internal standard peptide) are required for quantification of one protein. Therefore, 37 different proteins can be simultaneously quantified in a single analysis by using the currently available maximum of 300 SRM/MRM transitions (multiplexed SRM/MRM analysis).

3.2.2 In Silico Selection of Target Peptide Based on Amino Acid Sequence of Target Protein

The selection of the target peptide is a key issue to achieve highly sensitive and reliable protein quantification by SRM/MRM analysis. In most cases, global proteomics has been performed by using peptides obtained by trypsin digestion of biological samples that highly express the target protein, and peptides giving a high signal intensity have been chosen for quantification (Li et al. 2008; Wang et al. 2008). However, this strategy is time-consuming and it is necessary to prepare samples that highly express the target protein, so it is difficult to establish a quantification method for many molecules. Furthermore, trypsin digestion efficiency, peptide specificity, posttranslational modification (PTM), and polymorphism should be considered for accurate quantification, but the small number of peptides identified by global proteomics does not necessarily allow this.

To solve these problems, we have established a method to predict appropriate peptides for quantification based on the previous proteomic data and experience (Table 3.1). This allows us to design target peptides in silico from sequence information registered in protein databases, such as UniProtKB. Figure 3.3 shows the distribution of sensitivity and accuracy for all peptides of trypsin-digested human serum albumin (HSA); the sensitivity and accuracy vary by 1,000-fold and 30-fold,

Table 3.1 In silico peptide selection criteria

Necessary conditions

1. Amino acid sequence of peptide exists *only* in target protein (based on NCBI protein BLAST database)
2. Peptide is theoretically obtained by protease (such as trypsin) digestion of target protein, that is, arginine or lysine residue just before and at C-terminal of peptide if trypsin is used
3. Length between 6 and 16 amino acids (8–10 amino acids is better) for detection by Triple Q MS
4. *Not* including methionine or cysteine residues
5. *No* posttranslational modification and NO single nucleotide polymorphism for quantification of total amount of target protein
6. *No* continuous sequences of arginine or lysine residues (RR, KK, RK, KR) in the digestion region, to ensure efficient digestion by trypsin
7. *Not* including a sequence with a proline residue at the C-terminal side of arginine or lysine residue (RP or KP) in the digestion region, to ensure efficient digestion by trypsin
8. *Not* including a transmembrane region, to ensure efficient digestion by protease (such as trypsin)

Sufficient conditions

9. *Not* including a histidine residue, which would reduce peptide sensitivity of the mass spectrometer
10. Including glycine or proline residue, which increases peptide sensitivity of the mass spectrometer
11. Prediction of LC retention time based on hydrophobicity of amino acids
12. Select water-soluble peptide based on hydrophobicity of amino acids. Hydrophobic amino acids should preferably be less than 40 % of total residues in peptide

Taken from Kamiie et al. (2008) and modified

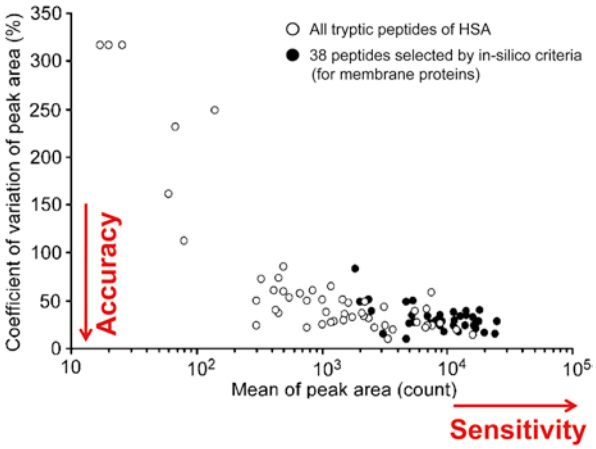

Fig. 3.3 Comparison of means and coefficients of variation of peak areas in 8 analyses between 38 peptides (10 fmol each) chosen by using in-silico criteria and all tryptic peptides of HSA. 36 membrane proteins were selected as models to evaluate whether the in-silico approach is workable to select probe peptides for highly sensitive and highly accurate quantitative analysis of target proteins. 38 probe peptides for the 36 membrane proteins were chosen by using in-silico criteria, and compared with all tryptic peptides of human serum albumin (HSA). Taken from Kamiie et al. (2008) and modified

respectively, among the peptides (Kamiie et al. 2008). In contrast, all 38 probe peptides of 36 membrane proteins chosen by using our in silico selection criteria were highly sensitive and highly accurate. Especially, 28 of the peptides (74 %) were detected at above 500 counts/fmol and their coefficients of variation were less than 40 %. We have also succeeded in developing software to automatically select appropriate peptides for target proteins within 10 min/protein, and have already established an LC-MS/MS quantification method for more than 500 proteins including transporters, enzymes, and receptors.

3.2.3 Experimental Procedure

The first step: the target peptide for a target molecule is chosen by employing our in silico selection criteria, and synthesized with >95 % peptide purity (Fig. 3.2). The concentration of peptide solution is determined by quantitative amino acid analysis, and MS conditions, including SRM/MRM transitions, declustering potentials, and collision energies, are optimized by direct infusion of 0.1–1 μM peptide solution into the mass spectrometer at a flow rate of 5 μL/min with a syringe pump. A dilution series of unlabeled peptide with a fixed amount of labeled peptide is then injected onto the C18 column of the LC coupled with the mass spectrometer to confirm appropriate elution of the peptide from the column, as well as the sensitivity and accuracy in SRM/MRM analysis.

The second step: protein expression level of a target molecule in target protein samples is determined by using the quantification method established in the first step. We have performed protein quantification in whole tissue lysates of human, monkey, and mouse brain capillaries, whole cell lysates of hCMEC/D3 and human breast cancer cell lines, microsomal fraction of liver, crude membrane fractions of human breast and stomach cancer cell lines, plasma membrane fractions of liver, kidney, platelets, meningioma, hCMEC/D3 cells and HUVECs, and cytosolic fractions of human pancreatic adenocarcinoma cell lines (Kamiie et al. 2008; Niessen et al. 2009, 2010; Ito et al. 2011; Kawakami et al. 2011; Uchida et al. 2011b; Obuchi et al. 2013; Ohmine et al. 2012; Ohtsuki et al. 2012, 2013; Yoshikawa et al. 2012). LC-MS/MS-based quantification is applicable to many kinds of protein samples, including those used in ELISA or immunoblotting. The proteins in the sample (50–100 μg protein) are first reduced and S-carbamoylmethylated under solubilizing conditions in the presence of 7 M guanidine hydrochloride (Fig. 3.2). The alkylated proteins are precipitated with a mixture of methanol and chloroform, and then the precipitates are treated with lysyl endopeptidase, trypsin, and trypsin enhancer to efficiently produce tryptic peptides.

The third step: a fixed amount of stable-isotope-labeled internal standard peptides is added, and the mixture is analyzed by multiplexed SRM/MRM to quantify expression of several molecules simultaneously (Fig. 3.2). Signal peaks with a peak area count of over 5,000 detected at the same retention time as an internal standard peptide are defined as positive. When positive peaks are observed in three or four

sets of SRM/MRM transitions, the molecules are considered to be expressed in the target protein samples. The absolute amount (fmol) of each target peptide is determined as the average of three or four quantitative values, which are calculated from the target-to-internal standard peptide peak area ratios in the target samples and the calibration curve. The protein expression level (fmol/μg protein) of target protein is obtained by dividing the determined absolute amount (fmol) of target peptide by the total protein amount (μg protein) of samples analyzed. We have confirmed the efficient solubilization and digestion of glut1 in mouse brain microvessels and human MDR1 in MDR1-overexpressing cells by comparing LC-MS/MS-based quantification and binding assays, including immunoblotting (Kamiie et al. 2008). Furthermore, no bands over 20 kDa were detected by SDS-PAGE after trypsin digestion. The results suggest that the solubilization and trypsin digestion proceeded efficiently, but do not necessarily indicate complete solubilization and digestion of all molecules.

3.2.4 Time Period

The rate-limiting step is synthesis of nonlabeled and stable-isotope-labeled peptides, which currently takes 2–3 weeks (Fig. 3.2). After synthesis, 3 days are necessary to establish the quantification method, including amino acid analysis and MS optimization. Sample preparation until trypsin digestion takes 3 days. The time required for a single analysis by LC-MS/MS depends on the HPLC gradient, and the total time for a series of analyses is proportional to the number of samples. Because a slow gradient is necessary to avoid significant ion suppression, it can take 2 h for a single analysis. If 6 different amounts of standard samples and 10 target protein samples are analyzed, it would take 32 h (16 samples × 2 h) for the whole analysis. In total, 1 month is sufficient to obtain a quantitative protein expression profile.

3.2.5 Cost

Since at least one stable isotope-labeled peptide is necessary for quantifying each protein, the cost of synthesizing the labeled peptides (about $1,000–$1,500 for 5 nmol each) is a critical issue for method development. However, the cost issue will be ameliorated by the establishment of peptide libraries. The AQUA peptide library (Sigma-Aldrich) provides 100 pmol peptide at about $300 each for the registered proteins. Another solution is to synthesize stable isotope-labeled protein containing the target peptides by using an *E. coli* or in vitro cell-free protein synthesis system (Kito et al. 2007). The sensitivity of the method also depends on the available equipment, and the cost of high-sensitivity LC and MS instruments can be significant.

3.3 Advantages and Limitations of Quantitative Targeted Absolute Proteomics

3.3.1 Comparison of Quantitative Targeted Absolute Proteomics and Global Proteomics

The use of tandem mass spectrometry (MS/MS) combined with the genome database has allowed large-scale identification of proteins expressed in biological and clinical materials (Aebersold and Mann 2003; Patterson and Aebersold 2003; Domon and Aebersold2006), so-called global proteomics (Fig. 3.4). Comprehensive analysis with the sequence-tag method using high-resolution mass spectrometers such as Q-TOF and Orbitrap can identify hundreds to thousands of proteins in biological materials in a single analysis (Nagano et al. 2005; Chen et al. 2006; Pshezhetsky et al. 2007). However, proteome coverage with the presently available global proteomic approaches is still insufficient. Highly abundant proteins are easy to identify, but low-abundance proteins are difficult to detect due to high background noise in the analysis of complex samples. The proteins that are difficult to detect include physiologically relevant molecules. Therefore, it is necessary to improve fractionation, purification, and separation techniques in sample preparation and liquid chromatography, and to increase the resolution and sensitivity of the mass spectrometer. These are still challenging problems.

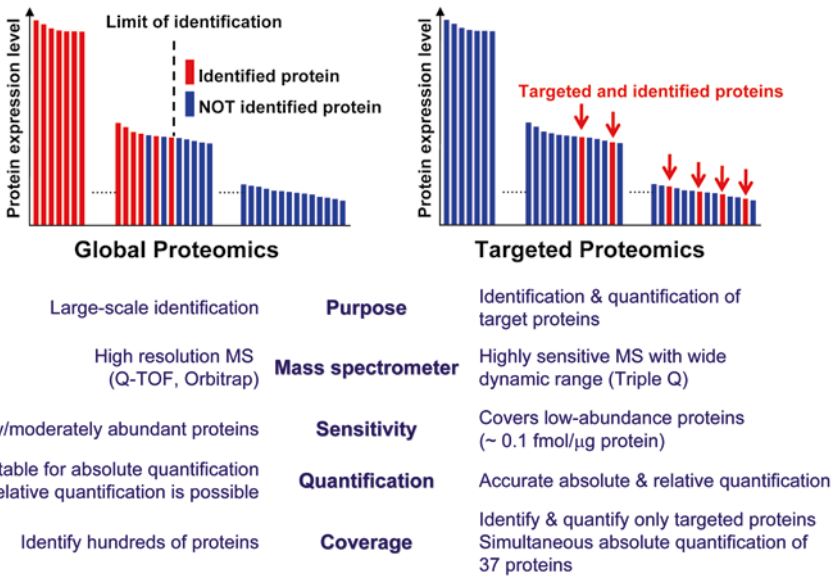

Fig. 3.4 Comparison of global proteomics and targeted proteomics

Compared to global proteomics, quantitative targeted absolute proteomics (QTAP) is suitable for detecting low-abundance molecules, and further can determine their absolute expression level (Fig. 3.4). The use of two mass filters, so-called SRM/MRM analysis, allows the target peptide to be distinguished in enormously complex samples, and provides high selectivity and a high signal-to-noise ratio. Because Triple Q MS has excellent sensitivity, SRM/MRM analysis with Triple Q MS permits highly sensitive detection of target peptides. Furthermore, the use of more than 95 % pure peptides and stable-isotope-labeled internal standard peptides with the same amino acid sequences as the nonlabeled peptides enables absolute quantification of target proteins. The high accuracy and wide dynamic range of Triple Q MS are also favorable for reliable quantification. For these reasons, once target proteins of interest are identified, QTAP provides superior detection ability to global proteomics, and further, can provide the absolute expression level of each target molecule, which may offer a clue to its physiological importance.

3.3.2 Comparison of Protein and mRNA Analysis

mRNA expression has been widely used as a surrogate marker for expression levels and activities of functional molecules. Ohtsuki et al. (2012) compared mRNA expression levels, protein expression levels, and functional activities of drug-metabolizing enzymes and transporters in 17 human liver biopsies. The mRNA expression levels of CYP3A4, CYP2B6, and CYP2C8 were each highly correlated with the corresponding enzyme activity and protein expression levels, whereas for 6 other P450s, the mRNA expression levels were less well correlated than the protein expression levels with the enzyme activities. Among transporters, the protein expression level of organic anion-transporting polypeptide 1B1 (OATP1B1) was relatively highly correlated with the mRNA expression level. However, 11 other transporters showed almost no correlation (Fig. 3.5). Another report indicated that mRNA expression levels and protein expression levels of ABCA7, B4, C1, C3, and C4 in human platelets were not correlated (Niessen et al. 2010). In the cases of P-glycoprotein (P-gp/MDR1) and Na^+/glucose cotransporter 1, the protein expression levels have been shown to correlate with the transport activities (Dyer et al. 1997; Shirasaka et al. 2008; Tachibana et al. 2010). Overall, these reports suggest that protein expression levels are to be preferred over mRNA expression levels for predicting the activities of drug-metabolizing enzymes and transporters.

On the other hand, mRNA analysis using PCR or DNA chip technology can comprehensively screen molecular expression. Therefore, screening of candidate molecules by mRNA analysis followed by the confirmation with QTAP should be an effective strategy to identify proteins expressed in target cells and tissues. Then, the protein expression level determined by QTAP would be useful information to decide on the order of priority for further study among a number of candidate proteins screened by mRNA analysis.

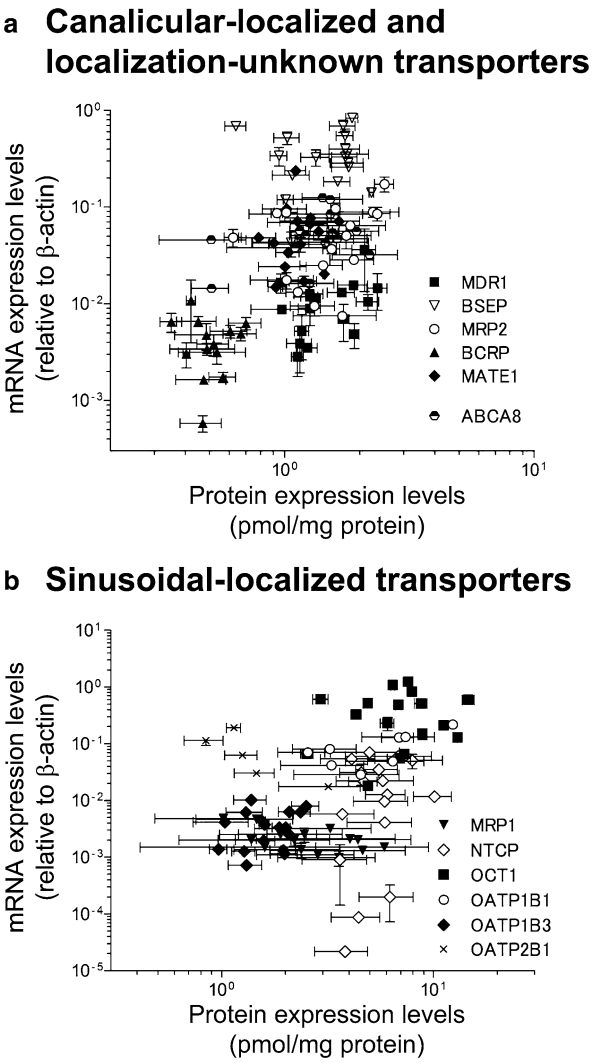

Fig. 3.5 Comparison between protein and mRNA expression levels of transporters in 17 human liver biopsies. Taken from Ohtsuki et al. (2012a) and modified

3.3.3 Comparison of LC-MS/MS and Antibody-Based Analysis

Binding assay using antibodies, such as quantitative western blotting or ELISA, is widely used for protein quantification. In Table 3.2, LC-MS/MS-based quantitative analysis is compared with antibody-based analysis.

As regards method development, it usually takes about a year to establish detection systems using antibodies, and sometimes a suitable specific antibody cannot be obtained at all. In contrast, it takes only a month to develop the quantification method using the LC-MS/MS-based system, and it is not necessary to prepare target

Table 3.2 Comparison of LC-MS/MS and antibody-based analysis

	LC-MS/MS-based analysis		Antibody-based analysis
Principle of quantification analysis	Quantification of peptides digested with protease		Binding assay using antibody, such as quantitative western blotting and ELISA
Essential material	Target peptide set (unlabeled and stable-isotope-labeled peptides)		Antibody
LC-MS/MS > antibody			
Method development	About 1 month for development, including target peptide selection, peptide synthesis, amino acid analysis, and MS optimization	>>	Long time for development, including antigen preparation, immunization, and specificity validation
	Target peptide is selected from sequence information	>>	Antigen protein or peptide is necessary
Specificity	High specificity due to mass filter, and specificity is confirmed by database	>>	Depends on antibody, and difficult to validate specificity
	Easy to distinguish modification and mutation by mass	>	Difficult to prepare specific antibodies for modifications and mutations in proteins
Multiprotein assay	37 proteins/1 assay	>>	1 protein/1 assay
LC-MS/MS < antibody			
Throughput	1 sample/1 run	<<	96 or more samples/1 run
Sensitivity	Medium sensitivity (ng/mL)	<	High sensitivity (pg/mL to ng/mL)
Localization analysis	Insufficient resolution and sensitivity	<<	High sensitivity and resolution, but depends on antibody
Instrument	Expensive and high-tech instrumentation	<	Simple instrumentation

">" or ">>" indicates advantages of LC-MS/MS-based analysis and "<" or "<<" indicates advantages of antibody-based analysis. Sensitivity, multiprotein assay, and throughput refer to ELISA as an antibody-based analysis. Taken from Ohtsuki et al. (2011) and modified

proteins, because in silico selection of target peptides is available. It is possible to make a decision as to whether or not the method is feasible within the first 10 min, based on the in silico target peptide selection. In contrast, antibody-based analysis first requires preparation of the antigens and it then takes several months to establish whether a suitable antibody can be obtained. Thus, the availability of in silico selection from a sequence database allows much more rapid and efficient development of a LC-MS/MS-based quantification method for target protein.

The specificity of the analytical system for the target protein is a key factor in interpreting the experimental results. In LC-MS/MS-based analysis, the specificity of the target peptide can be confirmed by database search, such as NCBI BLAST search (Table 3.2). Furthermore, MS selects the target peptide based on molecular weight (mass-to-charge ratio; m/z) with a mass filter, and selectively detects the target peptide in complex peptide mixtures obtained by digesting biological

samples. A single amino acid difference in a peptide changes the *m*/*z*, and can easily be distinguished by MS. Therefore, major advantages of this quantification method are very high specificity for the target protein and high selectivity, in contrast to the issue of cross-reactivity in antibody-based methods. An example of the superiority of LC-MS/MS can be seen in the separate quantification of mdr1a and mdr1b, for which the preparation of specific antibodies is difficult due to their high sequence similarity. Furthermore, single nucleotide polymorphism (SNP) or a PTM, such as phosphorylation, results in a change of *m*/*z*, so that LC-MS/MS can separately quantify both wild-type and mutated protein or both nonmodified and modified protein. It would be extremely difficult to prepare specific antibodies for these purposes. Quantification of phosphorylated proteins such as focal adhesion kinase, estradiol receptor α, and HER2 by LC-MS/MS has been reported (Ciccimaro et al. 2009; Domanski et al. 2010).

Simultaneous quantification of multiple proteins with multiplexed SRM/MRM is another advantage of LC-MS/MS-based quantification (Table 3.2). Up to 37 proteins can currently be quantified simultaneously (8 transitions per protein × 37 proteins = 296 transitions < 300 transitions at maximum in API5000 and QTRAP5500), and we have reported the simultaneous quantification of 34 transporters and 2 membrane proteins in mouse brain capillaries, liver, and kidney (Kamiie et al. 2008). It is also possible to increase the number of target proteins for quantification by repeating the LC-MS/MS analysis. We recently reported the quantification of 114 membrane proteins in human brain capillaries (Uchida et al. 2011b). Therefore, LC-MS/MS is an excellent tool to quantify large numbers of target proteins, such as transporters, enzymes, receptors, channels, and biomarker candidates.

On the other hand, a limitation of this method is the longer analysis time of LC-MS/MS compared to ELISA (Table 3.2). LC-MS/MS analyzes samples one by one, and a single analysis takes about 2 h using regular HPLC, so a maximum of 12 samples can be analyzed in a day. The use of ultra performance liquid chromatography (UPLC) can shorten the analysis time to a few minutes, but the shorter gradient causes significant ion suppression and it is necessary to reduce the number of proteins that can be quantified simultaneously to obtain accurate target peptide peaks. ELISA measures single proteins, but it is possible to analyze 96 or more samples in parallel. Therefore, ELISA is a useful methodology to determine the expression levels of one or several proteins in large numbers of samples, e.g., for clinical diagnosis.

Sensitivity is an important factor for quantification, as well as accuracy and reliability (Table 3.2). The sensitivity of ELISA is in the range from pg/mL to ng/mL, although it depends on the antibody (Ang et al. 2011). The sensitivity of LC-MS/MS-based quantification is of ng/mL order (0.1–1 pmol/mL) (Ang et al. 2011). Thus, LC-MS/MS-based quantification is less sensitive than ELISA. However, the continuing improvement of MS instruments is expected to increase the sensitivity. Alternatively, a step to purify and concentrate target proteins and peptides could be introduced.

Knowledge of protein localization in cells and tissues is essential to elucidate a protein's function. Antibodies are a good tool to clarify protein localization in

cells and tissues by means of immunocytochemical and immunohistochemical analyses, respectively. Recently, MS has also become available for localization analysis, with the introduction of imaging MS (Schwamborn and Caprioli 2010; Sugiura and Setou 2010). However, the current methodology does not have sufficient resolution and sensitivity (Table 3.2), so protein localization analysis by using imaging MS is still challenging issue. The laser microdissection technique has been adopted recently to obtain tissue samples exclusively from specific regions of interest, although the collected samples are very small in quantity (ng to μg protein). If a nano-LC system is coupled with a mass spectrometer, so-called nano-LC-MS/MS, the expression levels of target molecules can be determined by using as little as 1 μg protein of tissue sample, which is obtainable by laser microdissection. Therefore, the combination of laser microdissection and SRM/MRM analysis in nano-LC-MS/MS can improve the sensitivity in localization analysis and should be useful methodology to determine protein expression levels in specific tissue regions.

3.4 Recent Advances in LC-MS/MS-Based Quantification: Protein Quantification by High-Resolution Selected/Multiple Reaction Monitoring (HR-SRM/MRM)

Increasing the sensitivity of MS is important to quantify protein expression levels of target molecules that cannot be detected by existing LC-MS/MS systems. However, attempts to increase sensitivity usually cause an increase not only in the peak intensity of the target peptide but also in the noise level, so that the lower limit of quantification is not improved much. Protein samples of high complexity, such as whole tissue lysates, give high levels of background noise. Therefore, a reduction of noise levels is necessary to detect small amounts of proteins, as well as increasing the sensitivity. Q-TOF MS gives high mass resolution, which is favorable to distinguish a small target peak from background noise, but the dynamic range is narrow, being inadequate for quantification. Furthermore, Q-TOF MS is not suitable for multiprotein-targeted analysis such as multiplexed SRM/MRM because the scan time is longer. Recently, however, MS instrument development has led to an improvement in the dynamic range and scan speed of Q-TOF MS. High-resolution (HR)-SRM/MRM analysis with the latest Q-TOF MS (ABSCIEX TripleTOF5600) is able to simultaneously determine the protein expression levels of more than 20 proteins with a dynamic range of greater than 4 orders of magnitude. TripleTOF5600 gives a mass resolution of 0.02 unit, which is 35-fold superior to that of QTRAP5500 (0.7 unit). Indeed, TripleTOF5600 shows a significantly reduced noise level and can detect small peaks that are masked by background noise in the case of QTRAP5500 (Fig. 3.6). Therefore, HR-SRM/MRM analysis can be used to quantify protein expression of target molecules present in amounts too small to be detected by Triple Q MS.

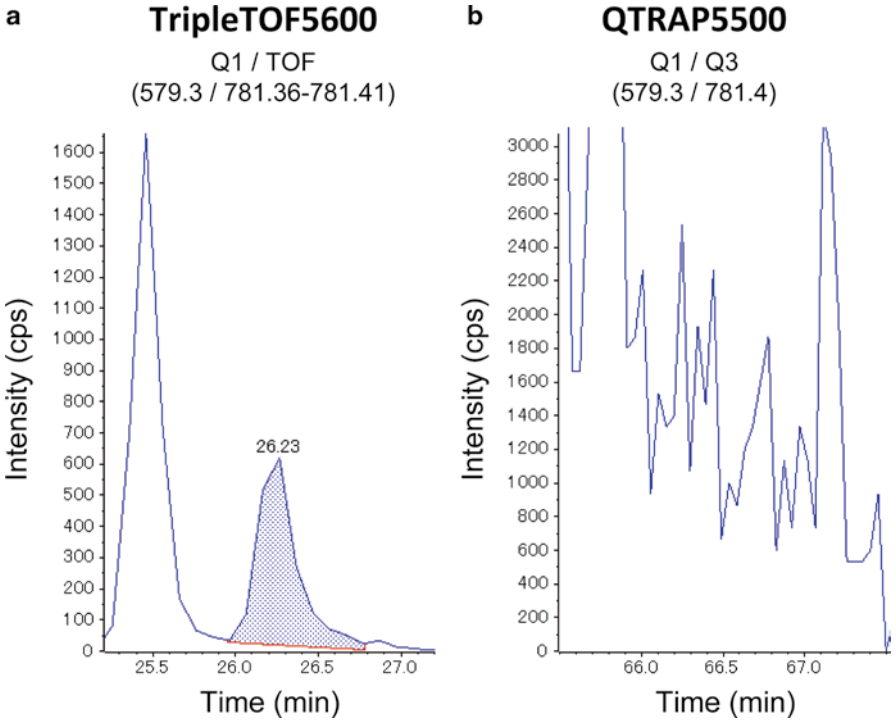

Fig. 3.6 Comparison of SRM/MRM chromatograms for cytochrome P450 2a5 (CYP2a5) in microsomal fraction of mouse liver between TripleTOF5600 (**a**) and QTRAP5500 (**b**). Microsomal fraction of mouse liver was digested with trypsin, and the digestion products were spiked with stable isotope-labeled peptides and subjected to LC-MS/MS analysis. (**a**) For the LC-TripleTOF5600 (Q-TOF), the digestion products were separated with a C18 column (3 μm, 75 μm × 150 mm, Eksigent Technologies) at a flow rate of 200 nL/min, and the peptide of CYP2a5 was analyzed by high-resolution SRM/MRM. (**b**) For the LC-QTRAP5500 (Triple Q), the digestion products were separated on Xbridge BEH130 C18, 3.5 μm, 1.0 mm × 100 mm (Waters) at a flow rate of 50 μL/min, and the peptide of CYP2a5 was analyzed by SRM/MRM. A signal peak was detected at the same retention time as the labeled peptide (26.2 min) and recognized as the peak of the target peptide of CYP2a5 on the LC-TripleTOF5600. In contrast, no signal peak was observed at the same retention time as the labeled peptide (66.4 min) on the LC-QTRAP5500

3.5 Applications in Blood–Brain Barrier Research

3.5.1 Interspecies Differences in Protein Expression Levels of Transporters and Receptors

Species differences and similarities between humans and experimental animals are key issues for efficient drug development, especially for increasing the success rate of progression of candidate drugs from preclinical to clinical studies. Therefore, we have clarified the absolute protein expression levels of transporters and receptors in

human, monkey, and mouse brain microvessels, providing basic information about species differences in molecular-level transport functions at the blood–brain barrier (BBB) (Table 3.3; Kamiie et al. 2008; Ito et al. 2011; Uchida et al. 2011b). This information is valuable for CNS drug discovery and development.

MDR1/mdr1a/P-gp/ABCB1 and BCRP/ABCG2 are major gatekeepers for multiple hydrophobic drugs, and function to pump out these drugs from brain capillary endothelial cells into the circulating blood and to attenuate drug distribution to the brain. MDR1 protein expression in human brain microvessels is 2.33-fold lower than that in mouse, whereas it is not significantly different between human and monkey (Table 3.3). The lower expression of MDR1 in human and monkey brain microvessels would lead us to predict higher distribution of MDR1 substrates to the brain of humans and monkeys compared to that of mice. Indeed, a PET study found that human brain penetration of [^{18}F]altanserin and [^{11}C]GR205171, substrates of MDR1, was 4.5- and 8.6-fold greater than in rodents, respectively, and monkey brain penetration of [^{11}C]verapamil and [^{11}C]GR205171 was 4.1- and 2.8-fold greater than in rodents, respectively, although the plasma protein bindings of these substrates did not show much difference among humans, monkeys, and rats (Syvanen et al. 2009). Furthermore, MDR1 inhibition with tariquidar in humans led to only a 2.7-fold increase in [^{1}C]verapamil brain uptake as compared with an 11.0-fold increase in rats, suggesting that MDR1 activity is less in humans than in rats (Bauer et al. 2012). These results indicate that, in addition to differences in substrate specificity and affinity, differences in the expression levels of transporters contribute to species differences in transporter function at the BBB.

BCRP protein expression was 1.74-fold greater in monkeys, but 1.85-fold lower in mice than in humans (Table 3.3). Although the species difference in BCRP transport activity at the BBB remains unknown, the higher expression level of BCRP than MDR1 in human and monkey BBB suggests that BCRP is mainly involved in limiting drug penetration into the brain in humans and monkeys. Various BCRP substrates, including imatinib, gefitinib, erlotinib, mitoxantrone, and topotecan (Kusuhara and Sugiyama 2009; Urquhart and Kim 2009), have been used for the treatment of glioblastoma, but their therapeutic benefit is minimal (Wen and Kesari 2008). In contrast, temozolomide is effective and is generally used as a first-line drug for glioma patients (Wen and Kesari 2008). Temozolomide is not transported well by human BCRP (de Vries 2009). Therefore, we postulate that the high efflux activity of BCRP at the human BBB is one of the reasons for the limited pharmacological activity of these anticancer agents, other than temozolomide, against glioblastoma.

MRP4 and OAT3 are well-characterized organic anion transporters at the rodent BBB, and, in vivo experiments with gene knockout mice have shown that mrp4 and oat3 play roles in drug efflux from brain to blood (Uchida et al. 2007; Ose et al. 2009). The protein expression of MRP4 is significantly smaller (8.1-fold) in humans than in mice, and that of OAT3 is at least 5.7-fold smaller (Table 3.3), raising the possibility that the efflux activities of MRP4 and OAT3 are low in human BBB compared to mouse BBB. Ro64-0802, an active form of the anti-influenza virus agent oseltamivir, undergoes active efflux mediated by OAT3 and MRP4 at the BBB

Table 3.3 Comparison of protein expression levels of transporters and receptors between human, cynomolgus monkey, and ddY mouse isolated brain microvessels

	Molecule (HUMAN/MONKEY/mouse)	Human (fmol/μg protein)	Individual difference (Max/Min) (-fold)	Cynomolgus monkey (fmol/μg protein)	ddY mouse (fmol/μg protein)
Drug transporters					
Efflux of lipophilic drugs	MDR1/MDR1/mdr1a	6.06 ± 1.69	2.10	4.71 ± 1.30	14.1 ± 2.1**
	BCRP/BCRP/bcrp	8.14 ± 2.26	2.86	14.2 ± 1.3**	4.41 ± 0.69*
Transport of organic anions	MRP4/MRP4/mrp4	0.195 ± 0.069	2.56	0.286 ± 0.042	1.59 ± 0.22**
	OAT3/OAT3/oat3	ULQ (<0.348)	–	ULQ (<0.404)	1.97 ± 0.11
	OATP1A2/OATP1A2/oatp1a4	ULQ (<0.695)	–	0.724 ± 0.041	2.11 ± 0.28
	OATP2B1/OATP2B1/oatp1a4	ULQ (<0.337)	–	ULQ (<0.135)	2.11 ± 0.28
	ABCA8/ABCA8/abca8a	1.21 ± 0.24	>1.75	Not measured	ULQ (<0.144)
	ABCA8/ABCA8/abca8b	1.21 ± 0.24	>1.75	Not measured	ULQ (<0.0324)
	ABCA8/ABCA8/abca9	1.21 ± 0.24	>1.75	Not measured	ULQ (<0.752)
Transporters for endogenous compounds					
Amino acid transport	LAT1/LAT1/lat1	0.431 ± 0.091	>2.03	ULQ (<0.326)	2.19 ± 0.21**
	4F2hc/4F2hc/4f2hc	3.47 ± 0.83	2.05	Not measured	16.4 ± 1.1**
	ASCT1/ASCT1/asct1	1.81 ± 0.53	2.23	Not measured	Not measured
	ASCT2/ASCT2/asct2	ULQ (<0.142)	–	ULQ (<0.114)	1.58 ± 0.06
	EAAT1/EAAT1/eaat1	24.5 ± 12.5	4.24	Not measured	Not measured
	EAAT2/EAAT2/eaat2	5.70 ± 1.89	2.65	Not measured	Not measured
	EAAT3/EAAT3/eaat3	ULQ (<0.256)	–	Not measured	Not measured
Energy source supply	GLUT1/GLUT1/glut1	139 ± 46	2.69	129 ± 21	90.0 ± 4.5
	GLUT3,14/GLUT3,14/glut3	4.40 ± 1.00	1.98	1.22 ± 0.21**	ULQ (<0.607)
	MCT1/MCT1/mct1	2.27 ± 0.85	3.18	0.834 ± 0.368*	23.7 ± 1.6**
	CD147/CD147/cd147	ULQ (<0.0828)	–	Not measured	19.5 ± 4.3

Thyroid hormone supply	OATP1C1/OATP1C1/oatp1c1	ULQ (<0.208)	–	ULQ (<0.365)	2.41 ± 0.25
	MCT8/MCT8/mct8	1.31 ± 0.37	2.15	1.35 ± 0.17	Not measured
Cholesterol transport	ABCA1/ABCA1/abca1	ULQ (<0.223)	–	ULQ (<0.271)	0.298 ± 0.098
	ABCA2/ABCA2/abca2	2.86 ± 0.58	1.88	Not measured	ULQ (<0.178)
Nucleoside transport	ENT1/ENT1/ent1	0.568 ± 0.134	1.85	0.541 ± 0.072	0.985 ± 0.363
Taurine transport	TAUT/TAUT/taut	ULQ (<0.0767)	–	ULQ (<0.236)	3.81 ± 0.64
Receptors					
	INSR/INSR/insr	1.09 ± 0.21	1.67	1.52 ± 0.25*	1.16 ± 0.74
	LRP1/LRP1/lrp1	1.51 ± 0.26	1.61	1.29 ± 0.05	1.07 ± 0.38
	TfR1/TfR1/tfr1	2.34 ± 0.76	2.63	Not measured	5.84 ± 0.87**
Marker proteins					
	γ-GTP/γ-GTP/γ-gtp	3.57 ± 0.71	1.57	Not measured	4.37 ± 0.86
	Na^+/K^+-ATPase/Na^+/K^+-ATPase/na^+/k^+-atpase	35.1 ± 12.6	2.37	35.1 ± 8.2	39.4 ± 2.2

Human data are taken from Uchida et al. (2011b) (average of 7 donors; 4 donors for ABCA8; 5 donors for LAT1 and γ-GTP), except for the data of ASCT1, EAAT2, and MCT8 taken from Shawahna et al. (2011) (average of 5 donors). Individual differences (Max/Min) were calculated by dividing the highest protein expression levels by the lowest protein expression levels among the 7 or 5 donors. For ABCA8 and LAT1, they were calculated by dividing the highest protein expression amounts by the limits of quantification (0.823 and 0.263 fmol/μg protein, respectively). Cynomolgus monkey data are taken from Ito et al. (2011). ddY mouse data are taken from Kamiie et al. (2008) or Uchida et al. (2011b). Nomenclature is given in capital letters for the human and monkey homologs and lower-case letters for the mouse homologs, and is described in order of HUMAN/MONKEY/mouse. Mouse abca8a, abca8b, and abca9 are possible homologs of human and monkey ABCA8. OATP1A2 and OATP2B1 of human and monkey are possible homologues of mouse oatp1a4 at the BBB. The data represent the mean ± S.D. (number of donors = 4–7; number of monkeys = 3–6; number of mouse samples = 6). ULQ, under the limit of quantification. *$p < 0.01$, **$p < 0.001$, significantly different from the protein expression levels in human isolated brain microvessels

(Ose et al. 2009). Recently, abnormal behavior has been reported in teenagers or younger people prescribed oseltamivir, though a rodent study showed no specific CNS or behavioral effects after administration of doses corresponding to at least 100 times the clinical dose (Toovey et al. 2008). Ro64-0802 is suspected to be one of the major causes of the CNS adverse effects in humans, because it is 30 times more potent than oseltamivir (Izumi et al. 2007). Hence, a possible explanation for oseltamivir toxicity in humans may be that low expression of MRP4 and OAT3 in the human BBB results in reduced efflux of Ro64-0802 from the brain, leading to greater accumulation in the brain, which in turn induces adverse effects on the CNS.

OATP is another family of organic anion transporters, and OATPs are thought to transport a variety of amphipathic drugs. In human brain microvessels, no protein expression of any the OATP subtypes was observed, as was also the case for OAT and MRP family members, except MRP4 (Uchida etal. 2011b). Therefore, not only OAT- and MRP-mediated transport but also OATP-mediated transport could be very limited at the human BBB. On the other hand, ABCA8 has been reported to transport organic anions, including substrates of rodent mrp4, oat3, and oatp1a4/oatp2 (Kusuhara et al. 1999; Tsuruoka et al. 2002; Ohtsuki and Terasaki 2007), and was detected in human brain microvessels in the amount of 1.21 fmol/μg protein, a level similar to those of mrp4, oat3, and oatp1a4 in mouse brain capillaries (Table 3.3). Therefore, ABCA8 could play a role corresponding to those of mouse mrp4, oat3, and oatp1a4 at the human BBB.

In addition to drug transporters, transporters and receptors for endogenous compounds also showed significant differences in protein expression levels between human and mouse, whereas the levels in monkeys were quite similar to those in humans. Thyroid hormones, such as thyroxine (T4) and triiodotyronine (T3), are essential for cell metabolism, normal growth and development, and supply of these hormones from blood to brain is vital. In rodents, mct8 and oatp1c1/oatp14 are expressed in isolated brain microvessel endothelial cells (Roberts et al. 2008), and are involved in the supply of thyroid hormones into the brain across the BBB (Tohyama et al. 2004; Trajkovic et al. 2007; Ceballos et al. 2009). In humans and monkeys, our QTAP analysis showed that MCT8 protein was expressed in isolated brain microvessels, whereas OATP1C1 protein was under the limit of quantification (Table 3.3). The levels in humans and monkeys were at least 11.6-fold and 6.60-fold lower than that in mice, respectively. Thyroid hormone insufficiency in the brain causes neurological abnormalities, such as Allan-Herndon-Dudley syndrome. Rather drastic abnormalities are observed in humans lacking functional MCT8, in contrast to mct8-null mice (Heuer 2007). These results suggest that, in humans and monkeys, MCT8 mainly contributes to the supply of thyroid hormones across the BBB, due to restricted expression of OATP1C1.

Excitatory amino acids, such as L-glutamic acid (L-Glu) and L-aspartic acid (L-Asp), play a role in excitatory neurotransmission in the CNS (Zorumski and Olney 1993). Since their accumulation in the brain results in excitatory neurotoxicity, the efflux transport system is required to act as a clearance system to maintain CNS function. L-Glu and L-Asp undergo efflux from the brain across the BBB (Hosoya et al. 1999). This transport system does not mediate efflux transport of D-aspartic

acid (D-Asp). Tetsuka et al. (2003) indicated that asct2 is involved in the L-ISOMER-SELECTIVE Asp efflux across the BBB in rodents. In humans, ASCT2 protein expression was not observed in isolated brain microvessels in QTAP analysis, and its level (<0.142 fmol/μg protein) was at least 11.1-fold lower than that in mouse (Table 3.3). However, ASCT1 protein was expressed in the amount of 1.81 fmol/μg protein, a level similar to that of asct2 in mouse brain capillaries (Table 3.3; Shawahna et al. 2011). As ASCT1 also mediates L-isomer-selective Asp transport (Tetsuka et al. 2003), ASCT1 appears to have a functional role similar to that of mouse asct2 at the human BBB.

As well as the ASCT family, excitatory amino acid transporters (EAATs) 1, 2, and 3 are also expressed in isolated brain capillary endothelial cells (O'Kane et al. 1999). Electrogenic transport experiments using *Xenopus* oocytes expressing EAAT subtypes have shown that all the three subtypes transport not only L-Glu and L-Asp but also D-Asp with similar transport rates [maximum current]/[K_m] for the three amino acids (Arriza et al. 1994). Therefore, EAATs cannot account for the stereoselective BBB efflux transport of Asp in rats (Hosoya et al. 1999), and the contribution of EAATs to the BBB transport system may be small compared with that of ASCTs. In isolated human brain microvessels, protein expression levels of EAATs were quantified in the rank order of EAAT1>EAAT2>EAAT3, and the protein levels of EAAT1 and EAAT2 (24.5 and 5.70 fmol/μg protein, respectively) were larger than those of human ASCT1 and mouse asct2 (Table 3.3). Because astrocytes express EAAT1 and EAAT2 (Kanai et al. 1997), the possibility cannot be excluded that high levels of EAAT1 and EAAT2 are partially due to astrocyte contamination, and the expression in brain capillary endothelial cells may not be large enough to provide a meaningful efflux transport function for excitatory amino acids. Another possible explanation may be that, unlike humans, the expression levels of EAATs in rats are very low in isolated brain microvessels, so that D-Asp does not undergo efflux from the brain across the BBB in rats (Hosoya et al. 1999).

3.5.2 *Interindividual Differences in Protein Expression Levels of Transporters and Receptors*

Among individuals, pharmacological and adverse effects of drugs in the CNS may differ even if systemic exposure to the drugs is same, because the effects are dependent upon brain concentration, which is influenced by drug penetration across the BBB. To evaluate individual differences in drug distribution into brain, individual differences in protein expression levels of transporters and receptors were examined in isolated brain microvessels from seven donors. As shown in Table 3.3, protein expression levels of most of the transporters and receptors were within threefold difference, although EAAT1 showed a 4.24-fold difference. According to our recent LC-MS/MS-based absolute quantification analysis, protein expression levels of transporters in plasma membrane of human liver showed more than threefold differences among 17 donors for most transporters (Ohtsuki et al. 2012). Furthermore, protein

expression levels of cytochrome P450 in human liver microsomes were remarkably different among individuals, e.g., over 20-fold differences for CYP1A2, 2A6, 2C19, and 3A4 (Kawakami et al. 2011). Compared to these differences in liver, the interindividual differences in protein expression levels of transporters and receptors at the human BBB are quite small. This may imply that a consistent transport function at the BBB is essential to maintain CNS function and to protect the brain from exposure to various xenobiotics, including environmental factors and drugs.

However, the data in Table 3.3 were obtained by using probe peptides located at regions other than the SNPs and PTMs registered in UniProtKB database. SNPs and PTMs may alter the intrinsic transport activity of transporters without any change of protein expression level. Therefore, we cannot rule out the possibility that, among the donors in Table 3.3, the transport activities per protein for certain transporters are different due to SNPs and/or PTMs, and so the extents of drug penetration into the brain are different. LC-MS/MS systems can distinguish wild-type and mutated protein or modified and nonmodified protein if peptides including the SNP(s) and/or PTM(s) are targeted. Therefore, QTAP will be available for studies of individual differences in transport activities arising from SNPs and/or PTMs.

MDR1 is one of the most influential transporters for drug penetration across the BBB, and individuals homozygous for C3435T (exon 26) polymorphism have significantly lower duodenal MDR1 protein expression and higher digoxin plasma levels after oral administration (Hoffmeyer et al. 2000). Hence, the effects of MDR1 SNPs on the transporter's efflux activity at the BBB and on drug distribution into the brain have been investigated. In contrast to small intestine, no significant difference was observed in the absolute values of brain uptake clearance of ^{11}C-verapamil between haplotypes (1236TT, 2677TT, 3435TT vs. 1236CC, 2677GG, 3435CC) in integration plot analysis, suggesting that MDR1 efflux activity at the BBB is not significantly different among the haplotypes (Takano et al. 2006). However, in the case of integration plot analysis, it is possible that the apparent change of efflux activity is underestimated, because the contribution of MDR1 to drug penetration across the BBB could be influenced by passive diffusion, other transport system(s) and protein binding in endothelial cells and brain parenchyma. As described in Sect. 3.6.1, it should be possible to use the concept of QTAP-based reconstruction to accurately clarify the differences in efflux activity of MDR1 among haplotypes by integrating the protein expression levels of MDR1 at the BBB with the efflux activity per MDR1 protein in individual haplotypes.

3.5.3 Developmental Changes in Protein Expression Levels of Transporters

Drug dosage regimen design in babies and children remains a significant challenge in clinical care. In order to understand how sensitive such patients are to the pharmacological and adverse effects of drugs in the brain, it is important to clarify developmental changes in transport function at the BBB. In rats, it has been reported that the brain-to-plasma concentration ratio of oseltamivir, an mdr1a substrate, was

decreased by about threefold with postnatal development, and the protein expression level of mdr1a was increased by about sixfold in the brain (Ose et al. 2008), suggesting that mdr1a efflux activity at the BBB is lower in the early developmental phase than in adult rats. However, in monkeys, differences in MDR1 protein levels in isolated brain microvessels were within 1.47-fold between neonate (1 day), child (16 months), and adult (4 years 3 months) (Ito et al. 2011). Although the brain-to-blood AUC ratio of oseltamivir decreased slightly with postnatal development, the changes were within 1.7-fold difference between infants (9 months), adolescents (24–27 months), and adults (5.6–6.6 years) (Takashima et al. 2011). A good MDR1 substrate, verapamil, exhibited a brain-to-blood AUC ratio of 2.3- and 1.6-fold higher in infants and adolescents than in adults, respectively, although no correction was made for developmental differences in plasma and brain protein binding levels (Takashima et al. 2011). Therefore, in monkeys too, MDR1 efflux activity might be lower in the early developmental phase than in adults, but the extent of developmental change seems to be smaller than that in rats.

Tachikawa et al. (2005) reported that bcrp expression in mouse brain did not significantly change from the E13 stage to adult, based on in situ hybridization. In contrast, the BCRP protein level in isolated monkey brain microvessels significantly increased with postnatal development and was 2.3-fold greater in adults than that at 1 day after birth (Ito et al. 2011).

Thus, the results of interspecies comparison of transporter protein expression levels (Table 3.3) indicates that the quantitative protein expression profile of BBB transporters in monkeys resembles that in humans more closely than does the pattern in rodents. Therefore, monkey data should be particularly helpful to understand changes in the brain distribution of drugs in the developmental phase in humans.

3.6 Advanced Applications in Blood–Brain Barrier Research

3.6.1 QTAP-Based Reconstruction of In Vivo Transporter Activity at the Blood–Brain Barrier

Transport functions of BBB transporters and contributions of individual transporters to drug distribution in the brain have been quantitatively evaluated by in vivo administration of various drugs in rodents, including gene-knockout mice. However, there are significant species differences between rodents and humans in the protein levels of transporters at the BBB and in the brain distribution of some substrates (Friden et al. 2009; Syvanen et al. 2009; Uchida et al. 2011b). This suggests that rodent experiments are not enough to quantitatively predict transport function at the human BBB, or the contributions of individual transporters to drug distribution in the human brain. Although imaging technologies such as PET and SPECT have recently become available for quantitative evaluation of in vivo transporter activity in humans, the number of suitable ligands, especially ligands specific for target transporters, is limited, and BBB penetration of the ligands can potentially be

masked by binding to brain tissue. Hence, the activities of only a few transporters at the human BBB can be evaluated with these technologies.

QTAP, however, can directly clarify differences in protein expression levels. Therefore, we postulated that it would be possible to reconstruct the in vivo transport activity of any target transporter at the human BBB from in vitro transport activity data in a transporter-overexpressing system by integrating the protein expression levels in brain capillaries and in the in vitro system. Mdr1a knockout mice are available, and the specific efflux activity of mdr1a at the BBB can be determined by comparing the brain distribution of substrates in knockout and wild-type mice. We therefore set out to test our idea by investigating whether the observed efflux activity of mdr1a at the mouse BBB can be reconstructed from in vitro experimental data by the application of QTAP and pharmacokinetic modeling.

The $K_{p,brain}$ ratio is the ratio of brain-to-plasma concentration ratio ($K_{p,brain}$) in mdr1a/1b knockout mice to that in wild-type mice, and is used as a parameter to describe in vivo mdr1a efflux activity at the BBB.

$$K_{p\,brain}\text{ratio} = \frac{K_{p\,brain}\text{in mdr1a / 1b}\left(-/-\right)\text{mice}}{K_{p\,brain}\text{in wild}-\text{type mice}} \tag{3.1}$$

Total drug concentration in brain (C_{brain}) is divided into unbound brain concentration ($C_{u,brain}$) and unbound fraction in brain ($f_{u,brain}$), and total drug concentration in plasma (C_{plasma}) is divided into unbound plasma concentration ($C_{u,plasma}$) and unbound fraction in plasma ($f_{u,plasma}$). Furthermore, $C_{u,brain}/C_{u,plasma}$ can be replaced with the ratio of the blood-to-brain clearance to the brain-to-blood clearance across the BBB ($PS_{blood\text{-}to\text{-}brain}/PS_{brain\text{-}to\text{-}blood}$), so $K_{p,brain}$ is given by

$$\begin{aligned} K_{p\,brain} &= \frac{C_{brain}}{C_{plasma}} \\ &= \frac{f_{u,plasma}}{f_{u,brain}} \times \frac{C_{u,brain}}{C_{u,plasma}} \\ &= \frac{f_{u,plasma}}{f_{u,brain}} \times \frac{PS_{blood\ to\ brain}}{PS_{brain\ to\ blood}} \end{aligned} \tag{3.2}$$

Using (3.1) and (3.2), the $K_{p,brain}$ ratio can be described as follows:

$$K_{p\,brain}\text{ratio} = \frac{PS_{blood\text{-}to\text{-}brain\,KO} / PS_{brain\text{-}to\text{-}blood\,KO}}{PS_{blood\text{-}to\text{-}brain\,wt} / PS_{brain\text{-}to\text{-}blood\,wt}} \tag{3.3}$$

According to the reported in vivo pharmacokinetic model illustrated in Fig. 3.7a (Adachi et al. 2001), four permeability clearances can be defined as follows:

$$PS_{blood\text{-}to\text{-}brain\,KO} = PS_{l,inf} \times \frac{PS_{al,eff}}{PS_{l,eff} + PS_{al,eff}} \tag{3.4}$$

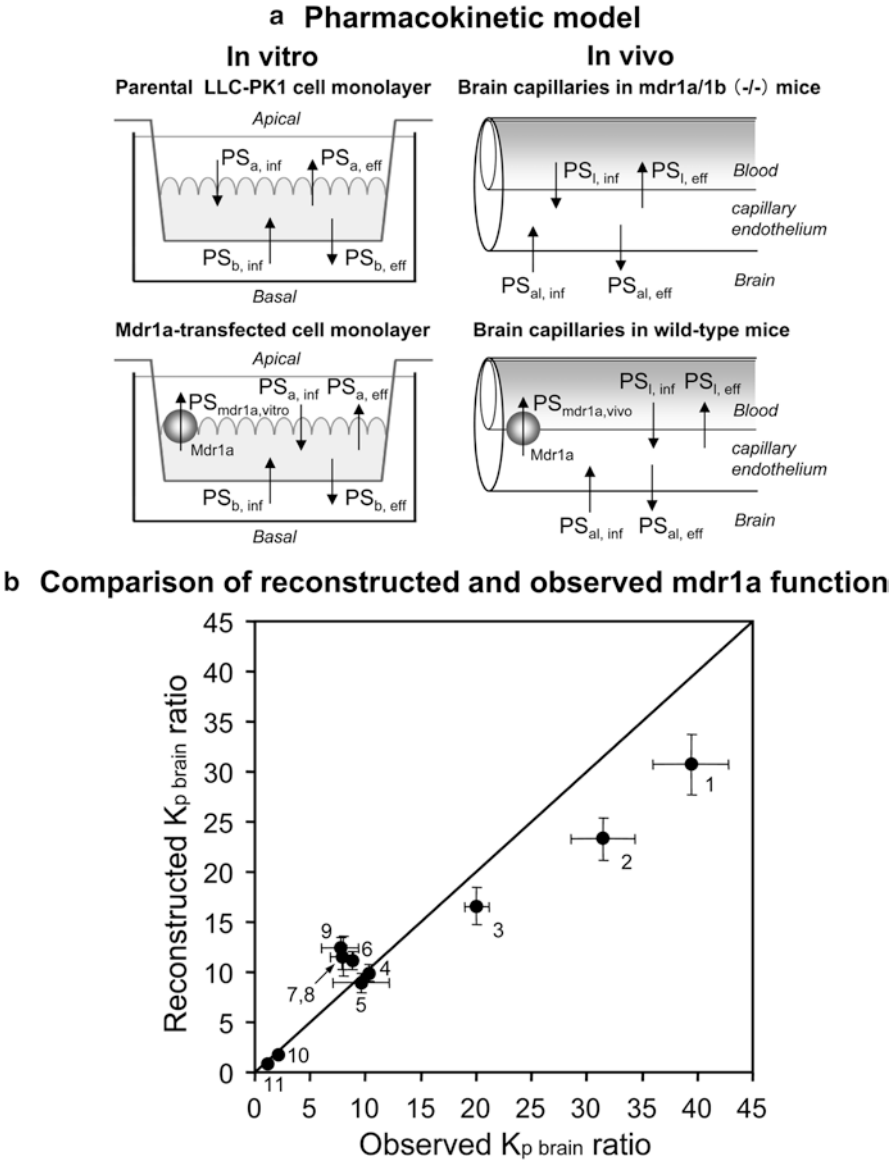

Fig. 3.7 Reconstruction of mdr1a function at the BBB by means of a pharmacokinetic model using mdr1a protein level and intrinsic transport activity. (**a**) $PS_{a,inf}$, $PS_{a,eff}$, $PS_{b,inf}$, $PS_{b,eff}$, and $PS_{mdr1a,vitro}$ represent the PS products for the apical influx, apical efflux (except for mdr1a efflux), basal influx, basal efflux, and mdr1a-mediated efflux in the mdr1a-transfected cells, respectively. $PS_{l,inf}$, $PS_{l,eff}$, $PS_{al,inf}$, $PS_{al,eff}$, and $PS_{mdr1a,vivo}$ represent the PS products for the luminal influx, luminal efflux (except for mdr1a efflux), abluminal influx, abluminal efflux, and mdr1a-mediated efflux in the brain capillary endothelium, respectively. Taken from Adachi et al. (2001) and Uchida et al. (2011a), and modified. (**b**) The solid line represents perfect agreement of reconstructed and observed $K_{p,brain}$ ratio. Each point represents the mean ± S.E.M. 1. Quinidine, 2. loperamide, 3. digoxin, 4. risperidone, 5. indinavir, 6. dexamethasone, 7. vinblastine, 8. paclitaxel, 9. verapamil, 10. loratadine, 11. diazepam. Taken from Uchida et al. (2011a) and modified. The observed $K_{p,brain}$ ratios for risperidone, indinavir, paclitaxel, verapamil, loratadine, and diazepam were taken from Hendrikse et al. (1998), Kim et al. (1998), Chen et al. (2003), Kemper et al. (2004) and Doran et al. (2005)

$$PS_{\text{brain-to-blood KO}} = PS_{\text{al,inf}} \times \frac{PS_{\text{l,eff}}}{PS_{\text{l,eff}} + PS_{\text{al,eff}}} \tag{3.5}$$

$$PS_{\text{blood-to-brain wt}} = PS_{\text{l,inf}} \times \frac{PS_{\text{al,eff}}}{PS_{\text{mdr1a,vivo}} + PS_{\text{l,eff}} + PS_{\text{al,eff}}} \tag{3.6}$$

$$PS_{\text{brain-to-blood wt}} = PS_{\text{al,inf}} \times \frac{PS_{\text{mdr1a,vivo}} + PS_{\text{l,eff}}}{PS_{\text{mdr1a,vivo}} + PS_{\text{l,eff}} + PS_{\text{al,eff}}} \tag{3.7}$$

where $PS_{\text{l,inf}}$, $PS_{\text{l,eff}}$, $PS_{\text{al,inf}}$, $PS_{\text{al,eff}}$, and $PS_{\text{mdr1a,vivo}}$ represent the PS products for luminal influx, luminal efflux (except for mdr1a efflux), abluminal influx, abluminal efflux, and mdr1a-mediated efflux in brain capillary endothelium, respectively (Fig. 3.7a). Therefore, the $K_{\text{p,brain}}$ ratio can be calculated as

$$K_{\text{p brain}}\,\text{ratio} = 1 + \frac{PS_{\text{mdr1a,vivo}}}{PS_{\text{l,eff}}} \tag{3.8}$$

Similarly, according to the reported in vitro pharmacokinetic model illustrated in Fig. 3.7a (Adachi et al. 2001), apical-to-basal ($PS_{\text{apical-to-basal}}$) and basal-to-apical ($PS_{\text{basal-to-apical}}$) flux across monolayers of parental LLC-PK1 cells and mouse mdr1a-transfected LLC-PK1 cells (L-mdr1a) can be given by

$$PS_{\text{apical-to-basal LLC-PK1}} = PS_{\text{a,inf}} \times \frac{PS_{\text{b,eff}}}{PS_{\text{a,eff}} + PS_{\text{b,eff}}} \tag{3.9}$$

$$PS_{\text{basal-to-apical LLC-PK1}} = PS_{\text{b,inf}} \times \frac{PS_{\text{a,eff}}}{PS_{\text{a,eff}} + PS_{\text{b,eff}}} \tag{3.10}$$

$$PS_{\text{apical-to-basal L-mdr1a}} = PS_{\text{a,inf}} \times \frac{PS_{\text{b,eff}}}{PS_{\text{mdr1a,vitro}} + PS_{\text{a,eff}} + PS_{\text{b,eff}}} \tag{3.11}$$

$$PS_{\text{basal-to-apical L-mdr1a}} = PS_{\text{b,inf}} \times \frac{PS_{\text{mdr1a,vitro}} + PS_{\text{a,eff}}}{PS_{\text{mdr1a,vitro}} + PS_{\text{a,eff}} + PS_{\text{b,eff}}} \tag{3.12}$$

where $PS_{a,inf}$, $PS_{a,eff}$, $PS_{b,inf}$, $PS_{b,eff}$, and $PS_{mdr1a,vitro}$ represent the PS products for the apical influx, apical efflux (except for mdr1a efflux), basal influx, basal efflux, and mdr1a-mediated efflux in L-mdr1a cells, respectively (Fig. 3.7a). The flux ratio ($PS_{basal\text{-}to\text{-}apical}/PS_{apical\text{-}to\text{-}basal}$) in LLC-PK1 and L-mdr1a cells can be calculated as

$$\text{flux ratio}_{\text{LLC-PK1}} = \frac{PS_{b,inf} \times PS_{a,eff}}{PS_{a,inf} \times PS_{b,eff}} \tag{3.13}$$

$$\text{flux ratio}_{\text{L-mdr1a}} = \frac{PS_{b,inf} \times \left(PS_{mdr1a,vitro} + PS_{a,eff}\right)}{PS_{a,inf} \times PS_{b,eff}} \tag{3.14}$$

Also, in vitro P-gp efflux ratio is defined as the ratio of the flux ratio in L-mdr1a cells to that in parental LLC-PK1 cells:

$$\text{In vitro P-gp efflux ratio} = 1 + \frac{PS_{mdr1a,vitro}}{PS_{a,eff}} \tag{3.15}$$

To reconstruct in vivo mdr1a efflux activity from in vitro activity, we linked $K_{p,brain}$ ratio (3.8) with in vitro P-gp efflux ratio (3.15) based on the following assumptions. If test compounds are specifically transported by mdr1a at the luminal membrane of the endothelium and the apical membrane of the L-mdr1a cell monolayer, $PS_{l,eff}$ can be assumed to be equal to $PS_{a,eff}$ because both processes occur by passive diffusion. Based on this assumption, the $K_{p,brain}$ ratio is given by (3.8) and (3.15) as follows:

$$K_{p\,brain}\,\text{ratio} = 1 + \left(\text{in vitro P-gp efflux ratio} - 1\right) \times \frac{PS_{mdr1a,vivo}}{PS_{mdr1a,vitro}} \tag{3.16}$$

Hoffmeyer et al. (2000) have suggested that the P-gp transport activity depends on P-gp protein expression level in vivo in humans. Shirasaka et al. (2008) and Tachibana et al. (2010) reported that P-gp transport activity was approximately proportional to P-gp protein expression level in vitro. Therefore, we assumed that the mdr1a activity is directly related to the mdr1a protein expression level, and the in vitro intrinsic transport activity of mdr1a (transport rate per mdr1a protein) is identical to that in vivo. Hence, (3.16) can be converted to

$$\begin{aligned} K_{p\,brain}\,\text{ratio} = {} & 1 + \left(\text{in vitro P-gp efflux ratio} - 1\right) \\ & \times \frac{\text{Mdr1a protein expression amounts in brain capillaries}}{\text{Mdr1a protein expression amounts in mdr1a-transfected cell monolayer}} \end{aligned} \tag{3.17}$$

Accordingly, the in vivo $K_{p,brain}$ ratio can be theoretically reconstructed from in vitro experimental data, i.e., transcellular transport study to determine the in vitro P-gp efflux ratio and QTAP to determine the mdr1a protein expression amounts.

To validate this reconstruction theory, transcellular transport of 11 mdr1a substrates was measured across monolayers of L-mdr1a and parental cells to determine the in vitro P-gp efflux ratios. Furthermore, the protein expression levels of mdr1a were determined in isolated mouse brain capillaries and L-mdr1a cell monolayers. The values obtained were 14.1 and 15.2 fmol/μg protein, respectively (Kamiie et al. 2008; Uchida et al. 2011a). Using these experimental data, we reconstructed the $K_{p,brain}$ ratio by using (3.17). As shown in Fig. 3.7b, all reconstructed $K_{p,brain}$ ratios were within a 1.6-fold range of observed values determined by in vivo administration study to wild-type and mdr1a/1b (–/–) mice (Uchida et al. 2011a). Therefore, we confirmed that the in vivo transport activity of mdr1a at the BBB can indeed be reconstructed from in vitro data integrated with absolute protein expression levels in mouse.

Using this QTAP-based reconstruction method, MDR1 transport activity at the BBB in humans can be reconstructed by integrating the protein level of P-gp in human brain capillaries (Uchida et al. 2011b), in vitro P-gp transport activity and P-gp protein level in human P-gp-transfected LLC-PK1 cell monolayers. It should also be possible to reconstruct the in vivo transport activities of other transporters at the human BBB similarly by using in vitro overexpression systems of target transporters and the protein expression levels. As already mentioned, imaging technologies such as PET and SPECT are currently applicable to evaluate in vivo activities of only a few transporters at the human BBB. From this point of view, we believe that QTAP-based reconstruction offers a rational methodology to clarify in vivo transporter activity in humans. QTAP avoids the issues associated with in vivo human studies, and is expected to be widely applicable, opening up the new research field of pharmacoproteomics (PPx).

3.6.2 QTAP-Based Reconstruction of Drug Distribution in Brain

Quantitative evaluation of drug distribution in human brain is a key issue in drug discovery and development, because the distribution of a drug is directly related to its pharmacological actions and toxic effects in the CNS. $K_{p,brain}$ and unbound brain-to-plasma concentration ratios ($K_{p,uu,brain}$) are the most commonly used parameters in this area, and are accepted as good indexes for identifying drugs that would be effective in treating CNS disorders, because CNS drugs have been shown to have higher $K_{p,brain}$ and $K_{p,uu,brain}$ values than non-CNS drugs (Friden et al. 2009). Therefore, after demonstrating that mdr1a efflux activity at the BBB could be successfully reconstructed from in vitro data (Uchida et al. 2011a), we examined whether $K_{p,brain}$

and $K_{p,uu,brain}$ can be reconstructed by integrating in vitro experimental data and reconstructed mdr1a efflux activity ($K_{p,brain}$ ratio).

The $K_{p,brain}$ ratio is defined as

$$K_{p\,brain}\text{ratio} = \frac{K_{p\,brain\,KO}}{K_{p\,brain\,WT}} \tag{3.18}$$

where $K_{p,brain\,WT}$ (= $K_{p,brain}$) and $K_{p,brain\,KO}$ represent the brain-to-plasma concentration ratios in wild-type and mdr1a/1b (–/–) mice, respectively. In addition, the $K_{p,brain\,KO}$ is defined in (3.19) based on unbound fractions in plasma ($f_{u,plasma}$) and brain ($f_{u,brain}$), and the ratio of the brain unbound concentration ($C_{u,brain\,KO}$) to the plasma unbound concentration ($C_{u,plasma\,KO}$).

$$K_{p\,brain\,KO} = \frac{f_{u,plasma}}{f_{u,brain}} \times \frac{C_{u,brain\,KO}}{C_{u,plasma\,KO}} \tag{3.19}$$

$C_{u,brain\,KO}/C_{u,plasma\,KO}$ can be replaced with the ratio of the blood-to-brain clearance to the brain-to-blood clearance across the BBB ($PS_{blood\text{-}to\text{-}brain\,KO}/PS_{brain\text{-}to\text{-}blood\,KO}$). For compounds transported only by mdr1a at the BBB, $PS_{blood\text{-}to\text{-}brain\,KO}$ can be assumed to be equal to $PS_{brain\text{-}to\text{-}blood\,KO}$ because both processes occur by passive diffusion in mdr1a/1b (–/–) mice (Fig. 3.8a). Therefore, $C_{u,brain\,KO}/C_{u,plasma\,KO} = 1$ and then $K_{p,brain\,KO}$ is obtained as

$$K_{p\,brain\,KO} = \frac{f_{u,plasma}}{f_{u,brain}} \tag{3.20}$$

Using (3.18) and (3.20), $K_{p,brain}$ can be finally described in terms of the $K_{p,brain}$ ratio and unbound fractions.

$$K_{p\,brain} = K_{p\,brain\,WT} = \frac{f_{u,plasma}}{f_{u,brain} \times K_{p\,brain}\text{ratio}} \tag{3.21}$$

In addition to $K_{p,brain}$, $K_{p,uu,brain}$ is defined as

$$K_{p,uu,brain} = \frac{C_{u,brain}}{C_{u,plasma}} = K_{p\,brain} \times \frac{f_{u,brain}}{f_{u,plasma}} \tag{3.22}$$

Using (3.21) and (3.22), $K_{p,uu,brain}$ can be described as the reciprocal of the $K_{p,brain}$ ratio.

$$K_{p,uu,brain} = \frac{1}{K_{p\,brain}\text{ratio}} \tag{3.23}$$

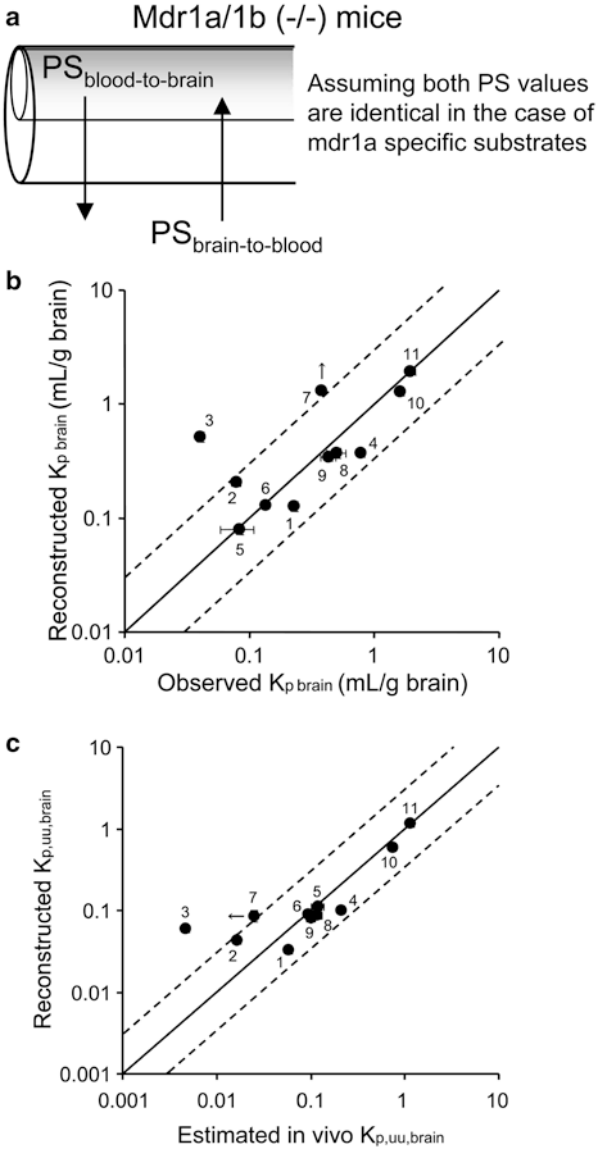

Fig. 3.8 Reconstruction of brain distribution of mdr1a substrates by means of a pharmacokinetic model using mdr1a function, plasma, and brain unbound fractions. (**a**) BBB in mdr1a/1b (−/−) mice. If a compound is actively transported only by mdr1a at the BBB of wild-type mice, the blood-to-brain permeability ($PS_{blood\text{-}to\text{-}brain}$) is assumed to be equal to the brain-to-blood permeability ($PS_{brain\text{-}to\text{-}blood}$) in mdr1a/1b (−/−) mice. (**b**) Comparison of the observed and reconstructed $K_{p,brain}$ for 11 mdr1a/P-gp substrates. (**c**) Comparison of reconstructed and estimated in vivo $K_{p,uu,brain}$ values for 11 mdr1a/P-gp substrates. The *solid line* passing through the origin represents the line of identity, and the broken lines represent threefold differences. *Each point* represents the mean ± S.E.M.. 1. Quinidine, 2. loperamide, 3. digoxin, 4. risperidone, 5. indinavir, 6. dexamethasone, 7. vinblastine, 8. paclitaxel, 9. verapamil, 10. loratadine, and 11. diazepam. Taken from Uchida et al. (2011a) and modified. The observed $K_{p,brain}$ values for risperidone, indinavir, paclitaxel, verapamil, loratadine, and diazepam were taken from Hendrikse et al. (1998), Kim et al. (1998), Chen et al. (2003), Kemper et al. (2004) and Doran et al. (2005)

To validate our reconstruction theory, we experimentally reconstructed $K_{p,brain}$ and $K_{p,uu,brain}$ of 11 mdr1a substrates according to (3.21) and (3.23), respectively, by using the reconstructed values of $K_{p,brain}$ ratio and in vitro experimental data of $f_{u,plasma}$ and $f_{u,brain}$. We found that the reconstructed $K_{p,brain}$ and $K_{p,uu,brain}$ agreed with the observed values within a threefold range for 9 of the 11 compounds (Fig. 3.8b, c; Uchida et al. 2011a). These results indicate that the $K_{p,brain}$ and $K_{p,uu,brain}$ of mdr1a substrates can be reconstructed from in vitro experimental data together with reconstructed mdr1a efflux activity and unbound fraction.

According to Friden et al. (2009), there is a 4.5-fold difference in $K_{p,brain}$ between CNS (4.31) and non-CNS (0.962) drugs, and there is also a 5.3-fold difference in $K_{p,uu,brain}$ between CNS (0.767) and non-CNS (0.145) drugs. Hence, in terms of brain distribution, the precision of QTAP-based predictions of $K_{p,brain}$ and $K_{p,uu,brain}$ could be high enough to evaluate whether compounds are likely to be suitable for use as CNS or non-CNS drugs. However, the ranges of these parameters, especially $K_{p,brain}$, among CNS or non-CNS drugs are large, so it would be difficult to identify CNS or non-CNS drugs on the basis of $K_{p,brain}$ alone or $K_{p,uu,brain}$ alone. A combination of $K_{p,brain}$ and $K_{p,uu,brain}$ predictions will be more reliable.

Human $K_{p,brain}$ and $K_{p,uu,brain}$ can be also predicted from in vitro data by integrating a reconstructed $K_{p,brain}$ ratio, $f_{u,plasma}$, and $f_{u,brain}$ in humans according to (3.21) and (3.23). Human brain tissue is necessary to measure $f_{u,brain}$, and is usually obtained in a frozen state. Therefore, human $f_{u,brain}$ may not be accurately determined by the brain slice method, because the cells in frozen brain could be partially ruptured. Alternatively, Summerfield et al. (2008) determined human $f_{u,brain}$ by the brain homogenate method with commercially available frozen human brain. Although $f_{u,brain}$ measured by the homogenate method alone is less relevant to the in vivo situation than that measured by the brain slice method (Friden et al. 2007), the combination of the homogenate method with a pH partition model is likely to give a value of $f_{u,brain}$ that is more relevant to the in vivo situation (Friden et al. 2011). Therefore, the homogenate method using a pH partition model might be useful for the prediction of human $K_{p,brain}$.

$K_{p,brain}$ and $K_{p,uu,brain}$ can be predicted from the results of only in vitro experiments including QTAP, in vitro transport experiments, the brain slice method (or equilibrium dialysis with brain homogenate) and equilibrium dialysis with plasma. All the experiments can be performed with LC-MS/MS to quantify compound concentrations, so that nonlabeled compounds can be used for the $K_{p,brain}$ and $K_{p,uu,brain}$ predictions. So far, imaging technologies such as PET and SPECT have been the only analytical methods able to quantitatively evaluate brain distribution of compounds in humans, but they require radio-labeled compounds, which have many disadvantages. Therefore, we believe that QTAP-based reconstruction represents a breakthrough in evaluating drug distribution in the brain, and should be useful to predict drug distribution in the human brain at an early stage of drug discovery and development.

3.7 Conclusions and Perspectives

QTAP is a highly sensitive (~0.1 fmol/μg protein at present) and selective protein quantification method that is able to determine absolute expression levels of many proteins simultaneously (37 proteins at present), and is applicable to a wide range of proteins, including transporters, enzymes, receptors, and channels. By applying QTAP to BBB research, we have shown that it is a useful tool to understand the molecular basis of transport functions at the BBB, as well as drug distribution in the brain, and species/interindividual/age differences. We have further demonstrated the usefulness of QTAP for reconstruction of BBB transporter activity and drug distribution in the brain from in vitro data. It is noteworthy that QTAP overcomes major limitations of previous methods available for BBB research, and we believe it represents a breakthrough that will open up a new research field, BBB pharmacoproteomics.

It has recently been reported that the activities and expression levels of various transporters at the BBB are changed in CNS disorders (Loscher and Potschka 2005; Miller et al. 2008; Sakata et al. 2011; Zhang et al. 2012). However, in humans, few quantitative data are available regarding the changes of transporter activities in CNS disorders compared to normal brain. QTAP provides a tool to address this issue and is expected to prove useful in discovery and development of drugs to treat CNS disorders. Moreover, it should be possible to validate the reconstruction of transporter activity at the human BBB and the prediction of drug distribution in the human brain with QTAP by comparison of the QTAP results with in vivo human data obtained with imaging technologies, where these are available. The combination of QTAP-based reconstruction and imaging technologies should open the way to prediction of the distribution of a variety of compounds in the human brain in normal and disease states.

3.8 Points for Discussion

1. How does the QTAP technique bring benefits to basic research or drug discovery and development?
2. Why is it necessary to use the QTAP technique to understand important variations including in vitro/in vivo, species, individual, age, gender, normal/disease, racial, and strain differences in the activities of functional proteins (transporters, receptors, channels, enzymes, and tight junction proteins) at the CNS barriers?
3. Can the QTAP technique replace antibody-based analysis?
4. What is the advantage of absolute quantification for protein expression, as opposed to relative comparisons?
5. How can we effectively use the QTAP technique in combination with others, e.g., global proteomics, mRNA analysis, and functional assays, in CNS barrier studies?

6. Are protein expression levels always correlated to the activities of functional proteins? That is, can we assume that the activity per molecule does not change? If not, what kinds of factors could affect the activity per molecule?
7. Why would QTAP-based reconstruction be useful to clarify in vivo activities of functional proteins (e.g., transporters, receptors, channels, enzymes, and tight junction proteins) at the CNS barriers?
8. How much can we increase the success rate of CNS drugs in clinical trials by using QTAP-based predictions of $K_{p,brain}$ and $K_{p,uu,brain}$ in human brain?
9. The protein expression profile at the mouse BBB is significantly different from that at the human BBB while cynomolgus monkeys show a similar profile to human. Based on these data, do you think that the mouse is a useful animal in CNS barriers research? How should we deal with the data obtained in mouse experiments in the future?
10. Except for P-gp, which molecules play an important role in controlling drug distribution in the human brain and need the QTAP-based prediction of in vivo activities in drug discovery and development?

Acknowledgements We thank N. Handa and A. Niitomi for secretarial assistance. The studies mentioned in this chapter were supported in part by four Grants-in-Aid for Scientific Research (S) [KAKENHI: 18109002], Scientific Research (A) [KAKENHI: 24249011], Young Scientists (B) [KAKENHI: 23790170], and the Japan Society for the Promotion of Science (JSPS) Fellows [KAKENHI: 207291] from the JSPS. The studies were also supported in part by a Grant-in-Aid for Scientific Research on Priority Area [KAKENHI: 17081002] from The Ministry of Education, Culture, Sports, Science and Technology (MEXT), three Grants for Development of Creative Technology Seeds Supporting Program for Creating University Ventures, Creation of Strategic Innovation Project and Revitalization Promotion Program (A-STEP) from Japan Science and Technology Agency (JST). Furthermore, the studies were also supported in part by the Industrial Technology Research Grant Program from New Energy and the Industrial Technology Development Organization (NEDO) of Japan, and a Health and Labour Sciences Research Grant from The Ministry of Health, Labour and Welfare.

Conflict of Interest

Tetsuya Terasaki and Sumio Ohtsuki are full professors of Tohoku University and Kumamoto University, respectively, and are also directors of Proteomedix Frontiers. This research was not supported by Proteomedix Frontiers and their positions at Proteomedix Frontiers do not present any financial conflicts. The other authors declared no conflict of interest.

References

Adachi Y, Suzuki H, Sugiyama Y (2001) Comparative studies on in vitro methods for evaluating in vivo function of MDR1 P-glycoprotein. Pharm Res 18:1660–1668

Aebersold R, Mann M (2003) Mass spectrometry-based proteomics. Nature 422:198–207

Ang CS, Phung J, Nice EC (2011) The discovery and validation of colorectal cancer biomarkers. Biomed Chromatogr 25:82–99

Arriza JL, Fairman WA, Wadiche JI, Murdoch GH, Kavanaugh MP, Amara SG (1994) Functional comparisons of three glutamate transporter subtypes cloned from human motor cortex. J Neurosci 14:5559–5569

Bauer M, Zeitlinger M, Karch R, Matzneller P, Stanek J, Jager W, Bohmdorfer M, Wadsak W, Mitterhauser M, Bankstahl JP, Loscher W, Koepp M, Kuntner C, Muller M, Langer O (2012)

Pgp-mediated interaction between (R)-[^{11}C]verapamil and tariquidar at the human blood-brain barrier: a comparison with rat data. Clin Pharmacol Ther 91:227–233

Ceballos A, Belinchon MM, Sanchez-Mendoza E, Grijota-Martinez C, Dumitrescu AM, Refetoff S, Morte B, Bernal J (2009) Importance of monocarboxylate transporter 8 for the blood-brain barrier-dependent availability of 3,5,3′-triiodo-L-thyronine. Endocrinology 150:2491–2496

Chen C, Hanson E, Watson JW, Lee JS (2003) P-glycoprotein limits the brain penetration of non-sedating but not sedating H1-antagonists. Drug Metab Dispos 31:312–318

Chen P, Li X, Sun Y, Liu Z, Cao R, He Q, Wang M, Xiong J, Xie J, Wang X, Liang S (2006) Proteomic analysis of rat hippocampal plasma membrane: characterization of potential neuronal-specific plasma membrane proteins. J Neurochem 98:1126–1140

Ciccimaro E, Hanks SK, Yu KH, Blair IA (2009) Absolute quantification of phosphorylation on the kinase activation loop of cellular focal adhesion kinase by stable isotope dilution liquid chromatography/mass spectrometry. Anal Chem 81:3304–3313

de Vries NA (2009) Preclinical models to study the impact of the blood-brain barrier in brain tumor chemotherapy. Doctor's thesis, Division of Clinical Chemistry, The Netherlands Cancer Institute/Antoni van Leeuwenhoek Hospital, Amsterdam, The Netherlands and Department of Pharmacy and Pharmacology, The Netherlands Cancer Institute/Slotervaart Hospital, Amsterdam, The Netherlands

Domanski D, Murphy LC, Borchers CH (2010) Assay development for the determination of phosphorylation stoichiometry using multiple reaction monitoring methods with and without phosphatase treatment: application to breast cancer signaling pathways. Anal Chem 82:5610–5620

Domon B, Aebersold R (2006) Mass spectrometry and protein analysis. Science 312:212–217

Doran A, Obach RS, Smith BJ, Hosea NA, Becker S, Callegari E, Chen C, Chen X, Choo E, Cianfrogna J, Cox LM, Gibbs JP, Gibbs MA, Hatch H, Hop CE, Kasman IN, Laperle J, Liu J, Liu X, Logman M, Maclin D, Nedza FM, Nelson F, Olson E, Rahematpura S, Raunig D, Rogers S, Schmidt K, Spracklin DK, Szewc M, Troutman M, Tseng E, Tu M, Van Deusen JW, Venkatakrishnan K, Walens G, Wang EQ, Wong D, Yasgar AS, Zhang C (2005) The impact of P-glycoprotein on the disposition of drugs targeted for indications of the central nervous system: evaluation using the MDR1A/1B knockout mouse model. Drug Metab Dispos 33: 165–174

Dyer J, Barker PJ, Shirazi-Beechey SP (1997) Nutrient regulation of the intestinal Na $^{+}$/glucose co-transporter (SGLT1) gene expression. Biochem Biophys Res Commun 230:624–629

Frank R, Hargreaves R (2003) Clinical biomarkers in drug discovery and development. Nat Rev Drug Discov 2:566–580

Friden M, Gupta A, Antonsson M, Bredberg U, Hammarlund-Udenaes M (2007) In vitro methods for estimating unbound drug concentrations in the brain interstitial and intracellular fluids. Drug Metab Dispos 35:1711–1719

Friden M, Winiwarter S, Jerndal G, Bengtsson O, Wan H, Bredberg U, Hammarlund-Udenaes M, Antonsson M (2009) Structure-brain exposure relationships in rat and human using a novel data set of unbound drug concentrations in brain interstitial and cerebrospinal fluids. J Med Chem 52:6233–6243

Friden M, Bergstrom F, Wan H, Rehngren M, Ahlin G, Hammarlund-Udenaes M, Bredberg U (2011) Measurement of unbound drug exposure in brain: modeling of pH partitioning explains diverging results between the brain slice and brain homogenate methods. Drug Metab Dispos 39:353–362

Fukumoto H, Cheung BS, Hyman BT, Irizarry MC (2002) Beta-secretase protein and activity are increased in the neocortex in Alzheimer disease. Arch Neurol 59:1381–1389

Hendrikse NH, Schinkel AH, De Vries EG, Fluks E, Van Der Graaf WT, Willemsen AT, Vaalburg W, Franssen EJ (1998) Complete in vivo reversal of P-glycoprotein pump function in the blood-brain barrier visualized with positron emission tomography. Br J Pharmacol 124: 1413–1418

Heuer H (2007) The importance of thyroid hormone transporters for brain development and function. Best Pract Res Clin Endocrinol Metab 21:265–276

Hoffmeyer S, Burk O, Von Richter O, Arnold HP, Brockmoller J, Johne A, Cascorbi I, Gerloff T, Roots I, Eichelbaum M, Brinkmann U (2000) Functional polymorphisms of the human multidrug-resistance gene: multiple sequence variations and correlation of one allele with P-glycoprotein expression and activity in vivo. Proc Natl Acad Sci U S A 97:3473–3478

Hosoya K, Sugawara M, Asaba H, Terasaki T (1999) Blood-brain barrier produces significant efflux of L-aspartic acid but not D-aspartic acid: in vivo evidence using the brain efflux index method. J Neurochem 73:1206–1211

Ito K, Uchida Y, Ohtsuki S, Aizawa S, Kawakami H, Katsukura Y, Kamiie J, Terasaki T (2011) Quantitative membrane protein expression at the blood-brain barrier of adult and younger cynomolgus monkeys. J Pharm Sci 100:3939–3950

Izumi Y, Tokuda K, O'dell KA, Zorumski CF, Narahashi T (2007) Neuroexcitatory actions of Tamiflu and its carboxylate metabolite. Neurosci Lett 426:54–58

Kamiie J, Ohtsuki S, Iwase R, Ohmine K, Katsukura Y, Yanai K, Sekine Y, Uchida Y, Ito S, Terasaki T (2008) Quantitative atlas of membrane transporter proteins: development and application of a highly sensitive simultaneous LC/MS/MS method combined with novel in-silico peptide selection criteria. Pharm Res 25:1469–1483

Kanai Y, Trotti D, Nussberger S, Hediger MA (1997) The highaffinity glutamate transporter family. In: Reith MEA (ed) Neurotransmitter transporters: structure, function, and regulation. Humana Press, Totowa, NJ, pp 171–213

Kawakami H, Ohtsuki S, Kamiie J, Suzuki T, Abe T, Terasaki T (2011) Simultaneous absolute quantification of 11 cytochrome P450 isoforms in human liver microsomes by liquid chromatography tandem mass spectrometry with In silico target peptide selection. J Pharm Sci 100:341–352

Kemper EM, Cleypool C, Boogerd W, Beijnen JH, Van Tellingen O (2004) The influence of the P-glycoprotein inhibitor zosuquidar trihydrochloride (LY335979) on the brain penetration of paclitaxel in mice. Cancer Chemother Pharmacol 53:173–178

Kim RB, Fromm MF, Wandel C, Leake B, Wood AJ, Roden DM, Wilkinson GR (1998) The drug transporter P-glycoprotein limits oral absorption and brain entry of HIV-1 protease inhibitors. J Clin Invest 101:289–294

Kito K, Ota K, Fujita T, Ito T (2007) A synthetic protein approach toward accurate mass spectrometric quantification of component stoichiometry of multiprotein complexes. J Proteome Res 6:792–800

Kola I, Landis J (2004) Can the pharmaceutical industry reduce attrition rates? Nat Rev Drug Discov 3:711–715

Kusuhara H, Sugiyama Y (2009) In vitro-in vivo extrapolation of transporter-mediated clearance in the liver and kidney. Drug Metab Pharmacokinet 24:37–52

Kusuhara H, Sekine T, Utsunomiya-Tate N, Tsuda M, Kojima R, Cha SH, Sugiyama Y, Kanai Y, Endou H (1999) Molecular cloning and characterization of a new multispecific organic anion transporter from rat brain. J Biol Chem 274:13675–13680

Langenfeld E, Zanger UM, Jung K, Meyer HE, Marcus K (2009) Mass spectrometry-based absolute quantification of microsomal cytochrome P450 2D6 in human liver. Proteomics 9: 2313–2323

Li N, Nemirovskiy OV, Zhang Y, Yuan H, Mo J, Ji C, Zhang B, Brayman TG, Lepsy C, Heath TG, Lai Y (2008) Absolute quantification of multidrug resistance-associated protein 2 (MRP2/ABCC2) using liquid chromatography tandem mass spectrometry. Anal Biochem 380:211–222

Loscher W, Potschka H (2005) Drug resistance in brain diseases and the role of drug efflux transporters. Nat Rev Neurosci 6:591–602

Miller DS, Bauer B, Hartz AM (2008) Modulation of P-glycoprotein at the blood-brain barrier: opportunities to improve central nervous system pharmacotherapy. Pharmacol Rev 60: 196–209

Nagano K, Taoka M, Yamauchi Y, Itagaki C, Shinkawa T, Nunomura K, Okamura N, Takahashi N, Izumi T, Isobe T (2005) Large-scale identification of proteins expressed in mouse embryonic stem cells. Proteomics 5:1346–1361

Niessen J, Jedlitschky G, Grube M, Bien S, Schwertz H, Ohtsuki S, Kawakami H, Kamiie J, Oswald S, Starke K, Strobel U, Siegmund W, Rosskopf D, Greinacher A, Terasaki T, Kroemer HK (2009) Human platelets express organic anion-transporting peptide 2B1, an uptake transporter for atorvastatin. Drug Metab Dispos 37:1129–1137

Niessen J, Jedlitschky G, Grube M, Kawakami H, Kamiie J, Ohtsuki S, Schwertz H, Bien S, Starke K, Ritter C, Strobel U, Greinacher A, Terasaki T, Kroemer HK (2010) Expression of ABC-type transport proteins in human platelets. Pharmacogenet Genomics 20:396–400

Obuchi W, Ohtsuki S, Uchida Y, Ohmine K, Yamori T, Terasaki T (2013) Identification of transporters associated with etoposide sensitivity of stomach cancer cell lines and methotrexate sensitivity of breast cancer cell lines by quantitative targeted absolute proteomics. Mol Pharmacol 83:490–500. doi:10.1124/mol.112.081083

Ohmine K, Kawaguchi K, Ohtsuki S, Motoi F, Egawa S, Unno M, Terasaki T (2012) Attenuation of phosphorylation by deoxycytidine kinase is key to acquired gemcitabine resistance in a pancreatic cancer cell line: targeted proteomic and metabolomic analyses in PK9 cells. Pharm Res 29:2006–2016

Ohtsuki S, Terasaki T (2007) Contribution of carrier-mediated transport systems to the blood-brain barrier as a supporting and protecting interface for the brain; importance for CNS drug discovery and development. Pharm Res 24:1745–1758

Ohtsuki S, Uchida Y, Kubo Y, Terasaki T (2011) Quantitative targeted absolute proteomics-based ADME research as a new path to drug discovery and development: methodology, advantages, strategy, and prospects. J Pharm Sci 100:3547–3559

Ohtsuki S, Schaefer O, Kawakami H, Inoue T, Liehner S, Saito A, Ishiguro N, Kishimoto W, Ludwig-Schwellinger E, Ebner T, Terasaki T (2012) Simultaneous absolute protein quantification of transporters, cytochromes P450, and UDP-glucuronosyltransferases as a novel approach for the characterization of individual human liver: comparison with mRNA levels and activities. Drug Metab Dispos 40:83–92

Ohtsuki S, Ikeda C, Uchida Y, Sakamoto Y, Miller F, Glacial F, Decleves X, Scherrmann JM, Couraud PO, Kubo Y, Tachikawa M, Terasaki T (2013) Quantitative targeted absolute proteomic analysis of transporters, receptors and junction proteins for validation of human cerebral microvascular endothelial cell line hCMEC/D3 as a human blood-brain barrier model. Mol Pharm 10:289–296. doi:10.1021/mp3004308

O'kane RL, Martinez-Lopez I, Dejoseph MR, Vina JR, Hawkins RA (1999) Na(+)-dependent glutamate transporters (EAAT1, EAAT2, and EAAT3) of the blood-brain barrier. A mechanism for glutamate removal. J Biol Chem 274:31891–31895

Ose A, Kusuhara H, Yamatsugu K, Kanai M, Shibasaki M, Fujita T, Yamamoto A, Sugiyama Y (2008) P-glycoprotein restricts the penetration of oseltamivir across the blood-brain barrier. Drug Metab Dispos 36:427–434

Ose A, Ito M, Kusuhara H, Yamatsugu K, Kanai M, Shibasaki M, Hosokawa M, Schuetz JD, Sugiyama Y (2009) Limited brain distribution of [3R,4R,5S]-4-acetamido-5-amino-3-(1-ethylpropoxy)-1-cyclohexene-1-carboxyl ate phosphate (Ro 64-0802), a pharmacologically active form of oseltamivir, by active efflux across the blood-brain barrier mediated by organic anion transporter 3 (Oat3/Slc22a8) and multidrug resistance-associated protein 4 (Mrp4/Abcc4). Drug Metab Dispos 37:315–321

Pardridge WM (2002) Why is the global CNS pharmaceutical market so under-penetrated? Drug Discov Today 7:5–7

Patterson SD, Aebersold RH (2003) Proteomics: the first decade and beyond. Nat Genet 33 Suppl:311–323

Pshezhetsky AV, Fedjaev M, Ashmarina L, Mazur A, Budman L, Sinnett D, Labuda D, Beaulieu JF, Menard D, Nifant'ev I, Levy E (2007) Subcellular proteomics of cell differentiation: quantitative analysis of the plasma membrane proteome of Caco-2 cells. Proteomics 7:2201–2215

Roberts LM, Woodford K, Zhou M, Black DS, Haggerty JE, Tate EH, Grindstaff KK, Mengesha W, Raman C, Zerangue N (2008) Expression of the thyroid hormone transporters monocarboxylate transporter-8 (SLC16A2) and organic ion transporter-14 (SLCO1C1) at the blood-brain barrier. Endocrinology 149:6251–6261

Sakata S, Fujiwara M, Ohtsuka K, Kamma H, Nagane M, Sakamoto A, Fujioka Y (2011) ATP-binding cassette transporters in primary central nervous system lymphoma: decreased expression of MDR1 P-glycoprotein and breast cancer resistance protein in tumor capillary endothelial cells. Oncol Rep 25:333–339

Schwamborn K, Caprioli RM (2010) MALDI imaging mass spectrometry–painting molecular pictures. Mol Oncol 4:529–538

Shawahna R, Uchida Y, Decleves X, Ohtsuki S, Yousif S, Dauchy S, Jacob A, Chassoux F, Daumas-Duport C, Couraud PO, Terasaki T, Scherrmann JM (2011) Transcriptomic and quantitative proteomic analysis of transporters and drug metabolizing enzymes in freshly isolated human brain microvessels. Mol Pharm 8:1332–1341

Shirasaka Y, Sakane T, Yamashita S (2008) Effect of P-glycoprotein expression levels on the concentration-dependent permeability of drugs to the cell membrane. J Pharm Sci 97:553–565

Sugiura Y, Setou M (2010) Imaging mass spectrometry for visualization of drug and endogenous metabolite distribution: toward in situ pharmacometabolomes. J Neuroimmune Pharmacol 5:31–43

Summerfield SG, Lucas AJ, Porter RA, Jeffrey P, Gunn RN, Read KR, Stevens AJ, Metcalf AC, Osuna MC, Kilford PJ, Passchier J, Ruffo AD (2008) Toward an improved prediction of human in vivo brain penetration. Xenobiotica 38:1518–1535

Syvanen S, Lindhe O, Palner M, Kornum BR, Rahman O, Langstrom B, Knudsen GM, Hammarlund-Udenaes M (2009) Species differences in blood-brain barrier transport of three positron emission tomography radioligands with emphasis on P-glycoprotein transport. Drug Metab Dispos 37:635–643

Tachibana T, Kitamura S, Kato M, Mitsui T, Shirasaka Y, Yamashita S, Sugiyama Y (2010) Model analysis of the concentration-dependent permeability of P-gp substrates. Pharm Res 27:442–446

Tachikawa M, Watanabe M, Hori S, Fukaya M, Ohtsuki S, Asashima T, Terasaki T (2005) Distinct spatio-temporal expression of ABCA and ABCG transporters in the developing and adult mouse brain. J Neurochem 95:294–304

Takano A, Kusuhara H, Suhara T, Ieiri I, Morimoto T, Lee YJ, Maeda J, Ikoma Y, Ito H, Suzuki K, Sugiyama Y (2006) Evaluation of in vivo P-glycoprotein function at the blood-brain barrier among MDR1 gene polymorphisms by using 11C-verapamil. J Nucl Med 47:1427–1433

Takashima T, Yokoyama C, Mizuma H, Yamanaka H, Wada Y, Onoe K, Nagata H, Tazawa S, Doi H, Takahashi K, Morita M, Kanai M, Shibasaki M, Kusuhara H, Sugiyama Y, Onoe H, Watanabe Y (2011) Developmental changes in P-glycoprotein function in the blood-brain barrier of nonhuman primates: PET study with R-^{11}C-verapamil and ^{11}C-oseltamivir. J Nucl Med 52:950–957

Tetsuka K, Takanaga H, Ohtsuki S, Hosoya K, Terasaki T (2003) The l-isomer-selective transport of aspartic acid is mediated by ASCT2 at the blood-brain barrier. J Neurochem 87:891–901

Tohyama K, Kusuhara H, Sugiyama Y (2004) Involvement of multispecific organic anion transporter, Oatp14 (Slc21a14), in the transport of thyroxine across the blood-brain barrier. Endocrinology 145:4384–4391

Toovey S, Rayner C, Prinssen E, Chu T, Donner B, Thakrar B, Dutkowski R, Hoffmann G, Breidenbach A, Lindemann L, Carey E, Boak L, Gieschke R, Sacks S, Solsky J, Small I, Reddy D (2008) Assessment of neuropsychiatric adverse events in influenza patients treated with oseltamivir: a comprehensive review. Drug Saf 31:1097–1114

Trajkovic M, Visser TJ, Mittag J, Horn S, Lukas J, Darras VM, Raivich G, Bauer K, Heuer H (2007) Abnormal thyroid hormone metabolism in mice lacking the monocarboxylate transporter 8. J Clin Invest 117:627–635

Tsuruoka S, Ishibashi K, Yamamoto H, Wakaumi M, Suzuki M, Schwartz GJ, Imai M, Fujimura A (2002) Functional analysis of ABCA8, a new drug transporter. Biochem Biophys Res Commun 298:41–45

Uchida Y, Kamiie J, Ohtsuki S, Terasaki T (2007) Multichannel liquid chromatography-tandem mass spectrometry cocktail method for comprehensive substrate characterization of multidrug resistance-associated protein 4 transporter. Pharm Res 24:2281–2296

Uchida Y, Ohtsuki S, Kamiie J, Terasaki T (2011a) Blood-brain barrier (BBB) pharmacoproteomics: reconstruction of in vivo brain distribution of 11 P-glycoprotein substrates based on the BBB transporter protein concentration, in vitro intrinsic transport activity, and unbound fraction in plasma and brain in mice. J Pharmacol Exp Ther 339:579–588

Uchida Y, Ohtsuki S, Katsukura Y, Ikeda C, Suzuki T, Kamiie J, Terasaki T (2011b) Quantitative targeted absolute proteomics of human blood-brain barrier transporters and receptors. J Neurochem 117:333–345

Urquhart BL, Kim RB (2009) Blood-brain barrier transporters and response to CNS-active drugs. Eur J Clin Pharmacol 65:1063–1070

Wang MZ, Wu JQ, Dennison JB, Bridges AS, Hall SD, Kornbluth S, Tidwell RR, Smith PC, Voyksner RD, Paine MF, Hall JE (2008) A gel-free MS-based quantitative proteomic approach accurately measures cytochrome P450 protein concentrations in human liver microsomes. Proteomics 8:4186–4196

Wen PY, Kesari S (2008) Malignant gliomas in adults. N Engl J Med 359:492–507

Yagi T, Ohkubo M (2010) Cost and time period for drug discovery and development. JPMA Newslett 136:33–35

Yoshikawa A, Nakada M, Ohtsuki S, Hayashi Y, Obuchi W, Sato Y, Ikeda C, Watanabe T, Kawahara Y, Hasegawa T, Sabit H, Kita D, Nakanuma Y, Terasaki T, Hamada JI (2012) Recurrent anaplastic meningioma treated by sunitinib based on results from quantitative proteomics. Neuropathol Appl Neurobiol 38:105–110

Zhang C, Kwan P, Zuo Z, Baum L (2012) The transport of antiepileptic drugs by P-glycoprotein. Adv Drug Deliv Rev 64:930–942

Zorumski CF, Olney JW (1993) Excitotoxic neuronal damage and neuropsychiatric disorders. Pharmacol Ther 59:145–162

Chapter 4
Drug Metabolism at the Blood–Brain and Blood–CSF Barriers

Xavier Declèves, Nathalie Strazielle, Jean-Michel Scherrmann, and Jean-François Ghersi-Egea

Abstract Drug metabolism is in most cases a detoxification process allowing the organism to inactivate and eliminate foreign substances to which it is exposed. While the liver is the main site of drug metabolism, drug-metabolizing enzymes that catalyze functionalization and conjugation reactions have been detected in the brain, and several of these enzymes are notably enriched at blood–brain interfaces. This chapter summarizes the principles of drug metabolism, reviews the molecular and functional evidence for drug-metabolizing enzyme location at both the blood–brain barrier (BBB) and blood–CSF barrier (BCSFB), and discusses their functional significance for modulating cerebral drug delivery and brain toxin exposure.

4.1 Introduction and History of Cerebral Drug Metabolism

Drug metabolism is a process whereby xenobiotics (either exogenous non-nutrient organic compounds including pharmacological molecules, or environmental toxics) are enzymatically transformed in the body to form one or several metabolites. These biotransformation reactions largely take place in the liver and strongly influence

X. Declèves • J.-M. Scherrmann
INSERM, U705, CNRS UMR 8206, Universités Paris Descartes et Didero, Paris, France

N. Strazielle
Brain-i, Lyon, France

J.-F. Ghersi-Egea (✉)
Inserm U1028, CNRS UMR 5292, Lyon Neuroscience Research Center, Lyon-1 University, Lyon, France
e-mail: jean-francois.ghersi-egea@inserm.fr

M. Hammarlund-Udenaes et al. (eds.), *Drug Delivery to the Brain*, AAPS Advances in the Pharmaceutical Sciences Series 10, DOI 10.1007/978-1-4614-9105-7_4,

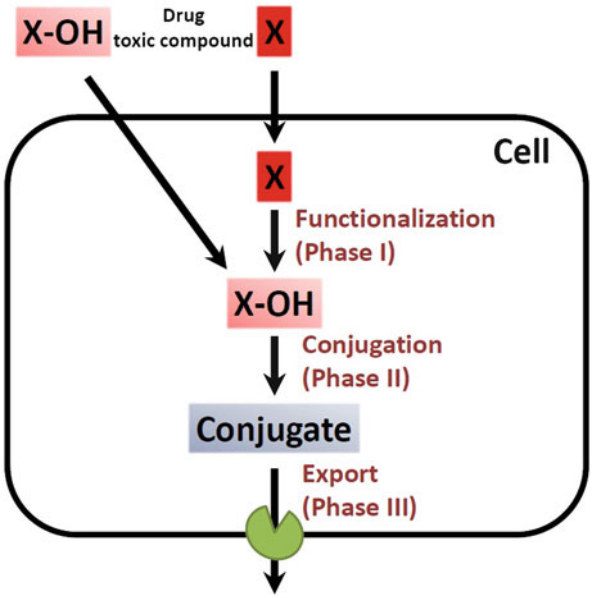

Fig. 4.1 General principle of drug metabolism

the transport and partitioning of a compound within the body, its toxicity, and its rate and route of elimination. About 50 multispecific enzymes catalyze the biotransformation of xenobiotics in human. Additional enzymes usually involved in endogenous metabolism also participate to the biotransformation of selected drugs. Drug metabolism is a multiphase process (Fig. 4.1). Phase I is functionalizing and generally oxidative, but can be reductive in some instances (Cashman 2000; Ghersi-Egea et al. 1998; Nebert and Russell 2002). Functionalization enzymes generate metabolites which are more polar than the parent compounds, and more readily eliminated. Phase II of drug metabolism correspond to conjugation processes whereby a hydrophilic moiety such as a glucuronic acid, a sulfate, or a cysteine-bearing molecule (e.g., glutathione) is bound to the parent drug or the phase I metabolite (Duffel et al. 2001; Eaton and Bammler 1999; King et al. 2000). Figure 4.2 summarizes the main pathways of drug metabolism and enzymes involved in these pathways. Phase III of metabolism involves transport processes mediating the efflux of metabolites out of the producing cells and their excretion from the body. The best known phase III transport proteins belong to the ATP binding cassette (ABC) C subfamily of transporters, and are often referred to as multidrug-related resistance proteins (Ishikawa 1992). They accept a large range of drug conjugates as substrates. Overall these different metabolic and transport steps allow the biotransformation of drugs to polar metabolites that are readily excreted out of the body. The produced metabolites are usually inactive or less active than the parent compounds. Yet, in some instances, they can be pharmacologically more active, such as for morphine-6-glucuronide which has stronger analgesic properties than morphine (Christrup 1997).

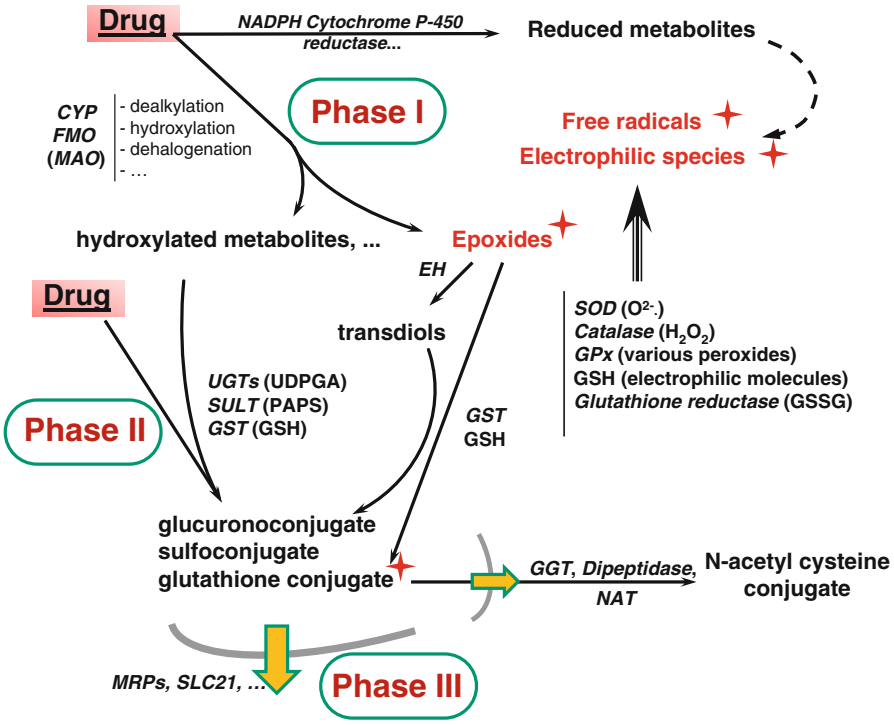

Fig. 4.2 Main pathways of drug metabolism. Functionalization enzymes (Phase I) generate metabolites which are more polar than the parent compounds, and more readily excretable. They include the numerous isoforms of cytochrome P-450 (CYP), also called mixed function oxidase, the flavin monoamine oxidases (FMO), and also more specific oxidation enzymes such as monoamine oxidases (MAO). They also include enzymes such as NADPH-cytochrome P-450 reductase responsible for xenobiotic (e.g., nitro-compounds) reduction. Oxidative and reductive processes can lead to the formation of reactive metabolites such as epoxides, or can generate oxygen derived free radicals. These are in turn inactivated by epoxide hydrolases (EH), conjugation to glutathione, or reactive oxygen species-inactivating enzymes. Phase II of drug metabolism corresponds to a conjugation process whereby a hydrophilic moiety such as a glucuronic acid, a sulfate or a cysteine-bearing molecule (e.g., glutathione) is bound to the drug or the phase I metabolites. This biotransformation is catalyzed by uridine diphosphoglucuronosyl transferases (UGTs), glutathione-S-transferases (GSTs), or sulfotransferases (SULTs). Glutathione conjugates can be further metabolized along the mercapturic acid pathway involving two ectoenzymes, gamma-glutamyltranspeptidase (GGT) and dipeptidase, and N-acetyltransferase (NAT). Usually inactive or less active than the parent compounds, the produced metabolites in some instances can be pharmacologically more active or toxic. *Red stars* refer to classes of metabolites that can be potentially harmful. Names or abbreviations of enzymes appear in *italic*. Phase III of drug metabolism refer to the efflux of the conjugates out of the cells, which primarily involves transporters of the multidrug resistance-associated protein family (MRPs) and of the SLC21 family of organic anion transport proteins. Other abbreviations: *SOD* superoxide dismutase, *GPx* glutathione peroxidase, *GSH* and *GSSG* reduced and oxidized glutathione, respectively. Modified from Strazielle et al. (2004)

They can also be more toxic as exemplified by the high carcinogenicity of hydroperoxide metabolites of benzo[a]pyrene (Gelhaus et al. 2011) (Fig. 4.2). A specific feature of drug metabolism is that at least in the liver the expression of many phase I and phase II isoenzymes and some phase III transporters can be transcriptionally induced upon exposure to drugs or other exogenous compounds. This occurs through different mechanisms. For instance, binding of polycyclic aryl hydrocarbons to the cytosolic aryl hydrocarbon receptor (AhR) induces the translocation of this receptor into the nucleus, which subsequently activates an enhancer DNA element called xenobiotic responsive element (XRE) present in the promoter of a number of drug-metabolizing enzyme genes. Other xenobiotics such as phenobarbital, dexamethasone, and fibrates interact with nuclear receptors such as the constitutive androstane receptor (CAR), the pregnane X receptor (PXR), and the peroxisome proliferator activated receptor (PPAR), respectively (Aleksunes and Klaassen 2012; Tolson and Wang 2010; Xu et al. 2005). Finally, electrophilic compounds can induce the nuclear translocation of the nuclear factor (erythroid-derived 2)-like 2 (nrf2). The activation of the nrf2 pathway enhances the transcription of genes bearing the antioxidant response element (ARE), which include genes of glutathione-S-transferases (GSTs) and enzymes involved in the antioxidant cellular capacity (Calkins et al. 2009). The overall benefit of these induction mechanisms is an increase in the protective activities towards drugs or xenobiotics to which cells are exposed.

Following the pioneer discovery of hepatic drug metabolism as a major process for xenobiotic detoxification in mammals, an era of research on extrahepatic sites for drug metabolism opened. Brain, as other organs, was scanned for drug-metabolizing enzyme (DME) activities. These enzymatic activities often measured in tissue homogenates were found to be low to very low in the whole brain compared with their liver activities, and have been considered insignificant, until the complexity and specificity of the morphological and cellular organization of this organ was taken into account to refine the findings.

The brain is constituted of numerous anatomically differentiated structures, whose parenchymal tissue is composed of intermingled cells of different types, namely, neurons, glial cells including astrocytes, myelin-producing oligodendrocytes, as well as microglial cells bearing immune functions. Besides, the brain has an internal circulatory system of its own. The cerebrospinal fluid (CSF) circulates through the ventricular cavities lined by the ependyma into various membrane-filled cisterns and subarachnoid spaces of the brain before being resorbed in the venous circulation. Exchanges between the brain and the periphery, i.e., blood, are controlled by specific cellular interfaces. Within the neuropil, the blood–brain barrier (BBB) is located at the endothelial wall of the brain microvessels, while the epithelium of the choroid plexuses forms a barrier between the blood and the CSF (BCSFB) (Fig. 4.3). Cells at both the BBB and BCSFB are sealed by tight junctions, so that only those drugs which are lipophilic enough to cross lipid membranes have access to the brain.

Given this extensive heterogeneity, differences in the expression levels of DME were therefore searched among cerebral regions and cell subpopulations. Both phase I and phase II enzymes were found to be heterogeneously distributed among

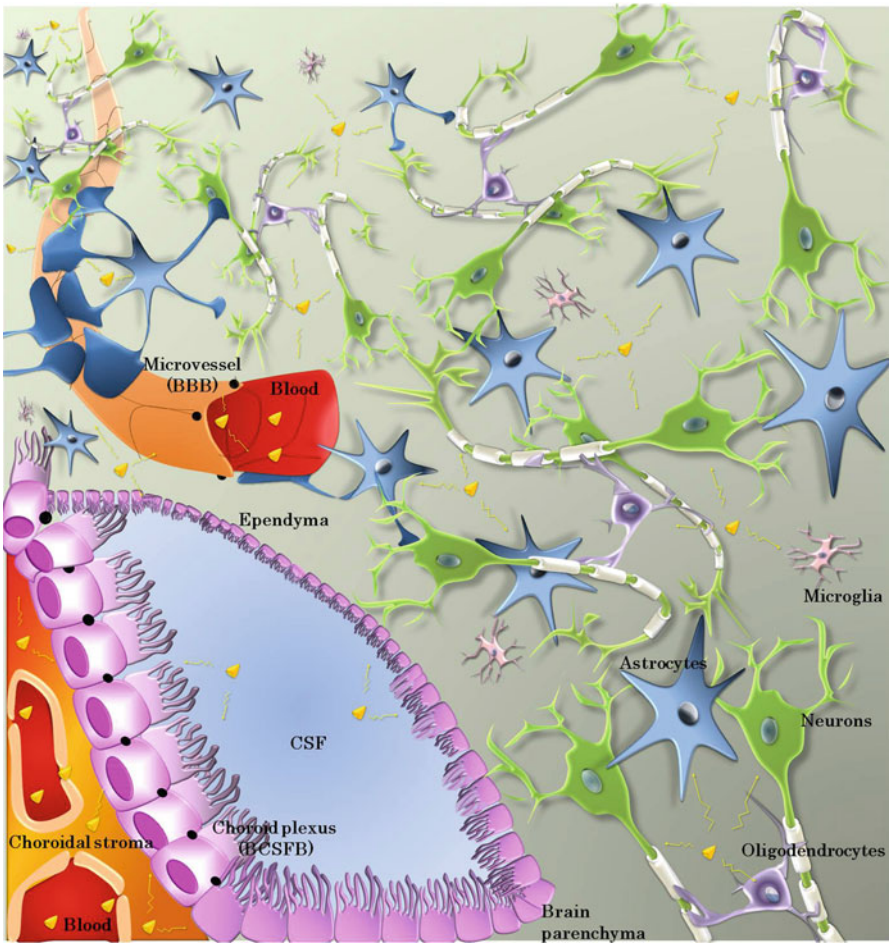

Fig. 4.3 Schematic drawing of the brain parenchyma illustrating the intermingled neural cell types and the main sites of exchange between the blood and the brain. Exchanges between the blood and the brain occur mainly across the microvessel walls forming the blood–brain barrier (BBB) and the choroid plexus epithelium forming the blood–cerebrospinal fluid barrier (BCSFB). The cells forming these barriers are sealed by tight junctions (*black dots and lines*). The fenestrated choroidal vessels allow extensive exchanges between the blood and the choroidal stroma. CSF–brain exchanges take place across the ependyma, or the pia–glia limitans (not shown here). Drug metabolism at these interfaces may influence the cerebral bioavailability of drugs and other xenobiotics. Within the neuropil, neurons, astrocytes, microglia, and oligodendrocytes harbor different levels of detoxification systems. Figure as originally published in: Gazzin et al. (2012) Transport and metabolism at blood–brain interfaces and in neural cells: relevance to bilirubin-induced encephalopathy *Front. Pharmacol.* 3:89. doi: 10.3389/fphar.2012.00089

regions and between neurons and glial cells (Bhamre et al. 1993; Miksys and Tyndale 2002; Minn et al. 1991; Monks et al. 1999; Teissier et al. 1998) In addition, a clear enrichment in cytochrome P-450 (CYP) dependent monooxygenases, monoamine oxidases (MAOs), epoxide hydrolases, several phase II enzymes, and antioxidant enzymes was demonstrated in the cells forming the blood–brain interfaces, both in rodent and human. Some of these enzymes proved to be sensitive to exogenous inducers (Ghersi-Egea et al. 1988, 1993, 1994; Hansson et al. 1990; Johnson et al. 1993; Riachi et al. 1988; Tayarani et al. 1989; Volk et al. 1991) This suggested a putative new function of these enzymes as a metabolic barrier between the blood and the brain (reviewed in Ghersi-Egea et al. 1995).

Since these pioneer works, various studies have explored this potential new barrier aspect of blood–brain interfaces. They initiated the identification of phase I and II enzyme isoforms and aimed at establishing the functional relevance of drug metabolism at the barriers. This paper describes our current understanding of drug metabolism at both the BBB and BCSFB and explores the mechanisms regulating the expression of DME in these interfaces.

4.2 Current Status

4.2.1 The Blood–Brain Barrier

4.2.1.1 Anatomical and Functional Features of the Blood–Brain Barrier

The BBB is formed by the endothelial cells lining the brain capillaries and microvessels (Ballabh et al. 2004; Cardoso et al. 2010; Zhang and Harder 2002) (Fig. 4.3). These cells are the main determinants of the BBB phenotype in humans and other animals (Khan 2005) and are referred to as brain microvessel endothelial cells (BMVECs) in this review. Only brain microvessels possess the properties of a fully efficient BBB, since the degree of leakiness across the endothelium varies inversely to the vessel diameter (Hawkins and Davis 2005). Although BMVECs are responsible for the BBB phenotype in vivo, these cells are in dynamic contact with other cells such as astrocytes, pericytes, and neurons that form the neurovascular unit. The mature BBB phenotype is believed to result from the particular interaction between the BMVECs and these other cells in the surroundings (Ballabh et al. 2004; Calabria and Shusta 2008; Cardoso et al. 2010; Lee et al. 2006). The walls of the brain microvessels are mainly lined with endothelial cells and BMVECs are fundamentally different from the endothelial cells lining the vessels in peripheral tissues (Choi and Kim 2008). The BMVECs have narrow junctional complexes (tight and adherens junctions), reducing gaps or spaces between cells and restricting free passive diffusion of blood-borne substances by paracellular route into the brain (also known as brain interstitial fluid) (Zlokovic 2008). BMVECs tightness is known to be 50–100-fold higher than that in peripheral microvessels (Abbott 2002).

It also provides this endothelium with a particularly high transendothelial electrical resistance (TEER) of 1,500–2,000 Ω cm^2 (Hawkins and Egleton 2006). BMVECs also differ from peripheral endothelial cells by several factors: (a) the uniform thickness of their cytoplasm, (b) absence or restricted fenestrae, (c) poor endocytotic activities, (d) continuous basement membrane, (e) negative charged surface, and (f) large number of mitochondria (Ballabh et al. 2004; Cardoso et al. 2010; de Boer and Gaillard 2006; Persidsky et al. 2006). In the following paragraph, the review focuses only on phase I and phase II drug-metabolizing enzymes at the BBB. Transporters potentially involved in phase III of drug metabolism are described in other chapters of this book.

4.2.1.2 Molecular Characterization, Relative Expression, and Functional Significance of Drug-Metabolizing Enzymes at the Blood–Brain Barrier

Phase I of Drug Metabolism

One of the primary functions of peripheral metabolism is to render substrates more polar, thus more water soluble, facilitating their removal from the body via the urine or bile. In the BBB, the presence of Phase I DME in BMVECs raises the question of their role in physiology and pharmacology. Rendering substrates more polar is probably not the primary function of phase I DME in the BBB. We may hypothesize that metabolism at the BBB may be more considered as a mechanism of brain protection by inactivating pharmacologically active compounds or toxic substances, thus preventing their access to the neuropil. While this is the general case, the opposite can happen in the case of prodrugs where an inactive parent compound may be transformed into a pharmacologically active metabolite as exemplified in the introduction. These metabolites can be beneficial to the brain if they are derived from a prodrug and harmful if they are toxic metabolites.

MAOs are phase I DME evidenced in the 1960s that metabolize neuroactive monoamines like adrenaline, noradrenalin, dopamine, serotonin, and their precursors and are thus important for controlling neurochemical signaling in the brain (Van Gelder 1968). MAOs are present in the mitochondria of BMVECs which contain up to 5-times more mitochondria than vascular endothelial cells in the periphery (Betz et al. 1980). The MAOs at the BBB may be considered as a second line of defense together with luminal drug transporters for the brain against chemical assault (Minn et al. 1991). They may also protect the brain from exogenous pyridine derivatives (Riachi and Harik 1988). The expression pattern of the genes encoding the two MAO subunits (*A* and *B*) was recently established in freshly isolated human brain microvessels (Shawahna et al. 2011). The metabolic hyperactivity of the BMVECs may explain the high concentration of *MAOA* transcripts quantified in the isolated human microvessels which were almost 6-times more abundant than *MAOB* transcripts.

The CYP superfamily contains a substantial number of enzymes that mainly catalyze phase I oxidative reactions. These CYPs are responsible for the transformation of at least 60 % of the FDA-approved drugs. Although they are present mainly in the liver, some extrahepatic isoforms may be important for inactivating drugs and toxicants. CYP activity and expression have already been found in isolated rat and human brain microvessels (Ghersi-Egea et al. 1993, 1994) and whole human brain (reviewed in Dutheil et al. 2008), but the expression pattern of the genes encoding the main CYP isoforms in isolated human brain microvessels was only recently established (Dauchy et al. 2008). The main CYPs responsible for metabolizing most of drugs in the liver were absent from the BBB (Decleves et al. 2011). The gene expression profile of CYPs showed that *CYP1B1* and *CYP2U1* were the main isoforms significantly expressed in isolated brain microvessels (over 90 % of all CYP mRNAs quantified). *CYP1B1* was 15-times more abundant in the brain microvessels than in the cerebral cortex. More recently, these transcriptomic data were confirmed at protein levels using a sophisticated targeted absolute quantitative proteomic approach. Using isolated human brain microvessels from brain biopsies sampled as far as possible of the disease focus in patients suffering from epilepsia or glioma, these two isoforms were detected among 13 CYP proteins studied (Shawahna et al. 2011). Despite the small amounts of their mRNAs, some CYP isoforms, like CYP1A1 and CYP3A4, are of special interest. Ghosh and collaborators recently colocalized by immunohistochemistry CYP3A4 with Von Willebrand factor (vWF) in endothelial cells isolated from epileptic patients (Ghosh et al. 2010). This suggests that some CYPs such as CYP3A4 can be induced at the BBB in this disease state. The high expression of CYP2UI observed by gene expression profile analysis (Dauchy et al. 2008) confirm the expression of this CYP observed previously at the genomic and proteomic level at the BBB (Karlgren et al. 2004). Since no drugs have been identified as metabolized by CYP2U1, its role in the detoxification of drugs is still poorly understood. CY2U1 may be implicated in the metabolism of endogenous compounds like arachidonic acid into hydroxyeicosatetraenoic acid, and thus may help to regulate cerebral blood flow. CYP1B1 is implicated in the metabolism of some xenobiotics but is well known in the metabolism of endogenous compounds like estradiol, melatonin, and arachidonic acid derivatives (Vasiliou and Gonzalez 2008). It is also readily induced via the regulatory pathway mediated by AhR (see Sect. 4.2.1.3). This raises the question of the influence of CYP1B1-mediated metabolic pathways on tampering the integrity of the BBB. These substances can penetrate the BMVECs because they are highly lipophilic and not substrates of ABC efflux transporters. CYP1B1 expressed in cells derived from human ovaries and intestine can be induced by cigarette smoke (Josserand et al. 2006; Vidal et al. 2006), a process that may occur also at the BBB. While epoxide hydrolase, well expressed at the BBB, is usually a detoxifying enzyme inactivating carcinogenic epoxides, the sequential action of CYP1B1 and epoxide hydrolase may substantially increase the number of reactive metabolites like diol-epoxides (Jacob et al. 2011) potentially deleterious for BBB integrity.

Phase II of Drug Metabolism

Phase I reactions often render substrates sufficiently polar to undergo excretion. However, many other substrates need additional phase II metabolism in which they are conjugated to other substrates to make them sufficiently polar to undergo excretion. While most substrates undergo phase I followed by phase II metabolism, some are directly conjugated and eliminated without any phase I reaction. Phase II reactions leading to more polar phase II metabolites are carried out by enzymes belonging to the following main families (Fig. 4.2): UDP-glucuronosyltransferases (UGTs), glutathione *S*-transferases (GSTs), sulfotransferases (SULTs). Two other conjugation enzyme families are *N*-acetyltransferases (NATs) and methyltransferases (MTs).

UGT transcripts or proteins were not detected in freshly isolated human brain microvessels (Shawahna et al. 2011), and UGT activity toward planar compounds such as 1-naphthol was not detected in human brain capillaries (Ghersi-Egea et al. 1993), suggesting the absence of glucuronidation at the human BBB. On the contrary, homogenates of rat brain microvessels have been found to be rich in this UGT activity (Ghersi-Egea et al. 1988). Similarly, results reported by Benzi and collaborators, based on in situ brain perfusion in the monkey indicated that this organ contained efficient glucuronidation (Benzi et al. 1967). This set of data suggests therefore interspecies differences. UGTs seem to be important for the conjugation of drugs in hepatic and intestinal tissues. While the presence of some isoforms in the brain, and particularly in neurons, could modulate the concentrations of neurotherapeutics like morphine within the brain, UGTs do not seem to interfere with the entry of drugs at the BBB. The UGT1A6 and UGT2B7 in human neurons seem to account for the glucuronidation of the neurotransmitter serotonin and endogenous morphine.

GSTs are dimeric proteins that also form a multigenic family of membrane-bound and cytosolic enzymes. Alpha, mu, and pi classes of cytosolic GSTs are considered to be mainly involved in drug metabolism and detoxification pathways (Hayes et al. 2005). Measureable quantities of GST mRNAs and proteins, GSTP1 being the most abundant GST enzyme, were found at the BBB (Shawahna et al. 2011). These findings are consistent with those of previous studies showing considerable expression of GSTs from the α, π, and μ isoforms in postmortem human brain tissues (Listowsky et al. 1998). Some GST isoforms, like GSTA4, are more abundant in fetal and adult human brains than in the liver (Liu et al. 1998). In the rat BBB, GSTpi colocalizes with Abcc2/Mrp2, the regulation of both genes being coordinated by the pregnane-X-receptor (PXR) (Bauer et al. 2008). In contrast, we detected neither ABCC2/MRP2 transcripts nor proteins in human microvessels (Shawahna et al. 2011). The high concentration of GSTs at the human BBB may be due to the need to neutralize oxidative compounds. GSTP1 has also been detected in the cerebral capillary endothelium of a sample obtained from epileptic patients (Shang et al. 2008). Although glutathione can interact directly with electrophiles, GST-mediated conjugation is quite often found in several tissues, including the CNS. The concentration of glutathione may differ from one brain region to another depending on the developmental stage of the neurons, with concentrations being higher in newly developed neurons, suggesting that it is involved in neuroprotection

(Sun et al. 2006). As glutathione is negatively charged at physiological pH it cannot penetrate the cell membrane. Its presence in the cytoplasm of BMVECs is due to the ability of selected cells to synthesize glutathione. Glutathione and glutathione conjugates are often transported from the cytoplasm to the mitochondria by SLC transporters (OATPs) and often extruded by phase III ABC efflux pumps, ABCCs (MRPs) and ABCG2/BCRP. We have found considerable amounts of the human γ-gamma-glutamyltranspeptidase (GGT) protein (Shawahna et al. 2011). This is the only enzyme that can cleave the γ-glutamyl bond of glutathione. Thus, GSTs at the BBB may neutralize reactive oxygen species (ROS) involved in oxidative stress. They could also be involved in drug-resistant epilepsy, preventing the accumulation of antiepileptic drugs by conjugating them with glutathione in the cerebral cortex where the epileptic foci are located.

SULTs are well characterized phase II metabolizing enzymes that were discovered in the 1960s. They catalyze the sulfation of numerous endogenous and exogenous substrates. There are two forms of SULT: the membrane-associated SULTs generally implicated in protein sulfation in the Golgi apparatus and the cytosolic SULTs that catalyze the sulfation of a wide range of soluble substrates including xenobiotics. Low concentrations of *SULT1A1* transcripts were detected in isolated human brain microvessels (Shawahna et al. 2011). Since SULTs are involved in the conjugation of numerous substrates including hormones and steroids, they play a key role in the metabolism of aromatic monoamines including catecholamine neurotransmitters, neurosteroids, and catecholamine metabolites in the CNS (Rivett et al. 1982). SULT isoforms are believed to be localized within the neurons where they control the activities of many substrates including thyroid hormone and neurosteroids. They are also implicated in the synthesis of chondroitin sulfate, keratan sulfate, and the proteoglycans that are involved in cell–cell interactions and differentiation. Lastly, SULTs may be implicated in the metabolism of drugs like acetaminophen and methyldopa (Gamage et al. 2006).

Some MTs like catechol-O-methyl transferase (COMT) and thiopurine methyltransferase (TPMT) are ubiquitous enzymes, being distributed throughout the body including the CNS. While COMT and TPMT metabolize exogenous substrates, their main function is to catalyze the O- and *S*-methylation of endogenous substrates like catecholamines and purines (Gottwald et al. 1997; McLeod et al. 2000). COMT was initially found in glia, but immunoreactivity investigations have also detected it in neurons (Karhunen et al. 1995). TPMT and histamine *N*-methyltransferase (HNMT) are soluble enzymes usually found in the cytosol of brain endothelial cells and neurons (Nishibori et al. 2000; Stanulla et al. 2009). The gene expression and protein level of these three MTs has been recently quantified in freshly isolated human brain microvessels (Shawahna et al. 2011), but no quantitative data are available for other animal species.

4.2.1.3 Regulation of Drug-Metabolizing Enzymes at the Blood–Brain Barrier

Certain phase III ABC efflux transporters and DMEs have shown common transcriptional regulatory pathways as it was first described for ABCB1/MDR1/P--glycoprotein and CYP3A4 (Synold et al. 2001). The transcription factors able to

up-regulate CYP as well as Phase II DMEs (UGT, GST, SULT, …) and phase III transporters are PXR, CAR, AhR, PPAR, and Nrf2. This is particularly true for tissues involved in the pharmacokinetics of drugs such as the liver and the gut but limited investigations have been carried out to understand regulator mechanisms and key factors at the BBB. PXR has been shown to be present and functional at the BBB of transgenic mice expressing human (hPXR) but few data are available on the presence of PXR at the human BBB. Zastre and collaborators showed that the ABCB1 gene in a human cerebral microvessel endothelial cell line (hCMEC/D3) was up-regulated by PXR agonists (Zastre et al. 2009). Only low amounts of *CAR* and *PXR* genes can be detected in freshly isolated human brain microvessels (Dauchy et al. 2008). The low levels of PXR transcripts are not in agreement with recent reports showing that hPXR induced P-gp activity at the BBB of transgenic mice (Bauer et al. 2006), and that pig PXR, which is very similar to hPXR, induced P-gp in pig cultured brain endothelial cells (Ott et al. 2009). Similarly, CAR has been shown to induce the expression of ABC transporters in isolated rat brain microvessels and in the hCMEC/D3 human brain endothelial cell line (Chan et al. 2010; Wang et al. 2010). Unfortunately, induction of DMEs via PXR or CAR activation has not yet been studied at the BBB. In contrast to PXR and CAR, high levels of *AhR* transcripts were found in rat (Jacob et al. 2011) and human BMVECs (Dauchy et al. 2009). AhR is another transcriptional factor implied in the regulation of certain genes involved in drug metabolism. AhR does not belong to the nuclear receptor superfamily unlike PXR and CAR. However, AhR belongs to a family known as basis helix–loop–helix/Per-ARNT-Sim (bHLH/PAS). This family includes also ARNT (AhR nuclear translocator), which functions as an AhR partner when it heterodimerizes. Similar to the nuclear receptors, AhR heterodimerizes in the nucleus to regulate the transcription of the target genes (Barouki et al. 2007) AhR ligands are hydrophobic in nature and can be endogenous or exogenous. Xenobiotics able to activate AhR are mainly polycyclic aromatic hydrocarbons such as dioxins (environmental pollutants), benzo[a]pyrene (tobacco), and β-naphthoflavone but also some medications such as omeprazole (Denison and Nagy 2003). The list of genes regulated by AhR differs from that of PXR and CAR. However, some similarities are observed as AhR appears to be involved in regulating the expression of ABC transporters like MRP3 and BCRP. The CYP1A1/CYP1A2 and CYP1B1 are the best known and most studied AhR target genes and these isoforms are able to metabolize many procarcinogens into reactive metabolites. Therefore, any prolonged exposure to AhR ligands, including many environmental pollutants, may lead to an increased formation of reactive metabolites to cause toxicity. Activation of AhR by dioxin, one of the most potent AhR ligand, strongly induced Cyp1a1 and Cyp1b1 in isolated rat brain microvessels (Jacob et al. 2011; Wang et al. 2011). Interestingly, CYP1B1 has been shown as one of the main CYP expressed at the BBB, its function at this location remaining unknown (see Sect. 4.2.1.2). We hypothesize that ligands of AhR, including polycyclic aromatic hydrocarbons (PAHs) like coplanar polychlorinated biphenyls (PCBs) and benzo[a]pyrene may induce some AhR target genes, including *CYP1A1* and *CYP1B1*, at the human BBB. The role of CYP1B1 as a metabolic activator of toxic pollutants to form potentially neurotoxic metabolites remains to be determined.

4.2.2 The Blood–Cerebrospinal Fluid Barrier and the Ependyma

4.2.2.1 Anatomical and Functional Features of the Blood–CSF Barrier

The bulk of CSF is secreted by the choroid plexuses. CSF represents 50 % of the extracellular fluid of the brain in human. It flows through the ventricular system, then into the midbrain and hindbrain cisterns, velae, and subarachnoid spaces before being absorbed into the venous blood via the arachnoid villi or drained into the lymphatic system. Exchanges between the CSF and fluid-filled extracellular spaces of the brain parenchyma are not restricted as cells forming most of the ependymal ventricular wall or the external glia limitans lack tight junctions (Fig. 4.3). Drug metabolism at these places may however impact on the distribution of xenobiotics in the brain (see infra). The BCSFB lies at the choroid plexus epithelium and, downstream of CSF flow, at the arachnoid membrane. The former site is therefore mainly involved in CSF drug delivery. The choroid plexus–CSF system adds a degree of complexity to the mechanisms that set the cerebral bioavailability of both endogenous and exogenous bioactive compounds. The CSF circulatory pathway, and the interplay between BBB, BCSFB, and CSF have been described elsewhere (Ghersi-Egea et al. 2009a, b; Strazielle and Ghersi-Egea 2000b).

The brain contains four choroid plexuses, located in the two lateral, the third and the fourth ventricles. The different choroid plexuses display a somewhat different gross anatomy but are all organized as an ensemble of villi formed by a monolayer of epithelial cells surrounding a highly vascularized conjunctive core (Fig. 4.3). The choroid plexuses display the highest local cerebral blood flow among brain structures. The fenestrated vessels present in the choroidal stroma are highly permeable even to polar solutes, and the actual barrier between blood and CSF is located at the epithelium whose cells are sealed by tight junctions (Strazielle and Ghersi-Egea 2000a). Besides the production of CSF from plasma by a tightly regulated secretory process (Brown et al. 2004), the choroid plexuses also fulfill neuroendocrine functions by secreting various biologically active polypeptides and hormone carrier proteins, and participate to the neuroimmune surveillance of the brain (reviewed in Chodobski and Szmydynger-Chodobska 2001; Engelhardt and Ransohoff 2005; Szmydynger-Chodobska et al. 2009). Choroid plexus functions also include the selective blood-to-CSF entry of required molecules such as inorganic anions, nutrients and hormones (Damkier et al. 2010; Redzic et al. 2005; Schmitt et al. 2011), as well as the CSF-to-blood export of toxic compounds and metabolites (Kusuhara and Sugiyama 2004; Strazielle et al. 2004). These transport processes are facilitated by several factors. The blood–CSF barrier (BCSFB) is located between two circulating fluids. The surface area of exchange is enhanced by the organization of the choroid plexus into numerous villi, and by the anatomical peculiarities of the choroidal epithelium which develops an extended apical brush border and basolateral interdigitations (Keep and Jones 1990). Nonetheless the molecular exchanges between the blood and the CSF across the choroidal epithelium are tightly regulated. Like at the

BBB, the presence of tight junctions that link the epithelial cells together strongly reduces the nonspecific paracellular leakage (Kratzer et al. 2012). Different types of influx and efflux transport systems account for the selectivity and directionality of solute transport. Relevant to efflux transport proteins, the choroid plexuses express high levels of basolaterally located transporters of the multidrug resistance-related ABCC protein family, which participate to the low brain penetration of various drugs (Gazzin et al. 2008; Leggas et al. 2004; Wijnholds et al. 2000).

The detoxification reactions that take place at the choroid plexuses represent another neuroprotective facet of CP functions toward toxic compounds, and may also decrease the delivery of some drugs into the brain.

4.2.2.2 Molecular Characterization and Relative Expression of Drug-Metabolizing Enzymes in Rodent and Human Choroid Plexuses

Choroid plexuses appear to be a major site of drug metabolism in the brain. In rat, the choroidal specific enzymatic activities of enzymes such as epoxide hydrolases (EHs), UDP-glucuronosyltransferases (UGTs) or glutathione-S-transferases (GSTs) do reach hepatic levels (Ghersi-Egea et al. 1994; Strazielle and Ghersi-Egea 1999). As in liver, some DME activities in choroid plexus are inducible by foreign compounds (Leininger-Muller et al. 1994). This metabolic detoxification capacity is another function shared by the choroid plexuses and the liver, besides their ability to synthesize and secrete the thyroid hormone carrier transthyretin (Schreiber and Richardson 1997). They are, however, differences in drug metabolism between the two organs, particularly in phase I proteins.

Phase I of Drug Metabolism

Some CYP-dependent monooxygenase activities have been measured in isolated rat choroid plexuses (Ghersi-Egea et al. 1994), albeit at lower levels than in the liver. The molecular identification and localization of CYPs in the choroid plexus is only partial. Immunohistochemical and in situ hybridization studies identified CYP1A1, but not 1A2 in rat and mouse choroid plexuses following induction by β-naphthoflavone, or the carcinogenic 3-methylcholanthrene. The enzyme was located at the choroidal vessel walls rather than at the BCSFB proper. It was shown to metabolize heterocyclic amines into reactive intermediates, a metabolic activity that is deleterious in this instance (Brittebo 1994; Dey et al. 1999; Morse et al. 1998). CYP1A1 was not detected prior to inductive treatment. Immunohistochemical evidence for the localization of a CYP2B1,2-like protein in the rat and mouse choroid plexus has been reported (Miksys et al. 2000a; Volk et al. 1991). An antibody raised against isoforms of the CYP2D subfamily generated a strong signal in the rat choroid plexus, possibly associated with the endothelium (Miksys et al. 2000b). CYP2B and 2D proteins metabolize a large range of xenobiotics including centrally acting drugs but no relevant metabolic activities have yet been measured in the

choroidal tissue. A thorough evaluation of the choroidal expression of all CYP isoforms involved in the metabolism of xenobiotics, and of associated metabolic activities, is therefore called for. No data on CYP expression in human choroid plexus have been reported so far. Of note, the activity of NADPH–cytochrome P-450 reductase, the enzyme that provides the electrons necessary to the activity of microsomal CYPs, is sizably measured in rat choroid plexus homogenate and in choroid plexus epithelial cells (Strazielle and Ghersi-Egea 1999). Besides its role in electron transfer to CYPs, this enzyme can generate free radicals by a CYP-independent reductive metabolism of drugs, a mechanism that participates in the toxicity of compounds able to undergo a single electron reduction (Ghersi-Egea et al. 1998). Besides CYP-dependent monooxygenases, flavin-containing monooxygenases (FMO) also play an important role in phase I metabolism of foreign chemicals, including psychoactive drugs (Cashman 2000). FMO1 mRNA has been localized in the mouse choroidal epithelium by in situ hybridization (Janmohamed et al. 2004). No other information is so far available concerning the choroidal expression and function of the different FMO isoforms.

Among all brain structures in rat, the choroid plexus display the highest level of EH activity toward carcinogenic epoxides. The brain vessels have the second highest level of activity (Ghersi-Egea et al. 1994; Strazielle and Ghersi-Egea 1999). Inactivation of carcinogenic epoxides is mainly attributed to the membrane-bound form of EH. The enzymatic data match immunohistochemical data showing that the highest signal for this isoform is associated with the choroidal epithelium in mice (Marowsky et al. 2009). One study investigated the localization of the soluble form of EH (sEH) in human brain. sEH is involved in the metabolism of lipid-derived biologically active endogenous epoxides rather than that of carcinogenic xenobiotics. A high immunohistochemical signal towards sEH was also associated with the human choroid plexus (Sura et al. 2008), while Marowsky and colleagues (2009) do not specifically report such localization in the mouse brain.

Finally, other choroidal enzymes with narrower substrate specificity such as MAOs or alcohol dehydrogenases can also participate to the phase I of drug metabolism (reviewed in Strazielle et al. 2004).

Phase II of Drug Metabolism

In the rat, the choroidal activity of the UGT isoenzyme(s) responsible for the conjugation of planar compounds is high, reaching the hepatic level. This enzymatic activity is located in the epithelium and is inducible by exogenous polycyclic aromatic hydrocarbons as it is in the liver (Ghersi-Egea et al. 1994; Leininger-Muller et al. 1994; Strazielle and Ghersi-Egea 1999). It is likely to be catalyzed by one or several UGT1A isoenzymes. High levels of mRNAs were measured in the rat choroid plexus with primers common to all genes of the UGT1A subfamily (unpublished results). There may however be species differences in the conjugation capacity to glucuronic acid in the choroid plexus, especially between rodent, primate and human as discussed for the BBB (See Sect. 4.2.1.2).

Detoxification by sulfoconjugation appears to be active in both human and rodent choroid plexuses. High levels of SULT1A1 activity towards phenolic compounds, and of SULT1A1 protein were reported in fetal human choroid plexus by comparison to other brain structures (Richard et al. 2001). Adult material was not tested in this study. SULT1A1 mRNA level is high in choroidal material of both developing and adult rat (unpublished results). Additional functional studies are needed to precisely evaluate the impact of sulfoconjugation in the detoxification properties of the BCSFB.

Immunohistochemical evidence for the presence of the three main, alpha, mu, and pi classes of GSTs involved in drug metabolism and detoxification in the rodent choroid plexuses has been reported (Cammer et al. 1989; Johnson et al. 1993; Philbert et al. 1995). Immunoreactivity of GST pi has also been demonstrated in human choroid plexus (Carder et al. 1990). More recently, a high GSTalpha 4 (GST 8-8) mRNA enrichment has been reported in the rat choroid plexus (Liang et al. 2004). The conjugation to GSH of 1-chloro-2,4-dinitrobenzene (CDNB), which is a substrate for several cytosolic forms and the microsomal form of GSTs, is higher by one order of magnitude in choroid plexus than brain parenchyma in the newborn rat. This activity is found associated with the epithelial cells in rat choroid plexus, and is also high in human choroidal tissue (Ghersi-Egea et al. 2006; Strazielle and Ghersi-Egea 1999). Finally choroid plexus epithelial cells have the ability to efficiently take up glutathione precursors and to synthesize and recycle GSH (Burdo et al. 2006; Lee et al. 2012; Monks et al. 1999; Tate et al. 1973). These data suggest an important role of GST-dependent detoxification pathways at the BCSFB. Of note, GSTs have also been detected or shown to be enriched in the ependyma lining the ventricle in rat (Abramovitz et al 1988; Cammer et al 1989; Liang et al 2004; Philbert et al 1995), mouse (Beiswanger et al. 1995), and human (Carder et al. 1990), suggesting that GST-dependent detoxification extents to the interface between the CSF and the neuropil.

Phase III of Drug Metabolism

Different transporters of the ABCC family, including MRP1 and MRP4 are ideally located at the basolateral, blood-facing membrane in both rodent and humans to export conjugated metabolites into the systemic circulation (Gazzin et al. 2008; Ginguene et al. 2010; Leggas et al. 2004). Other basolateral transporters such as Oatp1a4 (Oatp2) may also transport drug conjugates at the basolateral membrane. The expression and functional significance of drug transporters at the BCSFB have been reviewed elsewhere (e.g., Ghersi-Egea et al. 2009b; Leslie et al. 2005; Strazielle and Ghersi-Egea 2005, other chapters in this book).

Antioxidant Systems

In addition to be a cosubstrate for GSTs, reduced glutathione is also active as a main intracellular antioxidant. The reduced/oxidized glutathione redox cycle is active in choroid plexus which in rat display enriched levels of glutathione reductase activity

compared with the neuropil. Glutathione is also substrate for the glutathione peroxidase, an enzyme whose activity is 13 times higher in choroid plexus than in brain parenchyma. Catalase and superoxide dismutase also display significantly higher activities in the rat choroid plexus than in brain tissue (Tayarani et al. 1989). Thus the choroid plexuses appear to possess a powerful machinery to fight reactive chemical species including reactive oxygen species.

4.2.2.3 Pharmacotoxicological Significance and Regulation of Drug Metabolism at the Blood–CSF Barrier

As for the BBB, most of the data available about drug metabolism in the BCSFB are related to the molecular identity, level of expression and localization of the enzymes. They also comprise specific activities measured in homogenates or subcellular fractions with excess of substrates and cosubstrates. In vivo data demonstrating drug-metabolizing enzyme activities in the choroid plexus are scarce. Only one work identified a carcinogen metabolic activation at the choroidal endothelium through CYP1A1 metabolism following induction with β-naphthoflavone (Brittebo 1994; Granberg et al. 2003). The metabolite irreversibly bound to the site of production and could thus be detected. In vivo evidence for the efficacy of drug metabolism at the BCSFB is difficult to obtain. Blood-to-CSF concentration ratios for substrates and metabolites are difficult to interpret. They are not only influenced by drug metabolism at choroidal, cerebral and extracerebral sites, but also by BBB permeability, BCSFB permeability, CSF circulation and CSF–brain extracellular fluid diffusion. To overcome these limitations, cellular models of the BCSFB have been developed to address transport and metabolism across the BCSFB independently of other brain and peripheral parameters. Such a model has been developed in rat and has been validated for transport and metabolic studies (Strazielle et al. 2003; Strazielle and Ghersi-Egea 1999). It was used to show that the choroidal epithelium acts as a blood-to-CSF metabolic barrier towards selected xenobiotics through conjugation via either a UGT-dependent pathway (Strazielle and Ghersi-Egea 1999), or a GST-dependent pathway (Ghersi-Egea et al. 2006). In the latter case, the barrier was efficient even against high concentrations of substrate, as long as the intracellular glutathione pool was not limiting. Following glutathione depletion, the efficacy of the barrier effect was dependent on the rate of glutathione neosynthesis by the choroidal epithelial cells, a synthetic pathway that could be enhanced by exposing the cells to drugs such as N-acetylcysteine. In both conditions, the conjugated metabolites were mainly effluxed at the basolateral membrane, by mechanisms likely to involve MRP/ABCC transporters. These data showed that at least some of the choroidal enzymatic equipment is pharmacotoxicologically efficient. Additional in situ imaging and in vivo metabolic studies are eagerly needed to precisely delineate the role of choroidal metabolism in reducing the entry of xenobiotics into the CSF and brain or increasing their elimination rate from the brain, and in participating to the overall neuroprotective function of blood–brain interfaces.

As in liver, choroidal DMEs may be induced by a wide range of xenobiotics including drugs. Although examples of choroidal induction have been published

only for AhR ligands such as β-naphthoflavone or carcinogenic compounds like 3-methylcholantrene, (e.g., Leininger-Muller et al. 1994; Morse et al. 1998), other inductive processes mediated by drugs or oxidative stress are likely to take place at the BCSFB, because transcription factors such as CAR, PXR, or nrf2 are expressed at the choroid plexus (unpublished results). Such inductive mechanisms may increase the neuroprotective functions associated with this barrier.

4.2.2.4 Drug Metabolism Associated with the Blood–CSF Barrier During Development

The efficacy of blood–brain interfaces in protecting neural cells during the critical period of brain development has been a subject of debate throughout the last decades (Ek et al. 2012; Johansson et al. 2008). More recently evidence both in rodent and in human for an early and efficient establishment of the tight junctions that seal the cells forming both the BBB and BCSFB has been gathered. This prevents non specific paracellular leakage between blood and brain during fetal development (Ek et al. 2006; Kratzer et al. 2012). The BCSFB in particular appears to follow a specific pattern of early maturation during brain development. The choroid plexuses appears early during the embryonic life and seems to acquire an "adult" morphological and functional phenotype earlier than most brain structures. This highlights the special role of the choroidal tissue in regulating blood–brain exchanges during development (Dziegielewska et al. 2001). With respect to metabolic capacities towards drugs and toxic compounds, the choroid plexuses already possess high detoxification capacities in the newborn rat (Strazielle and Ghersi-Egea 1997). Overall GST activities are higher in newborn than in adult rat choroid plexuses, and are also very high in choroidal tissue from fetal human brain (Ghersi-Egea et al. 2006). Yet the developmental enzyme expression profile differs from one GST class to another (Beiswanger et al. 1995; Carder et al. 1990). High levels of SULT1A1 are also clearly associated with the choroidal tissue in developing human brain (Richard et al. 2001). The protein level of Mrp1/Abcc1 that can export drug conjugates is already high in the choroid plexus of developing animals, by contrast to the protein level of the prototypic BBB efflux transporter P-glycoprotein in microvessels of the same animals (Gazzin et al. 2008). Taken together, these data suggest that detoxification processes are especially active at the choroid plexuses during brain development, but additional work is needed to explore this hypothesis.

4.3 Future Challenge

While the presence of specific drug-metabolizing enzymes has been clearly established at both the BBB and BCSFB, definite proofs that their activity can influence either the cerebral bioavailability or the neurotoxicity of drugs and xenobiotics are scarce. Designing in vivo experiments and pharmacokinetic models oriented toward the study

of cerebral drug metabolism is therefore mandatory to assess the significance of such metabolic pathways. This should be done in both adult and developing animals, owing to the substantial metabolic activity of the BCSFB during brain development.

No information is available concerning the level of drug-metabolizing enzyme expression in brain microvessels from developing animals or from fetal/neonate human. The establishment of developmental expression profiles for relevant enzymes at both barriers will allow appreciating the degree of maturity of these protective interfaces in the developing brain.

An in-depth molecular characterization of choroidal DME isoforms is needed to build a comprehensive view of drug metabolism at blood–brain interfaces. In particular, species differences need to be assessed to appreciate the predictive value of experimental pharmacokinetic models used to determine the influence of metabolism on the cerebral bioavailability of drugs in adult and pediatric patients.

Finally, as detoxification processes appear to contribute to the neuroprotective functions of the blood–brain interfaces, their importance in protecting the brain in pathological situations, e.g., following exposure to environmental toxins or following oxidative insults, needs to be explored more thoroughly. The pharmacological enhancement of these metabolic functions could be a strategy to improve neuroprotection in a pathophysiological context. This could be explored by assessing whether the induction pathways known to be efficient in the liver are also active at the blood–brain interfaces.

4.4 Conclusions

Evidence for the presence and activity of several phase I and phase II drug-metabolizing enzymes at blood–brain interfaces has been gathered over the past decades. The functional significance of drug-metabolizing enzyme activities at the BBB and the fate of the produced metabolites remain to be explored. The high choroidal specific activities of selected drug-metabolizing enzymes, concurrent to efficient metabolite efflux transporters at the BCSFB confers a function of metabolic barrier and detoxification to the choroid plexus. The inducibility of these enzymatic systems in the BBB and BCSFB opens the interesting possibility to pharmacologically enhance neuroprotection at blood–brain interfaces.

Acknowledgement This work was supported by the European Union (HEALTH- F2-2009-241778) to Nathalie Strazielle and Jean-François Ghersi-Egea.

References

Abbott NJ (2002) Astrocyte-endothelial interactions and blood-brain barrier permeability. J Anat 200:629–638

Abramovitz M, Homma H, Ishigaki S, Tansey F, Cammer W, Listowsky I (1988) Characterization and localization of glutathione-S-transferases in rat brain and binding of hormones, neurotransmitters, and drugs. J Neurochem 50:50–57

Aleksunes LM, Klaassen CD (2012) Coordinated regulation of hepatic phase I and II drug-metabolizing genes and transporters using AhR-, CAR-, PXR-, PPARalpha-, and Nrf2-null mice. Drug Metab Dispos 40:1366–1379

Ballabh P, Braun A, Nedergaard M (2004) The blood-brain barrier: an overview: structure, regulation, and clinical implications. Neurobiol Dis 16:1–13

Barouki R, Coumoul X, Fernandez-Salguero PM (2007) The aryl hydrocarbon receptor, more than a xenobiotic-interacting protein. FEBS Lett 581:3608–3615

Bauer B, Yang X, Hartz AM, Olson ER, Zhao R, Kalvass JC, Pollack GM, Miller DS (2006) In vivo activation of human pregnane X receptor tightens the blood-brain barrier to methadone through P-glycoprotein up-regulation. Mol Pharmacol 70:1212–1219

Bauer B, Hartz AM, Lucking JR, Yang X, Pollack GM, Miller DS (2008) Coordinated nuclear receptor regulation of the efflux transporter, Mrp2, and the phase-II metabolizing enzyme, GSTpi, at the blood-brain barrier. J Cereb Blood Flow Metab 28:1222–1234

Beiswanger CM, Diegmann MH, Novak RF, Philbert MA, Graessle TL, Reuhl KR, Lowndes HE (1995) Developmental changes in the cellular distribution of glutathione and glutathione S-transferases in the murine nervous system. Neurotoxicology 16:425–440

Benzi G, Berte F, Crema A, Frigo GM (1967) Cerebral drug metabolism investigated by isolated perfused brain in situ. J Pharm Sci 56:1349–1351

Betz AL, Firth JA, Goldstein GW (1980) Polarity of the blood-brain barrier: distribution of enzymes between the luminal and antiluminal membranes of brain capillary endothelial cells. Brain Res 192:17–28

Bhamre S, Bhagwat SV, Shankar SK, Williams DE, Ravindranath V (1993) Cerebral flavin-containing monooxygenase-mediated metabolism of antidepressants in brain: immunochemical properties and immunocytochemical localization. J Pharmacol Exp Ther 267: 555–559

Brittebo EB (1994) Metabolism-dependent binding of the heterocyclic amine Trp-P-1 in endothelial cells of choroid plexus and in large cerebral veins of cytochrome P450-induced mice. Brain Res 659:91–98

Brown PD, Davies SL, Speake T, Millar ID (2004) Molecular mechanisms of cerebrospinal fluid production. Neuroscience 129:957–970

Burdo J, Dargusch R, Schubert D (2006) Distribution of the cystine/glutamate antiporter system xc- in the brain, kidney, and duodenum. J Histochem Cytochem 54:549–557

Calabria AR, Shusta EV (2008) A genomic comparison of in vivo and in vitro brain microvascular endothelial cells. J Cereb Blood Flow Metab 28:135–148

Calkins MJ et al (2009) The Nrf2/ARE pathway as a potential therapeutic target in neurodegenerative disease. Antioxid Redox Signal 11:497–508

Cammer W, Tansey F, Abramovitz M, Ishigaki S, Listowsky I (1989) Differential localization of glutathione-S-transferase Yp and Yb subunits in oligodendrocytes and astrocytes of rat brain. J Neurochem 52:876–883

Carder PJ, Hume R, Fryer AA, Strange RC, Lauder J, Bell JE (1990) Glutathione S-transferase in human brain. Neuropathol Appl Neurobiol 16:293–303

Cardoso FL, Brites D, Brito MA (2010) Looking at the blood-brain barrier: molecular anatomy and possible investigation approaches. Brain Res Rev 64:328–363

Cashman JR (2000) Human flavin-containing monooxygenase: substrate specificity and role in drug metabolism. Curr Drug Metab 1:181–191

Chan GN, Hoque MT, Cummins CL, Bendayan R (2010) Regulation of P-glycoprotein by orphan nuclear receptors in human brain microvessel endothelial cells. J Neurochem 118:163–175

Chodobski A, Szmydynger-Chodobska J (2001) Choroid plexus: target for polypeptides and site of their synthesis. Microsc Res Tech 52:65–82

Choi YK, Kim KW (2008) Blood-neural barrier: its diversity and coordinated cell-to-cell communication. BMB Rep 41:345–352

Christrup LL (1997) Morphine metabolites. Acta Anaesthesiol Scand 41:116–122

Damkier HH, Brown PD, Praetorius J (2010) Epithelial pathways in choroid plexus electrolyte transport. Physiology (Bethesda) 25:239–249

Dauchy S, Dutheil F, Weaver RJ, Chassoux F, Daumas-Duport C, Couraud PO, Scherrmann JM, De Waziers I, Decleves X (2008) ABC transporters, cytochromes P450 and their main transcription factors: expression at the human blood-brain barrier. J Neurochem 107: 1518–1528

Dauchy S, Miller F, Couraud PO, Weaver RJ, Weksler B, Romero IA, Scherrmann JM, De Waziers I, Decleves X (2009) Expression and transcriptional regulation of ABC transporters and cytochromes P450 in hCMEC/D3 human cerebral microvascular endothelial cells. Biochem Pharmacol 77:897–909

de Boer AG, Gaillard PJ (2006) Blood-brain barrier dysfunction and recovery. J Neural Transm 113:455–462

Decleves X, Jacob A, Yousif S, Shawahna R, Potin S, Scherrmann JM (2011) Interplay of drug metabolizing CYP450 enzymes and ABC transporters in the blood-brain barrier. Curr Drug Metab 12:732–741

Denison MS, Nagy SR (2003) Activation of the aryl hydrocarbon receptor by structurally diverse exogenous and endogenous chemicals. Annu Rev Pharmacol Toxicol 43:309–334

Dey A, Jones JE, Nebert DW (1999) Tissue- and cell type-specific expression of cytochrome P450 1A1 and cytochrome P450 1A2 mRNA in the mouse localized in situ hybridization. Biochem Pharmacol 58:525–537

Duffel MW, Marshal AD, McPhie P, Sharma V, Jakoby WB (2001) Enzymatic aspects of the phenol (aryl) sulfotransferases. Drug Metab Rev 33:369–395

Dutheil F, Beaune P, Loriot MA (2008) Xenobiotic metabolizing enzymes in the central nervous system: contribution of cytochrome P450 enzymes in normal and pathological human brain. Biochimie 90:426–436

Dziegielewska KM, Ek J, Habgood MD, Saunders NR (2001) Development of the choroid plexus. Microsc Res Tech 52:5–20

Eaton DL, Bammler TK (1999) Concise review of the glutathione S-transferases and their significance to toxicology. Toxicol Sci 49:56–164

Ek CJ, Dziegielewska KM, Stolp H, Saunders NR (2006) Functional effectiveness of the blood-brain barrier to small water-soluble molecules in developing and adult opossum (Monodelphis domestica). J Comp Neurol 496:13–26

Ek CJ, Dziegielewska KM, Habgood MD, Saunders NR (2012) Barriers in the developing brain and neurotoxicology. Neurotoxicology 33:586–604

Engelhardt B, Ransohoff RM (2005) The ins and outs of T-lymphocyte trafficking to the CNS: anatomical sites and molecular mechanisms. Trends Immunol 26:485–495

Gamage N, Barnett A, Hempel N, Duggleby RG, Windmill KF, Martin JL, McManus ME (2006) Human sulfotransferases and their role in chemical metabolism. Toxicol Sci 90:5–22

Gazzin S, Strazielle N, Schmitt C, Fevre-Montange M, Ostrow JD, Tiribelli C, Ghersi-Egea JF (2008) Differential expression of the multidrug resistance-related proteins ABCb1 and ABCc1 between blood-brain interfaces. J Comp Neurol 510:497–507

Gazzin S, Strazielle N, Tiribelli C, Ghersi-Egea JF (2012) Transport and metabolism at blood-brain interfaces and in neural cells: relevance to bilirubin-induced encephalopathy. Front Pharmacol 3:89

Gelhaus SL, Harvey RG, Penning TM, Blair IA (2011) Regulation of benzo[a]pyrene-mediated DNA- and glutathione-adduct formation by 2,3,7,8-tetrachlorodibenzo-p-dioxin in human lung cells. Chem Res Toxicol 24:89–98

Ghersi-Egea JF, Minn A, Siest G (1988) A new aspect of the protective functions of the blood-brain barrier: activities of four drug-metabolizing enzymes in isolated rat brain microvessels. Life Sci 42:2515–2523

Ghersi-Egea JF, Perrin R, Leininger-Muller B, Grassiot MC, Jeandel C, Floquet J, Cuny G, Siest G, Minn A (1993) Subcellular localization of cytochrome P450, and activities of several enzymes responsible for drug metabolism in the human brain. Biochem Pharmacol 45:647–658

Ghersi-Egea JF, Leninger-Muller B, Suleman G, Siest G, Minn A (1994) Localization of drug-metabolizing enzyme activities to blood-brain interfaces and circumventricular organs. J Neurochem 62:1089–1096

Ghersi-Egea JF, Leininger-Muller B, Cecchelli R, Fenstermacher JD (1995) Blood-brain interfaces: relevance to cerebral drug metabolism. Toxicol Lett 82–83:645–653

Ghersi-Egea JF, Maupoil V, Ray D, Rochette L (1998) Electronic spin resonance detection of superoxide and hydroxyl radicals during the reductive metabolism of drugs by rat brain preparations and isolated cerebral microvessels. Free Radic Biol Med 24:1074–1081

Ghersi-Egea JF, Strazielle N, Murat A, Jouvet A, Buenerd A, Belin MF (2006) Brain protection at the blood-cerebrospinal fluid interface involves a glutathione-dependent metabolic barrier mechanism. J Cereb Blood Flow Metab 4:4

Ghersi-Egea JF, Gazzin S, Strazielle N (2009a) Blood-brain interfaces and bilirubin-induced neurological diseases. Curr Pharm Des 15:2893–2907

Ghersi-Egea JF, Monkkonen KS, Schmitt C, Honnorat J, Fevre-Montange M, Strazielle N (2009b) Blood-brain interfaces and cerebral drug bioavailability. Rev Neurol (Paris) 165:1029–1038

Ghosh C, Gonzalez-Martinez J, Hossain M, Cucullo L, Fazio V, Janigro D, Marchi N (2010) Pattern of P450 expression at the human blood-brain barrier: roles of epileptic condition and laminar flow. Epilepsia 51:1408–1417

Ginguene C, Champier J, Maallem S, Strazielle N, Jouvet A, Fevre-Montange M, Ghersi-Egea JF (2010) P-glycoprotein (ABCB1) and breast cancer resistance protein (ABCG2) localize in the microvessels forming the blood-tumor barrier in ependymomas. Brain Pathol 20:926–935

Gottwald MD, Bainbridge JL, Dowling GA, Aminoff MJ, Alldredge BK (1997) New pharmacotherapy for Parkinson's disease. Ann Pharmacother 31:1205–1217

Granberg L, Ostergren A, Brandt I, Brittebo EB (2003) CYP1A1 and CYP1B1 in blood-brain interfaces: CYP1A1-dependent bioactivation of 7,12-dimethylbenz(a)anthracene in endothelial cells. Drug Metab Dispos 31:259–265

Hansson T, Tindberg N, Ingelman-Sundberg M, Kohler C (1990) Regional distribution of ethanol-inducible cytochrome P450 IIE1 in the rat central nervous system. Neuroscience 34:451–463

Hawkins BT, Davis TP (2005) The blood-brain barrier/neurovascular unit in health and disease. Pharmacol Rev 57:173–185

Hawkins BT, Egleton RD (2006) Fluorescence imaging of blood-brain barrier disruption. J Neurosci Methods 151:262–267

Hayes JD, Flanagan JU, Jowsey IR (2005) Glutathione transferases. Annu Rev Pharmacol Toxicol 45:51–88

Ishikawa T (1992) The ATP-dependent glutathione S-conjugate export pump. Trends Biochem Sci 17:463–468

Jacob A, Hartz AM, Potin S, Coumoul X, Yousif S, Scherrmann JM, Bauer B, Decleves X (2011) Aryl hydrocarbon receptor-dependent upregulation of Cyp1b1 by TCDD and diesel exhaust particles in rat brain microvessels. Fluids Barriers CNS 8:23

Janmohamed A, Hernandez D, Phillips IR, Shephard EA (2004) Cell-, tissue-, sex- and developmental stage-specific expression of mouse flavin-containing monooxygenases (Fmos). Biochem Pharmacol 68:73–83

Johansson PA, Dziegielewska KM, Liddelow SA, Saunders NR (2008) The blood-CSF barrier explained: when development is not immaturity. Bioessays 30:237–248

Johnson JA, el Barbary A, Kornguth SE, Brugge JF, Siegel FL (1993) Glutathione S-transferase isoenzymes in rat brain neurons and glia. J Neurosci 13:2013–2023

Josserand V, Pelerin H, de Bruin B, Jego B, Kuhnast B, Hinnen F, Duconge F, Boisgard R, Beuvon F, Chassoux F, Daumas-Duport C, Ezan E, Dolle F, Mabondzo A, Tavitian B (2006) Evaluation of drug penetration into the brain: a double study by in vivo imaging with positron emission tomography and using an in vitro model of the human blood-brain barrier. J Pharmacol Exp Ther 316:79–86

Karhunen T, Tilgmann C, Ulmanen I, Panula P (1995) Neuronal and non-neuronal catechol-O-methyltransferase in primary cultures of rat brain cells. Int J Dev Neurosci 13:825–834

Karlgren M, Backlund M, Johansson I, Oscarson M, Ingelman-Sundberg M (2004) Characterization and tissue distribution of a novel human cytochrome P450-CYP2U1. Biochem Biophys Res Commun 315:679–685

Keep RF, Jones HC (1990) A morphometric study on the development of the lateral ventricle choroid plexus, choroid plexus capillaries and ventricular ependyma in the rat. Brain Res Dev Brain Res 56:47–53

Khan E (2005) An examination of the blood-brain barrier in health and disease. Br J Nurs 14:509–513

King CD, Rios GR, Green MD, Tephly TR (2000) UDPglucuronosyltransferases. Curr Drug Metab 1:143–161

Kratzer I, Vasiljevic A, Rey C, Fevre-Montange M, Saunders N, Strazielle N, Ghersi-Egea JF (2012) Complexity and developmental changes in the expression pattern of claudins at the blood-CSF barrier. Histochem Cell Biol 138:861–879

Kusuhara H, Sugiyama Y (2004) Efflux transport systems for organic anions and cations at the blood-CSF barrier. Adv Drug Deliv Rev 56:1741–1763

Lee SW, Kim WJ, Park JA, Choi YK, Kwon YW, Kim KW (2006) Blood-brain barrier interfaces and brain tumors. Arch Pharm Res 29:265–275

Lee A, Anderson AR, Rayfield AJ, Stevens MG, Poronnik P, Meabon JS, Cook DG, Pow DV (2012) Localisation of novel forms of glutamate transporters and the cystine-glutamate anti-porter in the choroid plexus: Implications for CSF glutamate homeostasis. J Chem Neuroanat 43:64–75

Leggas M, Adachi M, Scheffer GL, Sun D, Wielinga P, Du G, Mercer KE, Zhuang Y, Panetta JC, Johnston B, Scheper RJ, Stewart CF, Schuetz JD (2004) Mrp4 confers resistance to topotecan and protects the brain from chemotherapy. Mol Cell Biol 24:7612–7621

Leininger-Muller B, Ghersi-Egea JF, Siest G, Minn A (1994) Induction and immunological characterization of the uridine diphosphate-glucuronosyltransferase conjugating 1-naphthol in the rat choroid plexus. Neurosci Lett 175:37–40

Leslie EM, Deeley RG, Cole SP (2005) Multidrug resistance proteins: role of P-glycoprotein, MRP1, MRP2, and BCRP (ABCG2) in tissue defense. Toxicol Appl Pharmacol 204:216–237

Liang T, Habegger K, Spence JP, Foroud T, Ellison JA, Lumeng L, Li TK, Carr LG (2004) Glutathione S-transferase 8-8 expression is lower in alcohol-preferring than in alcohol-nonpreferring rats. Alcohol Clin Exp Res 28:1622–1628

Listowsky I, Rowe JD, Patskovsky YV, Tchaikovskaya T, Shintani N, Novikova E, Nieves E (1998) Human testicular glutathione S-transferases: insights into tissue-specific expression of the diverse subunit classes. Chem Biol Interact 111–112:103–112

Liu S, Stoesz SP, Pickett CB (1998) Identification of a novel human glutathione S-transferase using bioinformatics. Arch Biochem Biophys 352:306–313

Marowsky A, Burgener J, Falck JR, Fritschy JM, Arand M (2009) Distribution of soluble and microsomal epoxide hydrolase in the mouse brain and its contribution to cerebral epoxyeicosatrienoic acid metabolism. Neuroscience 163:646–661

McLeod HL, Krynetski EY, Relling MV, Evans WE (2000) Genetic polymorphism of thiopurine methyltransferase and its clinical relevance for childhood acute lymphoblastic leukemia. Leukemia 14:567–572

Miksys SL, Tyndale RF (2002) Drug-metabolizing cytochrome P450s in the brain. J Psychiatry Neurosci 27:406–415

Miksys S, Hoffmann E, Tyndale RF (2000a) Regional and cellular induction of nicotine-metabolizing CYP2B1 in rat brain by chronic nicotine treatment. Biochem Pharmacol 59:1501–1511

Miksys S, Rao Y, Sellers EM, Kwan M, Mendis D, Tyndale RF (2000b) Regional and cellular distribution of CYP2D subfamily members in rat brain. Xenobiotica 30:547–564

Minn A, Ghersi-Egea JF, Perrin R, Leininger B, Siest G (1991) Drug metabolizing enzymes in the brain and cerebral microvessels. Brain Res Brain Res Rev 16:65–82

Monks TJ, Ghersi-Egea JF, Philbert M, Cooper AJ, Lock EA (1999) Symposium overview: the role of glutathione in neuroprotection and neurotoxicity. Toxicol Sci 51:161–177

Morse DC, Stein AP, Thomas PE, Lowndes HE (1998) Distribution and induction of cytochrome P450 1A1 and 1A2 in rat brain. Toxicol Appl Pharmacol 152:232–239

Nebert DW, Russell DW (2002) Clinical importance of the cytochromes P450. Lancet 360:1155–1162

Nishibori M, Tahara A, Sawada K, Sakiyama J, Nakaya N, Saeki K (2000) Neuronal and vascular localization of histamine N-methyltransferase in the bovine central nervous system. Eur J Neurosci 12:415–424

Ott M, Fricker G, Bauer B (2009) Pregnane X receptor (PXR) regulates P-glycoprotein at the blood-brain barrier: functional similarities between pig and human PXR. J Pharmacol Exp Ther 329:141–149

Persidsky Y, Ramirez SH, Haorah J, Kanmogne GD (2006) Blood-brain barrier: structural components and function under physiologic and pathologic conditions. J Neuroimmune Pharmacol 1:223–236

Philbert MA, Beiswanger CM, Manson MM, Green JA, Novak RF, Primiano T, Reuhl KR, Lowndes HE (1995) Glutathione S-transferases and gamma-glutamyl transpeptidase in the rat nervous systems: a basis for differential susceptibility to neurotoxicants. Neurotoxicology 16:349–362

Redzic ZB, Preston JE, Duncan JA, Chodobski A, Szmydynger-Chodobska J (2005) The choroid plexus-cerebrospinal fluid system: from development to aging. Curr Top Dev Biol 71:1–52

Riachi NJ, Harik SI (1988) Strain differences in systemic 1-methyl-4-phenyl-1,2,3,6-tetrahydropyridine neurotoxicity in mice correlate best with monoamine oxidase activity at the blood-brain barrier. Life Sci 42:2359–2363

Riachi NJ, Harik SI, Kalaria RN, Sayre LM (1988) On the mechanisms underlying 1-methyl-4-phenyl-1,2,3,6-tetrahydropyridine neurotoxicity. II. Susceptibility among mammalian species correlates with the toxin's metabolic patterns in brain microvessels and liver. J Pharmacol Exp Ther 244:443–448

Richard K, Hume R, Kaptein E, Stanley EL, Visser TJ, Coughtrie MW (2001) Sulfation of thyroid hormone and dopamine during human development: ontogeny of phenol sulfotransferases and arylsulfatase in liver, lung, and brain. J Clin Endocrinol Metab 86:2734–2742

Rivett AJ, Eddy BJ, Roth JA (1982) Contribution of sulfate conjugation, deamination, and O-methylation to metabolism of dopamine and norepinephrine in human brain. J Neurochem 39:1009–1016

Schmitt C, Strazielle N, Richaud P, Bouron A, Ghersi-Egea JF (2011) Active transport at the blood-CSF barrier contributes to manganese influx into the brain. J Neurochem 117:747–756

Schreiber G, Richardson SJ (1997) The evolution of gene expression, structure and function of transthyretin. Comp Biochem Physiol B Biochem Mol Biol 116:137–160

Shang W, Liu WH, Zhao XH, Sun QJ, Bi JZ, Chi ZF (2008) Expressions of glutathione S-transferase alpha, mu, and pi in brains of medically intractable epileptic patients. BMC Neurosci 9:67

Shawahna R, Uchida Y, Decleves X, Ohtsuki S, Yousif S, Dauchy S, Jacob A, Chassoux F, Daumas-Duport C, Couraud PO, Terasaki T, Scherrmann JM (2011) Transcriptomic and quantitative proteomic analysis of transporters and drug metabolizing enzymes in freshly isolated human brain microvessels. Mol Pharm 8(4):1332–1341

Stanulla M, Schaeffeler E, Moricke A, Coulthard SA, Cario G, Schrauder A, Kaatsch P, Dordelmann M, Welte K, Zimmermann M, Reiter A, Eichelbaum M, Riehm H, Schrappe M, Schwab M (2009) Thiopurine methyltransferase genetics is not a major risk factor for secondary malignant neoplasms after treatment of childhood acute lymphoblastic leukemia on Berlin-Frankfurt-Munster protocols. Blood 114:1314–1318

Strazielle N, Ghersi-Egea JF (1997) Drug metabolism in newborn rat choroid plexus from lateral, third and fourth ventricle. Dev Anim Vet Sci 27:895–901

Strazielle N, Ghersi-Egea JF (1999) Demonstration of a coupled metabolism-efflux process at the choroid plexus as a mechanism of brain protection toward xenobiotics. J Neurosci 19:6275–6289

Strazielle N, Ghersi-Egea JF (2000a) Choroid plexus in the central nervous system: biology and physiopathology. J Neuropathol Exp Neurol 59:561–574

Strazielle N, Ghersi-Egea JF (2000b) Implication of blood-brain interfaces in cerebral drug metabolism and drug metabolite disposition. In: Williams G, Aruoma OI (eds) Molecular drug metabolism and toxicology. OICA International, Saint Lucia, London, pp 181–200

Strazielle N, Ghersi-Egea JF (2005) Factors affecting delivery of antiviral drugs to the brain. Rev Med Virol 15:105–133

Strazielle N, Belin MF, Ghersi-Egea JF (2003) Choroid plexus controls brain availability of anti-HIV nucleoside analogs via pharmacologically inhibitable organic anion transporters. AIDS 17:1473–1485

Strazielle N, Khuth ST, Ghersi-Egea JF (2004) Detoxification systems, passive and specific transport for drugs at the blood-CSF barrier in normal and pathological situations. Adv Drug Deliv Rev 56:1717–1740

Sun X, Shih AY, Johannssen HC, Erb H, Li P, Murphy TH (2006) Two-photon imaging of glutathione levels in intact brain indicates enhanced redox buffering in developing neurons and cells at the cerebrospinal fluid and blood-brain interface. J Biol Chem 281:17420–17431

Sura P, Sura R, Enayetallah AE, Grant DF (2008) Distribution and expression of soluble epoxide hydrolase in human brain. J Histochem Cytochem 56:551–559

Synold TW, Dussault I, Forman BM (2001) The orphan nuclear receptor SXR coordinately regulates drug metabolism and efflux. Nat Med 7:584–590

Szmydynger-Chodobska J, Strazielle N, Zink BJ, Ghersi-Egea JF, Chodobski A (2009) The role of the choroid plexus in neutrophil invasion after traumatic brain injury. J Cereb Blood Flow Metab 29:1503–1516

Tate SS, Ross LL, Meister A (1973) The -glutamyl cycle in the choroid plexus: its possible function in amino acid transport. Proc Natl Acad Sci U S A 70:1447–1449

Tayarani I, Cloez I, Clement M, Bourre JM (1989) Antioxidant enzymes and related trace elements in aging brain capillaries and choroid plexus. J Neurochem 53:817–824

Teissier E, Fennrich S, Strazielle N, Daval JL, Ray D, Schlosshauer B, Ghersi-Egea JF (1998) Drug metabolism in in vitro organotypic and cellular models of mammalian central nervous system: activities of membrane-bound epoxide hydrolase and NADPH-cytochrome P-450 (c) reductase. Neurotoxicology 19:347–355

Tolson A, Wang H (2010) Regulation of drug-metabolizing enzymes by xenobiotics receptors: PXR and CAR. Adv Drug Deliv Rev 62:1238–1249

Van Gelder NM (1968) A possible enzyme barrier for gamma-aminobutyric acid in the central nervous system. Prog Brain Res 29:259–271

Vasiliou V, Gonzalez FJ (2008) Role of CYP1B1 in glaucoma. Annu Rev Pharmacol Toxicol 48:333–358

Vidal JD, VandeVoort CA, Marcus CB, Lazarewicz NR, Conley AJ (2006) In vitro exposure to environmental tobacco smoke induces CYP1B1 expression in human luteinized granulosa cells. Reprod Toxicol 22:731–737

Volk B, Hettmannsperger U, Papp T, Amelizad Z, Oesch F, Knoth R (1991) Mapping of phenytoin-inducible cytochrome P450 immunoreactivity in the mouse central nervous system. Neuroscience 42:215–235

Wang X, Sykes DB, Miller DS (2010) Constitutive androstane receptor-mediated up-regulation of ATP-driven xenobiotic efflux transporters at the blood-brain barrier. Mol Pharmacol 78:376–383

Wang X, Hawkins BT, Miller DS (2011) Aryl hydrocarbon receptor-mediated up-regulation of ATP-driven xenobiotic efflux transporters at the blood-brain barrier. FASEB J 25:644–652

Wijnholds J, deLange EC, Scheffer GL, van den Berg DJ, Mol CA, van der Valk M, Schinkel AH, Scheper RJ, Breimer DD, Borst P (2000) Multidrug resistance protein 1 protects the choroid plexus epithelium and contributes to the blood-cerebrospinal fluid barrier. J Clin Invest 105:279–285

Xu C, Li CY, Kong AN (2005) Induction of phase I, II and III drug metabolism/transport by xenobiotics. Arch Pharm Res 28:249–268

Zastre JA, Chan GN, Ronaldson PT, Ramaswamy M, Couraud PO, Romero IA, Weksler B, Bendayan M, Bendayan R (2009) Up-regulation of P-glycoprotein by HIV protease inhibitors in a human brain microvessel endothelial cell line. J Neurosci Res 87:1023–1036

Zhang C, Harder DR (2002) Cerebral capillary endothelial cell mitogenesis and morphogenesis induced by astrocytic epoxyeicosatrienoic acid. Stroke 33:2957–2964

Zlokovic BV (2008) The blood-brain barrier in health and chronic neurodegenerative disorders. Neuron 57:178–201

Part II
Pharmacokinetic Concepts and Methods for Studying Drug Delivery

Chapter 5
Pharmacokinetic Concepts in Brain Drug Delivery

Margareta Hammarlund-Udenaes

Abstract This chapter presents the pharmacokinetic principles of blood–brain barrier (BBB) transport and the intra-brain distribution of drugs in order to provide a basis for understanding drug delivery to the brain from a clinically relevant perspective. The most important concentrations to measure when determining drug distribution are those of the unbound drug, because it is the unbound drug that causes the pharmacological effect by interacting with the target. Therefore, this chapter also discusses the pharmacokinetic basis, the kind of information provided, and the in vivo relevance of the methods used to obtain reliable, therapeutically useful estimates of brain drug delivery. The main factors governing drug distribution to the brain are the permeability of the BBB to the drug (influx clearance), the extent of nonspecific binding to brain tissue, and the efflux clearance of the drug. The ratio of the influx and efflux clearances provides an estimation of the extent of drug equilibration across the BBB, described by $K_{p,uu,brain}$. This parameter is important, as active uptake and/or efflux transporters influence the absolute brain concentrations of unbound drug in relation to those in plasma. The advantage of using $K_{p,uu,brain}$ during the drug discovery process lies in its ability to predict the potential success of drugs intended for action within the brain or, conversely, of those with few or no side effects in the brain.

A_{brain}	Amount of drug per g brain tissue excluding blood
A_{slice}	Amount of drug per g of brain slice
$A_{tot.brain\_inc\_blood}$	Amount of drug per g brain tissue including blood
$AUC_{tot,brain}$	Area under the total brain concentration–time curve
$AUC_{tot,plasma}$	Area under the total plasma concentration–time curve
$AUC_{u,brainISF}$	Area under the unbound brain ISF concentration–time curve

M. Hammarlund-Udenaes (✉)
Translational PKPD Group, Department of Pharmaceutical Biosciences, Uppsala University, Uppsala, Sweden
e-mail: mhu@farmbio.uu.se

M. Hammarlund-Udenaes et al. (eds.), *Drug Delivery to the Brain*, AAPS Advances in the Pharmaceutical Sciences Series 10, DOI 10.1007/978-1-4614-9105-7_5,

$AUC_{u,plasma}$	Area under the unbound plasma concentration–time curve
BBB	Blood–brain barrier
BCSFB	Blood–cerebrospinal fluid barrier
BBMEC	Bovine brain microvessel endothelial cells
Caco-2	Human epithelial colorectal adenocarcinoma cells
C_{buffer}	Concentration of drug in the buffer (brain slice method)
C_i	Apparent concentration of drug in a peripheral brain compartment i
$C_{tot,blood}$	Total concentration of drug in blood
$C_{tot.plasma}$	Total concentration of drug in plasma
$C_{u,brainISF}$	Concentration of drug in the brain ISF (by definition unbound)
$C_{u,cell}$	Average concentration of unbound drug in brain cells
$C_{u,plasma}$	Unbound concentration in plasma
$C_{u,ss,plasma}$	Unbound steady-state concentration in plasma
$C_{u,ss,brainISF}$	Unbound steady-state concentration in brain ISF
CL_{act_efflux}	Active efflux clearance from brain to blood at the BBB (μl/min/g_brain)
CL_{act_uptake}	Active uptake clearance from blood to brain at the BBB (μl/min/g_brain)
CL_{bulk_flow}	Clearance by bulk flow from brain ISF to CSF (μl/min/g_brain)
CL_i	Intercompartmental clearance between brain ISF and the peripheral brain compartment i
CL_{in}	Net influx clearance of drug to the brain (μl/min/g_brain), also called permeability clearance
$CL_{metabolism}$	Metabolic clearance of drug in the brain or at the BBB (μl/min/g_brain)
CL_{out}	Net efflux clearance of drug from the brain (μl/min/g_brain)
$CL_{passive}$	Passive diffusional clearance of drug at the BBB
CNS	Central nervous system
CSF	Cerebrospinal fluid
ECF	Extracellular fluid in the brain (also called ISF, interstitial fluid)
$f_{u,plasma}$	Fraction of unbound drug in plasma
$f_{u,brain}$	Fraction of unbound drug in brain homogenate
$f_{u,brain,corrected}$	Fraction of unbound drug in brain homogenate after correction for pH partitioning based on the p*K*a(s) of the drug
$f_{u,D}$	Fraction of unbound drug in diluted brain homogenate
GI	Gastrointestinal
ICF	Intracellular fluid in the brain
ISF	Interstitial fluid in the brain (also called ECF, extracellular fluid)
K_i	Inhibition constant
K_{in}	In situ brain perfusion unidirectional transfer constant (a clearance estimate equal to PS or CL_{in}) (μl/min/g_brain)

$K_{p,brain}$	Partition coefficient (ratio) of total brain to total plasma drug concentrations
$K_{p,u,brain}$	Ratio of total brain drug concentration to plasma unbound drug concentration
$K_{p,uu,brain}$	Ratio of brain ISF to plasma unbound drug concentrations
$K_{p,uu,cell}$	Ratio of brain ICF to ISF unbound drug concentrations
$K_{p,uu,CSF}$	Ratio of CSF to plasma unbound drug concentrations
logBB	Logarithm of the ratio of total brain to total plasma drug concentrations (equal to K_p)
MDCK	Madin–Darby canine kidney cells
Mdr1	Gene encoding for P-glycoprotein
$[plasma]_{,u}/[brain]_{,u}$	Ratio of plasma to brain unbound drug concentrations
P_{app}	Unidirectional apparent permeability coefficient measured in the apical-to-basolateral direction (cm/s)
PBS	Phosphate-buffered saline
P-gp	P-glycoprotein
PET	Positron emission tomography
PS	Permeability surface area product (in this context equal to net influx clearance to the brain) (μl/min/g_brain)
V_{blood}	Volume of blood in brain tissue
V_f	Volume of buffer film remaining around the sampled brain slice
V_i	Apparent volume of distribution of a peripheral brain compartment i
V_{ISF}	Physiological (and apparent) volume of ISF
$V_{u,brain}$	Volume of distribution of unbound drug in brain (ml/g_brain)

5.1 Introduction

The delivery of drugs from the blood to the brain takes place across the brain capillary endothelial cells comprising the blood–brain barrier (BBB). This is depicted in Fig. 5.1 in a classical electron micrograph of a capillary, the extremely thin endothelial cell layer and the brain parenchymal cells. Despite its thinness, the BBB is a very important organ that controls the brain environment in relation to the blood, picking up nutrients, discarding waste products, and hindering the influx of potentially harmful substances, including many drugs. The large surface area of the BBB and the high rate of blood flow to the brain ensure fast delivery of drugs to the brain (see Chap. 1 for physiological details of the BBB) but do not always ensure adequate drug concentrations within the brain.

This fact, together with the often inadequate methods used for measuring brain drug delivery, has caused problems in central nervous system (CNS) drug discovery and development. The methods used in the industry are developing rapidly; these

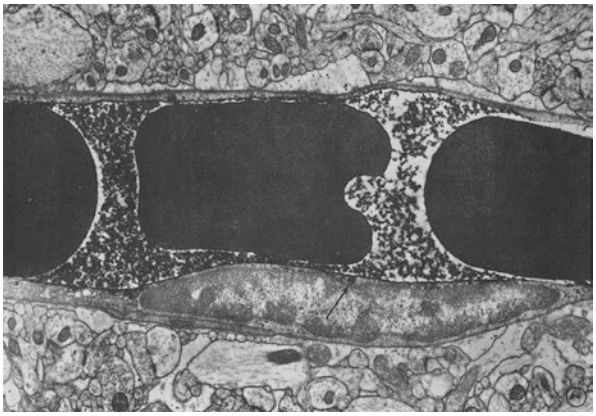

Fig. 5.1 An electron micrograph of a brain capillary with three erythrocytes, endothelial cell walls comprising the BBB, and brain parenchymal cells. The *black color* indicates intravenously administered peroxidase that does not pass the endothelial cells. The micrograph shows the two membranes of the BBB, the luminal membrane facing the blood and the abluminal membrane facing the brain parenchyma (×20,000). From Reese and Karnovsky with permission from the publisher (Reese and Karnovsky 1967)

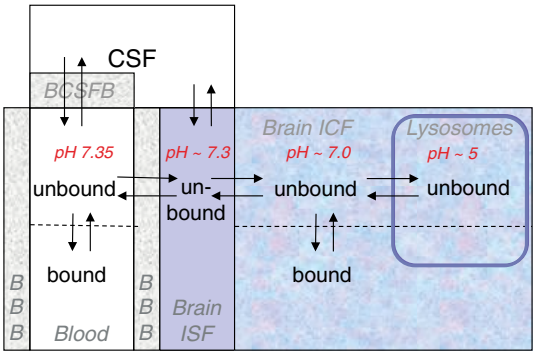

Fig. 5.2 Schematic illustration of drug distribution and equilibration across the BBB and other membranes within the brain parenchyma and unbound drug and drug bound to tissue components. The physiological volumes of the intra-brain compartments are brain interstitial fluid (ISF) 0.2 ml/g_brain and brain intracellular fluid (ICF) 0.8 ml/g_brain, of which the lysosomal compartment is 0.01 ml/g_brain. The figure is adapted from Hammarlund-Udenaes et al. (2008) with permission from the publisher

methods are discussed further in other chapters. This chapter focuses on the pharmacokinetic principles of drug delivery to the brain, on the rate and extent of drug transport as two separate factors governing drug delivery to the brain, and on the pharmacokinetic parameters needed to describe this.

Figure 5.2 provides a more schematic drawing of how drugs are distributed across the BBB and into the brain. As depicted, it is only the unbound drug molecules, i.e., those that are not bound to plasma proteins, that are able to transverse

membranes, in this case the BBB. The rate at which the drug enters the brain interstitial fluid (ISF, also called extracellular fluid (ECF)) depends on the permeability of the BBB to the particular molecule. Together with the passive and active uptake and efflux processes at the BBB, this will determine how much drug enters the brain ISF. The drug molecules will then be further distributed to and equilibrated within the brain cells, specific and nonspecific binding sites, and organelles, depending on the physicochemical interactions between the drug and the tissue.

Drug transport between blood and cerebrospinal fluid (CSF) takes place at the blood–CSF barrier (BCSFB). There is also some exchange between CSF and brain ISF. Transport from the CSF to the ISF involves passive diffusion, while transport from the ISF to the CSF involves both passive diffusion and the bulk flow of ISF (Cserr et al. 1977; Nicholson and Sykova 1998). See also Chap. 1. The pH of blood is 7.4 while that of the brain ISF is around 7.3, of the cell cytosol is 7.0, and of the lysosomes is around 5. These pH differences influence drug equilibration, with basic drugs accumulating more in low-pH organelles, especially in the lysosomes. By definition, the concentrations in the brain ISF are those of the unbound drug, as are the concentrations in the intracellular fluid (ICF). The extent of nonspecific binding is generally quantitatively much greater than that of specific binding to receptors or other target sites.

It is only the unbound drug that is in contact with receptor sites, and experimental data show that these concentrations are best correlated with clinical effects or side effects in the brain (Kalvass et al. 2007b; Large et al. 2009; Watson et al. 2009; Hammarlund-Udenaes 2010). The site of action of the particular drug will determine whether the brain ISF or the brain ICF concentration is more important in relation to the pharmacodynamic measurement. It has been clearly shown for dopamine agonists and other drugs that the unbound drug brain concentrations are much more closely related to receptor occupancy than the total brain concentrations or the concentrations of unbound drug in the blood (Watson et al. 2009; Stevens et al. 2012). This is clearly shown in Fig. 5.3, which depicts the receptor occupancy of several dopamine antagonists in relation to their plasma, total brain, and unbound drug brain concentrations.

The amount of drug to be delivered to the brain to achieve the desired effect is of course always an issue when deciding on the dose to be administered. However, a trade-off between side effects and the desired effects also needs to be taken into consideration. For drugs that are very efficiently effluxed at the BBB, there will be much lower unbound concentrations in the brain ISF than in plasma. This is advantageous if peripheral effects and avoidance of CNS side effects are desired but is less suitable if CNS effects are desired and peripheral side effects are to be avoided.

For measurements based on pharmacokinetic principles, drug delivery can be described by three distinctly different parameters. Two of these are important components of the transport of the drug across the BBB, and the third describes the intra-brain distribution of the drug. The first parameter describes the *rate of drug delivery to the brain* based on the permeability surface area product (PS), which in pharmacokinetic literature is often called the net influx clearance (CL_{in}, μl/min/g_brain). This describes the unidirectional net drug transport from blood to brain.

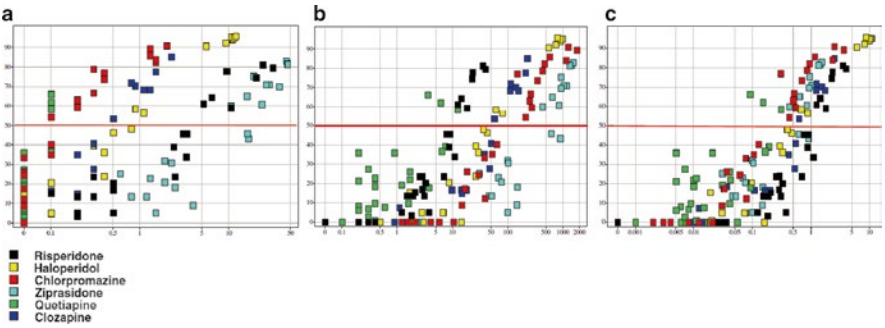

Fig. 5.3 Relationships between receptor occupancy and concentrations of neuroleptics normalized for their in vitro affinity for rat striatal D_2 receptors. (**a**) Total plasma concentrations, (**b**) total brain concentrations, and (**c**) unbound brain concentrations, illustrating the clear advantage of unbound brain concentrations when comparing drugs

The second parameter is the *extent of delivery*, which can be described either by the total drug concentrations in brain and plasma or by unbound drug concentrations at steady state. The total drug concentration ratio between brain and plasma is termed $K_{p,brain}$. Another way of describing the same parameter is logBB, which is also used for computational approaches (Young et al. 1988; Abraham et al. 1995; Norinder et al. 1998; Norinder and Haeberlein 2002; Sun 2004; Fan et al. 2010; Mensch et al. 2010a; Muehlbacher et al. 2011; Shityakov et al. 2013). The unbound drug concentration ratio between brain ISF and plasma is termed $K_{p,uu,brain}$ (Gupta et al. 2006). The relationship between the unbound and total drug concentrations in plasma is described by the fraction of drug that is not bound to plasma proteins, $f_{u,plasma}$. There are two alternative measurements in brain parenchymal tissue that can be used to describe *intra-brain distribution*, the third parameter. Both these correlate unbound to total drug concentrations in the brain. $f_{u,brain}$ is the fraction of unbound drug in the brain based on brain homogenate measurements (Kalvass and Maurer 2002), and $V_{u,brain}$ is the unbound volume of distribution within the brain in ml/g_brain tissue based on brain slice measurements (Kakee et al. 1996; Friden et al. 2007; Friden et al. 2009a). It should be noted that this volume term is not the same as that determined from in situ brain perfusion or PET studies. In the following sections, these three parameters are described in more detail. In vitro and in vivo methods used for determining brain drug delivery are further described in Chaps. 6–8 and 10.

5.2 Historical Aspects on Studying Brain Drug Delivery

Several expressions have been used to describe drug delivery to the brain in the literature: permeation (Tamai and Tsuji 2000; Abbott et al. 2008), brain penetration (Schinkel et al. 1996), extent of brain penetration (Liu et al. 2008), CNS penetration

(Summerfield et al. 2006), BBB penetration (Gunn et al. 2012), brain delivery (Pardridge et al. 1992), and CNS distribution (Dai et al. 2005; Kalvass et al. 2007a). The expressions used for the total brain-to-total plasma concentration ratio also vary: [brain]/[plasma] (Kalvass and Maurer 2002), K_p (a classical expression in pharmacokinetics for the partition coefficient between tissue and plasma (Rowland and Tozer 2011)), $K_{p,brain}$ (Gupta et al. 2006), and B/P (Maurer et al. 2005). Expressions for the brain-to-blood (or vice versa) unbound drug concentration ratios have been described as $K_{p,uu}$ (Gupta et al. 2006), $K_{p,free}$ (Liu et al. 2005), and $[plasma]_{,u}/[brain]_{,u}$ (Kalvass et al. 2007a).

Kalvass and Maurer made a seminal contribution in 2002 by initiating investigation into how to find out whether drugs are actively effluxed at the BBB (Kalvass and Maurer 2002), after P-glycoprotein (P-gp) had been found in the BBB (Cordon-Cardo et al. 1989; Thiebaut et al. 1989; Tsuji et al. 1992) and after the development of the P-gp knockout mouse model (Schinkel et al. 1996). They introduced the in vitro brain homogenate binding method in this context and simplified the estimation of extent of drug binding from diluted brain homogenate samples. The ratio of the fraction of unbound drug in plasma to that in brain ($f_{u,plasma}/f_{u,brain}$) was compared with the ratio of total brain to plasma concentrations ($K_{p,brain}$). Kalvass and Maurer concluded that, if the two ratios are the same, the drug will be transported across the BBB mainly by passive means. Efflux was indicated by differences between the ratios, i.e., this was an indirect way of describing BBB transport properties. We know today that the ratio of $f_{u,plasma}/f_{u,brain}$ itself as an indication of partitioning between brain and blood is misleading, as the main cause of deviations in $K_{p,brain}$ from this ratio is active transport at the BBB. The authors also compared CSF concentrations to brain and plasma concentrations and found that CSF concentrations overpredicted brain exposure for P-gp substrates.

Maurer et al. continued the work with a comparison of plasma and brain concentrations for 33 compounds (Maurer et al. 2005). Differences in $f_{u,plasma}/f_{u,brain}$ within a threefold range were allowed to cope with experimental errors and differences considered of little consequence for pharmacology or pharmacokinetics. The authors stated, "Because the brain to plasma ratio (K_p) is determined largely by nonspecific binding, efforts to optimize this parameter may actually lead to an unproductive or counterproductive design of drugs that are unnecessarily basic, lipophilic, and simply have a greater degree of nonspecific partitioning into brain tissue" (Maurer et al. 2005). This has proven to be a very relevant statement which partly explains the poor success rate in developing new drugs for CNS diseases (Kola and Landis 2004; Kaitin 2008). They also surmised that the underprediction of tissue distribution of bases, but not of neutral compounds and acids, based on $f_{u,brain}$ values could be the result of disruption of the subcellular acidic organelles such as lysosomes during homogenization.

Data from the literature were used by Kalvass and coauthors to compare more drugs, using the correlations developed earlier by Kalvass and Maurer (2002 and Kalvass et al. 2007a). They commented that $K_{p,brain}$ was still (in 2007) used to optimize brain delivery (values of ≥ 1 were arbitrarily given an interpretation of good brain delivery and values $<<1$ of poor brain delivery) and issued another warning

that this classification could be misleading, as $K_{p,brain}$ is also influenced by the relative extent of binding to plasma proteins and brain tissue (Kalvass et al. 2007a). A ratio based on plasma-to-brain concentrations of unbound drug was proposed ($[plasma]_{,u}/[brain]_{,u}$), and a log–log graph which plotted the in vivo P-gp efflux ratio vs. $[plasma]_{,u}/[brain]_{,u}$ was developed. Their conclusions on the BBB transport of the studied drugs were based on the quadrant into which the drug fell. This way of estimating BBB transport was further discussed by Avdeef in his book (Avdeef 2012). Kalvass et al. found indications of active uptake at the BBB and also found that efflux transport mediated by transporters other than P-gp was not able to be accurately predicted by the P-gp efflux ratios in Mdr1a(+/+) and Mdr1a(−/−) mice. For 10 of the 34 drugs studied, the extent of efflux in vivo was greater than could be explained by P-gp, and active uptake into the brain was indicated for 3 drugs. Thus, the in vivo P-gp efflux ratio for knockout and wild-type mice was not sufficient to predict brain delivery, and the $[plasma]_{,u}/[brain]_{,u}$ ratio was better predictive than the P-gp efflux ratio alone (Kalvass et al. 2007a). Despite this, most drug companies continue to trust P-gp efflux ratios in vivo or in vitro as the parameter of choice.

Concepts around the BBB transport of drugs were developed further by our group with the proposal of the term $K_{p,uu}$ by Gupta et al. to succinctly describe the brain ISF-to-blood concentration ratio for unbound drug (Gupta et al. 2006). Before the publication of this expression in 2006, the efficiency of net active efflux or uptake for individual drugs had been described as the "ratio of unbound brain to unbound blood concentrations" (Bouw et al. 2000; Xie et al. 2000; Bouw et al. 2001; Tunblad et al. 2003; Tunblad et al. 2004a; Tunblad et al. 2004b; Bostrom et al. 2005; Tunblad et al. 2005). BBB transport properties were thus separated from protein binding in plasma and binding to brain constituents, treating the three parameters as independent, individual properties of the drugs. It was indicated that the permeability of the brain to the drug (PS, CL_{in}) and the extent of equilibration across the BBB ($K_{p,uu,brain}$) were not correlated (Hammarlund-Udenaes et al. 1997; Hammarlund-Udenaes 2000; Hammarlund-Udenaes et al. 2008). The brain slice technique was also developed for studies of nonspecific binding to brain tissue in a high-throughput model and was compared with the brain homogenate method (Friden et al. 2007; Friden et al. 2009a; Friden et al. 2011).

Doran et al. concluded that most CNS drugs have some degree of P-gp-meditated transport and that this does not hamper their clinical use (Doran et al. 2005). They studied the total brain-to-plasma, CSF-to-plasma, and CSF-to-brain concentration ratios in Mdr1a(+/+) and Mdr1a(−/−) mice without taking into account differences between the drugs in nonspecific binding in the brain. They found that despite being a good P-gp substrate, risperidone has sufficient clinical effect in the CNS because of its high potency; the question of the correct dose in relation to peripheral side effects is also pertinent here.

At around the same time, Liu and co-workers published on properties that govern the equilibration of drug concentrations between brain and blood (Liu et al. 2005). They concluded that rapid permeation alone does not guarantee rapid equilibration. What is required is a combination of rapid permeation and low brain tissue binding. The authors used permeability as a surrogate for efflux clearance, although they are

not strictly interchangeable. Nonetheless, the combination of efflux clearance from the brain and the extent of brain binding determines the equilibration time across the BBB (Hammarlund-Udenaes et al. 1997; Liu et al. 2005; Syvanen et al. 2006).

Liu et al. proposed the direct extrapolation of $f_{u,plasma}$ to describe $f_{u,brain}$ as they (Liu et al. 2005) and others (Kalvass and Maurer 2002; Maurer et al. 2005) found a good correlation between the two ($r^2 = 0.69$ (Liu et al. 2005)). Although the use of $f_{u,plasma}$ for $f_{u,brain}$ has not been evaluated any further, its use can be questioned today if a good estimation of $K_{p,uu,brain}$ is the goal. Even a twofold difference between the two will result in a twofold difference in the value of $K_{p,uu,brain}$ and could skew information on the parameter needed for selection of the best drug candidates (see further Sect. 5.3.2.2).

Liu and Chen also discussed the extent and rate of brain penetration by looking at ways to increase the $K_{p,uu,brain}$ by reducing the efflux clearance or increasing the influx clearance (Liu and Chen 2005). In this chapter, $K_{p,brain}$ is considered unsuitable for evaluation of the potential success of a candidate as a CNS drug. Liu et al. later proposed strategies for studying transporters at the BBB, including "(1) Drug discovery screens should be used to eliminate good P-gp substrates for CNS targets. Special consideration could be given to moderate P-gp substrates as potential CNS drugs based on a high unmet medical need and the presence of a large safety margin. (2) Selection of P-gp substrates as drug candidates for non-CNS targets can reduce their CNS-mediated side effects" (Liu et al. 2008).

Several articles in the area have also been published by Summerfield and coworkers. In one study, they used Mdr1a/b(+(+) and Mdr1a/b(−/−) mice to investigate total brain-to-blood ratios ($K_{p,brain}$) in vitro, covering a wide range of physicochemical properties (Summerfield et al. 2006). They also compared $f_{u,brain}$ and $f_{u,blood}$. They concluded that the in vitro estimation of $f_{u,brain}/f_{u,blood}$ overpredicted the K_p observed in vivo because the in vitro ratio assumes that the concentrations in brain and blood are equal, while in reality they are not, because of active transport in the BBB. In their next study, they investigated 50 marketed drugs, compared in situ brain perfusion permeability with in vitro permeability, and then correlated these parameters with physicochemical information (Summerfield et al. 2007). In their 2008 publication they studied species differences in plasma and brain binding and found a good correlation in brain binding between rat, pig, and humans, thereby improving the prediction of drug distribution to the brain in humans; they also published a table defining PET and pharmacokinetic expressions (Summerfield et al. 2008). The use of PET and in vitro equilibrium dialysis to assess BBB transport of candidate drugs in CNS drug development was advocated in a recent publication (Gunn et al. 2012). An integrated approach involving permeability, active efflux, and brain distribution and focusing on unbound drug was proposed by Jeffrey and Summerfield (Jeffrey and Summerfield 2010).

Hakkarainen et al. compared the in vitro apparent permeability coefficient (P_{app}) from three cell culture systems with in vivo microdialysis measuring $K_{p,uu,brain}$ for nine drugs (Hakkarainen et al. 2010). Unfortunately, the use of an in vitro microdialysis probe recovery method in this otherwise thorough paper potentially affected the accurate measurement of the ISF concentrations and thus the $K_{p,uu,brain}$ values.

When the results for two P-gp substrates were omitted, the authors found an extremely good correlation between the permeability of BBMEC cells and the microdialysis results ($r=0.99$) and noted that the lower the permeability, the lower the $K_{p,uu,brain}$. When the drugs known to be P-gp substrates were included, the relationship became nonsignificant, as would be expected since lower $K_{p,uu,brain}$ values indicate more active efflux and are not correlated with permeability per se, as discussed below.

5.3 Parameters Describing Drug Delivery to the Brain

5.3.1 Rate of Brain Drug Delivery

5.3.1.1 What and Why

Permeability as a measurement of drug delivery to the brain has historically been the most common way of optimizing drug delivery to this area. Permeability measurements give an estimate of the unidirectional rate of transport of a drug across the BBB in situ or in a cell model in vitro. Rather than telling us how much drug has equilibrated across the BBB at steady state, these measurements tell us how fast the drug is transported across the BBB into the brain.

Permeability measurements are based on the tradition of studying gastrointestinal (GI) absorption. Physiological differences between the GI tract and the BBB, however, make this concept less translatable. Many articles have compared permeability values from in silico predictions, in vitro cell models, in situ methods, and in vivo methods (Levin 1980; Abbott 2004b; Liu et al. 2004; Bickel 2005; Garberg et al. 2005; Summerfield et al. 2007; Abbott et al. 2008; Di et al. 2009; Friden et al. 2009b; Hammarlund-Udenaes et al. 2009; Fan et al. 2010; Mensch et al. 2010a; Mensch et al. 2010b; Avdeef 2011; Avdeef and Sun 2011; Chen et al. 2011; Broccatelli et al. 2012; Di et al. 2012; Lanevskij et al. 2013). Quite commonly, methods measuring the rate of permeation are compared with those measuring the extent of permeation (Pardridge 2004; Hakkarainen et al. 2010).

5.3.1.2 Methods and Relationships

Permeability is described by the rate of permeation in cm/s, obtained by dividing the PS value estimated from in situ brain perfusion (called K_{in}) by the luminal surface area of the vascular space, estimated to be 150 cm^2/g_brain in vivo in rats (Fenstermacher et al. 1988), or by dividing by the surface area of the cell culture in vitro. The in vitro measurement is called P_{app}, the apparent permeability coefficient. In vitro methods include BBB-specific cell models as well as Caco-2 or MDCK cells (Chap. 6).

Table 5.1 Examples of in situ/in vivo CL_{in} values obtained by in situ brain perfusion or microdialysis

Drug	CL_{in} (µl/min/g_brain)	CL_{in} in Mdr1a (–/–) mice (µl/min/g_brain)	Species	Reference
Alfentanil	1,940	2,290	Mouse	(Zhao et al. 2009)
Antipyrine	492	–	Rat	(Avdeef and Sun 2011)
Atenolol	1.8	–	Rat	(Avdeef and Sun 2011)
Cimetidine	7	11	Mouse	(Zhao et al. 2009)
Colchicine	9	19	Mouse	(Zhao et al. 2009)
Diazepam	2,500	2,500	Mouse	(Zhao et al. 2009)
DPDPE	0.547	6.36	Mouse	(Dagenais et al. 2004)
Fentanyl	1,840	2,280	Mouse	(Dagenais et al. 2004)
Fexofenadine	3	13	Mouse	(Zhao et al. 2009)
Imipramine	1,860	–	Rat	(Avdeef and Sun 2011)
Loperamide	100	1,030	Mouse	(Dagenais et al. 2004)
Methadone	420	1,090	Mouse	(Dagenais et al. 2004)
Morphine	10.4	12.9	Mouse	(Dagenais et al. 2004)
Morphine	11.4	–	Rat	(Bouw et al. 2000; Tunblad et al. 2004b)
Morphine-3-glucuronide	0.11	–	Rat	(Xie et al. 2000)
Morphine-6-glucuronide	1.66	–	Rat	(Bouw et al. 2001; Tunblad et al. 2005)
Oxycodone	1,910	–	Rat	(Bostrom et al. 2006)
Phenytoin	334	347	Mouse	(Zhao et al. 2009)
Quinidine	34	541	Mouse	(Zhao et al. 2009)
Ritonavir	23	80	Mouse	(Zhao et al. 2009)
Sufentanil	340	295	Mouse	(Zhao et al. 2009)
Terfenadine	1,740	2,020	Mouse	(Zhao et al. 2009)
Valproate	243	181	Mouse	(Zhao et al. 2009)
Verapamil	315	1,370	Mouse	(Zhao et al. 2009)

The in situ brain perfusion method is a very elegant way of rapidly determining permeability in an animal model (Takasato et al. 1984). It can also be performed in genetically modified mice to study the influence of active transporters (Dagenais et al. 2000). Examples of CL_{in} (K_{in}) values from in situ brain perfusion and microdialysis studies are given in Table 5.1. It can be clearly seen, when Mdr1a(+/+) and

Mdra1a(−/−) mice are compared, that CL_{in} is decreased in the presence of P-gp. CL_{in} therefore describes the net influx clearance across the BBB. In general, the permeability of the BBB to a drug appears to be less critical to drug delivery than the influence of active efflux transporters. More about the pharmacokinetic aspects and relationships of the transport processes at the BBB can be found in Sect. 5.3.5.

5.3.2 Extent of Brain Drug Delivery

5.3.2.1 What and Why

The extent of drug delivery to the brain is based on steady-state measurements of the ratios of total concentrations in brain and plasma (the partition coefficient $K_{p,brain}$ or logBB), total concentrations in brain and unbound concentrations in plasma ($K_{p,u,brain}$), or unbound concentrations in brain ISF and plasma ($K_{p,uu,brain}$). In comparison to absorption from the GI tract, the amount of drug delivered to the brain can be compared with the bioavailability of drug in the brain, although the determining forces are somewhat different.

The most important advantage of using $K_{p,uu,brain}$ instead of $K_{p,brain}$ lies in its ability during the drug discovery process to predict the success of drugs intended for action within the brain or, conversely, for the avoidance of side effects in the brain. $K_{p,uu,brain}$ is the parameter that most closely relates to the drug's pharmacodynamic profile, if the receptors are situated facing the brain ISF. If the relevant receptors are intracellular, further investigations are required (see Sect. 5.3.4 and, in more detail, Chap. 10). The $K_{p,uu,brain}$ value is not influenced by plasma protein binding and brain parenchymal binding that would otherwise confound its interpretation. It gives a concrete value to the net result of passive and active transport across the BBB.

When $K_{p,uu,brain}$ is combined with the target binding properties of the drug, it is possible to estimate the required plasma concentrations, and thus the doses, for pharmacological success. There is no clear cutoff point below which a drug is not suitable for action within the brain, but the lower the $K_{p,uu,brain}$ value, the higher is the dose required to obtain pharmacologically relevant concentrations in the brain given similar potency. The trade-off is more between a dose that can be administered in relation to clinical effect vs. side effects and a dose that is economically defendable (Chap. 13).

5.3.2.2 Methods and Relationships

The $K_{p,brain}$ ratio can be determined by measuring steady-state drug concentrations or the area under the concentration–time curves in brain tissue, excluding capillary blood concentrations ($AUC_{tot,brain}$) and plasma ($AUC_{tot,plasma}$) after a single dose:

$$K_{\mathrm{p,brain}} = \frac{\mathrm{AUC}_{\mathrm{tot,brain}}}{\mathrm{AUC}_{\mathrm{tot,plasma}}}. \tag{5.1}$$

Measuring the AUC after a single dose is comparable to taking samples of brain and blood at one time point during steady state. The AUCs can then be substituted by the steady-state drug concentrations.

$K_{\mathrm{p,uu,brain}}$ can be determined directly from microdialysis samples from brain and plasma sites or by measuring total brain and plasma concentrations at steady state combined with plasma protein binding (giving the fraction of unbound drug in plasma, $f_{\mathrm{u,plasma}}$) and brain slice or brain homogenate measurements of nonspecific binding to brain parenchyma (Friden et al. 2007, 2009a, 2010:

$$K_{\mathrm{p,uu,brain}} = \frac{\mathrm{AUC}_{\mathrm{u,brainISF}}}{\mathrm{AUC}_{\mathrm{u,plasma}}} = \frac{\mathrm{AUC}_{\mathrm{tot,brain}}}{\mathrm{AUC}_{\mathrm{tot,plasma}} * V_{\mathrm{u,brain}} * f_{\mathrm{u,plasma}}}. \tag{5.2a}$$

Here, $\mathrm{AUC}_{\mathrm{u,brainISF}}$ describes the concentrations of unbound drug in brain ISF, and $\mathrm{AUC}_{\mathrm{u,plasma}}$ describes the concentrations of unbound drug in plasma. $V_{\mathrm{u,brain}}$ measured with the brain slice method may be replaced by $1/f_{\mathrm{u,brain}}$ after correction for pH partitioning if a brain homogenate is used to determine the nonspecific brain binding, as described in (5.2b):

$$K_{\mathrm{p,uu,brain}} = \frac{\mathrm{AUC}_{\mathrm{tot,brain}} * f_{\mathrm{u,brain,corrected}}}{\mathrm{AUC}_{\mathrm{tot,plasma}} * f_{\mathrm{u,plasma}}}. \tag{5.2b}$$

Thus, $V_{\mathrm{u,brain}}$ is similar but not equal to $1/f_{\mathrm{u,brain}}$, which can result in different results if pH partitioning is not compensated for (Friden et al. 2011). More about the similarities and differences between these parameters is given in Sect. 5.3.3 and in Chap 10. As the combined method involves measuring three individual parameters, the experimental error in each of them will affect the $\mathrm{K}_{\mathrm{p,uu,brain}}$ estimate (Kalvass et al. 2007a). Microdialysis is described in more detail in Chap. 7.

The concentration of drug in brain ISF is determined by diffusion, transport, metabolism, and binding processes, as described in Fig. 5.1. The differential equations describing the equilibration across the BBB between unbound drug in plasma and the brain ISF compartment are

$$\frac{V_{\mathrm{ISF}} * \mathrm{d}C_{\mathrm{u,brainISF}}}{\mathrm{dt}} = \mathrm{CL}_{\mathrm{in}} * C_{\mathrm{u,plasma}} - (\mathrm{CL}_{\mathrm{out}} + \mathrm{CL}_{\mathrm{i}}) * C_{\mathrm{u,brainISF}} + \mathrm{CL}_{\mathrm{i}} * C_{\mathrm{i}} \tag{5.3}$$

$$\frac{V_{\mathrm{i}} * \mathrm{d}C_{\mathrm{i}}}{\mathrm{dt}} = \mathrm{CL}_{\mathrm{i}} * (C_{\mathrm{u,brainISF}} - C_{\mathrm{i}}). \tag{5.4}$$

V_{ISF} describes both the physiological volume of the ISF and the apparent volume of distribution in the ISF, as it is assumed that there is no binding in this

compartment. CL_{in} and CL_{out} describe the net influx and efflux clearance across the BBB. CL_{in} is equivalent to PS. V_i and C_i are the apparent volume of and drug concentration in a possible deeper brain compartment i, and CL_i is the intercompartmental clearance between this compartment and the ISF. The plasma unbound drug concentration ($C_{u,plasma}$) is the driving force for the brain concentrations. Further equations necessary to describe the plasma concentration–time profile are beyond the scope of this chapter.

At steady state, there is no change in concentration in brain ISF, $dC_{u,brainISF}/dt = 0$, and the drug concentrations in plasma ($C_{u,ss,plasma}$) and brain ($C_{u,ss,brainISF}$) are in equilibrium. If $C_{u,brainISF} = C_i$, which can be assumed since C_i describes a hypothetical compartment, the relationship in (5.3) becomes

$$CL_{in} * C_{u,ss,plasma} = CL_{out} * C_{u,ss,brainISF}. \tag{5.5}$$

As $K_{p,uu,brain}$ is a steady-state parameter, it is not influenced by the further partitioning of the drug into brain cells:

$$K_{p,uu,brain} = \frac{C_{u,ss,brainISF}}{C_{u,ss,plasma}} = \frac{CL_{in}}{CL_{out}}. \tag{5.6}$$

It can be seen in (5.6) that $K_{p,uu,brain}$ is determined by the relative size of the net influx and efflux clearances. This means that influx and efflux clearances can both be small or large and still result in the same $K_{p,uu,brain}$. This explains why the permeability per se is not the most important parameter for estimating the extent of drug delivery to the brain. While rapid delivery to and elimination from the brain are clinically important for, for example, anesthetic drugs, the steady-state concentration in the brain is more important than the rate of delivery to the brain when a drug is to be administered repeatedly over time. The range of CL_{in} values within which brain delivery is still sufficient can, therefore, be quite wide. This is exemplified in Table 5.1 by the good clinical effects of morphine despite its low permeability clearance vs. the lack of clinical effect of loperamide despite its higher permeability clearance. This phenomenon is also illustrated in Fig. 5.4.

Equation 5.6 can be further developed to include the different processes governing the uptake and elimination of drug from brain ISF:

$$K_{p,uu,brain} = \frac{CL_{in}}{CL_{out}} = \frac{CL_{passive} + CL_{act\_uptake} - CL_{act\_efflux}}{CL_{passive} - CL_{act\_uptake} + CL_{act\_efflux} + CL_{bulk\_flow} + CL_{metabolism}}. \tag{5.7}$$

$CL_{passive}$ is the passive diffusional clearance across the BBB, which is assumed to be equal in both directions. CL_{act_efflux} describes the active efflux transport back across the BBB to the plasma (Syvanen et al. 2006). CL_{act_uptake} describes the active uptake transport across the BBB into the brain. Both active transport parameters can include

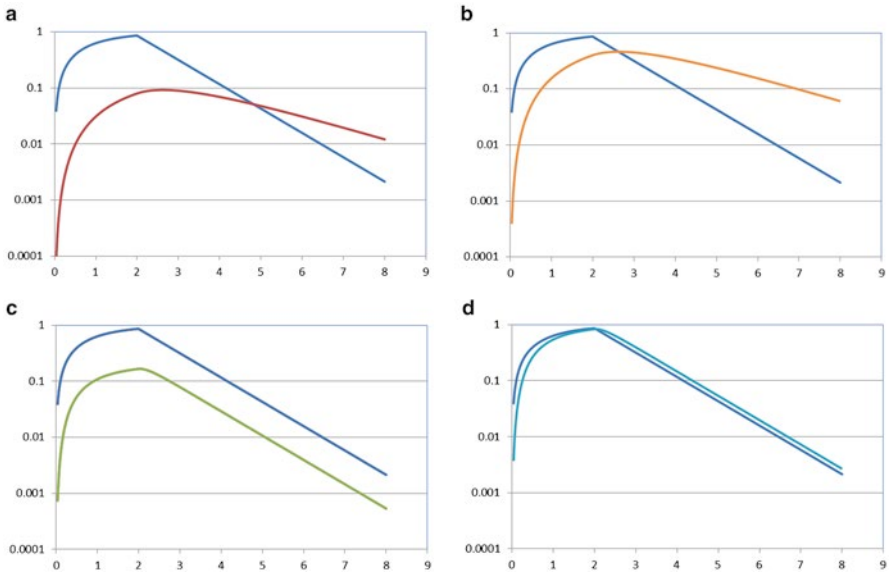

Fig. 5.4 Illustration of the absolute values of CL_{in} and CL_{out} and their relationships with the resulting brain concentration–time profile of unbound drug with time on the *x*-axis and concentration on the *y*-axis. The *blue line*, similar in all parts of the figure, describes the unbound drug concentration in blood after a short intravenous infusion of a fictive drug. The other lines describe the brain unbound drug concentrations. The relative values of CL_{in} and CL_{out} are in (**a**) $CL_{in} = 1$ and $CL_{out} = 5$ giving a $K_{p,uu,brain}$ of 0.2; (**b**) $CL_{in} = 5$ and $CL_{out} = 5$, giving a $K_{p,uu,brain}$ of 1.0; (**c**) $CL_{in} = 10$ and $CL_{out} = 50$ giving a $K_{p,uu,brain}$ of 0.2; and (**d**) $CL_{in} = 50$ and $CL_{out} = 50$, giving a $K_{p,uu,brain}$ of 1.0. In (**a**) and (**b**), CL_{out} values together with the size of $V_{u,brain}$ (the same in all simulations) result in a longer half-life for the drug in the brain than in blood. In (**c**) and (**d**), the half-life in the brain follows that in blood because of the more rapid processes in the brain than in blood. A comparison of (**a**) and (**c**), and (**b**) and (**d**), respectively, shows that the $K_{p,uu,brain}$ is the same, independent of a tenfold difference in CL_{in} and independent of differences in half-lives in the brain

one or several transporter functions and can, if of interest, be further divided into the individual processes. CL_{bulk_flow} is the bulk flow of ISF from brain to CSF, reported to be 0.1–0.3 μl/min/g_brain (Cserr et al. 1977; Rosenberg et al. 1980; Abbott 2004a). $CL_{metabolism}$ describes the elimination of a drug through metabolism within the brain.

Equation 5.7 assumes that $CL_{passive}$ is the same, independent of direction of transport across the BBB. In reality, this may not be correct for the two membranes of the BBB (luminal vs. abluminal), as a result of different fluid flow rates and diffusion properties. The equation suggests that active efflux of a drug will reduce CL_{in} and that active uptake will reduce CL_{out}. An experimental illustration of this is provided by the clear effect of P-gp on CL_{in} that was found by Dagenais et al. (Dagenais et al. 2004). They used in situ brain perfusion methodology in Mdr1a(+/+) and Mdr1a (−/−) mice. The PS of loperamide increased tenfold from 100 μl/min/g_brain in Mdr1a(+/+) mice to 1,030 μl/min/g_brain in Mdr1a (−/−) mice (Table 5.1). It should also be borne in mind that CL_{in} and CL_{out} are the net clearances across both the luminal and abluminal membranes of the brain endothelial cells when, in reality,

Table 5.2 Relationship between the rate and the extent of equilibration across the BBB. More than one transporter may be acting on the drug, and transport can be in either direction. Further examples from a combination of iv infusion, brain slice, and plasma protein binding measurements can be found in Friden et al. (2009b)

Parameter value	Relationship	Interpretation	In vivo examples and references
$K_{p,uu} \approx 1$	$CL_{in} \approx CL_{out}$	Net influx and efflux clearances are similar either because the drug is only passively transported across the BBB or because the active influx and efflux rates are similar. Note that the absolute sizes of the clearances are not important, only the relationship between the two.	Codeine (Xie and Hammarlund-Udenaes 1998) Diazepam (Dubey et al. 1989)
$K_{p,uu} < 1$	$CL_{in} < CL_{out}$	Elimination processes from the brain are more efficient than influx processes. This may be because of more active efflux transport at the BBB, metabolism within the brain parenchyma, or bulk flow (the latter requires clearances to be quite low, as bulk flow is 0.1–0.3 µl/min/g_brain)	Morphine (Bouw et al. 2000; Tunblad et al. 2003; Bostrom et al. 2008) Risperidone and 9-hydroxyrisperidone (Liu et al. 2009; Doran et al. 2012) Ofloxacin, perfloxacin (Ooie et al. 1997) 6-Mercaptopurine, probenecid (Deguchi et al. 2000) Atenolol, methotrexate, paclitaxel (Friden et al. 2009b) Quinidine, indinavir, dexamethasone (Uchida et al. 2011a)
$K_{p,uu} > 1$	$CL_{in} > CL_{out}$	Influx processes across the BBB are quantitatively more efficient than efflux/metabolism/bulk flow processes. This can only be accomplished if the drug is actively transported from blood to brain	Oxycodone (Bostrom et al. 2006) Diphenhydramine (Sadiq et al. 2011) Nicotine (Tega et al. 2013)

transporters are usually situated in either the apical or the basolateral membrane and are rarely situated in both membranes (Chap. 2).

If the only method of transport is passive or if the influx and elimination processes are of the same magnitude, the unbound concentrations in the brain will equal those in plasma when equilibrium is reached between the two sites. $K_{p,uu,brain}$ will be smaller than unity if efflux dominates the transport process (Gupta et al. 2006; Hammarlund-Udenaes et al. 2008) and greater than unity if active uptake dominates (Bostrom et al. 2006; Hammarlund-Udenaes et al. 2008). The relationships and their interpretation are further described in Table 5.2.

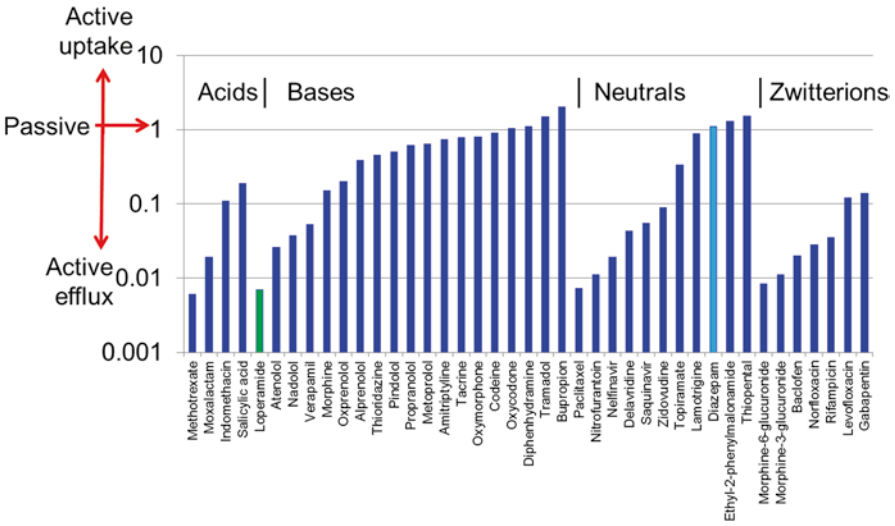

Fig. 5.5 $K_{p,uu,brain}$ values from a combined study of $K_{p,brain}$, $f_{u,plasma}$, and $V_{u,brain}$ in rats. $K_{p,uu,brain}$, to the extent that it can be extrapolated to humans, indicates the clinical usefulness of the drug for action in the brain. The brain ISF concentrations are similar ($K_{p,uu,brain} \approx 1$), lower ($K_{p,uu,brain} < 1$), or higher ($K_{p,uu,brain} > 1$) than the unbound concentrations in plasma. Data from Fridén et al. (2009b)

Most drugs seem to be effluxed at the BBB. This can be seen in Fig. 5.5, which provides the $K_{p,uu,brain}$ values for drugs that are acids, bases, neutrals, and zwitterions (Friden et al. 2009b).

5.3.3 Intra-brain Distribution

5.3.3.1 What and Why

Estimation of the extent of nonspecific binding of a drug to brain tissue is necessary in order to relate the total brain concentrations, which are easily measured, to the unbound drug concentrations, which are more difficult to measure but more valuable for optimizing drug treatment. This is an intra-brain measurement and is not related to BBB function.

5.3.3.2 Methods and Relationships

The three methods by which intra-brain distribution can be estimated include microdialysis in the brain in conjunction with a brain sample to provide total brain concentrations at steady state (Wang and Welty 1996), the brain homogenate method (Kalvass and Maurer 2002; Mano et al. 2002), and the brain slice method (Kakee

et al. 1996; Friden et al. 2009a; Friden et al. 2010). The microdialysis and brain slice methods result in an estimate of $V_{u,brain}$ in ml/g_brain tissue, while the brain homogenate method results in an estimate of $f_{u,brain}$.

Microdialysis

Microdialysis can be used to determine both $K_{p,uu,brain}$ and $V_{u,brain}$. In order to calculate $V_{u,brain}$, it is necessary to measure total brain concentrations at steady state at the same time as obtaining the concentration of unbound drug in brain ISF by microdialysis.

The expression $V_{u,brain}$ was introduced by Wang and Welty in their microdialysis study of gabapentin influx and efflux across the BBB (Wang and Welty 1996). The paper was seminal for improving understanding of how the BBB transport of drugs can be evaluated (Hammarlund-Udenaes et al. 2008). $V_{u,brain}$ can be described by (5.8)

$$V_{u,brain} = \frac{A_{tot,brain\_incl\_blood} - V_{blood} * C_{tot,blood}}{C_{u,brainISF}}, \tag{5.8}$$

where $A_{tot,brain\_incl\_blood}$ is the amount of drug present per g brain, obtained from chemical analysis of the brain tissue sample. It is then necessary to subtract the amount of drug in the brain capillaries in order to obtain the amount present in the brain tissue itself. V_{blood} is the physiological volume of blood present in the brain tissue sample, and $C_{tot,blood}$ is the total concentration of the drug in the blood. The volume used here is critical for correct estimation of $V_{u,brain}$ (Friden et al. 2010).

Brain Homogenate

The brain homogenate method results in an estimate of $f_{u,brain}$. In short, this method uses fresh or frozen brain homogenate that is diluted with phosphate-buffered saline (PBS) and equilibrated across a dialysis membrane. The method is described in detail in Chap. 10. Samples of buffer and homogenate are analyzed, and the fraction of unbound drug in the original sample is calculated using (5.9) to compensate for the dilution:

$$\text{Undiluted}\_f_{u,brain} = \frac{1/D}{((1/f_{u,D})-1)+1/D}. \tag{5.9}$$

D is the dilution factor of the brain tissue sample, and $f_{u,D}$ is the fraction of unbound drug in the diluted brain homogenate sample.

There are several advantages associated with the brain homogenate method: it is easy to carry out, using the same equipment as that used for plasma protein binding;

high-throughput methodology can be used; and the process can be based on frozen tissue. However, it should be borne in mind that homogenizing the sample can expose sites that normally do not bind the drug in vivo (Liu and Chen 2005). Furthermore, membrane structures are destroyed by homogenization. This excludes the measurement of the influence of possible transport processes and pH differences between the brain parenchymal cells and organelles.

The brain homogenate method was used by Di et al. to compare $f_{u,brain}$ values between species, with subsequent important potential for using animal brain homogenates to estimate the nonspecific binding of drugs in human brain (Di et al. 2011). Summerfield had earlier studied species differences between rat, pig, and humans regarding binding to brain tissue (Summerfield et al. 2008).

Brain Slice

The brain slice method results in an estimate of $V_{u,brain}$ in ml/g_brain tissue. This method, which provides information that is relevant for issues such as nonspecific binding of drug to tissues, lysosomal trapping, and active uptake of drug into cells, is described in detail in Chap. 10. The brain slice method has been optimized for high throughput of drugs, using cassettes of 5–10 drugs that can be studied simultaneously, although it is important that the total combined concentration of drugs in buffer in the cassette does not exceed 1 μM (Friden et al. 2007; Friden et al. 2009a).

$V_{u,brain}$ is obtained by dividing the total brain concentration found in the slices by the buffer concentration, which describes the ISF unbound concentration. Equation 5.10 is adapted from (5.8) to the in vitro situation:

$$V_{u,brain} = \frac{A_{slice} - V_f * C_{buffer}}{C_{buffer} * (1 - V_f)}. \tag{5.10}$$

A_{slice} is the amount of drug per gram of slice, and C_{buffer} is the concentration of drug in the buffer. V_f is the volume of buffer film that remains around the sampled slice due to incomplete absorption of buffer by the filter paper. Fridén et al. confirmed the value of V_f as 0.094 ml/g_slice (Friden et al. 2009a), in agreement with the original observation by Kakee et al. (1996).

5.3.3.3 Interpretations and Caveats

The relevant physiological volumes in brain tissue include the volume of brain ISF at 0.2 ml/g_brain (Nicholson and Phillips 1981; Nicholson and Sykova 1998) and the volume of total brain water at 0.8 ml/g_brain (Reinoso et al. 1997). Thus, drugs with values of $V_{u,brain}$ lower than 0.8 ml/g_brain are predominantly distributed outside the brain cells, with minimal binding to proteins or membranes [e.g., moxalactam, which has a $V_{u,brain}$ of 0.46 ml/g_brain (Friden et al. 2010)]. As the values for

Table 5.3 Interpretation of $V_{u,brain}$ information. For practical purposes, the value of 0.8 ml/g_brain can be approximated to 1 ml/g_brain. The values were obtained using the brain slice method; for further descriptions, see Friden et al. (2009b)

Parameter value	Interpretation	Examples (ml/g_brain)
$V_{u,brain} < 0.8$ ml/g_brain	Restricted distribution of the drug to the interstitial fluid. Probably very low entrance into cells and very little binding to proteins or membranes	Morphine-3-glucuronide (0.7) Moxalactam (0.6)
$V_{u,brain} \approx 0.8$ ml/g_brain	Free distribution of the drug in ISF and intracellular fluid and/or slight binding to proteins or membranes	Salicylic acid (1.0) Zidovudine (1.1)
$V_{u,brain} > 0.8$ ml/g_brain	Binding to proteins or membranes, or distribution to subcellular organelles such as lysosomes. The higher the value, the more drug is bound or distributed	Amitriptyline (310) Atenolol (2.5) Diazepam (20) Gabapentin (4.6) Indomethacin (14) Levofloxacin (1.7) Loperamide (370) Nelfinavir (860) Paclitaxel (769) Thioridazine (3,300) Verapamil (54)

$V_{u,brain}$ increase further above 0.8 ml/g_brain, intracellular distribution and/or binding to proteins or membranes also increase [e.g., loperamide, which has a $V_{u,brain}$ of 370 ml/g_brain (Friden et al. 2010)]. $V_{u,brain}$ varies between 0.2 and 3,300 ml/g_brain for the drugs studied to date. Table 5.3 provides examples of known $V_{u,brain}$ values and the interpretations that can be made based on this information; currently, the highest value is for thioridazine (Friden et al. 2009b).

When using $V_{u,brain}$ to determine $K_{p,uu,brain}$ (5.2a), Fridén et al. indicated that the value of V_{blood} from the literature (5.8) may be too high (Friden et al. 2010). This appeared especially true for drugs with low $K_{p,brain}$ values. A low $K_{p,brain}$ can be the result of either very efficient efflux at the BBB or a level of plasma protein binding that greatly exceeds the nonspecific binding of the drug in the brain. The latter situation causes a problem when the value for V_{blood} used in (5.8) is too high. An improved method was developed for this estimation (Friden et al. 2010). It should be noted that the remaining brain vascular space can vary with the method used to sacrifice the animal.

5.3.4 Intracellular Drug Distribution

The intracellular concentrations of drugs cannot be measured directly. However, information on the intracellular distribution of the drug can be obtained by combining brain slice and homogenate data (Friden et al. 2007; Friden et al. 2009a; Friden

et al. 2011). $K_{p,uu,cell}$ describes the steady-state ratio of intracellular to brain ISF concentrations of unbound drug, assuming an average concentration ratio for all cell types within the brain. In the drug discovery process, this will extend the available information about the distribution of new chemical entities and will help in selecting optimal drug candidates. It is important to measure $K_{p,uu,cell}$, and subsequently estimate the average concentration of unbound drug in brain cells ($C_{u,cell}$), in relation to the pharmacodynamic measurements when the drug has an intracellular site of action or when information about possible active transport processes at the ISF–cellular interface is required. $K_{p,uu,cell}$ is calculated as

$$K_{p,uu,cell} = \frac{C_{u,cell}}{C_{u,brainISF}} = V_{u,brain} * f_{u,brain}. \quad (5.11)$$

$V_{u,brain}$ is determined from brain slice experiments, and $f_{u,brain}$ is determined from equilibrium dialysis of brain homogenates. The details of how to estimate $K_{p,uu,cell}$ and the further division of this parameter into cytosolic and lysosomal components are further described in Chap. 11. Maurer et al. have mentioned lysosomal accumulation as a possible reason for differences in the distribution of acidic, neutral, and basic drugs between homogenates and in vivo measurements in tissues other than brain (Maurer et al. 2005). This appears also to be important in brain tissue when comparing brain slice data with data from brain homogenates (Friden et al. 2011).

5.3.5 *Combining Rate, Extent, and Intra-brain Drug Distribution in Brain Pharmacokinetics*

It will be obvious by now that the three main properties of brain drug delivery, CL_{in}, $K_{p,uu,brain}$, and $V_{u,brain}$, describe three individual properties of a drug. Fig. 5.6 provides the $V_{u,brain}$ and $K_{p,uu,brain}$ values for 41 drugs (Friden et al. 2009b).

It can be seen from the figure that these two properties are not correlated. Two examples in the figure highlight this: loperamide and diazepam. The very low $K_{p,uu,brain}$ of loperamide (0.007) indicates that only 0.7 % of the concentration of unbound loperamide in plasma will be present in brain ISF and thus that the efflux of loperamide at the BBB is very efficient. At the same time, loperamide has a high affinity for brain tissue, with a $V_{u,brain}$ of 370 ml/g_brain. The transport of diazepam at the BBB, on the other hand, is mainly passive, with a $K_{p,uu,brain}$ close to 1 and a lower $V_{u,brain}$ of 12 ml/g_brain. Similarly, the permeability clearance has little in common with the size of $K_{p,uu,brain}$. As discussed earlier (Fig. 5.4 and Eq. 5.6), the influx and efflux clearances can both be small or large but can still result in the same $K_{p,uu,brain}$.

The time for drug concentrations to reach equilibrium between brain and blood, on the other hand, is determined by the efflux clearance and the extent of intra-brain binding ($V_{u,brain}$), giving rise to an intrinsic half-life in brain, which can be shorter or longer than that in plasma. If the plasma half-life is longer than the intrinsic

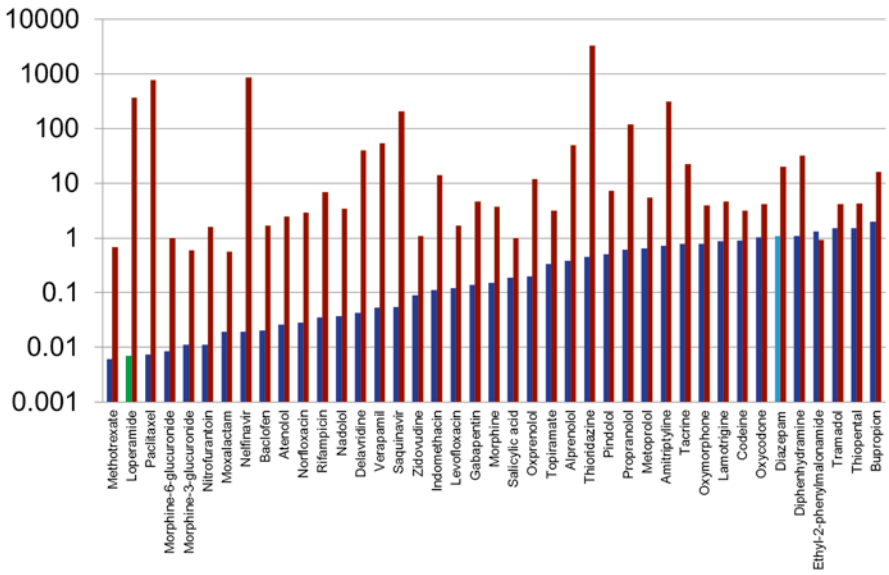

Fig. 5.6 Connections between nonspecific binding in the brain, as shown by $V_{u,brain}$ values (ml/g_brain), and $K_{p,uu,brain}$ ratios for 41 drugs. The scale on the logarithmic *y*-axis shows the experimentally obtained values for $K_{p,uu,brain}$ and $V_{u,brain}$. The drugs are sorted according to their $K_{p,uu,brain}$ value from smallest to largest. The individual $V_{u,brain}$ values are plotted alongside the $K_{p,uu,brain}$ values and show that there is very little correlation between the two parameters. Data are from Fridén et al. (2009b)

half-life, it will also determine the half-life in brain which will be equal to that in plasma, and the intrinsic half-life will not be observed. Thus, the unbound drug concentration in plasma is the driving force for the half-life in the brain, and the pharmacokinetic profile in plasma is therefore an important determinant of the concentration–time profile in the brain. Only when elimination of the drug is slower from the brain than from plasma will the intrinsic half-life in the brain be observable.

The determinants of the concentration–time profile of a drug in the brain are comparable to the parameters determining the pharmacokinetics in plasma: the plasma concentration–time profile is similarly determined by the absorption and elimination rates and the extent of binding to tissues. The relative unbound concentrations in brain and plasma are determined by the transport process that dominates the movement of the drug at the BBB. This may be active efflux, active influx, or passive transport as discussed earlier. CL_{in} therefore only influences the brain concentrations (cf. bioavailability) in relation to the efflux clearance but will not influence the concentration–time profile, including the time to reach equilibrium.

Active efflux of a drug will not only decrease CL_{in} but will also increase CL_{out}, as described in (5.7), thus increasing the rate of the equilibration processes across the BBB, although this depends on how the efflux transporter functions. If it only hinders influx (the so-called vacuum cleaner model), the efflux from the brain parenchyma

will not be influenced, and the active process will not influence the brain elimination half-life (Syvanen et al. 2006). It is, however, more likely that the transporter will both hinder influx and increase efflux (e.g., P-gp). In this case, the part that increases efflux will subsequently affect the elimination process and therefore the time to reach equilibrium across the BBB, while the part that hinders influx will not affect the elimination process and therefore neither the time to equilibrium.

Equilibrium across the BBB is thus reached more quickly for strong P-gp substrates than for drugs that are weaker substrates or that are only passively transported but otherwise have similar properties. Active efflux also has an important influence on the time aspects of equilibration across the BBB in the studies comparing drug uptake into the brains of Mdr1a/b(−/−) and Mdr1a/b(+/+) mice. Equilibration is expected to take longer in Mdr1a/b (−/−) mice. When sampling at a specific time after a single dose, this can influence the difference between the two groups of mice. Possible differences in equilibration time therefore need to be taken into consideration.

Padowski and Pollack have discussed the theoretical effects of P-gp on the time to equilibrium across the BBB (Padowski and Pollack 2011), and the theoretical consequences of active uptake and efflux have also been discussed by several authors (Hammarlund-Udenaes et al. 1997; Golden and Pollack 1998; Syvanen et al. 2006). Liu and Chen have suggested that the parameters determining the half-life of equilibration are the permeability of the BBB to the respective drug and the extent of binding in the brain (Liu and Chen 2005). As explained in this chapter, they could be more clearly described as the efflux permeability and the extent of binding in the brain. The slower of the half-lives in plasma and brain will determine the half-life in the brain.

Cooperation between P-gp and breast cancer resistance protein (BCRP) in increasing the efficiency of the efflux process at the BBB has been clearly described by Kusuhara and Sugiyama (2009). The presence and contributions of other, including as yet unknown, transporters should also be included in speculations about the fate of drugs at the BBB (Kalvass et al. 2007a; Hammarlund-Udenaes et al. 2008; Agarwal et al. 2012).

As stated earlier, measurement of unbound drug concentrations in plasma is not enough to determine the unbound concentrations in the brain. Binding to brain parenchymal tissue is also too different from binding to plasma proteins to allow prediction of one from the other. The presence of active transport at the BBB does not allow the ratio of the fraction of unbound drug in plasma to that in brain ($f_{u,plasma}/f_{u,brain}$) to be used to predict brain penetration, as discussed in Sect. 5.2.

5.4 CSF Pharmacokinetics vs. Brain ISF Pharmacokinetics

The CSF is an accessible sampling site for measuring human brain concentrations of unbound drug, given that CSF concentrations follow brain concentrations. However, the role of the CSF as an alternative site for measuring unbound brain

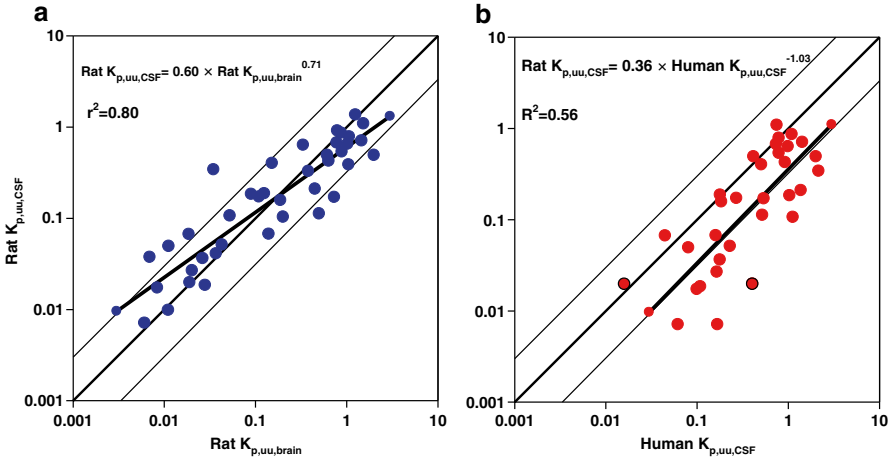

Fig 5.7 (**a**) Correlations between rat $K_{p,uu,brain}$ and $K_{p,uu,CSF}$ for 41 drugs. The *middle diagonal line* is the line of identity. The two *parallel lines* show a threefold difference in range from the line of identity. (**b**) Correlations between $K_{p,uu,CSF}$ in humans [*x*-axis, data from Shen et al. (2004)] and $K_{p,uu,CSF}$ in rats (*y*-axis). Although there is a good correlation between the species, there is a threefold deviation from the line of identity. Reprinted with permission from Fridén et al. (2009b). Copyright 2009 American Chemical Society

concentrations is still under discussion and has not been well established. De Lange and Danhof proposed that the CSF may be of limited value in the prediction of unbound brain concentrations (de Lange and Danhof 2002). There are both similarities and differences in drug concentrations between brain ISF and CSF. The BCSFB, situated between the epithelial cells of the choroid plexus, is different from the BBB as a transport site for drugs, and the cells have different origins (epithelial vs. endothelial), which could influence transporter expression. The relevant question for drug discovery is whether the transporter functions in the BBB are similar enough to those in the BCSFB to allow the extrapolation of CSF data to obtain data on the exposure of the brain to unbound drug.

While CSF sampling could be useful in the selection of drug candidates for entry into development programs, Lin cautions that CSF concentrations could differ from brain unbound drug concentrations (Lin 2008). Fridén et al. have actually demonstrated the correlations between rat CSF and rat brain ISF concentrations for 41 compounds (Friden et al. 2009b). In this study, 33 of the $K_{p,uu,brain}$ values were within a ±3-fold range of the $K_{p,uu,CSF}$ values, which is considered quite good (r^2=0.80). However, Fig. 5.7a shows that the regression line deviates from the line of identity for these compounds. CSF concentrations were lower than the unbound brain concentrations at high $K_{p,uu,brain}$ values and higher at low $K_{p,uu,brain}$ values. This confirms earlier work by Kalvass and Maurer, who found that unbound brain concentrations were overpredicted by CSF concentrations for drugs with low $K_{p,uu,brain}$ values (Kalvass and Maurer 2002). While the results from Fridén et al. support the use of $K_{p,uu,CSF}$ for comparisons of brain exposure between drugs (Friden et al. 2009b), it

should be borne in mind that other drug groups could behave differently and that individual drug concentrations could deviate from the predicted value quite extensively.

Differences in the location and expression of P-gp between the BBB and the BCSFB could explain the concentration differences at low $K_{p,uu,brain}$ values. P-gp and BCRP are located in the luminal membranes of the endothelial cells in the BBB. According to an early report, P-gp was thought to be located in the apical membrane of the epithelial cells of the choroid plexus, which would result in substrates being transported towards the CSF (Rao et al. 1999). This has, however, been questioned (Sun et al. 2003). It seems unlikely that P-gp would transport substrates into the CSF in the epithelial cells of the BCSFB and in the opposite direction, into the blood, at the BBB. If this was the case, the CSF would be an even less suitable site of measurement for estimating brain ISF concentrations. Although studies have shown less efficient P-gp functioning at the BCSFB than at the BBB, the findings do not actually support the transport of drugs towards the CSF (Fig. 5.4a). The reason for the differences in P-gp function may have been found by Gazzin et al., who measured the relative content of P-gp and Mrp1 protein in rat and human brain capillaries and choroid plexi (Gazzin et al. 2008). They showed that the P-gp content in rat choroid plexus homogenates was only 0.5 % of that in brain endothelial cells, while the opposite trend was seen with Mrp1—the microvessel content was only 4 % of that in the choroid plexus. The human data showed a similar picture. Thus, although it is present at the BCSFB, P-gp seems to have a significantly smaller role than at the BBB because of its lower expression.

The correlation between human and rat $K_{p,uu,CSF}$ is unexpectedly good; however, the threefold deviation from the line of identity, with higher CSF-to-plasma concentration ratios in humans than in rats (Fig. 5.7b), is an issue not yet explained (Shen et al. 2004; Friden et al. 2009b).

Issues on differences in the time between dosage and sampling, and the sites of sampling, in humans vs. rodents should also be taken into consideration when studying the use of CSF sampling to estimate drug distribution to the brain. The timing aspects of CSF concentration–time profiles vs. brain ISF profiles have been studied by Westerhout et al., using a multiple microdialysis probe approach in rats (Westerhout et al. 2012). It takes only slightly longer to reach similar concentrations of acetaminophen in rat CSF from the cisterna magna and third/fourth ventricles than in brain ISF, although the difference is extended for CSF from the subarachnoid space furthest away from the brain ISF, which is of relevance when sampling CSF in humans. Westerhout et al. developed a physiological pharmacokinetic model for multiple brain compartments, based on these rat data. After translation of the model by changing the physiological parameters to those in humans, they were able to successfully predict lumbar CSF data on acetaminophen comparable to those available from humans. The model also predicted human ISF concentration–time profiles (Westerhout et al. 2012).

In summary, it appears that CSF is an adequate sampling site for obtaining a preliminary understanding of unbound brain concentrations, with the caveats of taking into account the deviations at low and high $K_{p,uu,brain}$ values. The results support

the use of $K_{p,uu,CSF}$ for reasonable comparisons of brain exposure to drugs. However, it should be borne in mind that individual drugs could deviate quite extensively from the general correlation.

5.5 Drug Interactions at the BBB

Because transporters play such an important role at the BBB in controlling the traffic of drug molecules into and out of the brain, they are also the targets of clinically significant drug interactions. Unfortunately, interaction studies at the BBB in humans are few. Cyclosporin is the most potent P-gp inhibitor on the market, doubling the brain concentrations of verapamil and loperamide (Sasongko et al. 2005; Hsiao and Unadkat 2012). Quinidine also inhibits P-gp in humans, causing a 20 % reduction in the response to CO_2 (opiate-induced respiratory depression) when administered with loperamide (Sadeque et al. 2000).

The $K_{p,uu,brain}$ value of a drug can give information on its interaction potential at the BBB (Hammarlund-Udenaes et al. 2008). For a $K_{p,uu,brain}$ close to unity, the interaction potential is likely to be very low, given that the drug is mainly passively transported. The lower the $K_{p,uu,brain}$, the higher the theoretical possibility of an interaction with other drugs, depending on whether the low $K_{p,uu,brain}$ was caused by efflux via a single transporter or if there are several transporters acting on one drug. Inhibition of the main efflux transporter would thus result in increased brain concentrations, while an interaction at an uptake transporter would decrease brain concentrations. In practice, it appears that interactions at the BBB are very rare, irrespective of the direction of active transport (Sasongko et al. 2005; Liu et al. 2008; Sadiq et al. 2011). This low incidence of interaction is possibly the result of relatively low concentrations of both victim drug and perpetrator in plasma. For example, the inhibition constant K_i for an interaction between diphenhydramine and oxycodone at the uptake transporter in cell cultures was much higher than the maximum possible concentration (Sadiq et al. 2011). This is quite different from the situation in the gastrointestinal tract and the liver after oral administration, where much higher concentrations are present and the likelihood of an interaction is subsequently much greater.

5.6 Species Comparisons

Species differences in the extent of drug transport at the BBB are the result of differences in transporter expression and the capacity/specificity of substrates. It is now well known that the expression of P-gp and BCRP proteins in humans is different from that in other species; for example, BCRP content is higher than P-gp content in humans, and P-gp content is higher than BCRP content in rats/mice (Ito et al. 2011; Uchida et al. 2011b) (see also Chap. 2). This could explain the differences in

the results obtained when studying three PET tracers that are P-gp substrates in several species (Syvanen and Hammarlund-Udenaes 2010).

While the behavior of morphine at the BBB is very similar in rats, pigs, and humans ($K_{p,uu,brain}$ values are about 0.3–0.6), the $K_{p,uu,brain}$ in sheep deviates from this (1.2–1.9, depending on age) (Bouw et al. 2000; Tunblad et al. 2003; Ederoth et al. 2004; Tunblad et al. 2004a; Bengtsson et al. 2009). This could be because of differences in transporter expression between sheep and the other species, i.e., possibly a lack of an efflux transporter.

There is a clear need for further translational studies between experimental animals and humans to learn more about species differences in transporter function at the BBB.

5.7 Current Status and Future Challenges

The understanding of the pharmacokinetics of drug delivery to the brain has developed rapidly, although there is still some confusion on rate vs. extent measurements and methods and what they describe. There are now ways of measuring unbound concentrations in the brain using high-throughput methodology. However, in vivo studies have shown that there are still transport proteins acting as efflux or uptake transporters at the BBB that have not yet been identified. The presence and actions of transporters other than P-gp therefore need to be included in future thinking about brain penetration.

The scientific community and the drug industry are continuously striving to find correlations that will simplify measurements and enable prediction of successful new CNS drugs. There is, however, a difference between finding a correlation coefficient that is good enough and predicting the fate of an individual compound based on this correlation or based on measuring a substitute parameter. The use of log–log comparisons and correlation coefficients could actually hide important information. Considering what we now know about individual BBB transport properties, it is actually easier to select the new compounds that have high and low $K_{p,uu}$ values and assign them to potential clinical use depending on whether the desired effect is therapeutic efficacy or the avoidance of side effects in the CNS. Other aspects, such as peripheral side effects and affinity to target, are also included in the decision-making process (Chap. 13). It is recommended to put as much effort into the decision on the kind of measurements to be made as into finding correlations between measures that may or may not be clinically relevant. The area of BBB transport of drugs clearly illustrates the time lag between new scientific findings and adoption of these findings in the drug industry. Shortening this time lag would significantly improve the success rate in drug discovery/development.

More research is needed before we can extrapolate information from animal studies to prediction of clinically relevant brain drug delivery. Some progress has recently been made in demonstrating the expression of transporters at the BBB for different species, but in vivo examples are needed to confirm these findings and

more experimental studies are required. When we have identified most of the transporters, there is a real chance that predictive science will be able to help in the selection of good compounds for use in the CNS. There is also a need for better predictive disease models, understanding of disease mechanisms, and understanding of how disease states can influence drug transport into the brain, although these are beyond the scope of this chapter.

In an era of increased use of peptides and proteins, there is hope that some of these compounds will be available to the brain. The task before us, of understanding and improving their uptake into the brain from a quantitative and mechanistic perspective, is vast (Chap. 16). A greater understanding and quantitative investigation of the role of nanocarrier delivery of drugs to the brain are also required. The achievement of successful delivery by these means in humans will require biocompatible carriers, and these should be a particular focus.

5.8 Conclusions

The rate and extent of drug delivery to the brain are two individual properties that are not numerically related. Data on intra-brain distribution are required to obtain the full brain delivery picture in relation to total drug concentrations. The pharmacokinetic relationship between the permeability of the BBB (influx clearance) and the extent of drug delivery to the brain explains why the permeability per se is of lesser importance for brain drug delivery. Recent findings have confirmed the great value of focusing measurements on the extent of delivery of unbound drug to the brain. This is governed by the net flux of drug across the BBB and ultimately determines the clinical success rate when receptor occupancy is taken into account.

5.9 Points for Discussion

- What are the reasons for the extent of delivery being more clinically relevant than the rate of delivery for estimating the delivery of drugs into the brain?
- What are the essential processes governing the net influx and efflux clearances at the BBB, CL_{in}, and CL_{out}?
- For which purposes can $V_{u,brain}$ measurements be used?
- In what way could estimation of CNS exposure of drugs by the use of ratio of total brain to total plasma drug concentrations be flawed?
- How does the exchange of drugs between blood and CSF differ from the exchange between blood and brain ISF?
- How is the CSF concentration of the drug related to the brain ISF concentration? Discuss the rationale of using a surrogate approach for approximation of brain ISF concentration in preclinical and clinical studies (i.e., using other measurements than the direct ones).

- How may the understanding of intracellular distribution of drug contribute to establishment of a link between PK and PD?
- What are the clinically relevant sites of drug–drug interaction regarding brain drug delivery?
- What are the key components of interspecies differences in brain drug delivery?

References

Abbott NJ (2004a) Evidence for bulk flow of brain interstitial fluid: significance for physiology and pathology. Neurochem Int 45:545–552

Abbott NJ (2004b) Prediction of blood–brain barrier permeation in drug discovery from in vivo, in vitro and in silico models. Drug Discov Today Technol 1:407–416

Abbott NJ, Dolman DE, Patabendige AK (2008) Assays to predict drug permeation across the blood–brain barrier, and distribution to brain. Curr Drug Metab 9:901–910

Abraham MH, Chadha HS, Mitchell RC (1995) Hydrogen-bonding. Part 36. Determination of blood brain distribution using octanol-water partition coefficients. Drug Des Discov 13:123–131

Agarwal S, Uchida Y, Mittapalli RK, Sane R, Terasaki T, Elmquist WF (2012) Quantitative Proteomics of Transporter Expression in Brain Capillary Endothelial Cells Isolated from P-gp, BCRP, and P-gp/BCRP Knockout Mice. Drug Metab Dispos 40(6):1164–1169

Avdeef A (2011) How well can in vitro brain microcapillary endothelial cell models predict rodent in vivo blood–brain barrier permeability? Eur J Pharm Sci 43:109–124

Avdeef A (2012) Absorption and drug development. Solubility, permeability and charge state. Wiley, New York

Avdeef A, Sun N (2011) A new in situ brain perfusion flow correction method for lipophilic drugs based on the pH-dependent Crone-Renkin equation. Pharm Res 28:517–530

Bengtsson J, Ederoth P, Ley D, Hansson S, Amer-Wahlin I, Hellstrom-Westas L, Marsal K, Nordstrom CH, Hammarlund-Udenaes M (2009) The influence of age on the distribution of morphine and morphine-3-glucuronide across the blood–brain barrier in sheep. Br J Pharmacol 157:1085–1096

Bickel U (2005) How to measure drug transport across the blood–brain barrier. NeuroRx 2:15–26

Bostrom E, Hammarlund-Udenaes M, Simonsson US (2008) Blood–brain barrier transport helps to explain discrepancies in in vivo potency between oxycodone and morphine. Anesthesiology 108:495–505

Bostrom E, Simonsson US, Hammarlund-Udenaes M (2005) Oxycodone pharmacokinetics and pharmacodynamics in the rat in the presence of the P-glycoprotein inhibitor PSC833. J Pharm Sci 94:1060–1066

Bostrom E, Simonsson US, Hammarlund-Udenaes M (2006) In vivo blood–brain barrier transport of oxycodone in the rat: indications for active influx and implications for pharmacokinetics/pharmacodynamics. Drug Metab Dispos 34:1624–1631

Bouw MR, Gardmark M, Hammarlund-Udenaes M (2000) Pharmacokinetic-pharmacodynamic modelling of morphine transport across the blood–brain barrier as a cause of the antinociceptive effect delay in rats—a microdialysis study. Pharm Res 17:1220–1227

Bouw MR, Xie R, Tunblad K, Hammarlund-Udenaes M (2001) Blood–brain barrier transport and brain distribution of morphine-6-glucuronide in relation to the antinociceptive effect in rats–pharmacokinetic/pharmacodynamic modelling. Br J Pharmacol 134:1796–1804

Broccatelli F, Larregieu CA, Cruciani G, Oprea TI, Benet LZ (2012) Improving the prediction of the brain disposition for orally administered drugs using BDDCS. Adv Drug Deliv Rev 64:95–109

Chen H, Winiwarter S, Friden M, Antonsson M, Engkvist O (2011) In silico prediction of unbound brain-to-plasma concentration ratio using machine learning algorithms. J Mol Graph Model 29:985–995

Cordon-Cardo C, O'Brien JP, Casals D, Rittman-Grauer L, Biedler JL, Melamed MR, Bertino JR (1989) Multidrug-resistance gene (P-glycoprotein) is expressed by endothelial cells at blood–brain barrier sites. Proc Natl Acad Sci U S A 86:695–698

Cserr HF, Cooper DN, Milhorat TH (1977) Flow of cerebral interstitial fluid as indicated by the removal of extracellular markers from rat caudate nucleus. Exp Eye Res 25(Suppl): 461–473

Dagenais C, Graff CL, Pollack GM (2004) Variable modulation of opioid brain uptake by P-glycoprotein in mice. Biochem Pharmacol 67:269–276

Dagenais C, Rousselle C, Pollack GM, Scherrmann JM (2000) Development of an in situ mouse brain perfusion model and its application to mdr1a P-glycoprotein-deficient mice. J Cereb Blood Flow Metab 20:381–386

Dai H, Chen Y, Elmquist WF, Yang H, Wang Q, Elmquist WF (2005) Distribution of the novel antifolate pemetrexed to the brain. J Pharm Exp Ther 315:222–229

de Lange EC, Danhof M (2002) Considerations in the use of cerebrospinal fluid pharmacokinetics to predict brain target concentrations in the clinical setting: implications of the barriers between blood and brain. Clin Pharmacokinet 41:691–703

Deguchi Y, Yokoyama Y, Sakamoto T, Hayashi H, Naito T, Yamada S, Kimura R (2000) Brain distribution of 6-mercaptopurine is regulated by the efflux transport system in the blood–brain barrier. Life Sci 66:649–662

Di L, Artursson P, Avdeef A, Ecker GF, Faller B, Fischer H, Houston JB, Kansy M, Kerns EH, Kramer SD, Lennernas H, Sugano K (2012) Evidence-based approach to assess passive diffusion and carrier-mediated drug transport. Drug Discov Today 17:905–912

Di L, Kerns EH, Bezar IF, Petusky SL, Huang Y (2009) Comparison of blood–brain barrier permeability assays: in situ brain perfusion, MDR1-MDCKII and PAMPA-BBB. J Pharm Sci 98:1980–1991

Di L, Umland JP, Chang G, Huang Y, Lin Z, Scott DO, Troutman MD, Liston TE (2011) Species independence in brain tissue binding using brain homogenates. Drug Metab Dispos 39:1270–1277

Doran A, Obach RS, Smith BJ, Hosea NA, Becker S, Callegari E, Chen C, Chen X, Choo E, Cianfrogna J, Cox LM, Gibbs JP, Gibbs MA, Hatch H, Hop CE, Kasman IN, Laperle J, Liu J, Liu X, Logman M, Maclin D, Nedza FM, Nelson F, Olson E, Rahematpura S, Raunig D, Rogers S, Schmidt K, Spracklin DK, Szewc M, Troutman M, Tseng E, Tu M, Van Deusen JW, Venkatakrishnan K, Walens G, Wang EQ, Wong D, Yasgar AS, Zhang C (2005) The impact of P-glycoprotein on the disposition of drugs targeted for indications of the central nervous system: evaluation using the MDR1A/1B knockout mouse model. Drug Metab Dispos 33:165–174

Doran AC, Osgood SM, Mancuso JY, Shaffer CL (2012) An evaluation of using rat-derived single-dose neuropharmacokinetic parameters to project accurately large animal unbound brain drug concentrations. Drug Metab Dispos 40:2162–2173

Dubey RK, McAllister CB, Inoue M, Wilkinson GR (1989) Plasma binding and transport of diazepam across the blood–brain barrier. No evidence for in vivo enhanced dissociation. J Clin Invest 84:1155–1159

Ederoth P, Tunblad K, Bouw R, Lundberg CJ, Ungerstedt U, Nordstrom CH, Hammarlund-Udenaes M (2004) Blood–brain barrier transport of morphine in patients with severe brain trauma. Br J Clin Pharmacol 57:427–435

Fan Y, Unwalla R, Denny RA, Di L, Kerns EH, Diller DJ, Humblet C (2010) Insights for predicting blood–brain barrier penetration of CNS targeted molecules using QSPR approaches. J Chem Inf Model 50:1123–1133

Fenstermacher J, Gross P, Sposito N, Acuff V, Pettersen S, Gruber K (1988) Structural and functional variations in capillary systems within the brain. Ann N Y Acad Sci 529:21–30

Friden M, Bergstrom F, Wan H, Rehngren M, Ahlin G, Hammarlund-Udenaes M, Bredberg U (2011) Measurement of unbound drug exposure in brain: modeling of pH partitioning explains diverging results between the brain slice and brain homogenate methods. Drug Metab Dispos 39:353–362

Friden M, Ducrozet F, Middleton B, Antonsson M, Bredberg U, Hammarlund-Udenaes M (2009a) Development of a high-throughput brain slice method for studying drug distribution in the central nervous system. Drug Metab Dispos 37:1226–1233

Friden M, Gupta A, Antonsson M, Bredberg U, Hammarlund-Udenaes M (2007) In vitro methods for estimating unbound drug concentrations in the brain interstitial and intracellular fluids. Drug Metab Dispos 35:1711–1719

Friden M, Ljungqvist H, Middleton B, Bredberg U, Hammarlund-Udenaes M (2010) Improved measurement of drug exposure in the brain using drug-specific correction for residual blood. J Cereb Blood Flow Metab 30:150–161

Friden M, Winiwarter S, Jerndal G, Bengtsson O, Wan H, Bredberg U, Hammarlund-Udenaes M, Antonsson M (2009b) Structure-brain exposure relationships in rat and human using a novel data set of unbound drug concentrations in brain interstitial and cerebrospinal fluids. J Med Chem 52:6233–6243

Garberg P, Ball M, Borg N, Cecchelli R, Fenart L, Hurst RD, Lindmark T, Mabondzo A, Nilsson JE, Raub TJ, Stanimirovic D, Terasaki T, Oberg JO, Osterberg T (2005) In vitro models for the blood–brain barrier. Toxicol in Vitro 19:299–334

Gazzin S, Strazielle N, Schmitt C, Fevre-Montange M, Ostrow JD, Tiribelli C, Ghersi-Egea JF (2008) Differential expression of the multidrug resistance-related proteins ABCb1 and ABCc1 between blood–brain interfaces. J Comp Neurol 510:497–507

Golden PL, Pollack GM (1998) Rationale for influx enhancement versus efflux blockade to increase drug exposure to the brain. Biopharm Drug Dispos 19:263–272

Gunn RN, Summerfield SG, Salinas CA, Read KD, Guo Q, Searle GE, Parker CA, Jeffrey P, Laruelle M (2012) Combining PET biodistribution and equilibrium dialysis assays to assess the free brain concentration and BBB transport of CNS drugs. J Cereb Blood Flow Metab 32:874–883

Gupta A, Chatelain P, Massingham R, Jonsson EN, Hammarlund-Udenaes M (2006) Brain distribution of cetirizine enantiomers: comparison of three different tissue-to-plasma partition coefficients: K(p), K(p, u), and K(p, uu). Drug Metab Dispos 34:318–323

Hakkarainen JJ, Jalkanen AJ, Kaariainen TM, Keski-Rahkonen P, Venalainen T, Hokkanen J, Monkkonen J, Suhonen M, Forsberg MM (2010) Comparison of in vitro cell models in predicting in vivo brain entry of drugs. Int J Pharm 402:27–36

Hammarlund-Udenaes M (2000) The use of microdialysis in CNS drug delivery studies. Pharmacokinetic perspectives and results with analgesics and antiepileptics. Adv Drug Deliv Rev 45:283–294

Hammarlund-Udenaes M (2010) Active-site concentrations of chemicals—are they a better predictor of effect than plasma/organ/tissue concentrations? Basic Clin Pharmacol Toxicol 106:215–220

Hammarlund-Udenaes M, Bredberg U, Friden M (2009) Methodologies to assess brain drug delivery in lead optimization. Curr Top Med Chem 9:148–162

Hammarlund-Udenaes M, Friden M, Syvanen S, Gupta A (2008) On the rate and extent of drug delivery to the brain. Pharm Res 25:1737–1750

Hammarlund-Udenaes M, Paalzow LK, de Lange EC (1997) Drug equilibration across the blood–brain barrier–pharmacokinetic considerations based on the microdialysis method. Pharm Res 14:128–134

Hsiao P, Unadkat JD (2012) P-glycoprotein-based loperamide-cyclosporine drug interaction at the rat blood–brain barrier: prediction from in vitro studies and extrapolation to humans. Mol Pharm 9:629–633

Ito K, Uchida Y, Ohtsuki S, Aizawa S, Kawakami H, Katsukura Y, Kamiie J, Terasaki T (2011) Quantitative membrane protein expression at the blood–brain barrier of adult and younger cynomolgus monkeys. J Pharm Sci 100:3939–3950

Jeffrey P, Summerfield S (2010) Assessment of the blood–brain barrier in CNS drug discovery. Neurobiol Dis 37:33–37

Kaitin KI (2008) Obstacles and opportunities in new drug development. Clin Pharm Ther 83:210–212

Kakee A, Terasaki T, Sugiyama Y (1996) Brain efflux index as a novel method of analyzing efflux transport at the blood–brain barrier. J Pharm Exp Ther 277:1550–1559

Kalvass JC, Maurer TS (2002) Influence of nonspecific brain and plasma binding on CNS exposure: implications for rational drug discovery. Biopharm Drug Dispos 23:327–338

Kalvass JC, Maurer TS, Pollack GM (2007a) Use of plasma and brain unbound fractions to assess the extent of brain distribution of 34 drugs: comparison of unbound concentration ratios to in vivo p-glycoprotein efflux ratios. Drug Metab Dispos 35:660–666

Kalvass JC, Olson ER, Cassidy MP, Selley DE, Pollack GM (2007b) Pharmacokinetics and pharmacodynamics of seven opioids in P-glycoprotein-competent mice: assessment of unbound brain EC50, u and correlation of in vitro, preclinical, and clinical data. J Pharm Exp Ther 323:346–355

Kola I, Landis J (2004) Can the pharmaceutical industry reduce attrition rates? Nat Rev Drug Discov 3:711–715

Kusuhara H, Sugiyama Y (2009) In vitro-in vivo extrapolation of transporter-mediated clearance in the liver and kidney. Drug Metab Pharmacokinet 24:37–52

Lanevskij K, Japertas P, Didziapetris R (2013) Improving the prediction of drug disposition in the brain. Expert Opin Drug Metab Toxicol 9(4):473–486

Large CH, Kalinichev M, Lucas A, Carignani C, Bradford A, Garbati N, Sartori I, Austin NE, Ruffo A, Jones DN, Alvaro G, Read KD (2009) The relationship between sodium channel inhibition and anticonvulsant activity in a model of generalised seizure in the rat. Epilepsy Res 85:96–106

Levin VA (1980) Relationship of octanol/water partition coefficient and molecular weight to rat brain capillary permeability. J Med Chem 23:682–684

Lin JH (2008) CSF as a surrogate for assessing CNS exposure: an industrial perspective. Curr Drug Metab 9:46–59

Liu X, Chen C (2005) Strategies to optimize brain penetration in drug discovery. Curr Opin Drug Discov Dev 8:505–512

Liu X, Chen C, Smith BJ (2008) Progress in brain penetration evaluation in drug discovery and development. J Pharm Exp Ther 325:349–356

Liu X, Smith BJ, Chen C, Callegari E, Becker SL, Chen X, Cianfrogna J, Doran AC, Doran SD, Gibbs JP, Hosea N, Liu J, Nelson FR, Szewc MA, Van Deusen J (2005) Use of a physiologically based pharmacokinetic model to study the time to reach brain equilibrium: an experimental analysis of the role of blood–brain barrier permeability, plasma protein binding, and brain tissue binding. J Pharm Exp Ther 313:1254–1262

Liu X, Tu M, Kelly RS, Chen C, Smith BJ (2004) Development of a computational approach to predict blood–brain barrier permeability. Drug Metab Dispos 32:132–139

Liu X, Van Natta K, Yeo H, Vilenski O, Weller PE, Worboys PD, Monshouwer M (2009) Unbound drug concentration in brain homogenate and cerebral spinal fluid at steady state as a surrogate for unbound concentration in brain interstitial fluid. Drug Metab Dispos 37:787–793

Mano Y, Higuchi S, Kamimura H (2002) Investigation of the high partition of YM992, a novel antidepressant, in rat brain—in vitro and in vivo evidence for the high binding in brain and the high permeability at the BBB. Biopharm Drug Dispos 23:351–360

Maurer TS, Debartolo DB, Tess DA, Scott DO (2005) Relationship between exposure and nonspecific binding of thirty-three central nervous system drugs in mice. Drug Metab Dispos 33:175–181

Mensch J, Jaroskova L, Sanderson W, Melis A, Mackie C, Verreck G, Brewster ME, Augustijns P (2010a) Application of PAMPA-models to predict BBB permeability including efflux ratio, plasma protein binding and physicochemical parameters. Int J Pharm 395:182–197

Mensch J, Melis A, Mackie C, Verreck G, Brewster ME, Augustijns P (2010b) Evaluation of various PAMPA models to identify the most discriminating method for the prediction of BBB permeability. Eur J Pharm Biopharm 74:495–502

Muehlbacher M, Spitzer GM, Liedl KR, Kornhuber J (2011) Qualitative prediction of blood–brain barrier permeability on a large and refined dataset. J Comput Aided Mol Des 25:1095–1106

Nicholson C, Phillips JM (1981) Ion diffusion modified by tortuosity and volume fraction in the extracellular microenvironment of the rat cerebellum. J Physiol 321:225–257
Nicholson C, Sykova E (1998) Extracellular space structure revealed by diffusion analysis. Trends Neurosci 21:207–215
Norinder U, Haeberlein M (2002) Computational approaches to the prediction of the blood–brain distribution. Adv Drug Deliv Rev 54:291–313
Norinder U, Sjoberg P, Osterberg T (1998) Theoretical calculation and prediction of brain–blood partitioning of organic solutes using MolSurf parametrization and PLS statistics. J Pharm Sci 87:952–959
Ooie T, Terasaki T, Suzuki H, Sugiyama Y (1997) Kinetic evidence for active efflux transport across the blood–brain barrier of quinolone antibiotics. J Pharm Exp Ther 283:293–304
Padowski JM, Pollack GM (2011) Influence of time to achieve substrate distribution equilibrium between brain tissue and blood on quantitation of the blood–brain barrier P-glycoprotein effect. Brain Res 1426:1–17
Pardridge WM (2004) Log(BB), PS products and in silico models of drug brain penetration [comment]. Drug Discov Today 9:392–393
Pardridge WM, Boado RJ, Black KL, Cancilla PA (1992) Blood–brain barrier and new approaches to brain drug delivery. West J Med 156:281–286
Rao VV, Dahlheimer JL, Bardgett ME, Snyder AZ, Finch RA, Sartorelli AC, Piwnica-Worms D (1999) Choroid plexus epithelial expression of MDR1 P glycoprotein and multidrug resistance-associated protein contribute to the blood-cerebrospinal-fluid drug-permeability barrier. Proc Natl Acad Sci U S A 96:3900–3905
Reese TS, Karnovsky MJ (1967) Fine structural localization of a blood–brain barrier to exogenous peroxidase. J Cell Biol 34:207–217
Reinoso RF, Telfer BA, Rowland M (1997) Tissue water content in rats measured by desiccation. J Pharmacol Toxicol Methods 38:87–92
Rosenberg GA, Kyner WT, Estrada E (1980) Bulk flow of brain interstitial fluid under normal and hyperosmolar conditions. Am J Physiol 238:F42–F49
Rowland M, Tozer T (2011) Clinical pharmacokinetics and pharmacodynamics. Concepts and applications. Lippincott, Williams & Wilkins, Baltimore and Philadephia
Sadeque AJ, Wandel C, He H, Shah S, Wood AJ (2000) Increased drug delivery to the brain by P-glycoprotein inhibition. Clin Pharm Ther 68:231–237
Sadiq MW, Borgs A, Okura T, Shimomura K, Kato S, Deguchi Y, Jansson B, Bjorkman S, Terasaki T, Hammarlund-Udenaes M (2011) Diphenhydramine active uptake at the blood–brain barrier and its interaction with oxycodone in vitro and in vivo. J Pharm Sci 100:3912–3923
Sasongko L, Link JM, Muzi M, Mankoff DA, Yang X, Collier AC, Shoner SC, Unadkat JD (2005) Imaging P-glycoprotein transport activity at the human blood–brain barrier with positron emission tomography. Clin Pharm Ther 77:503–514
Schinkel AH, Wagenaar E, Mol CA, van Deemter L (1996) P-glycoprotein in the blood–brain barrier of mice influences the brain penetration and pharmacological activity of many drugs. J Clin Invest 97:2517–2524
Shen DD, Artru AA, Adkison KK (2004) Principles and applicability of CSF sampling for the assessment of CNS drug delivery and pharmacodynamics. Adv Drug Deliv Rev 56:1825–1857
Shityakov S, Neuhaus W, Dandekar T, Forster C (2013) Analysing molecular polar surface descriptors to predict blood–brain barrier permeation. Int J Comput Biol Drug Des 6:146–156
Stevens J, Ploeger BA, Hammarlund-Udenaes M, Osswald G, van der Graaf PH, Danhof M, de Lange EC (2012) Mechanism-based PK-PD model for the prolactin biological system response following an acute dopamine inhibition challenge: quantitative extrapolation to humans. J Pharmacokinet Pharmacodyn 39(5):463–477
Summerfield SG, Lucas AJ, Porter RA, Jeffrey P, Gunn RN, Read KR, Stevens AJ, Metcalf AC, Osuna MC, Kilford PJ, Passchier J, Ruffo AD (2008) Toward an improved prediction of human in vivo brain penetration. Xenobiotica 38:1518–1535

Summerfield SG, Read K, Begley DJ, Obradovic T, Hidalgo IJ, Coggon S, Lewis AV, Porter RA, Jeffrey P (2007) Central nervous system drug disposition: the relationship between in situ brain permeability and brain free fraction. J Pharm Exp Ther 322:205–213

Summerfield SG, Stevens AJ, Cutler L, del Carmen Osuna M, Hammond B, Tang SP, Hersey A, Spalding DJ, Jeffrey P (2006) Improving the in vitro prediction of in vivo central nervous system penetration: integrating permeability, P-glycoprotein efflux, and free fractions in blood and brain. J Pharm Exp Ther 316:1282–1290

Sun H (2004) A universal molecular descriptor system for prediction of logP, logS, logBB, and absorption. J Chem Inf Comput Sci 44:748–757

Sun H, Dai H, Shaik N, Elmquist WF, Bungay PM (2003) Drug efflux transporters in the CNS. Adv Drug Deliv Rev 55:83–105

Syvanen S, Hammarlund-Udenaes M (2010) Using PET studies of P-gp function to elucidate mechanisms underlying the disposition of drugs. Current Top Med Chem 10:1799–1809

Syvanen S, Xie R, Sahin S, Hammarlund-Udenaes M (2006) Pharmacokinetic consequences of active drug efflux at the blood–brain barrier. Pharm Res 23:705–717

Takasato Y, Rapoport SI, Smith QR (1984) An in situ brain perfusion technique to study cerebrovascular transport in the rat. Am J Physiol 247:H484–H493

Tamai I, Tsuji A (2000) Transporter-mediated permeation of drugs across the blood–brain barrier. J Pharm Sci 89:1371–1388

Tega Y, Akanuma S, Kubo Y, Terasaki T, Hosoya K (2013) Blood-to-brain influx transport of nicotine at the rat blood–brain barrier: involvement of a pyrilamine-sensitive organic cation transport process. Neurochem Int 62:173–181

Thiebaut F, Tsuruo T, Hamada H, Gottesman MM, Pastan I, Willingham MC (1989) Immunohistochemical localization in normal tissues of different epitopes in the multidrug transport protein P170: evidence for localization in brain capillaries and crossreactivity of one antibody with a muscle protein. J Histochem Cytochem 37:159–164

Tsuji A, Terasaki T, Takabatake Y, Tenda Y, Tamai I, Yamashima T, Moritani S, Tsuruo T, Yamashita J (1992) P-glycoprotein as the drug efflux pump in primary cultured bovine brain capillary endothelial cells. Life Sci 51:1427–1437

Tunblad K, Ederoth P, Gardenfors A, Hammarlund-Udenaes M, Nordstrom CH (2004a) Altered brain exposure of morphine in experimental meningitis studied with microdialysis. Acta Anaesthesiol Scand 48:294–301

Tunblad K, Hammarlund-Udenaes M, Jonsson EN (2004b) An integrated model for the analysis of pharmacokinetic data from microdialysis experiments. Pharm Res 21:1698–1707

Tunblad K, Hammarlund-Udenaes M, Jonsson EN (2005) Influence of probenecid on the delivery of morphine-6-glucuronide to the brain. Eur J Pharm Sci 24:49–57

Tunblad K, Jonsson EN, Hammarlund-Udenaes M (2003) Morphine blood–brain barrier transport is influenced by probenecid co-administration. Pharm Res 20:618–623

Uchida Y, Ohtsuki S, Kamiie J, Terasaki T (2011a) Blood–brain barrier (BBB) pharmacoproteomics: reconstruction of in vivo brain distribution of 11 P-glycoprotein substrates based on the BBB transporter protein concentration, in vitro intrinsic transport activity, and unbound fraction in plasma and brain in mice. J Pharmacol Exp Ther 339:579–588

Uchida Y, Ohtsuki S, Katsukura Y, Ikeda C, Suzuki T, Kamiie J, Terasaki T (2011b) Quantitative targeted absolute proteomics of human blood–brain barrier transporters and receptors. J Neurochem 117:333–345

Wang Y, Welty DF (1996) The simultaneous estimation of the influx and efflux blood–brain barrier permeabilities of gabapentin using a microdialysis-pharmacokinetic approach. Pharma Res 13:398–403

Watson J, Wright S, Lucas A, Clarke KL, Viggers J, Cheetham S, Jeffrey P, Porter R, Read KD (2009) Receptor occupancy and brain free fraction. Drug Metab Dispos 37:753–760

Westerhout J, Ploeger B, Smeets J, Danhof M, de Lange EC (2012) Physiologically based pharmacokinetic modeling to investigate regional brain distribution kinetics in rats. AAPS J 14:543–553

Xie R, Bouw MR, Hammarlund-Udenaes M (2000) Modelling of the blood–brain barrier transport of morphine-3-glucuronide studied using microdialysis in the rat: involvement of probenecid-sensitive transport. Br J Pharm 131:1784–1792

Xie R, Hammarlund-Udenaes M (1998) Blood–brain barrier equilibration of codeine in rats studied with microdialysis. Pharm Res 15:570–575

Young RC, Mitchell RC, Brown TH, Ganellin CR, Griffiths R, Jones M, Rana KK, Saunders D, Smith IR, Sore NE et al (1988) Development of a new physicochemical model for brain penetration and its application to the design of centrally acting H2 receptor histamine antagonists. J Med Chem 31:656–671

Zhao R, Kalvass JC, Pollack GM (2009) Assessment of blood–brain barrier permeability using the in situ mouse brain perfusion technique. Pharm Res 26:1657–1664

Chapter 6
In Vitro Models of CNS Barriers

N. Joan Abbott, Diana E.M. Dolman, Siti R. Yusof, and Andreas Reichel

Abstract This chapter reviews the history and modern applications of isolated preparations of the three main CNS barrier layers and cell culture preparations derived from them. In vitro models give valuable mechanistic information but also provide useful assay systems for drug discovery and delivery programmes. However, it is important to take into account practical issues including species differences and the degree to which the differentiated state of the in vivo barrier is retained. The range of models available is reviewed, with a critical evaluation of their strengths and weaknesses, and guidance in selecting and optimizing a suitable model for particular applications. New understanding of the unstirred water layers and paracellular leak pathway in in vitro preparations gives greater insights into the "intrinsic permeability" of the membrane, and a variety of techniques permit characterization of the transport systems and enzymes contributing to barrier function. Increasingly, aspects of CNS pathology are being modelled in cell culture, aiding the optimization of drug delivery regimes in pathological conditions.

N.J. Abbott (✉) • D.E.M. Dolman
BBB Group, Institute of Pharmaceutical Science, King's College London, Franklin Wilkins Building 3.10, 150 Stamford St, London, SE1 9NH, UK
e-mail: joan.abbott@kcl.ac.uk

S.R. Yusof
HICoE Centre for Drug Research, Universiti Sains Malaysia, Minden, Penang 11800, Malaysia

A. Reichel
Bayer Pharma AG, Global Drug Discovery, DMPK, Berlin D-13353, Germany

M. Hammarlund-Udenaes et al. (eds.), *Drug Delivery to the Brain*, AAPS Advances in the Pharmaceutical Sciences Series 10, DOI 10.1007/978-1-4614-9105-7_6,

6.1 Introduction

From the earliest demonstration of restricted exchange between the blood and the brain (Ehrlich 1885) leading to the modern understanding of the blood–CNS barriers, animal experiments and clinical observations have provided valuable information about the physiology and pathology of the barrier layers. However, obtaining mechanistic information from such studies at the cellular and molecular level is complex and time-consuming, and it is often difficult to obtain sufficient spatial and temporal resolution. The situation was dramatically improved by the introduction of in vitro methods (reviewed in Joó 1992).

6.1.1 Background and Early History

The first successful isolation of cerebral microvessels (Siakotos and Rouser 1969; Joó and Karnushina 1973) prepared the way for development of in vitro models of the blood–brain barrier (BBB), which have contributed to current understanding of its physiology, pharmacology and pathophysiology (reviewed in Joó 1992). Methods have also been developed for in vitro models of the choroid plexus and of the arachnoid epithelium (blood–CSF barrier, BCSFB). However, this proliferation of in vitro models and techniques causes problems for attempts at comparison between models and transferability of results obtained with different models, and makes it hard for scientists entering the field to select an optimal model for their particular interests. This chapter gives an overview of the current status of the most widely used in vitro CNS barrier models, with an update on an earlier review (Reichel et al. 2003), and offers guidance in model selection for specific applications, including permeability assay for drugs and "new chemical entities" (NCEs).

Isolated brain microvessels were the first model system for studying the BBB in vitro, offering new opportunities to investigate physiological and pathological processes at the cellular, subcellular and molecular level (Pardridge 1998). A new generation of in vitro models emerged with the first successful isolation of viable brain endothelial cells (BECs), which could be maintained in cell culture (Brendel et al. 1974; Panula et al. 1978; Bowman et al. 1981; see Joó 1992). There followed a number of advances which allowed improved isolation of endothelial cells from brain capillaries with minimal contamination from cells of arterioles and venules, both improving the "barrier phenotype" of the endothelial monolayer and minimizing the contamination by smooth muscle cells, pericytes and glia (Krämer et al. 2001). The first successful growth of endothelial cells on filters (Fig. 6.1a) allowed measurement of transendothelial permeability, and adopting technology developed for epithelia (Grasset et al. 1984) allowed monitoring of transendothelial electrical resistance (TEER) as a measure of tightness to small ions (Rutten et al. 1987; Hart et al. 1987). Many of the techniques for understanding ways to improve the yield, viability and expression of differentiated phenotype benefited from parallel developments in growing epithelial cells especially Caco-2 (Wilson 1990).

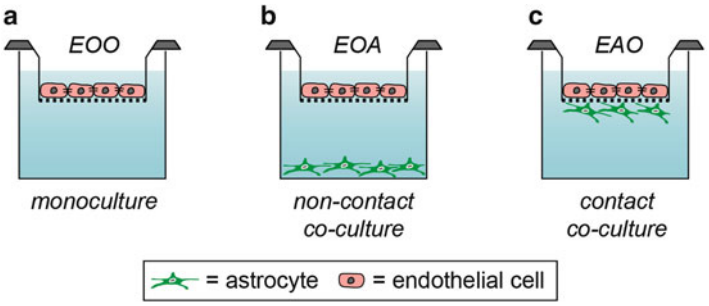

Fig. 6.1 Configurations for brain endothelial cell–astrocyte co-culture models. The three-letter label indicates cell location, in the following order: on the top of filter, on the underside of filter, and in the base of well. Thus panel (**a**) shows a typical monolayer culture with endothelial cells E on top of the filter and no other cell types present, hence E00, (**b**) shows non-contact co-culture with astrocytes A or mixed glia in the base of the well (E0A) and (**c**) shows "contact" (Note that depending on the size of the filter pores and time in co-culture, the glia may or may not actually send fine processes through the filter to contact the endothelial cells) co-culture with astrocytes growing on the underside of the filter, no cells in the base of the well (EA0). Redrawn by R Thorne, based on Nakagawa et al. 2009, with permission

Protocols for isolating and maintaining brain endothelial cells have been described for a large number of species including mouse, rat, cow, sheep, pig, monkey and human, typically producing confluent cell monolayers after about 9 days in culture (Garberg 1998; Deli et al. 2005). However, with passage, cultured BECs tend to show diminished characteristics of the in vivo BBB, e.g. tight junctional complexity, specific transporters, enzymes and vesicular transport, reverting towards the "default" non-brain endothelial phenotype characteristic of early BBB development (Daneman et al. 2010b). DeBault and Cancilla (1980) first reported that many of these BBB features can be at least partly re-established by co-culturing the BECs with astrocytes in arrangements allowing either direct contact or humoral exchange. Co-cultures with astrocytes followed (Fig. 6.1b, c) (Dehouck et al. 1990; Rubin et al. 1991; Kasa et al. 1991; see Cecchelli et al. 1999)

6.1.2 Model Development, Standardization, Refinement, and Innovation

During the next stage of development, some of the more sophisticated primary cultured models became so complex to prepare and maintain that they were not practical for routine assays; this was at least partly the motivation for the generation of much simpler models employing immortalized cell lines. However, unlike the well-accepted Caco-2 cell line employed for studies of intestinal absorption, or Madin–Darby canine kidney (MDCK) cells used as reliable epithelial models, there were no uniformly satisfactory cell line models for studying the BBB and other CNS

barriers in vitro, mainly because of the poor development of tight junctions and hence generation of models on filters that were too leaky for study of transendothelial or transepithelial permeation.

The ready availability of molecular biological techniques led to creation of many new immortalized and transfected CNS barrier cell line models (Reichel et al. 2003; Deli et al. 2005). There were also attempts to reintroduce lost features by means of transfection/transduction, but recent improvements in methods to produce practical primary cultures closer to the original has made this approach less attractive. Rather, molecular techniques allowing more subtle manipulation of cells for experimental purposes (e.g. to introduce imaging tracers, Huber et al. 2012) are proving practical and popular.

In vitro systems generally do not express fully the in vivo properties of the BBB, so specific modifications continued to be introduced to study particular aspects of BBB function. As the in vitro systems developed differed with respect to isolation procedures, cell culture conditions and configuration (mono/co-culture), and the cell type (origin and species), attempts were made in a European Union Concerted Action Programme (1993–1997) to standardize the most popular models to facilitate comparison of the data collated from different laboratories (de Boer and Sutanto 1997). ECVAM (European Centre for Validation of Alternative Methods) also sponsored a comparison between different in vitro BBB and epithelial models as CNS drug permeability assay systems (Garberg et al. 2005; see also Avdeef 2011). However, since no consensus emerged as to the "best model", most groups have continued to improve, optimize and extend the range of applications of the models they selected or developed for historical and practical reasons. Indeed, over the last 10 years, significant progress has been made, to the point that scientists new to the field have a range of good and practical options and can make informed choices. Some key landmarks in development of in vitro CNS barrier models are shown in Table 6.1.

6.1.3 Criteria for Useful In Vitro CNS Barrier Models

The ideal in vitro CNS barrier model would preserve in a reproducible way all the features of the in vivo equivalent, and be straightforward and inexpensive to prepare. The features to reproduce would include all aspects of the "physical, transport and enzymatic barrier" functions outlined in Chap. 1, and where relevant, also their immunological features. In the context of this volume, the models should also provide easy to use, readily available and reproducible assay tools for the reliable prediction of the penetration of compounds including drugs into the CNS in relation to both the route and rate of brain entry.

Thus far, no single BBB or BCSFB model fulfils these stringent requirements. However, satisfactory results may be obtained with models expressing the most critical features of the BBB or BCSFB in vivo that are relevant for the particular interest of the study. This means that it is important that users undertake basic model characterization to include the specific BBB feature(s) for which the model is then applied.

Table 6.1 Landmarks in development of in vitro BBB models

Landmark advance	Reference
Isolation of brain microvessels	Siakatos and Rouser (1969), Joó and Karnushina (1973)
Growth of brain endothelial cells in culture	Panula et al. (1978), Bowman et al. (1981)
Growth of brain endothelial cells on filters, TEER measurement (bovine, human)	Rutten et al. (1987), Hart et al. (1987)
Clonal bovine brain endothelial cell culture to avoid contaminating pericytes, co-culture with astrocytes (base of well) TEER >600 Ω cm^2	Dehouck et al. (1990)
Addition of differentiating factors to medium to improve BBB phenotype (bovine, porcine)	Rubin et al. (1991) (CPT-cAMP), Hoheisel et al. (1998) (hydrocortisone)
Development of immortalized cell line models mouse, rat, bovine, porcine, human	1988 onwards, see text and Table 6.2
"Dynamic" BBB model with intraluminal flow (DIV-BBB)	Stanness et al. (1996, 1997)
Tight porcine brain endothelial cell layer without astrocytes, TEER 700 (up to 1,500) Ω cm^2	Franke et al. (1999, 2000)
Further option for co-culture—astrocytes on the underside of filter, tighter layer (bovine)	Gaillard and de Boer (2000)
Confocal microscopy method for transport studies in isolated brain microvessels	Miller et al. (2000)
Conditionally immortalized rat, mouse cell lines from brain and retina endothelium, choroid plexus	Terasaki and Hosoya (2001)
First BBB genomics screen, isolated rat brain microvessels	Li et al. (2001, 2002)
Addition of puromycin to kill contaminating pericytes (rat)	Perrière et al. (2005)
Introduction of hCMEC/D3 human immortalized brain endothelial cell line	Weksler et al. (2005)
Quantitative proteomics of brain endothelium	Kamiie et al. (2008)
Tri-culture models—endothelium, pericytes, astrocytes	Nakagawa et al. (2009)
Transcriptome analysis of purified brain endothelium	Daneman et al. (2010a)
Method to measure and correct for unstirred water layers, paracellular permeability for cells on filters, allowing improved in vitro–in vivo correlation (IVIVC):	Adveef (2011)
Introduction of promising in vitro BBB model from human pluripotent stem cells (hPSCs)	Lippmann et al. (2012)
Microfluidic BBB model prototypes	Booth and Kim (2012), Prabhakarpandian et al. (2013), Griep et al. (2013)

6.1.4 The Physical Barrier and Tight Junctions: Monitoring CNS Barrier Tightness In Vitro

The expression of functional tight junctions between the BECs is one of the most critical features due to their consequences for the function of the BBB. In the in vivo BBB, complex and extensive tight junctions contribute significantly to the control over CNS ion and molecular penetration. This is achieved by (1) very severe restriction of the

paracellular pathway, and thus (2) limitation of flux of permeant molecules mainly to transendothelial pathways, (3) associated expression of specific carrier systems for hydrophilic solutes essential for the brain (e.g. nutrients) and (4) differential (i.e., polarized) expression of receptors, transporters and enzymes at either the luminal or abluminal cell surface allowing the BBB to act as a truly dynamic interface between the body periphery (blood) and the central compartment (brain), capable of vectorial transport of certain solutes.

As discussed in Chap. 1, the tight junctions of the choroid plexus and arachnoid express different claudins than those of brain endothelium, and are leakier than those of the BBB; however, their presence in the epithelial barrier layers has a similar effect on the properties of these epithelia, e.g. in polarization of function and regulation of transepithelial transport.

6.1.4.1 Methods to Measure Barrier Permeability and TEER

In vitro models to be used for transendothelial/transepithelial drug permeation studies need to have sufficiently restrictive tight junctions to impede paracellular permeation, mimicking the in vivo situation. Paracellular permeability can be assessed using inert extracellular tracers (Avdeef 2011, 2012); for tighter layers, small tracer molecules can be used, such as radiolabelled sucrose (MWt 342, hydrodynamic radius r: 4.6 Å or 0.46 nm) or mannitol (MWt 182, r 3.6 Å), or fluorescent markers such as Lucifer Yellow (MWt 443, r 4.2 Å) or sodium fluorescein (MWt 376, r 4.5 Å), and for leakier layers larger tracers used such as inulin, dextrans and serum albumin. However, the use of these tracers is labour-intensive and time-consuming, inevitably involving additional assays and analytical delays, has poor time-resolution, and fluorescent tracers may interfere with analysis of permeation of for example fluorescent substrates of membrane transporters.

For less-invasive monitoring, measurement of transendothelial/epithelial electrical resistance (TEER) is simpler, gives real-time readout and has a variety of applications: (1) to monitor the status of the barrier layer, especially for cells grown on opaque filters where visual inspection of confluence is not possible, (2) to determine the culture day on which optimum tightness is reached for experiments, (3) in quality control of cells grown on filters, establishing the baseline permeability of cell monolayers on individual filters to allow exclusion of poor monolayers that fall below a satisfactory threshold tightness and (4) to follow changes in resistance over time, e.g. to follow the effects of particular growth conditions or a drug or pharmacological agent on barrier integrity and tight junction function.

Two main types of system are used (Fig. 6.2) (Benson et al. 2013). In the first and simplest (Fig. 6.2a), voltohmmeter (VO), a pair of current and voltage electrodes in "chopstick" array are used; in the second, more recently developed instruments use the method of impedance spectroscopy (IS) (Fig. 6.2b). Both permit monitoring of TEER across cell layers but IS allows continuous analysis over hours to days, and also gives information about the electrical capacitance which can reveal additional

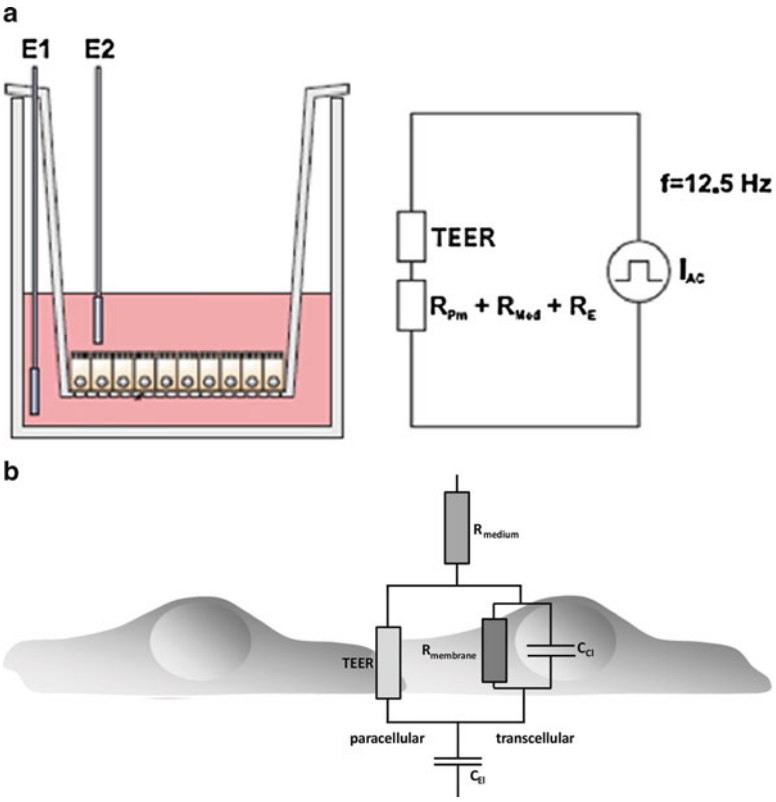

Fig. 6.2 Methods to measure TEER. (**a**) Resistance measurement in voltohmmeter (VO) system using "chopstick" electrodes. The electrodes (E1, E2) either side of the cell monolayer on the porous filter are used to determine the electrical resistance. The ohmic resistance across the cell layer (TEER), the cell culture medium in the upper and lower compartments (R_{Med}), the membrane of the filter inserts (R_{pm}) and electrode-medium interface (R_E) all contribute to the total electrical resistance. I_{AC}, alternating square wave current. (**b**) Measurement of TEER and capacitance in Impedance Spectroscopy (IS) system. Equivalent circuit diagram showing the contribution of the transcellular and paracellular pathways to the total impedance, Z, of the cellular system. *TEER* transendothelial electrical resistance, C_{EL} capacitance of the electrodes, C_{Ci} capacitance of the cell layer, R_{medium} ohmic resistance of the medium, $R_{membrane}$, ohmic resistance of the membranes. For tight endothelia and epithelia, TEER is dominated by the transcellular pathway. TEER is determined from the circuit analysis using Z measured at different frequencies of alternating current. From Benson et al. 2013, with permission

features of the barrier properties such as cell shape and the degree of cell-substrate adhesion. The earliest IS devices involved growing cells on solid microstructured electrodes, so these systems were not suitable for use in association with drug permeability screening. More recently developed systems permit use of cells grown on porous filters, and simultaneous monitoring of multiple filters, e.g. in a 12- or 24-well format.

6.1.4.2 TEER Measurement Based on Ohm's Law: V = IR (Voltage = Current × Resistance)

In the most widely used VO applications (Fig. 6.2a), such as the WPI (World Precision Instruments) "EVOM" system (or Millipore/Millicell equivalent), an AC (alternating current) square wave, here at 12.5 Hz, is passed between voltage electrodes either side of the cell layer, and the resulting current measured, giving the ohmic resistance R. When multiplied by the surface area of the membrane this gives TEER in Ω cm^2. A few papers in the literature give the units of TEER as "Ω/cm^2" which is incorrect, and this suggests that the authors do not fully understand the theory or methodology. An AC voltage source is preferred over DC as the latter can have polarizing effects on the electrodes or damage the cells. Earlier designs of chopstick electrode pairs (e.g. WPI STX2) were flexible, making difficult the placement of the electrodes and maintenance of a constant distance apart; recent improvements in design give fixed electrode spacing (e.g. STX100C) and hence better reproducibility. The "Endohm" chamber system with large plate electrodes to fit in the filter cup (above) and the well (below) the cells on the filter, samples a larger area of membrane including the more uniform central area, and can give more reproducible readings (Cohen-Kashi Malina et al. 2009; Helms et al. 2010, 2012; Patabendige et al. 2013a, b); however, the "plunger" action of inserting the upper electrode can disturb the cells, particularly the brain endothelial cells, which are much thinner and more fragile than the CNS barrier epithelial cells.

6.1.4.3 Impedance Spectroscopy Systems

An IS device (Fig. 6.2b) that has proved reliable in the context of BBB and choroid plexus epithelial (CPE) models is the "cellZscope" system (nanoAnalytics), available in different formats capable of accommodating 6, 12 or 24 filter inserts and giving continuous readout of TEER (Benson et al. 2013). The system is computer-controlled, and TEER and capacitance are derived from an electric equivalent circuit model within the software. There is an optimum frequency range appropriate for deriving TEER and capacitance. One drawback of this system is the indirect method for calculating TEER, which relies on use of the equivalent circuit and certain assumptions about the way current will flow through the system at different frequencies. A nanoAnalytics technical note comparing TEER measured with the cellZscope system and with chopstick electrodes shows good correspondence when the system parameters are set correctly. However, there are some discrepancies in the impedance literature measuring TEER across cultured choroid plexus epithelial (CPE) cells. Wegener et al. (1996, 2000) grew porcine CPE cells on gold film electrodes and recorded TEER 100–150 Ω cm^2, rising to 210 Ω cm^2 in presence of the differentiating agent 250uM CPT-cAMP, while other studies reported TEER >1,500 Ω cm^2 in serum-free medium (reviewed in Angelow et al. 2004). Using a VO device Stazielle and Ghersi-Egea (1999) recorded 187 Ω cm^2 in primary rat CPE, while Baehr et al. (2006) reported 100–150 Ω cm^2 in pig choroid plexus, and

commented this would be equivalent to ~600 Ω cm^2 in an impedance system. Using a VO system with a stable continuous subcultivatable porcine CPE cell line, Schroten et al. (2012) reported TEER >600 Ω cm^2. In general the values up to ~600 Ω cm^2 fit better with evidence for leakier tight junctions in CPE than BBB (Bouldin and Krigman 1975), but it is clear that more "side-by-side" comparisons of VO and IS systems using a particular in vitro model would be helpful to clarify the situation. .

6.1.4.4 Relation Between Permeability and TEER

Since 1990 steady progress has been made in the standard (flat filter) in vitro systems, to the point where some of the best are able to reach the level of tightness of the in vivo BBB (>1–2 kΩ cm^2) which is essential for the ionic homeostasis of the brain interstitial fluid required for neuronal function. For assessing solute and drug transport across the BBB, the tighter the monolayer the better the resolution (dynamic range) for determination of transendothelial permeability. Dynamic range can be established experimentally from the permeability ratio between a high and low permeant compound e.g. propranolol *vs*. sucrose. High dynamic range gives better discrimination and rank-ordering of compounds with similar physical chemical properties within a series. However, even models with medium-range tightness are capable of providing adequate resolution for certain applications, particularly if the models show reproducible tightness reflected in consistent values for solute permeability. Recent improvements in understanding, separating and correcting for the components of in vitro systems that affect cell permeation (unstirred water layer/aqueous boundary layer, and porosity of paracellular pathway) also provide ways to determine the true transcellular endothelial permeability, P_C (Avdeef 2011, 2012).

TEER effectively measures the resistance to ion flow ("charge" transfer) across the cell layer, carried by the chief charge carriers in body fluids and physiological saline solutions, Na^+ and Cl^-. The *conductance* "*g*" is the reciprocal of resistance ($g = 1/R$), and is a combined measure of both the ionic permeability of the cell layer and the total number (concentration) of available ions. *Permeability* (cm s^{-1}) is the ability of a solute (including ions) to move through a membrane channel or pore, i.e. is a measure of "mass" transfer, and is a property of the membrane or cell layer. Hence conductance is related to permeability.

Traditionally BBB groups have measured either the apparent permeability of the monolayer (P_{app}) or the endothelial permeability P_e, corrected for permeability of the filter. Since TEER is inversely related to permeability, a plot of permeability vs. TEER will give a falling exponential curve. Measuring TEER and permeability of a paracellular marker (e.g. sucrose, mannitol, some small fluorescent tracers) on the same filter with attached monolayer are a useful way of monitoring the status and reproducibility of the preparation, both for quality control and for experimental studies (Gaillard and de Boer 2000; Lohmann et al. 2002).

Where the monolayer properties including P_{app} are reproducible, a VO-measured TEER above ~150 Ω cm^2 may be sufficient to ensure P_{app} is relatively independent

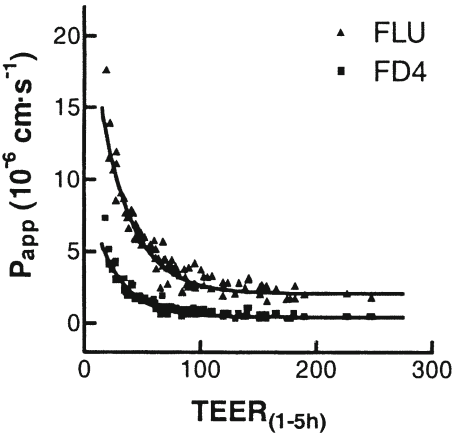

Fig. 6.3 Relationship between apparent permeability P_{app} and TEER. TEER was measured at the start of permeability experiment (0 h) then hourly up to 5 h and mean values (1–5 h) calculated; fitted profiles are from permeability data for sodium fluorescein (FLU) and FITC-labelled 4kDA dextran (FD4) calculated over the 5 h experiment. Above ~150 Ω cm^2 the scatter of data points is less and permeability is relatively independent of TEER, meaning that where TEER >150 Ω cm^2 the measured P_{app} accurately reflects permeability of the monolayer. The graphs illustrate the point that for leaky monolayers (here <~120 Ω cm^2), permeability measurements are less reliable. From Gaillard and de Boer 2000 with permission

of TEER, i.e. giving accurate values for P_{app} (Gaillard and de Boer 2000) (Fig. 6.3). Indeed, many groups have adopted a quality threshold of 200–250 Ω cm^2 for permeability assays. Lohmann et al. (2002) using monocultured porcine brain endothelial cells and measuring TEER with an impedance system found TEER in the range 300–1,500 Ω cm^2; P_e was quite variable at low TEER so they set a threshold of 600 Ω cm^2 for cells to be used for experiments. It is clear that the appropriate threshold should be selected for the particular cell model, TEER measuring system used and type of study.

6.1.5 Barrier Features Related to Transporters, Enzymes, Transcytosis, and Immune Responses

As with TEER, reasonable compromises may also be made with other aspects of the BBB. Indeed, it is generally accepted that for a particular application the model needs only to be characterized for those features which are both relevant and critical for the point of interest. For example, for an in vitro BBB system useful to screen small drug compounds for their CNS penetrability the model needs to be sufficiently tight and should possess relevant polarized carrier and efflux systems in order to produce useful information. Similarly, for examination of transendothelial

or transepithelial permeation of large molecules and nanocarrier systems where vesicular routes may be involved it is important that the cell system chosen reflects the specialized features of such transport in the polarized in vivo barrier system. However, for many drug permeability projects the model may not need to show the full complement of immunological responses which will only be necessary in those systems used to study the immune response of the CNS barriers. The existing in vitro model systems have very different levels of characterization, and have generally been chosen for utility in a particular area of research interest.

6.2 Current Status: Overview of Current In Vitro BBB Models

Isolated brain capillaries can be used in suspension or fixed onto glass slides. By contrast, all cell-based systems require specific growth surface coatings and cell culture media for growing BECs. Although the cell preparations and culture conditions are all based on the same principle, in order to obtain functional in vitro BBB models several small but significant differences between the systems, as well as preferences between laboratories have been introduced (Garberg 1998; de Boer and Sutanto 1997), an ongoing process as shown by recent papers (Abbott et al. 2012; Patabendige et al. 2013b; Watson et al. 2013). In the following sections current in vitro models of the BBB are briefly surveyed; for greater detail on specific systems the reader is referred to the corresponding key publications.

6.2.1 Isolated Brain Capillaries

Brain capillaries can be isolated from animal as well as human autopsy brains using mechanical and/or enzymatic procedures (Pardridge 1998; Miller et al. 2000). Typically, the capillary fragments consist of endothelial cells ensheathed by a basement membrane containing pericytes to which remnants of astrocytic foot processes and nerve endings may cling. Often preparations contain small venules and precapillary arterioles and hence smooth muscle cells. Isolated brain capillaries are metabolically active, although a significant loss of ATP and hence activity during the isolation procedure has been reported (Pardridge 1998). As the luminal surface of isolated brain microvessels cannot easily be accessed in vitro, most studies investigate the abluminal properties and function of the BBB. More recently, transendothelial transport of fluorescent drugs from the brain side to the blood side has been studied in real time using functionally intact brain microvessels by means of confocal microscopy (Miller et al. 2000) (Fig. 6.4). The technique has been used with porcine, rat and mouse microvessels and has given detailed insights into the cellular and molecular mechanisms regulating transport at the BBB and blood–spinal cord barrier, especially for P-glycoprotein (P-gp) (Miller 2010; Campos et al. 2012).

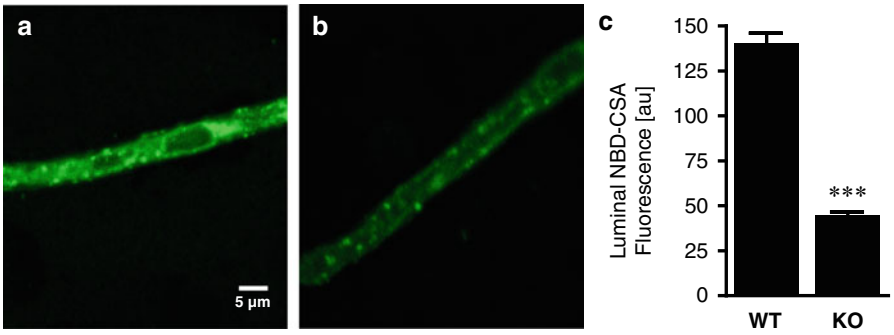

Fig. 6.4 Isolated mouse brain capillaries to study P-glycoprotein function. P-glycoprotein transport function measured as luminal accumulation of fluorescent P-gp-specific substrate NBD-CSA (NBD-cyclosporin A) in isolated brain capillaries from (**a**) Wild type and (**b**) CF-1 P-gp-deficient mice. (**c**) Image analysis. *Methods*: Brain capillaries were isolated from wild type (CF-1™) and CF-1 P-glycoprotein-deficient mice (KO; CF1-*Abcb1a*mds). P-glycoprotein transport activity was determined by exposing capillaries to 2 µM NBD-CSA for 1 h and measuring luminal fluorescence using confocal microscopy and image analysis. Data are mean ± SEM for 7 capillaries for each preparation of 20 mice; shown are arbitrary units (0–255). Statistics: *** $P < 0.001$ (Student's *t*-test). (Hartz AMS and Bauer B, unpublished data, with permission)

After isolation, brain microvessels can be stored frozen at −70 °C, thereby providing a versatile tool for several applications and a viable source for the cultivation of brain microvessel endothelial cells (Audus et al. 1998). In earlier studies isolated brain capillaries were used to examine receptor- and adsorptive-mediated endocytosis and solute transporter systems (Pardridge 1998; Fricker 2002) and more recently to isolate and identify BBB mRNA and proteins (Shawahna et al. 2011; Ito et al. 2011a). Isolated brain capillaries from both animals and humans with a neurological disorder or genetic alteration are contributing to elucidation of the role of the BBB in CNS pathophysiology (Wang et al. 2012; Hartz et al. 2012).

6.2.2 Primary and Low Passage Brain Endothelial Cells

Apart from isolated brain microvessels, the system next closest to in vivo are primary BECs which are isolated from or grow out of brain capillary fragments. Primary as well as low passage BECs retain many of the endothelial and BBB-specific characteristics of the BBB in vivo although many of the features are down-regulated or even lost if not re-induced.

6.2.2.1 Rat and Mouse Models

Due to the much higher yield of BECs from bovine and porcine brains compared to rat brains (up to 200 million, compared to 1–2 million cells per rat brain), the former

species currently represent the most popular source for in vitro BBB models both in academia and industry. However, primary cultured rat and mouse systems continue to be useful for investigation of pharmacology and transport, in studies where specific antibodies for larger species are lacking, and for comparison with standard in vivo rodent (rat, mouse) models used for PKPD analysis. The use of primary rodent models for transendothelial permeability measurements was until recently limited by the relatively leaky monolayers generated (TEER 150–200 Ω cm^2) due to the small flaws caused by contaminating pericytes, which are less of a problem in the bovine and porcine systems (Patabendige et al. 2013a, b). However, recent improvements in methods have allowed generation of purer primary cultures and co-cultures with glia (Fig. 6.1b), giving higher TEER up to ~500 Ω cm^2 or more (Coisne et al. 2005; Abbott et al. 2012; Watson et al. 2013). The advantage of growing glia in the base of the well (Fig. 6.1b) is that the filter with endothelial cells can be easily moved to a fresh well away from the glial "feeder" layer during experiments.

6.2.2.2 Bovine Models

Bovine BEC cultures are widely used, but differences between the procedures have developed historically in different BBB groups. Pioneered by Bowman et al. (1983) and later modified by Audus and Borchardt (1986) in the USA, bovine BEC are typically isolated by a combination of mechanical and enzymatic protocols and generally grown in mono-culture (Miller et al. 1992). These endothelial cell monolayers typically give TEER in the range 160–200 Ω cm^2 and sucrose permeability $10–20 \times 10^{-6}$ cm/s (Raub et al. 1992; Shah et al. 2012). The model has been used especially in US groups to study BBB transport (e.g. Wallace et al. 2011) and the mechanisms of drug action and permeation. Early studies also tested its ability to act as a drug permeability screen (Priya Eddy et al. 1997), but the relatively leaky paracellular pathway makes it less suitable than other models (see below, and Avdeef 2011).

In Europe, the group of Cecchelli and co-workers (Dehouck et al. 1990; Cecchelli et al. 1999) pioneered the omission of enzymatic steps in the bovine BEC isolation, using instead micro-trypsinization and sub-culturing of endothelial cell islands (clones) that grow out of brain capillaries selectively attached to a defined extracellular matrix. The BECs, which can be further subcultured (~8 passages) and stored, are grown in co-culture above rat astrocytes (base of well, Fig. 6.1b) to halt or counteract the loss of specific BBB markers. Due to the inductive effect of astrocytes typical TEER values are 200–400 Ω cm^2 higher than for mono-cultures (e.g. ~660 Ω cm^2 co-culture cf 420 Ω cm^2 monoculture, Dehouck et al. 1990). The model has been successfully used to rank-order compounds according to their BBB permeability (Lundquist et al. 2002); higher throughput variants of the model have been introduced for drug screening and toxicity testing (Culot et al. 2008; Vandenhaute et al. 2012). The model has also been used for proteomic (Pottiez et al. 2011) and transporter study, and it is one of the few models which have proved suitable for study of receptor-mediated transcytosis (Candela et al. 2010).

A co-culture involving bovine brain endothelial cells and rat astrocytes grown on either side of a porous membrane (Fig. 6.1c) was reported by the group of de Boer (Gaillard and de Boer 2000), advocating its use as permeability screen which simultaneously allows detection of drug-induced changes in BBB integrity as monitored by TEER. Basal TEER values in this model are in the range 350–800 Ω cm^2. A complication is the continuing presence and influence of the astrocytes during any transport experiment, particularly for lipophilic compounds which may become trapped in the astrocytes, or compounds subject to metabolism by enzymes highly expressed in the astrocyte layer (Dutheil et al. 2010). However, it is argued that the close association of endothelium and astrocytes mimics that in vivo, hence providing a good model for studying flux across the "combined barrier".

A recent variant of this model using increased buffer capacity in the medium gives higher TEER, allowing high-resolution examination of polarized solute transport (Helms et al. 2010, 2012).

6.2.2.3 Porcine Models

Galla and co-workers (Franke et al. 1999, 2000) developed a model based on porcine BECs (PBEC model) cultured without serum or astrocytic factors but in the presence of the endogenous differentiating agent hydrocortisone. In their hands, this model gives among the highest TEER values measured in vitro thus far (400–1500 Ω cm^2 with VO monitoring, or higher in IS systems, with sucrose permeability down to $1–4 \times 10^{-6}$ cm/s). The model has been used as a screening tool for CNS penetration of small drugs (Lohmann et al. 2002) and nanocarriers (Qiao et al. 2012) and for a number of mechanistic studies of BBB transporters and cell–cell interaction in the neurovascular unit (NVU). Using this model Cohen-Kashi Malina et al. (2009, 2012) showed an increased TEER of the PBECs, from 415 Ω cm^2 in monoculture, to 680 Ω cm^2 in non-contact co-culture with astrocytes (Fig. 6.1b), to 1,112 Ω cm^2 in contact co-culture (Fig. 6.1c). The model was sufficiently tight and polarized to examine the role of endothelial and glial cells in glutamate transport from brain to blood (Cohen-Kashi Malina et al. 2012). A different PBEC method originally developed in the group of Rubin (Eisai, London), based on the method for isolation of bovine brain endothelial cells (Rubin et al. 1991) has recently been reintroduced (Skinner et al. 2009) and further optimized (Patabendige et al. 2013a, b), able to give (VO) TEER >500 Ω cm^2 in monoculture and higher in co-culture with astrocytes (Fig. 6.1b). The model shows good functional expression of transport proteins (Patabendige et al. 2013a) and receptor-mediated transcytosis (RMT) for interleukin-1 (Skinner et al. 2009).

6.2.2.4 Human Models

The poor availability of human brain tissue makes primary human BECs a precious tool for the study of the human BBB at the cellular and molecular level

(Dorovini-Zis et al. 1991). The source material usually derives either from autopsies or biopsies (e.g. temporal lobectomy of epilepsy patients) and the most popular applications are studies related to the BBB in CNS diseases. Some human brain endothelial cells are commercially available, although batch-batch variation may pose problems. Human BEC monolayers are fragile in culture, contributing to low TEER values (~120–180 Ω cm^2, Mukthar and Pomerantz 2000; Giri et al. 2002) but, nevertheless, these models have been used to study (among others) drug transport (Riganti et al. 2013), nanoparticle permeation (Gil et al 2012) and conditions relevant to Alzheimer's disease (Giri et al. 2002) and multiple sclerosis (Larochelle et al. 2012; Liu and Dorovini-Zis 2012).

6.2.3 Immortalized Brain Endothelial Cell Lines

Primary cultured BECs have been successfully used as in vitro model of the BBB; however, their widespread and routine use has been restricted mainly by the time-consuming and often difficult preparation of the system which limits the continuous and homogeneous supply of biological assay material. Therefore, attempts have been made by several laboratories to immortalize primary BECs thereby avoiding the lengthy process of cell isolation.

The first generation of immortalized CNS barrier cell lines (first publication 1988–2000) involved introducing genes such as polyoma virus T antigen (bEND3 cells), Adenovirus EIA gene (RBE4) or SV40 large T antigen (many) (Table 6.2). More recently, conditionally immortalized cell lines have been established by using transgenic mice and rats harbouring the temperature-sensitive SV40 large T antigen gene (tsA58 T antigen gene) (Terasaki and Hosoya 2001; Terasaki et al. 2003). The advantage is that only small amounts of tissue are needed to establish a cell line, and the cell lines generated show better maintenance of in vivo functions. The gene is stably expressed in all tissues and cell cultures can easily be immortalized by activating the gene at 33 °C (Ribeiro et al. 2010). The technique has been used to generate both brain endothelial and choroid plexus cell lines.

Of immortalized brain endothelial cell lines introduced 1988–2000, several have proved reliable and popular and are still in use (Table 6.2). The models have been characterized to varying degrees, but all share a common weakness, i.e. insufficient tightness when grown as a cell monolayer on a porous membrane. Moreover, a good and robust immortalized human model was still lacking. Since then the situation has significantly improved, as detailed further below.

6.2.3.1 Comparison of Immortalized Cell Line Models Created

Bovine and porcine cell lines. As good primary cultured bovine and porcine BECs are now routinely produced in several groups, the use of immortalized bovine and porcine models showing more restricted features (Reichel et al. 2003) is less widespread.

Table 6.2 The most widely used current immortalized cell line models of BBB

Cell line	Species, transfection	1st publication	Recent references	Number of publications to 6–2013	Publication rate/year, rank order 2013
RBE4	Rat (2)	Roux et al. (1994)	Roux and Couraud (2005); Karstedt et al. (2013); Vilas-Boas et al. (2013)	137	2
hCMEC/D3	Human (5)	Weksler et al. (2005)	Weksler et al. (2013)	111	1
MBEC4	Mouse (1)	Shirai et al. (1994)	Watanabe et al. (2013)	40	4
*bEND3	Mouse (3)	Williams et al. (1988, 1989)	Watanabe et al. (2013)	37	5
TR-iBRB2	Rat retina (4)	Hosoya et al. (2001)	Usui et al. (2013)	33	3
GP8.3	Rat (1)	Greenwood et al. (1996)	Giurdanella et al. (2011)	21	6
GPNT	Rat (1)	Regina et al. (1999)	Thornton et al. (2010)	14	
TR-BBB13	Rat (4)	Hosoya et al. (2000)	Tega et al. (2013)	12	9
RBEC1	Rat (1)	Kido et al. (2000)	Okura et al. (2007)	10	10
cEND	Mouse (3)	Förster et al. (2005)	Burek et al. (2012)	9	7
*bEND5	Mouse (3)	Wagner and Risau (1994)	Steiner et al. (2011)	9	11
SV-HCEC	Human (1)	Muruganandam et al. (1997)	Dasgupta et al. (2011)	5	12

Transfection vectors/method (1) SV40 large T antigen; (2) Adenovirus E1A gene; (3) Polyoma virus middle T antigen; (4) Transgenic (Tg) rat or mouse harbouring temperature-sensitive SV40 large T antigen; (5) Sequential lentiviral transduction of hTERT and SV40 large T antigen
*Available from ECACC (European Collection of Animal Cell Cultures) and ATCC (American Type Culture Collection)

Rat and mouse cell lines. For rat, the RBE4 and GP8/GPNT cell lines remain popular, and have proved useful for a broad array of topics ranging from mechanistic transport studies to receptor-mediated modulation and inflammatory responses. Many of the currently available immortalized rat and mouse cell lines, especially conditionally immortalized lines, have been generated in Japan and are widely used, often in parallel in vivo/in vitro studies, and especially for identification and examination of carrier-mediated transport (Ito et al. 2011b, c; Lee et al. 2012; Tega et al. 2013). In an interesting breakthrough, Förster et al. (2005) returned to the earlier cell transduction technology used for bEND3 and bEND5 to generate mouse cEND cells, which uniquely among immortalized brain endothelial cell lines can produce tight

monolayers, with reported TEER up to >800 Ω cm^2. The details of the immortalization method have been published and the cells have been used for studies on the involvement of glucocorticoids on tight junction regulation, and on hypoxia and multiple sclerosis (Burek et al. 2012).

Human cell lines. A good human in vitro system is clearly an invaluable asset for BBB studies, and several attempts have been made to generate immortalized human BECs suitable for examination of the physiology, pharmacology and pathology of the human BBB in vitro, and as a screening tool for CNS penetration. Immortalization proved much more difficult than for BECs of other species, but several human cell line models were reported (Reichel et al. 2003; Deli et al. 2005). A major advance was the introduction of the hCMEC/D3 cell line by Weksler et al. (2005), building on significant prior experience of the authors in developing the rat RBE4, GP8.3 and GPNT cell lines. Several papers reporting the characterization of the model followed, and it was made widely available to other laboratories. Like most cell line models it suffers from poor development of tight junctions, but it has rapidly been adopted as the immortalized model of choice for studies where TEER is not a major issue, e.g. some studies of uptake and efflux. A recent review has summarized many of the useful applications of the model, and gives a balanced view of its strengths and weaknesses (Weksler et al. 2013). The model has been used for studies of transport systems including receptor-mediated transcytosis, but it is important to check that the properties reflect the in vivo condition, more fully expressed in primary cultures grown with astrocytes (see Sects. 6.2.2.1–3).

6.2.3.2 Applications of Immortalized Cell Lines

It is generally difficult to make BEC cell lines switch from the exponential growth phase after cell seeding to a more static phase of cell differentiation after the cells have reached confluence. Therefore, immortalized cell lines are less applicable for studies requiring a tight and stable in vitro barrier, but they have proved useful for mechanistic and biochemical studies requiring large amounts of biological material, e.g. to establish kinetics and structure-affinity relationships for BBB carrier systems and intracellular regulatory pathways. As continuous cell lines may gradually deviate from the normal BEC phenotype, both the basic characteristics and the particular feature of interest should be monitored through successive passages and the results validated with primary cells or in vivo data in order to ensure the relevance of the information obtained.

Of the 20 or so BBB (and blood–retinal barrier) cell line models mentioned in the literature since 1988, only 12 have 5 or more publications currently traceable in PubMed (Table 6.2), the top 5 being RBE4, hCMEC/D3, MBEC4, bEND3 and (retinal) TR-iBRB2. Groups that have developed immortalized cell lines tend to use these in their own studies, and pairing of in vivo studies (typically rat or mouse) to measure barrier permeation, and examination of cellular and molecular events in one or more cell lines is a popular and helpful approach.

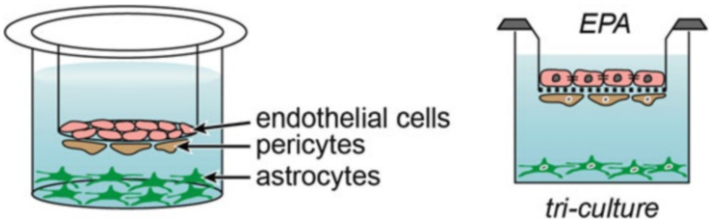

Fig. 6.5 Configuration for tricellular BBB co-culture model, reflecting the organization of the neurovascular unit (NVU). As for Fig. 6.1b, but here with addition of pericytes. Endothelial cells E on the top of the filter, pericytes P on the underside of the filter and astrocytes A in the base of the well (EPA arrangement). Redrawn by R Thorne, based on Nakagawa et al. (2009), with permission

One of the greatest limitations of the most readily available immortalized BEC lines is still their insufficient tightness, rendering these systems unsuitable for use in simple BBB permeability screens. Therefore, some groups have turned to other cell lines which, although of non-brain origin, either express sufficient brain endothelial features for functional and permeation studies such as ECV304/C6 (Hurst and Fritz, 1996; Neuhaus et al. 2009; Wang et al. 2011), or prove on validation to be useful predictors of passive and P-gp-mediated CNS penetrability of compounds, such as MDCK cells engineered to over-express human P-gp (MDCK- MDR1) and Caco-2 cells (Summerfield et al. 2007; Hellinger et al. 2012).

6.2.4 Tri-Culture, Dynamic Flow and 3-D Models

It would be expected that in vitro models that retain more features of the in vivo NVU would be more successful in showing a functional BBB phenotype. In cell culture models the inclusion of pericytes can be beneficial, depending on the differentiation state of the pericytes (Thanabalasundaram et al. 2011); barrier-inducing and -stabilizing effects of pericytes (plus astrocytes, tri-culture model) on BBB function have been demonstrated (Fig. 6.5) (e.g. Nakagawa et al. 2009; Vandenhaute et al. 2011), and a practical commercial rat tri-culture model is available.

Growth in porous tubes with luminal flow, and external astrocytes to aid barrier induction (Stanness et al. 1996, 1997; Janigro et al. 1999), proved an important innovation, with convincing demonstration from this “dynamic in vitro” (DIV) BBB model (Fig. 6.6) not only of improved tight junctional tightness, but also of other BBB features, reflecting the differentiating effects of flow (Cucullo et al. 2011; Naik and Cucullo 2012). Indeed, even the hCMEC/D3 cells show improved TEER (reported up to ~1,200 Ω cm^2 with or without astrocytes) in the DIV-BBB format (Cucullo et al. 2008). However, the complexity of the geometry (multiple hollow fibres) in this model, and the assumptions made in calculating TEER from the current measured, make it difficult to compare TEER values with those from flat filter configurations.

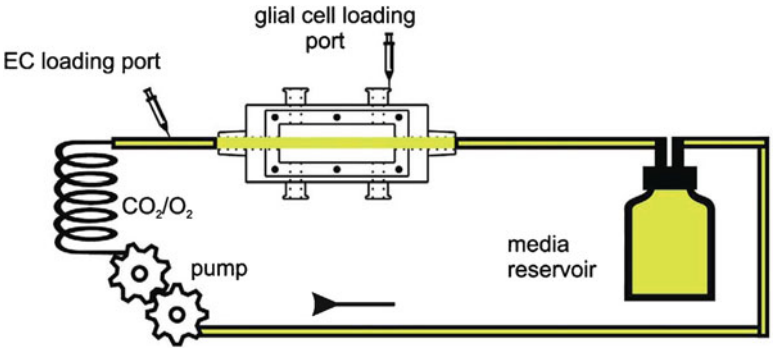

Fig. 6.6 Dynamic in vitro BBB model, DIV-BBB. Diagram showing cartridge containing replaceable bundle of hollow porous polypropylene fibres (capillary tubes) (*yellow*) suspended in the chamber and in continuity with a medium source through a flow path consisting of gas-permeable silicon tubing. A servo-controlled variable-speed pulsatile pump generates flow from the medium source through the capillary tube bundle and back. The circulatory pathway feeds both endothelial cells (EC) growing on the luminal surface of the capillary tubes and glia growing abluminally on their outer walls. The model has been used to assess the effects of flow on endothelial physiology, pathophysiology and leukocyte trafficking. From Cucullo et al. (2002), with permission

Generation of more-complex 3-D cultures has also been reported (Duport et al. 1998; Hatherell et al. 2011). However, tri-culture, DIV and 3-D models are more difficult to set up and maintain than standard mono or co-cultured models (Fig. 6.1), and have not yet been fully assessed for the whole range of BBB features including vesicular transport (Naik and Cucullo 2012; Abbott 2013). It is possible to isolate brain slices that preserve semi-intact capillaries and some BBB features (Kovács et al. 2011) with promise for studies of cell–cell interaction within the NVU, but such preparations are not suitable for quantitative studies to assess compound permeability and transport.

6.2.5 *Application of In Vitro Models for BBB Drug Permeability Assay*

A realistic in vitro assay system for screening and optimizing NCEs should combine as many features as possible of the in vitro BBB yet be suitable for medium-to-high throughput screening. Most pharmaceutical/biotech companies already have screens for intestinal permeability (generally Caco-2), and for "P-gp-liability", often MDCK-MDR1 cells (Summerfield et al. 2007), so a convenient and pragmatic system is to expect early stage screening on such models, and later refinement in a more "brain-like" system. A possible "screening cascade" involving early in silico modelling, then non-brain epithelial models, and final CNS barrier models may be practical (Abbott 2004). However, given the very different morphologies of endothelial cells and these epithelial cells (Fig. 6.7) (especially in cell thickness, luminal

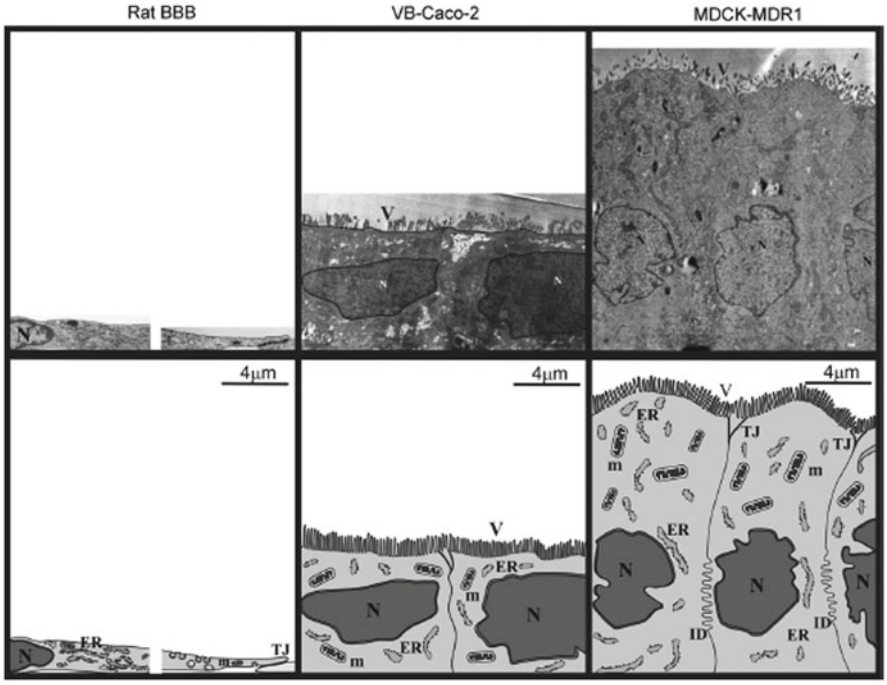

Fig 6.7 Electron micrographs of cell cultured rat brain endothelium, VB-Caco-2 and MDCK-MDR1 cell cytoarchitecture, with drawings below. VB-Caco-2 cells were created by growing Caco-2 cells in 10 nM vinblastine (VB, P-gp substrate) for at least six passages to elevate P-gp expression. *ER* endoplasmic reticulum, *ID* interdigitations, *m* mitochondrion, *N* nucleus, *TJ* intercellular tight junctions, *V* microvilli. From Hellinger et al. (2012), with permission

membrane microstructure and glycocalyx composition, junctional structure and organelle content) together with physiological differences in transporter and enzyme function and transcytosis mechanisms, caution still needs to be applied in such a sequential screen (see also Lohmann et al. 2002).

Most studies for CNS-specific permeability screening have focused on the BBB as the largest surface area blood–CNS interface, closest to neurons, but there is growing awareness of the need for assay systems of the choroid plexus reflecting especially the transport and enzymatic importance of this barrier (Strazielle and Ghersi-Egea 2013). A medium-high throughput BBB system using bovine endothelial cells exposed to glial-conditioned medium is available (Culot et al. 2008), and primary cultured porcine cells are also suitable either as monocultures or co-cultures with astrocytes (Patabendige et al. 2013a). Hellinger et al. (2012) compared a rat tri-culture model (TEER ~200 Ω cm^2) with Caco-2 and MDCK-MDR1 cells in screening 10 compounds (selected for predominantly passive permeation, efflux transport or both), and concluded that for passive permeability and P-gp-liability the epithelial layers gave better resolution, while the BBB model would have advantage in reflecting other in vivo BBB transporters. The situation would be improved with use of a tighter in vitro BBB model, e.g. bovine or porcine.

6.2.6 *In Vitro–In Vivo Correlations (IVIVC)*

Since the earliest in vitro BBB permeability assays (e.g. Dehouck et al. 1990; Cecchelli et al. 1999) there has been interest in comparing the performance of the in vitro models against permeability data generated in vivo, typically by constructing an in vitro *vs*. in vivo permeability plot and determining the correlation (IVIVC). In vivo data used have been either measurements of Brain Uptake Index (BUI) or permeability data derived from in situ brain perfusion, the K_{in} (unidirectional influx coefficient) or the derived P_c (transcellular permeability). However, the relatively leaky tight junctions (high paracellular permeability), and presence of unstirred water layers (or aqueous boundary layers, ABL) in vitro (Youdim et al. 2003) weaken the correlation (Avdeef 2011).

6.2.6.1 Unstirred Water Layer, Paracellular Permeability, Intrinsic Permeability Calculation

Building on quantitative biophysical models validated in epithelia, and applying his software *p*CEL-X, Avdeef (2011) used literature values (to 2008) of permeability from several different in vitro BBB and epithelial models, and deconvoluted the apparent permeability P_e of the endothelial barrier into its three components: P_{ABL}, P_C and P_{para}: ABL, transcellular and paracellular permeabilities, respectively. Finally, P_0, the intrinsic (charge-corrected) permeability was calculated from P_C by incorporating the pK_a value(s) of the molecule; P_0 represents the uncharged form of an ionizable molecule. Figure 6.8 shows the log-log IVIVC of P_0 data from mono-cultured porcine brain endothelium *vs*. P_0 data from rodent in situ brain perfusion studies. The correlation coefficient r^2 for the IVIVC (0.58) was greater than that for the uncorrected in vitro data, P_e *vs.* P_C in situ (0.33). The porcine BBB model also performed better than bovine, rodent and human models in this study. By applying the method to permeability data from the tightest current in vitro BBB models the correlations are expected to improve. The method helps to identify the most reliable in vitro models for predicting in vivo permeability, and to correct the data obtained from leakier models.

6.2.7 *How to Select an Appropriate In Vitro BBB Model*

It is clear that a wide range of models is available for studies of the BBB relevant to normal physiology and pathological situations, and to test and optimize CNS delivery of appropriate therapies. Careful selection with a variety of controls in place can give valuable information about the role of the BBB in pathology, and the rate and extent of entry of therapeutics into the CNS. These models are helping to refine a variety of formulations and constructs to improve their value in a range of diseases.

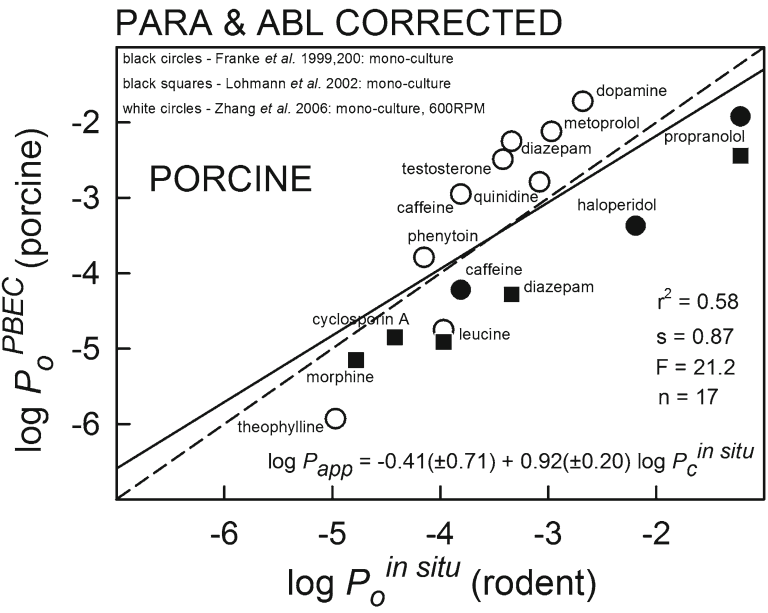

Fig 6.8 In vitro–in vivo correlation (IVIVC) analysis of brain endothelial permeability. Log intrinsic endothelial permeability P_0 calculated from P_e permeability data from four data sets generated in two different monocultured porcine brain endothelial cell (PBEC) models (Franke et al. 1999, 2000; Lohmann et al. 2002; Zhang et al. 2006) is plotted against log P_0 derived from an extensive rodent in situ brain perfusion data set; see text and Avdeef (2011) for details of the calculation method using *p*CEL-X software (from "*in-ADME.com*" http://www.in-adme.com/Index.html). The correlation coefficient from the data is greater than that for the raw P_e *vs.* P_C data, P_e being uncorrected for aqueous boundary layer (ABL) and paracellular permeability P_{para}. From Avdeef (2011), with permission

For scientists starting a new BBB project without prior experience, collaboration with an established group or groups is recommended, including adopting their well-characterized cell or cell line models if these are suitable for the application planned (Table 6.3).

6.2.8 Epithelial CNS Barriers

6.2.8.1 Choroid Plexus Epithelial (CPE) Cells

The choroid plexus is relatively straightforward to isolate with cell viability maintained for several hours, permitting studies of uptake and efflux, but without defined polarity (Gibbs and Thomas 2002). When polarity of transport is important, perfusion and isolation of sheep choroid plexus permits studies of vectorial transport across the epithelium (Preston et al. 1989). Primary culture models of rodent, porcine

Table 6.3 How to select an appropriate in vitro BBB model (see text)

Property of interest	Recommended cell model(s)	Check
Transendothelial permeability of small compounds (<500 MWt), detecting both passive and transporter-mediated flux	Primary cultured cells: –without astrocytes: porcine –with astrocytes: bovine, porcine –with astrocytes and pericytes: bovine, rat; porcine	Check TEER; aim for high TEER and high dynamic range, giving better discrimination and rank ordering within a drug series
ABC efflux transporters	Primary cultured system showing in vivo pattern, polarity/localization (bovine, porcine)	Check relative expression compared to human BBB, may permit prediction of PK in human
Transporters mediating brain entry or exit of small compounds via SLCs, ABC transporters	Many models including cell lines show sufficient expression, suitable for uptake and efflux studies	Check expression of transport system of interest, compare with in vivo or primary culture
Metabolic enzymes affecting drug permeation	Many models show sufficient expression	Check model has been characterized for enzymes
Receptor-mediated endocytosis and transcytosis	Primary cultured cells with astrocytes, found critical for full expression and function	Check receptor expression and polarity show features of BBB-type transcytosis rather than "default" non-BBB phenotype

and human CPE have been developed (see Baehr et al. 2006), but the most readily available human material is from foetal material or CP papilloma, which may not accurately reflect normal function (Redzic 2013). Resistances of 100–600 Ω cm^2 have been observed (see also Sect. 6.1.4.3), some models are tight enough for demonstration of CSF secretion, and the models have been used for a variety of studies of transport, metabolism and leukocyte traffic (Redzic 2013; Strazielle and Ghersi-Egea 2013; Monot and Zheng 2013). A stable continuous sub-cultivatable porcine cell line (PCP-R) (Schroten et al. 2012) and some immortalized cell lines (human Z310, Monot and Zheng 2013; rat TR-CSFB3, Terasaki and Hosoya 2001) have been introduced. The models have generally not been used for drug permeability screening.

6.2.8.2 Arachnoid Epithelial Cells

It has recently proved possible to culture arachnoid cells in vitro, which express claudin 1 and generate a TEER of ~160 Ω cm^2 with restriction of larger solute permeation (Lam et al. 2011, 2012; Janson et al. 2011). Characterization of the expression patterns of drug transporters and enzymes in arachnoid tissue and arachnoid barrier (AB) cells shows expression of both P-gp and breast cancer resistance protein (BCRP); an immortalized cell line of AB cells showed P-gp expression on the

apical (dura-facing) membrane, and BCRP on both apical and basal (CSF-facing) membranes (Yasuda et al. 2013). Microarray analysis of mouse and human arachnoid tissue showed expression of many drug transporters and some drug metabolizing enzymes. The consistency across in vitro models and isolated tissue makes it likely that these proteins contribute to the blood–CSF barrier function, and confirm that useful in vitro models can be generated and applied to examine these functions in detail.

6.3 Future Directions and Challenges

It is clear that in vitro models will continue to play important roles in generating mechanistic information about cellular and intercellular events in CNS barrier layers, capable of informing a range of applications in health and disease, drug discovery and drug delivery. Some emerging technologies and their combination offer clear future directions—the challenge will be to make them effective and advance understanding.

6.3.1 Human Pluripotent Stem Cells

A promising new development from the Shusta group is an in vitro BBB model derived from human pluripotent stem cells (hPSCs), involving initial co-differentiation of endothelial and neural cells, then purification and further maturation of the endothelial cells to develop a full BBB-like phenotype (Lippmann et al. 2012, 2013). It will be interesting to see how well this model replicates the in vivo behaviour in further characterization studies and applications, and whether it proves suitable for screening BBB permeation of a range of drug chemistries, including those subject to transfer by carrier-mediated mechanisms, and nanocarriers and engineered peptides and proteins, candidates for RMT. The reproducibility and transferability of the methods will also be critical features of this new model.

6.3.2 Microfluidics

Modern CNS barrier investigation involves many new and expanding technologies. The growing sophistication of live cell imaging allows real-time monitoring of intracellular events (e.g. transport function, transcytosis, metabolism, regulation) and intercellular events including signalling. Electrical measurement with VO and IS systems (see Sects. 6.1.4.1–6.1.4.3) gives information about barrier integrity, cell shape, cell–substrate interaction and the differentiating effects of flow. Hence there is growing interest in developing in vitro models that permit use of many of these

technologies in a single "microfluidic" platform capable of mimicking more closely the in vivo conditions. Pioneering studies have recently been published, establishing the feasibility of the method and scope for miniaturization (Booth and Kim 2012; Griep et al. 2013; Prabhakarpandian et al. 2013), so far with BBB cell-line models RBE4, bEND3 and hCMEC/D3. Many questions could be addressed in such systems, including the contribution of differential flow rates/shear stress to the observed heterogeneity of endothelial cytoarchitecture and function in different segments of the vasculature (Ge et al. 2005; Macdonald et al. 2010; Saubaméa et al. 2012; Paul et al. 2013; *cf* Ballermann et al. 1998). Given the complexity of the microfluidics chambers these are not likely to be suitable for high-throughput permeability assays at least in the short term, but meanwhile the generation of detailed mechanistic information is likely to be the most valuable output. An important advantage will be the ability to test barrier cells from different species, and with different pathologies, under equivalent conditions.

6.3.3 Transcriptomics, Proteomics and PKPD Modelling and In Vitro–In Vivo Extrapolation

Transcriptome examination and quantitative proteomics of freshly isolated brain capillaries and purified brain endothelial cells have helped determine the degree to which in vitro models reflect the in vivo condition, and how closely models from other species resemble the phenotype of the human CNS barriers (Kamiie et al. 2008; Daneman et al 2010a; Ohtsuki et al 2011; Hoshi et al. 2013). In future it should be possible to combine information from in vivo and in vitro studies (Ito et al. 2011b, c) with quantitative proteomics (Uchida et al. 2011a, b, 2013) to generate data for PKPD and "physiologically based pharmacokinetic" (PBPK) modelling, and for prediction of human CNS free drug concentrations (Shawahna et al. 2013), based on data including information generated in in vitro models from different species (Ball et al. 2012). The ultimate aim will be to permit reliable in vitro–in vivo extrapolation (IVIVE) to human brain (Ball et al. 2013).

6.3.4 Challenges for the Field

We need:

1. Generation of reliable and tight in vitro models of the human BBB, choroid plexus and arachnoid barriers, reproducing the in vivo condition.
2. Development of an accepted "industry standard" in vitro BBB model, robust, reliable, predictive of human drug PK and capable of operation in medium-to-high throughput screening of NCEs.
3. Better understanding of TEER measurement in different systems, with accepted calibration protocols, reference thresholds, and inter-system correlations.

4. Better integration of in silico, in vitro and in vivo models to provide complementary information and more complete characterization of permeability routes and transport systems; we need more projects designed with parallel in vitro and in vivo assessment.
5. More computational modelling with software optimized for CNS barrier models, before, during and after experiments to better understand and correct for artefacts in permeability-measuring systems.
6. Microfluidics platforms integrating flow, TEER and other sensors and permitting advanced live cell imaging, suitable for studies of a single barrier cell type, or co-cultures reflecting the in vivo condition as within the NVU.

6.4 Conclusions

In the ~40 year history of in vitro CNS barrier models there have been a number of major advances, and of course also many false starts, with natural evolution of the field by which useful, reliable and informative models become more widely used, so building up the critical mass of basic information from which new developments can take off. Groups developing and adopting in vitro models can learn from the history and current status of the field to ensure that further progress is soundly based and effective, and results reliable and applicable between laboratories and across the field. New investigators have available a range of good models and excellent tools, and increasingly will work by collaboration to apply them. Exciting times!

6.5 Points for Discussion

1. Imagine a new project in your lab that requires an in vitro model; (a) define the requirements of the model, (b) decide on the most suitable model(s) to use and justify this choice.
2. Why are leakier BBB models (TEER <200 $\Omega\,cm^2$) less suitable for transendothelial permeability screening?
3. For transendothelial permeability measurement, why is it useful to (a) measure the TEER of each filter with cells, (b) make parallel measurements of TEER and permeability of a paracellular marker (P_{app} or P_e), ideally in each experimental run?
4. What are appropriate paracellular markers for the model(s) you selected in (1)?
5. Why has it proved difficult to develop good primary-cultured human BBB models?
6. What is an unstirred water layer (aqueous boundary layer, ABL), and why is it a problem for in vitro but not in vivo BBB studies? For transendothelial permeation, which types of compound are most affected by the ABL? If the ABL is not considered, minimized and corrected for, how would transendothelial permeability measurements be affected?

7. How can in vitro models from different species contribute to prediction of drug PK in human brain interstitial fluid using a process of PBPK?
8. As an exercise, design a microfluidic chamber suitable for studies of transendothelial and transepithelial permeability using CNS barrier cells. What additional features would it provide not generally available for "flat" ("transwell") filter systems? In what ways could these features be important?
9. What are the main differences in generating an in vitro BBB model from human pluripotent stem cells and from freshly isolated human brain microvessels? How would you select the most "BBB-like" clones from a variety of clones generated from hPSCs using different growth conditions and media?

Acknowledgements We are grateful for discussions and comments from many colleagues especially Dr. Alex Avdeef, and Prof Margareta Hammarlund-Udenaes; for redrawing of Fig. 6.1 by Dr. Robert Thorne; and for Fig. 6.4 from Dr. Anika Hartz and Dr. Björn Bauer.

References

Abbott NJ (2004) Prediction of blood-brain barrier permeation in drug discovery from in vivo, in vitro and in silico models. Drug Discov Today Technol 1:407–416

Abbott NJ (2013) Blood-brain barrier structure and function and the challenges for CNS drug delivery. J Inherit Metab Dis 36:437–449

Abbott NJ, Dolman DE, Drndarski S, Fredriksson SM (2012) An improved in vitro blood-brain barrier model: rat brain endothelial cells co-cultured with astrocytes. Methods Mol Biol 814:415–430

Angelow S, Zeni P, Galla HJ (2004) Usefulness and limitation of primary cultured porcine choroid plexus epithelial cells as an in vitro model to study drug transport at the blood-CSF barrier. Adv Drug Deliv Rev 56:1859–1873

Audus KL, Borchardt RT (1986) Characterisation of an in vitro blood-brain barrier model system for studying drug transport and metabolism. Pharm Res 3:81–87

Audus KL, Rose JM, Wang W, Borchardt RT (1998) Brain microvessel endothelial cell culture systems. In: Pardridge WM (ed) Introduction to the blood-brain barrier: methodology, biology and pathology. Cambridge University Press, Cambridge

Avdeef A (2011) How well can in vitro brain microcapillary endothelial cell models predict rodent in vivo blood-brain barrier permeability? Eur J Pharm Sci 43:109–124

Avdeef A (2012) Absorption and drug development: solubility, permeability and charge state, 2nd edn. Wiley, Hoboken, NJ

Baehr C, Reichel V, Fricker G (2006) Choroid plexus epithelial monolayers - a cell culture model from porcine brain. Cerebrospinal Fluid Res 3:13

Ball K, Bouzom F, Scherrmann JM, Walther B, Declèves X (2012) Development of a physiologically based pharmacokinetic model for the rat central nervous system and determination of an in vitro-in vivo scaling methodology for the blood-brain barrier permeability of two transporter substrates, morphine and oxycodone. J Pharm Sci 101:4277–4292

Ball K, Bouzom F, Scherrmann JM, Walther B, Declèves X (2013) Physiologically based pharmacokinetic modelling of drug penetration across the blood-brain barrier – towards a mechanistic IVIVE-based approach. AAPS J 15:913–932

Ballermann BJ, Dardik A, Eng E, Liu A (1998) Shear stress and the endothelium. Kidney Int Suppl 67:S100–S108

Benson K, Cramer S, Galla HJ (2013) Impedance-based cell monitoring: barrier properties and beyond. Fluids Barriers CNS 10(1):5. doi:10.1186/2045-8118-10-5

Booth R, Kim H (2012) Characterization of a microfluidic in vitro model of the blood-brain barrier (μBBB). Lab Chip 12:1784–1792

Bouldin TW, Krigman MR (1975) Differential permeability of cerebral capillary and choroid plexus to lanthanum ion. Brain Res 99:444–448

Bowman PD, Betz AL, Ar D, Wolinsky JS, Penney JB, Shivers RR, Goldstein GW (1981) Primary culture of capillary endothelium from rat brain. In Vitro 17:353–362

Bowman PD, Ennis SR, Rarey KE, Betz AL, Goldstein GW (1983) Brain microvessel endothelial cells in culture: a model for study of blood-brain barrier permeability. Ann Neurol 14:396–402

Brendel K, Meezan E, Carlson EC (1974) Isolated brain microvessels: a purified, metabolically active preparation from bovine cerebral cortex. Science 185:953–955

Burek M, Salvador E, Förster CY (2012) Generation of an immortalized murine brainmicrovascular endothelial cell line as an in vitro blood brain barrier model. J Vis Exp 29(66):e4022. doi:10.3791/4022

Campos CR, Schröter C, Wang X, Miller DS (2012) ABC transporter function and regulation at the blood-spinal cord barrier. J Cereb Blood Flow Metab 32:1559–1566

Candela P, Gosselet F, Saint-Pol J, Sevin E, Boucau MC, Boulanger E, Cecchelli R, Fenart L (2010) Apical-to-basolateral transport of amyloid-β peptides through blood-brain barrier cells is mediated by the receptor for advanced glycation end-products and is restricted by P-glycoprotein. J Alzheimers Dis 22:849–859

Cecchelli R, Dehouck B, Descamps L, Fenart L, Buée-Scherrer V, Duhem C, Lundquist S, Rentfel M, Torpier G, Dehouck MP (1999) In vitro model for evaluating drug transport across the blood-brain barrier. Adv Drug Deliv Rev 36:165–178

Cohen-Kashi Malina K, Cooper I, Teichberg VI (2009) Closing the gap between the in-vivo and in-vitro blood-brain barrier tightness. Brain Res 1284:12–21

Cohen-Kashi-Malina K, Cooper I, Teichberg VI (2012) Mechanisms of glutamate efflux at the blood-brain barrier: involvement of glial cells. J Cereb Blood Flow Metab 32:177–189

Coisne C, Dehouck L, Faveeuw C, Delplace Y, Miller F, Landry C, Morissette C, Fenart L, Cecchelli R, Tremblay P, Dehouck B (2005) Mouse syngenic in vitro blood-brain barrier model: a new tool to examine inflammatory events in cerebral endothelium. Lab Invest 85:734–746

Cucullo L, Couraud PO, Weksler B, Romero IA, Hossain M, Rapp E, Janigro D (2008) Immortalized human brain endothelial cells and flow-based vascular modeling: a marriage of convenience for rational neurovascular studies. J Cereb Blood Flow Metab 28:312–328

Cucullo L, Hossain M, Puvenna V, Marchi N, Janigro D (2011) The role of shear stress in blood-brain barrier endothelial physiology. BMC Neurosci 12:40

Cucullo L, McAllister MS, Kight K, Krizanac-Bengez L, Marroni M, Mayberg MR, Stanness KA, Janigro D (2002) A new dynamic in vitro model for the multidimensional study of astrocyte-endothelial cell interactions at the blood-brain barrier. Brain Res 951:243–254

Culot M, Lundquist S, Vanuxeem D, Nion S, Landry C, Delplace Y, Dehouck MP, Berezowski V, Fenart L, Cecchelli R (2008) An in vitro blood-brain barrier model for high throughput (HTS) toxicological screening. Toxicol In Vitro 22:799–811

Daneman R, Zhou L, Agalliu D, Cahoy JD, Kaushal A, Barres BA (2010a) The mouse blood-brain barrier transcriptome: a new resource for understanding the development and function of brain endothelial cells. PLoS One 5(10):e13741. doi:10.1371/journal.pone.0013741

Daneman R, Zhou L, Kebede AA, Barres BA (2010b) Pericytes are required for blood-brain barrier integrity during embryogenesis. Nature 468:562–566

Dasgupta S, Wang G, Yu RK (2011) Sulfoglucuronosyl paragloboside promotes endothelial cell apoptosis in inflammation: elucidation of a novel glycosphingolipid-signaling pathway. J Neurochem 119:749–759

De Boer AG, Sutanto W (eds) (1997) Drug transport across the blood-brain barrier. Harwood, Amsterdam

DeBault LE, Cancilla PA (1980) Gamma-glutamyl transpeptidase in isolated brain endothelial cells: induction by glial cells in vitro. Science 207:653–655

Dehouck MP, Méresse S, Delorme P, Fruchart JC, Cecchelli R (1990) An easier, reproducible, and mass-production method to study the blood-brain barrier in vitro. J Neurochem 54:1798–1801
Deli MA, Abrahám CS, Kataoka Y, Niwa M (2005) Permeability studies on in vitro blood-brain barrier models: physiology, pathology, and pharmacology. Cell Mol Neurobiol 25:59–127
Dorovini-Zis K, Prameya R, Bowman PD (1991) Culture and characteristics of microvascular endothelial cells derived from human brain. Lab Invest 64:425–436
Duport S, Robert F, Muller D, Grau G, Parisi L, Stoppini L (1998) An in vitro blood-brain barrier model: cocultures between endothelial cells and organotypic brain slice cultures. Proc Natl Acad Sci U S A 95:1840–1845
Dutheil F, Jacob A, Dauchy S, Beaune P, Scherrmann JM, Declèves X, Loriot MA (2010) ABC transporters and cytochromes P450 in the human central nervous system: influence on brain pharmacokinetics and contribution to neurodegenerative disorders. Expert Opin Drug Metab Toxicol 6:1161–1174
Ehrlich P (1885) Das Sauerstoffbeduerfnis des Organismus, In: Eine Farbenanalytische Studie. Hirschwald, Berlin
Förster C, Silwedel C, Golenhofen N, Burek M, Kietz S, Mankertz J, Drenckhahn D (2005) Occludin as direct target for glucocorticoid-induced improvement of blood-brain barrier properties in a murine in vitro system. J Physiol 565:475–486
Franke H, Galla HJ, Beuckmann CT (1999) An improved low-permeability in vitro-model of the blood-brain barrier: transport studies on retinoids, sucrose, haloperidol, caffeine and mannitol. Brain Res 818:65–71
Franke H, Galla HJ, Beuckmann CT (2000) Primary cultures of brain microvessel endothelial cells: a valid and flexible model to study drug transport through the blood-brain barrier in vitro. Brain Res Brain Res Protoc 5:248–256
Fricker G (2002) Drug transport across the blood-brain barrier. In: Pelkonen O, Baumann A, Reichel A (eds) Pharmacokinetic challenges in drug discovery. Springer, Berlin
Gaillard PJ, de Boer AG (2000) Relationship between permeability status of the blood-brain barrier and in vitro permeability coefficient of a drug. Eur J Pharm Sci 12:95–102
Garberg P (1998) In vitro models of the blood-brain barrier. ATLA 28:821–847
Garberg P, Ball M, Borg N, Cecchelli R, Fenart L, Hurst RD, Lindmark T, Mabondzo A, Nilsson JE, Raub TJ, Stanimirovic D, Terasaki T, Oberg JO, Osterberg T (2005) In vitro models for the blood-brain barrier. Toxicol In Vitro 19:299–334
Ge S, Song L, Pachter JS (2005) Where is the blood-brain barrier … really? J Neurosci Res 79:421–427
Gibbs JE, Thomas SA (2002) The distribution of the anti-HIV drug, 2'3'-dideoxycytidine (ddC), across the blood-brain and blood-cerebrospinal fluid barriers and the influence of organic anion transport inhibitors. J Neurochem 80:392–404
Gil ES, Wu L, Xu L, Lowe TL (2012) β-Cyclodextrin-poly(β-amino ester) nanoparticles for sustained drug delivery across the blood-brain barrier. Biomacromolecules 13:3533–3541
Giri R, Selvaraj S, Miller CA, Hofman F, Yan SD, Stern D, Zlokovic BV, Kalra VK (2002) Effect of endothelial cell polarity on beta-amyloid-induced migration of monocytes across normal and AD endothelium. Am J Physiol Cell Physiol 283:C895–C904
Giurdanella G, Motta C, Muriana S, Arena V, Anfuso CD, Lupo G, Alberghina M (2011) Cytosolic and calcium-independent phospholipase A(2) mediate glioma-enhanced proangiogenic activity of brain endothelial cells. Microvasc Res 81:1–17
Grasset E, Pinto M, Dussaulx E, Zweibaum A, Desjeux JF (1984) Epithelial properties of human colonic carcinoma cell line Caco-2: electrical parameters. Am J Physiol 247:C260–C267
Greenwood J, Pryce G, Devine L, Male DK, dos Santos WL, Calder VL, Adamson P (1996) SV40 large T immortalised cell lines of the rat blood-brain and blood-retinal barriers retain their phenotypic and immunological characteristics. J Neuroimmunol 71:51–63
Griep LM, Wolbers F, de Wagenaar B, ter Braak PM, Weksler BB, Romero IA, Couraud PO, Vermes I, van der Meer AD, van den Berg A (2013) BBB ON CHIP: microfluidic platform to

mechanically and biochemically modulate blood-brain barrier function. Biomed Microdevices 15:145–150
Hart MN, VanDyk LF, Moore SA, Shasby DM, Cancilla PA (1987) Differential opening of the brain endothelial barrier following neutralization of the endothelial luminal anionic charge in vitro. J Neuropathol Exp Neurol 46:141–153
Hartz AM, Bauer B, Soldner EL, Wolf A, Boy S, Backhaus R, Mihaljevic I, Bogdahn U, Klünemann HH, Schuierer G, Schlachetzki F (2012) Amyloid-β contributes to blood-brain barrier leakage in transgenic human amyloid precursor protein mice and in humans with cerebral amyloid angiopathy. Stroke 43:514–523
Hatherell K, Couraud PO, Romero IA, Weksler B, Pilkington GJ (2011) Development of a three-dimensional, all-human in vitro model of the blood-brain barrier using mono-, co-, and tri-cultivation Transwell models. J Neurosci Methods 199:223–229
Hellinger E, Veszelka S, Tóth AE, Walter F, Kittel A, Bakk ML, Tihanyi K, Háda V, Nakagawa S, Duy TD, Niwa M, Deli MA, Vastag M (2012) Comparison of brain capillary endothelial cell-based and epithelial (MDCK-MDR1, Caco-2, and VB-Caco-2) cell-based surrogate blood-brain barrier penetration models. Eur J Pharm Biopharm 82:340–351
Helms HC, Waagepetersen HS, Nielsen CU, Brodin B (2010) Paracellular tightness and claudin-5 expression is increased in the BCEC/astrocyte blood-brain barrier model by increasing media buffer capacity during growth. AAPS J 12:759–770
Helms HC, Madelung R, Waagepetersen HS, Nielsen CU, Brodin B (2012) In vitro evidence for the brain glutamate efflux hypothesis: brain endothelial cells cocultured with astrocytes display a polarized brain-to-blood transport of glutamate. Glia 60:882–893
Hoheisel D, Nitz T, Franke H, Wegener J, Hakvoort A, Tilling T, Galla HJ (1998) Hydrocortisone reinforces the blood-brain barrier properties in a serum free cell culture system. Biochem Biophys Res Commun 247:312–315
Hoshi Y, Uchida Y, Tachikawa M, Inoue T, Ohtsuki S, Terasaki T (2013) Quantitative atlas of blood-brain barrier transporters, receptors, and tight junction proteins in rats and common marmoset. J Pharm Sci 102:3343–3355
Hosoya KI, Takashima T, Tetsuka K, Nagura T, Ohtsuki S, Takanaga H, Ueda M, Yanai N, Obinata M, Terasaki T (2000) mRNA expression and transport characterization of conditionally immortalized rat brain capillary endothelial cell lines; a new in vitro BBB model for drug targeting. J Drug Target 8:357–370
Hosoya K, Tomi M, Ohtsuki S, Takanaga H, Ueda M, Yanai N, Obinata M, Terasaki T (2001) Conditionally immortalized retinal capillary endothelial cell lines (TR-iBRB) expressing differentiated endothelial cell functions derived from a transgenic rat. Exp Eye Res 72:163–172
Huber O, Brunner A, Maier P, Kaufmann R, Couraud PO, Cremer C, Fricker G (2012) Localization microscopy (SPDM) reveals clustered formations of P-glycoprotein in a human blood-brain barrier model. PLoS One 7(9):e44776. doi:10.1371/journal.pone.0044776
Hurst RD, Fritz IB (1996) Properties of an immortalised vascular endothelial/glioma cell co-culture model of the blood-brain barrier. J Cell Physiol 167:81–88
Ito K, Uchida Y, Ohtsuki S, Aizawa S, Kawakami H, Katsukura Y, Kamiie J, Terasaki T (2011a) Quantitative membrane protein expression at the blood-brain barrier of adult and younger cynomolgus monkeys. J Pharm Sci 100:3939–3950
Ito S, Ohtsuki S, Katsukura Y, Funaki M, Koitabashi Y, Sugino A, Murata S, Terasaki T (2011b) Atrial natriuretic peptide is eliminated from the brain by natriuretic peptide receptor-C-mediated brain-to-blood efflux transport at the blood-brain barrier. J Cereb Blood Flow Metab 31:457–466
Ito S, Ohtsuki S, Nezu Y, Koitabashi Y, Murata S, Terasaki T (2011c) 1α,25-Dihydroxyvitamin D3 enhances cerebral clearance of human amyloid-β peptide(1-40) from mouse brain across the blood-brain barrier. Fluids Barriers CNS 8:20. doi:10.1186/2045-8118-8-20
Janigro D, Leaman SM, Stanness KA (1999) Dynamic modeling of the blood-brain barrier: a novel tool for studies of drug delivery to the brain. Pharm Sci Technolo Today 2:7–12
Janson C, Romanova L, Hansen E, Hubel A, Lam C (2011) Immortalization and functional characterization of rat arachnoid cell lines. Neuroscience 177:23–34

Joó F (1992) The cerebral microvessels in culture, an update. J Neurochem 58:1–17
Joó F, Karnushina I (1973) A procedure for the isolation of capillaries from rat brain. Cytobios 8:41–48
Kamiie J, Ohtsuki S, Iwase R, Ohmine K, Katsukura Y, Yanai K, Sekine Y, Uchida Y, Ito S, Terasaki T (2008) Quantitative atlas of membrane transporter proteins: development and application of a highly sensitive simultaneous LC/MS/MS method combined with novel in-silico peptide selection criteria. Pharm Res 25:1469–1483
Karlstedt K, Jin C, Panula P (2013) Expression of histamine receptor Hrh3 and Hrh4 in rat brain endothelial cells. Br J Pharmacol 170:58–66
Kasa P, Pakaski M, Joó F, Lajtha A (1991) Endothelial cells from human fetal brain microvessels may be cholinoceptive, but do not synthesize acetylcholine. J Neurochem 56:2143–2146
Kido Y, Tamai I, Okamoto M, Suzuki F, Tsuji A (2000) Functional clarification of MCT1-mediated transport of monocarboxylic acids at the blood-brain barrier using in vitro cultured cells and in vivo BUI studies. Pharm Res 17:555–562
Kovács R, Papageorgiou I, Heinemann U (2011) Slice cultures as a model to study neurovascular coupling and blood brain barrier in vitro. Cardiovasc Psychiatry Neurol 2011:646958. doi:10.1155/2011/646958
Krämer SD, Abbott NJ, Begley DJ (2001) Biological models to study blood-brain barrier permeation. In: Testa B, van de Waterbeemd H, Folkers G, Guy R (eds) Pharmacokinetic optimization in drug research: biological, physicochemical and computational strategies. Wiley-VCH, Weinheim
Lam CH, Hansen EA, Hubel A (2011) Arachnoid cells on culture plates and collagen scaffolds: phenotype and transport properties. Tissue Eng Part A 17:1759–1766
Lam CH, Hansen EA, Janson C, Bryan A, Hubel A (2012) The characterization of arachnoid cell transport II: paracellular transport and blood-cerebrospinal fluid barrier formation. Neuroscience 222:228–238
Larochelle C, Cayrol R, Kebir H, Alvarez JI, Lécuyer MA, Ifergan I, Viel É, Bourbonnière L, Beauseigle D, Terouz S, Hachehouche L, Gendron S, Poirier J, Jobin C, Duquette P, Flanagan K, Yednock T, Arbour N, Prat A (2012) Melanoma cell adhesion molecule identifies encephalitogenic T lymphocytes and promotes their recruitment to the central nervous system. Brain 135:2906–2924
Lee NY, Choi HO, Kang YS (2012) The acetylcholinesterase inhibitors competitively inhibited an acetyl L-carnitine transport through the blood-brain barrier. Neurochem Res 37:1499–1507
Li YJ, Boado RJ, Pardridge WM (2001) Blood-brain barrier genomics. J Cereb Blood Flow Metab 21:61–68
Li JY, Boado RJ, Pardridge WM (2002) Rat blood-brain barrier genomics. II. J Cereb Blood Flow Metab 22:1319–1326
Lippmann ES, Azarin SM, Kay JE, Nessler RA, Wilson HK, Al-Ahmad A, Palecek SP, Shusta EV (2012) Derivation of blood-brain barrier endothelial cells from human pluripotent stem cells. Nat Biotechnol 30:783–791
Lippmann ES, Al-Ahmad A, Palecek SP, Shusta EV (2013) Modeling the blood-brain barrier using stem cell sources. Fluids Barriers CNS 10(1):2. doi:10.1186/2045-8118-10-2
Liu KK, Dorovini-Zis K (2012) Differential regulation of CD4+ T cell adhesion to cerebral microvascular endothelium by the chemokines CCL2 and CCL3. Int J Mol Sci 13:16119–16140
Lohmann C, Hüwel S, Galla HJ (2002) Predicting blood-brain barrier permeability of drugs: evaluation of different in vitro assays. J Drug Target 10:263–276
Lundquist S, Renftel M, Brillault J, Fenart L, Cecchelli R, Dehouck MP (2002) Prediction of drug transport through the blood-brain barrier in vivo: a comparison between two in vitro cell models. Pharm Res 19:976–981
Macdonald JA, Murugesan N, Pachter JS (2010) Endothelial cell heterogeneity of blood-brain barrier gene expression along the cerebral microvasculature. J Neurosci Res 88:1457–1474
Miller DS (2010) Regulation of P-glycoprotein and other ABC drug transporters at the blood-brain barrier. Trends Pharmacol Sci 31:246–254
Miller DW, Audus KL, Borchardt RT (1992) Application of cultured endothelial cells of the brain microvasculature in the study of the blood-brain barrier. J Tiss Cult Meth 14:217–224

Miller DS, Nobmann SN, Gutmann H, Toeroek M, Drewe J, Fricker G (2000) Xenobiotic transport across isolated brain microvessels studied by confocal microscopy. Mol Pharm 58:1357–1367

Monnot AD, Zheng W (2013) Culture of choroid plexus epithelial cells and in vitro model of blood-CSF barrier. Methods Mol Biol 945:13–29

Mukhtar M, Pomerantz RJ (2000) Development of an in vitro blood-brain barrier model to study molecular neuropathogenesis and neurovirologic disorders induced by human immunodeficiency virus type 1 infection. J Hum Virol 3:324–334

Muruganandam A, Herx LM, Monette R, Durkin JP, Stanimirovic DB (1997) Development of immortalized cerebromicrovascular endothelial cell line as an in vitro model of the human blood-brain barrier. FASEB J 11:1187–1197

Naik P, Cucullo L (2012) In vitro blood-brain barrier models: current and perspective technologies. J Pharm Sci 101:1337–1354

Nakagawa S, Deli MA, Kawaguchi H, Shimizudani T, Shimono T, Kittel A, Tanaka K, Niwa M (2009) A new blood-brain barrier model using primary rat brain endothelial cells, pericytes and astrocytes. Neurochem Int 54:253–263

Neuhaus W, Germann B, Plattner VE, Gabor F, Wirth M, Noe CR (2009) Alteration of the glycocalyx of two blood-brain barrier mimicking cell lines is inducible by glioma conditioned media. Brain Res 1279:82–89

Ohtsuki S, Uchida Y, Kubo Y, Terasaki T (2011) Quantitative targeted absolute proteomics-based ADME research as a new path to drug discovery and development: methodology, advantages, strategy, and prospects. J Pharm Sci 100:3547–3559

Okura T, Ito R, Ishiguro N, Tamai I, Deguchi Y (2007) Blood-brain barrier transport of pramipexole, a dopamine D2 agonist. Life Sci 80:1564–1571

Panula P, Joó F, Rechardt L (1978) Evidence for the presence of viable endothelial cells in cultures derived from dissociated rat brain. Experientia 34:95–97

Pardridge WM (1998) Isolated brain capillaries: an in vitro model of blood-brain barrier research. In: Pardridge WM (ed) Introduction to the blood-brain barrier: methodology, biology and pathology. Cambridge University Press, Cambridge UK

Patabendige A, Skinner RA, Abbott NJ (2013a) Establishment of a simplified in vitro porcine blood-brain barrier model with high transendothelial electrical resistance. Brain Res 1521:1–15

Patabendige A, Skinner RA, Morgan L, Abbott NJ (2013b) A detailed method for preparation of a functional and flexible blood-brain barrier model using porcine brain endothelial cells. Brain Res 1521:16–30

Paul D, Cowan AE, Ge S, Pachter JS (2013) Novel 3D analysis of Claudin-5 reveals significant endothelial heterogeneity among CNS microvessels. Microvasc Res 86:1–10

Perrière N, Demeuse P, Garcia E, Regina A, Debray M, Andreux JP, Couvreur P, Scherrmann JM, Temsamani J, Couraud PO, Deli MA, Roux F (2005) Puromycin-based purification of rat brain capillary endothelial cell cultures. Effect on the expression of blood-brain barrier-specific properties. J Neurochem 93:279–289

Pottiez G, Duban-Deweer S, Deracinois B, Gosselet F, Camoin L, Hachani J, Couraud PO, Cecchelli R, Dehouck MP, Fenart L, Karamanos Y, Flahaut C (2011) A differential proteomic approach identifies structural and functional components that contribute to the differentiation of brain capillary endothelial cells. J Proteomics 75:628–641

Prabhakarpandian B, Shen MC, Nichols JB, Mills IR, Sidoryk-Wegrzynowicz M, Aschner M, Pant K (2013) SyM-BBB: a microfluidic blood brain barrier model. Lab Chip 13:1093–1101

Preston JE, Segal MB, Walley GJ, Zlokovic BV (1989) Neutral amino acid uptake by the isolated perfused sheep choroid plexus. J Physiol 408:31–43

Priya Eddy E, Maleef BE, Hart TK, Smith PL (1997) In vitro models to predict blood-brain barrier permeability. Adv Drug Deliv Rev 23:185–198

Qiao R, Jia Q, Hüwel S, Xia R, Liu T, Gao F, Galla HJ, Gao M (2012) Receptor-mediated delivery of magnetic nanoparticles across the blood-brain barrier. ACS Nano 6:3304–3310

Raub TJ, Kuentzel SL, Sawada GA (1992) Permeability of bovine brain microvessel endothelial cells in vitro: barrier tightening by a factor released from astroglioma cells. Exp Cell Res 199:330–340

Redzic ZB (2013) Studies on the human choroid plexus in vitro. Fluids Barriers CNS 10(1):10. doi:10.1186/2045-8118-10-10

Régina A, Romero IA, Greenwood J, Adamson P, Bourre JM, Couraud PO, Roux F (1999) Dexamethasone regulation of P-glycoprotein activity in an immortalized rat brain endothelial cell line, GPNT. J Neurochem 73:1954–1963

Reichel A, Begley DJ, Abbott NJ (2003) An overview of in vitro techniques for blood-brain barrier studies. Methods Mol Med 89:307–324

Ribeiro MM, Castanho MA, Serrano I (2010) In vitro blood-brain barrier models–latest advances and therapeutic applications in a chronological perspective. Mini Rev Med Chem 10:262–270

Riganti C, Salaroglio IC, Pinzòn-Daza ML, Caldera V, Campia I, Kopecka J, Mellai M, Annovazzi L, Couraud PO, Bosia A, Ghigo D, Schiffer D (2013) Temozolomide down-regulates P-glycoprotein in human blood-brain barrier cells by disrupting Wnt3 signaling. Cell Mol Life Sci

Roux F, Couraud PO (2005) Rat brain endothelial cell lines for the study of blood-brain barrier permeability and transport functions. Cell Mol Neurobiol 25:41–58

Roux F, Durieu-Trautmann O, Chaverot N, Claire M, Mailly P, Bourre JM, Strosberg AD, Couraud PO (1994) Regulation of gamma-glutamyl transpeptidase and alkaline phosphatase activities in immortalized rat brain microvessel endothelial cells. J Cell Physiol 159:101–113

Rubin LL, Hall DE, Porter S, Barbu K, Cannon C, Horner HC, Janatpour M, Liaw CW, Manning K, Morales J, Tanner LI, Tomaselli KJ, Bard F (1991) A cell culture model of the blood-brain barrier. J Cell Biol 115:1725–1735

Rutten MJ, Hoover RL, Karnovsky MJ (1987) Electrical resistance and macromolecular permeability of brain endothelial monolayer cultures. Brain Res 425:301–310

Saubaméa B, Cochois-Guégan V, Cisternino S, Scherrmann JM (2012) Heterogeneity in the rat brain vasculature revealed by quantitative confocal analysis of endothelial barrier antigen and P-glycoprotein expression. J Cereb Blood Flow Metab 32:81–92

Schroten M, Hanisch FG, Quednau N, Stump C, Riebe R, Lenk M, Wolburg H, Tenenbaum T, Schwerk C (2012) A novel porcine in vitro model of the blood-cerebrospinal fluid barrier with strong barrier function. PLoS One 7(6):e39835. doi:10.1371/journal.pone.0039835

Shah KK, Yang L, Abbruscato TJ (2012) In vitro models of the blood-brain barrier. Methods Mol Biol 814:431–449

Shawahna R, Uchida Y, Declèves X, Ohtsuki S, Yousif S, Dauchy S, Jacob A, Chassoux F, Daumas-Duport C, Couraud PO, Terasaki T, Scherrmann JM (2011) Transcriptomic and quantitative proteomic analysis of transporters and drug metabolizing enzymes in freshly isolated human brain microvessels. Mol Pharm 8:1332–1341

Shawahna R, Decleves X, Scherrmann JM (2013) Hurdles with using in vitro models to predict human blood-brain barrier drug permeability: a special focus on transporters and metabolizing enzymes. Curr Drug Metab 14:120–136

Shirai A, Naito M, Tatsuta T, Dong J, Hanaoka K, Mikami K, Oh-hara T, Tsuruo T (1994) Transport of cyclosporin A across the brain capillary endothelial cell monolayer by P-glycoprotein. Biochim Biophys Acta 1222:400–404

Siakotos AN, Rouser G (1969) Isolation of highly purified human and bovine brain endothelial cells and nuclei and their phospholipid composition. Lipids 4:234–239

Skinner RA, Gibson RM, Rothwell NJ, Pinteaux E, Penny JI (2009) Transport of interleukin-1 across cerebromicrovascular endothelial cells. Br J Pharmacol 156:1115–1123

Stanness KA, Guatteo E, Janigro D (1996) A dynamic model of the blood-brain barrier “in vitro”. Neurotoxicology 17:481–496

Stanness KA, Westrum LE, Fornaciari E, Mascagni P, Nelson JA, Stenglein SG, Myers T, Janigro D (1997) Morphological and functional characterization of an in vitro blood-brain barrier model. Brain Res 771:329–342

Steiner O, Coisne C, Engelhardt B, Lyck R (2011) Comparison of immortalized bEnd5 and primary mouse brain microvascular endothelial cells as in vitro blood-brain barrier models for the study of T cell extravasation. J Cereb Blood Flow Metab 31:315–327

Strazielle N, Ghersi-Egea JF (1999) Demonstration of a coupled metabolism-efflux process at the choroid plexus as a mechanism of brain protection toward xenobiotics. J Neurosci 19: 6275–6289

Strazielle N, Ghersi-Egea JF (2013) Physiology of blood-brain interfaces in relation to brain disposition of small compounds and macromolecules. Mol Pharm 10:1473–1491

Summerfield SG, Read K, Begley DJ, Obradovic T, Hidalgo IJ, Coggon S, Lewis AV, Porter RA, Jeffrey P (2007) Central nervous system drug disposition: the relationship between in situ brain permeability and brain free fraction. J Pharmacol Exp Ther 322:205–313

Tega Y, Akanuma S, Kubo Y, Terasaki T, Hosoya K (2013) Blood-to-brain influx transport of nicotine at the rat blood-brain barrier: involvement of a pyrilamine-sensitive organic cation transport process. Neurochem Int 62:173–181

Terasaki T, Hosoya K (2001) Conditionally immortalized cell lines as a new in vitro model for the study of barrier functions. Biol Pharm Bull 24:111–118

Terasaki T, Ohtsuki S, Hori S, Takanaga H, Nakashima E, Hosoya K (2003) New approaches to in vitro models of blood-brain barrier drug transport. Drug Discov Today 8:944–954

Thanabalasundaram G, Schneidewind J, Pieper C, Galla HJ (2011) The impact of pericytes on the blood-brain barrier integrity depends critically on the pericyte differentiation stage. Int J Biochem Cell Biol 43:1284–1293

Thornton P, McColl BW, Cooper L, Rothwell NJ, Allan SM (2010) Interleukin-1 drives cerebrovascular inflammation via MAP kinase-independent pathways. Curr Neurovasc Res 7: 330–340

Uchida Y, Ohtsuki S, Kamiie J, Terasaki T (2011a) Blood-brain barrier (BBB) pharmacoproteomics: reconstruction of in vivo brain distribution of 11 P-glycoprotein substrates based on the BBB transporter protein concentration, in vitro intrinsic transport activity, and unbound fraction in plasma and brain in mice. J Pharmacol Exp Ther 339:579–588

Uchida Y, Ohtsuki S, Katsukura Y, Ikeda C, Suzuki T, Kamiie J, Terasaki T (2011b) Quantitative targeted absolute proteomics of human blood-brain barrier transporters and receptors. J Neurochem 117:333–345

Uchida Y, Tachikawa M, Obuchi W, Hoshi Y, Tomioka Y, Ohtsuki S, Terasaki T (2013) A study protocol for quantitative targeted absolute proteomics (QTAP) by LC-MS/MS: application for inter-strain differences in protein expression levels of transporters, receptors, claudin-5, and marker proteins at the blood-brain barrier in ddY, FVB, and C57BL/6J mice. Fluids Barriers CNS 10(1):21. doi:10.1186/2045-8118-10-21

Usui T, Kubo Y, Akanuma SI, Hosoya KI (2013) β-Alanine and l-histidine transport across the inner blood-retinal barrier: potential involvement in l-carnosine supply. Exp Eye Res 113:135–142

Vandenhaute E, Dehouck L, Boucau MC, Sevin E, Uzbekov R, Tardivel M, Gosselet F, Fenart L, Cecchelli R, Dehouck MP (2011) Modelling the neurovascular unit and the blood-brain barrier with the unique function of pericytes. Curr Neurovasc Res 8:258–269

Vandenhaute E, Sevin E, Hallier-Vanuxeem D, Dehouck MP, Cecchelli R (2012) Case study: adapting in vitro blood-brain barrier models for use in early-stage drug discovery. Drug Discov Today 17:285–290

Vilas-Boas V, Silva R, Nunes C, Reis S, Ferreira L, Vieira C, Carvalho F, Bastos MD, Remião F (2013) Mechanisms of P-gp inhibition and effects on membrane fluidity of a new rifampicin derivative, 1,8-dibenzoyl-rifampicin. Toxicol Lett 220:259–266

Wagner EF, Risau W (1994) Oncogenes in the study of endothelial cell growth and differentiation. Semin Cancer Biol 5:137–145

Wallace BK, Foroutan S, O'Donnell ME (2011) Ischemia-induced stimulation of Na-K-Cl cotransport in cerebral microvascular endothelial cells involves AMP kinase. Am J Physiol Cell Physiol 301:C316–C326

Wang Q, Luo W, Zhang W, Liu M, Song H, Chen J (2011) Involvement of DMT1+IRE in the transport of lead in an in vitro BBB model. Toxicol In Vitro 25:991–998

Wang S, Qaisar U, Yin X, Grammas P (2012) Gene expression profiling in Alzheimer's disease brain microvessels. J Alzheimers Dis 31:193–205

Watanabe T, Dohgu S, Takata F, Nishioku T, Nakashima A, Futagami K, Yamauchi A, Kataoka Y (2013) Paracellular barrier and tight junction protein expression in the immortalized brain endothelial cell lines bEND.3, bEND.5 and mouse brain endothelial cell 4. Biol Pharm Bull 36:492–495

Watson PM, Paterson JC, Thom G, Ginman U, Lundquist S, Webster CI (2013) Modelling the endothelial blood-CNS barriers: a method for the production of robust in vitro models of the rat blood-brain barrier and blood-spinal cord barrier. BMC Neurosci 14(1):59

Wegener J, Sieber M, Galla HJ (1996) Impedance analysis of epithelial and endothelial cell monolayers cultured on gold surfaces. J Biochem Biophys Methods 32:151–170

Wegener J, Hakvoort A, Galla HJ (2000) Barrier function of porcine choroid plexus epithelial cells is modulated by cAMP-dependent pathways in vitro. Brain Res 853:115–124

Weksler BB, Subileau EA, Perrière N, Charneau P, Holloway K, Leveque M, Tricoire-Leignel H, Nicotra A, Bourdoulous S, Turowski P, Male DK, Roux F, Greenwood J, Romero IA, Couraud PO (2005) Blood-brain barrier-specific properties of a human adult brain endothelial cell line. FASEB J 19:1872–1874

Weksler B, Romero IA, Couraud PO (2013) The hCMEC/D3 cell line as a model of the human blood brain barrier. Fluids Barriers CNS 10(1):16. doi:10.1186/2045-8118-10-16

Williams RL, Courtneidge SA, Wagner EF (1988) Embryonic lethalities and endothelial tumors in chimeric mice expressing polyoma virus middle T oncogene. Cell 52:121–131

Williams RL, Risau W, Zerwes HG, Drexler H, Aguzzi A, Wagner EF (1989) Endothelioma cells expressing the polyoma middle T oncogene induce hemangiomas by host cell recruitment. Cell 57:1053–1063

Wilson G (1990) Cell culture techniques for the study of drug transport. Eur J Drug Metab Pharmacokinet 15:159–163

Yasuda K, Cline C, Vogel P, Onciu M, Fatima S, Sorrentino BP, Thirumaran RK, Ekins S, Urade Y, Fujimori K, Schuetz EG (2013) Drug transporters on arachnoid barrier cells contribute to the blood-cerebrospinal fluid barrier. Drug Metab Dispos 41:923–931

Youdim KA, Avdeef A, Abbott NJ (2003) In vitro trans-monolayer permeability calculations: often forgotten assumptions. Drug Discov Today 8:997–1003

Zhang Y, Li CS, Ye Y, Johnson K, Poe J, Johnson S, Bobrowski W, Garrido R, Madhu C (2006) Porcine brain microvessel endothelial cells as an in vitro model to predict in vivo blood-brain barrier permeability. Drug Metab Dispos 34:1935–1943

Chapter 7
In Situ and In Vivo Animal Models

Quentin R. Smith and Ramakrishna Samala

Abstract An important property in any central nervous system drug is the ability to cross the blood–brain barrier (BBB) and to reach therapeutic concentrations in brain at safe and acceptable doses. Multiple parameters influence brain drug bioavailability, including solubility, membrane permeation, and affinity for influx and efflux transporters. This chapter overviews the primary in vivo methods to assess brain drug distribution in preclinical and clinical reports. In most studies, two parameters, the BBB permeability-surface area product (PS) and brain distribution volume or partition coefficient ($K_{p,brain}$), are used to characterize the ability of a drug compound to gain access to and distribute in brain. Together with the time course of systemic drug exposure, these two parameters can be used to predict total drug concentration within brain. Further, because unbound drug concentration often correlates better with drug activity, a number of studies also determine the drug free fraction (f_u) so that the free concentrations can be calculated. Specific methods, such as in situ brain perfusion, brain efflux index, and brain microdialysis, are valuable to dissect specific elements of BBB drug permeation or transport as well as equilibration in brain interstitial fluid and cellular elements. Overall, these approaches complement in vivo drug distribution studies and in vitro BBB permeation methods.

Q.R. Smith, Ph.D. (✉) • R. Samala, Ph.D.
Department of Pharmaceutical Sciences, Texas Tech University Health Sciences Center, 1300 Coulter, Amarillo, TX 79106, USA
e-mail: Quentin.Smith@ttuhsc.edu

M. Hammarlund-Udenaes et al. (eds.), *Drug Delivery to the Brain*, AAPS Advances in the Pharmaceutical Sciences Series 10, DOI 10.1007/978-1-4614-9105-7_7,

7.1 Introduction

The blood–brain barrier (BBB) system represents a series of dynamic cellular interfaces at the border between the blood stream and the brain interstitial fluid (ISF) as well as cerebrospinal fluid (CSF), which together control drug access to the central nervous system (CNS) (Chap. 1). The BBB system is often called the "gate keeper to the CNS," determining the ability of drugs and other compounds to cross into and reach therapeutic concentrations in brain ISF. As brain ISF is in direct contact with the extracellular faces of many neuronal and glial plasma membrane receptors, drug concentration within it correlates best with much of in vivo CNS neuronal signaling (Kalvass et al. 2007; Liu et al. 2009). The barrier is thought to be critical to insulate the brain from circulating toxins, metals, and neuroactive substances and to provide a stable microenvironment for higher synaptic communication.

The BBB is located in mammals at the vascular endothelium which lines the blood vessels of the brain. The BBB endothelial cells possess a series of properties which are not static but can change with diet, development, gender, disease, drug or toxin exposure, and age (Cardoso et al. 2010). The brain vascular endothelial cells, like their counterparts in other organs, is their cellular plasma membranes, which are highly permeable to metabolic gases oxygen and carbon dioxide, and to many lipophilic solutes, such as the neutral lipophilic drugs, antipyrine, diazepam, ethanol, and caffeine (Smith 2003). However, unlike the vasculature of many organs, the hallmark of the brain endothelium is that it lacks open paracellular channels and fenestra which are the primary conduits for vascular exchange for many small polar solutes (MW < 5,000). As a consequence, in the brain, plasma-to-tissue ISF equilibration times ($t_{1/2}$) for small polar solutes, such as sodium, sucrose, and inulin, can fall in the range of hours to tens of hours, instead of being in the range of seconds to minutes, as in other organs (Crone 1986). Such low BBB permeability impedes exchange and dampens fluctuations in brain ISF concentration achieved from vascular exposure to such solutes. Further, the BBB expresses a number of other critical properties, such as active efflux transport, enzymatic catabolism, and CSF sink effect, which—when coupled with the low passive permeability of the barrier—markedly reduce brain equilibrium exposure to a wide range of compounds, including many therapeutic drugs. The restriction is not absolute, as indicated above; a number of small, moderately lipophilic solutes cross readily into brain by passive diffusion or, in some cases, by facilitated transport. The overall impact is that the BBB phenotype is highly complex and comprises multiple static and dynamic properties.

Because of the complexity of the BBB and the realization that many BBB properties are not constant but vary with disease, development, and drug exposure, it has been difficult to develop a small cassette of in vitro or in silico models that adequately predict drug transport and availability to the CNS. As a consequence in vivo testing of brain drug uptake and equilibration is still considered the "gold standard" of any CNS drug discovery program.

In this chapter, the primary techniques used to assay in vivo drug availability to brain and CSF are reviewed, assessing strengths and weaknesses of different methods, with the goal of guiding biomedical researchers in the design of their CNS drug screening program. Many newcomers to the field ask the following question: "Does a compound cross the BBB?" In truth, all compounds studied to date cross the BBB to some extent, albeit for some to a very limited degree. The real questions are "To what extent can a compound cross the BBB and reach active concentrations in brain at safe and tolerable doses?" and "If a compound shows poor brain distribution, how can this be improved?" This chapter aims to guide investigators through these critical questions, highlighting the latest methods used to assess brain uptake and exposure and to probe limiting factors that can be modified to improve brain distribution and effect.

7.2 Current Status

7.2.1 Two Parameters Commonly Used in In Vivo Brain Drug Distribution Experiments

In many cases, in vivo CNS drug exposure experiments are designed along classic pharmacokinetic lines to measure two primary parameters—the rate at which a compound crosses into brain (i.e., BBB permeability-surface area product—PS) and the extent to which the compound distributes within the CNS (i.e., brain distribution volume or partition coefficient—$K_{p,brain}$) (Hammarlund-Udenaes et al. 2008; Liu et al. 2008). These two parameters have parallels to the clearance and volume of distribution in systemic blood pharmacokinetics. As the systemic drug clearance and volume of distribution can be used to calculate the concentration of drug in serum or blood at a time point after *i.v.* administration, so can the BBB PS and $K_{p,brain}$ be used to calculate the total drug in brain at any point after systemic administration given a defined serum exposure.

The BBB PS for influx (PS_{in}) is generally determined from the initial rate of drug uptake into brain or from pharmacokinetic analysis of the time course of brain total drug concentration relative to that in plasma (Ohno et al. 1978; Smith and Rapoport 1986; Duncan et al. 1991; Liu et al. 2005). Measured BBB PS_{in} for compounds ranges >5 orders of magnitude from 1×10^{-6} ml/s/g (inulin) to $>5 \times 10^{-1}$ ml/s/g (diazepam) and is strongly influenced by solute lipophilicity as well as BBB influx or efflux transport (Rapoport et al. 1979; Smith 2003). It is defined in terms of free drug in the circulation and thus differs somewhat from the BBB K_{in}, which is defined in terms of serum total drug or solute concentration, as noted below. Just as there is a PS_{in} for influx of a given drug, there is also a matching PS_{out} for free drug efflux, and often they are not equal. PS_{in} can differ from PS_{out} due to facilitated or active transport, enzymatic conversion, or bulk flow. In many cases, $PS_{out} > PS_{in}$. The matching BBB efflux parameter for total drug is k_{out}.

Equilibrium drug distribution within brain ($K_{p,brain}$), on the other hand, is more complex and is influenced by multiple parameters, including BBB active transport, enzymatic conversion, tissue binding, cellular transport, drug ionization, and lysosomal pH trapping (Fridén et al. 2009). $K_{p,brain}$ is commonly determined from the steady-state ratio of total drug concentration in brain divided by that in serum or plasma:

$$K_{p,brain} = C_{tot,brain} / C_{tot,\ plasma} \tag{7.1}$$

where $C_{tot,brain}$ = total drug concentration in brain and $C_{tot,plasma}$ = total drug concentration in plasma. $K_{p,\ brain}$ can also be determined from the ratio of area-under-the-curve drug concentration in brain divided by that in serum or plasma. Both approaches are commonly used in the literature (Kemper et al. 2003):

$$K_{p,brain} \approx \int C_{tot,brain}\,dt / \int C_{tot,\ plasma}\,dt \tag{7.2}$$

At steady state, looking only at the average brain concentration or with constant rate *i.v.* infusion, just a single parameter is necessary. Once $K_{p,brain}$ is measured, the steady-state $C_{tot,brain}$ can be calculated as $K_{p,brain} \times C_{tot,plasma}$.

However, ultimately to describe the full time course of drug concentration in brain under nonsteady-state or most steady-state conditions, two parameters are required in *i.v.* bolus dose or oral dose administration experiments. Most drugs are given orally in discreet doses, and thus there will be maximum drug concentration in brain followed by a declining curve as the drug is eliminated, if given as a single-dose administration. If administered in repeat oral doses to steady state, brain concentration will fluctuate between a maximum and a minimum during the dosing interval, depending upon the brain K_p, BBB PS, dose and dosing interval, as well as plasma concentration. BBB PS is valuable as it gives insight into the time required to obtain brain steady-state distribution and thus an accurate estimate of $K_{p,brain}$ (Liu et al. 2005). As pointed out by Padowski and Pollack (2011), brain exposure may require longer time for equilibration than 2–5 h, as used in a number of studies. For paclitaxel, brain equilibration required 2–4 days. The half time for brain equilibration can be calculated as

$$t_{1/2} = \ln 2 / (PS / K_{p,brain}) \tag{7.3}$$

Brain equilibration requires $4–5 \times t_{1/2}$.

7.2.2 Systemic Administration Method

The "gold standard" approach for in vivo characterization of the pharmacokinetics of drug penetration and distribution in brain is the intravenous administration

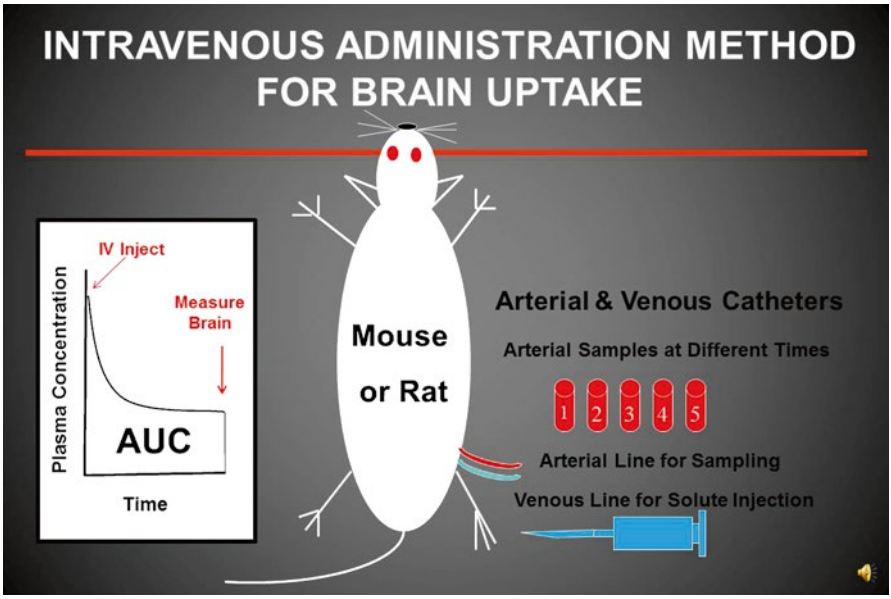

Fig. 7.1 Schematic diagram illustrating the intravenous *(i.v.)* administration method where a test drug is delivered as an *i.v.* bolus injection into the venous circulation and then arterial blood samples are collected at different times until brain drug concentration measurement. The plasma drug area-under-the-curve (AUC) concentration integral is calculated using the trapezoidal rule. Brain concentration, after vascular correction, is related to the time course of plasma concentration to calculate the brain tissue $K_p = AUC_{brain}/AUC_{plasma}$

method (Fig. 7.1). Drug or test compound is delivered directly into the circulation by bolus injection or constant rate infusion. The time course of drug concentration is determined in brain and serum by LC-MS/MS or other quantitative analytical techniques. The data are then fit to a kinetic model to provide BBB PS and $K_{p,\,brain}$ (Ohno et al. 1978; Duncan et al. 1991; Liu et al. 2005) (Fig. 7.2). Exposure time can be manipulated to allow the analysis of initial brain uptake, equilibrium distribution, or brain efflux, depending upon the mode of drug delivery into the circulation and penetration characteristics of the compound under study. Autoradiography or scanning mass spectrometry can be utilized to map drug distribution within brain lesions in diseases, such as stroke, infection, inflammation, neurodegenerative disease, or brain tumors (Fig. 7.3) (Lockman et al. 2010; Taskar et al. 2012). With disease-induced damage to the BBB, drug concentrations within brain parenchyma can become highly heterogeneous with values ranging >100-fold. Under such condition, the average concentration within the lesion reflects only part of the variation observed under the disease condition. The systemic administration technique is the reference standard because it is based upon the in vivo BBB and CNS parenchymal tissue, with all their complexity and unique differences. Most preclinical studies

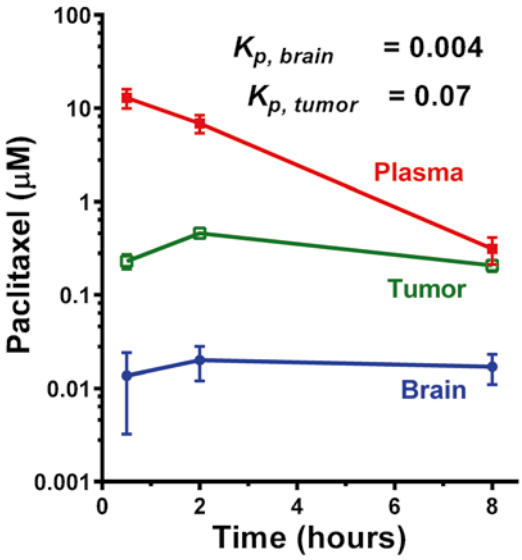

Fig. 7.2 Example of time course of drug concentration in brain, brain tumor, and plasma following vascular injection of paclitaxel (Taxol) to immune-compromised NuNu mice. Points equal mean ± SD for $n = 3–6$ animals. K_p is calculated from total drug concentration measurements as $AUC_{tissue}/AUC_{plasma}$

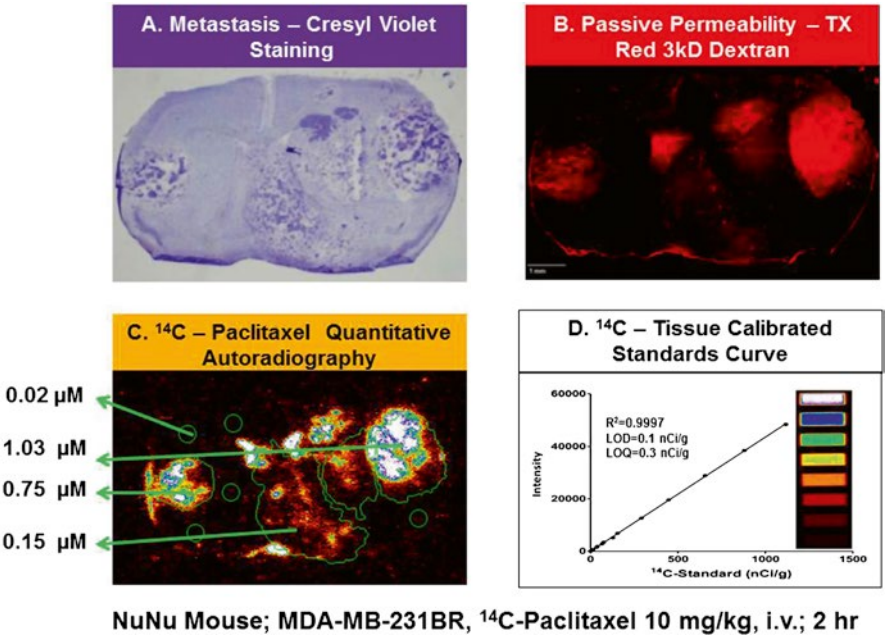

Fig. 7.3 Regional difference in brain and brain tumor uptake of paclitaxel at 2 h after *i.v.* injection of Taxol to immune-compromised NuNu mice, as determined using quantitative autoradiography. Coronal sections (20 **μ**m) were prepared from frozen brain tissue using a cryostat. Matching sections were analyzed for brain distribution of ^{14}C-paclitaxel using autoradiography or stained for tumor using Cresyl violet. Texas red dextran was administered 10–15 min prior to death to measure BBB permeability. The vasculature of the brain was washed out after death using transcardial perfusion (1 min)

utilize rodents, such as rats or mice. Eventually, extension to primates or humans can be made with in vivo imaging, such as positron emission tomography. Care must be employed to distinguish metabolites from intact drug and drug within brain from that residing within the blood circulation within the vasculature of the brain (Lockman et al. 2010). Further, in some cases, it is important to distinguish drug that has crossed the BBB from that sitting bound to the vascular endothelium or concentrated within the BBB endothelial space (Thomas et al. 2009). However, the small volume of the vascular endothelium within brain tissue (<1 μL/g) limits the impact of BBB partitioning on overall brain tissue pharmacokinetics. Depending upon the drug and where it acts within the CNS, results can be expressed as BBB PS and $K_{p,\ brain}$ for whole brain or for specific regions within the CNS. In normal healthy brain, BBB PS varies only about three- to fivefold across the CNS and for many solutes correlates with regional differences in capillary surface area (Takasato et al. 1984).

7.2.3 *Free Versus Total Drug in BBB Kinetic Analyses and Brain Microdialysis*

In many cases, it is valuable to distinguish the concentration of drug that is free or unbound from the total drug concentration in brain and serum, because the free drug concentration at the receptor site correlates best with pharmacodynamics models of activity. Many drugs bind significantly to proteins and lipids based upon lipophilicity and other factors. In such cases, total concentration can differ greatly from the free drug concentration that is usually the driving force for drug diffusion and equilibration. The fraction of drug that is unbound (f_u) can be determined from total concentration by ex vivo equilibrium dialysis or ultrafiltration (Hammarlund-Udenaes et al. 2008). Once f_u is measured, the free concentration (C_u) can be calculated as

$$C_u = f_u \times C_{tot.} \tag{7.4}$$

C_u can also be measured directly in brain by microdialysis (de Lange et al. 1997; Hammarlund-Udenaes et al. 2008).

The unbound drug concentration in brain ISF is useful for comparison with pharmacodynamic studies (Kalvass et al. 2007; Liu et al. 2009) as well as for evaluation of the role of the BBB in hindering brain drug equilibration. The steady-state ratio of unbound drug concentration in brain to that in the circulation is termed $K_{p,uu}$ and is calculated as

$$K_{p,uu} = C_{u,brain} / C_{u,\ plasma} = K_{p\ brain} \times f_{u,brain} / f_{u,plasma} \tag{7.5}$$

A $K_{p,uu}$ value significantly less than 1.0 indicates restriction in brain drug availability as a consequence of the BBB, most commonly a result of active efflux

transport, enzymatic breakdown, or CSF sink effect. In some cases, $K_{p,uu}$ exceeds 1.0, which is usually attributed to active influx transport at the BBB. A $K_{p,uu}$ value of ~1.0 indicates good brain drug bioavailability, especially when accompanied by a reasonably rapid BBB PS for rapid equilibration.

7.2.4 Brain Vascular Correction

Most analytical methods measure total brain drug concentration, and thus a vascular correction is usually required in order to obtain that drug which has crossed the BBB. This correction can be made either by (a) washing out residual blood in brain vasculature at the end of the experiment or (b) subtracting the vascular content, calculated as product of the brain blood volume and the blood drug concentration at the end of the experiment. Brain blood volume is usually measured using radiotracers, such as [^{125}I]albumin, [^{14}C]dextran, or [^{3}H]inulin which, under normal condition, minimally cross the BBB. The vascular correction is most important at early uptake times, where blood concentration is frequently large (such as after bolus *i.v.* injection) and parenchymal brain concentrations are small. Brain vascular volume varies from 0.005 to 0.025 mL/g, and thus $K_{p,brain}$ values >0.25 are minimally influenced by vascular contribution.

7.2.5 Influence of Flow on Initial Brain Uptake and BBB PS

In most studies, the initial rate of drug uptake into brain does not directly measure BBB PS but the transfer coefficient (K_{in}) for drug uptake into brain. K_{in} is related to PS as it gives an excellent index of the ease with which a solute can move from plasma into brain, but it is not permeability (P). This is because, if the solute is sufficiently permeant at the BBB, the flow rate by which the solute is presented to brain can influence its initial rate of brain uptake. The net result is that brain uptake also depends upon cerebral blood flow (F) which varies between brain regions and with neuronal activity. Brain uptake is also influenced by the capillary surface area (S). Renkin (1959) and Crone (1963) modeled this flow dependence using the Krogh single-capillary model and derived the following relationship between flow (F), capillary permeability (P), free fraction of drug in plasma ($f_{u,plasma}$), and capillary surface area (S),

$$K_{in} = F\left[\,1\text{-}e^{-(fu,\,plasma\times PS/F)}\,\right] \tag{7.6}$$

(Mandula et al. 2006; Parepally et al. 2006). Thus, in most experiments, K_{in} is directly measured and BBB PS is calculated. Two limiting conditions in (7.6) are worth noting, (a) when $F >> PS$, $K_{in} \rightarrow PS$, and (b) when $PS >> F$, $K_{in} \rightarrow F$. For practical purposes, BBB $K_{in} \approx PS$ with less than 10 % error when $F > 5 \times PS$, and $K_{in} \approx F$

with less than 10 % error when $PA > 2.3 \times F$. Thus, K_{in} is an acceptable estimate of BBB PS when $F/PS > 5$. When $F/PS < 5$, K_{in} is influenced by both PS an F.

7.2.6 *In Situ Brain Perfusion and Brain Efflux Index*

In some situations, additional information is required regarding the mechanisms involved that restrict drug uptake into brain at the BBB. With the normal in vivo approach, limits are placed on the degree to which an investigator can control or change brain blood flow and free drug concentration or block transport or metabolic mechanisms. Knockout animals are available for several key BBB transporters, such as p-glycoprotein, breast cancer resistance protein, multidrug resistance protein-4, and organic acid-transporting polypeptide. However, with current transporter knockouts, the alteration is not just at the BBB but at all sites within the CNS that usually express the transporter. This can lead to complexity in evaluating the separate role of the BBB in overall brain distribution of the compound.

As alternatives to direct in vivo analysis, in situ perfusion and brain efflux index methods are available for more specific studies of BBB transport. These approaches complement the standard *i.v.* administration method but allow greater flexibility in studying factors that may alter transport. The in situ perfusion method utilizes the in vivo structure of the BBB and cerebral tissues and simply superimposes its own vascular perfusion fluid in replacement to the animal's circulating blood (Fig. 7.4). The particular key advantage of this method is the facile control of perfusate solute concentration which can be altered over a much greater range than generally tolerated in vivo. The concentration dependence of transport is readily measured, as are the effects of ion concentrations and inhibitors. The perfusion approach was originally developed for rats (Takasato et al. 1984) but has been expanded to mice and used in multiple studies of BBB drug transport (e.g., André et al. 2013).

Mechanisms of brain-to-plasma efflux can also be investigated with the brain efflux index technique of Kakee et al. (1996a, b). This method involves direct microinjection of test solute and impermeant reference tracers into brain. At various times thereafter, the ratio of test tracer to impermeant reference marker (R) is determined in brain and expressed as a "brain efflux index" value (BEI), defined as

$$\mathrm{BEI} = 100 \times \left(\left[1 - \left(R \right)_{\mathrm{brain}} / \left(R \right)_{\mathrm{injectate}} \right] \right) \tag{7.7}$$

From this data a rate coefficient for efflux (k_{out}) from brain is calculated and is converted to a transfer coefficient (i.e., clearance) for efflux, as $K_{out} = k_{out} \times K_{pu}$ where K_{pu} as determined from the steady-state distribution of test solute versus free drug concentration in brain slices in vitro. Caution must be exercised with the technique as BBB damage from needle tract injections may alter BBB transport or blood flow. Similarly, solute dilution in brain parenchyma is significant (>50-fold), forcing the necessity to use high levels (e.g., >100 mM) of competitor or transport inhibitor in the injection solution in some experiments. Finally, because of the transient nature of

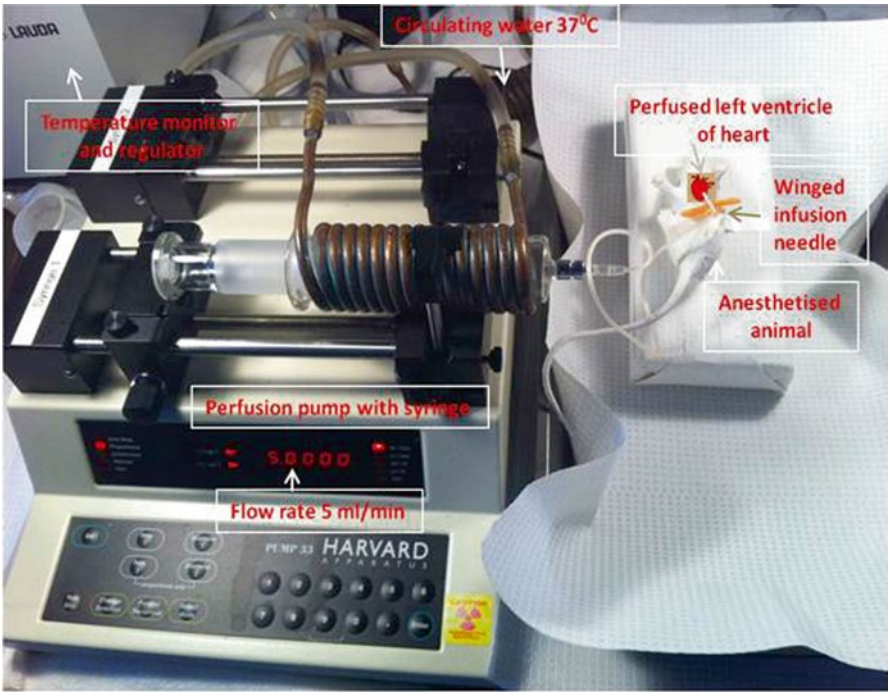

Fig. 7.4 Typical setup for in situ brain perfusion with syringe, infusion pump, temperature control, and circulating water bath

the experimental design, it is hard to precisely know the free drug concentration in ISF at the BBB as a function of time. K_{pu} assumes equilibration, but under normal circumstances, the efflux index is determined under conditions of changing drug concentration. Regardless, the brain efflux index method provides valuable insight into the role and characterization of a number of efflux transport systems at the BBB.

7.2.7 Cerebrospinal Fluid

The CSF is in direct contact with brain ISF and can be used to gain some insight as to drug distribution in the CNS. CSF is particularly useful when measured at steady state, where it provides a reasonable (±two- to threefold) estimate of the drug concentration in brain ISF. As CSF is low in protein content, it provides an estimate of free drug concentration in brain ISF. Under nonsteady-state conditions, the CSF provides a poor index of brain concentration due to multiple factors influencing its formation and circulation within brain. This is particularly true when the BBB is disrupted in one location, whereas the CSF is sampled from distant locations, such as from the lumbar space.

7.3 Future (Challenges/Directions)

Considerable progress has been made over the last 10 years in methods to assess in vivo drug distribution and availability to brain, and in correlating drug availability with in vivo pharmacodynamic effects. Challenges continue to be the low-throughput nature of the experimental setup and the complexity of factors impacting measurements. In many cases, studies are performed only in healthy subjects and do not accurately reflect circumstances in the diseased brain. Further, marked continued progress is needed in dissecting out the roles of individual transporters beyond P-gp and BCRP. A recent publication by Lin et al. (2013) highlights the importance of MRP4 together with P-gp and BCRP in limiting brain distribution of camptothecin analogs. Further, species differences in some cases can be important, where rodent models do not reflect the situation in human brain. Cassette dosing in some cases allows the simultaneous analysis of drug distribution for a series of agents at low doses that do not alter drug transport, distribution, binding, or clearance (Liu et al. 2012).

7.4 Conclusions

An array of accurate and readily utilized procedures are available to investigators to assess the uptake and distribution of drugs in vivo in preclinical models and in humans. The gold standard continues to be direct in vivo assessment and offers the advantage that all the parameters are present that have importance. Results are obtained using the true BBB, not a model, and alterations from disease are readily incorporated. More recent studies linking free drug concentration to effect are critically important as most agents cross to some degree the BBB. By comparing the attained free drug concentration in brain to the EC_{50} for drug effect, one can more clearly assess the extent to which BBB transport is limiting and how improvement can be made by increasing brain delivery or reducing EC_{50} with more potent agents.

7.5 Points for Discussion (Questions)

- How do direct measurements of brain drug availability differ from those obtained with in vitro models?
- How do BBB PS, brain K_p, and brain $K_{p,uu}$ differ in what they tell us about brain drug availability?
- To what extent is the ratio of brain free drug concentration to EC_{50} a better index of BBB availability than BBB PS or $K_{p,uu}$?

- How do selected methods like in situ brain perfusion, microdialysis, and brain efflux index provide additional insights of brain drug distribution and transport?
- How does the presence of the BBB alter drug distribution to brain distinct from other organs of the body?
- What impact does altered BBB function in disease have on drug distribution and availability to the CNS?

References

André P, Saubaméa B, Cochois-Guégan V, Marie-Claire C, Cattelotte J, Smirnova M, Schinkel AH, Scherrmann JM, Cisternino S (2013) Transport of biogenic amine neurotransmitters at the mouse blood–retina and blood–brain barriers by uptake1 and uptake2. AAPS J 32:1989–2001

Cardoso FL, Brites D, Brito MA (2010) Looking at the blood–brain barrier: molecular anatomy and possible investigation approaches. Brain Res Rev 64:328–363

Crone C (1963) Permeability of capillaries of various organs as determined using the "indicator diffusion" method. Acta Physiol Scand 58:292–305

Crone C (1986) Modulation of solute permeability in microvascular endothelium. Fed Proc 45:77–83

de Lange ECM, Danhof M, de Boer AG, Breimer DD (1997) Methodological considerations of intracerebral microdialysis in pharmacokinetic studies of drug transport across the blood–brain barrier. Brain Res Rev 25:27–49

Fridén M, Winiwarter S, Jerndal G, Bengtsson O, Wan H, Bredberg U, Hammarlund-Udanaes M, Antonsson M (2009) Structure-brain exposure relationships in rat and human using a novel set of unbound drug concentrations in brain interstitial and cerebrospinal fluids. J Med Chem 52:6233–6243

Duncan MW, Villacreses N, Pearson PG, Wyatt L, Rapoport SI, Kopin IJ, Markey SP, Smith QR (1991) 2-Amino-3- (methylamino)-propanoic acid (BMAA) pharmacokinetics and blood-brain barrier permeability in the rat. J Pharmacol Exp Ther 258:27–35

Hammarlund-Udenaes M, Fridén M, Syvänen S, Gupta A (2008) On the rate and extent of drug delivery to the brain. Pharm Res 25:1737–1750

Kakee A, Terasaki T, Sugiyama Y (1996a) Brain efflux index as a novel method of analyzing efflux transport at the blood–brain barrier. J Pharmacol Exp Ther 277:1550–1559

Kakee A, Terasaki T, Sugiyama Y (1996b) Selective brain to blood efflux transport of para-aminohippuric acid across the blood–brain barrier: in vivo evidence by use of the brain efflux index method. J Pharmacol Exp Ther 283:1018–1025

Kalvass JE, Olson ER, Cassidy MP, Selley DE, Pollack GM (2007) Pharmacokinetics and pharmacodynamics of seven opioids in p-glycoprotein-competent mice; assessment of unbound brain EC50,u and correlation of in vitro, preclinical, and clinical data. J Pharmacol Exp Ther 323:346–355

Kemper EM, van Zandbergen AE, Cleypool C, Mos HA, Boogerd W, Beijnen JH, van Tellingen O (2003) Increased penetration of paclitaxel into the brain by inhibition of P-glycoprotein. Clin Cancer Res 9:2849–2855

Lin F, Marchetti S, Pluim D, Iusuf D, Mazzanti R, Schellens JH, Beijnen JH, van Tellingen O (2013) Abcc4 together with abcb1 and abcg2 form a robust cooperative drug efflux system that restricts the brain entry of camptothecin analogues. Clin Cancer Res 19:2084–2095

Liu X, Chen C, Smith BJ (2008) Progress in brain penetration evaluation in drug discovery and development. J Pharmacol Exp Ther 325:349–356

Liu X, Ding X, Deshmukh G, Liederer BM, Hop CE (2012) Use of the cassette-dosing approach to assess brain penetration in drug discovery. Drug Metab Dispos 40:963–969

Liu X, Smith BJ, Chen C, Callegari E, Becker SL, Chen X, Cianfrogna J, Doran AC, Doran SD, Gibbs JP, Hosea N, Liu J, Nelson FR, Szewc MA, Van Deusen J (2005) Use of a physiologically based pharmacokinetic model to study the time to reach brain equilibrium: an experimental analysis of the role of blood–brain barrier permeability, plasma protein binding, and brain tissue binding. J Pharmacol Exp Ther 313:1254–1262

Liu X, Vilenski O, Kwan J, Apparsundaram S, Weikert R (2009) Unbound brain concentration determines receptor occupancy: a correlation of drug concentration and brain serotonin and dopamine reuptake transporter occupancy for eighteen compounds. Drug Metab Dispos 37:1548–1556

Lockman PR, Mittapalli RK, Taskar KS, Rudraraju V, Gril B, Bohn KA, Adkins CE, Roberts A, Thorsheim HR, Gaasch JA, Huang S, Palmieri D, Steeg PS, Smith QR (2010) Heterogeneous blood-tumor barrier permeability determines drug efficacy in mouse brain metastases of breast cancer. Clin Cancer Res 16:5664–5678

Mandula H, Parepally JMR, Feng R, Smith QR (2006) Role of site-specific binding to plasma albumin in drug availability to brain. J Pharmacol Exp Ther 317:667–675

Ohno K, Pettigrew KD, Rapoport SI (1978) Lower limits of cerebrovascular permeability to non-electrolytes in the conscious rat. Am J Physiol 235:H299–H307

Padowski JM, Pollack GM (2011) Influence of time to achieve substrate distribution equilibrium between brain tissue abd blood on quantitation of the blood–brain barrier p-glycoprotein effect. Brain Res 1426:1–17

Parepally JMR, Mandula H, Smith QR (2006) Brain uptake of nonsteroidal anti-inflammatory drugs—ibuprofen, flurbiprofen and indomethacin. Pharm Res 23:873–881

Rapoport SI, Ohno K, Pettigrew KD (1979) Drug entry into the brain. Brain Res 172:354–359

Renkin EM (1959) Transport of potassium from blood to tissue in isolated mammalian skeletal muscles. Am J Physiol 197:1205–1210

Smith QR, Rapoport SI (1986) Cerebrovascular permeability coefficients to sodium, potassium, and chloride. J Neurochem 46:1732–1742

Smith QR (2003) A review of blood–brain barrier transport techniques. Meth Mol Med 10:191–2003

Takasato Y, Rapoport SI, Smith QR (1984) An in situ brain perfusion technique to study cerebrovascular transport in the rat. Am J Physiol 247:H484–H493

Taskar KS, Rudraraju V, Mittapalli RK, Samala R, Thorsheim HR, Lockman J, Gril B, Hua E, Palmieri D, Polli JW, Castellino S, Rubin SD, Lockman PR, Steeg PS, Smith QR (2012) Lapatinib distribution in HER2 overexpressing experimental brain metastases of breast cancer. Pharm Res 29(3):770–781

Thomas FC, Taskar K, Rudraraju V, Goda S, Thorsheim HR, Gaasch JA, Palmieri D, Steeg PS, Lockman PR, Smith QR (2009) Uptake of ANG1005—a novel paclitaxel-peptide derivative, through the blood–brain barrier into brain and experimental brain metastases of breast cancer. Pharm Res 26:2486–2492

Chapter 8
Principles of PET and Its Role in Understanding Drug Delivery to the Brain

Stina Syvänen and Roger N. Gunn

Abstract Positron emission tomography (PET) is a non-invasive medical imaging technique that enables the investigation of drug pharmacokinetics in vivo. The technique is especially powerful for pharmacokinetic studies of new CNS drug candidates as tissue samples from the brain are understandably difficult to obtain. The PET technique involves the administration of a radiolabelled molecule whose spatio-temporal distribution can be measured using tomography. The radiolabelled molecule can be the drug under investigation, a structurally different molecule that binds to the same target as the drug candidate or a molecule that interacts with a downstream target that is believed to be affected by the action of the drug candidate. Such radiolabelled probes allow PET to address several questions central for CNS drug development: Does the drug candidate reach the target site? Does the drug candidate interact with the desired target? Is the concentration of the drug at the target site sufficient to illicit an effect? What is the temporal nature of such an interaction? What is the relationship between the target site concentration and the administered dose and/or plasma concentrations?

S. Syvänen (✉)
Department of Public Health and Caring Sciences, Uppsala University, Uppsala, Sweden
e-mail: stina.syvanen@pubcare.uu.se

R.N. Gunn
Department of Medicine, Imperial College London, London, UK

Department of Engineering Science, University of Oxford, Oxford, UK

Imanova, London, UK

M. Hammarlund-Udenaes et al. (eds.), *Drug Delivery to the Brain*, AAPS Advances in the Pharmaceutical Sciences Series 10, DOI 10.1007/978-1-4614-9105-7_8,

8.1 Introduction

8.1.1 Background

Positron emission tomography (PET) is a medical imaging technique that allows for the measurement of a range of biological processes involving receptors, enzymes and transporters in addition to the bio-distribution of labelled drugs. The development of PET imaging was initiated in the early 1970s with the first operational human PET scanner in 1975. Early PET work was dominated by [^{18}F]fluorodeoxyglucose ([^{18}F]FDG), a marker for glucose metabolism, which has subsequently been translated into a diagnostic tool in the clinic for the detection of tumours in oncology. [^{18}F]FDG, a glucose analogue, allows the direct measurement of regional glucose consumption in the body. A high uptake of [^{18}F]FDG indicates increased metabolism in a viable tumour and is founded on the Warburg effect (Warburg 1956) which determines that cancer cells have a higher rate of glycolysis. The effect of anti-cancer treatments may be monitored by serial [^{18}F]FDG PET examinations, although the long-term response to treatment may not be well predicted by the short-term reduction in glycolysis for all drugs. The brain is another organ with high glucose consumption, and [^{18}F]FDG can be used to study brain physiology and function in health and disease. For example, it has been used in diagnosing Alzheimer's disease which is characterised by a decreased [^{18}F]FDG uptake particularly in temporoparietal areas of the brain.

The number of available PET radiotracers increased during the late 1980s, and PET has utilised these imaging tools to study other neurological disorders such as anxiety, epilepsy and Parkinson's disease. In the late 1990s many pharmaceutical companies realised the potential of PET in drug development and started to apply it particularly in neuroscience applications (Table 8.1). In the past and to some extent still today, the selection of new drug candidates for neurosciences relies mainly on in vitro techniques which are good and often preferable for studying specific drug–target interactions but which may fail to mimic the complexity of the in vivo situation. Although preclinical in vivo studies are used the results can be confounded by species differences. The potential to actually study new drug candidates in vivo in man at an early phase in drug candidate selection was obviously appealing to the pharmaceutical industry. What hampered the use of PET for drug development in the 1990s was the availability of lab facilities sufficiently equipped for radiopharmaceutical research, the lack of labelling methods for introducing the PET radionuclide into drug candidates and to some extent the cost. Today, the cost associated with PET is still high, but PET is available at more locations, and most small drugs or drug-like molecules can be labelled with one of the available PET radionuclides which has increased utilisation of PET in the development of new CNS drugs, especially antipsychotic and anti-depressive drugs (Bergström et al. 2003; Pike 2009; Matthews et al. 2012).

Table 8.1 Application of PET in CNS drug development

Early phase	• Biodistribution studies to confirm that the drug reaches the brain or a specific target site in the brain at sufficient concentrations • Brain pharmacokinetics, for example as a guide for dose selection • Drug–target (receptor occupancy) interactions, for example as a guide for dose selection • Pharmacodynamic biomarkers for proof of concept (reasons to believe) • Translational preclinical imaging to aid candidate selection or to identify and validate biomarkers • In vivo measures for monitoring safety or toxicity
Late phase	• Surrogate markers of response (may be more sensitive and faster to measure than clinical outcome) • Stratification of patients based on potential for successful treatment (personalised medicine) • Pharmacological differentiation of competitor compounds (best in class)
Marketed drugs	• Evaluation of ongoing treatment based on biomarkers • Differentiation between available treatments • Patient stratification based on disease sub-phenotype or early treatment response • Improved disease classification/diagnosis • Earlier diagnosis

8.1.2 Principles of PET

A PET radiotracer is a molecule labelled with a positron-emitting radionuclide such as ^{11}C, ^{13}N, ^{15}O, ^{18}F or ^{68}Ga. Nearly all endogenous and drug-like molecules contain carbon (C) which makes them amenable to PET labelling with ^{11}C. By replacing a naturally occurring carbon isotope in the molecule with ^{11}C it is possible to generate PET tracer whose chemical structure and pharmacokinetic properties are the same as the original compound. In addition, nitrogen (N) or oxygen (O) are also common in endogenous and drug-like molecules and may also be replaced by positron-emitting isotopes. Further, most molecules also contain hydrogen (H). Non-acidic hydrogen can often be substituted by fluorine (F) with minor changes of the molecule's pharmacological or physiochemical properties. These commonly used PET radionuclides have a relatively short half-life, 20.3 min for ^{11}C and 110 min for ^{18}F (see Table 8.2), and thus the tracer synthesis time has to be short. All ^{11}C-tracers must be injected into the subject shortly after being synthesised, while ^{18}F-tracers have the benefit of a longer half-life often resulting in a shelf life of several hours. The short half-life of these radionuclides is challenging for the synthesis and production of PET radiotracers but allows for repeated scans in single subjects on the same day.

All PET radionuclides contain an excess of protons compared to neutrons, and to increase stability one proton is converted into a neutron and during this decay event a single positron is emitted. It is the emission of these positrons which is the basis for the PET signal. Each emitted positron will travel a few mm in the tissue until it collides with an electron causing a positron–electron annihilation that produces two photons emitted at an angle of 180°. These photons are detected by a ring

Table 8.2 Radionuclides used in PET and their half-lives

Isotope	Half-life	Comments
^{15}O	122 s	Oxygen (O) is common in drug-like molecules, and ^{15}O labelling does therefore not change pharmacokinetic properties. However, the very short half-life is a drawback
^{13}N	9.97 min	Although not as abundant as O and C in drug-like molecules, nitrogen (N) is still fairly common in drug-like molecules, and ^{13}N labelling may also be used to avoid alteration in pharmacokinetic properties
^{11}C	20.4 min	Essentially all endogenous and drug-like molecules contain carbon (C) and ^{11}C labelling, where an isotopically unmodified carbon atom is replaced by ^{11}C and is often desirable as this approach does not alter the molecule with respect to its pharmacokinetic properties
^{68}Ga	68.3 min	Used for labelling of peptides and antibody fragments
^{18}F	110 min	Can often replace hydrogen (H) without any major effects on pharmacokinetic properties
^{89}Zr	78.4 h	Used for labelling of macromolecules such as antibodies with slow pharmacokinetics
^{124}I	100 h	Used for labelling of macromolecules such as antibodies with slow pharmacokinetics

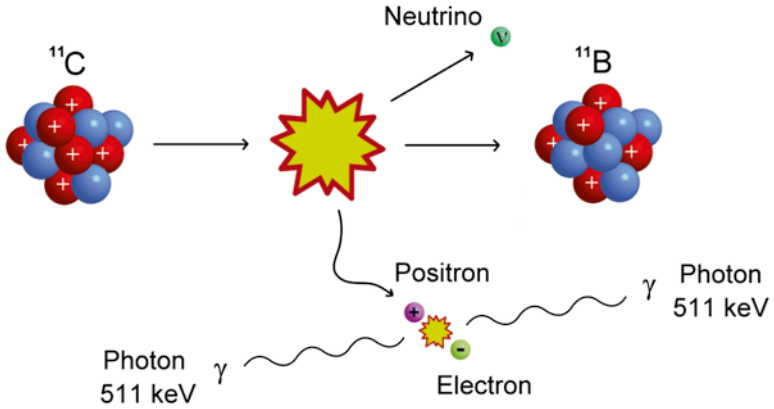

Fig. 8.1 Decay of ^{11}C. A positron-emitting nuclide, in this figure ^{11}C, is unstable due to a surplus of protons. Therefore, one proton is converted to a neutron to increase stability and, at the same time, a positron is emitted from the nucleus. The positron travels through tissue for up to a few mm until it collides with an electron. The positron–electron annihilation produces two photons that are emitted at an angle of approximately 180°. These photons are then detected by the PET scanner, and knowledge of which detector pairs registered the coincidence events and their precise timings enables the reconstruction of the spatial distribution of the emitted positrons

of detectors in the PET scanner (Fig. 8.1). The acquisition of PET data may simply be a single 3D image representing the average concentration over a particular time period (static image) or it can be a 4D image that measures the changing concentration over time (dynamic image). The raw tomographic data is reconstructed into

quantitative images by applying appropriate corrections for confounding factors such as attenuation and scatter. For image quantification, a region of interest is often delineated on the PET image around the tissue or the part of a tissue that is of interest for the study. The outlined region can be applied to images from different time frames to generate a dynamic time–activity curve for the particular region (or simply to measure the radiotracer concentration for static acquisitions). Many regions can be outlined in the set of PET images, allowing for assessment of regional differences in pharmacokinetics. The application of appropriate bio-mathematical models to the dynamic data allows for the estimation of quantitative biological parameters (Gunn et al. 2001) such as those presented in Sect. 8.1.3.

There are three principal ways in which PET can be used to understand drug behaviour in vivo:

- Using a labelled drug to understand its administration, distribution, metabolism or elimination (ADME)
- Using a separate labelled compound which allows imaging of the target and drug action on the target
- Using a separate labelled compound which reflects the effects of drug action on cellular or organ physiology

In the first scenario, PET can be used to study the pharmacokinetics of the drug molecule directly so that drug uptake in the brain, time to maximum concentrations in the brain and brain concentrations over time can easily be obtained. However, if the drug is only slowly distributed to the brain, the information obtained in this experimental setting might have limited value since a PET investigation cannot be extended beyond 3–4 half-lives of the radionuclide. In the second scenario, a radiotracer is used as a marker for specific target system. In this case, it is the changes in the uptake of the radiotracer after administration of the drug that are studied in the PET investigation. For example, if a radiotracer is known to bind to a specific receptor, a PET scan before drug administration will allow for a quantitative estimate of the receptor availability in the absence of the drug. A subsequent scan following the administration of the drug then measures the change in receptor availability caused by binding of the unlabelled drug and enables the construction of a dose–occupancy relationship. By performing multiple PET scans at different time points it is possible to measure the kinetics of the drug candidate at its target site in relation to the plasma pharmacokinetics in order to provide a more comprehensive characterisation of the drug (Abanades et al. 2011). The characterisation of drug–target occupancy in relation to dose (or concentration) and time in the brain provides valuable information to drug development teams that addresses both the questions of brain entry and also optimisation of dose levels for larger clinical studies of efficacy. Finally, a radiotracer might be used to monitor the effect of the drug on cellular function. For example, [^{18}F]FDG is frequently used for studying cancer tumours; in this case, a high uptake indicates extensive metabolism and a viable tumour, and decreased uptake after treatment may suggest that the treatment was successful.

8.1.3 PET Concepts and Nomenclature

PET measures the total amount of radioactive material in the tissue of interest. At its most simplest, this can be quantified as the measured radioactivity, normalised to injected dose or normalised to injected dose per body weight, given as

$$\%\text{injected dose}(\%\text{ID}) = \frac{\text{Radioactivity per tissue weight}}{\text{Injected radio activity}} \times 100 \tag{8.1}$$

or

$$\text{SUV} = \frac{\text{Radioactivity per tissue weight}}{\text{Injected radioactivity per body weight}} \tag{8.2}$$

where SUV is the standardised uptake value. Both of these measurements reflect the radioactive concentration at the site of measurement in relation to the amount of radioactivity injected. However, since the amount of radioactivity in the tissue is dependent on the amount supplied to it via the plasma, further analysis is required to derive parameters that are specific for the tissue, and this involves the parallel measurement of radioactivity in whole blood or plasma.

The most common parameter estimated from measurements of radioactivity in both tissue and plasma is the brain-to-plasma partition coefficient. The nomenclature for this parameter in PET and pharmacokinetic literature differs, although Innis et al. (Innis et al. 2007) have published a suggestion for standardisation of the PET nomenclature and Summerfield et al. have presented a table clarifying the PET nomenclature in relation to standard pharmacokinetic terminology (Summerfield et al. 2008; Syvänen and Hammarlund-Udenaes 2010). In PET, the brain-to-plasma partition coefficient is often referred to as the volume of distribution (V_T), while, in pharmacokinetic studies, it is called K_p (Table 8.3). This PET nomenclature can be confusing, since the distribution volume in standard pharmacokinetics refers to the apparent volume of distribution for a drug, given in volume units. K_p (V_T) can be determined from PET data in a number of different ways: by compartmental modelling (Gunn et al. 2001), by model-independent graphical analysis (Patlak et al. 1983; Logan et al. 1990) or simply by comparing steady-state concentrations in brain and plasma (Carson et al. 1993). In its most simple definition it is defined as the ratio of the concentration in tissue to that in plasma at equilibrium.

The net rate of drug transfer to the brain can be measured with PET if radioactivity concentrations are measured in plasma in parallel to PET scanning. The permeability surface area product PS, which is equal to the net influx clearance CL_{in}, measured in ml min^{-1} g_$brain^{-1}$, is comparable to the PET parameter K_1, measured in ml min^{-1} cm^{-3}.

In addition to V_T and K_1, other common outcome measures from PET studies are binding potential (BP) and receptor occupancy. BP is a composite parameter that

Table 8.3 Terms explaining relationship between PET and pharmacokinetic nomenclature in brain biodistribution studies

PET	Description	Relation to field of standard pharmacology
SUV	Standardised uptake value; total tissue concentrations normalised for injected dose per body weight	Not used
% Inj dose	Total tissue concentrations normalised for injected dose	Not used
V_T	Equilibrium partition coefficient; total brain-to-total plasma concentration ratio	K_p
V_{ND}	Non-displaceable equilibrium partition coefficient; total brain-to-total plasma concentration ratio when no specific binding exists	K_p in a region devoid of specific binding
K_1 (mL min^{-1} cm^{-3})	Rate constant for drug transfer from arterial plasma to tissue	PS (permeability surface product) or CL_{in} (net influx clearance)
$\frac{f_{ND}}{f_P}\frac{C_{ND}}{C_P}$	Equilibrium partition coefficient; unbound brain-to-unbound plasma concentration ratio, where f_{ND} and f_p are the free fractions in the brain tissue and plasma, respectively, and can be determined by equilibrium dialysis and C_{ND} and C_p are total concentrations in tissue (devoid of specific binding) and plasma and can be obtained from PET and blood sampling, respectively	$K_{p,uu}$

includes both the density of "available" binding sites (receptors) and the affinity of the radiotracer for that target. BP can be calculated from separate estimates of V_T in a target and reference region (devoid of the target site):

$$\mathrm{BP} = \frac{V_T^{\mathrm{Target}} - V_T^{\mathrm{Reference}}}{V_T^{\mathrm{Reference}}} \tag{8.3}$$

As a rule of thumb, BP should be between 0.5 and 15 for a good radiotracer candidate, as values below 0.5 indicate that the signal-to-noise ratio will likely be too low, while BP above 15 indicates near-irreversible kinetics and problems in accurately estimating BP. The receptor occupancy after administration of a drug candidate can be calculated based on BP before drug administration ($BP_{baseline}$) and BP after drug administration (BP_{drug}) according to (8.4):

$$\text{Receptor Occupancy}(\%) = \frac{\mathrm{BP}_{\mathrm{baseline}} - \mathrm{BP}_{\mathrm{drug}}}{\mathrm{BP}_{\mathrm{baseline}}} \times 100 \tag{8.4}$$

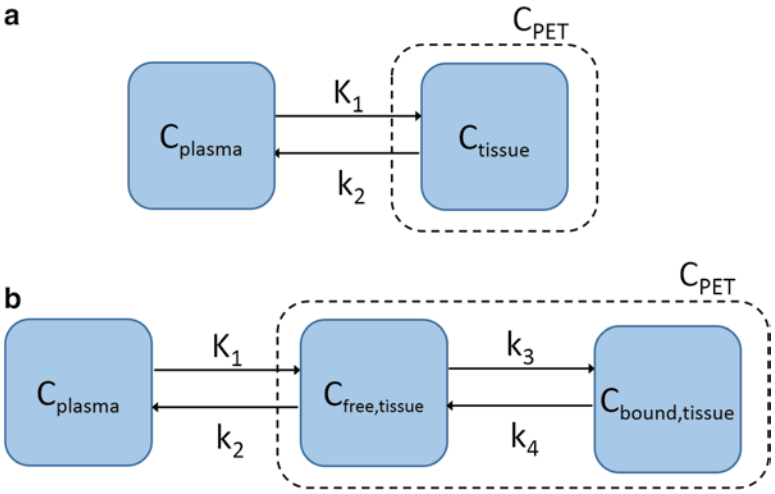

Fig. 8.2 Schematic overview of PET compartment models. (**a**) A standard single-tissue compartment model (1T2k in PET nomenclature). (**b**) A two-tissue compartment model (2T4k in PET nomenclature). K_1 is the transfer of tracer from plasma into tissue, k_2 is the rate constant describing the transport of tracer back to plasma, k_3 is the rate constant describing the association of the tracer with the specific binding sites and k_4 is considered as the dissociation rate constant of the receptor–tracer complex. For clarity, the blood volume in the PET compartments has been omitted

8.1.4 Study Protocols

As discussed above the pharmacokinetic parameter of interest in most PET studies is the brain-to-plasma concentration ratio K_p (V_T in PET nomenclature). K_p is usually estimated from PET experiments in which the tracer is administered as a single bolus and application of pharmacokinetic modelling (Gunn et al. 2001; Slifstein and Laruelle 2001). For example, K_p can be obtained from K_1 and k_2 for a single-tissue compartment model ($K_p = K_1/k_2$) or from K_1, k_2, k_3, and k_4 ($K_p = K_1/k_2\,(1 + k_3/k_4)$) for a two-tissue compartment model (Gunn et al. 2001), or from the slope of a Logan graphical analysis ($K_p = 1/\text{slope}$) (Logan et al. 1990). Single-tissue and two-tissue compartment models and rate constants are shown in Fig. 8.2. K_p can also be directly calculated from the steady-state concentrations of the drug in brain and plasma. Steady-state concentrations can be obtained by appropriate infusion protocols based on elimination kinetics of the tracer. Using the steady-state approach no assumptions have to be made regarding the pharmacokinetic model. There are advantages and disadvantages with each of these designs. For example, bolus injections are technically easier than infusions as a single bolus dose of the radiotracer does not require an infusion pump and the injection can be given manually. In addition, it may not be possible to get the system into equilibrium within the duration of the scan.

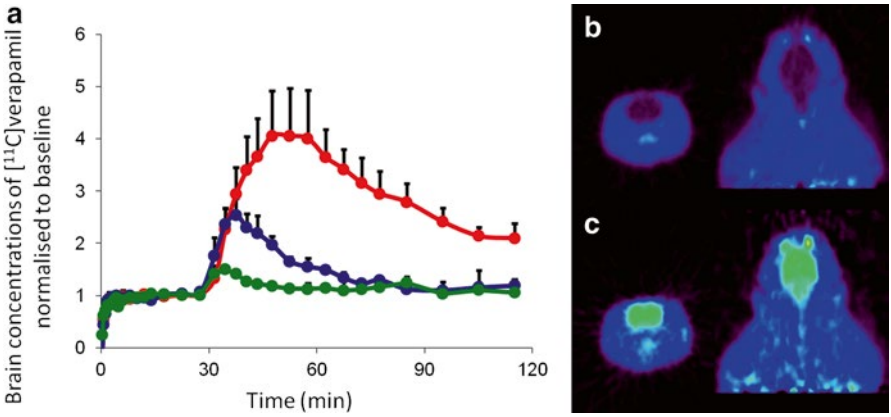

Fig. 8.3 Effect of P-glycoprotein inhibitor tariquidar on brain distribution of [^{11}C]verapamil. (**a**) [^{11}C]verapamil concentrations in the brain before (0–30 min) and after (30–120 min) P-glycoprotein inhibition with 3 (*green*), 10 (*blue*) and 25 (*red*) mg/kg cyclosporine. (**b**) PET images before P-glycoprotein inhibition and (**c**) after P-glycoprotein inhibition. Intense colours indicate high concentrations

The outcome of a drug intervention is often compared between individuals that are treated with the drug and individuals that act as controls (non-treated or placebo treated). If bolus protocols are used, two groups are needed or, alternatively, each individual can serve as its own control, which requires two PET scans: one before and one after intervention. When separate control and intervention groups are used, it can be difficult to know whether a possible difference between the control and the intervention group is due to inter-individual/inter-occasion variability or due to an effect of the intervention drug. In this setting, steady-state protocols are appealing as the dynamics of drug intervention or drug interaction can be studied in each subject. For example chemical inhibition of efflux transporters at the BBB can be studied in real time with infusion of a radiotracer that is an efflux transporter substrate (Fig. 8.3) (Syvänen et al. 2006). Also, displacement of radiotracer from specific targets by intervention drugs can be visualised with steady-state approaches (Carson et al. 1993). The main disadvantage of using infusions is the increase in radioactive exposure to both the subject and the attending personnel. A special shield for the syringe containing the radiotracer has to be used both for protection of the subject/personnel and also to avoid any influence on the scanner. The radioactivity in the bolus component of the steady-state protocol may have to be decreased somewhat in comparison to the amount of radioactivity injected using a single bolus protocol since additional radioactivity is infused during the infusion component. However, compared to acquiring two separate PET scans, e.g., one before and one after intervention, the steady-state protocols normally result in less radioactivity dose. Steady-state protocols have been used in human subjects with both ^{11}C and ^{18}F radiotracers (Pinborg et al. 2003; Lee et al. 2013).

8.2 Current Status

8.2.1 Brain Distribution Studies

PET biodistribution studies use the radiolabelled version of the drug as the radiotracer. Hence, PET can be used to study the pharmacokinetics of a drug candidate. When the radiotracer is injected in tracer dose this set-up is often referred to as microdosing (Bergström et al. 2003). The radiotracer (i.e., the labelled drug) can also be co-injected with unlabelled drug, and, since the relationship between labelled and unlabelled drug concentrations is known, the tissue pharmacokinetics can then be deduced quantitatively at clinically relevant doses. Further, such co-injections with unlabelled compound may also reveal whether any BBB efflux transporters that are active at tracer dose become saturated at therapeutic dose and allow for sufficient drug to enter the brain to elicit a pharmacological response. In addition, application of transporter inhibitors with these experimental set-ups may provide further confidence about transporter influence on drug distribution into the brain (Syvänen and Hammarlund-Udenaes 2010; Syvänen and Eriksson 2013).

Regardless of whether the study is performed as a microdosing study or at clinical doses, a number of factors need to be considered. First, PET measures the total radioactivity; so any metabolites carrying the radioactive label will also contribute to the signal, thus potentially confounding the results. Hence, the radiotracer data needs to be evaluated with respect to metabolism and the appearance of radioactive metabolites in plasma and in tissue. The position of the radioactive label will determine which radioactive metabolites are produced and thus contribute to the signal. Ideally for a CNS tracer, the position of the label should be such that only hydrophilic metabolites are produced, i.e., metabolites that are unlikely to enter the lipophilic environment of the brain to the same extent as the tracer. Second, radioactivity measured with PET will originate from both radioactivity in the brain tissue as well as in the vascular component of the brain. Negligence to correct for vascular activity, especially for compounds that do not enter the brain readily, may lead to overestimation of brain concentrations of the investigational compound. As initial biodistribution studies with new drug candidates are often preclinical, a third factor to consider is the choice of preclinical species. Ultimately the drug candidates need to be effective in humans, but for different reasons, mainly toxicological, it is not always possible to directly study a new drug candidate in humans (even when using microdosing). Translation between species is complex for CNS active drugs as the passage of drugs into the brain is governed not only by passive diffusion but also by the presence of active transport mechanisms and protein binding in both plasma and brain tissue. Compared to other organs, where molecules can easily diffuse between cells, making active transport processes less important for the target site concentrations, the brain concentrations will be dependent on active influx and efflux from the brain. These processes may, in addition to systemic elimination and protein binding, differ between species, and significant differences in brain concentrations have been reported for both unlabelled drugs and radiotracers

across species (Syvänen et al. 2009). In the development of new drug candidates or radiotracers it is important to consider this when taking a decision on whether or not to proceed with the development of a molecule when it has been discovered that it interacts with for example an efflux transporter. Even when a molecule is a clear P-glycoprotein (P-gp) substrate in cell lines or rodents, it could reach relatively high brain concentrations in humans. In fact, several radiotracers, e.g. [^{11}C]2, 3, 4, 5, 6, 7-hexahydro-1{4-[1[4-(2-methoxyphenyl)-piperazinyl]]-2-phenyl butyry}-1*H*-azepine ([^{11}C]RWAY), 4-(2′-methoxyphenyl)-1-[2′-(N-2″-pyridinyl)-*p*-[^{18}F]fluorobenzamido]ethylpiperazine ([^{18}F]MPPF), [^{18}F]altanserin and [^{11}C](*S*)- (2-methoxy-5-(5-trifluoromethyltetrazol-1-yl)-phenylmethylamino)-2(*S*)-phenyl piperidine (GR205171), have been successfully used as PET CNS tracers in humans before they were found to be P-gp substrates. These findings are important for the interpretation of studies investigating drug delivery to the brain, when extrapolating in vitro and preclinical data to humans.

8.2.2 Drug–Target Interactions

PET studies that measure receptor occupancy of a ligand are usually performed with a PET radiotracer that is structurally different from the ligand but which binds to the same binding site. This is a consequence of the fact that only a small subset of ligands actually produces PET radiotracers with a measurable specific signal. The successful subset is dependent on good brain penetration and delivery, low non-specific binding and suitable affinity for the target of interest. For a ligand to be a successful therapeutic drug the rate of entrance is often not as important since drugs are dosed to steady-state concentrations and often optimised for high target affinity which leads to a slow dissociation. Development of PET probes for a novel target should proceed in parallel with the drug development programme itself as the process of obtaining an applicable tool in humans will require at least 18 months' lead time. Candidate molecules for the new PET radiotracer can be screened in parallel as they will often originate from the same series of molecules and may benefit from concomitant medicinal chemistry support. Thus, it is important to start the development of the PET radiotracer in parallel to the development of the novel drug so that the PET imaging tools are available to be used in first time in human studies. It should also be mentioned that performing these measurements in man as early as possible is important because there may be species differences that mean that preclinical estimates of the in vivo IC_{50} are not applicable in humans. For example H_3 histamine occupancy of a candidate drug has been shown to be significantly different between preclinical species and humans (Ashworth et al. 2010).

The main application of PET receptor occupancy studies is in dose finding studies which can involve exploring the relationship between temporal occupancy profiles and the plasma concentration of the drug. These studies consist, initially, of the acquisition of baseline scans in the absence of the drug to measure the baseline receptor availability and subsequently involve the acquisition of further scans at

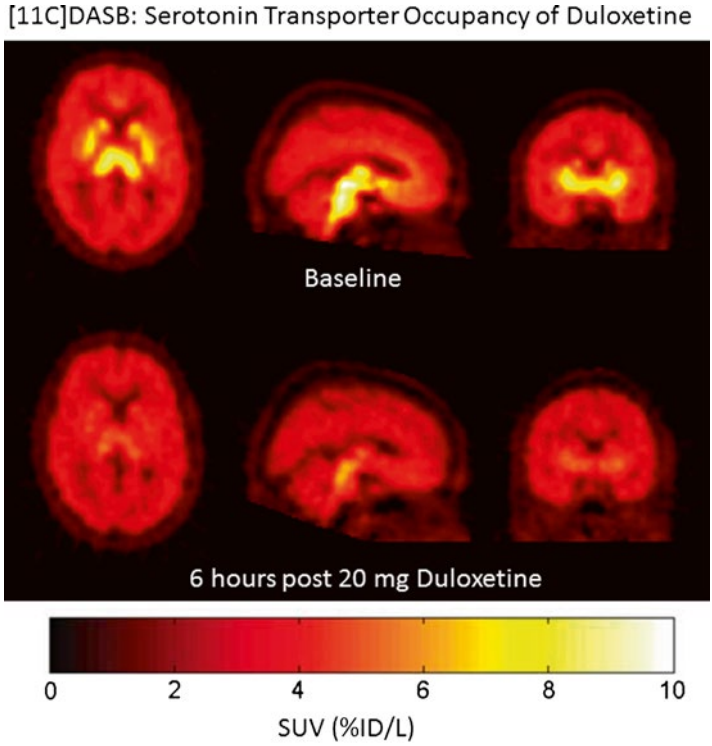

Fig. 8.4 Dose–receptor occupancy. Radioligand signal before (*upper panel*) and after (*lower panel*) administration of cold drug, duloxetine, competing for the same binding site. PET scanning after different doses of cold drug and at different time points post dose administration enables characterisation of drug–target occupancy in relation to dose (or concentration) and time

different time points post dosing with the drug (Fig. 8.4). Comparison of the receptor availability post dose with the baseline values allows for the calculation of the fractional receptor occupancy. Combined with knowledge of the desired receptor occupancy, these studies provide confidence in selecting doses for larger later phase clinical studies. For example, the cost in terms of time and money (10s of millions of dollars) in performing a study at either non-pharmacological doses or at doses that produce side effects must be avoided. Receptor occupancy studies may be performed at single dose or repeat dose to characterise the relationship between the plasma concentration time course and the target occupancy. A recent study by Abanades et al. (2011) has demonstrated how the application of plasma–target occupancy models to single-dose PET occupancy data can be used to predict the target occupancy data at repeat dose even if the drug kinetics are not direct (i.e. there is an increased target residence time of the molecule which means that the effective IC_{50} of the drug is different following single and repeat dose). This is important as repeat dosing is the usual dosing regimen applied in patients, and thus the ability to characterise this as early in the drug development process as possible is valuable.

8.2.3 Drug Effects on Cellular or Organ Physiology

Glucose metabolism in tissue is a classical example of PET as a tool to monitor cellular function, and as mentioned above the glucose analogue [^{18}F]FDG has been used to study brain glucose utilisation. Certain dementias are characterised by region-specific decreases in glucose turn-over, and these can be visualised with PET, and thus it can aid in their diagnosis. Another example is amyloid imaging with the PET radiotracer [^{11}C]PIB (N-methyl-[^{11}C]2-(4′-methylamino-phenyl)-6-hydroxybenzothiazole), a derivate of thioflavin-T, which is the most frequently used radiotracer in the assessment of amyloid plaques in Alzheimer's disease. The clinical experiences with [^{11}C]PIB amyloid imaging are that it detects Alzheimer's disease pathogenesis early in the course of disease and helps distinguish Alzheimer's disease from other types of dementia, e.g. Lewy body dementia and fronto-temporal dementia in the differential diagnosis. However, [^{11}C]PIB amyloid imaging is of limited value to measure disease progression, since the signal does not further increase as the disease progresses, i.e. there is a ceiling effect with amyloid levels plateauing early in the disease process (Engler et al. 2006). Despite this, one recent study reported that [^{11}C]PIB brain uptake was significantly lower in patients with Alzheimer's disease treated with a new anti-amyloid antibody compared to patients treated with placebo (Rinne et al. 2010). The study also showed that the different doses used had similar therapeutic effects but that side effects (vasogenic oedema) were observed only at higher doses. The study illustrates the use of PET imaging of surrogate markers to evaluate and aid in the dose selection of novel treatments.

Drug development for many CNS diseases is hampered by the lack of knowledge about the disease mechanism. Imaging of cellular or organ physiology can be useful in the development of a new therapeutic when the exact target site for drug action is unknown or when no PET radiotracer is available for the target. Thus, these types of studies may provide some indirect evidence about successful drug delivery to the target tissue.

8.2.4 Challenges When Using PET for Studies of BBB Transport

The effect of a drug intended for a target inside the brain is generally related to the unbound (free) drug concentration inside the brain (Hammarlund-Udenaes et al. 2008; Jeffrey and Summerfield 2009; Watson et al. 2009). PET measures total radioactivity, including that associated with both unbound and bound drug as well as any metabolites carrying the positron-emitting radionuclide, and hence only K_p and $K_{p,u}$ (ratio of total concentration in brain and unbound concentration in plasma) can be calculated. The unbound ratio of drug in brain interstitial fluid to unbound in plasma, $K_{p,uu}$, cannot be estimated from a PET investigation unless the unbound fraction in the brain is deduced by other means. This can be done by combining PET

data with in vitro equilibrium dialysis assays of the free fraction of drug molecules in brain tissue and plasma (Gunn et al. 2012). Whilst the free fraction in brain may be difficult to obtain for human tissue, Summerfield et al. and Di et al. have shown that this fraction is well conserved across species (in contrast to the plasma free fraction) for a number of test compounds, and thus the estimated tissue free fraction obtained in preclinical species might be used (with caution) together with clinical PET data (Summerfield et al. 2008; Di et al. 2011). The free fraction in plasma should always be estimated in the species under investigation, as species differences in plasma protein binding are common.

As a true translational technique PET experiments can be performed according to similar protocols in vivo in animals as well as in humans. This means that preclinical studies can precede clinical studies and provide valuable parameter estimates that help refine clinical experimental designs. However, in addition to potential species differences, the need for anaesthesia may limit the use of preclinical data for prediction of human response. For example, a number of studies have shown that differences in brain uptake may be a consequence of different anaesthesia (Harada et al. 2004). It is important to make an educated choice regarding anaesthesia method in preclinical studies so that the anaesthetics used do not interfere with the studied target system.

Lastly, when studying a new CNS drug candidate with PET it is always important to study the radiotracer concentrations in plasma or, if available, in a reference region, since intervention with a new drug candidate could potentially change the metabolism or the plasma protein binding of the radiotracer and thus alter the fraction of radiotracer molecules available for transport into and binding within the brain. Measurement of radiotracer concentrations in blood is also required for correction of radioactivity in the blood volume in the brain.

8.3 Future

8.3.1 Macromolecules and Biologics

For decades, the development of small molecular drugs has been the main focus for the pharmaceutical industry. Today there is an increasing interest in macromolecules and biologics such as peptides, proteins, oligonucleotides and monoclonal antibodies. In line with this trend in the development of new drugs, there is also an increasing use of PET to explore the biodistribution of macromolecules, and given the slow kinetics of these molecules this has led to the use of longer lived radionuclides such as ^{89}Zr ($t_{1/2}$ = 78.4 h) and ^{124}I ($t_{1/2}$ = 100.3 h) (Hooker 2010; van Dongen and Vosjan 2010; van Dongen et al. 2012). These new PET studies have without exception been applied in the oncology field, and most studies have focused on quantitative evaluation of monoclonal antibody binding to specific targets such as B-lymphocyte antigen CD20, cMet (proto-oncogene encoding hepatocyte growth

factor) and prostate-specific membrane antigen (PSMA) as a scouting procedure prior to radioimmunotheraphy (van Dongen et al. 2012). For this purpose the radiotracer should show similar biodistribution as the antibody used in the therapeutic radioimmunotheraphy. All published studies so far describe targets outside the CNS. However, as macromolecular drugs are also more frequently developed for CNS targets, PET biodistribution studies will be important for estimating brain distribution of these molecules. For example, several pharmaceutical companies are developing anti-amyloid antibodies that aim to reduce the cerebral amyloid-β load. The exact mechanism is debated; it is not completely clear whether the antibodies act within the blood as amyloid binders and thus decrease amyloid concentrations in the brain and prevent the subsequent formation of senile plaques which are central in Alzheimer's disease pathogenesis or if they actually exert their action within the brain. Hence, it is also of interest to image the levels of these anti-amyloid antibodies inside the brain, and labelled antibodies could potentially be used as diagnostics to examine the levels of intrabrain-soluble amyloid (as opposed to insoluble amyloid measured with the available PET radiotracers today). The large size of antibodies limits the diffusion from the blood into the brain, and for this purpose the use of antibody fragments or engineered proteins like diabodies and nanobodies might be an option. In addition to being smaller, these proteins are also more rapidly cleared from the body and can thus be labelled with shorter lived radionuclides. Radiolabelling with ^{68}Ga ($t_{1/2}$ = 1.13 h) is attractive as generation of ^{68}Ga does not require a cyclotron but can be produced from commercially available ^{68}Ge/^{68}Ga generators. Taken together, PET imaging using macromolecular CNS radiotracers is still in its infancy, but interest in the area is likely to increase in parallel to focus on new CNS active macromolecular drugs and biologics.

8.3.2 Novel Technologies

The development of dual-modality scanners, i.e. PET combined with computerised tomography (CT) or magnetic resonance imaging (MRI), has facilitated co-registration of structural and functional data. PET scanners are now available with integrated high-end multi-detector-row CT scanners. Recently dual-PET/MRI scanners have also become available. Thus, PET and CT/MRI scans can be performed in immediate sequence during the same session, with the study subject not changing position between the two types of scans. The co-registered images display both functional and anatomical information so that areas of abnormality on the PET imaging can be correlated with anatomy on the CT/MRI images. The combination of PET–MRI should enable methods for correction of motion during the scans which degrade image quality but is difficult to avoid in long PET scans.

The possibility to reliably quantify drug concentrations in brain has contributed to the increasing use of PET in pharmaceutical research. However, in line with the different nomenclature in PET pharmacokinetics, different pharmacokinetics

methods are often applied in the PET field compared to the field of standard pharmacokinetics. In the field of standard pharmacokinetics it is widely accepted that non-linear mixed effects modelling, often referred to as population modelling, is a preferable choice compared to analyses on solely individual level or naïve pooling (Pillai et al. 2005). Mixed effects modelling resolves both intra- and inter-subject variability, i.e. it gives a description of the pharmacokinetics in the typical subject as well as information about variation in the study population through simultaneous analysis of all study subjects. Further, estimates of covariate effects such as age, sex, weight and disease severity can be obtained. By far, most PET studies are today analysed at the individual level, i.e. all pharmacokinetic analyses are made for each individual separately, and, after this analysis, population averages and variability are computed based on the individual pharmacokinetic (PK) model parameter estimates. This method requires either rich individual data and/or simple models for the individual parameters to be identifiable. If this is the case, this two-stage approach to obtaining population parameter estimates has been shown to be generally unbiased in estimation of the mean parameters, but the variances and covariances of the estimates are likely to be overestimated in all realistic situations (Steimer et al. 1984). Recently population approaches have been applied to PET receptor studies, mainly as a method to estimate receptor occupancy of a therapeutic drug but also for brain distribution and receptor density studies (Lim et al. 2007; Kim et al. 2011; Syvänen et al. 2011; Zamuner et al. 2012). As PET studies are expensive and although the radioactivity that the study subject is exposed to is relatively low, there is still a need for keeping the number of PET scans required at a minimum. The use of mixed effects modelling also in the PET field could potentially make PET studies more cost-effective and more informative. Especially in receptor occupancy studies adaptive designs that use information obtained in previous subjects and scans for changing scan protocols for subsequent studies are emerging (Zamuner et al. 2010; Abanades et al. 2011; Gunn et al. 2011).

8.3.3 PET Chemistry

During the last decade new labelling methods have increased the number of possible radiotracers. ^{11}C is most often introduced via a reaction with labelling precursors [^{11}C]methyl iodide and, to a lesser extent, [^{11}C]methyl triflate, which are both obtained from [^{11}C]carbon dioxide. [^{11}C]Carbon monoxide ([^{11}C]CO) is interesting as a synthon (synthetic building block) as PET applications for CNS targets often require that the labelled molecule has high specific activity (specific activity = amount of radioactivity per mole of molecule), something that favours the use of [^{11}C]CO in labelling synthesis as the relatively low abundance of carbon monoxide in air, in contrast to carbon dioxide, reduces the risk for isotopical dilution. However, the general use in radiopharmaceutical synthesis has been hampered by the low

solubility of carbon monoxide in most solvents and the resulting challenge to confine [^{11}C]CO in low-volume reaction vessels. Recently two new methods have been described which will enable easy use of [^{11}C]CO for labelling (Kealey et al. 2009; Eriksson et al. 2012). High specific activity allows for administration of low amounts of drug (nanomolar range), i.e. a subpharmacological dose. Thus, even toxic compounds can be labelled and visualised with PET. Further, as drug doses are low, less extensive toxicology testing is required for new labelled drug candidates to be studied with PET, and hence, these can be studied in vivo in man at an early stage in candidate selection.

8.4 Conclusions

The development of new drugs that elicit their effect inside the brain is complicated because of both the protective nature of the BBB and the technical difficulties in studying drug concentrations at the CNS target site in humans. With PET, it is possible to measure drug concentrations non-invasively in the brain, and this has meant that the method is playing an increasingly important role in drug development processes. Advances in labelling methods, novel tracers, study design, analysis of PET data and the introduction of multimodality scanners are likely to further increase the number of PET applications in pharmaceutical research.

8.5 Points for Discussion

- How can V_T/K_p be estimated from PET measurements?
- Mention three radionuclides that can be used with PET.
- Discuss the advantages and disadvantages when using a radionuclide with a short half-life.
- Why is ^{11}C useful for radiolabelling of endogenous and small drug-like molecules?
- When is it relevant to perform PET studies at tracer dose (microdosing)? And at pharmacological dose?
- Discuss the advantages and disadvantages of bolus-only and bolus-plus-infusion regimens.
- Why are metabolites of PET radiotracers a potential confounding factor for the read-out?
- Why is it important to correct the PET signal obtained in the brain area for radioactivity in the vascular space of the brain?
- How can PET be used in drug development?
- What information can be obtained from a receptor occupancy study?

References

Abanades S, van der Aart J, Barletta JA, Marzano C, Searle GE, Salinas CA, Ahmad JJ, Reiley RR, Pampols-Maso S, Zamuner S, Cunningham VJ, Rabiner EA, Laruelle MA, Gunn RN (2011) Prediction of repeat-dose occupancy from single-dose data: characterisation of the relationship between plasma pharmacokinetics and brain target occupancy. J Cereb Blood Flow Metab 31(3):944–952

Ashworth S, Rabiner EA, Gunn RN, Plisson C, Wilson AA, Comley RA, Lai RY, Gee AD, Laruelle M, Cunningham VJ (2010) Evaluation of 11C-GSK189254 as a novel radioligand for the H3 receptor in humans using PET. J Nucl Med 51(7):1021–1029

Bergström M, Grahnen A, Långström B (2003) Positron emission tomography microdosing: a new concept with application in tracer and early clinical drug development. Eur J Clin Pharmacol 59(5–6):357–366

Carson RE, Channing MA, Blasberg RG, Dunn BB, Cohen RM, Rice KC, Herscovitch P (1993) Comparison of bolus and infusion methods for receptor quantitation: application to [^{18}F] cyclofoxy and positron emission tomography. J Cereb Blood Flow Metab 13(1):24–42

Di L, Umland JP, Chang G, Huang Y, Lin Z, Scott DO, Troutman MD, Liston TE (2011) Species independence in brain tissue binding using brain homogenates. Drug Metab Dispos 39(7):1270–1277

Engler H, Forsberg A, Almkvist O, Blomquist G, Larsson E, Savitcheva I, Wall A, Ringheim A, Langström B, Nordberg A (2006) Two-year follow-up of amyloid deposition in patients with Alzheimer's disease. Brain 129(Pt 11):2856–2866

Eriksson J, van den Hoek J, Windhorst AD (2012) Transition metal mediated synthesis using [^{11}C] CO at low pressure—a simplified method for ^{11}C-carbonylation. J Label Compd Radiopharm 55:223–228

Gunn RN, Gunn SR, Cunningham VJ (2001) Positron emission tomography compartmental models. J Cereb Blood Flow Metab 21(6):635–652

Gunn RN, Murthy V, Catafau AM, Searle G, Bullich S, Slifstein M, Ouellet D, Zamuner S, Herance R, Salinas C, Pardo-Lozano R, Rabiner EA, Farre M, Laruelle M (2011) Translational characterization of [(11) C]GSK931145, a PET ligand for the glycine transporter type 1. Synapse 65(12):1319–1332

Gunn RN, Summerfield SG, Salinas CA, Read KD, Guo Q, Searle GE, Parker CA, Jeffrey P, Laruelle M (2012) Combining PET biodistribution and equilibrium dialysis assays to assess the free brain concentration and BBB transport of CNS drugs. J Cereb Blood Flow Metab 25(10):1

Hammarlund-Udenaes M, Friden M, Syvänen S, Gupta A (2008) On the rate and extent of drug delivery to the brain. Pharm Res 25(8):1737–1750

Harada N, Ohba H, Fukumoto D, Kakiuchi T, Tsukada H (2004) Potential of [(18)F]beta-CFT-FE (2beta-carbomethoxy-3beta-(4-fluorophenyl)-8-(2-[(18)F]fluoroethyl)nortropane) as a dopamine transporter ligand: a PET study in the conscious monkey brain. Synapse 54(1):37–45

Hooker JM (2010) Modular strategies for PET imaging agents. Curr Opin Chem Biol 14(1): 105–111

Innis RB, Cunningham VJ, Delforge J, Fujita M, Gjedde A, Gunn RN, Holden J, Houle S, Huang SC, Ichise M, Iida H, Ito H, Kimura Y, Koeppe RA, Knudsen GM, Knuuti J, Lammertsma AA, Laruelle M, Logan J, Maguire RP, Mintun MA, Morris ED, Parsey R, Price JC, Slifstein M, Sossi V, Suhara T, Votaw JR, Wong DF, Carson RE (2007) Consensus nomenclature for in vivo imaging of reversibly binding radioligands. J Cereb Blood Flow Metab 27(9):1533–1539

Jeffrey P, Summerfield S (2009) Assessment of the blood–brain barrier in CNS drug discovery. Neurobiol Dis 37(1):33–37

Kealey S, Miller PW, Long NJ, Plisson C, Martarello L, Gee AD (2009) Copper(I) scorpionate complexes and their application in palladium-mediated [^{11}C]carbonylation reactions. Chem Commun 25:3696–3698

Kim E, Howes OD, Kim BH, Yu KS, Jeong JM, Lee JS, Kim SJ, Jang IJ, Park JS, Kim YG, Shin SG, Turkheimer FE, Kapur S, Kwon JS (2011) The use of healthy volunteers instead of patients to inform drug dosing studies: a [^{11}C]raclopride PET study. Psychopharmacology 217(4):515–523

Lee DE, Gallezot JD, Zheng MQ, Lim K, Ding YS, Huang Y, Carson RE, Morris ED, Cosgrove KP (2013) Test-retest reproducibility Of [^{11}C]-(+)-propyl-hexahydro-naphtho-oxazin positron emission tomography using the bolus plus constant infusion paradigm. Mol Imaging 12(2):77–82

Lim KS, Kwon JS, Jang IJ, Jeong JM, Lee JS, Kim HW, Kang WJ, Kim JR, Cho JY, Kim E, Yoo SY, Shin SG, Yu KS (2007) Modeling of brain D2 receptor occupancy-plasma concentration relationships with a novel antipsychotic, YKP1358, using serial PET scans in healthy volunteers. Clin Pharmacol Ther 81(2):252–258

Logan J, Fowler JS, Volkow ND, Wolf AP, Dewey SL, Schlyer DJ, MacGregor RR, Hitzemann R, Bendriem B, Gatley SJ et al (1990) Graphical analysis of reversible radioligand binding from time-activity measurements applied to [N-^{11}C-methyl]-(-)-cocaine PET studies in human subjects. J Cereb Blood Flow Metab 10(5):740–747

Matthews PM, Rabiner EA, Passchier J, Gunn RN (2012) Positron emission tomography molecular imaging for drug development. Br J Clin Pharmacol 73(2):175–186

Patlak CS, Blasberg RG, Fenstermacher JD (1983) Graphical evaluation of blood-to-brain transfer constants from multiple-time uptake data. J Cereb Blood Flow Metab 3(1):1–7

Pike VW (2009) PET radiotracers: crossing the blood–brain barrier and surviving metabolism. Trends Pharmacol Sci 30(8):431–440

Pillai GC, Mentre F, Steimer JL (2005) Non-linear mixed effects modeling—from methodology and software development to driving implementation in drug development science. J Pharmacokinet Pharmacodyn 32(2):161–183

Pinborg LH, Adams KH, Svarer C, Holm S, Hasselbalch SG, Haugbol S, Madsen J, Knudsen GM (2003) Quantification of 5-HT2A receptors in the human brain using [^{18}F]altanserin-PET and the bolus/infusion approach. J Cereb Blood Flow Metab 23(8):985–996

Rinne JO, Brooks DJ, Rossor MN, Fox NC, Bullock R, Klunk WE, Mathis CA, Blennow K, Barakos J, Okello AA, Rodriguez Martinez de Liano S, Liu E, Koller M, Gregg KM, Schenk D, Black R, Grundman M (2010) 11C-PiB PET assessment of change in fibrillar amyloid-beta load in patients with Alzheimer's disease treated with bapineuzumab: a phase 2, double-blind, placebo-controlled, ascending-dose study. Lancet Neurol 9(4):363–372

Slifstein M, Laruelle M (2001) Models and methods for derivation of in vivo neuroreceptor parameters with PET and SPECT reversible radiotracers. Nucl Med Biol 28(5):595–608

Steimer JL, Mallet A, Golmard JL, Boisvieux JF (1984) Alternative approaches to estimation of population pharmacokinetic parameters: comparison with the nonlinear mixed-effect model. Drug Metab Rev 15(1–2):265–292

Summerfield SG, Lucas AJ, Porter RA, Jeffrey P, Gunn RN, Read KR, Stevens AJ, Metcalf AC, Osuna MC, Kilford PJ, Passchier J, Ruffo AD (2008) Toward an improved prediction of human in vivo brain penetration. Xenobiotica 38(12):1518–1535

Syvänen S, Blomquist G, Sprycha M, Höglund AU, Roman M, Eriksson O, Hammarlund-Udenaes M, Långström B, Bergström M (2006) Duration and degree of cyclosporin induced P-glycoprotein inhibition in the rat blood–brain barrier can be studied with PET. Neuroimage 32(3):1134–1141

Syvänen S, de Lange EC, Tagawa Y, Schenke M, Molthoff CF, Windhorst AD, Lammertsma AA, Voskuyl RA (2011) Simultaneous in vivo measurements of receptor density and affinity using [(11)C]flumazenil and positron emission tomography: comparison of full saturation and steady state methods. Neuroimage 57(3):928–937

Syvänen S, Eriksson J (2013) Advances in PET imaging of P-glycoprotein function at the blood–brain barrier. ACS Chem Neurosci 4(2):225–237

Syvänen S, Hammarlund-Udenaes M (2010) Using PET studies of P-gp function to elucidate mechanisms underlying the disposition of drugs. Curr Top Med Chem 10(17):1799–1809

Syvänen S, Lindhe Ö, Palner M, Kornum BR, Rahman O, Långström B, Knudsen GM, Hammarlund-Udenaes M (2009) Species differences in blood–brain barrier transport of three positron emission tomography radioligands with emphasis on P-glycoprotein transport. Drug Metab Dispos 37(3):635–643

van Dongen GA, Poot AJ, Vugts DJ (2012) PET imaging with radiolabeled antibodies and tyrosine kinase inhibitors: immuno-PET and TKI-PET. Tumour Biol 33(3):607–615
van Dongen GA, Vosjan MJ (2010) Immuno-positron emission tomography: shedding light on clinical antibody therapy. Cancer Biother Radiopharm 25(4):375–385
Warburg O (1956) On the origin of cancer cells. Science 123(3191):309–314
Watson J, Wright S, Lucas A, Clarke KL, Viggers J, Cheetham S, Jeffrey P, Porter R, Read KD (2009) Receptor occupancy and brain free fraction. Drug Metab Dispos 37(4):753–760
Zamuner S, Di Iorio VL, Nyberg J, Gunn RN, Cunningham VJ, Gomeni R, Hooker AC (2010) Adaptive-optimal design in PET occupancy studies. Clin Pharmacol Ther 87(5):563–571
Zamuner S, Rabiner EA, Fernandes SA, Bani M, Gunn RN, Gomeni R, Ratti E, Cunningham VJ (2012) A pharmacokinetic PET study of NK(1) receptor occupancy. Eur J Nucl Med Mol Imaging 39(2):226–235

Chapter 9
PKPD Aspects of Brain Drug Delivery in a Translational Perspective

Elizabeth C.M. de Lange

Abstract The development and optimization of CNS drug is hampered by the inaccessibility of the human brain and the difficulty to quantify human CNS drug effects. The use of serial CSF sampling in animals and mathematical modeling of plasma pharmacokinetics, in conjunction with CNS effects, provided only useful information for drugs that distribute to the brain target site by simple diffusion and having direct and reversible CNS effects. Active transport processes across blood–brain barriers and brain cell membranes may be applicable for many drugs and should be taken into account. Also, context dependencies of the rates and extents of all transport processes should be included. This indicates the need for cross-compare designed preclinical experimental approaches and mathematical modeling to provide information on contributions of the (main) individual processes, in terms of rate and extent, as well as their interplay, to be able to predict human CNS drug effects.

Abbreviations

AR	Agonist receptor complex density
BBB	Blood–brain barrier
BCSFB	Blood–cerebrospinal fluid barrier
Ce	Concentration of the drug in the effect compartment
CNS	Central nervous system
CSF	Cerebrospinal fluid
E	Effect

E.C.M. de Lange (✉)
Target Site Equilibration Group, Division of Pharmacology,
Leiden Academic Center of Drug Research, Leiden, The Netherlands
e-mail: l.lange@lacdr.leidenuniv.nl

M. Hammarlund-Udenaes et al. (eds.), *Drug Delivery to the Brain*, AAPS Advances in the Pharmaceutical Sciences Series 10, DOI 10.1007/978-1-4614-9105-7_9,

E0	Effect in the absence of the agonist
EC_{50}	Concentration of agonist at half-maximal effect
ECF	Extracellular fluid
Em	Maximal effect in the biological system
Emax	Maximal effect of the agonist
K_A	Agonist-receptor binding dissociation equilibrium constant
Ke	Density of agonist receptor complex that elicits the half maximal effect
K_{1e}	First-order rate constant for influx K_{1e}
Keo	Rate constant for drug efflux from the hypothetical effect compartment
P-gp	P-glycoprotein
PD	Pharmacodynamics
PK	Pharmacokinetics
PKPD	Pharmacokinetic-pharmacodynamic
RT	Total receptor density
τ	Transducer constant (efficacy parameter)
Ve,app	Apparent volume of distribution in the brain

9.1 Introduction

Despite enormous advances in CNS research, CNS disorders remain the world's leading cause of disability and account for more hospitalizations and prolonged care than almost all other diseases combined. This indicates a high unmet need for good CNS drugs and drug therapies. For a proper CNS effect the drug should have the ability to access the CNS "at the right place, at the right time, and at the right concentration." To that end a number of key issues need to be considered.

- Only the unbound drug is able to pass the BBB and to interact with its target to drive the effect (Urien et al. 1987; Jolliet et al. 1997; Tanaka and Mizojiri 1999; Liu et al. 2005; Hammarlund-Udenaes et al. 2008; Hammarlund-Udenaes 2009; Stevens et al. 2012).
- Transport across the blood–brain barrier (BBB) needs to take place for adequate drug delivery to the CNS. It is of great importance to understand the mechanisms involved in uptake into and efflux from the brain, on one hand being governed by BBB functionality (in terms of passive paracellular and transcellular diffusion), facilitated diffusion, active influx, active efflux, and absorptive or receptor-mediated endocytosis and on the other hand by drug physicochemical properties and structure (Mayer et al. 1959; Oldendorf 1974; Betz and Goldstein 1986; Suzuki et al. 1997; Kalvass and Maurer 2002; Danhof et al. 2005, 2007; Westerhout et al. 2011).
- Not only BBB transport is of importance but also plasma pharmacokinetics and intrabrain distribution, the latter indicating spatial and temporal exchange of a drug between brain ECF, brain cells, and CSF (De Lange et al. 1995c; Kalvass and Maurer 2002; Liu et al. 2005; Westerhout et al. 2011, 2012).

- Mechanisms that underlie BBB functionality and brain tissue characteristics all have their specific rate and extent, being dynamically regulated. Therefore, heterogeneity in species, gender, genetic background, tissue, age, diet, disease conditions, drug treatment, etc., (Letrent et al. 1999; Karssen et al. 2001; Kooij et al. 2010; De Lange et al. 2005; Mulder et al. 2001; Danhof et al. 2007; Ravenstijn et al. 2007, 2012; Syvänen et al. 2009; Westerhout et al. 2011, 2012) contributes to context-dependent variability in CNS target site PK.
- Then, not only CNS target site distribution is context dependent so is the observed effect or the biomarker(s) of the effect. Context-dependent PKPD relationships of CNS drugs most of all underlies the relative high failure of CNS drug candidates. Therefore the link between target concentration and CNS response should preferentially be obtained within the same subject (De Lange 2013a).
- Information on time-dependency is crucial (De Lange et al. 2005; Hammarlund-Udenaes et al. 2008).

The inaccessibility of the human brain for sampling hampers obtaining relevant human target site concentrations of CNS drugs, while also it is often difficult to quantify human CNS drug effects. This indicates that CNS drug distribution and effects in humans should be predicted by other measures.

To decipher and learn more on the factors that govern plasma pharmacokinetics, BBB transport intrabrain distribution, as well as their interrelationships and consequences for CNS effects in the different settings, systematic preclinical research on CNS drugs will be of help. To that end, investigations should be performed such that variables are systematically varied (e.g., inhibition of an efflux transporter, or induction of pathological state) in which time-dependency is explicitly included. As our brains do not have the capacity to integrate all these data and determine contributions of individual mechanisms in PKPD relationships, we need to organize, condense, and store knowledge in mathematical frameworks, by the use of advanced mathematical modeling. This provides the links to the human situation.

This chapter deals with more classical, current, and future approaches to PKPD aspects of brain drug delivery in a translational perspective.

9.2 History

9.2.1 CSF Concentrations to Predict CNS Target Site Concentration

For a long time monitoring approaches have been searched for to obtain information that could be used to predict human target site kinetics and CNS effects. As it is the free drug that is available for target binding, in the early 1980s it was anticipated that the drug concentration in the cerebrospinal fluid (CSF) could serve as a biomarker of the free brain target site concentrations, because in CSF, at least under physiological conditions, no binding of drugs to proteins occurs (Bonati et al. 1984).

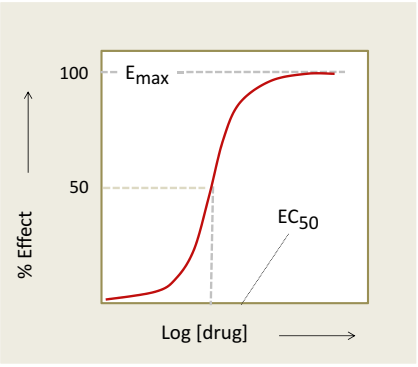

Fig. 9.1 Plasma concentration–effect profiles often have a sigmoidal shape when the percentage of the maximal response (Emax) of a drug (agonist) is plotted against the logarithm of the drug concentration

A step forward was then made by the development of the methodology of serial CSF sampling. Experiments were designed to obtain the time-course of concentrations in relation to parallelly obtained CNS drug effects, and many samples could be obtained from single animals providing the possibility of within-subject cross-over designed studies, and minimizing the number of animals to be used. Serial CSF sampling in conjunction with measuring CNS effects was applied for pento- and heptabarbital, ethanol, and pentylenetetrazole, and by varying the rate and duration of an intravenous infusion of a single dose, it could be clearly demonstrated that the CSF compartment was pharmacokinetically indistinguishable from the site of action of this drug (Danhof and Levy 1984; Dingemanse et al. 1988; Ramzan and Levy 1986). On that basis CSF concentrations were considered to be of key value for studying PKPD relationships of CNS active drugs, and methodologies for sequential CSF sampling in human became available (Bruce and Oldfield 1988).

9.2.2 Predictions of CNS Drug Response by Compartmental PKPD Modeling

In the early 1990s, as an alternative to serial CSF sampling, mathematical modeling techniques were developed to describe the effect–time course of a CNS drug on the basis of its plasma pharmacokinetics (Campbell 1990). Concentration–response profiles often have a sigmoidal shape when the percentage of the maximal response (Emax) is plotted against the logarithm of the drug concentration (Fig. 9.1). Therefore, the sigmoid Emax model is (still) most generally used to fit a plasma concentration–effect profiles to provide estimates of EC_{50} and Emax values of drugs. The sigmoid Emax equation (9.1) is the following:

$$E = \mathrm{E0} + [(\mathrm{E\,max} \times [\mathrm{A}]^N) / (\mathrm{EC}_{50}{}^N + [\mathrm{A}]^N)] \tag{9.1}$$

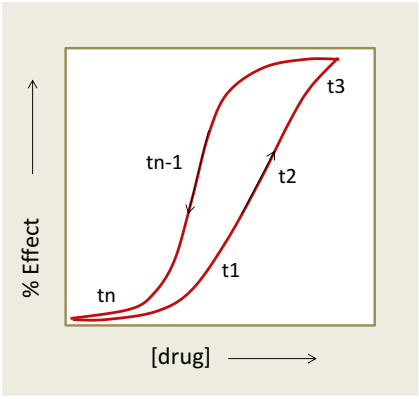

Fig. 9.2 Time developments of plasma concentration and effect are not usually in phase. A number of processes may cause a delay in effect relative to plasma concentrations of the drug. This will result in a so-called hysteresis loop for the effect versus drug concentration in the climbing and falling phase of drug concentrations in plasma

With E0, the baseline response, *E* the response observed for a given drug concentration [A] at time *t*, Emax, the maximal effect of the drug, EC_{50} is the plasma concentration of the drug that produces 50 % of Emax, and *h*, the Hill coefficient, which determines the steepness of the concentration–effect relationship. The EC_{50} ("potency") is simply the concentration of agonist required to provoke a response halfway between the baseline and maximum responses. It is usually not the same as the dissociation equilibrium constant (KA) for the binding of agonist to its receptor. If drug concentrations at the target site are in equilibrium with those in plasma (site of measurement) and drug effects are direct and in case the effect is (assumed to be) direct and reversible this is a very useful approach, especially as it can also be applied to humans.

However, when the drug concentration in plasma is not in equilibrium with its site of action, hysteresis occurs and drug levels are out of phase with activity. So-called counter-clockwise hysteresis (Fig. 9.2) is observed when the effect increases with time for a given drug concentration in plasma. Such situation can be caused by pharmacokinetic processes such as slow diffusion of the drug towards the target site taking time, active influx of the drug towards the target site, formation of active agonistic metabolites, but also by pharmacodynamic processes like relatively slow signal transduction processes and sensitization. Clockwise hysteresis, in which the effect decreases with time for a given drug concentration, can be caused by tolerance, active antagonistic metabolites, learning effects, and feedback regulation.

Hysteresis can be mathematically dealt with by incorporating an "effect site compartment" using the COLLAPS algorithm (Sheiner et al. 1979; Veng-Pedersen et al. 1991), also called the "link model," that contains a compartment with hypothetical target site concentrations (the effect site compartment), being linked to the plasma concentration by a first-order rate constant for influx k_{1e} and a rate constant k_{eo} for drug efflux from the hypothetical effect compartment.

$$E = \mathrm{E0} + [(\mathrm{Emax} \times [\mathrm{Ce}]^N) / [\mathrm{EC}_{50}{}^N + [\mathrm{Ce}]^N)] \tag{9.2}$$

In which Ce is the concentration of the drug (agonist) in the effect compartment.

With inclusion of the effect compartment, simultaneous PKPD modeling may provide estimates of EC_{50}, Emax, and Hill factor, as well as the rate of CNS target site equilibration as has been shown for benzodiazepines, baclofen, antiepileptic drugs, and adenosine receptor agonists and antagonists (Mandema and Danhof 1992; Mandema et al. 1992; Danhof et al. 1993). Therewith it was demonstrated that by using PKPD modeling in preclinical investigations, useful quantitative information on the pharmacodynamics of new drugs in vivo could be obtained (Breimer and Danhof 1997a, b).

However, compartmental direct effect PKPD modeling cannot distinguish between slow diffusion and other active pharmacokinetic processes determining the concentration of the drug at the target site, nor does it allow the discrimination between drug affinity (binding of the drug to its receptor) and efficacy (ability of the drug to cause an effect after binding to the receptor) (De Lange et al. 2005). It, therefore, lacks the power to predict drug responses under different physiologic or pathologic conditions, where active transport processes are involved, or where both affinity and efficacy may be affected. This means that for prediction of CNS drug effects a more in depth investigation on PKPD relationships is needed on one hand by incorporating information on target site distribution and on the other hand by including information on target site interaction and signal transduction.

9.3 More in Depth Investigation on PKPD Relationships Is Needed

9.3.1 Drug Transport Processes Between Blood and CNS Target Site

In the last decades it has become clear that exchange of drugs between blood and brain (Fig. 9.3; Davson and Segal 1996; Fenstermacher et al. 1974) is to a high extent governed by active transport processes, and may therefore affect CNS target site pharmacokinetics (Greig et al. 1987; Hammarlund-Udenaes et al. 1997, 2008; Bouw et al. 2001a, b; De Lange et al. 2005; Girardin 2006; Westerhout et al. 2011), as depicted in Fig. 9.4. This indicates that for building a proper PKPD model for CNS drugs it is of importance to determine BBB transport as that will help to reveal the mechanisms that play a role in the relation between plasma concentrations and CNS drug effects, in other words to distinguish target site distribution from target interaction and signal transduction processes (Fig. 9.5).

9.3.1.1 Blood–Brain Barrier (BBB) Transport

Among the transporters present at the BBB the P-glycoprotein efflux transporter (P-gp) is the earliest discovered best characterized one. By the development of the

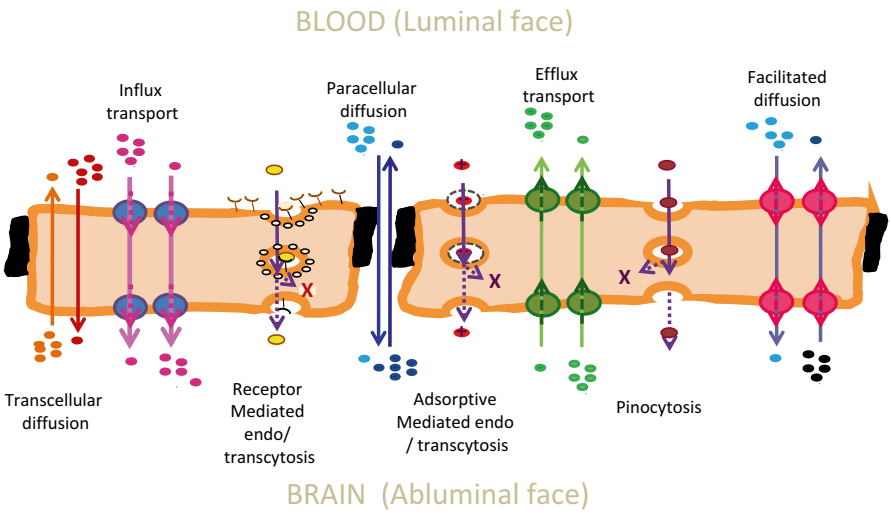

Fig. 9.3 Exchange of drugs between blood and brain may occur via different transport processes, among which multiple active transport mechanisms (Influx transport, efflux transport, pinocytosis, and transcytosis). *Arrows* indicate possible direction and *circles* indicate drugs with concentration gradient

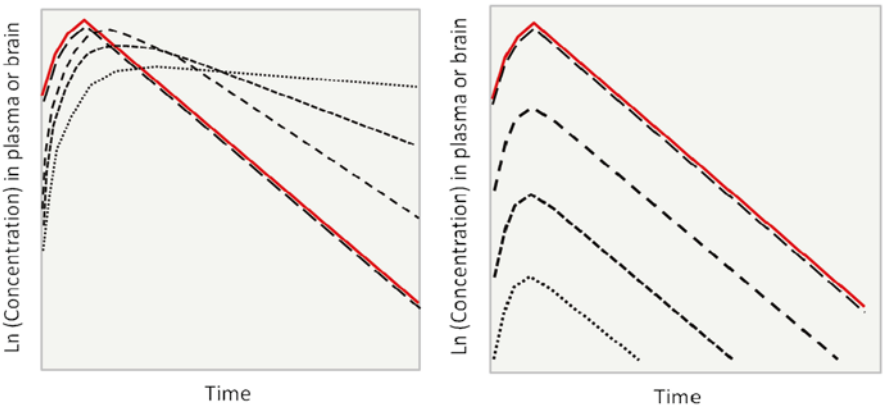

Fig. 9.4 Using simulations on a simple plasma and brain compartment model in which only unbound drug concentrations are present, one can clearly see that plasma and brain pharmacokinetics may be considerably different, depending on the (virtual) values of CL_{in} and Cl_{out}. *Left*: For $CL_{in} = Cl_{out}$, both varying from high (1.0) to low (0.1) values, with that showing greater discrepancy between plasma and brain PK. *Right*: For a fixed value for $CL_{out} = 0.5$, varying of Cl_{in} from high (0.5) to low (0.01) shows a decrease of the PK in brain in parallel to plasma PK. Adapted from (Hammarlund-Udenaes et al. 1997)

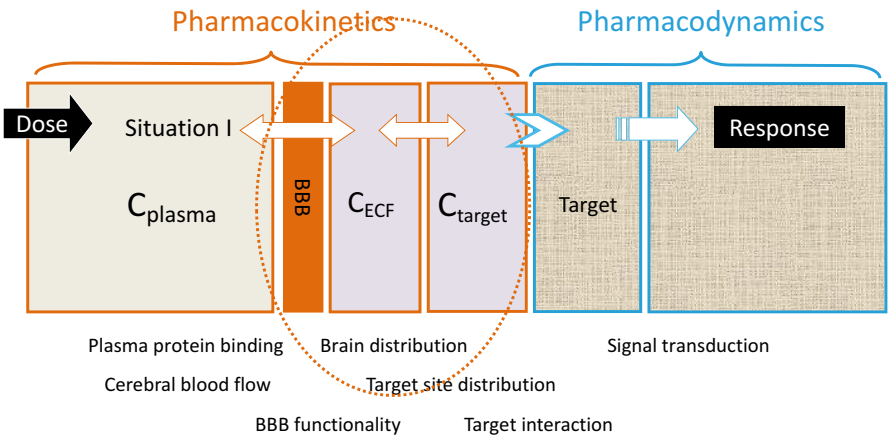

Fig. 9.5 Factors between drug dose and CNS effect. For building a proper PKPD model for CNS drugs it is of importance to determine BBB transport and target site distribution to be distinguished from target interaction and signal transduction processes

so-called P-gp knockout or mdr1a(–/–) mice, Schinkel et al. (1994) demonstrated the importance of the efflux by P-gp for brain distribution of many clinically important drugs and revolutionized research on active transport mechanisms at the level of the BBB. Later, also the multidrug-related transport proteins (MRP'S; Borst et al. 2000; Wijnholds et al. 2000) and the breast cancer-resistance protein (BCRP; Enokizono et al. 2008) were found to play a role in the brain disposition of many drugs, with partial overlap on substrates with each other.

For quantitative determination of P-gp efflux at the level of the BBB unbound concentrations at either side of the BBB are needed, i.e. unbound plasma and brain extracellular (brain ECF) concentrations. Microdialysis is widely considered to be the best technique to monitor concentrations in the brain ECF over time (Cremers et al. 2009), which combined with simultaneous serial blood sampling from the same animal is a powerful approach to study pharmacokinetic properties related to BBB transport and intracerebral distribution mechanisms (Wang and Welty 1996; De Lange et al. 1994, 1997; Hammarlund-Udenaes et al. 1997). Rate and extent of BBB transport for the unbound drug can be determined using this technique, without confounding influence of binding in plasma or brain (Hammarlund-Udenaes et al. 2008).

Furthermore, in many cases, CNS targets are membrane bound receptors facing the brain ECF, or enzymes within the brain ECF. This makes information on brain ECF concentrations highly valuable (De Lange and Danhof 2002; Watson et al. 2009; Jeffrey and Summerfield 2010; Westerhout et al. 2011). For intracellular targets, however, obtaining in vivo information is more complicated. There are no means to directly monitor brain intracellular concentration–time profiles. At best, (at equilibrium), brain intracellular concentrations can be derived by combining different experimental approaches (Fridén et al. 2007; Hammarlund-Udenaes et al. 2008).

The use of the microdialysis technique showed that even if drugs cross the BBB by passive diffusion, important differences may exist between brain ECF and plasma concentration profiles (Wong et al. 1992; Malhotra et al. 1994; De Lange et al. 1994, 1995a, b, c-critical factors; Yang et al. 1997; Wang et al. 1997; Bouw et al. 2000, 2001a, b) which are influenced upon (induced) changes in BBB properties (de Lange et al. 1995a, b). That has led to a more general theoretical framework on the rate and extent of BBB transport and influences thereof on the relationship between plasma and brain ECF concentration profiles (Hammarlund-Udenaes et al. 1997, 2008).

Also active transport processes could be determined by microdialysis, with P-gp-mediated efflux at the BBB being addressed first. De Lange et al. (1998) studied the BBB transport and P-gp functionality in mdr1a(−/−) mice and wild-type for the model P-gp substrate rhodamine-123 (R123), and Xie et al. (1999) studied the effect of P-gp functionality at the BBB for morphine in these mice, indicating that P-gp participates in regulating morphine transport across the BBB, with an approximately twofold higher extent of brain distribution in the absence of P-gp efflux transport. Likewise, for the fluoroquinolone sparfloxacin, a clear effect of P-gp functionality on BBB transport was found, with about a fivefold increase in brain ECF distribution in the absence of P-gp efflux (De Lange et al. 2000). Another example is the increase of imipramine brain distribution by inhibition of P-gp (O'Brien et al. 2012). Other active transporters at the BBB were indicated by the use of intracerebral microdialysis with probenecid as inhibitor of other active transport at the level of the BBB. Xie studied the BBB transport characteristics of morphine-3-glucuronide (M3G) in the rat and found that its extent of BBB transport increased about twofold upon coadministration of probenecid (Xie et al. 2000). The possible influence of probenecid on morphine transport across the BBB was studied by Tunblad with a ~1.3-fold increase of extent of BBB transport of morphine (Tunblad et al. 2005). As final example, microdialysis studies by Sun in rats indicated that multidrug-resistance-related proteins (MRPs) or MRP-like transport system(s) play a role in fluorescein distribution across both BBB and BCSFB, formerly considered as a marker for passive paracellular transport (Sun et al. 2001).

Actually, apart from P-gp and MRP's many more active transporters have been found at the level of the BBB (Begley 2004; de Boer et al. 2003; Kusuhara and Sugiyama 2004, 2005; Löscher and Potschka 2005; Boström et al. 2006; Uchida et al. 2011, 2012)

9.3.1.2 Intracerebral Distribution

Apart from plasma pharmacokinetics and BBB transport also other factors processes may be important determinants for actual target site concentrations. These factors may include extracellular metabolism, extra-intracellular distribution, and exchange of the drug between ECF and CSF (Cserr and Bundgaard 1984; Wong et al. 1992; Malhotra et al. 1994; Williams et al. 1995; De Lange et al. 1995c; Yang et al. 1997; Shen et al. 2004; Westerhout et al. 2012; Syvänen et al. 2012). As an example, for a

drug with low BBB permeability but fast accumulation into brain cells, the ECF concentrations will be lower than in case no intracellular accumulation takes place. Therefore, it is a prerequisite to take total brain concentrations into account, because otherwise the extent and rate of transport into the brain will be underestimated. Moreover, intra-extracellular exchange may include active transport mechanisms (Lee et al. 2001) and potential change in this transport by coadministration of transport inhibitors, intended to modify BBB transport, could as well modify extra-intracellular exchange. The effect of brain ECF to parenchymal exchange has been clearly demonstrated by the microdialysis study by Scism on valproate in rabbits. Coadministration of probenecid via the probe increased the intracellular concentrations without affecting brain ECF concentrations, indicating the presence of a probenecid-sensitive efflux transporter at the brain parenchymal cells (Scism et al. 1997).

9.3.1.3 Blood–Cerebrospinal Fluid-Barrier (BCSFB) Transport

With time, the potential contribution of the BCSFB in drug transport into and out of the brain has become clear. The BCSFB is based in the epithelial cells of the choroid plexus in which also transporters are expressed (Nishino et al. 1999; Wijnholds et al. 2001; De Lange 2004). To date there is no full consensus on the transport direction and subcellular localization of all the different transporters. As presented above, it has been well established that P-gp functions as an efflux transporter at the BBB, either by efflux enhancement or by influx hindrance (Tunblad et al. 2004b; Syvänen et al. 2006). However, the transport direction of P-gp at the level of the BCSFB is unclear. There have been some indications that P-gp functions as an influx transporter at the BCSFB. Noninvasive single-photon-emission computed tomography (SPECT) studies with 99mTc-sestamibi, a membrane-permeant radiopharmaceutical that is a substrate of both P-gp and MRP, were performed by Rao et al. (1999). It was concluded that P-gp localizes subapically at the choroid plexus epithelium, with transport into the direction of the CSF. Also Kassem et al. (2007) came to the same conclusion based on their studies on thyroxine transfer from CSF to choroid plexus and ventricular brain regions in rabbit. A recent study of the detailed kinetics of the strong P-gp substrate quinidine in different sites of the brain (brain extracellular, lateral ventricle, and cistern magna) could not confirm active influx of quinidine from blood into the ventricles (Westerhout et al. 2012). This is in line with findings of only minimal expression of P-gp at the choroid plexus cells of the lateral and fourth ventricle by Gazzin et al. (2008).

Interestingly, the BBB and the BCSFB have many similarities but also differences with regard to location and surface, but also both qualitatively and quantitatively between the plethora of active transport properties being expressed. It can be seen that this may impact on drug distribution at different sites/parts of the brain (Fig. 9.6).

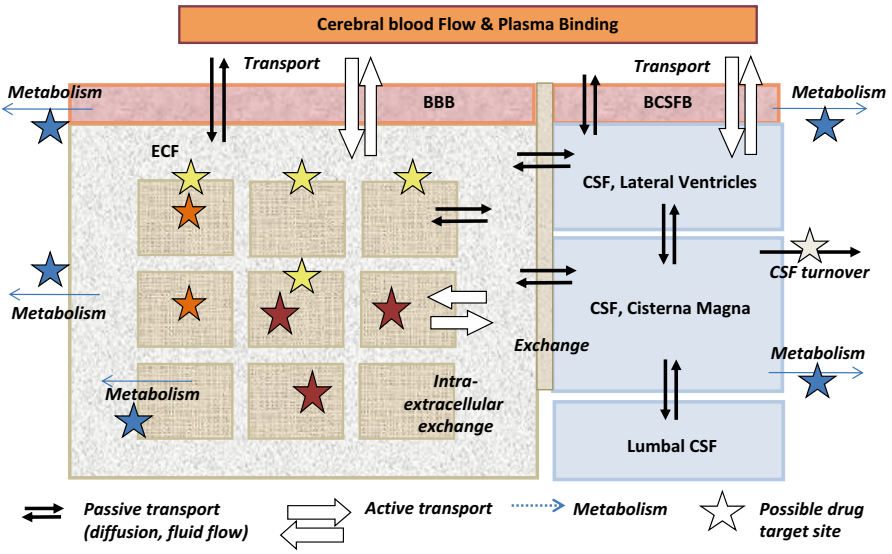

Fig. 9.6 Simplified and schematic representation of the brain, with passive and active transport processes, and metabolism, that all govern the concentration–time profile of the free drug at different locations in the CNS and therewith CNS drug effects

9.3.1.4 Pathologic Conditions

An important feature is that the BBB is under continuous physiologic control by surrounding astrocytes, pericytes, neurons, and plasma components. All together, these factors determine the delicate homeostasis of the brain environment. This dynamic regulation of the BBB indicates that different situations may result in different BBB functionalities and changes in pathological conditions (Zlokovic et al. 1989; Oztaş and Küçük 1995; Oztaş et al. 2004; Oztas et al. 2007; Mulder et al. 2001; Ederoth et al. 2004; Langford et al. 2004; De Lange et al. 2005; Bell and Zlokovic 2009; Bengtsson et al. 2009; Zlokovic 2010). BBB functionality changes may influence drug transport across the BBB and, therefore, they may have important implications for the target site kinetics.

9.3.1.5 Impact of Blood–Brain Transport and Brain Distribution on PKPD Relationships

Wang and Welty (1993) studied the concentration–time profile of gabapentin in plasma and brain ECF by microdialysis, and end-of-experiment whole brain tissue in rats, and determined the anticonvulsant effects of gabapentin by maximal electroshock. Brain ECF concentrations of gabapentin were very small (~5 %) in comparison with those in plasma, while brain tissue concentrations were equal to or greater than

those in plasma. Wang and Welty were the first to introduce the term "volume of distribution in brain" (Ve,app) as the extent of drug distribution between brain unbound to brain tissue. For gabapentin a large Ve,app was found (5.5 mL/g-brain). Furthermore, the maximal anticonvulsant effect of gabapentin lagged behind both plasma and brain ECF gabapentin concentrations indicating that the anticonvulsant effect of gabapentin is delayed relative to plasma concentrations by time-dependent events in distribution from blood to brain and even deeper into the brain.

Stain-Texier et al. (1999) showed that M6G brain ECF concentrations were ~125-fold (!) higher than the calculated intracellular levels, showing that M6G is almost exclusively distributed into brain ECF, which is highly favorable for exposure to the opioid receptors. Bouw et al. (2001a, b) further investigated the contribution of the blood–brain barrier (BBB) transport to the delay in antinociceptive effect of morphine-6-glucuronide (M6G), and studied the equilibration of M6G in vivo across the BBB with microdialysis measuring unbound concentrations. They found a significant longer half-live of M6G in brain ECF than in blood. Active efflux in BBB transport of M6G was indicated by the extent of BBB transport being far below unity (~25 %). Ve,app of M6G was ~20 % of the brain, corresponding with the brain ECF space, in line with the data of Stain-Texier et al. (1999). Furthermore, it was found that about half of the delay between blood concentrations and antinociceptive effect of M6G was attributed to slow transport across the BBB. For morphine the contribution of BBB transport of to the delay in antinociceptive effect was even larger (Bouw et al. 2000). Lötsch et al. (2002) further assessed the relationship between spinal concentrations and antinociceptive effects of M6G in rats, and showed that pharmacological inhibition of P-gp resulted in approximately twofold increase in the M6G spinal cord/plasma concentration ratio while also the antinociceptive effects of M6G were significantly enhanced.

For the antiepileptic drug oxcarbamazepine Clinckers et al. (2008) studied simultaneously the concentration–time profile of oxcarbamazepine and effects on hippocampal monoamines as pharmacodynamic markers for the anticonvulsant activity, in absence or presence of locally administered P-gp inhibitors in a rat model of epilepsy. Although systemic oxcarbazepine administration alone failed in preventing the animals from developing seizures, coadministration with verapamil (as P-gp blocker) or probenecid (as MRP's blocker) offered complete protection. Concomitantly, significant increases in extracellular hippocampal dopamine and serotonin levels were observed.

All together these studies clearly demonstrate that (active) transport processes at the BBB and brain distribution beyond have an impact on the response and should be taken into account to better understand PKPD relationships of CNS drugs.

9.3.2 Target Site Interaction and Signal Transduction

Many times brain distribution is studied without measuring associated (biomarkers of the) effects. Actually, it would be of great added value if PK and associated PD

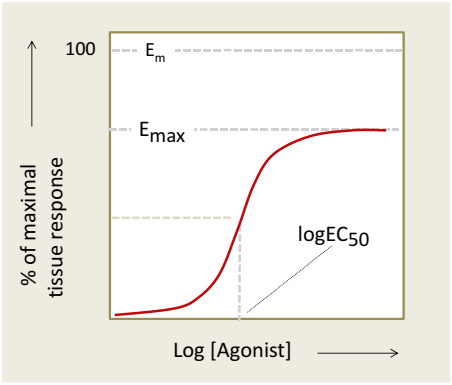

Fig. 9.7 The maximal tissue response is termed Em. It is important to note that this is not necessarily equal to maximal response, Emax, that can be produced by a particular agonist

would be obtained in a single experimental subject or at least single experimental context. So, therefore, it is of importance to learn more about factors in target activation and signal transduction, as addressed in this chapter.

Here we assume the target being a receptor. At equilibrium, the relationship between agonist concentration ([A]) and agonist-occupied receptor ([AR]) is described by (9.3):

$$[AR] = ([RT] \times [A]) / ([A] + KA) \tag{9.3}$$

in which [RT] represents total receptor concentration and KA represents the agonist-receptor equilibrium dissociation constant.

9.3.2.1 Operational Model of Agonism

Receptor theory as included in the operational model of agonism assigns mathematical rules to biological systems in order to quantify drug effects and define what biological systems can and cannot do, leading to the design of experiments that may further modify the model. For the relation between agonist-occupied receptors [AR] and receptor activation Black and Leff (1983) derived a practical or "operational" equation. If agonist binding to the target is hyperbolic and the concentration–response curve has a Hill slope of 1.0, the equation linking the concentration of "agonist-occupied receptors" to the response must also be hyperbolic. This leads to the "transducer function," as the mathematical representation of the transduction of receptor occupation into a response, in (9.4):

$$E = (Em \times [AR]) / ([AR] + KE) \tag{9.4}$$

The parameter, Em, is the maximum response possible in the system (tissue). It is important to note that this is not necessarily equal to the maximum response that a particular agonist actually produces (Fig. 9.7). The parameter KE is the concentration of [AR] that elicits half the maximal tissue response, Em. The efficacy of

an agonist is determined by both KE and the total receptor density of the tissue ([RT]). Black and Leff (1983) combined those two parameters into a ratio ([RT]/KE) and called this parameter tau (τ), the "transducer constant."

It actually indicates that two agents in a setting with equivalent sets of receptors may not produce equal degrees of effect even if both agents are given in maximally effective doses. This is due to differences in "Intrinsic activity" (or efficacy) that can be defined as the property of a drug that determines the amount of biological effect produced per unit of drug–receptor complex formed. Thus, the drug that produces the greater maximum effect has the greater intrinsic activity. It is important to note that intrinsic activity is not the same as "potency" and may be completely independent of it.

Activation of the receptor should be "transduced" to elicit the response. Combining the hyperbolic occupancy equation with the hyperbolic transducer function yields an explicit equation (9.5) describing the effect at any concentration of agonist:

$$E = (\mathrm{Em} \times \tau^n \times [\mathrm{A}]^n) / (\mathrm{KA} + [\mathrm{A}]^n) + \tau^n \times [\mathrm{A}]^n) \tag{9.5}$$

in which E = effect, Em = maximum response achievable in system, KA = agonist dissociation equilibrium constant, and n = slope index of the receptor occupancy effect function. It actually describes a 3-dimensional interrelationship as can be seen in Fig. 9.8.

Intrinsic activity—like affinity—depends on the characteristics of both the drug and the receptor, but intrinsic activity and affinity apparently can vary independently. This means that the EC_{50} does not equal KA but rather KA/(1 + τ). As an example, having a strong agonist that reaches a 50 % response upon binding fewer than half the available receptors, its EC_{50} will be much less than KA.

Receptor affinity and intrinsic activity are "drug-specific" properties and can be estimated in in vitro bioassays, with the maximal response of the drug being determined, not from single dose–response curves but from using pairs of dose–response curves (usually treatment and control) for a particular tissue, here CNS, sharing some parameters.

Subsequent simultaneous analysis of the resulting different PKPD relationships must be performed to build a mechanism-based model that explicitly distinguishes between the drug-specific and the system-specific properties to allow prediction of the intrinsic activity and potency of another drug for a particular pharmacological effect or response. These different PKPD relationships may be obtained in different ways.

- Studying one agonist under control conditions and conditions in which the number of receptors available for binding is reduced (Furchgott 1966; Garrido et al. 2000).
- Studying series of chemically similar drugs with varying degrees of agonism for the specific receptor and simultaneous analysis of the PKPD relationships (Cox et al. 1998; Groenendaal et al. 2008).

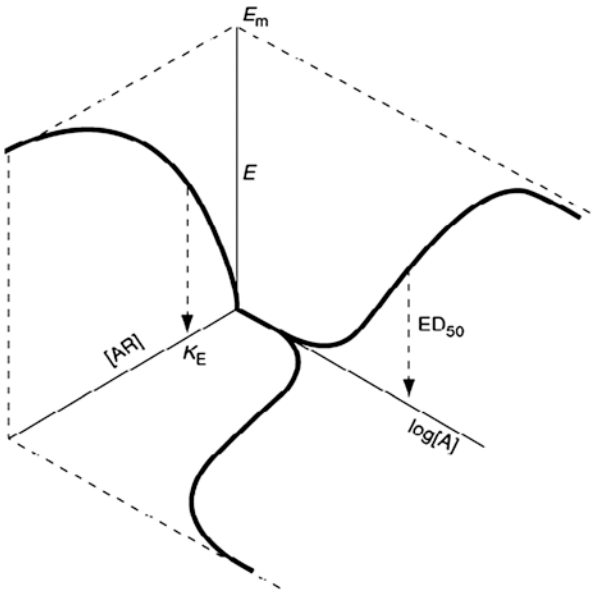

Fig. 9.8 A certain agonist concentration [A] leads to a certain occupancy of the receptor (concentration of the receptor–agonist complex [AR]). Then, receptor occupancy should be "transduced" to elicit the response *E*. The relation between agonist concentration, receptor occupancy, and elicited effect can be described by a 3-dimensional interrelationship. Em = maximum response achievable in system, K_A = agonist dissociation equilibrium constant, n = slope index of the occupancy effect function, R_0 = total number of available receptors, Ke = concentration occupied receptors [AR] that produces 50 % of maximal effect, τ = transducer constant or efficacy parameter ($=R_0$/Ke)

The operational model of agonism has been successfully applied in numerous in vitro studies and later also in mechanisms-based PKPD analysis of in vivo drug effects (Kenakin 2004; Danhof et al. 2005, 2007). For adenosine A_1 receptor agonists a good correlation was observed between the in vivo pK_A and the in vitro pK_i and also between the in vivo efficacy parameter (τ) and the in vitro GTP shift (as measure for intrinsic activity), thus enabling the prediction of in vivo concentration–effect relationships (Van der Graaf and Danhof 1997a, b; Van der Graaf et al. 1999). In addition, excellent in vitro–in vivo correlations have also been observed for benzodiazepines (Tuk et al. 1999, 2002; Visser et al. 2003) and neuroactive steroids (Visser et al. 2002).

Taken together, incorporation of receptor theory into PKPD models on in vivo concentration–effect relationships could provide information on:

- Tissue selectivity of drug effects (Van Schaick et al. 1998)
- Interspecies differences in concentration–effect relationships
- Tolerance and sensitization (Cleton et al. 2000)
- Intra- and interindividual variability

Of course, life is not that simple that in all cases the incorporation of receptor theory in mechanism-based PKPD models was successful. For the opioids alfentanil, fentanyl, and sufentanil, it was shown by simulation that the concentration–effect relationships could be explained by the operational model of agonism under the assumption of a considerable receptor reserve (Cox et al. 1998), while also, a shift in the concentration–effect relationship of alfentanil was observed following pretreatment with the irreversible μ-opioid receptor antagonist β-funaltrexamine, which was consistent with the 40–60 % reduction in the available number of specific μ-opioid binding sites as shown in an in vitro receptor bioassay (Garrido et al. 2000). However, a proper incorporation of the receptor theory in a mechanism-based PKPD model of the opioid receptor agonists could not been accomplished.

Also, for the 5-HT_{1A} receptor agonists, a rather poor correlation was found between the in vivo pK_A and the in vitro pK_i, despite a good correlation between in vivo and the in vitro GTP shift (Zuideveld et al. 2007). Failure of successful inclusion of the receptor theory in the PKPD models of the opioid and 5-HT_{1A} agonists could be due to complexities at the level of blood–brain transport and intracerebral distribution which was not addressed in these studies, as estimates of hypothetical target site concentrations were made using the link model.

When solving shortcomings in knowledge on target site distribution of drugs, the principles of the operational model will provide the basis for future developments in drug development by classifying drugs and predicting their mechanism of action in pharmacology (Kenakin and Christopoulos 2011)

9.3.3 Mechanism-Based PKPD Modeling Including Complex Target Site Distribution

As indicated above, the mechanism-based PKPD analysis of the EEG effects of the opioids alfentanil, fentanyl, and sufentanil, using the operational model of agonism (Cox et al. 1998) did not predict in vivo efficacies of these opioids. Moreover, alfentanil, fentanyl, and sufentanil all appeared to behave as high-efficacy (full) agonists. However, for the development of a mechanism-based PKPD model for the central effects of opioids, additional PKPD data on low-efficacy (partial) agonists were needed, as well as information on the target site equilibration. Therefore, also in vivo PKPD studies on the EEG effects of nalbuphine, butorphanol, and morphine were included to contribute to further data analysis (Groenendaal et al. 2007a, b, 2008). In addition, in vitro studies on passive permeability rates of membrane transport and P-gp interaction of all opioids were performed using cell systems comprised of epithelial cells transfected with either the human MDR1 or the rodent MDR1a gene. The results of these investigations confirmed that morphine is a P-gp substrate and that its transport could be inhibited by the P-gp inhibitor GF120918 (elacridar). Alfentanil, fentanyl, and sufentanil were found to be inhibitors of P-gp, but could not be identified as substrates for this efflux transporter. No interaction with P-gp was observed for butorphanol. For alfentanil, fentanyl, sufentanil, and

butorphanol, the passive permeability across the monolayers was very high, whereas for morphine and nalbuphine the passive permeability was low. For morphine more information was needed on its BBB transport in conjunction to its EEG effect. To quantitatively determine the influence of BBB transport on the PKPD relationship of morphine, including P-gp-mediated efflux, the combined EEG/microdialysis technique was developed and used. For morphine the functionality of transporters at the BBB was found to be a major determinant of the time-course of brain ECF concentrations as well as on the EEG effect though brain ECF concentrations could not be used to directly predict EEG effects. Still, the data of all opioids could not be condensed into one mechanism-based model on the central effects of opioids using the operational model of agonism. So, this indicates that lots of insights on PKPD relationships of opioids have been gained, but remaining parts between brain unbound morphine concentration and EEG effect remaining to be determined.

9.4 Current Status

9.4.1 Quantitative Translational Systems Approach in PKPD Modeling

Since biological systems operate at different set points in the body under different conditions, the ability to predict drug effects under a variety of circumstances is important (Ingss 1990; Van der Graaf and Danhof 1997a, b; Kenakin 2008; Gabrielsson and Green 2009; Van Steeg et al. 2007, 2009, 2010). Moreover, as biological system mechanisms are *concurrently working*, there is a need for *integrated* in vivo experiments, e.g., that the experiments *address multiple mechanisms* (/biomarkers) *at the same time*. Using animals, we can learn more on the interrelationship of the different pharmacokinetic processes, by performing integrative studies in which variables are systematically varied (e.g., inhibition of an efflux transporter or induction of pathological state, or using a different drug or route of administration). By these are so-called integrative cross-compare designed studies (Westerhout et al. 2011, 2012; De Lange 2013a, b) we can dissect contributions of individual mechanisms in animals using mechanism-based mathematical modeling. This provides the links to the human situation based on the parsimony of the biological system.

9.4.2 Classification of Biomarkers

In translational models, specific expressions are needed that quantitatively characterize processes on the causal path between drug administration and effect. These include target site distribution, target binding and activation, transduction, PD interactions, and homeostatic feedback mechanisms (Mandema et al. 1991; Cox et al. 1998;

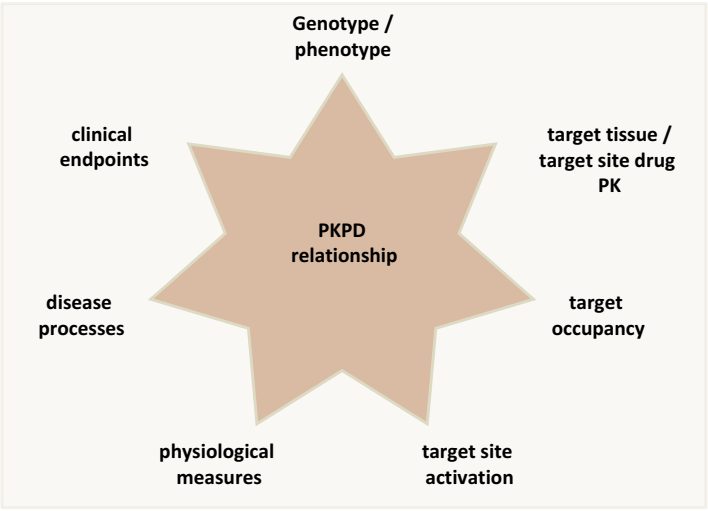

Fig. 9.9 In translational models, specific expressions are needed that quantitatively characterize processes on the causal path between drug administration and effect. These can be characterized by different types of biomarkers according to the presented classification

Van der Graaf and Danhof 1997a, b; van Steeg et al. 2009). Ultimately also the effects on and of disease processes and disease progression have to be considered. These can be characterized by biomarkers according to the following classification of biomarkers (Danhof et al. 2005; Fig. 9.9):

- Type 0 biomarkers refer to the *genotype or phenotype* as determinant of the drug response, that influences target site exposure or response due to variation in the expression of e.g., enzymes or receptors. They are commonly used as covariates in PKPD models.
- Type 1 biomarkers refer to *drug concentrations in general and at the target site in particular*. As previously pointed out, quantitative biomarkers that represent the target site distribution of drugs and metabolites for compounds that act in the CNS are difficult to obtain in man, but readily available in vivo in animals (De Lange et al. 2005).
- Type 2 biomarkers refer to the *degree of target occupancy*. In theory, effects may occur at different degrees of target occupancy and may be species dependent. The relationship between target occupancy and effect is therefore important for the understanding of inter- and intraindividual variability. Information on target occupancy is available by bioassays in vitro and can also be noninvasively measured in humans by positron emission tomography (Kapur et al. 2000; Kvernmo et al. 2006, 2008).
- Type 3 biomarkers refer to *quantification of the target site activation*. By means of in vitro bioassays information can be obtained on receptor activation in animal and man. Techniques like electroencephalograms (EEG) (Kropf and Kuschinsky

1993; Vorobyov et al. 2003) and functional-magnetic resonance imaging (fMRI) can obtain specific receptor activation in preclinical and clinical in vivo setting.
- Type 4 biomarkers refer to *physiological measures* in the integral biological system, which are often controlled by homeostatic feedback mechanisms (Bagli et al. 1999). Such measures can for example be on pituitary hormones that play a very important role in communication between CNS and periphery (Freeman et al. 2000).
- Type 5 biomarkers characterize *disease processes* and are particularly useful in clinical settings. (However, an important question is whether type 5 biomarkers can be identified in animal models of disease; Holford and Nutt 2008).
- Type 6 biomarkers refer to *clinical endpoints*, such as occurrence of a disease, symptom, sign, or laboratory abnormality that links to target outcomes (Holford and Nutt 2008).

Obtaining combined information on a number of biomarker types (preferable in parallel, within a single biological system) will allows the development of better models, with increased accuracy and predictability. The better we will be able to develop predictive models in preclinical studies, the more the number of often extremely costly clinical studies can be reduced.

The focus should therefore be on the design of quantitative in vivo animal studies such that translational pharmacology approaches can be applied (Boxenbaum 1982; Danhof et al. 2008; Fridén et al. 2009). Especially, to that end, in refined animal models the biomarkers of the effect that can be measured in both animals and human will be useful.

9.4.3 Development of a Translational PKPD Model on D2 Receptor Inhibition

Investigations on drugs that interact with the dopaminergic system in the brain are of interest as many diseases, including Parkinson's disease, schizophrenia, and depression, are related to dysfunctions in the dopaminergic system. Since dopamine is an important neurotransmitter in hypothalamic control, pituitary hormones have high potential as type 4 biomarkers for dopaminergic activity in the brain (Freeman et al. 2000), as these are secreted into blood and blood levels can be assessed in both animal and human. One of these hormones is prolactin. Prolactin is synthesized in the lactotrophs of the pituitary, and its release into plasma will occur upon dopaminergic inhibition (specifically the D2 receptor; Fig. 9.10).

Remoxipride is a weak, but selective, dopamine-D2 receptor antagonist (Farde and Von Bahr 1990; Köhler 1990) and was prescribed as an atypical antipsychotic (Roxiam®) at the end of the 1980s. Due to a few cases of aplastic anemia, the drug was withdrawn from the market (Philpott 1993). The data that have been obtained before that time in clinical setting can still be used and extensive clinical PKPD datasets are available for remoxipride and prolactin plasma data (Movin-Osswald

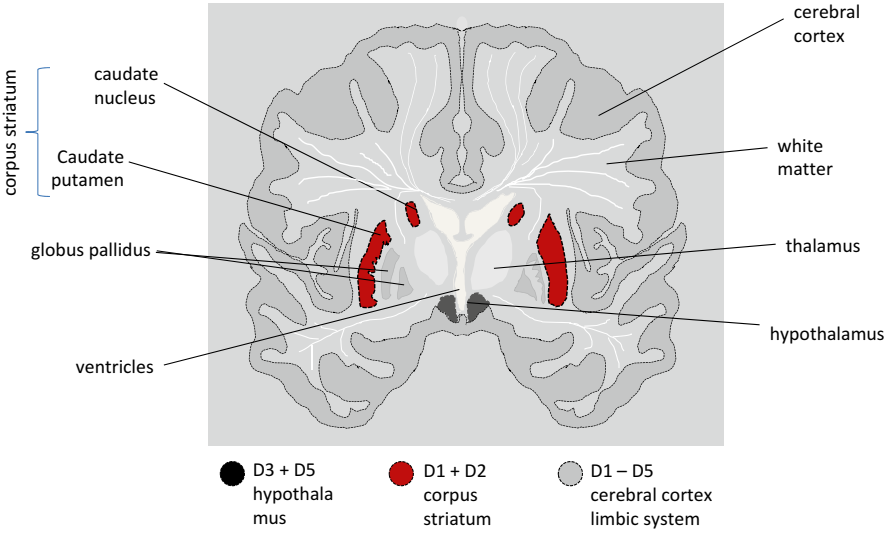

Fig. 9.10 Cartoon of transversal cross section of human brain with dopaminergic areas dopaminergic receptor-type distributions

et al. 1995). In recent studies, remoxipride was used as a paradigm compound in rats, finally enabling investigation of animal to human extrapolation of dopaminergic drug effects (Stevens et al. 2012) and the development of the translational model, first for intravenous to intranasal administration, then from rat to human, is presented below.

9.4.3.1 Development of the PKPD Model Following Intravenous Administration in Rats

Following intravenous administration of remoxipride as a model drug for dopaminergic D2 receptor inhibition, using the levels of the pituitary hormone prolactin in plasma as a pharmacodynamic readout (Fitzgerald and Dinan 2008; Stevens et al. 2011, 2012). Remoxipride pharmacokinetics was determined in plasma, and in brain ECF by microdialysis, as the latter was anticipated to allow better prediction of pharmacodynamic effects in a PKPD model. After assessment of baseline variation in prolactin plasma concentrations, the prolactin response (increase in plasma concentrations) upon intravenous administration of three different single doses of remoxipride was obtained. Also, the prolactine response was measured following double low dosing of remoxipride with different time intervals to get information on the synthesis of prolactin in the lactotrophs of the pituitary similar to the data obtained in human (Movin-Osswald and Hammarlund-Udenaes 1995; Fig. 9.11)

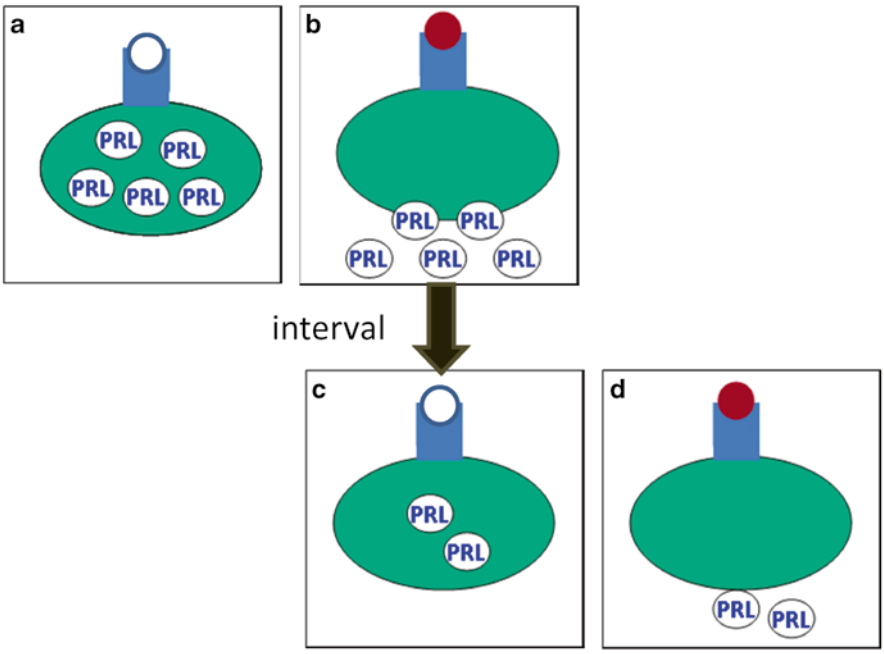

Fig. 9.11 Information on the synthesis rate of prolactin in the lactotrophs can be obtained by the double dosing approach (Movin-Osswald and Hammarlund-Udenaes 1995). After the first dose of the D2 antagonist the lactotroph is depleted from prolactin. The time to the second dose (interval) will determine how much prolactin has been newly synthesized and can be released by the D2 antagonist at that time. (**a**) Fully filled lactotroph with dopaminergic inhibition (**b**) release of prolactin content from the lactotroph upon antagonizing dopaminergic inhibition by the D2 antagonist (**c**) partly filled lactotroph after some time and (**d**) release of the newly synthesized prolactin by the second dose of the D2 antagonist

The PKPD model was developed in multiple steps, comparing different structural models and model quality testing. The final mechanistic PKPD model consisted of a:

- Pharmacokinetic model for plasma and brain unbound remoxipride concentrations.
- Pool model for prolactin synthesis and storage and its release into- and elimination from plasma.
- Positive feedback of prolactin plasma concentrations on prolactin synthesis.
- (Not unbound plasma but specifically) the unbound brain concentrations of remoxipride for the inhibition of the D2 receptor, and resulting stimulation of prolactin release into plasma.

It is of interest that plasma prolactin concentrations had a positive feedback on prolactin synthesis in the lactotrophs and that brain unbound remoxipride concentrations were indistinguishable from target site concentrations to drive the release of prolactin into plasma.

Although the strong positive feedback by plasma prolactin suggested in this study is not consistent with a few previous findings (Movin-Osswald et al. 1995; Friberg et al. 2008; Ma et al. 2010), other literature seems to support our current observation of a positive feedback (Freeman et al. 2000; Phelps 1986; Ben Jonathan et al. 2008). Since prolactin receptors are present in the cell membranes of lactotrophs and their activation can result in synthesis of prolactin, this demonstrates that lactotrophs can perceive and respond to prolactin concentrations in a paracrine manner by which release of prolactin by lactotrophs (depletion) increases the prolactin synthesis to "refill" the lactotrophs.

9.4.3.2 Extension of the PKPD Model for Intranasal Administration in Rats

Next to rapid systemic uptake of compounds, intranasal administration may provide a direct way for delivery of therapeutics into the CNS (Hanson and Frey et al. 2008; Baker and Spencer 1986; Bagger and Bechgaard 2004; Constantino et al. 2007). If direct transport into the brain would be possible, intranasal administration could enhance the CNS target site bioavailability and therewith a more selective effect of CNS drugs (Graff and Pollack 2004; Illum 2000, 2004; Jansson and Bjork 2002). Intranasal administration could be a promising alternative for dopaminergic drugs because oral administration is often limited due to active first-pass clearance by the liver while also frequently restricted BBB transport of dopaminergic drugs has been reported (Dhuria et al. 2009).

Using a previously reported minimum stress, freely moving rat model for intranasal drug administration (Stevens et al. 2009), plasma- and brain ECF samples were obtained over time, after giving remoxipride intranasally at the same dosages as in the intravenous study, and measuring the resulting prolactine levels in plasma within the same rats.

The remoxipride PKPD model as developed on intravenous data was extended by adding an absorption compartment to allow simultaneous fitting of the intravenous and intranasal datasets. However, for proper description of the intranasal data by the model, a second absorption compartment with transport of remoxipride direct from nose to brain had to be included. The visual predictive check of the final model showed good prediction of the plasma- and brain ECF observations after intravenous and intranasal administration (Stevens et al. 2011; Fig. 9.12). Thus, a multicompartment pharmacokinetic model with two distinct absorption compartments, nose-to-systemic and direct nose-to-brain was found to best describe the observed pharmacokinetic data. Absorption was described in terms of bioavailability and rate. Total bioavailability following intranasal administration was ~90 % of which ~75 % was attributed to direct nose-to brain transport. The advanced mathematical model and appropriate data allowed further for having information not only on the extent of brain distribution but also on the rates of transport. The direct nose-to-brain absorption did not turn out to be a rapid route to the brain. The rate was slow, explaining prolonged brain ECF exposure after intranasal compared to intravenous administration. Thus, by the experimental combined with mathematical

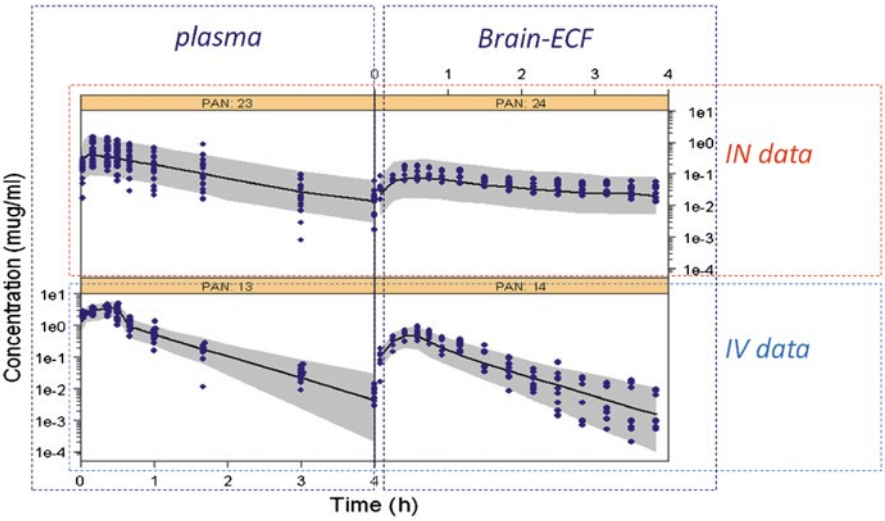

Fig. 9.12 Visual predictive check of the PK model for plasma and brainECF data (*dots*) (95 % percentiles inclusion as *gray* areas) for remoxipride following intravenous (IV) and intranasal (IN) administration

modeling approach explicit separation and quantitation of systemic- and direct nose-to-brain transport after intranasal administration of remoxipride in the rat could be made.

An important finding was that brain ECF (brain unbound) concentrations could directly be linked to the observed effect on prolactin plasma concentrations following intranasal administration, while the model did not converge with using plasma concentration data of remoxipride. It shows the importance of having kinetic information of unbound concentrations as close to the receptor as possible, as was indicated by study of Watson et al. (2009), in which brain unbound concentrations were found to be a better predictor of dopamine D2 receptor occupancy than total brain concentration, CSF concentration, or blood unbound concentration.

9.4.3.3 Use of the Structural Preclinical PKPD Model to Finally Predict Human PKPD

When drug-specific and biological system-specific parameters are quantified in a PKPD model it provides the opportunity to scale the system-specific parameters from animal to human to translate PKPD relationship to man. Allometric scaling of drug pharmacokinetic properties and biological system-specific parameters has been used in translational investigations, with reasonable degree of success, to predict drug effects in humans (Yassen et al. 2007; Zuideveld et al. 2007). But, pharmacodynamic properties are more difficult to scale compared to pharmacokinetic properties, since pharmacodynamic parameters are often not related to bodyweight (e.g., receptor

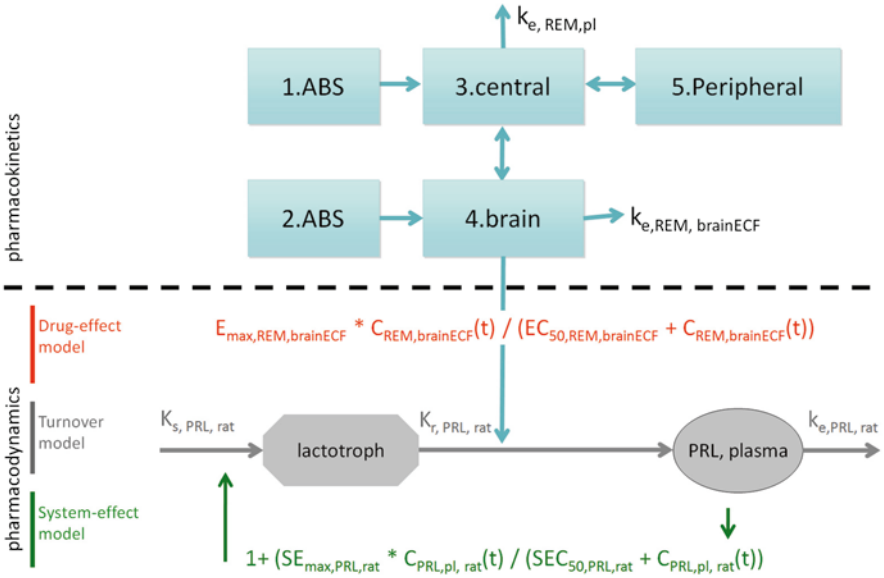

Fig. 9.13 Preclinical-derived translational PKPD model for remoxipride and its effect on plasma concentrations of prolactin

occupancy). Such information may be available by in vitro bioassays. For many drugs and endogenous compounds, clinical information is often readily available, like for target binding characteristics of dopaminergic compounds (Kvernmo et al. 2006, 2008) and on prolactin in animals and human (Ben Jonathan et al. 2008). BBB transport of remoxipride in humans was assumed to be comparable to that in rat (in essence based on passive diffusion). The preclinical translational human PKPD model successfully predicted the system prolactin response in humans, indicating that positive feedback on prolactin synthesis and allometric scaling thereof could be a new feature in describing complex homeostatic mechanisms (Fig. 9.13).

9.5 Future Directions

We have to accept that CNS drug delivery and CNS disease research is complex, and we need to (continue to) put efforts in performing the type of investigations that provide data that we learn from in having a CNS drug "at the right place, at the right time, and at the right concentration."

Since biological systems operate at different set points in the body under different conditions, the ability to predict drug effects under a variety of circumstances is important and more advanced experimental designs are needed to decipher and learn more on the factors that govern plasma pharmacokinetics, BBB transport intrabrain distribution, as well as their interrelationships and consequences for CNS

effects in the different settings (Garrido et al. 2000; Grime and Riley 2006; Gabrielsson and Green 2009; Danhof et al. 2007, 2008; Ploeger et al. 2009; Kenakin and Christopoulos 2011). Therefore, individual processes on the causal path between drug dose and CNS effect should be systematically varied (e.g., inhibition of an efflux transporter, or induction of pathological state, and so on and so forth) to study the impact on the PKPD relationships are measured in a time-dependent manner. Therefore, in the design of future experiments we always need to consider the following.

- Combining different levels of biomarkers (see all types Sect. 9.4.2) in single subjects as outcomes are context dependent (most important!).
- Measuring unbound drug concentrations as it is the unbound drug that is able to interact with its target and therefore drives the effect.
- Involving time dependencies.
- Understanding the mechanisms involved in uptake into and efflux from the brain, but also plasma pharmacokinetics and intrabrain distribution and their mutual interrelationships.
- Including drug receptor theory as a tool for quantifying the activity of drugs in a system-independent manner.
- Identifying the heterogeneity in rate and extent of mechanisms on the causal chain between dose and CNS effects (including challenges/disease conditions).
- Using advanced mathematical modeling to integrate all these data to build preclinical mathematical models (generalized frameworks).
- Using human data to test validity of the models after tuning this to human conditions.
- Improving interspecies extrapolation of pharmacokinetics, by using a more physiologically based pharmacokinetic modeling approach.

Such approach may be referred to as the "Mastermind Research Approach," in analogy of the game (Fig. 9.14, De Lange 2013a). It makes that the predictive value of the models on PKPD relationships of CNS drugs will increase significantly and the outlook is therefore that clinical studies would suffice with fewer individuals and less samples per individual, for proof of concept in man.

9.6 Challenges

Performing integrative studies is not without big challenges.

- From the perspective of the subject, it is of course impossible to integrate research at all biomarker levels within a single subject, but a combination of a subset of major aspects will do.
- From a technical perspective, there are limitations to what level subjects can be instrumented, and development, improvement, and refinement of techniques remain important.
- When it comes down to challenges applied to the subject, there are limitations, for humans much more than for animals. Integrity of the physiology of subjects remains to be a high priority. Then, intentionally inducing a disease state can be performed only in animals, and animal disease may at best partly reflect that in human.

Fig. 9.14 The approach of using integrative cross-compared designed studies, literature data, and advanced mathematical modeling to dissect contributions of rate and extent of individual mechanisms in dose–CNS effect relationships in different conditions, as the basis for translation between conditions. This approach may be shortly abbreviated as the "Mastermind Research Approach," in analogy of the strategic approach that is needed to "decipher the code" in the game called "Mastermind." This approach makes that the predictive value of the models on PKPD relationships of CNS drugs will increase significantly

- With increasing complexity of experiments, the chance of failures will increase. Thus, from the people perspective, performing advanced surgeries, complex experimentation, and the use of apparatus needed for monitoring techniques, advanced mathematical data analysis, and model development can be performed only by well-trained and skilled persons.
- In an overall perspective, Good Academic (/Clinical) Research Practice in terms of preparation of experiments, administration of files, data storage and use in building mathematical models, and last but not least communication, should be effectuated.

9.7 Conclusions

For a proper CNS effect the drug should have the ability to access the CNS "at the right place, at the right time, and at the right concentration." To that end a number of key issues need to be considered:

- To develop treatments with improved safety and efficacy, one of the scientific challenges is to understand the biological mechanisms underlying the PKPD relationships of CNS drugs. Knowledge on an only one individual processes is worthless and its role should be investigated in multiple contexts.

- PKPD modeling is the golden standard to investigate such complex mechanisms. Often, these models include plasma drug concentration–effect relationships. However, when the target site is in a tissue, a discrepancy between unbound plasma concentrations and unbound tissue concentrations should be considered.
- Investigations on the kinetics of the unbound drug are indispensable. These are the concentrations seen by the target and a more mechanistic approach should be aimed at understanding the factors that control unbound drug concentrations at the target site.
- To have information on what concentrations can actually represent target site concentrations, measurement of concomitant effects of the drug is needed.
- Advanced mathematical modeling techniques are needed to reveal complex relationships of body processes and interactions of the body and the drug, to be ultimately settled down in mathematical models.

9.8 Points for Discussion

- Body is a total system in which processes are interdependent. Studies need to be designed such that mutual dependence gets clear. How can studies be best designed to have the most valuable data collected?
- What concentrations in human can be assessed and used best to predict CNS target site concentrations?
- Can we address sources of variability between drug responses in human populations, aiming at personalized CNS medicine?

References

Bagger M, Bechgaard E (2004) A microdialysis model to examine nasal drug delivery and olfactory absorption in rats using lidocaine hydrochloride as a model drug. Int J Pharm 269:311–322

Bagli M, Suverkrup R, Quadflieg R, Hoflich G, Kasper S, Moller HJ, Langer M, Barlage U, Rao ML (1999) Pharmacokinetic-pharmacodynamic modeling of tolerance to the prolactin-secreting effect of chlorprothixene after different modes of drug administration. J Pharmacol Exp Ther 291:547–554

Baker H, Spencer RF (1986) Transneuronal transport of peroxidase-conjugated wheat germ agglutinin (WGA-HRP) from the olfactory epithelium to the brain of the adult rat. Exp Brain Res 63(3):461–473

Begley DJ (2004) ABC transporters and the blood-brain barrier. Curr Pharm Des 10:1295–1312

Bell RD, Zlokovic BV (2009) Neurovascular mechanisms and blood-brain barrier disorder in Alzheimer's disease. Acta Neuropathol 118(1):103–113

Ben Jonathan N, LaPensee CR, LaPensee EW (2008) What can we learn from rodents about prolactin in humans? Endocr Rev 29:1–41

Bengtsson J, Ederoth P, Ley D, Hansson S, Amer-Wåhlin I, Hellström-Westas L, Marsál K, Nordström CH, Hammarlund-Udenaes M (2009) The influence of age on the distribution of morphine and morphine-3-glucuronide across the blood-brain barrier in sheep. Br J Pharmacol 157(6):1085–1096

Betz AL, Goldstein GW (1986) Specialized properties and solute transport in brain capillaries. Annu Rev Physiol 48:241–250

Black J, Leff P (1983) Operational model of pharmacological agonism. Proc R Soc Lond B 220:141–162

Bonati M, Latini R, Tognini G, Young JF, Garattini S (1984) Interspecies comparison of in vivo caffeine pharmacokinetics in man, monkey, rabbit, rat and mouse. Drug Metab Rev 15: 1355–1383

Borst P, Zelcer N, van Helvoort A (2000) ABC transporters in lipid transport. Biochim Biophys Acta 1486(1):128–144

Borst P, Elferink RO (2002) Mammalian ABC transporters in health and disease. Annu Rev Biochem 71:537–592

Boström E, Simonsson US, Hammarlund-Udenaes M (2006) In vivo blood-brain barrier transport of oxycodone in the rat: indications for active influx and implications for PK/PD. Drug Metab Dispos 34(9):1624–1631

Bouw MR, Ederoth P, Lundberg J, Ungerstedt U, Nordstrom CH, Hammarlund-Udenaes M (2001a) Increased blood-brain barrier permeability of morphine in a patient with severe brain lesions as determined by microdialysis. Acta Anesthesiol Scand 45:390–392

Bouw MR, Gardmark M, Hammarlund-Udenaes M (2000) PK-PD modelling of morphine transport across the blood-brain barrier as a cause of the antinociceptive effect delay in rats—a microdialysis study. Pharm Res 17:1220–1227

Bouw MR, Xie R, Tunblad K, Hammarlund-Udenaes M (2001b) Blood-brain barrier transport and brain distribution of morphine-6-glucuronide in relation to the antinociceptive effect in rats—pharmacokinetic/pharmacodynamic modelling. Br J Pharmacol 134:1796–1804

Boxenbaum H (1982) Interspecies scaling, allometry, physiological time, and the ground plan of pharmacokinetics. J Pharmacokinet Biopharm 10:201–227

Breimer DD, Danhof M (1997a) Prediction of the time course of drug effects in vivo in health and disease (intensity and duration). Clin Pharmacokinet 32:259–267

Breimer DD, Danhof M (1997b) Relevance of the application of pharmacokinetic-pharmacodynamic modelling concepts in drug development. The 'wooden shoe' paradigm. Clin Pharmacokinet 32:259–267

Bruce JN, Oldfield EH (1988) Method for sequential sampling of cerebrospinal fluid in humans. Neurosurgery 23:788–790

Campbell DB (1990) The use of kinetic-dynamic interactions in the evaluation of drugs. Psychopharmacology (Berl) 100(4):433–450

Cleton A, Odman J, Van der Graaf PH, Ghijsen W, Voskuyl R, Danhof M (2000) Mechanism-based modeling of functional adaptation upon chronic treatment with midazolam. Pharm Res 17:321–327

Clinckers R, Smolders I, Meurs A, Ebinger G, Michotte Y (2005) Quantitative in vivo microdialysis study on the influence of multidrug transporters on the blood-brain barrier passage of oxcarbazepine: concomitant use of hippocampal monoamines as pharmacodynamic markers for the anticonvulsant activity. J Pharmacol Exp Ther 14(2):725–731

Clinckers R, Smolders I, Michotte Y, Ebinger G, Danhof M, Voskuyl RA, Della Pasqua O (2008) Impact of efflux transporters and of seizures on the pharmacokinetics of oxcarbazepine metabolite in the rat brain. Br J Pharmacol 155(7):1127–1138

Costantino HR, Illum L, Brandt G, Johnson PH and Quay SC (2007) Intranasal delivery: physicochemical and therapeutic aspects. Int J Pharm 337:1–24

Cox EH, Kerbusch T, van der Graaf PH, Danhof M (1998) Pharmacokinetic-pharmacodynamic modeling of the electroencephalogram effect of synthetic opioids in the rat. Correlation with binding at the μ-opioid receptor. J Pharmacol Exp Ther 284:1095–1103

Cremers TI, de Vries MG, Huinink KD, Loon JP, Hart MV, Ebert B, Westerink BH, De Lange EC (2009) Quantitative microdialysis using modified ultraslow microdialysis: direct rapid and reliable determination of free brain concentrations with the MetaQuant technique. J Neurosci Methods 178(2):249–254

Cserr HF, Bundgaard M (1984) Blood-brain interfaces in vertebrates: a comparative approach. Am J Physiol 246:R277–R288

Danhof M, Alvan G, Dahl SG, Kuhlmann J, Paintaud G (2005) Mechanism-based pharmacokinetic-pharmacodynamic modeling-a new classification of biomarkers. Pharm Res 22:1432–1437

Danhof M, de Jongh J, de Lange ECM, Della Pasqua OE, Ploeger BA, Voskuyl RA (2007) Mechanism-based pharmacokinetic-pharmacodynamic modeling: biophase distribution, receptor theory, and dynamical systems analysis. Annu Rev Pharmacol Toxicol 47:357–400

Danhof M, de Lange EC, Della Pasqua OE, Ploeger BA, Voskuyl RA (2008) Mechanism-based pharmacokinetic-pharmacodynamic (PKPD) modeling in translational drug research. Trends Pharmacol Sci 29:186–191

Danhof M, Levy G (1984) Kinetics of drug action in disease states. I. Effect of infusion rate on phenobarbital concentrations in serum, brain and cerebrospinal fluid of normal rats at onset of loss of righting reflex. J Pharmacol Exp Ther 229(1):44–50

Danhof M, Mandema JW, Hoogerkamp A, Mathot RA (1993) Pharmacokinetic-pharmacodynamic modeling in pre-clinical investigations: principles and perspectives. Eur J Drug Metab Pharmacokinet 18(1):41–47

Davson H, Segal MB (1996) Physiology of the CSF and blood-brain barriers. CRC, Boca Raton, FL

De Boer AG, van der Sandt I, Gaillard PJ (2003) The role of drug transporters at the blood-brain barrier. Annu Rev Pharmacol Toxicol 43:629–656

De Lange EC, Danhof M (2002) Considerations in the use of cerebrospinal fluid pharmacokinetics to predict brain target concentrations in the clinical setting: implications of the barriers between blood and brain. Clin Pharmacokinet 41:691–703

De Lange EC, Danhof M, de Boer AG, Breimer DD (1994) Critical factors of intracerebral microdialysis as a technique to determine the pharmacokinetics of drugs in rat brain. Brain Res 666:1–8

De Lange EC, de Bock G, Schinkel AH, de Boer AG, Breimer DD (1998) BBB transport and P-glycoprotein functionality using MDR1A (–/–) and wild-type mice. Total brain versus microdialysis concentration profiles of rhodamine-123. Pharm Res 15(11):1657–1665

De Lange EC, Marchand S, van den Berg D, van der Sandt IC, de Boer AG, Delon A, Bouquet S, Couet W (2000) In vitro and in vivo investigations on fluoroquinolones; effects of the P-glycoprotein efflux transporter on brain distribution of sparfloxacin. Eur J Pharm Sci 12(2):85–93

De Lange EC, Ravenstijn PGM, Groenendaal D, van Steeg TS (2005) Toward the prediction of CNS drug effect profiles in physiological and pathological conditions using microdialysis and mechanism-based pharmacokinetic-pharmacodynamic modeling. AAPS J 7(3), 54

De Lange EC (2004) Potential role of ABC transporters as a detoxification system at the blood-cerebrospinal fluid-barrier. Adv Drug Deliv Rev 56(12):1793–1809

De Lange EC (2013a) Utility of CSF in translational neuroscience. J Pharmacokinet Pharmacodyn 40(3):315–326

De Lange ECM, Bouw MR, Danhof M, De Boer AG, Breimer DD (1995a) Application of intracerebral microdialysis to study regional distribution kinetics of drugs in rat brain. Br J Pharmacol 116:2538–2544

De Lange ECM, Danhof M, De Boer AG, Breimer DD (1997) Methodological considerations of intracerebral microdialysis in pharmacokinetic studies on blood-brain barrier transport of drugs. Brain Res Rev 25:27–49

De Lange ECM, de Vries JD, Zurcher C, Danhof M, De Boer AG, Breimer DD (1995b) The use of intracerebral microdialysis to study blood-brain barrier transport of anticancer drugs in tumor-bearing rat brain. Pharm Res 12:1924–1931

De Lange ECM, Hesselink MB, Danhof M, De Boer AG, Breimer DD (1995c) The use of intracerebral microdialysis to determine changes in blood-brain barrier transport characteristics. Pharm Res 12:129–133

De Lange ECM (2013b) The use of the mastermind research approach: factors in brain distribution and prediction of human brain target site kinetics and CNS drug effects. Fluids Barriers CNS 10:12

Dhuria SV, Hanson LR, Frey WH (2009) Intranasal delivery to the central nervous system: Mechanisms and experimental considerations. J Pharm Sci 99:1654–1673

Dingemanse J, Hutson PH, Langemeijer MW, Curzon G, Danhof M (1988) Application of serial sampling of cerebrospinal fluid in pharmacodynamic studies with a drug active in the CNS: heptabarbital concentrations at onset and offset of loss of righting reflex in rats. Neuropharmacology 27(5):467–474

Ederoth P, Tunblad K, Bouw R, Lundberg CJ, Ungerstedt U, Nordström CH, Hammarlund-Udenaes M (2004) Blood-brain barrier transport of morphine in patients with severe brain trauma. Br J Clin Pharmacol 57(4):427–435

Enokizono J, Kusuhara H, Ose A, Schinkel AH, Sugiyama Y (2008) Quantitative investigation of the role of breast cancer resistance protein (Bcrp/Abcg2) in limiting brain and testis penetration of xenobiotic compounds. Drug Metab Dispos 36(6):995–1002

Faraci FM (1993) Endothelium-derived vasoactive factors and regulation of the cerebral circulation. Neurosurgery 33(4):648–659

Farde L, von Bahr C (1990) Distribution of remoxipride to the human brain and central D2-dopamine receptor binding examined in vivo by PET. Acta Psychiatr Scand Suppl 358:67–71

Fenstermacher JD, Patlak CS, Blasberg RG (1974) Transport of material between brain extracellular fluid, brain cells and blood. Fed Proc 33:2070–2074

Fenstermacher JD, Wei L, Acuff V, Lin SZ, Chen JL, Bereczki D, Otsuka T, Nakata H, Tajima A, Hans FJ, Ghersi-Egea JF, Finnegan W, Richardson G, Haspel H, Patlak C (1995) The dependency of influx across the blood-brain barrier on blood flow and the apparent flow-independence of glucose influx during stress. In: Greenwood J et al (eds) New concepts of a blood-brain barrier. Plenum, New York, pp 89–101

Fitzgerald P, Dinan TG (2008) Prolactin and dopamine: what is the connection? A review article. J Psychopharmacol 22(2 Suppl):12–19

Freeman ME, Kanyicska B, Lerant A, Nagy G (2000) Prolactin: structure, function, and regulation of secretion. Physiol Rev 80:1523–1631

Frey WH (2002) Intranasal delivery: bypassing the blood-brain barrier to deliver therapeutic agents to the brain and spinal cord. Drug Deliv Technol 2:46–49

Friberg LE, Vermeulen AM, Petersson KJF, Karlsson MO (2008) An agonist-antagonist interaction model for prolactin release following risperidone and paliperidone treatment. Clin Pharmacol Ther 85:409–417

Fridén M, Gupta A, Antonsson M, Bredberg U, Hammarlund-Udenaes M (2007) In vitro methods for estimating unbound drug concentrations in the brain interstitial and intracellular fluids. Drug Metab Dispos 35:1711–1719

Fridén M, Winiwarter S, Jerndal G, Bengtsson O, Wan H, Bredberg U, Hammarlund-Udenaes M, Antonsson M (2009) Structure—brain exposure relationships in rat and human using a novel data set of unbound drug concentrations in brain interstitial and cerebrospinal fluids. J Med Chem 52:6233–6243

Furchgott RF (1966) The use of β-haloalkylamines in the differentiation of receptors and in the determination of dissociation constants of receptor-agonist complexes. Adv Drug Res 3:21–55

Gabrielsson J, Green AR (2009) Quantitative pharmacology or pharmacokinetic pharmacodynamic integration should be a vital component in integrative pharmacology. J Pharmacol Exp Ther 331:767–774

Garrido M, Gubbens-Stibbe J, Tukker E, Cox E, von Frijtag J, Künzel DM, Ijzerman A, Danhof M, Van der Graaf PH (2000) Pharmacokinetic-pharmacodynamic analysis of the EEG effect of alfentanil in rats following beta-funaltrexamine-induced mu-opioid receptor “knockdown” in vivo. Pharm Res 17:653–659

Gazzin S, Strazielle N, Schmitt C, Fevre-Montange M, Ostrow JD, Tiribelli C, Ghersi-Egea JF (2008) Differential expression of the multidrug resistance-related proteins ABCb1 and ABCc1 between blood-brain interfaces. J Comp Neurol 510(5):497–507

Ghersi-Egea JF, Leininger-Muller B, Cecchelli R, Fenstermacher JD (1995) Blood-brain interfaces: relevance to cerebral drug metabolism. Toxicol Lett 82–83:645–653
Girardin F (2006) Membrane transporter proteins: a challenge for CNS drug development. Dialogues Clin Neurosci 8:311–321
Gjedde A, Crone C (1983) Biochemical modulation of blood-brain barrier permeability. Acta Neuropathol Suppl 8:59–74
Graff CL, Pollack G (2004) Drug transport at the blood-brain barrier and the choroid plexus. Curr Drug Metab 5:95–108
Greig NH, Momma S, Sweeney DJ, Smith QR, Rapoport SI (1987) Facilitated transport of melphalan at the rat blood-brain barrier by the large neutral amino acid carrier system. Cancer Res 47:1571–1576
Grime K, Riley RJ (2006) The impact of in vitro binding on in vitro-in vivo extrapolations, projections of metabolic clearance and clinical drug-drug interactions. Curr Drug Metab 7(3):251–264
Groenendaal D, Freijer J, de Mik D, Bouw MR, Danhof M, De Lange EC (2007a) PK-PD modelling of the electroencephalogram effects of morphine: the influence of biophase equilibration and P-glycoprotein interaction. Br J Pharmacol 151(5):713–720
Groenendaal D, Freijer J, de Mik D, Bouw MR, Danhof M, De Lange EC (2007b) Population pharmacokinetic modelling of non-linear brain distribution of morphine: influence of active saturable influx and P-glycoprotein mediated efflux. Br J Pharmacol 151(5):701–712
Groenendaal D, Freijer J, Rosier A, de Mik D, Nicholls G, Hersey A, Ayrton AD, Danhof M, de Lange EC (2008) Pharmacokinetic/pharmacodynamic modelling of the EEG effects of opioids: the role of complex biophase distribution kinetics. Eur J Pharm Sci 34(2–3):149–163
Hammarlund-Udenaes M, Fridén M, Syvänen S, Gupta A (2008) On the rate and extent of drug delivery to the brain. Pharm Res 25(8):1737–1750
Hammarlund-Udenaes M, Paalzow LN, De Lange ECM (1997) Drug equilibration across the blood-brain-barrier—pharmacokinetic considerations based on the microdialysis method. Pharm Res 14:128–134
Hammarlund-Udenaes M (2009) Active-site concentrations of chemicals—are they a better predictor of effect than plasma/organ/tissue concentrations? Basic Clin Pharmacol Toxicol 106:215–220
Hanson LR, Frey WH (2008) 2nd. Intranasal delivery bypasses the blood-brain barrier to target therapeutic agents to the central nervous system and treat neurodegenerative disease. BMC Neurosci 2008 Dec 10;9 Suppl 3:S5
Holford N, Nutt JG (2008) Disease progression, drug action and Parkinson's disease: why time cannot be ignored. Eur J Clin Pharmacol 64(2):207–216
Illum L (2004) Is nose-to-brain transport of drugs in man a reality? J Pharm Pharmacol 56:3–17
Illum L (2000) Transport of drugs from the nasal cavity to the central nervous system. Eur J Pharm Sci 11:1–18
Ings RMJ (1990) Interspecies scaling and comparisons in drug development and toxicogenetics. Xenobiotica 20:1201–1231
Jansson B, Bjork E (2002) Visualization of in vivo olfactory uptake and transfer using fluorescein dextran. J Drug Target 10:379–386
Jeffrey P, Summerfield S (2010) Assessment of the blood-brain barrier in CNS drug discovery. Neurobiol Dis 37:33–37
Jolliet P, Simon N, Bree F, Brée F, Urien S, Pagliara A, Carrupt PA, Testa B, Tillement JP (1997) Blood-to-brain transfer of various oxicams: effects of plasma binding on their brain delivery. Pharm Res 14:650–656
Kalvass JC, Maurer TS (2002) Influence of nonspecific brain and plasma binding of CNS exposure: implications for rational drug discovery. Biopharm Drug Dispos 23:327–338
Kapur S, Zipursky R, Jones C, Remington G, Houle S (2000) Relationship between dopamine D2 occupancy, clinical response, and side effects: a double-blind PET study of first-episode schizophrenia. Am J Psychiatry 157:514–520
Karssen AM, Meijer OC, van der Sandt ICJ, Lucassen PJ, de Lange ECM, de Boer AG, de Kloet ER (2001) Multidrug resistance P-glycoprotein hampers the access of cortisol but not of corticosterone to mouse and human brain. Endocrinology 142:2686–2694

Kassem NA, Deane R, Segal MB, Chen RL, Preston JE (2007) Thyroxine (T4) transfer from CSF to choroid plexus and ventricular brain regions in rabbit: contributory role of P-glycoprotein and organic anion transporting polypeptides. Brain Res 1181:44–50

Kenakin T, Christopoulos A (2011) Analytical pharmacology: the impact of numbers on pharmacology. Trends Pharmacol Sci 32(4):189–196

Kenakin T (2004) Principles: receptor theory in pharmacology. Trends Pharmacol Sci 25(4): 186–192

Kenakin T (2008) Receptor theory. Curr Protoc Pharmacol. Chapter 1:Unit 1.2

Kooij G, van Horssen J, de Lange EC, Reijerkerk A, van der Pol SM, van Het Hof B, Drexhage J, Vennegoor A, Killestein J, Scheffer G, Oerlemans R, Scheper R, van der Valk P, Dijkstra CD, de Vries HE (2010) T lymphocytes impair P-glycoprotein function during neuroinflammation. J Autoimmun 34(4):416–425

Köhler C, Hall H, Magnusson O, Lewander T, Gustafsson K (1990) Biochemical pharmacology of the atypical neuroleptic remoxipride. Acta Psychiatr Scand Suppl. 358:27–36

Kropf W, Kuschinsky K (1993) Effects of stimulation of dopamine D1 receptors on the cortical EEG in rats: different influences by a blockade of D2 receptors and by an activation of putative dopamine autoreceptors. Neuropharmacology 32:493–500

Kusuhara H, Sugiyama Y (2004) Efflux transport systems for organic anions and cations at the blood-CSF barrier. Adv Drug Deliv Rev 56:1741–1763

Kusuhara H, Sugiyama Y (2005) Active efflux across the blood-brain barrier: role of the solute carrier family. NeuroRx 2:73–85

Kvernmo T, Hartter S, Burger E (2006) A review of the receptor-binding and pharmacokinetic properties of dopamine agonists. Clin Ther 28:1065–1078

Kvernmo T, Houben J, Sylte I (2008) Receptor-binding and pharmacokinetic properties of dopaminergic agonists. Curr Top Med Chem 8(12):1049–1067

Langford D, Grigorian A, Hurford R, Adame A, Ellis RJ, Hansen L, Masliah E (2004) Altered P-gp expression in AIDS patients with HIV encephalitis. J Neuropathol Exp Neurol 63:1038–1047

Lee G, Dallas S, Hong M, Bendayan R (2001) Drug transporters in the central nervous system: brain barriers and brain parenchyma considerations. Pharmacol Rev 53:569–596

Letrent SP, Pollack GM, Brouwer KR, Brouwer KL (1999) Effects of a potent and specific P-glycoprotein inhibitor on the blood-brain barrier distribution and antinociceptive effect of morphine in the rat. Drug Metab Dispos 27:827–834

Liu X, Smith BJ, Chen C, Callegari E, Becker SL, Chen X, Cianfrogna J, Doran AC, Doran SD, Gibbs JP, Hosea N, Liu J, Nelson FR, Szewc MA, Van Deusen J (2005) Use of a physiologically based pharmacokinetic model to study the time to reach brain equilibrium: an experimental analysis of the role of blood–brain barrier permeability, plasma protein binding, and brain tissue binding. J Pharmacol Exp Ther 313:1254–1262

Löscher W, Potschka H (2005) Blood-brain barrier active efflux transporters: ATP-binding cassette gene family. Nat Rev Neurosci 6:591–602

Lötsch J, Schmidt R, Vetter G, Schmidt H, Niederberger E, Geisslinger G, Tegeder I (2002) Increased CNS uptake and enhanced antinociception of morphine-6-glucuronide in rats after inhibition of P-glycoprotein. J Neurochem 83(2):241–248

Ma G, Friberg LE, Movin-Osswald G, Karlsson MO (2010) Comparison of the agonist-antagonist interaction model and the pool model for the effect of remoxipride on prolactin. Br J Clin Pharmacol 70:815–824

Malhotra BK, Lemaire M, Sawchuk RJ (1994) Investigation of the distribution of EAB 515 to cortical ECF and CSF in freely moving rats utilizing microdialysis. Pharm Res 11:1223–1231

Mandema JW, Sansom LN, Dios-Viéitez MC, Hollander-Jansen M, Danhof M (1991) Pharmacokinetic-pharmacodynamic modelling of the EEG effects of benzodiazepines. Correlation with receptor binding and anticonvulsant activity. J Pharmacol Exp Ther 257:472–478

Mandema JW, Danhof M (1992) Electroencephalogram effect measures and relationships between pharmacokinetics and pharmacodynamics of centrally acting drugs. Clin Pharmacokinet 23(3):191–215

Mandema JW, Kuck MT, Danhof M (1992) Differences in intrinsic efficacy of benzodiazepines are reflected in their concentration-EEG effect relationship. Br J Pharmacol 105(1):164–170

Mayer S, Maickel RP, Brodie BB (1959) Kinetics of penetration of drugs and other foreign compounds into cerebrospinal fluid and brain. J Pharmacol Exp Ther 127:205–211

Movin-Osswald G, Hammarlund-Udenaes M (1995) Prolactin release after remoxipride by an integrated pharmacokinetic-pharmacodynamic model with intra- and interindividual aspects. J Pharmacol Exp Ther 274:921–927

Movin-Osswald G, Hammarlund-Udenaes M, Von Bahr C, Eneroth P, Walton-Bowen K (1995) Influence of the dosing interval on prolactin release after remoxipride. Br J Clin Pharmacol 39:503–510

Mulder M, Blokland A, van den Berg DJ, Schulten H, Bakker AH, Terwel D, Honig W, de Kloet ER, Havekes LM, Steinbusch HW, de Lange EC (2001) Apolipoprotein E protects against neuropathology induced by a high-fat diet and maintains the integrity of the blood-brain barrier during aging. Lab Invest 81(7):953–960

Nishino J, Suzuki H, Sugiyama D, Kitazawa T, Ito K, Hanano M, Sugiyama Y (1999) Transepithelial transport of organic anions across the choroid plexus: possible involvement of organic anion transporter and multidrug resistance-associated protein. J Pharmacol Exp Ther 290(1):289–294

O'Brien FE, Clarke G, Fitzgerald P, Dinan TG, Griffin BT, Cryan JF (2012) Inhibition of P-glycoprotein enhances transport of the antidepressant imipramine across the blood-brain barrier: microdialysis studies in the conscious freely moving rat. Br J Pharmacol. doi:10.1111/j.1476-5381.2012.01858.x

Oldendorf WH (1974) Lipid solubility and drug penetration of the blood-brain barrier. Proc Soc Exp Biol Med 14:813–816

Oztaş B, Akgül S, Arslan FB (2004) Influence of surgical pain stress on the blood-brain barrier permeability in rats. Life Sci 74(16):1973–1979

Oztas B, Akgul S, Seker FB (2007) Gender difference in the influence of antioxidants on the blood-brain barrier permeability during pentylenetetrazol-induced seizures in hyperthermic rat pups. Biol Trace Elem Res 118(1):77–83

Oztaş B, Küçük M (1995) Influence of acute arterial hypertension on blood-brain barrier permeability in streptozocin-induced diabetic rats. Neurosci Lett 188(1):53–56

Phelps CJ (1986) Immunocytochemical analysis of prolactin cells in the adult rat adenohypophysis: distribution and quantitation relative to sex and strain. Am J Anat 176:233–242

Philpott NJ (1993) Aplastic anaemia and remoxipride. Lancet 342:1244

Ploeger BA, van der Graaf PH, Danhof M (2009) Incorporating receptor theory in mechanism-based pharmacokinetic-pharmacodynamic (PK-PD) modeling. Drug Metab Pharmacokinet 24:3–15

Ramzan IM, Levy G (1986) Chronic theophylline administration has no apparent effect on theophylline concentrations required to produce seizures in rats. Proc Soc Exp Biol Med 182(2): 176–180

Rao VV, Dahlheimer JL, Bardgett ME, Snyder AZ, Finch RA, Sartorelli AC, Piwnica-Worms D (1999) Choroid plexus epithelial expression of MDR1 P-glycoprotein and multidrug resistance-associated protein contribute to the blood-cerebrospinal-fluid drug-permeability barrier. Proc Natl Acad Sci U S A 96:3900–3905

Ravenstijn PG, Merlini M, Hameetman M, Murray TK, Ward MA, Lewis H, Ball G, Mottart C, de Ville de Goyet C, Lemarchand T, van Belle K, O'Neill MJ, Danhof M, De Lange EC (2007) The exploration of rotenone as a toxin for inducing Parkinson's disease in rats, for application in BBB transport and PKPD experiments. J Pharmacol Toxicol Methods 57(2):114–130

Ravenstijn PGM, Drenth H, Baatje MS, O'Neill MJ, Danhof M, de Lange ECM (2012) Evaluation of BBB transport and CNS drug metabolism in diseased and control brain after intravenous L-DOPA in a unilateral rat model of Parkinson's disease. Fluids Barriers CNS 9:4

Schinkel AH, Smit JJM, van Tellingen O, Beijnen JH, Wagenaar E, van Deemter L, Mol CAAM, van der Valk MA, Robanus-Maandag EC, te Riele HPJ, Berns AJM, Borst P (1994) Disruption of the Mouse mdr1a P-glycoprotein gene leads to a deficiency in the blood-brain barrier and to increased sensitivity to drugs. Cell 77:491–502

Scism JL, Powers KM, Artru AA, Chambers AC, Lewis L, Adkison KK, Kalhorn TF, Shen DD (1997) Effects of probenecid on brain-cerebrospinal fluid-blood distribution kinetics of E-Delta(2)-valproic acid in rabbits. Drug Metab Dispos 25:1337–1346

Scism JL, Powers KM, Artru AA, Lewis L, Shen DD (2000) Probenecid-inhibitable efflux transport of valproic acid in the brain parenchymal cells of rabbits: a microdialysis study. Brain Res. 884(1–2):77–86

Sheiner LB, Stanski DR, Vozeh S, Miller RD, Ham J (1979) Simultaneous modeling of pharmacokinetics and pharmacodynamics: application to d-tubocurarine. Clin Pharmacol Ther 25(3): 358–371

Shen DD, Artru AA, Adkison KK (2004) Principles and applicability of CSF sampling for the assessment of CNS drug delivery and pharmacodynamics. Adv Drug Deliv Rev 56:1825–1857

Stain-Texier F, Boschi G, Sandouk P, Scherrmann JM (1999) Elevated concentrations of morphine 6-beta-D-glucuronide in brain extracellular fluid despite low blood-brain barrier permeability. Br J Pharmacol 128:917–924

Stevens J, Ploeger B, Hammarlund-Udenaes M, Osswald G, van der Graaf PH, Danhof M, de Lange ECM (2012) Mechanism-based PK–PD model for the prolactin biological system response following an acute dopamine inhibition challenge: quantitative extrapolation to humans. J Pharmacokinet Pharmacodyn 39(5):463–477

Stevens J, Ploeger B, van der Graaf PH, Danhof M, de Lange ECM (2011) Systemic- and direct nose-to-brain transport in the rat; a mechanistic pharmacokinetic model for remoxipride after intravenous and intranasal administration. Drug Metab Dispos 39(12):2275–2282

Stevens J, Suidgeest E, van der Graaf PH, Danhof M, de Lange EC (2009) A new minimal-stress freely-moving rat model for preclinical studies on intranasal administration of CNS drugs. Pharm Res 26(8):1911–1917

Sun H, Miller DW, Elmquist WF (2001) Effect of probenecid on fluorescein transport in the central nervous system using in vitro and in vivo models. Pharm Res 18(11):1542–1549

Suzuki H, Terasaki T, Sugiyama Y (1997) Role of efflux transport across the blood-brain barrier and blood-cerebrospinal fluid barrier on the disposition of xenobiotics in the central nervous system. Adv Drug Deliv Rev 25:257–285

Syvänen S, Lindhe Ö, Palner M, Kornum BR, Rahman O, Långström B, Knudsen GM, Hammarlund-Udenaes M (2009) Species differences in blood-brain barrier transport of three positron emission tomography radioligands with emphasis on P-glycoprotein transport. Drug Metab Dispos 37:635–643

Syvänen S, Schenke M, van den Berg D-J, Voskuyl RA, de Lange ECM (2012) Alteration in P-glycoprotein functionality affects intrabrain distribution of quinidine more than brain entry—a study in rats subjected to status epilepticus by kainate. AAPS J 14:87–96

Syvänen S, Xie R, Sahin S, Hammarlund-Udenaes M (2006) Consequences of active drug efflux at the blood–brain barrier. Pharm Res 23:705–717

Tanaka H, Mizojiri K (1999) Drug-protein binding and blood-brain barrier permeability. J Pharmacol Exp Ther 288:912–918

Tuk B, van Gool T, Danhof M (2002) Mechanism-based pharmacodynamic modeling of the interaction of midazolam, bretazenil, and zolpidem with ethanol. J Pharmacokinet Pharmacodyn 29(3):235–250

Tuk B, van Oostenbruggen MF, Herben VM, Mandema JW, Danhof M (1999) Characterization of the pharmacodynamic interaction between parent drug and active metabolite in vivo: midazolam and alpha-OH-midazolam. J Pharmacol Exp Ther 289(2):1067–1074

Tunblad K, Ederoth P, Gardenfors A, Hammarlund-Udenaes M, Nordstrom CH (2004a) Altered brain exposure of morphine in experimental meningitis studied with microdialysis. Acta Anaesthesiol Scand 48:294–301

Tunblad K, Hammarlund-Udenaes M, Jonsson E (2004b) An integrated model for the analysis of pharmacokinetic data from microdialysis experiments. Pharm Res 21:1698–1707

Tunblad K, Hammarlund-Udenaes M, Jonsson EN (2005) Influence of probenecid on the delivery of morphine-6-glucuronide to the brain. Eur J Pharm Sci 24:49–57

Tunblad K, Jonsson EN, Hammarlund-Udenaes M (2003) Morphine blood-brain barrier transport is influenced by probenecid co-administration. Pharm Res 20:618–623

Uchida Y, Ohtsuki S, Kamiie J, Terasaki T (2012) Blood-brain barrier (BBB) pharmacoproteomics (PPx): reconstruction of in vivo brain distribution of 11 P-glycoprotein substrates based on the BBB transporter protein concentration, in vitro intrinsic transport activity, and unbound fraction in plasma and brain in mice. J Pharmacol Exp Ther 339(2):579–588

Uchida Y, Ohtsuki S, Katsukura Y, Ikeda C, Suzuki T, Kamiie J, Terasaki T (2011) Quantitative targeted absolute proteomics of human blood-brain barrier transporters and receptors. J Neurochem 117(2):333–345

Urien S, Pinquier JL, Paquette B, Chaumet RP, Kiechel JR, Tillement JP (1987) Effect of the binding of isradipine and darodipine to different plasma proteins on their transfer through the blood-brain barrier. J Pharmacol Exp Ther 242:349–353

Van der Graaf PH, Danhof M (1997a) Analysis of drug-receptor interactions in vivo: a new approach in pharmacokinetic-pharmacodynamic modelling. Int J Clin Pharmacol Ther 35:442–446

Van der Graaf PH, Van Schaick EA, Visser SA, De Greef HJ, Ijzerman AP, Danhof M (1999) Mechanism-based pharmacokinetic-pharmacodynamic modeling of antilipolytic effects of adenosine A(1) receptor agonists in rats: prediction of tissue-dependent efficacy in vivo. J Pharmacol Exp Ther 290:702–709

Van der Graaf PH, Danhof M (1997b) On the reliability of affinity and efficacy estimates obtained by direct operational model fitting of agonist concentration-effect curves following irreversible receptor inactivation. J Pharmacol Toxicol Methods 38(2):81–85

Van Schaick EA, Tukker HE, Roelen HCPF, IJzerman AP, Danhof M (1998) Selectivity of action of 8-alkylamino analogues of N6-cyclopentyladenosine in vivo: haemodynamic versus antilipolytic responses in rats. Br J Pharmacol 124(3):607–618

Van Steeg T, Krekels EHJ, Danhof M, de Lange ECM (2007) Experimental alteration of serum AGP and albumin concentrations in the rat; an approach to assess the impact of changes in serum protein binding on pharmacodynamics. J Pharmacol Toxicol Methods 56:72–78

Van Steeg T, Krekels EHJ, Freijer J, Danhof M, de Lange ECM (2010) Effect of altered AGP plasma binding on heart rate changes by S(-)-propranolol in rats using mechanism-based estimations of in vivo receptor affinity (KB, vivo). J Pharm Sci 99(5):2511–2520

Van Steeg TJ, Boralli VB, Krekels EHJ, Slijkerman P, Freijer J, Danhof M, de Lange EC (2009) Influence of plasma protein binding on pharmacodynamics: estimation of in vivo receptor affinities of b blockers using a new mechanism-based PK–PD modelling approach. J Pharm Sci 98(10):3816–3828

Veng-Pedersen P, Mandema JW, Danhof M (1991) A system approach to pharmacodynamics. III: An algorithm and computer program, COLAPS, for pharmacodynamic modeling. J Pharm Sci 80(5):488–495

Visser SA, Wolters FL, Gubbens-Stibbe JM, Tukker E, Van Der Graaf PH, Peletier LA, Danhof M (2003) Mechanism-based pharmacokinetic/pharmacodynamic modeling of the electroencephalogram effects of GABAA receptor modulators: in vitro-in vivo correlations. J Pharmacol Exp Ther 304(1):88–101

Visser SAG, Gladdines WWFT, van der Graaf PH, Peletier LA, Danhof M (2002) Neuroactive steroids differ in potency but not in intrinsic efficacy at the GABAA receptor in vivo. J Pharmacol Exp Ther 303(6):616–626

Vorobyov VV, Schibaev NV, Morelli M, Carta AR (2003) EEG modifications in the cortex and striatum after dopaminergic priming in the 6-hydroxydopamine rat model of Parkinson's disease. Brain Res 97(2):177–185

Wang Y, Wei Y, Sawchuk RJ (1997) Zidovudine transport within the rabbit brain during intracerebroventricular administration and the effect of probenecid. J Pharm Sci 86(12):1484–1490

Wang YF, Welty DF (1996) The simultaneous estimation of the influx and efflux blood-brain barrier permeabilities of gabapentin using a microdialysis-pharmacokinetic approach. Pharm Res 13:398–403

Watson J, Wright S, Lucas A, Clarke KL, Viggers J, Cheetham S, Jeffrey P, Porter R, Read KD (2009) Receptor occupancy and brain free fraction. Drug Metab Dispos 37:753–760

Westerhout J, Danhof M, de Lange EC (2011) Preclinical prediction of human brain target site concentrations: considerations in extrapolating to the clinical setting. J Pharm Sci 100(9): 3577–3593

Westerhout J, Ploeger B, Smeets J, Danhof M, de Lange ECM (2012) Physiologically based pharmacokinetic modeling to investigate regional brain distribution kinetics in rats. AAPS J 14(3):543–553

Westerhout J, Smeets J, Danhof M, de Lange ECM (2013) The impact of P-gp functionality on non-steady state relationships between CSF and brain extracellular fluid. J Pharmacokinet Pharmacodyn 40(3):327–342

Wijnholds J, de Lange ECM, Scheffer GL, van den Berg D-J, Mol CAAM, van der Valk M, Schinkel AH, Scheper RJ, Breimer DD, Borst P (2000) Multidrug resistance protein 1 protects the choroid plexus epithelium and contributes to the blood-cerebrospinal fluid barrier. J Clin Invest 105:279–285

Williams SA, Davson H, Segal MB (1995) Transport of the nucleoside thymidine, in the central nervous system: the blood-cerebrospinal fluid and blood-brain barriers. In: Greenwood J, Begley DJ, Segal MB (eds) New concepts of a blood-brain barrier. Plenum, New York

Wong SL, Van Belle K, Sawchuk RJ (1993) Distributional transport kinetics of zidovudine between plasma and brain extracellular fluid/cerebrospinal fluid in the rabbit: investigation of the inhibitory effect of probenecid utilizing microdialysis. J Pharmacol Exp Ther 264(2):899–909

Wong SL, Wang Y, Sawchuk RJ (1992) Analysis of zidovudine distribution to specific regions in rabbit brain using microdialysis. Pharm Res 9(3):332–338

Xie R, Bouw MR, Hammarlund-Udenaes M (2000) Modelling of the blood-brain barrier transport of morphine-3-glucuronide studied using microdialysis in the rat: involvement of probenecid-sensitive transport. Br J Pharmacol 131(8):1784–1792

Xie R, Hammarlund-Udenaes M, de Boer AG, de Lange ECM (1999) The role of P-glycoprotein in blood-brain barrier transport of morphine: transcortical microdialysis studies in mdr1a (−/−) and mdr1a (+/+) mice. Br J Pharmacol 128:563–568

Yang Z, Brundage RC, Barbhaiya RH, Sawchuk RJ (1997) Microdialysis studies of the distribution of stavudine into the central nervous system in the freely-moving rat. Pharm Res 14(7):865–872

Yassen A, Olofsen E, Kan J, Dahan A, Danhof M (2007) Animal-to-human extrapolation of the pharmacokinetic and pharmacodynamic properties of buprenorphine. Clin Pharmacokinet 46:433–447

Zhang Y, Schuetz JD, Elmquist WF, Miller DW (2004) Plasma membrane localization of multidrug resistance-associated protein homologs in brain capillary endothelial cells. J Pharmacol Exp Ther 311:449–455

Zlokovic BV, Skundric DS, Segal MB, Colover J, Jankov RM, Pejnovic N, Lackovic V, Mackic J, Lipovac MN, Davson H et al (1989) Blood-brain barrier permeability changes during acute allergic encephalomyelitis induced in the guinea pig. Metab Brain Dis 4(1):33–40

Zlokovic BV (2010) Neurodegeneration and the neurovascular unit. Nat Med 16(12):1370–1371

Zuideveld KP, van der Graaf PH, Peletier LA, Danhof M (2007) Allometric scaling of pharmacodynamic responses: application to 5-Ht1A receptor mediated responses from rat to man. Pharm Res 24:2031–2039

Part III
Industrial Approaches for Investigation of Potential Central Nervous System Drugs

Chapter 10
Drug Discovery Methods for Studying Brain Drug Delivery and Distribution

Irena Loryan and Margareta Hammarlund-Udenaes

Abstract Methods used in drug discovery laboratories for assessing the delivery of small molecules to the brain have changed significantly in recent years. There is now more focus on measuring or estimating target unbound drug concentrations in the brain and evaluating the quantitative aspects of drug transport across the blood–brain barrier (BBB). The techniques for investigation of the rate and extent of BBB transport of new chemical entities (NCEs) are discussed in this chapter. Combinatory methodology for rapid mapping of the extent of brain drug delivery via assessment of the unbound drug brain partitioning coefficient is presented. The chapter also explains the procedures for approximation of subcellular distribution of NCEs, particularly into the lysosomes. The principles, technical issues, advantages, and potential applications of techniques for evaluation of intra-brain distribution, i.e., equilibrium dialysis-based brain homogenate and brain slice methods, are described. The assessment of extent of BBB transport and intracellular distribution of NCEs, the identification of intra-brain distribution patterns, and their integration with pharmacodynamic measurements are valuable implements for candidate evaluation and selection in drug discovery and development.

Abbreviations

A_{brain}	Amount of drug in brain tissue
$AUC_{tot,brain}$	Area under the total brain concentration–time curve
$AUC_{tot,plasma}$	Area under the total plasma concentration–time curve
BBB	Blood–brain barrier

I. Loryan (✉) • M. Hammarlund-Udenaes
Translational PKPD Research Group, Department of Pharmaceutical Biosciences, Uppsala University, Uppsala, Sweden
e-mail: Irena.loryan@farmbio.uu.se

M. Hammarlund-Udenaes et al. (eds.), *Drug Delivery to the Brain*, AAPS Advances in the Pharmaceutical Sciences Series 10, DOI 10.1007/978-1-4614-9105-7_10,

BCRP	Breast cancer resistance-associated protein
BCSFB	Blood-CSF barrier
CB	Cellular barrier
C_{buffer}	Concentration of compound in the buffer (brain slice method)
CNS	Central nervous system
CSF	Cerebrospinal fluid
$C_{tot,blood}$	Total drug concentration in blood
$C_{tot,brain}$	Total drug concentration in brain
$C_{tot,plasma}$	Total drug concentration in plasma
$C_{u,brainISF}$	Unbound drug concentration in brain interstitial fluid
$C_{u,cell}$	Unbound drug concentration in intracellular fluid
$C_{u,cyto}$	Unbound drug concentration in cytosol
$C_{u,lyso}$	Unbound drug concentration in lysosomes
$C_{u,plasma}$	Unbound drug concentration in plasma
DMPK	Drug metabolism and pharmacokinetics
ECF	Extracellular fluid (same as ISF)
ED	Equilibrium dialysis
ER	Efflux ratio
$f_{u,brain}$	Fraction of unbound drug in brain homogenate
$f_{u,brain,corrected}$	$f_{u,brain}$ Corrected for pH partitioning into cells
$f_{u,hD}$	Fraction of unbound drug in diluted brain homogenate
$f_{u,plasma}$	Fraction of unbound drug in plasma
HTS	High-throughput screening
ICF	Intracellular fluid in the brain
ISF	Interstitial fluid in the brain
K_d	Equilibrium dissociation constant
$K_{p,brain}$	Ratio of total brain to total plasma drug concentrations (also abbreviated as BB)
$K_{p,uu,brain}$	Ratio of brain ISF to plasma unbound drug concentrations
$K_{p,uu,cell}$	Ratio of brain ICF to ISF unbound drug concentrations
$K_{p,uu,cyto}$	Ratio of cytosolic to extracellular unbound drug concentrations
$K_{p,uu,lyso}$	Ratio of lysosomic to cytosolic unbound drug concentrations
LC-MS/MS	Liquid chromatography tandem mass spectrometry
logBB	Logarithm of $K_{p,brain}$ (BB)
MWCO	Molecular weight cut off
NCE	New chemical entity
neuroPK	Neuropharmacokinetics
P_{app}	Unidirectional apparent permeability coefficient measured in the apical-to-basolateral direction (cm/s)
PBS	Phosphate buffered saline
PD	Pharmacodynamics
PET	Positron emission tomography
P-gp	P-glycoprotein
PK	Pharmacokinetics
PLD	Drug-induced phospholipidosis

PS	Permeability surface area product (μL/min g/brain)
V_{ss}	Apparent volume of distribution at steady state
$V_{u,brain}$	Volume of distribution of unbound drug in brain (mL g/brain)

10.1 Introduction

The existing situation in the discovery and development of drugs for CNS-related conditions is unprecedentedly desperate, in the face of enormous unmet medical need (Eaton et al. 2008; Schoepp 2011; Schwab and Buchli 2012). The probability of success with emerging breakthrough first-in-class CNS drugs is small. Further, because neurotherapeutic drugs move more slowly in the development pipeline (compared to, for example, AIDS antivirals), they require a relatively extended time to get to market (Kaitin and DiMasi 2011). Despite immense efforts from the drug industry and academia, it could be thought that CNS drug discovery is currently almost in a blind alley. In contrast, however, Weaver and Weaver have used molecular modeling to reach the conclusion that the pharmaceutical industry is still in its infancy when it comes to exploring the neuroactive chemical space (Weaver and Weaver 2011).

The reasons for the apparent failure of CNS drug discovery, such as lack of clinically translatable animal disease models, lack of relevant biomarkers, and inadequate exposure of the CNS to potential drugs because of the blood–brain barrier (BBB), are generally acknowledged and are challenging to resolve (Jeffrey and Summerfield 2007; Hammarlund-Udenaes et al. 2008; Neuwelt et al. 2008; Kelly 2009; Reichel 2009; Abbott et al. 2010; Brunner et al. 2012).

This chapter is dedicated to the quantitative aspects of drug transport across the BBB and contemporary methods of assessing CNS exposure to NCEs in drug discovery and development programs. From drug discovery perspectives, it is important to mention that the BBB per se is not the only obstacle to drug delivery to the brain. Inadequate understanding of the principles of drug transport at the BBB and a lack of appropriate interpretation of target exposure could also be seen as hindrances to progression (Hammarlund-Udenaes et al. 2009).

As explained in the article by Elebring and colleagues, it is becoming more and more imperative to separate and define two crucial aspects of drug discovery: efficacy (i.e., doing the right things) and efficiency (i.e., doing things right) (Elebring et al. 2012). In the modern pharmaceutical industry we often observe the problems associated with "high-throughput" thinking (high efficiency) which typically biases biopharmaceutical scientists towards simple "one fits all" solutions. Alternatively, a tailored specific approach could be more effective. If this approach is to be applied to brain drug delivery, it is important initially to define what is meant by brain drug delivery and subsequently to identify the relevant core neuropharmacokinetic (neuroPK) parameters and applicable methods for the assessment of CNS exposure.

Because the novel strategies available for CNS drug delivery differ widely (invasive, noninvasive), the definitions of brain drug delivery, and consequently the

choice of appropriate neuroPK parameters, are also divergent (Pardridge et al. 1992; Thorne et al. 1995; Begley 1996; Huwyler et al. 1996; Pardridge 1997; Li et al. 1999; Scherrmann 2002; Reichel et al. 2003; Begley 2004; Garberg et al. 2005; Garcia-Garcia et al. 2005; Terasaki and Ohtsuki 2005; Pardridge 2006; de Boer and Gaillard 2007; Hammarlund-Udenaes et al. 2008; Wang et al. 2009; Gaillard et al. 2012; Stevens et al. 2012; de Lange 2013a). This chapter focuses on "classical" blood-to-brain delivery of small molecules, where drug delivery from the blood to the brain through the BBB can be described by *rate* and *extent* parameters (see Chap. 5, which discusses the pharmacokinetic concepts of brain drug delivery).

The *rate* of BBB transport is commonly characterized by the *permeability surface area product* (PS, mL min kg^{-1} body weight). Being unidirectional, the PS describes the speed at which the drug enters the brain (Fenstermacher 1992; Tanaka and Mizojiri 1999; Gaillard and de Boer 2000; Summerfield et al. 2007; Liu et al. 2008; Zhao et al. 2009). Generally, fast permeation is a key requirement for drugs when rapid CNS onset is wanted, e.g., for general anesthetics, and analgesics. Although only a limited number of compounds in a few pharmacological classes are required to permeate the brain quickly, the apparent BBB permeability (P_{app}; measured in vitro) is among the parameters considered by pharmaceutical industry to be essential for evaluation of BBB penetration in drug development programs (Liu et al. 2005; Jeffrey and Summerfield 2007; Summerfield et al. 2007). Moreover, combined with an in vitro P-glycoprotein (P-gp) assay, it is used as a basis for guiding the lead optimization and candidate selection (Di et al. 2012a). To make this point more explicit, it is worth mentioning that permeability-limited drug distribution in the brain (<10 % of cerebral blood flow or logPS < −2.9) is a very rare phenomenon associated with a slow equilibration time in the brain, and is not a matter of concern for potential CNS drugs intended for chronic administration (Abraham 2011; Kell et al. 2011; Deo et al. 2013; Kell et al. 2013). It is obvious that permeability as a test for BBB penetration is over-promoted in the pharmaceutical industry. The methods used for permeability measurements are not covered in this chapter, but are thoroughly discussed in Chaps. 6 and 7.

In the drug discovery setting, the *extent* of BBB transport is traditionally evaluated in rodents using the steady-state ratio of total brain to total plasma drug concentrations ($K_{p,brain}$, BB or logBB). Many generations of CNS drug discovery programs have been driven by optimizing $K_{p,brain}$, which has led to mass production of CNS compounds with high lipophilicity and development of the phenomenon known as the "lipidization trap": higher lipophilicity—higher $K_{p,brain}$ value—higher brain tissue binding—lower fraction of unbound drug in the brain (Deo et al. 2013). Because it is affected by nonspecific binding of the drug to plasma proteins and brain tissue, $K_{p,brain}$ masks the actual BBB net flux value (Lin et al. 1982; Lin and Lin 1990; Kalvass and Maurer 2002; Summerfield et al. 2007; Wan et al. 2007; Hammarlund-Udenaes et al. 2008; Read and Braggio 2010; Friden et al. 2011; Longhi et al. 2011). The use of $K_{p,brain}$ for optimizing novel neurotherapeutics has thus created further confusion in the field. In this regard, the steady-state *ratio of brain interstitial fluid* (*ISF*) *to plasma unbound drug concentrations*

($K_{p,uu,brain}$) is currently considered to be the most relevant measure of BBB function (Gupta et al. 2006; Jeffrey and Summerfield 2007; Hammarlund-Udenaes et al. 2008; Hammarlund-Udenaes et al. 2009; Liu et al. 2009b; Reichel 2009; Read and Braggio 2010; Di et al. 2012a; Doran et al. 2012).

$K_{p,uu,brain}$, the unbound drug brain partitioning coefficient, allows the assessment of the concentration of cerebral unbound drug, which is the main pharmacokinetic determinant of CNS activity of neurotherapeutics, based on a given plasma concentration (Harashima et al. 1984; Kalvass et al. 2007a; Liu et al. 2009b; Watson et al. 2009; Hammarlund-Udenaes 2010; Bundgaard et al. 2012b). Thus far, cerebral microdialysis has been the "gold" standard for the measurement of unbound cerebral concentrations in the brains of animals and humans (Elmquist and Sawchuk 1997; Hammarlund-Udenaes et al. 1997; de Lange et al. 1999; Elmquist and Sawchuk 2000). However, the practice of microdialysis for evaluation of BBB penetration in a drug discovery setup is limited mainly due to extensive adsorption to plastic tubing and probe. Nevertheless, a clinically relevant picture of the extent of brain drug delivery can be achieved by multidimensional evaluation of pharmacokinetic (PK) parameters such as $K_{p,brain}$, the volume of distribution of unbound drug in the brain ($V_{u,brain}$), and the fraction of unbound drug in the plasma ($f_{u,plasma}$) (Chap. 5 and Sect. 10.5).

A very important element of brain drug disposition, although it is unrelated to the BBB, is the *intracerebral distribution* of the drug, which is discussed in Sects. 10.2–10.4. Enhanced understanding of the distribution of the drug in the brain provides new perspectives on the pharmacodynamics of neurotherapeutics. Typically, brain tissue binding is measured as the *fraction of unbound drug in the brain* ($f_{u,brain}$) using an equilibrium dialysis (ED) technique to assess the extent of nonspecific binding to brain tissue (Kalvass and Maurer 2002; Kalvass et al. 2007a; Wan et al. 2007; Friden et al. 2011; Longhi et al. 2011; Di et al. 2012b). The method is mainly assessing intracellular binding (Friden et al. 2007; Friden et al. 2011).

Alternatively, the *volume of distribution of unbound drug in the brain* ($V_{u,brain}$), estimated using the fresh brain slice method, can allow assessment of the overall uptake by brain tissue (Kakee et al. 1997; Liu et al. 2006; Benkwitz et al. 2007; Friden et al. 2009a; Kodaira et al. 2011; Uchida et al. 2011a). In this chapter, we have chosen to express information from brain homogenate studies as $f_{u,brain}$ and information from brain slice studies as $V_{u,brain}$ to differentiate and clarify the information as much as possible. Both these parameters, $V_{u,brain}$ and $f_{u,brain}$, permit estimation of the concentration of unbound drug in brain ISF ($C_{u,brainISF}$) using total brain concentration ($C_{tot,brain}$) measurements, and give an indication of the probable extracellular target engagement. However, the intracellular concentration of unbound drug is also of great interest. In view of this, approximation of the *ratio of brain intracellular fluid (ICF) to ISF unbound drug concentrations* ($K_{p,uu,cell}$) may be beneficial for understanding the pharmacological query related to intracellular targets and may be strategically influential (Friden et al. 2007). The $K_{p,uu,cell}$ concept is innovative, as it provides the basis for an increased awareness of the impact of cellular barrier function on intracerebral drug distribution, which has hitherto been neglected in drug discovery programs.

The approaches applied for prediction, assessment and optimization (Chap. 12) of the BBB transport of NCEs, such as *in silico* (Chap. 11), in vitro (Chap. 6) and in vivo methods (Chap. 7), depend on the development phase of the drug and the questions of interest.

10.2 The Brain Homogenate Method for $f_{u,brain}$

The concentration of unbound drug in the brain, estimated using $C_{tot,brain}$ corrected for brain tissue binding, is a surrogate for $C_{u,brainISF}$. $C_{u,brainISF}$ is currently considered to be the most relevant parameter for measuring the pharmacological response of neurotherapeutics (Bouw et al. 2001; Bostrom et al. 2006; Bundgaard et al. 2007; Kalvass et al. 2007b; Liu et al. 2009b; Watson et al. 2009; Hammarlund-Udenaes 2010; Smith et al. 2010; Westerhout et al. 2011; Bundgaard et al. 2012b).

Brain tissue binding can be determined by various methods, including ED, stepwise ED, ultrafiltration, ultracentrifugation, gel filtration, and absorption by brain lipid membrane vesicles stabilized on silica beads (TRANSIL brain absorption kit) (Fichtl et al. 1991a; Kalvass and Maurer 2002; Mano et al. 2002; Vuignier et al. 2010; Longhi et al. 2011). This section focuses on the ED technique for the estimation of $f_{u,brain}$, which is presently used in drug discovery programs in a high-throughput manner.

Equilibrium Dialysis

In 2001, Kariv et al. presented the successful development of a 96-well ED plate suitable for evaluation of plasma protein binding for large numbers of biologically active NCEs during high-throughput screening (HTS) (Kariv et al. 2001). The special design of the dialysis apparatus permits dispensing and aspirating from both the sample and dialysate sides. This innovative 96-well ED apparatus allows the researcher to examine a large number of samples, time points, or replicates in the same experiment.

Using a similar approach in 2002, Kalvass and Maurer introduced a high-throughput ED technique designed for determination of brain tissue binding (Kalvass and Maurer 2002). The method rapidly became standard and it is currently widely used for estimation of $f_{u,brain}$ for a large number of chemically diverse compounds (Summerfield et al. 2006; Wan et al. 2007; Di et al. 2011; Friden et al. 2011; Longhi et al. 2011). The need for protein binding data in combination with the large number of compounds created from combinatorial chemistry has stimulated the development of a novel cassette-based pooling approach which allows simultaneous assessment of $f_{u,brain}$ or $f_{u,plasma}$ for more than five compounds per sample (Fung et al. 2003; Wan et al. 2007; Plise et al. 2010; Longhi et al. 2011).

Several research groups and pharmaceutical companies have validated the compatibility of the high-throughput ED techniques (96-, 48-well formats) with most standard laboratory supplies and robotics (Banker et al. 2003; van Liempd et al. 2011). Several devices based on a 96-well format are currently on the market [e.g., the Equilibrium Dialyzer-96 from Harvard Biosciences (Holliston, MA, USA), the Rapid Equilibrium Device from Thermo Scientific/Pierce (Rockford, IL, USA), and the Micro Equilibrium Dialysis Device from HTdialysis LLC (Gales Ferry, CT, USA)].

10.2.1 Principles

The semipermeable membrane between the buffer and the homogenate compartments in the ED apparatus acts as a molecular filter permitting diffusion against the concentration gradient of molecules smaller than a definite molecular weight. The drug (1–5 μM) is added to the brain homogenate (donor side) and is sampled from both the donor and the buffer (receiver) sides. To be able to perform ED, the brain homogenate needs to be diluted with phosphate-buffered saline (PBS; Sect. 10.2.1.2.2), commonly with dilution factors of either three (Kalvass and Maurer 2002) or five (Di et al. 2012b). As a general rule, the drug–tissue protein interaction is reversible and, in the majority of cases, equilibrium rapidly occurs between the unbound and bound molecular species. At equilibrium, the unbound fraction in diluted brain homogenate can be calculated as:

$$f_{\mathrm{u,hD}} = \frac{C_{\mathrm{receiver}}}{C_{\mathrm{donor}}}, \tag{10.1}$$

where $f_{\mathrm{u,hD}}$ is the measured experimental fraction of unbound compound in diluted (D) brain homogenate, C_{receiver} is the concentration of the compound in the buffer, and C_{donor} is the concentration of compound in the donor chamber at equilibrium.

The interaction between the compound/drug and brain tissue is, in most cases, a rapid and reversible process governed by the law of mass action, given that binding does not alter the drug or protein (Klotz 1973). The model assumes that binding between drug and brain tissue takes place in a single step and that the drug interacts with only one binding site on the protein. The equilibrium is described as:

$$[D]+[B] \leftrightarrow [DB], \tag{10.2}$$

where [D] and [B] represent the unbound drug and brain tissue protein concentrations, and [DB] represents the concentration of the drug–brain tissue protein complex.

The equilibrium dissociation constant (K_d) characterizes the concentration of unbound drug that occupies half of the binding sites on the protein at equilibrium:

$$K_d = \frac{k_{off}}{k_{on}} = \frac{[D][B]}{[DB]}. \tag{10.3}$$

Accordingly, the fraction of unbound drug can be described as:

$$f_{u,hD} = \frac{[DB]}{[B]+[DB]} = \frac{K_d}{[B]+K_d}. \tag{10.4}$$

Rearranging (10.4) gives:

$$K_d = \frac{f_{u,hD}[B]}{1 - f_{u,hD}}. \tag{10.5}$$

The unbound drug fraction usually increases as the brain homogenate is diluted. Therefore, $f_{u,hD}$ in the brain homogenate has to be corrected for dilution (Kurz and Fichtl 1983). There are several issues related to the dilution of the brain homogenate and subsequent adjustment methods (Fichtl et al. 1991b). The relationship between the measured unbound drug fraction and the dilution factor is typically not linear (Kurz and Fichtl 1983). The relative impact of dilution of the brain homogenate on the formation of drug–brain tissue protein complexes has been thoroughly discussed by Romer and Bickel (Romer and Bickel 1979). Assuming two different concentrations of brain tissue binding components $[B]_1$ and $[B]_2$ with unbound drug fractions $f_{u,brain}$ and $f_{u,hD}$, (10.5) can be rewritten as:

$$1 = \frac{f_{u,brain} \times [B]_1 \times (1 - f_{u,hD})}{f_{u,hD} \times [B]_2 \times (1 - f_{u,brain})}. \tag{10.6}$$

The ratio of $[B]_1/[B]_2$ is projected as the brain homogenate dilution factor D. Hence (10.6) can be reorganized to obtain the fraction of unbound drug in the undiluted brain tissue homogenate, which is used to calculate $f_{u,brain}$:

$$f_{u,brain} = \frac{\frac{1}{D}}{\left(\left(\frac{1}{f_{u,hD}}\right) - 1\right) + \frac{1}{D}}. \tag{10.7}$$

10.2.2 Technical Challenges

Implementation of a 96-well ED plate improved the robustness of the ED method and allowed the use of volumes of brain homogenate and/or plasma as small as 30 μL (e.g., HTdialysis LLC). Although ED is regarded as a "gold" standard method, it has drawbacks which need to be discussed along with the advantages of the method. The equilibration time, concentration of drugs and proteins, membrane surface area, membrane features, and molecular charges can all crucially affect the rate of dialysis.

10.2.2.1 Selection of Dialysis Membrane

Dialysis membranes consist of a spongy matrix of cross-linked polymers with different pore ratings or molecular weight cutoff points (MWCO). The MWCO is

defined by the molecular weight of solute that is 90 % retained by the membrane during a 17-h period. Various membranes (e.g., cellulose ester, regenerated cellulose, and polyvinylidene difluoride) with a range of MWCOs from 3.5 to 50 K are applicable for ED. The most commonly used MWCO range is 12–14 K.

A potential caveat of the ED method is the risk of nonspecific adsorption of drugs or proteins onto the chamber walls and the dialysis membrane (Vuignier et al. 2010). The use of an inert reusable 96-well Teflon construction minimizes nonspecific binding of test compounds to the apparatus. However, investigation of different types of dialysis membranes could be beneficial for selection of the most suitable material.

Recovery (also called mass balance) is traditionally evaluated to account for nonspecific binding and is used as an acceptance criterion for ED-based experiments. However, a recent investigation found that recovery had no influence on $f_{u,brain}$ or $f_{u,plasma}$ (Di et al. 2012b). These researchers recommended focusing on stability issues as a main cause of uncertainty in the binding experiments, instead.

10.2.2.2 Preparation of Brain Homogenate

Because undiluted brain tissue homogenate is paste-like in consistency and difficult to handle, it is diluted with PBS pH 7.4. However, this raises several questions concerning the trustworthy conversion of the brain tissue binding values estimated from diluted homogenate into values for the original protein concentrations in brain tissue. The dilution factor may not affect the final $f_{u,brain}$ measurement (unpublished observations), and various dilution factors have been used. For example, Kalvass and colleagues diluted with two volumes of PBS (Kalvass and Maurer 2002; Liu et al. 2005; Friden et al. 2007; Summerfield et al. 2007; Wan et al. 2007), while Di and coauthors diluted with four volumes of Dulbecco's PBS (Di et al. 2011).

Either frozen or fresh brain tissue can be used to prepare the brain homogenate. However, because of limited supplies of fresh brain homogenate, frozen brain homogenate is often used in drug discovery programs (Di et al. 2012b). To date, no systematic study has been carried out to confirm or reject the existence of differences in brain tissue binding measured using fresh and frozen brain homogenates.

Brain tissue is known to contain some serum albumin as a result of the residual blood left in the tissue (Glees and Voth 1988). The presence of residual blood in the brain homogenate could affect $f_{u,brain}$ measurement, predominantly for compounds with high affinity for serum albumin (Longhi et al. 2011). Fridén and coworkers demonstrated that the procedure of exsanguination of the animal before sampling the brain tissue could influence the residual volume of blood in the brain (Sect. 10.5) (Friden et al. 2010). Thus, the method of sacrificing animals should be standardized with the aim of reducing the residual volume of blood in the brain tissue. As a precautionary action, intracardial perfusion with cold PBS before extraction of the brain could be useful (Longhi et al. 2011). It has been proposed that determination of the serum albumin and total protein content in a brain tissue homogenate could aid the characterization and normalization of different batches (Kodaira et al. 2011; Longhi et al. 2011).

10.2.2.3 Equilibration Process

After spiking the diluted brain homogenate with the compound(s) of interest, 150 μL aliquots are usually loaded into the 96-well ED apparatus and dialyzed against 150 μL of PBS. Compounds with poor aqueous solubility are typically considered to be problematic and limit the use of ED. Equilibrium is generally achieved by incubating the 96-well ED apparatus in a 37 °C incubator at 155 rpm for 4–6 h (Kalvass and Maurer 2002). However, if more exact information is wanted it could be an advantage to perform an initial set of studies to determine the time required for the system to reach equilibrium, as slow drug–protein dissociation may occur.

The equilibration time needed in ED, normally 4–6 h, is considered to be one of the drawbacks of the method if the compounds studied are unstable in plasma or brain homogenate. Moreover, the equilibration time is associated with a volume shift that takes place because of the semipermeable membrane and the presence of proteins. This volume shift can be as large as 10–30 % for ED with plasma (Huang 1983). Measuring drug concentrations on both sides of the membrane is therefore required.

10.2.2.4 Bioanalysis

During the equilibration period, the buffer side becomes enriched with ions, amino acids, lipids, carbohydrates, and any other molecules smaller than the MWCO of the dialysis membrane that are not already present in the buffer. The brain homogenate composition also changes as a result of osmotic pressure. The modifications in the composition of the buffer and brain homogenate could result in a "matrix" effect during subsequent liquid chromatography tandem mass spectrometry (LC-MS/MS) analysis (e.g., ion suppression, enhancement of analyte signal) (Van Eeckhaut et al. 2009). Mixed-matrix and semi-automated mixed-matrix methods are currently being developed to decrease mass spectrometer run times and reduce the probability of experimental artifacts (Plise et al. 2010). For semi-automated mixed-matrix methods with a cassette-based approach, a single matrix is prepared following dialysis by mixing dialyzed plasma and buffer containing different test compounds from the same dialysis plate. The method should eliminate the need for standard curves, and increase the consistency of the sample matrix for LC-MS/MS analysis. This approach could easily be adopted when running the ED-based brain homogenate method and can be considered as a step towards further optimization of ED. Figure 10.1 describes the main steps of the proposed approach.

In conclusion, ED-based determination of $f_{u,brain}$ can be considered a proficient method. However, the biological and pharmacological meaning of the obtained values must be critically evaluated in relation to other neuroPK parameters (Sects. 10.4 and 10.5).

Recently, ED measures of the unbound fraction of drugs in plasma and brain were used as additional parameters for interpretation of in vivo positron emission tomography (PET) results, particularly for estimation of unbound drug concentrations in the CNS and accurate quantification of receptor binding (Gunn et al. 2012).

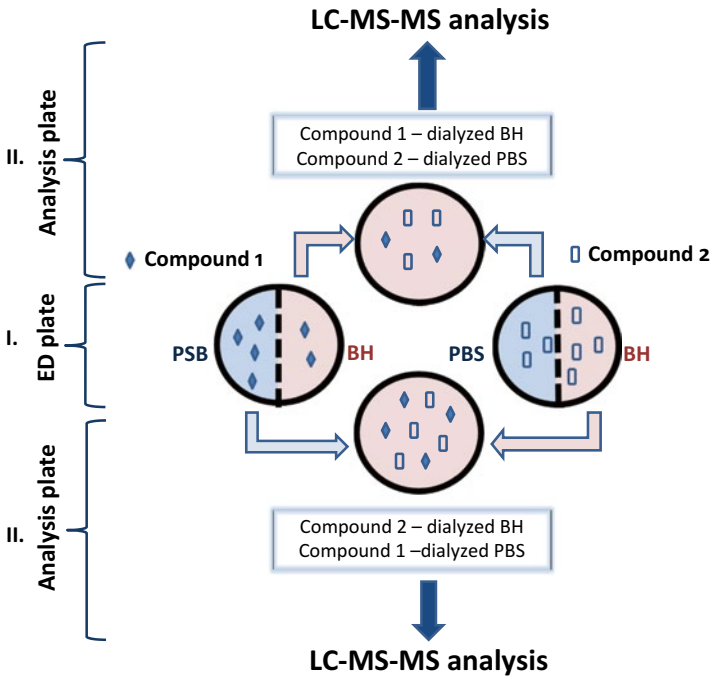

Fig. 10.1 Proposed sample preparation for the equilibrium dialysis (ED)-based brain homogenate method, modified from Plise and coworkers (Plise et al. 2010). This method allows eradication of the "matrix" effect often observed in LC-MS/MS when analyzing non-dialyzed vs. dialyzed buffer and homogenate samples, respectively. The method is based on a mixed matrix and can be used in a semi-automated fashion. After performing ED with the individual compounds in Step I, an aliquot of the dialyzed buffer (phosphate buffer saline, PBS) from Compound 1 is combined with an aliquot of the dialyzed brain homogenate (BH) from Compound 2. Similarly, an aliquot of dialyzed BH from Compound 1 is combined with an aliquot of dialyzed PBS from Compound 2. In Step II, the samples are analyzed by LC-MS/MS

10.3 The Brain Slice Method for $V_{u,brain}$

With respect to assessing the intracerebral distribution of small drug molecules, the ED-based brain homogenate method has drawbacks that are primarily linked to the disruption of brain parenchymal cells (Becker and Liu 2006; Liu et al. 2006; Friden et al. 2007; Friden et al. 2011). In this regard, the brain slice method is an advanced, well-functioning approach to the evaluation of the overall uptake of drugs into brain tissue via determination of the volume of distribution of unbound drug in the brain ($V_{u,brain}$; mL g brain^{-1}). This method has the benefits of being used in a regulated in vitro environment, while at the same time preserving much of the cellular complex integrity, including cellular barriers and circuitry, and as a result conserving the functionality of the in vivo brain. As a result, the technique delivers information that

is directly relevant to issues such as nonspecific binding to tissues, lysosomal trapping (Sect. 10.4.3), and active uptake into the cells.

The brain slice method was implemented by Henry McIlwain more than six decades ago and is nowadays widely used in neurobiology, electrophysiology and quantitative neuropharmacology (McIlwain 1951b; Collingridge 1995). The first use of this method for evaluation of intracerebral distribution of substances aimed to estimate the uptake of nutrients such as glucose and amino acids into the brain (McIlwain 1951a; Blasberg et al. 1970; Newman et al. 1988a; Newman et al. 1991; Smith 1991). Later, the method was proposed for in vitro investigation of the distribution of drugs in the brain (Van Peer et al. 1981; Kakee et al. 1996, 1997; Ooie et al. 1997). There have been several efforts to establish mechanistic pharmacokinetic/pharmacodynamics links using brain slice methodology, e.g., for propofol (Gredell et al. 2004), etomidate (Benkwitz et al. 2007), and volatile agents (Chesney et al. 2003).

$V_{u,brain}$ can also be measured using cerebral microdialysis and total brain concentration measurements; this is currently accepted as an in vivo reference method for evaluating intracerebral drug distribution. When the fresh brain slice method was validated against microdialysis, $V_{u,brain}$ was within a threefold range of the microdialysis results for 14 of 15 investigated compounds (Friden et al. 2007). In contrast, when $V_{u,brain}$ was recalculated using data from the brain homogenate method for the same list of compounds, the results were less accurate. In particular, the brain homogenate method over-predicted in vivo $V_{u,brain}$ for compounds limited to intracerebral ISF distribution (e.g., morphine-3- and morphine-6-glucuronide, R- and S-cetirizine) and under-predicted the distribution of gabapentin, which has predominantly active cellular uptake (Friden et al. 2007). However, these results have been challenged. Liu and colleagues demonstrated that, for eight of the nine studied compounds (carbamazepine, citalopram, ganciclovir, metoclopramide, *N*-desmethylclozapine, quinidine, risperidone, 9-hydroxyrisperidone, and thiopental), the $C_{u,brainISF}$ estimated using the brain homogenate method was within a threefold range of that obtained using cerebral microdialysis (Liu et al. 2009a). Nonetheless, these contrasting results should still be critically evaluated, since the microdialysis probes were calibrated using only in vitro recovery. Determination of $V_{u,brain}$ values that are more relevant to the in vivo situation, using fresh brain slices instead of brain homogenate, appears to be associated with more accurate assessment of $C_{u,brainISF}$ (i.e., $C_{u,buffer}$).

Despite the obvious benefits of the fresh brain slice method, it has not yet received wide acceptance in the drug industry compared to the brain homogenate method. The arguments against acceptance include that the method requires greater labor intensity. However, a high-throughput brain slice method has now been developed to fit the drug discovery format, thus offering new possibilities for the utilization of the method (Friden et al. 2009a; Loryan et al. 2013). Once the brain slice technique is established in a laboratory, one skilled assistant can perform up to four experiments per day. Up to ten compounds in one cassette can be tested simultaneously (prior consultation with an analytical chemist is obligatory). A series of three

experiments is enough to obtain consistent results for one cassette. The detailed protocol of how to perform brain slice studies can be found in the publication by Loryan et al. (Loryan et al. 2013).

10.3.1 Principles

The use of the apparent $V_{u,brain}$, obtained in vivo using cerebral microdialysis Equation (10.8), to assess the distribution of drugs in the brain was first suggested by Wang and Welty (they used the abbreviation $V_{e,app}$) (Wang and Welty 1996). $V_{u,brain}$ describes the relationship between the total drug concentration in the brain and the unbound drug concentration in the brain ISF, regardless of BBB function.

Assessment of $V_{u,brain}$ using the in vitro fresh brain slice method is based on the assumption that *at equilibrium*, $C_{u,brainISF}$ is equal to the drug concentration in protein-free artificial extracellular fluid buffer (aECF). Thus, $V_{u,brain}$ (mL g brain^{-1}) is calculated as the ratio of the amount of drug in the brain slice (A_{brain}, nanomoles g brain^{-1}) to the measured final aECF after reaching equilibrium (C_{buffer}, micromoles · L^{-1}):

$$V_{u,brain} = \frac{A_{brain}}{C_{u,brainISF}} = \frac{A_{brain}}{C_{buffer}}. \tag{10.8}$$

Because a certain volume of the aECF remains on the surface of the brain slice (V_i, mL g slice^{-1}), even after removing the excess with filter paper, this has to be accounted for. V_i is estimated in a separate experiment using [^{14}C] inulin as described in Fridén et al. (Friden et al. 2009a). Equation (10.8) is then rearranged to obtain $V_{u,brain}$ corrected for V_i ($1-V_i$):

$$V_{u,brain} = \frac{A_{brain} - V_i \times C_{buffer}}{C_{buffer} \times (1 - V_i)}. \tag{10.9}$$

As outlined by Wang and Welty $V_{u,brain}$ value that is higher than 1 mL g brain^{-1} indicates intracellular accumulation or excessive brain tissue binding because it exceeds the total volume of water in the brain which is 0.8 mL g brain^{-1} (Wang and Welty 1996). $V_{u,brain}$ values between 1 and 0.2 mL g brain^{-1} indicate limited distribution of drug in the brain ECF and ICF (Nicholson and Sykova 1998; Sykova and Nicholson 2008). As the volume of healthy adult rat brain ISF is 0.2 mL g brain^{-1}, a volume below 0.2 mL g brain^{-1} is not possible. However, it should be kept in mind that this technique does not account for possible intracerebral metabolism (Chap. 4).

In the literature, $V_{u,brain}$ is sometimes expressed as $f_{u,brain,slice}$ (Kodaira et al. 2011; Uchida et al. 2011a). It is important to keep in mind that $f_{u,brain,slice}$ could be considerably different from $f_{u,brain}$, as they obtained using different matrices, i.e., brain slice and brain tissue homogenate (Sect. 10.4).

10.3.2 Technical Challenges

10.3.2.1 Artificial Extracellular Fluid and Formation of Cassettes

It is important to preserve the viability of the brain slices during the experiment and to mirror the in vivo cellular milieu as closely as possible. There are two main approaches to achieving this, regarding the medium used. One approach is based on the use of either fresh or thawed *plasma* as a medium for the incubation, with subsequent evaluation of the brain slice-to-plasma drug concentration ratio (Becker and Liu 2006). The second and more commonly applied approach is to use a *protein-free* artificial cerebrospinal fluid (CSF) or aECF as an incubation medium (Kakee et al. 1996, 1997). The latter simplifies the interpretations of the results obtained. A large number of formulations for aECF can be found in the literature (Newman et al. 1991; Kakee et al. 1996, 1997; Gredell et al. 2004; Friden et al. 2009a; Uchida et al. 2011a). In many of these, ascorbic acid is used as a natural free radical scavenger to protect cell membranes from lipid peroxidation and swelling of the brain slices (Rice 1999). The HEPES-buffered aECF containing 129 mM NaCl, 3 mM KCl, 1.4 mM $CaCl_2$, 1.2 mM $MgSO_4$, 0.4 mM K_2HPO_4, 25 mM HEPES, 10 mM glucose, and 0.4 mM ascorbic acid is a robust and practical formulation for sustaining the physiological pH (around 7.3 at 37 °C after 5 h incubation) for the high-throughput setup (Friden et al. 2009a).

Another critical requirement is an adequate oxygen supply. Either 100 % humidified oxygen or carbogen (a mixture of 95 % oxygen and 5 % CO_2) can be used.

The brain slice method allows examination of up to ten compounds per experiment, covering a wide range of physicochemical properties and pharmacological targets, mixed together in the same *cassette* (the mixture of compounds under investigation is called the cassette) (Friden et al. 2009a; Kodaira et al. 2011). Low concentrations of compounds (e.g., 0.1–0.2 μM) are preferable. The summed concentration of all the drugs in the cassette should not exceed 1 μM (Friden et al. 2009a). Application of higher concentrations of various compounds can lead to accumulation of compounds in the acidic compartments of the cells (i.e., lysosomes) or competition for specific cell membrane transporters with subsequent incorrect values for $V_{u,brain}$. For instance, it is recognized that interactions between two weak bases are regulated by the free concentrations of the compounds in the cassette and the ability of these compounds to elevate intralysosomal pH (Daniel and Wojcikowski 1999b). Potential bioanalytical issues should be addressed when assembling the cassettes for investigation, so as to avoid technical hitches.

10.3.2.2 Preparation of Brain Slices and Incubation

It is important that the fresh brain slices are of high quality if the $V_{u,brain}$ values are to be relevant to the in vivo situation. This can be accomplished by keeping strictly to the protocol for preparation and maintenance of the brain slices during the

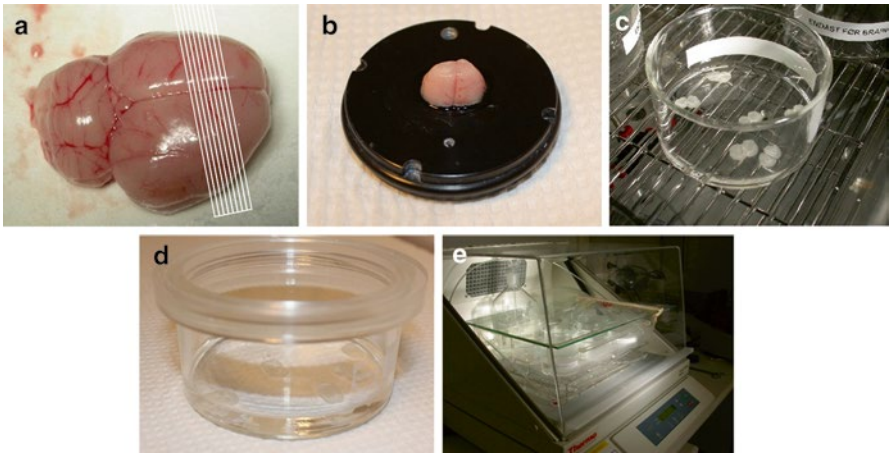

Fig. 10.2 Illustration of the main steps in the preparation of brain slices. (**a**) Schematic representation of the cutting direction. (**b**) Brain glued to the slicing platform in a coronal position. (**c**) Brain slices transferred into the Ø80 mm flat-bottomed glass beaker. (**d**) Beaker covered by the custom fabricated lid fitted with a Teflon fluorinated ethylene-propylene film. (**e**) Setup for the incubation–equilibration period. Reprinted with permission from BioMed Central (Loryan et al. 2013)

experiment (Friden et al. 2009a; Loryan et al. 2013). The key steps of the brain slice method are illustrated in Fig. 10.2.

The protocol for the fresh brain slice method (also called in vitro brain slice uptake technique) has not been unified among research laboratories, which makes comparison and interpretation of the results challenging. For instance, the brain can be sliced using a brain microslicer (Ooie et al. 1997; Benkwitz et al. 2007; Kodaira et al. 2011), a McIlwain tissue chopper (Becker and Liu 2006), or a vibrotome (Friden et al. 2009a; Loryan et al. 2013). Moreover, researchers have used slices from different planes of the brain, such as hypothalamic (Kakee et al. 1997), cortical (Kodaira et al. 2011), or striatal (Friden et al. 2009a, 2009b). The thickness of the brain slices also differs between protocols: 300 μm (Kakee et al. 1996, 1997; Friden et al. 2009a, b), 400 μm (Becker and Liu 2006), or even 1000 μm (Van Peer et al. 1981). Accordingly, the incubation time (time required to reach equilibrium) varies and could be 8 h or longer, which may be too long to sustain the viability of the slices.

The time needed to reach equilibrium is influenced by various factors such as the amount of brain tissue per unit of buffer volume, the stirring speed, and the initial concentration of the compound (Gredell et al. 2004; Benkwitz et al. 2007; Friden et al. 2009a). The ratio of six/ten (rat/mouse) 300 μm sequential brain slices to 15/10 mL (rat/mouse) of aECF has been found to be the most optimal for various diverse compounds to reach equilibrium in about 5 h (Friden et al. 2009a; Loryan et al. 2013). Very lipophilic compounds may require a longer equilibration time in some experimental setups, and this could compromise the viability of the brain slices. In this case, mathematical modeling of the data could be a reasonable alternative (Kodaira et al. 2011).

Sufficient viability of the brain slices is a critical prerequisite. The viability can be assessed indirectly by measuring the pH of the aECF (acidification of the medium is linked to low viability of the slices). However, more advanced methods such as measuring the ATP content of the slices (Friden et al. 2007; Kodaira et al. 2011; Uchida et al. 2011a) or the activity of released lactate dehydrogenase (Dos-Anjos et al. 2008; Loryan et al. 2013) are now recommended.

10.3.2.3 Bioanalysis

The drug concentrations in brain slices and aECF samples taken at equilibrium can be analyzed after homogenization using high-throughput techniques and LC-MS/MS as discussed for brain homogenate samples in Sect. 10.2.2.4. To avoid the preparation of calibration curves, tenfold and 100-fold dilutions of the samples are preferable (Friden et al. 2009a). Several groups normalize the protein concentrations to correct for dilution of brain homogenate (Kodaira et al. 2011).

In summary, the fresh brain slice method is a precise and robust technique for estimating the overall uptake of drugs into brain tissue. This method is recommended for the estimation of target-site PK in the early drug discovery process in order to guide candidate selection. One of the attractive features of the brain slice method is that it can be developed to scrutinize compound-specific molecular mechanisms of the intracerebral distribution of NCEs (Sects. 10.4 and 10.5). For instance, fresh brain slices could be prepared from different strains of wild type or genetically modified mice and rats to elucidate the effects of intracerebral transporters on the distribution of drugs within the brain (BBB transporters cannot be directly mapped with this technique). Furthermore, the brain slices could be manipulated genetically using various methods such as viral infection (Stokes et al. 2003) or biolistics (Wellmann et al. 1999). Disease models could also be used to study the diffusion and distribution of drugs or radiotracers within the brain (Newman et al. 1988b; Patlak et al. 1998). In addition, pharmacological inhibition or stimulation could be used to investigate particular distributional mechanisms, e.g., monesin or nigericin to study the impact of lysosomal accumulation on the intracellular distribution of drugs (Friden et al. 2011; Logan et al. 2012).

10.4 Intracellular Distribution

Historically, it has been presumed that the transport of small molecules between intracellular and extracellular neurocompartments is more efficient than BBB transport, which is considered to be a rate-limiting step for drug distribution to the brain (Wang and Welty 1996). Accordingly, from a PK point of view, assessment of the intracerebral distribution of NCEs is usually less prioritized, is often inadequate because of a lack of reliable methods, and is narrowed to estimation of the unbound drug fraction in a brain homogenate, with subsequent evaluation of its half-life in brain tissue (Liu et al. 2005). However, awareness of compound-specific intracerebral distributional mechanisms in early drug discovery could allow better directed

Table 10.1 Key components affecting drug distribution to and from the different compartments in the brain[a]

Extracellular neurocompartment	Cellular membranes	Intracellular neurocompartment
Diffusion in extracellular space	Membrane permeation	Nonspecific binding to intracellular membrane components (often quantitatively significant)
Hydraulic permeability	Active influx (e.g., organic cation transporters, L-type amino acid transporters)	pH differences causing accumulation of weak bases in acidic compartments (e.g., lysosomes, endosomes)
ISF bulk flow	Active efflux	Specific binding to the target (e.g., tubulin, enzymes)
	Nonspecific binding to cell membrane components (often quantitatively insignificant)	Drug metabolism (often insignificant)[b]
	Specific binding to the target (often quantitatively insignificant)	

[a]Differences between types of brain parenchymal cells and brain subregions are not taken into account

[b]Drug metabolism is discussed in more detail in Chap. 4

evaluation and selection of drug candidates, based on the location of the potential CNS target (i.e., extracellular or intracellular) and the probable side effects.

After passing the BBB, drugs are distributed in the extracellular space mainly by diffusion and convection (see Chap. 5 for a comprehensive analysis of the transport processes of drugs within the CNS). As pointed out in the state-of-the-art review by Wolak and Thorne (Wolak and Thorne 2013), the diffusion of molecules is governed by the features of the extracellular space (i.e., width, volume fraction, viscosity, geometry) as well as by any potential binding to the extracellular matrix or cellular membrane components (Fenstermacher and Kaye 1988). It should be highlighted that diffusion of compounds in the extracellular neurocompartment is a potentially limiting step for macromolecules, nanoparticles and viral vectors (Thorne et al. 2004; Thorne and Nicholson 2006; Thorne et al. 2008). The bulk flow of the ISF should be accounted for in addition to the diffusion and hydraulic permeability (see Chap.1 and Table 10.1). However, although it can be influential for poorly penetrating compounds, it is not a matter of concern for small highly lipophilic compounds (Cserr and Patlak 1992; Davson and Segal 1995; Abbott 2004). The bulk flow of the ISF has been measured as ~0.1–0.3 μL min^{-1} g^{-1} in the rat brain but the actual value may be greater than this (Chap. 1 and Joan Abbott personal communication).

Because ISF is virtually protein free (Davson et al. 1970; Davson and Segal 1995), the drug present in the ISF can be measured as unbound and accessible for interactions at a cellular membrane level (Hammarlund-Udenaes et al. 1997; Ooie et al. 1997; Kalvass and Maurer 2002; Mano et al. 2002; Shen et al. 2004; Doran et al. 2005; Liu et al. 2005; Summerfield et al. 2006; Friden et al. 2007; Watson et al. 2009). The permeation of unbound, un-ionized drug through the cell membrane

could be defined as the most significant distributional process of small molecules into the cell. Accumulation is a distributional process that is associated with asymmetry at the cellular barrier, is linked to the physiological pH gradient, and is driven by acidic intracellular compartments such as lysosomes, endosomes, peroxisomes, and the trans-Golgi network (Sect. 10.4.2). Asymmetry at the cellular barrier level can also occur as a consequence of active transport such as influx processes governed by organic cation transporters (e.g., 1-methyl-4-phenylpyridinium, tetraethylammonium, metformin) and L-type amino acid transporters (e.g., gabapentin), or efflux processes (Lee et al. 2001a; Lee et al. 2001b; Bendayan et al. 2002; Kusuhara and Sugiyama 2002; Ohtsuki et al. 2004; Syvanen et al. 2012). The specific and nonspecific binding of compounds to extracellular constituents of the cell membrane can be ignored because of their much smaller surface areas, i.e., the external surface area of a typical human cell membrane represents less than 0.5 % of the total cell membrane surface area (Nicholson and Sykova 1998; Sykova 2004).

After passing the cellular barrier, compounds can bind reversibly to intracellular constituents such as lipoproteins, phospholipids of the inner cellular membrane, or organelles. Nonspecific binding is often the dominant distributional component for small lipophilic compounds. In most cases, specific intracellular binding is irrelevant from a distributional perspective because of the low expression levels of the targets in relation to the extent of nonspecific binding. However, there are some exceptions; these are discussed at the end of Sect. 10.4.

Off-target or nonspecific binding of the drug to the cellular membranes is often not associated with any pharmacological response. However, progress has been made in recent decades towards an understanding of the interactions between the ligand and the target (i.e., receptor, ion channel, and enzyme). Primarily, the "passive" role of the cell membrane in target-binding kinetics has been questioned (Vauquelin and Packeu 2009). Novel membrane-connected concepts that reexamine the notion of so-called nonspecific plasma membrane partitioning are being proposed (Sargent et al. 1988; Vauquelin and Van Liefde 2005). It has been recognized that nonspecific ligand-membrane interactions could be favorable, although not in all cases, for ligand-target interactions (Sargent and Schwyzer 1986; Bean et al. 1988; Vauquelin et al. 2012). This process could be very important for peptide-target interactions (Sargent and Schwyzer 1986). Another crucial aspect of membrane partitioning is the increased in vivo residence time of hydrophobic ligands. Slow release from the cell membranes is commonly acknowledged to be strongly associated with the long lasting effects of highly lipophilic compounds (e.g., salmeterol). In other words, the cell membrane can be perceived as a depot/reservoir for hydrophobic ligands.

10.4.1 Using $K_{p,uu,cell}$ to Estimate the Extent of Cellular Barrier Transport

Frequently, as with plasma protein binding, scientists define the binding of drugs to brain tissue as "nonspecific." However, in comparison with plasma protein binding, less is known about the drug–brain tissue interaction, mainly because of

technical difficulties in obtaining data on the tissue-binding components and in the quantification of intracellular drug concentrations.

In most cases, intracerebral distribution is assessed by either the ED-based brain homogenate method, with evaluation of $f_{u,brain}$, or the fresh brain slice method, with assessment of $V_{u,brain}$. Combining the two methods provides further information on intracellular distribution. The main determinant of $f_{u,brain}$ is *brain tissue binding* which primarily consists of nonspecific binding of the drug to various *intracellular* lipids and proteins. $V_{u,brain}$ then provides complementary data on intracerebral distribution factors other than binding. The importance of $K_{p,uu,cell}$ in this respect has been discussed by Fridén et al. (Friden et al. 2007; Friden et al. 2009a; Friden et al. 2011). $K_{p,uu,cell}$ can be estimated by combining $f_{u,brain}$ (brain homogenate) with $V_{u,brain}$ (brain slice) using (10.10) (Friden et al. 2007):

$$K_{p,uu,cell} = V_{u,brain} \times f_{u,brain}. \tag{10.10}$$

$K_{p,uu,cell}$ describes the *steady-state* relationship of intracellular-to-extracellular unbound drug concentrations and provides the average concentration ratio for all cell types within the brain. The assumptions behind the $K_{p,uu,cell}$ concept are the following (Friden et al. 2007):

1. The ISF concentration is assumed to describe unbound drug (ISF is a practically protein-free fluid).
2. $C_{u,brainISF}$ represents the concentration of unbound drug in brain ISF from the entire brain (cranioregional and cell type dissimilarities are not accounted for).
3. Membrane permeation and binding to intracellular and extracellular constituents are the key distributional processes.
4. Intracellular drug molecules can be unbound or bound to intracellular components.
5. Drug binding to the outer part (surface) of the cell is negligible. However, this assumption could be incorrect for molecules with distribution entirely restricted to the ISF (e.g., large molecules) and/or those that are significantly bound to cellular membranes.

The derivation of the equations presented below is based on the definition of $V_{u,brain}$ as the ratio of the total amount of drug in the brain excluding blood (A_{brain}) to the concentration of unbound drug in brain ISF (10.8). According to the proposed distributional model (Friden et al. 2007), the total amount of drug in the brain can be presented as:

$$A_{brain} = V_{brainISF} \times C_{u,brainISF} + V_{cell} \times V_{u,cell} \times C_{u,cell}, \tag{10.11}$$

where $V_{brainISF}$ and V_{cell} are the physiological fractional volumes of ISF (~0.2 mL g brain^{-1}) (Nicholson and Sykova 1998; Sykova and Nicholson 2008) and brain parenchymal cells (~0.8 mL g brain^{-1}) and the density of brain tissue is assumed to be 1. $V_{u,cell}$ describes the volume of distribution of unbound drug in the cell (mL ICF · mL cell^{-1}), and relates the total amount of drug in the cell to the

intracellular concentration of unbound drug, $C_{u,cell}$. $V_{u,cell}$ can be compared with $V_{u,brain}$, describing the whole brain drug distribution.

Another way of explaining $V_{u,cell}$ is that it describes the affinity of the drug to bind inside the cell. The more drug is bound, the higher the value of $V_{u,cell}$. It can be estimated using the ED-based brain homogenate method:

$$V_{u,cell} = 1 + \frac{D}{V_{cell}} \times \left(\frac{1}{f_{u,hD}} - 1 \right), \tag{10.12}$$

where $f_{u,hD}$ is the buffer-to-brain homogenate concentration ratio measured using ED and D is the dilution factor associated with homogenate preparation (Sect. 10.2).

Rewriting (10.8) using (10.11), and dividing both sides by $C_{u,brainISF}$ gives:

$$V_{u,brain} = V_{brainISF} + V_{cell} \times V_{u,cell} \times \frac{C_{u,cell}}{C_{u,brainISF}}. \tag{10.13}$$

Consequently, the ratio of brain ICF to ISF unbound drug concentrations ($K_{p,uu,cell}$) can be derived as:

$$K_{p,uu,cell} = \frac{C_{u,cell}}{C_{u,brainISF}} = \frac{V_{u,brain} - V_{brainISF}}{V_{cell} \cdot V_{u,cell}} \tag{10.14}$$

When analyzing numerical values of $K_{p,uu,cell}$, it is important to remember its meaning. When cellular membrane permeation is predominantly passive, the unbound drug intracellular and extracellular concentrations are the same, giving a $K_{p,uu,cell}$ equal to unity. $K_{p,uu,cell}$ values higher than unity indicate intracellular accumulation and $K_{p,uu,cell}$ values below unity could indicate active efflux at the cellular barrier. Estimation of $K_{p,uu,cell}$ is valuable for interpreting and understanding the processes governing the distribution of drugs into the brain parenchymal cells. It should be remembered, however, that the numbers obtained are average values from all the cell types in the brain.

10.4.2 Lysosomal Trapping

Although they were discovered in the early 1970s, the role of lysosomes in drug tissue distribution kinetics can still be considered as *terra incognita* (De Duve 1971). Lysosomes are conventionally acknowledged as the cell's "garbage-disposal units." They are membrane-bound organelles containing about fifty hydrolytic enzymes that function at pH 4.5. Vacuolar type H^+-ATPase embedded in the lysosomal membrane maintains the intralysosomal acidic environment.

Lysosomotropism or lysosomal trapping is a phenomenon where compounds (*lysosomotropic agents*) with both a lipophilic moiety and a basic moiety are

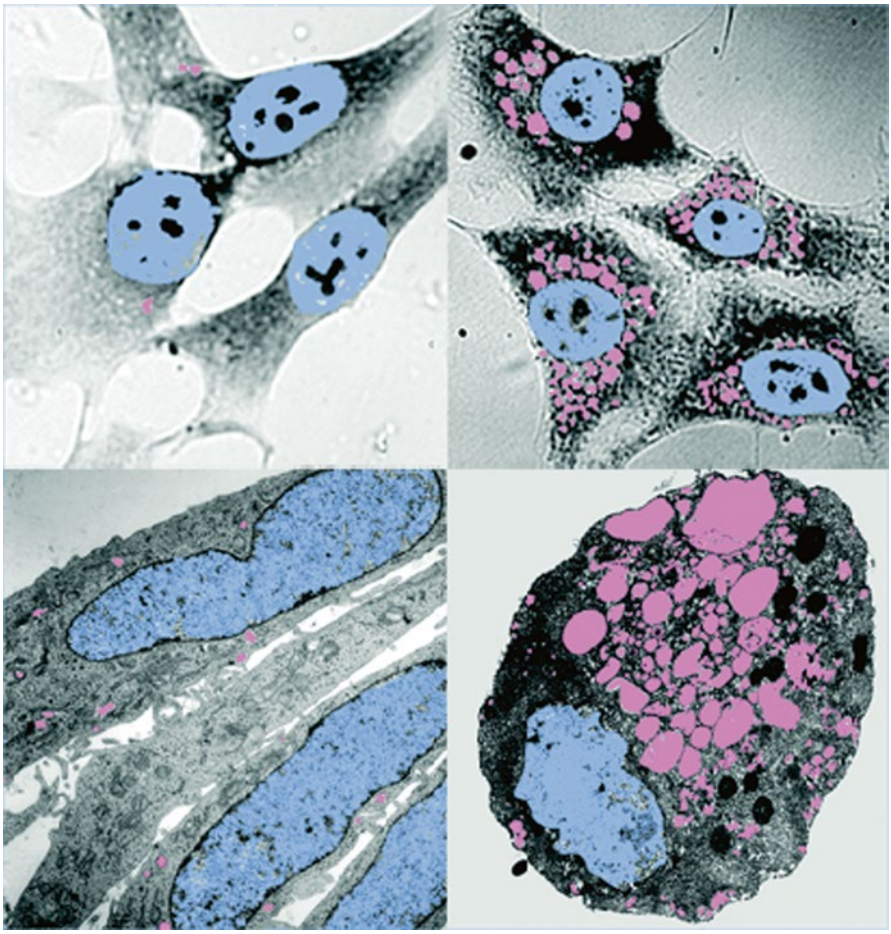

Fig. 10.3 Cells displaying the lysosomal trapping phenomenon. Picture from Boya et al. (Boya et al. 2003). In contrast to controls (*top left* and *bottom left panels*), the cells treated with the lysosomotropic drug ciprofloxacin (*top right* and *bottom right panels*) manifest multiple autophagic vacuoles (colored *pink*) in the cytoplasm, before undergoing apoptosis. The bottom microphotographs have been obtained by electron microscopy, while the top ones result from conventional light microscopy, after Giemsa staining. Nuclei are colored *blue*. Reprinted with permission from Rockefeller University Press (picture appeared on the cover page of J Exp Med, May 19, 2003)

accumulated in acidic intracellular compartments mainly in lysosomes (Fig. 10.3) (De Duve 1970; Nadanaciva et al. 2011).

Lysosomal trapping is governed by the large physiological pH gradient between ICF and lysosomes. The process of lysosomal trapping is saturable, energy-dependent (necessary for normal function of the H^+-ATPase), and requires cellular integrity (De Duve 1970; MacIntyre and Cutler 1988; Daniel and Wojcikowski 1999a). Weak bases in their un-ionized state permeate cellular and lysosomal membranes and accumulate in the acidic compartment of lysosomes (Fig. 10.4).

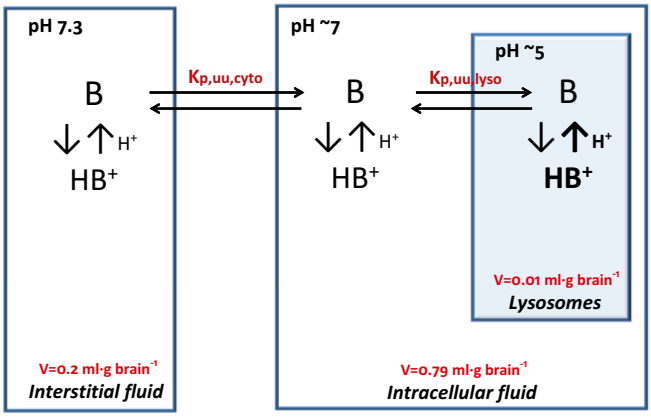

Fig. 10.4 Graphic illustration of the pH partitioning of a basic drug between extracellular and intracellular compartments, i.e., interstitial fluid, intracellular fluid, and lysosomes. Accumulation of the protonated form (HB^+) of the basic drug (B) in the compartments is driven by the physiological pH gradient. The cytosolic-to-interstitial fluid unbound drug concentration ratio ($K_{p,uu,cyto}$) and the lysosomic-to-cytosolic unbound drug concentration ratio ($K_{p,uu,lyso}$) can be estimated using a three-compartment pH partitioning model (Friden et al. 2011)

Diacidic bases are trapped more easily than monoacidic bases, with a subsequent impact on their distribution (MacIntyre and Cutler 1988). Because they are protonated within the lysosomes, the bases are not able to diffuse back into the cytosol (MacIntyre and Cutler 1988; Lloyd 2000; Kaufmann and Krise 2007). The intralysosomal concentrations of trapped compounds can reach high levels, with lysosome-to-cytosol accumulation ratios as high as 100:1 (Daniel and Wojcikowski 1997). Moreover, because the weak bases interact with phospholipids within the lysosome, the apparent lysosomal volume measured indirectly could be substantially greater than the physical (i.e., actual) lysosomal volume (MacIntyre and Cutler 1988; Duvvuri and Krise 2005). The physical volume of the lysosomes can also increase with time due to vesicle-mediated trafficking and fusion of lysosomes with the cell membrane (Kaufmann and Krise 2007; Logan et al. 2012).

Consequently, despite the very small physiological volume of the lysosomes (~0.01 mL g brain^{-1}), lysosomotropic compounds show extensive tissue accumulation (e.g., in lungs, liver, brain) which is reflected by a high apparent volume of distribution (Daniel and Wojcikowski 1999b). Moreover, lysosomal trapping can result in drug–drug interactions (Daniel et al. 1995; Daniel et al. 1998; Daniel and Wojcikowski 1999b; Daniel et al. 2000; Logan et al. 2012). For instance, because the process of lysosomal trapping is saturable, the lysosomal uptake of co-administered drugs could decline. All this suggests that lysosomal trapping is an important mechanism of drug distribution with potential impact on systemic PK.

Although brain tissue is not as lysosome-rich as the lungs, liver, and kidneys lysosomal trapping could also influence brain PK. Many marketed and novel neurotherapeutics are cationic amphiphilic compounds; it is thus not surprising that they

are lysosomotropic (Daniel 2003; Nadanaciva et al. 2011). Hence, it is recommended that particular attention be paid to lysosomotropism in CNS drug development programs.

Lysosomotropism is also interesting in that there are several lysosomal acidic hydrolases that may be useful pharmacological CNS targets (de Duve 1975; Boya and Kroemer 2008; Schultz et al. 2011). For instance, acid sphingomyelinase affects ceramide levels in several psychiatric and neurological disorders such as major depression, morphine antinociceptive tolerance, and Alzheimer's disease (Schwarz et al. 2008; Ndengele et al. 2009; He et al. 2010; Kornhuber et al. 2011). Inhibition of acid sphingomyelinase results in anti-apoptotic, proliferative, and anti-inflammatory effects. Consequently, functional acid sphingomyelinase inhibitors have potential in a number of new clinical therapies (Muehlbacher et al. 2012).

10.4.2.1 Compensation for pH Partitioning

Several researchers have suggested that lysosomal accumulation is a potential explanation for dissimilarities between in vitro (homogenates) and in vivo measurements when describing the distribution of acidic, neutral and basic drugs in tissues other than the brain (Harashima et al. 1984; Sawada et al. 1984; MacIntyre and Cutler 1988; Daniel and Wojcikowski 1997; Yokogawa et al. 2002; Maurer et al. 2005). For instance, it has been documented that predictions of the pharmacokinetic parameter apparent volume of distribution at steady state (V_{ss}) for 36 compounds, based on measurement of the unbound drug fraction in 15 different tissues, were less accurate for acidic and strongly basic substances (Berry et al. 2010). However, after making allowance for the ionic effects of tissue-to-blood pH gradients, the predictions for V_{ss} were accurate within a threefold range for 81 % of the compounds studied.

Inconsistencies between $C_{u,brainISF}$ values obtained using cerebral microdialysis and those projected from A_{brain} corrected for nonspecific binding using $f_{u,brain}$ for weak bases and acids are also thought to be linked to lysosomotropism (Friden et al. 2007). Lysosomotropism in brain tissue is also important when comparing brain slice and brain homogenate data (Friden et al. 2011).

The cell partitioning coefficient frequently deviates from unity. Intracellular accumulation as a result of the pH gradient is often suggested as one of the main reasons for the mismatch between the brain homogenate and brain slice data, i.e., $f_{u,brain} \neq 1/V_{u,brain}$. The lack of agreement is mainly due to the different properties of the two methods; cell and organelle membranes are retained in the slices, and pH differences are preserved. If the intracellular unbound drug concentration is similar to the brain ISF unbound drug concentration (i.e., $K_{p,uu,cell}$ is close to unity and $V_{u,brain}$ exceeding 1 mL g brain^{-1}) it can be assumed that intracellular nonspecific binding to membrane constituents is a major, quantitatively significant, distributional mechanism.

If only $K_{p,uu,brain}$ is of interest and brain homogenate data are used, the $f_{u,brain}$ values can be corrected to more in vivo-like values by compensating for pH partitioning according to the pKa of the drug (Friden et al. 2007; Friden et al. 2011).

A three-compartment (ISF, cytosol and lysosomes) pH partitioning model for $K_{p,uu,cell}$ based on the strong relationship between drug accumulation in acidic compartments due to lysosomal trapping and the pKa values of the compound has been developed (Fig. 10.4) (Friden et al. 2011). The starting point is described by (10.15):

$$K_{p,uu,cell} = V_{u,brain} \times f_{u,brain} = \frac{A_{brain}}{C_{u,brainISF}} \times f_{u,brain}. \tag{10.15}$$

The total amount of drug in the brain can be described as the sum of the total amounts in the ISF, the cytosol, and the lysosomes, denoted as A_{ISF}, A_{cyto}, and A_{lyso}, respectively. Each compartment is described by its physiological volume multiplied by the concentration of unbound drug in the compartment, divided by $f_{u,brain}$:

$$A_{brain} = A_{ISF} + A_{cyto} + A_{lyso} = \frac{V_{brainISF} \times C_{u,brainISF} + V_{cyto} \times C_{u,cyto} + V_{lyso} \times C_{u,lyso}}{f_{u,brain}}. \tag{10.16}$$

V_{ISF}, V_{cyto}, and V_{lyso} are the physiological volumes of the ISF (0.20 mL g brain^{-1}), cytosol (0.79 mL g brain^{-1}), and lysosomes (0.01 mL g brain^{-1}), respectively. $C_{u,cyto}$ and $C_{u,lyso}$ describe the unbound drug concentrations in cytoplasm and lysosomes, respectively. If (10.15) and (10.16) are combined, $K_{p,uu,cell}$, predicted from the three-compartment pH partition model, can be defined as:

$$K_{p,uu,cell} = V_{ISF} + K_{p,uu,cyto} \times \left(V_{cyto} + V_{lyso} \times K_{p,uu,lyso} \right). \tag{10.17}$$

Estimation of the cytosolic-to-interstitial fluid unbound drug concentration ratio ($K_{p,uu,cyto}$) and the lysosomic-to-cytosolic unbound drug concentration ratio ($K_{p,uu,lyso}$) can be computed by introducing the pKa values of the compounds (i.e., bases) in (10.18) and (10.19), respectively:

$$K_{p,uu,cyto} = \frac{C_{u,cyto}}{C_{u,brainISF}} = \frac{10^{pKa-pH_{cyto}} + 1}{10^{pKa-pH_{ISF}} + 1}, \tag{10.18}$$

$$K_{p,uu,lyso} = \frac{C_{u,lyso}}{C_{u,brain\ ISF}} = \frac{10^{pKa-pH_{lyso}} + 1}{10^{pKa-pH_{cyto}} + 1}, \tag{10.19}$$

where $pH_{cyto} = 7.06$, and $pH_{lyso} = 5.18$, as determined by Fridén and coworkers (Friden et al. 2011).

The main application of the pH partitioning model is related to $f_{u,brain}$, measured using the brain homogenate method. Based on pH partitioning, $V_{u,brain}$ ($1/f_{u,brain,corrected}$) can be estimated from $f_{u,brain}$ using (10.15), i.e., by dividing the calculated $K_{p,uu,cell}$ by $f_{u,brain}$ (10.17). As demonstrated after correction for pH partitioning, the discrepancy between brain homogenate and brain slice methods was practically abolished in a dataset consisting of 56 compounds (Friden et al. 2011). However, the pH partitioning model was still incapable of identifying and/or correcting other processes

governing the dissimilarities between the brain slice and homogenate methods, such as active uptake into the cells.

The three-compartment pH partitioning model can also be used for preliminary evaluation of $K_{p,uu,cell}$ and identification of potential lysosomotropic compounds already in the lead optimization phase. pKa values are frequently calculated in silico in the early discovery stages, and a critical approach is recommended since they may not reflect the real pKa values. pKa values measured at 25 °C can also diverge from actual in vivo values when using the pH partitioning model (Sun and Avdeef 2011). This can lead to some differences in experimental $K_{p,uu,cell}$ and computed $K_{p,uu,cell}$ values.

10.4.3 Intracerebral Distributional Patterns

Because of the physicochemical features and character of the pharmacological targets, the patterns of intracerebral distribution can differ for different drugs (Fig. 10.5). Thioridazine, salicylic acid, and gabapentin are used as model drugs and are discussed in detail in this section.

Figure 10.5a shows the intracerebral distribution of thioridazine. Thioridazine is a base, with a pKa of 8.9 and pronounced plasma and brain tissue binding mainly as a result of its high lipophilicity (ClogP 6.0). The experimental $f_{u,plasma,rat}$ is 0.002, and the $V_{u,brain}$ is around 3000 mL g brain^{-1}, the highest $V_{u,brain}$ observed so far (Friden et al. 2009a; Loryan et al. 2013). As a result, the determined $K_{p,brain}$ of 3.75 is significantly influenced by nonspecific binding to brain tissue and plasma proteins. The $K_{p,uu,brain}$ is 0.45 (Friden et al. 2009b). *Lysosomal trapping* is the main reason for thioridazine accumulating in the cells. When the intracellular compartment is viewed as 1 U, there is a 2.24-fold higher intracellular concentration of unbound thioridazine than in the brain ISF. Moreover, because of the presence of the physiological pH gradient, thioridazine as a base accumulates in the cytosol and then becomes trapped in the acidic intracellular compartments (Fig. 10.5b). The calculations (10.19) indicate that, when the cytosolic compartment is separated from the lysosomal compartment, thioridazine will reach a 75-fold higher intralysosomal than cytosolic concentration. This type of distribution could be considered as a *signature pattern* for basic compounds.

Acidic compounds such as salicylic acid (see Fig. 10.5c) have a different distribution pattern in the brain. Only 19 % of the unbound salicylic acid in the plasma crosses the BBB ($K_{p,uu,brain} = 0.19$). Moreover, about 60 % of the unbound salicylic acid in brain ISF equilibrates across the cellular barrier. Using the three-compartment pH partitioning model (Fig. 10.5d), it is possible to describe the unbound cytosolic and lysosomal partitioning coefficients and identify a lysosomal exclusion phenomenon ($K_{p,uu,lyso} = 0.015$).

Active carrier mediated transport into the cells is an alternative process which can be observed at the cellular barrier. Gabapentin provides a classic example of a compound lacking any nonspecific binding to brain tissue ($f_{u,brain} = 1$) while at the

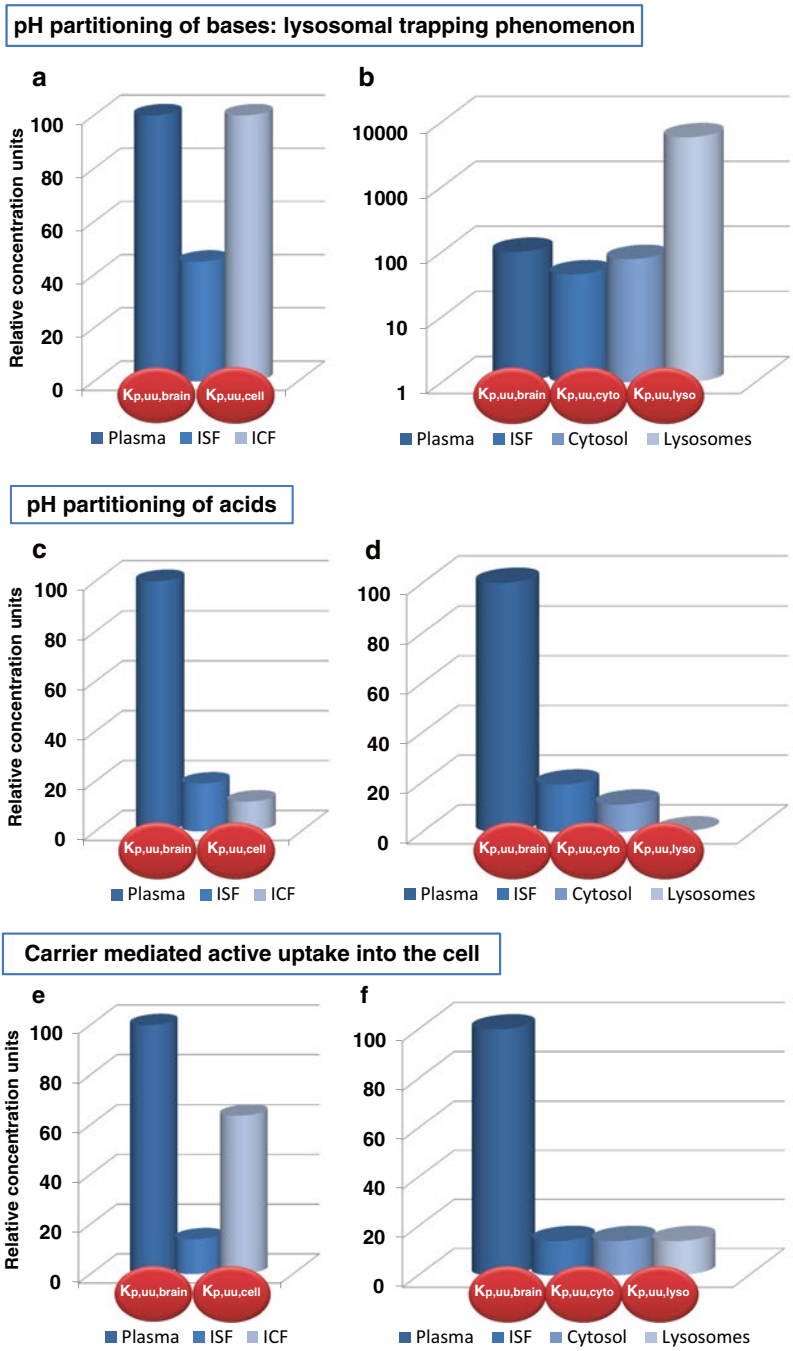

Fig. 10.5 The intracerebral unbound drug distribution patterns of prototypical drugs ((**a**) and (**b**) thioridazine; (**c**) and (**d**) salicylic acid; (**e**) and (**f**) gabapentin). The distributional pattern depends on both the physicochemical properties of the compound and the functional characteristics of the

same time exhibiting active uptake into the cells (Fig. 10.5e). Due to the active passage of gabapentin into the cells by the L-α-amino acid transporter (Su et al. 1995), it reaches nearly fivefold higher intracellular concentrations on average. Additional examples of compounds undergoing active cellular uptake include 1-methyl-4-phenylpyridinium (MPP, $K_{p,uu,cell} = 77$) and tetra-ethylammonium (TEA, $K_{p,uu,cell} = 8.95$) (Friden et al. 2011).

Because of the practical value of $K_{p,uu,cell}$ and its further division into $K_{p,uu,lyso}$ and $K_{p,uu,cyto}$, it is highly recommended that the unbound drug intracellular-to-extracellular concentration ratio be assessed in DMPK studies. Estimated neuroPK parameters are important contributors to the evaluation of the intracerebral distribution pattern of NCEs and their possible side effects.

10.5 Combination of in Vivo Infusion with Brain Slice or Homogenate to Estimate $K_{p,uu,brain}$

$K_{p,brain}$ estimated under steady-state conditions or using the area under the concentration–time curves in brain tissue ($AUC_{tot,brain}$) and plasma ($AUC_{tot,plasma}$) after a single dose (10.20) has historically been recognized as a driving force in CNS drug discovery screening programs (Pardridge 1989; Ghose et al. 1999; Ghose et al. 2012) (see Chap. 5 for an explanation of the doctrines of brain PK and Chap. 12 for a comprehensive review of old and new paradigms for assessing CNS penetration in drug discovery programs).

$$K_{p,brain} = \frac{A_{brain}}{C_{tot,plasma}} = \frac{AUC_{tot,brain}}{AUC_{tot,plasma}} \tag{10.20}$$

Fig. 10.5 (continued) compartments and membranes, defined by $K_{p,uu,brain}$ and $K_{p,uu,cell}$. The graphs were constructed from data in Fridén et al. (Friden et al. 2007; Friden et al. 2011). The unbound drug plasma concentration is set at 100 arbitrary units. (**a**) shows the efflux of thioridazine at the BBB ($K_{p,uu,brain} = 0.45$) and its accumulation in the cells as described by a $K_{p,uu,cell}$ of 2.24. Because thioridazine is a weak base with a pKa of 8.9, it is subject to lysosomal trapping and accumulation in the cells. The pH partitioning of thioridazine (**b**) is described by the unbound-thioridazine cytosolic ($K_{p,uu,cyto} = 1.72$) and lysosomal ($K_{p,uu,lyso} = 75$) partition coefficients computed using the three-compartment pH partitioning model. C and D demonstrate the distribution and pH partitioning of salicylic acid. Salicylic acid is poorly transported across the BBB ($K_{p,uu,brain} = 0.19$) and has reduced cellular penetration ($K_{p,uu,cell} = 0.62$). Moreover, as an acid (pKa 4.3), salicylic acid has limited distribution in brain tissue ($V_{u,brain} = 1$ mL g brain^{-1}). The pH partitioning model (D) supports the suggestion that salicylic acid is mainly distributed in the cytosol ($K_{p,uu,cyto} = 0.58$) and is almost completely absent from acidic compartments such as lysosomes ($K_{p,uu,lyso} = 0.015$). E and F represent the zwitterion gabapentin. Gabapentin transport in the BBB is restricted ($K_{p,uu,brain} = 0.14$). However, after passing the BBB, it is excessively accumulated in the cells ($K_{p,uu,cell} = 4.55$). The pH partitioning model is, however, incapable of identifying its uptake in the cells since the uptake is not related to lysosomal accumulation. Gabapentin is a substrate of the L-type amino acid transporter, which explains the observed active uptake into the cells (Wang and Welty 1996; Friden et al. 2011)

The identification and selection of drug candidates with "acceptable brain penetration" has typically been based on predefined cutoff values for $K_{p,brain}$ (BB or often logBB); however, these vary between groups/companies. For instance, logBB = 0.3 ($K_{p,brain} = 2$) has often been used as the cutoff point for NCE penetration of the BBB (Reichel 2006). Another approach uses an arbitrary cutoff point for $K_{p,brain}$ of greater than unity (Kalvass et al. 2007a; Padowski and Pollack 2011a). At Eli Lilly research laboratories, the cutoff point for $K_{p,brain}$, determined using a mouse brain uptake assay, was 0.3 (30 %) (Raub et al. 2006). Alternatively, substances with $K_{p,brain}$ values higher than 0.04 (determined using brain tissue with residual blood) have been considered "brain penetrants" by some, since this value exceeds the cerebral blood volume, approximated as 4 % of the total brain volume (Hitchcock and Pennington 2006; Shaffer 2010). Basically, higher $K_{p,brain}$ values have frequently been considered to be favorable for CNS penetration (Young et al. 1988; Pardridge 1989; Ghose et al. 1999; Ghose et al. 2012; Segall 2012). Despite the fact that it has been found to be inadequate for evaluation of the transport of drugs across the BBB and to be by no means foolproof, this type of "taxonomy" has been common practice in the pharmaceutical industry.

However, off-target binding of drug to plasma and brain tissues irrefutably masks the actual BBB net flux (see Chaps. 5, 11, and 12 for more detailed explanations). Currently, driven by abundant evidence supporting the "free-drug hypothesis," $K_{p,uu,brain}$ (also called $K_{p,free}$) is replacing $K_{p,brain}$.

Several scientists have tried to differentiate between the two main components of $K_{p,brain}$, i.e., nonspecific binding to tissues and free (unbound) drug (Lin et al. 1982; Kalvass and Maurer 2002; Mano et al. 2002; Maurer et al. 2005; Gupta et al. 2006; Summerfield et al. 2006; Friden et al. 2007; Hammarlund-Udenaes et al. 2008; Liu et al. 2009a). For instance, Becker and Liu categorize the ratio of $f_{u,plasma}$ to $f_{u,brain}$ as an "intrinsic" partition coefficient between brain and plasma ($K_{p,in}$) which could be considered a descriptor of nonspecific binding in brain and plasma (Becker and Liu 2006). It is, however, essential to bear in mind that $K_{p,in}$ and $K_{p,uu,brain}$ describe different properties of the compound, where $K_{p,in}$ describes the ratio of the binding properties without including BBB transport (if there is no observed active transport, $K_{p,brain} = K_{p,in}$), and $K_{p,uu,brain}$ specifically defines the BBB transport of unbound drug. $K_{p,in}$ cannot therefore be used to assess the $K_{p,uu,brain}$ of NCEs.

Alternative approaches to the use of microdialysis for determining $K_{p,uu,brain}$ that are based on the co-estimation of $K_{p,brain}$ and nonspecific binding to plasma and brain tissues have been established (Gupta et al. 2006; Friden et al. 2007; Hammarlund-Udenaes et al. 2008; Hammarlund-Udenaes et al. 2009). Hence, $f_{u,plasma}$ can be used to correct $C_{tot,plasma}$ (binding to formal elements of the blood is excluded):

$$C_{u,plasma} = C_{tot,plasma} \times f_{u,plasma}. \tag{10.21}$$

Correspondingly, $V_{u,brain}$ (mL g brain^{-1}) or $f_{u,brain}$ corrected for pH partitioning ($f_{u,brain,corrected}$) is used to estimate $C_{u,brainISF}$ (μmol g brain^{-1}):

$$C_{\text{u,brainISF}} = \frac{A_{\text{brain}}}{V_{\text{u,brain}}} = A_{\text{brain}} \times f_{\text{u,brain,corected}}. \tag{10.22}$$

Accordingly, $K_{p,uu,brain}$ can be derived from (10.20) as:

$$K_{\text{p,uu,brain}} = \frac{K_{\text{p,brain}}}{V_{\text{u,brain}} \times f_{\text{u,plasma}}} \approx \frac{K_{\text{p,brain}}}{\frac{1}{f_{\text{u,brain,corrected}}} \times f_{\text{u,plasma}}}. \tag{10.23}$$

Because this method (10.23) is based on several individually determined parameters obtained using various techniques, the level of uncertainty and variability in the final $K_{p,uu,brain}$ estimates is increased. Therefore, reduction of the potential uncertainty in each measurement ($K_{p,brain}$, $V_{u,brain}$, $f_{u,brain}$, $f_{u,plasma}$) will make assessment of the brain partitioning coefficient for unbound drug more secure in drug discovery. Some critical steps in determining the brain partitioning coefficient for total drug, required for assessment of $K_{p,uu,brain}$, are described below.

Ideally, the brain partitioning coefficient would be determined using steady-state total brain and plasma concentrations after constant-rate intravenous infusion (Friden et al. 2009b; Hammarlund-Udenaes et al. 2009). However, in drug discovery and development setups, intravenous infusions can be challenging and consequently are often not an option. Alternatively, $K_{p,brain}$ can be determined as the $AUC_{tot,brain}/AUC_{tot,plasma}$ ratio (10.20), using various time points (up to five animals per time point) after a single (discrete) dose. In fact, subcutaneous administration is most commonly used, because it decreases the inter-experimental variability, mainly as a result of the compounds circumventing oral absorption and first-pass metabolism. In some cases, $K_{p,brain}$ is assessed using total brain and plasma concentrations obtained at a specific point in time after drug administration. However, this approach has been heavily criticized since it is known that $K_{p,brain}$ is a time-dependent parameter. In this regard, Padowski and Pollack have suggested the use of different notations of $K_{p,brain}$ with the intention of specifying the conditions under which brain exposure has been determined, i.e., $K_{p,brain,t}$ (single time point), $K_{p,brain,DE}$ (distributional equilibrium reached), and $K_{p,brain,SS}$ (in a steady-state system) (Padowski and Pollack 2011a). These researchers have also used a simulation approach to study the links between $K_{p,brain,t}$ with a sampling time prior to the point of distribution equilibrium, and the experimentally obtained $K_{p,brain}$ in the presence vs. absence of P-gp efflux transport. In some cases, an initial overshoot or increase in $K_{p,brain,t}$ values was followed by a decline to a value which remained constant with time. Consequently, it was concluded that the P-gp effect estimated based on a $K_{p,brain}$ value prior to reaching distribution equilibrium could be significantly inaccurate. The experimental design will thus greatly influence the conclusions made. The simulations also indicated that assessment of the P-gp effect was more precise and less variable with intravenous constant-rate infusions than with bolus administration, i.e., $K_{p,brainSS}$ was the most appropriate choice (Gibaldi 1969; Padowski and Pollack 2011b). Although the proposed ranking of these parameters certainly introduces clarity and flags the

importance of potential time-dependent differences in BBB equilibration, it has not been followed up in practice to any great extent.

The correlation between $K_{p,brain}$ derived from a single (discrete) dose and that derived at steady-state has also been investigated in an attempt to improve throughput in neuroPK studies in the industrial setting. For instance, $K_{p,brain}$ values derived from a single dose differed maximally 2.5-fold from the steady-state values for eight of the nine commercial and two proprietary compounds tested (>2.5-fold for thiopental) (Liu et al. 2009a; Doran et al. 2012). These results give the impression that the single-dose approach, which is more time-efficient, may not compromise data quality to any great extent.

Another approach, which was introduced with the intention of reducing the use of animals and improving the efficiency of investigations into CNS exposure in drug discovery programs, uses a mixture of up to five NCEs administered together, termed a *cocktail*, *cassette* or *Nin1* (Manitpisitkul and White 2004; Friden et al. 2009b; Liu et al. 2012). Liu and colleagues investigated the brain partitioning coefficients of 11 model compounds using discrete and cassette dosing and discovered that drug–drug interactions at the BBB level are unlikely at these low subcutaneous cassette doses (Liu et al. 2012). Nevertheless, it is advisable to administer low doses of the drugs during the experiment to prevent any interactions at the BBB as well as potential side effects. Overall, the route and duration of administration, the dose (discrete or cassette dosing), and the brain and plasma tissue sampling times should be critically evaluated prior to the experiment to avoid potential pitfalls.

Methods for correcting the residual blood in the sampled brain tissue also need to be considered. Using $V_{u,brain}$ to determine $K_{p,uu,brain}$, Fridén et al. showed that the literature values for V_{blood} may be too high when used for correcting A_{brain} for the residual blood (Friden et al. 2010). This was especially observed for drugs with low $K_{p,brain}$ values. A low $K_{p,brain}$ value can be caused by either very efficient efflux at the BBB or plasma protein binding that greatly exceeds the nonspecific binding of the drug in the brain. The latter becomes a problem when using a value for V_{blood} that is too high. An improved method has been developed for this estimation (Friden et al. 2010). It should be noted that the remaining brain vascular space varies with the method used to sacrifice the animal.

The correction for residual blood can be calculated from the effective plasma space in the brain for a given drug, V_{eff}, which in turn can be calculated from the measured plasma protein binding according to:

$$V_{\text{eff}} = f_{\text{u,plasma}} \times V_{\text{water}} + \left(1 - f_{\text{u,plasma}}\right) \times V_{\text{protein}}. \tag{10.24}$$

V_{water} and $V_{protein}$ in rat brain capillary blood have been estimated as 7.99 μL g brain^{-1} and 10.3 μL g brain^{-1}, respectively (Friden et al. 2010). This equation can be used when binding to blood elements is not significant. The amount of drug in brain tissue excluding the capillary contents, A_{brain}, can be calculated as:

$$A_{\text{brain}} = \frac{C_{\text{tot,brain}} - V_{\text{eff}} \times C_{\text{tot,plasma}}}{1 - V_{\text{water}}}. \tag{10.25}$$

$C_{tot,brain}$ is the concentration of drug in the whole brain tissue sample and $C_{tot,plasma}$ is the drug concentration in a regular (arterial) plasma sample. The total physical volume of residual blood in the rat brain after exsanguination by severing the heart has been estimated as 12.7 μL g brain^{-1} (Friden et al. 2010).

The complexity of the processes governing the drug concentrations in the brain requires the input of several methods, each providing a defined piece of the information required to assemble a more in-depth picture of drug disposition in the CNS. Using this combined approach, it is possible in the early drug-development phases to map the concentrations of unbound drug in the main pharmacokinetic compartments relevant to drug disposition in the brain, such as plasma, ISF, ICF (and if necessary lysosomes) and CSF. The compartments and relevant concentration relationships are illustrated in Fig. 10.6, using the atypical antidepressant bupropion as a model.

The main benefit of this mapping approach is the visualization and better understanding of the target-site PK. Additionally, it allows ranking of the compounds based on the target-compartment unbound drug concentration normalized by the PD parameters (EC50, IC50, Ki, etc.) as well as in the design of new PKPD studies.

10.6 Translational Aspects of the Methods

In the drug discovery process, in vitro assays and preclinical animal studies are widely used to evaluate the potency of NCEs and to identify candidates that may have desirable clinical responses.

However, when there is no correlation between in vivo and in vitro potencies, the validity of the in vitro assay, the animal model, and the target can be questioned (Brunner et al. 2012). Translational science is the study of the extrapolation of experimental findings to clinical solutions. It is important to improve the proficiency of clinical trial design by planning clinical doses based on nonclinical results. Animal brain PK studies are a routine tool for predicting drug behavior in humans. Thus far, it has been extremely challenging to master the translation of in vitro-to-in vivo and animal-to-human data in the drug discovery process, primarily because of the shortage of supportive data and the underlying multiple assumptions. Some translational aspects linked to methodologies described in this chapter are discussed below.

10.6.1 Translational Aspects of Brain Tissue Binding Assays

It is important to estimate the cerebral concentrations of unbound neurotherapeutic drugs in various species and related these to the potential CNS activity and target engagement of the drugs in preclinical and clinical PK studies. The $f_{u,brain}$ of drug candidates is routinely determined in several species to account for possible species dependence, as is the case with plasma protein binding, although this does not fit

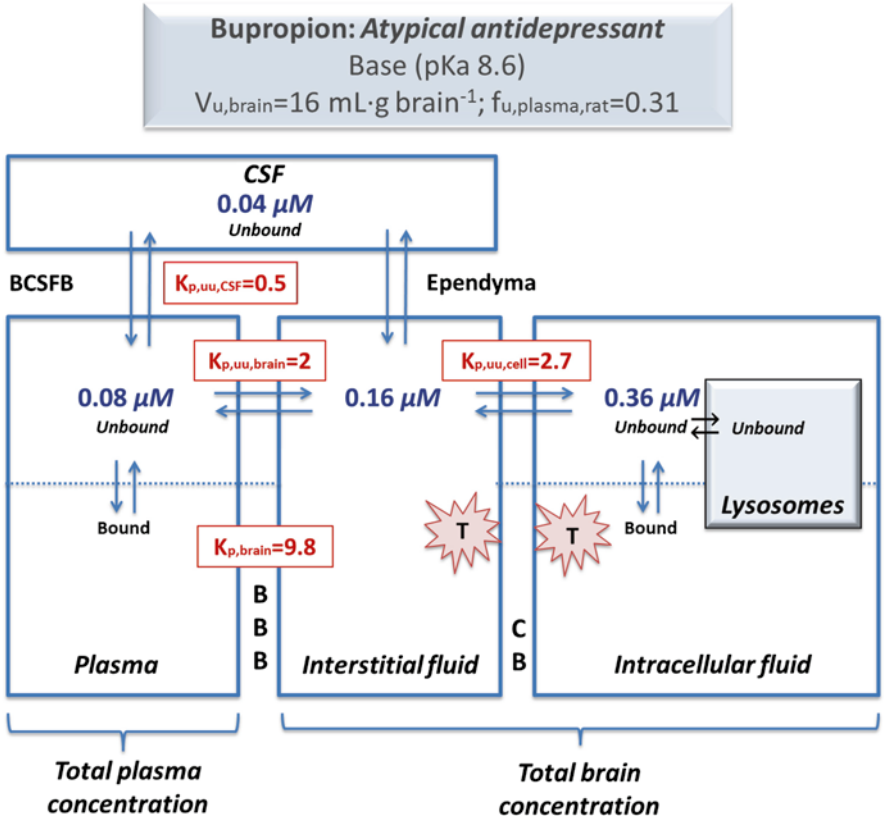

Fig. 10.6 Schematic representation of the distribution of a drug, here exemplified by the atypical antidepressant bupropion, into the different compartments (plasma, brain ISF, brain ICF, lysosomes, and CSF) involved in the disposition of drugs across the barriers (BBB, CB, and BCSFB), with the resulting concentrations obtained in each compartment. T represents the possible target sites of the drug, facing either the ISF or the ICF. The graph was constructed using steady-state total plasma, total brain, and CSF concentration determinations in rats after a 4 h constant-rate intravenous infusion of bupropion 2 µmol kg h^{-1} (Friden et al. 2009b). Using this model and given the unbound drug plasma concentration, it is possible to estimate the target site concentrations. This approach can be used in drug discovery programs for establishing the link between the PK and engagement of the target. The $K_{p,uu,CSF}$ is quite different from the $K_{p,uu,brain}$ for bupropion, which means that estimations of the target site concentrations will be less valuable if based on CSF measurements

with experimental results demonstrating that brain tissue binding is less sensitive to interspecies dissimilarities than plasma protein binding (Summerfield et al. 2007; Wan et al. 2009; Read and Braggio 2010). In fact, when Di et al. evaluated the degree and nature of potential species differences in brain tissue binding, they found that brain tissue binding is species independent (Di et al. 2011). This finding was very beneficial for translational medicine because it meant that a single representative species such as the rat could replace multispecies determinations of $f_{u,brain}$.

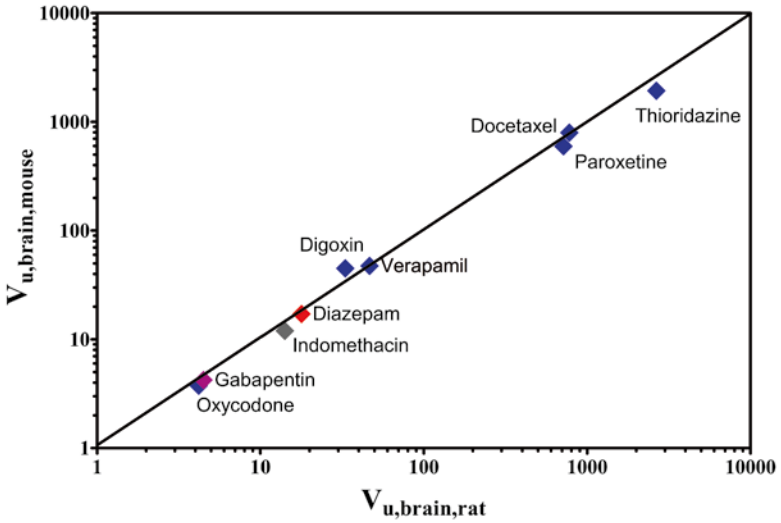

Fig. 10.7 Relationship between rat (*x*-axis) and mouse (*y*-axis) brain slices for estimation of the volume of distribution of unbound drug in the brain of ten compounds ($V_{u,brain}$; mL g brain^{-1}). The *solid line* represents the line of identity. The color of the *diamonds* represents the ion class of the compound (bases: thioridazine, docetaxel, paroxetine, verapamil, digoxin, oxycodone; neutral: diazepam; acid: indomethacin; zwitterion: gabapentin). Constructed from data in Loryan et al. (Loryan et al. 2013)

Laboratory studies have not found any significant dissimilarities in estimated $V_{u,brain}$ values from fresh brain slices between Sprague-Dawley rats and NMRI mice (Fig. 10.7). However, more systematic investigations are required to support the possibility of the interchangeable use of $V_{u,brain}$ measurements for translational studies.

10.6.2 Translational Aspects of Brain Exposure Assessment

In the drug industry, the translation of drug tissue distribution data between species is grounded on the assumption that the tissue-to-plasma drug partitioning coefficient for passive transport is tissue- and species-independent. However, the available information in the literature supports the existence of interspecies differences in the lipid composition of the tissues, which is considered to be the main factor in drug binding to tissues (Rouser et al. 1969; Simon and Rouser 1969). Elaborate investigation of tissue lipid composition with regard to drug distribution in dogs and rats has demonstrated clear differences between the animals; for example the proportion of neutral lipids was fivefold lower in dog brain than in rat brain (Rodgers et al. 2012). The authors suggested that the assumption of constancy in

tissue-to-plasma partitioning should be used with caution when species-specific tissue distribution is of interest. Nevertheless, based on a widely accepted measure of prediction that describes the number of compounds that fall within a twofold to threefold range, various groups have demonstrated the reliability of rodent-derived PK parameters for predicting BBB net flux in humans and large animals, although this has mainly been for compounds with predominantly passive transport (Friden et al. 2009b; Di et al. 2012a; Doran et al. 2012; Kielbasa and Stratford 2012; Westerhout et al. 2012). For instance, Doran and colleagues showed that preclinical rat-derived neuroPK parameters, particularly $K_{p,uu,brain}$, can be used to extrapolate $C_{u,brainISF}$ in dogs and nonhuman primates for freely permeating non-P-gp substrates (Doran et al. 2012). In contrast, prediction of $C_{u,brainISF}$ for P-gp substrates such as risperidone and 9-hydroxyrisperidone using a similar approach was significantly flawed, with under-prediction of $K_{p,uu,brain}$ in dogs and nonhuman primates from rat-derived data. Reports describing species differences in brain exposure measurements have also been documented (Dagenais et al. 2001; Syvanen et al. 2008; Syvanen et al. 2009; Bundgaard et al. 2012a).

Issues related to the disequilibrium of drug concentrations at the BBB make it difficult to rank the importance of the PK parameters for the translation. Consequently, it is critical to assess the extent of human BBB transport and evaluate the potential impact of the degree of asymmetry on brain exposure in relation to target engagement or pharmacological activity early in drug discovery and development programs. The main reason for the observed asymmetry in BBB equilibration is the species-specific presence of efflux and influx transporters (see Chap. 2 and 3 for an overview of BBB transporters and pharmacoproteomics). There is no doubt that P-gp is one of the most important efflux transporters at the BBB (Tsuji et al. 1992; Tsuji et al. 1993; Terasaki and Hosoya 1999; Demeule et al. 2002; Mizuno et al. 2003; Lin 2004; Syvanen et al. 2008; Kodaira et al. 2011; Uchida et al. 2011a; Agarwal et al. 2012). However, the relative importance of P-gp in humans and rats was questioned after the breast cancer resistance protein (BCRP) was found to be the most abundant protein expressed in the human BBB (Uchida et al. 2011b). Nonetheless, cell lines transfected with human transporters, mostly only P-pg, are often used in lead optimization and candidate selection in the preclinical phases of drug discovery (see Chap. 6 for a comprehensive overview of cell culture models of the BBB). Transporter knockout animals or chemically "knocked-out" animals (i.e., after administration of P-gp or BCRP inhibitors) are used in drug discovery projects (see Chap. 7 for an exploration of in situ and in vivo animal models and Chap. 12 for the current thinking on this topic in the drug industry). Regardless of the "solid" status of in vitro and in vivo P-gp assays in drug discovery, both the rationale of the applied methods and the interpretation of the obtained results are debatable. Overall, it remains challenging to predict the BBB net flux of potential transporter substrates from rodent data. Consequently, due to the lack of translational knowledge the recommendation not to advance efflux transporter substrates is often promoted in the drug industry (Di et al. 2012a).

10.7 Current Status and Future Directions

Notwithstanding immense progress in the understanding of drug delivery to the brain and improved screening cascades in drug discovery programs, the clinical success rate for novel neurotherapeutics is exceptionally low at present. The approaches to the selection and optimization of compounds with sufficient delivery to the brain in drug discovery are currently stereotypical, high-throughput methods in most pharmaceutical companies. The complications associated with the measurement of active-site concentrations for potential CNS drugs have made surrogate methodologies (such as the assessment of brain ISF drug concentrations using matrices such as CSF and plasma) popular. There have been advancements in methodologies related to the assessment of $C_{u,brainISF,}$ making it easier to measure the actual value rather than a surrogate. The use of the CSF as a relevant surrogate for $C_{u,brainISF}$ has been extensively investigated to support the rationale of its use in drug discovery (de Lange and Danhof 2002; de Lange et al. 2005; Liu et al. 2006; Lin 2008; Friden et al. 2009b; Liu et al. 2009a; Di et al. 2012a; de Lange 2013b). Issues related to the sampling of CSF and interpretations of the data are discussed in Chaps. 5 and 9. However, despite the progress made, problems related to the veracity of the predicted values remain. It is important to remember that "you get what you measure" (Elebring et al. 2012), meaning that the definitions of the parameters and/or appropriate surrogates including critical interpretation are crucial.

The establishment of a PKPD stage very early in drug development is a great advance for drug discovery (Chap. 9) (Westerhout et al. 2011). Strategies to minimize neurotoxicity for non-CNS compounds are also of great interest (Wager et al. 2012). Exploration of the potential of mathematical modeling, particularly physiologically based PKPD modeling in drug discovery programs, will facilitate better understanding of the BBB transport of small molecules.

The role of the efflux and influx transporters and their potential interactions require investigation to provide further insight into active BBB transport. We need to learn how to incorporate our knowledge of proteomics into drug transport modeling. Advancements in our understanding of pathological conditions (Part V) and their influences on the most important neuroPK parameters ($K_{p,uu,brain}$, $V_{u,brain}$ and $K_{p,uu,cell}$) will also improve the translational aspects of drug discovery.

10.8 Points for Discussion (Questions)

- What are the conceptual differences between the brain homogenate and brain slice methods?
- What allows the combination of the brain homogenate and brain slice methods to approximate the cellular unbound drug partitioning coefficient?
- Discuss the driving forces of BBB and CB drug transport.

- What is the physiological basis and pharmacokinetic impact of lysosomotropism for basic compounds?
- How can information about whether the compound is lysosomotropic influence the drug discovery and development processes?
- What are the pros and cons of using cutoff values for $K_{p,uu,brain}$ in relation to evaluation of drug target engagement?
- Which neuroPK parameters are critical for translational medicine?
- Discuss the impact of the threefold difference cutoff point for methods in drug discovery.
- In which phase of drug discovery is it best to investigate the BBB transport and brain drug distribution of NCEs?

References

Abbott NJ (2004) Evidence for bulk flow of brain interstitial fluid: significance for physiology and pathology. Neurochem Int 45(4):545–552

Abbott NJ, Patabendige AA, Dolman DE, Yusof SR, Begley DJ (2010) Structure and function of the blood–brain barrier. Neurobiol Dis 37(1):13–25

Abraham MH (2011) The permeation of neutral molecules, ions, and ionic species through membranes: brain permeation as an example. J Pharm Sci 100(5):1690–1701

Agarwal S, Uchida Y, Mittapalli RK, Sane R, Terasaki T, Elmquist WF (2012) Quantitative proteomics of transporter expression in brain capillary endothelial cells isolated from P-gp, BCRP, and P-gp/BCRP knockout mice. Drug Metab Dispos 40(6):1164–9

Banker MJ, Clark TH, Williams JA (2003) Development and validation of a 96-well equilibrium dialysis apparatus for measuring plasma protein binding. J Pharm Sci 92(5):967–974

Bean JW, Sargent DF, Schwyzer R (1988) Ligand/receptor interactions–the influence of the microenvironment on macroscopic properties. Electrostatic interactions with the membrane phase. J Recept Res 8(1–4):375–389

Becker S, Liu X (2006) Evaluation of the utility of brain slice methods to study brain penetration. Drug Metab Dispos 34(5):855–861

Begley DJ (1996) The blood–brain barrier: principles for targeting peptides and drugs to the central nervous system. J Pharm Pharmacol 48(2):136–146

Begley DJ (2004) Delivery of therapeutic agents to the central nervous system: the problems and the possibilities. Pharmacol Ther 104(1):29–45

Bendayan R, Lee G, Bendayan M (2002) Functional expression and localization of P-glycoprotein at the blood brain barrier. Microsc Res Tech 57(5):365–380

Benkwitz C, Liao M, Laster MJ, Sonner JM, Eger EI 2nd, Pearce RA (2007) Determination of the EC50 amnesic concentration of etomidate and its diffusion profile in brain tissue: implications for in vitro studies. Anesthesiology 106(1):114–123

Berry LM, Roberts J, Be X, Zhao Z, Lin MH (2010) Prediction of V(ss) from in vitro tissue-binding studies. Drug Metab Dispos 38(1):115–121

Blasberg R, Levi G, Lajtha A (1970) A comparison of inhibition of steady state, new transport, and exchange fluxes of amino acids in brain slices. Biochim Biophys Acta 203(3):464–483

Bostrom E, Simonsson US, Hammarlund-Udenaes M (2006) In vivo blood–brain barrier transport of oxycodone in the rat: indications for active influx and implications for pharmacokinetics/pharmacodynamics. Drug Metab Dispos 34(9):1624–1631

Bouw MR, Xie R, Tunblad K, Hammarlund-Udenaes M (2001) Blood–brain barrier transport and brain distribution of morphine-6-glucuronide in relation to the antinociceptive effect in rats–pharmacokinetic/pharmacodynamic modelling. Br J Pharmacol 134(8):1796–1804

Boya P, Andreau K, Poncet D, Zamzami N, Perfettini JL, Metivier D, Ojcius DM, Jaattela M, Kroemer G (2003) Lysosomal membrane permeabilization induces cell death in a mitochondrion-dependent fashion. J Exp Med 197(10):1323–1334

Boya P, Kroemer G (2008) Lysosomal membrane permeabilization in cell death. Oncogene 27(50):6434–6451

Brunner D, Balci F, Ludvig EA (2012) Comparative psychology and the grand challenge of drug discovery in psychiatry and neurodegeneration. Behav Processes 89(2):187–195

Bundgaard C, Jensen CJ, Garmer M (2012a) Species comparison of in vivo P-glycoprotein-mediated brain efflux using mdr1a-deficient rats and mice. Drug Metab Dispos 40(3):461–466

Bundgaard C, Jorgensen M, Mork A (2007) An integrated microdialysis rat model for multiple pharmacokinetic/pharmacodynamic investigations of serotonergic agents. J Pharmacol Toxicol Methods 55(2):214–223

Bundgaard C, Sveigaard C, Brennum LT, Stensbol TB (2012b) Associating in vitro target binding and in vivo CNS occupancy of serotonin reuptake inhibitors in rats: the role of free drug concentrations. Xenobiotica 42(3):256–265

Chesney MA, Perouansky M, Pearce RA (2003) Differential uptake of volatile agents into brain tissue in vitro. Measurement and application of a diffusion model to determine concentration profiles in brain slices. Anesthesiology 99(1):122–130

Collingridge GL (1995) The brain slice preparation: a tribute to the pioneer Henry McIlwain. J Neurosci Methods 59(1):5–9

Cserr HF, Patlak CS (1992) Secretion and bulk flow of interstitial fluid. In: Bradbury MWB (ed) Physiology and pharmacology of the blood–brain barrier. Springer, Berlin, pp 245–261

Dagenais C, Zong J, Ducharme J, Pollack GM (2001) Effect of mdr1a P-glycoprotein gene disruption, gender, and substrate concentration on brain uptake of selected compounds. Pharm Res 18(7):957–963

Daniel WA (2003) Mechanisms of cellular distribution of psychotropic drugs. Significance for drug action and interactions. Prog Neuropsychopharmacol Biol Psychiatry 27(1):65–73

Daniel WA, Bickel MH, Honegger UE (1995) The contribution of lysosomal trapping in the uptake of desipramine and chloroquine by different tissues. Pharmacol Toxicol 77(6):402–406

Daniel WA, Syrek M, Haduch A, Wojcikowski J (1998) Pharmacokinetics of phenothiazine neuroleptics after chronic coadministration of carbamazepine. Pol J Pharmacol 50(6):431–442

Daniel WA, Syrek M, Haduch A, Wojcikowski J (2000) Different effects of amitriptyline and imipramine on the pharmacokinetics and metabolism of perazine in rats. J Pharm Pharmacol 52(12):1473–1481

Daniel WA, Wojcikowski J (1997) Contribution of lysosomal trapping to the total tissue uptake of psychotropic drugs. Pharmacol Toxicol 80(2):62–68

Daniel WA, Wojcikowski J (1999a) Lysosomal trapping as an important mechanism involved in the cellular distribution of perazine and in pharmacokinetic interaction with antidepressants. Eur Neuropsychopharmacol 9(6):483–491

Daniel WA, Wojcikowski J (1999b) The role of lysosomes in the cellular distribution of thioridazine and potential drug interactions. Toxicol Appl Pharmacol 158(2):115–124

Davson H, Hollingsworth G, Segal MB (1970) The mechanism of drainage of the cerebrospinal fluid. Brain 93(4):665–678

Davson H, Segal MB (1995) Physiology of the CSF and blood–brain barriers. CRC Press, Boca Raton, USA

de Boer AG, Gaillard PJ (2007) Drug targeting to the brain. Annu Rev Pharmacol Toxicol 47:323–355

De Duve C (1970) The role of lysosomes in cellular pathology. Triangle 9(6):200–208

De Duve C (1971) Tissue fractionation. Past and present. J Cell Biol 50(1):20d–55d

de Duve C (1975) The role of lysosomes in the pathogeny of disease. Scand J Rheumatol Suppl 12:63–66

de Lange EC (2013a) The mastermind approach to CNS drug therapy: translational prediction of human brain distribution, target site kinetics, and therapeutic effects. Fluids Barriers CNS 10(1):12

de Lange EC (2013b) Utility of CSF in translational neuroscience. J Pharmacokinet Pharmacodyn 40(3):315–26
de Lange EC, Danhof M (2002) Considerations in the use of cerebrospinal fluid pharmacokinetics to predict brain target concentrations in the clinical setting: implications of the barriers between blood and brain. Clin Pharmacokinet 41(10):691–703
de Lange EC, de Boer BA, Breimer DD (1999) Microdialysis for pharmacokinetic analysis of drug transport to the brain. Adv Drug Deliv Rev 36(2–3):211–227
de Lange EC, Ravenstijn PG, Groenendaal D, van Steeg TJ (2005) Toward the prediction of CNS drug-effect profiles in physiological and pathological conditions using microdialysis and mechanism-based pharmacokinetic-pharmacodynamic modeling. AAPS J 7(3):E532–543
Demeule M, Regina A, Jodoin J, Laplante A, Dagenais C, Berthelet F, Moghrabi A, Beliveau R (2002) Drug transport to the brain: key roles for the efflux pump P-glycoprotein in the blood–brain barrier. Vascul Pharmacol 38(6):339–348
Deo AK, Theil FP, Nicolas JM (2013) Confounding parameters in preclinical assessment of blood–brain barrier permeation: an overview with emphasis on species differences and effect of disease states. Mol Pharm 10(5):1581–95
Di L, Rong H, Feng B (2012a) Demystifying brain penetration in central nervous system drug discovery. J Med Chem 56(1):2–12
Di L, Umland JP, Chang G, Huang Y, Lin Z, Scott DO, Troutman MD, Liston TE (2011) Species independence in brain tissue binding using brain homogenates. Drug Metab Dispos 39(7):1270–1277
Di L, Umland JP, Trapa PE, Maurer TS (2012b) Impact of recovery on fraction unbound using equilibrium dialysis. J Pharm Sci 101(3):1327–1335
Doran A, Obach RS, Smith BJ, Hosea NA, Becker S, Callegari E, Chen C, Chen X, Choo E, Cianfrogna J, Cox LM, Gibbs JP, Gibbs MA, Hatch H, Hop CE, Kasman IN, Laperle J, Liu J, Liu X, Logman M, Maclin D, Nedza FM, Nelson F, Olson E, Rahematpura S, Raunig D, Rogers S, Schmidt K, Spracklin DK, Szewc M, Troutman M, Tseng E, Tu M, Van Deusen JW, Venkatakrishnan K, Walens G, Wang EQ, Wong D, Yasgar AS, Zhang C (2005) The impact of P-glycoprotein on the disposition of drugs targeted for indications of the central nervous system: evaluation using the MDR1A/1B knockout mouse model. Drug Metab Dispos 33(1):165–174
Doran AC, Osgood SM, Mancuso JY, Shaffer CL (2012) An evaluation of using rat-derived single-dose neuropharmacokinetic parameters to project accurately large animal unbound brain drug concentrations. Drug Metab Dispos 40(11):2162–73
Dos-Anjos S, Martinez-Villayandre B, Montori S, Salas A, Perez-Garcia CC, Fernandez-Lopez A (2008) Quantitative gene expression analysis in a brain slice model: influence of temperature and incubation media. Anal Biochem 378(1):99–101
Duvvuri M, Krise JP (2005) A novel assay reveals that weakly basic model compounds concentrate in lysosomes to an extent greater than pH-partitioning theory would predict. Mol Pharm 2(6):440–448
Eaton WW, Martins SS, Nestadt G, Bienvenu OJ, Clarke D, Alexandre P (2008) The burden of mental disorders. Epidemiol Rev 30:1–14
Elebring T, Gill A, Plowright AT (2012) What is the most important approach in current drug discovery: doing the right things or doing things right? Drug Discov Today 17(21–22): 1166–1169
Elmquist WF, Sawchuk RJ (1997) Application of microdialysis in pharmacokinetic studies. Pharm Res 14(3):267–288
Elmquist WF, Sawchuk RJ (2000) Use of microdialysis in drug delivery studies. Adv Drug Deliv Rev 45(2–3):123–124
Fenstermacher J, Kaye T (1988) Drug diffusion within the brain. Ann N Y Acad Sci 531:29–39
Fenstermacher JD (1992) The blood–brain barrier is not a “barrier” for many drugs. NIDA Res Monogr 120:108–120
Fichtl B, v Nieciecki A, Walter K (1991a) Tissue binding versus plasma binding of drugs: general principles and pharmacokinetic consequences. In: Testa B (ed) Advances in drug research , vol 20. Academic Press, London, pp 117–166

Fichtl B, Von Nieciecki A, Walter K (1991b) ChemInform abstract: tissue binding versus plasma binding of drugs: general principles and pharmacokinetic consequences. ChemInform 22

Friden M, Bergstrom F, Wan H, Rehngren M, Ahlin G, Hammarlund-Udenaes M, Bredberg U (2011) Measurement of unbound drug exposure in brain: modeling of pH partitioning explains diverging results between the brain slice and brain homogenate methods. Drug Metab Dispos 39(3):353–362

Friden M, Ducrozet F, Middleton B, Antonsson M, Bredberg U, Hammarlund-Udenaes M (2009a) Development of a high-throughput brain slice method for studying drug distribution in the central nervous system. Drug Metab Dispos 37(6):1226–1233

Friden M, Gupta A, Antonsson M, Bredberg U, Hammarlund-Udenaes M (2007) In vitro methods for estimating unbound drug concentrations in the brain interstitial and intracellular fluids. Drug Metab Dispos 35(9):1711–1719

Friden M, Ljungqvist H, Middleton B, Bredberg U, Hammarlund-Udenaes M (2010) Improved measurement of drug exposure in the brain using drug-specific correction for residual blood. J Cereb Blood Flow Metab 30(1):150–161

Friden M, Winiwarter S, Jerndal G, Bengtsson O, Wan H, Bredberg U, Hammarlund-Udenaes M, Antonsson M (2009b) Structure-brain exposure relationships in rat and human using a novel data set of unbound drug concentrations in brain interstitial and cerebrospinal fluids. J Med Chem 52(20):6233–6243

Fung EN, Chen YH, Lau YY (2003) Semi-automatic high-throughput determination of plasma protein binding using a 96-well plate filtrate assembly and fast liquid chromatography-tandem mass spectrometry. J Chromatogr B Analyt Technol Biomed Life Sci 795(2):187–194

Gaillard PJ, de Boer AG (2000) Relationship between permeability status of the blood–brain barrier and in vitro permeability coefficient of a drug. Eur J Pharm Sci 12(2):95–102

Gaillard PJ, Visser CC, Appeldoorn CC, Rip J (2012) Targeted blood-to-brain drug delivery – 10 key development criteria. Curr Pharm Biotechnol 13(12):2328–2339

Garberg P, Ball M, Borg N, Cecchelli R, Fenart L, Hurst RD, Lindmark T, Mabondzo A, Nilsson JE, Raub TJ, Stanimirovic D, Terasaki T, Oberg JO, Osterberg T (2005) In vitro models for the blood–brain barrier. Toxicol In Vitro 19(3):299–334

Garcia-Garcia E, Andrieux K, Gil S, Couvreur P (2005) Colloidal carriers and blood–brain barrier (BBB) translocation: a way to deliver drugs to the brain? Int J Pharm 298(2):274–292

Ghose AK, Herbertz T, Hudkins RL, Dorsey BD, Mallamo JP (2012) Knowledge-based, central nervous system (CNS) lead selection and lead optimization for CNS drug discovery. ACS Chem Neurosci 3(1):50–68

Ghose AK, Viswanadhan VN, Wendoloski JJ (1999) A knowledge-based approach in designing combinatorial or medicinal chemistry libraries for drug discovery. 1. A qualitative and quantitative characterization of known drug databases. J Comb Chem 1(1):55–68

Gibaldi M (1969) Effect of mode of administration on drug distribution in a two-compartment open system. J Pharm Sci 58(3):327–331

Glees P, Voth D (1988) Clinical and ultrastructural observations of maturing human frontal cortex. Part I (Biopsy material of hydrocephalic infants). Neurosurg Rev 11(3–4):273–278

Gredell JA, Turnquist PA, Maciver MB, Pearce RA (2004) Determination of diffusion and partition coefficients of propofol in rat brain tissue: implications for studies of drug action in vitro. Br J Anaesth 93(6):810–817

Gunn RN, Summerfield SG, Salinas CA, Read KD, Guo Q, Searle GE, Parker CA, Jeffrey P, Laruelle M (2012) Combining PET biodistribution and equilibrium dialysis assays to assess the free brain concentration and BBB transport of CNS drugs. J Cereb Blood Flow Metab 32(5):874–83

Gupta A, Chatelain P, Massingham R, Jonsson EN, Hammarlund-Udenaes M (2006) Brain distribution of cetirizine enantiomers: comparison of three different tissue-to-plasma partition coefficients: K(p), K(p, u), and K(p, uu). Drug Metab Dispos 34(2):318–323

Hammarlund-Udenaes M (2010) Active-site concentrations of chemicals - are they a better predictor of effect than plasma/organ/tissue concentrations? Basic Clin Pharmacol Toxicol 106(3): 215–220

Hammarlund-Udenaes M, Bredberg U, Friden M (2009) Methodologies to assess brain drug delivery in lead optimization. Curr Top Med Chem 9(2):148–162

Hammarlund-Udenaes M, Friden M, Syvanen S, Gupta A (2008) On the rate and extent of drug delivery to the brain. Pharm Res 25(8):1737–1750

Hammarlund-Udenaes M, Paalzow LK, de Lange EC (1997) Drug equilibration across the blood–brain barrier–pharmacokinetic considerations based on the microdialysis method. Pharm Res 14(2):128–134

Harashima H, Sugiyama Y, Sawada Y, Iga T, Hanano M (1984) Comparison between in-vivo and in-vitro tissue-to-plasma unbound concentration ratios (Kp, f) of quinidine in rats. J Pharm Pharmacol 36(5):340–342

He X, Huang Y, Li B, Gong CX, Schuchman EH (2010) Deregulation of sphingolipid metabolism in Alzheimer's disease. Neurobiol Aging 31(3):398–408

Hitchcock SA, Pennington LD (2006) Structure-brain exposure relationships. J Med Chem 49(26):7559–7583

Huang JD (1983) Errors in estimating the unbound fraction of drugs due to the volume shift in equilibrium dialysis. J Pharm Sci 72(11):1368–1369

Huwyler J, Wu D, Pardridge WM (1996) Brain drug delivery of small molecules using immunoliposomes. Proc Natl Acad Sci U S A 93(24):14164–14169

Jeffrey P, Summerfield SG (2007) Challenges for blood–brain barrier (BBB) screening. Xenobiotica 37(10–11):1135–1151

Kaitin KI, DiMasi JA (2011) Pharmaceutical innovation in the 21st century: new drug approvals in the first decade, 2000-2009. Clin Pharmacol Ther 89(2):183–188

Kakee A, Terasaki T, Sugiyama Y (1996) Brain efflux index as a novel method of analyzing efflux transport at the blood–brain barrier. J Pharmacol Exp Ther 277(3):1550–1559

Kakee A, Terasaki T, Sugiyama Y (1997) Selective brain to blood efflux transport of para-aminohippuric acid across the blood–brain barrier: in vivo evidence by use of the brain efflux index method. J Pharmacol Exp Ther 283(3):1018–1025

Kalvass JC, Maurer TS (2002) Influence of nonspecific brain and plasma binding on CNS exposure: implications for rational drug discovery. Biopharm Drug Dispos 23(8):327–338

Kalvass JC, Maurer TS, Pollack GM (2007a) Use of plasma and brain unbound fractions to assess the extent of brain distribution of 34 drugs: comparison of unbound concentration ratios to in vivo p-glycoprotein efflux ratios. Drug Metab Dispos 35(4):660–666

Kalvass JC, Olson ER, Cassidy MP, Selley DE, Pollack GM (2007b) Pharmacokinetics and pharmacodynamics of seven opioids in P-glycoprotein-competent mice: assessment of unbound brain EC50, u and correlation of in vitro, preclinical, and clinical data. J Pharmacol Exp Ther 323(1):346–355

Kariv I, Cao H, Oldenburg KR (2001) Development of a high throughput equilibrium dialysis method. J Pharm Sci 90(5):580–587

Kaufmann AM, Krise JP (2007) Lysosomal sequestration of amine-containing drugs: analysis and therapeutic implications. J Pharm Sci 96(4):729–746

Kell DB, Dobson PD, Bilsland E, Oliver SG (2013) The promiscuous binding of pharmaceutical drugs and their transporter-mediated uptake into cells: what we (need to) know and how we can do so. Drug Discov Today 18(5–6):218–239

Kell DB, Dobson PD, Oliver SG (2011) Pharmaceutical drug transport: the issues and the implications that it is essentially carrier-mediated only. Drug Discov Today 16(15–16):704–714

Kelly J (2009) Principles of CNS drug development: from test tube to clinic and beyond

Kielbasa W, Stratford RE Jr (2012) Exploratory translational modeling approach in drug development to predict human brain pharmacokinetics and pharmacologically relevant clinical doses. Drug Metab Dispos 40(5):877–883

Klotz IM (1973) Physiochemical aspects of drug-protein interactions: a general perspective. Ann N Y Acad Sci 226:18–35

Kodaira H, Kusuhara H, Fujita T, Ushiki J, Fuse E, Sugiyama Y (2011) Quantitative evaluation of the impact of active efflux by p-glycoprotein and breast cancer resistance protein at the blood–brain barrier on the predictability of the unbound concentrations of drugs in the brain using cerebrospinal fluid concentration as a surrogate. J Pharmacol Exp Ther 339(3):935–944

Kornhuber J, Muehlbacher M, Trapp S, Pechmann S, Friedl A, Reichel M, Muhle C, Terfloth L, Groemer TW, Spitzer GM, Liedl KR, Gulbins E, Tripal P (2011) Identification of novel functional inhibitors of acid sphingomyelinase. PLoS One 6(8):e23852

Kurz H, Fichtl B (1983) Binding of drugs to tissues. Drug Metab Rev 14(3):467–510

Kusuhara H, Sugiyama Y (2002) Role of transporters in the tissue-selective distribution and elimination of drugs: transporters in the liver, small intestine, brain and kidney. J Control Release 78(1–3):43–54

Lee G, Dallas S, Hong M, Bendayan R (2001a) Drug transporters in the central nervous system: brain barriers and brain parenchyma considerations. Pharmacol Rev 53(4):569–596

Lee G, Schlichter L, Bendayan M, Bendayan R (2001b) Functional expression of P-glycoprotein in rat brain microglia. J Pharmacol Exp Ther 299(1):204–212

Li JY, Sugimura K, Boado RJ, Lee HJ, Zhang C, Duebel S, Pardridge WM (1999) Genetically engineered brain drug delivery vectors: cloning, expression and in vivo application of an anti-transferrin receptor single chain antibody-streptavidin fusion gene and protein. Protein Eng 12(9):787–796

Lin JH (2004) How significant is the role of P-glycoprotein in drug absorption and brain uptake? Drugs Today (Barc) 40(1):5–22

Lin JH (2008) CSF as a surrogate for assessing CNS exposure: an industrial perspective. Curr Drug Metab 9(1):46–59

Lin JH, Sugiyama Y, Awazu S, Hanano M (1982) In vitro and in vivo evaluation of the tissue-to-blood partition coefficient for physiological pharmacokinetic models. J Pharmacokinet Biopharm 10(6):637–647

Lin TH, Lin JH (1990) Effects of protein binding and experimental disease states on brain uptake of benzodiazepines in rats. J Pharmacol Exp Ther 253(1):45–50

Liu X, Chen C, Smith BJ (2008) Progress in brain penetration evaluation in drug discovery and development. J Pharmacol Exp Ther 325(2):349–356

Liu X, Ding X, Deshmukh G, Liederer BM, Hop CE (2012) Use of cassette dosing approach to assess brain penetration in drug discovery. Drug Metab Dispos 40(5):963–9

Liu X, Smith BJ, Chen C, Callegari E, Becker SL, Chen X, Cianfrogna J, Doran AC, Doran SD, Gibbs JP, Hosea N, Liu J, Nelson FR, Szewc MA, Van Deusen J (2005) Use of a physiologically based pharmacokinetic model to study the time to reach brain equilibrium: an experimental analysis of the role of blood–brain barrier permeability, plasma protein binding, and brain tissue binding. J Pharmacol Exp Ther 313(3):1254–1262

Liu X, Smith BJ, Chen C, Callegari E, Becker SL, Chen X, Cianfrogna J, Doran AC, Doran SD, Gibbs JP, Hosea N, Liu J, Nelson FR, Szewc MA, Van Deusen J (2006) Evaluation of cerebrospinal fluid concentration and plasma free concentration as a surrogate measurement for brain free concentration. Drug Metab Dispos 34(9):1443–1447

Liu X, Van Natta K, Yeo H, Vilenski O, Weller PE, Worboys PD, Monshouwer M (2009a) Unbound drug concentration in brain homogenate and cerebral spinal fluid at steady state as a surrogate for unbound concentration in brain interstitial fluid. Drug Metab Dispos 37(4): 787–793

Liu X, Vilenski O, Kwan J, Apparsundaram S, Weikert R (2009b) Unbound brain concentration determines receptor occupancy: a correlation of drug concentration and brain serotonin and dopamine reuptake transporter occupancy for eighteen compounds in rats. Drug Metab Dispos 37(7):1548–1556

Lloyd JB (2000) Lysosome membrane permeability: implications for drug delivery. Adv Drug Deliv Rev 41(2):189–200

Logan R, Funk RS, Axcell E, Krise JP (2012) Drug-drug interactions involving lysosomes: mechanisms and potential clinical implications. Expert Opin Drug Metab Toxicol 8(8):943–958

Longhi R, Corbioli S, Fontana S, Vinco F, Braggio S, Helmdach L, Schiller J, Boriss H (2011) Brain tissue binding of drugs: evaluation and validation of solid supported porcine brain membrane vesicles (TRANSIL) as a novel high-throughput method. Drug Metab Dispos 39(2):312–321

Loryan I, Friden M, Hammarlund-Udenaes M (2013) The brain slice method for studying drug distribution in the CNS. Fluids Barriers CNS 10(1):6

MacIntyre AC, Cutler DJ (1988) The potential role of lysosomes in tissue distribution of weak bases. Biopharm Drug Dispos 9(6):513–526
Manitpisitkul P, White RE (2004) Whatever happened to cassette-dosing pharmacokinetics? Drug Discov Today 9(15):652–658
Mano Y, Higuchi S, Kamimura H (2002) Investigation of the high partition of YM992, a novel antidepressant, in rat brain - in vitro and in vivo evidence for the high binding in brain and the high permeability at the BBB. Biopharm Drug Dispos 23(9):351–360
Maurer TS, Debartolo DB, Tess DA, Scott DO (2005) Relationship between exposure and nonspecific binding of thirty-three central nervous system drugs in mice. Drug Metab Dispos 33(1):175–181
McIlwain H (1951a) Glutamic acid and glucose as substrates for mammalian brain. J Ment Sci 97(409):674–680
McIlwain H (1951b) Metabolic response in vitro to electrical stimulation of sections of mammalian brain. Biochem J 48(4):1vi
Mizuno N, Niwa T, Yotsumoto Y, Sugiyama Y (2003) Impact of drug transporter studies on drug discovery and development. Pharmacol Rev 55(3):425–461
Muehlbacher M, Tripal P, Roas F, Kornhuber J (2012) Identification of drugs inducing phospholipidosis by novel in vitro data. ChemMedChem
Nadanaciva S, Lu S, Gebhard DF, Jessen BA, Pennie WD, Will Y (2011) A high content screening assay for identifying lysosomotropic compounds. Toxicol In Vitro 25(3):715–723
Ndengele MM, Cuzzocrea S, Masini E, Vinci MC, Esposito E, Muscoli C, Petrusca DN, Mollace V, Mazzon E, Li D, Petrache I, Matuschak GM, Salvemini D (2009) Spinal ceramide modulates the development of morphine antinociceptive tolerance via peroxynitrite-mediated nitroxidative stress and neuroimmune activation. J Pharmacol Exp Ther 329(1):64–75
Neuwelt E, Abbott NJ, Abrey L, Banks WA, Blakley B, Davis T, Engelhardt B, Grammas P, Nedergaard M, Nutt J, Pardridge W, Rosenberg GA, Smith Q, Drewes LR (2008) Strategies to advance translational research into brain barriers. Lancet Neurol 7(1):84–96
Newman GC, Hospod FE, Patlak CS (1988a) Brain slice glucose utilization. J Neurochem 51(6):1783–1796
Newman GC, Hospod FE, Schissel SL (1991) Ischemic brain slice glucose utilization: effects of slice thickness, acidosis, and K+. J Cereb Blood Flow Metab 11(3):398–406
Newman GC, Hospod FE, Wu P (1988b) Thick brain slices model the ischemic penumbra. J Cereb Blood Flow Metab 8(4):586–597
Nicholson C, Sykova E (1998) Extracellular space structure revealed by diffusion analysis. Trends Neurosci 21(5):207–215
Ohtsuki S, Takizawa T, Takanaga H, Hori S, Hosoya K, Terasaki T (2004) Localization of organic anion transporting polypeptide 3 (oatp3) in mouse brain parenchymal and capillary endothelial cells. J Neurochem 90(3):743–749
Ooie T, Terasaki T, Suzuki H, Sugiyama Y (1997) Quantitative brain microdialysis study on the mechanism of quinolones distribution in the central nervous system. Drug Metab Dispos 25(7):784–789
Padowski JM, Pollack GM (2011a) The influence of distributional kinetics into a peripheral compartment on the pharmacokinetics of substrate partitioning between blood and brain tissue. J Pharmacokinet Pharmacodyn 38(6):743–767
Padowski JM, Pollack GM (2011b) Influence of time to achieve substrate distribution equilibrium between brain tissue and blood on quantitation of the blood–brain barrier P-glycoprotein effect. Brain Res 1426:1–17
Pardridge WM (1989) Strategies for drug delivery through the blood–brain barrier. Neurobiol Aging 10(5):636–637, discussion 648-650
Pardridge WM (1997) Drug delivery to the brain. J Cereb Blood Flow Metab 17(7):713–731
Pardridge WM (2006) Molecular Trojan horses for blood–brain barrier drug delivery. Curr Opin Pharmacol 6(5):494–500
Pardridge WM, Boado RJ, Black KL, Cancilla PA (1992) Blood–brain barrier and new approaches to brain drug delivery. West J Med 156(3):281–286

Patlak CS, Hospod FE, Trowbridge SD, Newman GC (1998) Diffusion of radiotracers in normal and ischemic brain slices. J Cereb Blood Flow Metab 18(7):776–802

Plise EG, Tran D, Salphati L (2010) Semi-automated protein binding methodology using equilibrium dialysis and a novel mixed-matrix cassette approach. J Pharm Sci 99(12):5070–5078

Raub TJL, Lutzke BS, Andrus PK, Sawada GA, Staton BA (2006) Early preclinical evaluation of brain exposure in support of hit identification and lead optimization. In: Borchardt RT, Middagh CR (eds) Optimization of drug-like properties during lead optimization, Biotechnology: pharmaceutical aspects series. Am Assoc Pharm Sci Press, Arlington, VA

Read KD, Braggio S (2010) Assessing brain free fraction in early drug discovery. Expert Opin Drug Metab Toxicol 6(3):337–344

Reichel A (2006) The role of blood–brain barrier studies in the pharmaceutical industry. Curr Drug Metab 7(2):183–203

Reichel A (2009) Addressing central nervous system (CNS) penetration in drug discovery: basics and implications of the evolving new concept. Chem Biodivers 6(11):2030–2049

Reichel A, Begley D, Abbott N (2003) An overview of in vitro techniques for blood–brain barrier studies. In: Nag S (ed) The blood–brain barrier: biology and research tools, Methods in molecular medicine (Vol. 89). Humana Press Inc., Totowa, NJ

Rice ME (1999) Use of ascorbate in the preparation and maintenance of brain slices. Methods 18(2):144–149

Rodgers T, Jones HM, Rowland M (2012) Tissue lipids and drug distribution: dog versus rat. J Pharm Sci 101(12):4615–4626

Romer J, Bickel MH (1979) A method to estimate binding constants at variable protein concentrations. J Pharm Pharmacol 31(1):7–11

Rouser G, Simon G, Kritchevsky G (1969) Species variations in phospholipid class distribution of organs. I. Kidney, liver and spleen. Lipids 4(6):599–606

Sargent DF, Bean JW, Schwyzer R (1988) Conformation and orientation of regulatory peptides on lipid membranes. Key to the molecular mechanism of receptor selection. Biophys Chem 31(1–2):183–193

Sargent DF, Schwyzer R (1986) Membrane lipid phase as catalyst for peptide-receptor interactions. Proc Natl Acad Sci U S A 83(16):5774–5778

Sawada Y, Hanano M, Sugiyama Y, Harashima H, Iga T (1984) Prediction of the volumes of distribution of basic drugs in humans based on data from animals. J Pharmacokinet Biopharm 12(6):587–596

Scherrmann JM (2002) Drug delivery to brain via the blood–brain barrier. Vascul Pharmacol 38(6):349–354

Schoepp DD (2011) Where will new neuroscience therapies come from? Nat Rev Drug Discov 10(10):715–716

Schultz ML, Tecedor L, Chang M, Davidson BL (2011) Clarifying lysosomal storage diseases. Trends Neurosci 34(8):401–410

Schwab ME, Buchli AD (2012) Drug research: plug the real brain drain. Nature 483(7389): 267–268

Schwarz E, Prabakaran S, Whitfield P, Major H, Leweke FM, Koethe D, McKenna P, Bahn S (2008) High throughput lipidomic profiling of schizophrenia and bipolar disorder brain tissue reveals alterations of free fatty acids, phosphatidylcholines, and ceramides. J Proteome Res 7(10):4266–4277

Segall MD (2012) Multi-parameter optimization: identifying high quality compounds with a balance of properties. Curr Pharm Des 18(9):1292–1310

Shaffer CL (2010) Defining neuropharmacokinetic parameters in CNS drug discovery to determine cross-species pharmacologic exposure-response relationships. Annu Rep Med Chem 45:55–70

Shen DD, Artru AA, Adkison KK (2004) Principles and applicability of CSF sampling for the assessment of CNS drug delivery and pharmacodynamics. Adv Drug Deliv Rev 56(12): 1825–1857

Simon G, Rouser G (1969) Species variations in phospholipid class distribution of organs. II. Heart and skeletal muscle. Lipids 4(6):607–614

Smith DA, Di L, Kerns EH (2010) The effect of plasma protein binding on in vivo efficacy: misconceptions in drug discovery. Nat Rev Drug Discov 9(12):929–939

Smith QR (1991) The blood–brain barrier and the regulation of amino acid uptake and availability to brain. Adv Exp Med Biol 291:55–71

Stevens J, Ploeger BA, Hammarlund-Udenaes M, Osswald G, van der Graaf PH, Danhof M, de Lange EC (2012) Mechanism-based PK-PD model for the prolactin biological system response following an acute dopamine inhibition challenge: quantitative extrapolation to humans. J Pharmacokinet Pharmacodyn 39(5):463–477

Stokes CE, Murphy D, Paton JF, Kasparov S (2003) Dynamics of a transgene expression in acute rat brain slices transfected with adenoviral vectors. Exp Physiol 88(4):459–466

Su TZ, Lunney E, Campbell G, Oxender DL (1995) Transport of gabapentin, a gamma-amino acid drug, by system l alpha-amino acid transporters: a comparative study in astrocytes, synaptosomes, and CHO cells. J Neurochem 64(5):2125–2131

Summerfield SG, Read K, Begley DJ, Obradovic T, Hidalgo IJ, Coggon S, Lewis AV, Porter RA, Jeffrey P (2007) Central nervous system drug disposition: the relationship between in situ brain permeability and brain free fraction. J Pharmacol Exp Ther 322(1):205–213

Summerfield SG, Stevens AJ, Cutler L, del Carmen OM, Hammond B, Tang SP, Hersey A, Spalding DJ, Jeffrey P (2006) Improving the in vitro prediction of in vivo central nervous system penetration: integrating permeability, P-glycoprotein efflux, and free fractions in blood and brain. J Pharmacol Exp Ther 316(3):1282–1290

Sun N, Avdeef A (2011) Biorelevant pK(a) (37 degrees C) predicted from the 2D structure of the molecule and its pK(a) at 25 degrees C. J Pharm Biomed Anal 56(2):173–182

Sykova E (2004) Extrasynaptic volume transmission and diffusion parameters of the extracellular space. Neuroscience 129(4):861–876

Sykova E, Nicholson C (2008) Diffusion in brain extracellular space. Physiol Rev 88(4): 1277–1340

Syvanen S, Hooker A, Rahman O, Wilking H, Blomquist G, Langstrom B, Bergstrom M, Hammarlund-Udenaes M (2008) Pharmacokinetics of P-glycoprotein inhibition in the rat blood–brain barrier. J Pharm Sci 97(12):5386–5400

Syvanen S, Lindhe O, Palner M, Kornum BR, Rahman O, Langstrom B, Knudsen GM, Hammarlund-Udenaes M (2009) Species differences in blood–brain barrier transport of three positron emission tomography radioligands with emphasis on P-glycoprotein transport. Drug Metab Dispos 37(3):635–643

Syvanen S, Schenke M, van den Berg DJ, Voskuyl RA, de Lange EC (2012) Alteration in P-glycoprotein functionality affects intrabrain distribution of quinidine more than brain entry-a study in rats subjected to status epilepticus by kainate. AAPS J 14(1):87–96

Tanaka H, Mizojiri K (1999) Drug-protein binding and blood–brain barrier permeability. J Pharmacol Exp Ther 288(3):912–918

Terasaki T, Hosoya K (1999) The blood–brain barrier efflux transporters as a detoxifying system for the brain. Adv Drug Deliv Rev 36(2–3):195–209

Terasaki T, Ohtsuki S (2005) Brain-to-blood transporters for endogenous substrates and xenobiotics at the blood–brain barrier: an overview of biology and methodology. NeuroRx 2(1):63–72

Thorne RG, Emory CR, Ala TA, Frey WH 2nd (1995) Quantitative analysis of the olfactory pathway for drug delivery to the brain. Brain Res 692(1–2):278–282

Thorne RG, Hrabetova S, Nicholson C (2004) Diffusion of epidermal growth factor in rat brain extracellular space measured by integrative optical imaging. J Neurophysiol 92(6):3471–3481

Thorne RG, Lakkaraju A, Rodriguez-Boulan E, Nicholson C (2008) In vivo diffusion of lactoferrin in brain extracellular space is regulated by interactions with heparan sulfate. Proc Natl Acad Sci U S A 105(24):8416–8421

Thorne RG, Nicholson C (2006) In vivo diffusion analysis with quantum dots and dextrans predicts the width of brain extracellular space. Proc Natl Acad Sci U S A 103(14):5567–5572

Tsuji A, Tamai I, Sakata A, Tenda Y, Terasaki T (1993) Restricted transport of cyclosporin A across the blood–brain barrier by a multidrug transporter, P-glycoprotein. Biochem Pharmacol 46(6):1096–1099

Tsuji A, Terasaki T, Takabatake Y, Tenda Y, Tamai I, Yamashima T, Moritani S, Tsuruo T, Yamashita J (1992) P-glycoprotein as the drug efflux pump in primary cultured bovine brain capillary endothelial cells. Life Sci 51(18):1427–1437

Uchida Y, Ohtsuki S, Kamiie J, Terasaki T (2011a) Blood–brain barrier (BBB) pharmacoproteomics: reconstruction of in vivo brain distribution of 11 P-glycoprotein substrates based on the BBB transporter protein concentration, in vitro intrinsic transport activity, and unbound fraction in plasma and brain in mice. J Pharmacol Exp Ther 339(2):579–588

Uchida Y, Ohtsuki S, Katsukura Y, Ikeda C, Suzuki T, Kamiie J, Terasaki T (2011b) Quantitative targeted absolute proteomics of human blood–brain barrier transporters and receptors. J Neurochem 117(2):333–345

Van Eeckhaut A, Lanckmans K, Sarre S, Smolders I, Michotte Y (2009) Validation of bioanalytical LC-MS/MS assays: evaluation of matrix effects. J Chromatogr B Analyt Technol Biomed Life Sci 877(23):2198–2207

van Liempd S, Morrison D, Sysmans L, Nelis P, Mortishire-Smith R (2011) Development and validation of a higher-throughput equilibrium dialysis assay for plasma protein binding. J Lab Autom 16(1):56–67

Van Peer AP, Belpaire FM, Bogaert MG (1981) Binding of drugs in serum, blood cells and tissues of rabbits with experimental acute renal failure. Pharmacology 22(2):146–152

Vauquelin G, Bostoen S, Vanderheyden P, Seeman P (2012) Clozapine, atypical antipsychotics, and the benefits of fast-off D(2) dopamine receptor antagonism. Naunyn Schmiedebergs Arch Pharmacol 385(4):337–372

Vauquelin G, Packeu A (2009) Ligands, their receptors and … plasma membranes. Mol Cell Endocrinol 311(1–2):1–10

Vauquelin G, Van Liefde I (2005) G protein-coupled receptors: a count of 1001 conformations. Fundam Clin Pharmacol 19(1):45–56

Vuignier K, Schappler J, Veuthey JL, Carrupt PA, Martel S (2010) Drug-protein binding: a critical review of analytical tools. Anal Bioanal Chem 398(1):53–66

Wager TT, Liras JL, Mente S, Trapa P (2012) Strategies to minimize CNS toxicity: in vitro high-throughput assays and computational modeling. Expert Opin Drug Metab Toxicol 8(5): 531–542

Wan H, Ahman M, Holmen AG (2009) Relationship between brain tissue partitioning and microemulsion retention factors of CNS drugs. J Med Chem 52(6):1693–1700

Wan H, Rehngren M, Giordanetto F, Bergstrom F, Tunek A (2007) High-throughput screening of drug-brain tissue binding and in silico prediction for assessment of central nervous system drug delivery. J Med Chem 50(19):4606–4615

Wang Y, Welty DF (1996) The simultaneous estimation of the influx and efflux blood–brain barrier permeabilities of gabapentin using a microdialysis-pharmacokinetic approach. Pharm Res 13(3):398–403

Wang YY, Lui PC, Li JY (2009) Receptor-mediated therapeutic transport across the blood–brain barrier. Immunotherapy 1(6):983–993

Watson J, Wright S, Lucas A, Clarke KL, Viggers J, Cheetham S, Jeffrey P, Porter R, Read KD (2009) Receptor occupancy and brain free fraction. Drug Metab Dispos 37(4):753–760

Weaver DF, Weaver CA (2011) Exploring neurotherapeutic space: how many neurological drugs exist (or could exist)? J Pharm Pharmacol 63(1):136–139

Wellmann H, Kaltschmidt B, Kaltschmidt C (1999) Optimized protocol for biolistic transfection of brain slices and dissociated cultured neurons with a hand-held gene gun. J Neurosci Methods 92(1–2):55–64

Westerhout J, Danhof M, De Lange EC (2011) Preclinical prediction of human brain target site concentrations: considerations in extrapolating to the clinical setting. J Pharm Sci 100(9): 3577–3593

Westerhout J, Ploeger B, Smeets J, Danhof M, de Lange EC (2012) Physiologically based pharmacokinetic modeling to investigate regional brain distribution kinetics in rats. AAPS J 14(3):543–553

Wolak D, Thorne R (2013) Diffusion of macromolecules in the brain: implications for drug delivery. Mol Pharm 10(5):1492–504

Yokogawa K, Ishizaki J, Ohkuma S, Miyamoto K (2002) Influence of lipophilicity and lysosomal accumulation on tissue distribution kinetics of basic drugs: a physiologically based pharmacokinetic model. Methods Find Exp Clin Pharmacol 24(2):81–93

Young RC, Mitchell RC, Brown TH, Ganellin CR, Griffiths R, Jones M, Rana KK, Saunders D, Smith IR, Sore NE et al (1988) Development of a new physicochemical model for brain penetration and its application to the design of centrally acting H2 receptor histamine antagonists. J Med Chem 31(3):656–671

Zhao R, Kalvass JC, Pollack GM (2009) Assessment of blood–brain barrier permeability using the in situ mouse brain perfusion technique. Pharm Res 26(7):1657–1664

Chapter 11
Prediction of Drug Exposure in the Brain from the Chemical Structure

Markus Fridén

Abstract The level of drug exposure in the brain is long known to relate to the physico-chemical properties of the drug. The study of this relationship has attracted much attention through the years as it holds a promise that this drug property can be predicted in silico from the chemical drug structure. Various in vivo methodologies have been used to define and quantify drug exposure in the brain, the most commonly used parameter being logBB, which is the brain-to-blood ratio of *total* drug concentrations. From datasets of logBB it has been inferred that drug exposure in the brain is promoted by the lipophilicity, i.e. lipid solubility, of the drug and restricted by its hydrogen bonding potential. Recent work with the $K_{p,uu,brain}$ parameter, representing a pharmacologically relevant brain-to-blood ratio of *unbound* drug concentrations, has confirmed the limiting effect of hydrogen bonding on drug exposure in the brain, but also indicated no dependence on lipophilicity. The challenges associated with obtaining high predictivity models for $K_{p,uu,brain}$ confirm the contemporary view of the blood–brain barrier (BBB) as not only being physical and passive in nature but also involving specific carrier-mediated processes. It follows that in silico approaches need to compliment and merge with experimental methodologies to advance the field of brain exposure predictions.

M. Fridén, Ph.D. (✉)
Department of Drug Metabolism and Pharmacokinetics, AstraZeneca Research and Development, Respiratory, Inflammation and Autoimmunity Innovative Medicines, Pepparedsleden 1, Mölndal 43183, Sweden
e-mail: Markus.Friden@astrazeneca.com

M. Hammarlund-Udenaes et al. (eds.), *Drug Delivery to the Brain*, AAPS Advances in the Pharmaceutical Sciences Series 10, DOI 10.1007/978-1-4614-9105-7_11,

11.1 Introduction

For decades it has been recognized that a drug's ability to cross the blood–brain barrier (BBB) is related to its physicochemical properties. This idea is not only supported by experimental data in animals but also by clinical notions of for example the hydrophilic beta-blocker atenolol having less CNS related side effects than do the more lipophilic propranolol (McAinsh and Cruickshank 1990) (see Fig 11.1 for molecular structures). The relationship with lipophilicity seems to have become common knowledge even amongst clinicians and it has nourished an idea that BBB transport is essentially predictable. This chapter critically reviews the various approaches that have been taken during the years to predict the level of drug exposure in the brain form the chemical structure of the drug. While the computational

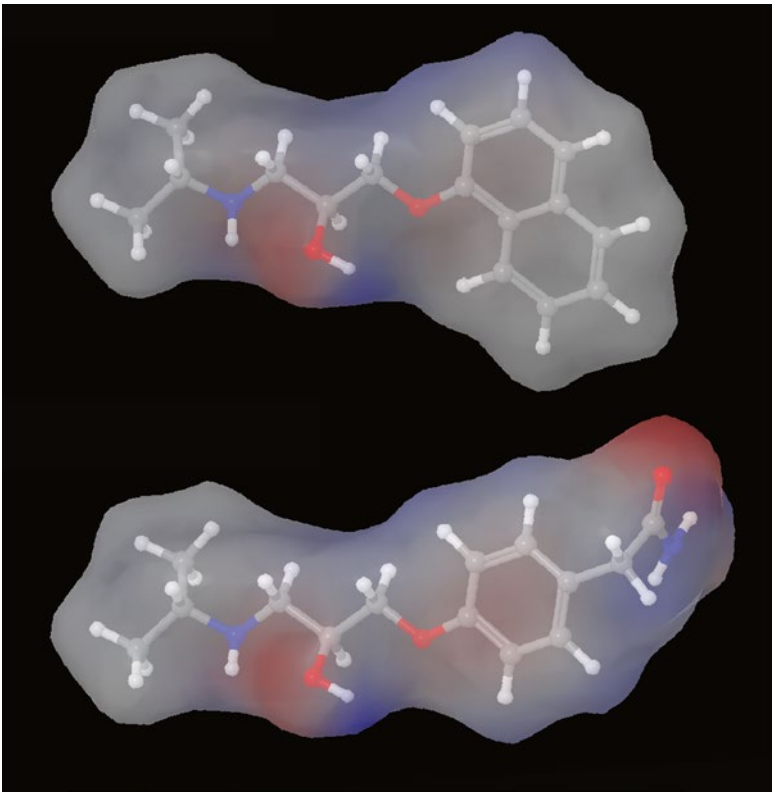

Fig. 11.1 Three-dimensional structures of propranolol (*top*) and atenolol (*bottom*) coloured according to the electrostatic potential where red and blue areas indicate the negative and positive charges of oxygen and nitrogen atoms (MacroModel v. 8.0, MM3* force field). Note that the drugs differ only in the substitution of the aromatic ring where propranolol has a fused benzene ring, i.e. a naphthyl group, and atenolol has an amide, i.e. two additional hydrogen bond acceptors

approaches have reached advanced levels, the weakest spot can be considered to be the quality and relevance of the underlying experimental data that is used to derive the prediction models (Mehdipour and Hamidi 2009). Therefore, a discussion is included on the various endpoints of drug exposure in brain that are currently used as basis for in silico prediction models. The actual analysis of the relationship with chemical drug properties is focused on the parameter that is currently regarded as the most appropriate: the unbound brain-to-plasma ratio $K_{p,uu,brain}$ (Sect. 11.2.2), commonly determined in the rat. The reader will also be provided with some basic knowledge of how to derive and validate prediction models (Sect. 11.1.2.5) and some tactics of how to utilize them for drug design (Sect. 11.3.2).

11.1.1 Various Measurements of Brain Exposure and Availability of Data

Needless to say, the vast majority of data on drug exposure in the brain and related measurements are from rodents. The validity of these data for making predictions in humans resides with the extent to which the drug transport properties of the BBB are "conserved" across the mammalian species. There are distinct pharmacokinetic aspects to consider for drug transport across the BBB such as the rate and extent to which it occurs (see Chap. 5). When attempting to experimentally quantify these aspects there are associated drug properties need to be considered such as the degree of non-specific binding in blood plasma and in brain tissue. While Chap. 10 covers the various experimental in vivo methodologies to determine each of these aspects or properties, this section highlights those that have been commonly used for deriving the relationship with the chemical structure of the drug.

11.1.1.1 LogBB

With respect to prediction of drug exposure in the brain, the by far most commonly used measurement is the (steady-state) ratio of total brain to total plasma or blood concentrations. This total brain-to-blood or brain-to-plasma ratio is referred to as the partitioning coefficient of the brain $K_{p,brain}$, or BB and the logarithm thereof (logBB). The relative ease of its experimental determination in animals has made this parameter the choice of preference for many modellers and the datasets are commonly as large as ~150 logBB values while some workers have compiled up to 470 values (Lanevskij et al. 2011). Rather recently there has been an increased awareness that only the free, *unbound*, drug is available for transport across the BBB and binding to target proteins. This has raised serious concerns regarding any work based on logBB since this is a measure of total drug in brain (bound + unbound) relative to plasma. Notwithstanding that the logBB value contains some information

about the BBB, drug compounds generally differ with respect to the balance between bound and unbound drug in brain tissue versus blood plasma, thus making logBB very misleading (van de Waterbeemd et al. 2001; Martin 2004; Hammarlund-Udenaes et al. 2008). This topic is expanded on in Sect. 11.2.3.

11.1.1.2 $K_{p,uu,brain}$

Given the acceptance of the free drug hypothesis and that the extent of drug transport is probably more important than the rate for most CNS and non-CNS drugs it is currently argued that the most useful measurement of brain exposure is the steady-state unbound brain-to-plasma ratio $K_{p,uu,brain}$ (Gupta et al. 2006), also called the unbound partition coefficient of the brain. As described in Chap. 10, $K_{p,uu,brain}$ can be directly determined in vivo using microdialysis or derived from $K_{p,brain}$ (logBB) values by determining the binding in blood plasma and brain tissue in vitro (Friden et al. 2007). However, it is only rather recently that data has been generated for this parameter and systematically compiled to publically available datasets (Sect. 11.2.2).

11.1.1.3 BBB Permeability Surface Area Product (PS)

It has been proposed that the rate of transport, i.e. the BBB permeability surface area product (PS) should be used to derive predictive models (Pardridge 2004); however, it is difficult to rationalize this choice of parameter since rate and extent are not necessarily correlated. Relative to logBB it is technically more challenging to determine logPS and as result the datasets are smaller, as has been the interest in modelling this parameter. Liu et al. determined and modelled logPS for a set of 28 compounds (Liu et al. 2004), which is a similar number of compounds as in earlier work (Gratton et al. 1997; Abraham 2004b).

11.1.1.4 Classification Approaches

In order to remedy the relatively limited availability of logBB values, larger datasets have been created by classifying marketed or investigational drugs as CNS active (CNS^+) or inactive (CNS^-) according to the presence or lack of central drug effects or side effects. The underlying assumption of this approach is that CNS^+ drugs "cross" the BBB, whereas CNS^- drugs do not. This is obviously correct for all CNS^+ drugs but the lack of CNS effects of CNS^- drugs can arguably have different backgrounds. Recently a BBB^+/BBB^- classification scheme has been proposed based on actual measurements of drug concentrations in human brain or cerebrospinal fluid (Broccatelli et al. 2012). Experimentally determined values of rodent logBB have also been added to these datasets by using arbitrary cut-off values for classification as CNS^+ or CNS^-. A justified objection to categorical modelling is that brain

exposure is a continuous variable by nature, and strictly speaking, CNS^- drugs do not exist since all drugs enter the brain to some extent. The size of CNS^+/CNS^- datasets ranges from less than one hundred to more than fifty thousand compounds depending on the databases that are used (Abraham and Hersey 2007).

11.1.2 Modelling Strategies

The significant number of different approaches to predicting drug exposure in the brain poses a challenge to scientists that enter the field of in silico modelling. To assess the value of existing approaches or to develop new methods for a particular situation it is therefore useful to know some basics of modelling strategies. The procedure for developing predictive computational models for, say, brain exposure can be divided into five general steps: (1) selecting a relevant set of drug molecules, (2) generating experimental data for the drug property of interest, (3) describing the chemical structure of the molecules in terms of numerical descriptor values, (4) relating the structural description to the experimental data using a mathematical relationship and (5) validating the predictivity of the model (Matsson 2007). This section (Sect. 11.1.2) describes the general basis of developing predictive models in the context of being able to predict drug exposure in brain for a new chemical entity. Strategies for drug design are discussed in Sect. 11.3.2.

11.1.2.1 Compound Selection

The selection of a *training-set* of compounds on which to build the relationship between brain exposure and molecular structure is not an arbitrary choice, since it will define the *applicability domain* of the model. The desired applicability domain can be larger, e.g. to encompass drugs in general (global models) or small to encompass only structures that are relevant to for example a particular drug discovery programme (local models). A higher level of predictivity is expected from local models than from global models though it comes at the expense of a more restricted applicability domain. Regardless of whether global or local models are considered, one should strive for a structurally diverse selection within the domain.

11.1.2.2 Molecular Descriptors

Molecular structures need to be translated into numerical representations before a mathematical relationship can be derived with the measured drug property. This is done by molecular descriptors encoding various properties of the molecule. There are several sets of descriptors which are associated with the different computational approaches or software (Winiwarter et al. 2007). Some of these are derived from the three-dimensional structure of the molecule. For prediction of BBB transport,

Table 11.1 Commonly used molecular descriptors

Property	Abbreviation	Molecular descriptor
Lipophilicity	ClogP	Prediction of octanol–water partition coefficient for molecules in their neutral state
	ClogD (ACDLogD7.4)	Prediction of octanol–water partition coefficient at pH 7.4 using ACD/Labs software
Size/shape	MW	Molecular weight
	VOL	Molecular volume as defined by a Gaussian volume
	RotBond	Number of rotatable bonds in molecule
	RingCount	Number of rings in molecule
	NPSA	Non-polar surface area in Å^2
Hydrogen bonding	HBA	Number of hydrogen bond acceptors (number of oxygen plus nitrogen atoms, N + O)
	HBD	Number of hydrogen bond donors (number of hydroxyls + amine hydrogen atoms (OH + NH)
	PSA	Polar surface area in Å^2
Charge/polarity	Acid	Presence of an acidic function
	Base	Presence of a basic function
	Neutral	Absence of acidic and basic functions
	Zwitterion	Presence of at least one acidic and one basic function

however, standard physicochemical descriptors have been commonly used (Table 11.1). Physicochemical descriptors provide information about the molecular size, shape, lipid solubility (lipophilicity) as well as information on the hydrogen bonding potential of the drug. Acid–base properties, i.e. proton dissociation constants (pK_a), can also be predicted from the structure and used to classify drugs as neutrals, acids, bases or zwitterions.

11.1.2.3 Generation of Experimental Data

This step is often considered the most costly and time-demanding step of model development. There is consequently always a risk of using inadequate experimental methods or not applying sufficiently stringent criteria for inclusion of experimental data from literature. It is well known that good quality data are a *conditio sine qua non*, an absolutely essential condition. A prediction model can never make better predictions than the experimental data used for its generation.

11.1.2.4 Relating Experimental Data to Molecular Descriptors

There are several mathematical or statistical modelling approaches collectively referred to as machine learning that can be used in the process of identifying and describing the relationship between molecular descriptors and a measured parameter. The very simplest form would be to look at the correlation between the

measured parameter and individual molecular descriptors. If a strong relationship is found (linear or not), the equation describing the relationship could be used as a computational prediction model for future compounds. If a strong relationship cannot be seen with any one descriptor, it is possible that several descriptors can give a better prediction when combined in, for example, *multiple linear regression* (MLR) analysis. A related technique is *partial least squares projection to latent structures* (PLS) (Wold 2001). By this method of modelling, a larger number of molecular descriptors can be reduced to a smaller number of latent super-variables or *principal components*, which are then related to experimental data. Advantages of using PLS include that descriptors that are irrelevant to the problem are handled as well as closely related (correlated) descriptors. PLS models are also easily interpreted in terms of how the molecular properties could be changed. A major drawback is that PLS is a linear method that does not handle non-linear relationships unless variables are transformed prior to analysis. Novel and computationally more advanced machine learning algorithms include support vector machine, random forest and neural networks (Mehdipour and Hamidi 2009).

11.1.2.5 Validation of the Model

Before a computational prediction model can be taken into practice it must be validated. While the coefficient of determination (R^2) describes the correlation between observed and predicted values for the training-set, it cannot be taken for granted that the predictivity is equally good for drugs not used in the training of the model. In fact, R^2 should never be used to compare prediction models or be expected to reflect the real model predictivity for new compounds. Cross-validation or *leave-many-out* is a method for validating a model (Wold 1991). By dividing the compounds in groups, a model can be generated based on all groups but one, for which the values are instead predicted. The procedure is repeated until all groups have been withheld from the model and predicted. The cross-validated coefficient of determination (Q^2) is generally the first method of validating a PLS model, and is used continuously to assess the predictivity of rivalling models. Unfortunately, a high value for Q^2 is neither a guarantee for a predictive model. The only way to really validate a prediction model is to use an external *test-set* of compounds which have not at all been used in the training of the model. Failure of a high Q^2 model to satisfactorily predict compounds in a test-set indicates that there are unresolved issues with defining the applicability domain of the model. This highlights the importance of the compound selection procedure which, if made appropriately for the problem at hand, increases the chances of obtaining a model that is fit-for-purpose.

11.1.3 Overview of BBB Prediction Models

While there are several exhaustive reviews of modelling brain exposure (Mehdipour and Hamidi 2009; Abraham and Hersey 2007; Ecker and Noe 2004; Clark 2003;

Norinder and Haeberlein 2002; Hitchcock and Pennington 2006) this section briefly highlights some of the historical studies that have been influential. The era of computational modelling of BBB transport began in 1980 when Levin observed a strong relationship between the BBB permeability (PS) and the octanol–water partitioning coefficient (LogP) for a set of 27 compounds (Levin 1980). Interestingly, four compounds with molecular weight greater than 400 Da were excluded from the analysis since they were considered "extremely restricted" owing to their size. In retrospect it is realized that these were substrates of P-glycoprotein. It was, however, concluded that there exists a molecular weight cut-off for "significant BBB passage". A relationship between descriptors of lipophilicity and logBB was also found by Young et al. in 1988 for a set of 20 antihistamines (Young et al. 1988). Since then, the public dataset of logBB values has expanded well over a hundred compounds, and several computational approaches have been used by different groups (Abraham et al. 1994; Abraham et al. 2002; Abraham 2004a; Luco 1999; Osterberg and Norinder 2000; Bendels et al. 2008). These studies taken together indicate that brain penetration as measured by logBB is negatively correlated to descriptors of hydrogen bonding, e.g. the number of hydrogen bond donors (HBD), acceptors (HBA) or polar molecular surface area (PSA). A positive correlation with logBB is seen for descriptors related to lipophilicity such as LogP. Furthermore, acids having a negative charge at physiological pH generally have lower logBB than do basic drugs with a net positive charge (Clark 2003). The underlying mechanisms of these findings are identified and discussed in Sect. 11.2.3. The predictivity levels achieved using the various datasets and approaches are sometimes considered to "approach experimental error", since the predictions are on average ~threefold away from the measured value (Clark 2003).

With respect to classification approaches, Palm and co-workers demonstrated that orally administered drugs should not exceed a PSA greater than 120 $Å^2$ (Palm et al. 1997). Inspired by this work, Kelder and co-workers published a prediction model for logBB based on PSA together with an analysis showing that the majority of CNS^+ drugs have PSA 60 $Å^2$ or less (Kelder et al. 1999). The accuracy of classification of CNS^+/CNS^- datasets is generally >80 % correct and slightly better for CNS^+ compounds than CNS^- compounds (Clark 2003). Table 11.2 summarizes a number classification rules-of-thumb that indicate the characteristics of CNS drugs.

11.2 Current Status

11.2.1 Which Parameter of Drug Exposure in Brain Should Be Used?

A challenge that is currently posed to the community of in silico modellers of drug exposure in the brain is the flagrant lack of common understanding of which parameter that should be predicted. While recent years' debate has highlighted again and

Table 11.2 Characteristics of CNS drugs

Reference	Type of dataset	Property	Favourable value for CNS drugs
(van de Waterbeemd et al. 1998)	CNS^+/CNS^-	PSA	<90 Å^2
		MW	<450
		logD(7.4)	1–3
(Kelder et al. 1999)	CNS^+/CNS^-	PSA	<60–70 Å^2
(Norinder and Haeberlein 2002)	CNS^+/CNS^-	N + O	≤5
	logBB	logP-(N + O)	>0
(Friden et al. 2009)	$K_{p,uu,brain}$	HBA	≤2
(Chen et al. 2011)	$K_{p,uu,brain}$	Kappa2	≤8
(Wager et al. 2010)	CNS+	ClogP	2.8[a]
		ClogD	1.7[a]
		MW	305.3[a]
		TPSA	44.8[a]
		HBD	1[a]
		pK_a	8.4[a]
(Broccatelli et al. 2012)	CNS^+/CNS^-	Volsurf+ $CACO_2$	>−0.3
		Substrate for Pgp[b]	Not substrate
		BDDCS[c]	Class 1

[a]Median (optimal) values for CNS+
[b]For compounds with Volsurf+ $CACO_2 > -0.3$
[c]For P-gp substrates with Volsurf+ $CACO_2 > -0.3$

again the pitfalls of the logBB parameter (Mehdipour and Hamidi 2009; Martin 2004; Hammarlund-Udenaes et al. 2009), the discussions seem not to have resulted in a consensus view of what is the appropriate alternative; logBB, PS, $K_{p,uu,brain}$, $f_{u,brain}$, CNS^+/CNS^- and BBB^+/BBB^- are all used in parallel. Let alone that logBB is still often used; virtually every published modelling work seems to be accompanied by a new interpretation of drug transport kinetics across the BBB. To the extent that this diversity has become problematic, one of its causes are factual misunderstandings of pharmacokinetic principles such as muddling up unbound fractions with unbound concentrations or not appreciating the (in)-dependence of the two. In addition there could be challenges in communicating the intentions of a prediction model. There can for example be different ways of using a logBB prediction model that are based on compounds whose BBB transport is supposedly "governed by passive diffusion". Such a prediction model could be used either with the intention to "optimize logBB" (not recommended) or for comparison with experimental logBB data to indirectly deduce information on drug efflux and unbound drug exposure in the brain (sound).

Recently, focus may have shifted towards characterizing CNS^+ datasets or modelling CNS^+/CNS^- datasets (Sect. 11.2.4), which highlights that the optimization of CNS drugs should be done in a more holistic manner that doesn´t treat drug exposure in the brain separately from other critical drug properties that need optimization.

With respect to in silico modelling of experimental measurements, the fundamentals of pharmacokinetics make a clear case that the $K_{p,uu,brain}$ is an appropriate and adequate parameter. The experimental methodology for $K_{p,uu,brain}$ determination has been available since microdialysis became a quantitative methodology in the 1990s (Elmquist and Sawchuk 1997; de Lange et al. 1999; Hammarlund-Udenaes 2000). More efficient methods were described around the turn of the century (Kakee et al. 1996; Kalvass and Maurer 2002), yet there are currently only a couple of reports including explicit analysis of its relationship with the chemical properties of the drug (Friden et al. 2009; Chen et al. 2011).

11.2.2 Emerging Understanding of Determinants of Unbound Drug Exposure in the Brain, $K_{p,uu,brain}$

In 2009, Fridén et al. published a dataset of $K_{p,uu,brain}$ for 41 structurally diverse compounds obtained using a combination of in vivo brain tissue sampling and in vitro brain slice method (Friden et al. 2009). With respect to the values of $K_{p,uu,brain}$ it clearly showed that active efflux dominates drug disposition in the brain, since a majority of drugs had $K_{p,uu,brain}$ values less than unity and few drugs had values greater than unity (Fig 11.2). The range of $K_{p,uu,brain}$ was from 0.006 for methotrexate to 2.0 for bupropion, i.e. 300-fold. In contrast, $K_{p,brain}$ from the same dataset ranged from ~0.002 for sulphasalazine to 20 for amitriptyline, i.e. 10,000-fold, which is considerably larger than for $K_{p,uu,brain}$. The relationship between $K_{p,uu,brain}$ and 16 conventional molecular descriptors was analyzed using PLS. The most significant molecular descriptors for the relationship with $K_{p,uu,brain}$ were those that relate to hydrogen bonding, i.e. PSA and HBA (Fig. 11.3). Most other descriptors, including those of lipophilicity, did not add to the predictivity and a simple model was put forth that used HBA as a single descriptor (Fig. 11.4).

$$\log K_{p,uu,brain} = -0.04 - 0.14 \times \mathrm{HBA} \tag{11.1}$$

The model was interpreted as follows; in order to achieve a twofold increase in $K_{p,uu,brain}$, it is necessary to remove 2 HBAs from the molecular structure. Conversely, a twofold reduction in $K_{p,uu,brain}$ can be achieved by addition of 2 HBAs. The moderate predictivity of the models, explaining only 40–50 % of the variability in $K_{p,uu,brain}$ between drugs was rationalized as being due to the smaller range of values compared to $K_{p,brain}$ (logBB) and the fact that any deviation of $K_{p,uu,brain}$ from unity reflects the involvement of carrier-mediated transport.

Using similar experimental methodology Chen and co-workers expanded this dataset to 246 with AstraZeneca proprietary compounds (Chen et al. 2011). The analysis was made with 196 molecular descriptors and various machine learning algorithms. The best model was a consensus model that incorporated several submodels. The predictivity on a subset (test-set) of 73 compounds ($R^2 = 0.56$) suggests a substantial improvement versus the previous study (Friden et al. 2009); however,

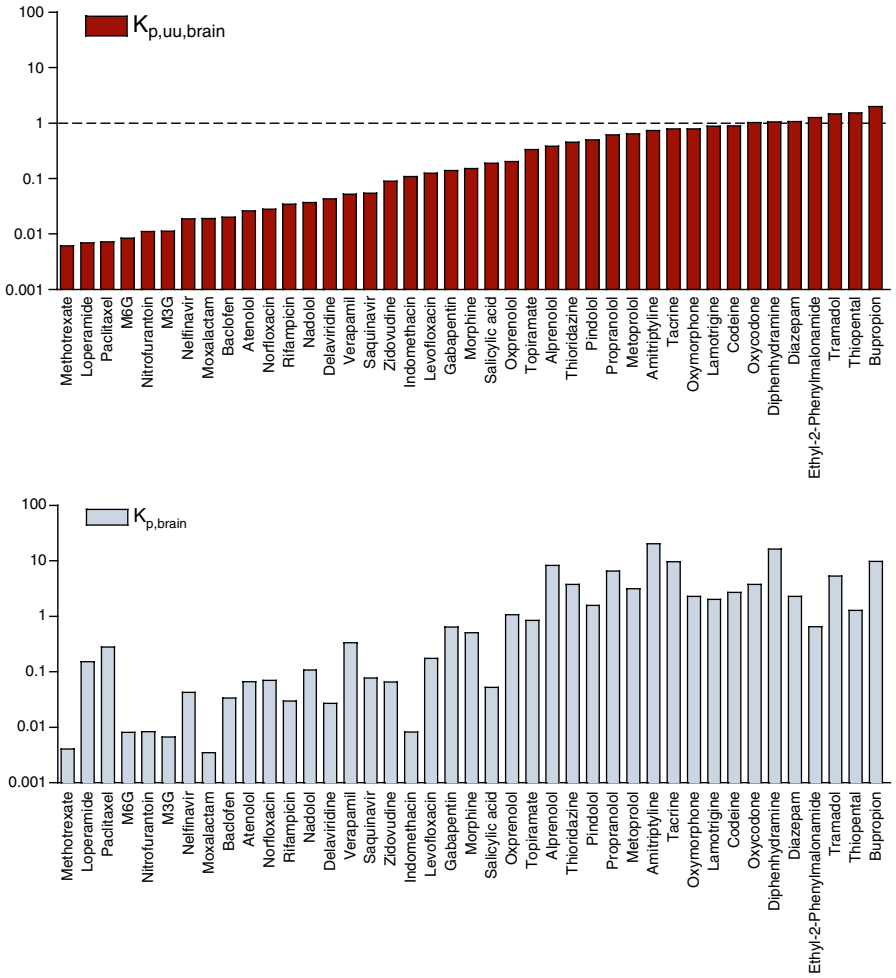

Fig. 11.2 Distribution of $K_{p,uu,brain}$ and $K_{p,brain}$ values for 41 diverse drugs. Constructed from data in reference (Friden et al. 2009)

it is much worse than reported for models of logBB. The analysis of the importance of individual descriptors identified several descriptors relating to hydrogen bonding; however, the single most important descriptor was Kappa2 that describes the molecular shape in terms of its linearity. Interestingly, extensively branched compounds with Kappa2 greater than 8 had lower values for $K_{p,uu,brain}$ than did more linear compounds with Kappa2 values of 8 or below (Fig 11.5).

While the importance of hydrogen bonding is in line with models of logBB and CNS^+/CNS^- classification, it is intriguing that lipophilicity, which is normally correlated with passive transport, did not increase the value of $K_{p,uu,brain}$. This is a remarkable finding since it directly contradicts the common perception amongst

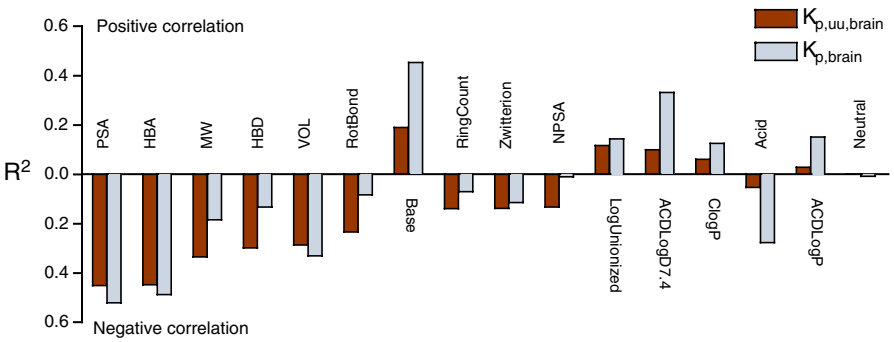

Fig. 11.3 Linear correlation coefficient, R^2, for $K_{p,uu,brain}$, $K_{p,brain}$, and each of the 16 molecular descriptors for the selected drugs in the training dataset. The upward and downward orientations of the bars represent positive and negative correlations, respectively, with $K_{p,uu,brain}$ and $K_{p,brain}$. Constructed from data in reference (Friden et al. 2009)

clinicians that drug access to the brain is determined by the lipid solubility of the drug. It was proposed as a plausible explanation that the effect of increased passive transport by increased lipophilicity is paralleled and offset by increased efflux owing to increased drug concentrations in the membrane where the interaction takes place between drug and P-glycoprotein or other transporters (Friden et al. 2009). Hence, the dominating position of hydrogen bonding for structure–brain exposure relationships seems to arise from its additive effects on passive and active transport independently of lipophilicity; a less lipophilic drug with many HBAs has very limited passive transport and is thus sensitive to low capacity active efflux, while a lipophilic drug with many HBAs is a probable transporter substrate, e.g. a P-gp substrate (Seelig and Landwojtowicz 2000).

The example of beta-blockers introduced above can be analyzed in this context (Fig 11.1); it suggests that the lower $K_{p,uu,brain}$ of atenolol versus propranolol is due to its 2 additional hydrogen bond acceptors (and the increased potential for transporter interactions) rather than being related to reduced passive diffusion as governed by lipophilicity (ACDlogD7.4). Note the similar structures of atenolol and propranolol in Fig 11.1.

11.2.3 Relationship Between Prediction Models for log BB and $K_{p,uu,brain}$

The evident discrepancy between the interpretations of the classical work with logBB and the recent work with $K_{p,uu,brain}$ warrants a more detailed discussion. The key to understanding the difference is to grasp how logBB (11.2) is a composite parameter of $K_{p,uu,brain}$ (the actual effect of the BBB), plasma protein binding ($f_{u,p}$),

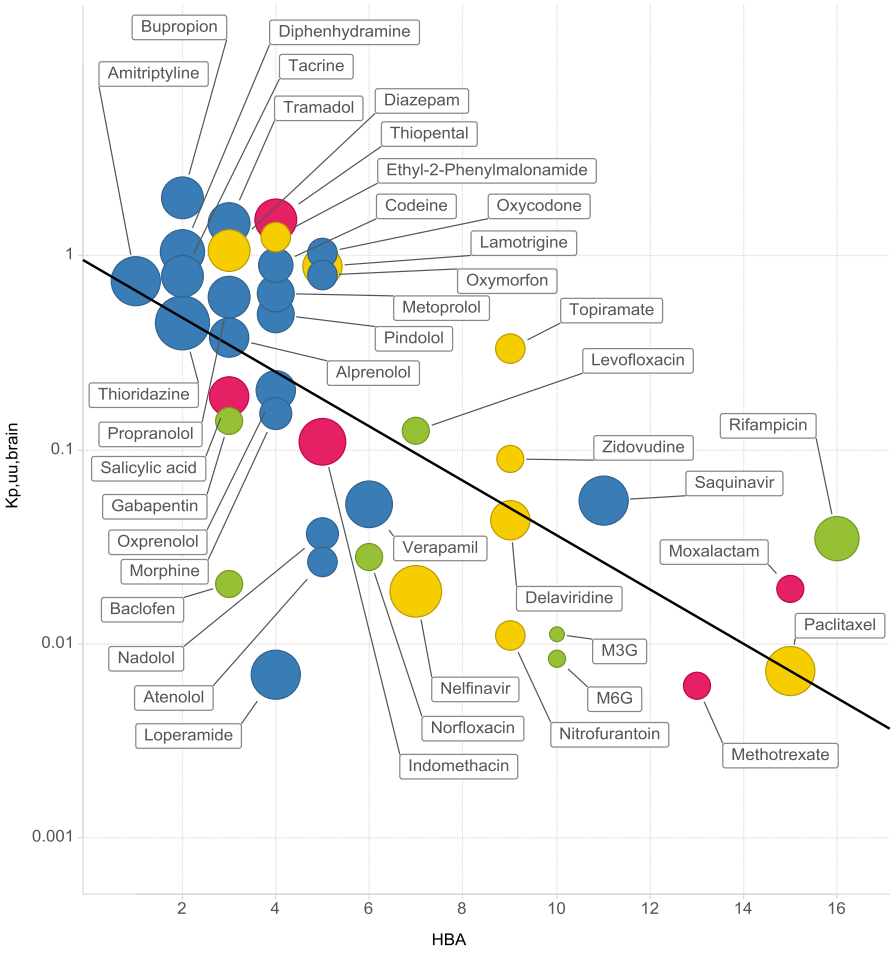

Fig. 11.4 Observed versus predicted rat $K_{p,uu,brain}$ based on HBA (11.1). There is no obvious relationship between $K_{p,uu,brain}$ and lipophilicity (marker size by cLogP) or ion class (bases *blue*, acids *red*, neutral *yellow* and zwitterions *green*). Constructed form data in reference (Friden et al. 2009)

and non-specific binding in the brain tissue described by the unbound volume of distribution in brain ($V_{u,brain}$).

$$\mathrm{BB} = K_{p,uu,brain} \times V_{u,brain} \times f_{u,p} \tag{11.2}$$

As such, any model of logBB is "contaminated" with $V_{u,brain}$ and $f_{u,p}$; $K_{p,uu,brain}$ is in itself the pharmacologically relevant concentration gradient of unbound drug across the BBB, and its steady-state value is independent of $V_{u,brain}$ and $f_{u,p}$. A logBB PLS model was developed using the same molecular descriptors and dataset (Friden et al. 2009). The relationship between logBB and structure was dominated by hydrogen bonding similar to $K_{p,uu,brain}$ (Fig. 11.3). In contrast to $K_{p,uu,brain}$, however, logBB was also positively correlated with descriptors of lipophilicity.

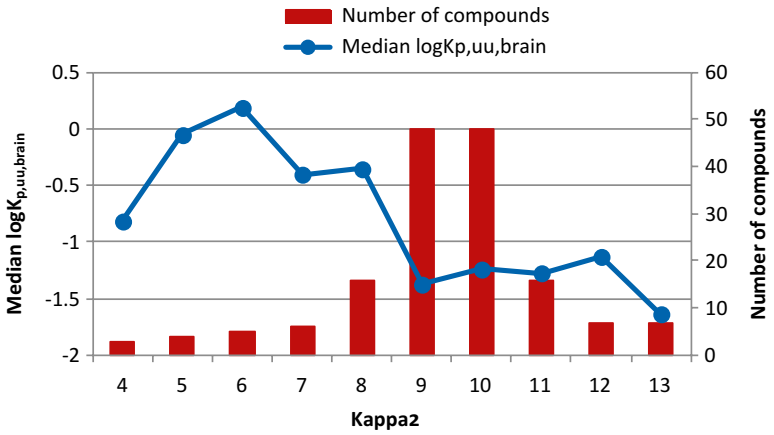

Fig. 11.5 The relationship between the median log $K_{p,uu,brain}$ and Kappa2. Note the drop in $K_{p,uu,brain}$ as Kappa2 exceeds 8 for increasingly branched molecules. Constructed from data in reference (Chen et al. 2011)

Furthermore, logBB was higher for basic drugs than for acidic drugs (Fig. 11.3). The PLS model that was developed contained one descriptor for hydrogen bonding (HBA), one descriptor of lipophilicity (ACDLogD7.4) and the ion class of the drug (acid or base):

$$\log BB = -0.18 - 0.097\text{HBA} + 0.10\text{ACD}\log\text{D7.4} + 0.68\text{Base} - 0.67\text{Acid} \quad (11.3)$$

The predictivity of the logBB model was better than the $K_{p,uu,brain}$ model based on comparison of Q^2 (0.693 vs. 0.426). The better Q^2 value of the logBB model should be seen in the light of the 30-fold greater range of observed values. In contrast, similar predictivity is seen based on the root of mean squared error (RMSE, 4.0-fold vs. 3.9-fold). The logBB model was mechanistically rationalized as follows: HBA accounts for the part of logBB which is, in fact, related to $K_{p,uu,brain}$; ACDLogD7.4 and the drug being basic accounts for binding to phospholipid in tissue ($V_{u,brain}$); and the drug being acidic accounts for extensive binding to albumin in plasma ($f_{u,p}$). A plot of $K_{p,brain}$ versus $K_{p,uu,brain}$ (Fig 11.6) clearly shows that the ion class explains much of the differences between the two. The imminent risk of relying on logBB-derived prediction models is the design of drugs that are unnecessarily lipophilic or basic without improved unbound brain exposure; or if restricted brain exposure is desired, the design of albumin bound acidic compounds that later prove to have significant CNS effects at therapeutic plasma concentrations.

11.2.4 Recent Developments in CNS⁺/CNS⁻ Classification

Possibly pushed by the debate around logBB, many workers have recently used CNS^+/CNS^- classification as parameter for in silico model development. The CNS^+/

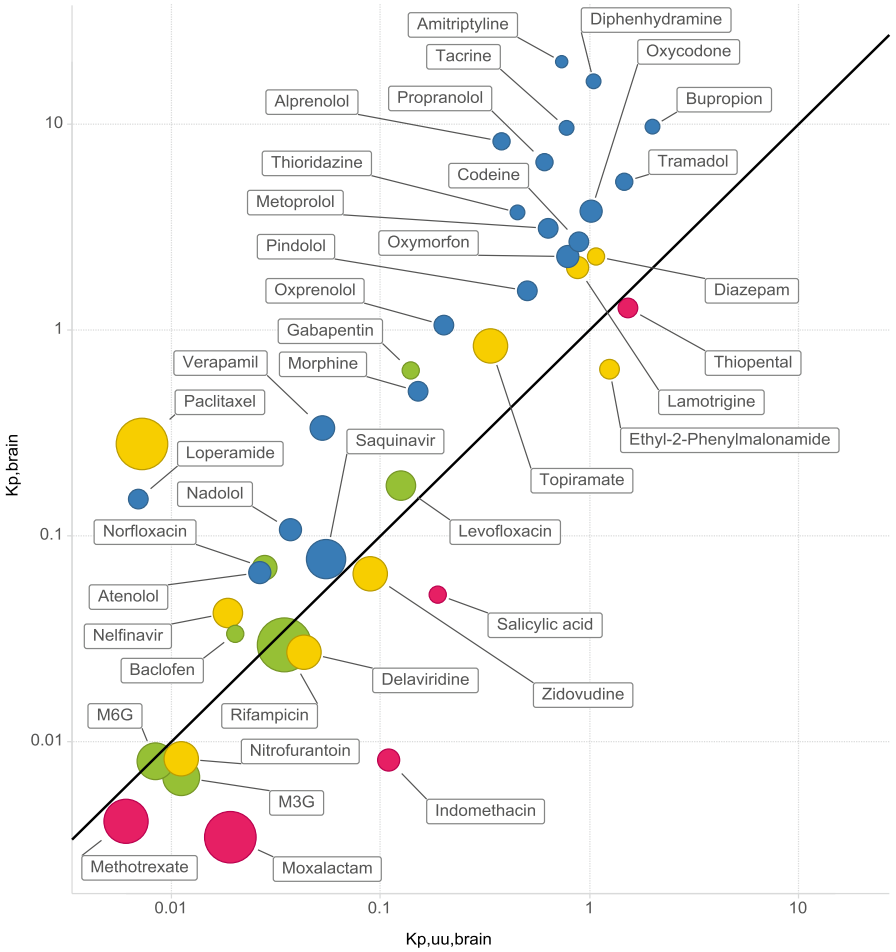

Fig. 11.6 The relationship between $K_{p,brain}$ and $K_{p,uu,brain}$ is largely dependent on the ion class of the drug; relative to their $K_{p,uu,brain}$ basic drugs (*blue* markers) have high $K_{p,brain}$ and acids (*red* markers) low $K_{p,brain}$. This is because basic drugs tend to bind to brain tissue constituents more strongly than to plasma proteins, whereas the opposite is observed for acidic drugs. For neutrals (*yellow* markers) and zwitterions (*green* markers) there is better agreement and no clear trend. Markers are sized according to the number of hydrogen bond acceptors. The solid line represents identity. Constructed from data in (Friden et al. 2009)

CNS^- datasets have been trimmed in various ways; some have chosen not to include any investigational drugs on the basis of that the majority of investigational CNS^+ drugs fail to reach the market (Ghose et al. 2012). Others have also carefully scrutinized the CNS^- class by applying a cut-off value for actual measurements in humans using positron emission tomography (PET) or sampling of cerebrospinal fluid and named the classification scheme BBB^+/BBB^- (Broccatelli et al. 2012). Much work is also done to analyse the group of CNS drugs on the market as it stands. The philosophy is that there are so many other pivotal CNS drug properties in addition to

brain exposure that need consideration in drug design: metabolic clearance, safety risks, etc. Wager and co-workers developed a CNS multiparameter optimization (MPO) approach to assess the alignment of a drug candidate's chemical properties to those of marketed CNS drugs (Wager et al. 2010). Using this approach they showed that the CNS MPO score of 108 Pfizer candidates were distributed considerably less favourably thus suggesting that the CNS MPO score could indicate the chances of a candidate becoming a registered drug. Recently, a pipeline of rules has been proposed based on a combination of in silico predicted permeability, experimental classification as substrate or non-substrate of P-gp and the class belonging to the Biopharmaceutics Drug Disposition Classification System (BDDCS) (Broccatelli et al. 2012). The prediction model performed better than a number of purely computationally based classification models based on the same BBB^+/BBB^- dataset. Recent classification approaches are summarized in Table 11.2 together with older rules of thumb.

Carefully scrutinized CNS^+/CNS^- classification is arguably a convincing parameter of drug exposure in brain in the sense that it is based on human in vivo information. A major drawback of classification approaches, however, is that information on brain exposure is reduced from its natural (continuous) ratio measurement to the binary CNS^+/CNS^-. By introducing cut-off values to compile data-sets one is not only removing potentially useful information but also adding in new by the arbitrary choice of cut-off. This problem is obvious when considering a group of equivalent drugs around the cut-off value.

11.3 Future Directions and Challenges

Recent work on $K_{p,uu,brain}$ datasets has shed new light on the significance of molecular properties for drug exposure in the brain; lipophilicity does not seem to play a major role. Equally important, it became evident that the predictivity of $K_{p,uu,brain}$ models was much lower than that for logBB models assessed by cross-validated Q^2 on training-sets or R^2 on test-sets. This is related to the smaller range of values for $K_{p,uu,brain}$ than that for logBB; to date at best, only 50–60 % of the variability in $K_{p,uu,brain}$ between compounds has been possible to relate to descriptors of molecular properties. There are three messages in this observation that need to be appreciated. First, the smaller range of $K_{p,uu,brain}$ compared to BB or PS means that the extent to which drugs differ with respect to exposure in the brain has been somewhat exaggerated. Second and related to the first, the established perception that "brain penetration" is a predictable drug property needs reconsideration; the apparent success of in silico models of logBB or PS is due to the parameter being inclusive of additional drug properties such as non-specific binding in brain, which are easily predicted yet not relevant to the problem. Third, the remaining hardship of predicting $K_{p,uu,brain}$ reflects the fact that any variability in $K_{p,uu,brain}$ between compounds is caused by drug-specific, multi-specific molecular interactions with the drug transporters at the BBB.

11.3.1 Improving Predictions of $K_{p,uu,brain}$ by Integration of Approaches

Drug exposure in the brain is primarily determined by specific interactions with the transporters at the BBB. It therefore appears likely that the approaches used so far have already delivered close to their full potential. An interesting way forward can be molecular modelling of the BBB drug transporters. Molecular modelling of transporters can be applied either by using a transporter-based approach, which utilizes the three-dimensional crystal structure of the protein, or if this is not known as is generally the case, a substrate-based approach, e.g. comparative molecular field analysis (CoMFA) yielding a pharmacophore model of the transporter. Several review articles have featured the developments in this field (Demel et al. 2009; Ecker et al. 2008; Ekins et al. 2007; Winiwarter and Hilgendorf 2008). However successful these models may become in terms of discriminating substrates from non-substrates, it is just a first step of being able to make quantitative predictions of $K_{p,uu,brain}$. This is because a drug can be substrate of several different transporters at the BBB and there is interplay with passive transport as well as additional mechanisms of drug elimination from brain including metabolism and bulk flow of brain interstitial fluid. Integration of molecular modelling (of several transporters) with passive diffusion and physiologically based pharmacokinetic (PBPK) models would seem like a logic and appealing approach but it is likely to remain a utopia for years to come. The success of progressing the field of $K_{p,uu,brain}$ predictions is more likely to depend on the development of new and imaginative ways of integrating different computational and experimental methodologies with machine learning algorithms. As a simple example it would be feasible to use experimental measurements of, for example, passive diffusion and molecular modelling "docking scores" as variables alongside molecular descriptors in, for example, a PLS analysis. Moreover, novel machine learning algorithms previously used to predict $K_{p,uu,brain}$ (or logBB) from computed molecular descriptors could also find an application to predict $K_{p,uu,brain}$ from a battery of in vitro transporter assays. While for preclinical species in vivo methodologies will remain the mainstay for drug discovery, it is important to progress predictions of drug exposure in the brain using in vitro and in silico methodologies in order to conduct a proper translation to humans.

11.3.2 Drug Design Strategies

As discussed in Sect. 11.2.2 a default and crude strategy to "optimize" drug exposure in the brain would be to add or remove hydrogen bond acceptors to the molecular structure; for every addition or removal of two hydrogen bond acceptors one should expect a twofold reduction or increase, respectively, in $K_{p,uu,brain}$. Even though the

accuracy of this kind of prediction is improved by using more complex modelling approaches it comes at the expense of the model being difficult to comprehend for the modeller. This lack of transparency can be very unhelpful for the chemist who needs an idea of *how* to change the molecular structure to obtain the desired change in $K_{p,uu,brain}$. In an investigation of the trade-off between model accuracy and comprehensibility it was shown for a set of 16 biopharmaceutical classification tasks that in general there is a limited cost of prediction accuracy when choosing a comprehensible model (Johansson et al. 2011). Lack of transparency of a model is commonly mitigated by construction of virtual compound libraries that can be screened in the prediction model whereby promising compound structures can be identified for synthesis.

The discussed challenges of making $K_{p,uu,brain}$ predictions based on in silico models should not shadow its utility for drug design. Frequently, more predictive models can be obtained for a set of compounds with a more limited range of properties, i.e. with a smaller applicability domain. This is typically the case when optimizing a chemical drug series for a particular drug target. The limited applicability domain of this situation is a double edged sword; on the one hand it helps the understanding of what molecular features are associated with high or low $K_{p,uu,brain}$ for the particular series, but it also does not tell the chemist how to make molecules that are different and even better than the ones already made and used in the model. An approach recently taken at AstraZeneca to extend the $K_{p,uu,brain}$ beyond the existing domain is to pay attention to structural modifications that result in compounds that deviate from the prediction model in a favourable direction (Plowright et al. 2012). The idea was that in spite of such a compound having a mediocre $K_{p,uu,brain}$, it possesses a new structural element that when combined with the favourable molecular properties as described by the model achieves a step-change in $K_{p,uu,brain}$ (Fig 11.7). This approach exemplifies how computational methods can not only be used to derive prediction models as such, but also be used to discover and exploit hidden patterns in the experimental data.

11.4 Conclusions

In silico prediction of a compounds ability to efficiently cross the BBB has been an area of development for decades; computational methodologies have evolved and experimental datasets have increased in size. Yet the (lack of) pharmacologic meaning of the commonly used logBB measurement has been generally overlooked and it is rather recently that the focus of modellers has either turned to classification approaches on CNS^+/CNS^- datasets or to datasets of *unbound* drug exposure in the brain ($K_{p,uu,brain}$), which is considered a pharmacologically meaningful parameter. In silico modelling of $K_{p,uu,brain}$ has corroborated some findings from logBB models but disputed others; whereas the importance of hydrogen bonding stands strong, there is no evidence based on $K_{p,uu,brain}$ that compound lipophilicity has any influence on drug exposure in the brain. As should be expected from a parameter that is

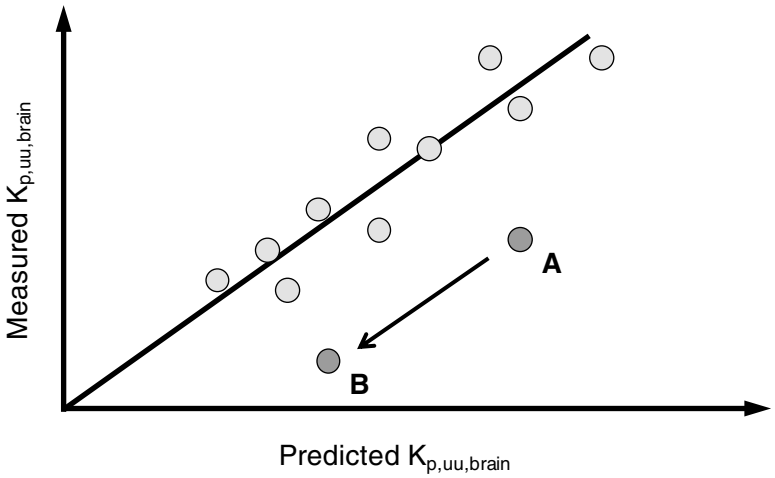

Fig. 11.7 A prediction model can be used to identify outliers with promising properties for optimization. In the figure, compound A is predicted substantially higher than the experimental value for whatever reason, but the value is not as low as desired. Structural modification of A as guided by the prediction model results in a new compound B with superior properties. Adapted from (Plowright et al. 2012)

determined by multiple specific and unspecific molecular interactions, the success of $K_{p,uu,brain}$ predictions has been moderate even when applying state-of-the-art modelling methodologies. Hence, there appears to be rather limited scope for improvement in this field with the toolbox used to date, i.e. modelling of molecular descriptors. Instead, the advancement of predictions of drug exposure in the brain from the chemical structure requires the inclusion of additional sources of information such as in vitro measurements and clever ways of integrating the data. Future work with predictions of drug exposure in the brain will facilitate the translation from the preclinical species to humans, and thus raise the power of in silico modelling to the desired level for successful development of new drug treatments.

11.5 Topics for Discussion

- What is meant by the applicability domain of a model and why is it important to define it?
- Why is it necessary to use a test-set of compounds to validate a model?
- What aspects of a molecule's properties are not covered by the descriptors listed in Table 11.1?
- What are the mechanistic reasons why hydrogen bonding plays such an important role for unbound drug exposure in the brain?
- What could be the reasons for prediction models of $K_{p,uu,brain}$ not requiring descriptors of lipophilicity?

- At which stages in the drug discovery process is it more useful to have an in silico model for drug exposure in the brain?
- To what an extent can in silico models replace in vitro or in vivo experiments?
- Which measurement logPS or logBB would you expect to correlate more closely with lipophilicity and why?
- What are the strengths and weaknesses of modelling categorical CNS^{+}/CNS^{-} datasets versus the continuous $K_{p,uu,brain}$ variable?

References

Abraham MH, Hersey A (2007) In silico models to predict brain uptake. In: Comprehensive medicinal chemistry II (anonymous), John B. Taylor and David J. Triggle. Elsevier Ltd., London, p 745

Abraham MH (2004a) The factors that influence permeation across the blood–brain barrier. Eur J Med Chem 39:235–240

Abraham MH (2004b) The factors that influence permeation across the blood–brain barrier. Eur J Med Chem 39:235–240

Abraham MH, Ibrahim A, Zissimos AM, Zhao YH, Comer J, Reynolds DP (2002) Application of hydrogen bonding calculations in property based drug design. Drug Discov Today 7: 1056–1063

Abraham MH, Chadha HS, Mitchell RC (1994) Hydrogen bonding. 33. Factors that influence the distribution of solutes between blood and brain. J Pharm Sci 83:1257–1268

Bendels S, Kansy M, Wagner B, Huwyler J (2008) In silico prediction of brain and CSF permeation of small molecules using PLS regression models. Eur J Med Chem 43:1581–1592

Broccatelli F, Larregieu CA, Cruciani G, Oprea TI, Benet LZ (2012) Improving the prediction of the brain disposition for orally administered drugs using BDDCS. Adv Drug Deliv Rev 64:95–109

Chen H, Winiwarter S, Friden M, Antonsson M, Engkvist O (2011) In silico prediction of unbound brain-to-plasma concentration ratio using machine learning algorithms. J Mol Graph Model 29:985–995

Clark DE (2003) In silico prediction of blood–brain barrier permeation. Drug Discov Today 8:927–933, see comment

de Lange EC, de Boer BA, Breimer DD (1999) Microdialysis for pharmacokinetic analysis of drug transport to the brain. Adv Drug Deliv Rev 36:211–227

Demel MA, Kramer O, Ettmayer P, Haaksma EE, Ecker GF (2009) Predicting ligand interactions with ABC transporters in ADME. Chem Biodivers 6:1960–1969

Ecker GF, Stockner T, Chiba P (2008) Computational models for prediction of interactions with ABC-transporters. Drug Discov Today 13:311–317

Ecker GF, Noe CR (2004) In silico prediction models for blood–brain barrier permeation. Curr Med Chem 11:1617–1628

Ekins S, Ecker GF, Chiba P, Swaan PW (2007) Future directions for drug transporter modelling. Xenobiotica 37:1152–1170

Elmquist WF, Sawchuk RJ (1997) Application of microdialysis in pharmacokinetic studies. Pharm Res 14:267–288

Friden M, Winiwarter S, Jerndal G, Bengtsson O, Wan H, Bredberg U, Hammarlund-Udenaes M, Antonsson M (2009) Structure-brain exposure relationships in rat and human using a novel data set of unbound drug concentrations in brain interstitial and cerebrospinal fluids. J Med Chem 52:6233–6243

Friden M, Gupta A, Antonsson M, Bredberg U, Hammarlund-Udenaes M (2007) In vitro methods for estimating unbound drug concentrations in the brain interstitial and intracellular fluids. Drug Metabol Dispos 35:1711–1719

Ghose AK, Herbertz T, Hudkins RL, Dorsey BD, Mallamo JP (2012) Knowledge-based, central nervous system (CNS) lead selection and lead optimization for CNS drug discovery. ACS Chem Neurosci 3:50–68

Gratton JA, Abraham MH, Bradbury MW, Chadha HS (1997) Molecular factors influencing drug transfer across the blood–brain barrier. J Pharm Pharmacol 49:1211–1216

Gupta A, Chatelain P, Massingham R, Jonsson EN, Hammarlund-Udenaes M (2006) Brain distribution of cetirizine enantiomers: comparison of three different tissue-to-plasma partition coefficients: K(p), K(p, u), and K(p, uu). Drug Metabol Dispos 34:318–323

Hammarlund-Udenaes M, Bredberg U, Friden M (2009) Methodologies to assess brain drug delivery in lead optimization. Curr Top Med Chem 9:148–162

Hammarlund-Udenaes M, Friden M, Syvänen S, Gupta A (2008) On the rate and extent of drug delivery to the brain. Pharm Res 25:1737–1750

Hammarlund-Udenaes M (2000) The use of microdialysis in CNS drug delivery studies. Pharmacokinetic perspectives and results with analgesics and antiepileptics. Adv Drug Deliv Rev 45:283–294

Hitchcock SA, Pennington LD (2006) Structure-brain exposure relationships. J Med Chem 49:7559–7583

Johansson U, Sonstrod C, Norinder U, Bostrom H (2011) Trade-off between accuracy and interpretability for predictive in silico modeling. Future Med Chem 3:647–663

Kakee A, Terasaki T, Sugiyama Y (1996) Brain efflux index as a novel method of analyzing efflux transport at the blood–brain barrier. J Pharmacol Exp Therapeut 277:1550–1559

Kalvass JC, Maurer TS (2002) Influence of nonspecific brain and plasma binding on CNS exposure: implications for rational drug discovery. Biopharm Drug Dispos 23:327–338

Kelder J, Grootenhuis PD, Bayada DM, Delbressine LP, Ploemen JP (1999) Polar molecular surface as a dominating determinant for oral absorption and brain penetration of drugs. Pharm Res 16:1514–1519

Lanevskij K, Dapkunas J, Juska L, Japertas P, Didziapetris R (2011) QSAR analysis of blood-brain distribution: the influence of plasma and brain tissue binding. J Pharm Sci 100:2147–2160

Levin VA (1980) Relationship of octanol/water partition coefficient and molecular weight to rat brain capillary permeability. J Med Chem 23:682–684

Liu X, Tu M, Kelly RS, Chen C, Smith BJ (2004) Development of a computational approach to predict blood–brain barrier permeability. Drug Metab Dispos 32:132–139

Luco JM (1999) Prediction of the brain-blood distribution of a large set of drugs from structurally derived descriptors using partial least-squares (PLS) modeling. J Chem Inf Comput Sci 39:396–404

Martin I (2004) Prediction of blood–brain barrier penetration: are we missing the point? Drug Discov Today 9:161–162, see comment

Matsson P (2007) ATP-Binding cassette efflux transporters and passive membrane permeability in drug absorption and disposition. Digital Comprehensive Summaries of Uppsala Dissertations from the Faculty of Pharmacy 67:68

McAinsh J, Cruickshank JM (1990) Beta-blockers and central nervous system side effects. Pharmacol Therapeut 46:163–197

Mehdipour AR, Hamidi M (2009) Brain drug targeting: a computational approach for overcoming blood–brain barrier. Drug Discov Today 14:1030–1036

Norinder U, Haeberlein M (2002) Computational approaches to the prediction of the blood–brain distribution. Adv Drug Deliv Rev 54:291–313

Osterberg T, Norinder U (2000) Prediction of polar surface area and drug transport processes using simple parameters and PLS statistics. J Chem Inf Comput Sci 40:1408–1411

Palm K, Stenberg P, Luthman K, Artursson P (1997) Polar molecular surface properties predict the intestinal absorption of drugs in humans. Pharm Res 14:568–571

Pardridge WM (2004) Log(BB), PS products and in silico models of drug brain penetration. Drug Discov Today 9:392–393, see comment

Plowright AT, Nilsson K, Antonsson M, Amin K, Broddefalk J, Jensen J, Lehmann A, Jin S, St-Onge S, Tomaszewski MJ, Tremblay M, Walpole CS, Wei Z, Yang H, Ulander J (2012)

Discovery of agonists of cannabinoid receptor 1 with restricted CNS penetration aimed for treatment of gastroesophageal reflux disease. J Med Chem. doi:10.1021/jm301511h
Seelig A, Landwojtowicz E (2000) Structure-activity relationship of P-glycoprotein substrates and modifiers. Eur J Pharm Sci 12:31–40
van de Waterbeemd H, Smith DA, Jones BC (2001) Lipophilicity in PK design: methyl, ethyl, futile. J Comput Aided Mol Des 15:273–286
van de Waterbeemd H, Camenisch G, Folkers G, Chretien JR, Raevsky OA (1998) Estimation of blood–brain barrier crossing of drugs using molecular size and shape, and H-bonding descriptors. J Drug Target 6:151–165
Wager T, Hou X, Verhoest PR, Villalobos A (2010) Moving beyond rules: the development of a central nervous system multiparameter optimization (CNS MPO) approach to enable alignment of druglike properties. ACS Chem Neurosci 1:435–449
Winiwarter S, Hilgendorf C (2008) Modeling of drug-transporter interactions using structural information. Curr Opin Drug Discov Devel 11:95–103
Winiwarter S, Ridderström M, Ungell AL, Andersson TB, Zamora I, Zamora I (2007) Use of molecular descriptors for absorption, distribution, metabolism, and excretion predictions. In: comprehensive medicinal chemistry II (anonymous), John B. Taylor and David J. Triggle. Elsevier Ltd., London, p 745
Wold S (2001) PLS-regression: a basic tool of chemometrics. Chemometr Intell Lab 58:109–130
Wold S (1991) Validation of QSAR's. Quant Struct: Act Relat 10:191–193
Young RC, Mitchell RC, Brown TH, Ganellin CR, Griffiths R, Jones M, Rana KK, Saunders D, Smith IR, Sore NE (1988) Development of a new physicochemical model for brain penetration and its application to the design of centrally acting H2 receptor histamine antagonists. J Med Chem 31:656–671

Chapter 12
Integrated Approach to Optimizing CNS Penetration in Drug Discovery: From the Old to the New Paradigm and Assessment of Drug–Transporter Interactions

Andreas Reichel

Abstract Assessing CNS penetration in drug discovery and development is important for both CNS projects *and* non-CNS projects that aim to improve desired or to avoid unwanted central effects of their drug candidates. After a brief reasoning on the flawed old concept of maximising total brain levels, the chapter describes the key principles of the new paradigm of examining CNS penetration and distribution by integrating those parameters and processes that are crucial in controlling unbound brain concentrations as surrogate for the pharmacologically active drug concentration in brain. As a consequence, $K_{p,uu,brain}$ is about to replace the total brain/plasma ratio $K_{p,brain}$ as measure of the extent of brain penetration. The chapter outlines strategies, methods and approaches both for the optimisation of CNS penetration as well as for avoiding it, including exemplary lead optimisation screening trees of CNS and non-CNS projects. A comprehensive framework is given linking the pharmacokinetics of a compound in the body's periphery to its central (unbound) exposure and subsequent PKPD relation in animal models of efficacy, including considerations for the translation of the PKPD relationships from rodents to larger animals and human. The chapter furthermore summarises current knowledge of drug–transporter interactions at the level of the BBB, and outlines the potential of the new concept for refueling the fading interest in CNS drug discovery and development as a result of too many clinical trial failures and an insufficient understanding of the reasons.

A. Reichel (✉)
Research Pharmacokinetics, DMPK, Global Drug Discovery,
Bayer Pharma AG, Müllerstrasse 178, Berlin 13353, Germany
e-mail: andreas.reichel@bayer.com

M. Hammarlund-Udenaes et al. (eds.), *Drug Delivery to the Brain*, AAPS Advances in the Pharmaceutical Sciences Series 10, DOI 10.1007/978-1-4614-9105-7_12,

12.1 Introduction

Knowledge about the CNS penetration of new compounds is important in all drug discovery projects regardless of whether the drug target resides within the CNS or outside of it in the body's periphery. While this is very obvious for CNS drug discovery programmes where sufficient brain penetration is prerequisite for a successful drug candidate to reach its site of action, it may be less so for non-CNS projects. However, ignoring brain penetration for peripherally acting drugs may pose severe safety concerns for the patient. Reviewing more than 250 divers compounds Easter et al. (2009) showed that more than 50 % of them cause seizures or convulsions despite their primary targets being outside of the CNS. A recent analysis of the group of Les Benet suggests that almost all BDDCS class 1 drugs markedly distribute into brain regardless of whether their primary drug target is in the CNS or in the periphery of the body (Broccatelli et al. 2012). Therefore, early information on the ability of new chemical entities (NCEs) to penetrate the CNS has become vital in drug discovery and development in order to better understand and control drug safety and drug efficacy (Wager et al. 2012).

The astonishing complexity of the brain's anatomy, function and diseases makes CNS drug discovery notoriously difficult. Indeed developing new drugs for mental health disorders and neurological diseases takes considerably longer and costs much more while clinical success rates are significantly lower than in any other therapeutic area (Kola and Landis 2004; Tufts CSDD Impact Report 2012). With clinical success rates of new CNS drug candidates continuing to decline many pharma companies currently reduce or even abandon their efforts in this field in spite of a growing medical need (Abbott 2011). The quest is high for analysis of the reasons for failure and the deduction of lessons-learned for CNS drug discovery programmes to become more successful.

In a recent meta-analysis Griebel and Holsboer (2012) have shown that there are multiple factors contributing to the very poor success rate of new medications for psychiatric disorders. Although most often programmes on new CNS targets fail because they do not demonstrate a benefit of new drug candidates in patients in spite of compelling preclinical data in animal disease models it remains difficult to clearly delineate whether this is due to an incomplete understanding of the role the proposed molecular target plays in the disease, inappropriate animal models of the clinical condition in patients, and/or insufficient drug target exposure in human (Palmer and Alavijeh 2012).

Therefore, it is becoming absolutely vital to generate an integrated view on drug target exposure, mode of action, and efficacy which translates reliably from animal models to the clinical setting. Clinical trials can become more successful only if high-quality scientific evidence from preclinical research can be thoroughly tested in patients which are carefully selected for their potential to respond to the proposed mode of action unbiased of any doubt of whether or not there was sufficient drug substance engaging with the target at the site of action in the CNS. A sound link between brain target exposure and target engagement which ensures that the mode of action could principally take place in the patient is fundamental in enabling

clinical research to rigorously test new treatment paradigms based on new CNS targets and to establish how the interference with them can positively affect the course of the disease.

After a brief look at the old CNS drug discovery paradigm and its shortcomings, the present chapter describes the development of the evolving new paradigm of addressing, optimising and characterising CNS penetration and distribution and how it is implemented in today's drug discovery and development process. The chapter also contains a brief overview of transporter-mediated drug–drug interactions at the level of the BBB.

12.2 The Old Paradigm of Addressing CNS Penetration

While the interstitial fluid of many tissues in the body is in relatively free exchange with the blood circulation, brain tissue is not. The brain's parenchyma is completely separated from blood by the tight layer of brain capillary endothelial cells forming, together with other cell types, the so-called blood–brain barrier (BBB) (see Chap. 1). The BBB controls the movement between blood and brain of solutes and nutrients, ions and hormones as well as of peptides, proteins, antibodies and cells. It does, of course, also limit the free entry of drugs into the CNS which lead to the much cited evocation that only some 1–2 % of drugs are able to enter the CNS (Pardridge 2007).

Although this figure may well be exaggerated, it has become paramount for CNS drug discovery programmes to test new compounds—besides of their general ADME properties—also for their ability to enter the CNS (Reichel 2006; Cecchelli et al. 2007; Mangas-Sanjuan et al. 2010; Avdeef 2012). The classical approach to assess brain entry typically involves both in vitro and in vivo testing of new compounds (Fig. 12.1). As all compounds entering the brain have to cross the brain endothelium, in vitro permeability assays have been applied early on, even though a generally accepted in vitro model of the BBB has not been accomplished in spite of many years of intense research (Reichel et al. 2003; Tóth et al. 2011; Naik and Cucullo 2012). For more detailed information on in vitro models of the BBB please refer to Chap. 6. In the absence of an ideal in vitro model of the BBB, surrogate screening tools have become very popular in industry which allows addressing two of the most critical BBB features, the ability of a compound to permeate across a very tight monolayer of cells and the ability to be recognised by efflux pumps, for instance P-glycoprotein (P-gp). P-gp is very highly active at the BBB and efficiently functions to keep many drugs out of the brain (Löscher and Potschka 2005; Broccatelli et al. 2010). MDCK-MDR1 cells have become the most widely used in vitro model screen compounds for their (i) permeability, and (ii) susceptibility to efflux by P-gp. As this cell line is very easy to use, the MDCK-based in vitro permeability assay is run in an automated format, generating information of a compounds permeability and efflux ratio at high throughput. The large amount of data that has been produced in the past has become the basis to build in silico tools for both endpoints assisting medicinal chemistry to design compounds with improved permeation and efflux properties (see Chap. 11).

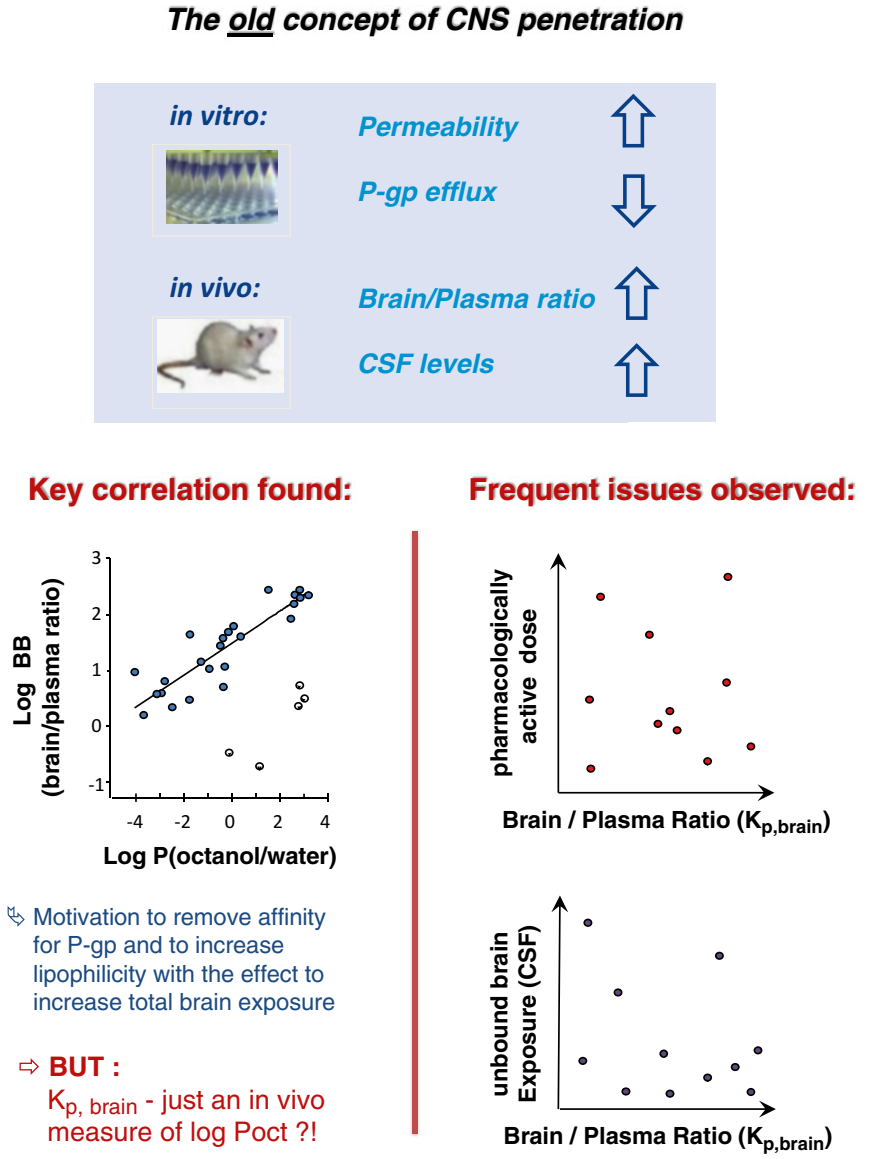

Fig. 12.1 Schematic illustration of the old concept of optimizing CNS penetration. The correlation in the *left panel* is redrawn from Levin (1980), solid points: compounds distributing passively into brain, open points: P-gp substrates as outliers. The two graphs on the right show typical findings and correlations a project team would find when pursuing the optimisation path in the *top panel*, i.e. a very good correlation between lipophilicity (logPoct) and brain penetration ($K_{p,brain}$) (*left panel*), but no clear relationship of the optimised $K_{p,brain}$ with efficacy (e.g. efficacious dose) or unbound levels in brain as estimated from CSF (*right panel*). The persisting disconnect between $K_{p,brain}$ and unbound brain levels is the fundamental flaw of the old concept

To complement these in vitro assays, animal studies to quantify compound levels in the brain have been carried out to verify the anticipated improvements in CNS penetrability in vivo. The results were also used to inform the initiation of in vivo pharmacology studies. The following two methods to quantify compound levels in brain became favourites in CNS drug discovery: the brain/plasma ratio, and measuring CSF levels.

Measuring the concentration ratio of a compound between brain and plasma at different time points after administration had become *the* backbone of in vivo PK support for CNS projects. At given time points after either iv, ip, sc or po administration of a compound to rodents both blood and brain are removed to generate plasma and brain homogenate samples which are then quantified by LC/MS/MS analysis. Brain homogenate levels are calculated back to total brain levels. Since concentration-time profiles in plasma and brain may have different shapes, the brain/plasma ratio (or $K_{p,brain}$) is not calculated from one (arbitrary) time point, but from the area under the concentration-time curve (AUC) of plasma and brain recorded over typically 3–5 time points. In addition to $K_{p,brain}$, compound levels in CSF can be measured at designated time points or even continuously from the cisterna magna in rat (Shen et al. 2004; Lin 2008).

Although this combined in vitro permeability/efflux and in vivo brain levels approach to optimise compounds for their CNS penetrability sounds reasonable, it has caused a lot of frustration and dismay of many CNS project teams spoiling their progress and leading them nowhere (Martin 2004; Jeffrey and Summerfield 2007; Reichel 2009). So where is the concept flawed?

With the intention to enhance in vivo efficacy, project teams have been rapidly learning how to modify the physicochemical properties of their discovery compounds to favour overall CNS penetration by increasing their brain/plasma ratio $K_{p,brain}$. Unfortunately, this turned out all too simple since increasing lipophilicity generally leads to $K_{p,brain}$ going up as well. This is in line with the classic correlation between log BB (log of $K_{p,brain}$) and log P octanol/water from Levin (1980), with the main outliers being identified in the early 1990's to be substrates for the P-gp efflux pump at the BBB (Begley 1996). Hence, increasing in vivo efficacy was attempted by removing affinity for P-gp and by increasing the compound's lipophilicity (Fig. 12.1, left) which in many cases has the additional benefit of increasing the potency against the drug target at the same time (van de Waterbeemd et al. 2001; Martin 2004).

However, many of these attempts were deemed to fail. They did not result in meaningful correlations between brain levels, potency and efficacy leaving teams without a clear rationale of what parameter(s) to modify in order to improve in vivo activity (Fig. 12.1, right). Why is a compound with high brain levels AND high potency not acting in vivo? Why is increasing both $K_{p,brain}$ and potency not enhancing efficacy, but in contrast actually diminishing it in the majority of cases?

In recent years, a number of excellent studies have elucidated this conundrum and in the course fundamentally threw over the "old" paradigm of enhancing CNS penetration (Kalvass et al. 2007; Jeffrey and Summerfield 2007; Hammarlund-Udenaes et al. 2008). Instrumental in the understanding was the concept that it is not the total but only the *unbound* drug that can—upon binding to its target protein—elicit

pharmacodynamic effects. While this concept—also known as the "*free drug hypothesis*"—has been a firm basis for the understanding of the in vivo action in many disease areas (Trainor 2007), it did not touch base in the field of CNS drug discovery until very recently.

The poor acceptance was also a result of a technology gap since experimental access to the relevant effect compartment in the brain is impractical, i.e. very cumbersome and prone to a variety of technical issues. Thus, in spite of important progress being made in establishing meaningful PKPD relationships using either CSF levels as ISF surrogate (Lin 2008) or directly measuring brain ISF levels using brain microdialysis (de Lange et al. 1997), both techniques are limited in their use since CSF levels do not always correlate well with ISF levels (de Lange and Danhof 2002), and microdialysis is unsuitable for routine use in drug discovery if the test compounds are very lipophilic and extensively stick to the material of the dialysis probe (Hammarlund-Udenaes et al. 2009). Nevertheless, the technique can be used to address well-defined questions as illustrated by Kielbasa et al. (2009) and Darvesh et al. (2011). Although brain microdialysis is less suitable for routine drug discovery, the technique became fundamental in carving out the theory of the new concept of CNS penetration (Hammarlund-Udenaes et al. 2008; Westerhout et al. 2011).

Looking at a group of 7 opioid μ-receptor antagonists, Kalvass et al. (2007) have demonstrated that it is the unbound brain concentration that correlated most closely with in vivo efficacy, while total brain and total or unbound plasma levels showed a very poor ranking. Likewise, the similar extent of the in vivo CNS action of morphine and its metabolite morphine-6-glucuronide cannot be conceived based on the classic concept according to which the latter would not be CNS penetrant ($K_{p,brain}$ <0.05), but fully makes sense when comparing the unbound concentrations of both compounds in the brain interstitial fluid (ISF) which is the effect compartment in the brain, i.e. where their target receptors reside (Hammarlund-Udenaes 2009). Despite morphine-6-glucuronide having a much lower brain/plasma ratio ($K_{p,brain}$ of 0.05 vs 0.74) and much slower rate of permeability (PS of 1.66 vs 11.4 μl/min/g brain) compared to morphine itself, its concentration in the brain ISF is higher with an AUC of 336 vs 79 μM*min for morphine (see Hammarlund-Udenaes et al. 2008). Having a just slightly lower in vitro potency (3–5-fold), the pharmacologically active exposure in the relevant effect compartment in the brain (i.e. brain ISF) of morphine-6-glucuronide is thus in full accordance with its in vivo efficacy being comparable to morphine itself.

While it seems easy to follow why the unbound brain concentration is the most relevant parameter for efficacy, why does an increase in total brain concentrations not consistently lead to an increase in unbound concentrations? Whereas plasma consists to 18 % of protein and only to 0.65 % of lipid, the composition of brain tissue is very different showing almost a 20-fold higher lipid content than plasma: brain protein 7.9 %, brain lipid content 11 % (Di et al 2008). Hence an increase in the lipophilicity of compounds will preferentially lead to an increase in lipid binding (van de Waterbeemd et al. 2001). Consequently, compounds with high $K_{p,brain}$ values have a very low fraction unbound in brain ($f_{u,brain}$ < 0.2), while only compounds with $K_{p,brain}$ values around and below 1 tend to have high unbound fractions in brain

(Reichel 2009). Increasing the $K_{p,brain}$ values, therefore, simply drives compounds into (non-specific) brain lipid binding rather than increasing their concentration in the brain ISF (Fig. 12.1, right). The persisting disconnect between $K_{p,brain}$ and unbound brain exposure is the *fundamental flaw* of the old concept.

Jeffrey and Summerfield (2007) came thus to conclude that the traditional backbone of "optimising brain/plasma ratios ($K_{p,brain}$) may transpire to be one of the most misleading exercises within modern CNS drug discovery", emerging as nothing more than an in vivo representation of the log P octanol/water partition coefficient. Indeed this flawed strategy lead teams on a "*lipid escalator*" path toward "*molecular obesity*" (Hann 2011) with all the adverse effects that come with it, in particular (i) no IVIVC between in vitro potency and in vivo activity in pharmacology, and (ii) no clear structure–property relation to inform medicinal chemists on how to improve the new compounds in the project.

A retrospective analysis by Doran et al. (2005), examining the $K_{p,brain}$ of 34 diverse CNS drugs including P-gp substrates and non-substrates, revealed that their $K_{p,brain}$ values span a 400-fold range from as low as 0.06 to as much as 24. This work showed clearly that a high $K_{p,brain}$ is not at all necessary for CNS activity, e.g. 9-OH risperidone ($K_{p,brain}=0.06$) sulpiride (0.078) and midazolam (0.23). The analysis also demonstrated that P-gp recognition per se is not prohibitive for drugs to be active in the CNS. A recent study by Salphati et al. (2012) also illustrates this with the PI3K inhibitor GDC-0980. Even though this compound is recognised by both P-gp and BCRP having a more than 20-fold higher $K_{p,brain}$ in Mdr1a/b/Bcrp triple knockout mice, the unbound levels in brain even in wild-type mice were sufficiently above the IC50 of the target to fully inhibit the PI3K pathway in vivo.

Furthermore, Benet and co-workers suggest that almost all (98 %) BDDCS class 1 drugs (high solubility, high permeability, clearance mainly by metabolism) distribute well into CNS and are only little influenced by (efflux) transporters at the BBB, e.g. verapamil and bromocriptine (Broccatelli et al. 2012).

Current thinking is thus moving away from screening in simple assays but engaging in a more integrated approach which involves *all* key aspects at the same time with regard to peripheral PK as well as CNS distribution and pharmacology. The clear focus on *unbound* drug concentrations in brain is the main difference compared to the old paradigm of addressing CNS penetration.

12.3 The New Paradigm of CNS Penetration in Drug Discovery

The new paradigm of addressing CNS penetration in drug discovery operates more consequently on the brain PK compartments that have direct relevance for drug efficacy/safety and quantitatively takes into account rate and extent of the distribution processes between these compartments as described in the seminal review by Hammarlund-Udenaes et al. (2008). Pharmacological effects are determined by the exposure at the target site, the binding kinetics of the drug, the dynamics of the

drug-target complex (signal transduction) and the phenotypic changes elicited in the target cells. Consequently, receptor theory is forming the basis for in vivo drug concentration–effect relationships (Ploeger et al. 2009). Key effect compartment within the CNS is the brain ISF whose drug concentration is dependent on influx across the BBB, brain tissue binding, back flux into blood as well as bulk flow into the CSF (Westerhout et al. 2011).

While the "old" concept was very inconsistent on these aspects, the new integrative concept allows (i) to link pharmacokinetics with pharmacodynamics, (ii) to integrate data from various in vitro assays into a physiological context which is meaningful for the situation in vivo, and (iii) to be fully incorporated into the existing screening and profiling procedures of the drug discovery process as established across industry (Reichel 2009).

12.3.1 Optimisation of CNS Compounds

The optimisation of lead structures to transform them into viable drugs is by no means one-dimensional but highly complex and multivariate indeed (Zhang and Surapaneni 2012). It is the multidimensionality which poses the biggest challenge to drug discovery, i.e. to select the most suitable drug candidate out of the thousands of molecules a project team has been looking at during high throughput screening for hit structures, the optimisation of lead compounds and the selection process for a viable drug development candidate. As for any other project, during the course of a CNS project the team has to learn iteratively what the optimal property balance for a viable candidate out of the available chemical space can be. Since there is no one optimal balance—otherwise there would be only one drug per disease mechanism or drug target—there is also no preset property mix that leads discovery teams straight away to the final drug candidate by simply tick-boxing assay data until a compound is found with all desired property values being met.

It should always be kept in mind that pharmacokinetics is not a purpose in itself but an enabler of drug efficacy, drug safety, treatment convenience and, hence, patient compliance. Thus, PK optimisation including CNS penetration must be addressed and guided with this ultimate goal in mind.

In exercising out this "thinking from the end approach", this chapter lays down how the new paradigm to CNS penetration can be filled with life to increase the odds for new CNS drug discovery programmes to become more viable.

A meta-analysis of 44 proof-of-concept (PoC) projects of Pfizer by Morgan et al. (2012) has revealed that there are "three pillars of survival" that determine the likelihood of clinical candidates to have a positive outcome in Phase II trials: *Pillar* (1) exposure at the target site of action, *Pillar* (2) binding to the pharmacological target incl. level of target engagement, and *Pillar* (3) functional modulation of the target as prerequisite for pharmacological activity according to the supposed mode-of-action (MoA) and to demonstrate that target engagement results in a sufficient level of response. Ultimately, there needs to be a sound understanding in the relation between primary pharmacology (i.e. potency), unbound concentrations at the site of

action (and hence receptor occupation) and the in vivo efficacy in pharmacodynamic (MoA) and animal disease models (Morgan et al. 2012).

Drug exposure at the site of action within the brain should be examined very carefully in vivo, ensuring not only that the target is being exposed, but to generate information as to what type of exposure profile is needed for in vivo efficacy to be robust, i.e. answering the questions of how much is drug exposure exceeding pharmacological potency for how long a period of time. As the actual site of pharmacological action is not accessible in most cases—and not only so for CNS programmes—a surrogate (PK) compartment is being used instead. There is a wealth of data suggesting that unbound drug concentration (–time profile) in plasma but *not the total* drug levels in plasma or target tissue is a reliable surrogate of the effect compartment (Gabrielsson and Hjorth 2012). For CNS compounds, due to the existence of an effective barrier between blood and brain as described above, it is the unbound concentration in brain interstitial fluid (ISF) rather than in plasma which is the most reliable effect compartment for most CNS drug targets (Hammarlund-Udenaes 2009; Westerhout et al. 2011; Liu et al. 2009, 2012). This may be different though for particular drug targets and if so, attempts should be made early on to identify a relevant surrogate for the effect compartment which is suitable to guide the programme through drug discovery and development. A wrong compromise between feasibility and relevance may turn out fatal only at hindsight once the initial small saving has grown to become very expensive. Thus, Pillar 1 has to be addressed very carefully right from the start of the project.

In order to determine what type of exposure profile is driving efficacy the following steps need to be taken: (1) define the suite of in vitro assays and in vivo studies to measure exposure incl. a surrogate for target exposure, (2) identify compounds that are likely to reach sufficient exposure at the target, (3) apply varying doses and dosing regimens to establish the PKPD relationship that drives in vivo efficacy.

Steps (1) and (2) should all be covered by the screening tree which also should take into account the target drug profile as well as the key liabilities of the chemical starting points, i.e. lead compounds (Ballard et al. 2012). The screening tree forms the basis of the design-make-test-analyse (DMTA) cycles which rationally guide compound optimisation and ultimately lead to the selection of a suitable drug development candidate (Plowright et al. 2012).

12.3.2 Screening Tree for CNS vs Non-CNS Projects

A CNS project team may design a tiered screening tree with the following in silico parameters, in vitro assays and in vivo studies in place (Fig. 12.2):

(1a) *Physicochemical* (*PC*) *properties* along the "Lipinski rules for CNS-likeness" (Wager et al. 2010a) and aqueous solubility to eliminate totally unsuitable compounds (Avdeef 2012). Typical values for PC properties supporting CNS penetration are shown in Fig. 12.3. Aqueous solubility should be compatible with the dose size, route of application and formulation anticipated.

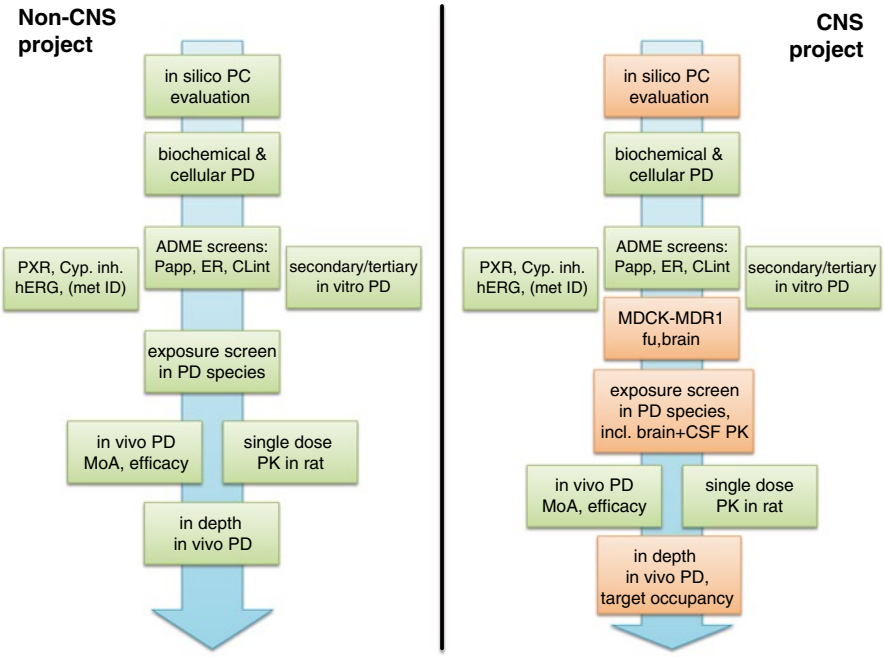

Fig. 12.2 Schematic of the early parts of generic lead optimisation screening trees for a hypothetical CNS and Non-CNS projects with the key differences for CNS projects marked in orange. Note that depending on the compound liabilities of the specific lead structure in a real project, the screening tree may well deviate from the generic version. Studies being performed at later steps such as non-rodent PK, toxicology tests, etc., are not shown for clarity reasons

Compound Property	CNS +	CNS -
MW	≤ 380	> 500
TPSA	90-40	> 120, < 20
clogP	≤ 3	> 5
clogD	≤ 2	> 4
pKa	≤ 8	> 10
HBD	≤ 1	> 3-4
Papp	> 100	< 50
ER	< 2-3	> 5
CLint	< 1/3 LBF	< 2/3 LBF

Fig. 12.3 In silico (physicochemical) and in vitro (ADME) compound properties favouring or disfavoring CNS penetration. ADME: absorption, distribution, metabolism and elimination, TPSA: topological surface area, HBD: hydrogen bonding donors, Papp: apparent permeability in units of nm/s, ER: efflux ratio, Clint: intrinsic metabolic CL scaled up to an in vivo CL, LBF—liver blood flow. Based on Wager et al. (2010a,b; 2012), and Ghose et al. (2012)

(*1b*) *Potency and Selectivity* in biochemical and cellular assays to ensure minimal pharmacology requirements. Potency values should ideally be in the nM range, and selectivity >50-100-fold vs non-target receptors as sound starting point for a sufficiently large therapeutic window.

(*2a*) *ADME screens*: Metabolic stability (CLint) in liver microsomes and/or hepatocytes, Permeability (Papp) and efflux ratio (ER) in Caco-2 and/or MDCK-MDR1 cells to enable sufficient in vivo exposure of the body. High metabolic stability (i.e. low intrinsic metabolic clearance, CLint <1/3 liver blood flow), high permeability (Papp >100 nm/s) and low susceptibility to drug efflux (efflux ratio, ER <2-3) should be aimed at in order to achieve high and lasting concentrations in the blood circulation. Compounds with poor in vitro ADME properties shall be discarded, and the learnings be built into structure–property relationships for the chemical space of the project. For a more detailed description of CLint, Papp and ER the reader is referred to Kerns and Di (2008) or Zhang and Surapaneni (2012).

(*2b*) *PXR*, *Cyp inhibition*, *and hERG assays*, (*metabolite ID*) to address basic drug metabolism and safety aspects. These in vitro assays typically run on high throughput and examine the potential of compounds for CYP450 induction, CYP450 inhibition and hERG channel binding as surrogate for a potential QT prolongation. Again, compounds with poor in vitro properties shall be discarded, and the learnings be built into structure–property relationships for the chemical space of the project. For selected compounds, metabolite identification (ID) is being performed in order to reveal soft metabolic spots suitable for compound stabilisation and to identify potentially reactive metabolites. For a more detailed description of the PXR, CYP inhibition, hERG and metabolite ID assays the reader is referred to Kerns and Di (2008) or Zhang and Surapaneni (2012).

(*2c*) *Secondary and tertiary* in vitro *pharmacology assays* facilitate a deeper understanding of the primary pharmacology and the mode-of-action (MoA) in cellular systems in relation to disease hypothesis and treatment paradigm.

(*3*) *Rapid exposure screen in PD species* at the intended route of application and pharmacologically active (high) doses at 3–5 time points to select doses and formulations that provide sufficient target exposure as prerequisite for in vivo efficacy. The exposure screen is a central element in the screening and decision tree and is complemented by in vitro plasma protein and brain tissue binding data to produce the following readouts: (i) plasma concentration-time profile, (ii) brain concentration-time profile (same time points), (iii) calculation of the AUC for the plasma and brain concentration-time profiles, (iv) unbound plasma and unbound brain concentration-time profiles, (v) $K_{p,brain}$ (total AUC brain / total AUC plasma) and $K_{p,uu,brain}$ (unbound AUC brain / unbound AUC plasma), (vi) unbound brain concentration vs in vitro potency (e.g. IC50 or Kd) relationship.

(*4a*) in vivo *PD experiment* at a dose expected to expose the target to provide first evidence of the in vivo mode-of-action (MoA) and, if possible, to get first evidence for in vivo efficacy in a disease model. Dose, route and formulation shall be selected based on the data obtained in step 3.

(*4b*) *Low dose full PK in rat* to identify PK deficits which cause exposure limitations in vivo and that need to be optimised in order to reduce/eliminate PK-related risks for drug development and in human. Key liabilities to watch out for are high clearance, short half-life, low bioavailability, or non-linearity. The total clearance in vivo will be compared with the in vitro CL (CLint) obtained in step 2a to delineate the main clearance pathways in vivo.

(*5*) *In-depth* in vivo *PD at different doses* (dose–response) and if possible different dose regimens (e.g. infusions, split dose) to explore exposure–MoA relation, exposure–efficacy relation, and/or exposure–biomarker/efficacy surrogate relation supported by PKPD modelling. The selection of suitable endpoints is key for the translatability of the results to the human situation and the validity of dose and dosing schedule predictions to be made later in the project. Although it may be tempting to go ahead with the first compound getting to this stage, balancing speed against competition and level of removal of uncertainty to avoid failure in clinical proof-of-concept (PoC) trials often pays out later on (Cartwright et al. 2010). It is the relation between PK and PD which should be carefully worked out not only to avoid failure but also to be able to define what type of parameter(s) actually should be optimised and what is the best property mix in a compound for robust efficacy in vivo. The better the PK–exposure–efficacy relationship is being understood in the animal, the more certainty will accompany the course of the project.

(*6*) *Further studies and activities to complete the profiling of potential development candidates* such as non-rodent PK, PK at different doses to examine dose-linearity and to establish multiples of exposures, PK of micronised crystalline material to inform pharmaceutical development, toxicology and safety pharmacology testing, PBPK and species scaling of PK to human, prediction of human therapeutic dose and safety margins.

12.3.3 Key Elements of the New Concept of CNS Penetration

While several of the above aspects are central to drug discovery projects in most therapeutic areas, the following elements are more *specific to CNS projects* (Fig. 12.2) taking specific consideration of the effect compartment (i.e. brain ISF) being separated from the blood circulation (i.e. plasma compartment) by the BBB or BCSFB:

12.3.3.1 Permeability and Susceptibility to Drug Efflux

A high intrinsic permeability and a low efflux ratio in both MDR1 and BCRP overexpressing cells are both very important for a good CNS penetration as otherwise non-CNS availability is very likely to occur (Cole et al. 2012). With the cell membranes of brain endothelial cells being more enriched with cholesterol and hence

providing more resistance to passive transmembrane permeation and at the same time making the impact of efflux pumps stronger (Aänismaa et al. 2008; Nervi et al. 2010), it is important to optimise compounds toward both a high permeability *and* a low efflux ratio. While the Caco-2 cell permeability screen may suffice to demonstrate rapid permeability, cell lines overexpressing MDR1 and BCRP may be used to optimise the efflux ratio against these two ABC transporters. It is important to note that the combined effort of MDR1 and BCRP as occurring at the BBB in vivo can pose a significant limitation to the CNS penetration of drugs despite only showing moderate efflux in cells overexpressing just one of the two efflux transporters (Kusuhara and Sugiyama 2009; Agarwal et al. 2011).

12.3.3.2 Fraction Unbound in Brain Tissue

As stated under 12.2, the in vivo activity of a CNS compounds depends on whether the unbound concentration in brain (i.e. brain ISF levels) reaches levels that match the in vitro potency of the drug. In order to calculate the free concentrations in brain, the fraction unbound in brain needs to be determined in vitro. There are now two different methods available to determine fu,brain (Fridén et al. 2007): (i) equilibrium dialysis against brain homogenate of rodents, and (ii) distribution into freshly isolated rodent brain slices ex vivo. Both experimental methods are being discussed in detail in Chap. 10. The equilibrium brain homogenate dialysis technique has earned rapid and wide acceptance as standard method for fu,brain in industry. The method can be run at high throughput in an automated fashion, utilising the same equipment as used for the in vitro determination of plasma protein binding. This type of data is thus being obtained very easily. The brain homogenate method can also be used in a cassette format (Wan et al. 2007). Since brain composition and fu,brain shows little differences across species (Summerfield et al. 2008; Di et al 2011), it is enough to measure this parameter in only one species, typically the pharmacodynamic species (rat or mouse) (Read and Braggio 2010). It has been argued that destroying the brain compartments during the homogenisation procedure does no longer reflect tissue binding and distribution as occurring in vivo, a fact that would speak in favour of the brain slice technique. To make this very elaborate technique more attractive, a high throughput format has been put forward (Fridén et al. 2009a). However, the experimental advantages of the homogenate technique and the accumulating evidence of its value give little reason to switch to the more laborious brain slice technique. Even more so, as the fu,brain readout of homogenate technique can be improved by correcting for pH partitioning as proposed by Fridén et al. (2011). This is because intra-brain distribution is affected not only by non-specific binding to brain tissue but also by pH partitioning of charged drugs between interstitial fluid and the cells' cytosol and sub-compartments as well as transport processes at the level of brain cells. Although the latter process cannot be taken into account by the proposed pH partitioning method it suffices to get the fu,brain results within 2-fold of brain slice method. The brain slice method may be of advantage in cases where the CNS target resides within brain cells with

cytosolic compound levels being different to those in the ISF due to active transport at the level of the target brain cells (Westerhout et al. 2011; Ballard et al. 2012).

Both in vitro methods, however, are much easier than brain microdialysis, are amenable to higher throughput, cost effective and thereby fully compatible with assay needs in a drug discovery setting. With the arrival of these in vitro tissue binding methods, the missing link between the theoretical concept and its practical implication has finally materialised bringing the new concept to its full fruition now.

Last but not least, there is an important note to be made: The fraction unbound, i.e. fu,brain as well as fu,plasma, has only to be seen as descriptive property and shall *not* become an optimisation parameter in itself as has been explained convincingly by Smith et al. (2010) and Liu et al. (2011). The only exception to this may be the requirement for a very rapid onset of action (e.g. in the case of anaesthetics, anti-epileptics or some stroke treatments) as a short time to achieve equilibrium distribution between plasma and brain will require both a high permeability *and* a high fraction unbound in brain, according to the equation t1/2 = ln2 x Vbrain / PS x fu,brain (Liu et al. 2005). For the more often used chronic drug administration, however, time to achieve equilibrium is only of minor relevance.

12.3.3.3 $K_{p,brain}$, $K_{p,uu,brain}$ and $C_{u,brain}$

Total concentrations in brain and plasma and the corresponding $K_{p,brain}$ ratio are typically determined in rodents, with the selection between rat or mouse depending on which species will be used for pharmacodynamic studies. As the result for $K_{p,brain}$ may depend on the route of administration (Sane et al. 2012), careful consideration should be given as to which route of application will be tested. Ideally this shall be the route which is also going to be used in the clinic and in in vivo pharmacology studies. An abbreviated concentration-time (c-t) profile is preferable (about 4 time points) over a single time point. It allows to calculate AUC values for both plasma and brain and to assess whether or not the c-t profiles run in parallel. Parallel c-t courses in brain and plasma suggest that both compartments are in equilibrium and that their unbound concentrations are in correspondence (Gabrielsson and Hjorth 2012). In the absence of barriers between both compartments, the unbound levels would be identical—an assumption that holds true for most peripheral tissues. However, because plasma and CNS tissue are separated by the BBB, the unbound concentrations in plasma and brain ISF will differ by the factor equivalent to $K_{p,uu,brain}$ if either active transport is involved or if there is a significant gradient between the diffusion rate from blood to brain ISF (PS + CLuptake) vs that from brain ISF into CSF (CL,bulk) (Fig. 12.4).

A $K_{p,uu,brain}$ of approximately 1 is indicative of a purely passive distribution of the test compound between blood and brain. Note, if the blood:plasma ratio differs from unity, fu,blood should be taken instead of fu,plasma in all calculations (fu,blood = fu,plasma/blood:plasma ratio).

$K_{p,uu,brain}$ is far better suited than $K_{p,brain}$ as measure of the extent of brain penetrations, since $K_{p,uu,brain}$ purely reflects the ratio of the free equilibrium concentrations between brain and plasma unbiased of binding to tissue or plasma proteins as is the case for $K_{p,brain}$ which hence is a mixed parameter. In contrast, $K_{p,uu,brain}$ provides a

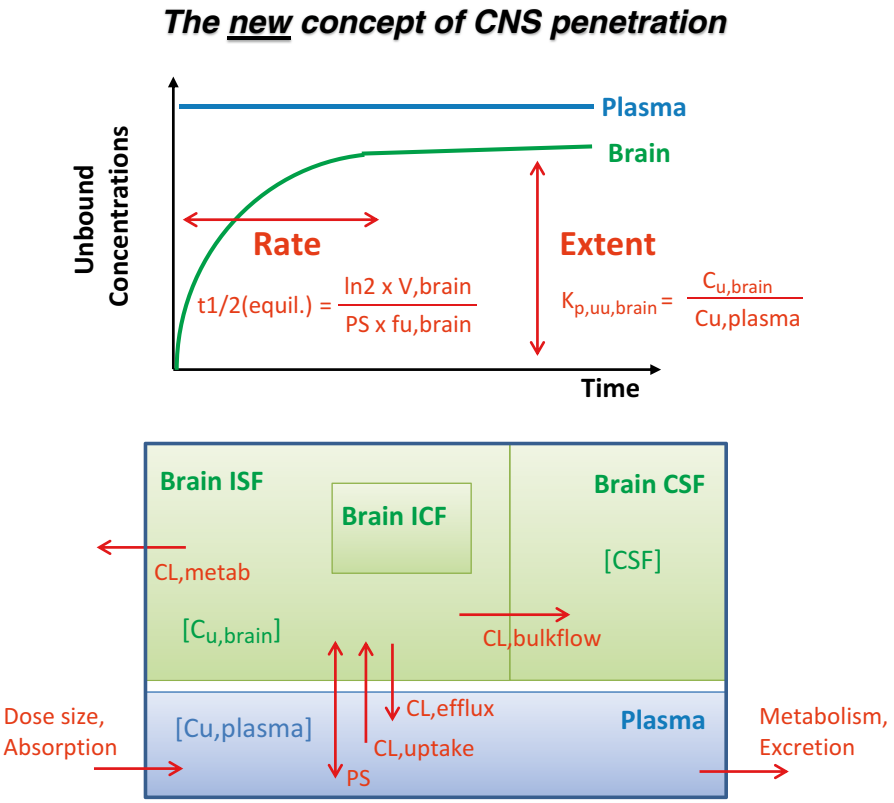

$$C_{u,plasma} = C,plasma(total) \times fu,plasma$$

$$C_{u,brain} = C,brain(total) \times fu,brain$$

$$K_{p,brain} = \frac{C,brain(total)}{C,plasma(total)} = \frac{fu,plasma}{fu,brain}$$

$$K_{p,uu,brain} = \frac{C_{u,brain}}{Cu,plasma} = \frac{PS + CL,uptake}{PS + CL,efflux + CL,bulkflow + CL,metab}$$

$$C_{u,brain}(t) = Cu,plasma(t) \times K_{p,uu,brain}$$

Fig. 12.4 Key elements of the new concept of addressing CNS penetration. The *top panel* illustrates the importance of differentiating between rate and extent as two independent key aspects of brain penetration. The *middle panel* shows the different brain compartments and the distributional processes between them that ultimately drive the unbound concentration in brain interstitial fluid. The processes which control intracellular brain concentrations have not been depicted for clarity reasons. For the same reason some other processes, e.g. transport between plasma and CSF have been omitted from the scheme. The *bottom panel* lists key equations which are fundamental to the new concept. For abbreviations see text

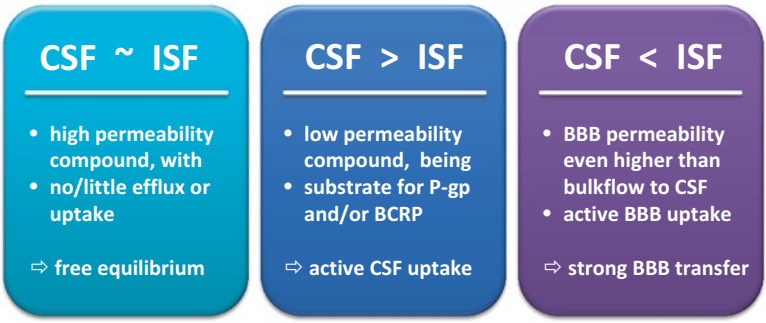

Fig. 12.5 Different scenarios for the relation between compound concentrations in brain CSF and brain ISF and how they can be interpreted or predicted based on the permeability and efflux characteristics of a test compound

direct measure for the extent of BBB transport and allows to directly derive the unbound brain exposure from the unbound systemic exposure of a compound.

The unbound brain concentrations, unbound c-t profile and unbound AUC for a given dose can be calculated by multiplying the total brain concentration with fu,brain. The comparison of $K_{p,brain}$ as determined from AUCbrain/AUCplasma in vivo vs the $K_{p,brain}$ as calculated from fu,plasma/fu,brain in vitro can provide additional insights as to whether the data are consistent and—if not—give rise to search for the causes of the inconsistency, e.g. strong involvement of transport processes, blood:plasma ratio different from unity, non-specific binding to equipment affecting the in vitro fu readouts, etc.

To make this in vivo technique more efficient, Liu et al. (2012) have developed and validated an adaptation which uses cassette dosing combined with the estimation of $K_{p,brain}$ directly from the LC/MS/MS mass spectrometer responses without using any standard curves to quantitate the actual plasma and brain concentrations.

12.3.3.4 CSF Levels

Because the cerebrospinal fluid is in close correspondence with the brain interstitial fluid, i.e. not separated by a tight cell layer because the ependyma lining the ventricles is very leaky, CSF has always been a popular surrogate for brain ISF. Its composition is relatively similar to that of ISF (yet both are very different to plasma) and it is relatively easily accessible in vivo. CSF can be collected by puncture of the cisterna magna from rat and mouse, but also more continuously by serial sampling from an inserted catheter therein (Shen et al. 2004; Lin 2008). Owing to its very little amount of proteins, sample preparation for LC/MS/MS analysis is much easier compared to plasma or brain tissue and effectively represents unbound concentration.

When using CSF levels as surrogate for drug ISF concentrations, it has to be kept in mind that CSF levels do not necessarily reflect ISF levels. If they differ, they may

either be overpredictive or underpredictive (Fig. 12.5). In two systematic studies of 39 compounds by Fridén et al. (2009b) and 25 compounds by Kodaira et al. (2011), both groups demonstrated that good correspondence is to be expected for compounds that show a high permeability and little or no drug efflux. For those compounds, CSF levels can be a reliable surrogate for the concentration in the effect compartment of the brain. Deviations, however, occur for those compounds which show a relevant net transport by P-gp and/or BCRP across the BBB (e.g. verapamil, loperamide, quinidine or cimetidine). While P-gp or BCRP substrates show higher levels in CSF than in ISF, the opposite may occur for compounds with a very high rate of BBB permeation and low brain tissue binding causing the rate at which the brain ISF volume fills up to exceed the bulk flow of the ISF into the CSF (Fig. 12.5).

With regard to species scaling and translating rodent data to larger animals and human, Doran et al. (2012) have demonstrated that CSF sampling in higher species may be more relevant for compounds that are substrates for efflux and show a low permeability. Apparently, for compounds with a $K_{p,uu,brain}$ deviating from unity, the error from using the rodent $K_{p,uu,brain}$ across species is larger than from using CSF levels of the very species, presumably due to species differences in the expression, function and impact BBB transporters have on the $K_{p,uu,brain}$ of such compounds between species. As pointed out by Fridén et al. (2009b) care must be taken when interpreting CSF data between species and attempts should be made to discriminate real species differences from experimental bias.

12.3.3.5 PKPD Relationships and Target Receptor Occupancy

The establishment of sound PKPD relationships is a key element of any drug discovery programme and serves (i) to understand and translate the in vitro pharmacology to in vivo efficacy with regard to the mode-of-action (MoA) in vivo and how it relates to the therapeutic effects in an animal disease model, (ii) this in turn serves as basis to translate the results to the human situation, (iii) and forms the rational basis for the estimation of a human therapeutic dose, optimal dose regimens and the anticipated therapeutic window in human.

Crucial to the validity of any PKPD model is the availability of pharmacokinetic data of the effect compartment, i.e. the concentration-time profile at the proposed site of action or a relevant surrogate measure of it. In case of most CNS compounds by far the best correlations are found using the unbound concentrations in brain, i.e. $C_{u,brain}$ (Hammarlund-Udenaes 2009; Read and Braggio 2010; Westerhout et al. 2011; Liu et al. 2012).

Attention shall be paid to establish a relation between the in vitro potency of the compound at the target, the target site occupancy in vivo and how this translates to the expected MoA in the target cells and further to the efficacy in the in vivo disease model (Shaffer 2010). Computing unbound drug concentrations vs in vitro potency data from cellular assays is a straight forward approach to see what pattern is required for a positive in vivo MoA and efficacy result. In CNS research, the determination of receptor occupancy (RO) is common place to determine how much

target site occupancy is required for the therapeutic effect (Grimwood and Hartig 2009). The level of receptor occupancy for a given unbound brain concentration can be predicted using the equation

$$RO = C_{u,brain} / (C_{u,brain} + Kd) \quad (12.1)$$

with Kd being the in vitro potency, providing a theoretical estimate of the occupancy target receptor. This theoretical estimate should be verified using experimental data from dose–response studies, e.g. from ex vivo receptor occupancy studies (Suzuki et al. 2009) or PET studies in animals (Gunn et al. 2012) in order to verify the RO estimate, and the reliability of the estimation of $C_{u,brain}$ as surrogate for the concentration in the effect compartment. It also aids to the team's understanding of the level of RO needed for efficacy. The earlier this understanding is available, the better the compound optimisation can be guided to deliver the optimal drug candidate (Read and Braggio 2010). Typically, antagonists require approximately 60-90 % target occupancy to elicit a sufficient functional response, while there is no such rule of thumb for agonists since their optimal RO depends on a number of variables that are specific to the target and the compound (Grimwood and Hartig 2009). It should be kept in mind that high receptor occupancy per se may not necessarily translate into therapeutic effects as reported by Borsook et al. (2012) for NK-1 receptor antagonists and pain, despite their impressive efficacy in emesis.

Once the level of receptor occupancy needed for in vivo efficacy and the relevance of $C_{u,brain}$ as suitable surrogate for the effect compartment are established, this information needs to be linked to dose and peripheral PK using typical PKPD models, paying specific attention to the link between plasma PK and brain PK essentially following the equation $C_{u,brain} = Cu,plasma \times K_{p,uu,brain}$ (Fig. 12.4). The confidence in this relationship becomes high if the concentration-time profile of the compound in plasma and brain run in parallel. Note again, if the blood:plasma ratio of the compound differs from equity Cu,blood should be used instead of Cu,plasma.

12.3.3.6 Translating PKPD from Rodents to Larger Animals and Human

Once the relation between dose (route, size and regimen), plasma PK, brain PK (target exposure), target binding (receptor occupancy), functional response (MoA) and in vivo efficacy is established in an animal disease model, translation to larger animals for safety testing and to human for projecting a clinically effective dose is required.

For toxicological studies it may be of interest to estimate the level of brain exposure at the (high) doses tested in order to evaluate the therapeutic window for CNS side effects via off-target receptors, transporters or ion channels. Doran et al. (2012) have proposed an approach of how to translate the brain PK as determined in rodents to larger animals where there is limited or even no access to brain samples. In a study examining the species extrapolation to dog and non-human primate of unbound brain concentrations of 11 compounds as determined in rat, they

concluded that the best estimates for $C_{u,brain}$ in the species is obtained using the following equation, which also contains a term for the molecular weight (MW) of the compound:

$$C_{u,brain}(\text{species}) = \text{Cu,plasma}(\text{species}) \times K_{p,uu,brain}(\text{rat}) \times 1{,}000 / \text{MW} \quad (12.2)$$

While this equation works well for compounds with high permeability and low susceptibility to drug efflux across the BBB in vitro, this approach is less reliable for low permeability compounds that are also substrates for P-gp and/or BCRP (see above). For such compounds, CSF levels appeared to provide the better estimate of free brain concentrations in the respective species (Doran et al. 2012).

In addition, it should be kept in mind that the disease state as well as the treatments the patient is under may change the state and the function of the BBB and hence $K_{p,uu,brain}$, e.g. by breakdown of the barrier function (PS may increase) or up- and downregulation of transport processes (CLuptake and CLefflux may change accordingly) (Reichel 2006).

The effective concentration-time profile both for plasma and brain (including unbound plasma and brain) as identified in animal disease model(s) will provide the corresponding target c-t profiles in human as required for efficacy in patients. Applying PK scaling approaches, e.g. allometric species scaling or physiologically based PK scaling, estimates for the principal PK parameters, such as total clearance, volume of distribution, half-life and oral bioavailability can be obtained which in turn allow to simulate a dose and dosing schedule which is most likely to obtain the desired target c-t profile in human (Rowland et al. 2011; Jones et al. 2012; Peters 2012; Ballard et al. 2012; Zhang and Surapaneni 2012). This is done with the aim to propose a dose (size and regimen) which will generate a drug exposure profile in human that is likely to achieve the same level of target exposure and occupancy as was required for efficacy in the animal disease model(s). If validated PET tracers are available, the estimate may be confirmed or adjusted in human PET studies thereby aiding further clinical development (Borsook et al. 2012; Wong et al. 2012). Additional examples of translational PKPD modelling from preclinical species to the clinical situation can also be found in Westerhout et al. (2011), Kielbasa and Stratford (2012) and Chap. 9.

As stated above, the most reliable extrapolations can be made for compounds whose c-t profiles in plasma and brain run in parallel, which have a $K_{p,uu,brain}$ near unity, high permeability and no/low efflux. For such compounds Cu,plasma can reliably be taken as surrogate for the effect compartment in the brain. This biomatrix is also the matrix of choice during preclinical and clinical drug development and for which there is a wealth of experience with regard to inter-species extrapolations of PK parameters (Zhang and Surapaneni 2012).

While such a compound profile may sound very ideal, stringent optimisation of physicochemical and pharmacokinetic compound properties may well put such a profile into the reach of the chemical space available. In any case increased effort toward obtaining such a profile is very likely to pay out later on, as compounds with a strong non-parallel c-t profile between plasma and brain will carry a high level uncertainty with regard to (i) accurate estimation of their unbound brain concentrations in the

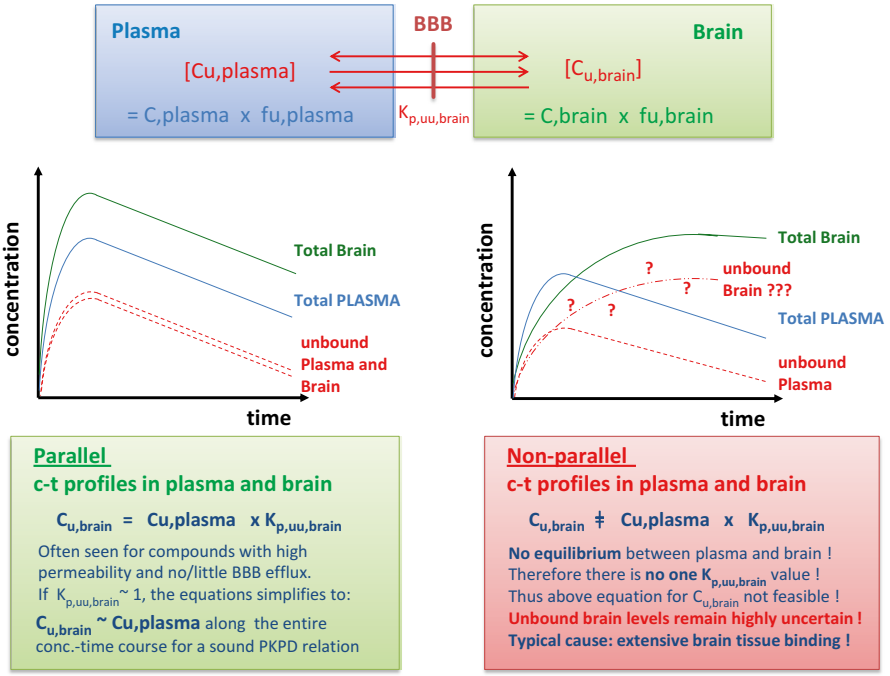

Fig. 12.6 Advantages and disadvantages with regard to the predictivity of unbound brain concentrations for compounds with parallel and non-parallel concentration-time (c-t) profiles between plasma and brain. While parallel c-t profiles make both $K_{p,uu,brain}$ and Cu,plasma very solid parameters for calculating unbound brain levels, both these parameters cannot be used with any confidence to predict the unbound concentrations in the brain for compounds which have not reached equilibrium, most often due to very extensive non-specific binding to brain tissue

effect compartment even in the lab animal where brain samples can be taken, and (ii) reliable prediction of relevant brain concentrations across species and to human. This is because a strong non-parallel c-t profile in plasma and brain does not permit calculation of $C_{u,brain}$ based on the key equation $C_{u,brain}$=Cu,plasma x $K_{p,uu,brain}$, because $K_{p,uu,brain}$ applies to equilibrium conditions which obviously have not been reached in this case and non-specific brain tissue binding is still dominating the PK profile (Fig. 12.6). $C_{u,brain}$ may be estimated based on $C_{u,brain}$=C,brain(total) x fu,brain, but the limitation becomes obvious when attempting to get the input for this equation from higher animal species and human, i.e. C,brain(total). Keeping in mind these serious limitations of a non-parallel c-t profile in plasma and brain may spur optimisation efforts to remove this liability from the current compounds by reducing the excessive lipophilicity-driven non-specific binding to brain tissue.

12.3.4 Strategies to Improve Brain Penetration

If compounds show poor efficacy in vivo as a result of insufficient target receptor occupancy, there are principally two ways to improve on compounds: either by

boosting their target affinity (i.e. reducing Kd) and/or by boosting their target exposure (increase $C_{u,brain}$). For instance, if $C_{u,brain}$ and Kd can be brought in a relation of 3:1, the target receptor occupancy will be 75 %. Hence, it is not the absolute values that are important but their ratio to one another and an improvement can be made on either one, depending on which of the two has the greatest potential for improvement in the chemical space available to the project team. In the following, a path for improvement is described for $C_{u,brain}$ only.

Since $C_{u,brain}$ depends on both Cu,plasma and $K_{p,uu,brain}$, the levers to improve brain target exposure can be derived if one delineates the corresponding mechanisms that determine Cu,plasma and $K_{p,uu,brain}$, respectively.

12.3.4.1 Improving $K_{p,uu,brain}$

$K_{p,uu,brain}$ may be improved only if its value is much below unity to begin with. Based on the below equation, this can result either from the compound being a very strong efflux substrate (i.e. CLefflux dominates), or having a very low BBB permeability (PS) compared to the interstitial bulk flow (CLbulkflow ~0.1–0.3 μl/min/g brain; Abbott 2004). For example, mannitol is a compound of low permeability with a PS value <1 μl/min/g, and thus bulk flow becomes significant, resulting in a very low $K_{p,uu,brain}$ of 0.01 (Liu and Chen 2005). Since drug metabolising enzymes are less active in the brain, CLmetab rarely is a relevant parameter, although it may become significant for some compounds (see Chap. 4).

$$K_{p,uu,brain} = (PS + CLuptake) / (PS + CLefflux + CLbulkflow + CLmetab) \quad (12.3)$$

Consequently, the most straight forward pathway to bring $K_{p,uu,brain}$ to unity is to increase the intrinsic permeability of the compound while removing its recognition by efflux pumps, both of which can relatively easily be achieved using cell-based systems such as MDCK cells overexpressing P-gp and BCRP or Caco-2 cells (Kerns and Di 2008; Wang and Skolnik 2010; Zhang and Surapaneni 2012).

Theoretically, $K_{p,uu,brain}$ can be lifted up to become greater than one, but there is little experience in rationally designing in compound recognition by active uptake transporters at the BBB (i.e. increasing CLuptake) (Reichel et al. 2000), although there are examples of CNS compounds using drug transporters to enter the CNS (see Chap. 2).

12.3.4.2 Improving Cu,plasma

Since $C_{u,brain}$ depends on the unbound plasma concentration and $K_{p,uu,brain}$, the second key lever is the improvement of the (unbound) systemic exposure of the test compounds.

According to the relation Cu,plasma = C,plasma(total) × fu,plasma, the reduction in plasma protein binding has occasionally been attempted to improve the systemic exposure of new compounds in a chemical series. However, it has now become very clear, that any reduction in fu,plasma will have counterproductive effects on the

systemic clearance of the compounds, leaving the resulting Cu,plasma levels effectively the same as explained very eloquently by Smith et al. (2010).

The unbound systemic exposure of a compound depends on the oral bioavailability (F), the dose size administered (Dose), the total systemic clearance of the compound and, of course, it's free fraction according to following equation:

$$\mathrm{AUCu} = \mathrm{fu,plasma} \times \mathrm{F} \times \mathrm{Dose} / \mathrm{CL} \tag{12.4}$$

Since a high total clearance is likely to result in a low oral bioavailability, *improving the systemic CL is an essential* element in improving the systemic exposure of any compound in any project, including CNS projects. As liver metabolism is often the key driver of total clearance, reducing the rate of degradation of compounds in a series is being accomplished by measuring the intrinsic metabolic CL (CLint,Liver) in liver microsomes or hepatocytes, an assay which has become a cornerstone of early ADME screening (Kerns and Di 2008; Ballard et al. 2012; Zhang and Surapaneni 2012).

Upon transforming the oral exposure measure of AUC to plasma concentrations, the above equation changes to the following relation (for a stepwise deviation of the equation see for instance Liu et al. 2011 or Gabrielsson and Hjorth 2012):

$$\mathrm{Cu,plasma} = \left(\mathrm{Dose\ rate} \times \mathrm{Fabs}\right) / \left(\mathrm{CLint,Liver}\right) \tag{12.5}$$

Consistent with the statement above, the following strategies improve unbound plasma exposure (and in turn unbound brain exposure):

1. Reducing CLint,Liver, i.e. the intrinsic susceptibility to degradation by the drug metabolizing enzymes in the liver, by *metabolic stabilisation* of the compounds. Metabolite ID may be used to identify the location of the metabolic soft spots in a molecule.
2. Increasing the fraction of dose absorbed (Fabs), which can be achieved by increasing the *solubility* of the compound and/or its *intestinal permeability* (see also Kerns and Di 2008, Ballard et al. 2012, Zhang and Surapaneni 2012),
3. Although equation 12.5 implies that increasing the dose rate, i.e. the dose size per dosing interval will be beneficial, in reality this often is not feasible as increasing the dose may become counterproductive for the fraction absorbed (Fabs) if intestinal absorption becomes solubility limited, or higher doses simply increase the occurrence of unwanted side effects. It may however be possible to change the *dosing regimen*, i.e. to split the dose and give it more often during the treatment period (e.g. BID instead of QD).

Taken together (Fig. 12.7), unbound brain concentration can be described pharmacokinetically by the following equation which delineates what the most powerful levers are to optimise this key driver of efficacy in CNS drug discovery programmes:

$$\mathrm{C_{u,brain}} = \left(\mathrm{Dose\ rate} \times \mathrm{Fabs} \times \mathrm{K_{p,uu,brain}}\right) / \left(\mathrm{CLint,Liver}\right) \tag{12.6}$$

The equation makes again clear, that neither permeability as such nor total brain levels or the brain/plasma ratio control the drug concentration in brain ISF as a key effect compartment of the CNS.

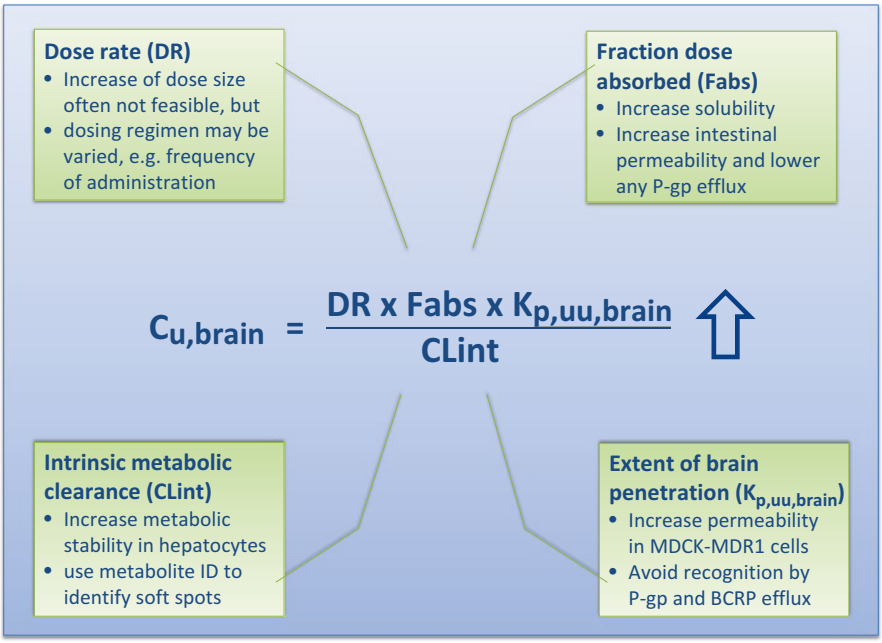

Fig. 12.7 Schematic illustrating the PK properties which determine unbound concentrations in the CNS and how corresponding in vitro physchem and ADME assays can be used to guide the improvement of the brain penetration of new compounds

For compounds which require a rapid onset of action (e.g. for anaesthesia, stroke, epilepsy), the time to achieve equilibrium (t1/2) will have to be short:

$$t1/2 = \ln 2 \times Vbrain / PS \text{ x } fu,brain \tag{12.7}$$

According to the above equation which was derived by (Liu et al. 2005), such compounds should be optimised toward a high BBB permeability and a low brain tissue binding, to be able to rapidly fill the interstitial fluid compartment of the brain.

Some recent examples of how to optimise the CNS penetration from a medicinal chemistry point of view can be found in Wager et al. (2010a,b) who used a multi-parameter optimisation (MPO) strategy with a simple scoring system related to potency, PK and safety aspects to rank order compounds and to inform chemical synthesis toward improved compounds along the design-make-test-analyse (DMTA) cycle. The group describe how they have used this approach for hypothesis-driven optimisation cycles to obtain drug-like, effective and safe H3 receptor antagonists to treat CNS disorders including the incorporation of specific safety aspects and the projection to clinical efficacious concentrations (Wager et al. 2011). In silico approaches to guide the chemical synthesis of compounds with improved CNS penetration properties are also described by Ghose et al. (2012) and in Chap. 11. Recently, the biopharmaceutical drug disposition classification system (BDDCS) has been expanded to aid the prediction of CNS penetration (Broccatelli et al. 2012).

12.3.5 Strategies to Avoid Brain Penetration

Avoiding CNS penetration may be an important aspect for peripherally acting drugs whose pharmacological target receptors (or off-target receptors) also reside in the CNS, but shall not be activated in vivo in order to avoid CNS side effects (Easter et al. 2009; Wager et al. 2012). A well-known example where this has been achieved are the second generation antihistaminic agents which despite being active on central histamine receptors in vitro, do not elicit central effects, what their first generation counterparts do (Yanai et al. 2012). After some other hypotheses, affinity for P-glycoprotein-mediated drug efflux at the level of the BBB has been identified as main reason why 2nd generation antihistamines show little CNS side effects (Chishty et al. 2001; Obradovic et al. 2007). While this protecting mechanism was discovered only later on in the case of the antihistamines, it is now becoming a rational element in optimising the separation between the peripheral and the central activity of compounds in drug discovery projects aiming at a very low/no central activity to avoid CNS side effects (Broccatelli et al. 2010; Cole et al. 2012).

Revisiting the equation given in Fig. 12.4, $C_{u,brain}$ could principally be diminished by either reducing Cu,plasma and/or $K_{p,uu,brain}$. Obviously, reducing Cu,plasma would be counterproductive as the compound's peripheral activity will require a certain minimum unbound exposure in the blood circulation. Hence, the only handle remaining is to reduce $K_{p,uu,brain}$, so to lower $C_{u,brain}$ below a level at which it no longer sufficiently occupies central receptors, while the occupation of the peripheral targets still suffices to elicit the desired effects due to the relatively higher Cu,plasma.

Cole et al. (2012) have reported recently how they have accomplished this "peripherally restrictive" profile with a couple of in-house examples from Pfizer. They report that compounds with a low intrinsic permeability (MDCK cells, Papp < 100 nm/s) and a high efflux ratio (P-gp- and BCRP-overexpressing MDCK cells, ER > 10-20) best fulfil this profile (Fig. 12.3). They have validated these compounds in vivo by showing their CSF levels to be <10 % of their unbound plasma concentrations and most importantly by absence of a functional response in pharmacological in vivo studies.

Benet and co-workers describe that drugs having one or two violations of the Lipinski "rule-of-five" are very likely to be substrates for P-gp, 61 % and 89 %, respectively (Broccatelli et al. 2012). This finding may very easily be welcomed by the medicinal chemist's toolbox for avoidance of CNS-penetration. The group of Benet further concludes, that P-gp substrates are excluded from brain significantly only in case the compound is a non-BDDCS class 1 drug. Hence, drugs for peripheral use should avoid to be in BDDCS class 1, while BDDCS class 2 may be ideal in order to escape CNS side effects (Broccatelli et al. 2012).

It follows from the theory laid out in this chapter that a complete avoidance of CNS penetration cannot be achieved, but rather a reduction in ISF levels relative to unbound plasma levels. Thus, for such compounds $K_{p,uu,brain}$ effectively becomes the basis for the safety margin between peripheral and central effects. Currently, it is not very clear yet how $K_{p,uu,brain}$ values from rodents translate quantitatively to human

(see Doran et al. 2012). It remains to be seen how differences in the expression levels of transporters contribute to species differences in transporter function at the BBB as well as drug distribution to the brain (Ohtsuki et al. 2011). It also remains to be seen whether co-medications potentially can lead to an inhibition of drug efflux at the BBB, and hence whether switching off the "$K_{p,uu,brain}$ barrier" can affect the safety of such compounds in the clinical situation with patients.

12.4 Drug–Transporter Interactions at the BBB

In a world of an ageing multi-morbid population requiring polypharmacology, one of the biggest challenges is to ensure that new chemical entities (NCE) can be applied safely along with the co-medications a patient is already on. Drug–drug interactions (DDI) can occur at the level of drug metabolising enzymes and/or drug transporters (both uptake and efflux) leading to an increase in the exposure if both the NCE and the co-medication are being cleared predominantly by the same enzymatic or transporter pathway. The inhibiting drug is called "perpetrator", while the drug whose exposure will change due to the inhibition is called "victim". Either the NCE or the co-medication can act as victim or perpetrator (Fig. 12.8). A change in the exposure can lead to an increase in the exposure which in turn can cause serious or

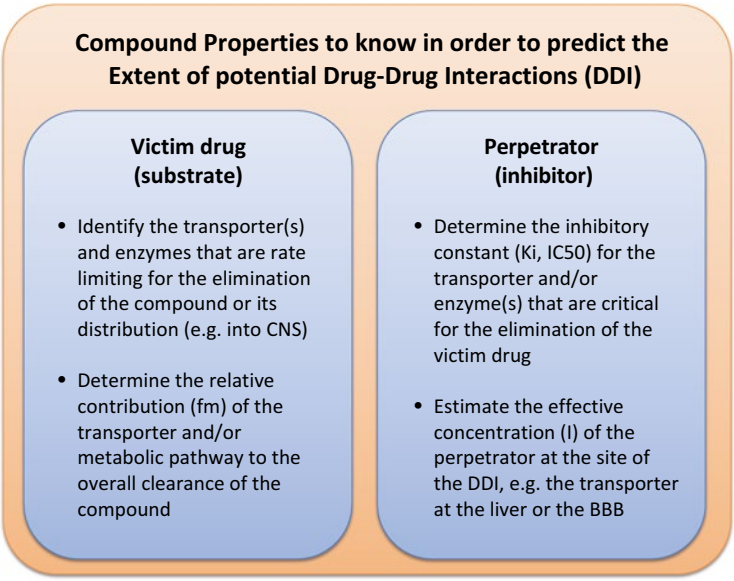

Fig. 12.8 Compound properties which have to be determined in order to predict the effect of drug–drug interactions (DDI). There are different parameters to be acquired depending on whether the compound acts as perpetrator or as victim of the DDI. Equations to predict the extent of transporter-mediated DDIs based on these parameters can be found in Yoshida et al. (2012)

even fatal adverse effects, or to a decrease in the exposure rendering the NCE or the co-medication ineffective. For more details about the broad field of DDIs the reader is referred to special monographs, e.g. by Pang et al. (2010).

Avoiding any DDI risk is essential for the safe administration of a new drug candidate to patients under co-medication(s). Thus, regulators demand particular attention to this subject, as can be seen from the recently released guidelines for sponsors, both from the FDA and the EMA (see websites under list of references).

Although DDIs can occur from interaction at the level of drug metabolising enzymes (DMEs) and drug transporters, the following chapter will deal only with the latter, since the expression of DMEs is much lower at the BBB as compared to the liver (see also Chap. 4), whereas the expression of drug transporters at the BBB is significant (see Chap. 2).

Given that P-gp is very highly expressed in the BBB where it acts to restrict the distribution of many compounds into brain, it is surprising to learn that CNS drug–transporter interactions are very rare. Indeed, thus far there are only two reports for P-gp-mediated DDIs affecting CNS distribution: (i) verapamil (victim) and cyclosporine (perpetrator) (Sasongko et al. 2005), (ii) loperamide (victim) and quinidine (perpetrator) (Sadeque et al. 2000; Skarke et al. 2003). These studies involve unusually high doses of the perpetrator (2.5 mg/kg iv of cyclosporine; 600 mg of loperamide vs the recommended 4–8 mg recommended against diarrhoea), and the higher brain concentrations of the victim drug most likely are simply a consequence of the higher plasma concentrations resulting from an interaction occurring at other sites in the body, rather than an inhibition at the level of BBB since the brain/plasma ratio remained unchanged (Cole et al. 2012). Furthermore, a study of these interactions in rodents suggests that they are unlikely to occur at the typical therapeutic doses that are actually used in human patients (Sugimoto et al. 2011).

A similar picture emerges looking at a human study of the endothelin receptor antagonist tezosentan which was dosed with cyclosporine for inhibition of P-gp in humans, as the drug is eliminated into the bile (van Giersbergen et al. 2002). The authors note an increased incidence of adverse events, including headache, hot flushes, and nausea, that may have been caused by increased brain distribution of the drug, although it is not clear whether the mechanism is at the level of P-gp inhibition at the BBB or simply a result of the increase in plasma exposure, which in turn will also increase brain exposure, and yet again is only secondary to a peripherally occurring DDI.

Because liver and kidneys express the greatest level and variety of transporters, Grover and Benet (2009) denote these organs as the primary location of transporter-based interactions. They conclude that while altered distribution due to secondary interactions at tissues other than the liver and kidneys may have a pharmacodynamic effect, these interactions, at least at the BBB, do not appear to significantly influence overall distribution volume. Thus, while brain distribution may change, even dramatically as in the case of ABC-transporter knockout mice, these changes do not necessarily manifest in a change in the volume of distribution (Grover and Benet 2009). An inhibitor of P-gp may hence affect the distribution of a P-gp substrate into brain, as observed for the verapamil–cyclosporine A interaction, without

significantly affecting the plasma concentration-time profile of the substrate (Sasongko et al. 2005). This is possible because the amount of drug distributing into the tissue of interest (e.g. the brain) is only a small fraction of the total amount of the drug in the body, and the clearance of the drug from the body may be mediated by processes other than the affected transporter, e.g. metabolism (Endres et al. 2006). While most clinically significant interactions result in noticeable changes in plasma concentrations, there are cases where a change in plasma concentrations is not evident, as is the case for tissues with a low volume of distribution, e.g. brain. In these instances, a transporter-based interaction could indeed occur, but the resulting effect on tissue concentrations may not be evident from the corresponding plasma concentration (Thompson 2011).

Therefore, due to the complexity of transporter-mediated clearance and distribution processes occurring simultaneously in different organs, much remains to be learned with regard to DDIs at the BBB. For an elaborate review on the subject the reader is referred to the publication of Eyal et al. (2009).

The importance of transporter-mediated DDIs has been emphasised in a recent draft guidance document by the FDA, and a final guidance document from the EMA (see websites under list of references). These documents are intended to give a comprehensive, systematic and mechanistic approach to the evaluation of the interaction potential of NCEs. They propose the use of (i) well-characterised in vitro assay systems to define the roles of the different transporters in drug absorption, distribution and elimination, and (ii) clinically relevant, selective probe substrates, inhibitors for the most important transporter subtypes. They further propose decision trees that attempt to define what can be extrapolated from current knowledge to aid in guiding the need, or lack thereof, for clinical DDI studies. A recent "ITC White Paper on transporters" of The International Transporter Consortium (ITC) has highlighted major uptake and efflux transporters that could be relevant in terms of the potential clinical outcome (Giacomini et al. 2010) mitigating efficacy and safety as well as the potential of genetic polymorphisms to become an issue in the clinic. The paper states "that current clinical data indicate that there are no consistent examples in which inhibition of P-gp in the BBB resulted in adverse effects".

A quantitative framework for examining P-gp-mediated DDI at the BBB in vitro and extrapolating the results to in vivo (rat) and further to human has been proposed by Sugimoto et al. (2011) and Hsiao and Unadkat (2012). An important step in the evaluation is to elucidate the relative contribution of the target transporter to the overall membrane transport of a given drug (Kusuhara and Sugiyama 2009). Sugimoto et al. (2011) used a MDR-1 overexpressing cell line as in vitro P-gp inhibition system from which they derived Ki values for a number of compounds. The Ki values were then related to the unbound plasma concentrations of the inhibitor in vivo (I,unbound). DDIs, as determined by changes in $K_{p,brain}$, were predicted for compounds where the ratio I,unbound/Ki was greater than 1. The conclusions were confirmed in the rat in vivo and compared with data from human.

Of the other transporter systems mentioned by Giacomini et al. 2010 to be expressed at the BBB (e.g. BCRP, MRP4/5, OATP1A2/2B1), there is no reported evidence for clinical DDIs (Kalvass et al. 2013).

Noteworthy, there seems to be a combined or even synergistic effect of P-gp and BCRP at the BBB with both efflux pumps cooperating to very strongly reduce CNS levels of tyrosine kinase inhibitors such as lapatinib, gefitinib, imatinib, dasatinib, sorafenib, axitinib, and cediranib (see Giacomini et al. 2010). Thus, compounds inhibiting both P-gp and BCRP at the same time could potentially have a strong impact on the brain distribution of these drugs (Kusuhara and Sugiyama 2009).

Regarding the L-system amino acid transporter at the BBB, there have been concerns in the past for the safe use of the artificial sweetener Aspartam as voiced by Pardridge (1986). Blood phenylalanine levels are known to increase following aspartame consumption. Thus, fivefold increases in the plasma phenylalanine level are expected in the up to 20 million individuals with impairment in phenylalanine metabolism who consume high amounts of aspartame per day. This unilateral increase may saturate the L-system amino acid transporter thereby leading to a distortion of the transport of the essential amino acids all entering the brain via this route, potentially impacting brain development and in particular those processes within the CNS which require constant supply with essential amino acids (e.g. neurotransmitter and protein synthesis), ultimately causing a subtle yet distinct impairment in brain (Pardridge 1986). L-Dopa and melphalan are drugs that also utilise this carrier system to gain access to the CNS. An interaction study with high doses of Aspartam in Parkinson patients on L-Dopa, however, did not reveal any adverse effects (Karstaedt and Pincus 1993).

The area of transporter-mediated processes and their consequences on PK, efficacy and safety, including DDIs, is currently one of the fastest growing areas in pharmacokinetic and clinical research. The field is on a very steep learning curve with new insights accumulating rapidly, but waiting to be integrated into a comprehensive and predictive framework.

12.5 Summary and Conclusions

The complex structure of the CNS also makes brain penetration and distribution a complex multi-parameter process which cannot be rationalised on the basis of any single parameter. Not adequately addressing this complexity has resulted in many CNS drug discovery programmes to go on a troubled path too often ending up in clinical failures. Clinical trials costs but also failure rates in CNS drug development are higher than in any other therapeutic area today making R&D into new CNS drug targets economically non-viable and unattractive. Several Big Pharma companies have responded by downsizing their efforts or even departing the field very recently (Abbott 2011; Tufts CSDD Impact Report 2012). In spite of Neurosciences research being very exciting in many areas, current understanding of the neuropathology of many CNS diseases is incomplete and not seen mature enough to make drug discovery both efficient for drug development and effective in patient trials (Palmer 2011a,b; Tufts CSDD Impact Report 2012).

Re-entering the field will require that the right conclusions are drawn very carefully from both preclinical and clinical failures, and that the lessons are learned at a level which allows implementing a new CNS drug discovery and development paradigm that encompasses the high complexity of a drug's action at CNS targets in their full spatial and temporal resolution in conjunction with disease aetiology. A high level of understanding and confidence on the drug's CNS penetration and distribution to the site of action will be a fundamental basis of this new paradigm allowing more clearly to differentiate between lack of response due to a flawed disease hypothesis and failures due to technical reasons.

The past strategy of (simply) optimising total brain levels, i.e. Kp, has turned out to be part of the problem. Abandoning the old strategy very rapidly makes way for a broad acceptance of the new concept of CNS penetration and distribution that acknowledges the interplay between the different PK compartments in blood and brain, BBB transport, and drug distribution to the site of action within the CNS in an integrative fashion. The new concept gives a comprehensive framework of the essential science as well as a methodological spectrum which is fully compatible with routine implementation in today's drug discovery process.

For many CNS drugs, their target site concentrations are directly linked to drug concentrations in the brain ISF, i.e. their unbound levels in brain (Westerhout et al. 2011). Unbound brain concentrations are therefore a reliable surrogate of the driving force of drug action in the CNS. The *new definition of CNS exposure thus is unbound drug concentration in brain* as surrogate for the pharmacologically active drug concentration in brain. Furthermore, $K_{p,uu,brain}$ *is to replace* $K_{p,brain}$ *as measure of the extent of brain penetration* as $K_{p,uu,brain}$ is not distorted by non-specific binding to brain tissue and hence directly reflects the processes affecting brain interstitial fluid concentrations, i.e. the unbound drug levels in the key effect compartment of many CNS targets.

With the strategy essentially being in place to be able to follow the concentration–time profile at the target site in the brain, disease hypotheses and therapeutic potential of new CNS drug targets can be examined much more rigorously than has been possible in the past. This will greatly benefit the extraction of powerful conclusions from failed clinical trials as it may help to identify those mechanisms out of the complex pattern of reported reasons that are key to the solution (Reichel 2009; Palmer and Alavijeh 2012).

Many CNS diseases have been defined more than a century ago by clinical symptoms rather than pharmacological mechanisms, hence there often is a large fraction of non-responders in the patient population masking the effect in a potentially responding sub-population of a drug that is very selectively acting on one particular molecular CNS target. Our understanding of the mechanisms underlying the pathophysiology of CNS diseases is still seen to be very insufficient or even in its infancy, as for instance in the case of stroke but also in other neuropathological diseases. More than too often, there were no effects in human despite significant effects in the lab questioning the clinical relevance of animal disease models. Also, short-term favourable effects may reverse over longer-term applications, pointing toward temporal response patterns which change between acute and during chronic treatment

as the CNS appears to respond to treatment in a complex spatial and temporal mode. Another problem to this day is to identify an appropriate dose and schedule in the clinical trial which is both efficacious and safe, this difficulty being further aggravated if the drug candidate has a very narrow therapeutic window and validated biomarkers are not available. Failures due to insufficient CNS penetration have also been reported, but should soon be a matter of the past (Reichel 2009; Enna and Williams 2009; Palmer 2011a,b; Palmer and Alavijeh 2012).

Based on the new concept of CNS penetration allowing to determine and control brain target exposure, therapeutic hypotheses can be tested much more stringently than has been possible in the past. By systematically changing some key properties of new compounds or experimental conditions, one can decipher the impact these changes will have on plasma and brain PK, BBB transport, CNS distribution and target engagement using the integrative power of PKPD modelling and simulation. The concept will thus form a solid basis for the systematic investigation of the relation between target engagement, functional target response and its potential therapeutic role in the course of a disease. Aspirations are high that this approach will be one key to solve the conundrum why positive effects in animal disease models do not translate to the human patient.

PET studies in patients to examine target receptor occupancy in the human brain, to define effective plasma concentrations and hence clinical doses, and to study treatment paradigms in human are becoming another key methodology (Wong et al. 2009). The use of receptor occupancy PET imaging allows to study the pharmacodynamic consequences of target engagement, and to follow "downstream" pharmacology, i.e. the pharmacodynamic consequences of target engagement to verify the disease hypothesis as related to the proposed action of the drug to a specific biological effect that is the basis for the therapeutic rationale of the programme. If available, PET occupancy studies may also help stratifying patients to select the right patients for Phase II proof-of-concept trials.

Such imaging studies will not only facilitate the development of new CNS medications but also help redefining dose and dosing regimens of already existing "old" medications as suggested by Gründer et al. (2011). The authors show that many classical antipsychotics have never undergone any rational dose-finding study. They now will be subjected to PET occupancy studies in patients to readjust the recommended doses in order to make their use more efficient and safer compared to the traditional doses and hopefully also improving their often poor response rates within the patient population.

In view of the enormous potential of the new concept of brain penetration, it would be great to see it becoming a turning point that refuels the fading interest in CNS drug research. With the CNS drug market currently being valued at more than $50bn worldwide and growing at an annual rate of ~15 % (Enna and Williams 2009), with CNS disorders to affect over 1.5bn people worldwide accounting for about one-third of the global disease burden (Palmer 2011a), there is a lot waiting for us to be accomplished by future CNS drug discovery and development.

References

Aänismaa P, Gatlik-Landwojtowicz E, Seelig A (2008) P-glycoprotein senses its substrates and the lateral membrane packing density: consequences for the catalytic cycle. Biochemistry 47(38):10197–10207

Abbott NJ (2004) Evidence for bulk flow of brain interstitial fluid: significance for physiology and pathology. Neurochem Int 45(4):545–552

Abbott A (2011) Novartis to shut brain research facility. Drug giant redirects psychiatric efforts to genetics. Nature 480:161–162

Agarwal S, Hartz AM, Elmquist WF, Bauer B (2011) Breast cancer resistance protein and P-glycoprotein in brain cancer: two gatekeepers team up. Curr Pharm Des 17(26):2793–2802

Avdeef A (2012) Absorption and drug development: Solubility, permeability, and charge state. John Wiley & Sons, New Jersey, p 744

Ballard P, Brassil P, Bui KH, Dolgos H, Petersson C, Tunek A, Webborn PJ (2012) The right compound in the right assay at the right time: an integrated discovery DMPK strategy. Drug Metab Rev 44(3):224–252

Begley DJ (1996) The blood–brain barrier: principles for targeting peptides and drugs to the central nervous system. J Pharm Pharmacol 48(2):136–146

Borsook D, Upadhyay J, Klimas M, Schwarz AJ, Coimbra A, Baumgartner R, George E, Potter WZ, Large T, Bleakman D, Evelhoch J, Iyengar S, Becerra L, Hargreaves RJ (2012) Decision-making using fMRI in clinical drug development: revisiting NK-1 receptor antagonists for pain. Drug Discov Today 17(17–18):964–973

Broccatelli F, Carosati E, Cruciani G, Oprea TI (2010) Transporter-mediated efflux influences CNS side effects: ABCB1, from antitarget to target. Mol Inform 29(1–2):16–26

Broccatelli F, Larregieu CA, Cruciani G, Oprea TI, Benet LZ (2012) Improving the prediction of the brain disposition for orally administered drugs using BDDCS. Adv Drug Deliv Rev 64(1):95–109

Cartwright ME, Cohen S, Fleishaker JC, Madani S, McLeod JF, Musser B, Williams SA (2010) Proof of concept: a PhRMA position paper with recommendations for best practice. Clin Pharmacol Ther 87(3):278–285

Chishty M, Reichel A, Siva J, Abbott NJ, Begley DJ (2001) Affinity for the P-glycoprotein efflux pump at the blood–brain barrier may explain the lack of CNS side-effects of modern antihistamines. J Drug Target 9(3):223–238

Cecchelli R, Berezowski V, Lundquist S, Culot M, Renftel M, Dehouck MP, Fenart L (2007) Modelling of the blood–brain barrier in drug discovery and development. Nat Rev Drug Discov 6(8):650–661

Cole S, Bagal S, El-Kattan A, Fenner K, Hay T, Kempshall S, Lunn G, Varma M, Stupple P, Speed W (2012) Full efficacy with no CNS side-effects: unachievable panacea or reality? DMPK considerations in design of drugs with limited brain penetration. Xenobiotica 42(1):11–27

de Lange EC, Danhof M, de Boer AG, Breimer DD (1997) Methodological considerations of intracerebral microdialysis in pharmacokinetic studies on drug transport across the blood–brain barrier. Brain Res Brain Res Rev 25(1):27–49

de Lange EC, Danhof M (2002) Considerations in the use of cerebrospinal fluid pharmacokinetics to predict brain target concentrations in the clinical setting: implications of the barriers between blood and brain. Clin Pharmacokinet 41(10):691–703

Darvesh AS, Carroll RT, Geldenhuys WJ, Gudelsky GA, Klein J, Meshul CK, Van der Schyf CJ (2011) In vivo brain microdialysis: advances in neuropsychopharmacology and drug discovery. Expert Opin Drug Discov 6(2):109–127

Di L, Kerns EH, Carter GT (2008) Strategies to assess blood–brain barrier penetration. Exp Opin Drug Disc 3(6):677–687

Di L, Umland JP, Chang G, Huang Y, Lin Z, Scott DO, Troutman MD, Liston TE (2011) Species independence in brain tissue binding using brain homogenates. Drug Metab Dispos 39(7):1270–1277

Doran A, Obach RS, Smith BJ, Hosea NA, Becker S, Callegari E, Chen C, Chen X, Choo E, Cianfrogna J, Cox LM, Gibbs JP, Gibbs MA, Hatch H, Hop CE, Kasman IN, Laperle J, Liu J, Liu X, Logman M, Maclin D, Nedza FM, Nelson F, Olson E, Rahematpura S, Raunig D, Rogers S, Schmidt K, Spracklin DK, Szewc M, Troutman M, Tseng E, Tu M, Van Deusen JW, Venkatakrishnan K, Walens G, Wang EQ, Wong D, Yasgar AS, Zhang C (2005) The impact of P-glycoprotein on the disposition of drugs targeted for indications of the central nervous system: evaluation using the MDR1A/1B knockout mouse model. Drug Metab Dispos 33(1):165–174

Doran AC, Osgood SM, Mancuso JY, Shaffer CL (2012) An evaluation of using rat-derived single-dose neuropharmacokinetic parameters to project accurately large animal unbound brain drug concentrations. Drug Metab Dispos 40(11):2162–2173

Easter A, Bell ME, Damewood JR Jr, Redfern WS, Valentin JP, Winter MJ, Fonck C, Bialecki RA (2009) Approaches to seizure risk assessment in preclinical drug discovery. Drug Discov Today 14(17–18):876–884

EMA Guideline on the Investigation of Drug Interactions, Final, (2012). http://www.ema.europa.eu/docs/en_GB/document_library/Scientific_guideline/2012/07/WC500129606.pdf

Enna SJ, Williams M (2009) Challenges in the search for drugs to treat central nervous system disorders. J Pharmacol Exp Ther 329(2):404–411

Endres CJ, Hsiao P, Chung FS, Unadkat JD (2006) The role of transporters in drug interactions. Eur J Pharm Sci 27(5):501–517

Eyal S, Hsiao P, Unadkat JD (2009) Drug interactions at the blood–brain barrier: fact or fantasy? Pharmacol Ther 123(1):80–104

FDA Guidance for Industry: Drug Interaction Studies—Study Design, Data Analysis, Implications for Dosing, and Labeling Recommendations, Draft Guidance, (2012). http://www.fda.gov/downloads/Drugs/GuidanceComplianceRegulatoryInformation/Guidances/ucm292362.pdf

Fridén M, Gupta A, Antonsson M, Bredberg U, Hammarlund-Udenaes M (2007) In vitro methods for estimating unbound drug concentrations in the brain interstitial and intracellular fluids. Drug Metab Dispos 35(9):1711–1719

Fridén M, Ducrozet F, Middleton B, Antonsson M, Bredberg U, Hammarlund-Udenaes M (2009a) Development of a high-throughput brain slice method for studying drug distribution in the central nervous system. Drug Metab Dispos 37(6):1226–1233

Fridén M, Winiwarter S, Jerndal G, Bengtsson O, Wan H, Bredberg U, Hammarlund-Udenaes M, Antonsson M (2009b) Structure-brain exposure relationships in rat and human using a novel data set of unbound drug concentrations in brain interstitial and cerebrospinal fluids. J Med Chem 52(20):6233–6243

Fridén M, Bergström F, Wan H, Rehngren M, Ahlin G, Hammarlund-Udenaes M, Bredberg U (2011) Measurement of unbound drug exposure in brain: modeling of pH partitioning explains diverging results between the brain slice and brain homogenate methods. Drug Metab Dispos 39(3):353–362

Gabrielsson J, Hjorth S (2012) Quantitative Pharmacology. An introduction to integrative pharmacokinetic-pharmacodynamic analysis. Apotekearsocieteten, Stockholm, p 263

Ghose AK, Herbertz T, Hudkins RL, Dorsey BD, Mallamo JP (2012) Knowledge-based, central nervous system (CNS) lead selection and lead optimization for CNS drug discovery. ACS Chem Neurosci 3(1):50–68

Giacomini KM, Huang S-M, Tweedie DJ, Benet LZ, Brouwer KLR, Chu X, Dahlin A, Evers R, Fischer V, Hillgren KM, Hoffmaster KA, Ishikawa T, Keppler D, Kim RB, Lee CA, Niemi M, Polli JW, Sugiyama Y, Swaan PW, Ware JA, Wright SH, Yee SW, Zamek-Gliszczynski MJ, Zhang L, for The International Transporter Consortium, (2010) Membrane transporters in drug development. Nat Rev Drug Disc 9(3):215–236

Griebel G, Holsboer F (2012) Neuropeptide receptor ligands as drugs for psychiatric diseases: the end of the beginning? Nat Rev Drug Discov 11(6):462–478

Grimwood S, Hartig PR (2009) Target site occupancy: emerging generalizations from clinical and preclinical studies. Pharmacol Ther 122(3):281–301

Grover A, Benet LZ (2009) Effects of drug transporters on volume of distribution. AAPS J 11(2):250–261

Gründer G, Hiemke C, Paulzen M, Veselinovic T, Vernaleken I (2011) Therapeutic plasma concentrations of antidepressants and antipsychotics: lessons from PET imaging. Pharmacopsychiatry 44(6):236–248

Gunn RN, Summerfield SG, Salinas CA, Read KD, Guo Q, Searle GE, Parker CA, Jeffrey P, Laruelle M (2012) Combining PET biodistribution and equilibrium dialysis assays to assess the free brain concentration and BBB transport of CNS drugs. J Cereb Blood Flow Metab 32(5):874–883

Hammarlund-Udenaes M, Fridén M, Syvänen S, Gupta A (2008) On the rate and extent of drug delivery to the brain. Pharm Res 25(8):1737–1750

Hammarlund-Udenaes M (2009) Active-site concentrations of chemicals - are they a better predictor of effect than plasma/organ/tissue concentrations? Basic Clin Pharmacol Toxicol 106(3):215–220

Hammarlund-Udenaes M, Bredberg U, Fridén M (2009) Methodologies to assess brain drug delivery in lead optimization. Curr Top Med Chem 9(2):148–162

Hann MM (2011) Molecular obesity, potency and other addictions in drug discovery. Med Chem Commun 2:349–355

Hsiao P, Unadkat JD (2012) P-glycoprotein-based loperamide-cyclosporine drug interaction at the rat blood–brain barrier: prediction from in vitro studies and extrapolation to humans. Mol Pharm 9(3):629–633

Jeffrey P, Summerfield SG (2007) Challenges for blood–brain barrier (BBB) screening. Xenobiotica 37(10–11):1135–1151

Jones HM, Dickins M, Youdim K, Gosset JR, Attkins NJ, Hay TL, Gurrell IK, Logan YR, Bungay PJ, Jones BC, Gardner IB (2012) Application of PBPK modelling in drug discovery and development at Pfizer. Xenobiotica 42(1):94–106

Kalvass JC, Olson ER, Cassidy MP, Selley DE, Pollack GM (2007) Pharmacokinetics and pharmacodynamics of seven opioids in P-glycoprotein-competent mice: assessment of unbound brain EC50, u and correlation of in vitro, preclinical, and clinical data. J Pharmacol Exp Ther 323(1):346–355

Kalvass JC, Polli JW, Bourdet DL, Feng B, Huang SM, Liu X, Smith QR, Zhang LK, Zamek-Gliszczynski MJ (2013) Why clinical modulation of efflux transport at the human blood-brain barrier is unlikely: the ITC evidence-based position. Clin Pharmacol Ther 94(1):80–94

Karstaedt PJ, Pincus JH (1993) Aspartame use in Parkinson's disease. Neurology 43(3 Pt 1):611–613

Kerns E, Di L (2008) Drug-like properties: Concepts, structure design and methods: From ADME to toxicity optimization. Academic Press, Amsterdam, p 552

Kielbasa W, Kalvass JC, Stratford R (2009) Microdialysis evaluation of atomoxetine brain penetration and central nervous system pharmacokinetics in rats. Drug Metab Dispos 37(1):137–142

Kielbasa W, Stratford RE Jr (2012) Exploratory translational modeling approach in drug development to predict human brain pharmacokinetics and pharmacologically relevant clinical doses. Drug Metab Dispos 40(5):877–883

Kodaira H, Kusuhara H, Fujita T, Ushiki J, Fuse E, Sugiyama Y (2011) Quantitative evaluation of the impact of active efflux by p-glycoprotein and breast cancer resistance protein at the blood–brain barrier on the predictability of the unbound concentrations of drugs in the brain using cerebrospinal fluid concentration as a surrogate. J Pharmacol Exp Ther 339(3):935–944

Kola I, Landis J (2004) Can the pharmaceutical industry reduce attrition rates? Nat Rev Drug Discov 3(8):711–715

Kusuhara H, Sugiyama Y (2009) In vitro-in vivo extrapolation of transporter-mediated clearance in the liver and kidney. Drug Metab Pharmacokinet 24(1):37–52

Levin VA (1980) Relationship of octanol/water partition coefficient and molecular weight to rat brain capillary permeability. J Med Chem 23(6):682–684

Lin JH (2008) CSF as a surrogate for assessing CNS exposure: an industrial perspective. Curr Drug Metab 9(1):46–59

Liu X, Chen C (2005) Strategies to optimize brain penetration in drug discovery. Curr Opin Drug Discov Devel 8(4):505–512
Liu X, Smith BJ, Chen C, Callegari E, Becker SL, Chen X, Cianfrogna J, Doran AC, Doran SD, Gibbs JP, Hosea N, Liu J, Nelson FR, Szewc MA, Van Deusen J (2005) Use of a physiologically based pharmacokinetic model to study the time to reach brain equilibrium: an experimental analysis of the role of blood–brain barrier permeability, plasma protein binding, and brain tissue binding. J Pharmacol Exp Ther 313(3):1254–1262
Liu X, Van Natta K, Yeo H, Vilenski O, Weller PE, Worboys PD, Monshouwer M (2009) Unbound drug concentration in brain homogenate and cerebral spinal fluid at steady state as a surrogate for unbound concentration in brain interstitial fluid. Drug Metab Dispos 37(4):787–793
Liu X, Chen C, Hop CE (2011) Do we need to optimize plasma and tissue binding in drug discovery? Curr Topics Med Chem 11(4):450–466
Liu X, Ding X, Deshmukh G, Liederer BM, Hop CE (2012) Use of the cassette-dosing approach to assess brain penetration in drug discovery. Drug Metab Dispos 40(5):963–969
Löscher W, Potschka H (2005) Drug resistance in brain diseases and the role of drug efflux transporters. Nat Rev Neurosci 6(8):591–602
Mangas-Sanjuan V, González-Alvarez M, Gonzalez-Alvarez I, Bermejo M (2010) Drug penetration across the blood–brain barrier: an overview. Ther Deliv 1(4):535–562
Martin I (2004) Prediction of blood–brain barrier penetration: are we missing the point? Drug Discov Today 9(4):161–162
Morgan P, Van Der Graaf PH, Arrowsmith J, Feltner DE, Drummond KS, Wegner CD, Street SD (2012) Can the flow of medicines be improved? Fundamental pharmacokinetic and pharmacological principles toward improving Phase II survival. Drug Discov Today 17(9–10):419–424
Naik P, Cucullo L (2012) In vitro blood–brain barrier models: current and perspective technologies. J Pharm Sci 101(4):1337–1354
Nervi P, Li-Blatter X, Aänismaa P, Seelig A (2010) P-glycoprotein substrate transport assessed by comparing cellular and vesicular ATPase activity. Biochim Biophys Acta 1798(3):515–525
Obradovic T, Dobson GG, Shingaki T, Kungu T, Hidalgo IJ (2007) Assessment of the first and second generation antihistamines brain penetration and role of P-glycoprotein. Pharm Res 24(2):318–327
Ohtsuki S, Uchida Y, Kubo Y, Terasaki T (2011) Quantitative targeted absolute proteomics-based ADME research as a new path to drug discovery and development: methodology, advantages, strategy, and prospects. J Pharm Sci 100(9):3547–3559
Palmer AM (2011a) The role of the blood brain barrier in neurodegenerative disorders and their treatment. J Alzheimers Dis 24(4):643–656
Palmer AM (2011b) Neuroprotective therapeutics for Alzheimer's disease: progress and prospects. Trends Pharmacol Sci 32(3):141–147
Palmer AM, Alavijeh MS (2012) Translational CNS medicines research. Drug Discov Today 17(19–20):1068–1078
Pang KS, Rodrigues AD, Peter RM (2010) Enzyme- and transporter-based drug-drug interactions: Progress and future challenges. Springer, New York
Pardridge WM (1986) The safety of aspartame. JAMA 256(19):2678
Pardridge WM (2007) Drug targeting to the brain. Pharm Res 24(9):1733–1744
Peters SA (2012) Physiologically-based pharmacokinetic modeling and simulations. John Wiley & Sons, New Jersey, pp 430
Ploeger BA, van der Graaf PH, Danhof M (2009) Incorporating receptor theory in mechanism-based pharmacokinetic-pharmacodynamic (PK-PD) modeling. Drug Metab Pharmacokinet 24(1):3–15
Plowright AT, Johnstone C, Kihlberg J, Pettersson J, Robb G, Thompson RA (2012) Hypothesis driven drug design: improving quality and effectiveness of the design-make-test-analyse cycle. Drug Discov Today 17(1–2):56–62
Read KD, Braggio S (2010) Assessing brain free fraction in early drug discovery. Expert Opin Drug Metab Toxicol 6(3):337–344

Reichel A, Begley DJ, Abbott NJ (2000) Carrier-mediated delivery of metabotrophic glutamate receptor ligands to the central nervous system: structural tolerance and potential of the L-system amino acid transporter at the blood–brain barrier. J Cereb Blood Flow Metab 20(1):168–174

Reichel A, Begley DJ, Abbott NJ (2003) An overview of in vitro techniques for blood–brain barrier studies. Methods Mol Med 89:307–324

Reichel A (2006) The role of blood–brain barrier studies in the pharmaceutical industry. Curr Drug Metab 7(2):183–203

Reichel A (2009) Addressing central nervous system (CNS) penetration in drug discovery: basics and implications of the evolving new concept. Chem Biodivers 6(11):2030–2049

Rowland M, Peck C, Tucker G (2011) Physiologically-based pharmacokinetics in drug development and regulatory science. Annu Rev Pharmacol Toxicol 51:45–73

Sadeque AJ, Wandel C, He H, Shah S, Wood AJ (2000) Increased drug delivery to the brain by P-glycoprotein inhibition. Clin Pharmacol Ther 68(3):231–237

Sane R, Agarwal S, Elmquist WF (2012) Brain distribution and bioavailability of elacridar after different routes of administration in the mouse. Drug Metab Dispos 40(8):1612–1619

Salphati L, Pang J, Plise EG, Lee LB, Olivero AG, Prior WW, Sampath D, Wong S, Zhang X (2012) Preclinical assessment of the absorption and disposition of the phosphatidylinositol 3-kinase/mammalian target of rapamycin inhibitor GDC-0980 and prediction of its pharmacokinetics and efficacy in human. Drug Metab Dispos 40(9):1785–1796

Sasongko L, Link JM, Muzi M, Mankoff DA, Yang X, Collier AC, Shoner SC, Unadkat JD (2005) Imaging P-glycoprotein transport activity at the human blood–brain barrier with positron emission tomography. Clin Pharmacol Ther 77(6):503–514

Shaffer CL (2010) Defining neuropharmacokinetic parameters in CNS drug discovery to determine cross-species pharmacologic exposure-response relationships. Ann Rep Med Chem 45:55–70

Shen DD, Artru AA, Adkison KK (2004) Principles and applicability of CSF sampling for the assessment of CNS drug delivery and pharmacodynamics. Adv Drug Deliv Rev 56(12): 1825–1857

Skarke C, Jarrar M, Schmidt H, Kauert G, Langer M, Geisslinger G, Lötsch J (2003) Effects of ABCB1 (multidrug resistance transporter) gene mutations on disposition and central nervous effects of loperamide in healthy volunteers. Pharmacogenetics 13(11):651–660

Smith DA, Di L, Kerns EH (2010) The effect of plasma protein binding on in vivo efficacy: misconceptions in drug discovery. Nat Rev Drug Discov 9(12):929–939

Sugimoto H, Hirabayashi H, Kimura Y, Furuta A, Amano N, Moriwaki T (2011) Quantitative investigation of the impact of P-glycoprotein inhibition on drug transport across blood–brain barrier in rats. Drug Metab Dispos 39(1):8–14

Summerfield SG, Lucas AJ, Porter RA, Jeffrey P, Gunn RN, Read KR, Stevens AJ, Metcalf AC, Osuna MC, Kilford PJ, Passchier J, Ruffo AD (2008) Toward an improved prediction of human in vivo brain penetration. Xenobiotica 38(12):1518–1535

Suzuki G, Kawagoe-Takaki H, Inoue T, Kimura T, Hikichi H, Murai T, Satow A, Hata M, Maehara S, Ito S, Kawamoto H, Ozaki S, Ohta H (2009) Correlation of receptor occupancy of metabotropic glutamate receptor subtype 1 (mGluR1) in mouse brain with in vivo activity of allosteric mGluR1 antagonists. J Pharmacol Sci 110(3):315–325

Thompson TN (2011) The clinical significance of drug transporters in drug disposition and drug interactions. In: Bonate PL, Howard DR (eds) Pharmacokinetics in drug development. AAPS Books, Springer, New York

Tóth A, Veszelka S, Nakagawa S, Niwa M, Deli MA (2011) Patented in vitro blood–brain barrier models in CNS drug discovery. Recent Pat CNS Drug Discov 6(2):107–118

Tufts CSDD Impact Reports (2012) Pace of CNS drug development and FDA approvals lags other drug classes, March/April 2012, Vol. 14, No. 2

Trainor GL (2007) The Importance of protein binding in drug discovery. Expert Opin Drug Discov 2(1):51–64

van de Waterbeemd H, Smith DA, Jones BC (2001) Lipophilicity in PK design: methyl, ethyl, futile. J Comput Aided Mol Des 15(3):273–286

van Giersbergen PL, Bodin F, Dingemanse J (2002) Cyclosporin increases the exposure to tezosentan, an intravenous dual endothelin receptor antagonist. Eur J Clin Pharmacol 58(4):243–245

Wager TT, Chandrasekaran RY, Hou X, Troutman MD, Verhoest PR, Villalobos A, Will Y (2010a) Defining desirable central nervous system drug space through the alignment of molecular properties, in vitro ADME, and safety attributes. ACS Chem Neurosci 1(6):420–434

Wager TT, Hou X, Verhoest PR, Villalobos A (2010b) Moving beyond rules: The development of a central nervous system multiparameter optimization (CNS MPO) approach to enable alignment of druglike properties. ACS Chem Neurosci 1(6):435–449

Wager TT, Pettersen BA, Schmidt AW, Spracklin DK, Mente S, Butler TW, Howard H, Lettiere DJ, Rubitski DM, Wong DF, Nedza FM, Nelson FR, Rollema H, Raggon JW, Aubrecht J, Freeman JK, Marcek JM, Cianfrogna J, Cook KW, James LC, Chatman LA, Iredale PA, Banker MJ, Homiski ML, Munzner JB, Chandrasekaran RY (2011) Discovery of two clinical histamine H(3) receptor antagonists: trans-N-ethyl-3-fluoro-3-[3-fluoro-4-(pyrrolidinylmethyl)phenyl] cyclobutanecarboxamide (PF-03654746) and trans-3-fluoro-3-[3-fluoro-4-(pyrrolidin-1-ylmethyl)phenyl]-N-(2-methylpropyl)-cyclobutanecarboxamide (PF-03654764). J Med Chem 54(21):7602–7620

Wager TT, Liras JL, Mente S, Trapa P (2012) Strategies to minimize CNS toxicity: in vitro high-throughput assays and computational modeling. Expert Opin Drug Metab Toxicol 8(5):531–542

Wan H, Rehngren M, Giordanetto F, Bergström F, Tunek A (2007) High-throughput screening of drug-brain tissue binding and in silico prediction for assessment of central nervous system drug delivery. J Med Chem 50(19):4606–4615

Wang J, Skolnik S (2010) Mitigating permeability-mediated risks in drug discovery. Expert Opin Drug Metab Toxicol 6(2):171–187

Westerhout J, Danhof M, De Lange EC (2011) Preclinical prediction of human brain target site concentrations: considerations in extrapolating to the clinical setting. J Pharm Sci 100(9): 3577–3593

Wong DF, Tauscher J, Gründer G (2009) The role of imaging in proof of concept for CNS drug discovery and development. Neuropsychopharmacology 34(1):187–203

Yanai K, Rogala B, Chugh K, Paraskakis E, Pampura AN, Boev R (2012) Safety considerations in the management of allergic diseases: focus on antihistamines. Curr Med Res Opin 28(4):623–642

Yoshida K, Maeda K, Sugiyama Y (2012) Transporter-mediated drug-drug interactions involving OATP substrates: Predictions based on in vitro inhibition studies. Clin Pharmacol Ther 91(6):1053–1064

Zhang D, Surapaneni S (2012) ADME-enabling technologies in drug design and development. John Wiley & Sons, New Jersey, p 622

Chapter 13
Pharmacoeconomic Considerations in CNS Drug Development

David Gray

Abstract Recent advances in understanding of the blood–brain barrier (BBB) suggest that we are entering an era in which basic discoveries of BBB structure and function may be parlayed into meaningful disease applications. The development of impactful human therapies is a difficult and lengthy process; nonetheless, many researchers desire to see their work applied to the treatment of human disease. Significant financial reward will follow functional solutions to BBB delivery challenges; however, validating a trans-BBB delivery strategy to support and sustain a clinical program is costly and risky and requires multidisciplinary expertise. Investigators must necessarily garner funding and expertise for such campaigns, mainly through government grants, private investment firms, and industrial partnerships. Among the many considerations for researchers looking to advance brain delivery technology are the commercial aspects of the technology and the requirements attached to the funding mechanisms for clinical development. Early choices about delivery modality and target therapy (indication) have important consequences for the development process. An understanding of the forces that currently drive the pricing of therapeutics and the factors considered by potential investors who can fund expensive clinical development programs is helpful for framing a discussion about the pharmacoeconomics of BBB delivery. Complex multimodal delivery technologies may have added challenges for demonstrating safety and significantly higher drug manufacturing costs that can influence the risk–benefit analysis made by potential investors. Both the therapeutic application and the delivery system influence the path to generating commercial or government interest in advancing a particular brain delivery approach toward the clinic.

D. Gray (✉)
Pfizer Pharmatherapeutics Research, 700 Main Street,
Cambridge, MA 02139, USA
e-mail: david.l.gray@pfizer.com

M. Hammarlund-Udenaes et al. (eds.), *Drug Delivery to the Brain*, AAPS Advances in the Pharmaceutical Sciences Series 10, DOI 10.1007/978-1-4614-9105-7_13,

Abbreviations

BBB	Blood–brain barrier
CNS	Central nervous system
GMP	Good manufacturing practice
NIH	National Institute of Health
QALY	Auality-adjusted life year

13.1 Introduction

As described in Chaps. 1 and 2, blood–brain barrier (BBB) functionally limits the access of many reagents to the brain. Clearly, strategies that overcome the drug-limiting aspects of the BBB could be important components to future treatment of CNS-based disease (Bisht 2011; Frank et al. 2011; Jain and Jain 2011; Malakoutikhah et al. 2011; Rajadhyaksha et al. 2011; Shinde et al. 2011; Tian et al. 2011; Tucker 2011). Significant progress in the development of protein, peptide, antibody, protein fusion, stem cell, viral, gene, and other therapeutic modalities (biotherapeutics) has redefined the landscape of investigational clinical drugs for non-CNS indications (Schneider et al. 2010), and a substantial portion of successful new pharmaceutical treatments are expected to be biotherapies (Zhong et al. 2011). In contrast to treatments in other disease areas, both existing drugs and current exploratory agents for common CNS disorders are almost exclusively small molecule entities (Pardridge 2005; Misra 2003). Effective or improved treatment of CNS disease is one of the most important unmet medical needs and could alleviate a significant financial burden on society. In a critical research area beset with poor translational disease models, the significant BBB-imposed restrictions on drug composition and modality are unwelcome impediments to progress.

For nearly 40 years, researchers have been looking for ways to circumvent the BBB to deliver otherwise brain-impaired molecules to CNS targets (Bodor et al. 1975). Until recently, the successful endpoint for these programs was an in vitro or rodent model demonstrating modified brain levels of a payload agent (Fig. 13.1). Chapters 16–22 of this text describe and reference many of these approaches and their success. With a maturing understanding of BBB structure and physiology, many BBB delivery researchers have shifted their focus from achieving laboratory success in vitro or in rodents to establishing methods or techniques that can effect brain delivery in a human clinical setting and thus contribute to the progress of CNS clinical research (see Fig. 13.1). Moving research objectives from the laboratory to the clinic brings a new set of funding challenges and decisions as well as potential financial reward.

Safety and efficacy are most critical and deterministic to the clinical success of any drug development program. Making a program attractive to investment, however, can be addressed and considered by investigators early in a BBB delivery

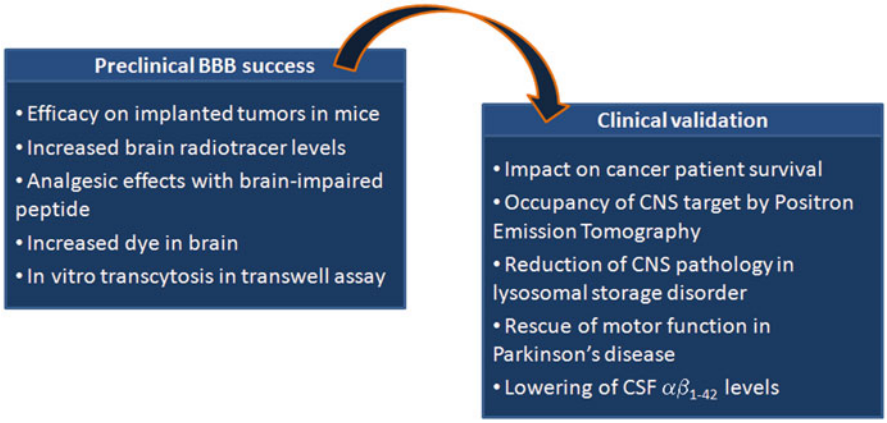

Fig. 13.1 Transition from successful preclinical demonstration of brain delivery to clinical validation

research program. In some cases, early choices about therapeutic application and reagent construction may impact opportunities to obtain support for clinical testing. This chapter discusses the orientation and prosecution of research within the larger picture clinical funding and provides context for cost-related considerations as they pertain to BBB delivery research.

13.1.1 Funding for BBB Delivery Research

BBB research that is not specifically directed toward clinical application is clearly valuable. Some public funding sources specifically foster research that is fundamental, speculative, or disconnected from the restrictions imposed by application. Presently, however, some of the largest sources of public research funding (NIH R01 grants in the USA, for example) are earmarked for health-related research. Given the increased difficulty in obtaining funding for basic science and the increased costs of laboratory research, lead investigators have become accustomed to aligning their research proposals to the requirements of funding sources. Some of these alignments are made primarily to satisfy the appearance of a human health application, whereas others genuinely attempt to assemble the elements necessary to advance a research idea toward a potential clinical application.

The most effective time to incorporate considerations about the clinical application of a BBB technology is often very early in research when pivotal decisions about potential human treatment are made; however, given the low conversion rate of BBB delivery research ideas into clinical trials, altering or constraining early stage BBB delivery research to align with an optimum path to clinical application may be counterproductive to innovation. As a technology gains momentum and its

proponents begin to think seriously about building toward human clinical studies, it is absolutely essential to begin planning a path that goes beyond "getting into the clinic" to consider what data will be necessary to make the opportunity attractive to investors.

13.1.2 Description of Stage Gates and Costs

The process of developing an idea into a market drug is often divided into a preclinical research stage and then into four development stages that roughly coincide with increasing levels of financial investment. The preclinical research stage culminates in the identification of a specific and defined therapeutic agent with sufficiently promising preclinical data to justify a development program that includes

- Late-stage preclinical research (meets regulatory requirements prior to human testing).
- Phase I, clinical testing (safety).
- Phase II, clinical research (efficacy).
- Phase III, large-scale clinical testing (robust safety and efficacy).

Most current BBB delivery concepts are in the early preclinical research stage. Relative to the development stage, preclinical research is less expensive, less subject to regulation, and less driven by timelines for progress. As a precursor to clinical work, preclinical biomedical research aims to generate a single reagent for testing and assemble an associated dataset to convince private investment to fund clinical exploration.

The first part of a development program is a late-stage preclinical phase that involves the manufacturing of test articles and gathering of safety data on the investigational agent under rigorous conditions that meet regulatory safety requirements. Once a therapeutic reagent enters development, any change in its molecular composition necessitates the restarting of preclinical or clinical research to generate data on the new material. Practically speaking, from the point a reagent is selected for late preclinical development, most of the elements that will determine clinical success or failure are irreversibly locked in. All subsequent work is geared toward investigating the potential of the selected reagent without opportunities to change payloads, linkers, loading, or other fundamental aspects of the therapeutic that impact safety, indication, and efficacy. Some reagents have long polymers or other complex components (large polyethylene glycol chains, for example) that result in drug products that vary within precisely defined analytical specifications. Such reagents can be advanced provided that all development work is conducted with material that is rigorously shown to meet manufacturing control standards and lies within prespecified distribution ranges. Manufacturing and safety data together with information that justifies testing in human subjects are submitted to a regulatory authority that reviews them and can grant approval for human clinical testing.

13.1.3 Phases of Clinical Development

The clinical development of novel agents is extraordinarily expensive and almost entirely funded by private investment. As a consequence, such research must align to the goals of the individuals or institutions providing the funding. BBB researchers who are serious about contributing to clinical advances in BBB delivery should consider the challenging and frequently unfamiliar financial realities of later-stage clinical research as they make decisions early in their programs. Colleagues in pharmaceutical or biotechnology companies can be useful resources for early conversations on this topic.

In Phase I, regulators grant approval for limited human testing with the primary aim of establishing data to support the safety of a drug. With sufficient demonstration of human safety, approval may be granted to expand the clinical program into Phase II exploratory studies focused on assessing the efficacy of a drug in patients. The validity of the approach for impacting human disease is typically first assessed at this stage. If an investigational agent shows acceptable safety and sufficient promise of patient benefit in Phase II studies, approval can be obtained to initiate Phase III studies in broader groups of patients in which a thorough assessment of safety and efficacy can be conducted to support an application to bring the drug to market. In some cases, the developing company and regulators may agree that it is advantageous to evaluate safety and some measures of efficacy in patients simultaneously in a hybrid stage often called Phase I/II. Some important areas in which efficacy testing has recently occurred in very small numbers of patients in Phase I/II studies include life-threatening cancers and severely debilitating genetic illnesses. The most advanced clinical testing of the viability of BBB delivery strategies is directed toward these indications—specifically, brain cancers, lysosomal storage disorders, and advanced Parkinson's disease in which limited efficacy assessment can be conducted concomitantly with safety studies in patients during Phase I. Patients with these severe or terminal illnesses have limited treatment options, and their participation in Phase I/II efficacy studies can both accelerate the availability of new therapies for their illnesses and provide early data on brain delivery efficacy in a clinical setting. In these cases, definitive Phase II and Phase III studies in larger numbers of patients are still required for convincing demonstration of safety and efficacy.

13.1.4 Drug Partitioning Between Brain and Other Tissues

Much of the clinical failure of novel therapeutics or technologies can be directly attributed to insufficient safety or efficacy. Essentially all substances are toxic to the human body in excess (Rosenberg et al. 2003). When the BBB restricts the partitioning of a CNS therapeutic agent into the brain, other organs and tissues are generally exposed to much higher levels of that agent than those intended for brain targets, in turn increasing the risk of a toxic event related to elevated exposure in untargeted

tissue (Jeffrey and Summerfield 2010). Most drugs and biotherapeutics partition more effectively into other tissues than they do into the brain; however, data to date show that at steady state, nearly all substances (including large biotherapeutic reagents) can get into the brain to some (often very limited) extent even without the aid of a delivery technology (Gosk et al. 2004; Moos and Morgan 2001; Yu et al. 2011). In theory, if an effective agent posed no risk of toxicity but was inefficacious because of poor brain penetration at standard doses, the dose could be increased thousands or millions of fold to a point at which the concentration gradient outside of the brain would drive an equilibrium to achieve the necessary engagement of the therapeutic mechanism in the brain. In practice, however, dosing to extreme levels to overcome major CNS impairment is neither safe nor practical. Thus, a major focus in BBB delivery research is the validation of strategies that favorably alter the partitioning of an agent toward increased exposure at CNS targets relative to other tissues. Technologies that increase distribution into the brain and other tissues without altering the partition equilibrium across tissues are approached with caution by clinicians for all but the most terminal patients. Any serious BBB delivery approach must accumulate robust evidence of cost, safety, and efficacy advantages well beyond what can be achieved by simply dosing the payload at a higher level.

13.1.5 Next Horizons for BBB Delivery Research

Although many publications are describing preclinical evidence of increased partitioning of brain-impaired reagents, at the time of this writing, no technologies, platforms, or strategies have been clinically proven to mediate reliable, therapeutically significant increases in the partitioning of a drug to targets in the whole human brain parenchyma relative to levels achieved in non-CNS tissues, although several important human trials are currently under way (Bisht 2011). The ultimate goal for applied BBB delivery research is to achieve safe, functionally significant improvement in human disease status using therapeutics that would be otherwise unsafe or ineffective. An intermediate but still important advance would be the demonstration of unequivocal engagement of targets in the healthy parenchyma by reagents that do not engage the target unless assisted by a delivery technology. This type of clinical demonstration, particularly if coupled to evidence of enhanced partitioning into the brain relative to other organs (liver, spleen, lung, etc.), would advance the field even if the engagement did not lead to the desired functional improvement in patients.

The challenges associated with achieving the ultimate goal of successful human therapy are immense. Success requires, among other elements, the simultaneous juxtaposition of a safe and successful therapeutic agent, a safe and effective delivery approach, the design and execution of effective clinical trials in the appropriate patient populations, and substantial amounts of money (Fig. 13.2). If any of these elements is missing from a program, the end result, measured against the goal of improving clinical outcomes, will be a failure. In practical terms, even researchers

Fig. 13.2 Common failure modes in clinical development

with effective BBB delivery strategies may be unable to demonstrate success if their strategies are paired with ineffective therapies, applied to the wrong patient population, or insufficiently supported financially to conduct the necessary studies.

13.2 Basics of Pricing

Companies and investors must take substantial risks with large investments over extended periods to bring new drugs to market (Paul et al. 2010; Basu et al. 2008; Adams and Brantner 2006). The current intellectual property system in the USA, Europe, Japan, and many other countries provides a means for companies and investors to make a profit commensurate with the risk and investment shouldered during drug development based on the value that an effective therapy brings to society during a short period of legally protected exclusivity. Developing a potential therapeutic agent into a marketed drug requires a sustained investment of capital, skill, and research dedication that could potentially be applied to any other endeavor (opportunity cost). To encourage the application of those resources to the socially important goal of improved health, the patent system protects well-considered investments in innovative new drug therapies. Patients and society benefit from successful research funded by for-profit entities, and the government maintains regulatory control over the process for new drug approval to protect the safety of those taking the drug. After extensive review of the clinical data and risk–benefit profile, a regulatory agency may grant approval to market a new drug for a specific

indication, and the developing company can begin to sell the drug. Ultimately, drug prices during the period of patent exclusivity reflect the value of effective new therapies to patients and society. Examples of specific factors that influence drug pricing include the effectiveness of a drug compared with other treatment options, the magnitude of the beneficial effect, and the societal burden and functional significance of the illness being treated. Untreated illness frequently leads to lower quality of life, loss of productivity, and increased health care expenditures for hospitalization, emergency room treatment, family care, and doctor visits (Goldie et al. 2004). Effective pharmacotherapy often substantially lowers total health care costs for groups of patients (Arnold 2007; Lock et al. 2011) and can drive marked improvement in the quality of life for those patients and their families. The evaluation of drug pricing considers principles of both macroeconomics and humanity.

13.2.1 Placing a Value on Efficacy

Some pricing parameters are determined by society (and may differ from country to country), whereas others are defined by the outcome of controlled clinical studies on the safety and efficacy of a new drug. One highly debated subjective parameter that undergoes constant revision is the value that society (usually a specific country) places on an additional quality-adjusted life year (QALY). Cost-effectiveness analyses frequently compare a chosen QALY value to the cost of the therapy (Marino et al. 2008). At the time of this writing, QALY values vary by country and methodology from US$30,000 to US$130,000. A readily understood example in which these factors could combine to support a significant valuation for a successful and innovative therapy is the treatment of a deadly cancer. The safety and efficacy of a potential new cancer drug are defined in carefully controlled clinical studies that assess specified patient outcomes such as survival and measures of quality of life. The outcomes for each patient in the trials are frequently combined to derive average outcomes across all patients or for defined subgroups in the study, and the overall effectiveness and safety of the new drug is put into context with expected or concomitantly measured outcomes of other available therapies. If the studies show that the treatment is beneficial, the additional months or years of life or improved functional outcomes (QALY) have a substantial value to the cancer patient and to society, which is reflected in a high valuation. Debilitating illnesses exist for which most or all patients currently lack treatment options. Unmet medical needs are high in these diseases, and society places great value on therapeutic advances.

13.2.2 Evaluating Commercial Potential

Before assuming the enormous cost and risk of developing a new drug, investing organizations consider the commercial potential of the successful drug by forecasting

Fig. 13.3 General composition of brain delivery-enabled therapeutics

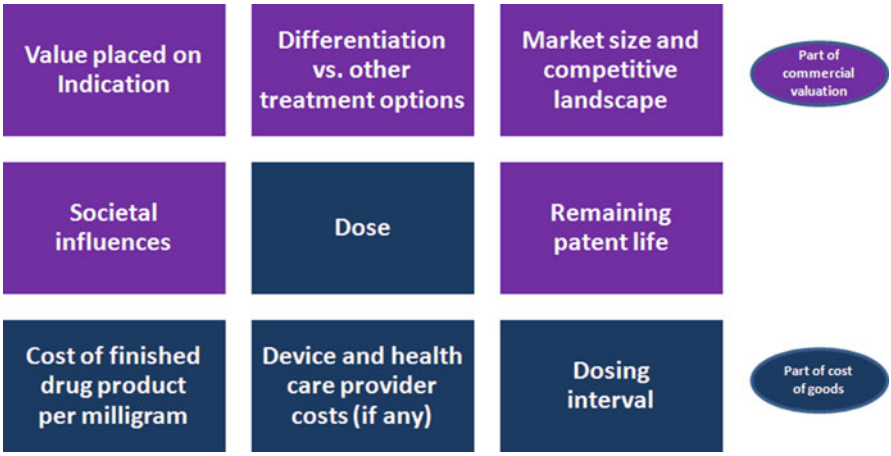

Fig. 13.4 Factors considered in commercial assessments

the number of patients it may treat (market size) and the societal, disease, and competitive factors that will influence pricing when it is launched. Frequently, these forecasts stretch many years into the future and have significant uncertainty. The investing organization will try to estimate the likelihood that an investigational agent will demonstrate the necessary safety and efficacy to become a marketed drug, the cost of the development program, and the length of remaining patent exclusivity at product launch (Wermeling 1993). Investors seek opportunities for which all of these factors combine to suggest a potential return on the total investment that is commensurate with its risk.

The expected cost of manufacturing a final drug product is another variable that can influence the commercial potential of a new therapy. Most current BBB delivery approaches can be conceptualized as having a payload component (the therapeutic agent), a targeting component, and frequently, additional components that join the payload to the targeting element (linker element; see Fig. 13.3). The costs for GMP synthesis and validation of these components together with the expense of combining, purifying, formulating, packaging, and storing the final drug product define the cost of goods per unit of active pharmaceutical ingredient (Fig. 13.4) (Basu et al. 2008). Manufacturing, storage, and distribution costs (cost of goods) that are too high relative to the market-established value of a therapy can erode the capability of a

developing company to make a profit and justify the investment. As a drug moves through the development process, a staged investment is made in the manufacture of the drug product itself with the aim of lowering the cost of goods via efficient production processes. Throughout the development process, companies frequently reevaluate the commercial potential of an investigational agent as new information on safety, efficacy, market size, regulatory environment, societal factors, and cost of manufacturing becomes available. These reevaluations can reveal that continued investment in the development of the agent is no longer justified for commercial reasons. For truly novel approaches such as BBB delivery strategies in which significant safety and technical hurdles remain unexplored, investors are more willing to assume the risk and expense of clinical development when they are applied to high-value therapeutic indications. Governments have established additional incentives to encourage research for rare illnesses with high unmet medical need (Sharma et al. 2010). These mechanisms can help make high-risk clinical research for rare or so-called orphan diseases financially attractive to private investment.

13.2.3 Expectations Accompanying Clinical Development Funding

Preclinical biomedical research is supported by many funding sources, including government grants, university budgets and endowments, charitable foundations, venture capital (VC) groups, and pharmaceutical and biotechnology companies. Public funding for early preclinical research is typically granted without any expectation of clinical advancement or application. The costs associated with advancing a successful preclinical laboratory demonstration of BBB delivery through early development to a completed, definitive clinical proof-of-concept trial (full Phase II) are substantially higher than most researchers might expect. Beyond the major costs of the trials themselves, the costs of manufacture, formulation, and storage of sufficient GMP material, required preclinical safety testing, legal and regulatory filings, analytical assay development, and compliance leading up to Phase I study are significant and only increase thereafter.

Limited publically funded or private charity programs are available to help move promising ideas into limited early stage clinical studies; however, the money to conduct full development is generally obtained only after private investors (VC groups or biotechnology/pharmaceutical companies) are convinced to finance a program based on its commercial potential or approach. Biomedically focused VC firms and biotechnology/pharmaceutical partners have access to the necessary capital, expertise, and perspective to evaluate the merits of exploratory ideas and invest in them on behalf of shareholders who desire a positive return. Researchers must realize that potential partners will view with great caution any opportunity lacking clinical validation, as failure in clinical development can lead to a nearly complete loss of investment. Among the many important consequences of this

reality is that the merits of an idea and the path to a return on investment are considered by an organization (VC or biotechnology/pharmaceutical partner) that is mainly focused on the financial merits of investments. Investigators must be prepared if potential funders propose directions and rigorous timelines for their programs that they did not envision.

13.2.4 Commercial Considerations Specific to BBB Delivery Technologies

The development of BBB delivery-enabled therapeutics may present specific considerations for potential investors. Increased reagent complexity and manufacturing costs, additional uncertainty about the safety of such technologies, and unclear development paths weigh negatively, whereas the potential for a successful strategy to have expanded commercial potential as a platform for the delivery of multiple therapeutic agents increases attractiveness.

13.2.4.1 Minimizing Risk with Robust Demonstration of Preclinical Safety

Before clinical studies, the safety of a new therapy is assessed in studies prescribed by regulatory agencies. For larger constructs, specific considerations of immunogenicity, persistence/accumulation, metabolism, and storage/handling may be required in addition to the demonstration of appropriate safety margins in prescribed in vitro and in vivo studies. Conducting definitive safety studies during the preclinical research phase to allay the concerns of a potential investor is not always possible; however, risk mitigation strategies can include using materials (including drug payloads) with demonstrated safety and completing some non-GMP in vitro or in vivo safety studies before seeking VC or industry funding. The safety of any investigational agent is always discussed as the therapeutic index between safe and efficacious exposures. Drug safety has an important empirical component; therefore, actual safety data in appropriate in vitro toxicity models and results from extended studies in appropriate animal species at multiples of targeted efficacious exposure and via the proposed route of administration are most convincing.

13.2.4.2 Maximizing Clinical Efficacy

Managing large clinical trials is a specialized and difficult endeavor. In general, VC or biotechnology/pharmaceutical partners will lead these activities for the programs in which they invest. Currently, a major failure mode for CNS drug development programs is the lack of clinical criteria necessary to support additional advancement. Many important CNS diseases (depression, schizophrenia, and Alzheimer's

for example) lack validated predictive preclinical models in which novel agents can be vetted with confidence. Many BBB delivery researchers look to mitigate clinical failure by deploying their delivery technology in the context of a therapeutic with established efficacy in human studies.

Two companies that have advanced brain delivery approaches into the clinic are Angiochem and to-BBB. Angiochem's clinical agent, ANG1005, is currently in Phase II studies for the treatment of brain tumors (Regina et al. 2008; Thomas et al. 2009). Scientists at Angiochem covalently attached the marketed anticancer drug paclitaxel (Taxol) to a peptide-based recognition sequence for a putative BBB transcytosis effector (see Chap. 18). The approach by to-BBB, 2B3-101, uses a liposomally encapsulated payload of the marketed chemotherapeutic doxorubicin (see Chap. 17) (Ranson et al. 2001). In both cases, the BBB delivery vector payloads are approved drugs, and the delivery systems use materials from classes with demonstrated preclinical safety. Both companies have lowered the efficacy-related failure risk of the payload by choosing proven efficacious drugs and successfully convinced investors to provide millions of dollars for clinical studies on the potential that their technologies will carry these proven agents more effectively into brain tumors.

13.3 Drug/Reagent Costs

Substantial research investment goes into the safe and reliable manufacture, formulation, quality control, and packaging of drug products. The cost of a finished therapeutic includes many elements that are not part of the drug product itself, including regulated storage, transportation, process development, and validation of any devices that are part of drug administration (Pinheiro et al. 2006). Although these costs are part of the manufacturing expense and investment, they do not define the value of a new drug the way efficacy and societal benefits do. In a simplified hypothetical example, if two drugs had identical safety, efficacy, and patient outcomes for a particular illness and one of the drugs cost ten times more to manufacture, the market and society would likely place a similar value on both drugs. The manufacturer of the more expensive drug would be at a competitive disadvantage owing to the higher cost of goods.

13.3.1 Importance of Dose Amount and Frequency

The frequency and amount of drug administration are important drivers of the cost of goods. Some drugs can be given as weekly or monthly injections, whereas others are administered orally or must be dosed multiple times each day. The value of a therapy for a particular illness depends on an effective response and is less influenced by the number of doses or the amount of drug in each dose necessary to achieve that response. A convenient way to normalize drug costs across modalities

and dosing schedules is to consider the total amount of drug required for a complete therapeutic response during a 1-month period. This calculation also connects drug costs to the way in which drugs are normally purchased. The cost of goods combines all manufacturing and production costs for the total amount of drug needed for a therapeutic response during a specified (often 1-month) period or, for acute illnesses, the amount of drug necessary to achieve of a full therapeutic response.

As ideas about a brain delivery technology and its human therapeutic application begin to crystallize, researchers must use available efficacy data to refine estimates of the dose amount and frequency that may be required for a therapeutic response in human trials and use that information to estimate the impact of the cost of goods on viability of the program. Scenarios can unfold in which a high cost of goods driven by either expensive manufacturing or large drug requirement destroys the value proposition for the investors and discourages the initiation or continuation of clinical development of an agent. Monoclonal antibodies are expensive to produce relative to small molecules; however, marketed antibodies are often dosed infrequently owing to their long circulation half-life, which helps lower the cost of goods. Modifications to antibodies or other complex reagents necessary to enable brain delivery may result in agents with shorter half-lives, in turn driving up monthly drug requirements and the cost of goods for therapy.

13.3.2 Drug Manufacturing Costs and Economy of Scale

The costs to manufacture a certain quantity of finished GMP drug products vary widely. Preclinical and early clinical research is carried out with smaller amounts of material and fit-for-purpose processes. Additional investment in new synthetic routes, formulation processes, and production methods along with the construction of dedicated manufacturing facilities and sourcing of raw materials on larger scales can optimize the cost of a final drug product. These expensive activities to lower the cost of goods are typically initiated in a staged fashion as the drug progresses through development.

The impacts of scale and dedicated manufacturing processes on pricing are illustrated in the case of β-cyclodextrin, which is now widely used in the formulation of final drug products and to enhance solubility in other industrial processes. When this reagent was first available in high purity in 1980, it cost US$10,000/kg (Loftsson and Duchene 2007; Zulsdorf et al. 2011). As demand for cyclodextrin increased, market forces encouraged suppliers to invest in developing new synthetic routes and, later, dedicated manufacturing capabilities for this product. At present, cyclodextrin can be purchased on large scale for less than US$10/kg—a greater than 1,000-fold decrease in the cost per gram driven by increased demand and investment in improved manufacturing processes. Although such dramatic reductions in price do not occur for all drug components, researchers can reasonably assume that the cost of goods for the first dose of investigational material will be much higher than that calculated when the drug is launched to market owing to process improvements and increased scale of production.

13.3.3 Impact of Drug Complexity

The number of processing and purification steps, the cost of the raw materials, the amount of time needed on large-scale equipment, and any special handling requirements are important contributors to reagent cost. A good example of a complex reagent is the 36-residue peptide drug enfuvirtide (Fuzeon). This drug was brought to market after demonstrating clinical efficacy in slowing the proliferation of the human immunodeficiency virus in patients via a novel mechanism of action. The manufacture of this drug was complicated, involving more than 100 processing and synthesis steps, many kilograms of raw materials for each kilogram of product, and a large amount of time on processing and purification equipment. The developing companies worked to bring costs down and even constructed a dedicated plant for production. When the drug was launched in 2003, however, it was priced at approximately US$1,650/month, and sales did not meet expectations. In a securities filing dated March 2008, the codeveloper of Fuzeon™ made the following statement about the impact of the cost of goods to the company: "If sufficient amounts of Fuzeon™ cannot be manufactured on a cost-effective basis, our financial condition and results of operations will be materially and adversely affected." Millions of dollars were spent to reduce the cost of goods for this drug, but its complex manufacturing process as well as the moderately high daily dose (approximately 180 mg/day is typical) required for efficacy have made pricing an issue for the developing companies since its launch.

13.4 Current Status of Commercial Considerations by Modality

Although every reagent has unique parameters that drive the cost of goods and commercial potential, some generalizations can be made about the cost of various BBB delivery approaches. Some of the inputs for the commercial potential of investigational drugs are depicted in Fig. 13.4. To illustrate some of these considerations, several BBB delivery approaches are discussed in the sections that follow.

13.4.1 Intranasal Delivery

Numerous companies and researchers are exploring nasal delivery as a potential privileged access route to the brain (see Chap. 16) (Rajadhyaksha et al. 2011; Landis et al. 2012; Malerba et al. 2011; Ugwoke et al. 2005). Nasal delivery is most often deployed in conjunction with a physical delivery device. In principle, nasal delivery systems could deliver small molecule therapies, administer complex drugs, or even be paired with BBB delivery strategies. The costs of the drug payload and additional BBB delivery technology must be added to the expenses specific to nasal delivery

additives and devices. The drug formulations used in most current strategies contain relatively simple excipients and proprietary reagents to increase permeability and transport at the nasal membrane. Many of these systems feature materials with demonstrated biocompatibility and safety to mitigate development risk (Ugwoke et al. 2005). The total amount of material that can be absorbed nasally is bounded by the constraints of the nasal mucous membrane; therefore, nasal delivery is limited to a relatively small total amount of drug and excipients. Many permeability enhancers are bulk commodities, but even custom excipients and permeability enhancers of the types currently being explored can be expected to contribute only modestly to the overall cost of the finished drug product unless they are complex to manufacture. If a nasal delivery system meaningfully increases the partitioning of a therapy to targets in the brain beyond what can be achieved by other routes of administration, few indications exist for which the *nasal-specific* costs of a device and modest amounts of excipient would destroy its value proposition.

The total cost of goods of the drug payload must still be considered. For example, if only a small fraction of a hypothetical therapeutic can be absorbed nasally and frequent administrations of an expensive drug are needed, the total cost of a nasal therapy could become considerable even if brain delivery is effective. Depending on the pricing expectations for the targeted indication and the magnitude of the therapeutic advance, the cost of goods might become commercially unattractive owing to excessive payload costs. The keys to making nasal delivery approaches to BBB delivery attractive to investors include pairing the delivery technology with a reagent that has demonstrated clinical safety/efficacy via another route of administration, a deep understanding of the mechanism for enhanced BBB delivery and how it will translate from animals to humans (considering anatomical and expression differences), and unequivocal demonstration that nasal delivery represents a privileged access point for the BBB beyond that achievable via other peripheral routes of administration.

13.4.2 Nanocarriers

Nanocarrier brain delivery systems are often based on polymers of established biocompatible materials or chemically modified variants and are typically not discrete entities but rather a distribution of nanoparticles within a specific size range (see Chap. 17) (Beg et al. 2011; Blasi et al. 2011; Celia et al. 2011; De Rosa et al. 2012; Martin-Banderas et al. 2011; Nair et al. 2012; Raudino et al. 2011; Panagiotou and Fisher 2011; Crunkhorn 2012). In some instances, they contain inorganic cores such as gold or feature coatings of polyethylene glycol or other polymers proposed to enhance delivery (Haque et al. 2012; Malhotra and Prakash 2011; Su et al. 2011; Wankhede et al. 2012; Herve et al. 2008). The drug payload is loaded onto the nanoparticles via non-covalent interactions, meaning that a given nanocarrier system could potentially be deployed to deliver many drugs without modification to the drug or the nanocarrier. The types of biocompatible nanomaterials under investigation to facilitate BBB delivery are frequently available in bulk or synthesized via well-established chemistries.

Some challenges, such as controlling aggregation and size distribution, are inherent in the manufacture of nanoparticles, but simple inorganic, polymeric, or coated nanoparticle delivery systems derived from established supply chains can largely be expected to have low to modest contributions to total drug cost.

Some nanoparticle systems are composed of highly specialized monomers or are complex multicomponent or multilayer systems. Cost can become significant in these systems and may factor into investor decisions depending on the indication for the therapy. At the extreme, a multilayer nanoparticle carrier may be functionalized with complex antibody or peptide ligands, and such a delivery system would add substantially to the total cost of the active pharmaceutical ingredient (Frank et al. 2011). Despite many publications that chronicle laboratory success, nanocarrier BBB delivery approaches have not advanced into clinical development. The keys to making this approach attractive to investors are strong safety data that support a low risk of toxicity after chronic administration of a therapeutically relevant concentration of the drug to the brain and the pairing of delivery technologies with reagents that have demonstrated clinical safety/efficacy.

13.4.3 Receptor-Mediated Approaches

Several delivery approaches under preclinical examination operate via an endothelially expressed transporter to facilitate BBB entry of cargo (see Chap. 18) (Tian et al. 2011; Rip et al. 2009). The manufacturing of these reagents is expected to be more complicated than that in the other approaches discussed in this section, and most are administered intravenously. These properties dictate that cost of goods will be more particularly considered as part of decisions about clinical development of receptor-mediated delivery systems. Several of the current receptor-mediated technologies are based on peptide ligands that engage with the endocytosis receptor (Gabathuler 2010). Peptide-based reagents are attractive owing to the substantial multi-decade global investments that have been made in the synthesis of complex peptides and the established supply chains for bulk availability of starting materials. For example, the aforementioned ANG1005 is a 19-residue peptide composed of natural amino acids covalently attached to three molecules of Taxol. The cost and complexity of its synthesis certainly far exceed that of most small molecule drugs, but it can be made using established chemistries and widely available materials. Ongoing trials of ANG1005 for the treatment of solid tumors are targeting a dose of approximately 1 g of active drug given as an infusion every 3 weeks. If the clinical trials show adequate safety and advantageous efficacy relative to other treatment options, the high value of the cancer indication combined with the modest monthly amount of drug and the accessibility of manufacturing methods will likely encourage continued investment in the clinical program.

The to-BBB investigational agent, 2B3-101, is a multicomponent liposome composed of relatively accessible monomers. Drug-loaded liposomes are currently on the market, and some production methods have been established (Ranson et al. 2001; Cagnoni et al. 2000). 2B3-101 adds a putative brain-targeting element to the

approved liposomal doxorubicin (Caelyx™) by mixing a low percentage of a custom polyethylene glycol to the liposome assembly. Despite the elegant simplicity of the manufacturing approach, the expense of making and loading customized liposomes while maintaining sufficient control over particle size could lead to a comparatively expensive drug product. The relatively low doses (20–100 mg every 21 days) being investigated in the clinic should mitigate reagent costs. Protein- and antibody-derived delivery systems and drugs are currently more expensive and complex than peptides. Some progress has being made to lower the cost of goods of antibody reagents, and additional decrease can be expected. Production costs are high for this reagent, and the total monthly dose must be carefully considered in the context of indication.

Other receptor-mediated transport targeting approaches can become quite complex—for example, Ding and coworkers (Ding et al. 2010) describe a malic acid polymer that includes multiple antibodies, a tracking dye, oligonucleotide elements, and a endosomal escape element. Although this construct was not intended as a therapy, it illustrates a potential disconnect between the types of reagents that can be used in laboratory setting and those that might be accessible for clinical work using current productions methods. The GMP manufacture of multicomponent materials that incorporate antibody-targeting vectors is certain to trigger addition scrutiny from potential investors with regard to the cost of goods. Researchers considering clinical work with complex delivery technologies may need to invest extra time to simplify manufacturing and increase the efficiency of brain delivery or reagent potency to reduce dose.

13.4.4 Neurosurgical Direct Delivery Approaches

Device-based delivery systems represent an interesting case study in the cost of therapy (see Chap. 20) (Ferguson et al. 2007; Bidros et al. 2010). The initial surgical procedure for implanting a direct CNS delivery system is substantial; the combination of surgery and device can be expected to exceed $10,000 in the USA. Once the device is implanted, ongoing drug material and maintenance costs are incurred specific to the drug. Directly implanted systems are widely used for intrathecal drug delivery in patients with chronic pain that cannot be managed with traditional pharmacotherapy (Kumar et al. 2001). Implanted devices demonstrate benefits—for example, decreases in the amount of drug used and increased tissue selectivity—similar to those sought with BBB delivery technologies, and device companies are making major investments to study applications in CNS disease (de Lissovoy et al. 2007; Bensmail et al. 2009). If such a system can achieve selective delivery of therapeutically effective payloads that otherwise have insufficient access to the brain, an interplay occurs between the high initial cost of the surgery and the therapeutic benefits. Making a device-based direct delivery system commercially viable for indications with low reimbursement would be challenging after considering the surgical costs. For life-threatening illnesses or conditions with significant unmet need, however, the economics are different and would need to be considered case by

case. In recent years, limited clinical exploration of direct delivery to the brain in severely ill patients has been funded by private charities, public research monies, or medical device manufacturers (Hall et al. 2003; Mehta et al. 2011). In general, these studies are approached as highly experimental and commercial considerations have not been rigorously analyzed. A clinical validation of device-based direct drug delivery to the brain from these efforts would certainly catalyze efforts to match this technology to commercially viable indications or pair it with payload modalities that may require only infrequent dosing (such as gene therapy).

13.4.5 Transient BBB Opening

The use of hyperosmotic mannitol or focused ultrasound with microbubbles as described in Chaps. 21 and 22 for transient disruption of the BBB is unlikely to add substantial reagent cost to a development program because the opening agents currently proposed are inexpensive and the procedures infrequent (although requiring considerable involvement from a health care provider) (Jain and Jain 2011; Rajadhyaksha et al. 2011; Shinde et al. 2011; Etame et al. 2012). Parallel research exists between transient BBB opening and direct delivery approaches because limited experimental studies have been carried out in which transient BBB opening has being attempted in terminally ill patients in a context disconnected from commercial considerations (Shawkat et al. 2012; Iwadate et al. 1993). A key next step for brain delivery via transient opening is the gathering of clear data defining the safety and efficacy of this approach and, from there, the identification of a subset of illnesses for which this approach is commercially attractive.

13.4.6 CNS Gene Therapy

Gene therapy has been proposed as a means to achieve persistent disease modification, often in patients with severe dysfunction. Gene therapy vectors could potentially be delivered in combination with other BBB delivery techniques, and dosing would be infrequent. Insufficient information is available from which to draw clear conclusions about the impact of drug reagent costs on the economics of gene therapy and viral vector approaches. With these emerging technologies, current research is appropriately focused on safety and efficacy; commercial aspects can be addressed as the scope of the technique is defined.

13.5 Conclusions

Any researcher with a true desire to advance BBB delivery technologies to a clinical proof of concept must eventually consider the means through which funding for that endeavor will be obtained. As a program moves along, key decisions about payload,

indication, safety data, and manufacturing can strongly influence how the opportunity will be viewed by VC, biotechnology, or pharmaceutical partners, and as the technology for the manufacture of certain biologic constructs improves, some of the cost-of-goods pressures will likely ease. Investigators must be prepared, however, for a future research environment in which the demonstration of safety and efficacy will be even more challenging than it is today. An increasing drive toward conducting high-risk/high-reward BBB delivery research in the context of innovative partnerships, pre-competitive research consortiums, and cost-sharing models may emerge in which the control of research objectives shifts toward those providing financial backing (Kessel and Frank 2007). Important societal conversations about the value of innovation and mechanisms to reward high-risk investment in drug research are playing out in various countries and governing bodies, and their outcomes may have a substantial influence on the way that capital is deployed to support cutting-edge research and development (Meropol et al. 2009).

Many BBB delivery researchers appreciate that the intersection of clinically validated or high-confidence therapeutics (lower failure risk owing to mechanism efficacy or study design) and life-threatening illness (strong valuation for successful therapies) represents an important opportunity to validate novel brain delivery strategies in a way that attracts needed investment from VC, biotechnology, or pharmaceutical partners. When a delivery technology adds substantially to final drug costs, researchers would be wise to consider addressing cost-of-goods issues by investing additional time and effort to improve delivery efficiency or payload efficacy. Both primary and business development literature describing novel brain delivery methods frequently tout cost savings or safety advantages associated with using a particular brain delivery approach to lower the payload needed for efficacy. Although these theoretical advantages are part of the opportunity for BBB delivery technologies, any such expectations need to be grounded in data before they can be factored into an analysis of commercial potential. In truth, brain delivery systems will bring additional safety risks and costs to clinical development until compelling data demonstrate that their theoretical advantages can be realized. Robust clinical brain delivery is a challenging problem, but without a doubt, opening the door to the use of brain-impaired reagents in CNS-based disorders represents an important and commercially valuable medical advance.

13.6 Points for Discussion

1. What role should biomedical researchers play in the dialogue about how health care innovation is funded and directed?
2. Do mechanisms exist for scientists to debate these issues within the scientific community or to educate policymakers on the likely impact of various approaches? Is this type of dialogue important to the advancement of human health?
3. What are the pros and cons of the current system for drug pricing?
4. What might you approach differently in your research after reading this chapter? Did any of the information herein surprise you? Were there statements that "rubbed you the wrong way?" If so, why?

5. What value would you place on an extra year of life? Do you think accepted values for QALYs will change in the next 5 years? If so, in what direction?
6. Do you think that a lot of brain delivery "winners" are simply not getting a chance to advance owing to lack of funding?
7. How important is marketing when trying to attract private funding to develop a new therapy?
8. Are elements of the current privately funded drug development process counterproductive or inefficient? If so, which ones?
9. Should the emphasis of government funding for research change? Should increased requirements for applicability be put in place for grants such as NIH R01?
10. What kinds of brain delivery clinical studies do you anticipate in 5 years, and do you expect new funding mechanisms or arrangements to foster clinical research in exploratory areas?

References

Adams CP, Brantner VV (2006) Estimating the cost of new drug development: is it really 802 million dollars? Health Aff (Millwood) 25(2):420–428

Arnold RJG (2007) Cost-effectiveness analysis: should it be required for drug registration and beyond? Drug Discov Today 12(21–22):960–965

Basu P, Joglekar G, Rai S, Suresh P, Vernon J (2008) Analysis of manufacturing costs in pharmaceutical companies. J Pharm Innov 3(1):30–40

Beg S, Samad A, Alam MI, Nazish I (2011) Dendrimers as novel systems for delivery of neuropharmaceuticals to the brain. CNS Neurol Disord Drug Targets 10(5):576–588

Bensmail D, Ward AB, Wissel J, Motta F, Saltuari L, Lissens J, Cros S, Beresniak A (2009) Cost-effectiveness modeling of intrathecal baclofen therapy versus other interventions for disabling spasticity. Neurorehabil Neural Repair 23(6):546–552

Bidros DS, Liu JK, Vogelbaum MA (2010) Future of convection-enhanced delivery in the treatment of brain tumors. Future Oncol 6(1):117–125

Bisht R (2011) Brain drug delivery system: a comprehensive review on recent experimental and clinical findings. Int J Pharm Sci Res 2(4):792–806

Blasi P, Schoubben A, Giovagnoli S, Rossi C, Ricci M (2011) Solid lipid nanoparticles to improve brain drug delivery. Nanomater Life Sci 10:365–394

Bodor N, Shek E, Higuchi T (1975) Delivery of a quaternary pyridinium salt across the blood-brain barrier by its dihydropyridine derivative. Science 190(4210):155–156

Cagnoni PJ, Walsh TJ, Prendergast MM, Bodensteiner D, Hiemenz S, Greenberg RN, Arndt CA, Schuster M, Seibel N, Yeldandi V, Tong KB (2000) Pharmacoeconomic analysis of liposomal amphotericin B versus conventional amphotericin B in the empirical treatment of persistently febrile neutropenic patients. J Clin Oncol 18(12):2476–2483

Celia C, Cosco D, Paolino D, Fresta M (2011) Nanoparticulate devices for brain drug delivery. Med Res Rev 31(5):716–756

Crunkhorn S (2012) Neurological disorders: nanoparticle opens door to cerebral palsy treatment. Nat Rev Drug Discov 11(6):440–441

de Lissovoy G, Matza LS, Green H, Werner M, Edgar T (2007) Cost-effectiveness of intrathecal baclofen therapy for the treatment of severe spasticity associated with cerebral palsy. J Child Neurol 22(1):49–59

De Rosa G, Salzano G, Caraglia M, Abbruzzese A (2012) Nanotechnologies: a strategy to overcome blood-brain barrier. Curr Drug Metab 13(1):61–69
Ding H, Inoue S, Ljubimov AV, Patil R, Portilla-Arias J, Hu J, Konda B, Wawrowsky KA, Fujita M, Karabalin N, Sasaki T, Black KL, Holler E, Ljubimova JY (2010) Inhibition of brain tumor growth by intravenous poly (beta-L-malic acid) nanobioconjugate with pH-dependent drug release [corrected]. Proc Natl Acad Sci U S A 107(42):18143–18148
Etame AB, Diaz RJ, Smith CA, Mainprize TG, Hynynen K, Rutka JT (2012) Focused ultrasound disruption of the blood-brain barrier: a new frontier for therapeutic delivery in molecular neurooncology. Neurosurg Focus 32(1):E3
Ferguson SD, Foster K, Yamini B (2007) Convection-enhanced delivery for treatment of brain tumors. Expert Rev Anticancer Ther 7(12 Suppl):S79–S85
Frank RT, Aboody KS, Najbauer J (2011) Strategies for enhancing antibody delivery to the brain. Biochim Biophys Acta Rev Cancer 1816(2):191–198
Gabathuler R (2010) Approaches to transport therapeutic drugs across the blood-brain barrier to treat brain diseases. Neurobiol Dis 37(1):48–57
Goldie SJ, Kohli M, Grima D, Weinstein MC, Wright TC, Bosch FX, Franco E (2004) Projected clinical benefits and cost-effectiveness of a human papillomavirus 16/18 vaccine. J Natl Cancer Inst 96(8):604–615
Gosk S, Vermehren C, Storm G, Moos T (2004) Targeting anti-transferrin receptor antibody (OX26) and OX26-conjugated liposomes to brain capillary endothelial cells using in situ perfusion. J Cereb Blood Flow Metab 24(11):1193–1204
Hall WA, Rustamzadeh E, Asher AL (2003) Convection-enhanced delivery in clinical trials. Neurosurg Focus 14(2):E2
Haque S, Md S, Alam MI, Sahni JK, Ali J, Baboota S (2012) Nanostructure-based drug delivery systems for brain targeting. Drug Dev Ind Pharm 38(4):387–411
Herve F, Ghinea N, Scherrmann JM (2008) CNS delivery via adsorptive transcytosis. AAPS J 10(3):455–472
Iwadate Y, Namba H, Saegusa T, Sueyoshi K (1993) Intra-arterial mannitol infusion in the chemotherapy for malignant brain tumors. J Neurooncol 15(2):185–193
Jain A, Jain SK (2011) Drug targeting to the brain—a review. Curr Nanosci 7(1):21–36
Jeffrey P, Summerfield S (2010) Assessment of the blood-brain barrier in CNS drug discovery. Neurobiol Dis 37(1):33–37
Kessel M, Frank F (2007) A better prescription for drug-development financing. Nat Biotechnol 25(8):859–866
Kumar K, Kelly M, Pirlot T (2001) Continuous intrathecal morphine treatment for chronic pain of nonmalignant etiology: long-term benefits and efficacy. Surg Neurol 55(2):79–88
Landis MS, Boyden T, Pegg S (2012) Nasal-to-CNS drug delivery: where are we now and where are we heading? An industrial perspective. Ther Deliv 3(2):195–208
Lock K, Wilson K, Murphy D, Riesco JA (2011) A cost-effectiveness model of smoking cessation based on a randomised controlled trial of varenicline versus placebo in patients with chronic obstructive pulmonary disease. Expert Opin Pharmacother 12(17):2613–2626
Loftsson T, Duchene D (2007) Cyclodextrins and their pharmaceutical applications. Int J Pharm 329(1–2):1–11
Malakoutikhah M, Teixido M, Giralt E (2011) Shuttle-mediated drug delivery to the brain. Angew Chem Int Ed 50(35):7998–8014
Malerba F, Paoletti F, Capsoni S, Cattaneo A (2011) Intranasal delivery of therapeutic proteins for neurological diseases. Expert Opin Drug Deliv 8(10):1277–1296
Malhotra M, Prakash S (2011) Targeted drug delivery across blood-brain-barrier using cell penetrating peptides tagged nanoparticles. Curr Nanosci 7(1):81–93
Marino P, Roche H, Moatti JP (2008) High-dose chemotherapy for patients with high-risk breast cancer: a clinical and economic assessment using a quality-adjusted survival analysis. Am J Clin Oncol 31(2):117–124
Martin-Banderas L, Holgado MA, Venero JL, Alvarez-Fuentes J, Fernandez-Arevalo M (2011) Nanostructures for drug delivery to the brain. Curr Med Chem 18(34):5303–5321

Mehta AI, Choi BD, Raghavan R, Brady M, Friedman AH, Bigner DD, Pastan I, Sampson JH (2011) Imaging of convection enhanced delivery of toxins in humans. Toxins 3(3):201–206
Meropol NJ, Schrag D, Smith TJ, Mulvey TM, Langdon RM Jr, Blum D, Ubel PA, Schnipper LE (2009) American Society of Clinical Oncology guidance statement: the cost of cancer care. J Clin Oncol 27(23):3868–3874
Misra A (2003) Drug delivery to the central nervous system: a review. J Pharm Pharm Sci 6(2): 252–273
Moos T, Morgan EH (2001) Restricted transport of anti-transferrin receptor antibody (OX26) through the blood-brain barrier in the rat. J Neurochem 79(1):119–129
Nair SB, Dileep A, Rajanikant GK (2012) Nanotechnology based diagnostic and therapeutic strategies for neuroscience with special emphasis on ischemic stroke. Curr Med Chem 19(5):744–756
Panagiotou T, Fisher RJ (2011) Enhanced transport capabilities via nanotechnologies: impacting bioefficacy, controlled release strategies, and novel chaperones. J Drug Deliv 902403:ePub Apr 26, 1–14
Pardridge WM (2005) The blood-brain barrier: bottleneck in brain drug development. NeuroRx 2(1):3–14
Paul SM, Mytelka DS, Dunwiddie CT, Persinger CC, Munos BH, Lindborg SR, Schacht AL (2010) How to improve R&D productivity: the pharmaceutical industry's grand challenge. Nat Rev Drug Discov 9(3):203–214
Pinheiro E, Vasan A, Kim JY, Lee E, Guimier JM, Perriens J (2006) Examining the production costs of antiretroviral drugs. AIDS 20(13):1745–1752
Rajadhyaksha M, Boyden T, Liras J, El-Kattan A, Brodfuehrer J (2011) Current advances in delivery of biotherapeutics across the blood-brain barrier. Curr Drug Discov Technol 8(2):87–101
Ranson MR, Cheeseman S, White S, Margison J (2001) Caelyx (stealth liposomal doxorubicin) in the treatment of advanced breast cancer. Crit Rev Oncol Hematol 37(2):115–120
Raudino G, Caffo M, Caruso G, Alafaci C, Tomasello F (2011) Nanoparticle-based cerebral drug-delivery systems and antiangiogenic approach in gliomas treatment. Recent Pat Nanotechnol 5(3):239–244
Regina A, Demeule M, Che C, Lavallee I, Poirier J, Gabathuler R, Beliveau R, Castaigne JP (2008) Antitumour activity of ANG1005, a conjugate between paclitaxel and the new brain delivery vector Angiopep-2. Br J Pharmacol 155(2):185–197
Rip J, Schenk GJ, de Boer AG (2009) Differential receptor-mediated drug targeting to the diseased brain. Expert Opin Drug Deliv 6(3):227–237
Rosenberg J, Nicas M, Yomashiro Y (2003) Understanding toxic substances. California Hazard Evaluation and Information Service–Occupational Health Branch Service. http://www.lni.wa.gov/wisha/p-ts/pdfs/toxicsubstances.pdf. Accessed 7 Jul 2012
Schneider CK, Salmikangas P, Jilma B et al (2010) Challenges with advanced therapy medicinal products and how to meet them. Nat Rev Drug Discov 9(3):195–201
Sharma A, Jacob A, Tandon M, Kumar D (2010) Orphan drug: development trends and strategies. J Pharm Bioallied Sci 2(4):290–299
Shawkat H, Westwood M-M, Mortimer A (2012) Mannitol: a review of its clinical uses. Contin Educ Anaesth Crit Care Pain
Shinde RL, Jindal AB, Devarajan PV (2011) Microemulsions and nanoemulsions for targeted drug delivery to the brain. Curr Nanosci 7(1):119–133
Su X, Zhan X, Tang F, Yao J, Wu J (2011) Magnetic nanoparticles in brain disease diagnosis and targeting drug delivery. Curr Nanosci 7(1):37–46
Thomas FC, Taskar K, Rudraraju V, Goda S, Thorsheim HR, Gaasch JA, Mittapalli RK, Palmieri D, Steeg PS, Lockman PR, Smith QR (2009) Uptake of ANG1005, a novel paclitaxel derivative, through the blood-brain barrier into brain and experimental brain metastases of breast cancer. Pharm Res 26(11):2486–2494
Tian X, Canton I, Battaglia G (2011) Targeting transcytosis across the blood-brain-barrier. Nanotech conference & expo 2011: an interdisciplinary integrative forum on nanotechnology, biotechnology and microtechnology, vol 3, Boston, 13–16 June 2011, pp 459–462

Tucker IG (2011) Drug delivery to the brain via the blood–brain barrier: a review of the literature and some recent patent disclosures. Ther Deliv 2(3):311–327

Ugwoke MI, Agu RU, Verbeke N, Kinget R (2005) Nasal mucoadhesive drug delivery: background, applications, trends and future perspectives. Adv Drug Deliv Rev 57(11):1640–1665

Wankhede M, Bouras A, Kaluzova M, Hadjipanayis Costas G (2012) Magnetic nanoparticles: an emerging technology for malignant brain tumor imaging and therapy. Expert Rev Clin Pharmacol 5(2):173–186

Wermeling DP (1993) Value of investigational drugs. Am J Hosp Pharm 50(8):1576

Yu YJ, Zhang Y, Kenrick M, Hoyte K, Luk W, Lu Y, Atwal J, Elliott JM, Prabhu S, Watts RJ, Dennis MS (2011) Boosting brain uptake of a therapeutic antibody by reducing its affinity for a transcytosis target. Sci Transl Med 3(84):84ra44

Zhong XP, NewmanP CM, Loh E (2011) Recent advances in biotherapeutics drug discovery and development. InTech, Shanghai, pp 363–378

Zulsdorf TB, Coenen C, Fiedeler AF, Milburn C, Weinroth M (2011) Quantum engagements: social reflections of nanoscience and emerging technologies. PA, IOS Press, Lansdale

Part IV
Strategies for Improved Central Nervous System Drug Delivery

Chapter 14
Intranasal Drug Delivery to the Brain

Jeffrey J. Lochhead and Robert G. Thorne

Abstract Drug delivery into the central nervous system (CNS) compartment is often restricted by the blood–brain barrier (BBB) and blood–cerebrospinal fluid barriers (BCSFB) that separate the blood from brain interstitial and cerebrospinal fluids, respectively. New strategies to circumvent the BBB are greatly needed to utilize polar pharmaceuticals and large biotherapeutics for CNS disease treatment because the BBB is typically impermeable to such compounds. Intranasal administration is a noninvasive method of drug delivery that potentially allows even large biotherapeutics access to the CNS along extracellular pathways associated with the olfactory and trigeminal nerves. Rapid effects, ease of self-administration, and the potential for frequent, chronic dosing are among the potential advantages of the intranasal route. This chapter provides an overview of the unique anatomic and physiologic attributes of the nasal mucosa and its associated cranial nerves that allow small but significant fractions of certain intranasally applied drugs to transfer across the nasal epithelia and subsequently be transported directly into the CNS. We also review the preclinical and clinical literature related to intranasal targeting of biotherapeutics to the CNS and speculate on future directions.

J.J. Lochhead
Pharmaceutical Sciences Division, University of Wisconsin—Madison
School of Pharmacy, Madison, WI, USA

R.G. Thorne (✉)
Pharmaceutical Sciences Division, University of Wisconsin—Madison
School of Pharmacy, Madison, WI, USA

Center for Neuroscience & Neuroscience Training Program,
University of Wisconsin—Madison, Madison, WI, USA

Cellular and Molecular Pathology Graduate Training Program,
University of Wisconsin—Madison, Madison, WI, USA

Clinical Neuroengineering Training Program, University of Wisconsin—Madison,
Madison, WI, USA
e-mail: rthorne@wisc.edu

M. Hammarlund-Udenaes et al. (eds.), *Drug Delivery to the Brain*, AAPS Advances in the Pharmaceutical Sciences Series 10, DOI 10.1007/978-1-4614-9105-7_14,

14.1 Introduction

The blood–brain barrier (BBB) and blood–cerebrospinal fluid barriers (BCSFB) are critical for maintenance of central nervous system (CNS) homeostasis. Although these barriers restrict neurotoxic substances from entering the brain, they also restrict many potential therapeutics from reaching the CNS. The BBB, formed by brain endothelial cells lining microvessels, exhibits a low rate of pinocytosis and possesses tight junction (TJ) protein complexes on neighboring cells that limit paracellular permeability (Reese and Karnovsky 1967). These TJ create a high transendothelial electrical resistance of 1,500–2,000 Ω cm^2 compared to 3–30 Ω cm^2 across most peripheral microvessels (Crone and Olesen 1982; Butt et al. 1990). This high resistance is associated with very low paracellular permeability, and typically, only small (<600 Da) lipophilic molecules appreciably cross the healthy BBB via transcellular passive diffusion, although some limited transport of certain peptides and peptide analogs has been reported (Banks 2009). Additionally, many potential therapeutics that would otherwise be predicted to cross the BBB based on their molecular weight (MW) and lipophilicity are restricted by the expression of drug transporters (e.g., P-glycoprotein) (Miller 2010; Ronaldson et al. 2007).

Nearly all CNS drugs in clinical use today can be categorized as small MW pharmaceuticals that either cross the BBB transcellularly (e.g., barbiturates) or utilize endogenous transporters expressed on endothelial cells (e.g., the Parkinson's therapeutic levodopa). Just about all large MW substances are severely restricted from crossing the BBB under normal (non-pathological) physiological conditions. Indeed, the only examples of large MW drugs approved for clinical use in treating neurological illnesses are those that act outside the CNS (e.g., type I interferons for treating multiple sclerosis), those with the chance to cross compromised endothelial barriers associated with some CNS tumors (e.g., the humanized monoclonal antibody bevacizumab for the treatment of recurrent glioblastoma), and a peptide administered intrathecally to treat severe, chronic pain (the ~3 kDa cone snail toxin ziconotide). Many other large MW peptides, proteins, oligonucleotides, and gene therapy vectors have been identified as potential CNS therapeutics based on studies utilizing in vitro systems and animal models; however, new drug delivery strategies are needed to allow these potential drugs to cross or bypass the BBB and BCSFB for these studies to translate to the clinic (Neuwelt et al. 2008).

Central input of substances through intraparenchymal, intracerebroventricular, or intrathecal injections/infusions represent one strategy, but these routes of administration are invasive and typically not ideal for chronic administration. Increasing evidence suggests that the intranasal (IN) route of administration provides a noninvasive method to bypass the BBB and directly deliver therapeutics to the CNS along extracellular pathways associated with the olfactory and trigeminal nerves (Fig. 14.1). In addition to its noninvasiveness, the IN administration route has long been associated with a number of advantages (Lochhead and Thorne 2012), mostly based on the application of drugs with a systemic mode of action; these include typically rapid onset of effects, ease of administration by nasal drops or sprays,

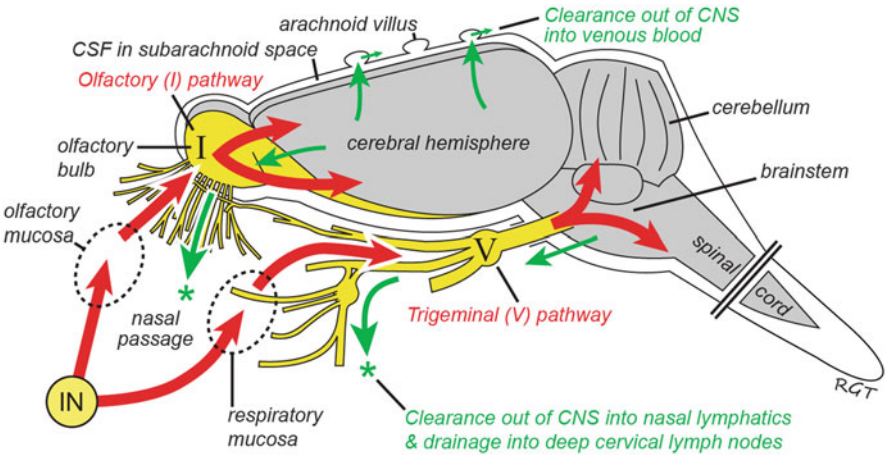

Fig. 14.1 Intranasal (IN) administration provides access to olfactory and trigeminal pathways (shown in *red* for the rat), potentially allowing certain peptides, proteins, and even cells to reach widespread CNS regions. Based on work utilizing radiolabeled proteins in rats and primates (Thorne et al. 2004b, 2008), a small fraction of intranasally applied drug may be rapidly transported via components associated with the olfactory nerves (the first cranial nerve) to the olfactory bulbs and rostral brain regions or via components associated with the trigeminal nerves (the fifth cranial nerve) to the brainstem and caudal brain regions. Drug entry into the brain appears to occur rapidly following transport across the olfactory or respiratory epithelia. Other work has shown that a variety of substances may also be cleared out of the brain along possibly related pathways (shown in *green*) connecting CNS parenchymal tissue and cerebrospinal fluid (CSF) in the subarachnoid spaces with lymphatics in the nasal passages and, ultimately, the deep cervical lymph nodes of the neck (Bradbury and Cserr 1985; Kida et al. 1993). The principal clearance of CSF into the venous blood occurs through arachnoid villi that extend from the subarachnoid space into the dural sinuses

simple dose adjustment, avoidance of hepatic first-pass elimination, and a developing record of experience with clinically approved formulations (e.g., nasal spray of the 3.5 kDa polypeptide hormone calcitonin has been used for many years to treat postmenopausal osteoporosis) (Lansley and Martin 2001; Illum 2012). The main disadvantages of the IN route comprise a limitation typically to potent drugs due to low nasal absorption (particularly for hydrophilic drugs, peptides and proteins), limited solution volumes (typically, 25–200 μl in humans), active mucociliary clearance processes resulting in limited contact time with the absorptive epithelia, nasal enzymatic degradation for some drugs, interindividual variability and low CNS delivery efficiencies (<0.05 %) for most proteins measured thus far (Lochhead and Thorne 2012; Costantino et al. 2007). Epithelial transporter activity (e.g., P-glycoprotein) for certain xenobiotics may also play a role in limiting or altering drug transport across either the olfactory or nasal respiratory mucosa (Kandimalla and Donovan 2005; Graff and Pollack 2005; Thiebaud et al. 2011).

The IN administration route has a long, successful history of clinical application, where it has been used to deliver a number of drugs to the systemic circulation that cannot be given orally (Lansley and Martin 2001; Costantino et al. 2007).

The possibility that IN administration may also deliver potentially therapeutic amounts of large MW drugs directly from the nasal passages to the CNS was first described relatively recently (Thorne et al. 1995; Frey et al. 1997). Delivery of small molecules, macromolecules, gene vectors, and even cells from the nasal passages to the brain has now been documented in numerous animal and clinical studies (Lochhead and Thorne 2012; Stevens et al 2011; Dhuria et al. 2010; Baker and Genter 2003; Illum 2004). This chapter provides an overview of relevant nasal anatomy and physiology as well as the potential pathways and transport mechanisms that are involved in the distribution of therapeutics from the nasal cavity to the CNS. We also summarize some of the most relevant preclinical and clinical studies that have presented evidence of brain entry and/or efficacy following intranasal targeting of biotherapeutics to the CNS and speculate on future directions.

14.2 Nasal Anatomy and Physiology

14.2.1 General Overview

The nasal chamber is divided into two separate passages by the nasal septum, with each nasal passage principally consisting of an olfactory region (containing the olfactory epithelium) and a respiratory region (containing the respiratory epithelium) extending from the nostrils (nares) to the nasopharynx. The general organization of the rat nasal passage is shown in Fig. 14.2. The olfactory region contains olfactory

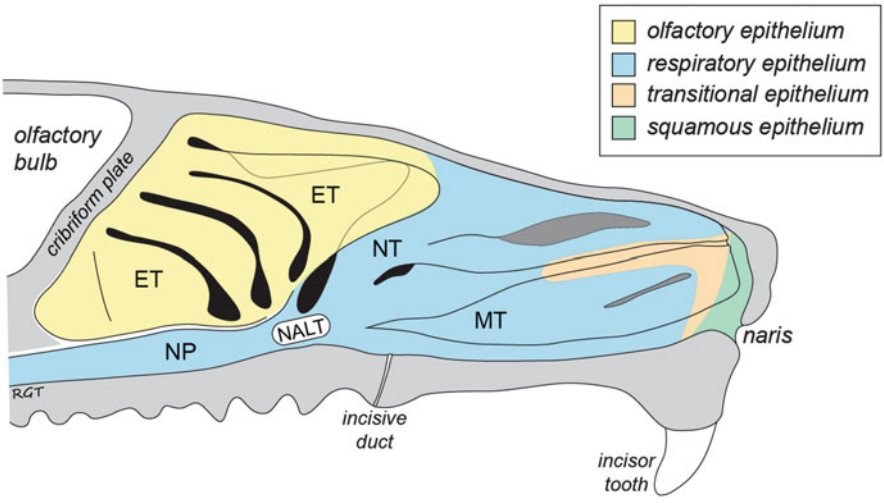

Fig. 14.2 Schematic diagram of the nasal passage showing the distribution of the surface epithelia on the lateral wall of the rat. *ET* ethmoturbinates, *MT* maxilloturbinate, *NALT* nasal-associated lymphoid tissue, *NP* nasopharynx, *NT* nasoturbinate (figure partly based on Mery et al. 1994; Harkema et al. 2006)

sensory neurons that are responsible for the detection of airborne odorants (i.e., mediating the sense of smell). Most of the non-olfactory epithelium in the nasal passages of laboratory animals and human beings consists of a respiratory epithelium specialized for warming and humidifying inspired air as well as the removal of allergens, microorganisms and particulates (Harkema et al. 2006). The human nasal cavity has a large absorptive surface area of ~160 cm^2 due to three, comma shaped bony structures called turbinates or conchae (inferior, middle, and superior) (Harkema et al. 2006). Differences in nasal structure, organization, and physiology between primates and rodents may potentially be important in evaluating experimental data in support of nose-to-brain transport pathways (Lochhead and Thorne 2012), e.g., humans and monkeys are oronasal breathers, while rats are obligate nasal breathers with a turbinate architecture that is considerably more complex than that in primate species. Additionally, the olfactory region accounts for only about 10 % of the total absorptive surface area in the human nasal cavity, whereas it comprises ~50 % of the total nasal surface area in the rat, likely reflecting the greater importance of this sense for macrosmatic mammals such as rodents. By contrast, the absolute olfactory surface area does not differ too greatly between human beings (~12.5 cm^2), rhesus monkeys (6–9 cm^2) and rats (7 cm^2) (Lochhead and Thorne 2012). While it is not yet clear if significant differences in nose-to-brain transport occur with different species, most investigations have utilized rodents simply because it has not been practical to conduct certain types of research in monkeys and human beings; further developments in noninvasive imaging may allow better comparisons between species in the future.

In addition to the olfactory and respiratory regions, the nasal cavity also contains squamous and transitional regions, along with a small specialized area of lymphoepithelium (Harkema et al. 2006). The squamous region extends from just inside the nares to the anterior portion of the inferior turbinates and is lined with stratified squamous epithelium containing coarse hairs in addition to sebaceous and sweat glands. The transitional region is a non-ciliated cuboidal or columnar epithelium located between the squamous and respiratory epithelia. Nasal-associated lymphoid tissue (NALT) contains the lymphoepithelium, a region on both sides of the nasopharyngeal duct in rodents (Fig. 14.2) that appears to play a role in the induction of antigen-specific immune responses (Kiyono and Fukuyama 2004). The stimulation of protective systemic/mucosal immunity resulting from intranasal administration of specific antigens (usually requiring co-administration of an enhancing adjuvant for adequate stimulation of NALT) provides the basis for nasal vaccine development. It is generally considered that the olfactory and respiratory epithelia are by far the most important sites for nasal absorption so these regions will be covered individually in greater detail below.

14.2.2 Blood Supply and Lymphatic Drainage

The nasal mucosa is extremely vascular, a feature which allows efficient absorption into the systemic circulation for drugs possessing the right properties for this to

occur (e.g., drugs that are sufficiently small to cross through the interendothelial clefts of nasal capillaries). Once in the systemic circulation, a substance would need to cross the BBB or BCSFB to enter the CNS. Although some nasal endothelial cells express TJ proteins such as zona occludens (ZO)-1, occludin, and claudin-5, capillaries in the nasal submucosa appear fenestrated with porous basement membranes, suggesting higher permeability than capillaries comprising the BBB (Cauna and Hinderer 1969; Wolburg et al. 2008). Nasal venules and arterioles are continuous and lack fenestrations. Differences may exist in the permeability of blood vessels in the respiratory and olfactory regions of the nasal submucosa but this is an area that has received little attention; interestingly, injection of Evans blue dye into the tail vein of rats has been shown to result in greater staining of the respiratory region of the nasal epithelium than the olfactory region while the brain remains unstained (Wolburg et al. 2008). Therefore, greater absorption of drugs into the systemic circulation following intranasal administration may result from targeting the respiratory region rather than the olfactory region of the nasal epithelium. It is also possible that targeting the olfactory region may result in reduced drug loss due to clearance into nasal capillaries; indeed, intranasal devices have been designed to target the olfactory region with the goal of enhancing direct delivery to the CNS (Hoekman and Ho 2011). Clearly, the utility of targeting different regions of the nasal passage with intranasally administered drugs for the purpose of enhancing brain targeting is an area that merits further study.

Blood supplying the nasal passages is chiefly provided by (1) branches of the opthalmic artery, (2) the sphenopalatine artery, and (3) branches of the facial artery (Greene 1935; Gray's Anatomy 2008; Schuenke et al. 2010). The anterior and posterior ethmoidal arteries branch from the ophthalmic artery to supply the olfactory region, anterior septum, and anterior lateral wall. The sphenopalatine artery mostly supplies the posterior septum and posterior lateral wall with smaller branches extending to further areas. Branches of the facial artery supply the antero-inferior septum and lateral wall. Species differences between rats and humans exist upstream of the ophthalmic and sphenopalatine arteries. The internal carotid artery gives rise to the opthalmic artery in humans while the opthalmic artery branches from the pterygopalatine artery in rats. In humans, the sphenopalatine artery is a branch from the maxillary artery via the external carotid artery. The rat sphenopalatine artery, however, arises from the pterygopalatine artery via the internal carotid artery. It is also relevant that both olfactory and trigeminal arteries have been described in the rat and in other mammals, including human beings (Coyle 1975; Scremin 2004; Favre et al. 1995); these vessels travel at least some distance with their respective nerve bundles and likely provide complex anastomoses between nasal arteries in the nasal passages and cerebral arterial branches from the anterior and posterior brain circulations. Venous drainage in the posterior nasal passage occurs primarily through the sphenopalatine vein while veins accompanying the ethmoidal arteries drain the anterior nasal passage. Some veins in the nasal passage connect with cerebral veins on the frontal lobe after passing through the cribriform plate.

There are no lymph nodes in the CNS but a number of studies have shown that extracellular and cerebrospinal fluids in the brain may drain either through

arachnoid villi to the venous blood or through the cribriform plate to the nasal lamina propria and then subsequently to the deep cervical lymph nodes in the neck (Fig. 16.1) (Bradbury and Cserr 1985). Intranasally administered substances that are absorbed to the nasal lamina propria but do not enter into nasal capillaries (i.e., the systemic circulation) may therefore drain to the deep cervical lymph nodes. Radiolabeled protein tracers or dyes injected into the brain or CSF are cleared to the nasal lamina propria to reach the deep cervical lymph nodes at high concentrations (Bradbury and Cserr 1985; Kida et al. 1993). Sealing the cribriform plate with kaolin or acrylate glue significantly reduced drainage of [^{125}I]-albumin following intraventricular infusion (Bradbury and Cserr 1985). It has long been known that dyes can be found in the perineural sheaths of the fila olfactoria as well as the deep cervical lymph nodes following intranasal administration (Faber 1937; Yoffey and Drinker 1938). This localization of intranasally administered dyes is similar to the localization of dyes injected into the subarachnoid space CSF (Kida et al. 1993), suggesting that pseudo-lymphatic pathways leading out of the brain may be similar to pathways leading into the brain. These studies suggest that the subarachnoid space, nasal lamina propria, and deep cervical lymph nodes are in communication. Importantly, the localization of microfil (a silicone rubber compound typically used to visualize the microcirculation) following injection into the CSF compartment of cadavers has confirmed that some of these connections also appear to be present in humans (Johnston et al. 2004).

14.2.3 The Olfactory Region of the Nasal Passage

The olfactory region consists of a pseudostratified columnar epithelium (Fig. 14.3a) located on the most superior aspect of the nasal cavity where the olfactory sensory neurons (OSN) reside. The OSN are the only first order neurons possessing cell bodies located in a distal epithelium. The tips of their dendritic processes contain several nonmotile cilia which extend into the overlying mucus layer; odorant receptors are found in the plasma membrane of the olfactory cilia, where they are positioned to respond to olfactory stimuli in the external environment. The OSN are bipolar cells possessing unmyelinated axons which extend through the epithelial basal lamina and converge with axons from other OSN to form nerve bundles called fila olfactoria. Interlocking olfactory ensheathing cells (OEC) form continuous channels around the fila olfactoria from their origin to the olfactory bulb. Multicellular sheets of olfactory nerve fibroblasts enclose the OEC to form a perineural-like sheath around the fila olfactoria (Field et al. 2003). The olfactory nerve is comprised of the ensheathed fila olfactoria and travels through the cribriform plate of the ethmoid bone into the brain where its axons terminate on dendrites of mitral, periglomerular, and tufted cells in glomeruli of the olfactory bulb. Axons of the mitral and tufted cells project to a number of areas, including the anterior olfactory nucleus, olfactory tubercle, piriform cortex, amygdala and entorhinal cortex (Carmichael et al. 1994).

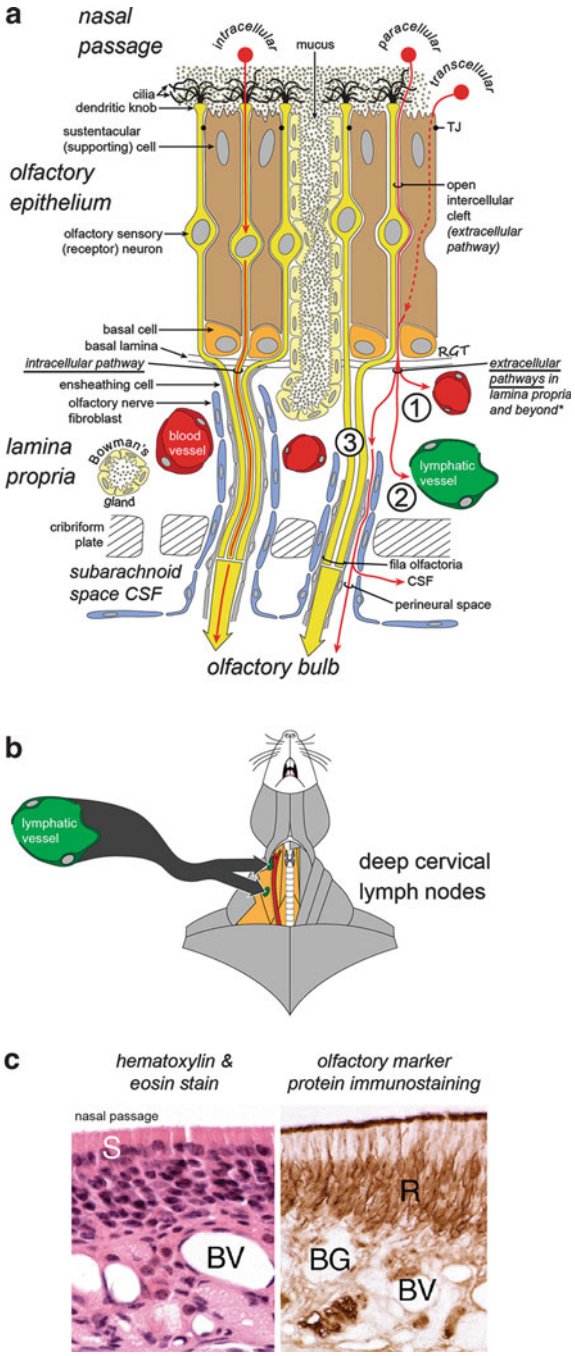

Fig. 14.3 The olfactory region: organization and histology. (**a**) The olfactory mucosa consists of the olfactory epithelium and the lamina propria. Axonal processes of olfactory sensory neurons converge into bundles (fila olfactoria), surrounded by ensheathing cells and fibroblasts, before projecting to the olfactory bulb. Red arrows indicate potential pathways for drug delivery across

In addition to OSN, several other cell types are located in the olfactory epithelium and the underlying lamina propria. Sustentacular (supporting) cells extend from the apical region of the epithelium to the basal lamina and possess long, irregular microvilli which intermingle with the cilia of the OSN (Hegg et al. 2009). In the lamina propria, the Bowman's gland forms tubular-type ducts which traverse the basal lamina to produce and secrete a serous fluid which serves as a solvent for inhaled odorants and intranasally applied drugs. Globose basal cells (GBC), located in the lamina propria, are neural progenitors which provide a source for continuous replacement of the OSN throughout life (Caggiano et al. 1994). Horizontal basal cells are located superficial to the GBC and function as multipotent progenitors to the GBC, sustentacular cells, and cells of the Bowman's gland and ducts (Iwai et al. 2008). Microvillar cells also reside in the olfactory epithelium although their functions are not well defined (Elsaesser and Paysan 2007). Endothelial cells of blood and lymphatic vessels as well as inflammatory cells are also present in the lamina propria of the olfactory region (Fig. 14.3b, c).

14.2.4 The Respiratory Region of the Nasal Passage

The nasal respiratory region consists of a pseudostratified columnar secretory epithelium (Fig. 14.4a). Cell types of the human respiratory epithelium include goblet

Fig. 14.3 (continued) the olfactory epithelium and into the brain following intranasal administration. Intranasally applied drugs may be transported by an intracellular pathway from the olfactory epithelium to the olfactory bulb within olfactory sensory neurons following adsorptive, receptor-mediated, or nonspecific fluid phase endocytosis. Other drugs may cross the olfactory epithelial barrier by paracellular or transcellular transport to reach the lamina propria, where a number of different extracellular pathways for distribution are possible: (1) Absorption into olfactory capillaries and entry into the general circulation; (2) Absorption into olfactory lymphatics draining to the deep cervical lymph nodes of the neck; (3) Extracellular diffusion or convection in compartments associated with olfactory nerve bundles and entry into the cranial compartment. Transport within the perineural space bounded by olfactory nerve fibroblasts is shown but other possibilities exist, e.g., transport within the fila olfactoria compartment contained by ensheathing cells, transport within the perivascular spaces of blood vessels traversing the cribriform plate with olfactory nerves (not shown) or transport within lymphatics traversing the cribriform plate with olfactory nerves (not shown). Possible pathways for distribution of substances from the perineural space into the olfactory subarachnoid space cerebrospinal fluid (CSF) or into the olfactory bulb are shown. (Figure adapted with permission from Lochhead and Thorne 2012.) (b) Lymphatic drainage of the nasal mucosa is principally to the deep cervical lymph nodes. The deep cervical lymph nodes are present in the viscera of the neck deep to the superficial muscles and just lateral to the common carotid artery. (c) Rodent olfactory mucosa sections stained with hematoxylin and eosin or immunostained using an antibody to olfactory marker protein, a protein specific to mature olfactory sensory neurons (not sustentacular or basal cells). Sections show the pseudostratified layers of the olfactory epithelium with the relative positions of the cell bodies of sustentacular (S) cells and olfactory sensory (receptor, R) neurons indicated. Numerous blood vessels (BV) and Bowman's glands (BG) are also visible within the lamina propria. (Images of sections kindly provided by Professor Harriet Baker, Weill Medical College of Cornell University.)

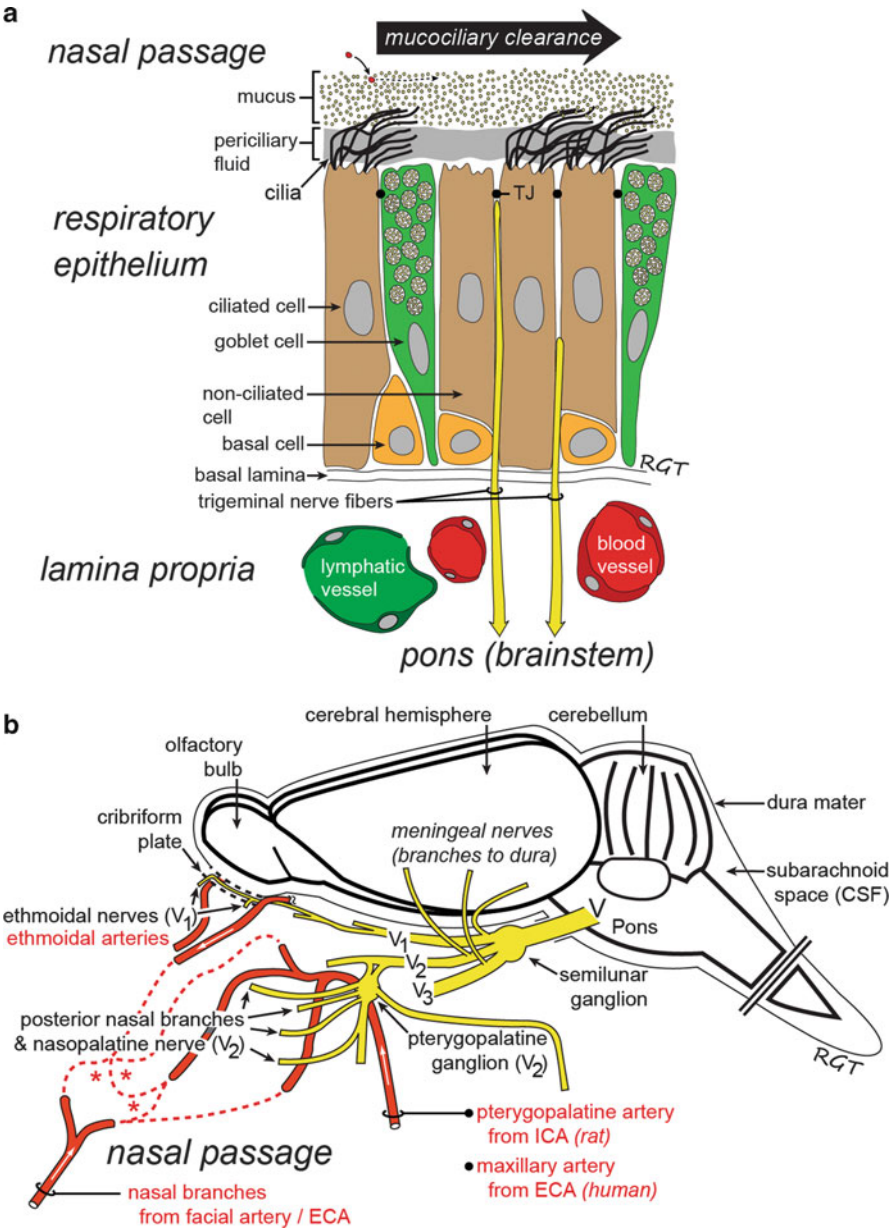

Fig. 14.4 The nasal respiratory region: general organization, trigeminal innervation and blood supply. (**a**) The respiratory mucosa includes the respiratory epithelium and its underlying lamina propria. The trigeminal nerve, important for conveying chemosensory, nociceptive, touch, and temperature information, is found throughout the nasal epithelium; free nerve endings extend nearly to the epithelial surface, just beneath tight junctions (TJ). (**b**) Central projections of the trigeminal nerve shown together with the nasal blood supply. The cell bodies of the trigeminal nerve fibers are located in the semilunar ganglion; their axons project into the brainstem at the level of

cells, ciliated cells, intermediate cells, and basal cells (Jafek 1983). Serous glands, seromucous glands, and intraepithelial glands are also associated with the nasal respiratory epithelium. Most nasal secretions are produced by seromucous glands although goblet cells also secrete mucus. The primary role of the ciliated cells in primates is to propel mucus with their motile cilia towards the nasopharynx where it is either swallowed or expectorated. In rodents, mucus is propelled mostly in the anterior direction. Basal cells are relatively undifferentiated cells which give rise to the other cell types in the nasal respiratory epithelium.

Both the nasal respiratory and olfactory epithelia are innervated by branches of the trigeminal nerve (cranial nerve V), the largest of the 12 cranial nerves (Schuenke et al. 2010). Fibers from trigeminal ganglion cells ramify extensively within the nasal submucosa so that their free nerve endings stop at the TJ level near the epithelial surface (Finger et al. 1990). The trigeminal nerve exits the pons bilaterally and consists of a very large sensory root and a small motor root. Its motor fibers innervate the muscles of mastication and the sensory fibers transmit information from the face, scalp, mouth and nasal passages. The trigeminal nerve consists primarily of somatic afferent fibers which convey sensory information to nuclei located within the brainstem and spinal cord.

The trigeminal nerve is comprised of three major branches: the ophthalmic nerve (V_1), the maxillary nerve (V_2), and the mandibular nerve (V_3) (Fig. 14.4b). V_1 and V_2 are sensory nerves that also carry autonomic fibers while V_3 contains the mixed portion of the trigeminal nerve. Importantly, ethmoidal (part of V_1), nasopalatine (part of V_2), and nasal (part of V_2) branches of the trigeminal nerve provide sensory innervation to the nasal passages (Tucker 1971; Bojsen-Moller 1975). A portion of trigeminal ganglion cells with sensory endings located in the nasal epithelium also send collaterals directly into the olfactory bulb in addition to the brainstem (Schaefer et al. 2002). Two other nerves, the nervus terminalus (terminal nerve; cranial nerve zero) and the vomeronasal nerve and organ (Jacobson's organ), are also located in the nasal passages but have so far not been viewed as important for CNS delivery following intranasal administration, particularly in adult human beings where they may be vestigial or even absent.

Fig. 14.4 (continued) the pons and ultimately synapse with neurons in a number of areas including the principal sensory and spinal trigeminal nuclei. Of the three main trigeminal nerve divisions (V_1, the ophthalmic nerve; V_2, the maxillary nerve; and V_3, the mandibular nerve), only V_1 and V_2 send branches to the nasal epithelium. Blood supply to the nasal passages is provided by ethmoidal branches of the ophthalmic artery, sphenopalatine branches of either the external carotid artery (ECA)/maxillary artery (in humans) or the internal carotid artery (ICA)/pterygopalatine artery (in rats), and nasal branches from the ECA/facial artery. Numerous anastomoses (*asterisks*) are indicated; these specialized connections between arteries may experience directional change in blood flow depending on the relative pressures within parent arteries. (Figures adapted from Lochhead and Thorne 2012 with permission.)

14.3 Mechanisms and Pathways for Transport into the CNS from the Nasal Passages

14.3.1 Transport Across the Olfactory and Respiratory Epithelial Barriers

The pathways and mechanisms governing the transport of substances from the nasal epithelium to various regions of the CNS are not fully understood. Substances which distribute throughout the CNS following intranasal administration must initially cross the nasal epithelial barrier through intracellular or extracellular (paracellular) routes. Proteins (e.g., albumin, horseradish peroxidase (HRP), wheat germ agglutinin-horseradish peroxidase (WGA-HRP)), and viruses (e.g., herpes, poliomyelitis, rhabdoviruses) endocytosed by OSN may reach the CNS (olfactory bulb) through intracellular axonal transport in the anterograde direction (Doty 2008; Kristensson and Olsson 1971; Broadwell and Balin 1985; Thorne et al. 1995; Baker and Spencer 1986; Kristensson 2011). HRP is taken up by OSN to a limited extent via pinocytosis, whereas WGA-HRP is internalized by OSN preferentially by adsorptive endocytosis (Broadwell and Balin 1985). Following intranasal administration, WGA-HRP is also endocytosed and transported intracellularly through the trigeminal nerve to the brainstem (Anton and Peppel 1991; Deatly et al. 1990). Viruses and bacteria may also be transmitted to the CNS along trigeminal nerve components within the nasal passages (Deatly et al. 1990; Jin et al. 2001). Endocytosis by peripheral trigeminal nerve processes and subsequent intracellular transport to the brainstem could potentially occur at either the olfactory or respiratory regions of the nasal epithelium.

Substances may also cross the nasal epithelial barrier through transcytosis or paracellular diffusion to access the lamina propria. Electron micrographs of nasal epithelial cells have demonstrated the existence of TJ, but the paracellular permeability of the nasal epithelia remains poorly defined (Altner and Altner-Kolnberger 1974; Kerjaschki and Horander 1976); this is partly due to the difficulty in establishing and utilizing in vitro models to predict transport for epithelia having neurons as integral components. The TJ proteins ZO-1, 2, and 3, occludin, and claudins-1, 3, 4, 5, and 19 are expressed at the olfactory epithelium of rats (Wolburg et al. 2008; Steinke et al. 2008). Measurements across excised rabbit nasal epithelium have yielded electrical resistance values ranging from 40 Ω cm^2 (Hosoya et al. 1993), suggesting a relatively permeable barrier, to 261 Ω cm^2 (Rojanasakul et al. 1992), suggesting barrier properties comparable to the intestinal epithelium. The regular turnover of cells in the nasal epithelium may lead to continual rearrangement and loosening of the TJ as basal cells replace epithelial cells throughout life (Altner and Altner-Kolnberger 1974), resulting in a relatively high permeability compared to other epithelial sites. Electron microscopic studies in the intestinal epithelium have demonstrated colloidal gold nanoparticles cross the epithelial barrier and distribute to other tissues through spaces created by single, degrading enterocytes as they are extruded from the villus in a process known as persorption (Hillyer and Albrecht 2001).

The replacement of cells throughout life at the nasal epithelial barrier may create similar potential spaces which may allow paracellular transport of substances to the lamina propria. Substances that reach the lamina propria through transcellular or paracellular routes may be absorbed into the systemic circulation, drain to the deep cervical lymph nodes, or enter the CNS by direct pathways utilizing components of the peripheral olfactory and/or trigeminal systems.

14.3.2 Transport from the Nasal Lamina Propria to Sites of Brain Entry

IN administration of [^{125}I]-insulin-like growth factor I (IGF-I, MW = 7.65 kDa) in rats and [^{125}I]-interferon-β1B (IFN-β1B, MW = 18.5 kDa) in monkeys suggests that delivery to the CNS occurs along components associated with the olfactory and trigeminal nerves followed by widespread distribution to other sites of the CNS within 30–60 min (Fig. 14.5; Thorne et al. 2004b, 2008). Substances may reach the brain from the nasal mucosa intracellularly following endocytosis by OSN or neurons of the trigeminal ganglion, as discussed above. There also appear to be extracellular pathways into the brain following transcytosis or paracellular diffusion across the nasal epithelium to the lamina propria; these pathways have been proposed on the basis of much experimental evidence obtained by a large number of different groups (reviewed in several sources, including: Thorne et al. 2004b; Illum 2004; Dhuria et al. 2010; Lochhead and Thorne 2012). The extracellular pathways potentially providing nose-to-brain transport routes include diffusion or convection within perineural, perivascular, or lymphatic channels associated with olfactory and trigeminal nerve bundles extending from the lamina propria to the olfactory bulb and brainstem, respectively.

Perineural distribution around olfactory nerve bundles extending from the lamina propria to the outermost layer of the olfactory bulb has been observed following IN administration of potassium ferrocyanide and iron ammonium citrate solutions as well as 3 kDa fluorescein-dextran, suggesting that perineural spaces may act as pathways for molecules to distribute to the CNS from the nasal cavity (Faber 1937; Jansson and Bjork 2002). OEC maintain continuous open spaces in the nerve bundles to allow regrowth of olfactory nerve fibers (Li et al. 2005). These compartments provide a potential path that substances may take to reach the brain from the perineural space of entering olfactory nerve bundles. The perineural spaces of the olfactory and trigeminal nerves appear to also allow distribution of certain substances to the CSF of the subarachnoid space, particularly smaller peptides and proteins, although the anatomical/physiological aspects of this perineural space-to-CSF distribution remain poorly understood. Indeed, the barrier between the perineural space and the CSF may be more permeable to some substances than others; for example, certain proteins, e.g., IGF-I, have not been detected in the CSF despite experimental evidence of brain entry following intranasal administration (Thorne et al. 2004b). For substances capable of accessing the CSF of the subarachnoid

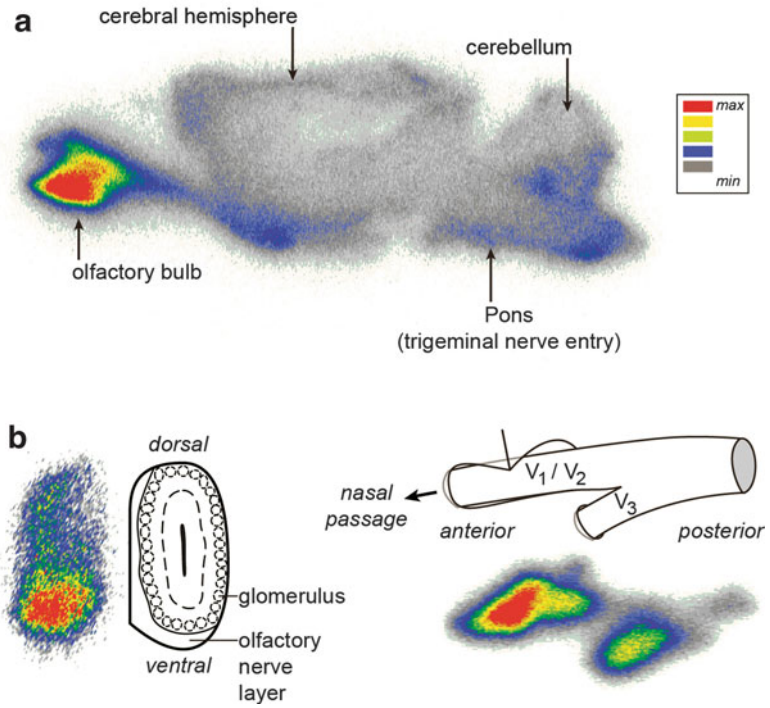

Fig. 14.5 The central distribution of [^{125}I]-labeled IGF-I following intranasal application in anesthetized adult rats is characterized by high levels within the olfactory bulbs and trigeminal nerves. (**a**) Sagittal brain section from a rat approximately 30 min following intranasal administration of a low specific activity solution of [^{125}I]-labeled IGF-I, allowing visualization of brain entry sites in the olfactory bulb (putative olfactory pathway) and pons (putative trigeminal pathway). (**b**) Coronal section through the olfactory bulb of a rat approximately 30 min following intranasal administration of a high specific activity solution of [^{125}I]-labeled IGF-I (*left image*). Signal intensity is highest in the ventral portion of the bulb in closer proximity to the olfactory nerve entry sites at the cribriform plate. Transverse section through the trigeminal nerve of a rat approximately 30 min following intranasal administration of a high specific activity solution of [^{125}I]-labeled IGF-I (*right image*). Signal intensity is highest in portions of the ophthalmic (V_1) and maxillary (V_2) nerve divisions which innervate the nasal passage. (Figures adapted from Thorne et al. (2004b) with permission.)

space following IN administration, further distribution to more distant sites of the CNS may occur along pathways of CSF flow.

The precise mechanisms underlying the rapid transport (30 min) of radiolabeled proteins from the rat nasal mucosa to widespread areas of the CNS after initial transfer along components of the olfactory and trigeminal nerves are at present unknown. Possible mechanisms responsible for the initial transport along olfactory/trigeminal components include intracellular (axonal) transport, extracellular diffusion, and extracellular convective (bulk) flow within perineural, perivascular, or lymphatic channels associated with olfactory and trigeminal nerve bundles. We have previously estimated the time it would take for a molecule to reach the olfactory bulb and brainstem of rats by intracellular transport, diffusion, or convective flow (Lochhead and

Thorne 2012). Intracellular (axonal) transport rates within olfactory or trigeminal nerves were estimated from experimental rates measured in fish olfactory nerves (Buchner et al. 1987). Rates of diffusion were based on experimental measurements and known correlations for protein free diffusion coefficients (Thorne et al. 2004a). Convective flow rates were estimated from experimentally measured albumin transport within the perivascular spaces of pial arteries using an open cranial window preparation in rats (Ichimura et al. 1991). In short, the previously reported distribution (Thorne et al. 2004b) of radiolabeled IGF-I to widespread areas of the CNS within 30 min of intranasal application strongly indicates that a convective (bulk) flow process along olfactory and trigeminal nerve components is the only plausible transport mechanism that can explain the experimental CNS distribution. This is an area clearly in need of further, careful study; more detailed discussion can be found elsewhere (Thorne et al. 2004b, 2008; Lochhead and Thorne 2012).

14.3.3 Transport from Brain Entry Sites to Widespread Areas Within the CNS

It has been speculated that the final distribution of substances which have reached the pial surface of the brain at the level of the olfactory bulb and brainstem to other areas of the CNS may occur via bulk flow within perivascular spaces of cerebral blood vessels (Thorne and Frey 2001; Thorne et al. 2004b). The normal expansion and contraction of cerebral blood vessels due to cardiac contractions could generate a pronounced fluid flow within the perivascular spaces. Different groups have attempted to understand the direction and characteristics for such a flow by modeling the process but thus far the results have produced conflicting ideas as to its directionality (Bilston et al. 2003; Schley et al. 2006; Wang and Olbricht 2011). It has been shown that increasing the blood pressure and heart rate results in a larger distribution of adeno-associated virus 2 capsids or fluorescent liposomes after injection into the striatum, suggesting involvement of arterial pulsations in the intraparenchymal distribution of these large substances via the perivascular spaces (Hadaczek et al. 2006). Several groups have also observed rapid distribution along perivascular spaces following tracer application into the CSF (Rennels et al. 1985; Iliff et al. 2012); however, others have seen limited perivascular distribution following injection of tracers into the subarachnoid CSF (Kida et al. 1993; Szentistvanyi et al. 1984). The precise role that perivascular flow plays in dictating CNS distribution following intranasal targeting of substances to the brain requires further study.

14.4 Current Status of the Intranasal Route of Administration for CNS Targeting

IN administration has become an increasingly popular method to bypass the BBB and deliver therapeutics directly to the CNS. Numerous preclinical studies have indicated IN administration offers advantages over other routes of administration

for delivery of some substances to the CNS. The published literature now includes a vast amount of animal work reporting positive effects following the intranasal administration of small molecules, peptides, proteins, oligonucleotides, gene vectors, or cell-based therapeutics using a number of different CNS disease models. Most importantly, several clinical trials involving IN administration for the treatment of CNS disorders either have been completed or are currently in progress or are in the process of planning/recruiting. The sections below provide a brief summary of some notable preclinical and clinical work that has been conducted to date. This review is by no means exhaustive; more comprehensive summaries may be found elsewhere (Lochhead and Thorne 2012; Dhuria et al. 2009).

14.4.1 Intranasal Delivery of Small Molecules to the CNS

Small molecules may be able to directly access the CNS through the IN route of administration. The paracellular permeability of substances across the nasal epithelium is likely inversely proportional to their size. This would favor a higher percentage of small molecules than macromolecules reaching the lamina propria following IN administration. Small molecules, however, may also be more easily absorbed into the nasal capillaries due to their smaller size. Therefore, intranasally administered small molecules may be more likely to access the nasal lamina propria than large molecules, but their size may favor absorption into the systemic circulation. Small molecules which escape absorption into the nasal vasculature may directly access the CNS through olfactory or trigeminal nerve-associated pathways. Absorption into the CSF may favor small molecules over macromolecules. Small molecules distributed in the perineural space of the olfactory or trigeminal nerve may also more easily cross the perineural barrier than large molecules. Therefore, small molecules may have greater access than large molecules to the CSF within the subarachnoid space surrounding the olfactory and trigeminal nerves. Upon entry into the CSF, small molecules may also have access to more distant sites in the CNS; conversely, small molecules may in some cases be cleared from the CNS compartment more quickly than larger molecules.

It has been questioned whether small molecules can directly access the brain following IN administration (Merkus et al. 2003). Merkus and coworkers measured the levels of *melatonin* (MW = 232 Da) in the CSF after IN or intravenous (IV) administration and concluded no direct delivery to the brain occurred. However, melatonin is able to cross the BBB, making it difficult to ascertain whether its detection in the CSF represents direct delivery from the nasal mucosa or delivery across the BBB or BCSFB from the systemic circulation. Furthermore, intranasally applied macromolecules such as IGF-I and vascular endothelial growth factor have been found in the brain but not the CSF following IN delivery, suggesting that drug levels in the CSF may not always correlate with brain levels (Thorne et al. 2004b; Yang et al. 2009). In another study, the dopamine-D2 receptor antagonist *remoxipride* (MW = 371 Da) was measured in brain extracellular fluid (ECF) using a

microdialysis probe placed within the striatum; brain ECF/plasma area under the curve (AUC) ratios were found to be significantly higher in rats administered remoxipride intranasally compared to intravenous application (Stevens et al. 2011). Elegant semi-physiologically based pharmacokinetic modeling by this group suggested that 75 % of remoxipride entering the brain following intranasal application did so using a direct nose-to-brain transport pathway. Similar results were obtained when levels of three glycine receptor antagonists and one angiotensin antagonist with varying degrees of BBB permeability (MW = 369–611 Da) were compared following IN or IV administration (Charlton et al. 2008). CNS/plasma AUC ratios were higher following IN versus IV administration for each compound. Autoradiographs further detected the angiotensin antagonist *GR138950* in the olfactory nerves, CSF, and brain within minutes following IN administration. Finally, the local anesthetic *lidocaine* (MW = 234 Da) has also been shown to be transported to the brain along the trigeminal nerve pathway (Johnson et al. 2010).

Several disease models have been successfully treated with intranasally administered small molecule drugs. For example, the angiotensin type II receptor antagonist *losartan* (MW = 423), which poorly penetrates the BBB, decreased amyloid β (Aβ) plaques and inflammation without inducing hypotension in an Alzheimer's disease (AD) transgenic mouse model (Danielyan et al. 2010). The iron chelator *deferoxamine* (MW = 561 Da) also exhibits neuroprotection in models of Parkinson's disease (PD), AD, and ischemic stroke (Febbraro et al. 2013; Guo et al. 2013; Hanson et al. 2009).

14.4.2 Intranasal Delivery of Peptides/Proteins to the CNS

Peptides and proteins are the most widely used drugs which have been administered intranasally to treat disorders of the CNS in both animal models and humans. Most preclinical studies utilizing the intranasal route of administration have shown behavioral or pharmacodynamic effects but not presented pharmacokinetic data indicating direct delivery of the drug to the CNS. This makes it difficult to determine if the drug entered the brain through direct pathways from the nasal cavity, crossed the BBB or accessed circumventricular areas from the systemic circulation, or exerted its effects through direct action on the BBB itself. For some peptides and proteins, there is pharmacokinetic data to support their ability to directly enter the CNS from the nasal cavity.

A pioneering study by Born and colleagues was among the first studies to obtain CNS pharmacokinetic data following IN delivery of peptides in humans. The peptides melanocortin (4–10) (MW = 980 Da), arginine-vasopressin (MW = 1.1 kDa), and insulin (5.8 kDa) were all detected in the CSF within 30 min in healthy volunteers with a lumbar puncture (Born et al. 2002). Importantly, there was no increase in plasma concentration of melanocortin (4–10), insulin, or glucose with intranasal dosing of melanocortin or insulin in this study. CSF levels of the peptides remained elevated for at least 80 min following IN administration.

Insulin is one of the most widely studied biologics with regards to its effects on the CNS following intranasal administration. A number of studies have intranasally administered insulin to treat metabolic and cognitive disorders in animal models as well as in humans. IN administration of [^{125}I]-insulin to mice yields significantly higher CNS levels after 1 h when compared to subcutaneous administration (Francis et al. 2008). [^{125}I]-insulin distributed widely throughout the mouse brain following IN administration, with the highest levels detected in the trigeminal nerve and the olfactory bulbs (Francis et al. 2008). Electron microscopic studies have found insulin within olfactory nerve bundles minutes following IN administration in mice (Renner et al. 2012b). A recently completed clinical trial showed IN insulin improved memory and preserved general cognition in patients with mild cognitive impairment or AD (Craft et al. 2012). Changes in memory and cognitive function were associated with changes in $A\beta_{42}$ levels and tau/$A\beta_{42}$ ratio in CSF (Craft et al. 2012). IN insulin has also suppressed food intake and increased brain energy levels in humans, suggesting potential as a treatment for obesity (Jauch-Chara et al. 2012). As already discussed above, IN administration of [^{125}I]-IGF-I results in significantly higher CNS levels than comparable intravenous dosing, with widespread CNS distribution occurring via olfactory and trigeminal nerve pathways, and activation of IGF-I signaling pathways in brain areas exhibiting high IGF-I receptor density such as the olfactory bulb and brainstem trigeminal nuclei (Thorne et al. 2004b); IGF-I brain entry and effects following IN application may also be relevant for understanding how IN insulin exerts its central actions because the two proteins share significant structural homology. A large multicenter trial examining the effects of intranasal insulin in AD and mild cognitive impairment is now underway in the USA.

Oxytocin (MW = 1 kDa) is a neuropeptide which exhibits a wide range of effects on human behavior. Oxytocin receptors are expressed centrally in the accessory olfactory bulb, anterior olfactory nucleus, islands of Calleja, amygdala, CA1 of hippocampus, ventral medial hypothalamus, nucleus accumbens, brainstem, and spinal cord (Stoop 2012). The BBB prevents passage of peripheral oxytocin (Ermisch et al. 1985; Kang and Park 2000) and IN administration of oxytocin has increasingly become a popular method for assessing oxytocin's central effects. Oxytocin is currently being administered intranasally in clinical trials to treat autism spectrum disorders, schizophrenia, and alcohol withdrawal. Despite the widespread use of oxytocin in clinical settings, little is known in animals or humans about oxytocin distribution in brain following IN administration, suggesting a need for further study in this area (Miller 2013).

Orexin-A (hypocretin-1, MW = 3.6 kDa) is a sleep-related peptide produced in the hypothalamus which has shown effects in monkeys and humans following IN administration. Intranasally administered orexin-A improved task performance and induced changes in brain metabolic activity in sleep deprived rhesus monkeys (Deadwyler et al. 2007). In humans suffering from narcolepsy with cataplexy, IN administration of orexin-A attenuates olfactory dysfunction, and induces and stabilizes REM sleep (Baier et al. 2008, 2011). In rats, intranasally administered orexin-A distributed to the brain within 30 min, yielding tissue-to-blood concentration ratios that were 5–8 times higher in the posterior trigeminal nerve, olfactory bulbs, hypothalamus, and cerebellum compared to rats given IV orexin-A (Dhuria et al. 2009).

High levels of orexin-A were found in cerebral blood vessel walls and low levels were found in the CSF of these rats, suggesting that transport pathways may have involved distribution within the perivascular spaces.

NAP (*davunetide*) is an eight amino acid neuroprotective peptide (MW = 825 Da) derived from activity-dependent neurotrophic factor. Intact levels of [^{3}H]-labeled NAP are found in the cortex and cerebellum of rats within 30 min following IN administration (Gozes et al. 2000). IN administration of NAP reduced levels of Aβ and hyperphosphorylated tau in an AD mouse model (Matsuoka et al. 2007) and decreased neurofibrillary tangles in a model of tauopathy (Shiryaev et al. 2009). IN NAP decreased hyperactivity and protected visual memory in a mouse model of schizophrenia (Powell et al. 2007). Unfortunately, IN NAP failed to show efficacy in a recent clinical trial to treat progressive supranuclear palsy. Clinical trials evaluating whether IN NAP is beneficial in the treatment of schizophrenia and tauopathies are currently in progress.

The 18.5 kDa protein *interferon-β1B* (IFN-β1B) is a cytokine therapeutic approved to treat the relapsing-remitting form of multiple sclerosis. Studies in rats have shown that IN application of [^{125}I]-labeled IFN-β1B results in significantly higher CNS levels than intravenous dosing (Ross et al. 2004). High IFN-β1B levels were measured in the olfactory bulbs and trigeminal nerves, with significant but lower levels in other brain regions and the spinal cord, approximately 30 min after the start of administration. A subsequent study evaluating CNS delivery following IN application of [^{125}I]-labeled IFN-β1B in cynomolgus monkeys (*Macaca fascicularis*) also demonstrated widespread distribution within the brain, with highest levels again in the olfactory bulbs and trigeminal nerves (Thorne et al. 2008). Importantly, this study also showed an anatomically unique and significant central localization of [^{125}I]-labeled IFN-β1B to regions of the basal ganglia that was remarkably consistent between different animals (Fig. 14.6). This study was among the first to describe the precise distribution and concentrations achievable in the CNS of a primate species following IN administration; [^{125}I]-IFN-β1B concentrations in the olfactory bulbs, trigeminal nerves and many other brain areas were found to be above the levels required for the antiviral, antiproliferative and immunomodulatory actions of IFN-β1B.

Antibodies are immunoglobulin proteins which are able to bind peptides and proteins with high affinity. This property makes them attractive drug candidates to treat diseases of the CNS, but antibodies have shown limited BBB penetration when administered systemically (Banks 2004). Anti-Aβ immunoglobulin G (IgG) has been administered intravenously in several clinical trials to treat or prevent AD. A few studies have intranasally administered antibodies or antibody fragments in mouse models of AD. Full length IgG (MW = 150 kDa) as well as a single chain variable fragment antibody (scFv) (MW = 26 kDa) directed against the C terminus of $A\beta_{1-42}$ reduced amyloid plaque levels following intranasal administration to APPswe/PS1dE9 transgenic mice (Cattepoel et al. 2011). The scFv was detected in brain immunohistochemically while the full length antibody was not, suggesting greater delivery of the smaller fragment. Another study in 5XFAD mice showed improved spatial learning and lower levels of Aβ following IN administration of an anti-Aβ oligomer antibody (Xiao et al. 2013). Limited levels of HRP-labeled

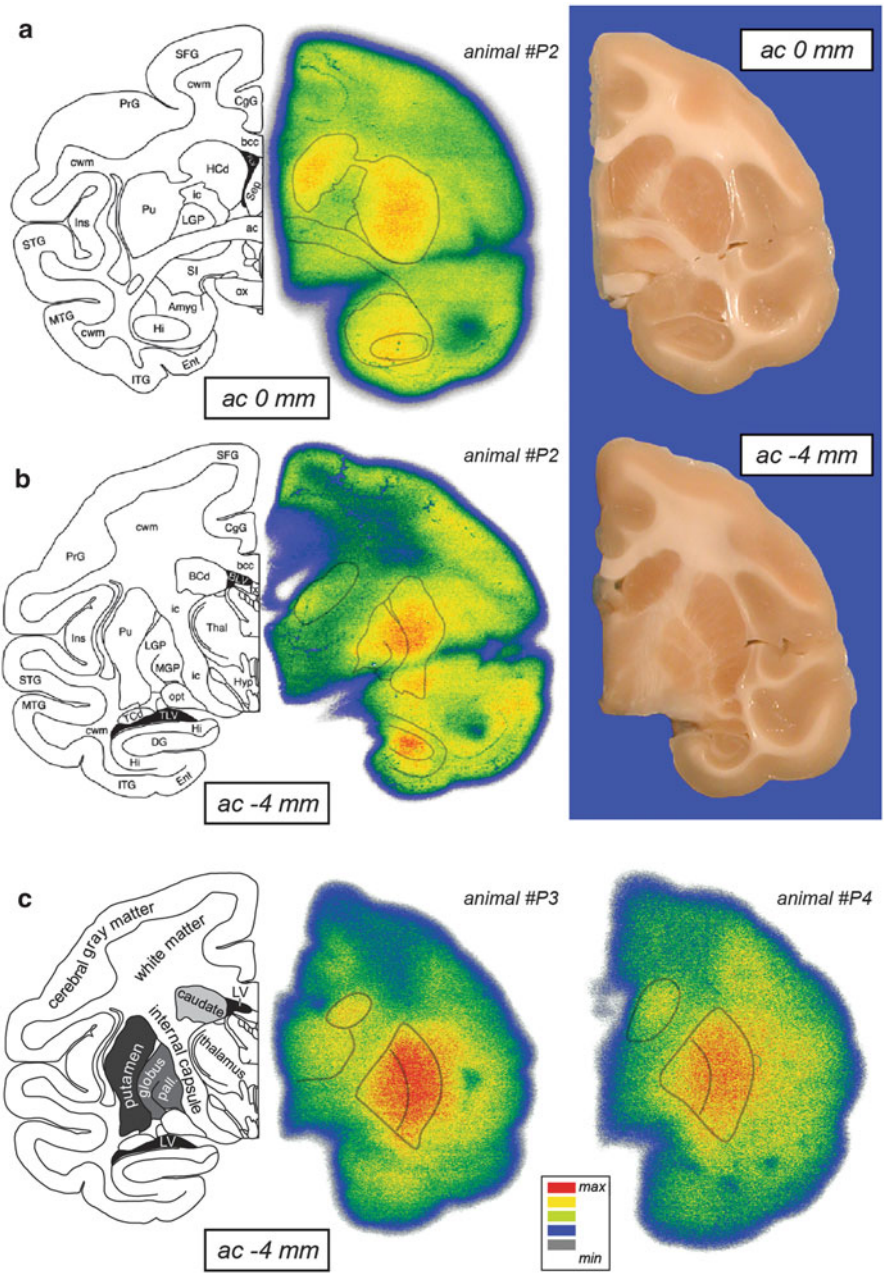

Fig. 14.6 Central distribution of [^{125}I]-labeled IFN-β1b following intranasal application in anesthetized cynomolgus monkeys. Coronal brain autoradiographs and labeled templates at (**a**) the level of the anterior commissure (ac 0 mm) or (**b**) 4 mm posterior to the anterior commissure (ac–4 mm) with corresponding brain sections provided to illustrate the highly anatomical distribution in a single monkey receiving a very high specific activity [^{125}I]-IFN-β1b solution.

antibody have been reported in the brain following development with diaminobenzidine (Xiao et al. 2013). However, a quantitative evaluation of IgG levels in different brain regions following IN administration has yet to be performed. The large size of IgG may prevent significant delivery to the brain via the intranasal route due to poor penetration across the nasal epithelial barrier.

14.4.3 Intranasal Delivery of Gene Vectors and Oligonucleotides to the CNS

Long term induction or suppression of gene products in the CNS has great potential to treat many neurological disorders. Many viral vectors, plasmids, and oligonucleotides exhibit low BBB permeability, making IN administration a potentially attractive alternative route. Several studies have investigated the IN route of administration to induce or repress gene products in the CNS.

Viral vectors such as the recombinant adenoviral vector ADRSVβgal (Draghia et al. 1995), the growth compromised herpes simplex virus type 2 mutant ΔRR (Laing and Aurelian 2008), and herpes simplex virus type 1 (Broberg et al. 2004), have all been reported to induce gene expression in widespread areas of the brain following IN administration. ΔRR encoded the anti-apoptotic gene ICP10PK and prevented kainic acid-induced seizures, neuronal loss, and inflammation in rats. IN administration was more efficient at delivering herpes simplex virus type 1 DNA in the brain than corneal or intralabial infection. A filamentous bacteriophage (1,000 nm long, 6 nm wide) expressing anti-Aβ scFv has also been shown to bind amyloid plaques in an AD mouse model following IN administration (Frenkel and Solomon 2002). While the filamentous phage was detected in the brain, a spheroid phage was not, suggesting that the shape of the phage may be important for IN delivery to the brain.

Plasmid DNA has also been delivered to the brain through the IN route. A 7.2 kb pCMVβ and a 14.2 kb pN2/CMVβ (encoding the gene for β-galactosidase) have been detected in the brain within 15 min of IN administration (Han et al. 2007). β-galactosidase activity was significantly higher in brain homogenates 48 h later and the brain-to-serum AUC ratio of pCMVβ levels was ~2,600-fold higher 10 min after IN administration when compared to IV administration. The authors also compared transfection efficiency in brain endothelial cells and microglia, finding higher levels of plasmid DNA in endothelial cells (neurons were not specifically examined).

Fig. 14.6 (continued) Highest concentrations were evident in regions of the basal ganglia (putamen, caudate, and globus pallidus) with slightly lower signal in other subcortical structures (e.g., hippocampus and amygdala). (**c**) Coronal brain autoradiographs and labeled templates from two different monkeys at the same level as in (**b**) demonstrating remarkably low variability in central distribution across different subjects. Distribution for each animal is shown approximately 60 min following intranasal administration of [^{125}I]-IFN-β1b. (Portions of (**a**), (**b**), and (**c**) adapted from Thorne et al. (2008) with permission.)

Finally, IN delivery of *oligonucleotides* to the CNS has also been reported. In one study, IN delivery of αB-crystallin small interfering RNA (siRNA) complexed with DharmaFECT 3 resulted in reduced expression of αB-crystallin in neurons and astrocytes in the olfactory bulb, amygdala, entorhinal cortex, and hypothalamus both 3 and 12 h following administration (Kim et al. 2009). In another study, a 21 base pair fluorescently labeled siRNA was delivered to the olfactory bulb following IN administration (Renner et al. 2012a). CNS delivery of the 22 base pair antagomir AM206 has also been reported following IN application in an AD transgenic mouse model (Lee et al. 2012). The authors concluded that AM206 increased brain-derived neurotrophic factor levels and memory function in mice by neutralizing microRNA-206.

14.4.4 Intranasal Delivery of Cell-Based Therapies to the CNS

Several recent studies have reported that the IN application of stem cells results in brain delivery and therapeutic effects in disease models. Fluorescently labeled rat *mesenchymal stem cells* (MSC) have been detected in the olfactory bulb, hippocampus, thalamus, cortex, and subarachnoid space of mice 1 h after IN delivery (Danielyan et al. 2009). Intranasally administered MSC have shown therapeutic potential in models of PD (Danielyan et al. 2011) and several models of stroke (Wei et al. 2013; Donega et al. 2013; van Velthoven et al. 2013). 1.5 h following IN administration, Hoechst labeled MSC could be found lining blood vessels as well as in the parenchyma after ischemic stroke in mice (Wei et al. 2013). A study in which neural stem/progenitor cells (NSPC) were administered by the IN route found that the cells were targeted to the site of an intracerebral glioma within 6 h (Reitz et al. 2012). The enhanced green fluorescent protein expressing NSPC were located in the olfactory bulb within 6 h and the olfactory tract at 24 h. Few cells were observed in the trigeminal nerve at 24 h, suggesting that NSPC migrated into the brain within the first 24 h by the olfactory pathway as well as via the systemic circulation. Finally, IN administration of T cells engineered to express a chimeric antigen receptor targeting myelin oligodendrocyte glycoprotein have been reported to result in brain delivery and to suppress inflammation in a mouse model of multiple sclerosis (Fransson et al. 2012).

14.5 Future Challenges and Directions for Intranasal Drug Delivery to the Brain

14.5.1 Methods to Enhance CNS Delivery Following Intranasal Administration

A number of absorption enhancers have been used in experimental and clinical settings to enhance intranasal drug delivery to the systemic circulation. In theory, absorption enhancers may also increase delivery of intranasally administered

substances to the brain by increasing access to transport pathways from the lamina propria to the CNS. The mechanisms by which most absorption enhancers typically work is by enhancing the permeability of compounds across the nasal epithelial barrier and/or decreasing mucociliary clearance (Deli 2009; Illum 2012). Materials that have been used as intranasal absorption enhancers include surfactants, bile salts, bile salt derivatives, phospholipids, cyclodextrins, cationic polymers, and lipids (Davis and Illum 2003). Enhancing the permeability of mucosal membranes is often associated with irritation or damage (Sezaki 1995). Most absorption enhancers have not been well tolerated when administered intranasally in humans; one exception may be chitosan, which is produced by the deacetylation of chitin, a polysaccharide found in crustacean cells. Chitosan transiently opens TJ in mucosal membranes, has bioadhesive properties, and has been shown to be nonirritating with low local and systemic toxicity (Illum 2012). The development of nontoxic, physiological absorption enhancers is needed and may increase delivery of substances to the brain following IN administration, particularly for larger substances that have difficulty crossing the nasal epithelial barriers.

14.5.2 Unresolved Questions

Despite the increasing use of IN administration as a means to bypass the BBB and deliver substances directly to the CNS, a number of basic questions remain with regards to mechanisms governing transport from the nasal mucosa to the brain. It is unknown if there is a size limit governing what can be delivered to the brain via the intranasal route. Studies with dextrans suggest that there is an inverse relationship between MW and the CSF concentration following IN administration (Sakane et al. 1995). The permeability of the nasal epithelial barrier is not well characterized and may differ between the olfactory and respiratory regions. As the trigeminal nerve innervates both the respiratory and olfactory regions, it is unclear whether preferentially targeting one of these regions favors delivery of substances to the brainstem along trigeminal nerve associated pathways. What are the sites and rates of bulk flow that govern the extracellular transport of substances from the lamina propria to the CNS? Is the bulk flow associated with perineural, perivascular, perilymphatic channels or some combination of these pathways? A summary of the hypothetical pathways into the brain from the nasal passages given our current state of knowledge is depicted in Fig. 14.7.

Another question is how or if disease states might affect brain delivery and/or the distribution of substances in the CNS following IN administration. It will be important to establish whether the capacity for nose-to-brain transport is compromised, unaffected or otherwise altered by specific pathology, disease or other factors. Finally, it is not yet clear how cells reach the brain by the IN route of administration; whether cells use the same or different pathways/mechanisms to gain entry to the brain from the nasal passage that have been identified for small molecules, peptides and proteins remains an open question. There is a clear need for further research to

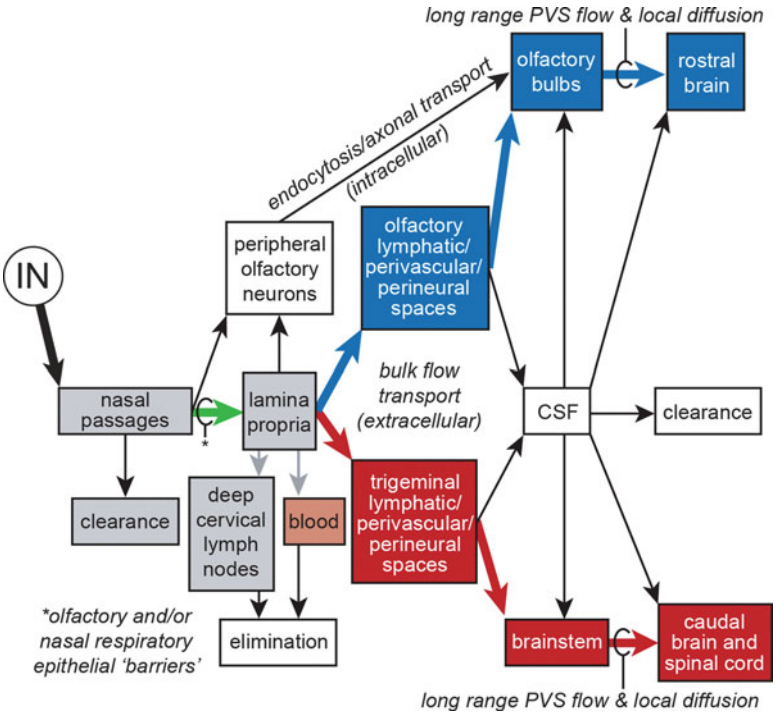

Fig. 14.7 Proposed pathways and mechanisms responsible for drug transport into the CNS following intranasal administration, based primarily upon studies utilizing radiolabeled proteins

address these questions and advance knowledge so that clinical applications utilizing intranasal targeting of drugs to the CNS can be evaluated with the best possible opportunities for success.

14.6 Conclusions

Drug delivery to the CNS remains a challenge due to the restrictive nature of the BBB and BCSFB. A number of studies suggest that the IN route of administration may allow rapid, noninvasive delivery of substances directly to the CNS along pathways associated with the olfactory or trigeminal nerves. These pathways are not yet fully characterized, presenting opportunities for further investigation. Methods to enhance delivery of substances from the nasal cavity to the CNS are also needed due to the typically low delivery efficiencies that have thus far been measured (<0.05 % for proteins). A better understanding of the mechanisms governing transport of substances into the CNS from the nasal mucosae may lead to improvements in the efficiency of IN administration. While IN drug delivery to the brain has shown great promise in animals and humans, it is clearly an area where more research is needed to fully exploit its potential.

14.7 Points for Discussion

- What advantages does the intranasal route of administration offer for chronic administration? Compare and contrast intranasal application requirements with those of other strategies designed to target biotherapeutics to the brain (e.g., Are trained health professionals required for administration? Can the administration be performed in an outpatient setting or is hospitalization necessary? What economic resources will likely be required to accomplish administration? Can the methods be easily applied in both developed and developing countries?).
- Why might knowledge of nasal epithelial organization and physiology be important for implementing, optimizing and adjusting brain targeting following intranasal drug administration?
- What are the likely pathways that underlie nose-to-brain transport? What are the likely mechanisms that underlie nose-to-brain transport? What additional information is needed to more fully understand the pathways/mechanisms responsible for intranasal targeting of drugs to the CNS?
- Discuss each of the steps that may be required for an intranasally applied drug to reach CNS target sites.
- How might the transport of small molecules, macromolecules and cell-based therapies into the brain following intranasal application be similar? How might their transport be different? What areas require further study?
- Compare and contrast how the rate and extent of nasal absorption may vary for different classes of drugs compared with other administration routes (e.g., oral delivery). Will such considerations apply equally well for both systemic delivery and delivery to the CNS? What additional information/knowledge is needed to advance the field?

Acknowledgements Portions of this work were supported by the University of Wisconsin-Madison School of Pharmacy, the Graduate School at the University of Wisconsin, the Michael J. Fox Foundation for Parkinson's Research, the Wisconsin Alzheimer's Disease Research Center (NIH P50-AG033514), and the Clinical and Translational Science Award (CTSA) program, through the NIH National Center for Advancing Translational Sciences (NCATS; grant UL1TR000427). All content is solely the responsibility of the authors and does not necessarily represent the official views of the NIH. Robert Thorne acknowledges periodically receiving honoraria for speaking to organizations within academia, foundations, and the biotechnology and pharmaceutical industry as well as occasional service as a consultant on CNS drug delivery to industry. Jeffrey Lochhead and Robert Thorne also acknowledge being inventors on patents and/or patent applications related to intranasal drug delivery.

References

Altner H, Altner-Kolnberger I (1974) Freeze-fracture and tracer experiments on the permeability of the zonulae occludentes in the olfactory mucosa of vertebrates. Cell Tissue Res 154(1): 51–59

Anton F, Peppel P (1991) Central projections of trigeminal primary afferents innervating the nasal mucosa: a horseradish peroxidase study in the rat. Neuroscience 41(2–3):617–628

Baier PC, Hallschmid M, Seeck-Hirschner M, Weinhold SL, Burkert S, Diessner N, Goder R, Aldenhoff JB, Hinze-Selch D (2011) Effects of intranasal hypocretin-1 (orexin A) on sleep in narcolepsy with cataplexy. Sleep Med 12(10):941–946

Baier PC, Weinhold SL, Huth V, Gottwald B, Ferstl R, Hinze-Selch D (2008) Olfactory dysfunction in patients with narcolepsy with cataplexy is restored by intranasal Orexin A (Hypocretin-1). Brain 131(Pt 10):2734–2741

Baker H, Genter MB (2003) The olfactory system and the nasal mucosa as portals of entry of viruses, drugs, and other exogenous agents into the brain. In: Doty RL (ed) Handbook of olfaction and gustation, 2nd edn. Marcel Dekker, Inc., New York, pp 549–573

Baker H, Spencer RF (1986) Transneuronal transport of peroxidase-conjugated wheat germ agglutinin (WGA-HRP) from the olfactory epithelium to the brain of the adult rat. Exp Brain Res 63(3):461–473

Banks WA (2004) Are the extracellular pathways a conduit for the delivery of therapeutics to the brain? Curr Pharm Des 10(12):1365–1370

Banks WA (2009) Characteristics of compounds that cross the blood-brain barrier. BMC Neurol 9(Suppl 1):S3

Bilston LE, Fletcher DF, Brodbelt AR, Stoodley MA (2003) Arterial pulsation-driven cerebrospinal fluid flow in the perivascular space: a computational model. Comput Methods Biomech Biomed Engin 6(4):235–241

Bojsen-Moller F (1975) Demonstration of terminalis, olfactory, trigeminal and perivascular nerves in the rat nasal septum. J Comp Neurol 159(2):245–256

Born J, Lange T, Kern W, McGregor GP, Bickel U, Fehm HL (2002) Sniffing neuropeptides: a transnasal approach to the human brain. Nat Neurosci 5(6):514–516

Bradbury MWB, Cserr HF (1985) Drainage of cerebral interstitial fluid and of cerebrospinal fluid into lymphatics. In: Johnston MG (ed) Experimental biology of the lymphatic circulation, vol 9. Elsevier, Amsterdam and New York, pp 355–391

Broadwell RD, Balin BJ (1985) Endocytic and exocytic pathways of the neuronal secretory process and trans-synaptic transfer of wheat germ agglutinin-horseradish peroxidase in vivo. J Comp Neurol 242(4):632–650

Broberg EK, Peltoniemi J, Nygardas M, Vahlberg T, Roytta M, Hukkanen V (2004) Spread and replication of and immune response to gamma134.5-negative herpes simplex virus type 1 vectors in BALB/c mice. J Virol 78(23):13139–13152

Butt AM, Jones HC, Abbott NJ (1990) Electrical resistance across the blood-brain barrier in anaesthetized rats: a developmental study. J Physiol 429:47–62

Buchner K, Seitz-Tutter D, Shonitzer K, Weiss DG (1987) A quantitative study of anterograde and retrograde axonal transport of exogenous proteins in olfactory nerve C-fibers. Neuroscience 22:697–707

Caggiano M, Kauer JS, Hunter DD (1994) Globose basal cells are neuronal progenitors in the olfactory epithelium: a lineage analysis using a replication-incompetent retrovirus. Neuron 13(2):339–352

Carmichael ST, Clugnet MC, Price JL (1994) Central olfactory connections in the macaque monkey. J Comp Neurol 346(3):403–434

Cattepoel S, Hanenberg M, Kulic L, Nitsch RM (2011) Chronic intranasal treatment with an anti-abeta(30-42) scFv antibody ameliorates amyloid pathology in a transgenic mouse model of Alzheimer's disease. PLoS One 6(4):e18296

Cauna N, Hinderer KH (1969) Fine structure of blood vessels of the human nasal respiratory mucosa. Ann Otol Rhinol Laryngol 78(4):865–879

Charlton ST, Whetstone J, Fayinka ST, Read KD, Illum L, Davis SS (2008) Evaluation of direct transport pathways of glycine receptor antagonists and an angiotensin antagonist from the nasal cavity to the central nervous system in the rat model. Pharm Res 25(7):1531–1543

Costantino HR, Illum L, Brandt G, Johnson PH, Quay SC (2007) Intranasal delivery: physicochemical and therapeutic aspects. Int J Pharm 337(1–2):1–24

Coyle P (1975) Arterial patterns of the rat rhinencephalon and related structures. Exp Neurol 49:671–690

Craft S, Baker LD, Montine TJ, Minoshima S, Watson GS, Claxton A, Arbuckle M, Callaghan M, Tsai E, Plymate SR, Green PS, Leverenz J, Cross D, Gerton B (2012) Intranasal insulin therapy for Alzheimer disease and amnestic mild cognitive impairment: a pilot clinical trial. Arch Neurol 69(1):29–38

Crone C, Olesen SP (1982) Electrical resistance of brain microvascular endothelium. Brain Res 241(1):49–55

Danielyan L, Klein R, Hanson LR, Buadze M, Schwab M, Gleiter CH, Frey WH (2010) Protective effects of intranasal losartan in the APP/PS1 transgenic mouse model of Alzheimer disease. Rejuvenation Res 13(2–3):195–201

Danielyan L, Schafer R, von Ameln-Mayerhofer A, Bernhard F, Verleysdonk S, Buadze M, Lourhmati A, Klopfer T, Schaumann F, Schmid B, Koehle C, Proksch B, Weissert R, Reichardt HM, van den Brandt J, Buniatian GH, Schwab M, Gleiter CH, Frey WH II (2011) Therapeutic efficacy of intranasally delivered mesenchymal stem cells in a rat model of Parkinson disease. Rejuvenation Res 14(1):3–16. doi:10.1089/rej.2010.1130

Danielyan L, Schafer R, von Ameln-Mayerhofer A, Buadze M, Geisler J, Klopfer T, Burkhardt U, Proksch B, Verleysdonk S, Ayturan M, Buniatian GH, Gleiter CH, Frey WH II (2009) Intranasal delivery of cells to the brain. Eur J Cell Biol 88(6):315–324

Davis SS, Illum L (2003) Absorption enhancers for nasal drug delivery. Clin Pharmacokinet 42(13):1107–1128

Deadwyler SA, Porrino L, Siegel JM, Hampson RE (2007) Systemic and nasal delivery of orexin-A (Hypocretin-1) reduces the effects of sleep deprivation on cognitive performance in nonhuman primates. J Neurosci 27(52):14239–14247

Deatly AM, Haase AT, Fewster PH, Lewis E, Ball MJ (1990) Human herpes virus infections and Alzheimer's disease. Neuropathol Appl Neurobiol 16(3):213–223

Deli MA (2009) Potential use of tight junction modulators to reversibly open membranous barriers and improve drug delivery. Biochim Biophys Acta 1788:892–910

Dhuria SV, Hanson LR, Frey WH II (2009) Intranasal drug targeting of hypocretin-1 (orexin-A) to the central nervous system. J Pharm Sci 98(7):2501–2515

Dhuria SV, Hanson LR, Frey WH II (2010) Intranasal delivery to the central nervous system: mechanisms and experimental considerations. J Pharm Sci 99(4):1654–1673

Donega V, van Velthoven CT, Nijboer CH, van Bel F, Kas MJ, Kavelaars A, Heijnen CJ (2013) Intranasal mesenchymal stem cell treatment for neonatal brain damage: long-term cognitive and sensorimotor improvement. PLoS One 8(1):e51253

Doty RL (2008) The olfactory vector hypothesis of neurodegenerative disease: is it viable? Ann Neurol 63(1):7–15

Draghia R, Caillaud C, Manicom R, Pavirani A, Kahn A, Poenaru L (1995) Gene delivery into the central nervous system by nasal instillation in rats. Gene Ther 2(6):418–423

Elsaesser R, Paysan J (2007) The sense of smell, its signalling pathways, and the dichotomy of cilia and microvilli in olfactory sensory cells. BMC Neurosci 8(Suppl 3):S1

Ermisch A, Barth T, Ruhle HJ, Skopkova J, Hrbas P, Landgraf R (1985) On the blood-brain barrier to peptides: accumulation of labelled vasopressin, DesGlyNH2-vasopressin and oxytocin by brain regions. Endocrinol Exp 19(1):29–37

Faber WM (1937) The nasal mucosa and the subarachnoid space. Am J Anat 62(1):121–148

Favre JJ, Chaffanjon P, Passagia JG, Chirossel JP (1995) Blood supply of the olfactory nerve: meningeal relationships and surgical relevance. Surg Radiol Anat 17:133–138

Febbraro F, Andersen KJ, Sanchez-Guajardo V, Tentillier N, Romero-Ramos M (2013) Chronic intranasal deferoxamine ameliorates motor defects and pathology in the alpha-synuclein rAAV Parkinson's model. Exp Neurol 247C:45–58

Field P, Li Y, Raisman G (2003) Ensheathment of the olfactory nerves in the adult rat. J Neurocytol 32(3):317–324

Finger TE, St Jeor VL, Kinnamon JC, Silver WL (1990) Ultrastructure of substance P- and CGRP-immunoreactive nerve fibers in the nasal epithelium of rodents. J Comp Neurol 294(2): 293–305

Francis GJ, Martinez JA, Liu WQ, Xu K, Ayer A, Fine J, Tuor UI, Glazner G, Hanson LR, Frey WH II, Toth C (2008) Intranasal insulin prevents cognitive decline, cerebral atrophy and white matter changes in murine type I diabetic encephalopathy. Brain 131(Pt 12):3311–3334

Fransson M, Piras E, Burman J, Nilsson B, Essand M, Lu B, Harris RA, Magnusson PU, Brittebo E, Loskog AS (2012) CAR/FoxP3-engineered T regulatory cells target the CNS and suppress EAE upon intranasal delivery. J Neuroinflammation 9:112

Frenkel D, Solomon B (2002) Filamentous phage as vector-mediated antibody delivery to the brain. Proc Natl Acad Sci U S A 99(8):5675–5679

Frey WH II, Liu L, Chen XQ, Thorne RG, Fawcett JR, Ala TA, Rahman YE (1997) Delivery of 125I-NGF to the brain via the olfactory route. Drug Deliv 4:87–92

Gozes I, Giladi E, Pinhasov A, Bardea A, Brenneman DE (2000) Activity-dependent neurotrophic factor: intranasal administration of femtomolar-acting peptides improve performance in a water maze. J Pharmacol Exp Ther 293(3):1091–1098

Graff CL, Pollack GM (2005) Nasal drug administration: potential for targeted central nervous system delivery. J Pharm Sci 94:1187–1195

Standring S, Borley NR, Collins P, Crossman AR, Gatzoulis MA, Healy JC, Johnson D, Mahadevan V, Newell RLM, Wigley CB (2008) Gray's anatomy, 40 edn. Elsevier, Philadelphia

Greene EC (1935) Anatomy of the rat. Braintree Scientific, inc., Braintree, MA

Guo C, Wang T, Zheng W, Shan ZY, Teng WP, Wang ZY (2013) Intranasal deferoxamine reverses iron-induced memory deficits and inhibits amyloidogenic APP processing in a transgenic mouse model of Alzheimer's disease. Neurobiol Aging 34(2):562–5759

Hadaczek P, Yamashita Y, Mirek H, Tamas L, Bohn MC, Noble C, Park JW, Bankiewicz K (2006) The "perivascular pump" driven by arterial pulsation is a powerful mechanism for the distribution of therapeutic molecules within the brain. Mol Ther 14(1):69–78

Han IK, Kim MY, Byun HM, Hwang TS, Kim JM, Hwang KW, Park TG, Jung WW, Chun T, Jeong GJ, Oh YK (2007) Enhanced brain targeting efficiency of intranasally administered plasmid DNA: an alternative route for brain gene therapy. J Mol Med 85(1):75–83

Hanson LR, Roeytenberg A, Martinez PM, Coppes VG, Sweet DC, Rao RJ, Marti DL, Hoekman JD, Matthews RB, Frey WH II, Panter SS (2009) Intranasal deferoxamine provides increased brain exposure and significant protection in rat ischemic stroke. J Pharmacol Exp Ther 330(3):679–686

Harkema JR, Carey SA, Wagner JG (2006) The nose revisited: a brief review of the comparative structure, function, and toxicologic pathology of the nasal epithelium. Toxicol Pathol 34(3):252–269

Hegg CC, Irwin M, Lucero MT (2009) Calcium store-mediated signaling in sustentacular cells of the mouse olfactory epithelium. Glia 57(6):634–644

Hillyer JF, Albrecht RM (2001) Gastrointestinal persorption and tissue distribution of differently sized colloidal gold nanoparticles. J Pharm Sci 90(12):1927–1936

Hoekman JD, Ho RJ (2011) Enhanced analgesic responses after preferential delivery of morphine and fentanyl to the olfactory epithelium in rats. Anesth Analg 113(3):641–651

Hosoya K, Kubo H, Natsume H, Sugibayashi K, Morimoto Y, Yamashita S (1993) The structural barrier of absorptive mucosae: site difference of the permeability of fluorescein isothiocyanate-labelled dextran in rabbits. Biopharm Drug Dispos 14(8):685–695

Ichimura T, Fraser PA, Cserr HF (1991) Distribution of extracellular tracers in perivascular spaces of the rat brain. Brain research 545(1–2):103–113

Iliff JJ, Wang M, Liao Y, Plogg BA, Peng W, Gundersen GA, Benveniste H, Vates GE, Deane R, Goldman SA, Nagelhus EA, Nedergaard M (2012) A paravascular pathway facilitates CSF flow through the brain parenchyma and the clearance of interstitial solutes, including amyloid beta. Sci Transl Med 4(147):147ra111

Illum L (2004) Is nose-to-brain transport of drugs in man a reality? J Pharm Pharmacol 56(1):3–17

Illum L (2012) Nasal drug delivery—recent developments and future prospects. J Control Release 161(2):254–263

Iwai N, Zhou Z, Roop DR, Behringer RR (2008) Horizontal basal cells are multipotent progenitors in normal and injured adult olfactory epithelium. Stem Cells 26(5):1298–1306

Jafek BW (1983) Ultrastructure of human nasal mucosa. Laryngoscope 93(12):1576–1599
Jansson B, Bjork E (2002) Visualization of in vivo olfactory uptake and transfer using fluorescein dextran. J Drug Target 10(5):379–386
Jauch-Chara K, Friedrich A, Rezmer M, Melchert UH, Scholand-Engler HG, Hallschmid M, Oltmanns KM (2012) Intranasal insulin suppresses food intake via enhancement of brain energy levels in humans. Diabetes 61(9):2261–2268
Jin Y, Dons L, Kristensson K, Rottenberg ME (2001) Neural route of cerebral Listeria monocytogenes murine infection: role of immune response mechanisms in controlling bacterial neuroinvasion. Infect Immun 69(2):1093–1100
Johnson NJ, Hanson LR, Frey WH (2010) Trigeminal pathways deliver a low molecular weight drug from the nose to the brain and orofacial structures. Mol Pharm 7(3):884–893
Johnston M, Zakharov A, Papaiconomou C, Salmasi G, Armstrong D (2004) Evidence of connections between cerebrospinal fluid and nasal lymphatic vessels in humans, non-human primates and other mammalian species. Cerebrospinal Fluid Res 1(1):2
Kandimalla KK, Donovan MD (2005) Localization and differential activity of p-glycoprotein in the bovine and nasal respiratory mucosae. Pharm Res 22:1121–1128
Kang YS, Park JH (2000) Brain uptake and the analgesic effect of oxytocin—its usefulness as an analgesic agent. Arch Pharm Res 23(4):391–395
Kerjaschki D, Horander H (1976) The development of mouse olfactory vesicles and their cell contacts: a freeze-etching study. J Ultrastruct Res 54(3):420–444
Kida S, Pantazis A, Weller RO (1993) CSF drains directly from the subarachnoid space into nasal lymphatics in the rat. Anatomy, histology and immunological significance. Neuropathol Appl Neurobiol 19(6):480–488
Kim ID, Kim SW, Lee JK (2009) Gene knockdown in the olfactory bulb, amygdala, and hypothalamus by intranasal siRNA administration. Korean J Anat 42(4):285–292
Kiyono H, Fukuyama S (2004) NALT-versus Peyer's patch-mediated mucosal immunity. Nat Rev Immunol 4:699–710
Kristensson K (2011) Microbes' roadmap to neurons. Nat Rev Neurosci 12(6):345–357
Kristensson K, Olsson Y (1971) Uptake of exogenous proteins in mouse olfactory cells. Acta Neuropathol 19(2):145–154
Laing JM, Aurelian L (2008) DeltaRR vaccination protects from KA-induced seizures and neuronal loss through ICP10PK-mediated modulation of the neuronal-microglial axis. Genet Vaccines Ther 6:1
Lansley AB, Martin GP (2001) Nasal drug delivery. In: Hillery AM, Lloyd AW, Swarbrick J (eds) Drug delivery and targeting. CRC Press, Boca Raton, pp 237–268
Lee ST, Chu K, Jung KH, Kim JH, Huh JY, Yoon H, Park DK, Lim JY, Kim JM, Jeon D, Ryu H, Lee SK, Kim M, Roh JK (2012) miR-206 regulates brain-derived neurotrophic factor in Alzheimer disease model. Ann Neurol 72(2):269–277
Li Y, Field PM, Raisman G (2005) Olfactory ensheathing cells and olfactory nerve fibroblasts maintain continuous open channels for regrowth of olfactory nerve fibres. Glia 52(3):245–251
Lochhead JJ, Thorne RG (2012) Intranasal delivery of biologics to the central nervous system. Adv Drug Deliv Rev 64(7):614–628
Matsuoka Y, Gray AJ, Hirata-Fukae C, Minami SS, Waterhouse EG, Mattson MP, LaFerla FM, Gozes I, Aisen PS (2007) Intranasal NAP administration reduces accumulation of amyloid peptide and tau hyperphosphorylation in a transgenic mouse model of Alzheimer's disease at early pathological stage. J Mol Neurosci 31(2):165–170
Merkus P, Guchelaar HJ, Bosch DA, Merkus FW (2003) Direct access of drugs to the human brain after intranasal drug administration? Neurology 60(10):1669–1671
Mery S, Gross EA, Joyner DR, Godo M, Morgan KT (1994) Nasal diagrams: a tool for recording the distribution of nasal lesions in rats and mice. Toxicol Pathol 22:353–372
Miller DS (2010) Regulation of P-glycoprotein and other ABC drug transporters at the blood-brain barrier. Trends Pharmacol Sci 31(6):246–254
Miller (2013) The promise and perils of oxytocin. Science 339:267–269

Neuwelt E, Abbott NJ, Abrey L, Banks WA, Blakley B, Davis T, Engelhardt B, Grammas P, Nedergaard M, Nutt J, Pardridge W, Rosenberg GA, Smith Q, Drewes LR (2008) Strategies to advance translational research into brain barriers. Lancet Neurol 7(1):84–96

Powell KJ, Hori SE, Leslie R, Andrieux A, Schellinck H, Thorne M, Robertson GS (2007) Cognitive impairments in the STOP null mouse model of schizophrenia. Behav Neurosci 121(5):826–835

Reese TS, Karnovsky MJ (1967) Fine structural localization of a blood-brain barrier to exogenous peroxidase. J Cell Biol 34(1):207–217

Reitz M, Demestre M, Sedlacik J, Meissner H, Fiehler J, Kim SU, Westphal M, Schmidt NO (2012) Intranasal delivery of neural stem/progenitor cells: a noninvasive passage to target intracerebral glioma. Stem Cells Transl Med 1(12):866–873

Rennels ML, Gregory TF, Blaumanis OR, Fujimoto K, Grady PA (1985) Evidence for a 'paravascular' fluid circulation in the mammalian central nervous system, provided by the rapid distribution of tracer protein throughout the brain from the subarachnoid space. Brain Res 326(1):47–63

Renner DB, Frey WH II, Hanson LR (2012a) Intranasal delivery of siRNA to the olfactory bulbs of mice via the olfactory nerve pathway. Neurosci Lett 513(2):193–197

Renner DB, Svitak AL, Gallus NJ, Ericson ME, Frey WH II, Hanson LR (2012b) Intranasal delivery of insulin via the olfactory nerve pathway. J Pharm Pharmacol 64(12):1709–1714

Rojanasakul Y, Wang LY, Bhat M, Glover DD, Malanga CJ, Ma JK (1992) The transport barrier of epithelia: a comparative study on membrane permeability and charge selectivity in the rabbit. Pharm Res 9(8):1029–1034

Ronaldson PT, Babakhanian K, Bendayan R (2007) Drug transport in the brain. In: You G, Morris ME (eds) Drug transporters: molecular characterization and role in drug disposition. Wiley-Interscience, Hoboken, pp 411–461

Ross TM, Martinez PM, Renner JC, Thorne RG, Hanson LR, Frey WH II (2004) Intranasal administration of interferon beta bypasses the blood-brain barrier to target the central nervous system and cervical lymph nodes: a non-invasive treatment strategy for multiple sclerosis. J Neuroimmunol 151(1–2):66–77

Sakane T, Akizuki M, Taki Y, Yamashita S, Sezaki H, Nadai T (1995) Direct drug transport from the rat nasal cavity to the cerebrospinal fluid: the relation to the molecular weight of drugs. J Pharm Pharmacol 47(5):379–381

Schaefer ML, Bottger B, Silver WL, Finger TE (2002) Trigeminal collaterals in the nasal epithelium and olfactory bulb: a potential route for direct modulation of olfactory information by trigeminal stimuli. J Comp Neurol 444(3):221–226

Schley D, Carare-Nnadi R, Please CP, Perry VH, Weller RO (2006) Mechanisms to explain the reverse perivascular transport of solutes out of the brain. J Theor Biol 238(4):962–974

Schuenke M, Schulte E, Schumacher U (2010) Head and neuroanatomy. Atlas of anatomy. Thieme, Stuttgart

Scremin OU (2004) Cerebral vascular system. In: Paxinos G (ed) The rat nervous system. Elsevier, Inc., San Diego, pp 1167–1202

Sezaki H (1995) Mucosal penetration enhancement. J Drug Target 3(3):175–177

Shiryaev N, Jouroukhin Y, Giladi E, Polyzoidou E, Grigoriadis NC, Rosenmann H, Gozes I (2009) NAP protects memory, increases soluble tau and reduces tau hyperphosphorylation in a tauopathy model. Neurobiol Dis 34(2):381–388

Steinke A, Meier-Stiegen S, Drenckhahn D, Asan E (2008) Molecular composition of tight and adherens junctions in the rat olfactory epithelium and fila. Histochem Cell Biol 130(2): 339–361

Stevens J, Ploeger BA, van der Graaf PH, Danhof M, de Lange EC (2011) Systemic and direct nose-to-brain transport pharmacokinetic model for remoxipride after intravenous and intranasal administration. Drug Metab Dispos 39(12):2275–2282

Stoop R (2012) Neuromodulation by oxytocin and vasopressin. Neuron 76(1):142–159

Szentistvanyi I, Patlak CS, Ellis RA, Cserr HF (1984) Drainage of interstitial fluid from different regions of rat brain. Am J Physiol 246(6 Pt 2):F835–F844

Thiebaud N, Menetrier F, Belloir C, Minn A-L, Neiers F, Artur Y, Le Bon A-M, Heydel J-M (2011) Expression and differential localization of xenobiotic transporters in the rat olfactory neuroepithelium. Neurosci Lett 505:180–185

Thorne RG, Emory CR, Ala TA, Frey WH II (1995) Quantitative analysis of the olfactory pathway for drug delivery to the brain. Brain research 692(1–2):278–282

Thorne RG, Frey WH II (2001) Delivery of neurotrophic factors to the central nervous system: pharmacokinetic considerations. Clin Pharmacokinet 40(12):907–946

Thorne RG, Hanson LR, Ross TM, Tung D, Frey WH II (2008) Delivery of interferon-beta to the monkey nervous system following intranasal administration. Neuroscience 152(3):785–797

Thorne RG, Hrabetova S, Nicholson C (2004a) Diffusion of epidermal growth factor in rat brain extracellular space measured by integrative optical imaging. J Neurophysiol 92(6):3471–3481

Thorne RG, Pronk GJ, Padmanabhan V, Frey WH II (2004b) Delivery of insulin-like growth factor-I to the rat brain and spinal cord along olfactory and trigeminal pathways following intranasal administration. Neuroscience 127(2):481–496

Tucker D (1971) Nonolfactory responses from the nasal cavity: Jacobson's organ and the trigeminal system. In: Biedler LM (ed) Handbook of sensory physiology, vol 4. Springer, New York, pp 151–181

van Velthoven CT, Sheldon RA, Kavelaars A, Derugin N, Vexler ZS, Willemen HL, Maas M, Heijnen CJ, Ferriero DM (2013) Mesenchymal stem cell transplantation attenuates brain injury after neonatal stroke. Stroke 44(5):1426–1432

Wang P, Olbricht WL (2011) Fluid mechanics in the perivascular space. J Theor Biol 274(1): 52–57

Wei N, Yu SP, Gu X, Taylor TM, Song D, Liu XF, Wei L (2013) Delayed intranasal delivery of hypoxic-preconditioned bone marrow mesenchymal stem cells enhanced cell homing and therapeutic benefits after ischemic stroke in mice. Cell Transplant 22(6):977–991

Wolburg H, Wolburg-Buchholz K, Sam H, Horvat S, Deli MA, Mack AF (2008) Epithelial and endothelial barriers in the olfactory region of the nasal cavity of the rat. Histochem Cell Biol 130(1):127–140

Xiao C, Davis FJ, Chauhan BC, Viola KL, Lacor PN, Velasco PT, Klein WL, Chauhan NB (2013) Brain transit and ameliorative effects of intranasally delivered anti-amyloid-beta oligomer antibody in 5XFAD mice. J Alzheimers Dis 35(4):777–788

Yang JP, Liu HJ, Cheng SM, Wang ZL, Cheng X, Yu HX, Liu XF (2009) Direct transport of VEGF from the nasal cavity to brain. Neurosci Lett 449(2):108–111

Yoffey JM, Drinker CK (1938) The lymphatic pathway from the nose and pharynx: the absorption of dyes. J Exp Med 68(4):629–640

Chapter 15
Blood-to-Brain Drug Delivery Using Nanocarriers

Pieter J. Gaillard, Corine C. Visser, Marco de Boer, Chantal C.M. Appeldoorn, and Jaap Rip

Abstract Brain and nervous system disorders represent a large, unmet medical need affecting two billion people worldwide; a number that is expected to grow with increasing life expectancy and the expanding global population. CNS drug development is hampered by the restricted transport of drug candidates across the blood-brain barrier (BBB). We will discuss blood-to-brain drug delivery strategies that make use of nanocarriers, like liposomes, albumin nanoparticles, and polymeric nanoparticles. The focus will be on the key pharmaceutical, pharmacological, and regulatory aspects towards the clinical development of nanocarriers. Clinical development of treatments employing nanocarriers is not as straightforward as for a single active moiety; therefore, we will highlight the issues that should be considered when translating basic research towards clinical development. Although it is still unrealistic to expect a magic bullet for exclusive CNS drug delivery, much progress has been made towards successful development of novel treatments for patients with devastating brain diseases.

15.1 Introduction

Current strategies to enhance drug delivery to the brain are either focused on locally circumventing the blood-brain barrier (BBB) through direct injections or globally through the blood stream (using targeted delivery approaches or by opening the blood-brain barrier). Since techniques such as convection-enhanced delivery, intranasal delivery, and (transiently) opening the blood-brain barrier are discussed elsewhere in this section on strategies for improved CNS drug delivery (Thorne 2014; Bankiewicz 2014; Fortin 2014; Konofagou 2014), we will not elaborate on this.

P.J. Gaillard (✉) • C.C. Visser • M. de Boer • C.C.M. Appeldoorn • J. Rip
to-BBB technologies BV, J.H. Oortweg 19, Leiden 2333 CH, The Netherlands
e-mail: PieterGaillard@toBBB.com

M. Hammarlund-Udenaes et al. (eds.), *Drug Delivery to the Brain*, AAPS Advances in the Pharmaceutical Sciences Series 10, DOI 10.1007/978-1-4614-9105-7_15,

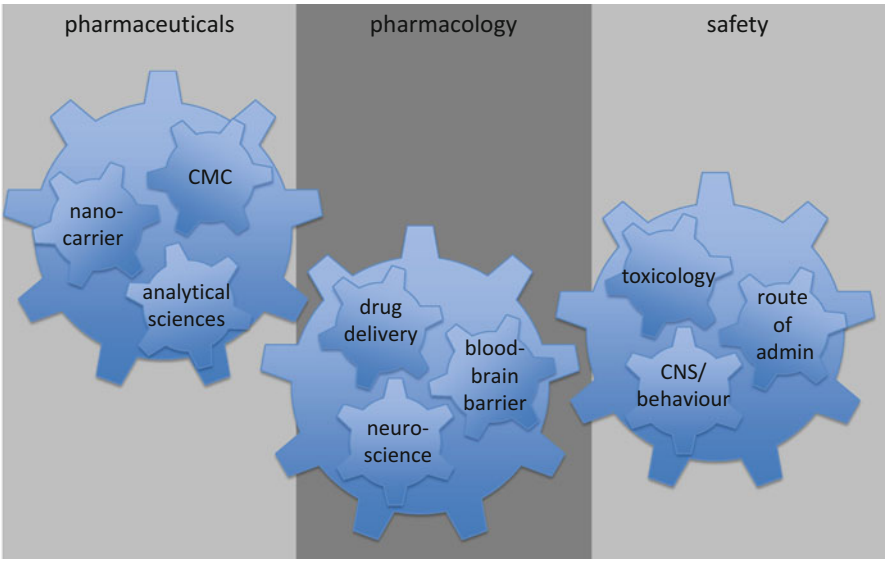

Fig. 15.1 Obtaining regulatory approval for clinical research using nanocarriers for drug delivery to the brain requires that many involved research areas connect with clockwork precision. Turning one wheel will influence the whole development process. *CMC* chemistry, manufacturing, and controls

Rather we will discuss drug delivery strategies that make use of nanocarriers, focusing on the carriers themselves. Although ligands are an essential part for targeting and delivery to the brain, this chapter's focus will be on the pharmaceutical development of the nanocarriers and their pharmacokinetics and biodistribution and not, or to a lesser extent, on the biology of ligand-receptor interactions at the blood-brain barrier.

Many approaches to enhance drug delivery across the blood-brain barrier are under development, both by academic research groups as well as pharmaceutical and biotechnology companies, albeit with little success. In order to translate basic (academic) research into safe and effective treatments for patients with devastating brain diseases, many steps in many different research areas are required (Fig. 15.1). Recently, we have summarized these aspects in ten key development criteria for targeted blood-to-brain drug delivery (Gaillard 2010; Gaillard et al. 2011). Of the currently active developments, only two brain-targeted delivery-based therapies have been approved for clinical research, i.e., Angiopep-2 conjugated to paclitaxel (ANG1005/GRN1005; based on the EPiC Technology) and glutathione pegylated liposomal doxorubicin (2B3-101; based on the G-Technology). Other brain-targeted delivery-based therapies that are currently in the research and development phase include, for example, fusion proteins of an active protein/enzyme with an antibody against the human insulin receptor (HIRMAb, Armagen), a heavy chain heterodimerization of a therapeutic antibody with a low-affinity antibody against the transferrin receptor (Genentech), and a direct conjugate between an anti-tumor drug and p97 (Bioasis). In our recent review we have reviewed these therapies and compared

them to our ten key development criteria (Gaillard et al. 2011). In this book chapter we will focus on the pharmaceutical, pharmacological, and regulatory aspects of the development of nanocarriers for blood-to-brain drug delivery. Throughout this chapter we will use the term nanocarrier as the European Medicine Agency (EMA) defined it: a drug formulation with the intention to form a particle in the nano-scale range. Examples of nanocarriers are liposomes, albumin nanoparticles, and polymeric nanoparticles.

15.2 Current Status of Nanocarrier Development

Currently there are two families of therapeutic nanocarriers, i.e., liposomes and albumin nanoparticles, firmly established in clinical practice worldwide. In addition, several therapeutic agents based on nanocarriers are in clinical trials, and still more in preclinical phases of development (Sanhai et al. 2008; Costantino and Boraschi 2012). Except for 2B3-101, which is in clinical phase I/IIa, none of these are specifically designed for enhanced drug delivery across the blood-brain barrier. Recently, Costantino and Boraschi (2012) presented an excellent overview of the development status of carrier-based drug delivery systems (nanocarriers and drug conjugates or fusion proteins) for CNS indications and especially brain tumors. In their overview, two other liposomal products are mentioned, however, these are not specifically designed for brain tumors. Marqibo (vincristine sulfate liposomes injection, OPTISOME™ (i.e., sphingomyelin-based liposomes)) is approved for treatment of leukemia and is currently investigated in a phase I trial in children and adolescents (2–21 years) with refractory cancer including primary brain tumors by the National Cancer Institute (clinicaltrials.gov; NCT01222780). NL-CPT11 (nanoliposomal CPT11, irinotecan) is investigated in patients with recurrent high-grade gliomas (clinicaltrials.gov; NCT00734682). Merrimack Pharmaceuticals is investigating a similar formulation (MM-398) for the treatment of pancreatic cancer, and the first-in-human trials were performed in patients with standard therapy-failure for solid tumors (Tsai et al. 2011). In addition to these intravenous administered therapies, treatment with cytarabine liposome injection (DepoCyt®) for lymphomatous meningitis is administered through local, intrathecal, injections.

When looking into the history of nanocarriers, pegylated liposomal doxorubicin (Doxil, Caelyx) was the first treatment based on a nanocarrier to be approved by the FDA (in 1995) and EMA (in 1996). Thereafter, several liposomal formulations have been approved, such as liposomal daunorubicin (Daunoxome), liposomal amphotericin B (Ambisome), and non-pegylated liposomal doxorubicin (Myocet; received only EMA approval). Another nanocarrier formulation, paclitaxel albumin nanoparticles (Abraxane), was approved more recently (by the FDA in 2005 and by the EMA in 2008). In addition to the liposomal amphotericin B formulation, a lipid complex formulation (Abelcet) has also been approved; however, this was less cost-effective compared to Ambisome for the treatment of persistently febrile neutropenic patients with presumed fungal infections (Gilead Sciences 2000; Morigi et al. 2012).

In addition to these clinically available nanocarrier drugs, several nanocarrier treatments are still in clinical or preclinical research (Kim et al. 2010; Duncan and Gaspar 2011; Costantino and Boraschi 2012); it would go too far to mention all of these in this chapter, therefore, we will first discuss general criteria that nanocarriers should adhere to in order to move into clinical practice. Subsequently, we will focus on the applicability of nanocarriers for drug delivery to the brain, and the points to consider for regulatory approval of nanocarriers.

15.2.1 Criteria for Nanocarriers to Move into Clinical Practice

Based on FDA and EMA recommendations (www.fda.gov; www.ema.europa.eu), product quality and product safety are most important to receive approval for clinical research. This is fully in line with the World Medical Association (WMA) Declaration of Helsinki, in which it is stated that "Every medical research study involving human subjects must be preceded by careful assessment of predictable risks and burdens to the individuals and communities involved in the research in comparison with foreseeable benefits to them and to other individuals or communities affected by the condition under investigation" (WMA 2008). Or to put it plain and simple: safety comes first. For all human drugs, and especially for neurotherapeutics, it is important to demonstrate safety of the drug with respect to the central nervous system (FDA 2001). However, governmental regulations are hindered by a lack of toxicology data for nanocarriers (Fernandes et al. 2010; Farrell et al. 2011). In addition, Wolf and Jones (2011) have recommended extra oversight for clinical research due to the uncertain but possibly significant risks of new science and technology associated with nanomedicine (including drug nanocarriers).

Clinical development of treatments employing nanocarriers is not as straightforward as for a single active moiety. Although there are no strict guidelines for treatments employing nanocarriers yet published, both the FDA and EMA are continuously working on guidance documents. Most advanced are the guidance documents on "Liposome drug products" (FDA 2002) and on "Early development considerations for innovative combination products" (FDA 2006). From these guidance documents it is clear that chemistry, manufacturing, and controls (CMC) should be investigated for each of the separate constituents of the nanocarrier, as well as the end product.

As for every drug product, efficacy of the drug-loaded nanocarrier should be shown in (GLP) preclinical research as well as in controlled clinical trials. Often, the benefit of nanocarriers is the prolonged circulation of a drug in plasma, which results in an improved therapeutic index. Although increased plasma availability may yield enhanced brain delivery by passive diffusion across the blood-brain barrier (Banks 2008), not all nanocarriers are optimized as brain-directed nanocarriers. Equally important, before developing a nanocarrier-based treatment, it is important to realize whether the amount of formulated (encapsulated) drug will actually result in the desired bioavailability of the free drug at the desired site of action.

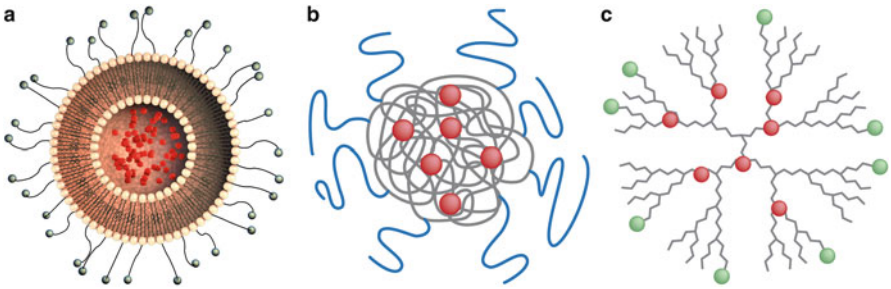

Fig. 15.2 Schematic presentation of the main nanocarriers discussed in this book chapter. (**a**) Liposomes; (**b**) Polymeric nanoparticles, including albumin nanoparticles; (**c**) Dendrimers. Liposome picture from to-BBB technologies BV, polymeric nanoparticle and dendrimer adapted from Zhang et al. (2008)

In addition, while for pegylated liposomal doxorubicin a drug loading efficiency of >90 % is reached (Jiang et al. 2011), polymeric nanoparticles usually have a drug loading of approximately 10 % (Costantino and Boraschi 2012). Although this might be acceptable for high-potency drugs, the therapeutic index might often not be positively influenced for drugs with a lower potency, as the desired target concentration cannot be met, or the cost of goods is too high because of the low drug loading.

Finally, when applying nanocarriers for CNS indications, the effect of the targeting ligands on the nanocarrier properties should be considered. These targeting ligands are necessary as homing devices to the blood-brain barrier, since nanocarriers themselves do not have this capacity. Targeting ligands may consist of antibodies, peptides, or proteins, as well as small molecules (Jones and Shusta 2007; Brasnjevic et al. 2009; Gabathuler 2014); importantly, these ligands may greatly affect pharmaceutical properties, e.g., charge, stability, and immunogenicity, as well as pharmacology, i.e., binding to plasma proteins, biodistribution (hopefully in favor of the brain), pharmacokinetics, and safety.

15.2.2 Nanocarriers Suitable for Brain Drug Delivery

Searching for the terms “nanocarriers” and “brain” in PubMed results in just over 50 articles; however, replacing “nanocarriers” with “nanoparticles” increases the results to almost 1,500, and “liposomes” and “brain” results in nearly 2,000 articles. Combining all this, and extending it with other specific nanocarriers, one may conclude that there is a wealth of research published on this topic. Rather than discussing all possible nanocarriers, we follow the FDA and EMA publications, in which nanocarriers for human use were discussed. For these nanocarriers (Fig. 15.2) we will also discuss their applicability as brain drug delivery vehicles.

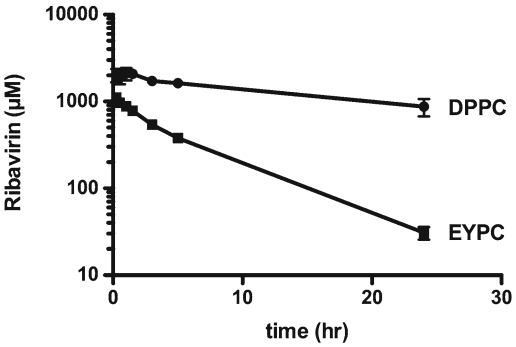

Fig. 15.3 The choice of lipids will influence the stability and circulation time of liposomal nanocarriers in plasma after intravenous injection in rats. Glutathione-pegylated liposomes were either made of DPPC (stable liposomes; dipalmitoyl phosphatidylcholine) or EYPC (less-stable liposomes; egg yolk phosphatidylcholine). The antiviral drug ribavirin was used as a model drug for this experiment. The total ribavirin concentration was measured, i.e., the liposomal encapsulated ribavirin and the free ribavirin

15.2.2.1 Liposomes

Liposomes have a strong presence in clinical use and research. There is not *one* liposomal formulation, as the constituents can vary. For example, we have shown that the selection of lipids can make a profound difference in the plasma circulation of different liposomal formulations containing the model drug ribavirin (Fig. 15.3). In general, by choosing the right constituents, liposomes are regarded as safe nanocarriers. Besides the more general "nanocarrier advantages" such as prolonged circulation time, liposomes have the additional benefit that they can encapsulate both lipophilic and hydrophilic compounds ranging from small molecules to larger biological compounds without modification of the encapsulated active pharmaceutical ingredient (API) (Gaillard et al. 2011).

With regard to the ability to deliver drugs across the blood-brain barrier, nontargeted liposomes most likely do not cross the blood-brain barrier in sufficient quantities, nor would they release their content specifically in the brain area. When blood-brain barrier integrity is compromised, e.g., in the newly formed blood vessels in brain tumors or as a consequence of trauma or disease, the likelihood of liposomal drugs to cross the blood-brain barrier is increased. In patients with a primary brain tumor (malignant glioblastoma multiforme), pegylated liposomal doxorubicin (alone or in combination with other chemotherapeutics) was considered safe and moderately effective (Fabel et al. 2001; Hau et al. 2004; Glas et al. 2007). This is, however, just an example that drugs from liposomes can mainly reach the center of larger brain tumors, since the integrity of the blood-brain barrier is maintained around the infiltrative growing tumor cells as well as in micrometastases (de Vries et al. 2006; Palmieri et al. 2007).

Many strategies have been developed to increase drug delivery to the brain, which can also be used together with liposomal drug delivery. These have been extensively discussed previously (Jones and Shusta 2007; Rip et al. 2010; Gaillard et al. 2011), as well as within this book (Gabathule 2014). Targeting ligands will not only alter the pharmaceutical properties of the liposomes but also influence their biodistribution. For example, repeated administration of identical doses of pegylated liposomal doxorubicin (Doxil/Caelyx) resulted in slightly higher plasma concentrations and lower clearance compared to glutathione pegylated liposomal doxorubicin (2B3-101) (Gaillard et al. 2012). Associated with this, higher tissue concentrations were found after Doxil/Caelyx administration, with the exception of brain and spleen. The doxorubicin retention in brain was almost three times higher ($p<0.02$) after repeated 2B3-101 administration compared to Doxil/Caelyx at the same dose (Gaillard et al. 2012).

Other examples of targeting ligands that are being combined with liposomal drug delivery include larger proteins, such as antibodies against the transferrin or insulin receptor. These antibodies have been used to produce the so-called Trojan horse liposomes for the delivery of plasmid DNA or antisense gene therapy (Pardridge 2010). Peptide targeting vectors for the delivery of liposomal drugs to the brain include COG133 (an ApoE-mimetic peptide), Angiopep-2 (with high affinity for the LRP receptor on brain endothelial cells), or GLA peptide (selected through phage display with brain uptake through a yet unknown mechanism) (van Rooy et al. 2010). Recently, van Rooy et al. (2012) have shown the importance of peptide conformation for the ability of GLA to improve drug targeting to the brain (van Rooy et al. 2012), a finding that may hold true for other (peptide) targeting ligands as well.

15.2.2.2 Albumin Nanoparticles

Albumin nanoparticles are formed by mixing albumin with a drug in aqueous solvent and then passing the product through filters to obtain 100–200 nm-sized particles (Kratz 2008). It was shown that enhanced uptake of an albumin-based drug delivery system for paclitaxel (Abraxane) in solid tumors is both passive, through enhanced permeability and retention (EPR), and potentially also active through binding to gp60 and SPARC receptors on the cell surface (Kratz 2008), although the paclitaxel dissociates from the albumin very shortly after administration in the blood stream. Therefore, the main advantage of Abraxane may be the replacement of Cremophor by albumin, since Cremophor can lead to severe side effects. Abraxane is currently the only nanoparticle form of albumin that is approved, although the use of albumin as a drug carrier through direct conjugations with small molecules or through covalent bonds with peptides or proteins is under investigation (Kratz 2008). Albumin, being present in high concentrations in circulation, is considered safe, since it is biodegradable and not immunogenic (Kratz 2008; Dadparvar et al. 2011). However, safety is not guaranteed, as it is a blood-derived product. The package insert of Abraxane literally states that it contains albumin derived from

human blood, which has a theoretical risk of viral transmission and therefore needs to be carefully controlled.

Albumin nanoparticles are also under investigation for their capability to deliver drugs to the brain. Dadparvar et al. recently showed that oximes (used as anti-nerve gas agents) adsorbed to the surface of albumin nanoparticles gave a higher protective response in vitro against chemical warfare agents compared to free oximes (Dadparvar et al. 2011), even though there was no targeting ligand present. In another study by the same research group, ApoE conjugated to the surface of the albumin nanoparticles resulted in an enhanced transport of oximes across an in vitro blood-brain barrier model compared to nontargeted albumin particles (Wagner et al. 2010). Conjugation of transferrin to albumin nanoparticles containing azidothymidine (AZT, an antiviral drug) resulted in an increased brain uptake of AZT compared to free drug, non-pegylated nanoparticles, and pegylated albumin nanoparticles (Mishra et al. 2006). In addition, using loperamide (an anti-nociceptive compound), Ulbrich et al (2009) have shown that transferrin, as well as antibodies against the transferrin receptor (OX26 and R17217) were able to enhance efficacy compared to nontargeted or albumin nanoparticles conjugated with a negative control antibody (Ulbrich et al. 2009); this same group has more recently shown that conjugation of albumin nanoparticles with insulin or an anti-insulin receptor antibody (29B4) also increased the anti-nociceptive response of loperamide formulated in these albumin particles (Ulbrich et al. 2011).

15.2.2.3 Polymeric Nanoparticles

In the last few decades several nanoparticle-based approaches for treatment of different diseases have been explored. A PubMed search using the words "polymeric" and "nanoparticles" results in greater than 14,000 publications and over 1,000 reviews. Nevertheless, it is important to realize that there is no clear definition of a polymeric nanoparticle. The search in PubMed also included different approaches including polymer-drug conjugates of which clinically approved formulations are available (Zhang et al. 2008). In this chapter, we will focus only on polymeric nanoparticles that are used for brain delivery of drugs.

Most nanoparticles were initially made of nonbiodegradable polymers that were unsuitable for clinical development due to their inherent chronic toxicity and immunological response. Biodegradable, biocompatible, and bioadhesive polymers have been developed and the most commonly used are poly(butylcyanoacrylate) PBCA, poly(lactic-co-glycolic acid) PLGA, and chitosan. PBCA particles can be produced easily, but they have a rapid biodegradation and an ineffective absorption of very hydrophobic and hydrophilic compounds. Chitosan is a natural product that is biodegradable and is available in different molecular weights and different degrees of deacetylation. Use of chitosan-based particles in preclinical studies and other related aspects have been recently reviewed (Nagpal et al. 2010; Wang et al. 2011). PLGA-based nanoparticles typically exhibit more controllable release kinetics and better encapsulation than most other polymeric materials. PLGA is approved by the US

FDA and the EMA and is already used in various (parenteral–topical) drug delivery systems in humans (Danhier et al. 2012). The polymers are commercially available with different molecular weights and copolymer composition.

Nanoparticles based on the above three polymers have also been investigated for CNS drug delivery. Different routes of administration have been explored, e.g., invasive direct injections in the brain (Garbayo et al. 2009), intranasal administration (Ali et al. 2010; Luppi et al. 2010), and intravenous administration (Costantino and Boraschi 2012). When focusing on intravenous administration, distribution of drugs in the brain from noncoated nanoparticles has been described. Nanoparticles may increase the availability of the drug by increasing the in vivo half-life and by protecting the drug from early degradation (Reddy et al. 2008). The slowly released drug can cross the blood-brain barrier and act in the brain. However, it is generally assumed that large nanoparticles cannot cross the blood-brain barrier without the use of a targeting ligand mediating transport. The above-mentioned polymeric nanoparticles have been combined with different targeting ligands for drug delivery to the brain, as extensively reviewed previously (Wilson 2009; Bhaskar et al. 2010; Patel et al. 2011; Costantino and Boraschi 2012); some of the targeting ligands that have been used are Apo E, Apo B100, Apo A1, folate, lactoferrin, simil-opioid peptide (g7), PEG TGN and Polysorbate 80 (Wohlfart et al. 2011), and glutathione (Geldenhuys et al. 2011).

15.2.2.4 Other Nanoparticles

Several other nanocarriers have been used to deliver drugs to the brain. Although some of the methods described in this section include the use of polymers and targeting ligands related to the methods presented in Sect. 15.2.2.3, we will describe them here separately. All approaches and their applicability for brain delivery with or without the already mentioned targeting ligands have been reviewed previously so we will therefore limit our discussion to a brief presentation of the methods and refer the reader to previous reviews for more detailed information.

The first approach is the use of dendrimers, of which poly(amido amine) (PAMAM) is perhaps the most well known. Dendrimers are macromolecules containing repetitive elements that can be used for drug delivery. This can be done by direct conjugation of drug to the dendrimer, noncovalent ionic interaction, or by encapsulation of drug in a micellar structure formed by the dendrimers. The use of dendrimers for brain delivery has recently been reviewed (Beg et al. 2011).

Solid lipid nanoparticles (SLNs) consist of spherical solid lipid particles in the nanometer range, which are dispersed in water or in aqueous surfactant solution and have the potential to carry lipophilic or hydrophilic drug(s) or diagnostics (Bondi et al. 2012). The possible use of these particles for drug delivery and a comparison with polymeric nanoparticles has been described previously (Kaur et al. 2008).

More recently, a new particle was introduced, i.e., drug nanocrystals, which are particles made from 100 % drug and are stabilized by surfactants. Nanocrystals have been used for oral drug administration but can potentially be used for delivery

Table 15.1 Main CMC criteria for product quality and product safety of nanocarriers [based on FDA guidance document on Liposome drug products; (FDA 2002)]

Main criteria	Details
Product quality	Characterization of physicochemical properties of the end-product, such as – Size, charge, and morphology – Encapsulation degree – Phase transition temperature – In vitro release of drug substance
Control of excipients	For each of the separate constituents it is necessary to have: – A full description and characterization – Manufacturing specifications – Stability data
Manufacturing process and process controls	During the manufacturing process reproducibility and sterility need to be demonstrated, also during the upscaling of the production process
Control of drug product	Assays for encapsulated and free drug substance and for nanocarrier components, including degradation products
Stability	Shelf-life; physical and chemical stability

of drugs to the brain after intravenous administration (Muller and Keck 2012). Finally, two more methods to mention are nanoemulsions (Ganta et al. 2010) and micellar formulations. These two methods include the use of several formulations made of different detergents, polymers, or lipids.

15.2.3 Points to Consider for Regulatory Approval

Translating basic (academic) findings into clinical practice requires regulatory approval from governmental bodies. However, it is not yet fully clear what exactly will be required for newer nanomedicine applications such as nanocarriers (Sanhai et al. 2008). Based on the Guidance for Industry documents from the FDA (2002, 2006), we found that a nanocarrier should meet many criteria (Fig. 15.1) related to pharmaceuticals, pharmacology, and safety before receiving approval to be tested in clinical research. These criteria are discussed in the sections below along with the idea that keeping to these criteria should result in a "definable product."

15.2.3.1 Pharmaceuticals

Besides the general CMC documentation supplied by the FDA (FDA-CMC overview), the Draft Guidance FDA document on Liposome drug products provides the most extensive regulatory information on liposomes (FDA 2002); this document can, to a large extent, also be applied for other nanoparticles. Table 15.1 provides an overview of criteria from this guidance document that should be taken into consideration.

In addition, a strict controlled manufacturing process should ensure that there are no batch-to-batch differences arising during the nanocarrier production. Reproducibility should also be demonstrated by multiple batches at different production scales. Critical manufacturing parameters (e.g., shear force, temperature) should be identified and evaluated, particularly during the scale-up of the production process (FDA 2002). Obtaining a sterilized end product can be challenging as nanoparticle components can block filters or interact with the filter matrix, causing the filters to be ineffective or a loss of material.

The size, particle size distribution, and charge are often the first characterization steps after preparation of nanocarriers. Using dynamic light scattering (DLS) techniques allows relatively easy measurements of these parameters. The size does influence the capacity for drug loading (encapsulation), especially since the volume of spherical vesicles increases or decreases with the radius to the third power ($V = {}^4/_3\pi r^3$). In addition, the size will also influence the biodistribution; this will be discussed in more detail in the section on pharmacological properties (Sect. 15.2.3.2). The drug loading efficiency, in turn, is dependent not only on size but also on the nanocarrier constituents and specific interaction with the drug. For example, the charge or hydrophilicity of the lipids or polymers will influence the interaction between nanocarrier constituents and the drug. Furthermore, the method of loading can greatly enhance the loading efficiency. For liposomes, the loading can be achieved either via passive loading (phospholipids dispersed in aqueous solvent containing the drug spontaneously forming concentric bilayers separated by narrow aqueous compartments with relatively low encapsulation efficiency (Mufamadi et al. 2011)) or via remote loading (drugs are loaded into preformed liposomes using a transmembrane pH or salt gradient reaching encapsulation efficiencies of 80–100 % (Zucker et al. 2009; Tazina et al. 2011)). The higher encapsulation efficiency associated with remote loading increases the drug-to-lipid ratio, which increases the chance to deliver enough drug without reaching the limits of lipid or particle toxicity.

An optimal and reproducible encapsulation efficiency needs to be demonstrated using validated analytical assays of the active substance as well as the nanocarrier components, targeting moiety, and other excipients. The analytical assay needs to discriminate between encapsulated and the released or non-encapsulated (free) drug substance. All nanocarrier components need to be well defined and the source (synthetic or biological) and certificates of origin and analysis need to be provided together with their stability data.

Once a nanocarrier product is manufactured and characterized, physical and chemical stability and shelf-life need to be determined. Nanoparticles are susceptible to fusion, aggregation, and leakage of the drug during storage. Both the drug and the nanocarrier itself are susceptible to change, and therefore this might influence the quality, safety, and efficacy of the product. This requires extensive testing of all components. Lipids can degenerate by oxidative stress or hydrolyze to form (toxic) lysolipids (Parnham and Wetzig 1993; Lutz et al. 1995). This process is studied using the normal storage conditions of the drug product (e.g., 2–8 °C), but nanocarriers are also exposed to stress conditions to characterize the physical state of the

carrier and to test the release of the drug from the carrier. All this should ultimately be performed in the final production scale and in the vials or containers intended for clinical use. For liposomal doxorubicin hydrochloride, the FDA has suggested several conditions for this in vitro drug leakage testing, including incubation in human plasma at 37 °C, exposure to a range of pH values and temperatures and low-frequency ultrasound disruption, all in an attempt to mimic in vivo conditions (FDA 2010).

Finally, in case changes in manufacturing processes are necessary, these changes should be made according to the guidance for Changes to an approved New Drug Application (NDA) or abbreviated NDA (ANDA) (FDA 2004) to assure that post-change products are identical to prechange products.

15.2.3.2 Pharmacology

Pharmacology criteria include the determination of pharmacokinetics (PK; see Hammarlund-Udenaes 2014) and biodistribution. It is important to determine the fate of the nanocarrier and the encapsulated drug in the body after administration and to answer some related questions: Is the drug released? Are there any (toxic) degradation products formed? Is there a prolonged circulation because of pegylation? Even if the answers are already known for the free drug, it is important to determine them for the nanocarrier encapsulated drug as well, as this will most likely influence the drug's disposition in the body (Gaillard et al. 2011; Nystrom and Fadeel 2012) and in the brain. In addition to the PK and biodistribution, the efficacy of brain delivery as well as the efficacy of the encapsulated drug needs to be determined. In this section we will therefore focus on the in vitro and in vivo models that can be used to determine transport across the blood-brain barrier.

In vivo models are generally less suitable for detailed mechanistic studies since the number of controls needed for solid experimental proof in such studies cannot easily be performed in that way. Therefore, reliable in vitro models may give a better insight into the mechanism of brain uptake. However, nanocarriers, like liposomes, may exhibit a nonspecific cell uptake in vitro, complicating in vitro brain uptake assays and potentially concealing the influence of specific drug release mechanisms that operate in vivo. Brain uptake in vitro is often studied in the so-called in vitro BBB models; there are many examples: monoculture models of (immortalized) brain capillary endothelial cells, coculture models of astrocytes or pericytes and endothelial cells, and even triculture models [see for reviews: (Deli et al. 2005; Wilhelm et al. 2011)].

To determine PK and biodistribution in vivo, no specific models are necessary, but one should keep in mind that metabolic pathways and/or tissue distribution patterns can be different in different species and may be different in diseased animals compared to healthy animals. The bioanalytical methods that are used to determine the PK and biodistribution should be validated; for nanocarriers, these methods should preferably be able to discriminate between the free drug and the nanocarrier-encapsulated drug (FDA 2002).

When investigating nanocarriers for drug delivery to the brain, brain uptake is of course an important hallmark of biodistribution studies. Most commonly used are measurements of drug in brain homogenates, often after whole body perfusion to remove blood from the brain. Although this method is useful, there will always be some blood contamination in the brain homogenates, which may lead to false positive results especially when long circulating nanocarriers are used. Therefore, other methods have been developed to quantify drug delivery to the brain. In situ brain perfusion avoids the blood contamination by perfusion of the brain with a known drug concentration in the perfusion fluid (e.g., plasma or saline) (Smith and Allen 2003); however, this method is limited to fast (max. 30 min) penetrating compounds, thereby missing the potential benefit of the long circulating properties of the nanocarriers. Taking brain homogenates, either after "normal" administration or after in situ brain perfusion, will allow for discrimination between encapsulated drug and free drug, assuming that homogenization alone does not affect the integrity of the nanocarrier.

In vivo brain microdialysis seems to be one of the most suitable techniques for characterizing the influx and efflux transport functions across the BBB under physiological and pathological conditions (de Lange et al. 2000; Deguchi 2002; Chaurasia et al. 2007). A microdialysis probe has a semipermeable membrane, which allows small, water-soluble solutes to cross by passive diffusion. Therefore, in contrast to brain homogenate samples, microdialysis reflects free drug concentrations, not the total drug loading of the nanocarriers. Together with researchers from Uppsala University, we have investigated the brain delivery of glutathione pegylated liposomal DAMGO and compared this to free DAMGO using microdialysis (Lindqvist et al. 2012); at a similar free drug concentration in plasma, approximately twofold more DAMGO was measured in brain interstitial fluid after administration in glutathione-pegylated liposomes. Microdialysis as a preclinical and clinical tool has been available for two decades, yet, there is still uncertainty about the use of microdialysis in drug research and development, both from a methodological and a regulatory point of view (Chaurasia et al. 2007), and this is further complicated by the use of nanocarriers that cannot cross the semipermeable membrane by themselves. Ultimately the acceptance of microdialysis as a regulatory tool will be dependent upon the correlation of microdialysis results with clinical responses. Thus, validation will be the key to regulatory acceptance of the methodology (Chaurasia et al. 2007).

More recently, open-flow microperfusion has been developed for continuous glucose and lactate monitoring, and subsequently for dermal drug sampling (Holmgaard et al. 2012). It is currently also in development for brain drug sampling [e.g., in ongoing collaborative studies with Drs. Frank Sinner and Thomas Birngruber, Joanneum Research, Graz, Austria]. Like microdialysis, this technique is based on measuring the concentration of compounds in tissue using a probe. The probe used for open-flow microperfusion, however, has microscopic perforations instead of a semipermeable membrane, which makes it suitable for larger and lipophilic compounds, including nanocarriers.

Cerebrospinal fluid (CSF) sampling is also used to determine brain uptake. However, it is important to realize that the CSF drug concentration may not always

represent the free drug concentration in the brain (de Lange and Danhof 2002; Lin 2008; Hammarlund-Udenaes 2009). Furthermore, in our experience CSF samples can be contaminated with blood, especially when the study is performed in smaller animals. Blood contamination of CSF samples is a particular problem when using long circulating nanocarriers, as plasma can still contain high concentrations of the investigated drug, creating high variability and a false-positive result of drug levels in CSF samples, even when performed at specialist contract laboratories (data not shown).

Other, more experimental methods to determine brain uptake of nanocarrier drugs include the (invasive) cranial window and noninvasive methods such as positron emission tomography (PET), single-photon emission computed tomography (SPECT), magnetic resonance imaging (MRI), or computed X-ray tomography (CT). The cranial window technology is based on in vivo imaging of brain tissue using two-photon laser scanning microscopy and animals (usually mice) with a cranial window or thinned skull (Helmchen and Denk 2005; Shih et al. 2012). Brain delivery of nanocarriers with fluorescent cargo can be imaged using this technology; however, no distinction can be made between free and encapsulated drug other than by particle morphology. In addition, BBB integrity can be altered locally by the experimental procedure, leading to local point bleeds and extravasation of drugs from the vasculature (personal observations). The noninvasive techniques require the addition of a radiolabel to be able to measure the brain uptake (Wong et al. 2011). For this it is important to take into account which part is labeled, i.e., the encapsulated drug or (part of) the nanocarrier, when interpreting the outcomes.

In vitro efficacy models that are used for single active moieties, such as tests for receptor occupancy, are not suitable for nanocarrier-based drugs, as the drug first needs to be released from the nanocarrier. Efficacy of a drug product should, therefore, be determined in a relevant animal model. It would go too far to discuss *all* available disease models in this chapter. However, we would like to point out that models should be validated and the right controls (free drug, targeted vs. nontargeted nanocarriers, targeting ligand controls, etc.) should be used to compare the efficacy of the investigated nanocarrier-encapsulated drug. Since nanocarriers influence the PK and biodistribution of a drug, one should take into account that the efficacy parameters might then also change. For example, the time points at which the efficacy is measured may need to be adapted compared to investigations into the free compound. Finally, from a development cost perspective, in vivo efficacy studies should preferably be short-term and in small animal models.

15.2.3.3 Safety

Since most publicly available information focuses on the content of nanocarriers, i.e., the active substance, only limited information is available about possible adverse effects of the nanocarrier components themselves. Szebeni and colleagues have investigated complement activation by liposomes that could occur after intravenous administration (Szebeni et al. 2010, 2011). In most people the symptoms

remain subclinical, even though significant complement activation may occur (Szebeni et al. 2010). Addition of PEG did not decrease complement activation in pigs (Szebeni et al. 2012), although opsonisation by proteins and scavenging by the reticuloendothelial system (RES) was decreased (Gabizon 2001). Complement activation-related pseudoallergy (CARPA), an acute hypersensitivity or infusion reaction, does occur not only with liposomal nanocarriers but also with other (polymeric) nanocarriers such as dendrimers, PEGs, and polaxamers, and its severity usually declines after repeated administration (Jiskoot et al. 2009; Duncan and Gaspar 2011). Other immunological risks include antibody formation against any of the substituents of the nanocarrier, including the targeting ligand and the active drug, and these antibodies can either lead to an accelerated blood clearance (reducing the bioavailability and efficacy) or to a burst-release through complement-mediated lysis of the nanocarrier (resulting in increased blood concentration and possibly toxicity) (Jiskoot et al. 2009). An immune response in itself does not need to be a problem as long as it is rapidly deactivated; however, a severe pathology can occur when the defense response is anomalous in extent or duration (Boraschi et al. 2012).

Toxicity of polymeric nanoparticles is an important issue, yet very difficult to discuss in general, since the different polymers and methods that are used in the large amount of studies undoubtedly lead to different toxicity profiles (Kean and Thanou 2010). General remarks on toxicity are probably not valuable, but safety has to be determined for each different nanoparticle formulation. Concerning brain delivery it is important to appreciate that toxicity may lead to (temporary) blood-brain barrier opening that will influence the delivery of drug to the brain and potentially even lead to neurotoxicity (Rempe et al. 2011).

For treatments that are being developed for brain diseases it is also important to show that, next to general toxicities, there are no particle- or drug-induced CNS-related toxicities, such as behavioral effects. In the preclinical development of 2B3-101, we have therefore included EEG measurements and a modified Irwin test to demonstrate that there was no change in neurobehavior (Gaillard et al. 2012).

15.2.3.4 Therapeutic Window

Together, the pharmacology and safety studies will determine the therapeutic window (also called therapeutic index). It is important to determine whether the drug delivered to the brain by a nanocarrier can exert an effect at a concentration that is below the maximum tolerated dose. Furthermore, side effects of the drug under investigation should be acceptable with respect to the severity of the disease/condition being treated; this consideration of potential costs versus benefits will obviously depend on the disease the drug is used for, e.g., the side effects of chemotherapy are usually more severe, yet acceptable, compared to anti-migraine treatments. To obtain regulatory approval and the possibility to continue the development of nanocarrier treatments for brain diseases, the therapeutic index is therefore a very important decision point.

15.3 Future Challenges/Directions

One can appreciate that if the clinical development of a single active moiety already requires a stringent development plan with ample decision points, this is even more complicated for nanocarrier drugs, consisting of multiple constituents besides the active pharmaceutical ingredient (API). Previously we have discussed ten key development criteria that are important for drug delivery to the brain [Table 15.2, (Gaillard 2010; Gaillard et al. 2011)]. We will now highlight some important considerations for optimizing the *nanocarrier* drug development process and minimizing costs as much as possible (Gray 2014).

15.3.1 Preparation and Characterization of Nanocarriers

Currently, the FDA and EMA only have draft guidelines for liposomal products and combined drug products. The criteria in these guidelines, therefore, need to be reviewed on a case-by-case basis for the development of other nanocarriers. For example, drug loading into liposomes can be done using a salt gradient of either ammonium sulfate (used for Doxil/Caelyx), or calcium acetate. Although this technique is not specifically mentioned in the draft guideline for liposome products, the remaining salt concentration after completing the drug loading needs to be determined from a CMC perspective.

15.3.2 Delivery and Efficacy of Brain-Targeted Nanocarriers

When it comes to evaluating the pharmacokinetics and efficacy, it is important to avoid false-positive and false-negative results by selecting the most suitable read-out/model and including the appropriate controls. Due to the complex nature of nanocarriers this will require more effort, compared to single moieties.

Table 15.2 Ten key development criteria for blood-to-brain drug delivery [from: (Gaillard 2010; Gaillard et al. 2011)]

Targeting the blood-brain barrier	Drug carriers	Drug development from lab to clinic
1. Proven inherently safe receptor biology in humans	6. No modification of active ingredient	8. Low costs and straightforward manufacturing
2. Safe and human applicable ligand	7. Able to carry various classes of molecules	9. Activity in all animal models
3. Receptor-specific binding		10. Strong IP protection
4. Applicable for acute and chronic indications		
5. Favorable pharmacokinetics		

Administration of brain-targeted nanocarriers has typically utilized either intravenous or intraparenchymal routes. For chronic disorders, it could be more patient friendly as well as cost-effective to use other administration routes, such as subcutaneous, intramuscular, or oral. These routes are, however, even more complex to explore initially so usually the intravenous route is preferred.

15.3.3 Safety of Brain-Targeted Nanocarriers

Many of the safety findings associated with the use of nanocarriers per se are immunologic in nature. Nanocarriers can be optimized with regard to their shape, size, surface charge, and chemical composition; these characteristics will influence whether the nanocarrier is eliminated, tolerated, or ignored by the immune system (Boraschi et al. 2012). In addition, the route of administration almost certainly influences the risk of immunological responses (Jiskoot et al. 2009). By changing the route of administration from intravenous to other routes, infusion reactions that are observed with several types of nanocarriers may also be avoided. Clinically, infusion reactions are often managed by dilution, a longer infusion time or patient premedication; however, it is still important to predict potential problems and, if possible, to eliminate them (Duncan and Gaspar 2011).

15.3.4 Clinical Research

There is still a strong need for the development of treatments for patients with devastating brain diseases and for this, clinical research in human subjects is necessary. Providing preclinical proof that the investigational product is safe is one consideration, while regulatory aspects make up another. Wolf and Jones (2011) have recently reviewed whether or not it is necessary to have extra oversight, i.e., additional approval processes beyond the current institutional review boards (IRB) for emerging technologies such as nanocarriers. They claim that there is a heightened uncertainty regarding the risks in fast-evolving science, yielding complex and increasingly active materials. This, together with the likelihood of research on vulnerable participants (e.g., cancer patients) and potential risks to others beyond the research participant could warrant the need for extra oversight, particularly for more chronic treatments.

15.4 Conclusions

Since the approval of the first nanocarrier (pegylated liposomal doxorubicin) in 1995, much progress has been made towards the clinical development of nanocarriers. However, brain-targeted nanocarriers are lagging behind mainly because of the

added challenges associated with delivery to the brain and other inherent difficulties in CNS drug development. It is not realistic to expect the development of a magic bullet for brain diseases; however, combining safe targeting ligands and receptors with well-known and safe nanocarrier technologies, brain-targeted nanocarriers may soon be able to enhance drug delivery to the brain and impact clinical treatment.

15.5 Points for Discussion

To strengthen research towards clinically applicable nanocarriers for drug delivery to the brain, we encourage a scientific discussion among researchers from industry and academia on the following points:

- Improving the safety of nanocarriers and ensuring the use of safe ligands and receptor biology, as this will improve clinical applicability
- Taking the cost of the product into account, i.e., it is of course exciting to design a complicated new drug product with many different components but this may come at a steep price when thinking about translation to successful clinical development!
- Taking the route of administration into account, especially for chronic administration

References

Ali J, Ali M, Baboota S, Sahani JK, Ramassamy C, Dao L, Bhavna (2010) Potential of nanoparticulate drug delivery systems by intranasal administration. Curr Pharm Des 16(14): 1644–1653

Bankiewicz K (2014) Neurosurgical approaches: drug infusion directly into the parenchyma or cerebrospinal fluid. In: Hammarlund-Udenaes M, de Lange E, Thorne R (eds) Drug delivery to the brain—physiological concepts, methodologies and approaches. Springer, New York, Chapter 20 of this book

Banks WA (2008) Delivery of peptides to the brain: emphasis on therapeutic development. Biopolymers 90(5):589–594

Beg S, Samad A, Alam MI, Nazish I (2011) Dendrimers as novel systems for delivery of neuropharmaceuticals to the brain. CNS Neurol Disord Drug Targets 10(5):576–588

Bhaskar S, Tian F, Stoeger T et al (2010) Multifunctional Nanocarriers for diagnostics, drug delivery and targeted treatment across blood-brain barrier: perspectives on tracking and neuroimaging. Part Fibre Toxicol 7:3

Bondi ML, Di Gesu R, Craparo EF (2012) Lipid nanoparticles for drug targeting to the brain. Methods Enzymol 508:229–251

Boraschi D, Costantino L, Italiani P (2012) Interaction of nanoparticles with immunocompetent cells: nanosafety considerations. Nanomedicine (Lond) 7(1):121–131

Brasnjevic I, Steinbusch HW, Schmitz C, Martinez-Martinez P (2009) Delivery of peptide and protein drugs over the blood-brain barrier. Prog Neurobiol 87(4):212–251

Chaurasia CS, Muller M, Bashaw ED et al (2007) AAPS-FDA workshop white paper: microdialysis principles, application and regulatory perspectives. Pharm Res 24(5):1014–1025

Costantino L, Boraschi D (2012) Is there a clinical future for polymeric nanoparticles as brain-targeting drug delivery agents? Drug Discov Today 17(7–8):367–378
Dadparvar M, Wagner S, Wien S, Kufleitner J, Worek F, von Briesen H, Kreuter J (2011) HI 6 human serum albumin nanoparticles–development and transport over an in vitro blood-brain barrier model. Toxicol Lett 206(1):60–66
Danhier F, Ansorena E, Silva JM, Coco R, Le Breton A, Preat V (2012) PLGA-based nanoparticles: an overview of biomedical applications. J Control Release 161(2):505–522
de Lange EC, Danhof M (2002) Considerations in the use of cerebrospinal fluid pharmacokinetics to predict brain target concentrations in the clinical setting: implications of the barriers between blood and brain. Clin Pharmacokinet 41(10):691–703
de Lange EC, de Boer AG, Breimer DD (2000) Methodological issues in microdialysis sampling for pharmacokinetic studies. Adv Drug Deliv Rev 45(2–3):125–148
de Vries NA, Beijnen JH, Boogerd W, van Tellingen O (2006) Blood-brain barrier and chemotherapeutic treatment of brain tumors. Expert Rev Neurother 6(8):1199–1209
Deguchi Y (2002) Application of in vivo brain microdialysis to the study of blood-brain barrier transport of drugs. Drug Metab Pharmacokinet 17(5):395–407
Deli MA, Abraham CS, Kataoka Y, Niwa M (2005) Permeability studies on in vitro blood-brain barrier models: physiology, pathology, and pharmacology. Cell Mol Neurobiol 25(1):59–127
Duncan R, Gaspar R (2011) Nanomedicine(s) under the microscope. Mol Pharm 8(6):2101–2141
Fabel K, Dietrich J, Hau P et al (2001) Long-term stabilization in patients with malignant glioma after treatment with liposomal doxorubicin. Cancer 92(7):1936–1942
Farrell D, Ptak K, Panaro NJ, Grodzinski P (2011) Nanotechnology-based cancer therapeutics–promise and challenge–lessons learned through the NCI Alliance for Nanotechnology in Cancer. Pharm Res 28(2):273–278
FDA (2001) Guidance for Industry: S7A Safety Pharmacology Studies for Human Pharmaceuticals. http://www.fda.gov/downloads/Drugs/GuidanceComplianceRegulatoryInformation/Guidances/UCM074959.pdf
FDA (2002) Guidance for Industry: Liposome Drug Products. http://www.fda.gov/downloads/Drugs/GuidanceComplianceRegulatoryInformation/Guidances/ucm070570.pdf
FDA (2004) Guidance for Industry: Changes to an approved NDA or ANDA. http://www.fda.gov/OHRMS/DOCKETS/98fr/1999d-0529-gdl0003.pdf
FDA (2006) Guidance for Industry and FDA Staff: Early Development Considerations for Innovative Combination Products. http://www.fda.gov/downloads/RegulatoryInformation/Guidances/ucm126054.pdf
FDA (2010) Draft Guidance on Doxorubicin Hydrochloride. http://www.fda.gov/downloads/Drugs/GuidanceComplianceRegulatoryInformation/Guidances/UCM199635.pdf
FDA-CMC Overview of CMC guidances. http://www.fda.gov/Drugs/GuidanceComplianceRegulatoryInformation/Guidances/ucm064979.htm
Fernandes C, Soni U, Patravale V (2010) Nano-interventions for neurodegenerative disorders. Pharmacol Res 62(2):166–178
Fortin D (2014) Osmotic Opening of the BBB for DRug Treatment for Brain Tumors (Focus on Methodological Issues). In: Hammarlund-Udenaes M, de Lange E, Thorne R (eds) Drug delivery to the brain—physiological concepts, methodologies and approaches. Springer, New York, Chapter 21 of this book
Gabathuler R (2014) Development of new protein vecotrs for the physiologic delivery of large therapeutic compounds to the CNS. In: Hammarlund-Udenaes M, de Lange E, Thorne R (eds) Drug delivery to the brain—physiological concepts, methodologies and approaches. Springer, New York, Chapter 18 of this book
Gabizon AA (2001) Stealth liposomes and tumor targeting: one step further in the quest for the magic bullet. Clin Cancer Res 7(2):223–225
Gaillard PJ (2010) Crossing barriers from blood-to-brain and academia-to-industry. Ther Deliv 1(4):495–500
Gaillard PJ, Visser CC, Appeldoorn CCM, Rip J (2011) Enhanced brain drug delivery: safely crossing the blood-brain barrier. Drug Discov Today Technol 9(2):e155–e160

Gaillard PJ, Gladdines W, Appeldoorn CCM, et al. (2012) Development of glutathione pegylated liposomal doxorubicin (2B3-101) for the treatment of brain cancer. [abstract]. In: Proceedings of the 103rd Annual Meeting of the American Association for Cancer Research; 2012 31 Mar–4 Apr; Chicago, Illinois. Philadelphia (PA): AACR; 2012. Abstract nr 5687

Ganta S, Deshpande D, Korde A, Amiji M (2010) A review of multifunctional nanoemulsion systems to overcome oral and CNS drug delivery barriers. Mol Membr Biol 27(7):260–273

Garbayo E, Montero-Menei CN, Ansorena E, Lanciego JL, Aymerich MS, Blanco-Prieto MJ (2009) Effective GDNF brain delivery using microspheres—a promising strategy for Parkinson's disease. J Control Release 135(2):119–126

Geldenhuys W, Mbimba T, Bui T, Harrison K, Sutariya V (2011) Brain-targeted delivery of paclitaxel using glutathione-coated nanoparticles for brain cancers. J Drug Target 19(9):837–845

Gilead Sciences, Inc. (2000) Press Release; http://www.gilead.com/pr_969296575

Glas M, Koch H, Hirschmann B et al (2007) Pegylated liposomal doxorubicin in recurrent malignant glioma: analysis of a case series. Oncology 72(5–6):302–307

Gray D (2014) Pharmacoeconomical considerations of CNS drug development. In: Hammarlund-Udenaes M, de Lange E, Thorne R (eds) Drug delivery to the brain—physiological concepts, methodologies and approaches. Springer, New York, Chapter 15 of this book

Hammarlund-Udenaes M (2009) Active-site concentrations of chemicals—are they a better predictor of effect than plasma/organ/tissue concentrations? Basic Clin Pharmacol Toxicol 106:215–220

Hammarlund-Udenaes M (2014) PK concepts for brain drug delivery. In: Hammarlund-Udenaes M, de Lange E, Thorne R (eds) Drug delivery to the brain—physiological concepts, methodologies and approaches. Springer, New York, Chapter 6 of this book

Hau P, Fabel K, Baumgart U et al (2004) Pegylated liposomal doxorubicin-efficacy in patients with recurrent high-grade glioma. Cancer 100(6):1199–1207

Helmchen F, Denk W (2005) Deep tissue two-photon microscopy. Nat Methods 2(12):932–940

Holmgaard R, Benfeldt E, Nielsen JB et al (2012) Comparison of open-flow microperfusion and microdialysis methodologies when sampling topically applied fentanyl and benzoic acid in human dermis ex vivo. Pharm Res 29:1808–1820

Jiang W, Lionberger R, Yu LX (2011) In vitro and in vivo characterizations of PEGylated liposomal doxorubicin. Bioanalysis 3(3):333–344

Jiskoot W, van Schie RM, Carstens MG, Schellekens H (2009) Immunological risk of injectable drug delivery systems. Pharm Res 26(6):1303–1314

Jones AR, Shusta EV (2007) Blood-brain barrier transport of therapeutics via receptor-mediation. Pharm Res 24(9):1759–1771

Kaur IP, Bhandari R, Bhandari S, Kakkar V (2008) Potential of solid lipid nanoparticles in brain targeting. J Control Release 127(2):97–109

Kean T, Thanou M (2010) Biodegradation, biodistribution and toxicity of chitosan. Adv Drug Deliv Rev 62(1):3–11

Kim BY, Rutka JT, Chan WC (2010) Nanomedicine. N Engl J Med 363(25):2434–2443

Konofagou EE (2014) Emerging engineering technologies for opening the BBB. In: Hammarlund-Udenaes M, de Lange E, Thorne R (eds) Drug delivery to the brain—physiological concepts, methodologies and approaches. Springer, New York, Chapter 22 of this book

Kratz F (2008) Albumin as a drug carrier: design of prodrugs, drug conjugates and nanoparticles. J Control Release 132(3):171–183

Lin JH (2008) CSF as a surrogate for assessing CNS exposure: an industrial perspective. Curr Drug Metab 9(1):46–59

Lindqvist A, Rip J, Gaillard PJ, Björkman S, Hammarlund-Udenaes M (2012) Enhanced brain delivery of the opioid peptide DAMGO in glutathione PEGylated liposomes: a microdialysis study. Mol Pharm 10:1533–1541

Luppi B, Bigucci F, Cerchiara T, Zecchi V (2010) Chitosan-based hydrogels for nasal drug delivery: from inserts to nanoparticles. Expert Opin Drug Deliv 7(7):811–828

Lutz J, Augustin AJ, Jager LJ, Bachmann D, Brandl M (1995) Acute toxicity and depression of phagocytosis in vivo by liposomes: influence of lysophosphatidylcholine. Life Sci 56(2):99–106

Mishra V, Mahor S, Rawat A, Gupta PN, Dubey P, Khatri K, Vyas SP (2006) Targeted brain delivery of AZT via transferrin anchored pegylated albumin nanoparticles. J Drug Target 14(1):45–53
Morigi V, Tocchio A, Pellegrini CB, Sakamoto JH, Arnone M, Tasciotti E (2012) Nanotechnology in medicine: from inception to market domain. J Drug Deliv Article ID 389485, 7 pages. doi:10.1155/2012/389485
Mufamadi MS, Pillay V, Choonara YE, Du Toit LC, Modi G, Naidoo D, Ndesendo VM (2011) A review on composite liposomal technologies for specialized drug delivery. J Drug Deliv Article ID 939851, 19 pages. doi:10.1155/2011/939851
Muller RH, Keck CM (2012) Twenty years of drug nanocrystals: where are we, and where do we go? Eur J Pharm Biopharm 80(1):1–3
Nagpal K, Singh SK, Mishra DN (2010) Chitosan nanoparticles: a promising system in novel drug delivery. Chem Pharm Bull (Tokyo) 58(11):1423–1430
Nystrom AM, Fadeel B (2012) Safety assessment of nanomaterials: implications for nanomedicine. J Control Release 161(2):403–408
Palmieri D, Chambers AF, Felding-Habermann B, Huang S, Steeg PS (2007) The biology of metastasis to a sanctuary site. Clin Cancer Res 13(6):1656–1662
Pardridge WM (2010) Preparation of Trojan horse liposomes (THLs) for gene transfer across the blood-brain barrier. Cold Spring Harb Protoc (4): pdb prot5407
Parnham MJ, Wetzig H (1993) Toxicity screening of liposomes. Chem Phys Lipids 64(1–3): 263–274
Patel T, Zhou J, Piepmeier JM, Saltzman WM (2011) Polymeric nanoparticles for drug delivery to the central nervous system. Adv Drug Deliv Rev 64(7):701–705
Reddy MK, Wu L, Kou W, Ghorpade A, Labhasetwar V (2008) Superoxide dismutase-loaded PLGA nanoparticles protect cultured human neurons under oxidative stress. Appl Biochem Biotechnol 151(2–3):565–577
Rempe R, Cramer S, Huwel S, Galla HJ (2011) Transport of Poly(n-butylcyano-acrylate) nanoparticles across the blood-brain barrier in vitro and their influence on barrier integrity. Biochem Biophys Res Commun 406(1):64–69
Rip J, Appeldoorn CC, Manca FM, Dorland R, Van Kregten JM and Gaillard PJ (2010) Receptor-mediated delivery of drugs across the blood-brain barrier. Front. Pharmacol. Conference Abstract: Pharmacology and Toxicology of the Blood-Brain Barrier: State of the Art, Needs for Future Research and Expected Benefits for the EU. doi:10.3389/conf.fphar.2010.02.00025
Sanhai WR, Sakamoto JH, Canady R, Ferrari M (2008) Seven challenges for nanomedicine. Nat Nanotechnol 3(5):242–244
Shih AY, Mateo C, Drew PJ, Tsai PS, Kleinfeld D (2012) A polished and reinforced thinned-skull window for long-term imaging of the mouse brain. J Vis Exp pii(61):3742
Smith QR, Allen DD (2003) In situ brain perfusion technique. Methods Mol Med 89:209–218
Szebeni J, Alving CR, Baranyi L, Bunger R (2010) Interaction of liposomes with complement leading to adverse reactions. In: Gregoriadis G (ed) Liposome technology—volume III interactions of liposomes with the biological milieu, 3rd edn. Informa Healthcare USA, Inc, Zug
Szebeni J, Muggia F, Gabizon A, Barenholz Y (2011) Activation of complement by therapeutic liposomes and other lipid excipient-based therapeutic products: prediction and prevention. Adv Drug Deliv Rev 63(12):1020–1030
Szebeni J, Bedocs P, Rozsnyay Z et al (2012) Liposome-induced complement activation and related cardiopulmonary distress in pigs: factors promoting reactogenicity of Doxil and AmBisome. Nanomedicine 8(2):176–184
Tazina EV, Kostin KV, Oborotova NA (2011) Specific features of drug encapsulation in liposomes (a review). Pharm Chem J 45(8):481–490
Thorne R (2014) Intranasal drug delivery to the brain. In: Hammarlund-Udenaes M, de Lange E, Thorne R (eds) Drug delivery to the brain—physiological concepts, methodologies and approaches. Springer, New York, Chapter 16 of this book
Tsai CS, Park JW, Chen LT (2011) Nanovector-based therapeis in advanced pancreatic cancer. J Gastrointest Oncol 2:185–194

Ulbrich K, Hekmatara T, Herbert E, Kreuter J (2009) Transferrin- and transferrin-receptor-antibody-modified nanoparticles enable drug delivery across the blood-brain barrier (BBB). Eur J Pharm Biopharm 71(2):251–256

Ulbrich K, Knobloch T, Kreuter J (2011) Targeting the insulin receptor: nanoparticles for drug delivery across the blood-brain barrier (BBB). J Drug Target 19(2):125–132

van Rooy I, Cakir-Tascioglu S, Couraud PO et al (2010) Identification of peptide ligands for targeting to the blood-brain barrier. Pharm Res 27(4):673–682

van Rooy I, Hennink WE, Storm G, Schiffelers RM, Mastrobattista E (2012) Attaching the phage display-selected GLA peptide to liposomes: factors influencing target binding. Eur J Pharm Sci 45(3):330–335

Wagner S, Kufleitner J, Zensi A et al (2010) Nanoparticulate transport of oximes over an in vitro blood-brain barrier model. PLoS One 5(12):e14213

Wang JJ, Zeng ZW, Xiao RZ, Xie T, Zhou GL, Zhan XR, Wang SL (2011) Recent advances of chitosan nanoparticles as drug carriers. Int J Nanomedicine 6:765–774

Wilhelm I, Fazakas C, Krizbai IA (2011) In vitro models of the blood-brain barrier. Acta Neurobiol Exp (Wars) 71(1):113–128

Wilson B (2009) Brain targeting PBCA nanoparticles and the blood-brain barrier. Nanomedicine (Lond) 4(5):499–502

WMA (2008) World Medical Association Declaration of Helsinki. http://www.wma.net/en/30publications/10policies/b3/17c.pdf

Wohlfart S, Gelperina S, Kreuter J (2011) Transport of drugs across the blood-brain barrier by nanoparticles. J Control Release 161(2):264–273

Wolf SM, Jones CM (2011) Designing oversight for nanomedicine research in human subjects: systematic analysis of exceptional oversight for emerging technologies. J Nanopart Res 13:1449–1465

Wong HL, Wu XY, Bendayan R (2011) Nanotechnological advances for the delivery of CNS therapeutics. Adv Drug Deliv Rev 64(7):686–700

Zhang L, Gu FX, Chan JM, Wang AZ, Langer RS, Farokhzad OC (2008) Nanoparticles in medicine: therapeutic applications and developments. Clin Pharmacol Ther 83(5):761–769

Zucker D, Marcus D, Barenholz Y, Goldblum A (2009) Liposome drugs' loading efficiency: a working model based on loading conditions and drug's physicochemical properties. J Control Release 139(1):73–80

Chapter 16
Development of New Protein Vectors for the Physiologic Delivery of Large Therapeutic Compounds to the CNS

Reinhard Gabathuler

Abstract The central nervous system (CNS) is a sanctuary protected by several barriers; the major one being the blood–brain barrier (BBB). The BBB is formed by the specific nature of the endothelial cells of the brain capillaries only allowing brain access to nutrients necessary for brain cell survival and function.

These properties of the BBB result in the incapacity of therapeutic compounds small and large to reach the brain at therapeutic concentrations. Various strategies are now being developed to enhance the amount and concentration of these compounds in the brain parenchyma. The development of new technologies such as peptide vectors will achieve the delivery of active agents in therapeutic concentration across the BBB to treat brain diseases such as cancer or neurodegenerative disorders. New technologies are being developed and will be presented. Critical opinions will be given on these different platforms to point out their advantages and disadvantages.

16.1 Introduction

The overwhelming majority of small molecules, proteins, and peptides do not efficiently cross the BBB. Usually therapeutics need to be present at high concentration in the blood in order to cross the BBB and reach the brain, often resulting in unacceptable toxicity in the periphery. The most important factors determining to what extent a small molecule will be delivered from blood into the CNS are lipid solubility, molecular mass, and charge (Lipinski et al. 2001). These structural characteristics allow for passive penetration of the molecules across the BBB.

R. Gabathuler (✉)
biOasis Technologies Inc., Suite 600, 1385 West 8th Avenue,
Vancouver, BC, Canada V6H 3V9
e-mail: rgaba@videotron.ca

M. Hammarlund-Udenaes et al. (eds.), *Drug Delivery to the Brain*, AAPS Advances in the Pharmaceutical Sciences Series 10, DOI 10.1007/978-1-4614-9105-7_16,

Larger molecules such as biologics which are usually hydrophilic and neutral present a very low brain penetration even with their much greater exposure due to a longer half-life in blood.

As the population ages, increasing numbers of patients will develop brain cancer or various neurodegenerative diseases, creating a great unmet need for therapies which can effectively cross the BBB. The existing market for CNS diseases was $65B in 2006, dominated by antidepressant, stroke, epilepsy, and Alzheimer's medications. This market is forecast to increase to $105B in 2015, and includes many unmet therapeutic needs: brain cancer (primary and metastatic), Alzheimer's disease (AD), Parkinson's disease (PD), amyotrophic lateral sclerosis (ALS), multiple sclerosis (MS), psychiatric disorders, stroke, and infections (Jain 2007). The entire CNS drug market would increase drastically if new therapeutics were developed with incorporation of a brain delivery technology allowing efficient entry into the brain.

16.2 Problem for Brain Delivery of Therapeutic Compounds

The capillaries of the brain have evolved to constrain the movement of molecules and cells between blood and brain, providing a natural defense against circulating toxic or infectious agents. The relative impermeability of the BBB results from tight junctions between capillary endothelial cells formed by cell adhesion molecules. Brain endothelial cells also possess few alternate transport pathways (e.g., fenestra, transendothelial channels, pinocytotic vesicles), and express high levels of active efflux transport proteins, including P-glycoprotein (P-gp, MDR-1 or ABCB1). The BBB maintains an essential brain homeostasis but as a result represents a great impediment to the effective treatment of many brain diseases (Pardridge 1993, 1998).

The BBB also has additional enzymatic aspects. Solutes crossing the cell membrane are subsequently exposed to degrading enzymes present in large numbers inside the endothelial cells that contain large densities of mitochondria, metabolically highly active organelles (Brownlees and Williams 1993).

The "classical" neuropharmaceutical agents in the market or in clinical trials are typically less than 600 Da in molecular weight with a sufficient degree of solubility allowing their passive BBB penetration. Based both on the lipid solubility and molecular mass, the passage of neuropharmaceuticals that fall into the category of peptide-based drugs, neuroactive peptides, neurotrophic factors, cytokines, monoclonal antibodies (mAb), and nucleotide-based agents such as oligonucleotides and genes will be impeded by the BBB. Therefore new technologies have to be developed to address this problem. Also, the development of an efficient gene vector is a key-limiting factor for brain gene therapy.

In recent years, convincing data have been published showing how neurotrophic factors can modulate neuronal transmission and prevent neuronal degeneration (Bonner and Peskind 2002; Tyler et al. 2002). The administration of nerve growth factor (NGF) and glial cells derived neurotrophic factor (GDNF) may slow down

the progression of neurodegenerative diseases such as Parkinson's disease (PD) and Alzheimer's Diseases (AD). However, NGF and other peptidic neurotrophic factors such as GDNF do not significantly penetrate the BBB from the circulation. For neurotrophic factors to be efficient for the treatment of brain disorders, they need to be administered intracranially, e.g., using catheters. Therefore any easy administration and greater clinical usefulness of NGF and other neurotrophic factors as a potential CNS therapy will depend on the use of a suitable carrier system that enhances its transport through the BBB.

Trastuzumab (Herceptin), a humanized monoclonal antibody, recognizes an extracellular domain of HER2 and when delivered together with chemotherapy, trastuzumab improves survival for patients with metastatic breast cancer that overexpress HER2 (Slamon et al. 2003). However, when patients with metastatic breast cancer are treated with trastuzumab, the breast cancer frequently progresses in the CNS (Bendell et al. 2003). 50 % of the women who developed CNS disease died from neurological decline. The correlation between HER2 overexpression of primary breast cancers and subsequent brain metastases is 97 % (Fuchs et al. 2002). Instead, progressive CNS disease probably results from poor penetration of trastuzumab into the brain. Trastuzumab is a relatively large protein with a molecular weight of 148,000. Therefore, it would not be expected to cross the BBB. Using intracerebral microinfusion of trastuzumab, Grossi et al. (2003) has demonstrated that HER2-overexpressing brain metastases are susceptible to HER2-targeted therapy. To maximally control this CNS disease, clinicians will need to overcome the challenge of delivering HER2-directed therapies across the BBB.

In response to the insufficiency in conventional delivery mechanisms, aggressive research efforts have recently focused on the development of new strategies to more effectively deliver drug molecules to the CNS.

16.3 Endogenous Mechanisms Used to Cross the BBB

Crossing the BBB remains a key obstacle in the development of drugs for brain diseases despite decades of research (De Boer and Gaillard 2007; Misra et al. 2003; Gabathuler 2010a, b). Multiple mechanisms are used by essential nutrients to reach brain cells, from the usage of transporters for small molecules like amino acids or glucose or of receptor-mediated transcytosis for larger molecules.

- Hydrophilic molecules such as amino acids, glucose, and other small molecules necessary for the survival of brain cells use transporters expressed at the luminal and basolateral side of the endothelial cells.
- Larger hydrophilic molecules such as hormones, transferrin for iron and lipoproteins use specific receptors that are highly expressed on the luminal side of the endothelial cells for transcytosis across the BBB to provide necessary nutrients to brain cells.

- Few small hydrophilic molecules can use the paracellular pathway between the endothelial cells forming the microvasculature of the brain.
- Lipophilic molecules can diffuse passively across the BBB into the brain. These molecules are exposed first to efflux transporters (P-gp and others) highly expressed on the luminal side of the BBB if not they will be exposed to degrading enzymes localized in the cytoplasm of endothelial cells.

16.4 Approaches Used to Cross the BBB

Three different approaches are currently used to reach the brain with therapeutic compounds: invasive, pharmacological, and physiological.

16.4.1 Invasive Approaches

Invasive approaches include all the methods associated with direct delivery of compounds in the brain parenchyma after surgery and comprise: (1) convection-enhanced delivery (CED), (2) intra-cerebro-ventricular (ICV) infusion, (3) intracerebral injection, (4) polymer or microchip systems which directly release therapeutics after implantation in the CNS and (5) disruption of the BBB using osmotic disruption, ultrasound, and bradykinin analogs such as RMP-7.

Invasive approaches usually need hospitalization of the patients which are costly and patient unfriendly. In addition drugs administered using such direct injection or infusion in the brain are obstructed to reach their site of action by a low diffusion rate in the cortex, resulting in an inability to reach therapeutic concentrations at the site of action.

16.4.2 Pharmacological Approaches

Lipidation and chemical modification of drugs are techniques used to improve their ability to diffuse across the BBB. In addition, formulation of drugs may facilitate brain delivery by passive diffusion due to the increased half-life and pharmacokinetic properties of the formulated drugs.

Chemical modifications of active drugs in order to increase their diffusion across the BBB may produce some unwanted effects such as decreasing their activity or increasing their interaction with plasma components and/or efflux pumps expressed at the BBB. These problems are associated with inefficient transport across the BBB and inability to reach therapeutic concentrations in the target area of the brain.

16.4.3 Physiological Approaches

Drugs can be modified to take advantage of BBB nutrient transport systems. Conjugation of drugs to ligands or antibodies against receptors expressed at the BBB will allow the drug to be transported across the BBB by receptor-mediated transcytosis. The physiological approach is recognized by the scientific community as the one with the most likely chance to succeed.

This chapter will address the development of active peptides and of new protein/peptide vectors, which are able to carry therapeutic compounds such as biologics across the BBB to reach efficient dosage in the brain parenchyma using a physiologic approach.

16.5 Physiological Approaches

The brain requires essential substances for its survival, i.e., glucose, insulin, growth hormone, Low Density Lipoprotein (LDL), etc. Specific receptor and transporter molecules implicated in active transport into the brain recognize these substances. These receptor and transporter molecules are in turn highly expressed on the endothelial cells of the BBB. Taking into account the high perfusion of the brain along with an average distance of 40 μm between capillaries, the most effective way of delivering biopharmaceutical drugs may likely be achieved by targeting these essential internalizing (uptake) transport receptors or transporters at the BBB.

The physiological approach takes advantage of the specific characteristics of the endothelial cells forming the BBB and uses an endogenous mechanism to transport a CNS active drug to the brain. It is specific, very efficient and applicable to small and large therapeutics such as chemotherapeutics or biologics.

16.6 Transporter Mediated

Some peptides and small molecules can use specific transporters expressed on the luminal and abluminal side of the endothelial cells forming the BBB, examples are the Glucose transporters (Glut-1), amino acid transporters (Pardridge 1993). The characterization of these transporters has been reported in other reviews (Pardridge 1993; Gabathuler 2009, 2010a, b).

At least eight different nutrient transport systems have been identified, with each transporting a group of nutrients of similar structure. Only drugs that closely mimic the endogenous carrier substrates will be taken up and transported into the brain.

One can modify drugs such that their transport is increased by using a carrier-mediated transporter expressed on the endothelial cells forming the BBB. Use of small molecules that directly target transporters to overcome BBB restrictions (Allen et al. 2003)

such as the choline transporter and the amino acid transporter has been done for few drugs. The BBB large neutral amino acid carrier has been used to deliver L-DOPA in Parkinson's disease (PD).

The use of transporters is usually not applicable for the transport of peptides and larger biologics across the BBB. The use of the glutathione transporter as a docking protein at the BBB is being developed for liposomes loaded with doxorubicin (Doxil) (Gaillard et al. 2009).

16.7 Receptor-Mediated Transcytosis

Large molecules necessary for the normal function of the brain are delivered to brain cells by specific receptors. These receptors are highly expressed on the endothelial cells forming the BBB. Some examples comprise the insulin receptor (IR), transferrin receptor (TR), and the Low-Density Lipoprotein Receptor-Related Protein (LRP).

It is thought that after ligand binding, the receptor is endocytosed at the luminal membrane, followed by the migration of vesicle across the cytoplasm or transcytosis and ends by the fusion of the vesicle to the abluminal side of the endothelial cell. The ligand is then exposed to the brain side and released from its receptor. The precise mechanism of the receptor transcytosis across polarized endothelial cells has not been determined. In addition, brain-targeted liposomes and nanoparticles with conjugated ligands and/or antibodies are used.

16.7.1 Use of Antibodies Against Receptors Expressed on Endothelial Cells of the BBB

Monoclonal antibodies (mAbs), ligands, and optimized ligand fragments binding to these receptor-mediated transcytosis systems are used to develop new peptide vectors for drug delivery to the brain. Monoclonal antibodies directed against highly expressed receptors at the BBB have been developed since the late 1980s (Pardridge 2010); receptors targeted by these antibodies have commonly been the transferrin and the insulin receptors. The ideal characteristics of these antibodies (also called BBB molecular Trojan horses) have historically been thought to include high-affinity binding (Pardridge 2010), but it has recently been shown that high-affinity mAbs may not have the adequate properties needed for efficient brain delivery of therapeutics. In short, high-affinity mAbs may be associated with inefficient release of the vector from the endothelial cells at the BBB (Yu et al. 2011; Atwal et al. 2011). It has also proven difficult to definitively identify receptor-mediated transport systems because receptors normally endocytosed in cells such as human brain endothelial cells can be transcytosed across these same cells when grown in astrocyte-conditioned medium as a monolayer mimicking the BBB (Benchenane

et al. 2005; Demeule et al. 2002). The use of high-affinity antibodies to TR for example may be a great way to deliver a payload to the endothelial cells but very little of this payload is seen associated with neurons or astrocytes in the brain parenchyma (Paris-Robidas et al. 2011; Moos and Morgan 2001).

16.7.1.1 Monoclonal Antibodies Against the Transferrin Receptor (TR)

Monoclonal antibodies generated against the TR expressed at the luminal membrane of the endothelial cells forming the BBB have been extensively used as vectors for the transport across the BBB of therapeutic molecules in the form of conjugates or on liposomes (Molecular Trojan Horse) (Pardridge 2007). These antibodies are characterized and selected for their high affinity for TR as described by Pardridge (2010) and do not affect the binding of holo-Tf to the TR. The function of the TR is to provide iron, an essential metal for cell survival. TR in endothelial cells is associated with the transcytosis of iron across the endothelial cells of the BBB. Drug targeting to the brain can be achieved by incorporating an anti-TR mAb (TRMAb) to the drug, which needs to be transported to the brain (Pardridge 2007, 2010).

Nanoparticles coated with TRMAb have been employed to transport drugs across the BBB. Human serum albumin nanoparticles covalently coupled to TRMAbs were used to transport loperamide across the BBB. Both types of nanoparticles were similarly efficient for the transport of loperamide across the BBB (Ulbrich et al. 2009).

16.7.1.2 Monoclonal Antibodies Against the Insulin Receptor (IR)

Pardridge et al. have extensively documented the use of IR for the targeted delivery of drugs to the brain using specific antibodies directed against the IR (Coloma et al. 2000), for example the 83-14 mouse mAb in Rhesus Monkey. These monoclonal antibodies have been selected for high affinity and no competition for insulin. Both chimeric antibody and a fully humanized form of the 83-14 antibody against human IR (HIR) have been created (Boado et al. 2008).

These BBB vectors based on mAb binding to specific receptors expressed at the BBB, also called Molecular Trojan Horses (Benchenane et al. 2005), are characterized by high-affinity binding (Pardridge 2007). These antibodies against IR have been extensively used by Pardridge et al. to deliver a variety of therapeutic compounds from antibodies, lysosomal enzymes, and neurotrophic factors to the brain in rodents and monkeys (Pardridge 2010). However, this technology has yet to go to human application.

16.7.1.3 Use of Bispecific Antibodies with Lower Affinities

Watts et al. (Atwal et al. 2011; Yu et al. 2011) showed that reducing the affinity of an antibody to the TR enhances the transport and release of the anti-TR antibody

across the BBB into the mouse brain where it can reach therapeutically relevant concentrations. Anti-TR antibodies that bind with high affinity to TR remain associated with the BBB, whereas lower affinity anti-TR antibody variants are released from the BBB into the brain and show a broad distribution 24 h after dosing (Atwal et al. 2011). The design of a bispecific antibody that binds with low affinity to TR and with high affinity to the enzyme β-secretase (BACE1) (Atwal et al. 2011) may allow its delivery to the brain at therapeutic concentration for the treatment of Alzheimer's disease. TR-facilitated transcytosis of this bispecific antibody across the BBB may enhance its potency as an anti-BACE1 therapy for treating Alzheimer's disease (Atwal et al. 2011).

16.7.1.4 Advantages and Problems with the Use of Monoclonal Antibodies to Receptors

High-affinity antibodies against the TR might be able to cross the BBB using a physiologic process called receptor-mediated transcytosis. However, recent work has suggested these antibodies bind to the endothelial cells forming the BBB but subsequently have difficulty detaching from the TR to be released into the brain parenchyma after transcytosis. Although the total brain uptake of antibodies against TR may appear high, with a large amount detected in the total brain fraction and accumulated in the brain endothelial cells, evidence of colocalization with neurons and astrocytes using specific antibodies against TR is lacking (Paris-Robidas et al. 2011). Using modified antibodies against TR with high, medium, and low affinities, anti-TR antibodies at trace doses showed a direct correlation between affinity and brain uptake, with lower-affinity antibodies showing the lowest uptake (Yu et al. 2011). In marked contrast to trace dosing, however, brain uptake of these same variants at much higher doses (20 mg/kg assessed at 1 and 24 h) showed an inverse correlation between affinity and brain uptake at 24 h and an increase in the brain-to-serum ratio of antibody (Yu et al. 2011). Furthermore, the lowest-affinity variant anti-TR showed a greater than fivefold increase in brain antibody concentration compared to control IgG 24 h after injection. This may be understood better by considering, for an antibody that recognizes only one site on TR, lowering antibody affinity for the TR may require a much higher amount (i.e., higher doses) to saturate all the TR. These high doses may produce unwanted side effects outside the brain. Any antibody manipulated in order to diminish its affinity for other targeted receptor developed for the transport of active molecules in the brain may have the same behavior and demonstrate potential side effects due to the high dosing needed.

It would be preferable to develop a vector with medium to low affinity for a receptor, which may demonstrate high-capacity binding. The lower affinity would be compensated by the high capacity of the receptor making such a receptor a good candidate for efficient transport across the BBB without the need to administer high concentration of drugs.

In addition, use of targeted liposomes and nanoparticles can have advantages: specific brain delivery properties, larger drug loading capacity, and the ability to disguise limiting characteristics of drugs using the physical nature of the liposomes or nanoparticles, thus minimizing toxicity and reduction of drug degradation in vivo.

Finally, the manufacturing of large fusion proteins composed of a targeting antibody and active molecule (heterodimers or trimers) may prove costly. Finally, the use of humanized antibodies in order to reduce immunogenicity may still result in immunogenicity of the new molecules synthesized.

16.7.2 Use of Ligand to Receptors Expressed on Endothelial Cells of the BBB

16.7.2.1 Use of Ligands to Low-Density Lipoprotein Receptor-Related Protein (LRP)-1

LRP is a multifunctional endocytosis receptor that mediates the internalization and degradation of ligands involved in diverse metabolic pathways [Hertz and Strickland 2001; Kounnas et al. 1995). LRP, a type I transmembrane protein, is synthesized as a 600 kDa precursor protein cleaved in the trans-golgi compartment by furin to generate a large 515 kDa subunit and a smaller 85 kDa subunit that remain noncovalently linked. The shorter cytoplasmic tail of LRP contains NPxY motifs and two dileucine-based motifs and interacts with a number of cytoplasmic adaptor and scaffold proteins (Yoon et al. 2007).

LRP interacts with a broad range of secreted proteins and resident cell surface molecules including apoE, α2M, tPA, PAI-1, APP, Factor VIII, and lactoferrin. LRP is expressed in many tissues including the CNS (Rebeck et al. 1993) and contains four putative-ligand binding domains (LBD) labeled with numerals I, II, III, and IV.

In the cerebellum, LRP expression was observed in neurons diffusely scattered throughout the granular cell layer and in astrocytes whereas moderate expression is reported in human cerebral and cerebellar astrocytes (Bu et al. 1994; Wolf et al. 1992; Moestrup et al. 1992). LRP expressed on neuronal cells functions similarly to the one found on other cell types in both binding and endocytosis of ligand. LRP is over-expressed in malignant astrocytomas, especially in glioblastomas (Yamamoto et al. 1997). A unique feature of LRP-1 is its rapid endocytosis rate, with the receptor on the cell surface able to internalize within 30 s ($t1/2 < 0.5$ min) (Li et al. 2000).

Tissue Plasminogen Activator (tPA) crosses the intact BBB independently of its proteolytic activity. This process is mediated through a receptor-dependent mechanism identified as a member of the LRP receptor family (Benchenane et al. 2005). LRP has been shown both in-vitro and in-vivo to be a high-capacity transport system that mediates transcytosis of protein (such as lactoferrin) from blood to brain (Yamamoto et al. 1997). These results confirm that in the in-vitro BBB model, LRP is a transcytosis receptor, in contrast to its role in other cell types such as glioblastomas or epithelial cells where LRP is an endocytosis receptor for clearance of

different ligands in the lysosomal compartment. This observation can be extended to other receptors such as TR for example (Paris-Robidas et al. 2011; Donoso et al. 2009; Nazer et al. 2008; Hussain et al. 1999).

The LRP-1 has recently been exploited to target drugs to the brain in a similar fashion as TR and IR. Contrary to descriptions (Pardridge 2010) referring to the work of Nazer et al. (2008) using a mini-LRP receptor mLRP4 (Obermoeller-McCormick et al. 2001) in an in-vitro barrier model composed of epithelial cells (MDCK), it has been demonstrated with multiple ligands that LRP is efficient in the transcytosis of molecules across the endothelial cells forming the BBB. This receptor, highly expressed at the BBB, presents some important advantages to the TR and IR system. LRP is characterized by a high transcytosis capacity due to its very short half-life at the cell surface, its constitutive internalization and multiple binding sites. LRP is able to bind multiple and diverse ligands from peptides to very large proteins such as activated α2-macroglobulin (700 kDa). No specific and unique amino acid sequence expressed on all these proteins is responsible for binding to LRP but certain configuration and contribution of positive charges may be responsible for interaction with LRP. Ligands to LRP have been shown to efficiently transport associated drugs across the BBB and be used as vectors for drug delivery to the brain.

Use of Apolipoprotein E, B, and A as a Vector for Brain Delivery

Apo E-, B-, and A-Coated Nanoparticles

Apolipoprotein E-, B-, and A- coated nanoparticles are able to transport drugs that normally cannot cross the BBB into the brain. An attractive aspect of this strategy for drug delivery to the CNS is that these particulate systems are nonspecific and that they can transport a wide range of drugs, peptides, proteins, and can carry a large payload of drug into the brain per particle which bypass efflux transporters (Zensi et al. 2009). Apo A-I human serum albumin nanoparticles are found within the endothelial cells of brain capillaries and within the brain parenchyma as detected by electron microscopy (Zensi et al. 2010).

The use of poly (butyl-cyanoacrylate) (PBCA) nanoparticles coated with polysorbate 80 (tween 80) loaded with active compounds such as analgesic peptides (dalargin) and chemotherapeutics such as doxorubicin results in a significant central pharmacological response in mice after intravenous injection (Wohlfart et al. 2011, 2012). It has been shown that polysorbate 80 (tween-80)-coated PBCA nanoparticles adsorb Apo E and B from the bloodstream after IV injection (Kreuter et al. 2002) and therefore use LRP for transcytosis across the BBB. The uptake mechanism of Apo-E modified nanoparticles on brain endothelial cells has been characterized and clearly demonstrates the participation of the LDL receptor-related protein, particularly LRP-1 (Wagner et al. 2011). These types of nanoparticles have been used for drug delivery to the brain since the mid-1990s (Kreuter et al. 2007; Kreuter et al. 2003; Steiniger et al. 2004). The precise mechanism of transcytosis has not been clarified (Olivier 2005) and is still debated.

Apolipoprotein A, B, or E Receptor Binding Sequence

Delivery of Apo B lysosomal enzyme fusion protein, glucocerebrosidase, and a secreted green fluorescent protein (GFP) to neurons and astrocytes in the CNS has been possible (Spencer and Verma 2007). Thus, the Apo B receptor (LDLR) binding peptide (38aa) can be used to deliver a protein to many tissues of the body in addition to delivery to the CNS. The length of the peptide (38aa) did not appear to greatly affect delivery or function of the recombinant protein. The Apo E receptor-binding site containing amino acid residues 152-168 functioned similarly to the Apo B sequence used (Spencer and Verma 2007).

Melanotransferrin (MTf, p97)

Melanotransferrin (MTf), also known as human melanoma-associated antigen p97, is expressed in two forms; a glycosyl-phosphatidyl-inositol (GPI) anchored membrane bound and secreted form (Jefferies et al. 1996; Food et al. 1994). Similar to transferrin (Tf), MTf is a sialoglycoprotein with a MW between 95 and 97 kDa (Food et al. 1994). Recombinant soluble form of MTf (80 kDa) is actively transported across the BBB in an in-vitro model of BBB trancytosis (Benchenane et al. 2005), with a transport rate 10–15 times higher than that of either Tf or lactoferrin (Demeule et al. 2002) and a preferential transport of MTf from the apical side to the basolateral side. Results from studies on the kinetics of binding and transport of MTf across the BBB are consistent with the presence of a medium-to-low affinity and high-capacity MTf receptor. The receptor is related to the family of LDL receptors and possibly involves a member of the low-density lipoprotein receptor-related protein family (LRP) that has been characterized as a transcytosis receptor at the BBB (Benchenane et al. 2005; Yamamoto et al. 1997; Li et al. 2000; Donoso et al. 2009).

Melanotransferrin (MTf, p97) is an endogenous shuttling protein that has clear potential as a BBB drug delivery vehicle with many advantages over existing delivery molecules or systems. First, MTf is a protein found at low levels (10 ng/mL) (Jefferies et al. 1996) in the blood of most normal individuals. Secondly, exogenously introduced MTf can be expected to localize in concert with the tissue distribution of the target receptor. Thirdly, because it is an autologous human protein, repeated treatments are unlikely to result in immune hypersensitivity or in elimination by neutralizing antibodies in clinical therapies. Finally, MTf having a relatively medium to low affinity for its receptor may not affect and compete for the binding and transport of other endogenous ligands of the receptor.

Previous studies have shown that p97 can cross the BBB and deliver iron (Moroo et al. 2003) and can also deliver doxorubicin and paclitaxel in the brain for the treatment of brain tumors (Gabathuler et al. 2005; Karkan et al. 2008). In addition, therapeutic compounds which are usually excluded from the brain by efflux pumps bypass these efflux carriers after association to MTf. Finally, it has been shown that MTf can direct and transcytose adenovirus (Ad5) through an in-vitro BBB model (Tang et al. 2007).

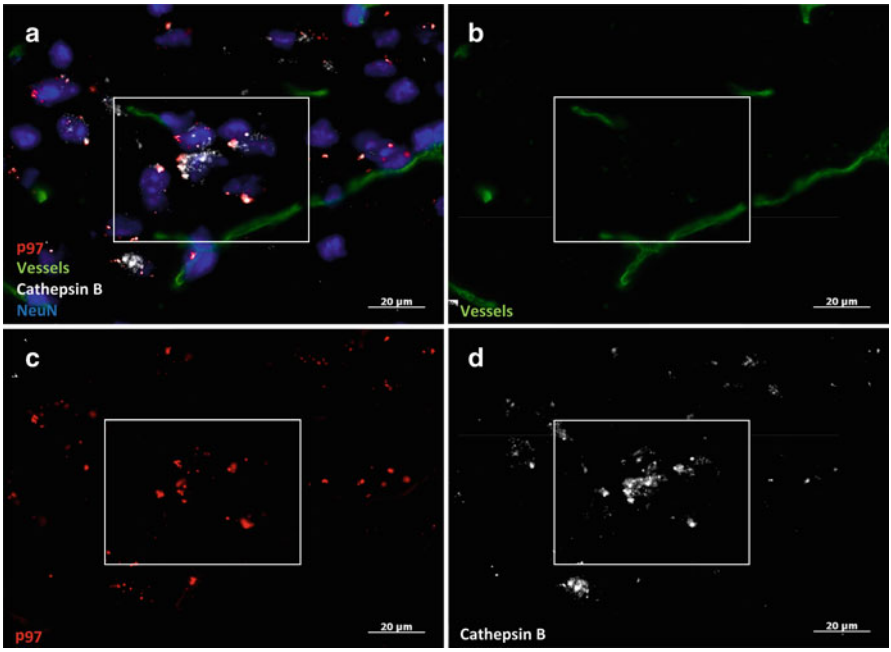

Fig. 16.1 Uptake of p97 in the lysosomes of neurons 2 h after IV administration in nude CD-1 mice: The fluorescent signals from Rhodamine-labeled p97 colocalized with cathepsin B, suggesting lysosomal localization for the p97-Rhodamine in vivo. Fluorescent microscopic images illustrating immunohistofluorescence staining for Cathepsin B (*white*) (**d**) in thin 10 µm brain sections of mice injected with p97-Rhodamine for 2 h (**c**). Cathepsin B is a lysosomal protein. On tissue sections, Cathepsin B, demonstrated staining around cell nuclei (i.e., perinuclear), similar to a lysosomal localization. Vessels are stained in *green* (**b**) and neuronal nuclei in *blue* (NeuN). Merged image shown in (**a**)

This technology is being developed for the design of new therapeutic compounds based on biologics such as enzymes and antibodies for their transport across the BBB at therapeutic concentrations.

Enzyme Replacement Therapy (ERT) has been developed to treat a number of lysosomal diseases. MPS I is a rare genetic Lysosomal Storage Disease (LSDs) which affects many systems of the body and which leads to organ damage. It is caused by a defect in the gene that codes an enzyme called alpha-L-iduronidase. After intravenous infusion the enzymes are picked up by the mannose-6-phosphate receptors expressed on the cells of the body and delivered to the lysosome. The lack of this receptor at the membrane of endothelial cells forming the BBB prevents them from entering the brain. MTf labeled with fluorescent dyes such as cy5.5 or rhodamine is transported 2 h after IV administration in mice in the lysosomal compartment of brain cells such as neurons, as shown by fluorescence microscopy (Fig. 16.1a–d). Our unpublished work has exploited MTf as a vehicle for delivery in the brain of the lysosomal enzyme alpha-L-iduronidase (IDU) in a mouse model of

Mucopolysaccharisosis I (MPS I). The results using the MTf-IDU fusion enzyme injected into mice MPS I show an increase in enzyme activity in the brain compared to the nonmodified enzyme. These results suggest that MTf can be used for the transport of the lysosomal enzymes in the brain for the treatment of lysosomal diseases affecting the CNS.

Other unpublished work conducted at biOasis Technologies Inc. and with the collaboration of the Institute for Biological Sciences at the NRC in Ottawa ON Canada, it has been demonstrated that MTf (Transcend) can transport and deliver large biologic molecules such as antibodies, e.g., anti-HER2 antibody (Trastuzumab, Herceptin), across the BBB into the brain after conjugation to MTf (Fig. 16.2a–c).

Receptor-Associated Protein

Other proteins such as receptor-associated protein (RAP) have been shown to be efficiently transported across the BBB into the brain parenchyma (Migliorini et al. 2003). RAP is found in the endoplasmic reticulum (ER) where it is a chaperone for the LDL receptor family, which includes LRP-1 facilitating its transport to the cell surface avoiding aggregation and interaction with endogenous ligands (Migliorini et al. 2003). The application of RAP as a drug carrier to the brain is being developed and currently under investigation with chemically conjugated anti-cancer agents and with fusion proteins (Prince et al. 2004).

Use of Angiopep Family of Peptides

Angiopep Family of Peptides Incorporated in Therapeutics

A new family of peptides derived from protein ligands of LRP (e.g., aprotinin) with high transcytosis capacity across the BBB has been designed as part of a new brain drug delivery system (Demeule et al. 2008a). Angiopep, a family of 19aa peptides derived from the putative LRP-1 binding sequence demonstrate high transcytosis rate (Demeule et al. 2008b; Che et al. 2010). This new platform technology is used as a brain delivery system for pharmaceutical agents that do not readily enter the brain and is applicable to small anticancer agents.

Fluorescence imaging studies of a cy5.5-Angiopep2 conjugate and immunohistochemical studies of injected Angiopep2 in mice demonstrated efficient transport across the BBB into the brain parenchyma and subsequent colocalization with the neuronal nuclei-selective marker NeuN and the glial marker Glial Fibrillary-Associated Protein (GFAP) (Fig. 16.3a–c) (Bertrand et al. 2010).

These Angiopep peptides are being developed as vectors to transport therapeutic agents to the brain parenchyma, the most advanced of which is ANG1005 formed by chemical conjugation of the peptide vector (Angiopep2) with three molecules of paclitaxel. Uptake of this new paclitaxel derivative, ANG1005, is related to the high level of expression of LRP-1 on the aggressive phenotype of glioblastoma cells

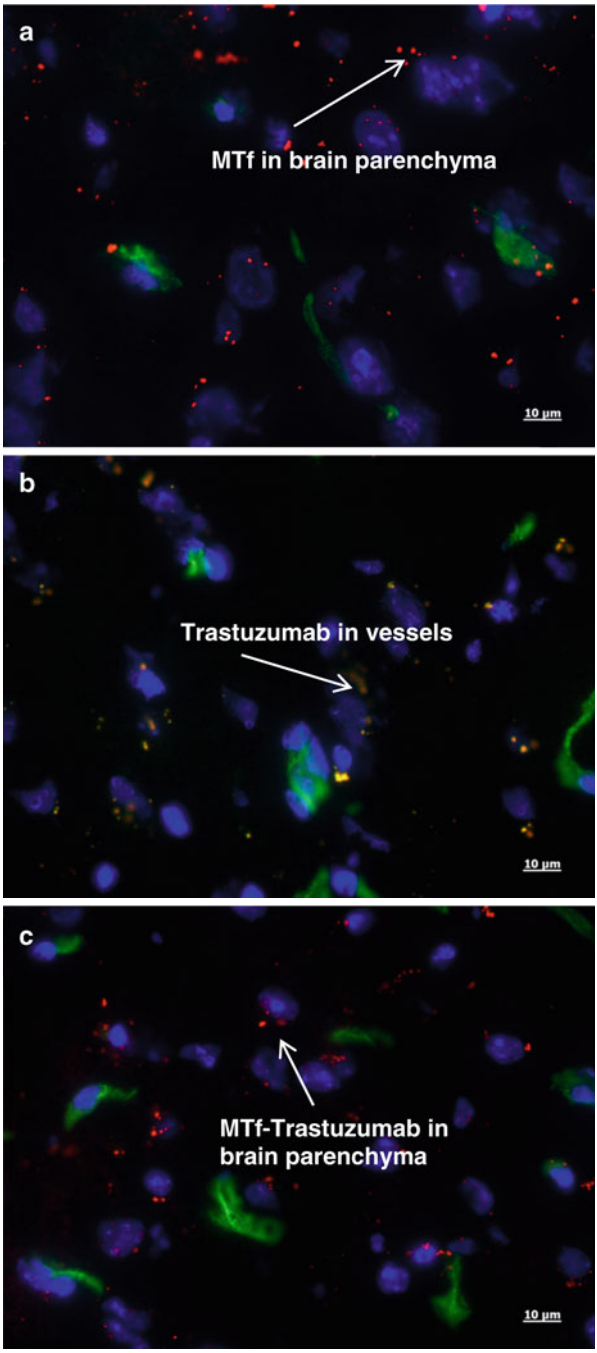

Fig. 16.2 Brain distribution of Rhodamine-labeled MTf, Trastuzumab, and MTf-trastuzumab conjugates 2 h after IV administration in nude CD-1 mice: The results indicate that there are more fluorescent signals in the brain for both MTf and MTf-Trastuzumab compared to Trastuzumab alone. Conjugation to MTf appears to allow for better delivery into the brain parenchyma. Trastuzumab appears to be present in most sections but appears to be associated with brain vessels at this time point (**b**) as seen in *yellow* when *green* and red are merged. (**a**) Fluorescent microscopic images of 10 **µ**m brain sections obtained from animals injected with MTf-Rhodamine (*red*, 2 h).

(Bertrand et al. 2011). Brain uptake measured by in-situ rat brain perfusion assay (Smith 2003; Takasato et al. 1984) shows 10 and 100-fold greater uptake into brain than peptide vector Angiopep2 and free drug paclitaxel, respectively (Thomas et al. 2009). Additional anticancer agents were manufactured in a similar way based on doxorubicin (ANG1007) and etoposide (ANG1009) as the active cytotoxic agents for the treatment of brain cancer and have shown high activity in preclinical studies (Demeule et al. 2010).

Following IV injection into mice, ANG1005 reached therapeutic concentrations in the brain parenchyma as measured by an increased survival of mice intracranially implanted with tumor cells and by analysis of the drug amount present in the brain parenchyma (Regina et al. 2008). This was confirmed in a set of data demonstrating regression of tumors in rats that had been intracranially implanted with U87 glioblastoma tumors cells and monitored by magnetic resonance imaging (MRI) (Bichat et al. 2008; Gabathuler 2010a, b).

This technology is to date the most advanced technology for brain delivery of drugs and is in clinical development with its most advanced product ANG1005. ANG1005 was in two phase II clinical trials in advanced cancer and brain metastases. This anti-cancer agent incorporating a peptide receptor targeting for brain uptake is the first such agent being evaluated in humans and demonstrates promising efficacy in the treatment of recurrent glioblastoma and brain metastasis in humans (Gabathuler 2010a, b; Drappatz et al. 2009; Kurzrock et al. 2009, 2011; Wen et al. 2011.

Angiopep-Coated Nanoparticles

Polyamidoamine dendrimers (PAMAM) were modified with angiopep through bifunctional PEG, then complexed with DNA, yielding PAMAM-PEG-Angiopep/DNA nanoparticles (NPs). The angiopep-modified NPs were observed to be internalized by brain capillary endothelial cells (BCECs) and showed higher efficiency in crossing the BBB with accumulation in brain (Ke et al. 2009). These angiopep-modified NPs were exploited to develop a brain-targeting gene delivery system. The Angiopep-modified gene delivery system exhibited enhanced brain-targeting capabilities and the Angiopep-modified vector/DNA NPs showed higher expression of

Fig. 16.2 (continued) Vessels are stained in *green* and cell nuclei in *blue*. (**b**) Fluorescent microscopic images of 10 μm brain sections obtained from animals injected with Trastuzumab-Rhodamine (*red*, 2 h). Vessels are stained in *green* and cell nuclei in *blue*. (**c**) Fluorescent microscopic images of 10 μm brain sections in animals injected with MTf-Trastuzumab-Rhodamine (*red*, 2 h). Vessels are stained in *green* and cell nuclei in *blue*. Brain vessels were stained with polyclonal anti-CD31 (1:100) and incubated with secondary anti-rabbit Alexa F680 antibody (1:300) in PBS for 1 h. Sections were washed five times and then stained with HOECHST (1:5000) diluted in Dako fluorescent mounting medium (DAKO) and cover slipped. Sections were visualized under an Olympus 1×81 inverted motorized microscope (Markham, ON, Canada) and analyzed using InVivo and ImagePro 6.2 Olympus acquisition and analysis software (Markham, ON, Canada)

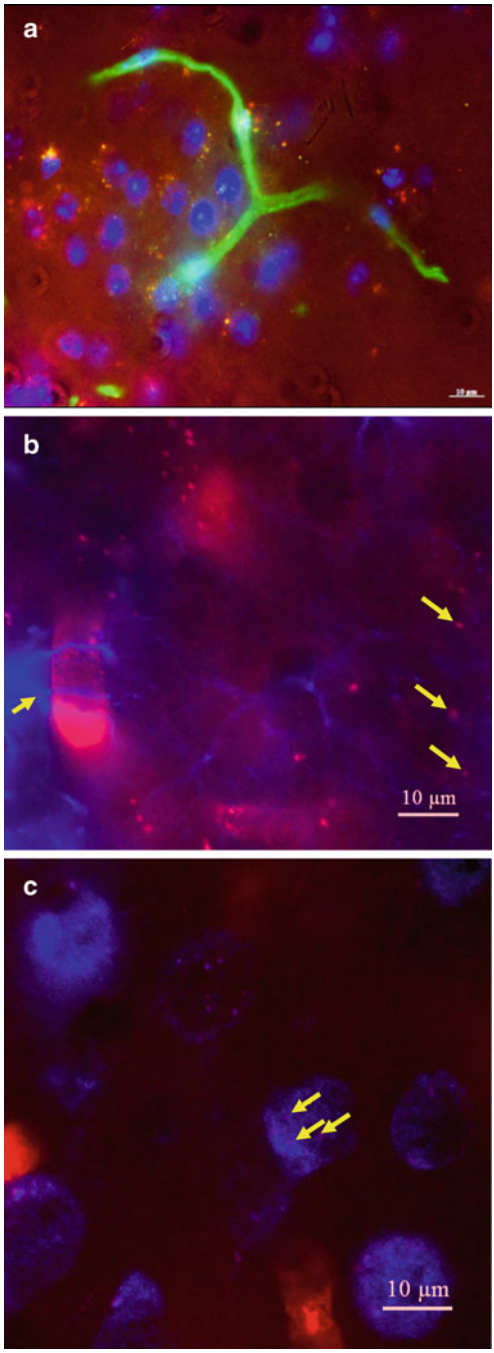

Fig. 16.3 Fluorescent microscopy of Cy5.5-Angiopep2 in brain sections and uptake of cy5.5-Angiopep2 in astrocytes and neurons. (**a**) 24 h after IV bolus injection of Cy5.5-Angiopep2 (100 µg), brains were fixed and fluorescence microscopy was performed on brain sections. Cy5.5-Angiopep2 was detected as *red spots*. Nuclei were labeled in blue with DAPI and brain capillaries were labeled in *green* with tomato lectin. (**b**) and (**c**) Fluorescent co-detection of the astrocyte (**b**) and neuron (**c**) markers after a 10 min brain perfusion with Cy5.5-Angiopep2. (**b**) Representative imaging of Cy5.5-Angiopep2 (*red*) colocalized with astrocyte marker GFAP (*blue*) (**c**) Representative imaging of Cy5.5-Angiopep2 (*red*) colocalized with neuron marker NeuN (*blue*)

exogenous genes in the brain (Ke et al. 2009). In this newly constructed vector, PAMAM served as a basic gene carrier, while Angiopep which was synthesized by adding a cysteine residue to the N-terminal of Angiopep2 was linked to PAMAM by bifunctional PEG. The apparent permeability (Papp) of PAMAM-PEG-Angiopep/DNA NPs at 60 min reached 85.3×10^{-6} cm/s (Ke et al. 2009). The Papp of PAMAM-PEG-Angiopep/DNA NPs was significantly increased with time while that of ^{14}C-sucrose maintained at a much lower level, about 1.4×10^{-3} cm/min as reported and indicated that these NPs do not affect the permeability of the in-vitro BBB model. The brain uptake of Angiopep-modified NPs increased with the ratio of Angiopep on NPs, indicating that Angiopep played a critical role in distribution of NPs in the brain involving LRP-1 receptor-mediated transcytosis across the BBB and endocytosis in brain cells (Ke et al. 2009).

Dual-targeting NPs were developed using conjugated angiopep with PEG-PCL (ANG-NP) through bifunctional PEG to overcome the low transport rate of chemotherapeutics. For examples, paclitaxel (Xin et al. 2011; Sun et al. 2012) or doxorubicin using PEGylated oxidized multi-walled carbon nanotubes (O-MWTs) (Ren et al. 2012) have shown efficient transport across the BBB and good penetration into tumor tissue.

16.7.2.2 Use of Other Ligands to BBB Receptors

Ligands other than those covered above have also been used to target receptors expressed at the BBB, not all of which have been precisely identified. These ligands or fragments of ligands have been linked to NPs in order to deliver a payload of active drug into the brain (Tosi et al. 2012).

The conjugation of the sequence 12–32 (g21) of leptin to poly-lactide-co-glycolide NPs resulted in their ability to cross the BBB and to penetrate the brain parenchyma as detected by electron microscopy (Tosi et al. 2012). The mechanism of transcytosis in this case is associated with the leptin receptor which has been shown to be expressed at the BBB (Banks et al. 1996; Corp et al. 1998; Burguera and Couce 2001). These NPs reach the brain parenchyma but the question remains as to whether the amount of drug accessing the brain is sufficient for therapeutic effects (Costantino and Boraschi 2012).

16.7.2.3 The BBB Transmigrating Llama Single Domain Antibodies (sdAb)

Using a Llama single domain antibody (sdAb) phage display library (Tanha et al. 2002), a new antigen-ligand system was identified for transvascular brain delivery [Muruganandam et al. 2002; Tanha et al. 2003; Abulrob et al. 2005). sdAbs are fragments of the heavy chain IgGs which occur naturally at a size of 13 kDa (Tanha et al. 2002). The transport of two sdAbs, FC5 and FC44 across the human brain

endothelial cells is polarized, charge independent, and temperature dependent, suggesting a receptor-mediated process. FC5 is targeted to early endosomes, bypass late endosomes/lysosomes, and remain intact after transcytosis. The receptor has been identified and is related to a novel isoform of the transmembrane domain protein 30A (TMEM 30A), also known as CDC50A. CDC50A is responsible for the cell surface expression of ATP8B1, which is hypothesized to be a flippase for phosphatidylserine (PS). CDC50A may be the potential β-subunit or chaperone for ATP8B1 (Paulusma et al. 2008). FC5 is now being developed to deliver therapeutic amounts of drugs (doxorubicin) into the brain after pentamerization and association to liposomes.

16.7.2.4 Advantages and Problems Associated with the Use of Ligands to BBB Receptors as Delivery Vectors

The use of ligands or fragments of ligands, which bind to specific receptors expressed on the luminal side of endothelial cells forming the BBB, has limitations. Ligands such as transferrin cannot be used as a vector for brain delivery across the BBB as transferrin concentration in the plasma is high (mg/ml levels), enough to saturate and compete out the administered transferrin. Anti-cancer agents conjugated to transferrin need to be locally injected in order to be therapeutically efficacious.

The use of LRP-1 and of ligands to the LRP such as LRP-1 have been characterized extensively and not all ligands are appropriate as brain delivery vectors. Targeting LRP-1 presents certain advantages. It is a receptor able to transcytose a variety of ligands from small peptides to very large proteins such as activated α2-macroglobulin (700 kDa). LRP-1 is a very fast endocytosed receptor with a half-life at the cell surface of less than 30 s, which is 20 times faster than the TR. In addition to its rapid endocytosis rate, LRP-1 has multiple binding sites and is constitutively endocytosed or internalized which results in a very high transcytosis rate across the BBB. These characteristics make LRP-1 a very high-capacity receptor able to transcytose high amounts of ligands very rapidly and making it an optimum brain delivery system.

Apo E associated with nanoparticles (NPs) by conjugation or adsorption on surfactant polysorbate-80 coated on NPs has been shown to target these NPs to the brain. The efficiency is not defined but certainly the fact that more than one molecule of Apo E may interact with the same receptor can allow it to bypass competition with endogenous plasma Apo E, and other ligands to LRP-1.

RAP, a chaperone protein for the LRP family of proteins, binds to LRP-1 in a noncompetitive way and modifies the 3D-conformation of the protein, inhibiting the binding of other ligands. Its function as a chaperone is to bind to LRP during its synthesis in the endoplasmic reticulum to avoid its aggregation with other proteins during transport to the cell surface. RAP may not be a good choice for a protein vector for brain delivery as it may hinder the transport of essential substances to the brain.

Aprotinin (trasylol) (6.7 kDa), its derived peptide sequence corresponding to angiopep peptides (angiopep2) (2.3 kDa), and recombinant soluble form of MTf (80 kDa) are ligands of the LRP family of proteins and bind with a medium affinity (100 nM–1 μM). LRP-1 is a receptor involved in the transcytosis of these ligands across the BBB. These ligands are very efficiently and rapidly transported across the BBB and are released in the brain parenchyma. Having medium affinity for LRP-1, these ligands will not compete with endogenous ligands of this receptor, some of which may be essential for the survival of brain cells. In addition, MTf is a human endogenous protein, which is present at very low concentration in plasma. Ligands to LRP-1 with medium affinity are the ideal protein vector for brain delivery as they are efficiently released in the brain parenchyma and they take advantage of the high capacity of this receptor.

16.8 Adsorptive-Mediated Transcytosis (AMT)

During the past decade, several peptides have been described that allow the intracellular delivery of polar, biologically active compounds in vitro and in vivo (Drin et al. 2002, 2003). All these peptides possess multiple positive charges, and some of them share common features, such as hydrophobicity and amphipathicity, the ability to interact with a lipid membrane and to adopt a significant secondary structure upon binding to lipids. Adsorptive transcytosis involves endocytosis in vesicles of charged substances similarly to a receptor-mediated mechanism but less specific. Peptides and proteins with a basic isoelectric point ("cationic" protein) bind initially to the luminal plasma membrane mediated by electrostatic interactions with anionic sites, which triggers adsorptive-mediated endocytosis (AME).

16.8.1 SynB and Protein Transduction Domains (PTDS)-Based Vectors

SynB vectors are a family of vectors derived from the antimicrobial peptide protegrin 1 (PG-1), an 18-amino acid peptide originally isolated from porcine leukocytes. As previously reported, the PG-1 peptide interacts with, and forms pores in, the lipid matrix of bacterial membranes. Researchers have designed various linear analogs of PG-1. These linear peptides (SynB vectors) are able to interact with the cell surface and cross the plasma membrane without their membrane-disrupting activity (Drin et al. 2003). Coupling of doxorubicin to either SynB1 (18aa) or SynB3 (10aa) vectors significantly enhances its brain uptake and bypasses the efflux transporters (Rousselle et al. 2000) without compromising the BBB integrity. Using this approach, brain uptake of an enkephalin analog (dalargin) was enhanced several 100-fold after vectorization (Rousselle et al. 2003). Improved

brain uptake and enhanced analgesic potency was observed after systemic administration of conjugated morphine-6-glucuronide to a peptide vector SynB3 (Temsamani et al. 2005).

Protein transduction domains (PTDs) are typically amino acid sequences located on transcription factors allowing transport of larger molecules across the cell membranes—examples include the homeodomain of Antennapedia, and penetratin. These peptides are basic, positively charged molecules, which bind to negatively charged phospholipids of cell membranes and are then taken up by adsorptive-mediated endocytosis.

16.8.2 Use of Cationic, Positively Charged, Peptides (Poly-Arginines)

Poly-arginines (9 mer of L-Arg, R9) have shown a very efficient cellular uptake 20-fold superior than Tat_{49-57} and greater than 100-fold superior than D-Arg oligomers (r9) (Wender et al. 2000). Uptake of basic peptides can be followed by using primary cultured bovine brain capillary endothelial cells (BBCEC). The steady state uptake was temperature dependent and significantly decreased in the presence of dansylcadaverine, protamine, and poly-L-Lysine. C-terminal structure and the basicity of the molecule rather than the number of constituent amino acids of the peptides were shown to be the most important determinants of uptake by AME in cultured BBCEC (Temsamani et al. 2001).

Cationic bovine serum albumin (CBSA) conjugated with poly(ethyleneglycol)-poly(lactide) (PEG-PLA) nanoparticles (CBSA-NP) have also been designed for brain drug delivery (Lu et al. 2005). CBSA-NPs incorporated with a lipophilic fluorescent probe, 6-coumarin, were tested in an in-vitro rat BBB model. CBSA-NP did not impact the integrity of BBB endothelial tight junctions and showed little toxicity against brain capillary endothelial cells. The permeability of CBSA-NP was significantly higher (7.8×) than that of BSA-NP (Lu et al. 2005).

For brain in-vivo imaging applications, the delivery module was conjugated to the NIR (near infrared) cy5.5 dye (Pham et al. 2005). To this end, a cys was deployed on a myristoylated poly-arginine peptide (MPAP) carboxyl-terminal where the thiol moiety reacted with the commercially available cy5.5 maleimide via a Michael addition reaction. To confirm that the observed fluorescence signal was truly from the brain, ex-vivo imaging was performed on excised mouse brain.

Additional peptides (g7 peptide) have been characterized which can cross the BBB. The mechanism of their transcytosis is not clearly defined and is probably dependent on their amphipathic conformation; these peptides have high affinity for luminal wall lipid bilayer components on endothelial cells (Tosi et al. 2011). These g7 peptides conjugated to poly-lactide-co-glycolide (PLGA) were shown to cross the BBB. Only loperamide delivered to the brain with g7-NPs created a high central analgesia, corresponding to 14 % of the injected dose (Tosi et al. 2011).

A short peptide derived from rabies virus glycoprotein (RVG) enables the transvascular delivery of small interfering RNA (siRNA) to brain cells (neurons) (Kumar et al 2007). This 29aa peptide specifically binds to the acetylcholine (Ach) receptor expressed on the neuronal cells. To enable siRNA binding, a chimaeric peptide was synthesized by adding nanomer arginine (9R) residues at the carboxy-terminus of RVG. This RVG-9R peptide was able to bind and transduce siRNA to neuronal cells in-vitro, resulting in efficient gene silencing. The mixture of component, peptide, and siRNA without covalent association was IV administered into mice. RVG-9R was delivered to the neuronal cells and resulted in specific gene silencing within the brain (Kumar et al. 2007).

16.8.3 PAMAM Dendrimers (Nanoparticles)

PAMAM dendrimers were first exploited as an efficient carrier of doxorubicin. The much higher cytotoxic activity of PAMAM/doxorubicin complexes over free doxorubicin implies that the cellular uptake of doxorubicin from the PAMAM/doxorubicin complex includes a transport mechanism other than simple diffusion. The mechanism for the increased brain doxorubicin levels (six times) likely consists of two aspects: (a) PAMAM/doxorubicin may change the mechanism of doxorubicin entry into cells from simple diffusion to AME due to the cationic PAMAM binding the negative cellular surface to enhance the uptake of doxorubicin and (b) doxorubicin complexed to PAMAM allows it to bypass efflux transporters (Cui et al. 2009).

PAMAM-PEG-RVG29/DNA nanoparticles (NPs) showed higher BBB crossing efficiency than PAMAM/DNA NPs in an in-vitro BBB model (Liu et al. 2009). This increase may be due to the specific targeting of RVG29 coated NPs to neuronal cells in the brain parenchyma.

16.8.4 Nanoparticles Coated with Tat (49-57) Peptides

Biologically active polymer core/shell nanoparticles (i.e., micelles) self-assembled from Tat peptide (49-57)-PEG-b-cholesterol (Tat-PEG-b-chol) have been fabricated and used as carriers for targeted BBB delivery of antibiotics. Ciprofloxin as a model antibiotic was efficiently loaded into the nanoparticles by a membrane dialysis method. The nanoparticles were spherical in nature, having an average size lower than 200 nm. The uptake of nanoparticles coated with Tat peptide by human brain endothelial cells was greater than without Tat peptide. Tat (49-57, YGRKKRRQRRR) peptide is the transduction domain from Tat protein of HIV-1 (Santra et al. 2005; Liu et al. 2008). Most importantly, the nanoparticles coated with Tat were able to cross the BBB and localize around the cell nucleus of neurons. These nanoparticles may provide a promising carrier to deliver antibiotics across the BBB for the treatment of brain infection (Liu et al. 2008).

Nanoparticles conjugated with Tat peptide demonstrate an increase in transport of encapsulated ritonavir, a protease inhibitor (PI), across the BBB to the CNS, bypassing efflux transporters. Localization of NPs in the brain parenchyma was confirmed by histological analysis of brain sections. The brain drug level with conjugated NPs was 800-fold higher than that obtained versus ritonavir alone at 2 weeks. In conclusion, Tat-conjugated NPs enhanced the CNS availability of the encapsulated PI and maintained therapeutic drug levels in the brain for a sustained period, a finding that could be important because reducing the viral load in the CNS may serve to decrease the brain's ability to serve as a reservoir for the replicating HIV-1 virus [Rao et al. 2008; Rao and Labhasetwar 2006; Dennisson et al. 2007).

Exosomes, endogenous nano-vesicles that transport RNAs and proteins, can deliver short interfering siRNA to the brain in mice (Alvarez-Erviti et al. 2011). Self-derived dendritic cells were used to produce exosomes in order to reduce immunogenicity. The rabies virus glycoprotein (RVG) peptide that specifically binds to the acetylcholine receptor in the brain was used for targeting these exosomes. The precise mechanism used by this exosome to deliver their payloads has not been investigated and may be associated with AMT induced by interaction of these vesicles with components on the luminal side of the endothelial cells. The therapeutic potential of exosome-mediated siRNA delivery was demonstrated by the strong mRNA (60 %) and protein (62 %) knockdown of BACE1, a therapeutic target in Alzheimer's Disease, in wild-type mice (Alvarez-Erviti et al. 2011).

16.8.5 Advantages and Problems with the Use of Cationic Molecules for Brain Delivery

The properties of these cationic peptides are related to the original proteins they were derived from (e.g., TAT), which are generally associated with transcription factors or membrane disrupting sequences. Cationic molecules such as peptides and nanoparticles with excess positive charge bind to negatively charged phospholipids composing the cellular membranes of the luminal side of the endothelial cells forming the BBB and are subsequently endocytosed/transcytosed across the cells using a nonspecific mechanism called adsorptive transcytosis. These peptides or molecules can be used to transfect cells in culture with nucleic acids or to introduce associated proteins such as antibodies into the cell's cytoplasm.

The charged properties of these molecules make them not very efficient to transport compounds across the BBB into the brain because they are usually adsorbed on other organs such as liver and lungs before reaching the brain and also present high adsorption to plasma proteins.

Cationic nanoparticles may also have a toxic effect at the BBB by increasing its permeability and allowing unwanted molecules and/or cells to enter the CNS (Lockman et al. 2004).

16.9 Conclusions

In addition to small-molecule drugs, there are many promising biopharmaceutical agents with potentially high activity for brain targets that, unfortunately, cannot enter the brain in sufficient quantities to be effective. Therefore, new technologies are in development to address this problem.

In this review new approaches in development to deliver small and large molecules such as biologics to the brain are described. Many techniques used thus far have involved injection or infusion of therapeutic compounds directly into the brain or the CSF (at the level of the cerebro-ventricles or the subarachnoid space), but these routes present great limitations for brain parenchyma distribution and necessitate hospitalization associated with high costs. Only the use of technologies able to cross the endothelial cells of the BBB will allow a homogenous distribution of therapeutics in the brain and provide a uniform exposure of brain cells.

The most promising new technologies use a physiological approach and take advantage of endogenous receptors or proteins highly expressed at the BBB, which provide brain cells with nutrients. Such proteins can include transporters such as amino acid transporters or receptors, e.g., LRP, TR, and IR among others. Ligands of these receptors can be used for transcytosis of therapeutic compounds to the CNS and are thought to be the best alternative for new brain delivery vectors. Technology associated with ligands and optimized fragments of ligands to the LDL receptor-related protein (LRP)-1 seem to offer among the most efficient brain targeting, as reviewed in this chapter.

A new peptide vector Angiopep demonstrates a high transport rate across the BBB and the ability to transport large quantities of drugs to the brain parenchyma. In addition, this technology may allow the transport of both small drugs and large biologics following conjugation. This technology has been developed for the transport of paclitaxel, a small anti-cancer agent, into the brain following systemic application; this product is the most advanced as it is now in two phase I clinical trials for the treatment of recurrent gliomas and brain metastasis and has been validated in human trials with encouraging results. The conjugate angiopep2-paclitaxel (ANG1005) was in two phase II clinical trials.

Melanotransferrin (MTf) a new protein vector for brain delivery has been developed for the transport of biologics such as lysosomal enzymes and antibodies to the brain. MTf has been characterized as a ligand of LRP-1 such that its transcytosis across the BBB and transport within brain cells is likely associated with this receptor.

More technologies need to be developed taking into account nanoparticles modified with targeting peptides such as Angiopep or MTf for brain delivery of biologics such as antibodies or nucleic acids for the treatment of brain diseases including neurodegenerative diseases, lysosomal storage diseases, and brain cancers. The use of nanoparticles may allow a higher payload to be delivered into the brain and ultimately allow therapeutic concentrations of active molecules in the brain parenchyma.

16.10 Points for Discussion

The major challenge in the area of brain delivery is first to find an efficient vector for brain delivery using a physiologic pathway mechanism in order to cross the BBB. These vectors can be in the form of peptides, proteins, antibodies, or some other specific formulation such as nanoparticles which target a specific receptor at the BBB and will cross the BBB by transcytosis. Some questions to be resolved with respect to brain delivery vectors include the following:

1. Can we find a unique vector that may be used as a universal brain delivery vector? This is very improbable as the types of active molecules that are thought to be useful in the brain are very diverse, from peptides to DNA.
2. It is important to consider not only brain delivery consisting of the release of cargo from its receptor in the brain parenchyma but also the final destination of the active molecules in the brain. Is the active compound being delivered to target cells, e.g., neurons, and ultimately is the active compound able to gain access to the correct intracellular compartment where it may exert its effects?
3. The active compound must not only be delivered to the brain parenchyma; it must also reach therapeutic concentrations within the brain. What in vivo assays using animals (most commonly mice and transgenic mouse models for specific diseases) will show therapeutic relevance with respect to brain delivery and in vivo efficacy?
4. Are the supporting data for a new delivery vector comparable to other data in other laboratories? It is important to have external validation of the published results and conclusions related to each vector's efficiency in crossing the BBB.
5. Should other approaches for brain delivery be considered for a specific application, e.g., intrathecal injection or intranasal delivery?

References

Abulrob A, Sprong H, Bergen en Henegouwen PV, Stanimirovic D (2005) The blood–brain barrier transmigrating single domain antibody: mechanisms of transport and antigenic epitopes in human brain endothelial cells. J Neurochem 95:1201–1214

Allen DD, Lockman PR, Roder KE, Dwoskin LP, Crooks PA (2003) Active transport of high-affinity choline and nicotine analogs into the central nervous system by the blood–brain barrier choline transporter. J Pharmacol Exp Ther 304:1268–1274

Alvarez-Erviti L, Seow Y, Yin H, Betts C, Lakhal S, Wood MJA (2011) Delivery of siRNA to the mouse brain by systemic injection of targeted exosomes. Nat Biotechnol 29:341–345

Atwal JK, Chen Y, Chiu C, Mortensen DL, Meilandt WJ, Liu Y, Heise CE, Hoyte K, Luk W, Lu Y, Peng K, Wu P, Rouge L, Zhang Y, Lazarus RA, Scearce-Levie K, Wang W, Wu Y, Tessier-Lavigne M, Watts RJ (2011) A therapeutic antibody targeting BACE1 inhibits amyloid-ß production in vivo. Sci Transl Med 3:84ra43

Banks WA, Kastin AJ, Huang W, Jaspan JB, Maness LM (1996) Leptin enters the brain by a saturable system independent of insulin. Peptides 17:305–311

Benchenane K, Berezowski V, Ali C, Fernández-Monreal M, López-Atalaya JP, Brillault J, Chuquet J, Nouvelot A, MacKenzie ET, Bu G, Cecchelli R, Touzani O, Vivien D (2005) Tissue-type plasminogen activator crosses the intact blood–brain barrier by low-density lipoprotein receptor - related protein—mediated transcytosis. Circulation 111:2241–2249

Bendell JC, Domchek SM, Burstein HJ, Harris L, Younger J, Kuter I, Bunnell C, Rue M, Gelman R, Winer E (2003) Central nervous system metastases in women who receive trastuzumab-based therapy for metastatic breast carcinoma. Cancer 97:2972–2977

Bertrand Y, Currie J-C, Demeule M, Regina A, Che C, Abulrob A, Fatehi D, Sartelet H, Gabathuler R, Castaigne J-P, Stanimirovic D, Beliveau R (2010) Transport characteristics of a novel peptide platform for CNS therapeutics. J Cell Mol Med 14(12):2827–2839

Bertrand Y, Currie JC, Poirier J, Demeule M, Abulrob A, Fatehi D, Stanimirovic D, Sartelet H, Castaigne J-P, Béliveau R (2011) Influence of glioma tumour microenvironment on the transport of ANG1005 via low-density lipoprotein receptor-related protein 1. Br J Cancer 105:1697–1707

Bichat F, Demeule M, Lawrence B, Raguin O, Sourzat B, Gabathuler R, Castaigne J-P, Genne P (2008) Enhanced drug delivery to brain tumours with a new paclitaxel-peptide conjugate. Eur J Cancer Suppl 6(45):139

Boado RJ, Zhang Y, Wang Y, Pardridge WM (2008) GDNF fusion protein for targeted-drug delivery across the human blood–brain barrier. Biotechnol Bioeng 100:387–396

Bonner LT, Peskind ER (2002) Pharmacologic treatments of dementia. Med Clin North Am 86:657–674

Brownlees J, Williams CH (1993) Peptidases, peptides, and the mammalian blood–brain barrier. J Neurochem 60:1089–1096

Bu G, Maksymovitch EA, Nerbonne JM, Schwartz AL (1994) Expression and function of the low density lipoprotein receptor-related protein (LRP) in mammalian central neurons. J Biol Chem 269:18521–18528

Burguera B, Couce ME (2001) Leptin access into the brain: a saturated mechanism in obesity. Physiol Behav 74:717–720

Che C, Yang G, Thiot C, Lacoste MC, Currie JC, Demeule M, Regina A, Beliveau R, Castaigne J-P (2010) New Angiopep-modified doxorubicin (ANG1007) and etoposide (ANG1009) chemotherapeutics with increased brain penetration. J Med Chem 53:2814–2824

Coloma MJ, Lee HJ, Kurihara A, Landaw EM, Boado RJ, Morrison SL, Pardridge WM (2000) Transport across the primate blood–brain barrier of a genetically engineered chimeric monoclonal antibody to the human insulin receptor. Pharm Res 17:266–274

Corp S, Conze DB, Smith F, Campfield LA (1998) Regional localization of specific [125]I-leptin binding sites in rat forebrain. Brain Res 789:40–47

Costantino L, Boraschi D (2012) Is there a clinical future for polymeric nanoparticles as brain-targeting drug delivery agents? Drug Discov Today 17:367–378

Cui D, Xu Q, Gu S, Shi J, Che X (2009) PAMAM-drug complex for delivering anticancer drug across the blood–brain barrier in-vitro and in-vivo. Afr J Pharm Pharmacol 3:227–233

De Boer AG, Gaillard PJ (2007) Drug targeting to the brain. Annu Rev Pharmacol Toxicol 47:323–355

Demeule M, Poirier J, Jodoin J, Bertrand Y, Desrosiers RR, Dagenais C, Nguyen T, Lanthier J, Gabathuler R, Kennard M, Jefferies WA, Karkan D, Tsai S, Fenart L, Cecchelli R, Béliveau R (2002) High transcytosis of melanotransferrin (p97) across the blood–brain barrier. J Neurochem 83:924–933

Demeule M, Currie J-C, Bertrand Y, Che C, Nguyen T, Regina A, Gabathuler R, Castaigne J-P, Béliveau R (2008a) Involvement of the low-density lipoprotein receptor-related protein in the transcytosis of the brain delivery vector Angiopep-2. J Neurochem 106:1534–1544

Demeule M, Regina A, Che C, Poirier J, Nguyen T, Gabathuler R, Castaigne JP, Béliveau R (2008b) Identification and design of peptides as a new drug delivery system for the brain. J Pharmacol Exp Ther 324:1064–1072

Demeule M, Regina A, Yang G, Che C, Beliveau R, Castaigne J-P (2010) New angiochem-modified doxorubicin with increased brain penetration and efficacy against brain tumors. Presented at: the Annual Meeting of the AACR, Washington DC, USA, 17–21 Apr 2010

Dennisson SR, Baker RD, Nicholl ID, Phoenix DA (2007) Interactions of cell penetrating peptide TAT with model membranes: a biophysical study. Biochem Biophys Res Commun 363:178–182

Donoso M, Cancino J, Lee J, van Kerkhof P, Retamal C, Bu G, Gonzalez A, Cáceres A, Marzolo M-P (2009) Polarized traffic of LRP1 involves AP1B and SNX17 operating on Y-dependent sorting motifs in different pathways. Mol Biol Cell 20:481–497

Drappatz J, Brenner A, Rosenfeld S, Schiff D, Wen P, Mikkelsen T, Groves M, Wong ET, Eichler A, Elian KM, Lawrence B, Demeule M, Castaigne J-P (2009) ANG1005: Development of a new Engineered Peptide Compound (EPiC) for the treatment of malignant glioma. Presented at: the Annual Neuroscience Conference 2009, Chicago IL, USA, 17–21 Oct 2009

Drin G, Rousselle C, Scherrmann J-M, Rees AR, Temsamari J (2002) Peptide delivery to the brain via adsorptive-mediated endocytosis: advances with SynB vectors. AAPS PharmSci 4(4):1–7

Drin G, Cottin S, Blanc E, Rees AR, Temsamari J (2003) Studies on the internalization mechanism of cationic cell-penetrating peptides. J Biol Chem 278:31192–31201

Food M, Rothenberger S, Gabathuler R, Haidl ID, Reid G, Jefferies WA (1994) Transport and expression in human melanomas of a transferrin like glycosylphosphatidylinositol-anchored proteins. J Biol Chem 269:3034–3040

Fuchs IB, Loebbecke M, Buhler H, Stoltenburg-Didinger G, Heine B, Lichtenegger W, Schaller G (2002) HER2 in brain metastases: issues of concordance, survival and treatment. J Clin Oncol 20:4130–4133

Gabathuler R (2009) Blood–brain barrier transport of drugs for the treatment of brain diseases. CNS Neurol Disord Drug Targets 8:195–294

Gabathuler R (2010a) An engineered peptide compound platform technology incorporating angiopep for crossing the BBB. In: Jain KK (ed) Drug delivery to the CNS neuromethods, vol 45. Humana Press, New York, pp 249–260, Chapter 12

Gabathuler R (2010b) Approaches to transport therapeutic drugs across the blood–brain barrier to treat brain diseases. Neurobiol Dis 37:48–57

Gabathuler R, Arthur G, Kennard ML, Chen Q, Tsai S, Yang J, Schoorl W, Vitalis T, Jefferies WA (2005) Development of a potential protein vector (NeuroTrans) to deliver drugs across the blood–brain barrier. In: AG de Boer (ed) Drug Transport(ers) and the diseased brain, Int Congress Series, Esteve Foundation Symposium XI, vol 1277, Elsevier, S'Agaró (Girona), Spain, p 171–184

Gaillard PJ, Leyssen P, Appeldoorn C, Dorland R, van Kregten J, Manca MF, Johan Neyts J (2009) Development of brain-targeted liposomes with antiviral drugs for treating lethal viral encephalitis. Presented at: 8th cerebral vascular biology (CVB) 2009 International Conference. Sendai, Japan, 28 June–2 July 2009

Grossi PM, Ochiai H, Archer GE, McLendon RE, Zalutsky MR, Friedman AH, Friedman HS, Binger DD, Sampson JH (2003) Efficacy of intracerebral microinfusion of trastuzumab in an athymic rat model of intracerebral metastatic breast cancer. Clin Cancer Res 9:5514–5520

Hertz J, Strickland DK (2001) LRP: a multifunctional scavenger and signalling receptor. J Clin Invest 108:779–784

Hussain MM, Strickland DK, Bakillah A (1999) The mammalian low-density lipoprotein receptor family. Annu Rev Nutr 19:141–172

Jain KK (2007) Drug delivery in central nervous system disorders, technology, companies and markets. Jain Pharmabiotechnology Report

Jefferies WA, Food M, Gabathuler R, Rothenberger S, Yamada T, McGeer PL (1996) Reactive microglia specifically associated with amyloid plaques in Alzheimer's disease brain tissue express melanotransferrin. Brain Res 712:122–126

Karkan D, Pfeifer C, Vitalis TZ, Arthur G, Ujiie M, Chen Q, Tsai S, Koliatis G, Gabathuler R, Jefferies WA (2008) A unique carrier for delivery of therapeutical compounds beyond the blood–brain barrier. PLoS One 3:e2469

Ke W, Shao K, Huang R, Han L, Liu Y, Li J, Kuang Y, Ye L, Lou J, Jiang C (2009) Gene delivery targeted to the brain using an Angiopep-conjugated polyethyleneglycol-modified polyamidoamine dendrimer. Biomaterials 30(36):6976–6985

Kounnas MZ, Moir RD, Rebeck GW, Bush AI, Argraves WS, Tanzi RE, Hyman BT, Strickland DK (1995) LDL receptor-related protein, a multifunctional ApoE receptor, binds secreted β-amyloid precursor protein and mediates its degradation. Cell 82:331–340

Kreuter J, Shamenkov D, Petrov V, Ramge P, Cychutek K, Koch-Brandt C, Alyautdin R (2002) Apolipoprotein-mediated transport of nanoparticles-bound drugs across the blood–brain barrier. J Drug Target 10:317–325

Kreuter J, Ramge P, Petrov V, Hamm S, Gelperina SE, Engelhardt B, Alyautdin R, von Briesen H, Begley DJ (2003) Direct evidence that polysorbate-80-coated poly(butylcyanoacrylate) nanoparticles deliver drugs to the CNS via specific mechanisms requiring prior binding of drug to the nanoparticles. Pharm Res 20:409–416

Kreuter J, Hekmatara T, Dreis S, Vogel T, Gelperina S, Langer K (2007) Covalent attachment of apolipoprotein A-I and apolipoprotein B-100 to albumin nanoparticles enables drug transport into the brain. J Control Release 118:54–58

Kumar P, Wu H, McBride JL, Jung KE, Kim MH, Davidson BL, Lee SK, Shankar P, Manjunath N (2007) Transvascular delivery of small interfering RNA to the central nervous system. Nature 448:33–40

Kurzrock R, Gabrail N, Moulder S, Brenner A, Guo Z, Bouchard D, Churchill W, Bento P, Fitsialos D, Fraitag B, Neale A, Castaigne J-P, Sarantopoulos J (2009) ANG1005: a promising new Engineered Peptide Compound (EPiC) for patients with advanced solid tumors and brain metastases. Presented at: the Annual Neuroscience Conference 2009, Chicago IL, USA, 17–21 Oct 2009

Kurzrock R, Gabrail N, Chandhasin C, Moulder S, Smith C, Brenner A, Sankhala K, Mita A, Elian K, Bouchard D, Sarantopoulos J (2011) Safety, pharmacokinetics, and activity of GRN1005, a novel conjugate of angiopep-2, a peptide facilitating brain penetration, and paclitaxel, in patients with advanced solid tumors. Mol Cancer Ther 11:308–316

Li Y, Marzolo MP, van Kerkhof P, Strous GJ, Bu G (2000) The YXXL motif, but not the two NPXY motifs, serves as the dominant endocytosis signal for low density lipoprotein receptor-related protein. J Biol Chem 275(22):17187–17194

Lipinski CA, Lombardo F, Dominy BW, Feeney PJ (2001) Experimental and computational approaches to estimate solubility and permeability in drug discovery and development settings. Adv Drug Deliv Rev 46:3–26

Liu L, Guo K, Lu J, Venkatraman SS, Luo D, Ng KC, Ling EA, Moochhala S, Yang YY (2008) Biologically active core/shell nanoparticles self-assembled from cholesterol-terminated PEG-TAT for drug delivery across the blood–brain barrier. Biomaterials 29:1509–1517

Liu Y, Huang R, Han L, Ke W, Shao K, Ye L, Lou J, Jiang C (2009) Brain-targeting gene delivery and cellular internalization mechanisms for modified rabies virus glycoprotein RVG29 nanoparticles. Biomaterials 30:4195–4202

Lockman PR, Koziara JM, Mumper RJ, Allen DD (2004) Nanoparticles surface charges alter the blood–brain barrier integrity and permeability. J Drug Target 12:635–641

Lu W, Tan Y-Z, Hu K-L, Jiang X-G (2005) Cationic albumin conjugated pegylated nanoparticles with its transcytosis ability and little toxicity against blood–brain barrier. Int J Pharm 295:247–260

Migliorini MM, Behre EH, Brew S, Ingham KC, Strickland DK (2003) Allosteric modulation of ligand binding to low density lipoprotein receptor-related protein by the receptor-associated protein requires critical lysine residues within the carboxy-terminal domain. J Biol Chem 278:17986–17992

Misra A, Ganesh S, Shahiwala A, Shah SP (2003) Drug delivery to the central nervous system: a review. J Pharm Pharm Sci 6:252–273

Moestrup SK, Gliemann J, Pallesen G (1992) Distribution of the alpha 2-macroglobulin receptor/low density lipoprotein receptor-related protein in human tissues. Cell Tissue Res 269: 375–382

Moos T, Morgan EH (2001) Restricted transport of anti-transferrin receptor antibody (OX26) through the blood–brain barrier in the rat. J Neurochem 103:119–129

Moroo I, Ujiie M, Walker BL, Tiong JW, Vitalis TZ, Karkan D, Gabathuler R, Moise AR, Jefferies WA (2003) Identification of a novel route of iron transcytosis across the mammalian blood–brain barrier. Microcirculation 10:457–462

Muruganandam A, Tanha J, Narang S, Stanimirovic D (2002) Selection of phage-displayed llama single-domain antibodies that transmigrate across human blood–brain barrier endothelium. FASEB J 16:240–242

Nazer B, Hong S, Selkoe DJ (2008) LRP promotes endocytosis and degradation, but not transcytosis, of the amyloid-β peptide in a blood–brain barrier in vitro model. Neurobiol Dis 30: 94–102

Obermoeller-McCormick LM, Li Y, Osaka H, FitzGerald DJ, Schwartz AL, Bu G (2001) Dissection of receptor folding and ligand-binding property with functional minireceptors of LDL receptor-related protein. J Cell Sci 114:899–908

Olivier J-C (2005) Drug transport to brain with targeted nanoparticles. NeuroRx 2:108–119

Pardridge WM (1993) Drug targeting to the brain. Pharm Res 24:1733–1744

Pardridge WM (1998) CNS drug design based on principles of blood–brain barrier transport. J Neurochem 70:1781–1792

Pardridge WM (2007) shRNA and siRNA delivery to the brain. Adv Drug Deliv Rev 59:141–152

Pardridge WM (2010) Biopharmaceutical drug targeting to the brain. J Drug Target 18:157–167

Paris-Robidas S, Emond V, Tremblay C, Soulet D, Calon F (2011) In vivo labeling capillary endothelial cells after intravenous injection of monoclonal antibodies targeting the transferrin receptor. Mol Pharmacol 80:32–39

Paulusma CC, Folmer DE, Ho-Mok KS, de Waart DR, Hilarius PM, Verhoeven AJ, Oude Elferink RP (2008) ATP8B1 requires an accessory protein for endoplasmic reticulum exit and plasma membrane lipid flippase activity. Hepatology 47:268–278

Pham W, Zhao B-Q, Lo EH, Medarova Z, Rosen B, Moore A (2005) Crossing the blood–brain barrier: a potential application of myristoylated polyarginine for in-vivo imaging. Neuroimage 28:287–292

Prince WS, McCormick LM, Wendt DJ, Fitzpatrick PA, Schwartz KL, Aguilera AI, Koppaka V, Christianson TM, Vellard MC, Pavloff N, Lemontt JF, Qin M, Starr CM, Bu G, Zankel TC (2004) Lipoprotein receptor binding, cellular uptake, and lysosomal delivery of fusions between the receptor-associated protein (RAP) and α-L-iduronidase or acid α-glucosidase. J Biol Chem 279:35037–35046

Rao KS, Labhasetwar V (2006) Trans-activating transcriptional activator (TAT) peptide-mediated brain drug delivery. J Biomed Nanotechnol 2:173–185

Rao KS, Reddy MK, Horning JL, Labhasetwar V (2008) TAT-conjugated nanoparticles for the CNS delivery of anti-HIV drugs. Biomaterials 29:4429–4438

Rebeck GW, Reiter JS, Strickland DK, Hyman BT (1993) Apolipoprotein E in sporadic Alzheimer's disease: allelic variation and receptor interactions. Neuron 11:575–580

Regina A, Demeule M, Che C, Lavallee I, Poirier J, Gabathuler R, Beliveau R, Castaigne J-P (2008) Antitumor activity of ANG1005, a conjugate between paclitaxel and the new brain delivery vector Angiopep-2. Br J Pharmacol 155:185–197

Ren J, Shen S, Wang D, Xi Z, Guo L, Pang Z, Qian Y, Sun X, Jiang X (2012) The targeted delivery of anticancer drugs to brain gliomas by PEFylated oxidized multi-walled carbon nanotubes modified with angiopep-2. Biomaterials 33:3324–3333

Rousselle C, Clair P, Lefauconnier J-M, Kaczorek M, Scherrmann J-M, Temsamani J (2000) New advances in the transport of doxorubicin through the blood–brain barrier by a peptide vector-mediated strategy. J Pharmacol Exp Ther 57:679–686

Rousselle C, Clair P, Smirnova M, Kolesnikov Y, Pasternak GW, Gac-Breton S, Rees AR, Scherrmann J-M, Temsamani J (2003) Improved brain uptake and pharmacological activity of dalargin using a peptide-vector-mediated strategy. J Pharmacol Exp Ther 306:371–376

Santra S, Yang H, Stanley JT, Holloway PH, Moudgil BM, Walter G, Mericle RA (2005) Rapid and effective labeling of brain tissue using TAT-conjugated CdS:Mn/ZnS quantum dots. Chem Commun 25:3144–3146

Slamon DJ, Leyland-Jones B, Shak S, Fuchs H, Paton V, Bajamonde A, Fleming T, Eiermann W, Wolter J, Pegram M, Baselga J, Norton L (2003) Use of chemotherapy plus a monoclonal antibody against HER2 for metastatic breast cancer that overexpresses HER2. N Engl J Med 344:783–792

Smith QR (2003) A review of blood–brain barrier transport techniques. Methods Mol Med 89:193–208

Spencer BJ, Verma IM (2007) Targeted delivery of proteins across the blood–brain barrier. Proc Natl Acad Sci U S A 104:7594–7599

Steiniger SCJ, Kreuter J, Khalansky AS, Skidan IN, Bobruskin AI, Smirnova ZS, Severin SE, Uhl R, Kock M, Geiger KD, Gelperina SE (2004) Chemotherapy of glioblastoma in rats using doxorubicin-loaded nanoparticles. Int J Cancer 109:759–767

Sun X, Pang Z, Ye H, Qiu B, Guo L, Li J, Ren J, Qian Y, Zhang Q, Chen J, Jiang X (2012) Co-delivery of pEGF-hTRAIL and paclitaxel to brain glioma mediated by an angiopep-conjugated liposome. Biomaterials 33:916–924

Takasato Y, Rapoport SI, Smith QR (1984) An in situ brain perfusion techniques to study cerebrovascular transport in the rat. Am J Physiol 247:484–493

Tang Y, Han T, Everts M, Zhu ZB, Gillespie GY, Curiel DT, Wu H (2007) Directing adenovirus across the blood–brain barrier via melanotransferrin (p97) transcytosis pathway in an in vitro model. Gene Ther 14:523–532

Tanha J, Dubuc G, Hirama T, Narang SA, MacKenzie CR (2002) Selection by phage display of llama conventional V_H fragments with heavy chain antibody V_HH properties. J Immunol Methods 263:97–109

Tanha J, Muruganandam A, Stanimirovic D (2003) Phage display technology for identifying specific antigens on brain endothelial cells. Methods Mol Med 89:435–449

Temsamani J, Rousselle C, Rees AR, Scherrmann J-M (2001) Vector-mediated drug delivery to the brain. Expert Opin Biol Ther 1:773–782

Temsamani J, Bonnafous C, Rousselle C, Fraisse Y, Clair P, Granier L-A, Rees AR, Kaczorek M, Scherrmann J-M (2005) Improved brain uptake and pharmacological activity profile of morphine-6-glucuronide using a peptide vector-mediated strategy. J Pharmacol Exp Ther 313:712–719

Thomas FC, Taskar K, Rudraraju V, Goda S, Thorsheim HR, Gaasch JA, Mittapalli RK, Palmieri D, Steeg PS, Lockman PR, Smith QR (2009) Uptake of ANG1005, a novel paclitaxel derivative, through the blood–brain barrier into brain and experimental brain metastases of breast cancer. Pharm Res 26:2486–2494

Tosi G, Fano RA, Bondioli L, Badiali L, Benassi R, Rivasi F, Ruozi B, Forni F, Vandelli MA (2011) Investigation on mechanisms of glycopeptide nanoparticles for drug delivery across the blood–brain barrier. Nanomedicine 6:423–436

Tosi G, Badiali L, Ruozi B, Vergoni AV, Bondioli L, Ferrari A, Rivasi F, Forni F, Vandelli MA (2012) Can leptin-derived sequence-modified nanoparticles be suitable tools for brain delivery? Nanomedicine 7:365–382

Tyler WJ, Perret SP, Pozzo-Miller LD (2002) The role of neurotrophins in neurotransmitter release. Neuroscientist 8:524–531

Ulbrich K, Hekmatara T, Herbert E, Kreuter J (2009) Transferrin- and transferrin-receptor-antibody-modified nanoparticles enable drug delivery across the blood–brain barrier (BBB). Eur J Pharm Biopharm 71:251–256

Wagner S, Zensi A, Wien SL, Tschickardt SE, Maier W, Vogel T, Worek F, Pietrzik CU, Kreuter J, von Briesen H (2011) Uptake mechanism of ApoE-modified nanoparticles on brain capillary endothelial cells as a blood–brain barrier model. PLoS One 7:e32568

Wen PY, Drappatz J, Brenner A, Mikkelsen T, Schiff D, Rosenfeld S, Groves M, Shen Y, Wang X, Shing M, Lawrence B, Castaigne J-P, Gabrail N, Sarantopoulos J, Kurzrock R (2011) GRN1005 Phase I studies final results. Molecular cancer therapeutics: Nov 2011; vol. 10, Supplement 1. doi: 10.1158/1535-7163.TARG-11-B49

Wender PA, Mitchell DJ, Pattabiraman K, Pelkey ET, Steinman L, Rothbard JB (2000) The design, synthesis, and evaluation of molecules that enable or enhance cellular uptake: peptoid molecular transporters. Proc Natl Acad Sci U S A 97:13003–13008

Wohlfart S, Khalansky AS, Gelperina S, Begley D, Kreuter J (2011) Kinetics of transport of doxorubicin bound to nanoparticles across the blood–brain barrier. J Control Release 154:103–107

Wohlfart S, Gelperina S, Kreuter J (2012) Transport of drugs across the blood–brain barrier by nanoparticles. J Control Release 161(2):264–273

Wolf GG, Lopes MBS, VandenBerg SR, Gonias SL (1992) Characterization and immunohistochemical localization of α2-macroglobulin receptor (Low-density lipoprotein receptor-related protein) in human brain. Am J Pathol 141:37–42

Xin H, Jiang X, Gu J, Sha X, Chen L, Law K, Chen Y, Wang X, Jiang Y, Fang X (2011) Angiopep-conjugated poly(ethylene glycol)-copoly(ϵ-caprolactone) nanoparticles as dual-targeting drug delivery system for brain glioma. Biomaterials 32:4293–4305

Yamamoto M, Ikeda K, Ohshima K, Tsugu H, Kimura H, Tomonaga M (1997) Increased expression of low density lipoprotein receptor-related protein/α2-macroglobulin receptor in human malignant astrocytomas. Cancer Res 57:2799–2805

Yoon I-S, Chen E, Busse T, Repetto E, Lakshmana MK, Koo EH, Kang DE (2007) Low-density lipoprotein receptor-related protein promotes amyloid precursor protein trafficking to lipid rafts in the endocytic pathway. FASEB J 21:2742–2752

Yu YJ, Zhang Y, Kenrich M, Hoyte K, Luk W, Lu Y, Atwal J, Elliott JM, Prabhu S, Watts RJ, Dennis MS (2011) Boosting brain uptake of a therapeutic antibody by reducing its affinity for a transcytosis target. Sci Transl Med 3(84):84ra44

Zensi A, Begley D, Pontikis C, Legros C, Mihoreanu L, Wagner S, Büchel C, von Briesen H, Kreuter J (2009) Albumin nanoparticles targeted with Apo E enter the CNS by transcytosis and are delivered to neurones. J Control Release 137:78–86

Zensi A, Begley D, Pontikis C, Legros C, Mihoreanu L, Buchel C, Kreuter J (2010) Human serum albumin nanoparticles with apolipoprotein A-I cross the blood–brain barrier and enter the rodent brain. J. Drug Target 18:842–848

Chapter 17
CNS Gene Therapy Utilizing Intravenously Administered Viral Vectors

Adam K. Bevan and Brian K. Kaspar

Abstract Gene therapy is an important emerging field of medicine that is already starting to make real impact on the lives of chronically ill patients. Nevertheless, with regard to treating neurologic disease, the blood–brain barrier is a significant obstacle to translation of theoretically beneficial therapeutics to the clinic. Recently, however, major strides have been made that allow for safe, effective transduction of central nervous system tissues via the bloodstream, including the use of blood–brain barrier disrupters and better appreciation of the innate abilities of certain adeno-associated viral and Simian virus 40-based vectors to enter into the brain across CNS barriers. The use of these new technologies is likely to have great impact on system-wide neurologic diseases such as spinal muscular atrophy, amyotrophic lateral sclerosis, lysosomal storage diseases, and many others.

17.1 Rationale for CNS Targeting via IV Gene Delivery

Over the last three decades, the number of diseases linked to aberrant expression of specific genes has increased exponentially. Appropriately, the field of gene therapy has been created to treat the root cause of these diseases by correcting gene expression.

A.K. Bevan, Ph.D.
Department of Gene Therapy, The Research Institute at Nationwide Children's Hospital and The Ohio State University School of Medicine, Columbus, OH, USA

B.K. Kaspar, Ph.D. (✉)
Department of Gene Therapy, The Research Institute at Nationwide Children's Hospital, Columbus, OH, USA

Department of Pediatrics, The Ohio State University Medical Center, Columbus, OH, USA

Department of Neuroscience, The Ohio State University Medical Center, Columbus, OH, USA
e-mail: Brian.Kaspar@NationwideChildrens.org

M. Hammarlund-Udenaes et al. (eds.), *Drug Delivery to the Brain*, AAPS Advances in the Pharmaceutical Sciences Series 10, DOI 10.1007/978-1-4614-9105-7_17,

While the basic concept of gene therapy is simple, i.e., to replace gene products where they were previously missing, there have been various barriers to implementing it in a clinically meaningful way. Targeting the correct cells and using safe vectors is the primary difficulty that needs to be overcome for clinical application of proposed therapies. The blood–brain barrier poses a significant challenge to any therapeutic strategy targeting the central nervous system (CNS), and this barrier has proven itself to be particularly formidable for gene therapy. Various techniques have been successfully employed to this end, such as direct injection, retrograde transport, and, more recently, system-wide targeting through the vasculature (Kaspar et al. 2003; Azzouz et al. 2004; Hollis et al. 2008; Foust et al. 2009).

For some focal neurologic diseases, such as Parkinson's disease, direct injection into neural tissue is a very good option (LeWitt et al. 2011). There are many diseases, though, that affect large portions of the brain and spinal cord, and meaningful treatment will need to target cells throughout the neuraxis. Direct injections into nervous tissue for these system-wide diseases such as spinal muscular atrophy (SMA), metabolic disorders (i.e., mucopolysaccharidoses (MPS)), and others would require multiple injections into very sensitive neuronal tissue, making it an impractical solution. Therefore, less damaging strategies to circumvent the blood–brain barrier need to be used in order to deliver genetic material over a substantial area. Delivery through the bloodstream using vectors that penetrate the BBB is a new and very helpful tool allowing for safe and effective gene transfer, and this will be the focus of this chapter.

17.2 Recent Advances in CNS-Wide Gene Therapy

For neurological research, the use of adeno-associated viruses (AAVs) has proven to be particularly advantageous (Weinberg et al. 2012). AAV is a small, single-stranded DNA virus of the parvoviridae family, and most of the known AAV serotypes have a strong tropism for neuronal tissue. Additionally, AAV has a marvelous, well-studied safety profile; it is not associated with any human disease, is unable to replicate on its own, and has very low immunogenicity compared to other viruses previously used for gene therapy. Researchers have taken advantage of naturally derived or rationally designed serotypes to expand the utility of the AAV family (Gao et al. 2002, 2004, 2005; White et al. 2008; Asokan et al. 2012; Lee et al. 2012).

17.2.1 Self-Complementary AAV Vectors

Wild-type AAV has a single-stranded genetic sequence of ~4.6 kb. Upon infection, host cell machinery is required to synthesize the complementary strand using the self-priming inverted terminal repeat (ITR) sequences flanking the AAV genetic payload. This process is somewhat inefficient, possibly leading to decreased expression potential.

While the mechanics of this process are beyond the intended scope of this chapter, manipulation of this mechanism has led to one of the most important innovations in AAV gene therapy. In 2001, Doug McCarty in the Samulski lab reported that by mutating one of the ITRs and halving the payload size, one could make a self-complementary, double-stranded vector that does not require second-strand synthesis (McCarty et al. 2001). This was found to significantly decrease the latency from infection to expression, with a resulting 5–20-fold increase in transduction efficiency. The obvious drawback of using self-complementary AAV (scAAV, a.k.a. double-stranded or dsAAV) is the decreased payload, with the maximum size being about 2.5 kb. In regard to systemic intravascular delivery to the CNS (discussed below), scAAV vectors are particularly important considering the high doses required (Gray et al. 2011).

17.2.2 Mannitol Improves CNS Penetration by Transient Disruption of the Blood–Brain Barrier

In 2003, Haiyan Fu and Doug McCarty found that it was possible to increase transduction of CNS structures after IV injection of AAV by transiently disrupting the BBB (Fu et al. 2003). Mannitol is a sugar alcohol that has been used to osmotically disrupt the BBB to improve CNS penetration after IV drug administration, and it has been used in human patients for various indications for years. Drs. Fu and McCarty found that AAV2 was almost completely unable to cross the BBB on its own, but widespread transduction was possible after pre-injection of IV mannitol. Furthermore, in a 2009 report, they defined a simple protocol that allowed AAV2 to escape around endothelial cells and infect both neuronal and nonneuronal cells of the CNS: IV inject 25 % mannitol 8 min prior to IV injection of vector (McCarty et al. 2009). The timing of mannitol pretreatment is crucial, with an 8-min separation of dosing being >100-fold more efficacious than either 5 or 10 min. Importantly, this report also included impressive preclinical efficacy in treating mucopolysaccharidosis IIIB (MPS IIIB, or Sanfilippo syndrome).

17.2.3 AAV Serotypes Expand the Capabilities of Gene Therapy

Almost all of the initial characterization of AAV was using DNA derived from serotype 2 until the 1990s (Carter 2004). However, the subsequent discovery and characterization of other serotypes have extended the possibilities of gene therapy since each serotype has its own tropism and ability to travel through different compartments in the body (Gao et al. 2002, 2004, 2005; Broekman et al. 2006; Wu et al. 2006; Zincarelli et al. 2008). An almost infinite arsenal of naturally occurring AAV serotypes remains to be characterized, and new useful gene therapy candidates continue to be unveiled.

Good examples of specific features of different capsids include AAV1 and AAV2 which are particularly good at being retrogradely transported by motor neurons from the musculature and AAV6, AAV8, and AAV9 which are able to transduce skeletal musculature with remarkable efficiency after IV injection (Kaspar et al. 2003; Wang et al. 2005; Bish et al. 2008; Hollis et al. 2008; Petruska et al. 2010). These findings led Kevin Foust and the Flotte lab to assess AAV8's ability to infect motor neuron fibers in the periphery and be retrogradely transported to the spinal cord (Foust et al. 2008). Ideally, this would obviate the need for multiple intramuscular injections in order to target the entire length of the spinal cord. The results of this experiment were somewhat underwhelming, as very few motor neurons were transduced. However, this study gave hope that if relatively few AAV8 particles could subvert the BBB, perhaps other serotypes would be discovered that could be even more efficient.

17.2.4 AAV9 Overcomes the Blood–Brain Barrier of Multiple Species

Similar to AAV8, AAV9 was found to efficiently escape vasculature and infect striated muscle. Using techniques similar to those used in his previous AAV8 study, Dr. Foust and the Kaspar group injected neonatal mice with high-titer scAAV9 (Foust et al. 2009). Surprisingly, neurons and glia throughout the brain and spinal cord were very well transduced. Throughout most areas of the brain, about 15–20 % of NeuN+ cells had detectable GFP expression, but in some distinct cell types, such as Purkinje cells of the cerebellum, >70 % were transduced. Interestingly, a substantial amount of glial cells throughout the brain were also transduced (Fig. 17.1a, b).

In the spinal cord of injected neonatal mice, there was a slightly different pattern of transduction. Glial cells were still moderately transduced similar to the brain, but the neuron population almost exclusively transduced were motor neurons. The initial attempt to quantify motor neuron transduction by immunofluorescence estimated that ~60 % of lumbar motor neurons were GFP+. Subsequent investigation using in situ hybridization to detect transgene expression was difficult to quantify, but estimates based on this technique confirm that at least 60–70 % of motor neurons expressed GFP transcript after neonatal injection with AAV9-GFP. Interestingly, most other neuronal cell bodies within the spinal cord were devoid of detectable gene expression, including sympathetic preganglionic cells of the intermediolateral column, despite the similarity of these cells to ventral horn motor neurons. However, it is clear that ascending fibers originating from the dorsal root ganglia are also transduced, as the posterior column fibers are strongly positive for GFP expression though these cells are found outside the parenchyma of the CNS (Fig. 17.1c). The reason why lower motor neurons are primarily transduced while others are not remains a mystery, but this phenomenon hints that there may be a different mechanism of CNS penetration in the brain versus the spinal cord or perhaps the makeup of the BBB or blood–spinal cord barrier could be different during the neonatal period.

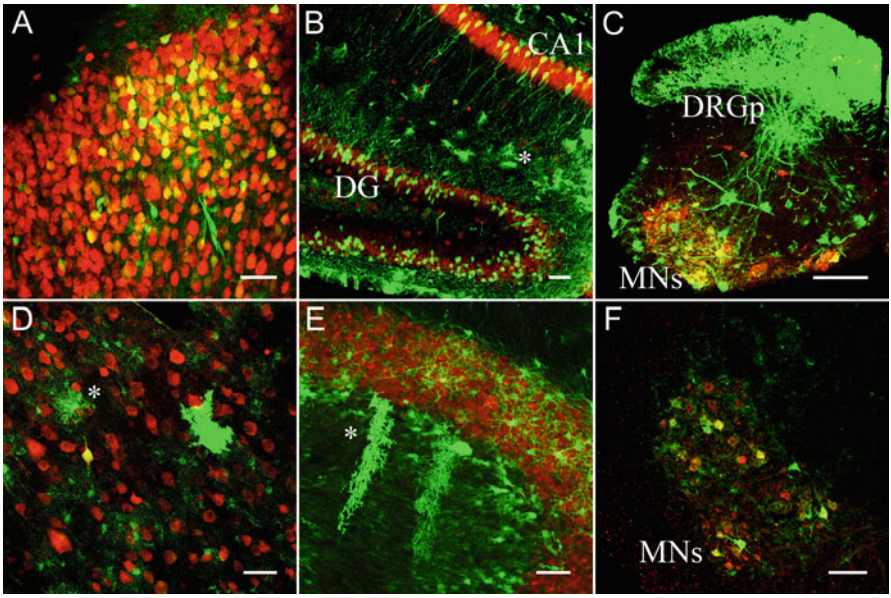

Fig. 17.1 Transgene expression after neonatal delivery of AAV9 encoding for a GFP transgene in mice (**a**–**c**) and nonhuman primates (**d**–**f**). Abundant transgene is expressed in cortical (**a**) and hippocampal (**b**) regions with neurons and astrocytes transduced. The dentate gyrus (DG) and CA1 regions of the hippocampus have numerous neurons targeting, and some astrocytes as depicted by the * AAV9 primarily target motor neurons and sensory fibers in the spinal cord of neonatally injected mice (**c**). The dorsal root ganglion projections (DRGp) are intensely bright, with large numbers of motor neurons (MNs) expressing GFP. In a neonatally injected Cynomolgus macaque, astrocytes (marked by a *) are mainly transduced in the cortex, with occasional neurons expressing the transgene (**d**). Both neurons and astrocytes (marked by a *) are well transduced in primate cerebellum (**e**), and motor neurons (MNs) are mainly transduced in the spinal cord (**f**). Neuronal marker, NeuN, in *red* for *panels* (**a**, **b**) and (**d**, **e**). Motor neuronal marker, ChAT in *red* for *panels* (**c**, **f**). Transgene, GFP, in *green* for all panels. Scale bars in all panels = 200 μm

Alternatively, it is reasonable to hypothesize that the site of cellular infection is outside the CNS parenchyma in the case of motor neurons, which allows for selective transduction of these cell types due to their large peripheral axonal exposure outside the BBB.

In older mice the ability of AAV9 to cross the BBB remained, although the transduction pattern was starkly different. In the brain, astrocyte transduction remained high, but neuron transduction was greatly diminished in most sections. The one exception to this was the hippocampus, in which the neurons of the cornu ammonis remained transduced, especially in the medial portions of the CA1 region as well as the dentate gyrus. In the spinal cords of adult injected mice, there was again an age-dependent change, where astrocytes were now even more prevalent and the numbers of motor neurons transduced decreased precipitously compared to the injected neonatal mice. Additionally, the ascending dorsal column neurons were no longer well transduced in adult mice. This shift in transduction pattern was first noted in mice

that were 6 weeks old when injected, but the shift was later found to start at ~4 days of age and be completed by about ~10–14 days. While the vascular component of the BBB is completely developed by birth, this age-dependent phenomenon corresponds well with the later phase of gliosis, when astrocyte arborization continues to occur and endfeet become more intimate with the vasculature over the first 3 weeks of life (Caley and Maxwell 1970).

Soon after the initial report in 2009, independent work in other labs further validated these findings, with almost identical results. Gray et al. also demonstrated that pairing AAV9 with mannitol pretreatment only increased expression intensity by ~50 %, and subsequent studies have shown similar results (Gray et al. 2011). The mannitol effect is very minor compared to previous results with AAV2, and it is likely due to the innate abilities of AAV9 to cross the endothelia, so disruption of the tight junctions is of relatively small benefit (Fu et al. 2011).

In addition to injecting neonatal and adult mice, the Barkats group from France found the same phenomenon existed in feline models (Duque et al. 2009). In 2-day-old kittens, neuronal and glial transduction mostly mirrored what was seen in mice, with motor neuron transduction being estimated between 30 and 40 % in the spinal cord. In older cats (~7 weeks old), motor neurons were well transduced but only at an estimated 15 %.

In late 2010, AAV9's ability to transduce beyond the BBB was reconfirmed in an in-depth study in neonatal rats (Wang et al. 2010). The results were almost identical with what was published in mice, with lower motor neuron transduction surpassing 75 % when a woodchuck post response enhancing element (WPRE) was used in the viral construct.

As species-specific differences in AAV transduction patterns had already been shown with other serotypes, it was of utmost importance to determine whether AAV9 could still transduce cells beyond the BBB in nonhuman primates (NHPs) (Wu et al. 2006). Details on the timing of BBB formation including astrocytosis are not available for NHPs, but it can reasonably be assumed that the entire process is complete by birth as it is in humans. Fortunately, despite this, AAV9 can indeed transduce beyond the BBB in newborn NHPs (*Macaca fascicularis*) (Foust et al. 2010; Bevan et al. 2011). In a subject injected within 24 h of birth, the Kaspar group found that, similar to mice, a large portion (>70 %) of spinal motor neurons was transduced, along with significant astrocytes and dorsal column sensory fibers. However, the transduction pattern in the brain was similar to the pattern seen in adult mouse brains, with glia being present throughout and only the occasional neuron being transduced in the cortex. Interestingly, the hippocampus in NHPs showed no specific bias for neuronal expression as it did in mice (Fig. 17.1d–f).

Soon, the NHP studies expanded to include 30- and 90-day-old subjects with similar results to the newborn (Bevan et al. 2011). The Samulski group independently investigated the transduction ability of AAV9 in adolescent NHPs (*Macaca mulatta*), though the dose was much lower than that used by the Kaspar lab in their infantile NHP study (Gray et al. 2011). Despite the lower dose, in subjects without preexisting AAV9 immunity, impressive transduction occurred throughout the CNS with similar neuron-to-astrocyte ratios seen by the Kaspar lab.

Table 17.1 Comparison of distribution in preclinical studies of intravenously delivered AAV9

	Neonatal				Adolescent/adult			
	Brain		Spinal cord		Brain		Spinal cord	
	Neurons	Glia	Neurons	Glia	Neurons	Glia	Neurons	Glia
Mice[a]	+++	++	+++	++	+	+++	+	+++
Rats[b]	+++	++	+++	++	?	?	?	?
Cat[c]	?	?	+++	?	?	?	+	?
Macaque[d]	+	+++	++	++	+	+++	+	++

"?" Denotes absence of experimental data for the specified category
[a]Mice neonates <4 days old, adult >14 days old
[b]Only neonatal (1-day-old) results published for rats
[c]Neonatal catst were 2 days old at the time of injection, and adolescent cats were 7 weeks old
[d]No difference in infants 1–90 days old (*Macaca fascicularis*), adolescents tested include 3–4-year-old *Macaca fascicularis* and *mulatta* species

Some attempts have been made to determine whether there is an optimal route for CNS-wide AAV9 delivery. In the report by Gray et al. in primates and in unpublished work by the Kaspar lab in mice, intracarotid arterial delivery was not shown to be significantly more efficacious than intravenous routes. This is somewhat expected since AAV9 is still found circulating in the bloodstream in injected subjects for hours post injection, thereby making the "first-pass" effect of arterially injected AAV likely of little significance; however, this remains to be fully determined (Table 17.1).

To complement the intravascular studies performed in NHPs, the Kaspar and Burghes labs also demonstrated impressive transduction of the spinal cord by intrathecal delivery of AAV9 (Bevan et al. 2011). In pigs, both motor neurons and astrocytes were extensively transduced in all regions of the spinal cord, regardless of the level at which AAV9 was introduced into the CSF. This and other more invasive techniques for gene delivery are discussed in the next chapter.

17.2.5 Emerging Viruses and Techniques

17.2.5.1 Emerging AAV Serotypes Provide a Potential Alternative to AAV9-Based Therapy

Shortly after the initial discovery that AAV9 could cross the BBB by Foust et al. a broader comparison of ten serotypes was performed to compare their abilities to cross the BBB by Zhang et al. from the Gao laboratory (Zhang et al. 2011). Among those tested, it was found that most had at least some ability to transduce CNS structures when introduced intravascularly, but the four serotypes that well outperformed the others were AAV9, AAV.rh10, AAV.rh39, and AAV.rh43. In many cases these

new serotypes were found to perform at least as well as AAV9 in specific areas of the brain, but there was significant variation that prohibited solid conclusions as to which serotype was most appropriate for intravascular gene therapy protocols. Additionally, the specific findings in the Zhang paper with regard to spinal cord transduction were less hopeful than what was reported previously by Foust and the Kaspar group.

These findings led to a head-to-head comparison of these four serotypes by the Kaspar group in collaboration with Dr. Gao to ensure that the correct product was moving forward to future clinical trials for treating SMA. Using more sensitive immunofluorescence, they found that all four serotypes highly transduced spinal cord motor neurons and scattered glia with very little difference, if any, in efficiency. The finding that other serotypes besides AAV9 exist which can transduce spinal motor neurons is very important, though, since some patients will be poor candidates for AAV9 therapy due to seropositivity for anti-AAV9 antibodies. With more serotype options, we hope fewer patients will be denied therapy or need more advanced procedures, such as plasmapheresis.

17.2.5.2 SV40

Simian virus 40 (SV40) is a different kind of virus from the polyomaviridae family. SV40 has a circular, double-stranded DNA genome about 5.2 kb in length. Many associate SV40 with the hype surrounding contamination of polio vaccines produced by NHP cell lines infected with the virus, although no pathology was proven to result directly from this (Mortimer et al. 1981). With manipulations of the wild-type genome and replacement with therapeutic transgenes, the safety profile seems similar to AAV (Louboutin et al. 2011). Like AAV, SV40 can remain episomally, but it can also integrate into the host genome with higher frequency than AAV (Chia and Rigby 1981).

In 2010, the Strayer lab reported that when introduced intravenously following mannitol pretreatment, recombinant SV40 is also able to transduce beyond the BBB in many regions of the CNS (Louboutin et al. 2010). Interestingly, some of these regions contrast the transduction pattern of AAV9, with cortical cells (mostly neurons) being highly transduced (~30–50 %), but the dentate, ventral hippocampus and cerebellum having the lowest transduction rates (<10 %). SV40 seems to transduce occasional microglia, which may be very important for diseases such as amyotrophic lateral sclerosis (ALS) (discussed below). Important to note is that when injected following mannitol, SV40 preferentially targets CNS structures at the expense of liver and kidney transduction, which may be extremely beneficial when trying to avoid peripheral expression of therapeutic transgenes specified for the CNS. While SV40 gene therapy has not been studied as in-depth as AAV-based protocols, the initial work provides strong evidence that SV40 is very well suited for gene therapy targeting the CNS and may appropriately complement AAV9-based approaches.

17.3 Potential Clinical Applications of AAV9-Based Therapies

17.3.1 scAAV9-SMN as a Treatment for Spinal Muscular Atrophy

Specifically due to the ability to selectively target lower motor neurons, the first application of this exciting new method of gene delivery was to determine whether systemically delivered AAV9-mediated gene replacement would be sufficient to rescue a model of proximal SMA.

SMA is a devastating disease affecting approximately 1 in 10,000 newborns worldwide (Roberts et al. 1970). Patients with this disease most often present with rapid onset of weakness prior to 6 months of age followed by respiratory failure by 18–24 months, although there is a spectrum of disease severity (Lefebvre et al. 1997). The weakness is due to dysfunction and loss of motor neurons that innervate skeletal muscle. The cause of SMA is decreased expression of the ubiquitous full-length survival motor neuron (SMN) protein (Lefebvre et al. 1995; Coovert et al. 1997). SMA is a premier candidate for systemic gene therapy as SMN is required in every cell, it is already present in low levels in every cell, and no toxicity has been demonstrated in overexpression models or in human subjects with excess copies of the gene. Immediately after discovery of AAV9's potential, the Kaspar lab found that a one-time dose of scAAV9 carrying the SMN transgene was sufficient to correct the phenotype in a mouse model of severe SMA (Foust, Wang et al. 2010). The relatively normal life-span of treated animals is far beyond any previous therapy has ever achieved, and a clinical trial of systemic scAAV9-SMN is imminent.

17.3.2 AAV9-hNAGLU as a Treatment for Mucopolysaccharidosis IIIB

MPS IIIB, a.k.a. Sanfilippo syndrome, is an autosomal recessive lysosomal storage disease, caused by homozygous deletion/mutation of the α-*N*-acetylglucosaminidase (*NAGLU*) gene. The result is an accumulation of heparan sulfate in various organ systems, including the brain, which leads to developmental and behavioral problems ultimately leading to premature mortality. MPS IIIB is a top candidate for gene therapy since the secreted NAGLU gene product leads to bystander effects, where a single transduced cell can support its neighbors (Fu et al. 2011). As previously discussed, AAV9 is able to transduce glial cells throughout the neuraxis at any age in NHP studies, so lower doses that lead to scant neuronal expression are likely to remain efficacious.

Systemic gene delivery attempts using mannitol prior to using AAV9 have been tried with some success, but the greatest benefit in both behavior and survival was

accomplished using a single-stranded AAV9-hNAGLU product (McCarty et al. 2009; Fu et al. 2011). A single dose was administered in 4–6-week-old mice, and the median survival increased from ~10 months to ~21 months. Of note, even though the less efficient single-stranded vector was used due to size restriction, the doses required for this effect are much smaller than what are required to treat SMA. This is likely due to bystander effects and the higher dose needed specifically for spinal motor neuron transduction. The success in MPS IIIB is likely just a first of many successful treatments for similar lysosomal storage disorders.

17.3.3 AAV9 for Modeling Amyotrophic Lateral Sclerosis

ALS is a devastating disease marked by loss of both upper and lower motor neurons, leading to a mixture of spastic and flaccid paralysis and ultimately death from respiratory failure. Unlike SMA, where disease progresses in a cell-autonomous fashion, almost all cells in the gray matter milieu have been implicated in the destruction of motor neurons in ALS, namely, astrocytes, oligodendrocytes, microglia, and even endothelia (Boillee et al. 2006a, b; Yamanaka et al. 2008; Zhong et al. 2008; Lasiene and Yamanaka 2011). Additionally, the definitive genetic cause of ALS has only been identified in ~2 % of cases, with ~90 % having no known genetic component at all. In the search for a therapeutic target, systemic AAV9 gene therapy may be a very useful tool.

In 2006 the transactive response DNA-binding protein-43 (*TDP43*) gene was identified as being aberrantly expressed in many ALS patients (Neumann et al. 2006). Multiple mutations have since been reported, leading to the creation of multiple versions of transgenic mouse models being made with varying success. In 2010, Wang et al. used intravascular AAV9 to overexpress TDP43 in glia and motor neurons throughout the CNS (Wang et al. 2010). The result was a robust model with an ALS-like phenotype that can be created in a fraction of the time compared to traditional transgenic modeling methods. This method can certainly be expanded for further screening of TDP43 variants and other potential targets for ALS. It also serves as an important "rapid transgenic" prototype for modeling other neurological diseases.

17.4 Intravenously Delivered AAV9 Is Safe

An important step in translation of systemic AAV9 therapy to the clinic is the preclinical demonstration of safety. To this end, the Kaspar lab has performed safety studies in mice and NHPs using the scAAV9-SMN product. Since the SMN transgene is expected to be completely benign, the data from this study are more generalizable as a toxicology study of high-dose systemically delivered AAV9 itself. Behavior, serum chemistry, hematology, immunologic, and histopathologic studies

all provide strong evidence that AAV9-based gene therapy is safe and well tolerated, even at doses 100-fold higher than have ever been attempted in human clinical trials. The confidence for a safe and effective therapy continues to increase.

17.5 Conclusions

As we are now in the thick of the "post-genomic era," we are increasingly confronted with new knowledge regarding genetic disease. Gene therapy, then, is naturally expanding in an attempt to answer the call for new modalities of genetic treatment. While targeting cells beyond the blood–brain barrier has presented a major hindrance in the past, emerging therapies using AAV and SV40 technologies provide safe, effective means for treating many neurological diseases.

Not 4 years have passed since the discovery of AAV9's ability to transcend the blood–brain barrier, but this finding has already impacted neurological research in remarkable ways. As the studies herein have outlined, SMA research and therapy development has primarily benefited from AAV9-based gene delivery thus far, but this technology may also prove very beneficial when applied to other CNS disorders.

Current IV-administered, AAV9-based therapies do have some limitations that must be considered for both basic research and clinical applications. First, those performing translational research using mouse models must remain cognizant that the pattern of transduction in the primate CNS is different than what is seen in both neonatal and adult mice. In the case of motor neuron targeting, as is needed for SMA gene therapy, the transduction remains the same. For certain other areas, such as the hippocampus, neuronal transduction is particularly lower in primate versus mouse studies, though astrocyte transduction remains similar. Another potential limitation is the high titer required for CNS penetration. While this has been shown to be very safe and well tolerated in both rodent and NHP studies, AAV9 is a promiscuous vector with particularly high tropism for striated muscle and liver. In the case of innocuous housekeeping transgenes such as SMN, this is of little importance, but off-target overexpression of other transgenes may not be acceptable. However, Pulicherla et al. have demonstrated that modifications can be made to detarget the liver for systemic applications of AAV9 (Pulicherla et al. 2011). Further modifications may be developed to further narrow the infection profile of AAV9.

In addition to the above, regardless of the vector system used, preexisting immunity is a potential hindrance to effective treatment of patients by almost any delivery route but especially when introduced via the bloodstream. Preclinical safety studies in the Kaspar lab demonstrate that AAV9 is safe and effective when introduced through the bloodstream of seronegative subjects (Foust et al. 2009; Foust, Wang et al. 2010; Bevan et al. 2011). Other studies show that seropositivity can decrease the effectiveness, but therapy remains safe (Gray et al. 2011). The maximum titer of anti-AAV9 antibodies that allows for effective transduction will need to be defined before widespread use of the vector, but even in cases of prohibitively high titers, this problem can be circumvented multiple ways. First, the emerging serotypes of

AAV.rh10, AAV.rh39, and AAV.rh43 provide alternatives, so when a given patient may be immune to one particular serotype, he or she may be immunologically naïve to another and still receive benefit from systemic gene therapy (Zhang et al. 2011). Of course, preclinical efficacy in mouse disease models has yet to be performed using these new vectors, but we assume that they will work similarly to AAV9. Second, moderately high titers can be lowered by plasmapheresis, and this will theoretically allow for efficacious systemic therapy (Monteilhet et al. 2011). Third, the possibility of utilizing SV40-based treatment is exciting, and it may be an acceptable alternative to AAV therapies should a patient be non-eligible (Louboutin et al. 2010). The efficacy of SV40 for specific disorders has yet to be determined, and supporting literature is limited, but initial studies do look very promising, and we look forward to seeing more data in the near future.

Gene therapy stands to make a substantial impact on the entire field of medicine, and neurological disease will especially benefit from the recent advances discussed herein. Where just a few years ago, system-wide gene therapy was completely unavailable, we now have multiple options for efficient gene delivery beyond the BBB. We are confident that we will see many patients benefit directly from these recent discoveries within the next decade.

17.6 Points for Discussion

How will age and various diseases affect the ability of viral vectors to cross the blood–brain barrier?

Can we identify the regions or the differences in the viral capsids that allows for crossing barriers?

Are NHPs predictive for the tropism we will find when viral vectors are delivered into humans?

What other neurological diseases may benefit from the advances from these viral vectors?

Will these vectors be found safe in humans?

How can viral vectors be improved, for safety, for efficacy? Will modifications based on rational design or evolutionary strategies of the viral capsid be effective towards these purposes?

References

Asokan A, Schaffer DV, Samulski RJ (2012) The AAV vector toolkit: poised at the clinical crossroads. Mol Ther 20:699–708

Azzouz M, Le T, Ralph GS, Walmsley L, Monani UR, Lee DC, Wilkes F, Mitrophanous KA, Kingsman SM, Burghes AH, Mazarakis ND (2004) Lentivector-mediated SMN replacement in a mouse model of spinal muscular atrophy. J Clin Invest 114:1726–1731

Bevan AK, Duque S, Foust KD, Morales PR, Braun L, Schmelzer L, Chan CM, McCrate M, Chicoine LG, Coley BD, Porensky PN, Kolb SJ, Mendell JR, Burghes AH, Kaspar BK (2011) Systemic gene delivery in large species for targeting spinal cord, brain, and peripheral tissues for pediatric disorders. Mol Ther 19:1971–1980

Bish LT, Morine K, Sleeper MM, Sanmiguel J, Wu D, Gao G, Wilson JM, Sweeney HL (2008) Adeno-associated virus (AAV) serotype 9 provides global cardiac gene transfer superior to AAV1, AAV6, AAV7, and AAV8 in the mouse and rat. Hum Gene Ther 19:1359–1368

Boillee S, Vande Velde C, Cleveland DW (2006a) ALS: a disease of motor neurons and their non-neuronal neighbors. Neuron 52:39–59

Boillee S, Yamanaka K, Lobsiger CS, Copeland NG, Jenkins NA, Kassiotis G, Kollias G, Cleveland DW (2006b) Onset and progression in inherited ALS determined by motor neurons and microglia. Science 312:1389–1392

Broekman ML, Comer LA, Hyman BT, Sena-Esteves M (2006) Adeno-associated virus vectors serotyped with AAV8 capsid are more efficient than AAV-1 or -2 serotypes for widespread gene delivery to the neonatal mouse brain. Neuroscience 138:501–510

Caley DW, Maxwell DS (1970) Development of the blood vessels and extracellular spaces during postnatal maturation of rat cerebral cortex. J Comp Neurol 138:31–47

Carter BJ (2004) Adeno-associated virus and the development of adeno-associated virus vectors: a historical perspective. Mol Ther 10:981–989

Chia W, Rigby PW (1981) Fate of viral DNA in nonpermissive cells infected with simian virus 40. Proc Natl Acad Sci U S A 78:6638–6642

Coovert DD, Le TT, McAndrew PE, Strasswimmer J, Crawford TO, Mendell JR, Coulson SE, Androphy EJ, Prior TW, Burghes AH (1997) The survival motor neuron protein in spinal muscular atrophy. Hum Mol Genet 6:1205–1214

Duque S, Joussemet B, Riviere C, Marais T, Dubreil L, Douar AM, Fyfe J, Moullier P, Colle MA, Barkats M (2009) Intravenous administration of self-complementary AAV9 enables transgene delivery to adult motor neurons. Mol Ther 17:1187–1196

Foust KD, Poirier A, Pacak CA, Mandel RJ, Flotte TR (2008) Neonatal intraperitoneal or intravenous injections of recombinant adeno-associated virus type 8 transduce dorsal root ganglia and lower motor neurons. Hum Gene Ther 19:61–70

Foust KD, Nurre E, Montgomery CL, Hernandez A, Chan CM, Kaspar BK (2009) Intravascular AAV9 preferentially targets neonatal neurons and adult astrocytes. Nat Biotechnol 27:59–65

Foust KD, Wang X, McGovern VL, Braun L, Bevan AK, Haidet AM, Le TT, Morales PR, Rich MM, Burghes AH, Kaspar BK (2010) Rescue of the spinal muscular atrophy phenotype in a mouse model by early postnatal delivery of SMN. Nat Biotechnol 28:271–274

Fu H, Muenzer J, Samulski RJ, Breese G, Sifford J, Zeng X, McCarty DM (2003) Self-complementary adeno-associated virus serotype 2 vector: global distribution and broad dispersion of AAV-mediated transgene expression in mouse brain. Mol Ther 8:911–917

Fu H, Dirosario J, Killedar S, Zaraspe K, McCarty DM (2011) Correction of neurological disease of mucopolysaccharidosis IIIB in adult mice by rAAV9 trans-blood–brain barrier gene delivery. Mol Ther 19:1025–1033

Gao G, Vandenberghe LH, Alvira MR, Lu Y, Calcedo R, Zhou X, Wilson JM (2004) Clades of Adeno-associated viruses are widely disseminated in human tissues. J Virol 78:6381–6388

Gao G, Vandenberghe LH, Wilson JM (2005) New recombinant serotypes of AAV vectors. Curr Gene Ther 5:285–297

Gao GP, Alvira MR, Wang L, Calcedo R, Johnston J, Wilson JM (2002) Novel adeno-associated viruses from rhesus monkeys as vectors for human gene therapy. Proc Natl Acad Sci U S A 99:11854–11859

Gray SJ, Matagne V, Bachaboina L, Yadav S, Ojeda SR, Samulski RJ (2011) Preclinical differences of intravascular AAV9 delivery to neurons and glia: a comparative study of adult mice and nonhuman primates. Mol Ther 19:1058–1069

Hollis ER 2nd, Kadoya K, Hirsch M, Samulski RJ, Tuszynski MH (2008) Efficient retrograde neuronal transduction utilizing self-complementary AAV1. Mol Ther 16:296–301

Kaspar BK, Llado J, Sherkat N, Rothstein JD, Gage FH (2003) Retrograde viral delivery of IGF-1 prolongs survival in a mouse ALS model. Science 301:839–842

Lasiene J, Yamanaka K (2011) Glial cells in amyotrophic lateral sclerosis. Neurol Res Int 2011:718987

Lee NC, Falk DJ, Byrne BJ, Conlon TJ, Clement N, Porvasnik S, Jorgensen ML, Potter M, Erger KE, Watson R, Ghivizzani SC, Chiu HC, Chien YH, Hwu WL (2012) An acidic oligopeptide displayed on AAV2 improves axial muscle tropism after systemic delivery. Genet Vaccines Ther 10:3

Lefebvre S, Burglen L, Reboullet S, Clermont O, Burlet P, Viollet L, Benichou B, Cruaud C, Millasseau P, Zeviani M et al (1995) Identification and characterization of a spinal muscular atrophy-determining gene. Cell 80:155–165

Lefebvre S, Burlet P, Liu Q, Bertrandy S, Clermont O, Munnich A, Dreyfuss G, Melki J (1997) Correlation between severity and SMN protein level in spinal muscular atrophy. Nat Genet 16:265–269

LeWitt PA, Rezai AR, Leehey MA, Ojemann SG, Flaherty AW, Eskandar EN, Kostyk SK, Thomas K, Sarkar A, Siddiqui MS, Tatter SB, Schwalb JM, Poston KL, Henderson JM, Kurlan RM, Richard IH, Van Meter L, Sapan CV, During MJ, Kaplitt MG, Feigin A (2011) AAV2-GAD gene therapy for advanced Parkinson's disease: a double-blind, sham-surgery controlled, randomised trial. Lancet Neurol 10:309–319

Louboutin JP, Chekmasova AA, Marusich E, Chowdhury JR, Strayer DS (2010) Efficient CNS gene delivery by intravenous injection. Nat Methods 7:905–907

Louboutin JP, Marusich E, Fisher-Perkins J, Dufour JP, Bunnell BA, Strayer DS (2011) Gene transfer to the rhesus monkey brain using SV40-derived vectors is durable and safe. Gene Ther 18:682–691

McCarty DM, Monahan PE, Samulski RJ (2001) Self-complementary recombinant adeno-associated virus (scAAV) vectors promote efficient transduction independently of DNA synthesis. Gene Ther 8:1248–1254

McCarty DM, DiRosario J, Gulaid K, Muenzer J, Fu H (2009) Mannitol-facilitated CNS entry of rAAV2 vector significantly delayed the neurological disease progression in MPS IIIB mice. Gene Ther 16:1340–1352

Monteilhet V, Saheb S, Boutin S, Leborgne C, Veron P, Montus MF, Moullier P, Benveniste O, Masurier C (2011) A 10 patient case report on the impact of plasmapheresis upon neutralizing factors against adeno-associated virus (AAV) types 1, 2, 6, and 8. Mol Ther 19:2084–2091

Mortimer EA Jr, Lepow ML, Gold E, Robbins FC, Burton GJ, Fraumeni JF Jr (1981) Long-term follow-up of persons inadvertently inoculated with SV40 as neonates. N Engl J Med 305:1517–1518

Neumann M, Sampathu DM, Kwong LK, Truax AC, Micsenyi MC, Chou TT, Bruce J, Schuck T, Grossman M, Clark CM, McCluskey LF, Miller BL, Masliah E, Mackenzie IR, Feldman H, Feiden W, Kretzschmar HA, Trojanowski JQ, Lee VM (2006) Ubiquitinated TDP-43 in frontotemporal lobar degeneration and amyotrophic lateral sclerosis. Science 314:130–133

Petruska JC, Kitay B, Boyce VS, Kaspar BK, Pearse DD, Gage FH, Mendell LM (2010) Intramuscular AAV delivery of NT-3 alters synaptic transmission to motoneurons in adult rats. Eur J Neurosci 32:997–1005

Pulicherla N, Shen S, Yadav S, Debbink K, Govindasamy L, Agbandje-McKenna M, Asokan A (2011) Engineering liver-detargeted AAV9 vectors for cardiac and musculoskeletal gene transfer. Mol Ther 19:1070–1078

Roberts DF, Chavez J, Court SD (1970) The genetic component in child mortality. Arch Dis Child 45:33–38

Wang DB, Dayton RD, Henning PP, Cain CD, Zhao LR, Schrott LM, Orchard EA, Knight DS, Klein RL (2010) Expansive gene transfer in the rat CNS rapidly produces amyotrophic lateral sclerosis relevant sequelae when TDP-43 is overexpressed. Mol Ther 18:2064–2074

Wang Z, Zhu T, Qiao C, Zhou L, Wang B, Zhang J, Chen C, Li J, Xiao X (2005) Adeno-associated virus serotype 8 efficiently delivers genes to muscle and heart. Nat Biotechnol 23:321–328

Weinberg MS, Samulski RJ, McCown TJ (2012) Adeno-associated virus (AAV) gene therapy for neurological disease. Neuropharmacology

White AF, Mazur M, Sorscher EJ, Zinn KR, Ponnazhagan S (2008) Genetic modification of adeno-associated viral vector type 2 capsid enhances gene transfer efficiency in polarized human airway epithelial cells. Hum Gene Ther 19:1407–1414

Wu Z, Asokan A, Samulski RJ (2006) Adeno-associated virus serotypes: vector toolkit for human gene therapy. Mol Ther 14:316–327

Yamanaka K, Boillee S, Roberts EA, Garcia ML, McAlonis-Downes M, Mikse OR, Cleveland DW, Goldstein LS (2008) Mutant SOD1 in cell types other than motor neurons and oligodendrocytes accelerates onset of disease in ALS mice. Proc Natl Acad Sci U S A 105:7594–7599

Zhang H, Yang B, Mu X, Ahmed SS, Su Q, He R, Wang H, Mueller C, Sena-Esteves M, Brown R, Xu Z, Gao G (2011) Several rAAV vectors efficiently cross the blood–brain barrier and transduce neurons and astrocytes in the neonatal mouse central nervous system. Mol Ther 19:1440–1448

Zhong Z, Deane R, Ali Z, Parisi M, Shapovalov Y, O'Banion MK, Stojanovic K, Sagare A, Boillee S, Cleveland DW, Zlokovic BV (2008) ALS-causing SOD1 mutants generate vascular changes prior to motor neuron degeneration. Nat Neurosci 11:420–422

Zincarelli C, Soltys S, Rengo G, Rabinowitz JE (2008) Analysis of AAV serotypes 1–9 mediated gene expression and tropism in mice after systemic injection. Mol Ther 16:1073–1080

Chapter 18
Neurosurgical Approaches: Drug Infusion Directly into the Parenchyma or the Cerebrospinal Fluid

Krystof Bankiewicz

Abstract Delivering drugs effectively to the central nervous system (CNS) has always presented a challenge. The blood–brain barrier prevents significant amounts of systemically administered therapeutics from reaching the brain. Traditional local CNS delivery (e.g., biodegradable polymers, cerebro-ventricular injection, cell implantation) has relied on diffusion, which is dependent on a concentration gradient. The rate of diffusion is inversely proportional to the size of the agent and is usually slow with respect to tissue clearance, resulting in a non-homogeneous distribution often restricted to a few millimeters from the source. By contrast, convection-enhanced delivery uses a pressure gradient established at the tip of an infusion catheter to create bulk flow, "pushing" drugs into a large volume of brain tissue. This displacement allows the infused material to engage the vasculature, with rhythmic blood vessel contractions acting as an efficient motive force to move particles along perivascular tracts. This chapter describes a fully integrated and FDA-approved drug delivery system for cerebral infusion that consists of an MR-compatible aiming device, a reflux-resistant cannula, and predictive software, allowing the monitoring of nanoparticle, viral vector, or small molecule distribution in "real time" during brain and brain tumor delivery.

18.1 Introduction

The delivery of high-molecular-weight therapeutic agents within selected regions of the brain holds promise for a number of evolving therapies, from the treatment of brain tumors and Parkinson's disease (PD) to rare genetic disorders. However, the

K. Bankiewicz (✉)
University of California, San Francisco, CA, USA
e-mail: Krystof.Bankiewicz@ucsf.edu

M. Hammarlund-Udenaes et al. (eds.), *Drug Delivery to the Brain*, AAPS Advances in the Pharmaceutical Sciences Series 10, DOI 10.1007/978-1-4614-9105-7_18,

precise introduction of these therapeutic agents into focally defined brain structures represents a significant challenge that presently does not have an adequate solution. Administration via intravenous or intra-arterial approaches is limited by the blood–brain barrier (BBB), which restricts the transfer of macromolecules across the capillary wall. An assortment of methods have been explored to overcome the BBB, as described in other chapters of this book, but many of these approaches do not provide targeted delivery with respect to specific anatomical targets. In addition, many methods will be limited to the production of transient effects and therefore may not be appropriate for chronic drug administration. Macromolecules further suffer from minimal ability to permeate tissue based on passive diffusion, limiting distribution even once the BBB has been traversed.

Direct brain administration of therapeutics has been applied to human studies, including patients with brain tumors (Kunwar et al. 2007) and in gene therapy trials for PD, but with inconsistent results (Eberling et al. 2008; Marks et al. 2010). These trials have suffered from poor drug distribution throughout the target structure and poor monitoring of the infusion, incurring enormous expense in both financial and patient costs. After promising initial studies showed a therapeutic benefit for chronic infusion of glial-derived neurotrophic factor into the putamen of patients with Parkinson's disease (Gill et al. 2003; Slevin et al. 2006), a larger follow-on study missed its primary endpoint (Lang et al. 2006). Similarly, a trial of neurturin gene transfer into the putamen of patients with Parkinson's disease suggested potential efficacy, but the Phase II trial failed to meet its primary endpoint, and retrospective analysis of brain tissue demonstrated that poor vector distribution likely contributed to the failure (Marks et al. 2010). Soon after, repeated delivery of antitumor IL13 for patients with glioblastoma multiforme failed to extend patient survival, and poor drug coverage was again indicated as the potential culprit (Kunwar et al. 2007). The failure of these trials has underscored the need to address the significant challenge of effective delivery in upcoming trials. As described below, research from our group and others has led the development of many key innovations to address the numerous technical challenges of convection-enhanced delivery (CED). These have included the design of a reflux-resistant infusion cannula and specifications for acceptable infusion cannulae positioning to distribute infused drugs throughout target structures. In 2005, we introduced real-time monitoring of viral vectors and nanoparticles to the brain with magnetic resonance imaging (MRI) (Krauze et al. 2005a, b; Saito et al. 2005), providing feedback on distribution volumes during infusions. We have since been involved in using MR data to produce and validate software to predict and plan brain infusions for a validated CED platform (iPlan Flow, BrainLAB, Inc). Through these projects, we have accumulated mounting evidence that improved planning coupled with vigilant monitoring of CED infusions can produce substantially superior results to those previously achieved (Rosenbluth et al. 2013).

18.2 Convection-Enhanced Drug Delivery

CED is an interstitial central nervous system (CNS) delivery technique (Bobo et al. 1994) that circumvents the BBB in delivering therapeutics into the CNS. Traditional local delivery of most therapeutic agents into the brain has relied on diffusion, which depends on a concentration gradient. The rate of diffusion is inversely proportional to the size of the therapeutic and is usually slow with respect to tissue clearance. Thus, diffusion results in a nonhomogeneous distribution of most delivered agents, often restricting achievement of therapeutic levels to distances of just a few millimeters from the source. In many cases, this limited distribution will not result in the desired therapeutic effect. By contrast, CED uses a fluid pressure gradient established at the tip of an infusion catheter and bulk flow to propagate substances within the extracellular fluid space (Bobo et al. 1994). CED allows the extracellularly infused material to further propagate via the perivascular spaces, with rhythmic contractions of blood vessels acting as an efficient motive force for spreading of the infusate (Hadaczek et al. 2006). As a result, a higher concentration of drug is distributed more evenly over a larger area of the targeted structure than what would be seen with a simple injection. CED has been developed as a drug delivery strategy and represents a powerful methodology for targeted therapy in the fields of neurodegenerative diseases, such as Parkinson's disease (Gill et al. 2003; Eberling et al. 2008), and neuro-oncology (Kunwar 2003; Mardor et al. 2001). Laboratory investigations with CED cover a broad field of application and include the delivery of small molecules (Carson et al. 2002; Lonser et al. 1999), macromolecules (Bobo et al. 1994), viral particles (Richardson et al. 2008), magnetic nanoparticles (Kroll et al. 1996), and liposomes (Krauze et al. 2006).

Our understanding of CED distribution has been amplified by the realization that arterial pulsations within the brain's perivascular spaces enhance the distribution of convected therapeutics (Hadaczek et al. 2006), by a better appreciation of the complexities of the extracellular matrix and its effects on convection (Hamilton et al. 2001; Nguyen et al. 2001; Neeves et al. 2007), and by consideration of biophysical properties of the extracellular microenvironment such as the volume fraction (Sykova 2004). Technical CED infusion parameters, such as cannula size and shape (Fig. 18.1), infusion rate, infusate concentration, and tissue sealing time, have been defined and refined to improve distribution of therapeutics (Chen et al. 1999; Morrison et al. 1999; Krauze et al. 2005a, b; Szerlip et al. 2007) while limiting potential toxicities and morbidities (Krauze et al. 2005a, b; Murad et al. 2007; Fiandaca et al. 2009a, b).

18.2.1 Imaging Drug Infusion as It Happens: Real-Time Convective Delivery

A major advance in the safe and efficacious use of CED in clinical neurosurgery has been the development of real-time convective delivery (RCD) (Nguyen et al. 2003;

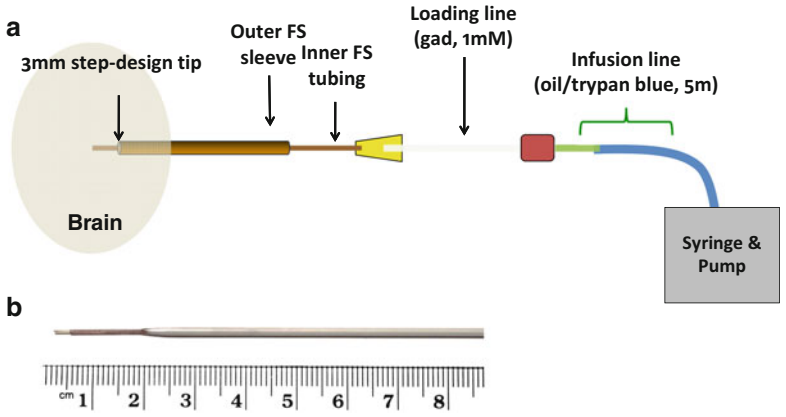

Fig. 18.1 (**a**) Schematic of the infusion setup used for real-time convective delivery (RCD). In clinical systems, no oil or loading lines are used. Inner fused silica (FS) tubing is extended to the Luer-type connector that connects with a syringe that contains the therapeutic agent mixed with 1 or 2 mmol Gd. It is important to pressurize the system by purging all the air from the line and the cannula and by beginning the infusion of the therapeutic agent prior to insertion. Cannulae should be inserted into the brain while running infusion at 1 μl/min to prevent any possible occlusion of the cannula tip. (**b**) Image of the step-design MR-compatible clinical cannula

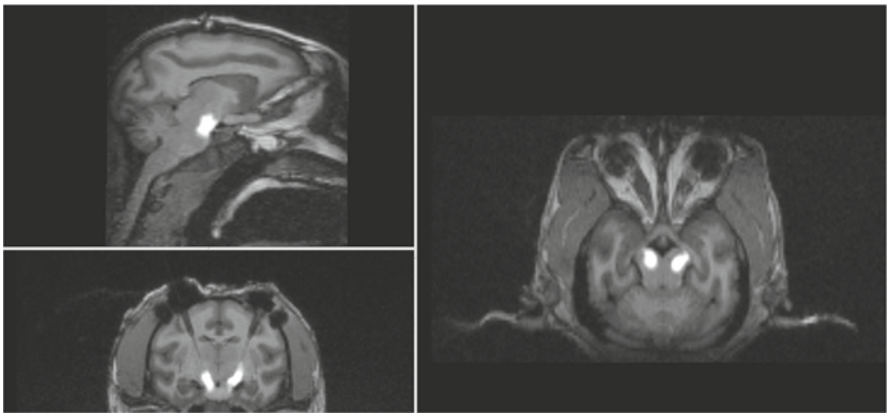

Fig. 18.2 Example of real-time convective delivery (RCD) of AAV2AADC vector into the NHP midbrain. Free gadolinium (Prohance) was used in this experiment

Krauze et al. 2005a, b). RCD utilizes MRI to visualize the CED process with the aid of co-convected contrast agents such as gadolinium-loaded liposomes (GDL) (Fig. 18.2) (Murad et al. 2006; Lonser et al. 2007; Fiandaca et al. 2009a, b); GDL is thought to co-distribute with the infused therapeutic, allowing real-time visualization of the infusion volume (Krauze et al. 2005b, c; Saito et al. 2005). RCD methodology has evolved through extensive modeling in nonhuman primate (NHP) over the years. Visualizing infusions in real time allows active feedback on (1) cannula

placement, (2) physical and anatomical diffusion parameters, and (3) control of drug delivery for optimizing gene transfer, thereby reducing the potential for adverse effects. Initially described by Oldfield and colleagues utilizing albumin-linked surrogate tracers (Nguyen et al. 2003), our current technique of RCD employs interventional MRI (iMRI) to monitor the distribution of therapeutic agents that are co-infused with gadolinium-based tracers (Richardson et al. 2009). Our initial work with GDL (Fiandaca et al. 2009a, b) has progressed to the co-infusion of free gadoteridol for predicting the distribution of protein (Gimenez et al. 2011) and adeno-associated virus serotype 2 (AAV2) vectors (Su et al. 2010; Fiandaca et al. 2009a, b; Richardson et al. 2009). A similar strategy was used to co-infuse therapeutic agent with Gd-diethylenetriamene pentaacetic acid (Gd-DTPA) in a clinical study in two patients with intrinsic brainstem lesions at the National Institutes of Health (Lonser et al. 2007). RCD has allowed us to monitor infusion of liposomal drugs into brain tumors (Dickinson et al. 2008) and viral gene therapy vectors into parenchyma (Fiandaca et al. 2008). Visualizing infused drug distribution was necessary to ensure accurate delivery of therapeutic agents into target sites while minimizing exposure of healthy tissue. Moreover, because infusions could be visualized, we were able to define quantitative relationships between infusate volume (Vi) and subsequent volume of distribution (Vd) for both white and gray matter (Krauze et al. 2005a, b). This method has given us the ability to directly monitor the local delivery of therapeutic agents and has improved the efficacy of CED in animals. The use of RCD has become critical in allowing treating physicians to directly monitor the distribution of therapeutics within the brain, as currently under investigation in GBM patients (Tocagen trial) and in Parkinson's patients using AAV2-GDNF (UCSF/NIH trial) or AAV2-AADC (UCSF/Genzyme trial). Reflux along the CED catheter or leakage outside the target area, especially at higher flow rates, can be monitored, allowing corrective steps such as retargeting the catheter or altering the rate of infusion (Varenika et al. 2008).

18.2.2 Cannula for Convection-Enhanced Drug Delivery

During RCD, the Vd for a given agent depends on the structural properties of the tissue being convected, such as hydraulic conductivity, vascular volume fraction, and extracellular fluid fraction (Sykova 2004). It also depends on the technical parameters of the infusion procedure, e.g., cannula design, cannula placement, infusion volume, and rate of infusion (Chen et al. 1999; Krauze et al. 2005b, c; Szerlip et al. 2007). The overall aim of RCD is to improve delivery efficiency while limiting the spread of the therapeutic into regions outside the target. Development of the optimal cannula type for effective CED delivery in the brain has also been critical. We have examined several types of cannulae with respect to size and design and concluded that a stepped design (Fig. 18.1) with a fused silica tip provided us with the most consistently robust brain delivery (Krauze et al. 2005b, c; Sanftner et al. 2005; Yin et al. 2010a, b). The stepped cannula dramatically reduces reflux along the infusion device by restricting initial backflow of fluid flow beyond the step.

18.2.2.1 CED Infusion Catheter Design

Reflux is defined as the phenomenon of the movement of infusate back up the outside of the cannula rather than into the tissue. A stepped design cannula for CED that effectively prevents reflux allows for reflux-free infusions at 10 μl/min rates that may significantly reduce infusion time as compared to initial gene therapy clinical trials that used CED to deliver AAV2 viral vector (Valles et al. 2010; Christine et al. 2006). Cannula design has been one of the most neglected features of brain delivery protocols. Although earlier studies showed that smaller cannula diameters permit better delivery, the crucial problem of reflux was either not assessed or not measurable. In our early studies, we confirmed that smaller cannula diameters allowed faster delivery rates, but the smallest available cannulae were associated with increasing reflux when the rate of infusion exceeded 0.5 μl/min (Krauze et al. 2005b, c), clearly a significant problem when infusing large volumes. Recently, we have been able to increase the infusion rate to 10 μl/min without reflux by means of an innovative stepped cannula (Rosenbluth et al. 2011; Krauze et al. 2005a, b), which dramatically reduces reflux along the infusion device by restricting initial backflow of fluid beyond the step. The early metal cannula has been replaced by one made of silica that also features sharp transitions in outer diameter that prevent reflux (Fig. 18.1) (Fiandaca et al. 2009a, b). The larger diameter of the stem of the cannula had an outer and inner diameter of 0.53 and 0.45 mm, respectively. The outer and inner diameters of the tip segment were 0.43 and 0.32 mm, respectively. The length of each infusion cannula was measured to ensure that the distal tip extended 3 mm beyond the length of the respective guide. This created a stepped design at the tip of the cannula to maximize fluid distribution during CED procedures and minimize reflux along the cannula tract. Our most recent experience with step cannula having a variable inner tip diameter allows for safe infusion rates above 10 μl/min (unpublished data). Robust reflux-free delivery and distribution of liposomes and AAV viral vectors have been achieved with stepped design cannula in rats, NHPs, and humans. The stepped design cannula also allows us to shorten the duration of infusion in ongoing clinical applications of CED in humans.

18.2.3 Optimizing CED into the Brain Parenchyma

A key component of successful CED is the site of cannula placement within a particular targeted area, e.g., the putamen, thalamus, or brainstem. The distance from the cannula step to its entry point in the target region was found to be critical for optimal distribution of therapeutics. We have developed the concept of red, green, and blue (RGB) zones for cannula placement during RCD. We defined these zones based on the containment of infusate within the target region. Within each region so far investigated, we have been able to define a subset of cannula locations associated with complete containment within the target (green), substantial containment (blue), or poor containment (red). Infusate escape into nearby ventricles or white matter tracts was driven by proximity to these structures. We have defined three-dimensional

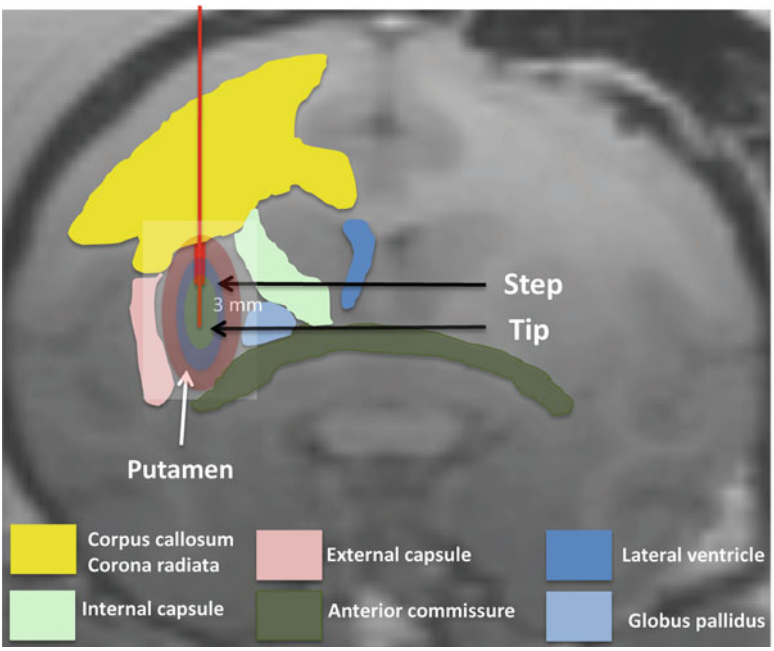

Fig. 18.3 Description of leakage pathways with the potential to affect distribution of therapeutic agents during CED in the putamen. Using a 3 mm step cannula placed within the "green zone," leakage can be minimized. Large blood vessels can also be responsible for leakage, as described in Krauze et al. (2005a, b)

RGB zones in the NHP putamen (Yin et al. 2009a, b), thalamus, and brainstem (Yin et al. 2010). To obtain the most effective distribution of the infused therapeutic within the intended target, it was essential to understand the optimal site of placement of the step and tip of the infusion cannula within that target, preferably within the green zone (Yin et al. 2009a, b, 2010a, b). Such optimal placement will reduce distribution into surrounding white matter tracts (corpus callosum, corona radiata, internal capsule, external capsule, and anterior commissure) that serve as leakage points (Varenika et al. 2008) (Fig. 18.3). Such consideration allows more precise delivery of the therapeutic to the target structure(s) but lessens the risk of inadvertent spread into surrounding brain regions. These factors may also explain some of the reported failures of CED in both NHP studies and human clinical trials, with limited distributions that may have been related to suboptimal targeting of the infusion cannula in relationship to fluid leakage pathways.

18.2.4 Cannula Placement Guidelines

Optimal results in the direct delivery of therapeutics into primate brain depend on reproducible distribution throughout the target region. In our recent studies,

we retrospectively analyzed MRI of RCD infusions into the putamen, thalamus, and brainstem of NHP and defined infusion parameters referred to as RGB zones for cannula placements that result in poor, suboptimal, and optimal volumes of distribution, respectively. The most robust data was achieved in putamen, and the reason for this is that problematic structures (ventricles, corpus callosum) surround this region. So it was relatively easy to define RGB zones in this setting (Fig. 18.3). By contrast, the thalamus and brainstem are larger structures with simpler 3D shapes that do not present as much challenge. Clearly, each new target region will impose its own anatomical constraints, and optimization of RCD will require empirical determinations to some extent. However, the three regions we have investigated suggest the following rules of thumb: When infusate emanates from the tip of stepped cannulae, the infusate forms an ovoid pattern with the cannula as the vertical axis. The upper dimension of the ovoid extends upwards somewhat less than the length of the step-tip. Thus, a 3 mm step-tip will generate a little less than 3 mm backflow. In the smaller rat striatum, we have adjusted the cannula tip to 1 mm and placed the step approximately 1–2 mm from the corpus callosum in order to place the cannula tip within the striatum while maintaining a clear separation of the leading edge of the backflow from the entry point (Yin et al. 2010a, b). These rules may be followed for the design of cannulae in smaller structures. With respect to periventricular zones for infusion into the putamen, we have found that the cannula should be placed at least 3 mm from the external and internal capsules. In general, a cannula trajectory that can maintain a distance of 3 mm or more from sensitive structures should ideally be considered for optimal infusions. The size of the striatum in humans is about fivefold that of the Rhesus monkey (Yin et al. 2009a, b), and consideration of such target volume differences is an important factor in clinical planning.

18.2.5 MRI-Guided Placement of CED Cannula

In order to further optimize the RCD technology, we have adopted the ClearPoint® system (MRI Interventions Inc, Irvine, CA) to translate targeting from the NHP brain into humans. ClearPoint is a novel, integrated hardware (skull-mounted SmartFrame device)/software platform for RCD that provides prospective stereotactic guidance for cannula placement and performance of RCD (Fig. 18.4). This platform is based on the concept of prospective stereotaxy, i.e., the alignment of a skull-mounted trajectory guide within an MRI system (Truwit and Liu 2001), and is already used in clinical studies to perform brain biopsies (Hall et al. 2001; Martin et al. 2008) and placement of DBS leads (Starr et al. 2010; Martin et al. 2005, 2008). In anticipation of upcoming gene therapy clinical trials, we adapted this "off-the-shelf" device to RCD of therapeutics via a customized infusion cannula. The targeting accuracy of this delivery system and the performance of the infusion cannula were validated in NHP. The ClearPoint system allows RCD to be performed with a high level of precision, safety, and predictability (Fig. 18.4b). This technique will increase the utility of RCD for expanding the scope of drug delivery studies. Clinical application of this

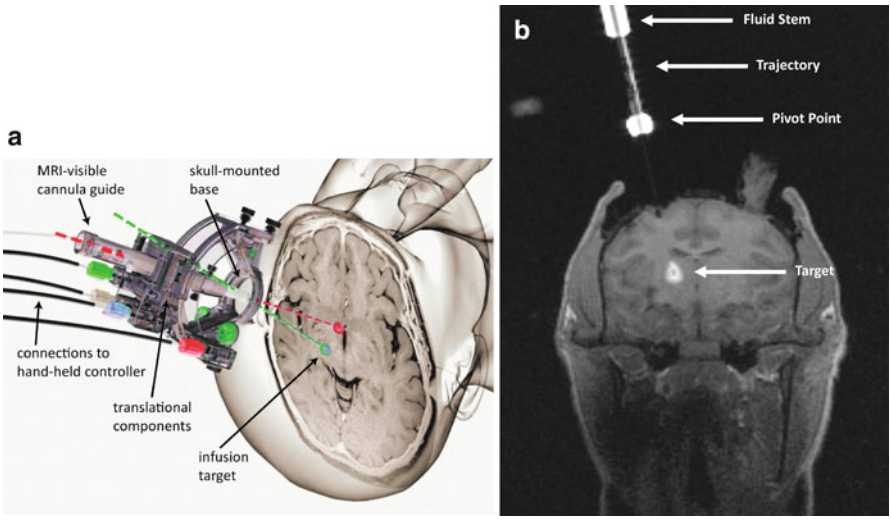

Fig. 18.4 (**a**) Schematic of the SmartFrame device used for RCD in monkey and human clinical studies. (**b**) Example for the RCD in the monkey thalamus using SmartFrame and Clinical cannula (SmartFlow)

guidance platform is likely to improve the success of clinical trials employing intracerebral drug delivery. Although continued refinements in RCD may be expected, our work over the past decade has resulted in a new paradigm for direct parenchymal delivery that may find increasing application in the treatment of currently intractable diseases like Alzheimer's and Parkinson's disease, brain tumors, and other movement disorders. Based on the results of RCD, the ClearPoint system appears to be highly accurate; satisfactory cannula placement has been achieved on the first attempt (without the need for repositioning) in all cases initially studied with the ClearPoint system (Richardson et al. 2011; Richardson et al. 2008). The ClearPoint system automatically calculated each targeting error, defined as the 3-dimensional distance between the expected cannula tip location and the actual location measured on post-insertion imaging. The average targeting error for all targets ($n = 11$) was 0.8 mm (95 % CI = 0.14 mm). We demonstrated that this system could place two infusions in close proximity without producing reflux in the initial cannula tract during the course of the second infusion. No technical limitations were encountered in redirecting the cannula for infusing multiple targets in the same hemisphere. No infusions in any target produced occlusion, cannula reflux, or leakage from adjacent tracts, and no signs of unexpected tissue damage were observed. In terms of cannula safety, no MRI-visible hemorrhages occurred during cannula placement, and no adverse events occurred during RCD. Standard postoperative care assessments also indicated that no RCD-related side effects were observed over the course of these experiments (2 months).

The accuracy of the ClearPoint system surpasses that of our previous experience with RCD in NHP where either a guide cannula or a multiport guide array was

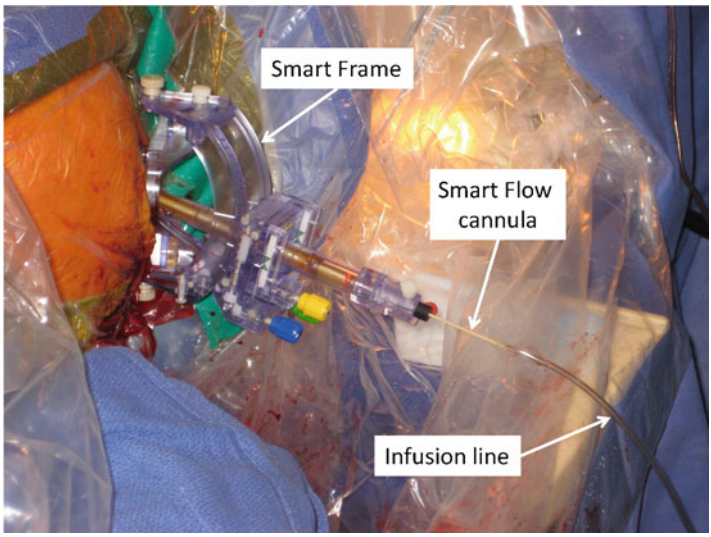

Fig. 18.5 RCD setup in brain tumor patient. Infusion line is directly connected to MR-compatible infusion pump

placed stereotactically in reference to a baseline MRI, prior to the iMRI procedure. Infusion data obtained by these methods were recently analyzed to determine the optimal zones for cannula placement within the putamen, thalamus, and brainstem (Yin et al. 2009a, b) that predict contained distribution within the target region. Images obtained during RCD in these studies showed that distribution of gadolinium tracer outside of the target structure occurred in 64 % of putaminal infusions and in 43 % of thalamic infusions, clearly demonstrating the need for prospective stereotaxy. In addition to the ability to choose the target and trajectory in real time, there are other advantages to the ClearPoint system that may explain improved performance over previous experimental studies. In comparison to the cannula used in our most recent NHP studies (Yin et al. 2010a, b), the internal diameter of the current cannula was smaller (200 vs. 324 mm). Additionally, the skull-mounted SmartFrame provides a rigid housing for the cannula that restricts axial movement during brain insertion. Therefore, the ClearPoint system allows RCD to be performed with a high level of precision, predictability, and safety. This technique should increase the utility of RCD for expanding the scope of drug delivery studies. Clinical application of this platform is likely to improve the success rate for clinical trials employing cerebral drug delivery by direct infusion (Fig. 18.5).

18.2.6 Simulation Algorithm for RCD

The theoretical groundwork describing how the infusion and tissue parameters affect infusate distribution has been previously described (Morrison et al. 1999).

This theory was developed into software that predicted the infusate distribution from MRI data by using diffusion tensor imaging (DTI) information to estimate the geometry of the underlying tissue (Sampson et al. 2003). This software was initially validated in a malignant glioma study by comparing the predicted distribution to the distribution detected with SPECT after co-infusing ^{123}I-labeled human serum albumin (HSA) into brain tissue surrounding resection cavity in eight patients receiving infusions of cintredekin besudotox. This validation showed the clinical utility of using software for planning trajectories and simulating infusion distribution. Recently we adopted the simulations for infusion techniques that will be used in ongoing clinical trials to do a highly accurate validation of the predictability of distributions. The validation data was a large series of gadoteridol (Prohance) infusions in 26 NHPs conducted with real-time MRI visualization. Using MRI to quantify the distribution provided submillimeter resolution with high signal contrast due to the T1-shortening effects of the gadoteridol. These infusions were part of protocols evaluating the safety and efficacy of using CED for gene therapy and hence followed the protocols of approved clinical studies. The gene therapy agents under evaluation were co-infused with the gadoteridol and included AAV2-GDNF, AAV2-hASM, AAV2-Tor1A mutant, and AAV2-AADC. The infusions used a cannula with a step design at the tip that required adapting the simulations. The simulation algorithm was validated by comparing the predicted volume of distribution to the distribution of gadoteridol observed in the MRI images. The goal was to inform clinicians using this method to plan surgeries how well they can expect the actual distribution to reflect the predicted infusion. This analysis showed that the simulation adequately predicted the measured gadolinium distribution volume even for challenging infusions involving short times or small volumes and demonstrated the algorithm's ability to predict the infusate distribution from a known cannula tip position (Rosenbluth et al. 2012a).

Accurate prediction is critical to allow a physician to plan optimal implantation of cannulae on a patient-by-patient basis to maximize therapeutic coverage with minimizing of target drug delivery. The next step will be to incorporate a stereotactic navigation system and evaluate the ability to predict the infusate distribution prior to cannula placement (Rosenbluth et al. 2012b).

18.3 Delivery of Therapeutic Proteins Directly into the Cerebrospinal Fluid Space

More global brain disorders such as Alzheimer's disease or lysosomal storage diseases (LSD) as well as spinal cord diseases, e.g., amyotrophic lateral sclerosis (ALS) and spinal muscular atrophy (SMA), could benefit from a therapy that provides a comprehensive treatment of the whole brain or the spinal cord, respectively.

Because the brain pathology in LSD diseases is global, it will be necessary to achieve widespread CNS distribution of therapeutic enzyme in these diseases.

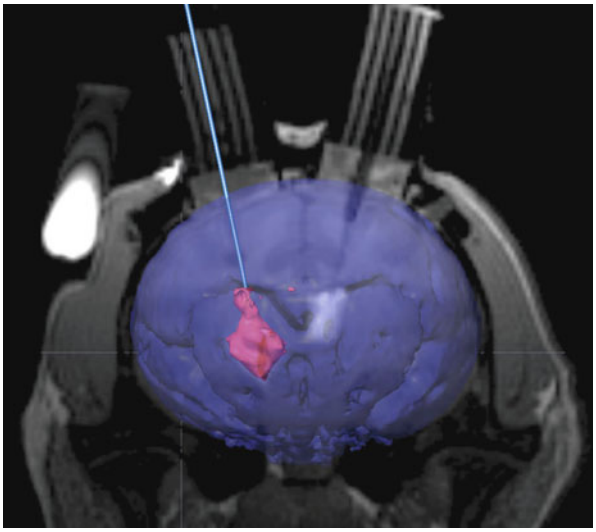

Fig. 18.6 3-D reconstruction of thalamic CED/RCD of Gd in NHP using step-design cannula and MR detection of the infusion (*left side*). By contrast, ICV infusion of Gd (*right side*) shows limited distribution surrounding the lateral ventricle with some limited diffusion of Gd into the caudate nucleus and septum

To date, protein infusions into the cerebrospinal fluid (CSF) has seen very limited success. It is currently unclear whether a therapeutic protein delivered to the brain by the CSF route can ever achieve therapeutic levels throughout the human brain with existing methods/paradigms (Fig. 18.6). While studies performed in mouse models of LSD utilizing ICV delivery may demonstrate global enzyme distribution and functional correction (Dodge et al. 2008), translation to the larger NHP brain has been limited (Ziegler et al. 2011), suggesting that this strategy faces significant challenges when applied in the human brain (Fig. 18.7).

The CSF compartment has been used as a conduit to achieve more global CNS distribution of proteins. Direct injections of sulfamidase into the cisterna magna have reduced pathologic substrate in the brains of mucopolysaccharidosis (MPS) IIIA mice (Hemsley et al. 2007, 2008) and within select brain regions of Huntaway dogs (Hemsley et al. 2009). Studies in MPS I animal models have also shown success with an intrathecal (IT) approach (Dickson et al. 2007). Intracerebroventricular (ICV) delivery could provide more widespread distribution of enzyme by taking advantage of the natural CSF flow from the ventricles. Widespread reduction of intracellular storage pathology has been demonstrated in rodent models after ICV administration of recombinant enzymes and has resulted in improved motor function in ASM knockout mice (Chang et al. 2008), along with increased survival in Gaucher mice (Cabrera-Salazar et al. 2010) and efficacy in additional LSD models (Chang et al. 2008; Lee et al. 2007).

In larger brains, ICV administration of high-molecular-weight molecules has given variable results. In primates, ICV infusions of glial cell line-derived neurotrophic factor (GDNF) led to behavioral/motor improvements in MPTP-induced

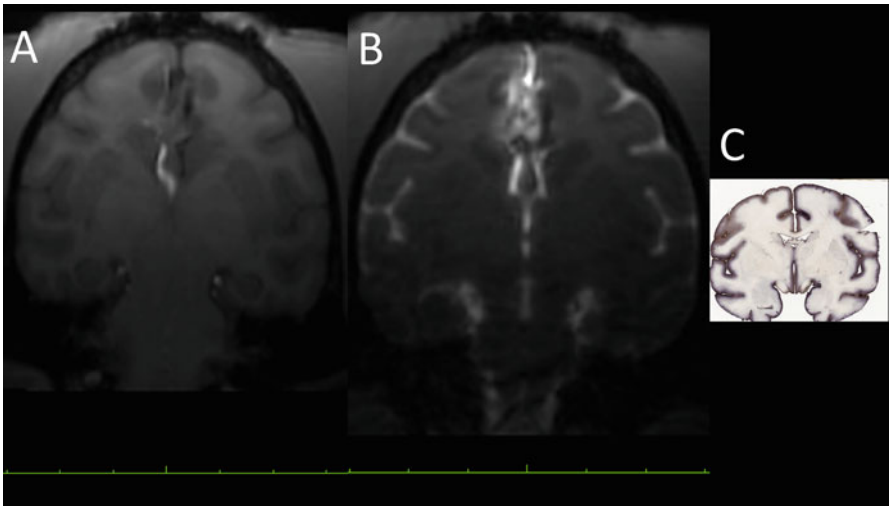

Fig. 18.7 Unilateral ICV administration of MRI tracer in a monkey. *Panel* (**a**) shows the initial distribution in the lateral ventricle on the side of the infusion. MRI tracer is present in the CSF in the brain and spinal cord after 30 min of infusion (**b**). The same animal was treated with a unilateral infusion of acid sphingomyelinase (ASM) recombinant protein (**c**). Note that ASM protein was primarily detected in the outer layer of cerebral cortex with just 1–2 mm diffusion into the parenchyma

hemi-parkinsonian NHPs (Gash et al. 1996; Zhang et al. 1997; Grondin et al. 2002) but in clinical translation failed to improve the parkinsonian condition of patients (Nutt et al. 2003). An autopsy of one trial patient (Kordower et al. 1999) indicated that the GDNF ICV infusion did not reach the intended target(s).

18.4 Delivery of AAV9 Directly into CSF Space

An alternative approach to IT delivery of therapeutic proteins is CSF delivery of viral vectors. Global gene therapy approaches have so far consisted of the intravenous delivery of viral vectors such as AAV9 that cross the BBB (Foust et al. 2009; Gray et al. 2011; Samaranch et al. 2012). Recently, we reported that injecting AAV9 into the cisterna magna (CM) provided a more extensive transduction of large structures like the brain cortex (Samaranch et al. 2013). Remarkably, AAV7 and AAV9 vector infusion into the cisterna magna and/or lumbar CSF region of NHPs is capable of significant transduction of either cortical neurons or glia cells, with the specific population transduced dependent upon the type of promoter used to drive gene expression (Samaranch et al. 2013). In addition, almost complete transduction of cerebellar Purkinje cells and spinal cord motor neurons was achieved after CSF delivery of AAV9 vector (Fig. 18.8). Despite these very promising results, the long-term consequences of AAV-9 delivery into the CSF to correct CNS deficits still need to be established. This route of delivery for AAV9 encoding secreteable proteins may yet have significant clinical application, especially in disorders such as SMA or LSDs.

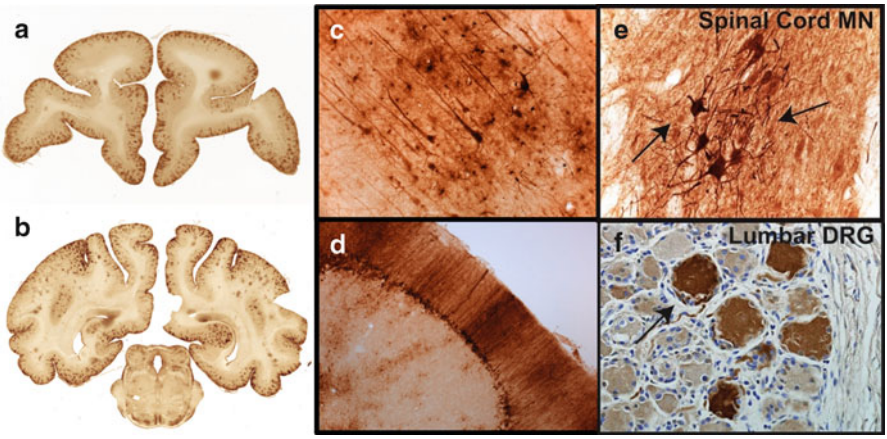

Fig. 18.8 NHP treated with AAV9 vector expressing GFP. Vector was infused into the cisternal and lumbar CSF. At 4 weeks robust GFP expression is detected in the brain ranging from prefrontal (**a**) to occipital (**b**) cortex. Mostly cortical regions show expression with very limited subcortical transduction. Neuronal expression (**c**) is evident in the cortex as well as in the cerebellum (**d**). *Panel* (**e**) represents motor neuron transduction in the spinal cord and (**f**) dorsal root ganglia (DRG). Transduction of the motor neurons is likely the result of axonal transport of AAV from DRG cells

18.5 Future Development

The ability of this RCD platform to deliver controlled volumes of drug to any structure in the NHP brain with highly accurate localization (on the order of 1 mm), and the capacity to monitor the infusion in real time, expands the utility of the NHP brain to model human disease and aids in the development of novel therapies. The NHP brain is uniquely suited for neurosurgical investigation of therapeutic delivery due to similarities between human and primate anatomy and physiology that cannot be closely modeled in other species (Richardson et al. 2008). We anticipate that this system will facilitate the creation of new NHP disease models due to the novel ability for precise infusion of therapeutic agents within discrete brain regions. Our recent investigations comparing linear measures in humans versus NHP will allow us to translate our NHP stereotactic (RGB) targeting data to humans, thereby facilitating advancement of these techniques into the clinic. In addition, we expect that ongoing studies will allow modeling of specific patterns of viral vector distribution and subsequent gene expression in structures to be targeted, such as mapping infusions in the putamen for Parkinson's disease. The evolution of this system may also include tools that aid the neurosurgeon in planning, delivering, and anticipating the functional outcome of infusions into multiple brain locations. For instance, initiatives to incorporate the auto-segmentation of target structures and surrounding anatomy, as well as auto-segmentation of infusion volumes in real time, are under way. Eventually, analysis of retrospective and prospective infusion data in the NHP brain

may allow the development of predictive algorithms where system software can forecast areas of drug distribution or transgene expression based on a selected location for cannula placement.

It remains critical, however, for investigators and clinicians to understand the basics of CED technology prior to considering its use for human trials. A lack of understanding will not allow the proper assessment of this delivery option and prevents a fair comparison to alternatives. Deciphering the mechanisms and critical points associated with CED has been painstakingly worked out over the last 25 years.

18.6 Points for Discussion

- Why should investigators work to understand how catheter size, shape, and correct placement are essential to minimize tissue trauma and enhance the convection of infusate while minimizing reflux?
- Why are flow rates critical to the CED process? Flow rates should typically not be used above 15 μl/min in an effort to avoid reflux or focal tissue cavitation.
- Why is it so important to understand optimal infusion catheter placement within the brain parenchyma, especially related to proximity to the ventricular system, subarachnoid space, or tumor resection cavity? Describe how catheter placement might be critical in maximizing effective Vd.
- Why is the ability to directly visualize the CED process with RCD essential for reproducible treatment strategies, improved patient safety, and a better determination of therapeutic efficacy?

References

Bobo RH, Laske DW et al (1994) Convection-enhanced delivery of macromolecules in the brain. Proc Natl Acad Sci U S A 91(6):2076–2080

Cabrera-Salazar MA, Bercury SD et al (2010) Intracerebroventricular delivery of glucocerebrosidase reduces substrates and increases lifespan in a mouse model of neuronopathic Gaucher disease. Exp Neurol 225:436–444

Carson BS Sr, Wu Q et al (2002) New approach to tumor therapy for inoperable areas of the brain: chronic intraparenchymal drug delivery. J Neurooncol 60(2):151–158

Chang M, Cooper JD et al (2008) Intraventricular enzyme replacement improves disease phenotypes in a mouse model of late infantile neuronal ceroid lipofuscinosis. Mol Ther 16(4):649–656

Chen MY, Lonser RR et al (1999) Variables affecting convection-enhanced delivery to the striatum: a systematic examination of rate of infusion, cannula size, infusate concentration, and tissue-cannula sealing time. J Neurosurg 90(2):315–320

Christine CW, Starr PA et al (2006) Aromatic L-amino acid decarboxylase gene transfer therapy for Parkinson's disease: initial results of an open-label, dose escalation, safety and tolerability study. Abstract S23.005. American Academy of Neurology, San Diego, CA

Dickinson PJ, LeCouteur RA et al (2008) Canine model of convection-enhanced delivery of liposomes containing CPT-11 monitored with real-time magnetic resonance imaging: laboratory investigation. J Neurosurg 108(5):989–998

Dickson P, McEntee M et al (2007) Intrathecal enzyme replacement therapy: successful treatment of brain disease via the cerebrospinal fluid. Mol Genet Metabol 91:61–68
Dodge JC, Clarke J et al (2008) Intracerebroventricular infusion of acid sphingomyelinase corrects CNS manifestations in a mouse model of Niemann–Pick A disease. Exp Neurol 215:349–357
Eberling JL, Jagust WJ et al (2008) Results from a phase I safety trial of hAADC gene therapy for Parkinson disease. Neurology 70(21):1980–1983
Fiandaca MS, Forsayeth JR et al (2008) Image-guided convection-enhanced delivery platform in the treatment of neurological diseases. Neurotherapeutics 5(1):123–127
Fiandaca MS, Varenika V et al (2009) Real-time MR imaging of adeno-associated viral vector delivery to the primate brain. Neuroimage 47(Suppl 2):T27–T35
Foust KD, Nurre E et al (2009) Intravascular AAV9 preferentially targets neonatal neurons and adult astrocytes. Nat Biotechnol 27(1):59–65
Gash DM, Zhang Z et al (1996) Functional recovery in parkinsonian monkeys treated with GDNF. Nature 380(6571):252–255
Gill SS, Patel NK et al (2003) Direct brain infusion of glial cell line-derived neurotrophic factor in Parkinson disease. Nat Med 9(5):589–595
Gimenez F, Krauze MT et al (2011) Image-guided convection-enhanced delivery of GDNF protein into Monkey Putamen. Neuroimage 54(1):S189–195
Gray SJ, Matagne V et al (2011) Preclinical differences of intravascular AAV9 delivery to neurons and glia: a comparative study of adult mice and nonhuman primates. Mol Ther 19(6):1058–1069
Grondin R, Zhang Z et al (2002) Chronic, controlled GDNF infusion promotes structural and functional recovery in advanced parkinsonian monkeys. Brain 125(Pt 10):2191–2201
Hadaczek P, Mirek H et al (2006) "Perivascular pump" driven by arterial pulsation is a powerful mechanism for the distribution of therapeutic molecules within the brain. Mol Ther 14(1): 69–78
Hall WA, Liu H et al (2001) Brain biopsy sampling by using prospective stereotaxis and a trajectory guide. J Neurosurg 94(1):67–71
Hamilton JF, Morrison PF et al (2001) Heparin coinfusion during convection-enhanced delivery (CED) increases the distribution of the glial-derived neurotrophic factor (GDNF) ligand family in rat striatum and enhances the pharmacological activity of neurturin. Exp Neurol 168(1): 155–161
Hemsley KM, Beard H et al (2008) Effect of high dose, repeated intra-cerebrospinal fluid injection of sulphamidase on neuropathology in mucopolysaccharidosis type IIIA mice. Genes Brain Behav 7:740–753
Hemsley KM, King B et al (2007) Injection of recombinant human sulfamidase into the CSF via the cerebellomedullrry cistern in MPS IIIA mice. Mol Genet Metab 90:313–328
Hemsley KM, Norman EJ et al (2009) Effect of cisternal sulfamidase delivery in MPS IIIA Huntaway dogs—a proof of principle study. Mol Genet Metabol 98:383–392
Kordower JH, Palfi S et al (1999) Clinicopathological findings following intraventricular glial-derived neurotrophic factor treatment in a patient with Parkinson's disease. Ann Neurol 46(3):419–424
Krauze MT, Forsayeth J et al (2006) Real-time imaging and quantification of brain delivery of liposomes. Pharm Res 23(11):2493–2504
Krauze MT, McKnight TR et al (2005a) Real-time visualization and characterization of liposomal delivery into the monkey brain by magnetic resonance imaging. Brain Res Brain Res Protoc 16:20–26
Krauze MT, Saito R et al (2005b) Effects of the perivascular space on convection-enhanced delivery of liposomes in primate putamen. Exp Neurol 196(1):104–111
Krauze MT, Saito R et al (2005c) Reflux-free cannula for convection-enhanced high-speed delivery of therapeutic agents. J Neurosurg 103(5):923–929
Kroll RA, Pagel MA et al (1996) Increasing volume of distribution to the brain with interstitial infusion: dose, rather than convection, might be the most important factor. Neurosurgery 38(4):746–752, discussion 752–754

Kunwar S (2003) Convection enhanced delivery of IL13-PE38QQR for treatment of recurrent malignant glioma: presentation of interim findings from ongoing phase 1 studies. Acta Neurochir Suppl 88:105–111

Kunwar S, Prados MD et al (2007) Direct intracerebral delivery of cintredekin besudotox (IL13-PE38QQR) in recurrent malignant glioma: a report by the Cintredekin Besudotox Intraparenchymal Study Group. J Clin Oncol 25(7):837–844

Lang AE, Gill S et al (2006) Randomized controlled trial of intraputamenal glial cell line-derived neurotrophic factor infusion in Parkinson disease. Ann Neurol 59(3):459–466

Lee WC, Tsoi YK et al (2007) Single-dose intracerebroventricular administration of galactocerebrosidase improves survival in a mouse model of globoid cell leukodystrophy. FASEB J 21(10):2520–2527

Lonser RR, Corthesy ME et al (1999) Convection-enhanced selective excitotoxic ablation of the neurons of the globus pallidus internus for treatment of parkinsonism in nonhuman primates. J Neurosurg 91(2):294–302

Lonser RR, Schiffman R et al (2007) Image-guided, direct convective delivery of glucocerebrosidase for neuronopathic Gaucher disease. Neurology 68(4):254–261

Mardor Y, Roth Y et al (2001) Monitoring response to convection-enhanced taxol delivery in brain tumor patients using diffusion-weighted magnetic resonance imaging. Cancer Res 61(13): 4971–4973

Marks WJ, Bartus RT et al (2010) Gene delivery of AAV2-neurturin for Parkinson's disease: a double-blind, randomised, controlled trial. Lancet Neurol 9:1164–1172

Martin AJ, Hall WA et al (2008) Minimally invasive precision brain access using prospective stereotaxy and a trajectory guide. J Magn Reson Imaging 27(4):737–743

Martin AJ, Larson PS et al (2005) Placement of deep brain stimulator electrodes using real-time high-field interventional magnetic resonance imaging. Magn Reson Med 54(5):1107–1114

Morrison PF, Chen MY et al (1999) Focal delivery during direct infusion to brain: role of flow rate, catheter diameter, and tissue mechanics. Am J Physiol 277(4 Pt 2):R1218–R1229

Murad GJ, Walbridge S et al (2006) Real-time, image-guided, convection-enhanced delivery of interleukin 13 bound to pseudomonas exotoxin. Clin Cancer Res 12(10):145–151

Murad GJ, Walbridge S et al (2007) Image-guided convection-enhanced delivery of gemcitabine to the brainstem. J Neurosurg 106(2):351–356

Neeves KB, Sawyer AJ et al (2007) Dilation and degradation of the brain extracellular matrix enhances penetration of infused polymer nanoparticles. Brain Res 1180:121–132

Nguyen JB, Sanchez-Pernaute R et al (2001) Convection-enhanced delivery of AAV-2 combined with heparin increases TK gene transfer in the rat brain. Neuroreport 12(9):1961–1964

Nguyen TT, Pannu YS et al (2003) Convective distribution of macromolecules in the primate brain demonstrated using computerized tomography and magnetic resonance imaging. J Neurosurg 98(3):584–590

Nutt JG, Burchiel KJ et al (2003) Randomized, double-blind trial of glial cell line-derived neurotrophic factor (GDNF) in PD. Neurology 60(1):69–73

Richardson RM, Kells AP et al (2011) Novel platform for MRI-guided convection-enhanced delivery of therapeutics: preclinical validation in nonhuman primate brain. Stereotact Funct Neurosurg 89(3):141–151

Richardson RM, Larson PS et al (2008) Gene and cell delivery to the degenerated striatum: status of preclinical efforts in primate models. Neurosurgery 63(4):629–642, dicussion 642–644

Richardson RM, Varenika V et al (2009) Future applications: gene therapy. Neurosurg Clin N Am 20(2):205–210

Rosenbluth KH, Eschermann JF et al (2012a) Analysis of a simulation algorithm for direct brain drug delivery. Neuroimage 59(3):2423–2429

Rosenbluth KH, Martin AJ et al (2012b) Evaluation of pressure-driven brain infusions in nonhuman primates by intra-operative 7 Tesla MRI. J Magn Reson Imaging 36(6):1339–1346

Rosenbluth KH, Luz M et al (2011) Design of an in-dwelling cannula for convection-enhanced delivery. J Neurosci Methods 196(1):118–123

Rosenbluth KH, Martin AJ et al (2013) Rapid inverse planning for pressure-driven drug infusions in the brain. PLoS One 8(2):e56397
Saito R, Krauze MT et al (2005) Gadolinium-loaded liposomes allow for real-time magnetic resonance imaging of convection-enhanced delivery in the primate brain. Exp Neurol 196(2):381–389
Samaranch L, Salegio EA et al (2013) Strong cortical and spinal cord transduction after AAV7 and AAV9 delivery into the cerebrospinal fluid of nonhuman primates. Hum Gene Ther 24(5): 526–532
Samaranch L, Salegio EA et al (2012) Adeno-associated virus serotype 9 transduction in the central nervous system of nonhuman primates. Hum Gene Ther 23(4):382–389
Sampson JH, Akabani G et al (2003) Progress report of a phase I study of the intracerebral microinfusion of a recombinant chimeric protein composed of transforming growth factor (TGF)-alpha and a mutated form of the Pseudomonas exotoxin termed PE-38 (TP-38) for the treatment of malignant brain tumors. J Neurooncol 65(1):27–35
Sanftner LM, Sommer JM et al (2005) AAV2-mediated gene delivery to monkey putamen: evaluation of an infusion device and delivery parameters. Exp Neurol 194(2):476–483
Slevin JT, Gash DM et al (2006) Unilateral intraputaminal glial cell line-derived neurotrophic factor in patients with Parkinson disease: response to 1 year each of treatment and withdrawal. Neurosurg Focus 20(5):E1
Starr PA, Martin AJ et al (2010) Subthalamic nucleus deep brain stimulator placement using high-field interventional magnetic resonance imaging and a skull-mounted aiming device: technique and application accuracy. J Neurosurg 112(3):479–490
Su X, Kells AP et al (2010) Real-time MR imaging with gadoteridol predicts distribution of transgenes after convection-enhanced delivery of AAV2 vectors. Mol Ther 18(8):1490–1495
Sykova E (2004) Diffusion properties of the brain in health and disease. Neurochem Int 45(4):453–466
Szerlip NJ, Walbridge S et al (2007) Real-time imaging of convection-enhanced delivery of viruses and virus-sized particles. J Neurosurg 107(3):560–567
Truwit CL, Liu H (2001) Prospective stereotaxy: a novel method of trajectory alignment using real-time image guidance. J Magn Reson Imaging 13(3):452–457
Valles F, Fiandaca MS et al (2010) Qualitative imaging of adeno-associated virus serotype 2-human aromatic L-amino acid decarboxylase gene therapy in a phase I study for the treatment of Parkinson disease. Neurosurgery 67(5):1377–1385
Varenika V, Dickenson P et al (2008) Detection of infusate leakage in the brain using real-time imaging of convection-enhanced delivery. J Neurosurg 109:874–880
Yin D, Forsayeth J et al (2010a) Optimized cannula design and placement for convection-enhanced delivery in rat striatum. J Neurosci Methods 187(1):46–51
Yin D, Richardson RM et al (2010) Cannula placement for effective convection-enhanced delivery in the nonhuman primate thalamus and brainstem: implications for clinical delivery of therapeutics. J Neurosurg 113(2):240–248
Yin D, Richardson RM et al (2010b) Cannula placement for effective convection-enhanced delivery in the nonhuman primate thalamus and brainstem: implications for clinical delivery of therapeutics. J Neurosurg 113(2):240–248
Yin D, Valles FE et al (2011) Optimal region of the putamen for image-guided convection-enhanced delivery of therapeutics in human and non-human primates. Neuroimage 54(1):S196–203
Yin D, Valles FE et al (2009a) Optimal region of the putamen for image-guided convection-enhanced delivery of therapeutics in human and non-human primates. Neuroimage
Yin D, Valles FE et al (2009b) Striatal volume differences between non-human and human primates. J Neurosci Methods 176(2):200–205
Zhang Z, Miyoshi Y et al (1997) Dose response to intraventricular glial cell line-derived neurotrophic factor administration in parkinsonian monkeys. J Pharmacol Exp Ther 282(3):1396–1401
Ziegler RJ, Salegio EA et al (2011) Distribution of acid sphingomyelinase in rodent and non-human primate brain after intracerebroventricular infusion. Exp Neurol 231(2):261–271

Chapter 19
Osmotic Opening of the BBB for Drug Treatment of Brain Tumors (Focus on Methodological Issues)

David Fortin

Abstract The blood–brain barrier (BBB) is a complex, functional barrier composed of endothelial cells, pericytes, astrocytic endfeet, and neuronal cells. This highly organized unit expresses a selective permeability for molecules that possess adequate molecular weight and sufficient liposolubility. Unfortunately, many potential therapeutic agents do not cross the BBB. As the BBB limitation has become more and more acknowledged, many innovative surgical and pharmacological strategies have been developed to circumvent it. This chapter focuses on the osmotic opening of the BBB. Since its inception by Rapoport in 1972, preclinical studies have provided important information on the extent of BBB permeation using this strategy. Neuwelt and colleagues further developed the osmotic opening of the BBB and brought it to the clinic. However, many questions remain as to the detailed physiology of the procedure, its long-term physiological impacts, and its best application to the clinic. Here we describe the results from ongoing studies relating to the spatial and temporal distribution of molecules after osmotic BBB breaching as well as the window of BBB permeabilization. We also summarize recent clinical series highlighting promising results in the application of this procedure. Finally, we discuss different approaches used to maximize the reach and efficacy of the procedure as well as to measure its physiological impact.

19.1 Introduction

The field of neuro-oncology is afflicted by several therapeutic limitations, one of which is the blood–brain barrier (BBB) (Van Den Bent 2003, Mathieu and Fortin 2006). Even though the BBB is universally recognized as a physiological entity, its

D. Fortin, M.D., F.R.C.S.C. (✉)
Department of Neurosurgery and Neuro-oncology,
Université de Sherbrooke, Sherbrooke, QC, Canada J1K 2R1
e-mail: David.fortin@usherbrooke.ca

M. Hammarlund-Udenaes et al. (eds.), *Drug Delivery to the Brain*, AAPS Advances in the Pharmaceutical Sciences Series 10, DOI 10.1007/978-1-4614-9105-7_19,

impact on brain tumor treatments is still controversial. As exemplified by contrast enhancement on CT or MRI scans, the function of the BBB is at least partially compromised in the presence of malignant tumors, whether it be glial (primary) or metastatic (secondary) (Provenzale et al. 2005). This breach in the integrity of the BBB is highly variable, heterogeneous, and dependent on tumor type and size (Rapoport et al. 1972, Kroll and Neuwelt 1998). As a consequence, systemically administered drugs often distribute unevenly, with a preferential accumulation in the necrotic core of brain tumors (Tosoni et al. 2004). Drug penetration at the edge of the tumor is negligible, as has been shown in an elegant in vivo study using fluorescein as a marker of vascular permeability (Sato et al. 1998).

The presence of the P-glycoprotein (P-gp) efflux pump and other ABC transporters at the luminal surface of the brain capillaries (as well as at the surface of tumor cells) further limits the entry of therapeutics, and the constant flow of cerebral spinal fluid (CSF) emanating from perivascular spaces toward the ventricular compartment also contributes to a decrease in the actual concentration and time of exposure of tumor cells to chemotherapy when treating CNS neoplasms (Bellavance et al. 2008).

As there is no doubt that the BBB suffers from variable degrees of breach in its integrity in the presence of malignant brain tumors, an impediment to drug delivery therefore remains significant, and strategies to optimize delivery should be considered if one is to really impact patient outcomes in neuro-oncology (Lockman et al. 2010).

19.1.1 The Blood–Brain Barrier as an Impediment to the Treatment of Brain Tumors: A Historic View

Ehrlich was the first to describe the BBB in 1906 (Bellavance et al. 2008). Ironically, he also coined the term "chemotherapy" and originated the idea of the "magic bullet," a concept that has become a current focus in oncology research with the advent of the so-called targeted therapy. In 1921, Stern and Gauthier observed that the barrier between the vascular compartment and the brain was selective to certain agents and called it "la barrière hémato-encéphalique" (Stern and Gautier 1921). Brodie et al. later detailed the significance of a molecule's lipid solubility as an indicator of its permeability through the barrier in 1960 (Brodie et al. 1960). A series of investigators next established that tight junctions between the cerebral capillary cells served as the prime anatomical basis for the barrier (Brightman et al. 1973). Muldoon et al. more recently investigated the possible role played by the basement membrane (basal lamina) as a secondary impediment to molecule delivery to the central nervous system by virtue of its negative charge (Muldoon et al. 1995). In addition to these factors, it has been found that the astrocytic foot processes as well as the pericytes also play a role in modulating BBB properties.

The "neurovascular unit" is a term used to refer to the complex functional barrier collectively composed of endothelial cells, pericytes, astrocytic endfeet, as well as neuronal cells (Davson and Oldendorf 1967; Cohen et al. 1996; Cohen et al. 1997;

Fenstermacher et al. 1988; Reese and Karnovsky 1967). This highly organized system confers unique properties to the CNS vasculature accounting for the selective permeability of the BBB. Endothelial tight junctions, lack of fenestrae, and low pinocytic/endosomal transport prevent the entry of hydrosoluble molecules into the brain across the BBB (Wolburg and Lippoldt 2002; Abbott et al. 2006; Deeken and Loscher 2007). Moreover, astrocytic endfeet apposition practically seals CNS vascular structures shut by covering nearly 99 % of their external surface (Abbott et al. 2006; Deeken and Loscher 2007; Smith and Gumbleton 2006). This peculiar organization of the BBB restrains passive transport (non-receptor- or non-carrier-mediated transport) to the CNS compartment from the blood.

19.2 Current Status

19.2.1 Altered BBB in the Context of Brain Neoplasia

The BBB can be modified by any CNS lesion, as is the case with brain tumors. Whereas there are different types of brain tumors, the pathophysiological alterations caused to the BBB need to be addressed differentially by stratifying tumor type as primary (glial) or secondary (metastatic), as the mechanisms involved and the implications to the BBB are quite different.

19.2.1.1 Glioma

The BBB is affected by the presence of a glial tumor. This breach in the integrity of the BBB is variable, heterogeneous, and dependent on tumor type, grade, and size (Rapoport et al. 1972; Kroll and Neuwelt 1998). As most low-grade and up to 30 % of high-grade glial tumors do not present contrast enhancement at MRI, a significant amount of these tumors may not greatly impact BBB permeability. However, for those that do, they do so in an extremely inconsistent fashion. As a consequence, drug distribution is uneven, with a preferential accumulation in the necrotic areas of high-grade tumors (Tosoni et al. 2004). Drug penetration at the proliferating edge of glial tumor is extremely low (Sato et al. 1998).

As an illustration of the potency of the BBB to impede drug delivery, Boyle and colleagues reported fascinating findings while studying vincristine penetration in a 9 L rat glioma model (Boyle et al. 2004). The authors found negligible vincristine delivery in tumors despite a clear increase in permeability, as evidenced by a marked Evans blue staining. Evans blue binds to albumin once in the circulation, so a macroscopic blue discoloration of the brain parenchyma suggested that the 66 kDa albumin could cross the blood–tumor barrier (BTB) to reach the CNS (Blanchette and Fortin 2011). Despite the fact that the authors elected to administer the vincristine intra-arterially to improve CNS delivery, drug concentration was 6–11-fold

higher in the liver when compared to tumor levels and 15–37-fold higher in the liver compared to the normal brain levels in non-implanted animals. The authors thus concluded that this observation was likely explainable by the activity of the P-gp efflux pumps blocking the entry of the vincristine xenobiotic.

Another interesting study performed by Sato et al. also support similar findings in humans (Sato et al. 1998). In a daring and elegant design, these investigators used fluorescein micro-angiograms to assess BBB integrity after having performed a neurosurgery in four patients. The authors found that although the BBB was partially permeable to the fluorescein, an important filling defect was observed at the immediate periphery of the tumor, suggesting competent barrier properties at that location. The administration of mannitol improved fluorescein delivery by increasing BBB permeability within the tumor, mostly at the venous capillary level as well as at the periphery of the tumors.

19.2.1.2 Metastatic Disease

The metastatic process involves different interactions altogether between the implanting cancer cell and the brain microenvironment, the so-called seed-and-soil concept. Resident CNS cells such as astrocytes and microglial cells play an active role in the way metastatic tumor cells seed, establish, and flourish in the brain (Deeken and Loscher 2007). This active process requires recruitment of blood vessels via different mechanisms, whether it be angiogenesis, vasculogenesis, co-option, intussusception, or vascular mimicry. Notwithstanding the process, these vessels and their associated BTB properties present certain morphological features: they have a significantly larger dilated diameter, have a thicker basal membrane, and present a lower microvessel density than the surrounding normal brain parenchyma (Eichler et al. 2011). More so, the tight junction structure is compromised, the perivascular space is increased, and fenestrations as well as pinocytic vacuoles can sometimes be found in these vessels (Deeken and Loscher 2007).

These brain tumor vessels also depict a different expression profile of efflux transporters, even though this difference is not very well characterized at the present time, as many discrepancies between the results of different studies have been reported (de Boer and Gaillard 2007; de Boer et al. 2003; Lee et al. 2001; Loscher and Potschka 2005; Guo et al. 2010). Some confusion arises because these proteins can also be expressed directly by tumor cells in addition to cerebral vessels (Shen et al. 2008). However, as a generalization, most studies looking at the expression of P-gp (and/or other ABC transporters) at the BTB in the context of brain metastasis have found either decreased or unchanged expression, relative to the levels in surrounding brain vessels (Deeken and Loscher 2007). To the contrary, tumor cells have often shown an increase in the expression profile of these transporters relative to normal glial cells (Shen et al. 2008).

All these observations support the caveat that even if the permeability of the BBB and BTB in malignant brain tumors is abnormal, it is nonetheless sufficiently preserved to represent an obstacle to delivery. Therapeutic drug levels are thereby

often insufficient within brain regions protected from the systemic circulation by this partially and heterogeneously breached barrier. By steeply reducing the concentration of intravenously administered chemotherapeutic agent at the periphery of the tumor, a sink effect is yet another mechanism that can contribute to chemotherapy failure in CNS neoplasm treatment. Although the BBB is breached in primary and secondary brain tumors, other factors can limit the delivery of antineoplastic agents, such as an increase in interstitial pressure within the tumor tissue as well as in the brain surrounding the tumor. The presence of numerous efflux pump systems targeting xenobiotics must also not be neglected as an additional impediment to brain entry.

Distressingly, when dealing with brain tumor patients, several iatrogenic factors may reestablish BBB integrity, thereby further impeding drug delivery. Anti-angiogenic therapies such as bevacizumab and the use of dexamethasone are commonly used medications exerting this effect.

19.2.2 Bypassing the BBB

Different approaches have been advocated to improve delivery across the BBB over the years. These approaches can be broadly classified as local, regional, or global in their ability to bypass the BBB. In this chapter, we focus the discussion on the osmotic permeabilization of the BBB, an invasive approach offering the potential of global delivery (Table 19.1).

19.2.3 Osmotic Blood–Brain Barrier Disruption

This approach involves the cerebral intravascular infusion of hypertonic solutions to produce a transient increase in permeabilization of the barrier, in one of the three selected vascular cerebral distributions (left and right carotid, vertebrobasilar). There is now extensive animal and human clinical data on the use of this strategy (Kroll and Neuwelt 1998; Fortin and Neuwelt 2002; Neuwelt 1989). When one considers the extensiveness of the vascular network supplying the brain, it becomes obvious that a global delivery strategy is plausible with the use of this vascular network as an avenue of delivery. The extensiveness of this network has already been illustrated by Bradbury and colleagues, stating that the entire network covers an area of 12 m^2/g of cerebral parenchyma (Neuwelt 1989). The extent of this network is further exemplified by the fact that the brain receives 20 % of the total cardiac output, while its weight constitutes only 2 % of the total body mass (Bradbury 1986). By increasing the permeability of these vessels, temporarily inactivating the function of the BBB, global drug delivery can be achieved (Fig. 19.1). This inactivation in the BBB function obviously needs to be transitory, with a time window of sufficient duration to allow the intra-arterial infusion and delivery of a therapeutic molecule.

Table 19.1 Strategies to circumvent the blood–brain barrier

Strategy	Methods	Potential applications
Surgical		
Convection-enhanced delivery	Catheters placed around the resection cavity at the time of surgery	To improve local control rates or prevent relapse after gross total resection
Osmotic BBB disruption	Intra-arterial infusion of hyperosmotic agent before intra-arterial infusion of chemotherapeutic, antibody, or nanoparticle drug	Multiple brain metastases from a chemosensitive primary tumor
Targeted ultrasound BBB disruption	Intravenous injection of preformed gas bubbles before pulsed ultrasound treatment	Single or limited number of brain metastases from a chemosensitive primary; single refractory or recurrent brain metastasis
Pharmacological		
Bradykinin analogs	Intravenous or intra-arterial b1 or b2 agonist delivery to transiently increase the permeability of the BTB	In combination with chemotherapy agents
Exploiting RMT: TfR, IR, IGF-1R, LRP-1	To achieve RMT, chemotherapy of choice linked to an antibody that targets the TfR, IR, IGF-1R, or LRP-1	Broad applicability for single or multiple brain metastases
P-gP inhibitors	Inhibiting the drug efflux pump (for example, HM30181A, cyclosporine A, valspodar, elacridir, zosuquidar)	Administration concurrently with chemotherapy for broad applications

BBB blood–brain barrier, *IGF-1R* insulin-like growth factor-1 receptor, *IR* insulin receptor, *LRP-1* low-density lipoprotein receptor-related protein 1, *P-gP* P-glycoprotein, *RMT* receptor-mediated transcytosis, *TfR* transferrin receptor

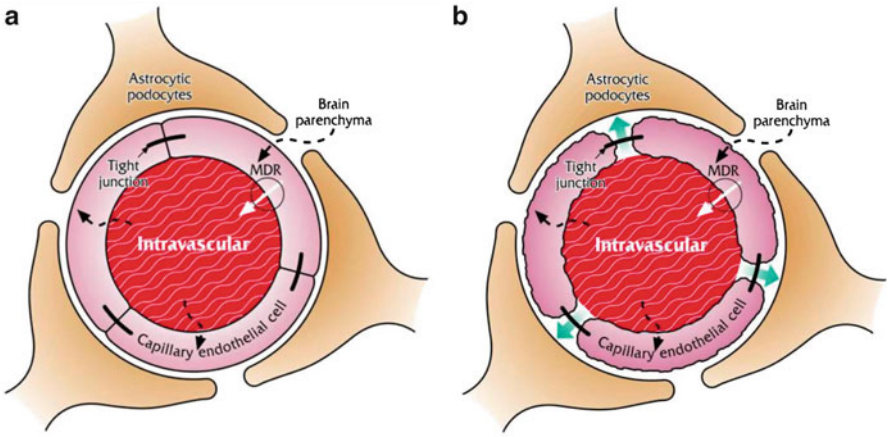

Fig. 19.1 Graphical sketch illustrating the hypothesis concerning the osmotic BBB modification. The tight junctions are shown (**a**) as devoid of any anatomic space between the endothelial cells. Moreover, the multidrug resistance gene product, or P-gp efflux pump, is also illustrated as it is integral to the mechanism of the barrier. The osmotic BBBD procedure induces a retraction in the cell membrane and a physical opening (**b**) accompanied by a modification of the Ca^{2+} metabolism in the cell

19.2.3.1 Preclinical Data

Different blood–brain barrier disruption (BBBD) animal models have been described in the literature; murine models have been the most commonly reported, likely due to their ease of use (Blasberg et al. 1990). In these animals, the procedure is standardized and has been described in detail in numerous studies (Oztas and Kucuk 1995; Kroll et al. 1998; Neuwelt et al. 1998). Briefly, after general anesthesia and endotracheal intubation, the carotid complex is surgically exposed, and the external carotid artery is isolated. After incision and retrograde cannulation of the external carotid artery with a PE-50 tubing, the tip of the catheter is positioned near the carotid bifurcation. A hypertonic solution of mannitol (25 %) is then infused in a precise predetermined volume and rate into the internal carotid artery, followed by the administration of the therapeutic agent (Fortin et al. 2004).

This procedure is influenced by many factors, one of which is the anesthetics used. Indeed, different investigators have suggested that the anesthetic agents must be chosen carefully because their hemodynamic effects can impact the intensity of the BBB opening (Gumerlock and Neuwelt 1990). As an example of this, we initiated our preclinical studies with *ketamine*/xylazine and had to modify the model to obliterate the negative impact of *ketamine* on the cerebral blood flow that ultimately affected the intensity of BBBD (Gumerlock and Neuwelt 1990). This was accomplished by simply isolating the perfused hemisphere from the systemic circulation by applying a temporary vascular clip to the common carotid artery, just prior to the infusion of mannitol (Fig. 19.2). This prevented backflow of mannitol in the cardiac chamber and increased the extent, intensity, and reliability of

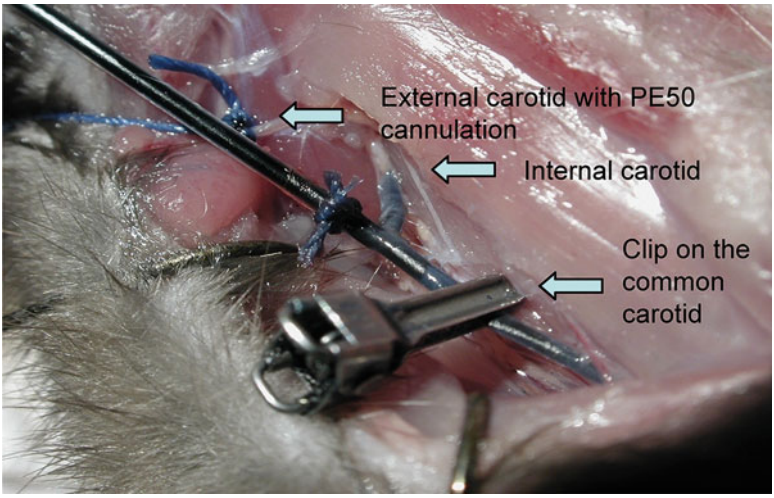

Fig. 19.2 Surgical setup for BBBD. The carotid complex was exposed, and the external carotid artery was ligated and incised. A PE50 tubing was inserted in a retrograde fashion and was positioned just above the bifurcation. The tubing was stabilized with a suture. Notice the clip on the common carotid artery, used to prevent backflow during mannitol infusion

the procedure (Fortin et al. 2004). As the infusion time is 30 s, the clip remains applied for an approximate 40 s.

Ultimately, however, propofol proved to be the anesthetic of choice, as it improved both the efficiency and consistency of the disruption procedure in animals (Remsen et al. 1999). Moreover, as propofol is infused continuously (iv) and has a very short half-life, it can be easily titrated, insuring a better control over vital signs than with *ketamine*. As an added benefit, propofol is an antiseizure medication and a cerebro-protectant, thus conferring to this anesthetic the ideal profile for the BBBD procedure.

However, as the use of propofol translates in a better delivery, the drawback we observed was an increase in neurotoxicity with some co-administered chemotherapeutic agents otherwise known to be safe when paired with other anesthetics (Fortin et al. 2000). This may have been related to an added delivery of potentially neurotoxic agents, e.g., cisplatin.

19.2.3.2 Preclinical Quantitative Studies

Albumin

Several factors can negatively impact the effectiveness of the BBBD: hemodynamic variables, anesthetic agent, and rate of infusion of hypertonic solutions are but a few examples (Remsen et al. 1999; Cosolo et al. 1989). As a consequence, even repeated BBBD procedures in the same subject can lead to highly variable BBB disruption intensities. It is therefore important to monitor the extent of BBBD for each procedure using systemic tracers to indicate the extent of brain entry, particularly if we wish to study the correlation in the intensity of delivery against different outcomes.

This can be accomplished in the clinic with the use of a contrast-enhanced CT scan performed shortly after BBBD. The magnitude of BBBD is then scored semi-quantitatively using a visual scale (Roman-Goldstein et al. 1994). A similar principle has been described by Rapoport in preclinical studies, where the contrast-enhanced CT scan is substituted by a macroscopic staining of the rat cerebrum using Evans blue, a marker that binds albumin (Rawson 1942, Freedman and Johnson 1969). The staining at the surface of the brain is evaluated against an arbitrary staining scale, returning a qualitative evaluation in the intensity of delivery (Kroll and Neuwelt 1998) (Fig. 19.3). As this technique is inherently subjective, the reliability of generated results thereby remains questionable. More so, the fact that the Evans blue so tightly binds albumin is questioned nowadays. This is obviously a critical issue on which the whole concept is based. Another important weakness of this technique arises from the global superficial evaluation, in that only the cortical surface is typically surveyed; if deeper structures are not visualized directly, then no data is gathered on the topographic extent of delivery.

To overcome these shortcomings, we adapted an approach based on albumin immunohistochemistry (Blanchette et al. 2012). This concept has been exploited in the past by Vorbrodt et al. to study the dynamics of BBBD (Vorbrodt et al. 1994).

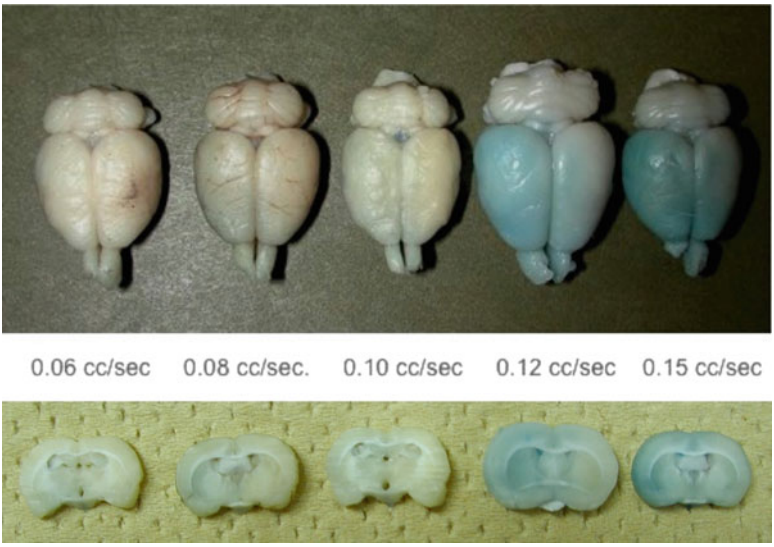

Fig. 19.3 Whole brain and corresponding coronal slices of samples extracted from one representative animal of each group exposed to different rates of mannitol (25 %) infusion as assessed by Evans blue staining. A sequential increment in blue discoloration is obvious, peaking at 0.15 cc/s

In their study, the authors used quantitative immunocytochemistry against albumin, followed by exposition to protein A-gold. They designed a score based on the square micrometer density of gold particles and used it to describe the dynamics in the BBB permeabilization in different brain compartments. The image analysis was performed on electron micrographs and thus did not allow a global estimation of delivery, thereby limiting the application of this technique.

In our search to improve the study of BBBD delivery, we designed a simple approach that allows precise data to be obtained regarding the extent of delivery (Blanchette et al. 2012).

Briefly, we conducted osmotic BBBD with mannitol in adult male Fisher rats, with infusion rates ranging from 0.01 to 0.15 cc/s. Brains were subsequently harvested, and slices were processed for albumin immunochemistry, using a rabbit polyclonal antibody against albumin in a dilution of 1/100. Biotinylated species-specific secondary antibody was applied (1/100) followed by an avidin–biotin amplification and peroxidase development. Afterwards, brain slices were digitized, and ratios of stained pixels to total brain pixels were calculated. Percentages of delivery may then be obtained from these ratios (Fig. 19.4).

This data allows the production of a conservative estimate on the extent of delivery, as albumin is a large protein. It is expressed as a percentage of the treated hemisphere on a single coronal slice and can also be used as a composite score translating global delivery, by simply summating the scores obtained on multiple contiguous slices. As the brain samples are processed and sliced in a standardized fashion using a brain matrix, the number of slices is consistent, thus ensuring that the composite

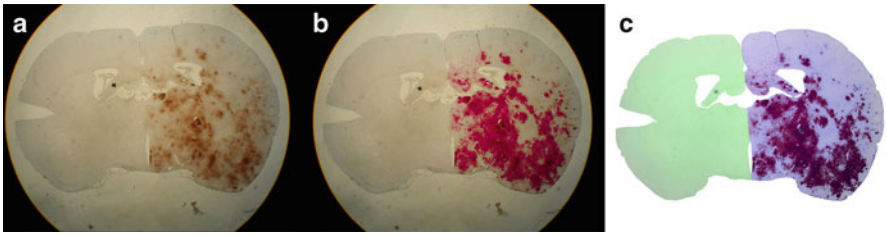

Fig. 19.4 Description of the steps involved in the calculation of the intensity of delivery ratio used in this study. (**a**) The albumin immunocytochemistry source image, displaying discolored areas in the treated hemisphere. (**b**) The image has been analyzed to identify pixels above a fixed threshold corresponding to the immunocytochemistry staining. These pixels are retained as the red overlay. (**c**) After having defined the pixel area of each hemisphere (*green* overlay is *left* hemisphere, whereas *blue* overlay is *right* hemisphere), the *red* overlay has been added to the image for final analysis. Results are expressed as the number of stained pixels (*red* overlay) as a fraction (%) of the treated (*right*) hemisphere (*blue* overlay). Results might also have been presented as the fraction of stained pixels (*red* overlay) over the entire slice area (*green* + *blue* overlays)

score is reproducible between samples. Its objectiveness will help investigators to evaluate the impact of various surrogates on CNS delivery and thus contribute to a better comprehension and characterization of the BBBD process. It does have, however, a significant drawback; test animal euthanasia is required, thereby preventing any kind of dynamic study over time.

MRI Quantification of BBB Permeability

To better study the temporal dynamics of the BBBD process, we have designed a methodology allowing osmotic BBBD to be conducted in the animal MRI gantry, allowing the acquisition of images throughout the course of the procedure (Blanchette et al. 2009). This setup allows us to study the distribution of contrast agents of different molecular weight, to estimate brain exposure against several surrogates following osmotic BBBD, and to estimate the window of barrier opening for each of these molecules.

We have studied the impact of the BBBD procedure in normal animals, and in tumor-bearing animals, using initially two contrast agents: Gd-DTPA, a *low-molecular-weight* contrast agent (0.9 kDa), and Gadomer, a higher molecular weight agent (17 kDa). To evaluate the distribution of these two molecules within the CNS of animals, MRI signal intensity was analyzed in several regions of interest (ROI) scattered across different areas of the brain over time.

Initial results with Gd-DTPA highlighted the heterogeneity in the CNS penetration and the subsequent diffusion of contrast agent from an area representing the cleft between the brain stem and the telencephalic structures (Fig. 19.5). This area was rapidly identified as consistently presenting the widest exposure to Gd-DTPA after BBBD. The study of the *dynamics* in the exposure of the CNS to Gd-DTPA

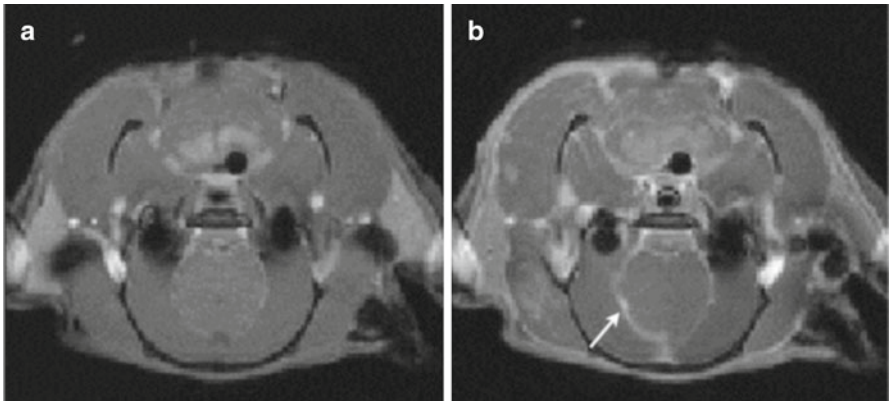

Fig. 19.5 An axial T1 enhanced cut, at the posterior aspect of the brain of a Wistar rat, prior (**a**) and after (**b**) BBBD. The *arrow* depicts the cleft area presenting the most intense increase in Gd-DTPA. It is from this area that a diffusion wave is observed

over time highlighted two different mechanisms by which the procedure increases BBB permeability: a direct and widespread permeabilization of the BBB (Mathieu and Fortin 2006) and a diffusion of the contrast agent within the brain from the ROI described above (Fig. 19.5).

The first *phenomenon* is a diffuse process of short duration observed in the entire disrupted hemisphere. It accounts for the initial T1 MRI signal drop, as water content increases in the extracellular space (Fig. 19.6). The second process involves a diffusion process in the interstitial compartment that spreads like a wave coming from the ROI representing the cleft between the brain stem and the telencephalic structures. This process is directly affected by the molecular size of the compound under study. It results in a delayed and broader distribution of the T1 MRI signal change that eventually reaches the *contralateral* hemisphere, thereby producing a delayed maximal exposure to the studied molecule.

This delay is 66 min for Gd-DTPA, whereas the Gadomer diffusion process is slower and of a lesser magnitude. We presume that this is related to the larger size of the molecule preventing free diffusion through CNS extracellular spaces (Blanchette et al. in preparation).

To quantify brain exposure, initial MRI signal intensities were recorded and subsequent signals measured during and after the BBBD were correlated to contrast agent concentrations by mathematical modeling. Brain exposure could thus be assessed as a function of the amount of contrast agent in a specified ROI (Fig. 19.7). As predicted, overall brain parenchyma is more exposed to Gd-DTPA than Gadomer because of its lower molecular weight, allowing a *wider* volume of distribution. As a corollary, Gd-DTPA is also washed out more rapidly from the brain parenchyma than Gadomer. In fact, the latter appears to remain trapped in the brain for a longer period, suggesting that both volume of distribution and persistence of a molecule in the CNS are related to its molecular weight. Therefore, an equilibrium between these two parameters is the key to maximize brain exposition.

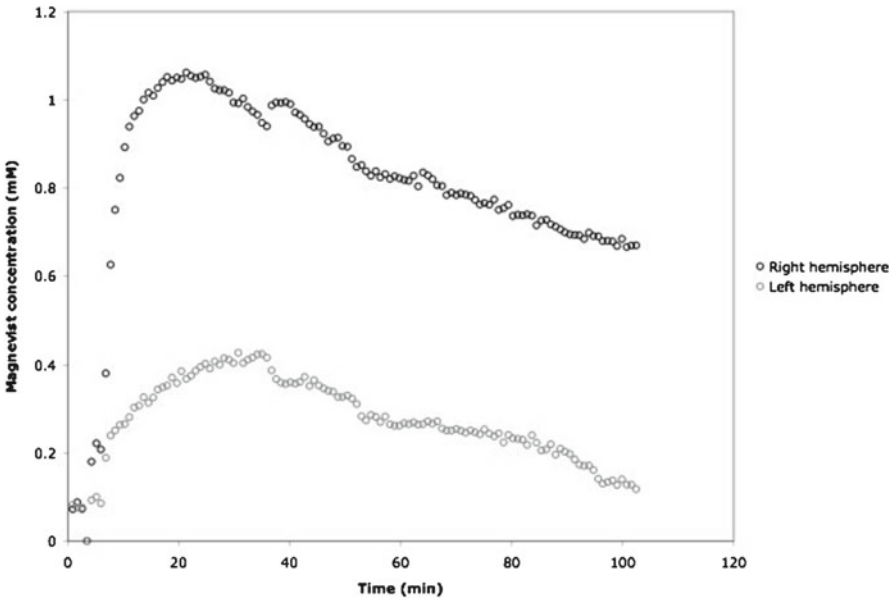

Fig. 19.6 Graphic depicting the Magnevist (Gd-DTPA) concentration over time in the disrupted hemisphere (*right*) and the non-disrupted hemisphere (*left*) in T1 MRI sequence acquisition. Notice the pronounced signal drop at time 3 min, immediately after BBBD, translating the increase in water content caused by the BBBD

To define the duration of BBB opening following the osmotic disruption, delayed administration of Gadomer (17 kDa) has been performed at different times after the osmotic BBBD procedure. We found that approximately 30 min after the mannitol infusion, the BBB seems to recover its normal permeability to Gadomer, displaying values similar to the control group. The same set of experiments for Gd-DTPA depicted a still permeable barrier at 30 min (Blanchette et al. 2009). When evaluating contrast agent exposure produced by BBBD in tumor-bearing animals (F98-Fischer rats), we observed that exposure to Magnevist increased twofold after BBBD, whereas Gadomer exposure showed a threefold increase after BBBD. Baseline tumor exposure was higher to Magnevist than Gadomer and remained so by a twofold factor post BBBD (Blanchettte et al. in preparation). Because of limitations related to the experimental design, the contrast agents were administered intravenously, instead of the intraarterial route normally used when combining the BBBD procedure to intra-arterial chemotherapy infusion. Thereby, these results may severely underestimate the delivery potency of this strategy.

19.2.3.3 Clinical Studies

Thanks to the pioneering work of many dedicated teams at multiple institutions, the BBBD procedure has made its way to the clinic.

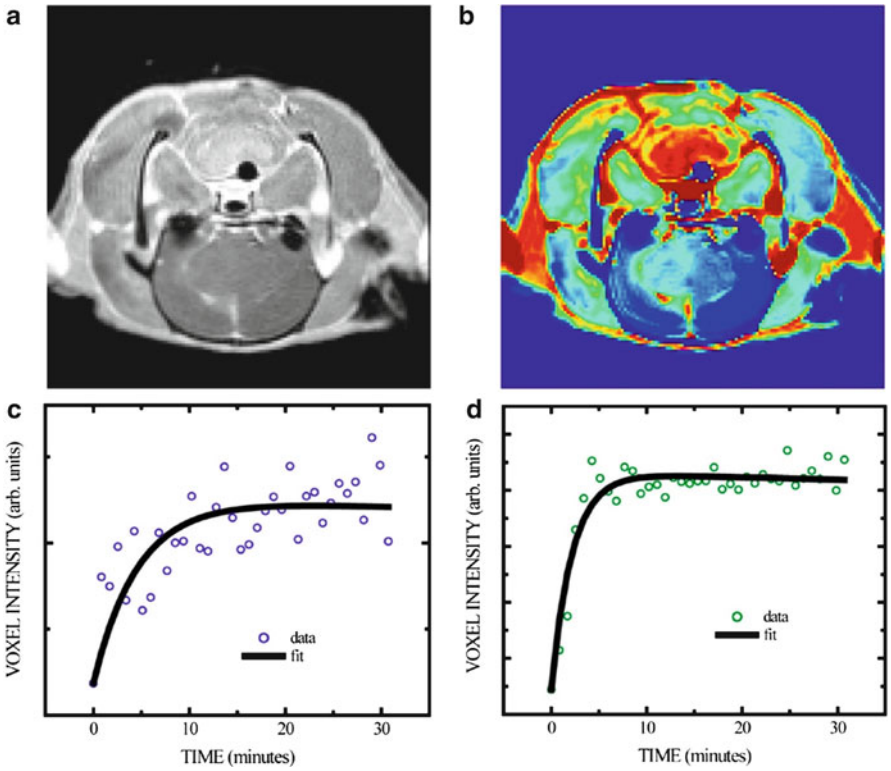

Fig. 19.7 An axial T1 Gd-DTPA-enhanced MRI immediately after BBBD is analyzed using an exposition map translating the area under the curve (AUC). In this animal in which the intensity of the BBBD was moderate at best, the *right* hemisphere presents a slight change in signal intensity (**a**). A map of the AUC produced by the permeabilization procedure is presented in (**b**). Mathematical function extracted for a single pixel in the white matter of the *right* hemisphere. The increase in intensity is studied over time (**c**). Mathematical function extracted for a single pixel in the subependymal region of the *right* hemisphere (**d**). This area consistently depicts the most intense signal variation after osmotic BBBD

Neuwelt and his group led the way and conducted the first clinical studies on osmotic opening of the BBB, beginning in 1979 (Neuwelt 1989). Ever since, this group has been leading the clinical research effort on BBBD, joined by other institutions under the umbrella of the international BBBD consortium. A brief description of the clinical procedure will be detailed, followed by results obtained so far in the treatment of brain tumors.

Description of the BBBD Clinical Procedure

Since the procedure needs to be performed under general anesthesia, the osmotic opening of the BBB is accomplished in the operating theater or in the angiography suite.

The human vascular cerebral system is organized in such a way that there are basically four major arteries taking charge of brain irrigation. However, the distal vascular anatomy is highly variable between different patients, and thus the precise anatomy must be detailed during the first treatment session by a formal cerebral angiography. The physiology of the procedure, by inducing a significant vasogenic edema in the treated vascular distribution and thereby a transient increase in intracranial pressure, does not allow for disruption of more than one vascular territory in a single treatment session. This implies that if a tumor covers more than one vascular distribution, or if there are multiple tumor nodules, the treatment will need to be *delivered* in different vascular distributions from cycle to cycle in order to cover all relevant cerebrum territory.

As hemodynamic parameters significantly impact the intensity of disruption, pharmacological manipulation is used to keep heart rate and systemic blood pressure stable and above certain threshold values (established for each patient) during the general anesthesia in preparation for BBBD (Doolittle et al. 2000).

After general anesthesia, the technique involves the following steps:

1. Percutaneous selective catheterization via transfemoral puncture of the parent cerebral arteries, namely, the left internal carotid artery, right internal carotid artery, left vertebral artery, or right vertebral artery. The tip of the catheter is positioned at the C2–C3 vertebral level in the carotid or at the C6–C7 vertebral level in the vertebral artery.
2. Estimation of the individual optimal rate of infusion of mannitol by iodinated contrast injection and fluoroscopy: This is determined as the highest obtainable infusion rate prior to the observation of a retrograde flow in the external carotid artery. The volume of mannitol infused will be the rate determined in cc/s × 30 s (usually between 4 and 10 cc/s in carotid circulation or between 4 and 8 cc/s in vertebral circulation). The ultimate goal is to fill the entire vascular compartment in the vessel distribution, without producing significant backflow of mannitol in the parent vessel.
3. The osmotic disruption is a physiologically stressful procedure. It can induce focal seizures in 5 % of procedures (Doolittle et al. 2000). It can also trigger a vaso-vagal response with bradycardia and hypotension. In order to prevent the occurrence of these adverse effects, different medications are administered just prior to the disruption to stabilize heart rate (atropine) and pressure (ephedrine) and to induce neuroprotection (benzodiazepine).
4. Osmotic disruption of the BBB is accomplished by infusing a 25 % mannitol solution in the previously catheterized artery at the previously defined rate.
5. During the infusion, interesting signs can be observed. The medial aspect of the forefront ipsilateral to the side of the infusion undergoes a whitish discoloration produced by the washout of blood from the ethmoidal branches, arteries known to connect the intracranial circulation to the extracranial circulation. Bilateral pupillary dilatation can also be observed during the mannitol infusion. During the initial phase of mannitol infusion, a slight bradycardia is observed followed by a brief period of tachycardia and systemic hypertension.

6. Intra-arterial contrast is infused to confirm catheter position and rule out arterial injury post disruption.
7. The therapeutic molecule is administered intra-arterially in the disrupted circulation. The concentration of the solution and the rate of infusion are critical factors when infusing intra-arterial solutions in avoiding neurotoxicity. The phenomenon of streaming defines an inhomogeneous distribution of the administered solution because of poor mixing at the infusion site. It is directly related to the Reynolds number, a crucial parameter in fluid dynamics that predicts the transition from streamlined to turbulent flow (Fortin et al. 1999). In the equation leading to the Reynolds number, the density and viscosity of fluid, lumen diameter of the infused vessels, and velocity of flow are all important determinants to control in order to avoid streaming (Saris et al. 1991).
8. Termination of procedure: The patient is taken to a recovery room, where his/her neurological status and state of consciousness are regularly evaluated until full recovery.
9. If the degree of BBBD opening needs to be assessed, a standard dose of IV nonionic contrast bolus can be administered 5 min after the mannitol infusion. At the end of the procedure, before proceeding to the recovery room, the patient is taken to the CT scan suit.

Contraindications to the BBBD Procedure

The BBBD procedure induces a transient rise in intracranial pressure (ICP) (baselines 3–9 cm H_2O to peaks of 16–23 cm at 30 min post disruption). This transient rise in ICP has been shown to correlate with an approximate 1.5 % increase in extracellular brain fluid content (Neuwelt 1989, Rapoport 1996). In preclinical studies, this transient increase in ICP was not associated with any clinical sequelae (Neuwelt 1989). It illustrates however the rationale behind the very first contraindication of osmotic BBBD: the presence of a significant mass effect associated to the tumor. The definition of mass effect is somewhat arbitrary, but we use standard radiological and clinical criteria to exclude patients deemed at risk.

Other contraindications to the procedure also include evidence of spinal cord block from tumor mass, significant increased risk for general anesthesia, and significant intra-arterial vascular pathologies.

Adverse Effects

In a seminal paper published by McAllister et al., the effect of the BBBD procedure combined with chemotherapy infusion (methotrexate) on neurocognitive function was evaluated in long-term survivors. Contrary to numerous established treatment modalities (e.g., cerebral radiotherapy), the BBBD procedure was not associated with any decline in formal neurocognitive assessment (McAllister et al. 2000).

Adverse effects can nevertheless occur and, for ease of discussion, are stratified in two groups:

- Catheter-related complications:
  - Asymptomatic subintimal tear during catheterization (incidence 5 %).
  - Significant groin hematoma post catheterization (incidence 0.5 %).
  - Parent vessel thrombosis (incidence 0.5 %): This complication could produce long-term neurological disability related to cerebral ischemia in the vascular distribution involved.
- Disruption-related complications:
  - Seizures (incidence 5 %): Seizures are typically focal and are immediately treated with IV thiopental and/or IV diazepam. This is typically a procedure-related event.
  - Temporary obtundation and/or increase in neurological symptoms (incidence 2.5 %): Complete recovery is the norm, with symptoms typically lasting less than 48 h. This adverse effect is associated with an excellent disruption.
  - Brain herniation: Obviously, the most serious complication. One patient expired from this complication (incidence 0.3 %). It is the only mortality event related to the procedure in 300 patients that have undergone a total of more than 3,000 instances of BBBD (Doolittle et al. 2000).

Based on an extensive review of the data across multiple centers using the procedure, Doolitle et al. concluded that the procedure was safe when performed in a standardized, multicenter controlled setting (Doolittle et al. 2000).

Clinical Results Obtained with the BBBD Procedure in the Treatment of Brain Tumors

Clinical results observed with the use of the BBBD procedure are briefly detailed below. However, before we initiate this discussion, a few key points first need to be addressed. Most clinical studies on the use of BBBD have been conducted in patients with brain tumors, as an adjunct to increase the intensity in the delivery of chemotherapy. Some of these tumors, such as malignant astrocytomas, are notoriously chemoresistant and, as such, are not as likely to respond to chemotherapy as other types of cancers. Thus, two distinct factors are at play: (1) the delivery intensity and (2) chemosensitivity of the tumor. However, it is very difficult to segregate these factors from each other in outcome studies, and this limitation must be recognized when analyzing the results. As such, a negative trial could be related to the choice of a poorly active therapeutic agent, even though this agent was adequately delivered to its target by the procedure. When reviewing clinical results on BBBD, all variables involved must be considered and adequately weighted against the surrogates under study to permit fine adjustments, ultimately allowing improvement in outcome.

In an attempt to decrease the number of variables involved, to nullify the choice of the chemotherapy agent in the analysis and to specifically isolate the impact of

delivery in the treatment of brain tumors, Kraemer et al. adopted an interesting approach (Kraemer et al. 2001). They studied the intensity of delivery against tumor response and survival in primary CNS lymphoma, a notoriously chemosensitive CNS tumor nonetheless presenting a poor overall outcome. Two surrogate measures of total dose intensity were used in the design of a delivery score: the total number of disruption procedures and a weighted quality of disruption score. In this study, the extent of the increase in permeability produced by the procedure correlated with long-term survival in a population of patients treated with the BBBD procedure combined with intra-arterial methotrexate infusion, emphasizing the importance of delivery on the patient's outcome.

The procedure has been used to treat different brain tumor types. Williams et al. reported on the use of BBBD in adjunct to a regimen composed of intra-arterial carboplatin and intravenous etoposide in 34 patients with various brain cancer histologies (Williams et al. 1995). Of these 34 patients, 22 had measurable disease, and 9 radiographic responses (50 % or more decrease in enhancing tumors) were observed in these patients. Carboplatin and etoposide delivered with BBBD was considered an active regimen in the treatment of malignant astrocytomas and showed dramatic responses in primitive neuroectodermal tumors and CNS lymphoma. Additionally, the durability of responses in patients with disseminated CNS germ cell tumors was considered encouraging, when compared to historical data.

Kraemer et al. reported on the use of a similar protocol in a series of 41 malignant astrocytoma patients, using a pre-disruption dose of i.v. cyclophosphamide in addition to the carboplatin and etoposide (Kraemer et al. 2002). In this trial, 28 patients were exposed to the BBBD treatment, whereas 13 patients received intra-arterial (IA) chemotherapy only. Treatment modality (BBBD vs. IA) scored as a highly significant variable both in uni- and multivariate analyses ($p = 0.0113$), suggesting that BBBD patients survived significantly longer than IA patients. However, bias cannot be accounted for in this type of uncontrolled study. Nevertheless, a median survival time of 90 weeks for the BBBD group was observed, compared to 50 weeks for the IA group.

The *Centre Hospitalier Universitaire de Sherbrooke* (CHUS) neuro-oncology group joined the consortium in 2000 and has reported results with the BBBD procedure combined with the administration of a carboplatin-based tri-drug regimen at first relapse, after radiation therapy (Fortin et al. 2005). We observed a prolonged median survival of 32.2 months in the treatment of glioblastoma (grade 4 astrocytomas), more than twice the reported median survivals of 9–14 months with standard therapeutic modalities (Huncharek et al. 1998; Huncharek and Muscat 1998, Stewart 2002, Stupp et al. 2002). We also recently reported our clinical data on brain metastasis (Fortin et al. 2007). We described a dramatic improvement in median survival for brain metastasis from ovarian carcinoma, lymphomas, and lung carcinoma (Fig. 19.8). Our series depicted median survival of 24 months for ovarian carcinoma (Fig. 19.9), 16 months for systemic lymphomas, and 13 months for lung carcinoma, compared to reported median survival of 12, 3, and 7 months, respectively, for ovarian, lymphoma, and lung brain metastasis patient series. At the time of this report, 38 patients were included in the analysis. We have now treated more than 150 patients with brain metastasis.

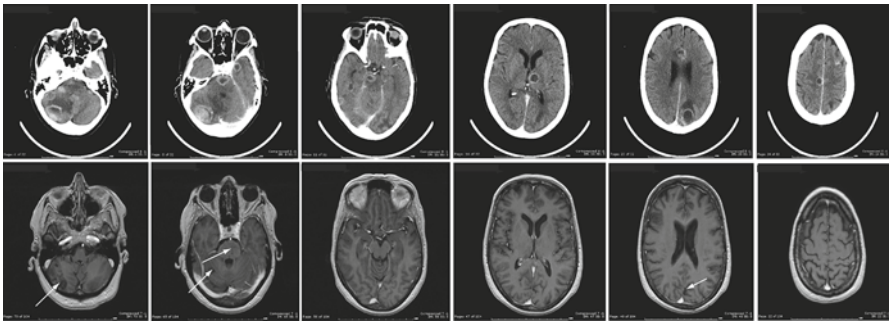

Fig. 19.8 Sixty-two-year-old woman with an initial presentation of headache, nausea, and dizziness. A CT scan revealed the presence of multiple brain lesions (*upper row*). Systemic investigation revealed the presence of a pulmonary nodule and of numerous abnormal lymph nodes. A biopsy of one of these lymph nodes revealed the diagnosis of an oat cell carcinoma. The patient was exposed to eight cycles of intra-arterial chemotherapy and presented a complete response (CR) (*lower row*). The white arrows depict the areas of hypointense signal related to encephalomalacia. These regions correspond to areas where significant tumor nodules were present prior to treatment; these nodules have now receded, thus producing encephalomalacia

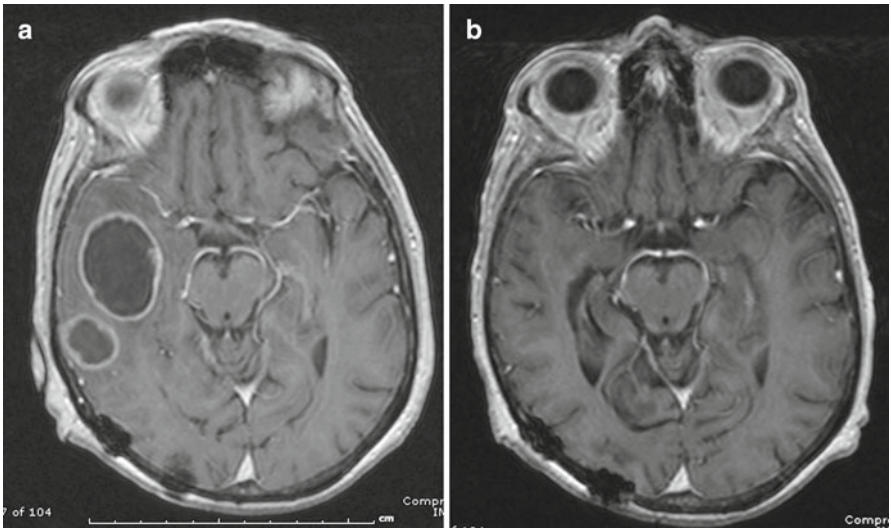

Fig. 19.9 A 69-year-old woman was diagnosed with poorly differentiated ovarian adenocarcinoma in May 2001, at which time she underwent extensive abdominal and gynecologic surgery, followed by six cycles of taxol/carboplatin. She presented a seizure in May 2002, and a metastatic lesion was identified in the right parietal region. She underwent a craniotomy for tumor resection, followed by eight cycles of the carboplatin regimen in conjunction with BBBD. She was considered in complete response (CR) after 2 cycles, and that condition was maintained until December 2005, when she relapsed in the right temporal lobe (**a**). BBBD treatments were resumed, and she was considered in CR after three cycles (**b**)

Recently, Hall et al. reported the experience of the consortium with diffuse pontine gliomas, a tumor type displaying a particularly poor prognosis and typically affecting young patients (Hall et al. 2006). In this small series of eight patients exposed to BBBD and carboplatin or methotrexate, a median time to progression of 15 months was reported along with a median survival of 27 months; indeed, survival beyond 2 years is unusual, and prior chemotherapy trials have not been reported to impact the outcome for this tumor type (Finlay and Zacharoulis 2005).

Recently, we completed a trial of glioblastoma with intra-arterial chemotherapy treatment at second relapse (Fig. 19.10). These patients were treated solely with intra-arterial infusion, without the use of BBBD. The median overall survival from diagnosis was 23 months, whereas a median survival of 11 months from study entry was observed. Twenty-five of 51 patients presented a radiological response to the treatment, whereas 14 remained stable (Fig. 19.11).

All in all, these results clearly hint at an improvement in outcomes for brain tumor patients undergoing chemotherapy regimens following BBBD. Ultimately, the real question is whether or not the procedure can impact tumor response and patient survival. To ascertain this question thoroughly, randomized phase III studies would need to be conducted. As only a few centers are offering the BBBD procedure and these tumors are not prevalent diseases, such studies are particularly difficult to put together. However, recent results showing major improvement in the survival of patients affected by different types of brain tumors and treated via the BBBD approach should prompt major oncology organizations to consider osmotic BBBD as a viable therapeutic option, even though the logistics of the procedure are complex. If more centers were to provide these treatments, multicenter randomized trials could be performed to more firmly establish the efficacy for BBBD.

19.3 Future Directions

Malignant gliomas are very aggressive tumors that remain resistant to treatment for a host of reasons; not only do they display an aggressive infiltrative phenotype that prevents a complete resection, but they also lie behind the BBB and BTB, which limit the bioavailability of the antineoplastic drugs to the CNS cancer cells. Efforts toward the use or the development of strategies to overcome or bypass the BBB and the BTB should thus be promoted in the field of neuro-oncology.

Recent clinical trials using new antineoplastic agents have failed to significantly impact the prognosis for glioma patients. Some drugs that work with high efficiency in vitro have low brain bioavailability because of the impediment imposed by the BBB. In a continuum of studies on the BBBD procedure, we have evaluated the BTB permeability to two molecules of different molecular weight, and we have characterized the dynamics of the BBBD process. Although BBBD significantly improved delivery for both molecules, we observed that drug size significantly impacted their brain penetration through the BTB and BBB following a BBBD procedure. BTB permeability therefore appears to depend on the physicochemical

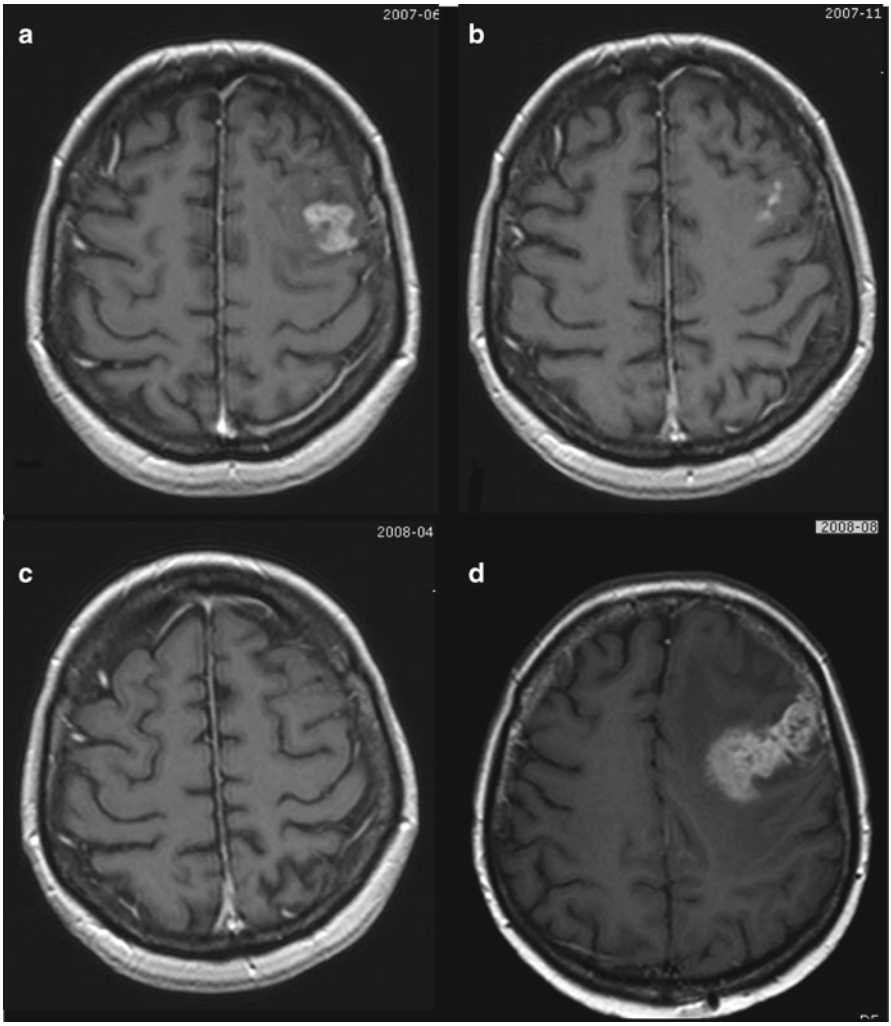

Fig. 19.10 Illustrative example of a good responding GBM patient enrolled in intra-arterial chemotherapy trial at tumor recurrence. A 50-year-old woman progressed 5 months after the beginning of the Stupp protocol (**a**). She underwent a biopsy to exclude a pseudo-progression and was accrued for a left carotid intra-arterial chemotherapy treatment. After only two cycles, she presented a good response (**b**) and, after 4 months of treatment, was considered in complete response (**c**). She progressed after 13 months of treatment (**d**) and survived 23 months after study entry. She was offered bevacizumab as a third line of treatment, after IA failure

characteristics of a given compound (e.g., molecular weight and possibly charge) as well as its affinity for the different multi-drug resistance protein transporters expressed at the BBB. The BBBD process thereby appears to be modulated in a drug-dependent manner. We hypothesize that the BBBD process may significantly increase delivery of drugs that are substrates of ABC transporters. We are currently conducting experiments to confirm this hypothesis.

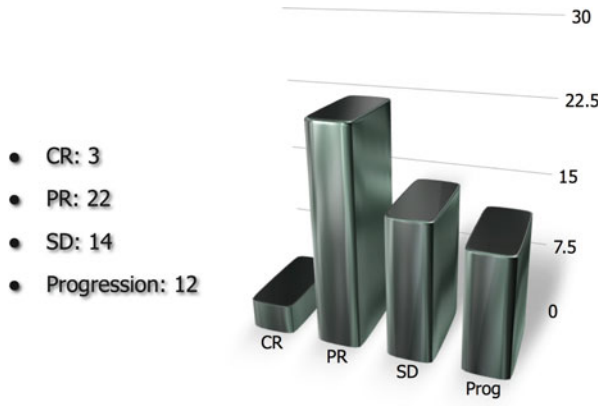

Fig. 19.11 Best radiological response obtained, according to the MacDonald criteria in the 51 patients treated, at second tumor relapse, with an intra-arterial infusion of carboplatin and Melphalan, without BBBD. Tumor responses are classified as *CR* complete response, *PR* partial response, *SD* stable disease or progression

The characterization of the BBBD process for drug molecules with different properties will help optimize drug administration protocols to the CNS using this strategy. This should hopefully translate to improved efficacy of chemotherapy treatment in glioma patients. As many recent clinical trials based on promising new drugs in neuro-oncology have failed to impact survival, the delivery issue should be addressed with greater attention.

19.4 Conclusions

The BBB can no longer be ignored as a factor greatly limiting the entry of therapeutics in the CNS. According to Pardridge, over 98 % of small molecules and close to 100 % of large molecules do not cross the BBB (Pardridge 2007). In neuro-oncology, clinical trials on brain tumor treatment are still *designed* with molecules that do not cross the BBB (e.g., vincristine, taxol). The unique challenge represented by the BBB in the treatment of CNS diseases can no longer be ignored. Less than 1 % of pharmaceutical companies *actually* have a BBB drug targeting effort. The BBBD strategy, *initially* proposed more than 3 decades ago, has now come a long way, with significant preclinical and clinical experience. However, its widespread acceptance has been hampered by many factors: the difficulty in setting teams dedicated to perform these procedures, the relative paucity of brain tumors, and the difficulty of putting together randomized studies. However, concerted efforts such as the international BBB consortium will allow the design of better multicenter trials eventually powered to answer whether or not this approach is worthwhile in the treatment of different CNS pathologies. As the overall clinical results obtained in the treatment of malignant gliomas and brain metastasis (representing the bulk of brain cancers)

remain poor with traditional treatments and very few major breakthroughs have been reported in the last decades despite active clinical research, clinical investigators have increasingly tended to adopt a more open-minded approach toward alternative treatment strategies emphasizing CNS delivery. The promising results obtained in trials published on BBBD in the last decade will allow a better accrual of patients in clinical studies. Hopefully, the promising results obtained thus far for BBBD will soon be followed by randomized clinical studies that show a clear advantage for this invasive technique on patient survival.

19.5 Points for Discussion

- The quintessential question is whether this invasive treatment clearly impacts the survival of patients with glial and metastatic disease. Phase III randomized studies should be designed to answer this question once and for all.
- If such a study was negative, the whole BBBD strategy should not be discredited, as the choice of the drug will obviously exert a paramount influence on results. In short, poor results could be attributable to bad drug selection for the study.
- The influence of the ABC transporters should be studied and considered as an integral component of the BBB.
- In neuro-oncology, the emphasis should not only be for a drug to cross the BBB but also for the drug to be taken up into tumor cells. Many tumor cells also express ABC transporters on their membrane. How is BBBD suited to this task?
- It is essential that the neuro-oncology scientific community acknowledges the importance of the BBB and BTB as delivery impediments and discusses these issues in their forums and publications. While this topic is often deemed esoteric by some neuro-oncologists, clinical studies continue to be designed with (1) drugs for which no knowledge exists regarding their capacity to cross the BBB (e.g., many kinase inhibitors) or (2) drugs which clearly do not cross the BBB (e.g., vincristine).

References

Abbott NJ, Ronnback L, Hansson E (2006) Astrocyte-endothelial interactions at the blood–brain barrier. Nat Rev Neurosci 7(1):41–53

Bellavance MA, Blanchette M, Fortin D (2008) Recent advances in blood–brain barrier disruption as a CNS delivery strategy. AAPS J 10(1):166–177

Blanchette M, Fortin D (2011) Blood–brain barrier disruption in the treatment of brain tumors. Methods Mol Biol 686:447–463

Blanchette M, Michaud K, Fortin D (2012) A new method of quantitatively assessing the opening of the blood–brain barrier in murine animal models. J Neurosci Methods 207(2):125–129. doi:10.1016/j.jneumeth.2012.03.012

Blanchette M, Pellerin M, Tremblay L, Lepage M, Fortin D (2009) Real-time monitoring of gadolinium diethylenetriamine penta-acetic acid during osmotic blood–brain barrier disruption

using magnetic resonance imaging in normal wistar rats. Neurosurgery 65(2):344–350. doi:10.1227/01.NEU.0000349762.17256.9E, discussion 350–351
Blanchette M, Tremblay L, Lepage M, Fortin D. Impact of Drug Size on Brain Tumor and Brain Parenchyma Delivery with and without Blood-Brain Barrier Disruption. submitted to Clinical cancer research (in preparation)
Blasberg R, Groothius D, Molnar P (1990) A review of hyperosmotic blood–brain barrier disruption in seven experimental brain tumor models. In: Johansson BB, Owman C, Widner H (eds) Pathophysiology of the blood–brain barrier. Elsevier, Amsterdam, pp 197–220
Boyle FM, Eller SL, Grossman SA (2004) Penetration of intra-arterially administered vincristine in experimental brain tumor. Neuro Oncol 6(4):300–305
Bradbury MWB (1986) Appraisal of the role of endothelial cells and glia in barrier breakdown. In: Suckling AJ, Rumsby MG, Bradbury MWB (eds) The blood–brain barrier in health and disease. Ellis Horwood, Chichester, England, pp 128–129
Brightman MW, Hori M, Rapoport SI, Reese TS, Westergaard E (1973) Osmotic opening of tight junctions in cerebral endothelium. J Comp Neurol 152:317–325
Brodie BB, Kurz H, Schanker LS (1960) The importance of dissociation constant and lipid-solubility in influencing the passage of drugs into the cerebrospinal fluid. J Pharmacol 130:20–25
Cohen Z, Bonvento G, Lacombe P, Hamel E (1996) Serotonin in the regulation of brain microcirculation. Prog Neurobiol 50(4):335–362
Cohen Z, Molinatti G, Hamel E (1997) Astroglial and vascular interactions of noradrenaline terminals in the rat cerebral cortex. J Cereb Blood Flow Metab 17(8):894–904
Cosolo WC, Martinello P, Louis WJ, Christophidis N (1989) Blood–brain barrier disruption using mannitol: time course and electron microscopy studies. Am J Physiol 256(2 Pt 2):R443–R447
Davson H, Oldendorf WH (1967) Symposium on membrane transport. Transport in the central nervous system. Proc R Soc Med 60(4):326–329
de Boer AG, Gaillard PJ (2007) Drug targeting to the brain. Ann Rev Pharmacol Toxicol 47:323–355
de Boer AG, van der Sandt IC, Gaillard PJ (2003) The role of drug transporters at the blood–brain barrier. Annu Rev Pharmacol Toxicol 43:629–656
Deeken JF, Loscher W (2007) The blood–brain barrier and cancer: transporters, treatment, and Trojan horses. Clin Cancer Res 13(6):1663–1674
Doolittle ND, Miner ME, Hall WA et al (2000) Safety and efficacy of a multicenter study using intraarterial chemotherapy in conjunction with osmotic opening of the blood–brain barrier for the treatment of patients with malignant brain tumors. Cancer 88(3):637–647
Eichler AF, Chung E, Kodack DP, Loeffler JS, Fukumura D, Jain RK (2011) The biology of brain metastases-translation to new therapies. Nat Rev Clin Onc 6:344–356
Fenstermacher J, Gross P, Sposito N, Acuff V, Pettersen S, Gruber K (1988) Structural and functional variations in capillary systems within the brain. Ann N Y Acad Sci 529:21–30
Finlay JL, Zacharoulis S (2005) The treatment of high grade gliomas and diffuse intrinsic pontine tumors of childhood and adolescence: a historical—and futuristic—perspective. J Neurooncol 75(3):253–266
Fortin D, Adams R, Gallez A (2004) A blood–brain barrier disruption model eliminating the hemodynamic effect of ketamine. Can J Neurol Sci 31(2):248–253
Fortin D, Desjardins A, Benko A, Niyonsega T, Boudrias M (2005) Enhanced chemotherapy delivery by intraarterial infusion and blood–brain barrier disruption in malignant brain tumors: the Sherbrooke experience. Cancer 103(12):2606–2615
Fortin D, Gendron C, Boudrias M, Garant MP (2007) Enhanced chemotherapy delivery by intraarterial infusion and blood–brain barrier disruption in the treatment of cerebral metastasis. Cancer 109(4):751–760. doi:10.1002/(ISSN)1097-0142
Fortin D, McAllister LD, Nesbit G et al (1999) Unusual cervical spinal cord toxicity associated with intra-arterial carboplatin, intra-arterial or intravenous etoposide phosphate, and intravenous cyclophosphamide in conjunction with osmotic blood brain-barrier disruption in the vertebral artery. AJNR Am J Neuroradiol 20(10):1794–1802

Fortin D, McCormick CI, Remsen LG, Nixon R, Neuwelt EA (2000) Unexpected neurotoxicity of etoposide phosphate administered in combination with other chemotherapeutic agents after blood–brain barrier modification to enhance delivery, using propofol for general anesthesia, in a rat model. Neurosurgery 47(1):199–207

Fortin D, Neuwelt EA (2002) Therapeutic manipulation of the blood-brain barrier. Neurobase-neurosurgery. 1st edn. Medlink CD-ROM

Freedman FB, Johnson JA (1969) Equilibrium and kinetic properties of the Evans blue-albumin system. Am J Physiol 216(3):675–681

Gumerlock MK, Neuwelt EA (1990) The effects of anesthesia on osmotic blood–brain barrier disruption. Neurosurgery 26(2):268–277

Guo Z, Zhu J, Zhao L, Luo Q, Jin X (2010) Expression and clinical significance of multidrug resistance proteins in brain tumors. J Exp Clin Cancer Res 29:122

Hall WA, Doolittle ND, Daman M et al (2006) Osmotic blood–brain barrier disruption chemotherapy for diffuse pontine gliomas. J Neurooncol 77(3):279–284

Huncharek M, Muscat J, Geschwind JF (1998) Multi-drug versus single agent chemotherapy for high grade astrocytoma; results of a meta-analysis. Anticancer Res 18(6B):4693–4697

Huncharek M, Muscat J (1998) Treatment of recurrent high grade astrocytoma; results of a systematic review of 1,415 patients. Anticancer Res 18(2B):1303–1311

Kraemer DF, Fortin D, Doolittle ND, Neuwelt EA (2001) Association of total dose intensity of chemotherapy in primary central nervous system lymphoma (human non-acquired immunodeficiency syndrome) and survival. Neurosurgery 48(5):1033–1040, discussion 1040–1041

Kraemer DF, Fortin D, Neuwelt EA (2002) Chemotherapeutic dose intensification for treatment of malignant brain tumors: recent developments and future directions. Curr Neurol Neurosci Rep 2(3):216–224

Kroll RA, Neuwelt EA (1998) Outwitting the blood–brain barrier for therapeutic purposes: osmotic opening and other means. Neurosurgery 42(5):1083–1099, discussion 1099–1100

Kroll RA, Pagel MA, Muldoon LL, Roman-Goldstein S, Fiamengo SA, Neuwelt EA (1998) Improving drug delivery to intracerebral tumor and surrounding brain in a rodent model: a comparison of osmotic versus bradykinin modification of the blood-brain and/or blood-tumor barriers. Neurosurgery 43(4):879–886, discussion 886–879

Lee G, Dallas S, Hong M, Bendayan R (2001) Drug transporters in the central nervous system: brain barriers and brain parenchyma considerations. Pharmacol Rev 53(4):569–596

Lockman PR, Mittapalli RK, Taskar KS, Rudraraju V, Gril B, Bohn KA, Adkins CE, Roberts A, Thorsheim HR, Gaasch JA, Huang S, Palmieri D, Steeg PS, Smith QR (2010) Heterogeneous blood-tumor barrier permeability determines drug efficacy in experimental brain metastases of breast cancer. Clin Cancer Res 16(23):5664–5678

Loscher W, Potschka H (2005) Role of drug efflux transporters in the brain for drug disposition and treatment of brain diseases. Prog Neurobiol 1:22–76

Mathieu D, Fortin D (2006) The role of chemotherapy in the treatment of malignant astrocytomas. Can J Neurol Sci 33(2):127–140

McAllister LD, Doolittle ND, Guastadisegni PE et al (2000) Cognitive outcomes and long-term follow-up results after enhanced chemotherapy delivery for primary central nervous system lymphoma. Neurosurgery 46(1):51–60, discussion 60–51

Muldoon LL, Nilaver G, Kroll RA, Pagel MA, Breakefield XO, Chiocca EA, Davidson BL, Weissleder R, Neuwelt EA (1995) Comparison of intracerebral inoculation and osmotic blood–brain barrier disruption for delivery of adenovirus, herpesvirus and iron oxide particles to normal rat brain. Am J Pathol 147:1840–1851

Neuwelt EA (ed) (1989) Implications of the blood–brain barrier and its manipulation, vol 1 and 2. Plenum Press, New York

Neuwelt EA, Barnett PA, McCormick CI, Remsen LG, Kroll RA, Sexton G (1998) Differential permeability of a human brain tumor xenograft in the nude rat: impact of tumor size and method of administration on optimizing delivery of biologically diverse agents. Clin Cancer Res 4(6):1549–1555

Oztas B, Kucuk M (1995) Intracarotid hypothermic saline infusion: a new method for reversible blood–brain barrier disruption in anesthetized rats. Neurosci Lett 190(3):203–206
Pardridge WM (2007) Blood–brain barrier delivery. Drug Discov Today 12(1–2):54–61
Provenzale JM, Mukundan S, Dewhirst M (2005) The role of blood–brain barrier permeability in brain tumor imaging and therapeutics. Am J Roentgenol 185(3):763–767
Rapoport SI (1996) Modulation of blood–brain barrier permeability. J Drug Target 3(6):417–425
Rapoport SI, Hori M, Klatzo I (1972) Testing of a hypothesis for osmotic opening of the blood–brain barrier. Am J Physiol 223(2):323–331
Rawson RA (1942) The binding of T-1824 and structurally related diazo dyes by the plasma proteins. Am J Physiol 138:708–717
Reese TS, Karnovsky MJ (1967) Fine structural localization of a blood–brain barrier to exogenous peroxidase. J Cell Biol 34(1):207–217
Remsen LG, Pagel MA, McCormick CI, Fiamengo SA, Sexton G, Neuwelt EA (1999) The influence of anesthetic choice, $PaCO_2$, and other factors on osmotic blood–brain barrier disruption in rats with brain tumor xenografts. Anesth Analg 88(3):559–567
Roman-Goldstein S, Clunie DA, Stevens J et al (1994) Osmotic blood–brain barrier disruption: CT and radionuclide imaging. AJNR Am J Neuroradiol 15(3):581–590
Saris SC, Blasberg RG, Carson RE et al (1991) Intravascular streaming during carotid artery infusions. Demonstration in humans and reduction using diastole-phased pulsatile administration. J Neurosurg 74(5):763–772
Sato S, Kawase T, Harada S, Takayama H, Suga S (1998) Effect of hyperosmotic solutions on human brain tumour vasculature. Acta Neurochirurgica 140(11):1135–1141, discussion 1141–1142
Shen F, Chu S, Bence AK, Bailey B, Xue X, Erickson PA, Montrose MH, Beck WT, Erickson LC (2008) Quantitation of doxorubicin uptake, efflux, and modulation of multidrug resistance (MDR) in MDR human cancer cells. J Pharmacol Exp Ther 324(1):95–102
Smith MW, Gumbleton M (2006) Endocytosis at the blood–brain barrier: from basic understanding to drug delivery strategies. J Drug Target 14(4):191–214
Stern L, Gautier R (1921) Rapports entre le liquide céphalo-rachidien et la circulation sanquine. Arch Int Physiol 17:138–192
Stewart LA (2002) Chemotherapy in adult high-grade glioma: a systematic review and meta-analysis of individual patient data from 12 randomised trials. Lancet 359(9311):1011–1018
Stupp R, Dietrich PY, Ostermann Kraljevic S et al (2002) Promising survival for patients with newly diagnosed glioblastoma multiforme treated with concomitant radiation plus temozolomide followed by adjuvant temozolomide. J Clin Oncol 20(5):1375–1382
Tosoni A, Ermani M, Brandes AA (2004) The pathogenesis and treatment of brain metastases: a comprehensive review. Crit Rev Oncol Hematol 52:199–215
Van Den Bent MJ (2003) The role of chemotherapy in brain metastases. Eur J Cancer 39(15):2114–2120
Vorbrodt AW, Dobrogowska DH, Tarnawski M, Lossinsky AS (1994) A quantitative immunocytochemical study of the osmotic opening of the blood–brain barrier to endogenous albumin. J Neurocytol 23(12):792–800
Williams PC, Henner WD, Roman-Goldstein S et al (1995) Toxicity and efficacy of carboplatin and etoposide in conjunction with disruption of the blood-brain tumor barrier in the treatment of intracranial neoplasms. Neurosurgery 37(1):17–27, discussion 27–28
Wolburg H, Lippoldt A (2002) Tight junctions of the blood–brain barrier: development, composition and regulation. Vascul Pharmacol 38(6):323–337

Chapter 20
Emerging Engineering Technologies for Opening the BBB

Elisa E. Konofagou

Abstract Current treatments of neurological and neurodegenerative diseases are limited due to the lack of a truly noninvasive, transient, and regionally selective brain drug delivery method. The brain is particularly difficult to deliver drugs to because of the blood–brain barrier (BBB). The impermeability of the BBB is due to the tight junctions between adjacent endothelial cells and highly regulatory transport systems of the endothelial cell membranes. The main function of the BBB is ion and volume regulation to ensure the conditions necessary for proper synaptic and axonal signaling. However, the same permeability properties that keep the brain healthy also present tremendous obstacles to its pharmacological treatment. Until a solution to the trans-BBB delivery problem is found, treatments of neurological diseases will remain impeded. Over the past decade, methods that combine focused ultrasound (FUS) and microbubbles have been shown to offer the unique capability to noninvasively, locally, and transiently open the BBB. Four of the main challenges to the application of FUS are (1) to assess its safety profile, (2) to unveil the mechanism by which the BBB opens and closes, (3) to control and predict the opened BBB properties and duration of the opening, and (4) to assess its promise for brain drug delivery. In this chapter, we discuss all of these challenges, along with findings in both small (mice) and large (nonhuman primates) animals, and emphasize the clinical potential for this technique.

E.E. Konofagou (✉)
Department of Biomedical Engineering, Columbia University,
351 Engineering Terrace, 1210 Amsterdam Avenue, New York, NY 10027, USA

Department of Radiology, Columbia University, New York, NY USA
e-mail: ek2191@columbia.edu

M. Hammarlund-Udenaes et al. (eds.), *Drug Delivery to the Brain*, AAPS Advances in the Pharmaceutical Sciences Series 10, DOI 10.1007/978-1-4614-9105-7_20,

20.1 Introduction

20.1.1 The Blood–Brain Barrier (BBB) Physiology: Structure and Function

The BBB is a specialized substructure of the vascular system, consisting of endothelial cells connected together by tight junctions and surrounded by pericytes and astrocytes (Pardridge 2005). The luminal and abluminal membranes of the brain endothelial cells act as the permeability barrier (Fig. 20.1). The combination of tight junctions and these two membranes result in the BBB exhibiting low permeability to large and ionic substances. However, certain molecules such as glucose and amino acids are exceptions, because they are actively transported. It has also been shown that lymphocytes can traverse the BBB by going through temporarily opened tight junctions of the endothelial cells. The astrocytes have been proven to offer a protective mechanism of the neurons to any mechanical effect (Pardridge 2005; Abbott et al. 2006; Stewart and Tuor 1994).

20.1.2 The BBB and Neurotherapeutics

Several neurological disorders remain intractable to treatment by therapeutic agents because of the BBB, the brain's natural defense. By acting as a permeability barrier, the BBB impedes entry from blood to the brain of virtually all molecules greater than 400 Da molecular weight thus rendering many potent, neurologically active substances and drugs ineffective simply because they cannot be delivered to where they are needed. As a result, traversing the BBB remains the rate-limiting factor in brain drug delivery development (Pardridge 2005, 2006).

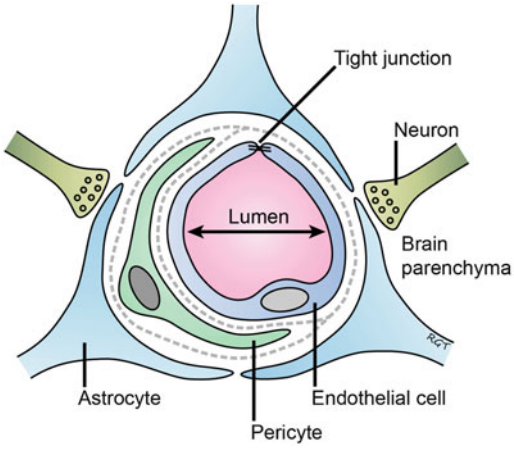

Fig. 20.1 Schematic illustration of the neurovascular unit. Tight junctions between endothelial cells comprise the blood–brain barrier

20.1.3 Focused Ultrasound (FUS)

Focused ultrasound (FUS) utilizes the same concept of acoustic wave propagation as the more widely known diagnostic ultrasound applications. However, instead of acquiring and displaying echoes generated at several tissue interfaces for imaging, FUS employs concave transducers that usually have either a single geometric focus or use phased arrays to electronically steer it, such that most of the power delivered during sonication induces mechanical effects, thermal effects, or both.

20.1.4 BBB Opening Using FUS and Microbubbles

Neuronal damage with BBB opening induced by ultrasound at or near ablation intensities was initially reported in some studies (Bakay et al. 1956; Ballantine et al. 1960; Patrick et al. 1990) but not in others (Vykhodtseva et al. 1995). After reducing the acoustic intensity and duty cycle, BBB opening was still observed, but macroscopic damage was avoided (Mesiwala et al. 2002). With the addition of intravenously (IV)-injected microbubbles prior to sonication, BBB opening was determined to be transient (Hynynen et al. 2001) in the presence of Optison™ (Optison™; Mallinckrodt, Inc., St. Louis, MO), which are albumin-coated, octafluoropropane-filled microbubbles of 3–4.5 μm in diameter and are usually used to enhance blood vessels on clinical ultrasound images through opacification. The BBB opening procedure could also be monitored with MRI and MR contrast agents (Hynynen et al. 2001). This showed the potential of opening the BBB without damaging parenchymal cells, such as neurons. Further investigations with Optison™ searched for a difference in the threshold of BBB opening and neuronal damage and assessed the mechanism of the opening in rabbits with (Hynynen et al. 2001; McDannold et al. 2004; Sheikov et al. 2004) or without (Hynynen et al. 2005) a craniotomy and skull heating in pigs (McDannold et al. 2004). The advantage of having microbubbles present in the blood supply is that they allow for the reduction of the ultrasound intensity, avoidance of thermal effects, and the reduction of the likelihood of irreversible neuronal damage (Hynynen et al. 2001, 2005, 2006; McDannold et al. 2004, 2005; Sheikov et al. 2004, 2006; Choi et al. 2005, 2006a, b, 2007a, b, c; Baseri et al. 2010). Although there are many indications that damage can be contained to minimal hemorrhage (Hynynen et al. 2003, 2006), the complete safety profile remains to be assessed. In addition, indications of various mechanisms such as the dilation of vessels, temporary ischemia, mechanically induced opening of the tight junctions, and the activation of various transport mechanisms have been reported (Mesiwala et al. 2002; Sheikov et al. 2004, 2006).

There are several reports over the past decade using FUS and microbubbles to disrupt the BBB, but this chapter will primarily focus on the main findings by our group. We have demonstrated the feasibility of BBB opening through intact skull and skin and successful imaging of the BBB opening in the area of the hippocampus

at submillimeter imaging resolution in both wild type (Choi et al. 2005, 2007a; Konofagou et al. 2009) and Alzheimer's mice (Choi et al. 2008) as well as non-human primates (Marquet et al. 2010, 2011). Our group has mainly concentrated on the hippocampus, which is a key drug delivery target in Alzheimer's disease to show that discrete brain areas can be successfully and reproducibly targeted (Konofagou and Choi 2008). However, another more recent focus is the treatment of Parkinson's disease with successful targeting of putamen and substantia nigra (Marquet et al. 2010, 2011). Delivery of molecules of up to 2,000 kDa in molecular weight has also been demonstrated (Baseri et al. 2012). Importantly, preliminary histology has indicated no structural damage in the area of the hippocampus within a specific pressure range (Baseri et al. 2010). Finally, it is important to note that the microbubbles used for BBB opening have been approved by the Food and Drug Administration (FDA) for human use in contrast echocardiography, e.g., for the detection of myocardial infarction (Kaufmann et al. 2007). It is equally important to specify that the pressure amplitudes used for BBB opening are of similar range to ultrasound diagnostic levels (<1.5–2 MPa) and, therefore, assumed safe for human use (Christensen 1988), while the pulse duration is orders of magnitude longer.

20.1.5 Microbubbles in Contrast Ultrasound and Associated Bioeffects

Currently, in the USA, microbubbles are only FDA-approved for echocardiography in patients with suboptimal images of the cardiac chambers. However, microbubbles have shown promise for imaging myocardial perfusion using intermittent contrast destruction pulses. Therefore, most in vivo studies of bioeffects have focused on the heart (Miller 2007). For a given frequency, separate pressure thresholds exist for microbubble destruction and the onset of bioeffects (Chen et al. 2002; Li et al. 2003, 2004). Safe cardiac perfusion imaging can then be achieved with the microbubble clearance pulse set between these thresholds. Doses for commercially available microbubbles used in contrast echocardiography could provide a useful benchmark for therapy trials. However, the human dose for imaging purposes varies widely. A typical dose ranges between 6 and 12×10^7 microbubbles per kg (60–120 microbubbles per mg). Mean diameters are given, but detailed information regarding the polydispersity of microbubble size distributions is lacking. Thus, the effects of microbubble size and concentration on safety are difficult to decouple from previous studies using these commercial agents. Our ability to generate and isolate microbubbles of distinct and narrow size distributions with well-defined concentrations has allowed us to probe these effects in the studies described.

Several studies have shown an increase in bioeffects with increasing microbubble dose. For Definity and Optison, increases in rat cardiomyocyte cell death and premature heart beats and microvessel leakage were found after insonation (Li et al. 2003; Miller et al. 2005). Similar dose–response relationships have been observed for BBB opening (Kaps et al. 2001; Liu et al. 2005; Yang et al. 2007). Miller et al. (2005) compared insonation of Optison, Definity and Imagent in the rat heart and

found that microvascular effects were similar when expressed as the number of microbubbles injected. They concluded that shell type and encapsulated gas have little effect on bioeffects. Given the polydispersed size distribution of the different formulations, however, the effects of size are difficult to glean from that study. However, little is known about the effects of microbubble size on bioeffects. Christiansen et al. (2003) found that intra-arterial injection was more effective than intravenous injection for gene transfection through sonoporation. This result was attributed to the difference in microbubble sizes delivered to the insonified region. Several biophysical studies have shown remarkable size dependence for microbubble oscillation and destruction (Chomas et al. 2001; Borden et al. 2005).

20.1.6 Clinical Relevance of BBB Disruption

20.1.6.1 Neurodegenerative Disease

According to the 2008 US News Health report, over 4 million US men and women suffer from Alzheimer's disease; 1 million from Parkinson's disease; 350,000 from multiple sclerosis; and 20,000 from ALS. Worldwide, these four diseases account for more than 20 million patients. Although great progress has been made in recent years toward understanding of neurodegenerative diseases like Alzheimer's, Parkinson's, multiple sclerosis, amyotrophic lateral sclerosis (ALS) and others, few effective treatments and no cures are currently available. Aging greatly increases the risk of neurodegenerative disease, and the average age of Americans is steadily increasing. Today, over 35 million Americans are over the age of 65. Within the next 30 years this number is likely to double, putting more and more people at increased risk of neurodegenerative disease. Alzheimer's disease, which has emerged as one of the most common brain disorders, severely affects the hippocampal formation with pathology gradually spreading to most brain areas as the disease progresses; this pathology is characterized partly by deposition of amyloid plaques in the brain tissue but also in the blood vessels themselves (Iadecola 2004). We have primarily therefore focused on the treatment of Alzheimer's disease through FUS-induced BBB opening targeted to the hippocampus.

20.1.6.2 Drug Delivery in Neurodegenerative Disease

Over the past decade, numerous small- and large-molecule products have been developed for treatment of neurodegenerative diseases with mixed success. When administered systemically in vivo, the BBB inhibits their delivery to the regions affected by those diseases. A review of the Comprehensive Medicinal Chemistry database indicates that only 5 % of the more than 7,000 small-molecule drugs treat the Central Nervous System (CNS) (Pardridge 2006). With these, only four CNS disorders can be treated: depression, schizophrenia, epilepsy, and chronic pain

(Ghose et al. 1999; Lipinski 2000). Despite the availability of pharmacological agents, potentially devastating CNS disorders and age-related neurodegenerative diseases such as Alzheimer's disease, Parkinson's disease, Huntington's disease, multiple sclerosis, and ALS remain undertreated mainly because of the impermeability of the BBB (Pardridge 2005, 2006). One of the goals of our studies has been to optimize the FUS method and elucidate the physical mechanism in order to ultimately deliver therapeutics to the brain and significantly facilitate treatment of currently intractable and devastating neurodegenerative diseases. As indicated before, there have been several hypotheses and reports on the physiological mechanism (Sheikov et al. 2006, 2008; Choi et al. 2011a), but the physical mechanism has been progressively unveiled and identified as being solely related to stable cavitation at low pressures (Tung et al. 2010, 2011a, b; Arvanitis et al. 2012) and a combination of stable and inertial cavitation at higher pressures (Tung et al. 2010, 2011a, b).

A successful drug delivery system requires transient, localized, and noninvasive targeting of a specific tissue region. None of the current techniques clinically used, or currently under research, address these issues within the scope of the treatment of neurodegenerative diseases. As a result, the present situation in neurotherapeutics enjoys few successful treatments for most CNS disorders. Some routes of administration/brain drug delivery strategies are listed and summarized in Table 20.1. Several pharmaceutical companies use the technique known as "lipidization," which is the addition of lipid groups to the polar ends of molecules to increase the permeability of the agent (Fischer et al. 1998). However, the effect is not localized as the permeability of the drug increases not only in the targeted region but also throughout the entire brain and body. There can thus be a limit to the amount absorbed before the side effects become deleterious (Fischer et al. 1998).

A second set of techniques under study are neurosurgically-based drug delivery methods, which involve the invasive implantation of drugs into a region by a needle (Blasberg et al. 1975; Fung et al. 1996). The drug spreads through diffusion and is often localized to the targeted region because diffusion does not allow molecules to travel far from their point of release. In addition to this, invasive procedures traverse untargeted brain tissue, potentially causing unnecessary damage. Other techniques utilize solvents mixed with drugs or adjuvants (pharmacological agents) attached to drugs to disrupt the BBB through dilation and contraction of the blood vessels (Pardridge 2005, 2006, 2007). However, this disruption is not localized within the brain, and the solvents and adjuvants used are potentially toxic. This technique may constitute a delivery method specific to the brain, but it requires special attention to each type of drug molecule and a specific transport system resulting in a time-consuming and costly process while still not being completely localized to the targeted region. FUS in combination with microbubbles therefore constitutes the only truly transient, localized, and noninvasive technique for opening the BBB. Due to these unique advantages over other existent techniques (Table 20.1), FUS may facilitate the delivery of already developed pharmacological agents and could significantly impact how devastating CNS diseases are treated.

Table 20.1 Techniques shown to induce trans-BBB transport or BBB disruption

Method	Description	Disadvantages	Noninvasive?	Localized?
Lipidization	Adds lipid groups to the drug Allows uptake in the BBB	Increases penetration across all biological membranes	Yes	No
Transcranial brain drug delivery	Neurosurgically based drug delivery method. Diffusion-based method	Invasive. Diffusion reduces the initial concentration by 90 % when traveling only 0.5 mm	No	Yes
Solvent/adjuvant-mediated BBB disruption	Solvent and adjuvants disrupt the BBB using dilation, contraction, and other methods	Disrupts the BBB in all of the brain. Potentially toxic	Yes	No
Delivery through endogenous transporters	Use endogenous transporters to traverse the BBB	Requires medicinal chemistry to modify drugs and knowledge of the endogenous transporters	Yes	No
Ultrasound	Focused ultrasound (FUS) with microbubbles	Possible irreversible damage may be induced at higher pressures	Yes	Yes

However, despite the fact that FUS is currently the only technique that can open the BBB locally and noninvasively, several key aspects of this phenomenon remain unexplored. A clear correlation of BBB opening with microbubbles has been shown (Hynynen et al. 2001; Choi et al. 2005; McDannold et al. 2006). Although the presence of microbubbles allows for a reduction in the necessary acoustic pressure for BBB opening, it also allows for the possibility of disrupting the microbubble through inertial cavitation (Pardridge 2007; Neppiras 1980; Leighton 1997). The resulting effects cannot only open the tight junctions, but also could induce irreversible damage to the blood vessels and its surrounding cells (Baseri et al. 2010). Recent studies have indicated that BBB opening may occur without necessarily incurring inertial cavitation, without (Hynynen et al. 2005) or with (McDannold et al. 2006) craniotomy. However, it is not clear how the different types of mechanical effects lead to BBB opening and how the role of the microbubble can be optimized. Given the strong coupling of microbubble size and concentration to the response to insonation, a mechanistic study to BBB opening by contrast-assisted FUS must include these parameters. Control over both ultrasound and microbubble parameters is essential for the proper optimization and understanding of the FUS technique.

20.1.6.3 FUS-Facilitated BBB Opening in Drug Delivery for Treatment of Neurodegenerative Disease

Realizing the strong premise of this technique for facilitation of drug delivery to specific brain regions, we showed that the BBB can be opened reliably and reproducibly in the hippocampal region in mice (Choi et al. 2005, 2007a, b, c, 2008, 2009; Konofagou and Choi 2008; Konofagou et al. 2009; Choi et al. 2011b). By developing a better understanding of the underlying physical parameters that are responsible for the opening of the BBB, namely, the ultrasound and microbubble parameters, we will be in a position to fully exploit this methodology and to do so safely. The feasibility of the technique using optimized ultrasound and microbubble parameters for reversible BBB opening, as determined in vivo, has been tested on wild-type mice under several different conditions to identify the potential of this technique in the treatment of neurodegenerative diseases (Choi et al. 2008, 2011a, b; Konofagou et al. 2009). The MR imaging methods developed allow for high sensitivity, high spatial resolution, and high temporal resolution. The latter is achieved through the slow diffusion of intraperitoneally injected gadolinium. The added potential of combining this ultrasound technique with any therapeutic agent may renew possibilities in potentially employing available pharmacological agents, whose development has currently been abandoned because of poor BBB penetration. This may thus result in the novel and effective treatment of several, potentially devastating, neurological and neurodegenerative diseases. As indicated above, we have concentrated on the feasibility of noninvasive and localized treatment Alzheimer's disease by specifically targeting the hippocampus. However, the FUS technique can, in principle, be combined and applied in the case of any neurological disease. Therefore, findings from our work may not only impact treatment of a specific disease but also the entire field of brain diseases. In summary, FUS stands to make an important impact in drug delivery to the brain, warranting its optimization through better understanding of the interactions that exist between the microbubble, the brain cells, and the FUS beam.

20.1.7 Drug Delivery Through the Opened BBB

The delivery of many large agents using FUS and microbubbles has been demonstrated in previous studies by our group and others using a variety of different agents: MRI contrast agents such as Omniscan (573 Da) (Choi et al. 2007b (and Magnevist® (938 Da) (Choi et al. 2007a), Evans Blue (Kinoshita et al. 2006), Trypan Blue (Raymond et al. 2008), Herceptin (148 kDa) (Kinoshita et al. 2006), horseradish peroxidase (40 kDa) (Sheikov et al. 2008), doxorubicin (544 Da) (Treat et al. 2007), multi-sized Dextran (Choi et al. 2008), rabbit anti-Aβ antibodies (Raymond et al. 2008), stem cells Burgess et al. 2011), adeno-associated viruses (Wang et al. 2013) and neurotrophic factors (Baseri et al. 2012). Despite the promise shown by the delivery of such a variety of compounds, several questions remain regarding the effectiveness of delivery with FUS. One of the questions that our group has addressed is whether the therapeutic molecules that cross the FUS-opened BBB can also enter into the neuronal cell and thereby trigger neuroprotection or neurogenesis (Baseri et al. 2012).

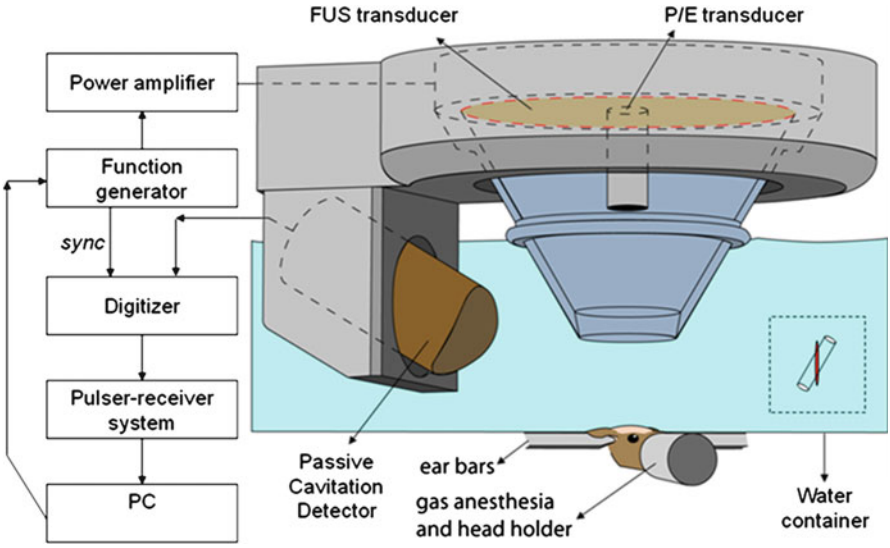

Fig. 20.2 Block diagram and illustration of the experimental setup. The PCD was positioned at 60° relative to the longitudinal axis of the FUS beam. The overlap between the focal regions of PCD (*blue*) and FUS (*red*) occurring inside the murine brain is illustrated in the inset

20.1.8 Methods for Inducing and Assessing BBB Opening

20.1.8.1 FUS and Microbubbles

A typical experimental setup is shown in Fig. 20.2. The FUS transducer (center frequency: 1.5 MHz; focal depth: 60 mm; outer radius: 30 mm; inner radius 11.2 mm, model: cdc7411-3, Imasonic, Besançon, France) is used to perform sonication immediately following bubble administration. The transducer is driven by a function generator (Agilent Technologies, Palo Alto, CA, USA) through a 50-dB power amplifier (ENI, Inc., Rochester, NY, USA). A cone filled with degassed and distilled water is attached to the transducer system. The transducer is attached to a computer-controlled positioner (Velmex, Inc., Bloomfield, NY). The passive cavitation detector (PCD), a 5-cm cylindrically focused broadband hydrophone (Sonic Concepts, Bothell, WA, USA), with a cylindrical focal region (height 19 mm, diameter 3.64 mm) is placed at 60° from the longitudinal axis of the FUS beam. The PCD and the FUS transducer are confocally aligned. The acoustic emissions from the microbubbles are captured with the PCD and collected using a digitizer (model 14200, Gage Applied Technologies, Inc., Lachine, QC, Canada) through a 20 dB amplifier (model 5800, Olympus NDT, Waltham, MA, USA). Microbubbles (Definity®: mean diameter range: 1.1–3.3 μm, Lantheus Medical Imaging, MA, USA, or lipid-shelled microbubbles manufactured in-house and size-isolated (using differential centrifugation; Feshitan et al. 2009) are activated and used within 24 h after activation.

Following activation, a 1:20 dilution solution is prepared using 1× phosphate-buffered saline (PBS) and slowly injected into the tail vein (1 μl per gram of mouse body weight). Both transducers use pulsed-wave FUS (burst rate: 10 Hz, burst duration: 20 ms, duty cycle: 20 %) in two 30-s sonication intervals with a 30-s intermittent delay. Peak-rarefactional acoustic pressures of 0.15, 0.30, 0.45, and 0.60 MPa are typically used as they have been shown to provide the best tradeoff between safety and BBB opening (Baseri et al. 2010). One side of the hippocampus in the horizontal orientation is sonicated in each mouse. Acoustic parameters other than the pressure have also been studied with respect to their role in BBB disruption. One of those is the pulse length (Choi et al. 2011a). In that study, mouse brains were pulse sonicated (center frequency: 1.5 MHz, peak-negative pressure: 0.3 MPa, pulse length (PL): 0.002–30 ms, pulse repetition frequency (PRF): 6.25, 25, 100 kHz) continuously or with a burst length of 1,000 pulses (burst repetition frequency (BRF): 0.1, 1, 2, or 5 Hz) through the intact scalp and skull for 11 min. One minute after the start of sonication, fluorescence-tagged dextran (60 μg/g, molecular weight: 3 kDa) and Definity® microbubbles (0.05 μl/g) were intravenously injected. After 20 min of circulation, the mice were transcardially perfused, and the brains were sectioned and imaged using fluorescence microscopy. In order to determine the microbubble size dependence, mice have been injected intravenously with lipid-shelled bubbles of either 1–2, 4–5, or 6–8 μm in diameter while the concentration was 10^7 numbers/ml (Choi et al. 2009).

20.1.8.2 Magnetic Resonance Imaging

A vertical-bore 9.4T MR system (Bruker Biospin, Billerica, MA, USA) was used to confirm the BBB opening in the murine hippocampus. Each mouse was anesthetized using 1–2 % of isoflurane gas and was positioned inside a single resonator. The respiration rate was monitored throughout the procedure using a monitoring or gating system (SA Instruments, Inc., Stony Brook, New York, USA). Prior to introducing the mouse into the scanner, intraperitoneal (IP) catheterization was performed. Two different protocols were used for MR imaging. The first protocol was a three-dimensional (3D), T1-weighted SNAP gradient echo pulse sequence, which acquired horizontal images using TR/TE = 20/4 ms, a flip angle of 25 deg, NEX of 5, a total acquisition time of 6 min and 49 s, a matrix size of 256 × 256 × 16 pixels, and a field of view (FOV) of 1.92 × 1.92 × 0.5 cm^3, resulting in a resolution of 75 × 75 × 312.5 μm^3. The second protocol was a 3D T2*-weighted GEFC gradient echo pulse sequence, which acquired horizontal images using TR/TE = 20/5.2 ms, a flip angle of 10 deg, NEX of 8, a total acquisition time of 8 min and 12 s, a matrix size of 256 × 192 × 16 pixels, and an FOV of 2.25 × 1.69 × 0.7 cm^3, resulting in a resolution of 88 × 88 × 437.5 μm^3. Both protocols were applied approximately 30 min after IP injection of 0.30 ml of gadodiamide (590 Da, Omniscan®, GE Healthcare, Princeton, NJ, USA), which allowed sufficient time for the gadodiamide to diffuse into the sonicated region.

20.1.8.3 Acoustic Emission Signal Acquisition and Analysis

The acoustic emission signals acquired by the PCD are sampled at 25 MHz to accommodate the highest memory limit of the digitizer involved in each case. A customized spectrogram function (30-cycles, i.e., 20 μs, Chebyshev window; 95 % overlap; 4096-point FFT) in MATLAB® (Choi et al. 2007b, Mathworks, Natick, MA) is used to generate a time–frequency map, which provides the spectral amplitude in time. The spectrogram can then clearly indicate how the frequency content of a signal changes over time. Therefore, the onset of the broadband response and its duration could be clearly demonstrated on the spectrogram.

The acoustic emissions are quantified in vivo. A high-pass, Chebyshev type 1 filter with a cut-off of 4 MHz was first applied to the acquired PCD signal. The acoustic emission collected by the focused hydrophone was used in the quantification of the ICD; the harmonic (nf, n = 1, 2, …,6), sub-harmonic ($f/2$), and ultra-harmonic ($nf/2$, $n = 3, 5, 7, 9$) frequencies produced by stable cavitation (Farny et al. 2009) were filtered out by excluding 300-kHz bandwidths around each harmonic and 100-kHz bandwidths around each sub- and ultra-harmonic frequencies. These bandwidths were designed to filter for the broadband response and to ensure that the stable cavitation response was not included in the ICD calculation. The root mean square (RMS) of the spectral amplitude (V_{RMS}) could then be obtained from the spectrogram after filtering. To maximize the broadband response compared to the sonication without microbubbles, only the first 50 μs of sonication was considered in the ICD calculation, which was performed by integrating the V_{RMS} variation within an interval of 0.75 μs (i.e., calculating the area below the V_{RMS} curve between 0.095 and 0.145 ms). In order to remove the effect of the skull in the ICD calculation, the V_{RMS} in the case without microbubbles was also calculated and was subtracted from the results with the microbubbles to obtain the net bubble response. A Student's t-test was used to determine whether the ICD was statistically different between different pressure amplitudes. A P-value of $P < 0.05$ was considered to denote a significant difference in all comparisons.

20.1.9 Acoustic Parameter Dependence and Mechanism of BBB Opening

We have found that the peak-rarefactional pressure and the microbubble diameter dictate the physical mechanism, i.e., whether the BBB opening occurs in the presence of stable or inertial cavitation [60]. The BBB opening pressure threshold is identified to fall between 0.30 and 0.45 MPa in the case of the 1–2-μm bubbles with inertial cavitation while the BBB opening occurs with stable cavitation only at pressures between 0.15 and 0.30 MPa in the 4–5 and 6–8-μm cases (Choi et al. 2009; Tung et al. 2010). At every acoustic pressure, both the region of contrast enhancement in the MRI imaging and the amplitude of broadband emissions increased with

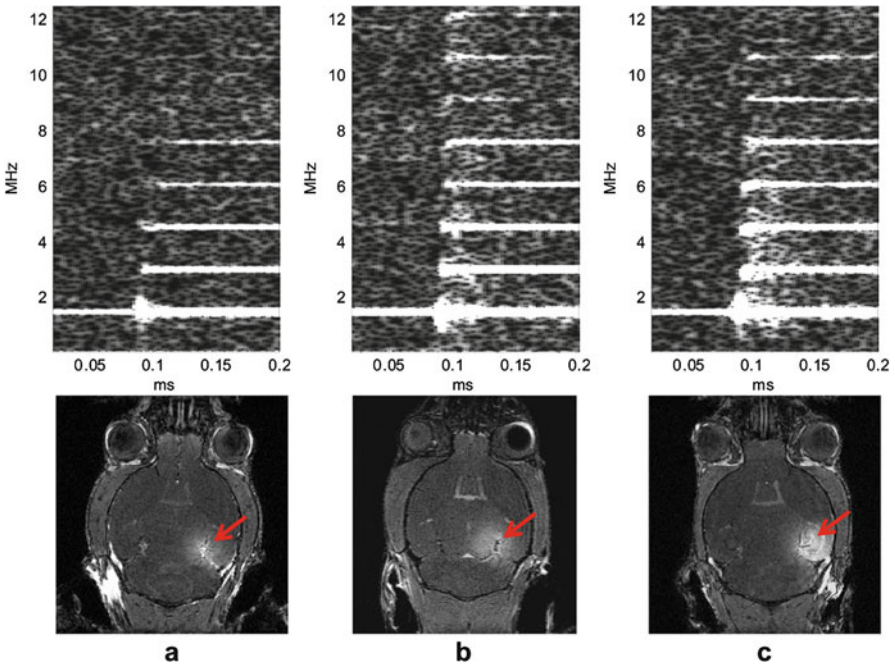

Fig. 20.3 Spectrogram during the first 0.2 ms sonication. Broadband acoustic emissions were detected at (**b**) 0.45 MPa and (**c**) 0.60 MPa but not at (**a**) 0.30 MPa. Corresponding MRI images confirm that the blood–brain barrier (BBB) could be opened at 0.30 MPa, i.e., without inertial cavitation (Tung et al. 2010). The red arrows indicate the location of BBB opening which is the hippocampus

the bubble diameter. The IC threshold is found to be bubble size independent and to lie between 0.30 and 0.45 MPa for all bubble sizes (Fig. 20.3). The underlying reason for this independence of the threshold on the bubble size is currently being investigated. In fluorescence imaging, the PL of 2.3 μs was found to be sufficient for BBB opening and Dextran delivery (Fig. 20.4).

20.1.10 Molecular Delivery Through the BBB Opening

A molecular delivery study (Choi et al. 2007b, 2011b) indicated that the range of molecular size for trans-BBB delivery spreads to well beyond the 574 Da (Gadolinium; Fig. 20.2) to 67 kDa (Albumin; Fig. 20.5) and 2,000 kDa (Dextrans; Fig. 20.5). As expected, at 2,000 kDa (~20 nm), the fluorescent region is the smallest (since the molecule is the largest and thus diffusion the slowest) and mostly outside of the hippocampus. Therefore, FUS-induced BBB opening was shown feasible for noninvasive, local, and transient opening of the BBB for drug delivery of agents of several tens of kDa.

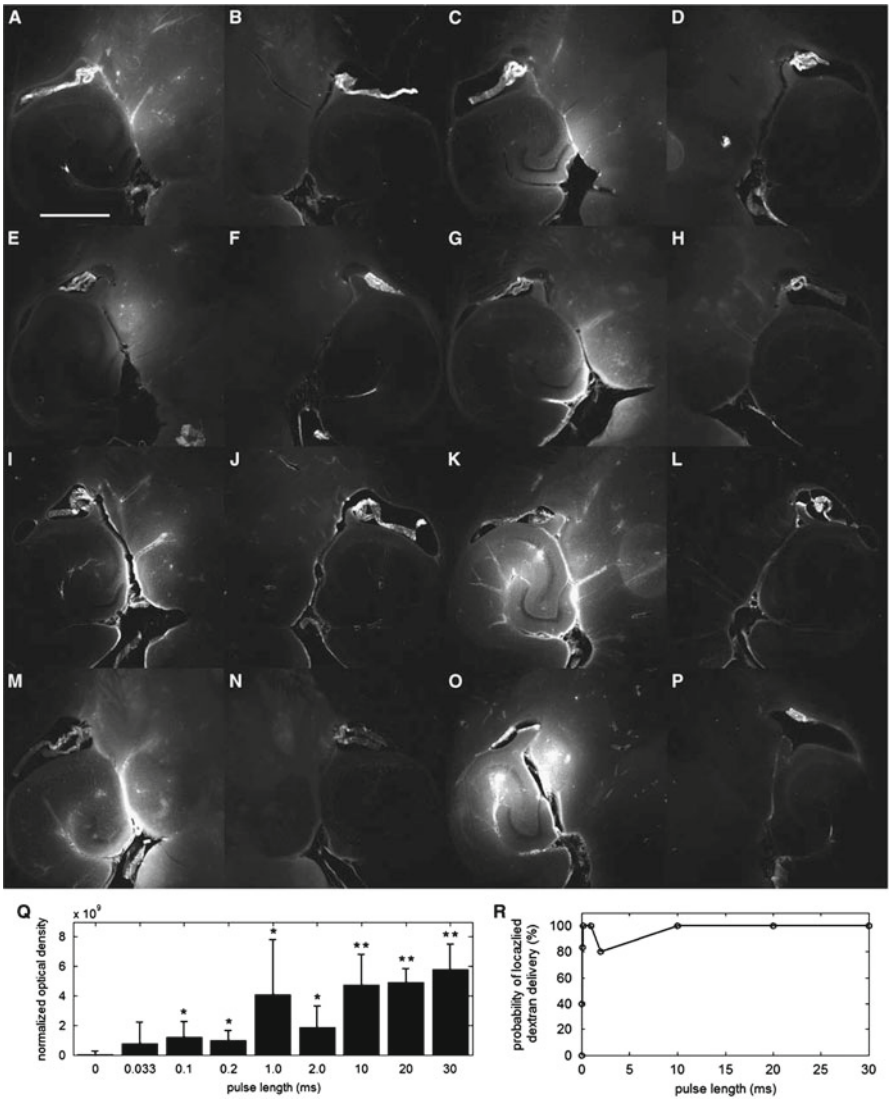

Fig. 20.4 Qualitative fluorescence images of the (**a**, **c**, **e**, **g**, **i**, **k**, **m**, **o**) *left* and (**b**, **d**, **f**, **h**, **j**, **l**, **n**, **p**) *right* brain regions of interest (ROI) that have been exposed to pulse length (PL) of (**a**) 0.033, (**c**) 0.1, (**e**) 0.2, (**g**) 1, (I) 2, (**k**) 10, (**m**) 20, and (**o**) 30 ms. The white scale bar in (**a**) indicates 1 mm. Quantitative (*Q*) normalized optical density (NOD) of the *left* focused ultrasound (FUS)-targeted ROI and (*R*) probability of localized dextran delivery. The *left* ROI was sonicated at different PLs. The single asterisk (*) indicates an NOD increase from the sham, whereas the *double asterisk* (**) indicates a significant increase ($p < 0.05$) compared with the 0.033-, 0.1-, and 0.2-ms PLs (Choi et al. 2011a)

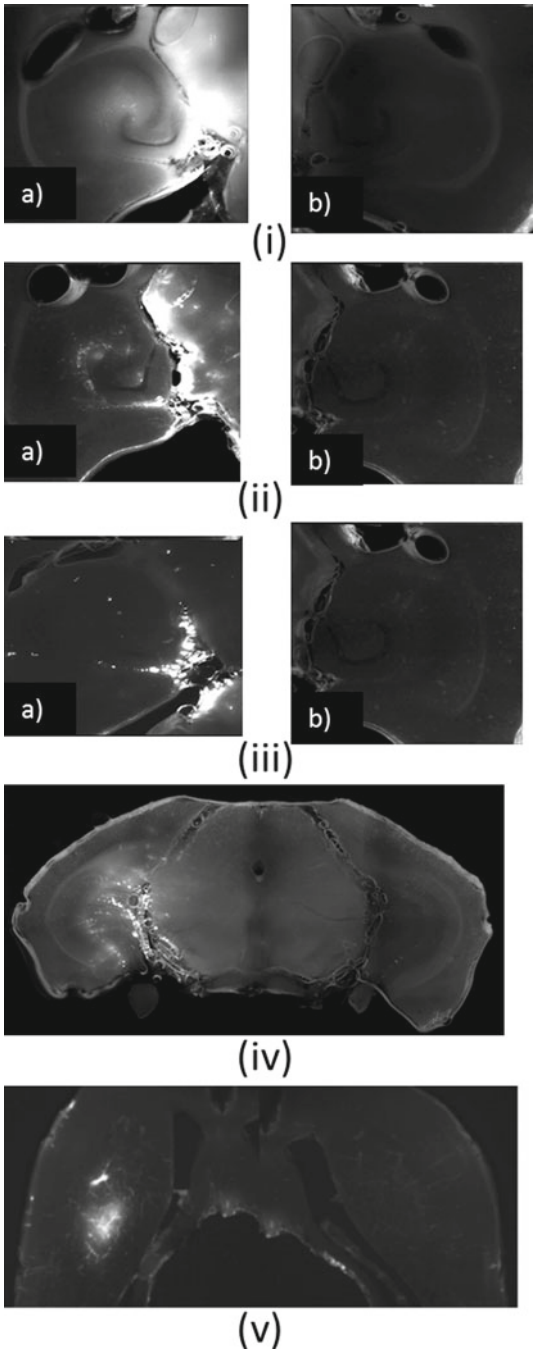

Fig. 20.5 *Study of the molecular size through the BBB opening using Dextrans or albumin and fluorescence imaging:* Horizontal slice of Dextran of molecular weight equal to (1) 3, (2) 70, and (3) 2,000 kDa on the (**a**) *left* (targeted) and (**b**) *right* (not targeted) hippocampus; (4) Coronal slice of the entire brain at 70 kDa Dextran showing the fluorescent *left* hippocampus (crescent-shaped); (5) Fluorescent albumin (67 kDa) permeated in the putamen through the opened BBB

20.1.11 Safety and Reversibility of BBB Opening

In order to determine the safety window of the FUS technique using histological and immunohistological techniques (Baseri et al. 2010), we sought to identify the safe operating parameters of ultrasound exposure for neurons, astrocytes, and endothelial cells (Fig. 20.6). Immunostaining studies to confirm these results have also been reported in neurons [65] and are ongoing in the other cases. In summary, BBB opening starts occurring at 0.3 MPa rarefactional pressure amplitude and beyond. At pressures under 0.6 MPa (Fig. 20.6a), no extravasation of red blood cells (RBC) or neuronal damage was observed in the regions of the hippocampus exhibiting the most pronounced BBB opening. Beyond 0.6 MPa (Fig. 20.6b), RBC extravasation was detected and beyond 0.9 MPa neuronal damage was observed. These preliminary findings suggest that there is overlap between the feasibility and safety windows within the pressure range of 0.3–0.6 MPa, i.e., the BBB can be opened throughout the entire hippocampus without endothelial or neuronal damage at those pressures (Fig. 20.6; Baseri et al. 2010). FUS-induced BBB opening was reported to close within 24 h under specific parameters in rabbits (Hynynen et al. 2001), mice (Howles et al. 2010; Samiotaki et al. 2012), and monkeys (Marquet et al. 2010, 2011;

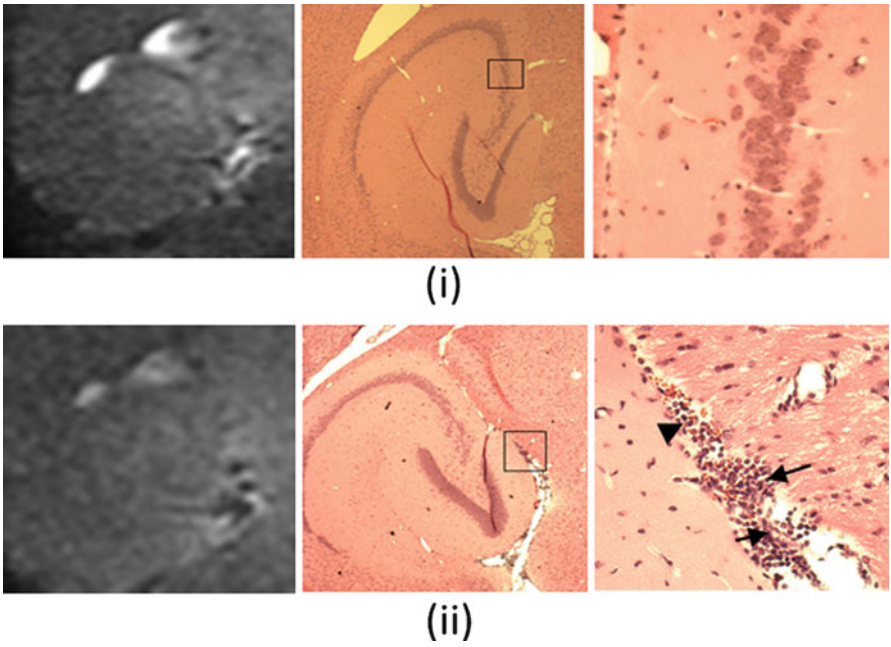

Fig. 20.6 Comparison between MRI (*left*) and histology (center (1×) and *right* (200× near the region of most enhanced BBB opening according to the MRI) after FUS-induced BBB opening on the *left* hippocampus at (**a**) 0.45 and (**b**) 0.75 MPa peak-rarefactional pressure. It shows that at lower pressures (**a**) the endothelial and neurons are intact (*red*), while at higher pressures (**b**) there is extravasation of red blood cells (indicated by *arrowhead*) and neuronal death (indicated by *arrow*). This indicates the safety window of the FUS technique in BBB opening

McDannold et al. 2012; Tung et al. 2011a, b). Figure 20.7 shows that BBB closure had occurred within the first 24 h after BBB opening.

Full assessment of the safety profile is more complex than the preliminary studies reported. Behavioral, cognitive, electrophysiological, and additional cell histology are warranted for maximal safety profile delineation. Although the preliminary studies by our group and others have identified that stable cavitation of the bubbles is sufficient to open the BBB (Fig. 20.8) and that histological sections indicate no damage (Fig. 20.6), both in vivo (fMRI, EEG, and PET as well as cognitive studies) and ex vivo immunostaining of glia, astrocytes, pericytes, and neurons still remain to be performed in order to fully characterize the safety profile of the technique.

20.1.12 Properties of BBB Opening

Dynamic contrast-enhanced (DCE) MRI has been performed before and after the intraperitoneal injection of gadodiamide over 60 min (Vlachos et al. 2010). The general kinetic model (GKM) is used to estimate the permeability in the entire brain (Vlachos et al. 2010). At 0.3 MPa and 4–5-μm bubbles, the permeability is found to

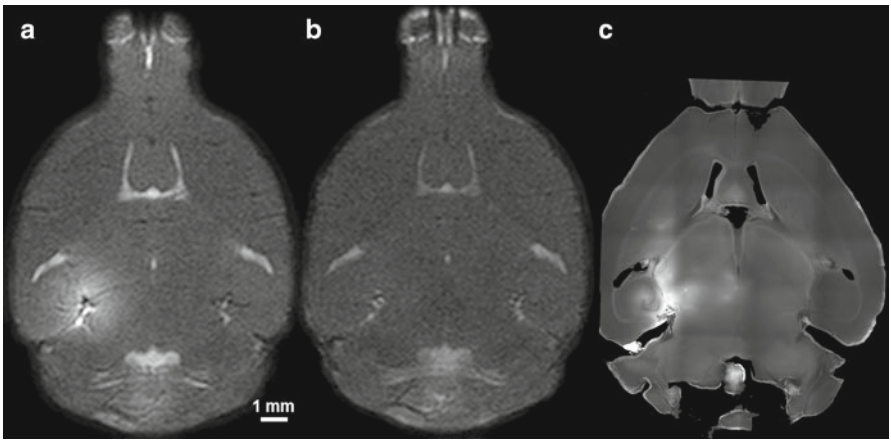

Fig. 20.7 T1 MRI images of (**a**) BBB opening, (**b**) BBB closing (24 h); and (**c**) fluorescence imaging with 3-kDa dextran of the *left* (sonicated) hippocampus

Fig. 20.8 MRI coronal and horizontal permeability images (first two images in first column in (i) and (ii)), coronal and horizontal T1-weighted images (first two images in second column in (i) and (ii)) of BBB opening in the *left* hippocampal formation (*right* one served as the control), H&E histology of both the *left* and *right* hippocampi (40×) (*last row* in (i) and (ii)) and cavitation spectrograms (*bottom row* in (iii) with corresponding T1 images on top) at 0.45 MPa ((i) and *right column* in (iii) and 0.30 MPa ((ii) and *left column* in (iii)). Note the harmonic peaks (*parallel lines*) in the spectrograms at 1.5, 3, 4.5 MHz, etc. at 0.3 MPa and the inertial cavitation (harmonics and broadband noise) on the spectrogram at 0.45 MPa. No structural damage was noted at either pressure or cavitation types in the 48 mice studied (Vlachos et al. 2011). The permeability maps show increase of a 100-fold in the area sonicated, i.e., the *left* hippocampal formation. The entorhinal cortex is designated using a *green arrow*

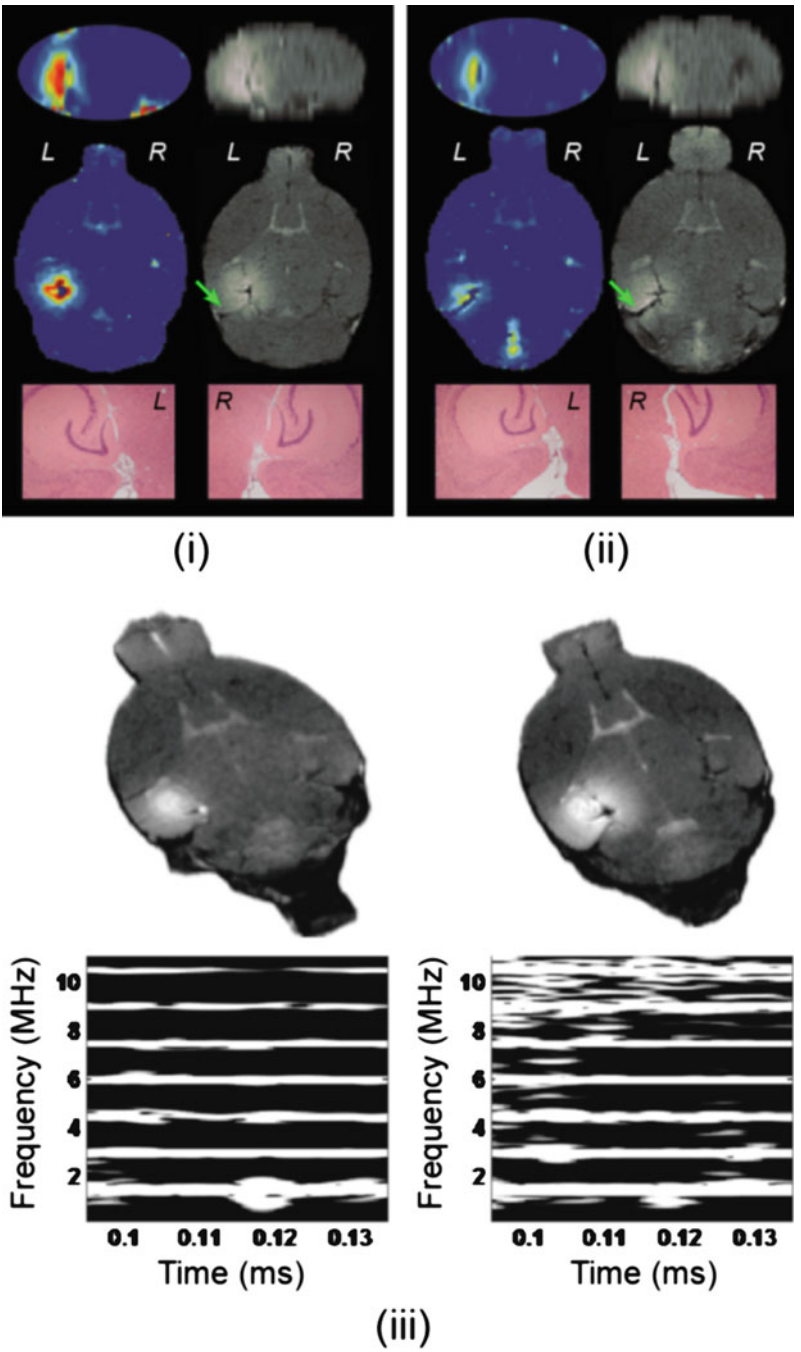

Fig. 20.8 (*see Caption on page 560*)

equal 0.02 ± 0.0123 min^{-1} and increase by at least 100 times in the region of BBB opening compared to the control side. Cavitation (Fig. 20.3) and permeability (Fig. 20.8) findings demonstrated that the inertial cavitation threshold is independent of the bubble size, while both the ICD and MR amplitude increased at larger bubble sizes, also indicating a correlation between the cavitation and permeability increase (Vlachos et al. 2010). The fact that the permeability increased with the pressure and microbubble size indicates that the BBB opening occurs at multiple sites within the capillary tree and that the BBB opening is larger with larger microbubbles, most likely due to the larger area of contact between the bubble and the capillary wall.

20.1.13 BBB Opening in Large Animals

A 3D finite-difference, time-difference simulation platform (Wave 3000, CyberLogic, New York, USA) simulation model (Fig. 20.9c; Deffieux and Konofagou 2010) was used to identify the optimal frequency for successful trans-skull propagation using CT scans (GE LightSpeed Ultrafast CT scanner; available in the department of radiology at) of ex vivo nonhuman primate and human skulls as inputs to model absorption and speed of sound maps. The targeted brain structures were extracted from publicly available 3D brain atlases registered with the skulls (Fig. 20.9a, b). The frequency of 500 kHz provided the best tradeoff in the human skull between phase aberrations due to transcranial propagation and standing wave effects due to multiple interfaces and longer wavelengths while the frequency of 800 kHz was most suitable in the case of the non-human primate skull. A fast periodic linear chirp method was developed and found capable of reducing the standing wave effects. The simple, single-element system that we have been using in mice was concluded to be feasible for BBB opening in primates and humans and the size of the focal spot dimensions fit the hippocampal sizes when targeting through the dorsal part of the skull (Fig. 20.10).

20.1.14 Therapeutic Delivery Through FUS-Induced Blood–Brain Barrier Opening

Neurotrophic delivery to the brain is thought to be essential in reversing neuronal degeneration processes but so far the application of growth factors to the CNS has been hindered by the BBB. In a recent study by our group, not only was it shown that brain-derived neurotrophic factor (BDNF) and neurturin (NTN) as well as AAV (Wang et al. 2013) can cross the ultrasound-induced BBB opening but also that it can trigger signaling pathways in the pyramidal neurons of mice in vivo from the membrane to the nucleus (Fig. 20.11) (Baseri et al. 2012). This opens entirely new avenues in brain drug delivery where FUS in conjunction with microbubbles can generate downstream effects at the cellular and molecular level and thus increase the drug's efficacy and potency in controlling or reversing disease.

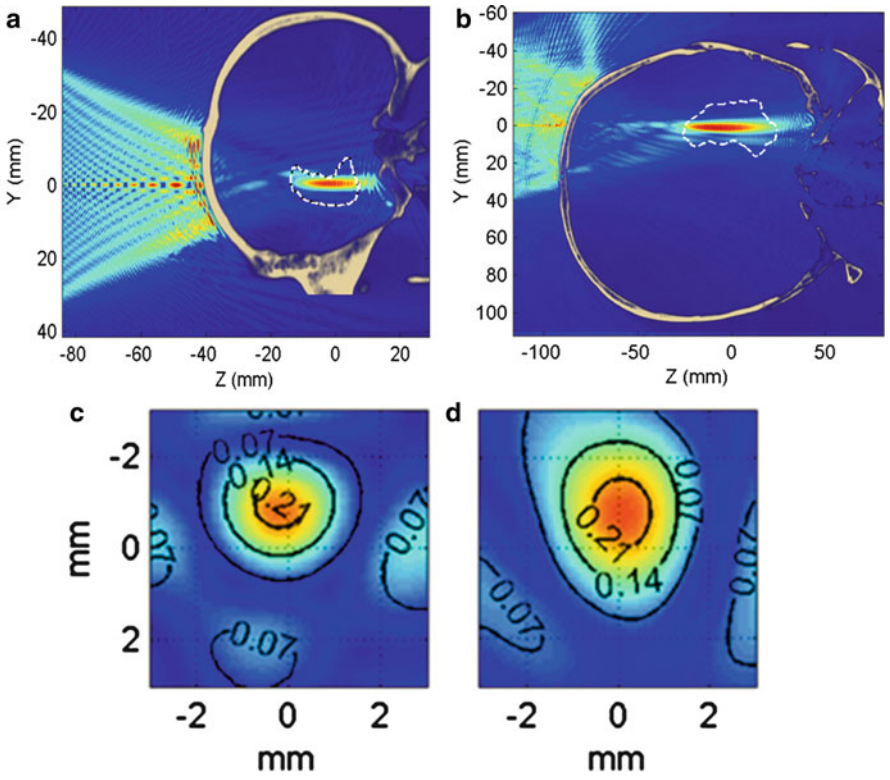

Fig. 20.9 Theoretical simulations with experimental validation for predicting the area of BBB opening (in *red*) relative to the hippocampus (*white dashed* contour through the skull) of (**a**) non-human primates at 800 kHz and (**b**) human at 500 kHz. In both cases, there is formation of a uniform focal spot with the largest dimension along the longest dimension of the hippocampus in both cases. (**c**) Experimental validation of a uniform focal spot (transverse view) through the ex vivo primate skull of the (**d**) simulated focal spot at 800 kHz (Deffieux and Konofagou 2010)

20.2 Discussion

Despite the fact that FUS is currently the only technique that can open the BBB locally and noninvasively (Table 20.1), several key aspects of the technique remain incompletely understood. Although the presence of microbubbles allows for a reduction in the necessary acoustic pressure for BBB opening, it also increases the probability of disrupting the microbubble through inertial cavitation. Not only can the resulting effects open the tight junctions, but they may also induce irreversible damage to the blood vessels and surrounding cells. While studies by most other groups have focused more globally, inducing BBB opening in arbitrary, multiple locations throughout the whole brain, studies from our group have focused on targeting a specific brain region such as the hippocampus and evaluating its properties locally. Furthermore, multielement phased arrays (with up to 1,024 elements) that

permit phase aberration correction have been proposed in order to increase flexibility of the location targeted, mainly used for tumor ablation with minimal aberration. However, these arrays are highly complex and difficult to manufacture and cumbersome in handling and positioning around a subject due to their typically bulky size and weight. Finally, the delivery of many large agents using FUS and microbubbles has been demonstrated in previous studies by our group and others. However,

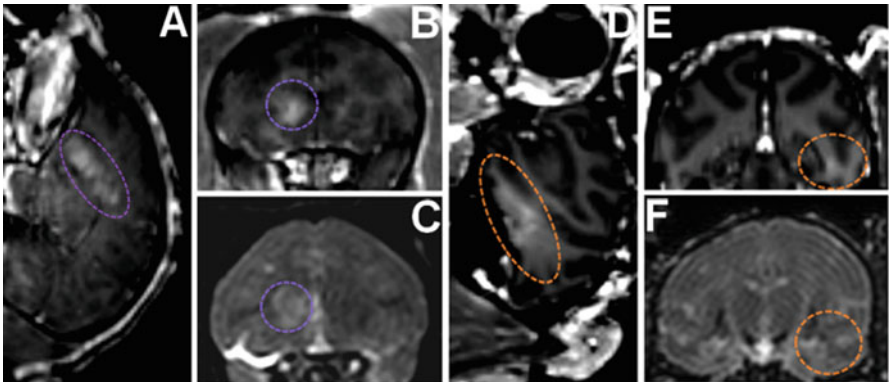

Fig. 20.10 In vivo *BBB opening in monkeys:* (**A**–**C**) BBB opening experiment targeting the caudate using custom made microbubbles and applying 0.6 MPa (*purple dashed* line shows region of interest). (**D**–**F**) BBB opening experiment targeting hippocampus using Definity® microbubbles and applying 0.6 MPa (*orange dashed line* shows region of interest). (**A**–**E**) 3D Spoiled Gradient-Echo (SPGR) T1-weighted sequence was applied after intravenous (IV) injection of gadodiamide 1 h after sonication. (**A**, **D**) Sagittal slices at the region of interest. (**B**, **E**) Corresponding coronal slices. (**C**, **F**) 3D T2-weighted sequence, an edema was visible using custom made microbubbles while no damage was detected using Definity® microbubbles at the highest pressure used

Fig. 20.11 (**a**) Fluorescent image of a 100-μm frozen brain section from a mouse that was sacrificed 20 min after sonication. The sonicated hippocampus (*left*) shows much higher fluorescent intensity than the un-sonicated hippocampus (*right*), depicting blood–brain barrier opening and the extravasation of fluorescent-tagged (Alexa Fluor 594) BDNF in the sonicated region; (**b**) a 5-μm frozen section from the same mouse was immunohistochemically stained using a primary antibody against phosphorylated MAPK (pMAPK). Consistent with the fluorescent image in (**a**), the intensity of DAB staining is much greater in the *left* sonicated hippocampus compared to the *right* control; the *black box* shows the enlarged area in (**c**), where immunoreactivity to pMAPK is shown in mossy fiber terminals (*arrowhead*), suprapyramidal CA3 dendrites (*black star*), and the axons of the Schaffer collateral system (*hollow star*); (**d**) immunohistochemical staining of a 5-μm frozen section from a mouse that was sacrificed 3 min after sonication; the same primary antibody against pMAPK was used. No difference in DAB intensity is observed between the sonicated and the control hippocampus; (**e**) Negative control for the same mouse in (**a**); no primary antibody (against pMAPK) was added to this 5-μm frozen section during the staining procedure. All magnifications are 40× and scale bars are 500 μm except for (**c**), which is 100× and 200 μm, respectively. In (**f**), immunohistology stain intensity analysis shows percentage change between the *left* (FUS) and the *right* (no FUS) sides of the mice brains. A significant difference ($p < 0.05$, $N = 3$; depicted by *asterisks*) was found between the BDNF administered animal group and the control (no BDNF) animal group for the TrkB, MAPK, and CREB antibodies. Bars represent mean ± standard deviation

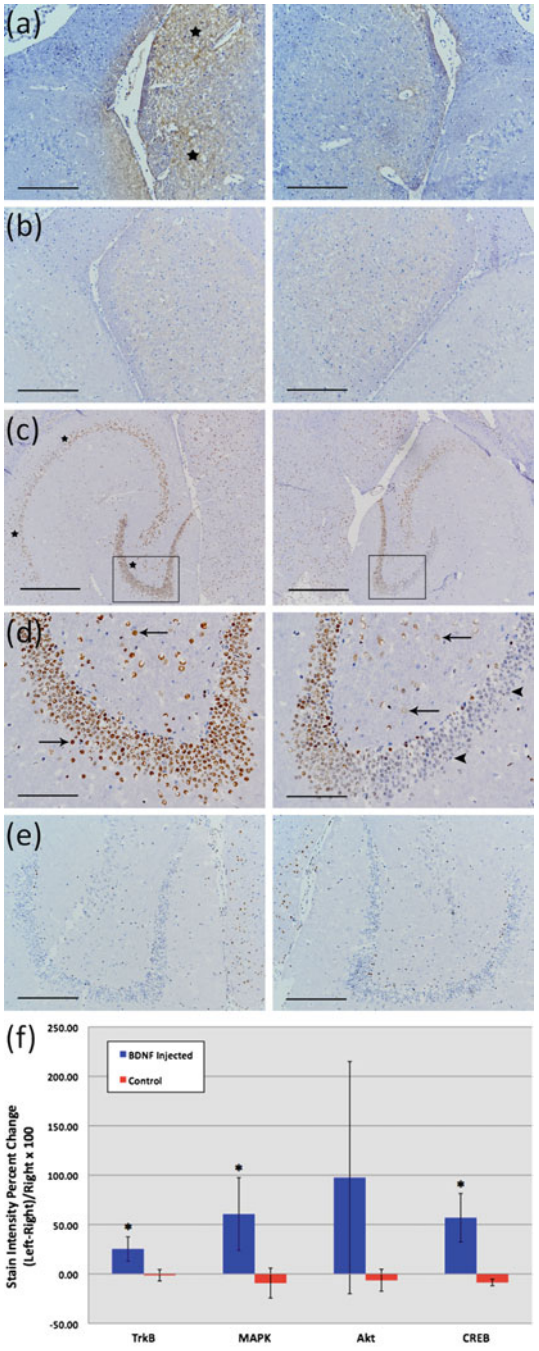

Fig. 20.11 (*see Caption on page 564*)

despite the promise shown by the delivery of such a variety of compounds, several questions on the effectiveness of the delivery remain. Our group has recently shown that a molecular cascade for neurogenesis is triggered by neurotrophic factors that penetrate the FUS-induced BBB opening and into the hippocampal neurons.

Given the established feasibility of FUS in BBB opening and its urgent need in brain drug delivery, the main findings summarized in this chapter are as follows:

1. The BBB can be reproducibly opened in a specific subcortical region associated with neurodegenerative disease, e.g., the hippocampus.
2. The BBB opening can be induced without requiring craniotomy or MRI for targeting in mice and monkeys.
3. A single-element transducer is sufficient to induce trans-skull wave propagation through both mouse and primate skulls ex vivo and can lead to a well-formed focal spot for BBB opening in both cases but at distinct ultrasound frequencies. More importantly, unlike tumor ablation using multielement arrays, lower pressures, and anatomy-specific (not tumor-specific) targeting are required, potentially rendering sonication with a single-element transducer sufficient.
4. An optimization study has been performed that has identified the pulse length and peak-rarefactional pressure safety range; H&E studies have shown that there is no structural damage associated with BBB opening using these optimized parameters.
5. Preliminary delivery of molecules on the order of 0.5–70 kDa, including dextrans and growth factors (BDNF), has been demonstrated. Our findings suggest FUS-induced BBB opening results in BDNF accessibility to neurons and the successful triggering of brain-specific signaling pathways.
6. Intraperitoneal (IP)-administered gadolinium allowed for spatiotemporal analysis of the BBB opening with MRI. A 100-fold increase in BBB permeability has been shown in the FUS-targeted hippocampus, as assessed in vivo by MRI.

20.3 Conclusion

FUS in conjunction with microbubbles has been shown to effectively and reproducibly open the BBB transcranially in vivo with its recovery occurring within the first 24 h. The permeability of the FUS-opened BBB has been shown to increase by at least two orders of magnitude, indicating facilitation of drug delivery through FUS. Molecules spanning a wide range of sizes appear capable of traversing the opened BBB without any associated structural damage and in some cases triggering specific neuronal pathways. A dependence of the BBB permeability on the pressure and the microbubble size indicates that multiple sites of BBB opening within the ultrasound beam occur simultaneously, while the microbubble size significantly affects the volume of BBB opening. Finally, it should be possible to utilize new pulse sequences for transcranial BBB opening in larger animals such as nonhuman primates and humans, opening up the technique to future clinical applications.

20.4 Points for Discussion

- Why is it necessary to open the BBB to treat CNS diseases?
- What are the main advantages of FUS in brain drug delivery?
- Which molecules would be most efficient to use with the ultrasound technology?
- Which diseases may benefit by such a treatment method?
- What are the main challenges that remain in its clinical translation?

Acknowledgements The work shown here was performed by Yao-Sheng Tung, James Choi, Thomas Deffieux, Babak Baseri, Fabrice Marquet, and Fotios Vlachos, previously with the Ultrasound and Elasticity Imaging Laboratory of the Biomedical Engineering Department at Columbia. Collaborators on the microbubble studies were Jameel Feshitan and Mark Borden (currently at the University of Colorado-Boulder) and on the non-human primate studies were Tobias Techert and Vincent Ferrera (Columbia University). The research was supported by NIH R01 EB009041, NIH R21 EY018505, NSF CAREER 064471, the Kinetics Foundation and the Kavli Institute.

References

Abbott NJ, Ronnback L, Hansson E (2006) Astrocyte-endothelial interactions at the blood–brain barrier. Nat Rev Neurosci 7:41–53

Arvanitis CD, Livingstone MS, Vykhodtseva N, McDannold N (2012) Controlled ultrasound-induced blood–brain barrier disruption using passive acoustic emissions monitoring. PloS One 7(9):e45783

Bakay L, Ballantine HT Jr, Hueter TF, Sosa D (1956) Ultrasonically produced changes in the blood–brain barrier. AMA Arch Neurol Psychiatry 76:457–467

Ballantine HT Jr, Bell E, Manlapaz J (1960) Progress and problems in the neurological applications of focused ultrasound. J Neurosurg 17:858–876

Baseri B, Choi JJ, Tung YS, Konofagou EE (2010) Safety assessment of blood–brain barrier opening using focused ultrasound and definity microbubbles: a short-term study. Ultrasound Med Biol 36(9):1445–1459

Baseri B, Choi JJ, Deffieux T, Samiotaki G, Tung YS, Olumolade O, Small SA, Morrison B, Konofagou EE (2012) Activation of signaling pathways following localized delivery of systemically administered neurotrophic factors across the blood–brain barrier using focused ultrasound and microbubbles. Phys Med Biol 57(7):N65–N81

Blasberg RG, Patlak C, Fenstermacher JD (1975) Intrathecal chemotherapy: brain tissue profiles after ventriculocisternal perfusion. J Pharmacol Exp Ther 195:73–83

Borden M, Kruse D, Caskey C et al (2005) Influence of lipid shell physicochemical properties on ultrasound-induced microbubble destruction. IEEE Trans Ultrason Ferroelect Freq Contr 52:1992–2002

Burgess A, Ayala-Grosso CA, Ganguly M, Jordão JF, Aubert I, Hynynen K (2011) Targeted delivery of neural stem cells to the brain using MRI-guided focused ultrasound to disrupt the blood–brain barrier. PLoS One 6(11):e27877

Chen S, Kroll MH, Shohet RV, Frenkel P, Mayer SA, Grayburn PA (2002) Bioeffects of myocardial contrast microbubble destruction by echocardiography. Echocardiagraphy 19:495–500

Choi JJ, Pernot M, Small SA, Konofagou EE (2005) Feasibility of transcranial, localized drug-delivery in the brain of Alzheimer's-model mice using focused ultrasound. IEEE Inter Ultrason Symp, Boston, MA, 988–991

Choi JJ, Pernot M, Small S, Konofagou EE (2006) Noninvasive blood–brain barrier opening in live mice. International symposium on therapeutic ultrasound. AIP conference proceedings, vol 829:271–275

Choi JJ, Small SA, Konofagou EE (2006) Optimization of blood–brain barrier opening in mice using focused ultrasound, In: IEEE proceedings of the symposium in ultrasonics, ferroelectrics and frequency control, pp 540–543

Choi JJ, Pernot M, Small SA, Konofagou EE (2007a) Noninvasive, transcranial and localized opening of the blood–brain barrier using focused ultrasound in mice. Ultrasound Med Biol 33:95–104

Choi JJ, Pernot M, Brown TR, Small SA, Konofagou EE (2007b) Spatio-temporal analysis of molecular delivery through the blood–brain barrier using focused ultrasound. Phys Med Biol 52:5509–5530

Choi JJ, Wang S, Morrison B III, Konofagou EE (2007) Focused ultrasound-induced molecular delivery through the blood-brain barrier. In: IEEE proceedings of the symposium in ultrasonics, ferroelectrics and frequency control, New York, NY, pp 1192–1195

Choi JJ, Wang S, Brown TR, Small SA, Duff KE, Konofagou EE (2008) Noninvasive and transient blood–brain barrier opening in the hippocampus of Alzheimer's double transgenic mice using focused ultrasound. Ultrason Imaging 30:189–200

Choi JJ, Feshitan JA, Wang S, Tung Y-S, Baseri B, Borden MA, Konofagou EE (2009) The dependence of the ultrasound-induced blood–brain barrier opening characteristics on microbubble size in vivo. In: Emad SE (ed) 8th international symposium on therapeutic ultrasound. AIP, Minneapolis, MN, USA, pp 58–62

Choi J, Selert K, Vlachos F, Wong A, Konofagou EE (2011a) Noninvasive and localized neuronal delivery using short ultrasonic pulses and microbubbles. Proc Natl Acad Sci U S A 108(40):16539–16544

Choi J, Selert K, Gao Z, Samiotaki G, Baseri B, Konofagou EE (2011b) Noninvasive and localized blood-brain barrier disruption using focused ultrasound can be achieved at short pulse lengths and low pulse repetition frequencies. Journal of Cerebral Flow and Metabolism, 31(2), 725–737

Christensen DA (1988) Ultrasonic bioinstrumentation. Wiley, New York

Christiansen J, French BA, Klibanov AL, Kaul S, Lindner JR (2003) Targeted tissue transfection with ultrasound destruction of plasmid-bearing cationic microbubbles. Ultrasound Med Biol 29:1759–1767

Chomas JE, Dayton P, May D, Ferrara K (2001) Threshold of fragmentation for ultrasonic contrast agents. J Biomed Opt 6:141–150

Deffieux T, Konofagou E (2010) Numerical study and experimental validation of a simple transcranial focused ultrasound system applied to blood–brain barrier opening. IEEE Trans Ultrason Ferroelectr Freq Control 57(12):2637–2653

Farny CH, Holt RG, Roy RA (2009) Temporal and spatial detection of HIFU-induced inertial and hot-vapor cavitation with a diagnostic ultrasound system. Ultrasound Med Biol 35:603–615

Feshitan JA, Chen CC, Kwan JJ, Borden MA (2009) Microbubble size isolation by differential centrifugation. J Colloid Interface Sci 329:316–324

Fischer H, Gottschlich R, Seelig A (1998) Blood–brain barrier permeation: molecular parameters governing passive diffusion. J Membr Biol 165:201–211

Fung LK, Shin M, Tyler B, Brem H, Saltzman WM (1996) Chemotherapeutic drugs released from polymers: distribution of 1,3-bis(2-chloroethyl)-1-nitrosourea in the rat brain. Pharmaceut Res 13:671–682

Ghose AK, Viswanadhan VN, Wendoloski JJ (1999) A knowledge-based approach in designing combinatorial or medicinal chemistry libraries for drug discovery. 1. A qualitative and quantitative characterization of known drug databases. J Comb Chem 1:55–68

Howles GP, Bing KF, Qi Y, Rosenzweig SJ, Nightingale KR, Johnson GA (2010) Contrast-enhanced in vivo magnetic resonance microscopy of the mouse brain enabled by noninvasive opening of the blood–brain barrier with ultrasound. Magn Reson Med 64(4):995–1004

Hynynen K, McDannold N, Vykhodtseva N, Jolesz FA (2001) Noninvasive MR imaging-guided focal opening of the blood–brain barrier in rabbits. Radiology 220:640–646

Hynynen K, McDannold N, Vykhodtseva N, Jolesz FA (2003) Non-invasive opening of BBB by focused ultrasound. Acta Neurochir Suppl 86:555–558

Hynynen K, McDannold N, Sheikov NA, Jolesz FA, Vykhodtseva N (2005) Local and reversible blood–brain barrier disruption by noninvasive focused ultrasound at frequencies suitable for trans-skull sonications. Neuroimage 24:12–20

Hynynen K, McDannold N, Vykhodtseva N, Raymond S, Weissleder R, Jolesz FA, Sheikov N (2006) Focal disruption of the blood–brain barrier due to 260-kHz ultrasound bursts: a method for molecular imaging and targeted drug delivery. J Neurosurg 105:445–454

Iadecola C (2004) Neurovascular regulation in the normal brain and in Alzheimer's disease. Nat Rev Neurosci 5:347–360

Kaps M, Seidel G, Algermissen C, Gerriets T, Broillet A (2001) Pharmacokinetics of echocontrast agent infusion in a dog model. J Neuroimaging 11:298–302

Kaufmann BA, Wei K, Lindner JR (2007) Contrast echocardiography. Curr Probl Cardiol 32:51–96

Kinoshita M, McDannold N, Jolesz FA, Hynynen K (2006) Noninvasive localized delivery of Herceptin to the mouse brain by MRI-guided focused ultrasound-induced blood–brain barrier disruption. Proc Natl Acad Sci U S A 103:11719–11723

Konofagou EE, Choi J, Baseri B, Lee A (2009) Characterization and optimization of trans-blood-brain barrier diffusion in vivo. In: Ebbini SE (ed) 8th international symposium on therapeutic ultrasound. AIP, Minneapolis, MN, USA, pp 418–422

Konofagou EE, Choi JJ (2008) Ultrasound-induced treatment of neurodegenerative diseases across the blood–brain barrier. In: Ahmed A-J, Alizad A (eds) Biomedical applications of vibration and acoustics in therapy, bioeffects and modeling. ASME Press, New York, NY, pp 63–80

Leighton RG (1997) The acoustic bubble. Academic, London, UK

Li P, Armstrong WF, Miller DL (2004) Impact of myocardial contrast echocardiography on vascular permeability: comparison of three different contrast agents. Ultrasound Med Biol 30:83–91

Li P, Cao LQ, Dou CY, Armstrong WF, Miller D (2003) Impact of myocardial contrast echocardiography on vascular permeability: an in vivo dose response study of delivery mode, pressure amplitude and contrast dose. Ultrasound Med Biol 29:1341–1349

Lipinski CA (2000) Drug-like properties and the causes of poor solubility and poor permeability. J Pharmacol Toxicol Methods 44:235–249

Liu GYP, Tan K et al (2005) Impact of microbubble enhanced ultrasound on blood–brain barrier permeability: an in vivo dose response study of ultrasound intensity and contrast dose. Circulation 112:U602–U605

Marquet F, Tung Y-S, Konofagou EE (2010) Feasibility study of a clinical blood–brain opening ultrasound system. Nano Life 1(3 & 4):309–322

Marquet F, Tung YS, Teichert T, Ferrera VP, Konofagou EE (2011) Noninvasive, transient and selective blood–brain barrier opening in non-human primates in vivo. PLoS One 6(7):e22598

McDannold N, Vykhodtseva N, Jolesz FA, Hynynen K (2004) MRI investigation of the threshold for thermally induced blood–brain barrier disruption and brain tissue damage in the rabbit brain. Magn Reson Med 51:913–923

McDannold N, Vykhodtseva N, Raymond S, Jolesz FA, Hynynen K (2005) MRI-guided targeted blood–brain barrier disruption with focused ultrasound: histological findings in rabbits. Ultrasound Med Biol 31:1527–1537

McDannold N, Vykhodtseva N, Hynynen K (2006) Targeted disruption of the blood–brain barrier with focused ultrasound: association with cavitation activity. Phys Med Biol 51:793–807

McDannold N, Arvanitis CD, Vykhodtseva N, Livingstone MS (2012) Temporary disruption of the blood–brain barrier by use of ultrasound and microbubbles: safety and efficacy evaluation in rhesus macaques. Cancer Res 72(14):3652–632012

Mesiwala AH, Farrell L, Wenzel HJ, Silbergeld DL, Crum LA, Winn HR, Mourad PD (2002) High-intensity focused ultrasound selectively disrupts the blood–brain barrier in vivo. Ultrasound Med Biol 28:389–400

Miller DL (2007) Overview of experimental studies of biological effects of medical ultrasound caused by gas body activation and inertial cavitation. Progr Biophys Mol Biol 93:314–330

Miller D, Li P, Dou C, Gordon D, Edwards CA, Armstrong WF (2005) Influence of contrast agent dose and ultrasound exposure on cardiomyocyte injury induced by myocardial contrast echocardiography in rats. Radiology 237:137–143

Neppiras EA (1980) Acoustic cavitation. Phys Rep 61:159–251

Patrick JT, Nolting MN, Goss SA, Dines KA, Clendenon JL, Rea MA, Heimburger RF (1990) Ultrasound and the blood–brain barrier. Adv Exp Med Biol 267:369–381

Pardridge WM (2005) The blood–brain barrier: bottleneck in brain drug development. NeuroRx 2:3–14

Pardridge WM (2006) Molecular trojan horses for blood–brain barrier drug delivery. Discov Med 6:139–143

Pardridge WM (2007) Drug targeting to the brain. Pharm Res 24:1733–1744

Raymond SB, Treat LH, Dewey JD, McDannold NJ, Hynynen K, Bacskai BJ (2008) Ultrasound enhanced delivery of molecular imaging and therapeutic agents in Alzheimer's disease mouse models. PLoS One 3(5):e2175

Samiotaki G, Vlachos F, Tung YS, Konofagou EE (2012) A quantitative pressure and microbubble-size dependence study of focused ultrasound-induced blood–brain barrier opening reversibility in vivo using MRI. Magn Reson Med 67(3):769–777

Sheikov N, McDannold N, Vykhodtseva N, Jolesz F, Hynynen K (2004) Cellular mechanisms of the blood–brain barrier opening induced by ultrasound in presence of microbubbles. Ultrasound Med Biol 30:979–989

Sheikov N, McDannold N, Jolesz F, Zhang YZ, Tam K, Hynynen K (2006) Brain arterioles show more active vesicular transport of blood-borne tracer molecules than capillaries and venules after focused ultrasound-evoked opening of the blood–brain barrier. Ultrasound Med Biol 32:1399–1409

Sheikov N, McDannold N, Sharma S, Hynynen K (2008) Effect of focused ultrasound applied with an ultrasound contrast agent on the tight junctional integrity of the brain microvascular endothelium. Ultrasound Med Biol 34(7):1093–1104

Stewart PA, Tuor UI (1994) Blood-eye barriers in the rat: correlation of ultrastructure with function. J Comp Neurol 340:566–576

Treat LH, McDannold N, Vykhodtseva N, Zhang Y, Tam K, Hynynen K (2007) Targeted delivery of doxorubicin to the rat brain at therapeutic levels using MRI-guided focused ultrasound. Int J Cancer 121:901–907

Tung YS, Vlachos F, Choi JJ, Deffieux T, Selert K, Konofagou EE (2010) In vivo noninvasive cavitation threshold detection during blood–brain barrier opening using FUS and Definity. Phys Med Biol 55(20):6141–6155

Tung YS, Marquet F, Teichert T, Ferrera V, Konofagou EE (2011a) Feasibility of noninvasive cavitation-guided blood–brain barrier opening using focused ultrasound and microbubbles in nonhuman primates. Appl Phys Lett 98(16):163704

Tung YS, Vlachos F, Feshitan JA, Borden MA, Konofagou EE (2011b) The mechanism of interaction between focused ultrasound and microbubbles in blood–brain barrier opening in mice. J Acoust Soc Am 130(5):3059–3067

Vlachos F, Tung Y, Konofagou EE (2010) Permeability assessment of the focused ultrasound-induced blood–brain barrier opening using dynamic contrast-enhanced MRI. Phys Med Biol 55:5451–5466

Vykhodtseva NI, Hynynen K, Damianou C (1995) Histologic effects of high intensity pulsed ultrasound exposure with subharmonic emission in rabbit brain in vivo. Ultrasound Med Biol 21:969–979

Wang S, Olumolade O, Osting S, Burger C, Konofagou EE (2013) Focused ultrasound induced blood-brain barrier opening in macromolecule delivery, 13th International Symposium on Therapeutic Ultrasound, Shanghai, China

Yang FY, Fu WM, Yang RS, Liou HC, Kang KH, Lin WL (2007) Quantitative evaluation of focused ultrasound with a contrast agent on blood–brain barrier disruption. Ultrasound Med Biol 33:1421–1427

Part V
Brain Drug Delivery in Disease Conditions

Chapter 21
Disease Influence on BBB Transport in Inflammatory Disorders

Geert J. Schenk, Gijs Kooij, Arie Reijerkerk, and Helga de Vries

Abstract During diseases of the central nervous system (CNS), such as Alzheimer's, Parkinson's, epilepsy, stroke and multiple sclerosis (MS), the protective function of the blood–brain barrier (BBB) is significantly impaired. The inflammatory response that is frequently associated with such brain diseases may underlie the loss of the integrity and function of the BBB. Consequentially, the delivery and disposition of drugs to the brain will be altered and may influence the treatment efficiency of CNS diseases. Altered BBB transport of drugs into the CNS during diseases may be the result of changes in both specific transport and non-specific transport pathways. Potential alterations in transport routes like adsorptive-mediated endocytosis and receptor-mediated endocytosis may affect drug delivery to the brain. As such, drugs that normally are unable to traverse the BBB may reach their target in the diseased brain due to increased permeability. On the contrary, the delivery of (targeted) drugs could be hampered during inflammatory conditions due to disturbed transport mechanisms. Therefore, the inventory of the neuro-inflammatory status of the neurovasculature (or recovery thereof) is of utmost importance in choosing and designing an adequate drug targeting strategy under disease conditions. Within this chapter we discuss how the function of the BBB can be affected during disease and how this may influence the delivery of drugs into the diseased CNS.

G.J. Schenk, Ph.D.
Department of Anatomy and Neurosciences, VU university medical center,
Van der Boechorststraat 7, Amsterdam 1081 BT, The Netherlands

G. Kooij, Ph.D. • A. Reijerkerk, Ph.D. • H. de Vries, Ph.D. (✉)
Department of Molecular Cell Biology and Immunology, VU university medical center,
Van der Boechorststraat 7, Amsterdam 1081 BT, The Netherlands
e-mail: he.devries@vumc.nl

M. Hammarlund-Udenaes et al. (eds.), *Drug Delivery to the Brain*, AAPS Advances in the Pharmaceutical Sciences Series 10, DOI 10.1007/978-1-4614-9105-7_21,

21.1 Introduction

The blood–brain barrier (BBB) is a complex cellular network consisting of brain endothelial cells lining the cerebral microvasculature which form a continuous cellular barrier between the central nervous system (CNS) and the bloodstream. The BBB plays a crucial role in maintaining brain homeostasis, which is necessary for the stability and activity of nerve cells (Abbott 2002; Abbott et al. 2006). The BBB is also the "firewall" that prevents the entry of toxic compounds and immune cells into the CNS (Quan 2006). The functionality of the BBB is achieved through the interactions of cells comprising the BBB: these include not only endothelial cells but also astrocytes, pericytes and neighbouring CNS cells (Hawkins and Davis 2005).

A number of specific transport and enzyme systems are in place at the BBB which regulate molecular traffic across the barrier (Abbott et al. 2006; Abbott and Romero 1996). While the BBB maintains brain homeostasis, inflammation and immune-related events are amongst the best described processes that cause disruption of the BBB and are associated with CNS disorders such as Alzheimer's disease (in particular capillary cerebral amyloid angiopathy (capCAA)), Parkinson's disease, epilepsy, stroke, HIV/neuroAIDS, traumatic brain injury and MS (Erickson et al. 2012; Boado and Pardridge 2011; Rip et al. 2009; DiNapoli et al. 2008; Friedman and Dingledine 2011). The inflammatory response is a process that is common to all of the above-mentioned brain diseases and is of influence on normal BBB function. Consequentially, drug delivery to the brain will be altered and disposition of drugs in the brain during different disease states may influence the treatment efficiency of CNS diseases. Altered BBB function during disease may be mediated through changes in paracellular transport and transcellular transport routes. This potentially enhances or reduces the efficacy of treatment for CNS disorders. As such, drugs that normally are unable to traverse the BBB may reach their target in the diseased brain due to increased permeability. Alternatively, drugs that are normally able to pass the BBB may be more actively extruded through elevated ATP-binding cassette (ABC)-transporter function or because of a reduction in receptor or transporter expression on the luminal side of the brain endothelium. Therefore, the state of neuro-inflammation and its reinforcing or inhibiting effects on various BBB transport routes should not be neglected in choosing and designing an adequate drug targeting strategy for such disorders.

21.2 Current Status

21.2.1 CNS Disorders with an Inflammatory Component and Their Treatment

Brain homeostasis is controlled by the BBB. Maintenance of a tightly regulated biochemical and immunological microenvironment is a prerequisite for proper CNS function and changes in its delicate balance has been associated with inflammation

in several CNS pathologies (Fung et al. 2012; Zlokovic 2008, 2010). Here, we will briefly mention Parkinson's disease (PD), Alzheimer's disease (AD), epilepsy and stroke and focus in more detail on multiple sclerosis (MS).

21.2.1.1 Parkinson's Disease

Parkinson's disease (PD) is known for the degeneration of dopaminergic neurons in the substantia nigra pars compacta causing characteristic movement impairments. In general, PD treatment includes a combination of L-DOPA[(-)-3-(3,4-dihydroxyphenyl)-L-arginine] and carbidopa [(2S)-3-(3,4-dihydroxphenyl)-2-hydrazine-2-methylpropanoic acid], which alleviates the PD movement phenotype by increasing CNS dopamine levels. L-DOPA is able to cross the BBB via the large neutral amino acid transporter and is converted to dopamine in the brain. Peripheral dopamine cannot pass the BBB, therefore combination therapy with carbidopa, a peripheral DOPA decarboxylase inhibitor, is used to increase L-DOPA bioavailability in the brain. Luminal efflux pumps, i.e. P-glycoprotein (P-gp, an ABC transporter), limit the bioavailability associated with oral treatment (Hawkins and Davis 2005; Bartels et al. 2008; Kortekaas et al. 2005). An important cytokine that may link inflammation and PD is tumour necrosis factor α (TNF-α), since TNF-α is known to mediate neurotoxicity at the level of the substantia nigra, thus providing a way by which this cytokine may promote Parkinson's disease (Qin et al. 2007; Erickson et al. 2012). In fact levels of several pro-inflammatory cytokines are affected in PD patient's brains, including IL-8, IFN-γ, IL-1β and TNF-α (Reale et al. 2009) and accumulating evidence suggests that neuro-inflammation plays both neuro-protective and neurotoxic role in PD (Chung et al. 2010). Better understanding of the complex mechanisms underlying neuro-inflammation may provide clues to the development of interventional therapeutic strategies for PD patients.

21.2.1.2 Alzheimer's Disease

The neuropathological changes associated with Alzheimer's disease (AD) are well characterized and consist of cortical atrophy, neurofibrillary tangles and neuritic plaques (Bell and Zlokovic 2009). Diminished cognition in AD, associated with the loss of cholinergic input, is partly a consequence of these pathological phenomena. The acetylcholine receptor plays a pivotal role in the cholinergic system and its expression is affected during CNS diseases. Reduced expression of the acetylcholine receptor has been found not only in patients with Alzheimer's disease, but an important role of the receptor has also been described in epilepsy and MS (Herholz et al. 2008; Kooi et al. 2011). Similar to PD treatment, current AD therapy aims to replace depleted neurotransmitters to treat symptoms. Donepezil, an acetylcholinesterase inhibitor, improves cognition in AD patients (Brousseau et al. 2007) by enhancing acetylcholine bioavailability. Donepezil crosses the BBB through the organic cation transporter (Kim et al. 2010), although P-gp, limits therapeutic

concentrations of acetylcholinesterase inhibitors in the brain (Ishiwata et al. 2007). An important mechanism by which inflammation contributes to AD is by reducing the ability of the BBB to remove amyloid-β from the brain. Amyloid-β accumulation in the brain is associated with AD pathology (Hardy and Selkoe 2002). Low-density lipoprotein receptor-related protein-1 (LRP-1) is highly expressed in the cerebellum, cortex, hippocampus and brain stem (de Boer and Gaillard 2007; Lillis et al. 2008). At the capillary endothelial cells of the BBB, it functions as an efflux transporter for amyloid-β at the abluminal side (Deane et al. 2004; Sagare et al. 2007). LRP-1 is down-regulated at the BBB in AD, causing decreased efflux of amyloid-β, thereby contributing to amyloid-β accumulation and pathogenesis (Erickson et al. 2012). The receptor for advanced glycation end products (RAGE) mediates amyloid-β peptide transport across the BBB barrier in the blood-to-brain direction and its expression can be altered during disease. Inflammation as occurs in AD potentially induces elevation of levels of amyloid-β within the CNS by three distinct mechanisms: increased brain influx, decreased brain efflux and increased neuronal production of amyloid-β, due to a change in the expression of mentioned efflux systems (Jaeger et al. 2009a, b; Reale et al. 2008).

21.2.1.3 Epilepsy

Epilepsy is characterized by spontaneous, recurrent seizures due to uncontrolled, repetitive firing of neuronal networks. Antiepileptic drugs provide symptomatic treatment by affecting neurotransmission by increasing inhibitory GABAergic output, decreasing excitatory glutaminergic activity or altering ion conductance. Epilepsy coincides with increased expression of P-gp or multidrug resistance efflux pumps at the BBB (Loscher et al. 2011; Luna-Tortos et al. 2010), which limits antiepileptic drugs from entering the brain at sufficient therapeutic concentrations (Lazarowski and Czornyj 2011). The role of the BBB and the regulation of its integrity during epilepsy are discussed in more detail elsewhere in this book (see Chap. 24: Disease influence on BBB transport in neurodegenerative disorders).

21.2.1.4 Stroke

Ageing affects both the vasculature and the immune system, rendering the aged BBB more prone to damage (Persky et al. 2010; Dinapoli et al. 2010; Rosen et al. 2005). Advanced age is an important risk factor for not only stroke but also other neurodegenerative diseases, including PD and AD. It is well established that ageing correlates with increased circulating inflammatory compounds following stroke. Peripheral inflammatory mediators may play a role in cerebrovascular disease (Tuttolomondo et al. 2008, 2009), thus indirectly affecting the incidence of stroke. Identifying and understanding the function of peripheral inflammatory mediators on the BBB will give insight to better clinical diagnosis for stroke (Vangilder et al. 2011). Stroke, although initially characterized by deprivation of blood flow, leading

to ischemic conditions, is typically followed by reperfusion, which is associated with tight junction (TJ) disruption. Hypoxic conditions are used in vitro to mimic ischemia in the brain, causing increased permeability by alterations in TJ protein expression (Witt et al. 2005; Fischer et al. 1999). Moreover, upregulation of TNF-α and IL-1 was shown in ischemia models (Yang et al. 1999; Schroeter et al. 2003), linking stroke directly to the inflammatory process.

21.2.1.5 Multiple Sclerosis

Multiple sclerosis (MS) is a chronic inflammatory disease of the CNS, marked by infiltration of monocyte-derived macrophages in the brain parenchyma. MS takes several forms, with new symptoms occurring either in discrete attacks (relapsing forms) or slowly accumulating over time (progressive forms). The pathophysiology of MS is characterized by massive influx of activated monocyte-derived macrophages, which subsequently induce BBB breakdown, demyelination, oligodendrocyte injury and axonal loss. During MS, changes at the level of the BBB are related to two main processes: disruption of the barrier, i.e. leakage and alterations of TJ proteins and the ability of BBB components, including endothelial cells and astrocytes to produce inflammatory mediators thereby influencing the recruitment of immune cells entering the brain (Alvarez et al. 2011; Larochelle et al. 2011). The breakdown of the BBB is believed to be transient, but recurrence may be observed at the same or different locations over time, as evidenced by gadolinium-enhanced magnetic resonance imaging (Harris et al. 1991). The subsequent development of MS plaques involves additional phases of BBB leakage, immunologically mediated demyelination and axonal transaction (Dutta and Trapp 2011; Alvarez et al. 2011). As described in Sect. 21.2.2.1 the expression levels and function of TJ proteins are known to change during inflammation in the brain as is the case for MS (Kirk et al. 2003). MS is characterized by leukocyte infiltration (Fig. 21.1) in the brain causing up regulation of pro-inflammatory cytokines and chemokines such as IL-1β, IL-17, IL-22, IFN-γ (Kebir et al. 2007; Cayrol et al. 2008) and increased cytokine levels coincide with a high BBB permeability in MS (Leech et al. 2007).

Since historically the main mechanism of injury in MS has been thought to be inflammation, current MS therapies are mostly focused on stopping the autoimmune response (Loma and Heyman 2011). Generally, MS medication can be subdivided in immunomodulatory and immunosuppressive drugs with interferon-beta (IFN-β) and glatimer acetate (Copaxone) being the first disease modifying drugs on the market for treatment of MS (Compston and Coles 2008; Lublin and Reingold 1996). Disease-modifying drugs include four different preparations of interferon-β (Avonex, Rebif, Betaseron and Extavia), glatiramer acetate (Copaxone), mitoxantrone (Novantrone), fingolimod (Gilenya) and steroids. (La Mantia et al. 2010; Cohen and Rivera 2010; Mellergard et al. 2010; Marriott et al. 2010; Morrow et al. 2009). The heterogeneity of MS pathophysiology, individual responses of patients to a certain prescription and side effects of medication contribute to the difficulty of adequately treating MS (Loma and Heyman 2011).

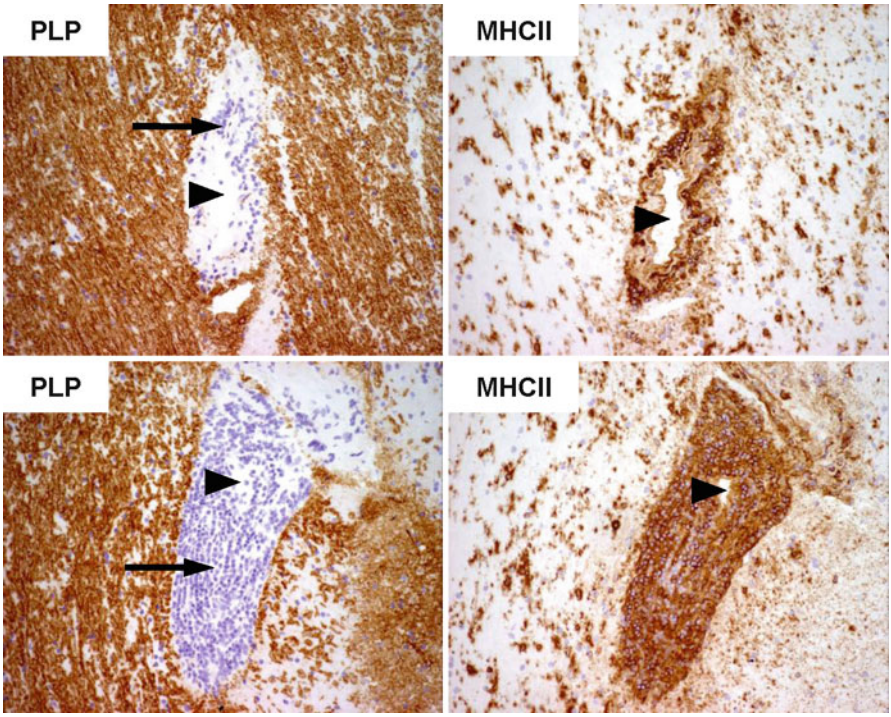

Fig. 21.1 Proteolipid protein (PLP) staining of NAWM MS brain tissue (*left panels*). Substantial peri-vascular cellular infiltrates are found (numerous purple nuclei, indicated by *arrows*). Leukocyte infiltates surrounding the vasculature show enhanced expression of major histocompatibility complex class II (MHCII; *right panels*). The blood vessel lumen is indicated by an *arrowhead* in each panel. Stainings were performed as described (Kooij et al. 2011), magnification 100×

The membrane expression of integrins on inflammatory leukocytes and their target adhesion molecules on the CNS vasculature has been a focus of therapeutic intervention in MS patients in recent years. Initially a monoclonal antibody blocking α4-integrin was used to prevent leukocyte transmigration across the BBB in vitro, and this approach was also able to alleviate disease in a rodent model of MS, experimental autoimmune encephalomyelitis (EAE) (Coisne et al. 2007, 2009). This has resulted in the generation of MS therapies currently used in the clinic. At the same time this provided solid evidence that therapies interfering with leukocyte transmigration are effective in controlling lesion formation in MS. A humanized form of this the α4-integrin blocking antibody, designated Natalizumab (Tysabri), was developed based on its established efficacy in treating EAE and is currently prescribed as second line of treatment for relapsing remitting MS (Engelhardt 2008; Banks and Erickson 2010).

21.2.2 Current Understanding of Transport Over the BBB Under Inflammatory Conditions

The BBB is diminished during inflammation in the brain (Neuwelt 2004). Not only can BBB disruption be disastrous to an organism, but drug delivery to the brain will also be altered (Abbott et al. 1999; de Boer et al. 2003). Changes in BBB function can be mediated through changes in both non-specific and specific transport pathways. This is exemplified for paracellular (TJ-controlled) and transcellular transport routes like adsorptive-mediated endocytosis and receptor-mediated endocytosis. In addition, expression of adhesion molecules and regulation of drug efflux transporters are altered under inflammatory disease conditions. Altogether, these changes may affect drug delivery into the brain. We highlight these different transport mechanisms in the next sections.

21.2.2.1 Paracellular Transport

Inflammatory conditions present in numerous neurological disorders lead to the production of cytokines that are known to result in TJ disruption. It is clear that some cytokines have effects on brain endothelial cells that could lead to either disruption or modulation of the restrictive aspects of the BBB. These effects include alterations of TJ protein expression (Erickson et al. 2012; Dohgu et al. 2004; Gloor et al. 2001; Alvarez et al. 2011) and cytoplasmic stress fibre formation of actin (Deli et al. 1995; Youakim and Ahdieh 1999). occludin, zona occludens (ZO)-1 and ZO-2 play crucial roles in TJ formation (Blasig and Haseloff 2011; Chiba et al. 2008). The use of in vitro and in vivo models has shown that an increase in BBB permeability can be induced by compounds that are released under inflammatory conditions, such as TNF-α, interferon (IFN)-γ, interleukin (IL)6, IL17 and IL22 (Burke-Gaffney and Keenan 1993; Deli et al. 1995; Wojciak-Stothard et al. 1998; Utech et al. 2005). Co-stimulation of endothelial cells with IFN-γ and TNF-α is known to affect their permeability through an altered distribution of the junction proteins claudin-5 and cadherin-5 (Ozaki et al. 1999; Wong et al. 1999). Interestingly, IFN-γ induces internalization of TJ proteins (Bruewer et al. 2005) thereby reducing the restrictive functions of the BBB, whereas removal of IFN-γ results in repositioning of TJ proteins in the cell membrane (Utech et al. 2010). IL-1β has been shown to destabilize the BBB via induction of matrix metalloproteinase-9 (MMP-9), a proteinase that has a.o. occludin, ZO-1 and claudin-5 as cleavable substrates (Bolton et al. 1998; Wachtel et al. 1999). Other studies show a direct effect of lipopolysaccharide (LPS) on BBB integrity, which has oftentimes been used to induce meningitis-like inflammation in BBB models (Tunkel et al. 1991; Tunkel et al. 1992; Banks and Erickson 2010). Moreover, oxidative stress that commonly occurs during inflammatory disease conditions results in a down-regulation of TJ expression (Abbott 2000; Krizbai et al. 2005; Lehner et al. 2011; Schreibelt et al. 2007; Fraser 2011). An important consequence of the TJ disruptions described above is elevated paracellular transport, which has consequences for drug delivery to and deposition in the diseased brain.

21.2.2.2 Adsorptive-Mediated Endocytosis

Cationic targeting moieties and cell penetrating peptides enter the brain via adsorptive-mediated endocytosis (Kumagai et al. 1987; Pardridge et al. 1987a, b; Kumar et al. 2007; Lossinsky and Shivers 2004; Drin et al. 2003). CNS endothelial cells have been shown to display increased adsorptive-mediated endocytosis in vitro after LPS, TNF-α or IL-6 treatment (Duchini et al. 1996; Banks et al. 1999). In addition, increased endocytotic activity has been observed in stroke models (Cipolla et al. 2004; Wong et al. 2012). Whether endocytosis is increased in humans during disease conditions is difficult to investigate and therefore incompletely understood, but given the generalized inflammatory response that often accompanies CNS diseases, induction of endocytotic activity is plausible. Changes in endocytotic activity of diseased CNS endothelial affect not only adsorptive-mediated endocytosis but also the more specific process of receptor-mediated endocytosis.

21.2.2.3 Receptor-Mediated Endocytosis

Another route by which macromolecular substances can pass the BBB and enter the brain is through receptor-mediated endo- and transcytosis. A wide variety of receptors and transporters involved in receptor-mediated endo- and transcytosis have been described (Abbott et al. 2010; Chishty et al. 2001; Reichel et al. 2000; Rip et al. 2009). Internalizing receptors, such as the transferrin and insulin receptors, expressed on the blood side of brain endothelial cells are amongst the most promising targets for drug transfer to the CNS (Shin et al. 1995; Lee et al. 2000; Pardridge et al. 1987a, b). Of note, transferrin receptor expression is often influenced by inflammatory conditions and disease progression (Harel et al. 2011). In addition, brain endothelial expression of transcytoting molecule Heparin-Binding Epidermal Growth Factor (HB-EGF) is strongly up regulated under inflammatory disease conditions, providing an opportunity for drug targeting to the inflamed CNS (Gaillard and de Boer 2006; Gaillard et al. 2005; Wang et al. 2011). Interestingly, not only is HB-EGF expressed at the BBB, but it is also present on the surface of leukocytes, potentially providing additional opportunities to interfere with leukocyte transmigration in inflammatory disorders such as MS (Schenk et al. 2012). Several transporters at the BBB are also altered or modulated by immune-related events (Banks and Erickson 2010; Begley 2004; Rip et al. 2009). The rate of receptor-mediated transport of TNF-α from blood to brain for instance is enhanced in mice with EAE, the animal model for MS. Despite disruption of the BBB, increased entry of TNF-α is caused by an enhancement of its transporter under inflammatory conditions (Pan et al. 1996). In contrast, the transport of another cytokine, IL-15, is diminished in the brain mice with EAE (Hsuchou et al. 2009), indicating that under disease conditions an altered transport of cytokines across the BBB determines the inflammatory status of the CNS.

21.2.2.4 Adhesion Molecule Expression

Cell adhesion molecules (CAMs) expressed on endothelial cells play a crucial role in transmigration of leukocytes across the BBB. Induction of CAMs is associated with disease states and the regulation of these molecules has been best described for stroke and even more so for MS (Rossi et al. 2011). BBB-leukocyte interaction is dependent upon expression of CAMs on the surface of BBB endothelial cells, such as intercellular CAM-1 (ICAM-1) and vascular CAM-1 (VCAM-1) on the one hand, and the expression of their ligands on leukocytes i.e. integrins αLβ2 and α4β1 on the other hand. Before being able to cross the endothelium and eventually move into the brain parenchyma, leukocytes have to perform a series of orchestrated actions, collectively designated diapedesis (Rossi et al. 2011; Engelhardt 2006; Owens et al. 2008; Engelhardt 2008). Migration of leukocytes through the endothelium increases BBB permeability, which facilitates future diapedesis (Biernacki et al. 2004; Prat et al. 2005; Seguin et al. 2003). Importantly, immune cells release inflammatory cytokines, reactive oxygen species and proteases that also facilitate the diapedesis process (Larochelle et al. 2011; Persidsky et al. 1997). Consequently, this neuro-inflammatory event indirectly affects drug transport to the brain via its influence on BBB permeability through altered TJ expression (Alvarez et al. 2011; Erickson et al. 2012; Gloor et al. 2001).

21.2.2.5 ABC Transporters

Next to the presence of complex TJs, barrier properties of the BBB are instated by the presence of specific endothelial ABC-transporters, which actively remove unwanted compounds from the brain. The ABC transporter family consists of a variety of efflux pumps (Loscher and Potschka 2005a, b), of which a few are generally regarded as key BBB transporters, including P-gp, breast-cancer resistance protein (BCRP) and the multidrug resistance-associated proteins-1 and -2 (MRP-1, -2). In general, ABC transporters drive cellular exclusion of a variety of exogenous compounds and drugs through the cell membrane against a concentration gradient at the cost of ATP hydrolysis (Loscher and Potschka 2005a, b), thereby preventing CNS entry. Expression and function of these transporters can be regulated by a broad variety of endogenous and exogenous factors, including nuclear receptors like steroid and xenobiotic receptors (Loscher and Potschka 2005a, b) or a variety of inflammatory molecules (Miller 2010). ABC transporters have been implicated in various neurological disorders, including Alzheimer's disease (Vogelgesang et al. 2002), Parkinson's disease (Bartels et al. 2008), epilepsy (Sisodiya et al. 2002; Aronica et al. 2012) and MS (Kooij et al. 2009, 2010, 2012). Interestingly, the altered vascular expression pattern and function of a crucial ABC transporter, P-gp, seems to be a general phenomenon in these neurological disorders. Consequently, since a number of substrates for P-gp such as statins (Kivisto et al. 2004) and corticosteroids (Dilger et al. 2004) are currently used in the treatment of such brain diseases, loss of P-gp

at the BBB as observed in MS has the advantage to specifically deliver drugs to affected brain areas at the site of the lesions, thereby increasing their effectiveness. Conversely, these drugs in turn may directly affect ABC transporter expression and function (Iqbal et al. 2011), thereby restoring these specific barrier properties of the BBB and preventing brain entry at the diseased sites. Therefore, further research is warranted to develop specific anti-inflammatory drugs that do not induce ABC transporter function, thereby allowing local delivery of therapeutic agents at the site of the diseased brain areas, preventing tissue damage.

21.3 Conclusions and Future Directions

As outlined above, CNS diseases with an inflammatory component affect BBB function. Consequentially, drug delivery to the brain will be altered and disposition of drugs in the brain during different disease states may limit efficient treatment. Altered BBB permeability and function during CNS diseases may be mediated via changes in various transport pathways and receptor systems. Conversely, disease state of the CNS also provide opportunities for drug targeting to sites of affected brain regions, since drugs that normally are unable to traverse the BBB (either due to ABC transporter activity or presence of TJs) may now reach their target in the diseased brain. To accurately treat complex CNS disorders future research should therefore aim to gain more and detailed insight into the effects of neuro-inflammation on different BBB properties.

Whether the described deregulation of transport and receptor systems are favourable or unfavourable for drug delivery across the BBB largely depends on the type of transport route or receptor involved, the regulation of its expression and specific localization of transporters or receptors in the brain. Thus, when relying on such mechanisms in delivery strategies, targeting efficiency may be changed during CNS disease states, potentially increasing or decreasing the therapeutic efficacy of drugs. In the past and also more recently, novel and specific drug delivery approaches have been developed to overcome the BBB (see Chaps. 17. Blood-to-brain drug delivery using nanocarriers and 18. Development of new protein vectors for the physiologic delivery of large therapeutic compounds to the CNS and (de Boer and Gaillard 2007; Gaillard and de Boer 2006; Gaillard et al. 2005; Wang et al. 2011; Erickson et al. 2012)). Since most of these targeting approaches are dependent on specific or non-specific targeting and trafficking mechanisms at the BBB, understanding the regulation of these mechanisms is of crucial importance. For proper selection of a suitable carrier or targeting moiety, the described deregulations of transport routes and potential target receptors during neuro-inflammatory conditions must be taken into account. For instance, paracellular transport is often increased in MS due to decreased TJ expression, this then would potentially allow for more efficient drug-targeting to affected brain regions. Likewise, the down-regulation of ABC-transporters during CNS diseases may lead to reduced efflux of exogenous compounds, thereby increasing brain retention of therapeutics and rendering the

application of drugs that are ABC transporter substrates more effective. In contrast, application of drugs may themselves cause an increase in ABC transporter expression and function, thus hampering drug delivery to the brain.

Drug delivery strategies that depend upon the expression of a specific internalizing receptor are at risk of missing their target if its expression is markedly reduced during disease status. On the other hand, enhanced or de novo expression of specific BBB ligands under inflammatory conditions holds promise for the development of new targeting strategies (van Rooy et al. 2012). Finally, it is of importance to realize that transport mechanisms and receptor expression may change during the course of the disease, complicating the selection of an efficient strategy even more. All these issues have to be taken into account when deciding which targeting and delivery strategy is the most adequate given disease conditions and experimental approaches and therapies should be constructed accordingly.

References

Abbott NJ (2000) Inflammatory mediators and modulation of blood–brain barrier permeability. Cell Mol Neurobiol 20:131–147

Abbott NJ (2002) Astrocyte-endothelial interactions and blood–brain barrier permeability. J Anat 200:629–638

Abbott NJ, Romero IA (1996) Transporting therapeutics across the blood–brain barrier. Mol Med Today 2:106–113

Abbott NJ, Chugani DC, Zaharchuk G, Rosen BR, Lo EH (1999) Delivery of imaging agents into brain. Adv Drug Deliv Rev 37:253–277

Abbott NJ, Ronnback L, Hansson E (2006) Astrocyte-endothelial interactions at the blood–brain barrier. Nat Rev Neurosci 7:41–53

Abbott NJ, Patabendige AA, Dolman DE, Yusof SR, Begley DJ (2010) Structure and function of the blood–brain barrier. Neurobiol Dis 37:13–25

Alvarez JI, Cayrol R, Prat A (2011) Disruption of central nervous system barriers in multiple sclerosis. Biochim Biophys Acta 1812:252–264

Aronica E, Sisodiya SM, Gorter JA (2012) Cerebral expression of drug transporters in epilepsy. Adv Drug Deliv Rev 64:919–929

Banks WA, Erickson MA (2010) The blood–brain barrier and immune function and dysfunction. Neurobiol Dis 37:26–32

Banks WA, Kastin AJ, Brennan JM, Vallance KL (1999) Adsorptive endocytosis of HIV-1gp120 by blood–brain barrier is enhanced by lipopolysaccharide. Exp Neurol 156:165–171

Bartels AL, Willemsen AT, Kortekaas R, de Jong BM, de Vries R, de Klerk O, van Oostrom JC, Portman A, Leenders KL (2008) Decreased blood–brain barrier P-glycoprotein function in the progression of Parkinson's disease, PSP and MSA. J Neural Transm 115:1001–1009

Begley DJ (2004) ABC transporters and the blood–brain barrier. Curr Pharm Des 10:1295–1312

Bell RD, Zlokovic BV (2009) Neurovascular mechanisms and blood–brain barrier disorder in Alzheimer's disease. Acta Neuropathol 118:103–113

Biernacki K, Prat A, Blain M, Antel JP (2004) Regulation of cellular and molecular trafficking across human brain endothelial cells by Th1- and Th2-polarized lymphocytes. J Neuropathol Exp Neurol 63:223–232

Blasig IE, Haseloff RF (2011) Tight junctions and tissue barriers. Antioxid Redox Signal 15:1163–1166

Boado RJ, Pardridge WM (2011) The trojan horse liposome technology for nonviral gene transfer across the blood–brain barrier. J Drug Deliv 2011:296151

Bolton SJ, Anthony DC, Perry VH (1998) Loss of the tight junction proteins occludin and zonula occludens-1 from cerebral vascular endothelium during neutrophil-induced blood–brain barrier breakdown in vivo. Neuroscience 86:1245–1257

Brousseau G, Rourke BP, Burke B (2007) Acetylcholinesterase inhibitors, neuropsychiatric symptoms, and Alzheimer's disease subtypes: an alternate hypothesis to global cognitive enhancement. Exp Clin Psychopharmacol 15:546–554

Bruewer M, Utech M, Ivanov AI, Hopkins AM, Parkos CA, Nusrat A (2005) Interferon-gamma induces internalization of epithelial tight junction proteins via a macropinocytosis-like process. FASEB J 19:923–933

Burke-Gaffney A, Keenan AK (1993) Modulation of human endothelial cell permeability by combinations of the cytokines interleukin-1 alpha/beta, tumor necrosis factor-alpha and interferon-gamma. Immunopharmacology 25:1–9

Cayrol R, Wosik K, Berard JL, Dodelet-Devillers A, Ifergan I, Kebir H, Haqqani AS, Kreymborg K, Krug S, Moumdjian R, Bouthillier A, Becher B, Arbour N, David S, Stanimirovic D, Prat A (2008) Activated leukocyte cell adhesion molecule promotes leukocyte trafficking into the central nervous system. Nat Immunol 9:137–145

Chiba H, Osanai M, Murata M, Kojima T, Sawada N (2008) Transmembrane proteins of tight junctions. Biochim Biophys Acta 1778:588–600

Chishty M, Reichel A, Siva J, Abbott NJ, Begley DJ (2001) Affinity for the P-glycoprotein efflux pump at the blood–brain barrier may explain the lack of CNS side-effects of modern antihistamines. J Drug Target 9:223–228

Chung YC, Ko HW, Bok E, Park ES, Huh SH, Nam JH, Jin BK (2010) The role of neuroinflammation on the pathogenesis of Parkinson's disease. BMB Rep 43:225–232

Cipolla MJ, Crete R, Vitullo L, Rix RD (2004) Transcellular transport as a mechanism of blood–brain barrier disruption during stroke. Front Biosci 9:777–785

Cohen BA, Rivera VM (2010) PRISMS: the story of a pivotal clinical trial series in multiple sclerosis. Curr Med Res Opin 26:827–838

Coisne C, Lyck R, Engelhardt B (2007) Therapeutic targeting of leukocyte trafficking across the blood–brain barrier. Inflamm Allergy Drug Targets 6:210–222

Coisne C, Mao W, Engelhardt B (2009) Cutting edge: Natalizumab blocks adhesion but not initial contact of human T cells to the blood–brain barrier in vivo in an animal model of multiple sclerosis. J Immunol 182:5909–5913

Compston A, Coles A (2008) Multiple sclerosis. Lancet 372:1502–1517

de Boer AG, Gaillard PJ (2007) Drug targeting to the brain. Annu Rev Pharmacol Toxicol 47:323–355

de Boer AG, van der Sandt IC, Gaillard PJ (2003) The role of drug transporters at the blood–brain barrier. Annu Rev Pharmacol Toxicol 43:629–656

Deane R, Wu Z, Sagare A, Davis J, Du Yan S, Hamm K, Xu F, Parisi M, LaRue B, Hu HW, Spijkers P, Guo H, Song X, Lenting PJ, Van Nostrand WE, Zlokovic BV (2004) LRP/amyloid beta-peptide interaction mediates differential brain efflux of Abeta isoforms. Neuron 43:333–344

Deli MA, Descamps L, Dehouck MP, Cecchelli R, Joo F, Abraham CS, Torpier G (1995) Exposure of tumor necrosis factor-alpha to luminal membrane of bovine brain capillary endothelial cells cocultured with astrocytes induces a delayed increase of permeability and cytoplasmic stress fiber formation of actin. J Neurosci Res 41:717–726

Dilger K, Schwab M, Fromm MF (2004) Identification of budesonide and prednisone as substrates of the intestinal drug efflux pump P-glycoprotein. Inflamm Bowel Dis 10:578–583

DiNapoli VA, Huber JD, Houser K, Li X, Rosen CL (2008) Early disruptions of the blood–brain barrier may contribute to exacerbated neuronal damage and prolonged functional recovery following stroke in aged rats. Neurobiol Aging 29:753–764

Dinapoli VA, Benkovic SA, Li X, Kelly KA, Miller DB, Rosen CL, Huber JD, O'Callaghan JP (2010) Age exaggerates proinflammatory cytokine signaling and truncates signal transducers and activators of transcription 3 signaling following ischemic stroke in the rat. Neuroscience 170:633–644

Dohgu S, Yamauchi A, Takata F, Naito M, Tsuruo T, Higuchi S, Sawada Y, Kataoka Y (2004) Transforming growth factor-beta1 upregulates the tight junction and P-glycoprotein of brain microvascular endothelial cells. Cell Mol Neurobiol 24:491–497

Drin G, Cottin S, Blanc E, Rees AR, Temsamani J (2003) Studies on the internalization mechanism of cationic cell-penetrating peptides. J Biol Chem 278:31192–31201

Duchini A, Govindarajan S, Santucci M, Zampi G, Hofman FM (1996) Effects of tumor necrosis factor-alpha and interleukin-6 on fluid-phase permeability and ammonia diffusion in CNS-derived endothelial cells. J Investig Med 44:474–482

Dutta R, Trapp BD (2011) Mechanisms of neuronal dysfunction and degeneration in multiple sclerosis. Prog Neurobiol 93:1–12

Engelhardt B (2006) Molecular mechanisms involved in T cell migration across the blood–brain barrier. J Neural Transm 113:477–485

Engelhardt B (2008) The blood-central nervous system barriers actively control immune cell entry into the central nervous system. Curr Pharm Des 14:1555–1565

Erickson MA, Dohi K, Banks WA (2012) Neuroinflammation: a common pathway in CNS diseases as mediated at the blood–brain barrier. Neuroimmunomodulation 19:121–130

Fischer S, Clauss M, Wiesnet M, Renz D, Schaper W, Karliczek GF (1999) Hypoxia induces permeability in brain microvessel endothelial cells via VEGF and NO. Am J Physiol 276: C812–C820

Fraser PA (2011) The role of free radical generation in increasing cerebrovascular permeability. Free Radic Biol Med 51:967–977

Friedman A, Dingledine R (2011) Molecular cascades that mediate the influence of inflammation on epilepsy. Epilepsia 52(Suppl 3):33–39

Fung A, Vizcaychipi M, Lloyd D, Wan Y, Ma D (2012) Central nervous system inflammation in disease related conditions: mechanistic prospects. Brain Res 1446:144–155

Gaillard PJ, de Boer AG (2006) A novel opportunity for targeted drug delivery to the brain. J Control Release 116:e60–e62

Gaillard PJ, Visser CC, de Boer AG (2005) Targeted delivery across the blood–brain barrier. Expert Opin Drug Deliv 2:299–309

Gloor SM, Wachtel M, Bolliger MF, Ishihara H, Landmann R, Frei K (2001) Molecular and cellular permeability control at the blood–brain barrier. Brain Res Brain Res Rev 36:258–264

Hardy J, Selkoe DJ (2002) The amyloid hypothesis of Alzheimer's disease: progress and problems on the road to therapeutics. Science 297:353–356

Harel E, Rubinstein A, Nissan A, Khazanov E, Nadler Milbauer M, Barenholz Y, Tirosh B (2011) Enhanced transferrin receptor expression by proinflammatory cytokines in enterocytes as a means for local delivery of drugs to inflamed gut mucosa. PLoS One 6:e24202

Harris JO, Frank JA, Patronas N, McFarlin DE, McFarland HF (1991) Serial gadolinium-enhanced magnetic resonance imaging scans in patients with early, relapsing-remitting multiple sclerosis: implications for clinical trials and natural history. Ann Neurol 29:548–555

Hawkins BT, Davis TP (2005) The blood–brain barrier/neurovascular unit in health and disease. Pharmacol Rev 57:173–185

Herholz K, Weisenbach S, Kalbe E (2008) Deficits of the cholinergic system in early AD. Neuropsychologia 46:1642–1647

Hsuchou H, Pan W, Wu X, Kastin AJ (2009) Cessation of blood-to-brain influx of interleukin-15 during development of EAE. J Cereb Blood Flow Metab 29:1568–1578

Iqbal U, Abulrob A, Stanimirovic DB (2011) Integrated platform for brain imaging and drug delivery across the blood–brain barrier. Methods Mol Biol 686:465–481

Ishiwata K, Kawamura K, Yanai K, Hendrikse NH (2007) In vivo evaluation of P-glycoprotein modulation of 8 PET radioligands used clinically. J Nucl Med 48:81–87

Jaeger LB, Dohgu S, Hwang MC, Farr SA, Murphy MP, Fleegal-DeMotta MA, Lynch JL, Robinson SM, Niehoff ML, Johnson SN, Kumar VB, Banks WA (2009a) Testing the neurovascular hypothesis of Alzheimer's disease: LRP-1 antisense reduces blood–brain barrier clearance, increases brain levels of amyloid-beta protein, and impairs cognition. J Alzheimers Dis 17:553–570

Jaeger LB, Dohgu S, Sultana R, Lynch JL, Owen JB, Erickson MA, Shah GN, Price TO, Fleegal-Demotta MA, Butterfield DA, Banks WA (2009b) Lipopolysaccharide alters the blood–brain barrier transport of amyloid beta protein: a mechanism for inflammation in the progression of Alzheimer's disease. Brain Behav Immun 23:507–517

Kebir H, Kreymborg K, Ifergan I, Dodelet-Devillers A, Cayrol R, Bernard M, Giuliani F, Arbour N, Becher B, Prat A (2007) Human TH17 lymphocytes promote blood–brain barrier disruption and central nervous system inflammation. Nat Med 13:1173–1175

Kim MH, Maeng HJ, Yu KH, Lee KR, Tsuruo T, Kim DD, Shim CK, Chung SJ (2010) Evidence of carrier-mediated transport in the penetration of donepezil into the rat brain. J Pharm Sci 99:1548–1566

Kirk J, Plumb J, Mirakhur M, McQuaid S (2003) Tight junctional abnormality in multiple sclerosis white matter affects all calibres of vessel and is associated with blood–brain barrier leakage and active demyelination. J Pathol 201:319–327

Kivisto KT, Zukunft J, Hofmann U, Niemi M, Rekersbrink S, Schneider S, Luippold G, Schwab M, Eichelbaum M, Fromm MF (2004) Characterisation of cerivastatin as a P-glycoprotein substrate: studies in P-glycoprotein-expressing cell monolayers and mdr1a/b knock-out mice. Naunyn Schmiedebergs Arch Pharmacol 370:124–130

Kooi EJ, Prins M, Bajic N, Belien JA, Gerritsen WH, van Horssen J, Aronica E, van Dam AM, Hoozemans JJ, Francis PT, van der Valk P, Geurts JJ (2011) Cholinergic imbalance in the multiple sclerosis hippocampus. Acta Neuropathol 122:313–322

Kooij G, Backer R, Koning JJ, Reijerkerk A, van Horssen J, van der Pol SM, Drexhage J, Schinkel A, Dijkstra CD, den Haan JM, Geijtenbeek TB, de Vries HE (2009) P-glycoprotein acts as an immunomodulator during neuroinflammation. PLoS One 4:e8212

Kooij G, van Horssen J, de Lange EC, Reijerkerk A, van der Pol SM, van Het Hof B, Drexhage J, Vennegoor A, Killestein J, Scheffer G, Oerlemans R, Scheper R, van der Valk P, Dijkstra CD, de Vries HE (2010) T lymphocytes impair P-glycoprotein function during neuroinflammation. J Autoimmun 34:416–425

Kooij G, Mizee MR, van Horssen J, Reijerkerk A, Witte ME, Drexhage JA, van der Pol SM, van Het Hof B, Scheffer G, Scheper R, Dijkstra CD, van der Valk P, de Vries HE (2011) Adenosine triphosphate-binding cassette transporters mediate chemokine (C-C motif) ligand 2 secretion from reactive astrocytes: relevance to multiple sclerosis pathogenesis. Brain 134:555–570

Kooij G, van Horssen J, Bandaru VV, Haughey NJ, de Vries HE (2012) The role of ATP-binding cassette transporters in neuro-inflammation: relevance for bioactive lipids. Front Pharmacol 3:74

Kortekaas R, Leenders KL, van Oostrom JC, Vaalburg W, Bart J, Willemsen AT, Hendrikse NH (2005) Blood–brain barrier dysfunction in parkinsonian midbrain in vivo. Ann Neurol 57: 176–179

Krizbai IA, Lenzser G, Szatmari E, Farkas AE, Wilhelm I, Fekete Z, Erdos B, Bauer H, Bauer HC, Sandor P, Komjati K (2005) Blood–brain barrier changes during compensated and decompensated hemorrhagic shock. Shock 24:428–433

Kumagai AK, Eisenberg JB, Pardridge WM (1987) Absorptive-mediated endocytosis of cationized albumin and a beta-endorphin-cationized albumin chimeric peptide by isolated brain capillaries. Model system of blood–brain barrier transport. J Biol Chem 262:15214–15219

Kumar P, Wu H, McBride JL, Jung KE, Kim MH, Davidson BL, Lee SK, Shankar P, Manjunath N (2007) Transvascular delivery of small interfering RNA to the central nervous system. Nature 448:39–43

La Mantia L, Munari LM and Lovati R (2010) Glatiramer acetate for multiple sclerosis. Cochrane Database Syst Rev (5):CD004678

Larochelle C, Alvarez JI, Prat A (2011) How do immune cells overcome the blood–brain barrier in multiple sclerosis? FEBS Lett 585:3770–3780

Lazarowski A, Czornyj L (2011) Potential role of multidrug resistant proteins in refractory epilepsy and antiepileptic drugs interactions. Drug Metabol Drug Interact 26:21–26

Lee HJ, Engelhardt B, Lesley J, Bickel U, Pardridge WM (2000) Targeting rat anti-mouse transferrin receptor monoclonal antibodies through blood–brain barrier in mouse. J Pharmacol Exp Ther 292:1048–1052

Leech S, Kirk J, Plumb J, McQuaid S (2007) Persistent endothelial abnormalities and blood–brain barrier leak in primary and secondary progressive multiple sclerosis. Neuropathol Appl Neurobiol 33:86–98

Lehner C, Gehwolf R, Tempfer H, Krizbai I, Hennig B, Bauer HC, Bauer H (2011) Oxidative stress and blood–brain barrier dysfunction under particular consideration of matrix metalloproteinases. Antioxid Redox Signal 15:1305–1323

Lillis AP, Van Duyn LB, Murphy-Ullrich JE, Strickland DK (2008) LDL receptor-related protein 1: unique tissue-specific functions revealed by selective gene knockout studies. Physiol Rev 88:887–918

Loma I, Heyman R (2011) Multiple sclerosis: pathogenesis and treatment. Curr Neuropharmacol 9:409–416

Loscher W, Potschka H (2005a) Blood–brain barrier active efflux transporters: ATP-binding cassette gene family. NeuroRx 2:86–98

Loscher W, Potschka H (2005b) Drug resistance in brain diseases and the role of drug efflux transporters. Nat Rev Neurosci 6:591–602

Loscher W, Luna-Tortos C, Romermann K, Fedrowitz M (2011) Do ATP-binding cassette transporters cause pharmacoresistance in epilepsy? Problems and approaches in determining which antiepileptic drugs are affected. Curr Pharm Des 17:2808–2828

Lossinsky AS, Shivers RR (2004) Structural pathways for macromolecular and cellular transport across the blood–brain barrier during inflammatory conditions. Review. Histol Histopathol 19:535–564

Lublin FD, Reingold SC (1996) Defining the clinical course of multiple sclerosis: results of an international survey. National Multiple Sclerosis Society (USA) Advisory Committee on Clinical Trials of New Agents in Multiple Sclerosi. Neurology 46:907–911

Luna-Tortos C, Fedrowitz M, Loscher W (2010) Evaluation of transport of common antiepileptic drugs by human multidrug resistance-associated proteins (MRP1, 2 and 5) that are overexpressed in pharmacoresistant epilepsy. Neuropharmacology 58:1019–1032

Marriott JJ, Miyasaki JM, Gronseth G, O'Connor PW (2010) Evidence report: the efficacy and safety of mitoxantrone (Novantrone) in the treatment of multiple sclerosis: Report of the Therapeutics and Technology Assessment Subcommittee of the American Academy of Neurology. Neurology 74:1463–1470

Mellergard J, Edstrom M, Vrethem M, Ernerudh J, Dahle C (2010) Natalizumab treatment in multiple sclerosis: marked decline of chemokines and cytokines in cerebrospinal fluid. Mult Scler 16:208–217

Miller DS (2010) Regulation of P-glycoprotein and other ABC drug transporters at the blood–brain barrier. Trends Pharmacol Sci 31:246–254

Morrow SA, Metz LM, Kremenchutzky M (2009) High dose oral steroids commonly used to treat relapses in Canadian MS clinics. Can J Neurol Sci 36:213–215

Neuwelt EA (2004) Mechanisms of disease: the blood–brain barrier. Neurosurgery 54:131–140, discussion 141–142

Owens T, Bechmann I, Engelhardt B (2008) Perivascular spaces and the two steps to neuroinflammation. J Neuropathol Exp Neurol 67:1113–1121

Ozaki H, Ishii K, Horiuchi H, Arai H, Kawamoto T, Okawa K, Iwamatsu A, Kita T (1999) Cutting edge: combined treatment of TNF-alpha and IFN-gamma causes redistribution of junctional adhesion molecule in human endothelial cells. J Immunol 163:553–557

Pan W, Banks WA, Kennedy MK, Gutierrez EG, Kastin AJ (1996) Differential permeability of the BBB in acute EAE: enhanced transport of TNT-alpha. Am J Physiol 271:E636–E642

Pardridge WM, Eisenberg J, Yang J (1987a) Human blood–brain barrier transferrin receptor. Metabolism 36:892–895

Pardridge WM, Kumagai AK, Eisenberg JB (1987b) Chimeric peptides as a vehicle for peptide pharmaceutical delivery through the blood–brain barrier. Biochem Biophys Res Commun 146:307–313

Persidsky Y, Stins M, Way D, Witte MH, Weinand M, Kim KS, Bock P, Gendelman HE, Fiala M (1997) A model for monocyte migration through the blood–brain barrier during HIV-1 encephalitis. J Immunol 158:3499–3510

Persky RW, Turtzo LC, McCullough LD (2010) Stroke in women: disparities and outcomes. Curr Cardiol Rep 12:6–13

Prat A, Biernacki K, Antel JP (2005) Th1 and Th2 lymphocyte migration across the human BBB is specifically regulated by interferon beta and copolymer-1. J Autoimmun 24:119–124

Qin L, Wu X, Block ML, Liu Y, Breese GR, Hong JS, Knapp DJ, Crews FT (2007) Systemic LPS causes chronic neuroinflammation and progressive neurodegeneration. Glia 55:453–462

Quan N (2006) Brain's firewall: blood–brain barrier actively regulates neuroimmune information flow. Brain Behav Immun 20:447–448

Reale M, Iarlori C, Feliciani C, Gambi D (2008) Peripheral chemokine receptors, their ligands, cytokines and Alzheimer's disease. J Alzheimers Dis 14:147–159

Reale M, Iarlori C, Thomas A, Gambi D, Perfetti B, Di Nicola M, Onofrj M (2009) Peripheral cytokines profile in Parkinson's disease. Brain Behav Immun 23:55–63

Reichel A, Begley DJ, Abbott NJ (2000) Carrier-mediated delivery of metabotrophic glutamate receptor ligands to the central nervous system: structural tolerance and potential of the L-system amino acid transporter at the blood–brain barrier. J Cereb Blood Flow Metab 20:168–174

Rip J, Schenk GJ, de Boer AG (2009) Differential receptor-mediated drug targeting to the diseased brain. Expert Opin Drug Deliv 6:227–237

Rosen CL, Dinapoli VA, Nagamine T, Crocco T (2005) Influence of age on stroke outcome following transient focal ischemia. J Neurosurg 103:687–694

Rossi B, Angiari S, Zenaro E, Budui SL, Constantin G (2011) Vascular inflammation in central nervous system diseases: adhesion receptors controlling leukocyte-endothelial interactions. J Leukoc Biol 89:539–556

Sagare A, Deane R, Bell RD, Johnson B, Hamm K, Pendu R, Marky A, Lenting PJ, Wu Z, Zarcone T, Goate A, Mayo K, Perlmutter D, Coma M, Zhong Z, Zlokovic BV (2007) Clearance of amyloid-beta by circulating lipoprotein receptors. Nat Med 13:1029–1031

Schenk GJ, Haasnoot PC, Centlivre M, Legrand N, Rip J, de Boer AG, Berkhout B (2012) Efficient CRM197-mediated drug targeting to monocytes. J Control Release 158:139–147

Schreibelt G, Kooij G, Reijerkerk A, van Doorn R, Gringhuis SI, van der Pol S, Weksler BB, Romero IA, Couraud PO, Piontek J, Blasig IE, Dijkstra CD, Ronken E, de Vries HE (2007) Reactive oxygen species alter brain endothelial tight junction dynamics via RhoA, PI3 kinase, and PKB signaling. FASEB J 21:3666–3676

Schroeter M, Kury P, Jander S (2003) Inflammatory gene expression in focal cortical brain ischemia: differences between rats and mice. Brain Res Mol Brain Res 117:1–7

Seguin R, Biernacki K, Rotondo RL, Prat A, Antel JP (2003) Regulation and functional effects of monocyte migration across human brain-derived endothelial cells. J Neuropathol Exp Neurol 62:412–419

Shin SU, Friden P, Moran M, Olson T, Kang YS, Pardridge WM, Morrison SL (1995) Transferrin-antibody fusion proteins are effective in brain targeting. Proc Natl Acad Sci U S A 92: 2820–2824

Sisodiya SM, Lin WR, Harding BN, Squier MV, Thom M (2002) Drug resistance in epilepsy: expression of drug resistance proteins in common causes of refractory epilepsy. Brain 125:22–31

Tunkel AR, Rosser SW, Hansen EJ, Scheld WM (1991) Blood–brain barrier alterations in bacterial meningitis: development of an in vitro model and observations on the effects of lipopolysaccharide. In Vitro Cell Dev Biol 27A:113–120

Tunkel AR, Wispelwey B, Quagliarello VJ, Rosser SW, Lesse AJ, Hansen EJ, Scheld WM (1992) Pathophysiology of blood–brain barrier alterations during experimental Haemophilus influenzae meningitis. J Infect Dis 165(Suppl 1):S119–S120

Tuttolomondo A, Di Raimondo D, di Sciacca R, Pinto A, Licata G (2008) Inflammatory cytokines in acute ischemic stroke. Curr Pharm Des 14:3574–3589

Tuttolomondo A, Pinto A, Corrao S, Di Raimondo D, Fernandez P, Di Sciacca R, Arnao V, Licata G (2009) Immuno-inflammatory and thrombotic/fibrinolytic variables associated with acute ischemic stroke diagnosis. Atherosclerosis 203:503–508

Utech M, Ivanov AI, Samarin SN, Bruewer M, Turner JR, Mrsny RJ, Parkos CA, Nusrat A (2005) Mechanism of IFN-gamma-induced endocytosis of tight junction proteins: myosin II-dependent vacuolarization of the apical plasma membrane. Mol Biol Cell 16:5040–5052

Utech M, Mennigen R, Bruewer M (2010) Endocytosis and recycling of tight junction proteins in inflammation. J Biomed Biotechnol 2010:484987

van Rooy I, Hennink WE, Storm G, Schiffelers RM, Mastrobattista E (2012) Attaching the phage display-selected GLA peptide to liposomes: factors influencing target binding. Eur J Pharm Sci 45:330–335

Vangilder RL, Rosen CL, Barr TL, Huber JD (2011) Targeting the neurovascular unit for treatment of neurological disorders. Pharmacol Ther 130:239–247

Vogelgesang S, Cascorbi I, Schroeder E, Pahnke J, Kroemer HK, Siegmund W, Kunert-Keil C, Walker LC, Warzok RW (2002) Deposition of Alzheimer's beta-amyloid is inversely correlated with P-glycoprotein expression in the brains of elderly non-demented humans. Pharmacogenetics 12:535–541

Wachtel M, Frei K, Ehler E, Fontana A, Winterhalter K, Gloor SM (1999) Occludin proteolysis and increased permeability in endothelial cells through tyrosine phosphatase inhibition. J Cell Sci 112(Pt 23):4347–4356

Wang P, Liu Y, Shang X, Xue Y (2011) CRM197-induced blood–brain barrier permeability increase is mediated by upregulation of caveolin-1 protein. J Mol Neurosci 43:485–492

Witt KA, Mark KS, Huber J, Davis TP (2005) Hypoxia-inducible factor and nuclear factor kappa-B activation in blood–brain barrier endothelium under hypoxic/reoxygenation stress. J Neurochem 92:203–214

Wojciak-Stothard B, Entwistle A, Garg R, Ridley AJ (1998) Regulation of TNF-alpha-induced reorganization of the actin cytoskeleton and cell-cell junctions by Rho, Rac, and Cdc42 in human endothelial cells. J Cell Physiol 176:150–165

Wong RK, Baldwin AL, Heimark RL (1999) Cadherin-5 redistribution at sites of TNF-alpha and IFN-gamma-induced permeability in mesenteric venules. Am J Physiol 276:H736–H748

Wong HL, Wu XY, Bendayan R (2012) Nanotechnological advances for the delivery of CNS therapeutics. Adv Drug Deliv Rev 64:686–700

Yang GY, Gong C, Qin Z, Liu XH, Lorris Betz A (1999) Tumor necrosis factor alpha expression produces increased blood–brain barrier permeability following temporary focal cerebral ischemia in mice. Brain Res Mol Brain Res 69:135–143

Youakim A, Ahdieh M (1999) Interferon-gamma decreases barrier function in T84 cells by reducing ZO-1 levels and disrupting apical actin. Am J Physiol 276:G1279–G1288

Zlokovic BV (2008) The blood–brain barrier in health and chronic neurodegenerative disorders. Neuron 57:178–201

Zlokovic BV (2010) Neurodegeneration and the neurovascular unit. Nat Med 16:1370–1371

Chapter 22
Disease Influence on BBB Transport in Neurodegenerative Disorders

Elizabeth C.M. de Lange

Abstract For the pharmacotherapy of neurodegenerative diseases, drugs have to pass the blood–brain barrier (BBB). Many changes in BBB properties in neurodegeneration have been reported. Furthermore, the BBB seems to play an important role in the disease initiation and or progression. While information on unbound drug concentrations in plasma and brain are needed to decipher BBB transport properties and target site concentrations, and changes thereof in disease conditions, surprisingly, only a very limited number of BBB transport studies in neurodegeneration have been performed on the basis of the unbound drug, and even fewer have taken into account disease conditions and/or measurements of an effect parameter. For better understanding and treatment, a much more integrative and translational pharmacometric research approach is needed, instead of studying neurodegenerative components in isolation. As the human brain is not accessible for sampling, we have to rely on animal models and translational approaches.

22.1 Introduction

Due to the aging population and perhaps also diet and lifestyle changes, we are facing a rapid increase in the prevalence of neurodegenerative diseases. Neurodegeneration can be defined as progressive loss of neuronal structure and function, finally culminating in neuronal cell death. Neurodegenerative diseases include Alzheimer's disease, amyotrophic lateral sclerosis, pharmacoresistant epilepsy, Huntington's disease, multiple sclerosis, Parkinson's disease, and traumatic brain injury (Kalaria 2010; Cholerton et al. 2011). Most neurodegenerative diseases start in mid-life

E.C.M. de Lange (✉)
Gorlaeus Laboratories, Division of Pharmacology, Leiden Academic Center for Drug Research, Leiden University, Leiden, The Netherlands
e-mail: l.lange@lacdr.leidenuniv.nl

M. Hammarlund-Udenaes et al. (eds.), *Drug Delivery to the Brain*, AAPS Advances in the Pharmaceutical Sciences Series 10, DOI 10.1007/978-1-4614-9105-7_22,

and can be characterized by motor and/or cognitive symptoms that progressively worsen with age and may reduce life expectancy.

The mechanisms of neurodegeneration are only partly understood and thus effective treatments for neurodegenerative diseases are lacking. Despite all efforts in research to develop new CNS drugs in the last few decennia, the results of clinical trials have been very disappointing. This indicates that we need to learn more about neurodegenerative processes and their interrelationships in order to develop better drug treatment approaches to combat, halt, or even reverse these processes. Adequate functioning of the blood–brain barrier (BBB) is essential for efficient brain function. Structural and functional disturbances in both the neurovascular unit and CNS fluid compartments may occur with advancing age or following epileptic seizures, traumatic brain injury, or stroke. These disturbances may include impairment in autoregulation and neurovascular coupling, BBB leakage, decreased cerebrospinal fluid (CSF) volume, and reduced vascular tone. Such processes make the brain vulnerable and appear to be responsible for varying degrees of neurodegeneration (Kalaria 2010).

As BBB dysfunction often leads to inflammatory changes such that immune cells and immune mediators get access to the brain and then contribute to the process of neurodegeneration, it seems that the BBB itself plays a key role in most (if not all) neurodegenerative disorders (Zlokovic 2008, 2010, 2011). Thus, for the development of drug treatment modalities for neurodegenerative conditions, we have to consider the complexity of the BBB and the brain together (Palmer 2011).

Despite all research efforts in this area, effective treatments for neurodegenerative diseases are still lacking. This is probably due to the fact that study designs thus far have not focused sufficiently on the interplay between the processes involved. The data obtained so far often do not provide information on the sensitivity of the obtained parameter values to the context in which they have been measured. Importantly, information on unbound drug concentrations has been lacking, while especially unbound concentrations in plasma and brain sites are most valuable with regard to specific information on BBB drug transport, intrabrain distribution, and target exposure. Moreover, systematic studies of disease state (or stage) compared to a proper control condition are almost absent.

In order to unravel the connections between neurodegeneration and transport at the BBB, multiple measures in a single system combined translational pharmacometric research approaches are needed to complement studies that focus on individual processes in isolation (see also Chap. 10). As the human brain is not accessible for in vivo sampling, a great deal of such studies must be performed in animal models (De Lange 2013).

In this chapter, neurodegenerative processes and disorders will be discussed, followed by specific information about BBB dysfunction in neurodegeneration. Though it is thought that the BBB is compromised in neurodegenerative disorders and therefore would be expected to allow enhanced access of drugs to the brain, the few studies on BBB transport and delivery to brain target sites in neurodegenerative diseases indicate that this is not necessarily always the case. The chapter finalizes with conclusions, points for discussion, and suggestions for future directions.

22.2 Neurodegenerative Processes and Disorders

Numerous disorders afflict the nervous system. Among those, neurodegenerative diseases are characterized by a long-lasting course of neuronal death and progressive nervous system dysfunction. The strongest risk factor for brain degeneration, whether it results from vascular or neurodegenerative mechanisms or both, is age. However, several modifiable risks such as cardiovascular disease, hypertension, dyslipidemia, diabetes, and obesity enhance the rate of cognitive decline and increase the risk of Alzheimer's disease in particular. The ultimate accumulation of pathological CNS lesions may be modified by genetic influences, such as the apolipoprotein E ε4 allele and the environment. Lifestyle measures that maintain or improve cardiovascular health, including consumption of healthy diets, moderate use of alcohol, and implementation of regular physical exercise are important factors for brain protection (Mulder et al. 2001; Kalaria 2010; Sagare et al. 2012).

22.2.1 Neurodegenerative Processes

The neurodegenerative diseases have many processes in common, though these processes may be qualititatively, quantitatively, temporally, and spatially distinct. These include gene defects, intracellular calcium and oxidative stress, (toxic) protein misfolding, and accumulation that will affect different biological signaling pathways or molecular machineries to cause neuronal cell death by necrosis or apoptosis.

Gene defects play a major role in the pathogenesis of neurodegenerative disorders. Knowledge gained from genetic studies has provided insight into molecular mechanisms underlying the etiology and pathogenesis of many neurodegenerative disorders (Bertram et al. 2005). Many genetic determinants for human neurodegeneration have been identified over the years, and many of these have been reflected in animal models. In the presence of genetic defects, the course of a progressive neurodegenerative disorder can be greatly modified by environmental elements (Coppedè et al. 2006).

Oxidative stress is the result of disturbances in the normal redox state of cells that can cause toxic effects through the production of peroxides and free radicals (reactive oxygen species) that damage all components of the cell, including proteins, lipids, and DNA. Furthermore, some reactive oxidative species act as cellular messengers in redox signaling. Thus, oxidative stress can cause disruptions in normal mechanisms of cellular signaling and seems to have a ubiquitous role in mechanisms that induce cell death in neurodegenerative disease states (Sayre et al. 2008; Navarro and Boveris 2010; Perez-Pinzon et al. 2012; Arnold 2012). The role of iron seems particularly prominent in oxidative stress. The so-called iron-mediated oxidative stress pathway includes a reduction in antioxidant enzymes (e.g., peroxiredoxin, cytochrome c oxidase) and an induction of ferritin (Berg and Youdim 2006). Potent neuroprotective compounds have often been found to reverse the effects of aging on the expression of various mitochondrial and key regulator genes involved

in neurodegeneration, cell survival, synaptogenesis, oxidation, and metabolism (Weinreb et al. 2007a).

Protein misfolding and accumulation can cause disease. Protein misfolding may happen spontaneously or it can result when a protein follows the wrong folding pathway. The change into a toxic configuration is most likely to occur in proteins that have repetitive amino acid motifs, such as the polyglutamine expansion in the Huntingtin protein that is associated with as Huntington's disease. Remarkably, the toxic configuration is often able to interact with other native copies of the same protein and catalyze their transition into a toxic state, known as an "infective conformation." The newly made toxic proteins repeat the cycle in a self-sustaining loop, amplifying the toxicity and thus leading to a catastrophic effect that eventually kills the cell or impairs its function. A prime example of proteins that catalyze their own conformational change into the toxic form is that of the prion proteins (Soto 2008; Jellinger 2012). Abnormal accumulations of proteins and organelles in neurodegenerative diseases will do further damage to the axon as part of the pathogenic process and, in particular, compromise axonal transport. It is known that disruption of axonal transport is an early and perhaps causative event in many of these diseases (Stokin and Goldstein 2006; De Vos et al. 2008).

Finally, *cell death* occurs, as a result of necrosis and/or apoptosis. Necrosis is a form of traumatic cell death that results from acute cellular injury. In contrast, apoptosis generally confers advantages during an organism's life cycle, being instrumental in development and in homeostatic processes. Necrosis, as a passive process, does not require new protein synthesis, has only minimal energy requirements, and is not regulated by any homeostatic mechanism. Inappropriate death of cells in the nervous system is associated with multiple neurodegenerative disorders (Price et al. 1998; Artal-Sanz and Tavernarakis 2005; Krantic et al. 2005; Bertram and Tanzi 2005; Lessing and Bonini 2009; Soto and Estrada 2008; Gorman 2008). Neuronal apoptosis, the programmed natural death of neurons, is triggered either by the activation of a death receptor upon binding of its ligand, recruitment of specific proteins at the "death domain," downstream signaling through a cascade of protein–protein interactions (extrinsic pathway), or via mitochondria and the release of pro-apoptotic factors into the cytosol with subsequent activation of executioner caspases (intrinsic pathway). While apoptosis is an important process during neurogenesis and CNS maturation, premature apoptosis and/or an aberration in apoptosis regulation is implicated in the pathogenesis of neurodegeneration. Reactive oxygen species can initiate apoptosis via the mitochondrial and death receptor pathways (Okouchi et al. 2007).

Besides the many-shared mechanisms in neurodegeneration, certain characteristic features are unique to particular diseases, such as the selective vulnerability of a neuronal population or brain structure involved in the lesion. The reasons for such specificity as well as the mechanisms responsible for its selective nature are largely unknown. Here the main features of different neurodegenerative diseases are shortly described together with the processes that influence BBB function for consideration of drug transport into and within the brain.

22.2.2 Alzheimer's Disease

Alzheimer's disease is the most common neurodegenerative disease. It usually starts with declarative memory loss and confusion, which is initially difficult to distinguish from normal aging. With progression of the disease, increasing behavior and personality changes are accompanied by a further decline in cognitive abilities as well as worsening problems recognizing family and friends. Alzheimer's disease ultimately leads to a severe loss of mental function. Alzheimer's disease is specifically characterized by a loss of neurons and synapses in the cerebral cortex and certain subcortical regions. This loss results in gross atrophy of the affected regions, including degeneration in the temporal lobe and parietal lobe, and parts of the frontal cortex and cingulate gyrus (Wenk 2003).

There are three major hallmarks in the brain that are associated with the disease processes of Alzheimer's disease (Finder 2010). The *first* is the presence of amyloid (senile) plaques. Alzheimer's disease has been hypothesized to be a protein misfolding disease caused by accumulation of abnormally folded small amyloid-beta (Aβ) peptides that can vary between 39 and 43 amino acids in length. Aβ is a fragment from a larger protein called the amyloid precursor protein (APP). APP is a transmembrane protein that penetrates through the neuron's membrane, and is critical to neuron growth, survival, and postinjury repair. In Alzheimer's disease, an unknown process causes APP to be divided into smaller fragments by enzymes through proteolysis. A toxic 42 amino acid form of Aβ (Aβ1-42) gives rise to fibrils that form the core of senile plaques. The *second* hallmark is the presence of neurofibrillary tangles in the intracellular space of neurons, with high content of the protein "tau." Normal tau is required for healthy neurons. However, in Alzheimer's disease, hyperphosphorylated tau aggregates as neurofibrillary tangles to cause neuronal dysfunction and eventual cell death. The *third* hallmark is brain atrophy and shrinkage. Neurons that lose their connection with other neurons will die; this occurs throughout the Alzheimer's disease brain, causing affected regions to atrophy and shrink. Current treatments of Alzheimer's disease are symptomatic, i.e., they affect symptoms while not slowing the progression of the disease process. These treatments include drugs such as Donepezil (Aricept), rivastigmine (Exelon), galantamine (Razadyne), and Memantine (Namenda); they mostly help patients to carry out daily tasks by maintaining thinking, memory, and/or speaking skills. Treatment modalities interfering with neurodegenerative processes of Alzheimer's disease are still elusive.

Available evidence suggests that alteration of the BBB plays an important role in Alzheimer's disease (Zlokovic 2011; Miyakawa 2010). The BBB plays a regulatory role in the deposition of brain Aβ. Active transport of Aβ seems to occur by putative Aβ receptors that control the level of the soluble isoform of Aβ in brain. Influx of circulating Aβ is achieved via a specific receptor for advanced glycation end products (RAGE) and by gp330/megalin (LRP-2)-mediated transcytosis (Chun et al. 1999). There are also indications of transcytosis by cellular prion protein (PrP(c)) that binds Aβ(1–40) (Pflanzner et al. 2012). Aβ accumulation in the Alzheimer's affected

brain is likely due to its faulty clearance from the brain (Zlokovic et al. 2000; Selkoe 2011; Tanzi et al. 2004; Holtzman and Zlokovic 2007). The BBB efflux of brain-derived Aβ into blood is accomplished by the low-density lipoprotein receptor-related protein-1 (LRP1) and P-glycoprotein (P-gp, MDR1, ABCB1) (Kuhnke et al. 2007; Bell and Zlokovic 2009; Brenn et al. 2011; Sharma et al. 2012; Sagare et al. 2012; Vogelgesang et al. 2011; Hartz et al. 2010). In plasma, a soluble form of LRP1 (sLRP1) is the major transport protein for peripheral Aβ. sLRP1 maintains a plasma "sink" activity for Aβ through binding of peripheral Aβ which in turn inhibits reentry of free plasma Aβ into the brain. LRP1 in the liver mediates systemic clearance of Aβ. In Alzheimer's disease, LRP1 expression at the BBB is reduced and Aβ binding to circulating sLRP1 is compromised by oxidation (Sagare et al. 2012). Significantly reduced expression of P-gp, LRP1, and RAGE mRNA has been found in mice treated with Aβ(1–42), while breast cancer-resistance protein transporter (BCRP, ABCG2) expression was not affected; notably, expression of the four proteins was unchanged in mice treated with Aβ1-40 or reverse-sequence peptides (Brenn et al. 2011). This indicates that, in addition to the age-related decrease of P-gp expression, Aβ1-42 itself downregulates the expression of P-gp and other Aβ-transporters, which could exacerbate the intracerebral accumulation of Aβ and thereby accelerate neurodegeneration in Alzheimer's disease and cerebral β-amyloid angiopathy. Furthermore, an increased BBB permeability in Alzheimer's disease is also likely since structural damage of brain endothelial cells is quite frequently observed. Defects in LRP-1- and P-gp-mediated Aβ clearance from the brain are thought be triggered by systemic inflammation by lipopolysaccharide (LPS), leading to increased brain accumulation of Aβ (Erickson et al. 2012). This indicates that inflammation could induce and promote the disease. In addition, there are indications that ischemic events may directly contribute to enhancement of the amyloidogenic metabolism within the BBB, leading to intracellular deposition of Aβ(42), which may contribute to impaired Aβ clearance and related BBB dysfunction in Alzheimer's disease (Bulbarelli et al. 2012). Moreover, Aβ damages its own LRP1-mediated transport by oxidating LRP1 (Owen et al. 2010).

Another contributor in risk for Alzheimer's disease is reduced insulin effectiveness. Insulin appears to play an important role in brain aging and cognitive decline that is associated with pathological brain aging (Cholerton et al. 2011).

For treatment of Alzheimer's disease, it seems that cell surface LRP1 and circulating sLRP1 represent druggable targets which can be therapeutically modified to restore the physiological mechanisms of brain Aβ homeostasis. Enhancement of P-gp functionality might also be a novel therapeutic strategy to increase Aβ clearance out of the brain (Hartz et al. 2010; Abuznait et al. 2011). In addition, lifestyle-related conditions such as insulin resistance are amenable to both pharmacologic and lifestyle interventions to reduce the deleterious impact on the aging brain (Cholerton et al. 2011). More information is needed on what processes result in impairment of the BBB functionality in Alzheimer's disease as well as in "normal aging." BBB leakage in temporal lobe cortex of human Alzheimer brain samples shows wide variation but overall significantly increased leakage of the BBB with progression of Alzheimer-type pathology (Viggars et al. 2011). In a PET study

using 11C verapamil as a P-gp functionality ligand, no evidence was found for additional BBB dysfunction of P-gp in Alzheimer's disease patients with microbleeds (van Assema et al. 2012). Thus, it is not entirely clear what mechanisms lead to BBB leakage in the aging brain (Viggars et al. 2011).

22.2.3 Amyotrophic Lateral Sclerosis

Amyotrophic lateral sclerosis (ALS) is a rapidly progressive, invariably fatal disease. Brainstem and spinal cord neurons that are responsible for controlling voluntary muscles are damaged, with affected muscles subject to progressively increasing weakness and atrophy. First symptoms of compromised voluntary movement include difficulty in speaking and swallowing (if brainstem motor nuclei are first affected) or muscle weakness in the limbs (if spinal cord motor nuclei are first affected). Ultimately, when muscles in the diaphragm and chest wall fail to function properly, affected individuals cannot breathe without ventilatory support and ultimately die. The cause of amyotrophic lateral sclerosis is not known and no cure has yet been found.

The drug riluzole prolongs life by an average of 2–3 months. Other ALS treatments are designed to relieve symptoms and improve quality of life without significantly extending survival. A promising lead to understanding the motoneuron degeneration of ALS came with the finding that missense mutations in the gene encoding the antioxidant enzyme Cu/Zn superoxide dismutase 1 (SOD1) are associated with ALS (Andersen et al. 2003). Unfortunately, the pathogenic mechanism underlying SOD1 mutant toxicity has yet to be resolved.

Recent reports suggest that functional or structural defects of the BBB are implicated in ALS pathology. Damage to endothelia (PCAM-1), tight junctions (occludin), and basement membranes (collagen IV), possibly resulting from activation of matrix metallopeptidase 9 (MMP-9), precede the sequential changes of the disease. This damage occurs prior to motor neuron degeneration and is accompanied by MMP-9 upregulation (Miyazaki et al. 2011). This suggests that the neurovascular unit is a potential target for therapeutic intervention in ALS. Another recent specific finding is that the blood–spinal cord barrier is damaged in ALS, with erythrocyte extravasation that may be secondary to pericyte loss (Winkler et al. 2013).

22.2.4 Huntington's Disease

Huntington's disease is a familial disease, passed from parent to child through a mutation in the normal gene. The genetically programmed degeneration of neurons in certain areas of the brain results in uncontrolled, jerky movements (chorea), loss of intellectual faculties, and emotional disturbance. With the progression of the disease, concentration on intellectual tasks becomes increasingly difficult and

the patient may have difficulty self-feeding and swallowing. The rate of disease progression and the age of onset vary from person to person.

Some drugs used to treat Huntington's disease help control emotional and movement problems (antipsychotics, antidepressants, tranquilizers, mood-stabilizers, and Botulinum toxin), while Tetrabenazine (Xenazine, USA) is used to treat chorea associated with Huntington's disease. At this time, there is no way to stop or reverse the course of Huntington's disease.

Huntington's disease causes astrogliosis and loss of medium spiny neurons. Areas of the brain are affected according to their structure and the types of neurons they contain, reducing in size as cell loss increases. Degeneration occurs mainly in the striatum (with the caudate more affected than the putamen) but the frontal and temporal cortex is also affected (Bano et al. 2011). Striatal input to the external globus pallidus is reduced and, ultimately, inhibition of the subthalamic nuclei leads to decreased activity of the basal ganglia output nuclei (the internal globus pallidus and the substantia nigra pars reticulata). The basal ganglia output nuclei have inhibitory connections to motor-related areas of the thalamus that contribute to initiating and modulating motion. The weaker signals from the subthalamic nuclei resulting in decreased basal ganglia output (with corresponding *increased* activity in motor-related thalamic areas) in Huntington's disease therefore lead to the characteristic hyperkinetic, involuntary movements of the disorder.

Also in Huntington's disease, protein misfolding occurs for the aggregate-prone protein named mutant huntingtin, encoded by the highly polymorphic CAG trinucleotide repeat expansion in exon-1 of the huntingin gene. Normally, these proteins are retrogradely transported to the cell body for destruction by lysosomes. It seems that the mutant proteins aggregate and therewith compromise the retrograde transport of important cargo such as brain-derived neurotrophic factor (BDNF) by damaging molecular motors as well as microtubules (Bano et al. 2011); altered transport of growth factors (e.g., BDNF) provides a mechanism for affecting brain regions beyond simply those in which mutant huntingtin is expressed (Van Raamsdonk et al. 2007).

Furthermore, in a 3-nitropropionic acid (3-NPA) animal model of Huntington's disease, BBB disruption has been reported in injured areas of the striatum that result from application of this inhibitor of the mitochondrial citric acid cycle. 3-NPA was found to induce lesions with several BBB alterations, including an increase in permeability to both blood components and exogenous fluorescent dyes, the degradation of brain endothelial cells, and alterations in tight junction proteins and the basement membrane that suggest a role for MMP-9 in the BBB disruption (Duran-Vilaregut et al. 2011).

Aggregated polyglutamines, not inherently toxic as such, constitute a biomarker for mutant huntingtin, and may be useful for developing therapeutics (Chopra et al. 2007). The small molecule C2-8 inhibits polyglutamine aggregation in cell culture and brain slices and rescues degeneration of photoreceptors in a Drosophila model of Huntington's disease. C2-8-treated mice also show improved motor performance and reduced neuronal atrophy with smaller huntingtin aggregates.

C2-8 may therefore help in the elucidation of neurodegeneration mechanisms in Huntington's disease as well as represent a therapeutic lead for further optimization and development.

22.2.5 Multiple Sclerosis

Multiple sclerosis is considered to be an autoimmune CNS demyelinating disease that targets oligodendrocytes with sparing of axons until advanced stages of the disease. It can range from relatively benign to somewhat disabling to devastating, as communication between the brain and other parts of the body is disrupted. Symptoms may also vary with time. Many multiple sclerosis patients initially experience symptoms consisting of impaired vision, muscle weakness in their extremities, and/or difficulty with coordination and balance (McDonald et al. 2001). These symptoms may be severe enough to impair walking or even standing. In the worst cases, multiple sclerosis can produce partial or complete paralysis. Approximately half of all people with multiple sclerosis experience cognitive impairments such as difficulties with concentration, attention, memory, and poor judgment, but such symptoms are usually mild and are frequently overlooked. Depression is another common feature of multiple sclerosis.

No cure is yet available for multiple sclerosis. Many patients do well with no therapy at all, especially since many medications have serious side effects and some carry significant risks. Typical therapies include i the use of beta interferon, Copaxone, Novantrone, and dalfampridine. Steroids can be used to reduce the duration and severity of attacks in some patients. Spasticity is usually treated with muscle relaxants and tranquilizers such as baclofen, tizanidine, diazepam, clonazepam, and dantrolene. Other drugs are used as well for other relatively minor symptoms.

Formation of multiple sclerosis focal lesions follows extravasation of activated leukocytes from blood through the BBB into the CNS. Once the activated leukocytes enter the CNS environment, they propagate massive destruction to finally result in the loss of both myelin/oligodendrocyte complex and neurodegeneration. Multiple clinical and basic scientific observations support endothelial cell 'stress' and apoptosis as a characteristic hallmark of multiple sclerosis. The manipulation of endothelial cell biology, with the aim of blocking trans-endothelial migration of activated immune cells into the CNS, is a potent form of MS treatment, with the potential for significant reductions in disease activity and new lesion formation (Alon and Feigelson 2002; Minagar et al. 2012; Holman et al. 2011).

Magnetic resonance imaging (MRI) studies have shown that focal lesions are not entirely responsible for the diffuse neurodegeneration in multiple sclerosis (Filippi and Rocca 2005). Relapse prevention with disease-modifying drugs does not markedly influence the onset of irreversible disability or the progression of cerebral atrophy. It is now thought that clinical progression and chronic diffuse neurodegeneration both play a key role, developing independently from relapses and focal lesions. If this is indeed the case, then successfully treating the acute focal inflammation of MS will not be enough to forestall the progression to neurodegeneration. It will also be necessary to nullify the ongoing diffuse inflammation within the brain, behind the BBB.

Multiple sclerosis is a typical inflammatory disease, but axonal loss and neurodegeneration have been observed even in its earliest stages (Hendriks et al. 2005; Engelhardt and Ransohoff 2005; Minagar et al. 2012; Stangel 2012). Increasing evidence suggests that excessive glutamate is released at the site of demyelination

and axonal degeneration in multiple sclerosis plaques, and the most probable candidates for this cellular release are infiltrating leukocytes and activated microglia. These observations are no longer simply preclinical results obtained in the multiple sclerosis animal model (experimental allergic encephalomyelitis), but have already been partially confirmed by postmortem studies and in vivo analysis in multiple sclerosis patients, thus raising the possibility that modulation of glutamate release and transport as well as receptor blockade might be relevant targets for the development of future therapeutic interventions (Confavreux and Vukusic 2006; Vigeveno et al. 2012; Frigo et al. 2012). Furthermore, P-gp functionality seems to be impaired in neuroinflammation and may play a role in immunomodulation (Kooij et al. 2009, 2010). Multiple sclerosis is discussed extensively in the previous chapter (Chap. 21).

22.2.6 Parkinson's Disease

Parkinson's disease is a chronic, progressive neurological disorder lacking a cure. It belongs to the group of motor system disorders and results from a loss of dopamine-producing brain cells mostly in the substantia nigra, for which the cause is unknown. Parkinson's disease is the second most common neurodegenerative disease. Although Parkinson's disease is most common for ages above 60 years, many people are diagnosed at ages younger than 40 years. The core symptoms are tremor, rigidity (stiffness), bradykinesia (slowness of movement), and postural instability (balance difficulties). These symptoms become more pronounced with time. Patients may have difficulty walking, talking, or completing other simple tasks. As the disease progresses, the shaking, or tremor, which affects the majority of Parkinson's disease patients may begin to interfere with daily activities. Nonmotor aspects of Parkinson's disease include depression and anxiety, cognitive impairment, sleep disturbances, sensation of inner restlessness, loss of smell (anosmia), and disturbances of autonomic function. In advanced Parkinson's disease, intellectual and behavioral deterioration, aspiration pneumonia, and bedsores (due to immobility) are common.

Current drugs available for the treatment of Parkinson's disease are L-DOPA (usually combined with a peripheral decarboxylase inhibitor), synthetic dopamine receptor agonists, centrally acting antimuscarinic drugs, amantadine, monoamine oxidase-B inhibitors, and catechol-O-methyltransferase inhibitors. These drugs in essence only ameliorate the symptoms of the disease and therapeutic strategies aimed at stopping or modifying disease progression are still being sought (Deleu et al. 2002). Usually, patients are given levodopa (L-DOPA) combined with carbidopa. L-DOPA helps in many cases of Parkinson's disease, with bradykinesia and rigidity responding best, while tremor may be only marginally reduced. Problems with balance and other symptoms may not be alleviated at all. Anticholinergics may help control tremor and rigidity. Dopamine agonists such as bromocriptine, pramipexole, and ropinirole may offer some advantages over levodopa as they likely do

not require a transporter to cross the BBB (levodopa uses the large neutral amino acid transporter for this purpose) nor is enzymatic conversion necessary for their activation (levodopa must be converted to dopamine by DOPA decarboxylase once in the brain (Puiu et al. 2008). An antiviral drug, amantadine, also appears to reduce symptoms. Animal experimentation has provided many insights into the features of Parkinson's disease. Indeed, the roles of oxidative stress, apoptosis, mitochondrial dysfunction, inflammation, and impairment of the protein degradation pathways have been highlighted by work with animal models (Grünblatt et al. 2000; Bové and Perier 2012).

The mechanism by which the brain cells in Parkinson's disease are lost may consist of an abnormal accumulation of the protein alpha-synuclein bound to ubiquitin in the damaged cells. The alpha-synuclein-ubiquitin complex cannot be directed to the proteosome. This protein accumulation forms proteinaceous cytoplasmic inclusions called Lewy bodies, which are one of the hallmarks of Parkinson's disease (De Vos et al. 2008). Impaired axonal transport of alpha-synuclein may contribute to its accumulation in the form of Lewy bodies, as reduced transport rates have been reported for both wild-type and two familial Parkinson's disease-associated mutant alpha-synucleins in cultured neurons. In addition, membrane damage by alpha-synuclein could be another Parkinson's disease mechanism (De Vos et al. 2008).

Inflammation might be a risk factor by itself and not only a factor contributing to neurodegeneration. Hernández-Romero et al. (2012) investigated the impact of mild to moderate peripheral inflammation by carrageenan on the degeneration of dopaminergic neurons by intranigral injection of lipopolysaccharide (LPS) in animals. Peripheral inflammation increased the effect of intranigral LPS on the loss of dopaminergic neurons in the substantia nigra, in addition to increasing serum levels of the inflammatory markers TNF-α, IL-1β, IL-6, and C-reactive protein. Peripheral inflammation is also associated with damage to the BBB as well as the activation of microglia, loss of astrocytes, and the increased expression of proinflammatory cytokines, the adhesion molecule ICAM, and the enzyme iNOS.

The possible implications of BBB rupture for the increased loss of dopaminergic neurons has been studied using another Parkinson's disease animal model based on the intraperitoneal injection of rotenone. In this experiment, loss of dopaminergic neurons was also strengthened by carrageenan although this was achieved without obvious effects at the BBB (Hernández-Romero et al. 2012). Intracerebral injection of rotenone may provide a better model of Parkinson's disease (Ravenstijn et al. 2008) although this model does not produce concomitant changes in BBB transport for fluorescein and L-DOPA (Ravenstijn et al. 2012). The transport of bromocriptine across the BBB has been investigated in mice with MPTP-induced dopaminergic degeneration (Vautier et al. 2009); transport of the small compounds [14C]-sucrose and [3H]-inulin across the BBB was unaffected while P-gp and BCRP functionality did not appear to change. Conversely, BCRP expression studied on brain capillaries from MPTP-treated mice was decreased (1.3-fold) and P-gp expression increased (1.4-fold). While MPTP intoxication did not seem to alter BBB permeability, bromocriptine brain distribution was increased in MPTP mice, probably by interaction

with another transport mechanism. Overall, for Parkinson's disease there is not really consensus about the changes in BBB functionality (Desai et al. 2007; Ravenstijn et al. 2008, 2012).

Although the etiology of Parkinson's disease has not been clarified as yet, it is believed that aging, diet, diabetes, and adiposity play a role (Lu and Hu 2012). Type 2 diabetes and lipid abnormalities share multiple common pathophysiological mechanisms with Parkinson's disease, as does the gradual impairment of neurovascular function with aging. Neurovascular impairment may include (focal) changes in the BBB that may result in the passage of harmful elements that would not normally be able to cross the BBB; for example, pro-inflammatory factors, reactive oxygen species, and neurotoxins may infiltrate into the brain and trigger neural injury (Reale et al. 2009).

Most recent studies suggest that both central and peripheral inflammation may be dysregulated in Parkinson's disease, not only in animal models but also Parkinson's disease patients. This strengthens and extends the idea that peripheral dysregulation in the cytokine network is associated with Parkinson's disease. Therefore, therapeutic strategies aimed at modulating systemic inflammatory reactions or energy metabolism may facilitate neuroprotection in Parkinson's disease (Reale et al. 2009; Lu and Hu 2012).

22.2.7 Pharmacoresistant Epilepsy

Epilepsy is a common and diverse set of chronic neurological disorders characterized by recurrent seizures and/or induced brain alterations. The seizures happen when neurons, in clusters or individually, send out the wrong signals. Affected people may have strange sensations and emotions or behave strangely; with severe forms, they can exhibit violent muscle spasms and loss of consciousness. Anything that disturbs the normal pattern of neuron activity can lead to seizures, including illness, brain injury, and abnormal brain development. In many cases, however, the cause is unknown. Thus, epilepsy has many possible causes and there are several types of seizures. Epilepsy becomes more common as people age. Onset of new cases occurs most frequently in infants and the elderly. Underlying causes of of epilepsy may be related to brain trauma, stroke, and brain tumors.

Epilepsy is usually controlled, but not cured, with medication. For about 70 % of individuals with epilepsy, seizures can be controlled with drugs and/or surgery. Some drugs are more effective for specific types of seizures. Drugs include carbamazapine for partial seizures, ethosuximide for absence seizures without generalized tonic-clonic seizure, valproate for primary generalized epilepsies as well as partial seizures. Phenytoin is used in the control of various kinds of epilepsy and of seizures associated with neurosurgery. Newer anti-epileptic drugs are often used as add-on therapies and include lamotrigine, oxcarbazepine, topiramate, gabapentin, and levetiracetam.).

Despite the availability of numerous medications for epilepsy, ~30 % of patients have seizures that remain uncontrolled. This epileptic condition is called

pharmacoresistant, drug refractory, or intractable epilepsy. In pharmacoresistent epileptic patients, status epilepticus (serious, potentially life-threatening, neurologic emergency characterized by prolonged seizure activity) is more common and ongoing, and uncontrolled seizure activity may result in brain damage and neurodegeneration, especially in young children (Bittigau et al. 2002). Seizures from (medial) Temporal Lobe Epilepsy are most commonly pharmacoresistant (Volk et al. 2006) and the underlying mechanisms are still elusive. There are two main hypotheses for the cause of (or major contribution to) pharmacoresistance in epilepsy (Volk et al. 2006; Bethmann et al. 2008):

1. The target hypothesis—anti-epileptic drug efficacy is diminished due to reduced target sensitivity (e.g., GABA(A) receptor binding changes) (Volk et al. 2006).
2. The transporter hypothesis—anti-epileptic drug efficacy is diminished due to decreased brain levels resulting from localized overexpression of drug efflux transporters (mainly P-gp) in epileptogenic brain tissue.

Network alterations in response to brain damage associated with epilepsy may also result in changes in anti-epileptic drug efficiency (Bethmann et al. 2008; Ndode-Ekane et al. 2010).

Much research has implicated P-glycoprotein in epilepsy treatment inefficiency and in epileptogenesis (Marchi et al. 2004; Bankstahl et al. 2011; Löscher et al. 2011). Seizures may induce BBB transport changes (Padou et al. 1995; Sahin et al. 2003) and increased expression of P-gp at the BBB, as determined from both epileptogenic brain tissue of patients with pharmacoresistant epilepsy (Dombrowski et al. 2001) and in rodent models of temporal lobe epilepsy, including the pilocarpine model. In the latter, Bankstahl et al. (2008) found that seizure-induced glutamate release seems to be involved in the regulation of P-gp expression, which can be blocked by dizocilpine (also known as MK-801), a noncompetitive antagonist of the *N*-methyl-d-aspartate (NMDA) receptor. The finding that MK-801 counteracts both P-p overexpression and neuronal damage when administered after status epilepticus may offer a clinically useful therapeutic option in patients with drug resistant status epilepticus.

In normal brain tissue, MDR1/P-gp is expressed almost exclusively by the BBB, while in epileptic cortex it has been found that both brain endothelial cells and perivascular astrocytes express MDR1/P-gp. This change in P-gp may act as a second line of defense that may have profound implications for the pharmacokinetic properties of antiepileptic drugs and their capacity to reach neuronal targets (Marroni et al. 2003; Lee and Bendayan 2004; Bendayan et al. 2006). Using (mdr1a) P-gp knockout mice and wild-type mice, Sills et al. (2002) investigated the brain-to-serum concentration ratio for seven anti-epileptic drugs. Only topiramate yielded a higher brain-to-serum ratio in mdr1a(−/−) mice compared to that in wild-type controls at all time points investigated. No consistent effects were observed with any of the other anti-epileptic drugs studied.

In vitro studies by Luna-Tortos et al. (2009) have indicated that topiramate is a substrate for human P-gp. Potschka et al. (2003a, b) reported that brain microdialysis concentrations of phenytoin in rats were increased by local application of the

MRP transporter inhibitor probenecid; similarly, brain microdialysis concentrations of phenytoin were significantly higher in MRP2-deficient TR—rats than in normal rats. In the kindling model of epilepsy, oadministration of probenecid significantly increased the anticonvulsant activity of phenytoin, while in kindled MRP2-deficient rats phenytoin exerted a markedly higher anticonvulsant activity than in normal rats. These microdialysis data indicate that MRP2 could substantially contribute to BBB function, and that phenytoin appears to be a MRP2 substrate. While Hoffmann et al. (2006) did not find MRP2 expression in the brain of normal rats, clear MRP2 staining became visible in brain capillary endothelial cells and, less frequently, in perivascular astroglia and neurons after pilocarpine-induced convulsive status epilepticus (a model of temporal lobe epilepsy).

Baltes et al. (2007b) found that phenytoin and levetiracetam were transported by mouse, but not human, P-gp, and that carbamazepine was not transported by any type of P-gp. These data indicated that substrate recognition or transport efficacy by P-gp differs between human and mouse for certain anti-epileptic drugs. In vitro studies indicated that none of the common anti-epileptic drugs carbamazepine, valproate, levetiracetam, phenytoin, lamotrigine, and phenobarbital is transported by MRP1, MRP2, or MRP5, while valproate was transported by a yet unknown transporter which could be inhibited by MK571 and probenecid (Luna-Tortós et al. 2010). When specifically measuring P-gp-related BBB transport and intracerebral distribution, Syvänen et al. (2012) found in rats subjected to status epilepticus by kainate that by P-gp inhibition the intrabrain distribution of the strong and selective P-gp substrate quinidine was more affected than was BBB transport and extracellular brain concentrations. The results of this study combined with those obtained by positron emission tomography (PET) study using the same animals suggest that P-gp function in epilepsy might be altered specifically at the brain parenchymal level (Syvänen et al. 2011, 2012).

While it is established that efflux transporters are upregulated in drug-resistant epileptogenic brain tissue in humans and rodents, their role in removal of antiepileptic drugs from the brain remains controversial (Anderson and Shen 2007; Löscher et al. 2011; van Vliet et al. 2007). Nevertheless, P-gp inhibition by verapamil, administered directly into rat cerebral cortex, has been reported to modestly increase (up to twofold) the brain ECF-to-plasma concentration ratios of phenobarbital, phenytoin, lamotrigine, felbamate, carbamazepine, or oxcarbazepine (Clinckers et al. 2005a, b; Potschka et al. 2001; Potschka and Löscher 2001a, b). Furthermore, in rats with induced seizures, cyclosporine and tariquidar can reverse resistance to several antiepileptic drugs and increased their brain-to-plasma concentration ratio without changing their plasma pharmacokinetics (Brandt et al. 2006; Clinckers et al. 2005a, b; Mazarati et al. 2002).

Apart from a transport restriction and changes in multidrug efflux transporters, there might be a role for P450 metabolic enzymes in reducing brain concentrations of CNS therapeutics in drug-resistant pathologies such as refractory forms of epilepsy (Ghosh et al. 2011) and changes in cerebrovascular hemodynamic conditions can affect expression of P450 enzymes and multidrug transporter proteins.

Focal epilepsies are often associated with BBB leakage. For example, BBB leakage to albumin-bound Evans blue has been found in PTZ-induced epilepsy, with the location and pattern depending on the rat strain (Ates et al. 1999). Selective modulation of claudin expression in the brain by kindling epilepsy has also been found (Lamas et al. 2002). It has been observed during the process by which a normal brain develops epilepsy (epileptogenesis), immunoglobulin G (IgG) leakage and neuronal IgG uptake increase concomitantly with the occurrence of seizures and that IgG-positive neurons show signs of neurodegeneration, such as shrinkage and eosinophilia. This may suggest that IgG leakage is related to neuronal impairment and may be a pathogenic mechanism in epileptogenesis and chronic epilepsy (Michalak et al. 2012; Ndode-Ekane et al. 2010). Other studies point to a profound role of seizure-induced neuronal cyclooxygenase-2 (COX-2) expression in neuropathologies that accompany epileptogenesis (Serrano et al. 2011) and it is thought that epileptic seizures drive expression of the BBB efflux transporter P-gp via a glutamate/COX-2-mediated signaling pathway. Targeting this pathway may represent an innovative approach to control P-gp expression in the epileptic brain and to enhance brain delivery of antiepileptic drugs (van Vliet et al. 2010).

Many studies indicate important links to activation of the immune system with epilepsy. Zattoni et al. (2011) found that BBB disruption and neurodegeneration in the kainate-lesioned hippocampus were accompanied by sustained intercellular adhesion molecule 1 (ICAM-1) upregulation, microglial cell activation, and infiltration of cluster of differentiation 3 (+) T-cells (CD3(+) T-cells). Moreover, macrophage infiltration was selectively observed in the hippocampal dentate gyrus, where prominent granule cell dispersion was evident. Neurodegeneration was aggravated in kainate-lesioned mice lacking T- and B-cells (RAG1-knockout) through delayed invasion by Gr-1(+) neutrophils. The fact that these mutant mice also exhibited early onset of spontaneous recurrent seizures emphasizes the strong role immune-mediated responses can play in network excitability (Deprez et al. 2011).

ApoE isoforms exhibit diverse effects on neurodegenerative and neuroinflammatory disorders. As with other neurodegenerative diseases (e.g., Alzheimer's disease), apolipoprotein E (ApoE) genotype seems to play a significant role in epilepsy (Zhang et al. 2012). Overexpression of apoE4 has been shown to worsen KA-induced hippocampal neurodegeneration in C57BL/6 mice, possibly through an enhanced activation of microglia as compared to wildtype and apoE2 or apoE3 transgenic mice. New epilepsy treatments may utilize insulin-like growth factor-1(IGF-I) or vitamin E, particularly where standard therapies do not show efficacy. Administration of IGF-I has been shown to decrease seizure severity, [increase?] hippocampal neurogenesis, protects against neurodegeneration and abolishes cognitive deficits in an animal model of temporal lobe epilepsy (Miltiadous et al. 2011). Vitamin E (α-tocopherol, α-T) is of interest as it has been proposed to alleviate glia-mediated inflammation in neurological diseases; indeed, α-T dietary supplementation was found to prevent the oxidative stress, neuroglial overactivation, and cell death that normally occurs after kainate-induced seizures (Betti et al. 2011).

22.2.8 Traumatic Brain Injury

Traumatic brain injury (TBI) occurs when head injury causes damage to the brain. The worst injuries can lead to permanent brain damage or death. Symptoms of a traumatic brain injury may not appear until days or weeks following the injury. Serious traumatic brain injuries need emergency treatment and their long-term outcome depends on both the severity of the injury and the effectiveness of treatment. Traumatic brain injury can cause a wide range of changes affecting thinking, sensation, language, or emotions. It can also be associated with posttraumatic stress disorder. People with severe injuries usually need rehabilitation (Amenta et al. 2012; Shlosberg et al. 2010). One-third of patients, who have died of TBI, have Aβ plaques, which are pathological features of Alzheimer's disease, indicating that traumatic brain injury acts as an important risk factor for Alzheimer's disease (Sivanandam and Thakur 2012). TBI survivors also have a significantly higher risk of developing epilepsy (Christensen 2012).

The pathophysiology of traumatic brain injury consists of two main phases, a primary (mechanical) phase of damage and a secondary (delayed) phase of damage. Primary damage occurs at the moment of insult and includes contusion and laceration, diffuse axonal injury, and intracranial hemorrhage. Secondary damage includes processes that are initiated at the time of insult, but do not appear clinically for hours or even days after injury. Such processes cause brain swelling, axonal injury and hypoxia, changes in cerebral blood flow, disruption of BBB function, increased inflammatory responses, oxidative stress, neurodegeneration, and cognitive impairment (Pop and Badaut 2011; Sivanandam and Thakur 2012; Weber 2012). The calcium ion contributes greatly to the delayed cell damage and death after traumatic brain injury. A large, sustained influx of calcium into cells can initiate cell death signaling cascades, through activation of several degradative enzymes, such as proteases and endonucleases (Weber 2012). Potential influence on traumatic brain injury outcomes by polymorphisms in the BDNF gene, and genes involved in dopaminergic and serotonergic system functionality have been proposed to influence six specific cognitive and social functions: working memory, executive function, decision making, inhibition and impulsivity, aggression, and social and emotional function (Weaver et al. 2012).

While neurons have been the major focus of translational research in all types of brain injury, it has become clear that more attention is needed to treat neurovascular unit dysfunction because posttraumatic changes in the BBB are one of the major factors determining the progression of injury (Weber 2012). BBB changes observed after injury are implicated in neuronal loss, altered brain function (impaired consciousness, memory loss, and motor impairment), and alterations in the response to therapy (Chodobski et al. 2011). The disruption of tight junctions and basement membrane integrity result in increased paracellular permeability. Injury causes oxidative stress, and the increased production of proinflammatory mediators. Upregulation of expression of cell adhesion molecules on the surface of the BBB promote the influx of inflammatory cells into the traumatized brain parenchyma.

There is also evidence suggesting that brain injury can change the expression and/or activity of BBB-associated monocarboxylate transporter 2 (MCT2) transporters (Prins and Giza 2006). These findings suggest that BBB breakdown and functionality changes might be useful as biomarkers in the clinic and in drug trials (Shlosberg et al. 2010; Pop and Badaut 2011).

Acute-phase treatment of traumatic brain injury has improved substantially, but prevention and management of long-term complications remains difficult (Rosenfeld et al. 2012; Shlosberg et al. 2010). Recently, lithium has been investigated for its medium-phase effect on traumatic brain injury-induced neuronal death, microglial activation, and cyclooxygenase-2 induction in mice; all of these factors were attenuated by lithium treatment, which also decreased matrix metalloproteinase-9 expression and preserved BBB integrity (Yu et al. 2012). As for behavioral outcomes, lithium treatment reduced anxiety-like behavior and improved short- and long-term motor coordination. Another recent preclinical finding is that zinc seems to play a role in resilience to traumatic brain injury, making it potentially useful in populations at risk for injury (Cope et al. 2012).

22.2.9 Potential Strategies and Targets for Treatment of Neurodegenerative Diseases

When it comes to drug treatment of the neurodegenerative diseases, there are many potential targets to modulate and treatment strategies that have been suggested (Lindsay et al. 1993; Hefti 1994; McIntosh et al. 1998; Chun et al. 2000; Grünblatt et al. 2000; Contestabile 2001; Sánchez-Pérez et al. 2003; Lee and bendayan 2004; Youdim and Buccafusco 2005; Alexander et al. 2006; Confavreux and Vukusic 2006; Van der Schyf et al. 2006); however, very few successful treatment strategies have emerged while the number of new concepts and proposed therapeutic targets have risen dramatically (Ohtsuki and Terasaki 2007; Allain et al. 2008; Schneider and Mandelkow 2008; Abuznait et al. 2011; Luessi et al. 2012; Lu et al. 2011; Pop and Badaut 2011; Freeman et al. 2012; Gaillard et al. 2012; Grunblatt et al. 2012; Minagar et al. 2012; Perez-Simon et al. 2012; Ronaldson and Davis 2012).

In how far BBB functionality could play a role in future success of brain delivery of therapeutics to the proposed targets remains to be determined.

22.3 Dysfunction of the BBB in Neurodegenerative Diseases

The BBB is the regulated interface between the peripheral circulation and the CNS. The anatomical substrate of the BBB is the cerebral microvascular endothelium. Together with astrocytes, pericytes, neurons, and the extracellular matrix, it constitutes a “neurovascular unit” that is essential for the health and function of the CNS

(Hawkins and Davis 2005). Dysfunction of the neurovascular unit is associated with both acute and chronic neurologic disorders (Sandoval and Witt 2008; Zlokovic 2008, 2010) and pathogenesis associated with BBB breakdown (Abbott et al. 2002; Zlokovic 2008, 2010, 2011; Freeman and Keller 2012; Al Ahmad et al. 2012).

Tight junctions regulate paracellular flux and contribute to the maintenance of homeostasis. Tight junctions are composed of transmembrane proteins such as occludin, claudin 5, claudin-8, claudin 12, and junctional adhesion molecules. Each of these transmembrane proteins is anchored into the endothelial cells by another protein complex that includes zonula occludens proteins (ZO-1, ZO-2, and ZO-3) (Aijaz et al. 2006). The components and function of tight junctions are both affected by neurodegenerative processes (Zlokovic 2011).

Occludin is vulnerable to attack by matrix metalloproteinases (MMPs) (Rosenberg and Yang 2007; Yang and Rosenberg 2011), which may be activated in ischemic conditions. Accumulation of occludin in neurons, astrocytes, and microglia has also been reported in the brain tissue of Alzheimer's patients (Romanitan et al. 2007), suggesting a role for occludin in Alzheimer's disease pathogenesis.. Furthermore, dephosphorylation of occludin in a multiple sclerosis mouse model precedes visible signs of disease, before changes in the BBB permeability were observed. Occludin could therefore regulate the response of the BBB to the inflammatory environment as seen in multiple sclerosis (Morgan et al. 2007).

Claudin-5 is degraded by MMP-2 and MMP-9 after an ischemic insult and claudin-5 has been found in surrounding astrocytes, but not in the brain endothelium, after ischemia-related BBB disruption (Yang et al. 2007). Selective downregulation of *claudin-8* by kindling epilepsy (Lamas et al. 2002) suggests that selective modulation of claudin expression in response to abnormal neuronal synchronization may lead to BBB breakdown and brain edema. Significant differences in the incidences of tight junction abnormalities related to reduced ZO-1 expression have been observed between different types of lesions in multiple sclerosis and between multiple sclerosis and control white matter (Kirk et al. 2003).

Actin is important in the cytoskeleton for establishing and maintaining the BBB (Nico et al. 2003). Tau-induced neurotoxicity in Alzheimer's disease might be related to a direct interaction between tau and actin (Tudor et al. 2007).

The *basal lamina* that surrounds brain endothelial cells consists of laminin, fibronectin, tenascin, collagens, and proteoglycan (Paulsson 1992; Erickson and Couchman 2000; Merker 1994) and provides mechanical support for cell attachment. It also serves as a substratum for cell migration, separates surrounding tissue, and restricts the passage of macromolecules. Cell adhesion to the basal lamina involves integrins (Hynes and Lander 1992). The composition of the extracellular matrix is altered upon BBB disruption and directly affects the progression of brain diseases (Baeten and Akassoglou 2011). For example, MMPs can be activated to degrade basal lamina proteins such as fibronectin, laminin, and heparan sulfate after an ischemic insult, a process, which may contribute to BBB breakdown (Cheng et al. 2006; Zlokovic 2006; Zlokovic 2011).

The specialized foot-processes of *perivascular astrocytes* have specialized functions in inducing and regulating BBB properties. Neuronal influence may also be of

importance in BBB regulation (Banerjee and Bhat 2007; Wolburg et al. 2009; Cohen-Kashi et al. 2009; Girouard et al. 2010). Astrocytes properties may be affected upon development of amyloid deposits (Yang et al. 2011; Zlokovic 2011). Abnormal astrocytic activity coupled to vascular instability has been observed in Alzheimer's disease models (Takano et al. 2007).

The impact of *pericytes* on BBB functionality has become more appreciated with time (Balabanov and Dore-Duffy 1998; Krueger and Bechmann 2010). In addition to providing mechanical stability, pericytes predominantly influence vessel stability by matrix deposition and by the release and activation of signals that promote brain endothelial cell differentiation and quiescence (Armulik et al. 2011a, b). Pericytes furthermore play a regulatory role in brain angiogenesis, cerebral endothelial cell tight junction formation, BBB differentiation, and contribute to microvascular structural stability. Pericytes cover 30–70 % of the abluminal endothelial cell surface of brain capillaries (von Tell et al. 2006). Pericytes might have a role in the development of neuropathology in Alzheimer's disease, and multiple sclerosis, (Wyss-Coray et al. 2000; Allt and Lawrenson 2001; von Tell et al. 2006; Zlokovic 2011). Loss of pericytes may damage the BBB due to an associated decrease in cerebral capillary perfusion, blood flow, and blood flow responses to brain activation. This will lead to more chronic perfusion problems like hypoxia, while BBB breakdown may further lead to brain accumulation of blood proteins and several macromolecules with toxic effects on the vasculature and brain parenchyma, ultimately leading to secondary neuronal degeneration (Bell et al. 2010; Zlokovic 2011).

While it is well appreciated that APOE4 homozygosity is associated with an increased risk of sporadic Alzheimer's disease, its effects on the brain microvasculature and BBB have been less appreciated. Interestingly, APOE(4,4) is associated with thinning of the microvascular basement membrane in Alzheimer's disease (Bell et al. 2012). In APOE4 transgenic mice, a high fat diet-induced deleterious effects on BBB permeability (Mulder et al. 2001). A recent study by Bell et al. (2012) suggested that CypA is a key target for treating APOE4-mediated neurovascular injury and the resulting neuronal dysfunction and degeneration; indeed, activating a proinflammatory CypA-nuclear factor-κB-matrix-metalloproteinase-9 pathway in pericytes is associated with increased susceptibility of the BBB to injury in APOE4 conditions.

The BBB is rich in mitochondria and contains many *metabolic enzymes* that may contribute to its barrier function. These enzymes include ATP-ase, nicotinamide adenine dinucleotide, monoamine oxidase, acid and alkaline phosphatases, various dehydrogenases, L-DOPA decarboxylase and gamma glutamyl transpeptidase, cytochrome P450 haemoproteins, cytochrome P450-dependent mono-oxygenases, NADPH-cytochrome P450 reductase, epoxide hydrolase, and also conjugating enzymes such as UDP-glucuronosyltransferase and α-class glutathion S-transferase (Maxwell et al. 1987; Williams et al. 1980; Fukushima et al. 1990; Kerr et al. 1984; Tayarani et al. 1989; Volk et al. 1991; Dutheil et al. 2010; Zlokovic 2011). Apart from metabolizing compounds coming from the blood, they also help to eliminate degradation products of neurotransmitters (Baranczyk-Kuzma et al. 1989).

BBB enzymes also recognize and rapidly degrade most peptides, including naturally occurring neuropeptides (Brownless and Williams 1993; Witt et al. 2001).

Specific *facilitative and active transport systems* exist to transport nutrients such as hexoses, neutral, basic, and acidic amino acids, monocarboxylic acids, nucleosides, purines, amines, and vitamins, mostly towards the brain (Hawkins et al. 2006; Simpson et al. 2007; Ohtsuki and Terasaki 2007; Deeken and Loscher 2007; Spector and Johanson 2007; Spector 2009). It has been suggested that glutamate excitotoxicity is implicated in the neurodegenerative processes in Alzheimer's disease (Lipton 2005), amyotrophic lateral sclerosis (Van Damme et al. 2005), epilepsy (Alexander and Godwin 2006), Huntington's disease (HD) (Cowan and Raymond 2006; Fan et al. 2009), and multiple sclerosis (Vallejo-Illarramendi et al. 2006). Glutamate transporters (EAAT1, EAAT2, and EAAT3) at the BBB determine the levels of brain extracellular glutamate and are essential to prevent excitotoxicity (Lipton 2005), prompting the question whether changes in these transporters may contribute to glutamate excess and excitotoxicity.

Facilitative glucose transport is mediated by one or more members of the closely related glucose transporter (GLUT) family. GLUT1 is the primary transporter of glucose across the BBB. Its distribution and expression in brain is affected in different pathophysiological conditions including Alzheimer's disease, epilepsy, ischemia, and traumatic brain injury. Recent investigations show that GLUT1 mediates BBB transport of some neuroactive drugs, such as glycosylated neuropeptides, low molecular weight heparin, and D-glucose derivatives (Guo et al. 2005). Protein expression of the glucose transporter GLUT1 is reduced in brain capillaries in Alzheimer's disease, without changes in GLUT1 mRNA structure (Mooradian et al. 1997) or levels of GLUT1 mRNA transcripts (Wu et al. 2005). Further, a reduction in CNS energy metabolites has been seen in several PET scanning studies of Alzhiemer's patients using FDG (Samuraki et al. 2007; Mosconi et al. 2006, 2008), likely because the surface area at the BBB available for glucose transport is substantially reduced in Alzheimer's disease (Bailey et al. 2004; Wu et al. 2005)

Active efflux transporters such as the ATP-binding cassette (ABC) transporters rapidly remove ingested toxic lipophilic metabolites and many structurally unrelated, often amphipathic cationic drugs from the brain or prevent their entry (Schinkel et al. 1994; Loscher and Potschka 2005; Hermann and Bassetti 2007; Dutheil et al. 2010). Arguably, the most important efflux transporter is P-gp. P-gp is expressed at the luminal and seems also to be expressed at the abluminal membrane of brain endothelial cells, as well as in pericytes and astrocytes (Bendayan et al. 2006). Subcellularly, P-gp is distributed along the nuclear envelope, in caveolae, cytoplasmic vesicles, the Golgi complex, and the rough endoplasmic reticulum (Bendayan et al. 2006). The possible role of the ABC transporters in the pathogenesis and treatment of neurodegenerative diseases is increasingly recognized. A positive association between the polymorphism in the MDR1 gene encoding P-gp (/ABCB1) and pharmacoresistant epilepsy has been reported in a subset of epilepsy patients (Siddiqui et al. 2003). However, the follow-up association genetics studies did not support a major role for this polymorphism, as recently reviewed (Tate and Sisodiya 2007; Sisodiya and Mefford 2011). Then, reports also suggest that

P-gp-mediated elimination of Aβ from the brain in Alzheimer's disease may be impaired (Hartz et al. 2007)

Although the brain was once considered to be an immune privileged site, today it is appreciated that (a) the brain is not isolated from the immune system, (b) complex immune responses do occur within the CNS, and (c) brain microglia provide important CNS immune surveillance along with macrophages and monocytes derived from the blood and bone marrow (Prinz et al. 2011). Mononuclear phagocytes from blood are also recruited to cross the BBB and enter the CNS in multiple sclerosis and other neurodegenerative diseases like Alzheimer's disease. Chemokines in the brain can recruit immune cells from the blood or from within the brain (Britschgi and Wyss-Coray 2007) to secrete MMP-2 and MMP-9 that increase BBB permeability (Feng et al. 2011). Inhibition of this process is linked to more rapid disease progression (Dimitrijevic et al. 2007).

Finally, *cerebral blood flow* (CBF) plays a role. Reduction of resting CBF or altered responses to brain activation may occur in different CNS regions in Alzheimer' s disease, Parkinson's disease, multiple sclerosis, and other CNS diseases (Lo et al. 2003; Iadecola 2010; Drake and Iadecola 2007; Lok et al. 2007). Even modest 20 % reductions in CBF, as seen in the aging brain, are associated with diminished cerebral protein synthesis (Hossmann 1994). Moderate regional reductions in CBF, as seen in chronic neurodegenerative disorders, lead to shifts in intracellular pH and water, and accummulation of glutamate and lactate in brain ISF (Drake and Iadecola 2007), while severe reductions in CBF (>80 %), such as that which occur in ischemic stroke, lead to electrolyte dysbalance and ischemic neuronal death.

It can be concluded that changes in the BBB and its surrounding cells (the neurovascular unit), degeneration of brain capillariesand reductions in resting CBF all may contribute to neurodegenerative processes.

22.4 Brain Target Site Drug Delivery in Neurodegenerative Diseases

Lots of investigations have dealt with processes involved in neurodegenerative conditions of which only a small portion has been described above. With regard to drug treatment of such diseases, a proper CNS effect can only result from having the drug in the CNS "at the right place, at the right time, and at the right concentration" (see Chap. 10). To that end, it is of importance to take into consideration the factors that play a role in producing CNS effects, e.g., drug properties, drug concentrations in plasma, multiple BBB transport mechanisms, drug concentrations in brain and intrabrain drug distribution, target interaction, and signal transduction processes. Information on unbound drug concentrations are by far the most valuable as these provide specific information on BBB drug transport and intrabrain distribution, for which total concentrations may be misleading, while also being the driving force in eliciting CNS drug effects.

In relation to neurodegenerative diseases, only a few quantitative pharmacological studies on small molecules have been performed on unbound drug concentrations in brain, without/with inclusion of disease conditions and/or concomitant measures of the effects.

22.4.1 Unbound Plasma and Brain Pharmacokinetics

Most of the research presented here has been performed with regard to anti-epileptic drugs. As discussed above, pharmacoresistance in epilepsy is thought to be caused by restricted BBB transport and/or unfavorable brain distribution. It is therefore important to learn about BBB transport mechanisms of antiepileptic drugs.

Luer (1999) studied whether the fraction of gabapentin crossing the BBB is linear over a broad range of doses, using the microdialysis technique for measuring gabapentin concentrations in the brain ECF, combined with plasma sampling. Although higher AUC brain ECF values were obtained with higher AUC plasma values, changes in AUC brain ECF were less than proportional to observed changes in AUC plasma. It seemed that BBB transport of gabapentin was saturable.

Christensen et al. (2001) investigated plasma and cerebrospinal fluid (CSF) samples from epileptic adults on topiramate and lamotrigin. CSF/plasma ratios of topiramate were around 0.85, based on total concentrations of topiramate in plasma and CSF (with protein binding fractions of 84 % in plasma and 97 % in CSF). Lamotrigine concentrations were also measured, for which free concentrations in CSF were about 50 % of those in plasma. The authors concluded that for topiramate unbound plasma concentrations are most relevant for therapeutic drug monitoring. The effect of brain ECF–parenchymal exchange has been clearly demonstrated by a study of valproate in rabbits by Scism et al. (2000). It was shown that the unfavorable brain-to-plasma gradient was the result of coupled efflux transport processes at both the parenchymal cells and the BBB. BBB transport and brain distribution of valproic acid were investigated in the absence and presence of probenecid, using microdialysis and total tissue sampling during steady-state iv infusion of valproic acid. In control conditions, the intracellular brain concentration (ICC) was about 2.8 times higher than the corresponding ECF concentrations. Co-infusion of probenecid elevated the ratio of ICC over ECF concentrations to 4.2 (Table 22.1). This indicated the presence of a probenecid-sensitive efflux transporter on brain parenchymal cell membranes. The ECF to unbound plasma concentration ratio was about 0.2, and was not significantly influenced by probenecid. This study's findings therefore suggested the presence of distinctly different organic anion transporters for the efflux of valproic acid at the parenchymal cells and capillary endothelium.

Potschka et al. (2001) used in vivo microdialysis in rats to study whether the concentration of carbamazepine in brain ECF could be enhanced through P-gp inhibition by verapamil or MRP inhibition by probenecid. Local perfusion of verapamil or probenecid via the microdialysis probe increased the microdialysate concentration of carbamazepine, and the authors concluded that both P-gp (verapamil) and

Table 22.1 Results of microdialysis studies in rabbits

Valproate	Control ($n=5$)	+Probenecid ($n=5$)
ECF (ug/ml)	1.72 ± 0.16	2.78 ± 0.36
ICC (ug/ml)	4.69 ± 0.27	11.6 ± 1.62
Brain: total plasma	0.069 ± 0.002	0.16 ± 0.024
Brain: free plasma	0.41 ± 0.052	0.70 ± 0.087
Brain: ECF	2.48 ± 0.23	3.66 ± 0.36
ECF: total plasma	0.029 ± 0.003	0.044 ± 0.005
ECF: free plasma	0.17 ± 0.034	0.19 ± 0.015
ICC: ECF	2.81 ± 0.28	4.24 ± 0.44
ICC: free plasma	0.46 ± 0.068	0.81 ± 0.10

Valproic acid concentrations were determined in brain extracellular fluid (ECF) of the cerebral cortex during steady-state i.v. infusion with valproic acid alone or with valproic acid plus probenecid. Probenecid co-infusion elevated VPA concentration in the brain tissue surrounding the tip of the microdialysis probe to a greater extent than in the ECF (230 % versus 47 %). Brain intracellular compartment (ICC) concentration was estimated. In control rabbits, the ICC concentration was 2.8 ± 0.28 times higher than the ECF concentration. Probenecid co-infusion elevated the ICC-to-ECF concentration ratio to 4.2 ± 0.44, which confirms the existence of an efflux transport system in brain parenchymal cells. The ECF-to-unbound plasma concentration ratio was well below unity (0.029), indicating an uphill efflux transport of VPA across the BBB. Co-infusion of probenecid did not have a significant effect on valproic acid efflux at the BBB as evidenced by a minimal change in the ECF-to-unbound plasma concentration ratio. This study suggests the presence of distinctly different organic anion transporters for the efflux of valproic acid at the parenchymal cells and capillary endothelium in the brain (Scism et al. 2000)

MRP (probenecid) participate in the regulation of brain ECF concentrations of carbamazepine. A similar study was performed for phenytoin (Potschka and Löscher 2001a, b) in which local perfusion of probenecid via the microdialysis probe significantly enhanced the microdialysate concentrations of phenytoin. The same group later studied the influence of P-gp inhibition by verapamil on BBB transport of phenobarbital, lamotrigine, and felbamate again using in vivo microdialysis (Potschka et al. (2002). Verapamil was found to increase the concentration of all three antiepileptic drugs in the cortical brain ECF. Importantly, these studies indicated that overexpression of P-gp and/or MRP in epileptic tissue might limit brain access of many antiepileptic drugs.

For levitiracetam, a new antiepileptic drug, the expectations were quite high as it seemed to be an effective and well-tolerated drug in many patients with otherwise pharmacoresistant epilepsy. Potschka et al. (2004) therefore investigated whether the concentration of levitiracetam in the cortical brain ECF could be modulated by inhibition of P-gp or MRPs, using the P-gp inhibitor verapamil and the MRP1/2 inhibitor probenecid. Local perfusion with verapamil or probenecid via the microdialysis probe did not increase the brain ECF concentration of levitiracetam, providing strong evidence that brain uptake of levitiracetam is not affected by P-gp or MRP1/2. This could explain levitiracetam's antiepileptic efficacy in patients whose seizures are poorly controlled by other antiepileptic drugs. While the above microdialysis studies elegantly suggest the importance of transporters in determining drug

efficacy and which drugs may have potential in treating pharmacoresistant epilepsy, some caution is warranted. It remains theoretically possible that other nonspecific changes, e.g., changing osmolarity, may contribute to observed results when a drug (inhibitor) is locally perfused into the brain using in vivo microdialysis. More work is clearly necessary in this area.

22.4.2 Unbound Brain PKPD

Feng et al. (2001) have studied the BBB influx and efflux of pregabalin with microdialysis. BBB influx (CLin) and efflux (CLout) permeability for pregabalin were ~5 and 37 μL/min/g brain, respectively, following intravenous infusion. The results indicate that pregabalin is able to enter the brain. Interestingly, a significant delay in anticonvulsant action of pregabalin was found relative to the estimated ECF drug concentrations. Using a PKPD link model, the counter-clockwise delay in the relationship between pregabalin brain ECF concentration and the anticonvulsant effect showed that the concentration in the hypothetical effect compartment (Ce) versus effect (PD) profile exhibits a sigmoidal curve and the calculated EC50 and Keo values were 95 ng/ml and 0.0092 min^{-1}, respectively. The small value for the Keo indicates that the effect is not directly proportional to the amount of pregabalin in the ECF compartment possibly due to inherent delay at steps other than BBB transport.

It has also been investigated whether ABCC2 (/MRP2) is functionally involved in transport of carbamazepine, lamotrigine and felbamate across the BBB. The distribution of these drugs into the brain was determined using ABCC2-deficient TR-rats. The microdialysis results gave no evidence that ABCC2 function modulates entry of carbamazepine, lamotrigine, or felbamate into the CNS. However, ABCC2 deficiency was associated with an increased anticonvulsant response of carbamazepine in the amygdala-kindling model of epilepsy (Potschka et al. 2003a, b).

22.4.3 Unbound Plasma and Brain Pharmacokinetics in Disease

Clinckers et al. (2008) examined unbound concentrations of 10,11-dihydro-10-hydroxy-carbamazepine (MHD) in plasma and in the hippocampus to study the impact of acute seizures and efflux transport mechanisms on MHD brain distribution. An integrated PK model describing simultaneously the PK of MHD in plasma and brain was developed. A compartmental model with combined zero- and first-order absorption, including lag time and biophase distribution best described the PK of MHD. A distribution process appeared to underlie the increased brain MHD concentrations observed following seizure activity and efflux transport inhibition, as reflected by changes in the volume of distribution of the biophase compartment. In contrast, no changes were observed in plasma PK.

To study potential changes in brain P-gp functionality after induction of status epilepticus (SE), Syvänen et al. (2012) used a quinidine microdialysis assay in kainate-treated rats to reveal differences in brain distribution upon changes in P-gp functionality by preadministration of tariquidar, a P-gp inhibitor. In control animals, total brain quinidine concentration increased ~40-fold while quinidine ECF concentration increased ~sevenfold following tariquidar pretreatment. After kainate treatment alone, however, no difference in quinidine transport across the BBB was found compared to saline-treated (control) animals, but kainate-treated rats tended to have a lower total brain concentration but a higher brain ECF concentration of quinidine than control rats. This could be concluded on the basis of a newly developed mathematical population pharmacokinetic model that includes statistical approaches to identify sources of variability in quinidine kinetics within the whole datset (Fig. 22.1a, b). Notably, this study did not provide evidence for the hypothesis that P-gp function at the BBB is altered at 1 week after status epilepticus induction, but rather suggests that P-gp function might be altered at the brain parenchymal level.

22.4.4 Unbound Brain PKPD in Disease

As already discussed above, by using local perfusion of the MRP inhibitor probenecid via a microdialysis probe, Potschka and colleagues (2003a, b) have shown an increase in brain microdialysate levels of phenytoin in rats (reflecting, but not neccessarlity equals, unbound brain concentrations of phenytoin in brain). This seems to indicate that phenytoin is a substrate of MRP2 at the BBB. This was also concluded from studies in MRP2-deficient TR-rats, in which brain microdialysate levels of phenytoin were significantly higher than in normal background strain rats (Then, in the kindling model of epilepsy, coadministration of probenecid significantly increased the anticonvulsant activity of phenytoin, while in kindled MRP2-deficient rats phenytoin exerted a markedly higher anticonvulsant activity than in normal rats. Altogether this supports the hypothesis that MRP2 may contribute to BBB function.

The relation between brain ECF concentrations following systemic administration of oxcarbazepine and its effects on local ECF levels of dopamine and serotonin was investigated by Clinckers et al. (2005a), including modulation of oxcarbazepine BBB transport. The intrahippocampal perfusion of verapamil, a P-gp inhibitor, and probenecid, a MRP inhibitor, on the BBB passage of oxcarbazepine was investigated. Simultaneously, the effects on hippocampal monoamines were studied as pharmacodynamic markers for oxcarbazepine anticonvulsant activity in the focal pilocarpine model for limbic seizures. Systemic oxcarbazepine administration alone did not prevent the rats from developing seizures; however, coadministration of verapamil or probenecid with oxcarbazepine yielded complete protection along with significant increases in hippocampal ECF levels of dopamine and serotonin. These findings indicate that oxcarbazepine is a substrate for multidrug transporters at the BBB and that coadministration of multidrug transporter inhibitors

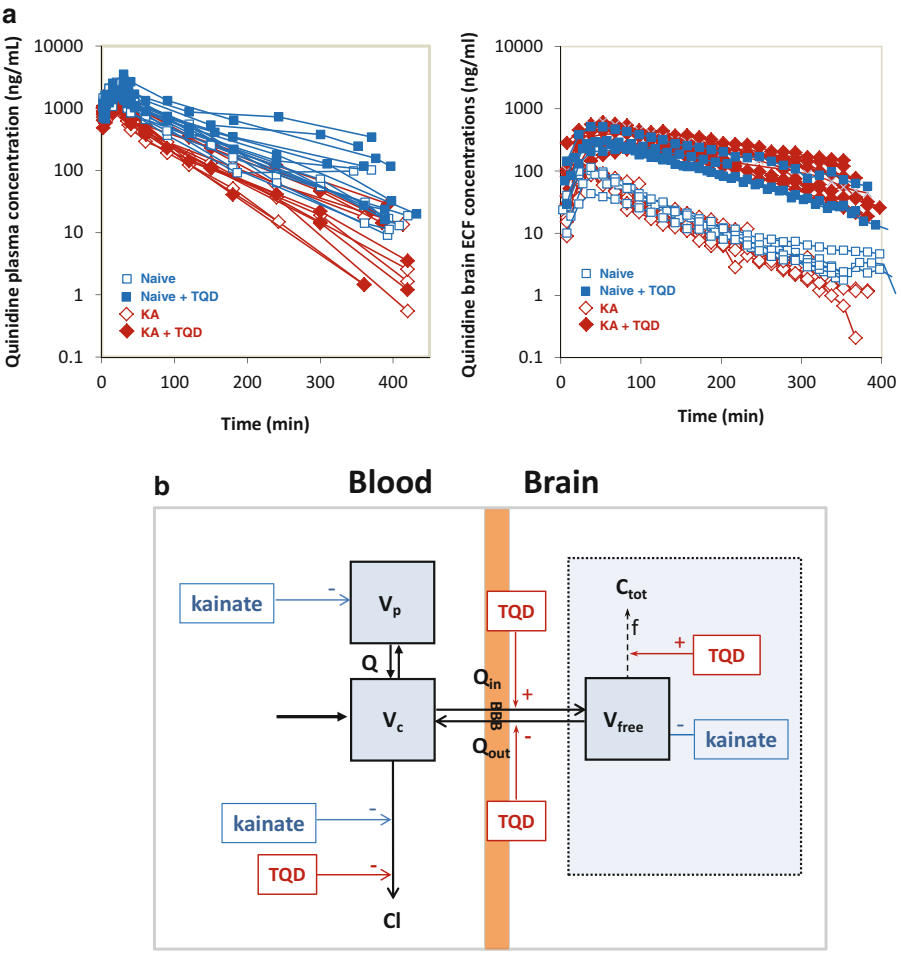

Fig. 22.1 (**a**) Pharmacokinetics of the P-gp substrate quinidine, in plasma (total concentrations) and brain (unbound concentrations) following an intravenous short infusion of 10 mg/kg in rats, for the naïve, naïve + Tariquidar (TQD), kainite treated, kaniate treated + Tarqiquidar (TQD) groups (Syvänen et al. 2012) (**b**) Pharmacokinetic model of quinidine distribution into the brain, including influences as determined by the so called covariate analysis, for P-gp inhibition by tariquidar (TQD) and of 1 week after kainate treatment induced Status Epilepticus (kainate). *Vc*, *Vp*, and *Vfree* are the volumes of distribution in central plasma, peripheral tissue and unbound brain, respectively. CL, *Q*, *Q*in, and *Q*out are the clearances from plasma, clearance between the two plasma compartments, and clearances into the brain and out from the brain, respectively. The distribution from the free brain compartment to the deeper brain compartment was described with a fraction, f, so that total brain concentration = *f*. unbound concentration in brain. The covariate analysis showed that kainate treatment decreased the systemic clearance, the volume of distribution in peripheral tissue and brain, while tariquidar coadministration decreased the systemic clearance, increased the quinidine clearance into the brain, decreased the clearance out from the brain and increased the distribution from the unbound brain compartment to the deeper brain compartment (Syvänen et al. 2012)

significantly potentiates oxcarbazepine anticonvulsant activity, highlighting the impact of BBB transport for the CNS effects of this antiepileptic drug.

Clinckers et al. (2005b) conducted an in vivo microdialysis study to investigate the impact of the transport kinetics of oxcarbazepine across the BBB on the observed treatment refractoriness. Also, the influence of intrahippocampal perfusion of verapamil, a P-gp inhibitor, and probenecid, a MPR inhibitor, on the BBB transport and anticonvulsant properties of oxcarbazepine were investigated, using the focal pilocarpine model for limbic seizures. Simultaneously, the effects on hippocampal monoamines were studied as pharmacodynamic markers for the anticonvulsant activity. Although systemic oxcarbazepine administration alone failed in preventing the animals from developing seizures, coadministration with verapamil or probenecid offered complete protection. Concomitantly, significant increases in extracellular hippocampal dopamine and serotonin levels were observed within our previously defined anticonvulsant monoamine range. The present data indicate that oxcarbazepine is a substrate for multidrug transporters at the blood–brain barrier. Coadministration with multidrug transporter inhibitors significantly potentiates the anticonvulsant activity of oxcarbazepine and offers opportunities for treatment of pharmacoresistant epilepsy.

To investigate potential changes in BBB transport of L-DOPA in conjunction with its intra-brain conversion in Parkinson's disease, Ravenstijn et al. (2012) used the unilateral rat rotenone model of Parkinson's disease (Ravenstijn et al. 2007). Microdialysis measurements were performed simultaneously in the control (untreated) and in the rotenone-treated cerebral hemisphere while L-DOPA was administered intravenously (10, 25 or 50 mg/kg). Serial blood samples and brain striatal microdialysates were analyzed for L-DOPA and dopamine metabolites (DOPAC and HVA). Ex-vivo brain tissue was analyzed for changes in tyrosine hydroxylase staining as a biomarker for disease model severity. An advanced mathematical model (Fig. 22.2a, b) was developed to evaluate BBB transport of L-DOPA along with the conversion of L-DOPA into DOPAC and HVA, and the results were compared between the control and rotenone-treated diseased cerebral hemispheres. As previously found for fluorescein (Ravenstijn et al. 2007), no difference in L-DOPA BBB transport was found in the rotenone-treated diseased hemisphere as compared to the untreated hemisphere. However, basal microdialysate levels of DOPAC and HVA were substantially lower in the rotenone-treated diseased hemisphere. Upon L-DOPA administration these elimination rates were higher at the rotenone-treated hemisphere. The higher elimination rate constant as found for DOPAC and HVA would be possible if dopamine concentrations were lower in the rotenone-treated diseased hemisphere such that metabolite formation rate-dependent elimination occurs. This is also called "flip-flop kinetics," i.e. [metabolite formation rate constant × amount of metabolite remaining to be formed] is about equal to the [metabolite elimination rate constant × amount of metabolite remaining to be eliminated]). Reduced dopamine concentrations in the rotenone-treated diseased hemisphere are indeed plausible with a diminished amount of dopaminergic neurons as indicated by substantially decreased TH staining. These studies show that it

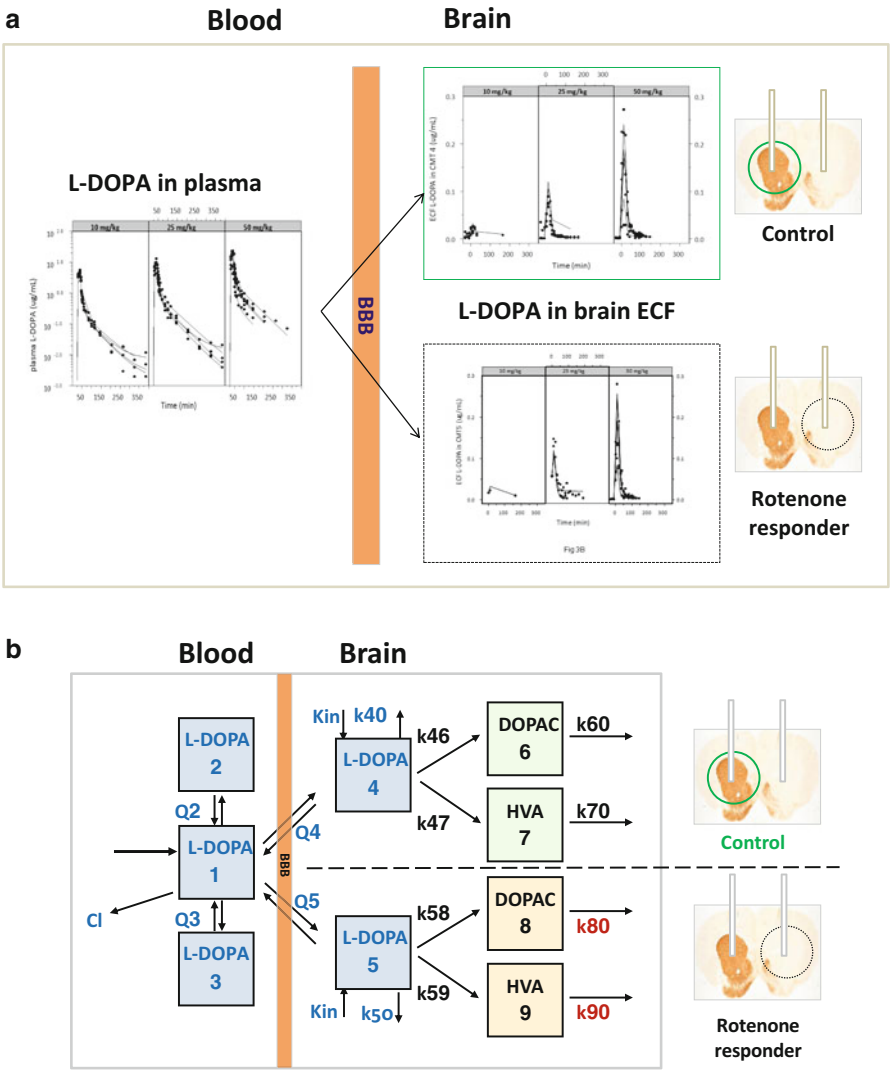

Fig. 22.2 (**a**) Pharmacokinetic profiles of L-DOPA obtained after a 20-min intravenous infusion in Lewis rats in plasma (*left*) and in brainECF in the control cerebral hemisphere (*right, upper part*) and in the rotenone-treated responder cerebral hemisphere (*right, lower part*) for three doses (10, 25, and 50 mg/kg). Depicted are the observed concentrations (*dots*) and individual model predictions (*solid lines*), separated by L-DOPA dose (Ravenstijn et al. 2012) (**b**) The population pharmacokinetic model for L-DOPA, DOPAC and HVA comprising of three compartments (*1–3*) describing the pharmacokinetics of L-DOPA in plasma, two compartments (*4* and *5*) describing the pharmacokinetics of L-DOPA in brainECF, one for the control cerebral hemisphere and one for the rotenone-treated responder cerebral hemisphere, two compartments (*6* and *8*) describing the kinetics of DOPAC in brainECF, one for the control cerebral hemisphere and one for the rotenone-treated responder cerebral hemisphere and two compartments (*7* and *9*) describing the kinetics of HVA in brainECF, one for the control cerebral hemisphere and one for the rotenone-treated responder cerebral hemisphere. (V = volume of distribution, Q = inter-compartmental clearance, k = elimination rate constant, Kin = endogenous formation rate constant of L-DOPA) (Ravenstijn et al. 2012)

is necessary to take into account both L-DOPA transport and conversion in order to appreciate whether or not specific changes in BBB transport may significantly influence L-DOPA PKPD in rodent models of Parkinson's disease.

22.5 Conclusions

The references presented in this chapter are by no means complete, as there is an extreme amount of publications in the area of neurodegeneration. Considerations of drug treatment have also been limited to small drugs with no information presented on biologics.

Most studies have focused exclusively on the processes underlying neurodegeneration when examining neurodegenerative diseases in human beings or animal models. However, it has become clear that the BBB/neurovascular unit may play an important role in neurodegenerative diseases by a number of different mechanisms, e.g., the exacerbation of neuroinflammation with increased entry of blood-borne immune cells into the diseased brain across the BBB.

There is a general consensus that delivery of drugs into the brain is among the most challenging problems in the treatment of neurodegeneration and that treatments should focus on increased BBB transport (Liu et al. 2012). However, the number of studies devoted to quantitative measurement of BBB transport of drugs, separate from intrabrain distribution, is surprisingly low. The few studies that have examined BBB transport and intrabrain distribution simultaneously (with the ability to separate the two factors) have shown a complex relationship between neurodegenerative disease states and BBB drug transport (Leroy et al. 2003; Cheng et al. 2010; Ravenstijn et al. 2007; Syvänen et al. 2012) (Potschka et al. 2003a, b; Clinckers et al. 2005a, b, 2008).

Moreover, many aspects of neurodegenerative processes have been studied more or less in isolation, so that information on interplay between these processes, as well as their time and context dependencies, has not been addressed. If we are to develop successful drug treatment modalities, we first need to have such information in hand, and we must aim to take more integrative research approaches combined with advanced mathematical modeling techniques. Otherwise, we risk missing out on critical information that would allow us to judge "what is wrong" on the causal path between drug dosing and effect (Chap. 9). It is possible that many drugs have more potential for treating neurodegeneration than currently appreciated, simply because they have not been studied thoroughly and quantitatively enough to reveal the right dosing, timing, and site of administration. Study designs too often suffer from a compromising superficiality (small sample sizes, variable practices in sample collection, variable contexts in sample collection, limiting numbers of parameters measured in conjunction), ultimately yielding inconsistent biomarker-related data and disparate outcome measures. New research approaches should bring us further and allow the kind of data collection necessary to better develop drug regimens for the treatment of neurodegenerative diseases.

Research on potential treatment strategies for neurodegenerative diseases is not an easy task. On the one hand, there are a large number of processes involved in neurodegenerative diseases with associated complexity. On the other hand, we have to work around the relative inaccessibility of the human brain to commonly used research tools. This means that we have to largely rely on animal models of neurodegenerative diseases, knowing that such animal models may only partly reflect the human conditions.

22.6 Points for Discussion

- How can studies be best designed to have the most valuable data collected?
- Why don't more studies aim to obtain quantitative and connected data?
- What biomarkers can be assessed in humans and in animals?
- What drug concentrations may be assessed in biological compartments, and, of these, which is best to predict CNS target site concentrations?
- How do animal models of disease provide valuable insights into human neurodegenerative processes and what are their limitations?
- How is the timescale of disease progression in animal models different from the human conditions?
- Given that neurodegeneration is highly heterogeneous, how can we address sources of variability between drug response in human populations to aim at personalized CNS medicine?
- What are the advantages of a "multitarget" drug treatment (/systems or network approach) compared to the more traditional "single target" drug treatment, given that neurodegenerative diseases are multifactorial?

22.7 Future Directions

Data on neurodegeneration so far has provided us with bits and pieces of information with valuable insights to a certain level, but much of this data is disconnected in the sense that different biological systems have been used, with disease conditions being induced by variable means. It is suggested that future studies should be designed to have a more structured and integrative nature, allowing us to learn about the interplay between processes and their sensitivity to the context in which they have been measured. The importance and challenge of performing integrative studies has already been addressed (Chap. 10) and also apply here. The following goals may facilitate future progress:

- To convert qualitative data (pictures, photographs, "increase" of parameter x, "decrease" of parameter y) into quantitative data.
- To include genomics, proteomics, and metabolomics data along with traditional measures of plasma and brain fluids.

- To increase the use of neuroimaging.
- To further include the outcomes of epidemiological studies on polymorphisms.
- To search for biomarkers of (early) disease processes and CNS drug effects.
- To include measurements of unbound drug concentrations as it is the unbound drug concentration that drives transport processes (BBB transport, intrabrain distribution, unbound brain concentrations) and target interactions that lead to drug effects.
- To include time-dependencies for drug kinetics, drug effects, and disease stage (progression).
- To obtain information on multiple parameters in parallel in a particular context (i.e., as much as possible; to obtain "connected data" (Paweletz et al. 2010) and vary the context in a systematic manner to learn about parameter sensitivity for the context (e.g., specific inhibition of processes). For example, it has been found that even in the same strain from two breeding locations, there are differences in seizure susceptibility, pharmacological response, and basal neurochemistry (Portelli et al. 2009).
- To obtain such "connected data" in animals by the use of both more- and less-invasive methods as well as noninvasive (imaging) techniques, the latter should also be applied in human studies (Greenhalgh et al. 2011).
- To include the use of advanced mathematical modeling to integrate all data, and by statistical approaches obtain insight into sources of variability (covariate), as this will improve interspecies extrapolation of pharmacokinetics to investigate the use of multiple drugs (a multitarget approach).

References

Abbott NJ, Khan EU, Rollinson CM, Reichel A, Janigro D, Dombrowski SM, Dobbie MS, Begley DJ (2002) Drug resistance in epilepsy: the role of the blood–brain barrier. Novartis Found Symp 243:38–47, discussion 47–53, 180–185

Abuznait AH, Cain C, Ingram D, Burk D, Kaddoumi A (2011) Up-regulation of P-glycoprotein reduces intracellular accumulation of beta amyloid: investigation of P-glycoprotein as a novel therapeutic target for Alzheimer's disease. J Pharm Pharmacol 63(8):1111–1118

Aijaz S, Balda MS, Matter K (2006) Tight junctions: molecular architecture and function. Int Rev Cytol 248:261–298

Al Ahmad A, Gassmann M, Ogunshola OO (2012) Involvement of oxidative stress in hypoxia-induced blood–brain barrier breakdown. Microvasc Res 84(2):222–225

Alexander GE, Chen K, Merkley TL, Reiman EM, Caselli RJ, Aschenbrenner M, Santerre-Lemmon L, Lewis DJ, Pietrini P, Teipel SJ, Hampel H, Rapoport SI, Moeller JR (2006) Regional network of magnetic resonance imaging gray matter volume in healthy aging. Neuroreport 17(10):951–956

Alexander GM, Godwin DW (2006) Metabotropic glutamate receptors as a strategic target for the treatment of epilepsy. Epilepsy Res 71:1–22

Allain H, Bentué-Ferrer D, Akwa Y (2008) Disease-modifying drugs and Parkinson's disease. Prog Neurobiol 84(1):25–39

Allt G, Lawrenson JG (2001) Pericytes: cell biology and pathology. Cells Tissues Organs 169:1–11

Alon R, Feigelson S (2002) From rolling to arrest on blood vessels: leukocyte tap dancing on endothelial integrin ligands and chemokines at sub-second contacts. Semin Immunol 14(2):93–104

Amenta PS, Jallo JI, Tuma RF, Elliott MB (2012) A cannabinoid type 2 receptor agonist attenuates blood–brain barrier damage and neurodegeneration in a murine model of traumatic brain injury. J Neurosci Res 90(12):2293–2305

Andersen PM, Sims KB, Xin WW, Kiely R, O'Neill G, Ravits J, Pioro E, Harati Y, Brower RD, Levine JS, Heinicke HU, Seltzer W, Boss M, Brown RH Jr (2003) Sixteen novel mutations in the Cu/Zn superoxide dismutase gene in amyotrophic lateral sclerosis: a decade of discoveries, defects and disputes. Amyotroph Lateral Scler Other Motor Neuron Disord 4(2):62–73

Anderson GD, Shen DD (2007) Where is the evidence that p-glycoprotein limits brain uptake of antiepileptic drug and contributes to drug resistance in epilepsy? Epilepsia 48(12):2372–2374

Armulik A, Genové G, Betsholtz C (2011a) Pericytes: developmental, physiological, and pathological perspectives, problems, and promises. Dev Cell 21(2):193–215

Armulik A, Mäe M, Betsholtz C (2011b) Pericytes and the blood–brain barrier: recent advances and implications for the delivery of CNS therapy. Ther Deliv 2(4):419–422

Arnold S (2012) The power of life–cytochrome c oxidase takes center stage in metabolic control, cell signalling and survival. Mitochondrion 12(1):46–56

Artal-Sanz M, Tavernarakis N (2005) Proteolytic mechanisms in necrotic cell death and neurodegeneration. FEBS Lett 579(15):3287–3296

Ates N, Esen N, Ilbay G (1999) Absence epilepsy and regional blood–brain barrier permeability: the effects of pentylenetetrazole-induced convulsions. Pharmacol Res 39(4):305–310

Baeten KM, Akassoglou K (2011) Extracellular matrix and matrix receptors in blood–brain barrier formation and stroke. Periodicals, inc. Dev Neurobiol 71:1018–1039

Bailey TL, Rivara CB, Rocher AB, Hof PR (2004) The nature and effects of cortical microvascular pathology in aging and Alzheimer's disease. Neurol Res 26:573–578

Balabanov R, Dore-Duffy P (1998) Role of the CNS microvascular pericyte in the blood–brain barrier. J Neurosci Res 53(6):637–644

Baltes S, Fedrowitz M, Tortós CL, Potschka H, Löscher W (2007a) Valproic acid is not a substrate for P-glycoprotein or multidrug resistance proteins 1 and 2 in a number of in vitro and in vivo transport assays. J Pharmacol Exp Ther 320(1):331–343

Baltes S, Gastens AM, Fedrowitz M, Potschka H, Kaever V, Löscher W (2007b) Differences in the transport of the antiepileptic drugs phenytoin, levetiracetam and carbamazepine by human and mouse P-glycoprotein. Neuropharmacology 52(2):333–346

Banerjee S, Bhat MA (2007) Neuron-glial interactions in blood–brain barrier formation. Annu Rev Neurosci 30:235–258

Bankstahl JP, Hoffmann K, Bethmann K, Löscher W (2008) Glutamate is critically involved in seizure-induced overexpression of P-glycoprotein in the brain. Neuropharmacology 54(6):1006–1016

Bankstahl JP, Bankstahl M, Kuntner C, Stanek J, Wanek T, Meier M, Ding XQ, Müller M, Langer O, Löscher W (2011) A novel positron emission tomography imaging protocol identifies seizure-induced regional overactivity of P-glycoprotein at the blood–brain barrier. J Neurosci 31(24):8803–8811

Bano D, Zanetti F, Mende Y, Nicotera P (2011) Neurodegenerative processes in Huntington's disease. Cell Death Dis 2(11):e228

Baranczyk-Kuzma A, Audus KL, Borchardt RT (1989) Catecholamine-metabolizing enzymes of bovine brain microvessel endothelial cell monolayers. J Neurochem 46(6):1956–1960

Bartels AL (2011) Blood–brain barrier P-glycoprotein function in neurodegenerative disease. Curr Pharm Des 17(26):2771–2777

Bell RD, Zlokovic BV (2009) Neurovascular mechanisms and blood–brain barrier disorder in Alzheimer's disease. Acta Neuropathol 118(1):103–113

Bell RD, Winkler EA, Sagare AP, Singh I, LaRue B, Deane R, Zlokovic BV (2010) Pericytes control key neurovascular functions and neuronal phenotype in the adult brain and during brain aging. Neuron 68(3):409–427

Bell RD, Winkler EA, Singh I, Sagare AP, Deane R, Wu Z, Holtzman DM, Betsholtz C, Armulik A, Sallstrom J, Berk BC, Zlokovic BV (2012) Apolipoprotein E controls cerebrovascular integrity via cyclophilin A. Nature 485(7399):512–516

Bendayan R, Ronaldson PT, Gingras D, Bendayan M (2006) In situ localization of P-glycoprotein (ABCB1) in human and rat brain. J Histochem Cytochem 54:1159–1167

Benkovic SA, O'Callaghan JP, Miller DB (2004) Sensitive indicators of injury reveal hippocampal damage in C57BL/6J mice treated with kainic acid in the absence of tonic-clonic seizures. Brain Res 1024(1–2):59–76

Berg D, Youdim MB (2006) Role of iron in neurodegenerative disorders. Top Magn Reson Imaging 17(1):5–17

Bertram L, Tanzi RE (2005) The genetic epidemiology of neurodegenerative disease. J Clin Invest 115(6):1449–1457

Bethmann K, Fritschy JM, Brandt C, Löscher W (2008) Antiepileptic drug resistant rats differ from drug responsive rats in GABA A receptor subunit expression in a model of temporal lobe epilepsy. Neurobiol Dis 31(2):169–187

Betti M, Minelli A, Ambrogini P, Ciuffoli S, Viola V, Galli F, Canonico B, Lattanzi D, Colombo E, Sestili P, Cuppini R (2011) Dietary supplementation with α-tocopherol reduces neuroinflammation and neuronal degeneration in the rat brain after kainic acid-induced status epilepticus. Free Radic Res 45(10):1136–1142

Bittigau P, Sifringer M, Genz K, Reith E, Pospischil D, Govindarajalu S, Dzietko M, Pesditschek S, Mai I, Dikranian K, Olney JW, Ikonomidou C (2002) Antiepileptic drugs and apoptotic neurodegeneration in the developing brain. Proc Natl Acad Sci U S A 99(23):15089–15094

Bové J, Perier C (2012) Neurotoxin-based models of Parkinson's disease. Neuroscience 211:51–76

Brandt C, Bethmann K, Gastens AM, Löscher W (2006) The multidrug transporter hypothesis of drug resistance in epilepsy: proof-of-principle in a rat model of temporal lobe epilepsy. Neurobiol Dis 24(1):202–211

Brenn A, Grube M, Peters M, Fischer A, Jedlitschky G, Kroemer HK, Warzok RW, Vogelgesang S (2011) Beta-amyloid downregulates MDR1-P-glycoprotein (Abcb1) expression at the blood–brain barrier in mice. Int J Alzheimers Dis 2011:690121

Britschgi M, Wyss-Coray T (2007) Immune cells may fend off Alzheimer disease. Nat Med 13:408–409

Brownless J, Williams CH (1993) Peptidases, peptides and the mammalian blood–brain barrier. J Neurochem 60:1089–1096

Bulbarelli A, Lonati E, Brambilla A, Orlando A, Cazzaniga E, Piazza F, Ferrarese C, Masserini M, Sancini G (2012) Aβ42 production in brain capillary endothelial cells after oxygen and glucose deprivation. Mol Cell Neurosci 49(4):415–422

Chalbot S, Zetterberg H, Blennow K, Fladby T, Andreasen N, Grundke-Iqbal I, Iqbal K (2011) Blood-cerebrospinal fluid barrier permeability in Alzheimer's disease. J Alzheimers Dis 25(3):505–515

Cheng T, Petraglia AL, Li Z, Thiyagarajan M, Zhong Z, Wu Z, Liu D, Maggirwar SB, Deane R, Fernandez JA, LaRue B, Griffin JH, Chopp M, Zlokovic BV (2006) Activated protein C inhibits tissue plasminogen activator-induced brain hemorrhage. Nat Med 12:1278–1285

Cheng Z, Zhang J, Liu H, Li Y, Zhao Y, Yang E (2010) Central nervous system penetration for small molecule therapeutic agents does not increase in multiple sclerosis- and Alzheimer's disease-related animal models despite reported blood–brain barrier disruption. Drug Metab Dispos 38(8):1355–1361

Chodobski A, Zink BJ, Szmydynger-Chodobska J (2011) Blood–brain barrier pathophysiology in traumatic brain injury. Transl Stroke Res 2(4):492–516

Cholerton B, Baker LD, Craft S (2011) Insulin resistance and pathological brain ageing. Diabet Med 28(12):1463–1475

Chopra V, Fox JH, Lieberman G, Dorsey K, Matson W, Waldmeier P, Housman DE, Kazantsev A, Young AB, Hersch S (2007) A small-molecule therapeutic lead for Huntington's disease: preclinical pharmacology and efficacy of C2-8 in the R6/2 transgenic mouse. Proc Natl Acad Sci U S A 104(42):16685–16689

Christensen J (2012) Traumatic brain injury: Risks of epilepsy and implications for medicolegal assessment. Epilepsia 53(Suppl 4):43–47
Christensen J, Højskov CS, Dam M, Poulsen JH (2001) Plasma concentration of topiramate correlates with cerebrospinal fluid concentration. Ther Drug Monit 23(5):529–535
Chun JT, Wang L, Pasinetti GM, Finch CE, Zlokovic BV (1999) Glycoprotein 330/megalin (LRP-2) has low prevalence as mRNA and protein in brain microvessels and choroid plexus. Exp Neurol 157(1):194–201
Chun HS, Son JJ, Son JH (2000) Identification of potential compounds promoting BDNF production in nigral dopaminergic neurons: clinical implication in Parkinson's disease. Neuroreport 11(3):511–514
Clinckers R, Smolders I, Meurs A, Ebinger G, Michotte Y (2005a) Quantitative in vivo microdialysis study on the influence of multidrug transporters on the blood–brain barrier passage of oxcarbazepine: concomitant use of hippocampal monoamines as pharmacodynamic markers for the anticonvulsant activity. J Pharmacol Exp Ther 314(2):725–731
Clinckers R, Smolders I, Meurs A, Ebinger G, Michotte Y (2005b) Hippocampal dopamine and serotonin elevations as pharmacodynamic markers for the anticonvulsant efficacy of oxcarbazepine and 10,11-dihydro-10-hydroxycarbamazepine. Neurosci Lett 390(1):48–53
Clinckers R, Smolders I, Michotte Y, Ebinger G, Danhof M, Voskuyl RA, Della PO (2008) Impact of efflux transporters and of seizures on the pharmacokinetics of oxcarbazepine metabolite in the rat brain. Br J Pharmacol 155(7):1127–1138
Cohen-Kashi MK, Cooper I, Teichberg VI (2009) Closing the gap between the in-vivo and in-vitro blood–brain barrier tightness. Brain Res 1284:12–21
Confavreux C, Vukusic S (2006) Accumulation of irreversible disability in multiple sclerosis: from epidemiology to treatment. Clin Neurol Neurosurg 108(3):327–332
Contestabile A (2001) Oxidative stress in neurodegeneration: mechanisms and therapeutic perspectives. Curr Top Med Chem 1(6):553–568
Cope EC, Morris DR, Levenson CW (2012) Improving treatments and outcomes: an emerging role for zinc in traumatic brain injury. Nutr Rev 70(7):410–413
Coppedè F, Mancuso M, Siciliano G, Migliore L, Murri L (2006) Genes and the environment in neurodegeneration. Biosci Rep 26(5):341–367
Cowan CM, Raymond LA (2006) Selective neuronal degeneration in Huntington's disease. Curr Top Dev Biol 75:25–71
Dalkara T, Gursoy-Ozdemir Y, Yemisci M (2011) Brain microvascular pericytes in health and disease. Acta Neuropathol 122(1):1–9
De Lange EC (2013) The mastermind approach to CNS drug therapy: translational prediction of human brain distribution, target site kinetics, and therapeutic effects. Fluids Barriers CNS 10(1):12
De Vos KJ, Grierson AJ, Ackerley S, Miller CJJ (2008) Role of axonal transport in neurodegenerative diseases. Annu Rev Neurosci 31:151–173
Deeken JF, Loscher W (2007) The blood–brain barrier and cancer: transporters, treatment, and Trojan horses. Clin Cancer Res 13:1663–1674
Deleu D, Northway MG, Hanssens Y (2002) Clinical pharmacokinetic and pharmacodynamic properties of drugs used in the treatment of Parkinson's disease. Clin Pharmacokinet 41(4): 261–309
Deprez F, Zattoni M, Mura ML, Frei K, Fritschy JM (2011) Adoptive transfer of T lymphocytes in immunodeficient mice influences epileptogenesis and neurodegeneration in a model of temporal lobe epilepsy. Neurobiol Dis 44(2):174–184
Desai BS, Monahan AJ, Carvey PM, Hendey B (2007) Blood–brain barrier pathology in Alzheimer's and Parkinson's disease: implications for drug therapy. Cell Transplant 16(3):285–299
Dimitrijevic OB, Stamatovic SM, Keep RF, Andjelkovic AV (2007) Absence of the chemokine receptor CCR2 protects against cerebral ischemia/reperfusion injury in mice. Stroke 38(4): 1345–1353

Dombrowski SM, Desai SY, Marroni M, Cucullo L, Goodrich K, Bingaman W, Mayberg MR, Bengez L, Janigro D (2001) Overexpression of multiple drug resistance genes in endothelial cells from patients with refractory epilepsy. Epilepsia 42(12):1501–1506

Dore-Duffy P, Cleary K (2011) Morphology and properties of pericytes. Methods Mol Biol 686:49–68

Drake CT, Iadecola C (2007) The role of neuronal signaling in controlling cerebral blood flow. Brain Lang 102:141–152

Duran-Vilaregut J, del Valle J, Manich G, Camins A, Pallàs M, Vilaplana J, Pelegrí C (2011) Role of matrix metalloproteinase-9 (MMP-9) in striatal blood–brain barrier disruption in a 3-nitropropionic acid model of Huntington's disease. Neuropathol Appl Neurobiol 37(5): 525–537

Dutheil F, Jacob A, Dauchy S, Beaune P, Scherrmann JM, Declèves X, Loriot MA (2010) ABC transporters and cytochromes P450 in the human central nervous system: influence on brain pharmacokinetics and contribution to neurodegenerative disorders. Expert Opin Drug Metab Toxicol 6(10):1161–1174

Engelhardt B, Ransohoff R (2005) The ins and outs of T-lymphocyte trafficking to the CNS: anatomical sites and molecular mechanisms. Trends Immunol 26:485–495

Erickson AC, Couchman JR (2000) Still more complexity in mammalian basement membranes. J Histochem Cytochem 48(10):1291–1306

Erickson MA, Hartvigson PE, Morofuji Y, Owen JB, Butterfield DA, Banks WA (2012) Lipopolysaccharide impairs amyloid beta efflux from brain: altered vascular sequestration, cerebrospinal fluid reabsorption, peripheral clearance and transporter function at the blood–brain barrier. J Neuroinflammation 9(1):150

Fan J, Cowan CM, Zhang LY, Hayden MR, Raymond LA (2009) Interaction of postsynaptic density protein-95 with NMDA receptors influences excitotoxicity in the yeast artificial chromosome mouse model of Huntington's disease. J Neurosci 29(35):10928–10938

Feng MR, Turluck D, Burleigh J, Lister R, Fan C, Middlebrook A, Taylor C, Su T (2001) Brain microdialysis and PK/PD correlation of pregabalin in rats. Eur J Drug Metab Pharmacokinet 26(1–2):123–128

Feng S, Cen J, Huang Y, Shen H, Yao L, Wang Y, Chen Z (2011) Matrix metalloproteinase-2 and −9 secreted by leukemic cells increase the permeability of blood–brain barrier by disrupting tight junction proteins. PLoS One 6(8):e20599

Filippi M, Rocca MA (2005) MRI evidence for multiple sclerosis as a diffuse disease of the central nervous system. J Neurol 252(Suppl 5):v16–v24

Finder VH (2010) Alzheimer's disease: a general introduction and pathomechanism. J Alzheimers Dis 22(Suppl 3):5–19

Freeman LR, Keller JN (2012) Oxidative stress and cerebral endothelial cells: regulation of the blood–brain-barrier and antioxidant based interventions. Biochim Biophys Acta 1822(5):822–829

Frigo M, Cogo MG, Fusco ML, Gardinetti M, Frigeni B (2012) Glutamate and multiple sclerosis. Curr Med Chem 19(9):1295–1299

Fukushima H, Fujimoto M, Ide M (1990) Quantitative detection of blood–brain barrier-associated enzymes in cultured endothelial cells of porcine brain microvessels. In Vitro Cell Dev Biol 26(6):612–620

Tudor AF, Elson-Schwab I, Khurana V, Steinhilb ML, Spires TL, Hyman BT, Feany MB (2007) Abnormal bundling and accumulation of F-actin mediates tau-induced neuronal degeneration in vivo. Nat Cell Biol 9:139–148

Gaillard PJ, Appeldoorn CC, Rip J, Dorland R, van der Pol SM, Kooij G, de Vries HE, Reijerkerk A (2012) Enhanced brain delivery of liposomal methylprednisolone improved therapeutic efficacy in a model of neuroinflammation. J Control Release 164(3):364–369

Ghosh C, Puvenna V, Gonzalez-Martinez J, Janigro D, Marchi N (2011) Blood–brain barrier P450 enzymes and multidrug transporters in drug resistance: a synergistic role in neurological diseases. Curr Drug Metab 12(8):742–749

Girouard H, Bonev AD, Hannah RM, Meredith A, Aldrich RW, Nelson MT (2010) Astrocytic endfoot Ca2+ and BK channels determine both arteriolar dilation and constriction. Proc Natl Acad Sci U S A 107(8):3811–3816

Gorman AM (2008) Neuronal cell death in neurodegenerative diseases: recurring themes around protein handling. J Cell Mol Med 12(6A):2263–2280
Götz ME, Künig G, Riederer P, Youdim MB (1994) Oxidative stress: free radical production in neural degeneration. Pharmacol Ther 63(1):37–122
Greenhalgh AD, Ogungbenro K, Rothwell NJ, Galea JP (2011) Translational pharmacokinetics: challenges of an emerging approach to drug development in stroke. Expert Opin Drug Metab Toxicol 7(6):681–695
Grünblatt E, Mandel S, Youdim MB (2000) MPTP and 6-hydroxydopamine-induced neurodegeneration as models for Parkinson's disease: neuroprotective strategies. J Neurol 247(Suppl 2): II95–II102
Guo X, Geng M, Du G (2005) Glucose transporter 1, distribution in the brain and in neural disorders: its relationship with transport of neuroactive drugs through the blood–brain barrier. Biochem Genet 43(3–4):175–187
Haass C, Selkoe DJ (2007) Soluble protein oligomers in neurodegeneration: lessons from the Alzheimer's amyloid beta-peptide. Nat Rev Mol Cell Biol 8(2):101–112
Hartz AM, Miller DS, Bauer B (2010) Restoring blood–brain barrier P-glycoprotein reduces brain amyloid-beta in a mouse model of Alzheimer's disease. Mol Pharmacol 77(5):715–723
Hawkins BT, Davis TP (2005) The blood–brain barrier/neurovascular unit in health and disease. Pharmacol Rev 57(2):173–185
Healy DP, Wilk S (1993) Localization of immunoreactive glutamyl aminopeptidase in rat brain. II. Distribution and correlation with angiotensin II. Brain Res 606:295–303
Hefti F (1994) Neurotrophic factor therapy for nervous system degenerative diseases. J Neurobiol 25(11):1418–1435
Hendriks JJ, Teunissen CE, de Vries HE, Dijkstra CD (2005) Macrophages and neurodegeneration. Brain Res Brain Res Rev 48(2):185–195
Hermann DM, Bassetti CL (2007) Implications of ATP-binding cassette transporters for brain pharmacotherapies. Trends Pharmacol Sci 28:128–134
Hernández-Romero MC, Delgado-Cortés MJ, Sarmiento M, de Pablos RM, Espinosa-Oliva AM, Argüelles S, Bández MJ, Villarán RF, Mauriño R, Santiago M, Venero JL, Herrera AJ, Cano J, Machado A (2012) Peripheral inflammation increases the deleterious effect of CNS inflammation on the nigrostriatal dopaminergic system. Neurotoxicology 33(3):347–360
Hoffmann K, Löscher W (2007) Upregulation of brain expression of P-glycoprotein in MRP2-deficient TR(−) rats resembles seizure-induced up-regulation of this drug efflux transporter in normal rats. Epilepsia 48(4):631–645
Hoffmann K, Gastens AM, Volk HA, Löscher W (2006) Expression of the multidrug transporter MRP2 in the blood–brain barrier after pilocarpine-induced seizures in rats. Epilepsy Res 69(1):1–14, Epub 2006 Feb 28
Holman DW, Klein RS, Ransohoff RM (2011) The blood–brain barrier, chemokines and multiple sclerosis. Biochim Biophys Acta 1812(2):220–230
Holtzman DM, Zlokovic BV (2007) Role of Ab transport and clearance in the pathogenesis and treatment of Alzheimer's disease. In: Sisodia S, Tanzi RE (eds) Alzheimer's disease: advances in genetics, molecular and cellular biology. Springer, New York, pp 179–198
Hossmann KA (1994) Viability thresholds and the penumbra of focal ischemia. Ann Neurol 36:557–565
Hynes RO, Lander AD (1992) Contact and adhesive specificities in the associations, migrations, and targeting of cells and axons. Cell 68(2):303–322
Iadecola C (2010) The overlap between neurodegenerative and vascular factors in the pathogenesis of dementia. Acta Neuropathol 120(3):287–296
Jellinger KA (2012) Interaction between pathogenic proteins in neurodegenerative disorders. J Cell Mol Med 16(6):1166–1183
Kalaria RN (2010) Vascular basis for brain degeneration: faltering controls and risk factors for dementia. Nutr Rev 68(Suppl 2):S74–S87
Kamouchi M, Ago T, Kuroda J, Kitazono T (2012) The possible roles of brain pericytes in brain ischemia and stroke. Cell Mol Neurobiol 32(2):159–165

Kannan P, John C, Zoghbi SS, Halldin C, Gottesman MM, Innis RB, Hall MD (2009) Imaging the function of P-glycoprotein with radiotracers: pharmacokinetics and in vivo applications. Clin Pharmacol Ther 86(4):368–377

Kaya M, Ahishali B (2011) Assessment of permeability in barrier type of endothelium in brain using tracers: Evans blue, sodium fluorescein, and horseradish peroxidase. Methods Mol Biol 763:369–382

Kaya M, Gurses C, Kalayci R, Ekizoglu O, Ahishali B, Orhan N, Oku B, Arican N, Ustek D, Bilgic B, Elmas I, Kucuk M, Kemikler G (2008) Morphological and functional changes of blood–brain barrier in kindled rats with cortical dysplasia. Brain Res 1208:181–191

Kerr IG, Zimm S, Collins JM, O'Neill D, Poplack DG (1984) Effect of intravenous dose and schedule on cerebrospinal fluid pharmacokinetics of 5-fluorouracil in the monkey. Cancer Res 44:4929–4932

Kirk J, Plumb J, Mirakhur M, McQuaid S (2003) Tight junctional abnormality in multiple sclerosis white matter affects all calibres of vessel and is associated with blood–brain barrier leakage and active demyelination. J Pathol 201:319–327

Kooij G, Backer R, Koning JJ, Reijerkerk A, van Horssen J, van der Pol SM, Drexhage J, Schinkel A, Dijkstra CD, den Haan JM, Geijtenbeek TB, de Vries HE (2009) P-glycoprotein acts as an immunomodulator during neuroinflammation. PLoS One 4(12):e8212

Kooij G, van Horssen J, de Lange EC, Reijerkerk A, van der Pol SM, van Het Hof B, Drexhage J, Vennegoor A, Killestein J, Scheffer G, Oerlemans R, Scheper R, van der Valk P, Dijkstra CD, de Vries HE (2010) T lymphocytes impair P-glycoprotein function during neuroinflammation. J Autoimmun 34(4):416–425

Krantic S, Mechawar N, Reix S, Quirion R (2005) Molecular basis of programmed cell death involved in neurodegeneration. Trends Neurosci 28(12):670–676

Krueger M, Bechmann I (2010) CNS pericytes: concepts, misconceptions, and a way out. Glia 58(1):1–10

Kuhnke D, Jedlitschky G, Grube M, Krohn M, Jucker M, Mosyagin I, Cascorbi I, Walker LC, Kroemer HK, Warzok RW, Vogelgesang S (2007) MDR1-P-glycoprotein (ABCB1) mediates transport of Alzheimer's amyloid-beta peptides–implications for the mechanisms of abeta clearance at the blood–brain barrier. Brain Pathol 17(4):347–353

Kunz J, Krause D, Kremer M, Dermietzel R (1994) The 140 kDa protein of blood–brain barrier-associated pericytes is identical to aminopeptidase N. J Neurochem 62:2375–2386

Kunz J, Krause D, Gehrmann J, Dermietzel R (1995) Changes in the expression pattern of blood–brain barrier-associated pericytic aminopeptidase N (pAPN) in the course of acute experimental auto-immune encephalomyelitis. J Neuroimmunol 59:41–55

Lamas M, González-Mariscal L, Gutiérrez R (2002) Presence of claudins mRNA in the brain. Selective modulation of expression by kindling epilepsy. Brain Res Mol Brain Res 104(2):250–254

Lee G, Bendayan R (2004) Functional expression and localization of P-glycoprotein in the central nervous system: relevance to the pathogenesis and treatment of neurological disorders. Pharm Res 21(8):1313–1330

Leroy C, Roch C, Koning E, Namer IJ, Nehlig A (2003) In the lithium-pilocarpine model of epilepsy, brain lesions are not linked to changes in blood–brain barrier permeability: an autoradiographic study in adult and developing rats. Exp Neurol 182(2):361–372

Lessing D, Bonini NM (2009) Maintaining the brain: insight into human neurodegeneration from Drosophila melanogaster mutants. Nature Rev Genet 10:359–370

Lindsay RM, Altar CA, Cedarbaum JM, Hyman C, Wiegand SJ (1993) The therapeutic potential of neurotrophic factors in the treatment of Parkinson's disease. Exp Neurol 124(1):103R–118R

Lipton SA (2005) The molecular basis of memantine action in Alzheimer's disease and other neurologic disorders: low-affinity, uncompetitive antagonism. Curr Alzheimer Res 2:155–165

Liu JY, Thom M, Catarino CB, Martinian L, Figarella-Branger D, Bartolomei F, Koepp M, Sisodiya SM (2012) Neuropathology of the blood–brain barrier and pharmacoresistance in human epilepsy. Brain 135(Pt 10):3115–3133

Lo EH, Dalkara T, Moskowitz MA (2003) Mechanisms, challenges and opportunities in stroke. Nat Rev Neurosci 4:399–415

Lok J, Gupta P, Guo S, Kim WJ, Whalen MJ, van Leyen K, Lo EH (2007) Cell-cell signaling in the neurovascular unit. Neurochem Res 32:2032–2045
Loscher W, Potschka H (2005) Drug resistance in brain diseases and the role of drug efflux transporters. Nat Rev Neurosci 6:591–602
Löscher W, Luna-Tortós C, Römermann K, Fedrowitz M (2011) Do ATP-binding cassette transporters cause pharmacoresistance in epilepsy? Problems and approaches in determining which antiepileptic drugs are affected. Curr Pharm Des 17(26):2808–2828
Lu M, Hu G (2012) Targeting metabolic inflammation in Parkinson's disease: implications for prospective therapeutic strategies. Clin Exp Pharmacol Physiol 39(6):577–585
Luer MS (1999) Interventions to achieve tonic exposure to levodopa: delaying or preventing the onset of motor complications. Pharmacotherapy 19(11 Pt 2):169S–179S
Luessi F, Siffrin V, Zipp F (2012) Neurodegeneration in multiple sclerosis: novel treatment strategies. Expert Rev Neurother 12(9):1061–1077
Luna-Tortós C, Rambeck B, Jürgens UH, Löscher W (2009) The antiepileptic drug topiramate is a substrate for human P-glycoprotein but not multidrug resistance proteins. Pharm Res 26(11):2464–2470
Luna-Tortós C, Fedrowitz M, Löscher W (2010) Evaluation of transport of common antiepileptic drugs by human multidrug resistance-associated proteins (MRP1, 2 and 5) that are overexpressed in pharmacoresistant epilepsy. Neuropharmacology 58(7):1019–1032
Marchi N, Hallene KL, Kight KM, Cucullo L, Moddel G, Bingaman W, Dini G, Vezzani A, Janigro D (2004) Significance of MDR1 and multiple drug resistance in refractory human epileptic brain. BMC Med 2:37
Marroni M, Marchi N, Cucullo L, Abbott NJ, Signorelli K, Janigro D (2003) Vascular and parenchymal mechanisms in multiple drug resistance: a lesson from human epilepsy. Curr Drug Targets 4(4):297–304
Maxwell K, Berliner JA, Cancilla PA (1987) Induction of gamma glutamyltranspeptidase in cultured cerebral endothelial cells by a product released by astrocytes. Brain Res 410:309–314
Mazarati AM, Sofia RD, Wasterlain CG (2002) Anticonvulsant and antiepileptogenic effects of fluorofelbamate in experimental status epilepticus. Seizure 11(7):423–430
McDonald WI, Compston A, Edan G, Goodkin D, Hartung HP, Lublin FD, McFarland HF, Paty DW, Polman CH, Reingold SC, Sandberg-Wollheim M, Sibley W, Thompson A, van den Noort S, Weinshenker BY, Wolinsky JS (2001) Recommended diagnostic criteria for multiple sclerosis: guidelines from the International Panel on the diagnosis of multiple sclerosis. Ann Neurol 50(1):121–127
McIntosh TK, Juhler M, Wieloch T (1998) Novel pharmacologic strategies in the treatment of experimental traumatic brain injury: 1998. J Neurotrauma 15(10):731–769
Merker HJ (1994) Morphology of the basement membrane. Microsc Res Tech 28(2):95–124
Meyer J, Mischek U, Vehyl M, Henzel K, Galla H-J (1990) Blood–brain barrier characteristic enzymatic properties in cultured brain capillary endothelial cells. Brain Res 514:305–309
Michalak Z, Lebrun A, Di Miceli M, Rousset MC, Crespel A, Coubes P, Henshall DC, Lerner-Natoli M, Rigau V (2012) IgG leakage may contribute to neuronal dysfunction in drug-refractory epilepsies with blood–brain barrier disruption. J Neuropathol Exp Neurol 71(9):826–838
Miltiadous P, Stamatakis A, Koutsoudaki PN, Tiniakos DG, Stylianopoulou F (2011) IGF-I ameliorates hippocampal neurodegeneration and protects against cognitive deficits in an animal model of temporal lobe epilepsy. Exp Neurol 231(2):223–235
Minagar A, Maghzi AH, McGee JC, Alexander JS (2012) Emerging roles of endothelial cells in multiple sclerosis pathophysiology and therapy. Neurol Res 34(8):738–745
Miyakawa T (2010) Vascular pathology in Alzheimer's disease. Psychogeriatrics 10(1):39–44
Miyazaki K, Ohta Y, Nagai M, Morimoto N, Kurata T, Takehisa Y, Ikeda Y, Matsuura T, Abe K (2011) Disruption of neurovascular unit prior to motor neuron degeneration in amyotrophic lateral sclerosis. J Neurosci Res 89(5):718–728
Mooradian AD, Chung HC, Shah GN (1997) GLUT-1 expression in the cerebra of patients with Alzheimer's disease. Neurobiol Aging 18:469–474

Morgan L, Shah B, Rivers LE, Barden L, Groom AJ, Chung R, Higazi D, Desmond H, Smith T, Staddon JM (2007) Inflammation and dephosphorylation of the tight junction protein occludin in an experimental model of multiple sclerosis. Neuroscience 147:664–673

Mosconi L, Sorbi S, de Leon MJ, Li Y, Nacmias B, Myoung PS, Tsui W, Ginestroni A, Bessi V, Fayyazz M, Caffarra P, Pupi A (2006) Hypometabolism exceeds atrophy in presymptomatic early-onset familial Alzheimer's disease. J Nucl Med 47(11):1778–1786

Mosconi L, De Santi S, Li J, Tsui WH, Li Y, Boppana M, Laska E, Rusinek H, de Leon MJ (2008) Hippocampal hypometabolism predicts cognitive decline from normal aging. Neurobiol Aging 29(5):676–692

Mulder M, Blokland A, van den Berg DJ, Schulten H, Bakker AHF, Terwel D, Honig W, de Kloet ER, Havekes LM, Steinbusch HWM, de Lange ECM (2001) Apolipoprotein E protects against neuropathology induced by a high-fat diet and maintains the integrity of the blood–brain barrier during aging. Lab Invest 81(7):953–960

Nakagawa S, Deli MA, Nakao S, Honda M, Hayashi K, Nakaoke R, Kataoka Y, Niwa M (2007) Pericytes from brain microvessels strengthen the barrier integrity in primary cultures of rat brain endothelial cells. Cell Mol Neurobiol 27(6):687–694

Navarro A, Boveris A (2010) Brain mitochondrial dysfunction in aging, neurodegeneration, and Parkinson's disease. Front Aging Neurosci 2:34

Ndode-Ekane XE, Hayward N, Gröhn O, Pitkänen A (2010) Vascular changes in epilepsy: functional consequences and association with network plasticity in pilocarpine-induced experimental epilepsy. Neuroscience 166(1):312–332

Nico B, Frigeri A, Nicchia GP, Corsi P, Ribatti D, Quondamatteo F, Herken R, Girolamo F, Marzullo A, Svelto M, Svelto M, Roncali L (2003) Severe alterations of endothelial and glial cells in the blood–brain barrier of dystrophic mdx mice. Glia 42:235–251

Ohtsuki S, Terasaki T (2007) Contribution of carrier-mediated transport systems to the blood–brain barrier as a supporting and protecting interface for the brain; importance for CNS drug discovery and development. Pharm Res 24:1745–1758

Okouchi M, Ekshyyan O, Maracine M, Aw TY (2007) Neuronal apoptosis in neurodegeneration. Antioxid Redox Signal 9(8):1059–1096

Owen JB, Sultana R, Aluise CD, Erickson MA, Price TO, Bu G, Banks WA, Butterfield DA (2010) Oxidative modification to LDL receptor-related protein 1 in hippocampus from subjects with Alzheimer disease: implications for Aβ accumulation in AD brain. Free Radic Biol Med 49(11):1798–1803

Padou V, Boyet S, Nehlig A (1995) Changes in transport of [14C] alpha-aminoisobutyric acid across the blood–brain barrier during pentylenetetrazol-induced status epilepticus in the immature rat. Epilepsy Res 22(3):175–183

Palmer AM (2011) The role of the blood brain barrier in neurodegenerative disorders and their treatment. J Alzheimers Dis 24(4):643–656

Patel NK, Gill SS (2007) GDNF delivery for Parkinson's disease. Acta Neurochir Suppl 97(Pt 2): 135–154

Pathan SA, Iqbal Z, Zaidi SM, Talegaonkar S, Vohra D, Jain GK, Azeem A, Jain N, Lalani JR, Khar RK, Ahmad FJ (2009) CNS drug delivery systems: novel approaches. Recent Pat Drug Deliv Formul 3(1):71–89

Paulsson M (1992) Basement membrane proteins: structure, assembly, and cellular interactions. Crit Rev Biochem Mol Biol 27(1–2):93–127

Paweletz CP, Wiener MC, Bondarenko AY, Yates NA, Song Q, Liaw A, Lee AY, Hunt BT, Henle ES, Meng F, Sleph HF, Holahan M, Sankaranarayanan S, Simon AJ, Settlage RE, Sachs JR, Shearman M, Sachs AB, Cook JJ, Hendrickson RC (2010) Application of an end-to-end biomarker discovery platform to identify target engagement markers in cerebrospinal fluid by high resolution differential mass spectrometry. J Proteome Res 9(3):1392–1401

Perez-Pinzon MA, Stetler RA, Fiskum G (2012) Novel mitochondrial targets for neuroprotection. J Cereb Blood Flow Metab 32(7):1362–1376

Persidsky Y, Ramirez SH, Haorah J, Kanmogne GD (2006) Blood–brain barrier: structural components and function under physiologic and pathologic conditions. J Neuroimmune Pharmacol 1(3):223–236

Pflanzner T, Petsch B, André-Dohmen B, Müller-Schiffmann A, Tschickardt S, Weggen S, Stitz L, Korth C, Pietrzik CU (2012) Cellular prion protein participates in amyloid-β transcytosis across the blood–brain barrier. J Cereb Blood Flow Metab 32(4):628–632

Pop V, Badaut J (2011) A neurovascular perspective for long-term changes after brain trauma. Transl Stroke Res 2(4):533–545

Portelli J, Aourz N, De Bundel D, Meurs A, Smolders I, Michotte Y, Clinckers R (2009) Intrastrain differences in seizure susceptibility, pharmacological response and basal neurochemistry of Wistar rats. Epilepsy Res 87(2–3):234–246

Potschka H, Löscher W (2001a) In vivo evidence for P-glycoprotein-mediated transport of phenytoin at the blood brain barrier of rats. Epilepsia 42:1231–1240

Potschka H, Löscher W (2001b) Multidrug resistance-associated protein is involved in the regulation of extracellular levels of phenytoin in the brain. Neuroreport 12(11):2387–2389

Potschka H, Fedrowitz M, Löscher W (2001) P-glycoprotein and multidrug resistance-associated protein are involved in the regulation of extracellular levels of the major antiepileptic drug carbamazepine in the brain. Neuroreport 12:3557–3560

Potschka H, Fedrowitz M, Loscher W (2002) P-Glycoprotein-mediated efflux of phenobarbital, lamotrigine, and felbamate at the blood–brain barrier, evidence from microdialysis experiments in rats. Neurosci Lett 327(3):173–176

Potschka H, Fedrowitz M, Loscher W (2003a) Multidrug resistance protein MRP2 contributes to the blood–brain barrier function and restricts antiepileptic drug activity. J Pharmacol Exp Ther 306:124–131

Potschka H, Fedrowitz M, Loscher W (2003b) Brain access and anticonvulsant efficacy of carbamazepine, lamotrigine, and felbamate in ABCC2/MRP2-deficient TR- rats. Epilepsia 44(12):1479–1486

Potschka H, Baltes S, Loscher W (2004) Inhibition of multidrug transporters by verapamil or probenecid does not alter blood–brain barrier penetration of levetiracetam in rats. Epilepsy Res 58(2–3):85–91

Price DL, Sisodia SS, Borchelt DR (1998) Genetic neurodegenerative diseases: the human illness and transgenic models. Science 282:1079–1083

Prins ML, Giza CC (2006) Induction of monocarboxylate transporter 2 expression and ketone transport following traumatic brain injury in juvenile and adult rats. Dev Neurosci 28(4–5): 447–456

Prinz M, Priller J, Sisodia SS, Ransohoff RM (2011) Heterogeneity of CNS myeloid cells and their roles in neurodegeneration. Nat Neurosci 14(10):1227–1235

Ravenstijn PG, Merlini M, Hameetman M, Murray TK, Ward MA, Lewis H, Ball G, Mottart C, de de Ville de Goyet C, Lemarchand T, van Belle K, O'Neill MJ, Danhof M, de Lange EC (2008) The exploration of rotenone as a toxin for inducing Parkinson's disease in rats, for application in BBB transport and PK-PD experiments. J Pharmacol Toxicol Methods 57(2):114–130

Ravenstijn PGM, Drenth H, Baatje MS, O'Neill MJ, Danhof M, de Lange ECM (2012) Evaluation of BBB transport and CNS drug metabolism in diseased and control brain after intravenous L-DOPA in a unilateral rat model of Parkinson's disease. Fluids Barriers CNS 9:4

Reale M, Iarlori C, Thomas A, Gambi D, Perfetti B, Di Nicola M, Onofrj M (2009) Peripheral cytokines profile in Parkinson's disease. Brain Behav Immun 23(1):55–63

Romanitan MO, Popescu BO, Winblad B, Bajenaru OA, Bogdanovic N (2007) Occludin is overexpressed in Alzheimer's disease and vascular dementia. J Cell Mol Med 11(3):569–579

Ronaldson PT, Davis TP (2012) Blood–brain barrier integrity and glial support: mechanisms that can be targeted for novel therapeutic approaches in stroke. Curr Pharm Des 18(25):3624–3644

Rosenberg GA, Yang Y (2007) Vasogenic edema due to tight junction disruption by matrix metalloproteinases in cerebral ischemia. Neurosurg Focus 22:E4

Rosenfeld JV, Maas AI, Bragge P, Morganti-Kossmann MC, Manley GT, Gruen RL (2012) Early management of severe traumatic brain injury. Lancet 380(9847):1088–1098

Sagare AP, Deane R, Zlokovic BV (2012) Low-density lipoprotein receptor-related protein 1: A physiological Aβ homeostatic mechanism with multiple therapeutic opportunities. Pharmacol Ther 136(1):94–105

Sahin D, Ilbay G, Ates N (2003) Changes in the blood–brain barrier permeability and in the brain tissue trace element concentrations after single and repeated pentylenetetrazole-induced seizures in rats. Pharmacol Res 48(1):69–73

Samuraki M, Matsunari I, Chen WP, Yajima K, Yanase D, Fujikawa A, Takeda N, Nishimura S, Matsuda H, Yamada M (2007) Partial volume effect-corrected FDG PET and grey matter volume loss in patients with mild Alzheimer's disease. Eur J Nucl Med Mol Imaging 34: 1658–1669

Sánchez-Pérez AM, Montoliu C, Felipo V (2003) Trialkylglycines: a new family of compounds with in vivo neuroprotective activity. CNS Drug Rev 9(3):263–274

Sandoval KE, Witt KA (2008) Blood–brain barrier tight junction permeability and ischemic stroke. Neurobiol Dis 32(2):200–219

Sayre LM, Perry G, Smith MA (2008) Oxidative stress and neurotoxicity. Chem Res Toxicol 21(1):172–188

Schinkel A, Smit J, van Tellingen O, Beijnen J, Wagenaar E, van Deemter L et al (1994) Disruption of the mouse mdr1a P-glycoprotein gene leads to a deficiency in the blood–brain barrier and to increased sensitivity to drugs. Cell 77:491–502

Schneider A, Mandelkow E (2008) Tau-based treatment strategies in neurodegenerative diseases. Neurotherapeutics 5(3):443–457

Scism JL, Powers KM, Artru AA, Lewis L, Shen DD (2000) Probenecid-inhibitable efflux transport of valproic acid in the brain parenchymal cells of rabbits: a microdialysis study. Brain Res 884(1–2):77–86

Selkoe DJ (2011) Alzheimer's disease. Cold Spring Harb Perspect Biol 1:3–7

Serrano GE, Lelutiu N, Rojas A, Cochi S, Shaw R, Makinson CD, Wang D, FitzGerald GA, Dingledine R (2011) Ablation of cyclooxygenase-2 in forebrain neurons is neuroprotective and dampens brain inflammation after status epilepticus. J Neurosci 31(42):14850–14860

Sharma HS, Castellani RJ, Smith MA, Sharma A (2012) The blood–brain barrier in Alzheimer's disease: novel therapeutic targets and nanodrug delivery. Int Rev Neurobiol 102:47–90

Sheng ZH, Cai Q (2012) Mitochondrial transport in neurons: impact on synaptic homeostasis and neurodegeneration. Nat Rev Neurosci 13:77–93

Shepardson NE, Shankar GM, Selkoe DJ (2011) Cholesterol level and statin use in Alzheimer disease: II. Review of human trials and recommendations. Arch Neurol 68(11):1385–1392

Shlosberg D, Benifla M, Kaufer D, Friedman A (2010) Blood–brain barrier breakdown as a therapeutic target in traumatic brain injury. Nat Rev Neurol 6(7):393–403

Shoham S, Youdim MB (2004) Nutritional iron deprivation attenuates kainate-induced neurotoxicity in rats: implications for involvement of iron in neurodegeneration. Ann N Y Acad Sci 1012:94–114

Shoulson I (1998) Experimental therapeutics of neurodegenerative disorders: unmet needs. Science 282(5391):1072–1074

Siddiqui A, Kerb R, Weale ME, Brinkmann U, Smith A, Goldstein DB, Wood NW, Sisodiya SM (2003) Association of multidrug resistance in epilepsy with a polmorhism in the drug-transporter gene ABCB1. N Engl J Med 348:1442–1448

Sills GJ, Kwan P, Butler E, de Lange EC, van den Berg DJ, Brodie MJ (2002) P-glycoprotein-mediated efflux of antiepileptic drugs: preliminary studies in mdr1a knockout mice. Epilepsy Behav 3(5):427–432

Simpson IA, Carruthers A, Vannucci SJ (2007) Supply and demand in cerebral energy metabolism: the role of nutrient transporters. J Cereb Blood Flow Metab 27(11):1766–1791

Sisodiya SM, Mefford HC (2011) Genetic contribution to common epilepsies. Curr Opin Neurol 24(2):140–145

Sivanandam TM, Thakur MK (2012) Traumatic brain injury: a risk factor for Alzheimer's disease. Neurosci Biobehav Rev 36(5):1376–1381

Soto C (2008) Endoplasmic reticulum stress, PrP trafficking, and neurodegeneration. Dev Cell 15(3):339–341

Soto C, Estrada LD (2008) Protein misfolding and neurodegeneration. Arch Neurol 65(2):184–189

Spector R (2009) Nutrient transport systems in brain: 40 years of progress. J Neurochem 111(2):315–320

Spector R, Johanson CE (2007) Vitamin transport and homeostasis in mammalian brain: focus on Vitamins B and E. J Neurochem 103:425–438

Stangel M (2012) Neurodegeneration and neuroprotection in multiple sclerosis. Curr Pharm Des 18(29):4471–4474

Stokin GB, Goldstein LSB (2006) Axonal transport and Alzheimer's disease. Annu Rev Biochem 75:607–627

Syvänen S, Luurtsema G, Molthoff CF, Windhorst AD, Huisman MC, Lammertsma AA, Voskuyl RA, de Lange EC (2011) (R)-[11C]verapamil PET studies to assess changes in P-glycoprotein expression and functionality in rat blood–brain barrier after exposure to kainate-induced status epilepticus. BMC Med Imaging 11:1

Syvänen S, Schenke M, van den Berg DJ, Voskuyl RA, de Lange EC (2012) Alteration in P-glycoprotein functionality affects intrabrain distribution of quinidine more than brain entry-a study in rats subjected to status epilepticus by kainate. AAPS J 14(1):87–96

Takano T, Tian GF, Peng W, Lou N, Libionka W, Han X, Nedergaard M (2006) Astrocyte-mediated control of cerebral blood flow. Nat Neurosci 9:260–267

Takano T, Han X, Deane R, Zlokovic B, Nedergaard M (2007) Two-photon imaging of astrocytic Ca2+ signaling and the microvasculature in experimental mice models of Alzheimer's disease. Ann N Y Acad Sci 1097:40–50

Tanzi RE, Moir RD, Wagner SL (2004) Clearance of Alzheimer's A beta peptide: the many roads to perdition. Neuron 43:605–608

Tate SK, Sisodiya SM (2007) Multidrug resistance in epilepsy: a pharmacogenomic update. Expert Opin Pharmacother 8:1441–1449

Tayarani I, Cloez I, Clément M, Bourre JM (1989) Antioxidant enzymes and related trace elements in aging brain capillaries and choroid plexus. J Neurochem 53:817–824

Vallejo-Illarramendi A, Domercq M, Pérez-Cerdá F, Ravid R, Matute C (2006) Increased expression and function of glutamate transporters in multiple sclerosis. Neurobiol Dis 21(1):154–164

Van Assema DM, Goos JD, van der Flier WM, Lubberink M, Boellaard R, Windhorst AD, Scheltens P, Lammertsma AA, van Berckel BN (2012) No evidence for additional blood–brain barrier P-glycoprotein dysfunction in Alzheimer's disease patients with microbleeds. J Cereb Blood Flow Metab 32(8):1468–1471

Van Damme P, Dewil M, Robberecht W, Van Den Bosch L (2005) Excitotoxicity and amyotrophic lateral sclerosis. Neurodegener Dis 2:147–159

Van der Schyf CJ, Gal S, Geldenhuys WJ, Youdim MB (2006) Multifunctional neuroprotective drugs targeting monoamine oxidase inhibition, iron chelation, adenosine receptors, and cholinergic and glutamatergic action for neurodegenerative diseases. Expert Opin Investig Drugs 15(8):873–886

Van Raamsdonk JM, Warby SC, Hayden MR (2007) Selective degeneration in YAC mouse models of Huntington disease. Brain Res Bull 72(2–3):124–131

Van Vliet EA, van Schaik R, Edelbroek PM, Voskuyl RA, Redeker S, Aronica E, Wadman WJ, Gorter JA (2007) Region-specific overexpression of P-glycoprotein at the blood–brain barrier affects brain uptake of phenytoin in epileptic rats. J Pharmacol Exp Ther 322(1):141–147

Van Vliet EA, Zibell G, Pekcec A, Schlichtiger J, Edelbroek PM, Holtman L, Aronica E, Gorter JA (2010) Potschka. COX-2 inhibition controls P-glycoprotein expression and promotes brain delivery of phenytoin in chronic epileptic rats. Neuropharmacology 58(2):404–412

Vautier S, Milane A, Fernandez C, Chacun H, Lacomblez L, Farinotti R (2009) Role of two efflux proteins, ABCB1 and ABCG2 in blood–brain barrier transport of bromocriptine in a murine model of MPTP-induced dopaminergic degeneration. J Pharm Pharm Sci 12(2):199–208

Vigeveno RM, Wiebenga OT, Wattjes MP, Geurts JJ, Barkhof F (2012) Shifting imaging targets in multiple sclerosis: from inflammation to neurodegeneration. J Magn Reson Imaging 36(1):1–19

Viggars AP, Wharton SB, Simpson JE, Matthews FE, Brayne C, Savva GM, Garwood C, Drew D, Shaw PJ, Ince PG (2011) Alterations in the blood brain barrier in ageing cerebral cortex in relationship to Alzheimer-type pathology: a study in the MRC-CFAS population neuropathology cohort. Neurosci Lett 505(1):25–30

Vogelgesang S, Jedlitschky G, Brenn A, Walker LC (2011) The role of the ATP-binding cassette transporter P-glycoprotein in the transport of β-amyloid across the blood–brain barrier. Curr Pharm Des 17(26):2778–2786

Volk B, Hettmansperger U, Papp TH, Amelizad Z, Oesch F, Knoth R (1991) Mapping of phenytoin-inducible cytochrome P450 immunoreactivity in the mouse central nervous system. Neuroscience 42:215–235

Volk HA, Arabadzisz D, Fritschy JM, Brandt C, Bethmann K, Löscher W (2006) Antiepileptic drug-resistant rats differ from drug-responsive rats in hippocampal neurodegeneration and GABA(A) receptor ligand binding in a model of temporal lobe epilepsy. Neurobiol Dis 21(3):633–646

Von Tell D, Armulik A, Betsholtz C (2006) Pericytes and vascular stability. Exp Cell Res 312:623–629

Vorbrodt AW (1988) Ultrastructural cytochemistry of blood–brain barrier endothelia. Prog Histochem Cytochem 18:1–99

Weaver SM, Chau A, Portelli JN, Grafman J (2012) Genetic polymorphisms influence recovery from traumatic brain injury. Neuroscientist 18(6):631–644

Weber JT (2012) Altered calcium signaling following traumatic brain injury. Front Pharmacol 3:60

Weinreb O, Amit T, Bar-Am O, Youdim MB (2007a) Induction of neurotrophic factors GDNF and BDNF associated with the mechanism of neurorescue action of rasagiline and ladostigil: new insights and implications for therapy. Ann N Y Acad Sci 1122:155–168

Weinreb O, Drigues N, Sagi Y, Reznick AZ, Amit T, Youdim MB (2007b) The application of proteomics and genomics to the study of age-related neurodegeneration and neuroprotection. Antioxid Redox Signal 9(2):169–179

Weiss HR (1988) Measurement of cerebral capillary perfusion with a fluorescent label. Microvasc Res 36:172–180

Wenk GL (2003) Neuropathologic changes in Alzheimer's disease. J Clin Psychiatry 64(Suppl 9):7–10

Whitton PS (2007) Inflammation as a causative factor in the aetiology of Parkinson's disease. Br J Pharmacol 150:963–976

Williams SK, Gillis JF, Matthews MA, Wagnert RC, Bitensky MW (1980) Isolation and characterization of brain endothelial cells: morphology and enzyme activity. J Neurochem 35(2):374–381

Winkler EA, Bell RD, Zlokovic BV (2011) Central nervous system pericytes in health and disease. Nat Neurosci 14(11):1398–1405

Winkler EA, Sengillo JD, Sullivan JS, Henkel JS, Appel SH, Zlokovic BV (2013) Blood-spinal cord barrier breakdown and pericyte reductions in amyotrophic lateral sclerosis. Acta Neuropathol 125(1):111–120

Witt KA, Gillespie TJ, Huber JD, Egleton RD, Davis TP (2001) Peptide drug modifications to enhance bioavailability and blood–brain barrier permeability. Peptides 22:2329–2343

Wolburg H (2006) The endothelial frontier. In: Dermietzel R, Spray DC, Nedergaard M (eds) Blood–brain interface: from ontogeny to artificial barriers. Wiley, Weinheim, pp 77–109

Wolburg H, Noell S, Mack A, Wolburg-Buchholz K, Fallier-Becker P (2009) Brain endothelial cells and the glio-vascular complex. Cell Tissue Res 335(1):75–96

Wu Z, Guo H, Chow N, Sallstrom J, Bell RD, Deane R, Brooks AI, Kanagala S, Rubio A, Sagare A, Liu D, Li F, Armstrong D, Gasiewicz T, Zidovetzki R, Song X, Hofman F, Zlokovic BV (2005) Role of the MEOX2 homeobox gene in neurovascular dysfunction in Alzheimer disease. Nat Med 11(9):959–965

Wyss-Coray T, Lin C, Sanan DA, Mucke L, Masliah E (2000) Chronic overproduction of transforming growth factor-beta1 by astrocytes promotes Alzheimer's disease-like microvascular degeneration in transgenic mice. Am J Pathol 156(1):139–150

Yang Y, Rosenberg GA (2011) MMP-mediated disruption of claudin-5 in the blood–brain barrier of rat brain after cerebral ischemia. Methods Mol Biol 762:333–345

Yang J, Lunde LK, Nuntagij P, Oguchi T, Camassa LM, Nilsson LN, Lannfelt L, Xu Y, Amiry-Moghaddam M, Ottersen OP, Torp R (2011) Loss of astrocyte polarization in the tg-ArcSwe mouse model of Alzheimer's disease. J Alzheimers Dis 27(4):711–722

Youdim MB, Buccafusco JJ (2005) Multi-functional drugs for various CNS targets in the treatment of neurodegenerative disorders. Trends Pharmacol Sci 26(1):27–35

Yu F, Wang Z, Tchantchou F, Chiu CT, Zhang Y, Chuang DM (2012) Lithium ameliorates neurodegeneration, suppresses neuroinflammation, and improves behavioral performance in a mouse model of traumatic brain injury. J Neurotrauma 29(2):362–374

Zattoni M, Mura ML, Deprez F, Schwendener RA, Engelhardt B, Frei K, Fritschy JM (2011) Brain infiltration of leukocytes contributes to the pathophysiology of temporal lobe epilepsy. J Neurosci 31(11):4037–4050

Zhang XM, Mao XJ, Zhang HL, Zheng XY, Pham T, Adem A, Winblad B, Mix E, Zhu J (2012) Overexpression of apolipoprotein E4 increases kainic-acid-induced hippocampal neurodegeneration. Exp Neurol 233(1):323–332

Zlokovic BV, Yamada S, Holtzman D, Ghiso J, Frangione B (2000) Clearance of amyloid beta-peptide from brain: transport or metabolism? Nat Med 6(7):718–719

Zlokovic BV (2006) Remodeling after stroke. Nat Med 12:390–391

Zlokovic BV (2008) The blood–brain barrier in health and chronic neurodegenerative disorders. Neuron 57(2):178–201

Zlokovic BV (2010) Neurodegeneration and the neurovascular unit. Nat Med 16:1370–1371

Zlokovic BV (2011) Neurovascular pathways to neurodegeneration in Alzheimer's disease and other disorders. Nat Rev Neurosci 12(12):723–738

Chapter 23
Drug Delivery in the Context of Stroke and Brain Trauma

Richard F. Keep, Jianming Xiang, Ningna Zhou, and Anuska V. Andjelkovic

Abstract Stroke and traumatic brain injury (TBI) cause marked changes in blood–brain barrier (BBB) function. These changes result in increased barrier permeability, vasogenic edema, and an influx of leukocytes into brain. As such, they are a therapeutic target. In addition, changes at the BBB can affect the entry of therapeutics into the brain. This chapter describes the changes in BBB function that occur after brain injury, the impact on drug delivery for stroke and TBI and potential ways of circumventing the BBB for therapy.

Abbreviations

ABC transporters	ATP-binding cassette transporters
BBB	Blood–brain barrier
BDNF	Brain-derived neurotrophic factor

R.F. Keep, Ph.D. (✉)
Department of Molecular and Integrative Physiology, R5018 Biomedical Science Research Building, University of Michigan, 109 Zina Pitcher Place, Ann Arbor, MI 48109-2200, USA

Department of Neurosurgery, R5018 Biomedical Science Research Building, University of Michigan, 109 Zina Pitcher Place, Ann Arbor, MI 48109-2200, USA
e-mail: rkeep@umich.edu

J. Xiang • N. Zhou
Department of Neurosurgery, R5018 Biomedical Science Research Building, University of Michigan, 109 Zina Pitcher Place, Ann Arbor, MI 48109-2200, USA

A.V. Andjelkovic
Department of Neurosurgery, R5018 Biomedical Science Research Building, University of Michigan, 109 Zina Pitcher Place, Ann Arbor, MI 48109-2200, USA

Department of Pathology, R5018 Biomedical Science Research Building, University of Michigan, 109 Zina Pitcher Place, Ann Arbor, MI 48109-2200, USA

M. Hammarlund-Udenaes et al. (eds.), *Drug Delivery to the Brain*, AAPS Advances in the Pharmaceutical Sciences Series 10, DOI 10.1007/978-1-4614-9105-7_23,

bFGF	Basic fibroblast growth factor
CSF	Cerebrospinal fluid
ICH	Intracerebral hemorrhage
IVH	Intraventricular hemorrhage
KO	Knockout
SAH	Subarachnoid hemorrhage
SVCT2	Na-dependent Vitamin C Transporter 2
TBI	Traumatic brain injury
TJ	Tight junction
tPA	Tissue plasminogen activator

23.1 Introduction

Stroke and traumatic brain injury (TBI) result in profound changes in blood–brain barrier (BBB) function. These changes have a role in brain injury (e.g., edema formation and leukocyte infiltration), but also impact drug delivery of potential therapeutics. The aim of this chapter is to (a) describe the changes that occur in BBB function during stroke and TBI, (b) the impact of those changes on the delivery of current and some potential therapeutics, and (c) potential methods of circumventing the BBB in stroke and TBI. While prior chapters have described the effects of the normal BBB on drug delivery and methods that are being used to enhance such delivery, this chapter focuses specifically on brain injury.

In cerebral ischemia, there is a reduction in blood flow to an area of brain that causes neural dysfunction. Reductions in flow are caused by thrombosis within a cerebral vessel, the lodging of emboli generated by a distant site, or temporary heart failure. The first two events cause focal cerebral ischemia, while the latter causes global cerebral ischemia. Focal ischemic events occur with and without restoration of blood flow (transient and permanent ischemia). Cerebral ischemia accounts for most strokes, but ~15% of strokes in the USA and 20–30% in Asia are hemorrhagic (Adeoye and Broderick 2010; Roger et al. 2012). Although the initial symptoms in hemorrhagic stroke are similar to cerebral ischemia, the underlying cause, a ruptured cerebral blood vessel, is different. Hemorrhages are defined by locations: intracerebral, subarachnoid, intraventricular, and subdural. There are differences in the mechanisms underlying brain injury in hemorrhagic and ischemic stroke (Xi et al. 2006). The components of brain injury after trauma are heterogeneous with physical damage to neural components, cerebral ischemia, and cerebral hemorrhage, and they vary with closed and penetrating brain injury (Maas et al. 2008).

Each year in the USA there are about 800,000 strokes (Roger et al. 2012) and 1.4 million cases of TBI (Shlosberg et al. 2010). It has also been estimated that there are ~9 million new silent ischemic strokes and ~2 million silent cerebral hemorrhages per year (Leary and Saver 2003). The impact of these asymptomatic strokes is the subject of current debate (Cordonnier and van der Flier 2011).

As described below, cerebral ischemia, cerebral hemorrhage, and TBI all cause BBB dysfunction (Hawkins and Davis 2005; Keep et al. 2008; Shlosberg et al. 2010).

That dysfunction contributes to the disease state and is, as such, a therapeutic target. Those changes also, though, impact the distribution of potential therapeutics into brain parenchyma.

23.2 The Blood–Brain Barrier During Stroke and Trauma

Cerebral ischemia, cerebral hemorrhage, and TBI all have major impacts on BBB function (Table 23.1). This is evinced by marked increases in permeability (for example to proteins, Fig. 23.1), edema formation, and leukocyte infiltration

Table 23.1 Changes in the blood–brain barrier after stroke and traumatic brain injury

Mechanism affected	Change	Consequence
Cerebral blood flow	Reduction[a]	Reduced uptake of highly permeable (flow dependent) compounds Potential reduction in endothelial ATP
Tight junction integrity	Disruption	Enhanced BBB permeability to small and large molecules
Endocytosis/transcytosis	Increase	Enhanced BBB permeability, particularly to large molecules
Leukocyte adhesion and transmigration	Increase	Inflammation and BBB disruption
Progenitor cell transmigration	Increase	Possible angiogenesis, reduced injury
ABC transporters	Increase	Reduced uptake of substrates into brain
Other transporters	Mixed	Altered uptake of substrates into brain

[a]In ischemic stroke, the reductions in blood flow are marked. In traumatic brain injury and subarachnoid hemorrhage, the reductions vary in magnitude between patients. In intracerebral hemorrhage, the reductions are limited

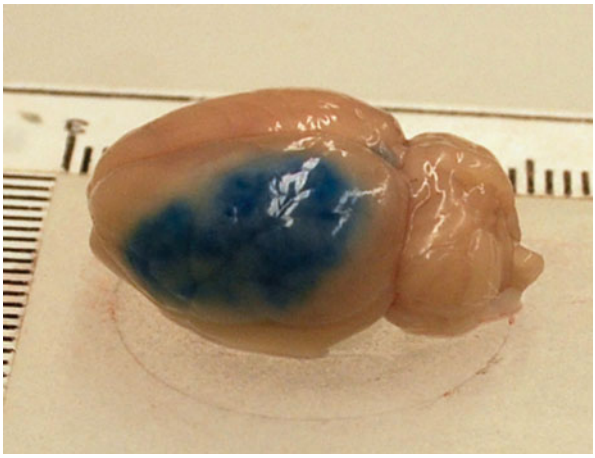

Fig. 23.1 Distribution of Evan's blue into brain after 2 h of focal middle cerebral artery occlusion with 2 h of reperfusion (transient focal ischemia) in an acutely hyperglycemic rat. Hyperglycemia exacerbates ischemia-induced BBB damage. Evan's blue binds to albumin within the bloodstream and the *blue color* in the ipsilateral hemisphere reflects increased BBB permeability to protein in the middle cerebral artery territory

into brain (Hawkins and Davis 2005; Keep et al. 2008; Shlosberg et al. 2010). These changes usually gradually resolve within 2–4 weeks (Menzies et al. 1993), although there is evidence of prolonged low level BBB leakiness after stroke (Topakian et al. 2010).

There can also be changes at the blood-CSF barrier (at the choroid plexuses) in cerebral ischemia and in TBI in relation to permeability and leukocyte infiltration (Ennis and Keep 2006; Johanson et al. 2000; Szmydynger-Chodobska et al. 2009; Szmydynger-Chodobska et al. 2012). However, this has been much less studied than effects on the BBB and this chapter focuses on that barrier.

23.2.1 Blood Supply

In cerebral ischemia, the extent and duration of reductions in blood flow depend on the underlying cause. In a heart attack, cerebral blood flow falls to zero and will result in death unless the heart resumes beating. In focal ischemia, the extent to which blood flow is reduced depends upon the blood vessel blocked and the degree of collateral blood flow (e.g., if the middle cerebral artery is blocked, how much flow will be supplied to a region by the anterior cerebral artery). In general, prolonged reductions in blood flow to less than ~20 ml/100g/min results in permanent brain damage (Jones et al. 1981).

Reduced blood flow (with reduced oxygen and glucose supply) is the underlying cause of ischemic brain injury. For some potential therapeutics reduced flow may also directly impact brain uptake. The BBB permeability of caffeine (~0.7 ml/g/min; (Tanaka and Mizojiri 1999)) is of the magnitude of cerebral blood flow, indicating that the uptake of caffeine into brain is flow limited as the concentration of caffeine will markedly decrease as it passes through the cerebrovasculature. Caffeine, in combination with ethanol (caffeinol), has undergone clinical trials for stroke (Piriyawat et al. 2003) and it should be noted that caffeine uptake into brain will be decreased by the reductions in blood flow in stroke.

The extent of blood flow reductions in other forms of stroke and TBI varies. In intracerebral hemorrhage (ICH), most evidence indicates that there are not pronounced reductions in flow (except probably for very large hemorrhages) (Xi et al. 2006). In subarachnoid hemorrhage (SAH), early and delayed cerebral ischemia is a large part of the injury (Etminan et al. 2011; Schubert and Thome 2008). In TBI, the extent of ischemia varies between different injuries and it can be widespread or perilesional (Maas et al. 2008).

23.2.2 Tight Junctions

Most potential therapeutics have much lower BBB permeabilities and brain uptake is not flow limited. There are though other changes that may impact uptake,

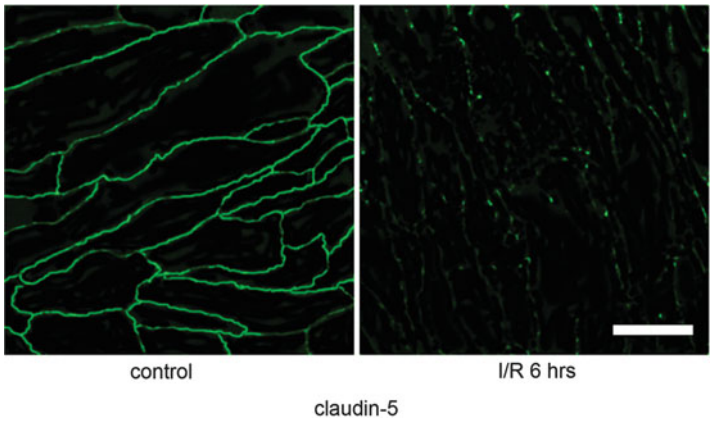

Fig. 23.2 Distribution of a tight junction protein, claudin-5, in mouse brain microvascular endothelial cells (mBMEC) in culture as determined by immunofluorescence. mBMEC were cocultured with astrocytes and then either exposed to normal culture conditions (control) or exposed to 5 h of oxygen glucose deprivation (OGD; a model of in vitro ischemia) and then returned to normal oxygen and glucose for 6 h ("ischemia/reperfusion", I/R). (A) Under control conditions, claudin-5 is located at the cell membrane between adjacent endothelial cells. (B) After OGD with reperfusion, claudin-5 is lost from the cell membrane (fragmented staining) and this is associated with increased permeability of the endothelial cell monolayers (Dimitrijevic et al. 2006). Scale bar = 50 μm

including changes in tight junction (TJ) structure. The TJs that link cerebral endothelial cells are comprised of transmembrane proteins (claudin 5, occludin, and junctional adhesion molecules (JAMs)), that are involved in occluding the paracellular space, and cytoplasmic plaque proteins (e.g., zonula occludens (ZO)-1), that are involved in stabilizing and regulating the TJ. Many studies have shown alterations in BBB TJ structure after cerebral ischemia (Dimitrijevic et al. 2006; Jiao et al. 2011; Rosenberg and Yang 2007) and TBI (Higashida et al. 2011; Walker et al. 2010) (Fig. 23.2). Changes in TJ structure can involve the loss of TJ proteins, the phosphorylation of particular proteins (which effects protein:protein interaction) and/or the relocation of proteins from their normal site at the plasma membrane (Dimitrijevic et al. 2006; Kago et al. 2006; Stamatovic et al. 2009; Yang et al. 2007). The role of each type of change varies dependent upon the type and duration of injury.

A number of factors are implicated in inducing changes in TJ structure. These include oxidative stress, cytokines, chemokines, and matrix metalloproteinases (Pun et al. 2009; Stamatovic et al. 2008; Yang et al. 2007). The latter can degrade occludin and claudin-5 (Yang et al. 2007). While the TJs of the cerebral endothelium limit paracellular permeability, other adjacent cells, astrocytes, and pericytes (cells of the neurovascular unit), can regulate that permeability. Recently, there has been considerable interest in the role of pericytes and those cells may protect the BBB during ischemia and pericyte movement away from the endothelium may contribute to ischemia-induced BBB disruption (Kamouchi et al. 2012).

The result of these TJ changes is an increase in paracellular permeability that allows entry of large compounds (e.g., plasma albumin; (Menzies et al. 1993))

into brain. It also enhances the permeability of low molecular weight polar compounds that normally have a low brain uptake across the BBB (e.g., sucrose, (Preston and Webster 2002)). Thus, these changes in TJ structure have the potential to alter the uptake of a wide range of therapeutics. The effects are dependent on the size of the molecule and the evolution of the injury (Nagaraja et al. 2007; Preston and Webster 2002).

23.2.3 Endocytosis/Transcytosis

Under normal conditions, the number of vesicles in the cerebral endothelium is low compared to other endothelia (Abbott et al. 2010). Vesicular trafficking plays multiple roles in cells, including the cerebral endothelium. At the BBB some trafficking is involved in the movement of compounds across the endothelium, i.e., transcytosis (Herve et al. 2008; Jones and Shusta 2007). Transcytosis plays an important role in the transport of compounds such as transferrin, LDL-receptor-related protein 1 (LRP1), and insulin between blood and brain (Abbott et al. 2010).

Under conditions of injury and other disease states there can be marked increases in the number of vesicles in the cerebral endothelium and evidence of increased transcytosis (Dietrich et al. 1988; Westergaard et al. 1976). Drug targeting to vesicular pathways during brain injury is, therefore, a method of potentially delivering those agents to the brain endothelial or brain parenchyma. Examples of this approach are the conjugation of brain-derived neurotrophic factor (BDNF) and basic fibroblast growth factor (bFGF) to an antibody recognizing the transferrin receptor which undergoes endocytosis. While BDNF and bFGF alone were not protective in a rat model of cerebral ischemia, their conjugates were (Song et al. 2002; Zhang and Pardridge 2001). With this type of approach, it is uncertain how big a role the increased vesicular traffic during injury has in the conjugate-induced protection (i.e., might the conjugated drugs be neuroprotective even without an increase in trafficking).

23.2.4 Cell Trafficking

Ischemic and hemorrhagic stroke and TBI all cause an influx of leukocytes into brain. That influx involves a coordinated action of adhesion molecules, cytokines, and chemokines, where the cerebral endothelium plays a central role (del Zoppo, 2010; Iadecola and Anrather 2011; Rhodes 2011; Wang 2010). There is considerable debate as to the mechanism by which leukocytes traverse the cerebral endothelium in different disease states, between or through the endothelial cells or both (Vestweber 2007; von Wedel-Parlow et al. 2011). In preclinical stroke and TBI models, inhibiting inflammation and leukocyte trafficking into brain reduces brain

and cerebrovascular injury (del Zoppo 2010; Rhodes 2011). As yet, though, there have been no successful clinical trials with that approach.

After stroke or brain injury, there is a migration of endogenous progenitor cells within the brain (e.g., from the subventricular zone) to the site of injury (Kernie and Parent 2010). In addition, though, progenitor cells within the bloodstream also target the injured brain (Borlongan et al. 2011). Those cells can integrate into the cerebrovasculature (participating in angiogenesis, (Borlongan et al. 2011)) and can migrate into brain parenchyma (Borlongan et al. 2011; Burns et al. 2009; Heile and Brinker 2011; Li and Chopp, 2009; van Velthoven et al. 2009). Such brain or bloodstream endogenous progenitors do not significantly integrate into the brain long term and, indeed, there may be aberrant integration (Kernie and Parent 2010). Exogenously derived progenitor cells are, though, being examined as a way of treating brain injury and, after transfection, as a way of delivering cells to the brain that will express potential therapeutics (Borlongan et al. 2011; Burns et al. 2009; Heile and Brinker 2011; Jenny et al. 2009; Li and Chopp 2009; van Velthoven et al. 2009).

23.2.5 Transport

The effects of brain injury on BBB transport have received relatively little attention. There is some evidence of upregulation of one of the ATP-binding cassette (ABC) transporters, p-glycoprotein (ABCB-1), at the mRNA and functional level after transient cerebral ischemia which may limit the access of potential therapeutics into brain (Patak and Hermann 2011). There is also evidence for upregulated Na/K/Cl cotransport (Wallace et al. 2011), increased Na-dependent Vitamin C Transporter 2 (SVCT2) mRNA and activity (Gess et al. 2011), and increased Na-dependent glucose transport (Vemula et al. 2009). In contrast, blood to brain transport of glutamine, taurine, and myo-inositol is reduced by cerebral ischemia (Kawai et al. 1999; Stummer et al. 1995) (Fig. 23.3). The changes in Na/K/Cl cotransport and Na-dependent glucose transport are important in the development of stroke-induced brain injury (Vemula et al. 2009; Wallace et al. 2011), but it has also been suggested that the increase in SVCT2 activity might be used to enhance drug delivery to the ischemic brain (Gess et al. 2011).

Reduced oxygen and glucose supply during cerebral ischemia depletes brain ATP levels causing failure of energy-dependent transport in parenchymal cells. As a result, there are marked changes in cellular ion gradients with an increase in intracellular Na and a decrease in K. This in turn may impact transporters that rely on those ion gradients (e.g., Na-dependent transporters). The extent to which cerebral ischemia impacts endothelial energy metabolism is uncertain. However, if endothelial ATP levels are depleted, this would impact ATP-dependent transporters, such as p-glycoprotein. It would also impact Na-dependent transport, and this has been suggested as the cause in the decline in BBB glutamine and taurine transport during permanent focal cerebral ischemia (Kawai et al. 1999; Stummer et al. 1995).

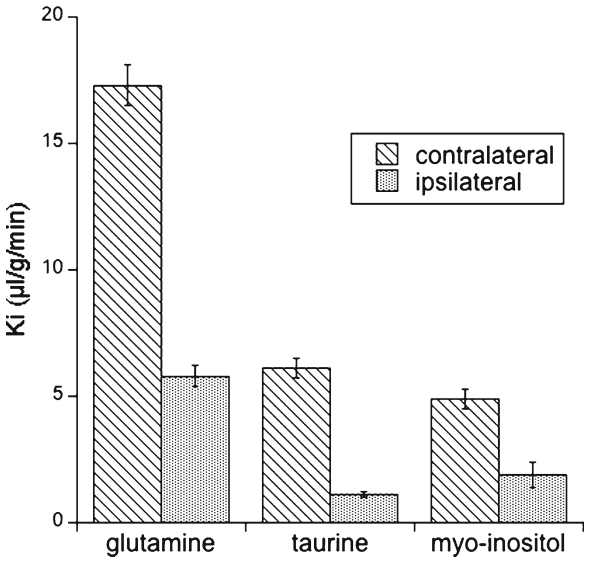

Fig. 23.3 Changes in the brain uptake (influx rate constant; K_i) of [^{14}C]glutamine, [^{3}H]taurine, and [3H]myo-inositol after 4 h of permanent focal cerebral ischemia (middle cerebral artery occlusion) in the rat (Kawai et al. 1999; Stummer et al. 1995). Note, in the core of the middle cerebral artery territory in the ipsilateral hemisphere to the occlusion, there was a marked decline in transport compared to the contralateral hemisphere. Reductions in transport during ischemia are reversed during reperfusion, suggesting that the changes in transport during ischemia may have been due to reduced endothelial ATP levels (glutamine, taurine, and myo-inositol transport at the BBB are Na-dependent and thus indirectly reliant on ATP; secondary active transport)

23.2.6 Metabolic Barrier

The BBB and the BCSFB possess a variety of enzymes that metabolize neuroactive compounds (el-Bacha and Minn 1999; Ghersi-Egea et al. 2006). These contribute to barrier function by degrading the compounds before they can enter the brain or by converting the compounds so they become substrates for brain efflux transporters. The effect of stroke and TBI on these enzymes has not received attention.

23.2.7 Modifiers of BBB Injury

As for brain injury as a whole, a number of conditions modify BBB damage after stroke and TBI. Thus, for example, hyperglycemia has a profound detrimental effect on the BBB damage induced by transient focal cerebral ischemia, indeed hyperglycemic animals are prone to hemorrhagic transformation (Ennis and Keep 2007; Kawai et al. 1997). Other factors that generally exacerbate BBB damage after stroke include hyperthermia (Noor et al. 2005), systemic inflammation (Denes et al. 2011), and smoking (Bradford et al. 2011).

Another potential modifier of BBB injury is age. Thus, Fernandez-Lopez et al. found much less BBB disruption after focal ischemia in neonatal compared to adult rats (Fernandez-Lopez et al. 2012). This was associated with less changes in tight junction proteins.

23.3 Impact of BBB Changes on the Delivery of Current Therapeutics in Stroke and Trauma

Most attention to the BBB in terms of drug delivery has focused on the effects of the BBB on the entry of neuroprotectants into the brain parenchyma. However, it should be noted that stroke is a cerebrovascular disease and, therefore, the target for some current and potential therapies is the cerebrovasculature itself. Thus, a therapeutic may not be required to cross the BBB and enter the brain parenchyma. It may act intravascularly or on endothelial cells. However, as indicated below, even for those therapies with intravascular targets, the BBB may have important effects.

23.3.1 Tissue Plasminogen Activator (tPA)

This agent is currently the only Food and Drug Administration (FDA) approved therapy for ischemic stroke. It acts to restore cerebral blood flow by lysing the intravascular clot. A major concern over the use of this drug is the potential for symptomatic ICH if blood flow is restored to a damaged blood vessel (Anonymous 1995). Initially, tPA could only be administered up to 3 h after the stroke, although this has more recently been extended to 4.5 h.

As the effects of tPA are intravascular, it does not need to cross the BBB to be effective. However, there has been interest in using vascular protectants in combination with tPA to reduce the incidence of ICH (Yamashita et al. 2009). There are also concerns over the potential effects of tPA if it crosses the BBB after a stroke. Although there is debate, there is substantial evidence that extravascular tPA increases brain damage (Zhang et al. 2002). Ways of limiting either the extravascular actions of tPA or the movement across the BBB after stroke while not affecting thrombolytic activity may be beneficial.

23.3.2 Ultrasound and Mechanical Thrombolysis

These alternate methods of inducing reperfusion after ischemic stroke have and are under clinical investigation (Alexandrov 2010; Bor-Seng-Shu et al. 2012). While mechanical thrombolysis may adversely affect the large diameter blood vessel containing the clot to be removed, which may cause hemorrhage and affect re-occlusion, the effects on the BBB are likely to be limited to those caused by any emboli that are shed during clot removal.

For ultrasound induced clot lysis (sonothrombolysis) in conjunction with tPA has been examined in a number of clinical studies (Bor-Seng-Shu et al. 2012). There is evidence that this combination increases reperfusion but there is still no evidence that it improves outcome (Alexandrov 2010; Bor-Seng-Shu et al. 2012). There was concern that it may cause hemorrhage but that hasn't been borne out by later clinical trials (Alexandrov 2010; Bor-Seng-Shu et al. 2012). There is also a concern that ultrasound may cause BBB disruption (Reinhard et al. 2006). Indeed, experimentally, ultrasound in combination with microbubbles has been used as a way of increasing BBB permeability in cerebral ischemia for drug delivery (McDannold et al. 2005).

23.3.3 Nimodipine

The calcium channel antagonist, nimodipdine, is approved for use in SAH in the USA (Bederson et al. 2009). Whether it acts as a vascular (e.g., preventing large vessel or microvessel-related ischemia) or a neuronal protectant is not certain (Bederson et al. 2009). Nimodipine has a relatively high BBB permeability (although it has significant protein binding) (Zlokovic et al. 1993) and does interact with *p*-glycoprotein (Hollt et al. 1992; Liu et al. 2003).

23.3.4 Glucocorticoids

This type of steroid, and particularly dexamethasone, is used to treat brain edema in tumor patients. They probably act via reducing capillary permeability, although glucorticoids also have profound anti-inflammatory effects. These steroids have been extensively examined in patients with cerebral ischemia, cerebral hemorrhage, and TBI with no evidence of benefit. However, there is some evidence of benefit of very high dose methylprednisolone (another glucocorticoid) in spinal cord injury, although this is controversial (Gomes et al. 2005). Methylprednisolone has a small but significant permeability at the uninjured BBB (Zlokovic et al. 1993).

There have been a number of studies examining brain uptake of dexamethasone. These have shown increased brain penetration in the Mdr-1 (p-glycoprotein) KO mouse (Meijer et al. 1998; Schinkel et al. 1995; Uchida et al. 2011). In addition, dexamethasone induces *p*-glycoprotein expression at the BBB (Bauer et al. 2004). This suggests that adequate brain dosing may be a problem in stroke and TBI, and whether this is the case has not been examined. An alternate explanation is suggested by the work of Kleinschnitz et al. (2011) who found that the endothelial glucocorticoid receptor becomes degraded under hypoxic conditions and that a proteasome inhibitor can restore that sensitivity (Kleinschnitz et al. 2011).

23.3.5 Hypothermia

In preclinical models, induced hypothermia has a profound effect on ischemic brain damage and TBI (Finkelstein and Alam 2010; MacLellan et al. 2009). The effects of hypothermia on ICH-induced brain injury are not as robust (MacLellan et al. 2009), probably reflecting a relative lack of ischemia. These preclinical effects on ischemia and TBI have led to multiple clinical trials and hypothermia has been accepted for use in cardiac arrest and neonatal hypoxic-ischemic encephalopathy (Finkelstein and Alam 2010). However, other trials on ischemic stroke and TBI have, as yet, been conflicting and disappointing, and induced hypothermia can result in significant complications (Finkelstein and Alam 2010).

There is evidence that one component of the effects of hypothermia during ischemic stroke and TBI is to protect the BBB (Smith and Hall, 1996; Yenari and Han, 2012). It should be noted that this may impact the delivery of other agents to the brain. Hypothermia may also affect the pharmacokinetics of drugs (e.g., metabolism; (Finkelstein and Alam 2010)).

23.4 Impact of BBB Changes on the Delivery of Potential Therapeutics in Stroke and Trauma

23.4.1 Proteins

Changes in TJ structure and/or changes in transcytosis during stroke and TBI increase the uptake of plasma proteins and protein therapeutics from blood to brain. In terms of drug delivery, this raises several questions, the answers to which are often uncertain:

(A) Does a protein therapeutic reach a high enough concentration to be neuroprotective? This depends on their pharmacokinetics, the distribution into the injured brain and the concentration required for neuroprotection. It also depends upon potential systemic toxicity.

The penetration of bFGF at the normal BBB is very low and this is enhanced after ischemic stroke where there is evidence of some neuroprotection (Fisher et al. 1995; Liu et al. 2006). However, Song et al. (2002) found that increasing BBB delivery using the conjugate to an antibody recognizing the transferrin receptor increased protection, suggesting that delivery of bFGF alone across the BBB after stroke may not the optimal (Fig. 23.4).

(B) Are the increased concentrations at the "correct" location? In ischemic stroke, there is an ischemic core with very low blood flows and a penumbra with higher blood flows. Little can be done to preserve the core, apart from a prompt restoration in blood flow, while the penumbra is regarded as potentially salvageable

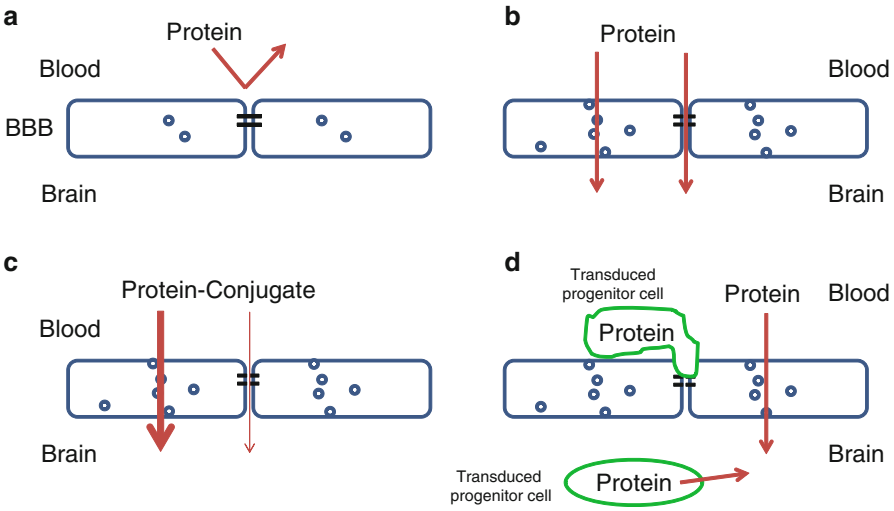

Fig. 23.4 Some alternative approaches to enhancing protein therapeutic delivery after stroke or brain injury. (**A**) Noninjury condition, where the therapeutic does not cross the BBB. (**B**) Injury condition where there is increased BBB permeability to proteins, with increased tight junction disruption and transcytosis. These changes will enhance the permeability of the protein therapeutic but this may not be sufficient to reach the brain concentrations necessary for efficacy. (**C**) Modifying the therapeutic to increase transcytosis, for example by conjugation to an antibody recognizing the transferrin receptor. By increasing the size of the molecule this may limit paracellular diffusion through the tight junction. (**D**) Transduction of progenitor cells so they express the protein therapeutic. The migration of those progenitor cells to the site of brain injury then results in local production of the therapeutic

with different therapeutics. However, the extent of BBB dysfunction also varies with location, with generally greater disruption and protein delivery in the core compared to the penumbra (Menzies et al. 1993).

(C) What is the relative importance of transcytosis vs. paracellular pathways in the uptake of specific proteins after a particular brain injury (cerebral ischemia, cerebral hemorrhage, TBI)? For proteins undergoing transcytosis, what are the relative roles of receptor-mediated and absorptive-mediated transcytosis, and how are these specific types of transcytosis affected by the brain injury type? Understanding the answers to these questions will give insight into the potential effects of a particular type of injury on the delivery of specific protein therapeutics.

(D) Do changes in the brain extracellular space affect drug delivery once the BBB is traversed? After cerebral ischemia, parenchymal cell swelling, particularly in astrocytes, affects diffusion through the brain extracellular space (Hrabetova et al. 2003; Sykova, 1997) which may impede the access of protein therapeutics to specific cell targets.

23.4.2 Small Molecular Weight Compounds

As for large proteins, there is an increased movement of many small molecular weight compounds across the BBB after stroke and TBI reflecting TJ disruption/transcytosis. Whether such changes are of relevance to the delivery of a therapeutic depends again on the answer to several questions some of which also applied to proteins therapeutics:

(A) Do the changes in movement through the TJ and transcytosis significantly impact the entry of the compound into brain? For lipophilic compounds the impact of changes in these pathways may be minor compared to the diffusional flux through the endothelial cell membrane.
(B) The impact of changes in TJ structure on brain uptake depends on the molecular weight of the compound. The absolute increases in uptake are larger for small molecular weight compounds, but the % increases are greater for large compounds (Preston and Foster 1997; Preston and Webster 2002).
(C) Is the uptake of the drug in the correct location? The greatest changes in BBB permeability are generally in the core of the injury (Menzies et al. 1993). This is the brain area that is most difficult to salvage. The penumbra is more amenable to treatment but in that region, the BBB changes may be smaller.
(D) Is the movement of the drug impeded by changes in the size of the brain extracellular space? The proximity of neurons to the cerebrovasculature is a great advantage of systemic delivery of therapeutics. Thus, all neurons within the brain are within about 50 μm of a capillary (Mabuchi et al. 2005) and this greatly limits the distance that a therapeutic agent has to penetrate through the brain. However, it should be noted that in cerebral ischemia there is marked swelling of the perivascular astrocyte endfeet (Kwon et al. 2009) and this, along with a reduction in the brain extracellular space, may impact diffusion of the therapeutic agent away from the vasculature.
(E) Is there an impact of changes in efflux transporter activity? Thus, do changes in ABC transporter expression at the BBB after injury result in greater efflux from brain to blood? This particularly applies to lipophilic drugs as these, as a whole, have greater affinity for the ABC transporter. Spudich et al. have found that inhibition of *p*-glycoprotein can enhance the delivery of a number of neuroprotectants in stroke (Spudich et al. 2006) implying that changes in *p-glycoprotein* activity after stroke will impact brain uptake of those agents. It should be noted that the affinity of drugs for ABC transporters may differ between humans and animals. The recent finding that humans pluripotent stem cells can be used to produce endothelial cells with BBB properties (Lippmann et al. 2012) should help facilitate examination of such differences and the impact of ischemia on transporter function.
(F) Is there an impact of changes in influx transporter activity? As described above, brain injury may also affect influx transporter activity (either down- or upregulation). However, most pharmaceutical compounds are unlikely to be a

substrate for such transporters. Levodopa (L-DOPA) is one of the few current therapeutics that utilizes a BBB transporter (system-L amino acid transport (Kageyama et al. 2000)).

23.4.3 Cell-Based Therapies

Cell-based therapies for treatment of stroke and TBI have used neural, mesenchymal, hematopoietic, and endothelial progenitor cells (Borlongan et al. 2011; van Velthoven et al. 2009). In preclinical models, progenitor cells have shown neuroprotection after transplantation directly into the brain or after administration into the bloodstream (Borlongan et al. 2011; Richardson et al. 2010; van Velthoven et al. 2009). It appears that this protection is via the secretion of pro-survival factors (e.g., growth factors) rather than cell replacement (e.g., production of new neurons) as few progenitor cells that migrate to the site of injury survive long term (Kernie and Parent 2010; Zhang and Chopp 2009). There are, though, efforts being made to increase survival. Given that progenitor cells given into the bloodstream can target the brain, there has also been interest in using these cells as a method for delivery of therapeutics to the brain, e.g., using gene transduction to induce overexpression of potentially protective proteins (van Velthoven et al. 2009). These approaches raise several questions in relation to the BBB and drug delivery:

(A) Can progenitors be used to repair the BBB? It is thought that low level of survival of endogenous and exogenous progenitors within an area of damaged brain is linked to adverse effects of the microenvironment within that area. It is possible that long-term effects on the cerebrovasculature may be more feasible. There is evidence that endothelial progenitors participate in angiogenesis after ischemia (Borlongan et al. 2011), but there has been less study of whether they form a fully mature BBB.

(B) Can the integration of endothelial progenitors into the cerebral endothelium be enhanced? There may be potential adverse effects either in terms of an immature BBB with increased leakiness or the production of cancerous growth (hemangiomas).

(C) Can the BBB be modulated to enhance the delivery of progenitor cells to the brain parenchyma? Most attention has focused on reducing cell (leukocyte) influx during brain injury. For progenitor cells, it may be advantageous to enhance influx. Potential overlaps in mechanism may make the latter difficult without altering leukocyte influx.

(D) How does the delivery of proteins via transduced progenitors compare to systemic delivery of those proteins? Although the approach using transduced progenitors is feasible, quantitatively how does that delivery compare to protein delivery from the bloodstream into the injured brain? It should be noted that because progenitors target the injury site, there may be higher local concentrations and there may be less risk of systemic toxicity.

23.5 Alternate (Nonvascular) Delivery Strategies

Although most studies have focused on delivering potential neuroprotectants from the bloodstream across the BBB, there are alternate strategies to avoid the BBB.

23.5.1 Intranasal

Intranasal administration avoids the BBB by allowing entry into brain across the olfactory epithelium along the olfactory and trigeminal neural pathways (Hanson and Frey 2008). In animal models of cerebral ischemia, intranasal administration of neuroprotectants such as caspase inhibitors and insulin-like growth factor has resulted in reduced ischemic brain damage (Akpan et al. 2011; Liu et al. 2001). A potential caveat to the use of intranasal delivery in human stroke/TBI trials relate to whether drug delivery will be homogeneous within the area affected by the brain injury. Thus, some potential therapeutics have a fairly narrow therapeutic range and may even be detrimental at high concentrations. There is, therefore, the potential for some areas of the brain to have subtherapeutic or harmful drug delivery. This may be particularly important in TBI where areas of brain may be affected that are distant from the initial injury site. Another potential caveat is whether the injury will significantly affect the drug delivery to the injured tissue (e.g., by affecting the extracellular space/CSF flow).

23.5.2 Direct Brain Administration

Direct intraparenchymal injections of therapeutics avoids the BBB, allows injection of large molecules, such as proteins, they can be administered to local regions and they limit potential systemic toxicity. However, in general, such direct administration raises concerns because of the need for surgery. In addition, single injections or slow release capsules that rely on diffusion for drug transport may only result in limited penetration into nearby parenchyma (1–2 mm; (Vogelbaum and Iannotti 2012)). To increase dispersion of agents, convection-enhanced delivery has been proposed where there is a prolonged infusion of the agent and bulk fluid flow serves to carry the drug away from the site of administration (Bobo et al. 1994; Vogelbaum and Iannotti 2012). The potential use of convection-enhanced delivery has been examined in cerebral ischemia with Gd-DPTA (Haar et al. 2010). They found that the Gd-DPTA distributed into a larger volume of brain at lower concentrations following ischemia compared to normal conditions. These changes probably reflect the effects of cellular edema which results in a shrinkage of the extracellular space.

23.5.3 CSF Administration

Intraventricular catheters are commonly placed in patients for CSF drainage. This makes this a more attractive route than direct parenchymal injection. The ependyma cells that line the cerebral ventricles are not linked by tight junctions permitting penetration of agents from CSF to brain parenchyma. However, the extent of that penetration may be limited without continuous drug administration (Smith et al. 2011), and this is likely to be exacerbated in the large human brain. Even with continuous infusion, there may be marked differences in drug concentration between the ependymal surface and brain areas distant from the ventricles (Milhorat et al. 1971). Confounding factors include fluid production in the brain parenchyma which flows towards the CSF system and the clearance of agents by brain parenchymal cells and the BBB.

Intraventricular administration has been used for administration of thrombolytics for intraventricular hemorrhage (IVH) in animal models and clinical trials. Intraventricular administration of tPA speeds the clearance of IVH and the potential benefit of this treatment on clinical outcome is currently being examined (CLEAR IVH trial (Webb et al. 2012)).

23.5.4 Extracranial Administration

It should be noted that some potential therapies may be administered extracranially. Thus, hypothermia can be administered to the head as well as by whole body cooling. Ultrasound for intravascular or intracerebral clot lysis is also administered through the skull.

23.6 Conclusion

Stroke and TBI cause marked changes in BBB properties and can result in marked increases in the brain uptake of compounds from the bloodstream. Understanding those changes and how they impact specific therapeutics may provide opportunities to enhance efficacy. However, broad statements about the BBB being disrupted after stroke and TBI and, therefore, drugs should have access to the brain, are a vast over simplification. Indeed the impact of stroke and TBI on drug delivery likely varies from patient to patient, changes between different impacted brain areas and evolves temporally within a single patient. The impact of such changes in delivery on past (failed) clinical trials for stroke and TBI, and future trials need to be addressed.

Acknowledgments This study was supported by grants NS-034709 (RFK), NS 062853 (AVA), and NS075757 (AVA) from the National Institutes of Health (NIH) and a grant from the Motor City Golf Classic (JX). The content is solely the responsibility of the authors and does not necessarily represent the official views of the NIH.

References

Abbott NJ, Patabendige AAK, Dolman DEM, Yusof SR, Begley DJ (2010) Structure and function of the blood–brain barrier. Neurobiol Dis 37:13–25

Adeoye O, Broderick JP (2010) Advances in the management of intracerebral hemorrhage. Nat Rev Neurol 6:593–601

Akpan N, Serrano-Saiz E, Zacharia BE, Otten ML, Ducruet AF, Snipas SJ, Liu W, Velloza J, Cohen G, Sosunov SA, Frey WH 2nd, Salvesen GS, Connolly ES Jr, Troy CM (2011) Intranasal delivery of caspase-9 inhibitor reduces caspase-6-dependent axon/neuron loss and improves neurological function after stroke. J Neurosci 31:8894–8904

Alexandrov AV (2010) Current and future recanalization strategies for acute ischemic stroke. J Intern Med 267:209–219

Anonymous (1995) Tissue plasminogen activator for acute ischemic stroke. The National Institute of Neurological Disorders and Stroke rt-PA Stroke Study Group. N Engl J Med 333**:** 1581–1587

Bauer B, Hartz AMS, Fricker G, Miller DS (2004) Pregnane X receptor up-regulation of P-glycoprotein expression and transport function at the blood–brain barrier. Mol Pharmacol 66:413–419

Bederson JB, Connolly ES Jr, Batjer HH, Dacey RG, Dion JE, Diringer MN, Duldner JE Jr, Harbaugh RE, Patel AB, Rosenwasser RH (2009) Guidelines for the management of aneurysmal subarachnoid hemorrhage: a statement for healthcare professionals from a special writing group of the Stroke Council, American Heart Association. Stroke 40:994–1025

Bobo RH, Laske DW, Akbasak A, Morrison PF, Dedrick RL, Oldfield EH (1994) Convection-enhanced delivery of macromolecules in the brain. Proc Natl Acad Sci U S A 91: 2076–2080

Bor-Seng-Shu E, Nogueira RDC, Figueiredo EG, Evaristo EF, Conforto AB, Teixeira MJ (2012) Sonothrombolysis for acute ischemic stroke: a systematic review of randomized controlled trials. Neurosurg Focus 32:E5

Borlongan CV, Glover LE, Tajiri N, Kaneko Y, Freeman TB (2011) The great migration of bone marrow-derived stem cells toward the ischemic brain: therapeutic implications for stroke and other neurological disorders. Prog Neurobiol 95:213–228

Bradford ST, Stamatovic SM, Dondeti RS, Keep RF, Andjelkovic AV (2011) Nicotine aggravates the brain postischemic inflammatory response. Am J Physiol - Heart Circ Physiol 300: H1518–H1529

Burns TC, Verfaillie CM, Low WC (2009) Stem cells for ischemic brain injury: a critical review. J Comp Neurol 515:125–144

Cordonnier C, van der Flier WM (2011) Brain microbleeds and Alzheimer's disease: innocent observation or key player? Brain 134:335–344

del Zoppo GJ (2010) Acute anti-inflammatory approaches to ischemic stroke. Ann N Y Acad Sci 1207:143–148

Denes A, Ferenczi S, Kovacs KJ (2011) Systemic inflammatory challenges compromise survival after experimental stroke via augmenting brain inflammation, blood- brain barrier damage and brain oedema independently of infarct size. J Neuroinflam 8:164

Dietrich WD, Prado R, Watson BD, Nakayama H (1988) Middle cerebral artery thrombosis: acute blood–brain barrier consequences. J Neuropathol Experimental Neurol 47:443–451

Dimitrijevic OB, Stamatovic SM, Keep RF, Andjelkovic AV (2006) Effects of the chemokine CCL2 on blood–brain barrier permeability during ischemia-reperfusion injury. J Cereb Blood Flow Metab 26:797–810

el-Bacha RS, Minn A (1999) Drug metabolizing enzymes in cerebrovascular endothelial cells afford a metabolic protection to the brain. Cell Mol Biol 45:15–23

Ennis SR, Keep RF (2006) The effects of cerebral ischemia on the rat choroid plexus. J Cereb Blood Flow Metab 26:675–683

Ennis SR, Keep RF (2007) Effect of sustained-mild and transient-severe hyperglycemia on ischemia-induced blood–brain barrier opening. J Cereb Blood Flow Metab 27:1573–1582

Etminan N, Vergouwen MDI, Ilodigwe D, Macdonald RL (2011) Effect of pharmaceutical treatment on vasospasm, delayed cerebral ischemia, and clinical outcome in patients with aneurysmal subarachnoid hemorrhage: a systematic review and meta-analysis. J Cereb Blood Flow Metab 31:1443–1451

Fernandez-Lopez D, Faustino J, Daneman R, Zhou L, Lee SY, Derugin N, Wendland MF, Vexler ZS (2012) Blood–brain barrier permeability is increased after acute adult stroke but not neonatal stroke in the rat. J Neurosci 32:9588–9600

Finkelstein RA, Alam HB (2010) Induced hypothermia for trauma: current research and practice. J Intensive Care Med 25:205–226

Fisher M, Meadows ME, Do T, Weise J, Trubetskoy V, Charette M, Finklestein SP (1995) Delayed treatment with intravenous basic fibroblast growth factor reduces infarct size following permanent focal cerebral ischemia in rats. J Cereb Blood Flow Metab 15:953–959

Gess B, Sevimli S, Strecker J-K, Young P, Schabitz W-R (2011) Sodium-dependent vitamin C transporter 2 (SVCT2) expression and activity in brain capillary endothelial cells after transient ischemia in mice. PLoS ONE [Electronic Resource] 6:e17139

Ghersi-Egea J-F, Strazielle N, Murat A, Jouvet A, Buenerd A, Belin M-F (2006) Brain protection at the blood-cerebrospinal fluid interface involves a glutathione-dependent metabolic barrier mechanism. J Cereb Blood Flow Metab 26:1165–1175

Gomes JA, Stevens RD, Lewin JJ 3rd, Mirski MA, Bhardwaj A (2005) Glucocorticoid therapy in neurologic critical care. Crit Care Med 33:1214–1224

Haar PJ, Broaddus WC, Chen Z-J, Fatouros PP, Gillies GT, Corwin FD (2010) Quantification of convection-enhanced delivery to the ischemic brain. Physiol Meas 31:1075–1089

Hanson LR, Frey WH 2nd (2008) Intranasal delivery bypasses the blood–brain barrier to target therapeutic agents to the central nervous system and treat neurodegenerative disease. BMC Neurosci 9 Suppl 3:S5

Hawkins BT, Davis TP (2005) The blood–brain barrier/neurovascular unit in health and disease. Pharmacol Rev 57:173–185

Heile A, Brinker T (2011) Clinical translation of stem cell therapy in traumatic brain injury: the potential of encapsulated mesenchymal cell biodelivery of glucagon-like peptide-1. Dialogues Clin Neurosci 13:279–286

Herve F, Ghinea N, Scherrmann J-M (2008) CNS delivery via adsorptive transcytosis. AAPS J 10:455–472

Higashida T, Kreipke CW, Rafols JA, Peng C, Schafer S, Schafer P, Ding JY, Dornbos D 3rd, Li X, Guthikonda M, Rossi NF, Ding Y (2011) The role of hypoxia-inducible factor-1alpha, aquaporin-4, and matrix metalloproteinase-9 in blood–brain barrier disruption and brain edema after traumatic brain injury. J Neurosurg 114:92–101

Hollt V, Kouba M, Dietel M, Vogt G (1992) Stereoisomers of calcium antagonists which differ markedly in their potencies as calcium blockers are equally effective in modulating drug transport by P-glycoprotein. Biochem Pharmacol 43:2601–2608

Hrabetova S, Hrabe J, Nicholson C (2003) Dead-space microdomains hinder extracellular diffusion in rat neocortex during ischemia. J Neurosci 23:8351–8359

Iadecola C, Anrather J (2011) The immunology of stroke: from mechanisms to translation. Nat Med 17:796–808

Jenny B, Kanemitsu M, Tsupykov O, Potter G, Salmon P, Zgraggen E, Gascon E, Skibo G, Dayer AG, Kiss JZ (2009) Fibroblast growth factor-2 overexpression in transplanted neural progenitors promotes perivascular cluster formation with a neurogenic potential. Stem Cells 27: 1309–1317

Jiao H, Wang Z, Liu Y, Wang P, Xue Y (2011) Specific role of tight junction proteins claudin-5, occludin, and ZO-1 of the blood–brain barrier in a focal cerebral ischemic insult. J Mol Neurosci 44:130–139

Johanson CE, Palm DE, Primiano MJ, McMillan PN, Chan P, Knuckey NW, Stopa EG (2000) Choroid plexus recovery after transient forebrain ischemia: role of growth factors and other repair mechanisms. Cell Mol Neurobiol 20:197–216

Jones AR, Shusta EV (2007) Blood–brain barrier transport of therapeutics via receptor-mediation. Pharm Res 24:1759–1771

Jones TH, Morawetz RB, Crowell RM, Marcoux FW, FitzGibbon SJ, DeGirolami U, Ojemann RG (1981) Thresholds of focal cerebral ischemia in awake monkeys. J Neurosurg 54:773–782
Kageyama T, Nakamura M, Matsuo A, Yamasaki Y, Takakura Y, Hashida M, Kanai Y, Naito M, Tsuruo T, Minato N, Shimohama S (2000) The 4F2hc/LAT1 complex transports L-DOPA across the blood–brain barrier. Brain Res 879:115–121
Kago T, Takagi N, Date I, Takenaga Y, Takagi K, Takeo S (2006) Cerebral ischemia enhances tyrosine phosphorylation of occludin in brain capillaries. Biochem Biophys Res Commun 339:1197–1203
Kamouchi M, Ago T, Kuroda J, Kitazono T (2012) The possible roles of brain pericytes in brain ischemia and stroke. Cell Mol Neurobiol 32:159–165
Kawai N, Keep RF, Betz AL (1997) Hyperglycemia and the vascular effects of cerebral ischemia. Stroke 28:149–154
Kawai N, Stummer W, Ennis SR, Betz AL, Keep RF (1999) Blood–brain barrier glutamine transport during normoglycemic and hyperglycemic focal cerebral ischemia. J Cereb Blood Flow Metab 19:79–86
Keep RF, Xiang J, Ennis SR, Andjelkovic A, Hua Y, Xi G, Hoff JT (2008) Blood–brain barrier function in intracerebral hemorrhage. Acta Neurochirurgica - Supplement 105:73–77
Kernie SG, Parent JM (2010) Forebrain neurogenesis after focal Ischemic and traumatic brain injury. Neurobiol Dis 37:267–274
Kleinschnitz C, Blecharz K, Kahles T, Schwarz T, Kraft P, Gobel K, Meuth SG, Burek M, Thum T, Stoll G, Forster C (2011) Glucocorticoid insensitivity at the hypoxic blood–brain barrier can be reversed by inhibition of the proteasome. Stroke 42:1081–1089
Kwon I, Kim EH, del Zoppo GJ, Heo JH (2009) Ultrastructural and temporal changes of the microvascular basement membrane and astrocyte interface following focal cerebral ischemia. J Neurosci Res 87:668–676
Leary MC, Saver JL (2003) Annual incidence of first silent stroke in the United States: a preliminary estimate. Cerebrovasc Dis 16:280–285
Li Y, Chopp M (2009) Marrow stromal cell transplantation in stroke and traumatic brain injury. Neurosci Lett 456:120–123
Lippmann ES, Azarin SM, Kay JE, Nessler RA, Wilson HK, Al-Ahmad A, Palecek SP, Shusta EV (2012) Derivation of blood–brain barrier endothelial cells from human pluripotent stem cells. Nat Biotechnol 30:783–791
Liu XD, Zhang L, Xie L (2003) Effect of P-glycoprotein inhibitors erythromycin and cyclosporin A on brain pharmacokinetics of nimodipine in rats. Eur J Drug Metab Pharmacokinet 28: 309–313
Liu XF, Fawcett JR, Thorne RG, DeFor TA, Frey WH 2nd (2001) Intranasal administration of insulin-like growth factor-I bypasses the blood–brain barrier and protects against focal cerebral ischemic damage. J Neurol Sci 187:91–97
Liu Y, Lu J-B, Ye Z-R (2006) Permeability of injured blood brain barrier for exogenous bFGF and protection mechanism of bFGF in rat brain ischemia. Neuropathology 26:257–266
Maas AI, Stocchetti N, Bullock R (2008) Moderate and severe traumatic brain injury in adults. Lancet Neurol 7:728–741
Mabuchi T, Lucero J, Feng A, Koziol JA, del Zoppo GJ (2005) Focal cerebral ischemia preferentially affects neurons distant from their neighboring microvessels. J Cereb Blood Flow Metab 25:257–266
MacLellan CL, Clark DL, Silasi G, Colbourne F (2009) Use of prolonged hypothermia to treat ischemic and hemorrhagic stroke. J Neurotrauma 26:313–323
McDannold N, Vykhodtseva N, Raymond S, Jolesz FA, Hynynen K (2005) MRI-guided targeted blood–brain barrier disruption with focused ultrasound: histological findings in rabbits. Ultrasound Med Biol 31:1527–1537
Meijer OC, de Lange EC, Breimer DD, de Boer AG, Workel JO, de Kloet ER (1998) Penetration of dexamethasone into brain glucocorticoid targets is enhanced in mdr1A P-glycoprotein knockout mice. Endocrinology 139:1789–1793
Menzies SA, Betz AL, Hoff JT (1993) Contributions of ions and albumin to the formation and resolution of ischemic brain edema. J Neurosurg 78:257–266

Milhorat TH, Hammock MK, Fenstermacher JD, Levin VA (1971) Cerebrospinal fluid production by the choroid plexus and brain. Science 173:330–332

Nagaraja TN, Keenan KA, Brown SL, Fenstermacher JD, Knight RA (2007) Relative distribution of plasma flow markers and red blood cells across BBB openings in acute cerebral ischemia. Neurol Res 29:78–80

Noor R, Wang CX, Shuaib A (2005) Hyperthermia masks the neuroprotective effects of tissue plaminogen activator. Stroke 36:665–669

Patak P, Hermann DM (2011) ATP-binding cassette transporters at the blood–brain barrier in ischaemic stroke. Curr Pharm Des 17:2787–2792

Piriyawat P, Labiche LA, Burgin WS, Aronowski JA, Grotta JC (2003) Pilot dose-escalation study of caffeine plus ethanol (caffeinol) in acute ischemic stroke. Stroke 34:1242–1245

Preston E, Foster DO (1997) Evidence for pore-like opening of the blood–brain barrier following forebrain ischemia in rats. Brain Res 761:4–10

Preston E, Webster J (2002) Differential passage of [14C]sucrose and [3H]inulin across rat blood–brain barrier after cerebral ischemia. Acta Neuropathol 103:237–242

Pun PBL, Lu J, Moochhala S (2009) Involvement of ROS in BBB dysfunction. Free Radic Res 43:348–364

Reinhard M, Hetzel A, Kruger S, Kretzer S, Talazko J, Ziyeh S, Weber J, Els T (2006) Blood–brain barrier disruption by low-frequency ultrasound. Stroke 37:1546–1548

Rhodes J (2011) Peripheral immune cells in the pathology of traumatic brain injury? Curr Opin Crit Care 17:122–130

Richardson RM, Singh A, Sun D, Fillmore HL, Dietrich DW 3rd, Bullock MR (2010) Stem cell biology in traumatic brain injury: effects of injury and strategies for repair. J Neurosurg 112:1125–1138

Roger VL, Go AS, Lloyd-Jones DM, Benjamin EJ, Berry JD, Borden WB, Bravata DM, Dai S, Ford ES, Fox CS, Fullerton HJ, Gillespie C, Hailpern SM, Heit JA, Howard VJ, Kissela BM, Kittner SJ, Lackland DT, Lichtman JH, Lisabeth LD, Makuc DM, Marcus GM, Marelli A, Matchar DB, Moy CS, Mozaffarian D, Mussolino ME, Nichol G, Paynter NP, Soliman EZ, Sorlie PD, Sotoodehnia N, Turan TN, Virani SS, Wong ND, Woo D, Turner MB (2012) Heart disease and stroke statistics–2012 update: a report from the American Heart Association. Circulation 125:e2–e220

Rosenberg GA, Yang Y (2007) Vasogenic edema due to tight junction disruption by matrix metalloproteinases in cerebral ischemia. Neurosurg Focus 22:E4

Schinkel AH, Wagenaar E, van Deemter L, Mol CA, Borst P (1995) Absence of the mdr1a P-Glycoprotein in mice affects tissue distribution and pharmacokinetics of dexamethasone, digoxin, and cyclosporin A. J Clin Investigation 96:1698–1705

Schubert GA, Thome C (2008) Cerebral blood flow changes in acute subarachnoid hemorrhage. Front Biosci 13:1594–1603

Shlosberg D, Benifla M, Kaufer D, Friedman A (2010) Blood–brain barrier breakdown as a therapeutic target in traumatic brain injury. Nat Rev Neurosci 6:393–403

Smith DE, Hu Y, Shen H, Nagaraja TN, Fenstermacher JD, Keep RF (2011) Distribution of glycylsarcosine and cefadroxil among cerebrospinal fluid, choroid plexus, and brain parenchyma after intracerebroventricular injection is markedly different between wild-type and Pept2 null mice. J Cereb Blood Flow Metab 31:250–261

Smith SL, Hall ED (1996) Mild pre- and posttraumatic hypothermia attenuates blood–brain barrier damage following controlled cortical impact injury in the rat. J Neurotrauma 13:1–9

Song B-W, Vinters HV, Wu D, Pardridge WM (2002) Enhanced neuroprotective effects of basic fibroblast growth factor in regional brain ischemia after conjugation to a blood–brain barrier delivery vector. J Pharmacol Exp Therap 301:605–610

Spudich A, Kilic E, Xing H, Kilic U, Rentsch KM, Wunderli-Allenspach H, Bassetti CL, Hermann DM (2006) Inhibition of multidrug resistance transporter-1 facilitates neuroprotective therapies after focal cerebral ischemia. Nat Neurosci 9:487–488

Stamatovic SM, Keep RF, Andjelkovic AV (2008) Brain endothelial cell-cell junctions: how to "open" the blood brain barrier. Curr Neuropharmacol 6:179–192

Stamatovic SM, Keep RF, Wang MM, Jankovic I, Andjelkovic AV (2009) Caveolae-mediated internalization of occludin and claudin-5 during CCL2-induced tight junction remodeling in brain endothelial cells. J Biol Chem 284:19053–19066

Stummer W, Betz AL, Shakui P, Keep RF (1995) Blood–brain barrier taurine transport during osmotic stress and in focal cerebral ischemia. J Cereb Blood Flow Metab 15:852–859

Sykova E (1997) Extracellular space volume and geometry of the rat brain after ischemia and central injury. Adv Neurol 73:121–135

Szmydynger-Chodobska J, Strazielle N, Zink BJ, Ghersi-Egea J-F, Chodobski A (2009) The role of the choroid plexus in neutrophil invasion after traumatic brain injury. J Cereb Blood Flow Metab 29:1503–1516

Szmydynger-Chodobska J, Strazielle N, Gandy JR, Keefe TH, Zink BJ, Ghersi-Egea J-F, Chodobski A (2012) Posttraumatic invasion of monocytes across the blood-cerebrospinal fluid barrier. J Cereb Blood Flow Metab 32:93–104

Tanaka H, Mizojiri K (1999) Drug-protein binding and blood–brain barrier permeability. J Pharmacol Exp Therap 288:912–918

Topakian R, Barrick TR, Howe FA, Markus HS (2010) Blood–brain barrier permeability is increased in normal-appearing white matter in patients with lacunar stroke and leucoaraiosis. J Neurol Neurosurg Psychiatry 81:192–197

Uchida Y, Ohtsuki S, Kamiie J, Terasaki T (2011) Blood–brain barrier (BBB) pharmacoproteomics: reconstruction of in vivo brain distribution of 11 P-glycoprotein substrates based on the BBB transporter protein concentration, in vitro intrinsic transport activity, and unbound fraction in plasma and brain in mice. J Pharmacol Exp Therap 339:579–588

van Velthoven CTJ, Kavelaars A, van Bel F, Heijnen CJ (2009) Regeneration of the ischemic brain by engineered stem cells: fuelling endogenous repair processes. Brain Res Rev 61:1–13

Vemula S, Roder KE, Yang T, Bhat GJ, Thekkumkara TJ, Abbruscato TJ (2009) A functional role for sodium-dependent glucose transport across the blood–brain barrier during oxygen glucose deprivation. J Pharmacol Exp Therap 328:487–495

Vestweber D (2007) Adhesion and signaling molecules controlling the transmigration of leukocytes through endothelium. Immunol Rev 218:178–196

Vogelbaum MA, Iannotti CA (2012) Convection-enhanced delivery of therapeutic agents into the brain. Handb Clin Neurol 104:355–362

von Wedel-Parlow M, Schrot S, Lemmen J, Treeratanapiboon L, Wegener J, Galla H-J (2011) Neutrophils cross the BBB primarily on transcellular pathways: an in vitro study. Brain Res 1367:62–76

Walker PA, Shah SK, Jimenez F, Gerber MH, Xue H, Cutrone R, Hamilton JA, Mays RW, Deans R, Pati S, Dash PK, Cox CS Jr (2010) Intravenous multipotent adult progenitor cell therapy for traumatic brain injury: preserving the blood brain barrier via an interaction with splenocytes. Exp Neurol 225:341–352

Wallace BK, Foroutan S, O'Donnell ME (2011) Ischemia-induced stimulation of Na-K-Cl cotransport in cerebral microvascular endothelial cells involves AMP kinase. Am J Physiol - Cell Physiol 301:C316–C326

Wang J (2010) Preclinical and clinical research on inflammation after intracerebral hemorrhage. Prog Neurobiol 92:463–477

Webb AJ, Ullman NL, Mann S, Muschelli J, Awad IA, Hanley DF (2012) Resolution of intraventricular hemorrhage varies by ventricular region and dose of intraventricular thrombolytic: The clot lysis: Evaluating Accelerated Resolution of IVH (CLEAR IVH) Program. Stroke 43:1666–1668

Westergaard E, Go G, Klatzo I, Spatz M (1976) Increased permeability of cerebral vessels to horseradish peroxidase induced by ischemia in Mongolian Gerbils. Acta Neuropathol 35:307–325

Xi G, Keep RF, Hoff JT (2006) Mechanisms of brain injury after intracerebral haemorrhage. Lancet Neurol 5:53–63

Yamashita T, Kamiya T, Deguchi K, Inaba T, Zhang H, Shang J, Miyazaki K, Ohtsuka A, Katayama Y, Abe K (2009) Dissociation and protection of the neurovascular unit after thrombolysis and reperfusion in ischemic rat brain. J Cereb Blood Flow Metab 29:715–725

Yang Y, Estrada EY, Thompson JF, Liu W, Rosenberg GA (2007) Matrix metalloproteinase-mediated disruption of tight junction proteins in cerebral vessels is reversed by synthetic matrix metalloproteinase inhibitor in focal ischemia in rat. J Cereb Blood Flow Metab 27:697–709

Yenari MA, Han HS (2012) Neuroprotective mechanisms of hypothermia in brain ischaemia. Nat Rev Neurosci 13:267–278

Zhang Y, Pardridge WM (2001) Neuroprotection in transient focal brain ischemia after delayed intravenous administration of brain-derived neurotrophic factor conjugated to a blood–brain barrier drug targeting system. Stroke 32:1378–1384

Zhang Z, Zhang L, Yepes M, Jiang Q, Li Q, Arniego P, Coleman TA, Lawrence DA, Chopp M (2002) Adjuvant treatment with neuroserpin increases the therapeutic window for tissue-type plasminogen activator administration in a rat model of embolic stroke. Circulation 106:740–745

Zhang ZG, Chopp M (2009) Neurorestorative therapies for stroke: underlying mechanisms and translation to the clinic. Lancet Neurol 8:491–500

Zlokovic BV, McComb JG, Lipovac MN, Chen TC, Mackic JB, Schneider J, Gianotta SL, Weiss MH (1993) Differential brain penetration of cerebroprotective drugs. Adv Exp Med Biol 331:117–120

Chapter 24
Which Drug or Drug Delivery Method Can Change Clinical Practice for Brain Tumor Therapy?

Tali Siegal

Abstract Despite advances in anticancer drug discovery and development, there has been little improvement in the prognosis and outcome of malignant brain tumors. Often and repeatedly it has been found that promising experimental agents for brain tumors have had little impact on the disease in clinical trials. These disappointing results can be partially explained by the inability to deliver therapeutic agents to the CNS across the physiological barriers (the blood–brain, blood–tumor, and blood–CSF barriers). The impediment posed by these barriers leads to failure of the delivered drug to reach the desired target in adequate concentrations. This chapter shortly reviews the leading strategies that try to improve drug delivery to brain tumors in view of their likelihood to change clinical practice. Strategies that use systemic delivery and those that utilize local delivery are critically reviewed. In addition challenges posed for drug delivery by the combined treatment with antiangiogenic therapy are outlined. For future development all new drugs or delivery systems must adhere to basic clinical expectations. These include besides an antitumor effect, a verified favorable toxicity profile, an easy introduction into clinical practice, feasibility of repeated or continuous administration and compatibility of the drug or strategy for any tumor size and brain location. Adherence to these essentials will enable a change in clinical practice

Abbreviation

AUC	Area under the curve
BBB	Blood–brain barrier
CED	Convection-enhanced delivery

T. Siegal, M.D. (✉)
Gaffin Center for Neuro-Oncology, Hadassah Hebrew University Medical Center, Ein Kerem, P.O.Box 12000, Jerusalem 91120, Israel
e-mail: siegal@hadassah.org.il

M. Hammarlund-Udenaes et al. (eds.), *Drug Delivery to the Brain*, AAPS Advances in the Pharmaceutical Sciences Series 10, DOI 10.1007/978-1-4614-9105-7_24,

CNS	Central nervous system
CSF	Cerebrospinal fluid
ECF	Extracellular fluid
EGF	Epidermal growth factor
HD-CTx	High-dose chemotherapy
MTX	Methotrexate
P-gp	P-glycoprotein
PEG	Polyethylene glycol
RES	Reticuloendothelial system
SAE	Severe adverse effects
VEGF	Vascular endothelial growth factor

24.1 Introduction

Despite advances in anticancer drug discovery and development, there has been little improvement in the prognosis and outcome of malignant brain tumors. Often and repeatedly it has been found that promising experimental agents for brain tumors have had little impact on the disease in clinical trials. These disappointing results can be partially explained by the inability to deliver therapeutic agents to the CNS across the blood–brain barrier (BBB) and failure of the delivered drug to reach the desired target in adequate concentration (Muldoon et al. 2007). This chapter shortly reviews the leading strategies that try to improve drug delivery to brain tumors in view of their likelihood to change clinical practice. The evaluation and judgments expressed in this chapter are based on perspective obtained from clinical experience. The content of this chapter does not relate to viral and DNA-based therapy or to immunotherapy although some extrapolations may be relevant particularly for the first two therapies.

24.2 Malignant Brain Tumors and Physiological Blood–Brain Barrier Function

Systemic chemotherapy for treatment of malignant brain tumors consists of traditional drugs that mostly belong to DNA alkylating agents which intervene in the cell cycle. Recently newer drugs that target cell surface receptors and associated pathways are being intensively investigated in clinical trials (Stewart 2002; Stupp et al. 2007). The ineffectiveness of drug therapy in the management of malignant brain tumors has been attributed to the physiological barriers namely, the BBB, blood–CSF barrier, and blood–tumor barrier (Muldoon et al. 2007). The BBB is a significant impediment to the transvascular extravasation of drugs into the extracellular compartment of brain tissue. However, the barrier is often porous in malignant brain tumors and this is demonstrated by the transvascular extravasation of contrast agents

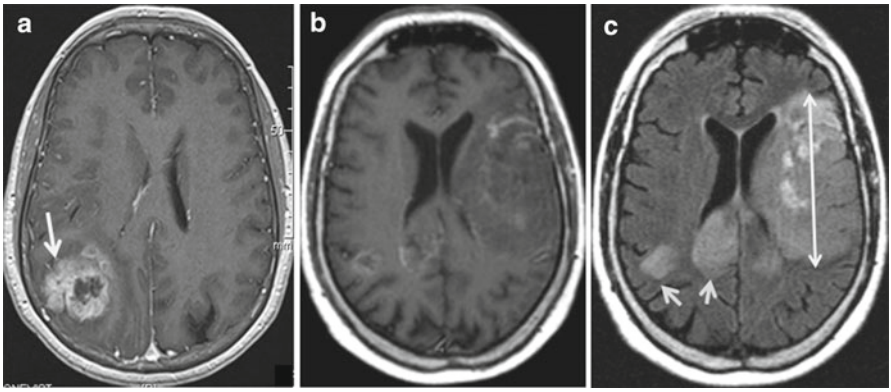

Fig. 24.1 Brain tumors and blood–brain barrier function. (**a**) Contrast enhancement of glioblastoma (*arrow*). The blood–tumor barrier is often porous in malignant brain tumors and this is demonstrated by the transvascular extravasation of the contrast agent that produces the contrast-enhancement effect on MRI study (T_1 weighted image with Gadolinium). (**b**) A MRI image of glioblastoma that demonstrates a mass effect on the left lateral ventricle with scanty areas of contrast enhancement (T_1 weighted image with Gadolinium). (**c**) The fluid attenuation reversion recovery (FLAIR) sequence of the MRI study of the tumor shown in (**b**). It demonstrates a large and extensive tumor (observed as hyperintensity) that involves the left hemisphere and produces the mass effect on the left lateral ventricle (the *double head arrow* delineates the longest diameter of the left hemispheric tumor). The tumor also crosses the splenium of the corpus callosum and involves the posterior aspect of the right hemisphere (*arrows*). Judged by the extent of the tumor on this FLAIR sequence most of the tumor mass is located behind an intact physiological barrier (no extravasation of the injected contrast agent on (**b**))

that produce the contrast enhancement effect during imaging of brain tumors (Fig. 24.1a) (Essig et al. 2006; Schneider et al. 2001). The contrast agent leaks into the extravascular extracellular compartment of the tumor tissue and therefore it has been argued that the BBB might not be a limiting factor for extravasation of small molecular weight drugs (Groothuis and Vick 1982; Vick et al. 1977). However, poor drug delivery to brain tumor is an outcome of multiple contributing factors such as low plasma concentration of the drug at tumor site, irregular vasculature of the tumor, increased interstitial pressure, and intratumoral hypoxia (Jain 1994, 2005; Netti et al. 1995). Still, a functioning physiological blood-barrier at the tumor site (Fig. 24.1b, c) may severely limit drug access into the extracellular space of the tumor.

When planning drug therapy for malignant brain tumor it is essential to figure out whether tumors actually reside behind intact BBB. Magnetic resonance imaging (MRI) often suggests that tumor infiltrates far beyond its enhancing part (Fig. 24.1c). With the advent of advanced neurosurgical techniques, contemporary imaging and precise localization of tissue sampling, it has become clear that significant portions of high-grade tumors reside behind intact barrier function. In fact, it has been demonstrated that glioblastomas, the most malignant brain tumors, contain heterogeneous cell populations with growth patterns which are characterized as either angiogenic or nonangiogenic, albeit similar proliferation rates (Naumov et al. 2006).

Recent experience with antiangiogenic treatment proved that glioblastoma can continue and grow and even increase cell invasion without a need for a second wave of angiogenesis (di Tomaso et al. 2011; Keunen et al. 2011). All these indicate that brain tumors proliferate behind an intact BBB function and this barricade has to be crossed by any drug aimed to affect tumor growth.

24.3 Requirements from a Drug Therapy and Practical Issues That Have to Be Faced

Many aspects and multiple components are involved in the ability of a certain drug to induce its anti-neoplastic effect. The first steps of drug development and evaluation engage the in vitro and subcutaneous xenografts proof that the agent in hand effectively kills tumor cells or enhances their killing by other modalities (e.g. radiation therapy). Once in vivo and human studies are involved other aspects have to be considered. These include the basic requirement that the drug should reach every brain tumor cell. For that to be possible the drug should first get to the desired target (the brain tumor) in adequate concentration and then maintain this concentration in the tumor's extracellular space for an adequate period of time in order to be effective (Blakeley and Portnow 2010). These prerequisites are major obstacles that are directly related to the method of drug delivery that should be carefully contemplated. In principle, the choices are between systemic deliveries versus local administration. Systemic delivery should face the impediment posed by the BBB. It relies on the existing vascular bed to serve as the delivery vehicle that will bring the drug to the desired site but, the drug has to cross the vascular wall to the abluminal side. On the other hand, local delivery is circumventing this impediment but has to confront with the limited ability to reach distant infiltrating tumor cells. Almost all recent drug developments in neuro-oncology either try to improve the technique of drug delivery or otherwise fail on this account (Bidros and Vogelbaum 2009; Laquintana et al. 2009; Soni et al. 2010).

Apart from the delivery method other relevant features for drug therapy includes the drug wash out from the extracellular space and the sink effect of the CSF which becomes major issues once local delivery is selected. Additional factors are the drug uptake by tumor cells and cellular targets, and the metabolic fate of the drug within tumor cells, features that are usually investigated in preclinical models but are largely not addressed in human studies.

Any drugs that finally reach the level of human study can be evaluated for its prospects to change clinical practice based on a set of five basic elements that include clinical expectations from a drug therapy. The expectations from drug therapy cannot be separated from issues related to the strategy which is used for the delivery of the agent to the brain. Those consist of the followings:

- Effectiveness
- Favorable adverse effects profile (including systemic toxicity and neurotoxicity)

- Easy introduction (assimilation) into clinical practice
- Repeated or continuous administration should be feasible (no agent is expected to cure a tumor by a single exposure to the drug)
- The agent and delivery strategy should be useful for any tumor size and every CNS location.

In the last three decades only one agent, temozolomide, did change clinical practice for malignant brain tumors. If we evaluate this agent by the above set of five expectations it becomes clear that temozolomide fulfills all of them. Temozolomide proved to significantly prolong both progression free survival and overall survival of patients with newly diagnosed glioblastoma (Stupp et al. 2005). The treatment is well tolerated with a favorable adverse effect profile and the regimen was easily assembled into clinical practice and became the standard therapy practiced in every clinic around the world. Repeated and continuous administration is feasible and constitutes part of the regimen, and finally it is probably useful for any tumor size at any CNS location.

24.4 Systemic Delivery of Drugs to Brain Tumors and Methods to Improve Drug Transport

Once systemic delivery of drugs is used to treat brain tumors an optimal effect depends on the ability to maintain drug concentration at the target site for sufficient duration while avoiding systemic toxicity. These basic elements are hardly ever achieved by standard chemotherapeutic agents used to treat brain tumors. For example, most small molecular weight drugs, like nitrosoureas, are rapidly eliminated by hepatic metabolism and renal excretion and due to the short blood half life only limited fraction of the drug gets to the target site of the brain tumor (Laquintana et al. 2009; Soni et al. 2010; Patel et al. 2009). The portion of the drug that does not get to the target site can be toxic to off-target organs and induce systemic toxicity. So the fraction of the drug that reaches the tumor, or the plasma concentration at the target area, is an elementary factor that determines the prospects to achieve adequate extracellular drug concentration at the tumor site. Once adequate plasma drug concentrations are achieved drugs still have to cross the physiological barriers in order to get to the extracellular space of the tumor and the surrounding brain. Basically there are two major types of transport mechanisms of drugs across the BBB: the passive diffusion mechanism which is concentration gradient dependent and the endogenous carrier mediated transport. These topics have been reviewed recently in relation to brain tumor drug therapy (Laquintana et al. 2009; Soni et al. 2010; Patel et al. 2009). An additional element that has to be faced is the active efflux transporters mechanisms that limit the ability to achieve effective drug concentration either at the extracellular space or within tumor cells due to active pumping of the drug away from its target (Haga et al. 2001; Rittierodt and Harada 2003; Becker et al. 1991).

24.4.1 Strategies to Improve Passive Drug Transport Across the BBB

Many strategies have been designed to overcome the poor transport of drugs across the barriers, and many are still under development. Those strategies that rely on systemic delivery of drugs are either trying to improve the passive drug transport across the barrier, or are exploiting the endogenous carrier transporters mechanism to carry the agents across the vascular wall. Improvement in passive drug transport may be achieved by manipulation of the drug, or by increasing the plasma concentration of the drug, or by transient opening of the BBB. An alternative approach is to block the active efflux transporters mechanism and thus maintain the drug in the abluminal side of the BBB.

Manipulation of the drug may include chemical modifications that improve the chances of the drug to passively cross the barrier namely, its lipophilicity may be increased (by lipidization), protein binding may be reduced or alternatively its plasma half life may be prolonged. For example, a sustained drug-release formulation can improve the plasma steady state concentration. Another approach is to formulate a prodrug that crosses the BBB. The most successful example is the case of temozolomide (Friedman et al. 2000) that converts under physiological pH to 5-(3-methyltriazen-1-yl)imidazole-4-carboxamide (MTIC) which is the active metabolite of dacarbazine (DTIC), a drug that has been in use for many years to treat systemic malignancy but is unable to cross the BBB.

24.4.1.1 Strategies That Increase Plasma Drug Concentration

Plasma concentration at the tumor site is an important factor in a mechanism which is dependent on concentration gradient as is the passive transport system of the BBB. Therefore, multiple approaches have tried to increase the fraction of the drug that reaches the brain. Those include the use of high-dose chemotherapy, bolus drug injection, and intra-arterial drug administration. High-dose chemotherapy increases plasma concentration of the drug at the cost of augmented systemic toxicity and therefore it requires systemic rescue maneuvers such as the use of folinic acid in the case of methotrexate (MTX), or granulocytic colony-stimulating factors with or without autologous bone marrow stem cell support when other agents are used.

An alternative method to increase plasma concentration with no need to modify the drug dose is to use bolus drug injection. Its effect on drug penetration into the extracellular space of a brain tumor model was demonstrated by the use of an osmotic pump device implanted within the tumor mass. This device enables dynamic in vivo evaluation of tumor's extracellular drug concentrations and at the same time plasma levels are measured as well (Dukic et al. 1999, 2000). These samplings demonstrated that a bolus injection of MTX (which is a water soluble drug) produced significantly higher pick drug concentrations in both plasma and tumor's extracellular fluid. The calculated ratio of the area under the curve of the tumor's

extracellular fluid/plasma (AUC_{ECF}/AUC_{plasma}) was significantly higher than the ratio that was obtained following continuous drug infusion. This ratio expresses drug penetration across the barrier and into the extracellular space of the tumor, and therefore the increased ratio indicates that the bolus injection augmented drug penetration. Similarly, a clinical study in patients with CNS lymphoma compared results of rapid versus slow infusion of MTX. The study showed higher CSF drug level and a trend toward improved outcome in patients treated with rapid MTX infusion (Hiraga et al. 1999). Of note is another human study that used implanted osmotic pumps in patients with malignant Gliomas for evaluation of MTX concentration in the extracellular space of the tumors. MTX was delivered by rapid infusion and the study demonstrated the profound effect of BBB permeability on drug concentration in the extracellular space of the tumor. The calculated AUC_{ECF}/AUC_{plasma} ratio was considerably greater in the region of contrast enhancing tumor (that contains leaky vasculature) than in the non-enhancing tissue (demonstrating intact barrier function) as can be expected for a passive transport of a small molecular weight water soluble drug such as MTX (Blakeley et al. 2009).

Intra-arterial drug administration has been used in various protocols in an attempt to increase plasma drug concentration and improve outcome (Gelman et al. 1999; Osztie et al. 2001; Tfayli et al. 1999; Angelov et al. 2009). The chemotherapy in this case is injected into the artery that supplies blood to the tumor and the surrounding brain. The advantage is that the perfused tissue receives higher plasma concentration during the first passage of the drug through the circulation, and the short duration of injection (5–15 min) is producing high plasma concentration (Cmax) due to the bolus injection. The disadvantages include the fact that this is an invasive procedure that induces only transient and short elevation of plasma concentration at the tumor area. Still, a study that evaluated cisplatin concentration in resected brain metastases showed significantly higher cisplatin tumor levels following pre-surgery intra-arterial infusion of the drug as compared to conventional intravenous cisplatin administration (Nakagawa et al. 1993).

24.4.1.2 Strategies That Induce Transient Disruption of the BBB

Strategies that try to induce transient disruption of the BBB in order to enhance the passive drug transport across the barrier include osmotic BBB disruption (BBBD) (Angelov et al. 2009), biochemical disruption (Borlongan and Emerich 2003) and ultrasound mediated BBBD (Chen et al. 2010; Liu et al. 2010; Deng 2010).

Osmotic disruption of the BBB is the only technique that is practiced by some centers for treatment of brain tumors as part of experimental treatment protocols. It entails transfemoral catheterization of the desired arterial territory and transient opening of the BBB which is induced by rapid intra-arterial infusion of hyperosmolar mannitol. Immediately after mannitol infusion intra-arterial and intravenous chemotherapy is given. The procedure is performed on two consecutive days under general anesthesia with assisted mechanical ventilation, requires a multidisciplinary expert team approach, and is repeated monthly as per protocol. Human studies

demonstrated that normalization of the BBB function following the osmotic disruption is a prolonged process that takes 6 h or more (Siegal et al. 2000), a period during which there is an increased risk for neurotoxic effects. Another study demonstrated a linear relationship between the semi-quantitative measurement of the degree of barrier disruption on post procedure imaging and MTX concentrations that were evaluated in the ventricular CSF of humans (Zylber-Katz et al. 2000). These findings fit the model of a water soluble drug, such as MTX, that penetrates the CNS by passive transport. That means that high degree of disruption will allow more drug penetration into the CNS. Yet, intense disruption is often associated with increased risk for complications including seizures or even fatal brain edema (Angelov et al. 2009; Marchi et al. 2007) and therefore the procedure is usually adjusted for moderate and safer degree of disruption. The available data from previous human studies (Siegal et al. 2000; Zylber-Katz et al. 2000) and a recent rabbit model (Joshi et al. 2011; Ergin et al. 2012) suggest that there are significant variations in the degree and duration of BBBD induced with intra-arterial mannitol. The inconsistency of the degree of BBBD has a profound effect on the passive drug delivery across the vascular wall (Zylber-Katz et al. 2000; Joshi et al. 2011) and on the reliability of this procedure for that effect. The largest published experience with the use of BBBD in conjunction with chemotherapy has been obtained from a multicenter study that treated patients with primary CNS lymphoma (Angelov et al. 2009). Unfortunately this study did not clearly demonstrated results which are superior to treatment outcome obtained with conventional administration of chemotherapy in this disease.

Biochemical disruption of the BBB relies on mediators of the inflammatory response. These mediators which include leukotrienes, histamine, and vasoactive peptides, can cause transient vascular leakage and increased permeability of blood vessels (Cloughesy and Black 1995). Bradykinin, a peripheral vasodilator, increases the tight junction permeability by activating B2 receptors of the endothelial cells (Bartus et al. 1996). The bradykinin agonist, RMP-7, transiently permeabilizes the BBB to hydrophilic compounds with greater impact in regions of the blood–tumor barrier as compared to nontumor BBB (Borlongan and Emerich 2003). Human studies showed that sequential intra-arterial injection of RMP-7 and the anticancer agent carboplatin were needed to enhance drug penetration into the tumor, which means that the method requires an invasive procedure. In a multinational clinical trial, intra-arterial RMP-7 was evaluated in combination with carboplatin for the treatment of malignant brain tumors (Ford et al. 1998) but due to high level of toxicity the trial was discontinued.

Ultrasound mediated BBBD (Chen et al. 2010; Liu et al. 2010; Deng 2010) is a new approach to focal CNS drug delivery. It produces consistent vascular leak without tissue damage in animal models. This effect is achieved by localizing cavitation-generated mechanical stresses to blood vessel walls by intravenous injection of preformed gas bubbles just before pulsed ultrasound treatment (Deng 2010; Hynynen et al. 2001). The focal opening of the BBB is reversible and does not last beyond 24 h. Animal studies showed that significantly higher liposomal doxorubicin concentrations were found in the brain regions exposed to the focused ultrasound effect (Treat et al. 2007). Clinical devices for magnetic resonance guided

focus ultrasound are available now but their use as a non invasive technique to treat brain disease is still under development. Future directions include further technology development for controlled and efficient drug transmission into the brain and demonstration of therapeutic efficacy. In addition, safety issues of cumulative effects of repeated procedures are important for eventual brain tumor therapy. The main drawback seems to be related to the limited focal disruption of the barrier defined to small areas. Therefore, the recently reported positive effects in small animal malignant Glioma models (Chen et al. 2010; Liu et al. 2010; Ting et al. 2012) might not be duplicated in large animals or in humans. Focal and limited volume of therapeutic exposure to drugs means that the technique may be applicable only for tumors of very limited size and that tumor cells that infiltrated away from the treated focus will escape the desired effect of enhanced exposure to chemotherapy.

24.4.1.3 Strategies That Block the Active Efflux Transporters Mechanisms

Active efflux of anticancer drugs contributes to drug resistance of brain tumors (Demeule et al. 2002; Ito et al. 2005). There are various efflux transporter systems that include the P-glycoprotein (P-gp) which is the most widely researched (Demeule et al. 2002), the breast cancer-resistance protein (BCRP) (Ito et al. 2005) and the multidrug-resistance-associated protein (MRP) family(Kruh and Belinsky 2003). Coadministration of chemotherapy with inhibitors of the active efflux transporters may increase drug concentration in the extracellular space. Preclinical and clinical studies have been performed to explore the potential of P-gp inhibition to improve CNS penetration of anticancer drugs. However, disappointing results were obtained in clinical trials using first generation P-gp inhibitors (e.g. verapamil, cyclosporin A) due to toxicity issues (Sikic et al. 1997). Novel P-gp inhibitors (e.g. valspodar, elacridar, zosuquidar) have an improved affinity profile and may prove to have a reduced clinical toxicity (Kemper et al. 2004). So far evidence is lacking to support routine use of these inhibitors.

24.4.1.4 Impact on Clinical Practice of Strategies Designed to Improve Passive Drug Transport Across the BBB (Tables 24.1 and 24.2)

The expected clinical impact of strategies that try to improve the passive drug transport across the BBB are discussed on the basis of the set of five expectations from drug therapy specified in Sect. 24.3.

Strategies that increase the plasma drug concentration namely, high-dose chemotherapy (HD-CTx) with systemic rescue maneuvers, bolus drug injection, and intra-arterial drug administration have had some impact on clinical practice (Table 24.1). HD-CTx is actually practiced routinely to treat both systemic malignancies and CNS tumors but its effectiveness regarding CNS involvement has been proved only in lymphoproliferative malignancies. In Burkitt's lymphoma and adult

Table 24.1 Strategies that increase the plasma drug concentration: Clinical impact based on expectations from drug therapy (for references please see text)

Strategy	Effectiveness for CNS malignancy	Toxicity/adverse effects profile	Introduction into clinical practice	Repeated/continuous administration	Tumor size and CNS location
High-dose chemotherapy with systemic rescue maneuvers	Established in Burkitt's lymphoma, ALL and PCNSL[a]	Usually manageable	Simple, widely practiced	Feasible but may be limited (by toxicity)	No limitations
Intravenous bolus drug injection	Suggested but not established in humans	Negligible	Simple, widely practiced	Feasible	No limitations
Intra-arterial drug injection	Suggested but not established (only phase II studies)	Invasive procedure. May be associated with SAE. Frequency varies	Limited. Requires expert team approach.	Feasible but limited by invasiveness of the procedure	No limitations

ALL adult lymphoblastic lymphoma, *PCNSL* primary CNS lymphoma, *SAE* severe adverse events

[a]Based on phase III clinical studies

Table 24.2 Strategies that induce transient disruption of the BBB in conjunction with intravenous and/or intra-arterial chemotherapy: Clinical impact based on expectations from drug therapy (for references please see text)

Strategy	Effectiveness for CNS malignancy	Toxicity/adverse effects profile	Introduction into clinical practice	Repeated/continuous administration	Tumor size and CNS location
Osmotic BBB disruption (I.A mannitol)	Not established (only phase II studies)	Invasive procedure. May be associated with SAE. Frequency varies	Limited. Requires multidisciplinary expert team approach	Feasible but limited by invasiveness of the procedure	Safety limited by tumor size, mass effect, and location
Biochemical disruption of the BBB(I.A RMP-7)	Not established (only phase II studies)	Invasive procedure. Associated with SAE	Clinical practice discontinued	Feasible but limited by invasiveness and toxicity of the procedure	Safety may be limited by tumor size, mass effect, and location
Focused ultrasound-mediated BBB disruption	No human studies only small animals studies	No human studies	No human studies	No human studies	Limited to small tumor size

BBB blood–brain barrier, *I.A.* intra-arterial, *SAE* severe adverse events

lymphoblastic lymphoma it has been shown that the use of HD-CTx significantly reduced the rate of CNS relapse (Hoelzer et al. 1996). Although it is widely used in other systemic lymphomas its effect on CNS involvement has not been established (Siegal and Goldschmidt 2012). Yet, systemic HD-CTx based on high-dose MTX is considered as standard therapy for primary CNS lymphoma (DeAngelis et al. 2002; Ferreri et al. 2009) although there is no consensus which regimen is the best. Table 24.1 shows that HD-CTx fulfills almost all expectations from drug therapy for those indications where effectiveness has been proved, and therefore it is not surprising that it gained wide acceptance in clinical practice.

The use of bolus drug injection can augment drug penetration into the extracellular space of brain tumors in animal studies (Dukic et al. 1999, 2000) as specified in Sect. 24.4.1.1. However, its clinical value has been suggested by a single small scale study that evaluated patients with CNS lymphoma (Hiraga et al. 1999). Nonetheless, the strategy gained irrefutable popularity in the clinic which is easily understandable once we view the favorable profile of all the other clinical expectations in Table 24.1. The situation is different for intra-arterial drug injection. Here Table 24.1 reveals that for four of the five clinical expectations the strategy's profile is disadvantageous and therefore it is not surprising that its clinical utility is limited to experimental regimens which are being practiced in a small number of centers.

Strategies that induce transient BBBD (Table 24.2): Despite the intriguing ability to facilitate the passive drug transport across the barrier these strategies have not gained wide clinical acceptance. This is not surprising once we evaluate the procedures by the set of clinical expectations as presented in Table 24.2. It is clear that all the procedures are either invasive or associated with severe adverse events. This limits the ability to use the strategy repeatedly and effectively. In addition, the superiority of these strategies over standard, less invasive, and safer therapies has not been proved. Finally, all these procedures are limited by their applicability to treat any tumor size at any CNS location. All together it is quite obvious that by the current status of these techniques none of them is expected to change clinical practice or become a standard therapy for primary brain tumors.

Finally, *strategies that block the active efflux transporters mechanisms* may have a theoretical chance to facilitated drug accumulation in the extracellular space of the tumor and the surrounding brain. However, more information is needed to predict the likelihood that it may change clinical practice (Table 24.3).

24.4.2 Strategies That Use Drug Carriers for Drug Delivery to Brain Tumors

Recent advances in nanotechnology have created exciting opportunities to improve the efficiency of drug delivery to the CNS (Laquintana et al. 2009; Soni et al. 2010; Sarin 2009; Wong et al. 2011; Invernici et al. 2011; Rajadhyaksha et al. 2011). In principle, a drug which is poorly distributed to the brain can be loaded on a nanocarrier system which interacts with the microvascular endothelium at the BBB.

Table 24.3 Strategies that use alternative methods to improve drug delivery: Clinical impact based on expectations from drug therapy (for references please see text)

Strategy	Effectiveness for CNS malignancy	Toxicity/ adverse effects profile	Introduction into clinical practice	Repeated/ continuous administration	Tumor size and CNS location
Efflux transport inhibition without/with nanocarriers	No studies	High toxicity for first generation compounds. No data for new generation compounds	No data. Potentially simple	No data. Potentially possible	No data No limitation expected
Systemic administration of drug nanocarriers without/with targeting molecules	Not established (few phase II studies)	Varies by carrier and compound. Require further investigation	Potentially simple	Potentially possible	No data No limitation expected
Systemic administration of CNS targeted drug carrier exosomes	No studies	Safe by preliminary in vivo animal studies	Potentially simple	Potentially possible	No data No limitation expected

CNS central nervous system

Eventually this may produce higher drug concentrations in brain parenchyma. These nanocarriers can be further modified for enhanced CNS selectivity and permeability with targeting moieties that will preferentially bind to putative receptors or transporters expressed at the BBB. In addition, this system can exploit the physiological barrier mechanisms for "drug trafficking" across the barrier structure making use, for example, of the endogenous carrier mediated transporters processes. At this stage no "ideal" nanocarrier can be identified but several classes of nanocarrier systems have been developed in the past decade and many are still undergoing intensive investigation. A detailed description of these systems is beyond the scope of this chapter but several recent reviews summarize the topic (Laquintana et al. 2009; Wong et al. 2011; Invernici et al. 2011; Rajadhyaksha et al. 2011). Shortly, the nanocarrier systems can be divided into two major categories: nanoparticles (or nanospheres) and a variety of other nanocarrier types. In principle nanoparticles are colloidal systems with compact structure where the therapeutic agent is either entrapped within the colloid matrix or coated on the particle surface by conjugation or adsorption. Nanoparticles include polymeric or solid lipid nanoparticles, lipid or albumin nanocapsule, liposomes, and micelles. The second group includes novel nanocarriers such as dendrimer, nanogel, nano-emulsion, and nano-suspension.

Only nanoparticles which are smaller than 12 nm in diameter, but not larger, can passively extravasate across the porous blood–tumor barrier microvasculature

(Sarin et al. 2008, 2009). In fact a subset of nanoparticles with diameter smaller than 10 nm was shown to maintain peak blood concentration for several hours and thus they accumulate over time to an effective concentration within the tumor extracellular space. This passive targeting is known as the enhanced permeability and retention effect. Although prolonged circulation time is an important requirement for an effective drug transport to the brain, it exposes the nanocarriers to interaction with the reticular endothelial system (RES) that removes particles depending on their size, charge, and surface properties. For most nanoparticles this is a major drawback and therefore attachment of polymers such as polyethylene glycol (PEG) is often necessary in order to "mask" the particles from the host's immune system (Jain and Jain 2008). However, PEGylated carriers are not easily transported through the barriers and their crossing via receptor-mediated trancytosis is often inefficient. Therefore, targeting strategies are frequently used to improve CNS delivery, exploiting "targeting molecules" that are conjugated to their surface (Wong et al. 2011). Targeting molecules may include monoclonal antibodies to transferin receptor (Huwyler et al. 1996; Pang et al. 2008), to insulin receptor (Zhang et al. 2002; Wu et al. 1997) or to EGF receptor (Mamot et al. 2005). Other targeting strategies may use coating of nanoparticles with cell penetrating peptides (Schwarze et al. 1999; Liu et al. 2008) or alternatively conjugate the carriers with endogenous molecules such as apolipoproteins (e.g. Apo A, B or E) (Goppert and Muller 2005; Kreuter et al. 2003; Michaelis et al. 2006).

Nanocarriers may be considered as good candidates for drug delivery across the BBB if they fulfill the following requirements: the particle diameter should be less than 100 nm, they should be nontoxic, biodegradable, and biocompatible, should be stable in blood, BBB-targeted with no activation of RES and be noninflammatory. They should not induce platelets aggregation, have prolonged circulation time, be amenable to small molecules, peptides, or nucleic acids and should exhibit controlled drug release profile (Invernici et al. 2011). Once nanocarriers will accomplish these multiple requirements and when human efficacy and toxicity studies will reveal favorable outcome, then nanotechnology for drug delivery will change clinical practice for brain tumor therapy (Table 24.3). However, this field is still in its infancy and many issues should be resolved before CNS nanomedicine becomes useful in clinical setting.

24.4.2.1 Exosomes Nanovesicles for Drug Delivery Across Biological Barriers

Exosomes are naturally occurring, membranous nanovesicles of 40–100 nm in diameter. They arise from the endocytic cellular pathway through inward budding of the limiting late endosomal membrane, giving rise to multivesicular bodies, which then fuse with the plasma membrane to release their vesicular content (exosome) (Lakhal and Wood 2011). Exosomes are natural carriers of protein and nucleic acids, including mRNA and microRNA (Valadi et al. 2007). Exosomes have pleiotropic biological functions while operating as natural vectors of intercellular

signaling within a given tissue or between different tissues. They appear to play an important role in many disease processes, most notably inflammation and cancer, where their efficient functional delivery of biological cargo seems to contribute to the disease progress (van Dommelen et al. 2011). Recent in vivo studies showed that systemic administration of ex-vivo derived exosomes could be used to deliver exogenous cargo to a targeted tissue type (van Dommelen et al. 2011; Alvarez-Erviti et al. 2011). The first proof of concept has been published recently. It demonstrated that by using a novel targeting strategy the systemically administered exosomes specifically targeted the brain, delivered their cargo, and induced a biological effect (Alvarez-Erviti et al. 2011).

The future utilization of the full potential of exosomes in the field of drug delivery hinges on the development of scalable approaches for the production of exosomes, as well as the refinement of targeting and loading methods. An important factor will be the establishment of a scalable source of well characterized exosomes. For that purpose induced pluripotent stem cells that can be derived from the patient's skin fibroblasts hold great promise as it also will eliminate immunogenicity(Aasen and Izpisua Belmonte 2010). In addition, neural stem cells-derived exosomes are likely to display intrinsic neurotropic behavior and enhanced brain specificity. Currently clinical translation is hindered by poor understanding of exosome trafficking across biological barriers, and the absence of exosome-tailored nanotechnologies for purification, characterization, and loading (Lakhal and Wood 2011). If technological advances permit, exosomes may revolutionize the field of drug delivery by enabling safe and effective tissue targeted drug delivery across impermeable biological barrier (Table 24.3).

24.5 Local Delivery of Drugs to Brain Tumors

Methods that deliver drugs directly to brain parenchyma (Buonerba et al. 2011) try to augment extracellular brain drug concentration by completely circumventing the physiological barriers. The main purpose is to achieve high local or interstitial drug concentration with low systemic exposure to the drug. All the available techniques require invasive brain procedures (Muldoon et al. 2007; Bidros and Vogelbaum 2009; Laquintana et al. 2009; Buonerba et al. 2011). Approaches to local drug delivery include the use of implantable controlled release polymer systems (Westphal et al. 2006; Brem et al. 1991), various catheters devices for intracavitary drug delivery (Zalutsky et al. 2008; Boiardi et al. 2005), and convection-enhanced delivery (CED) (Lidar et al. 2004; Kunwar et al. 2007; Sampson et al. 2008). The major limitation of these techniques is their failure to reach distant infiltrating tumor cells, a major requirement for therapy that aims to achieve a durable effect. Due to the invasive nature of these techniques and the restricted boundaries of drug distribution it is not surprising that these procedures largely remain experimental or that they already failed clinical trials (Table 24.4).

Table 24.4 Strategies for local drug delivery: Clinical impact based on expectations from drug therapy (for references please see text)

Strategy	Effectiveness for CNS malignancy	Toxicity/adverse effects profile	Introduction into clinical practice	Repeated/continuous administration	Tumor size and CNS location
Implantable polymers	Failed phase III clinical trials	Invasive procedure. Increase the rate of surgical complications	Relatively simple	Not feasible	Limited to resectable tumors and to distance from CSF pathways
Intracavitary drug delivery	Not established (few phase II studies)	Invasive procedure. Device associated infections, reversible and irreversible neurotoxicity for some agents	Limited. Requires multidisciplinary expert team approach	Pending on the agent may be possible for non-radioactive agents	Limited to small tumor size or to tumors accessible for GTR
Convection-enhanced delivery	Failed phase II/III clinical trials. Some studies are still ongoing	Invasive procedure. Some agents associated with neurotoxicity or chemical meningitis	Limited due to high complexity. Requires multidisciplinary expert team approach	Limited and associated with increased rate of infections	Limited by tumor size, mass effect, and CNS location

GTR gross total resection, *CSF* cerebrospinal fluid, *CNS* central nervous system

24.5.1 Implanted Polymers

The underlying concept is that a drug impregnated wafers that has a controlled, sustained release rate will provide a continuous local drug delivery. The biodegradable polymers release the drug by a combination of diffusion and hydrolytic polymer degradation. The only Food and Drug-approved form of local chemotherapy is carmustine wafers (Gliadel®) that has been studied in phase III clinical trials (Westphal et al. 2006; Brem et al. 1991). The carmustine wafers are implanted into the resection cavity of the tumor and therefore, a priori the therapy is limited to the subclass of resectable tumors with presumably small amount of residual neoplasm. It also means that the drug has to penetrate away from the resection cavity and affect the infiltrating tumor cells that invade the proximal and distal brain parenchyma. In addition, when the resection cavity is connected with the CSF pathways much of the released drug leak into the CSF rather than diffusing into the surrounding brain.

The flux of drug from the implant to the surrounding tissue is proportional to the concentration gradient. As the concentration at the implant site should deliberately be limited by the need to avoid toxicity to normal brain tissue, there is also an upper bound on the driving force for drug transport from the implant into surrounding tissue. Consequently, the concentration decreases rapidly as distance from the implant site increases. It has been found that drug diffusion delivers detectable concentrations for less than 0.5 mm from the implant site (Fung et al. 1996; Krewson et al. 1995) and by using a three-dimensional computerized model, it was concluded that the drug could not diffuse more that 1–2 cm away from the implantation site (Engelhard 2000). This by itself may explain why it has not resulted in improvement in patient outcome. But there are additional factors that contribute to ineffective delivery. As the drug diffuses, it is degraded, taken up into the vasculature, internalized by cells, and bind to extracellular matrix and so the transport is further hindered. In addition, the brain extracellular space is tortuous and the volume available for diffusion and fluid transport is low. Despite clinical ineffectiveness adverse effects have been recorded. These include mainly poor wound healing and increased risk of infections that may sometimes add significant morbidity.

24.5.2 Convection-Enhanced Delivery

CED relies on pressure-driven bulk flow of infusate as a means to deliver the desired agent to the extracellular space of the CNS. The bulk flow mechanism is created by a small pressure gradient from a pump that pushes solute through a catheter targeted within the CNS (Rajadhyaksha et al. 2011; Raghavan et al. 2006). The pressure-driven spreading of infused solutes through the interstitium does not depend on their intrinsic diffusivity and continues throughout the time CED is performed, to end abruptly when the procedure terminates (Allard et al. 2009). Because CED bypasses the BBB it can be used to infuse therapeutic agents with large or small molecular weight such as paclitaxel (Lidar et al. 2004; Tanner et al. 2007), or high molecular

weight targeted toxins (Kunwar et al. 2007; Sampson et al. 2008; Weber et al. 2003; Weaver and Laske 2003; Laske et al. 1997) as well as various types of nanocarriers loaded with different agents (Allard et al. 2009). Many factors affect the final distribution of the infused agent. Some of the investigated factors include the volume of infusion and infusion rate, catheter location and cannula size and shape and back flow along catheter track and air bubbles (Buonerba et al. 2011; Chen et al. 1999). Other determinants are infusate features (size, interstitial affinity, and octanol water coefficient), interstitial tissue properties (binding proteins, receptor uptake or binding, and tissue isotropy). Factors that affect efflux of the agent are diffusion or loss into capillaries and rate of metabolism. All the latter reduce the concentration over time and distance (Bidros and Vogelbaum 2009; Allard et al. 2009; Stukel and Caplan 2009).

Several clinical trials have been completed using CED including phase III trials—all have failed (Lidar et al. 2004; Sampson et al. 2008, 2010; Tanner et al. 2007; Weber et al. 2003; Weaver and Laske 2003; Kunwar et al. 2010; Bogdahn et al. 2011). Table 24.4 shows that if we assess the technique by the set of clinical expectations for drug delivery it discloses an unfavorable profile for each parameter. The technique is invasive, and entails placement of several catheters into the tumor bed and brain tissue. Adverse effects include surgical complications as well as significant neurological deterioration that were reported in about 13 % of patients (Shahar et al. 2012). Some of the agents also proved to be neurotoxic or caused aseptic meningitis when the infusate leaked to the CSF pathways (Lidar et al. 2004; Tanner et al. 2007). The technique is highly complex and as such often results with ineffective delivery and failure to get a therapeutic dose to the target (Buonerba et al. 2011; Shahar et al. 2012; Ding et al. 2010). Repeated and continuous administration is limited and associated with high rate of infections (Bogdahn et al. 2011). The method is also limited to a certain range of tumor size and does not fit all CNS location. Proximity to CSF pathways is an exclusion criterion because the infusate will leak into the CSF. It has been observed that adherence to catheter placement guidelines are hindered by lesion site, proximity to eloquent cortical areas, tissue density that interferes with trajectory, and technical limitations of stereotactic instruments (Shahar et al. 2012). Taken together, the current failure to prove clinical efficacy is expected and it is unlikely that in the near future the technique will change clinical practice for brain tumors.

24.5.3 Intracavitary Drug Delivery

Intracavitary drug delivery may entail simple manual drug injection into the resected tumor bed via an implanted reservoir device that can be accessed percutaneously. Alternatively, the injection may be performed by a motor pump that will provide prolonged and controlled intracerebral delivery of the therapeutic agent (Buonerba et al. 2011).

Intracavitary delivery has been exploited recently for delivery of radioactive ligands attached to monoclonal antibodies such as anti-tenascin antibodies

(for review see Buonerba et al. 2011). Tenascin is a glycoproteic antigen ubiquitously present in malignant Gliomas, but not in normal brain tissues. In Phase II clinical trials different types of radioactive monoclonal antibodies preparations were used and the experimental agents were injected into an implanted reservoir that has been left in the cavity after gross total resection of the tumor. Some of the humanized chimeric preparations were associated with hematologic toxicity and others with reversible or irreversible neurotoxicity (Buonerba et al. 2011).

Unfortunately the technique suffers from all the limitations associated with local drug delivery. As summarized in Table 24.4 it is unlikely that it will change clinical practice. Although, if refined, it may become applicable to a subclass of small resectable tumors once the efficacy will be established in phase III clinical trials.

24.6 Challenges for Drug Delivery Posed by Antiangiogeneic Therapy

Malignant brain tumors exhibit marked and aberrant blood vessel formation indicating angiogenic endothelial cells as potential target for brain tumor treatment. Yet, the tumor vasculature is often characterized by low vascularity, poor organization, and abnormal morphology, which result in inefficient transport of oxygen and therapeutic agents. In addition, the newly formed abnormal vascular network is highly permeable and consequently it is associated with propagation of surrounding brain edema and with high interstitial pressure within the tumor mass. The growth and expansion of the abnormal vasculature of the tumor is stimulated by vascular endothelial growth factor (VEGF), which is a validated therapeutic target for cancer treatment (Hurwitz et al. 2004; Sandler et al. 2006). One rational behind the use of anti-VEGF therapy for primary CNS malignancy is based upon the concept that normalization of tumor vasculature with a decrease in tumor interstitial pressure will improve drug delivery as well as oxygen supply which is essential for effective radiotherapy (Thompson et al. 2011; Ma et al. 2011). So far, it is unclear how antiangiogenic therapy affects tumor uptake of chemotherapeutic agents and what is the expected antitumor activity of combination therapies.

Several recent publications discuss the paradoxical effect of antiangiogenic therapy in the management of cancer and brain tumors (Thompson et al. 2011; Ma et al. 2011; Wurdinger and Tannous 2009). On one hand the induced morphological normalization of tumor vasculature can increase the transport efficiency of nutrients and drugs. But the total number of surviving blood vessels decreases and as a result tumor hypoxia is increasing. This affect tumor uptake of small molecules as has been demonstrated in experimental models (Ma et al. 2011; Ma and Waxman 2008). In brain tumors the restored BBB function is associated with decrease in tumor interstitial pressure, which is thought to improve delivery of chemotherapy to tumor cells (Ferrara 2005). But, the restored barrier function impedes the passive diffusion of drugs into the interstitial space of the tumor and to the surrounding brain parenchyma. Still, with the reduction in tumor interstitial pressure the rapid drug leakage

away from the tumor bulk into the surrounding brain or CSF pathways is decreased. As a result an increase in drug retention is observed (Ma et al. 2011). In an experimental glioma model it has been suggested that the observed complex effects on drug exposure can be exploited to improve outcome if a prodrug is used concomitantly with the antiangiogenic therapy. In that model systemic administration of a prodrug which is activated intratumorally served for that purpose. The study showed that the decrease in tumor drug uptake following antiangiogenic therapy could be fully reversed by the tumor drug retention effect induced by the same antiangiogenesis treatment (Ma et al. 2011). The increase in drug retention enhances the intratumoral activation of the prodrug and retains the active compounds longer thus escalating the anti-neoplastic effect of treatment.

Despite the remarkable effect of anti-VEGF therapy observed in recurrent glioblastoma (Nghiemphu et al. 2009) clinical and histological evidence suggest that tumor may adapt to antiangiogenic agents with increased tumor invasiveness and vessel cooption (Narayana et al. 2012; de Groot et al. 2010). Both clinical and animal studies show that the favorable effect of antiangiogenic therapy is short lasting and therefore coupling of this therapy with other anti-neoplasting agents is probably essential. However, a better understanding of the intricate issues related to drug delivery in face of antiangiogenic therapy is required for future rational integration of therapeutic modalities.

24.7 Conclusions and Future Directions

Despite tremendous efforts that were invested in development of drugs and delivery systems for the treatment of brain tumors the results are disappointing. Nonetheless, research into sophisticated, science-driven solutions is continuing. During the past decade, conceptual and practical advancements have been made in the design and implementation of various vectors that demonstrate desirable characteristics. Although optimal systems have not yet been developed, progress has been noticeable and expectations related to therapeutic efficacy have increased. The search in the field is now focused in the development of noninvasive therapies since all invasive methods to deliver drugs failed clinical expectations as delineated in this chapter. In order to achieve efficacious treatment, issues relevant to drug delivery need to be resolved. It seems plausible that nanomedicine approaches will improve the delivery of conventional drugs, targeted agents, and probably DNA-based therapy as well. All new drugs or delivery systems development must adhere to basic clinical expectations that include beside an anti-tumor effect a proof for favorable adverse effect profile, an easy introduction into clinical practice, feasibility of repeated or continuous administration and compatibility for any tumor size and brain location. Adherence to these essentials will enable a change in clinical practice once the antineoplastic effect is demonstrated in well-controlled clinical studies.

References

Aasen T, Izpisua Belmonte JC (2010) Isolation and cultivation of human keratinocytes from skin or plucked hair for the generation of induced pluripotent stem cells. Nat Protoc 5:371–382

Allard E, Passirani C, Benoit JP (2009) Convection-enhanced delivery of nanocarriers for the treatment of brain tumors. Biomaterials 30:2302–2318

Alvarez-Erviti L, Seow Y, Yin H, Betts C, Lakhal S et al (2011) Delivery of siRNA to the mouse brain by systemic injection of targeted exosomes. Nat Biotechnol 29:341–345

Angelov L, Doolittle ND, Kraemer DF, Siegal T, Barnett GH et al (2009) Blood-brain barrier disruption and intra-arterial methotrexate-based therapy for newly diagnosed primary CNS lymphoma: a multi-institutional experience. J Clin Oncol 27:3503–3509

Bartus RT, Elliott PJ, Dean RL, Hayward NJ, Nagle TL et al (1996) Controlled modulation of BBB permeability using the bradykinin agonist, RMP-7. Exp Neurol 142:14–28

Becker I, Becker KF, Meyermann R, Hollt V (1991) The multidrug-resistance gene MDR1 is expressed in human glial tumors. Acta Neuropathol 82:516–519

Bidros DS, Vogelbaum MA (2009) Novel drug delivery strategies in neuro-oncology. Neurotherapeutics 6:539–546

Blakeley J, Portnow J (2010) Microdialysis for assessing intratumoral drug disposition in brain cancers: a tool for rational drug development. Expert Opin Drug Metab Toxicol 6:1477–1491

Blakeley JO, Olson J, Grossman SA, He X, Weingart J et al (2009) Effect of blood brain barrier permeability in recurrent high grade gliomas on the intratumoral pharmacokinetics of methotrexate: a microdialysis study. J Neurooncol 91:51–58

Bogdahn U, Hau P, Stockhammer G, Venkataramana NK, Mahapatra AK et al (2011) Targeted therapy for high-grade glioma with the TGF-beta2 inhibitor trabedersen: results of a randomized and controlled phase IIb study. Neuro Oncol 13:132–142

Boiardi A, Bartolomei M, Silvani A, Eoli M, Salmaggi A et al (2005) Intratumoral delivery of mitoxantrone in association with 90-Y radioimmunotherapy (RIT) in recurrent glioblastoma. J Neurooncol 72:125–131

Borlongan CV, Emerich DF (2003) Facilitation of drug entry into the CNS via transient permeation of blood brain barrier: laboratory and preliminary clinical evidence from bradykinin receptor agonist, Cereport. Brain Res Bull 60:297–306

Brem H, Mahaley MS Jr, Vick NA, Black KL, Schold SC Jr et al (1991) Interstitial chemotherapy with drug polymer implants for the treatment of recurrent gliomas. J Neurosurg 74:441–446

Buonerba C, Di Lorenzo G, Marinelli A, Federico P, Palmieri G et al (2011) A comprehensive outlook on intracerebral therapy of malignant gliomas. Crit Rev Oncol Hematol 80:54–68

Chen MY, Lonser RR, Morrison PF, Governale LS, Oldfield EH (1999) Variables affecting convection-enhanced delivery to the striatum: a systematic examination of rate of infusion, cannula size, infusate concentration, and tissue-cannula sealing time. J Neurosurg 90:315–320

Chen PY, Liu HL, Hua MY, Yang HW, Huang CY et al (2010) Novel magnetic/ultrasound focusing system enhances nanoparticle drug delivery for glioma treatment. Neuro Oncol 12: 1050–1060

Cloughesy TF, Black KL (1995) Pharmacological blood-brain barrier modification for selective drug delivery. J Neurooncol 26:125–132

de Groot JF, Fuller G, Kumar AJ, Piao Y, Eterovic K et al (2010) Tumor invasion after treatment of glioblastoma with bevacizumab: radiographic and pathologic correlation in humans and mice. Neuro Oncol 12:233–242

DeAngelis LM, Seiferheld W, Schold SC, Fisher B, Schultz CJ et al (2002) Combination chemotherapy and radiotherapy for primary central nervous system lymphoma: Radiation Therapy Oncology Group Study 93-10. J Clin Oncol 20:4643–4648

Demeule M, Regina A, Jodoin J, Laplante A, Dagenais C et al (2002) Drug transport to the brain: key roles for the efflux pump P-glycoprotein in the blood-brain barrier. Vascul Pharmacol 38:339–348

Deng CX (2010) Targeted drug delivery across the blood-brain barrier using ultrasound technique. Ther Deliv 1:819–848
di Tomaso E, Snuderl M, Kamoun WS, Duda DG, Auluck PK et al (2011) Glioblastoma recurrence after cediranib therapy in patients: lack of "rebound" revascularization as mode of escape. Cancer Res 71:19–28
Ding D, Kanaly CW, Bigner DD, Cummings TJ, Herndon JE 2nd et al (2010) Convection-enhanced delivery of free gadolinium with the recombinant immunotoxin MR1-1. J Neurooncol 98:1–7
Dukic S, Heurtaux T, Kaltenbach ML, Hoizey G, Lallemand A et al (1999) Pharmacokinetics of methotrexate in the extracellular fluid of brain C6-glioma after intravenous infusion in rats. Pharm Res 16:1219–1225
Dukic SF, Heurtaux T, Kaltenbach ML, Hoizey G, Lallemand A et al (2000) Influence of schedule of administration on methotrexate penetration in brain tumours. Eur J Cancer 36:1578–1584
Engelhard HH (2000) The role of interstitial BCNU chemotherapy in the treatment of malignant glioma. Surg Neurol 53:458–464
Ergin A, Wang M, Zhang JY, Bruce JN, Fine RL et al (2012) The feasibility of real-time in vivo optical detection of blood-brain barrier disruption with indocyanine green. J Neurooncol 106:551–560
Essig M, Weber MA, von Tengg-Kobligk H, Knopp MV, Yuh WT et al (2006) Contrast-enhanced magnetic resonance imaging of central nervous system tumors: agents, mechanisms, and applications. Top Magn Reson Imaging 17:89–106
Ferrara N (2005) VEGF as a therapeutic target in cancer. Oncology 69(Suppl 3):11–16
Ferreri AJ, Reni M, Foppoli M, Martelli M, Pangalis GA et al (2009) High-dose cytarabine plus high-dose methotrexate versus high-dose methotrexate alone in patients with primary CNS lymphoma: a randomised phase 2 trial. Lancet 374:1512–1520
Ford J, Osborn C, Barton T, Bleehen NM (1998) A phase I study of intravenous RMP-7 with carboplatin in patients with progression of malignant glioma. Eur J Cancer 34:1807–1811
Friedman HS, Kerby T, Calvert H (2000) Temozolomide and treatment of malignant glioma. Clin Cancer Res 6:2585–2597
Fung LK, Shin M, Tyler B, Brem H, Saltzman WM (1996) Chemotherapeutic drugs released from polymers: distribution of 1,3-bis(2-chloroethyl)-1-nitrosourea in the rat brain. Pharm Res 13:671–682
Gelman M, Chakeres DW, Newton HB (1999) Brain tumors: complications of cerebral angiography accompanied by intraarterial chemotherapy. Radiology 213:135–140
Goppert TM, Muller RH (2005) Polysorbate-stabilized solid lipid nanoparticles as colloidal carriers for intravenous targeting of drugs to the brain: comparison of plasma protein adsorption patterns. J Drug Target 13:179–187
Groothuis D, Vick NA (1982) Brain tumors and the blood-brain barrier. Trends Neurosci 5:232
Haga S, Hinoshita E, Ikezaki K, Fukui M, Scheffer GL et al (2001) Involvement of the multidrug resistance protein 3 in drug sensitivity and its expression in human glioma. Jpn J Cancer Res 92:211–219
Hiraga S, Arita N, Ohnishi T, Kohmura E, Yamamoto K et al (1999) Rapid infusion of high-dose methotrexate resulting in enhanced penetration into cerebrospinal fluid and intensified tumor response in primary central nervous system lymphomas. J Neurosurg 91:221–230
Hoelzer D, Ludwig WD, Thiel E, Gassmann W, Loffler H et al (1996) Improved outcome in adult B-cell acute lymphoblastic leukemia. Blood 87:495–508
Hurwitz H, Fehrenbacher L, Novotny W, Cartwright T, Hainsworth J et al (2004) Bevacizumab plus irinotecan, fluorouracil, and leucovorin for metastatic colorectal cancer. N Engl J Med 350:2335–2342
Huwyler J, Wu D, Pardridge WM (1996) Brain drug delivery of small molecules using immunoliposomes. Proc Natl Acad Sci U S A 93:14164–14169
Hynynen K, McDannold N, Vykhodtseva N, Jolesz FA (2001) Noninvasive MR imaging-guided focal opening of the blood-brain barrier in rabbits. Radiology 220:640–646
Invernici G, Cristini S, Alessandri G, Navone SE, Canzi L et al (2011) Nanotechnology advances in brain tumors: the state of the art. Recent Pat Anticancer Drug Discov 6:58–69

Ito K, Suzuki H, Horie T, Sugiyama Y (2005) Apical/basolateral surface expression of drug transporters and its role in vectorial drug transport. Pharm Res 22:1559–1577
Jain RK (1994) Barriers to drug delivery in solid tumors. Sci Am 271:58–65
Jain RK (2005) Normalization of tumor vasculature: an emerging concept in antiangiogenic therapy. Science 307:58–62
Jain A, Jain SK (2008) PEGylation: an approach for drug delivery. A review. Crit Rev Ther Drug Carrier Syst 25:403–447
Joshi S, Ergin A, Wang M, Reif R, Zhang J et al (2011) Inconsistent blood brain barrier disruption by intraarterial mannitol in rabbits: implications for chemotherapy. J Neurooncol 104:11–19
Kemper EM, Boogerd W, Thuis I, Beijnen JH, van Tellingen O (2004) Modulation of the blood-brain barrier in oncology: therapeutic opportunities for the treatment of brain tumours? Cancer Treat Rev 30:415–423
Keunen O, Johansson M, Oudin A, Sanzey M, Rahim SA et al (2011) Anti-VEGF treatment reduces blood supply and increases tumor cell invasion in glioblastoma. Proc Natl Acad Sci U S A 108:3749–3754
Kreuter J, Ramge P, Petrov V, Hamm S, Gelperina SE et al (2003) Direct evidence that polysorbate-80-coated poly(butylcyanoacrylate) nanoparticles deliver drugs to the CNS via specific mechanisms requiring prior binding of drug to the nanoparticles. Pharm Res 20:409–416
Krewson CE, Klarman ML, Saltzman WM (1995) Distribution of nerve growth factor following direct delivery to brain interstitium. Brain Res 680:196–206
Kruh GD, Belinsky MG (2003) The MRP family of drug efflux pumps. Oncogene 22:7537–7552
Kunwar S, Prados MD, Chang SM, Berger MS, Lang FF et al (2007) Direct intracerebral delivery of cintredekin besudotox (IL13-PE38QQR) in recurrent malignant glioma: a report by the Cintredekin Besudotox Intraparenchymal Study Group. J Clin Oncol 25:837–844
Kunwar S, Chang S, Westphal M, Vogelbaum M, Sampson J et al (2010) Phase III randomized trial of CED of IL13-PE38QQR vs Gliadel wafers for recurrent glioblastoma. Neuro Oncol 12:871–881
Lakhal S, Wood MJ (2011) Exosome nanotechnology: an emerging paradigm shift in drug delivery: exploitation of exosome nanovesicles for systemic in vivo delivery of RNAi heralds new horizons for drug delivery across biological barriers. Bioessays 33:737–741
Laquintana V, Trapani A, Denora N, Wang F, Gallo JM et al (2009) New strategies to deliver anticancer drugs to brain tumors. Expert Opin Drug Deliv 6:1017–1032
Laske DW, Youle RJ, Oldfield EH (1997) Tumor regression with regional distribution of the targeted toxin TF-CRM107 in patients with malignant brain tumors. Nat Med 3:1362–1368
Lidar Z, Mardor Y, Jonas T, Pfeffer R, Faibel M et al (2004) Convection-enhanced delivery of paclitaxel for the treatment of recurrent malignant glioma: a phase I/II clinical study. J Neurosurg 100:472–479
Liu L, Guo K, Lu J, Venkatraman SS, Luo D et al (2008) Biologically active core/shell nanoparticles self-assembled from cholesterol-terminated PEG-TAT for drug delivery across the blood-brain barrier. Biomaterials 29:1509–1517
Liu HL, Hua MY, Chen PY, Chu PC, Pan CH et al (2010) Blood-brain barrier disruption with focused ultrasound enhances delivery of chemotherapeutic drugs for glioblastoma treatment. Radiology 255:415–425
Ma J, Waxman DJ (2008) Modulation of the antitumor activity of metronomic cyclophosphamide by the angiogenesis inhibitor axitinib. Mol Cancer Ther 7:79–89
Ma J, Chen CS, Blute T, Waxman DJ (2011) Antiangiogenesis enhances intratumoral drug retention. Cancer Res 71:2675–2685
Mamot C, Drummond DC, Noble CO, Kallab V, Guo Z et al (2005) Epidermal growth factor receptor-targeted immunoliposomes significantly enhance the efficacy of multiple anticancer drugs in vivo. Cancer Res 65:11631–11638
Marchi N, Angelov L, Masaryk T, Fazio V, Granata T et al (2007) Seizure-promoting effect of blood-brain barrier disruption. Epilepsia 48:732–742
Michaelis K, Hoffmann MM, Dreis S, Herbert E, Alyautdin RN et al (2006) Covalent linkage of apolipoprotein e to albumin nanoparticles strongly enhances drug transport into the brain. J Pharmacol Exp Ther 317:1246–1253

Muldoon LL, Soussain C, Jahnke K, Johanson C, Siegal T et al (2007) Chemotherapy delivery issues in central nervous system malignancy: a reality check. J Clin Oncol 25:2295–2305
Nakagawa H, Fujita T, Izumoto S, Kubo S, Nakajima Y et al (1993) cis-diamminedichloroplatinum (CDDP) therapy for brain metastasis of lung cancer. I. Distribution within the central nervous system after intravenous and intracarotid infusion. J Neurooncol 16:61–67
Narayana A, Kunnakkat SD, Medabalmi P, Golfinos J, Parker E et al (2012) Change in pattern of relapse after antiangiogenic therapy in high-grade glioma. Int J Radiat Oncol Biol Phys 82:77–82
Naumov GN, Bender E, Zurakowski D, Kang SY, Sampson D et al (2006) A model of human tumor dormancy: an angiogenic switch from the nonangiogenic phenotype. J Natl Cancer Inst 98:316–325
Netti PA, Baxter LT, Boucher Y, Skalak R, Jain RK (1995) Time-dependent behavior of interstitial fluid pressure in solid tumors: implications for drug delivery. Cancer Res 55:5451–5458
Nghiemphu PL, Liu W, Lee Y, Than T, Graham C et al (2009) Bevacizumab and chemotherapy for recurrent glioblastoma: a single-institution experience. Neurology 72:1217–1222
Osztie E, Varallyay P, Doolittle ND, Lacy C, Jones G et al (2001) Combined intraarterial carboplatin, intraarterial etoposide phosphate, and IV Cytoxan chemotherapy for progressive optic-hypothalamic gliomas in young children. AJNR Am J Neuroradiol 22:818–823
Pang Z, Lu W, Gao H, Hu K, Chen J et al (2008) Preparation and brain delivery property of biodegradable polymersomes conjugated with OX26. J Control Release 128:120–127
Patel MM, Goyal BR, Bhadada SV, Bhatt JS, Amin AF (2009) Getting into the brain: approaches to enhance brain drug delivery. CNS Drugs 23:35–58
Raghavan R, Brady ML, Rodriguez-Ponce MI, Hartlep A, Pedain C et al (2006) Convection-enhanced delivery of therapeutics for brain disease, and its optimization. Neurosurg Focus 20:E12
Rajadhyaksha M, Boyden T, Liras J, El-Kattan A, Brodfuehrer J (2011) Current advances in delivery of biotherapeutics across the blood-brain barrier. Curr Drug Discov Technol 8:87–101
Rittierodt M, Harada K (2003) Repetitive doxorubicin treatment of glioblastoma enhances the PGP expression—a special role for endothelial cells. Exp Toxicol Pathol 55:39–44
Sampson JH, Akabani G, Archer GE, Berger MS, Coleman RE et al (2008) Intracerebral infusion of an EGFR-targeted toxin in recurrent malignant brain tumors. Neuro Oncol 10: 320–329
Sampson JH, Archer G, Pedain C, Wembacher-Schroder E, Westphal M et al (2010) Poor drug distribution as a possible explanation for the results of the PRECISE trial. J Neurosurg 113:301–309
Sandler A, Gray R, Perry MC, Brahmer J, Schiller JH et al (2006) Paclitaxel-carboplatin alone or with bevacizumab for non-small-cell lung cancer. N Engl J Med 355:2542–2550
Sarin H (2009) Recent progress towards development of effective systemic chemotherapy for the treatment of malignant brain tumors. J Transl Med 7:77
Sarin H, Kanevsky AS, Wu H, Brimacombe KR, Fung SH et al (2008) Effective transvascular delivery of nanoparticles across the blood-brain tumor barrier into malignant glioma cells. J Transl Med 6:80
Sarin H, Kanevsky AS, Wu H, Sousa AA, Wilson CM et al (2009) Physiologic upper limit of pore size in the blood-tumor barrier of malignant solid tumors. J Transl Med 7:51
Schneider G, Kirchin MA, Pirovano G, Colosimo C, Ruscalleda J et al (2001) Gadobenate dimeglumine-enhanced magnetic resonance imaging of intracranial metastases: effect of dose on lesion detection and delineation. J Magn Reson Imaging 14:525–539
Schwarze SR, Ho A, Vocero-Akbani A, Dowdy SF (1999) In vivo protein transduction: delivery of a biologically active protein into the mouse. Science 285:1569–1572
Shahar T, Ram Z, Kanner AA (2012) Convection-enhanced delivery catheter placements for high-grade gliomas: complications and pitfalls. J Neurooncol 107:373–378
Siegal T, Goldschmidt N (2012) CNS prophylaxis in diffuse large B-cell lymphoma: if, when, how and for whom? Blood Rev 26(3):97–106

Siegal T, Rubinstein R, Bokstein F, Schwartz A, Lossos A et al (2000) In vivo assessment of the window of barrier opening after osmotic blood-brain barrier disruption in humans. J Neurosurg 92:599–605

Sikic BI, Fisher GA, Lum BL, Halsey J, Beketic-Oreskovic L et al (1997) Modulation and prevention of multidrug resistance by inhibitors of P-glycoprotein. Cancer Chemother Pharmacol 40(Suppl):S13–S19

Soni V, Jain A, Khare P, Gulbake A, Jain SK (2010) Potential approaches for drug delivery to the brain: past, present, and future. Crit Rev Ther Drug Carrier Syst 27:187–236

Stewart LA (2002) Chemotherapy in adult high-grade glioma: a systematic review and meta-analysis of individual patient data from 12 randomised trials. Lancet 359:1011–1018

Stukel JM, Caplan MR (2009) Targeted drug delivery for treatment and imaging of glioblastoma multiforme. Expert Opin Drug Deliv 6:705–718

Stupp R, Mason WP, van den Bent MJ, Weller M, Fisher B et al (2005) Radiotherapy plus concomitant and adjuvant temozolomide for glioblastoma. N Engl J Med 352:987–996

Stupp R, Hegi ME, Gilbert MR, Chakravarti A (2007) Chemoradiotherapy in malignant glioma: standard of care and future directions. J Clin Oncol 25:4127–4136

Tanner PG, Holtmannspotter M, Tonn JC, Goldbrunner R (2007) Effects of drug efflux on convection-enhanced paclitaxel delivery to malignant gliomas: technical note. Neurosurgery 61:E880–E882; discussion E882

Tfayli A, Hentschel P, Madajewicz S, Manzione J, Chowhan N et al (1999) Toxicities related to intraarterial infusion of cisplatin and etoposide in patients with brain tumors. J Neurooncol 42:73–77

Thompson EM, Frenkel EP, Neuwelt EA (2011) The paradoxical effect of bevacizumab in the therapy of malignant gliomas. Neurology 76:87–93

Ting CY, Fan CH, Liu HL, Huang CY, Hsieh HY et al (2012) Concurrent blood-brain barrier opening and local drug delivery using drug-carrying microbubbles and focused ultrasound for brain glioma treatment. Biomaterials 33:704–712

Treat LH, McDannold N, Vykhodtseva N, Zhang Y, Tam K et al (2007) Targeted delivery of doxorubicin to the rat brain at therapeutic levels using MRI-guided focused ultrasound. Int J Cancer 121:901–907

Valadi H, Ekstrom K, Bossios A, Sjostrand M, Lee JJ et al (2007) Exosome-mediated transfer of mRNAs and microRNAs is a novel mechanism of genetic exchange between cells. Nat Cell Biol 9:654–659

van Dommelen SM, Vader P, Lakhal S, Kooijmans SA, van Solinge WW et al (2011) Microvesicles and exosomes: opportunities for cell-derived membrane vesicles in drug delivery. J Control Release 161(2):635–644

Vick NA, Khandekar JD, Bigner DD (1977) Chemotherapy of brain tumors. Arch Neurol 34:523–526

Weaver M, Laske DW (2003) Transferrin receptor ligand-targeted toxin conjugate (Tf-CRM10) for therapy of malignant gliomas. J Neurooncol 65:3–13

Weber F, Asher A, Bucholz R, Berger M, Prados M et al (2003) Safety, tolerability, and tumor response of IL4-Pseudomonas exotoxin (NBI-3001) in patients with recurrent malignant glioma. J Neurooncol 64:125–137

Westphal M, Ram Z, Riddle V, Hilt D, Bortey E et al (2006) Gliadel wafer in initial surgery for malignant glioma: long-term follow-up of a multicenter controlled trial. Acta Neurochir (Wien) 148:269–275, discussion 275

Wong HL, Wu XY, Bendayan R (2011) Nanotechnological advances for the delivery of CNS therapeutics. Adv Drug Deliv Rev 64(7):686–700

Wu D, Yang J, Pardridge WM (1997) Drug targeting of a peptide radiopharmaceutical through the primate blood-brain barrier in vivo with a monoclonal antibody to the human insulin receptor. J Clin Invest 100:1804–1812

Wurdinger T, Tannous BA (2009) Glioma angiogenesis: towards novel RNA therapeutics. Cell Adh Migr 3:230–235

Zalutsky MR, Reardon DA, Akabani G, Coleman RE, Friedman AH et al (2008) Clinical experience with alpha-particle emitting 211At: treatment of recurrent brain tumor patients with 211At-labeled chimeric antitenascin monoclonal antibody 81C6. J Nucl Med 49:30–38

Zhang Y, Jeong Lee H, Boado RJ, Pardridge WM (2002) Receptor-mediated delivery of an antisense gene to human brain cancer cells. J Gene Med 4:183–194

Zylber-Katz E, Gomori JM, Schwartz A, Lossos A, Bokstein F et al (2000) Pharmacokinetics of methotrexate in cerebrospinal fluid and serum after osmotic blood-brain barrier disruption in patients with brain lymphoma. Clin Pharmacol Ther 67:631–641

Short Editors' Bios

Margareta Hammarlund-Udenaes (Ph.D.) is a Professor in Pharmacokinetics and Pharmacodynamics (PKPD) at Uppsala University and the Head of the Translational PKPD Group. Her research is focused at studying pharmacokinetic aspects of BBB transport of drugs in relation to CNS effects, which has led to the development of new concepts and methods within the BBB transport area, focusing on unbound drug relationships. Dr. Hammarlund-Udenaes is an Associate Editor of *Pharmaceutical Research* and a member of the Editorial Advisory Board of *Journal of Pharmaceutical Sciences* and *Fluids and Barriers of the CNS*. She became an American Association of Pharmaceutical Scientists' Fellow in 2005. She is a frequent lecturer at conferences and in drug industry. Her company gives courses and advice in PKPD and BBB transport issues. She cofounded and has cochaired several of the International Symposia on Microdialysis, and she is the Chair of the "Barriers of the CNS" Gordon Conference in 2014.

Elizabeth C.M. de Lange (Ph.D.) is Head of the Target Site Equilibration Group at the Division of Pharmacology of the Leiden Academic Center for Drug Research (LACDR). Her research program focuses on the development of generally applicable predictive PKPD models on CNS drugs using advanced in vivo animal models and mathematical modeling techniques, with a number of recent successes. She is an Editorial Board member of the journal *Fluids and Barriers of the CNS*, and an Editorial Advisory Board member of the *Journal of Pharmaceutical Sciences* and of *Pharmaceutical Research*. She has been the cofounder and (co-)Chair at the 1st, 2nd, and 5th International Symposia on Microdialysis and has been the Chair of the 9th International Conference on Cerebral Vascular Biology (2011). Among many other functions within the American Association of Pharmaceutical Scientists and being an AAPS fellow, she is the 2014 Chair of the Annual Meeting Programming Committee. With her company "In Focus" (www.infocus-ecmdelange.nl) she provides courses, training, and advice on microdialysis, pharmacokinetics, BBB transport, intra-brain distribution, and PKPD relationships.

M. Hammarlund-Udenaes et al. (eds.), *Drug Delivery to the Brain*, AAPS Advances in the Pharmaceutical Sciences Series 10, DOI 10.1007/978-1-4614-9105-7,

Robert G. Thorne (Ph.D.) is an Assistant Professor in Pharmaceutical Sciences at the University of Wisconsin-Madison School of Pharmacy and a KL2 scholar in the University of Wisconsin Institute for Clinical and Translational Research. He also serves as a Trainer in the Neuroscience, Cellular and Molecular Pathology, and Clinical Neuroengineering Training Programs at the University of Wisconsin-Madison. Dr. Thorne was previously a research scientist and Faculty member in the Department of Physiology and Neuroscience at the New York University School of Medicine. His background includes a Ph.D. in Pharmaceutics (University of Minnesota) and a B.S. in chemical engineering (University of Washington). His research focuses on diffusive and convective transport within the CNS and the development, refinement, and optimization of strategies for delivering biologics into the brain. He is a frequent invited speaker on topics related to CNS drug delivery for organizations within academia, foundations, and the biotechnology and pharmaceutical industry. Dr. Thorne serves on the editorial board of *Fluids and Barriers of the CNS*. He is also a founder and Council/Steering Committee member of the International Brain Barriers Society (http://www.ibbsoc.org/) as well as the 2016 Chair-elect for the "Barriers of the CNS" Gordon Research Conference.

Appendix
Primer on Central Nervous System Structure/ Function and the Vasculature, Ventricular System, and Fluids of the Brain

Robert G. Thorne

Abstract Detailed understanding of the various approaches for drug delivery to the brain necessitates some knowledge of central nervous system (CNS) anatomy and blood supply. The brain is different than other organs of the body in that it may not accurately be considered as a single compartment; its complex, heterogeneous structure is responsible for a multitude of functions with many different potential target sites for drug therapy. The cerebrovasculature is critically important from a drug delivery perspective because drugs will in many cases first reach the brain from the bloodstream. Additionally, stroke and other complications affecting the brain's blood vessels are a major cause of morbidity and mortality. The cerebrospinal fluid (CSF) of the brain is contained within the ventricles and the subarachnoid spaces and often assumes importance for drug delivery or as a sampling compartment. However, the CSF and the brain's interstitial fluids are in somewhat limited contact and may not always be assumed equivalent, particularly in the context of drug delivery. This chapter reviews the basic organization, function, blood supply, and fluids of the brain and spinal cord.

> [We] ought to know that from the brain, and from the brain only, arise our pleasures, joys, laughter and jests as well as our sorrows, pains, griefs and tears. Through it, in particular, we think, see, hear, and distinguish the ugly from the beautiful, the bad from the good, the pleasant from the unpleasant.
>
> —Attributed to Hippocrates, circa Fifth Century, BC

R.G. Thorne(✉)
Pharmaceutical Sciences Division, University of Wisconsin-Madison School of Pharmacy, Madison, WI, USA

Neuroscience Training Program, Clinical Neuroengineering Training Program, Cellular and Molecular Pathology Graduate Training Program, The Institute for Clinical and Translational Research, University of Wisconsin-Madison, Madison, WI, USA
e-mail: rthorne@wisc.edu

M. Hammarlund-Udenaes et al. (eds.), *Drug Delivery to the Brain*, AAPS Advances in the Pharmaceutical Sciences Series 10, DOI 10.1007/978-1-4614-9105-7,

> Among the various parts of an animated Body, which are subject to anatomical disposition, none is presumed to be easier or better known than the Brain; yet in the mean time, there is none less or more imperfectly understood.
>
> —Thomas Willis, 1681

> A great deal remains to be learned about the brain and spinal cord, a task that will take centuries, not years, to complete.
>
> —Santiago Ramón y Cajal 1909

A.1 Introduction to Neuroanatomy

Human brains weigh about 400 g at birth, nearly tripling in size during the first 3 years of life (due to the growth of neuronal processes and glia). The vast majority of human central nervous system (CNS) tissue is accounted for by the brain, which ranges from 1,050 to 1,800 g in normal young adults; by contrast, the spinal cord weighs only about 35 g. On average, the adult human male brain weighs 1,350 g and the adult human female brain weighs 1,250 g. This discrepancy may be explained by the observation that brain weight positively correlates with body size both within and across most species, e.g., an elephant weighing many thousand kilograms has a brain that weighs approximately 5 kg (although, interestingly, human brains tend to be smaller than expected relative to body size when compared to dolphins, rodents, and certain fish and primate species). Human cognition likely is shaped by our capacity for higher level processing. Indeed, our brains typically contain a much higher proportion of cerebral cortex than that found in lower mammals (e.g., cerebral cortex accounts for 77 % of the human brain's volume compared with only 31 % in the rat).

Microscopically, the CNS is principally composed of two types of cells: neurons and glia. Generally, neurons process information and signal to other neurons at synapses, while glia assist in the regulation of neuronal information by modulating synaptic activity as well as provide electrical insulation (myelin) to neuronal processes (axons). The cell bodies (somas) of neurons vary greatly in size, with diameters ranging from 5 to 10 μm (e.g., cerebellar granule cells) up to as large as ~100 μm for Betz cells in the primary motor cortex. Cell bodies are typically much larger than neuronal processes (axons and dendrites, collectively referred to as neurites), which range as small as 0.2 μm. Glia consist of macroglia (astrocytes and oligodendrocytes) and microglia (the resident immune cells of the brain). Glial sizes vary greatly, particularly across species. For example, human cortical protoplasmic astrocytes typically possess somas about ~10 μm in diameter and processes extending out 50–100 μm, both being severalfold larger than those found in the rodent. Glial cells outnumber neurons in most brain areas, with the exception of the cerebellum, e.g., there are likely well over ten times more glia than neurons in the thalamus and white matter.

Macroscopically, the CNS is divided into the brain and the spinal cord; major parts of the brain (the forebrain, midbrain, and hindbrain) can be divided based on

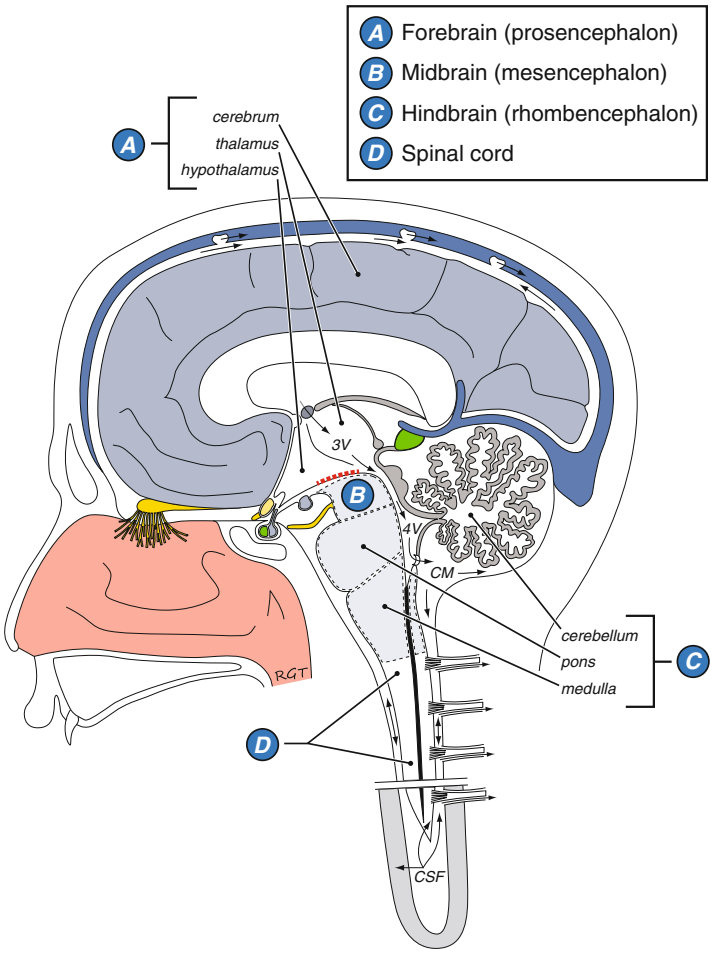

Fig. A.1 Schematic diagram showing a midsagittal view of the human central nervous system with the location of the brain and spinal cord in the cranial compartment. The cephalic flexure at the midbrain–diencephalic junction (diencephalon = thalamus + hypothalamus) is indicated by a *dashed red line*. Cerebrospinal fluid (CSF) flow from one of the lateral ventricles (not shown) through the third (3V) and fourth (4V) ventricles of the ventricular system and further circulation from the cisterna magna (CM) in the subarachnoid space are depicted with *arrows*

its embryological development (Fig. A.1). Further CNS divisions may be described through the use of several common terms for direction/orientation (Table A.1) and planes of section (Table A.2), e.g., it is often quite helpful to be able to use terms such as *rostral* (nearer to the front end of the neural axis, i.e., the front of the brain) and *caudal* (nearer to the tail end of the neural axis, i.e., the end of the spinal cord) when referring to specific CNS areas. For animals that move through the world horizontally and thus maintain a horizontal or a linearly oriented CNS, e.g., fish,

Table A.1 Directional terms used to refer to parts of the CNS

Direction/orientation	*Latin*	Meaning
Superior	*Superus* = "above"	Situated above
Inferior	*Inferus* = "below"	Situated below
Anterior	*Ante* = "before"	Situated in front
Posterior	*Post* = "after"	Situated behind
Dorsal	*Dorsum* = "back"	Toward the back
Ventral	*Venter* = "belly"	Toward the belly
Rostral	*Rostrum* = "beak"	Toward the snout
Caudal	*Cauda* = "tail"	Toward the tail

Table A.2 Planes used to refer to parts of the CNS

Planes	*Latin*	Meaning
Coronal	*Corona* = "crown"	Section in the plane of a tiara-like crown
Sagittal	*Sagitta* = "arrow"	Section in the plane of an arrow shot by an archer
Midsagittal		Sagittal section passing through the *mid*-line, dividing the brain into two halves
Parasagittal		Sagittal section *parallel* to the midsagittal plane
Horizontal		Section in the plane parallel to the *horizon* or the floor (also called *transverse* or *axial* in humans, i.e., perpendicular to the long axis of the body)

reptiles, and rodents, the *superior/inferior* and *anterior/posterior* terms are always equivalent to *dorsal/ventral* and *rostral/caudal*, respectively. Human beings have an upright posture, so it follows that the CNS contains a prominent bend (the cephalic flexure occurring at the level of the midbrain changes the rotation of the CNS by 80–90°); this bend results in different equivalencies whether we are above or below the midbrain. Above the human midbrain, *anterior* = *rostral*, *posterior* = *caudal*, *superior* = *dorsal*, and *inferior* = *ventral*. Below the human midbrain, *anterior* = *ventral*, *posterior* = *dorsal*, *superior* = *rostral*, and *inferior* = *caudal*. Examining a schematic view of the human CNS sectioned along the midsagittal plane (Fig. A.1), we can see the location of the cephalic flexure at the junction between the midbrain and the diencephalon.

The largest portion of the nervous system in human beings is the forebrain, represented by the telencephalon (*Greek*, "end brain") and the diencephalon (thalamus, hypothalamus, and associated structures). The telencephalon contains the cerebral cortex (tissue appearing gray in gross sections due to a relative abundance of cell bodies), white matter (made up mainly of myelinated axons, imparting a white appearance in gross sections), and subcortical structures such as the hippocampal formation, amygdala, and basal ganglia. The forebrain is connected to the hindbrain by the midbrain, and the hindbrain is in turn connected to the spinal cord. One may think of the forebrain sitting on top of the midbrain, pons, and medulla as broccoli or cauliflower would sit upon a stalk or a stem; indeed, the midbrain, pons, and medulla together are commonly referred to as the brain stem. As with many other

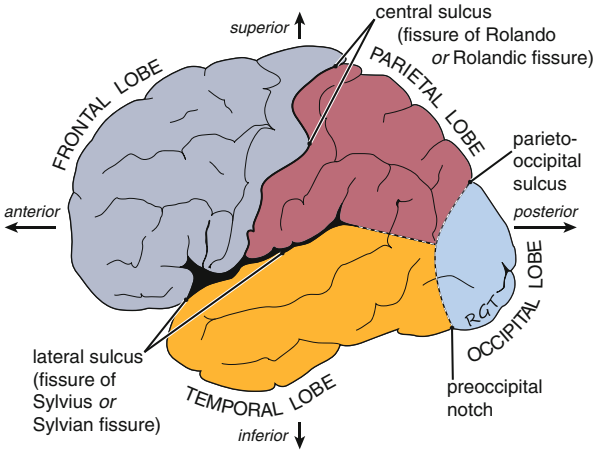

Fig. A.2 Diagram of the major lobes and sulci of the brain as seen from the lateral surface

parts of the body, the brain exhibits a high degree of bilateral symmetry. Dividing the brain longitudinally along the midsagittal plane yields two similar-appearing cerebral hemispheres that share a common pattern of surface landmarks between them. While this feature conveniently allows us to consider both hemispheres by learning the landmarks of only one, it must be kept in mind that important differences exist in the localization of function between the left and right sides, e.g., the majority of language processing is accomplished in the left hemisphere of most individuals.

Observing the human brain from the lateral surface (Fig. A.2) allows us to visualize the four major brain lobes, areas of cerebral cortex with specific functions that are separated from one another by identifiable surface landmarks. The surface of the human brain contains numerous folds with ridges that are termed gyri (singular, gyrus). These folds are often absent or much less elaborate in lower mammals because their cerebral cortex is less developed than in higher mammals. Separating the gyri are furrows or grooves termed sulci (singular, sulcus); particularly deep sulci are often termed fissures. The largest sulcus is the lateral sulcus (Sylvian fissure) which runs horizontally and separates the frontal and parietal lobes from the temporal lobe. The central sulcus (Rolandic fissure) runs vertically and separates the frontal from the parietal lobe. An imaginary line extending between the parieto-occipital sulcus (best seen on the brain's medial surface) and the preoccipital notch, an indentation in the brain created by the petrous part of the temporal bone, separates the occipital lobe from the temporal and parietal lobes; a second imaginary line extended from the middle of this first line to the lateral sulcus further separates the temporal and parietal lobes from each other. In addition to the four major lobes seen on the lateral surface, another region of tissue called the insular cortex is buried within the depths of the lateral sulcus, concealed from view by portions (termed opercula; *Latin*, "lid") of the frontal, parietal, and temporal lobes. Finally, references are often made to yet another lobe, the "limbic" lobe, which is separated from the frontal and parietal lobes by the cingulate sulcus; it is best appreciated when examining the cerebral hemisphere on its medial surface (Fig. A.3).

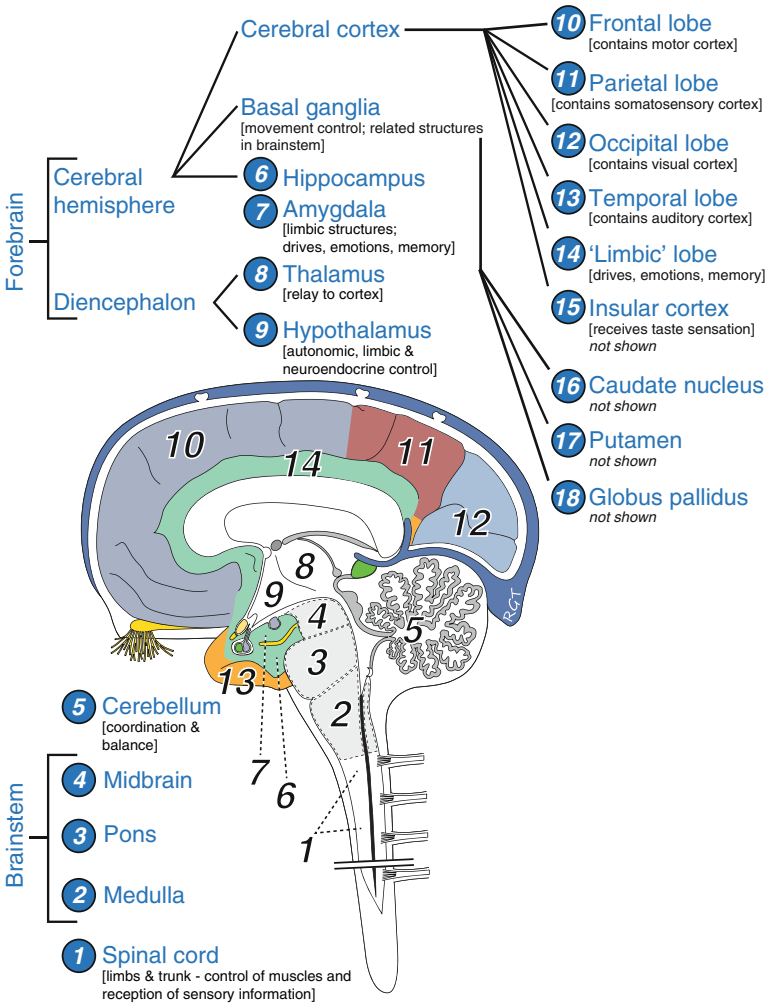

Fig. A.3 Functional subdivisions of the central nervous system. Adapted and redrawn from Nolte (2009)

A.2 Central Nervous System Functions

A vast array of functions may be identified for the many different brain and spinal cord areas that constitute the CNS. A simplified overview of some of the more important functional subdivisions is provided in Fig. A.3. Proceeding from caudal to rostral along the neural axis, we first encounter the spinal cord, a tubular structure which contains numerous nuclei (clusters or groups of cell bodies) corresponding to the spinal gray matter along with a large number of tracts or fasciculi (bundles of axons) corresponding to the spinal white matter. The spinal cord is concerned with the

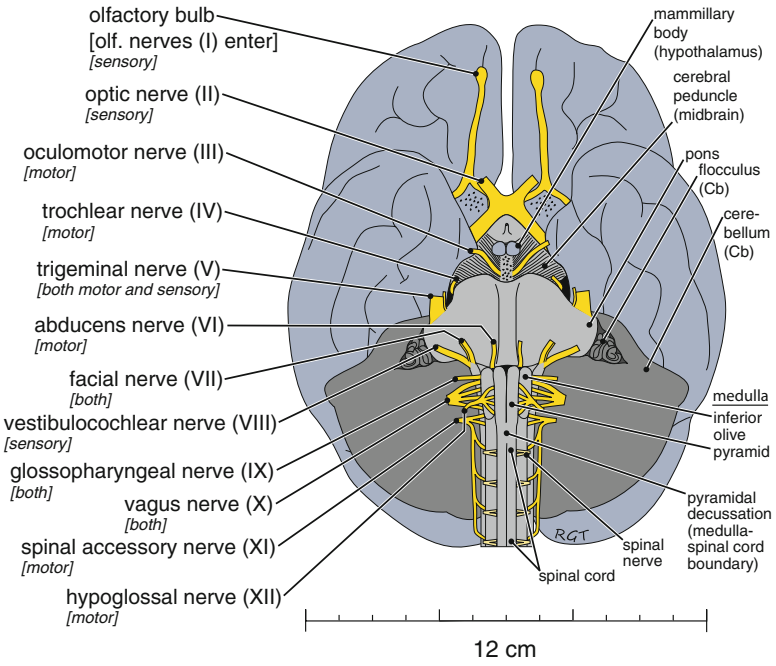

Fig. A.4 Diagram of the ventral brain surface showing the location of the 12 cranial nerves. The motor and/or sensory modality of each nerve is indicated

limbs and trunk of the body, primarily in the motor control of voluntary muscles and the reception of sensory information, although it also participates in the regulation of visceral functions. The human spinal cord has a total of 31 segments from which the motor (ventral) and sensory (dorsal) roots of spinal nerves arise (in order, from caudal to rostral): coccygeal (1), sacral (5), lumbar (5), thoracic (12), and cervical (8). The spinal gray matter is noticeably larger in two places that correspond to the lower and upper limbs, the lumbosacral (L2–S2) and cervical (C5–T1) enlargements, respectively.

Rostral to the spinal cord is the brain stem, a highly complex structure which regulates many basic physiological functions important for survival including arousal, blood pressure, and respiration. The brain stem is also associated with most of the 12 cranial nerves (only the olfactory and optic nerves are excluded), which provide cranial sensory information and allow for the control of head muscles, e.g., the extraocular muscles that move the eyes. The attachment sites for the cranial nerves are best seen in a ventral view of the brain (Fig. A.4); their varied functions and clinical tests commonly used to examine them are listed in Table A.3. The cerebellum, a structure embryologically related to the pons of the hindbrain, modulates motor information passing between the forebrain, brain stem, and spinal cord; its function may partly be inferred by the outcome of cerebellar lesions, which result in disorders of coordination and balance (ataxia).

Table A.3 Cranial nerve functions and their evaluation

Cranial nerve	Function	Test
I (Olfactory nerve)	Olfaction	Perception of an odorous substance
II (Optic nerve)	Vision	Perception of a vision chart
III (Oculomotor nerve)	Controls most extraocular eye muscles	Visual tracking of a moving object (e.g., following a finger)
IV (Trochlear nerve)	Controls superior oblique muscle (eye)	Visual tracking toward an object (e.g., looking down at the nose)
V (Trigeminal nerve)	Sensation of face, sinuses, and teeth; controls muscles of mastication	Touch, pain perception on face; ability to clench teeth
VI (Abducens nerve)	Controls lateral rectus muscle (eye)	Visual tracking toward an object (e.g., looking to the side)
VII (Facial nerve)	Controls muscles of facial expression; taste (ant. tongue)	Ability to smile and raise eyebrows; perception of sugar or salt
VIII (Vestibulo-cochlear nerve)	Hearing; balance	Perception of a tuning fork; evaluation for vertigo
IX (Glossopharyngeal nerve)	Pharynx sensation; swallowing; taste (post. tongue)	Elicit gag reflex; perception of sugar or salt
X (Vagus nerve)	Controls muscles of larynx and pharynx; visceral motor control and sensation	Check for hoarseness, sound production, and swallowing
XI (Spinal accessory nerve)	Controls trapezius and sternocleidomastoid muscles	Shoulder raise and turning the head against resistance
XII (Hypoglossal nerve)	Controls muscles of tongue	Tongue movements

Rostral to the brain stem is the diencephalon, which includes the hypothalamus and thalamus as well as the epithalamus. The hypothalamus serves as a control center for the autonomic system (a part of the peripheral nervous system that provides nonconscious control over the body's organs) in addition to the neuroendocrine and limbic systems; hypothalamic nuclei are involved in a wide variety of functions that include the regulation of thirst, body temperature, hunger, satiety, and circadian rhythms. The thalamus serves as a relay center for nearly all sensory information reaching the cerebral cortex (only olfactory projections bypass it); many non-sensory pathways, e.g., from the cerebellum, also reach the cerebral cortex after being processed by thalamic nuclei. The cerebrum sits above the diencephalon and consists of subcortical structures (the basal ganglia, hippocampal formation, and amygdala), the cerebral white matter, and the cerebral cortex. The basal ganglia consist of a group of nuclei including the globus pallidus, caudate, and putamen. The basal ganglia modulate motor information; dysfunction in components of its circuitry (often considered to also include the substantia nigra of the midbrain and the subthalamic nucleus) leads to movement disorders such as Parkinson's and Huntington's diseases. The hippocampus and amygdala are major limbic areas located in the medial temporal lobe (although, technically, often considered part of the limbic lobe); the hippocampus is involved in learning and memory, while the amygdala is thought to be important for emotional content and social behaviors.

The various sensory and motor functions of the human cerebral cortex are best appreciated after first dividing the four major lobes into component gyri (Fig. A.5a)

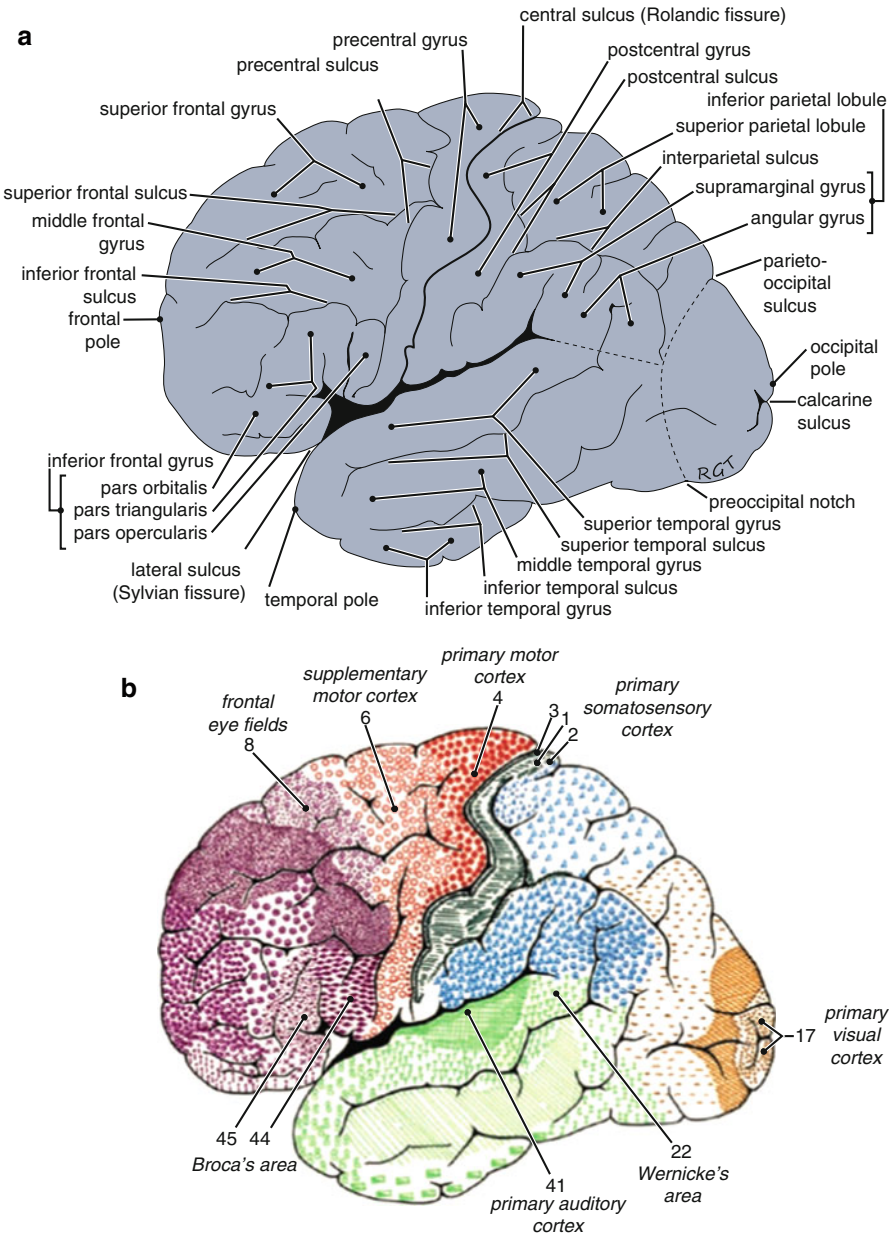

Fig. A.5 Schematic of the lateral brain surface—*detailed*. (**a**) Labeled view of the four visible lobes showing the location of the major gyri and sulci. (**b**) Brodmann's cytoarchitectonic map of the human cortex showing the location of major cortical units and their corresponding area number according to Brodmann's classification system (adapted from Zilles and Amunts 2010). The schematic in (**a**) has been drawn to closely match the view in (**b**)

and then considering a classification scheme such as the map developed by Korbinian Brodmann in his 1909 monograph (Fig. A.5b). Brodmann's map of the human cortex remains in wide use because his cytoarchitectonic divisions, based on differences in neuronal size, shape, and density observed in histological sections stained for cell bodies, correlate remarkably well with our current knowledge of structure–function relationships based on clinical observations, electrophysiological evidence, and neuroimaging. Brodmann divided the human cortex into 43 areas numbered between 1 and 52 (numbers 12–16 and 48–51 were not used in his map for the human brain). Numerous pathways connect the cerebral cortex with different levels of the neural axis below it; indeed, the nature of the information contained within the specific pathways arriving at and/or leaving a particular cortical area informs what is considered to be that area's function. Many pathways are longitudinally organized along the entire neural axis. For example, the dorsal column-medial lemniscal system provides information about fine touch, vibration, and position sense from the periphery, beginning at the level of the spinal cord and extending up through the brain stem and thalamus to the cerebral cortex (for this reason, it is called an ascending sensory pathway), while the corticospinal tract conveys impulses mediating voluntary movement from the cerebral cortex down to spinal cord motor neurons (for this reason, it is called a descending motor pathway). Most sensory and motor pathways cross (decussate) at some point as they travel up or down the neural axis; this crossing results in a given side of the brain controlling the muscles and receiving sensory information from the opposite side of the body.

The frontal lobe contains the primary and supplementary motor cortices, the frontal eye fields, Broca's area, and the prefrontal cortex. The primary motor cortex (Brodmann area 4), located in the precentral gyrus (the gyrus running just anterior and parallel to the central sulcus), is involved in the voluntary execution of movement for the opposite side of the body (i.e., the left primary motor cortex controls the body's right side). The supplementary motor cortex (area 6), located in the anterior part of the precentral gyrus and a portion of the adjacent superior and middle frontal gyri, is involved in the planning and initiation of movement for the opposite side of the body. The frontal eye fields (area 8) in the superior and middle frontal gyri initiate saccadic eye movements, e.g., voluntary gaze toward the opposite side. Broca's area, consisting of the pars opercularis and pars triangularis of the inferior frontal gyrus (areas 44 and 45, respectively) of one hemisphere (typically the left), is important for the production of speech. The prefrontal cortex comprises most of the remainder of the frontal lobe and is generally considered to be involved with personality, thought, cognition, and planning behavior.

The parietal lobe contains the primary somatosensory cortex and other cortical areas important for the perception and integration of the senses. The primary somatosensory cortex (areas 1, 2, and 3), located in the parietal lobe's postcentral gyrus (the gyrus running just posterior and parallel to the central sulcus), is involved in the perception of touch, pain, and position for the opposite side of the body. The superior parietal lobule of the parietal lobe is important for the formation of our self-image; lesions to this area can result in complicated neurological signs including neglect of the body on the opposite side. The inferior parietal lobule of the

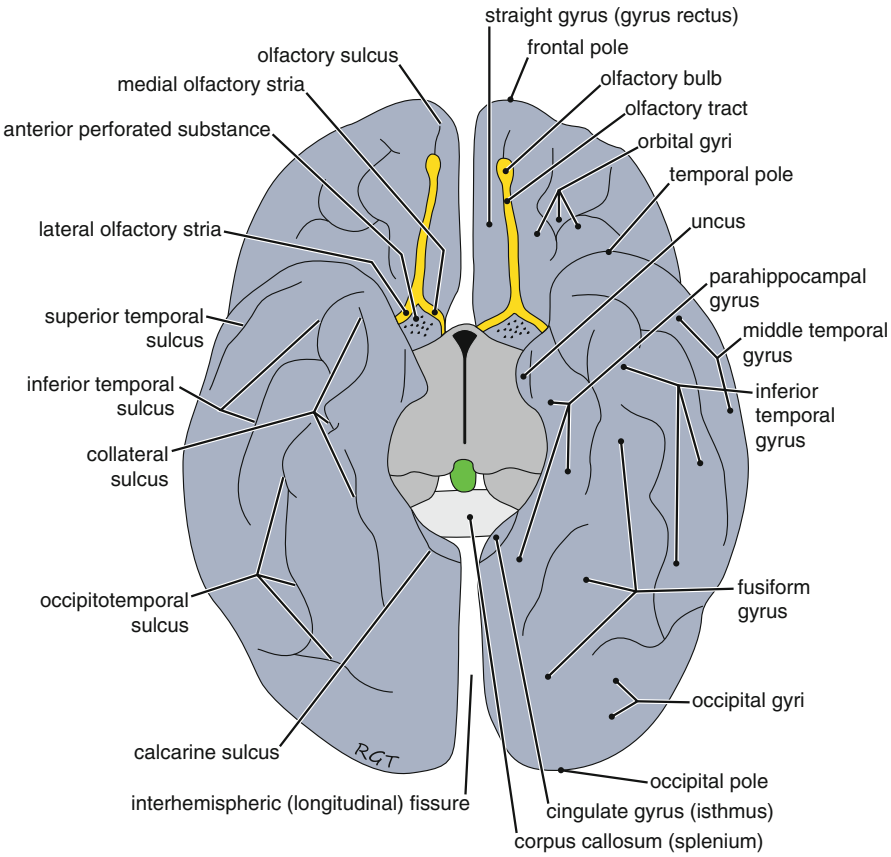

Fig. A.6 Schematic of the ventral brain surface with brain stem removed—*detailed*. All major gyri and sulci are labeled

parietal lobe is important for integrating diverse sensory information, e.g., content that is heard, read, and/or visualized.

The temporal lobe contains the auditory cortex and cortical tissue for recognizing speech and for the perception of visual forms, colors, emotions, and smells. The primary auditory cortex (area 41), located within the superior temporal gyrus and a transverse gyrus extending into the lateral sulcus (not well seen from the lateral view), and the secondary auditory cortex surrounding it are important for sound perception and localization. Wernicke's area (area 22), also located in the superior temporal gyrus (posterior aspect) of one hemisphere (typically the left), mediates the recognition of spoken language. Much of the middle and inferior temporal gyri are concerned with the perception of visual form and color. Cortical areas within the anterior-most portion of the temporal lobe (the temporal pole) and the parahippocampal gyrus (observed on the brain's ventral surface; see Fig. A.6) are important for the processing of emotions and smell.

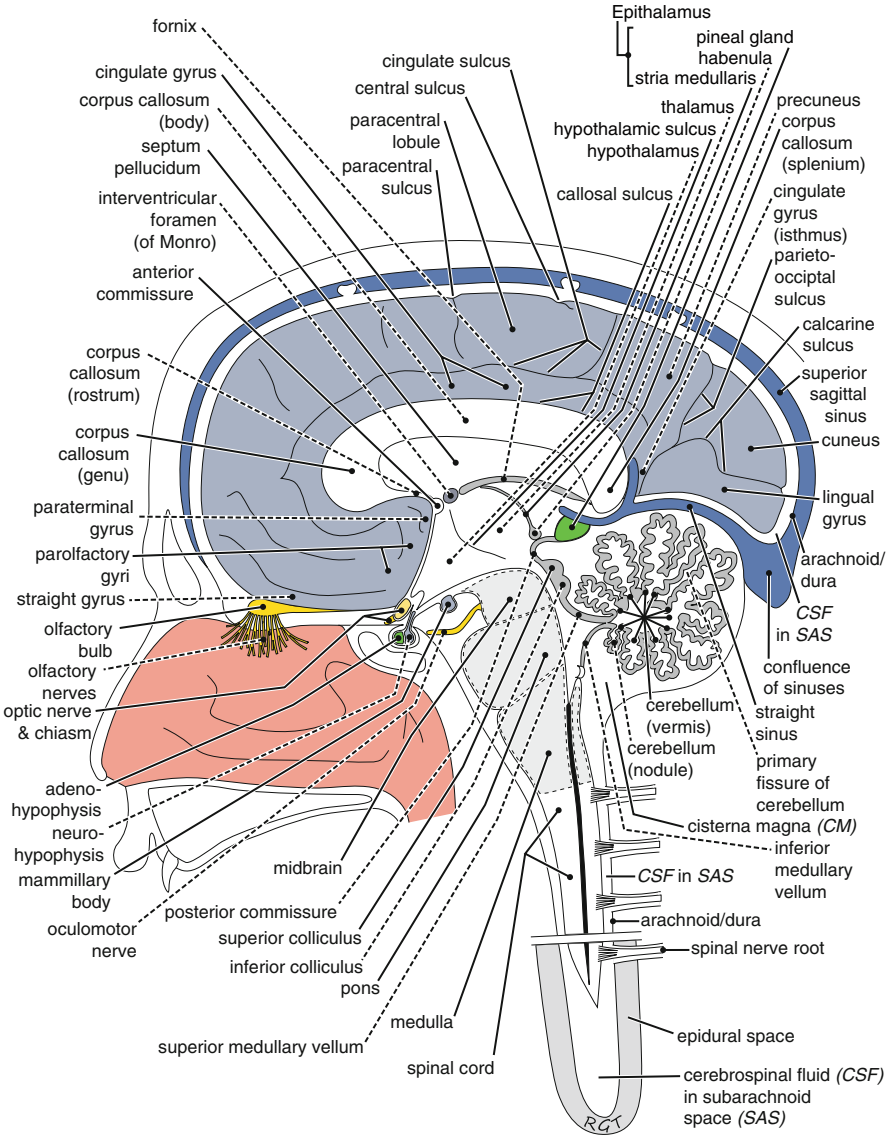

Fig. A.7 Schematic showing a midsagittal view (medial surface) of the CNS—*detailed*. All gyri, sulci, and other component structures are labeled

The occipital lobe contains the primary, secondary, and tertiary visual cortices subserving visual perception. The primary visual cortex (area 17), located in the banks of the calcarine sulcus (best appreciated in a medial view of the brain; see Fig. A.7), performs the initial processing of visual information. The secondary and tertiary visual cortices occupy most of the remainder of the occipital lobe and perform "higher" visual processing that allows us to perceive depth, motion, and color and to recognize faces.

A.3 Cerebrovasculature

The importance of the CNS vascular supply can obviously not be overstated. Neurons demand tremendous metabolic resources in order to function properly, e.g., a continuous supply of ATP is needed to maintain the ionic gradients essential for the membrane potentials underlying neurotransmission. Neurons have almost no ATP in reserve and must continuously be provided with glucose and oxygen so that aerobic metabolism can be utilized to produce the energy they require; even short periods of hypotension (low blood pressure) or ischemia (loss of blood supply) can lead to fainting or loss of consciousness; interruption of the cerebral blood supply to an area for just a few minutes can result in permanent damage. As with other body organs, CNS blood vessels may functionally be divided into distributing vessels (arteries), resistance vessels (arterioles), exchange vessels (capillaries and smaller post-capillary venules), and capacitance vessels (larger venules and veins). Brain capillaries are the smallest of these vessels, typically not larger than ~4–8 μm in diameter (approximately the same size or just a bit smaller than red blood cells).

In addition to facilitating the delivery of glucose, oxygen, and other endogenous blood substances to the CNS, the cerebrovasculature also provides among the most efficient routes for widespread drug access, provided the drug can pass the various barriers separating cerebral blood from the brain interstitial and cerebrospinal fluids. The most important of these barriers is the blood–brain barrier, represented by tight junctions between brain capillary endothelial cells forming the CNS microvasculature; this unique arrangement prevents nearly all but the smallest, lipophilic molecules from crossing the normal, healthy blood–brain barrier unless a specific transporter is present to facilitate their passage (e.g., as with glucose). Generally, gray matter is more highly perfused than white matter, although the normal perfusion rate of each is still much higher than that of muscle, skin, or fat. Cerebral capillary abundance can be as high as several thousand mm/mm^3 (total capillary length per tissue volume) in certain discrete areas of the adult gray matter, e.g., the rat paraventricular and supraoptic nuclei of the hypothalamus, while white matter areas exhibit much lower values (e.g., about 100–300 mm/mm^3 in the rat). This capillary abundance (also referred to as vascularity) varies dramatically over the life-span, with much lower values on average at birth than later in life (evidence suggests tissue vascularity correlates with the numbers of synapses, which increase with development and also exhibit notable differences across brain regions). Despite the brain's high capillary density, total cerebral blood volume under normal conditions across many species, including human beings and rodents, is only on the order of about 2–5 % of the total tissue volume, as measured using a variety of techniques (e.g., magnetic resonance imaging, positron emission tomography, and in situ brain perfusion). Cerebral blood volume is known to exhibit some regional variability, e.g., measurements in rats have yielded higher values (up to ~5 %) in areas such as the olfactory bulbs with lowest values in the white matter (~1 %).

The human brain and meninges are supplied with blood derived from the common carotid and vertebral arteries (Fig. A.8). The paired internal carotid arteries arise from the common carotids and feed the *anterior circulation*, supplying most, but not all, of the forebrain. The paired vertebral arteries arise from the subclavian arteries and

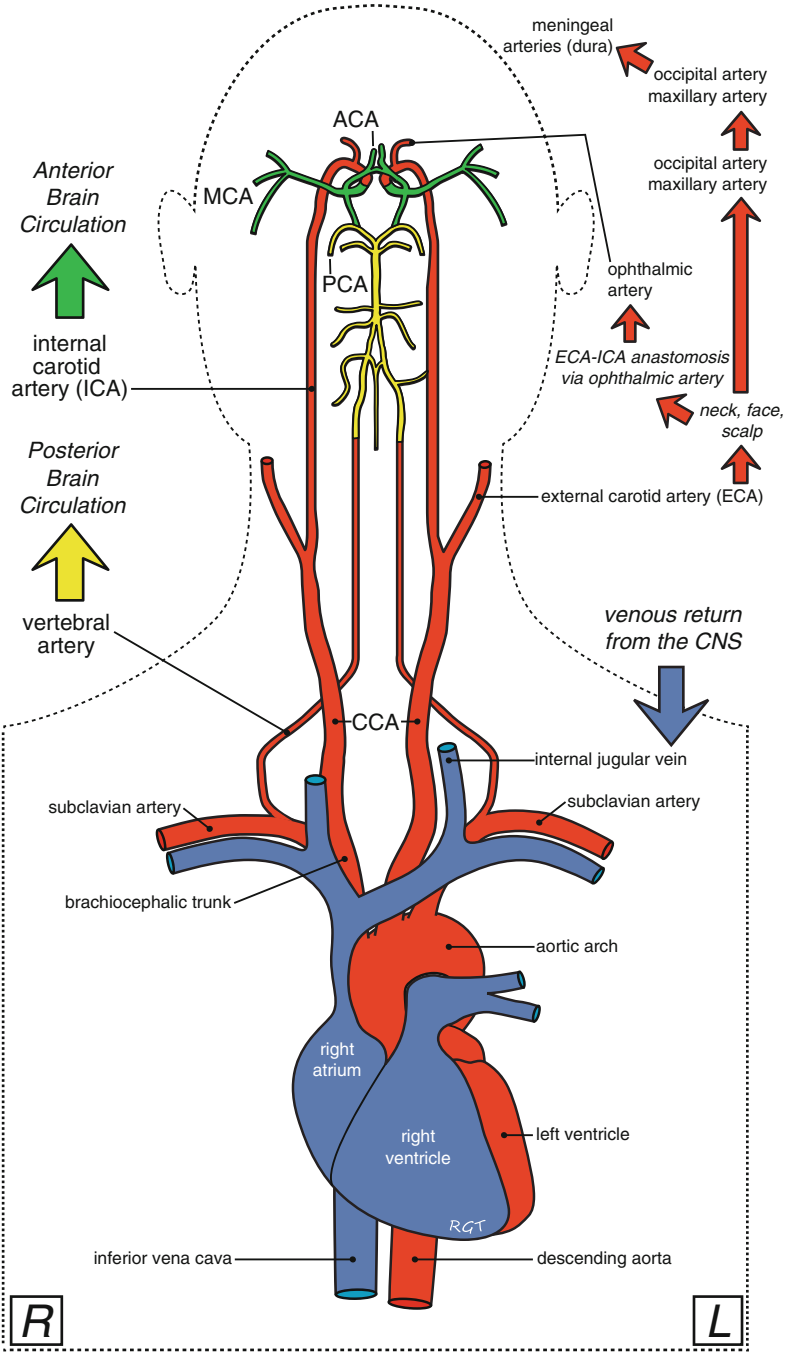

Fig. A.8 Blood supply to the brain showing the origin of the anterior and posterior circulations giving rise to the major cerebral vessels: the anterior (ACA), middle (MCA), and posterior (PCA) cerebral arteries. Points of anastomosis between the internal carotid artery (ICA) and external carotid artery (ECA) are also indicated. *CCA* common carotid artery

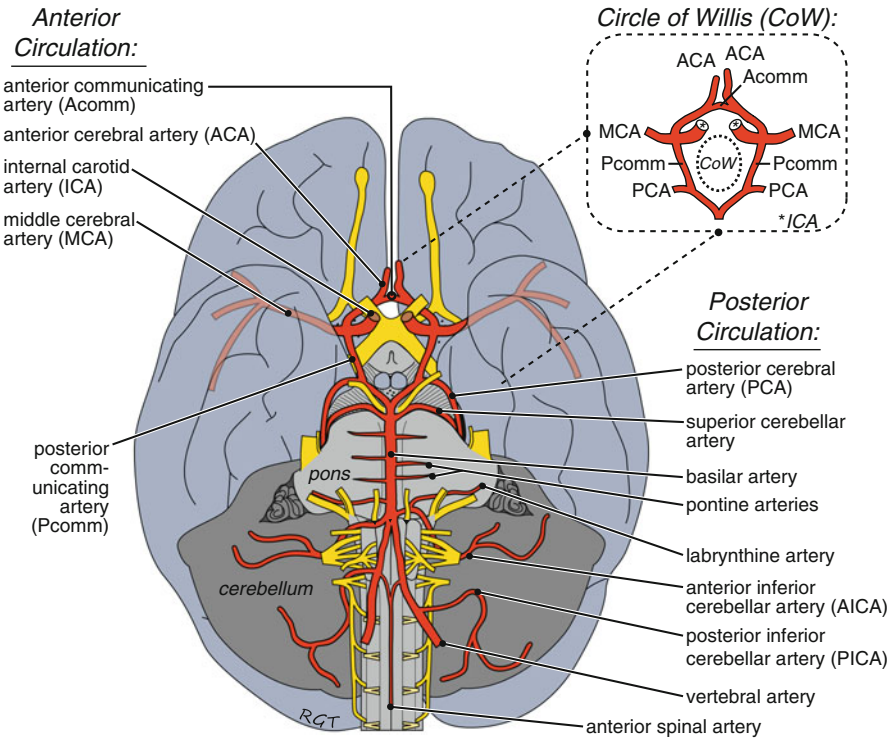

Fig. A.9 Diagram of the ventral brain surface showing the arterial supply. Components of the anterior circulation, posterior circulation, and the circle of Willis are emphasized

feed the *posterior circulation* to supply all of the hindbrain, nearly all of the midbrain, and parts of the diencephalon, spinal cord, and occipital and temporal lobes. The anterior and posterior circulations meet at the circulus arteriosus or circle of Willis (Fig. A.9); this important vascular feature bears the name of Sir Thomas Willis, among the first to accurately describe the cerebral arterial circle in 1664. The circle of Willis may be thought of as a nine-sided polygon (consisting of two each of the anterior, middle, posterior, and posterior communicating arteries along with a single anterior communicating artery); it forms a complete anastomotic ring in about 50 % of human beings, joining the anterior and posterior circulations. Arterial anastomoses, natural connections between two arteries, are important functionally because they can provide potential collateral circulation (a sort of "fail-safe system"), enlarging to compensate for occlusion or reduced supply in one of the segments. Under such conditions, a single artery may potentially supply blood to the normal territory of another in addition to its own territory following an obstruction.

All cortical areas of the cerebral hemispheres are supplied with blood via penetrating branches from one of the three main cerebral arteries (anterior, middle, and posterior); these vessels branch numerously, frequently penetrating into sulci as their leptomeningeal segments travel within the subarachnoid space just off the brain's surface (Fig. A.10). The cortical territories supplied by the cerebral arteries

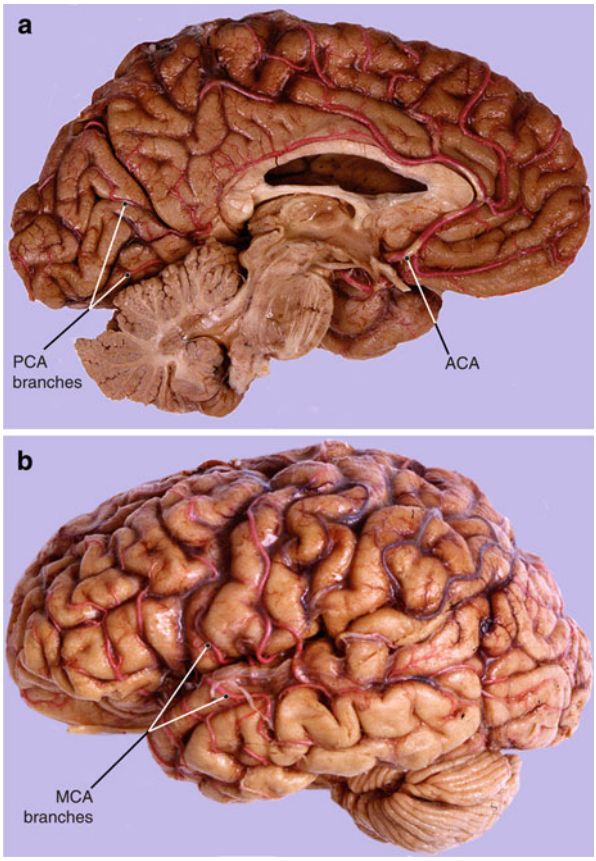

Fig. A.10 Midsagittal and lateral views of a human brain with arteries attached and visible. (**a**) The medial brain surface is supplied by branches of the anterior (ACA) and posterior (PCA) cerebral arteries. (**b**) The lateral brain surface is mostly supplied by branches of the middle cerebral artery (MCA). Adapted with permission from the Neuroanatomy Interactive Syllabus (Sundsten and Mulligan 1998)

are shown for the lateral, medial, and ventral brain surfaces in Figs. A.11a and A.12a and b, respectively (the most common territories are shown; however, considerable variability in their distribution is known to exist). In addition to the anastomotic ring at the circle of Willis, leptomeningeal anastomoses also exist between terminal branches of the cerebral arteries in areas called watershed or borderzone regions at the territorial boundaries (shown in detail in Fig. A.11a; similar watershed/borderzone regions are to be expected on the brain's medial and ventral brain surfaces but are not depicted in Fig. A.12a, b). The watershed regions are particularly vulnerable to ischemia and infarction when cerebral perfusion drops (e.g., when systemic blood pressure is dramatically reduced). Anastomoses between terminal branches of the cerebral arteries are also thought to play a role in providing collateral flow during ischemia (e.g., MCA occlusion), where they may help to save part of the penumbral tissue (potentially salvageable areas at the periphery of the core infarct). Penetrating vessels from the cerebral arteries also supply deep cerebral structures beneath the cortex (not shown); the most important of these are the lenticulostriate arteries (MCA branches that penetrate the anterior perforated substance (see Figs. A.6 and A.9)), providing blood to portions of the basal ganglia and

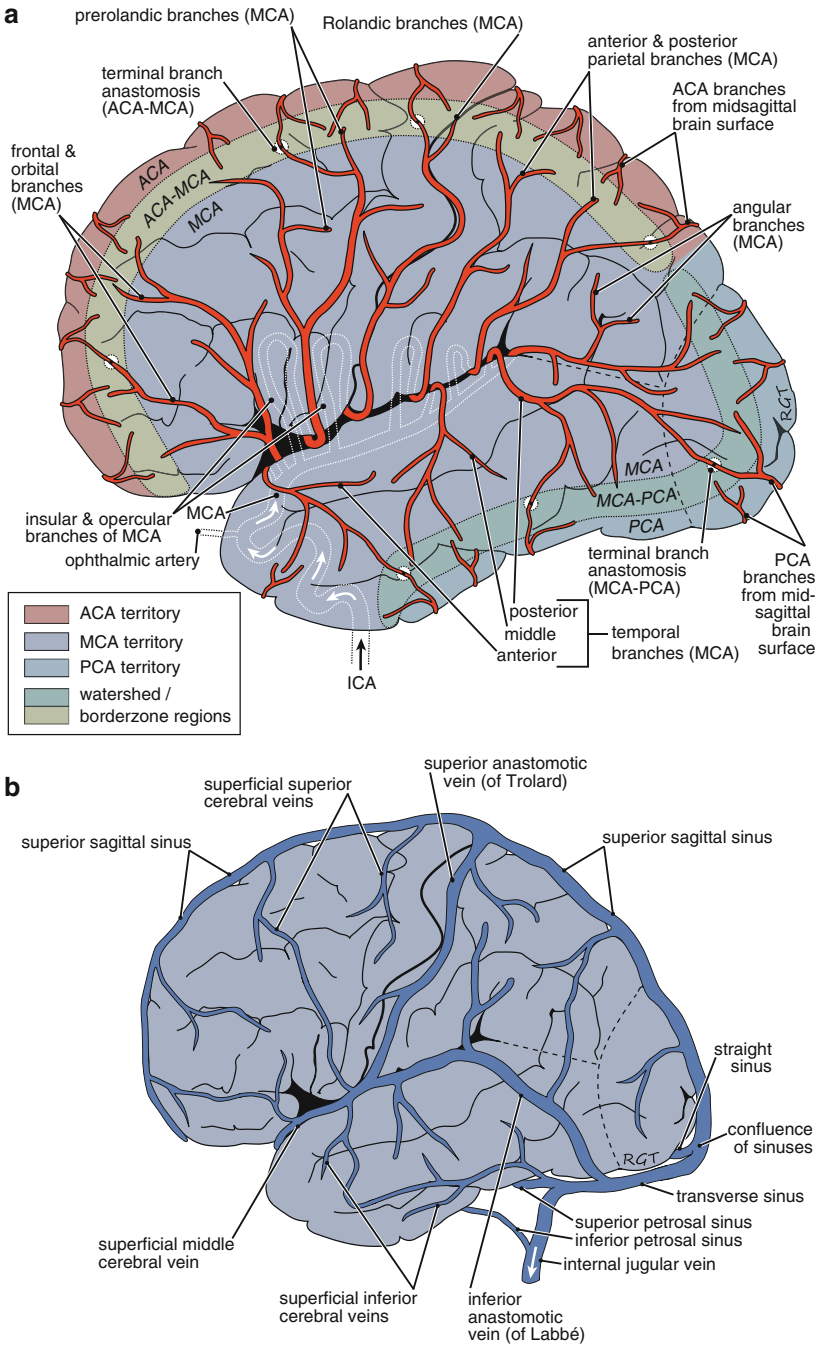

Fig. A.11 Diagram of the arterial supply (**a**) and venous drainage (**b**) on the brain's lateral surface—*detailed*. *ACA* anterior cerebral artery, *ICA* internal carotid artery, *MCA* middle cerebral artery, *PCA* posterior cerebral artery

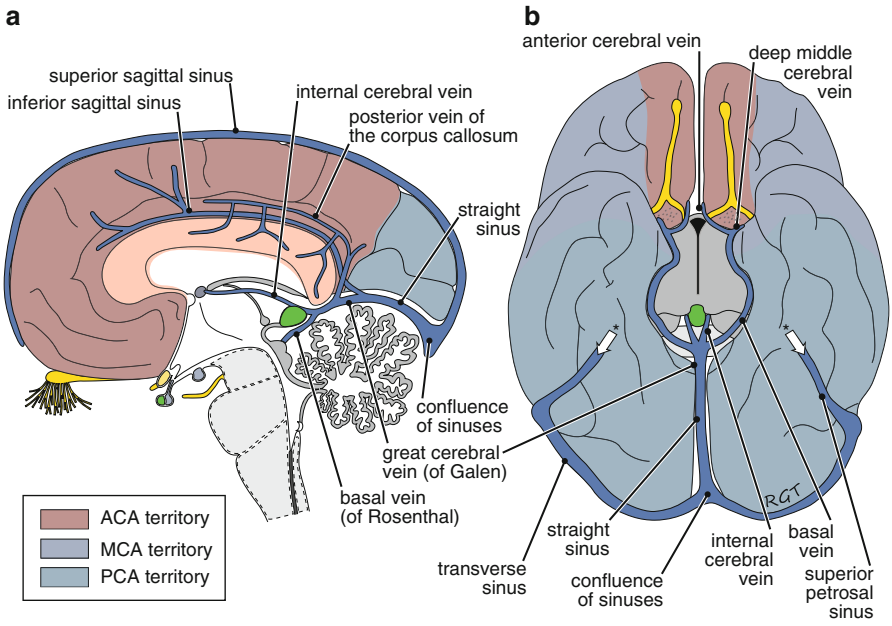

Fig. A.12 Diagram of the arterial supply and venous drainage on the brain's medial (**a**) and inferior (**b**) surfaces. *Venous blood draining from the cavernous sinus (not shown); *ACA* anterior cerebral artery, *MCA* middle cerebral artery, *PCA* posterior cerebral artery

the internal capsule. The anterior choroidal artery, arising off of the internal carotid artery, and the posterior choroidal artery, arising off of the posterior cerebral artery, also supply a variety of deep cerebral structures in addition to the choroid plexus of the ventricular system. A summary of the arterial supply to different CNS areas is provided in Table A.4.

Cerebral veins empty into the venous sinuses, large venous channels surrounded by the dura mater, which ultimately empty into the internal jugular veins (Fig. A.8). Cerebral veins are divided into superficial groups, which lie on the brain's surface and drain into the superior sagittal sinus (Fig. A.11b), and deep groups, which drain internal structures and empty into the straight sinus (Fig. A.12). Cerebral veins lack valves, contain numerous anastomoses, and do not usually run parallel to the arterial distribution.

A.4 Ventricular System and Brain Fluids

The CNS is immersed in cerebrospinal fluid (CSF), which helps to suspend the brain and avoid its distortion due to a buoyancy force that balances the downward force due to gravity. The CNS and CSF are together encased within the meninges

Table A.4 Arterial supply of the CNS

CNS area	Major arteries
Spinal cord	Anterior and posterior spinal arteries, radicular arteries
Medulla	Vertebral and posterior inferior cerebellar arteries (PICA)
Pons	Basilar and anterior inferior cerebellar arteries (AICA)
Cerebellum	*Superior surface*—superior cerebellar artery; *inferior surface*—AICA and PICA
Midbrain	Basilar, posterior cerebral, and superior cerebellar arteries, posterior and anterior choroidal arteries
Diencephalon	
Thalamus	Posterior cerebral (PCA), posterior communicating, and posterior choroidal arteries
Hypothalamus	Anterior cerebral (ACA), posterior communicating, and posterior cerebral arteries
Basal ganglia	
Globus pallidus	Anterior choroidal and middle cerebral (MCA) arteries (lenticulostriate arteries)
Putamen	ACA and MCA (lenticulostriate arteries)
Caudate nucleus	ACA and MCA (lenticulostriate arteries), anterior choroidal artery
Amygdala	Anterior choroidal artery
Hippocampus	PCA and anterior choroidal artery
Choroid plexus	Anterior and posterior choroidal arteries
Internal capsule	ACA, MCA, and anterior choroidal artery
Corpus callosum	ACA and PCA
Cerebral cortex	
Frontal lobe	ACA and MCA
Parietal lobe	ACA and MCA
Occipital lobe	MCA and PCA
Temporal lobe	MCA and PCA, choroidal arteries
Insular cortex	MCA

(the dura mater, arachnoid, and the pia mater) which provide additional stability; the dura mater is anchored to the skull, while the arachnoid, which forms the leptomeninges with the pia, is adherent to the dura mater. Arteries and veins run within the subarachnoid space surrounded by CSF.

The CSF of mammals occupies several cavities or chambers within the brain (the ventricular system) as well as a larger volume filling the subarachnoid space that surrounds the brain and spinal cord. The human brain contains four ventricles (Fig. A.13a–c): two large, c-shaped lateral ventricles; a single third ventricle between the thalamus and hypothalamus of each hemisphere; and a single tent-shaped fourth ventricle located between the cerebellum, pons, and medulla. CSF is actively secreted by the choroid plexuses of the lateral, third, and fourth ventricles (Fig. A.13c) such that there is a brisk flow of CSF within the system. CSF flows from the lateral ventricles to the third ventricle via two interventricular foramina, then from the third ventricle to the fourth ventricle via the cerebral aqueduct, and, finally, exits into several cisterns and the subarachnoid space via three apertures, one located medially and two located laterally in the fourth ventricle (Fig. A.13d). CSF is ultimately reabsorbed back into the blood supply through arachnoid projections into the venous sinuses (Figs. A.11b and A.12) and also along cranial and spinal nerve roots to extracranial lymphatics. Additional CSF outflow may also

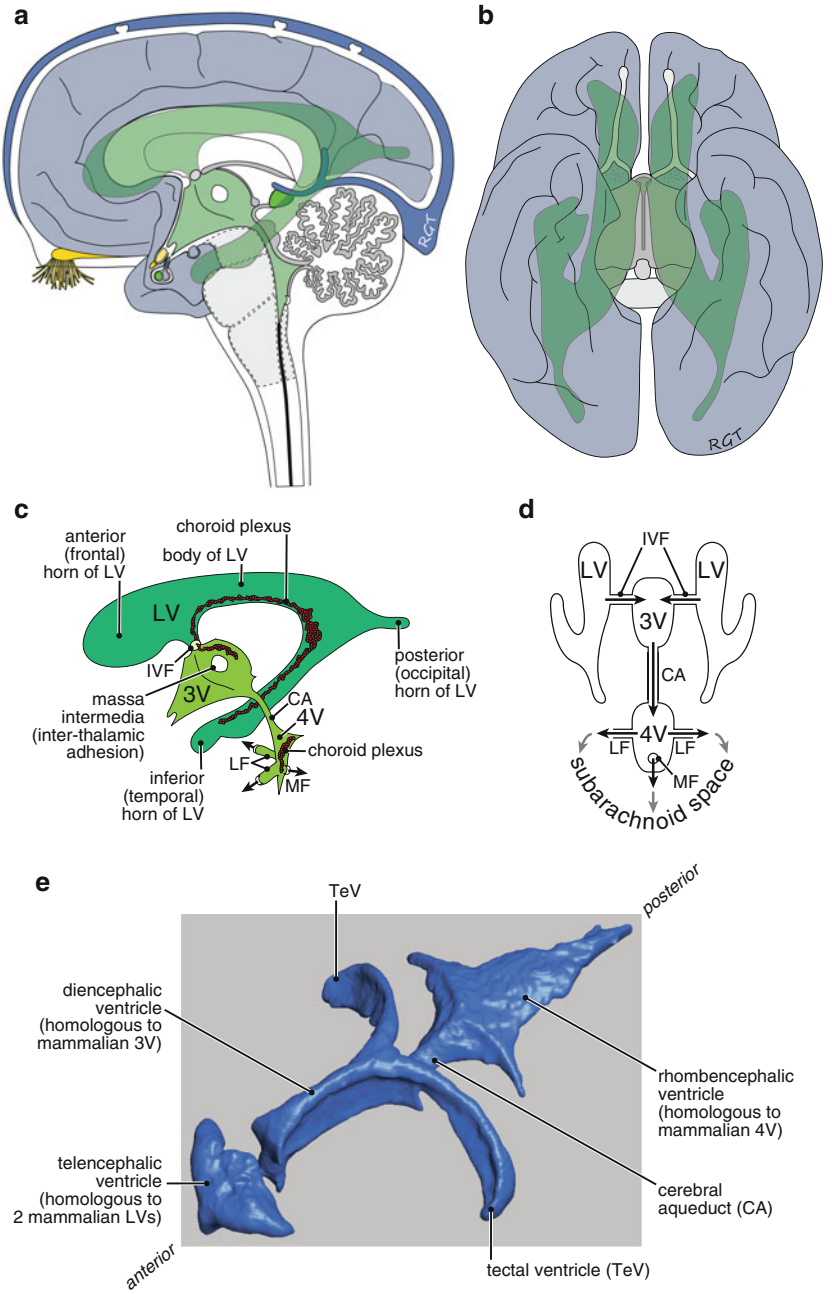

Fig. A.13 Anatomy of the ventricular system. Schematic 3-D representations of the ventricles and their drainage pathways in human beings as viewed from either the midsagittal (**a**) or the inferior (**b**) brain surfaces; the approximate position of the ventricular system within the brain is depicted. Schematics of the isolated human ventricular system (**c**) and flow pathways (**d**). (**e**) 3-D rendering of larval zebrafish ventricular anatomy, based on in vivo confocal microscopy (image kindly provided by Drs. Maxwell Turner, Jeremy Richardson, and Alan Kay). Homology to mammalian ventricular structures is indicated. *3V* third ventricle, *4V* fourth ventricle, *CA* cerebral aqueduct (of Sylvius), *IVF* interventricular foramen (of Monro), *LF* lateral foramina (of Luschka), *MF* medial foramen (of Magendie), *LV* lateral ventricle

Table A.5 Approximate physiological parameters for the cerebrospinal fluids (CSF) and ventricular systems of adult humans and rats

Parameter	Human	Rat
Ventricular CSF volume	25 ml	10–12 µl
Subarachnoid space CSF volume	115 ml	190 µl
Total CSF volume	140–150 ml	200–300 µl
CSF secretion rate	350–370 µl/min	2–5 µl/min
Rate, % per minute (turnover time)	0.3–0.4 (6–7 h)	0.7–1.7 (1–2.5 h)

occur along the perivascular sheaths of major blood vessels. In adult human beings, roughly 15 % of the total CSF volume is present within the ventricular system, with the remainder located within the fluid-filled cisterns and subarachnoid spaces outside of the brain and spinal cord; in rats, about 5 % or less of the total CSF volume is contained within the ventricles. Some differences in physiological parameters for the CSF and ventricular systems of adult humans and rats are listed in Table A.5. While the relative amounts of CSF obviously differ dramatically across species due to differences in brain size, with total CSF volumes ranging from ~150 ml (human) to ~290 µl (rat) to ~40 µl (mouse) to 2 nl (larval zebrafish), the general organization of the ventricular system appears to be remarkably preserved (Fig. A.13e).

It is often necessary to differentiate the CSF from brain interstitial fluid. The interstitial fluid of the CNS is contained within narrow extracellular spaces (ECS), approximately 40–60 nm in width on average, that exist between neurons and glia. Interstitial fluid is in contact with the CSF at the ventricular surfaces as well as the pial surfaces facing the subarachnoid space. The ECS occupies about 20 % of the total tissue volume in most brain areas of normal, adult animals. The ECS is critical to the distribution of neurotransmitters, nutrients, and all drugs within the CNS. Diffusion is an essential mechanism for the extracellular transport of most substances through the brain interstitial fluid. Diffusion is extremely fast and efficient over short distances like the synaptic cleft (~15 nm) and quite effective even for distances spanning a few cell bodies (~10–100 µm), but it can be quite limiting over the larger distances often necessary for effective drug distribution from the ventricular or the pial brain surfaces or from a syringe placed directly within the brain parenchyma. Neurons are rarely further than ~10–20 µm from their closest neighboring brain capillaries likely because the efficient diffusion of O_2, nutrients (e.g., glucose), and other molecules into the brain across the blood–brain barrier has necessitated such organization. While the composition of the CSF and brain interstitial fluid are generally thought to be quite similar, this may be strictly true only near the interface at the ventricular and pial surfaces, for at least two reasons: (1) diffusion is thought to greatly limit the exchange at distances greater than a few mm from these surfaces, and (2) certain components of the interstitial fluid (e.g., the extracellular matrix) are bound to cell surfaces and therefore not freely available for exchange. There is some evidence that convective transport (also referred to as bulk flow) of brain extracellular and cerebrospinal fluids can occur along certain preferential pathways within the CNS, e.g., within the perivascular spaces and possibly also along axon tracts, but interstitial fluid transport within the neuropil ECS of gray matter is likely restricted to diffusion.

Finally, it is important to appreciate the bony cranial compartment that the CNS tissue, CSF, and cerebrovasculature all occupy as it is rigid and unaccommodating of volume expansions except early in life. Given that the entire cerebrovascular system occupies about 2–5 % of the total tissue volume and the CNS extracellular space occupies about 20 % tissue volume, a normal adult human being with a brain and spinal cord weighing 1,300 g will have approximately 150 ml cerebrospinal fluid, 260 ml interstitial fluid within the extracellular space, and 30–70 ml of cerebral blood. It is therefore easy to appreciate the rising intracranial pressure that often results from a significant expansion of the CSF compartment (e.g., hydrocephalus), brain tissue compartment (e.g., a growing primary or metastatic brain tumor), or cerebral blood compartment (e.g., intracerebral or subarachnoid hemorrhage).

A.5 Conclusions

The brain is the most complex organ of the body. It directs our communication with the external world, what we do to our surroundings through our behaviors and what we perceive of our surroundings through our senses. It also monitors and controls our internal world, maintaining the delicate, exquisite balance among our internal organs that is necessary for sustained life. Any of these functions may be affected by disease or injury. It is in this context that it becomes necessary to consider how and where to deliver drugs to restore or improve the human condition. This chapter has attempted to summarize and briefly introduce the first considerations one must make in contemplating drug delivery to the brain, namely, to account for its diverse structure, function, and physiology.

Acknowledgements This work was supported by the University of Wisconsin-Madison School of Pharmacy, the Graduate School at the University of Wisconsin, the Michael J. Fox Foundation for Parkinson's Research, and the Clinical and Translational Science Award (CTSA) program, through the NIH National Center for Advancing Translational Sciences (NCATS; grant UL1TR000427). All content is solely the responsibility of the author and does not necessarily represent the official views of the NIH.

Sources/Further Reading

Abbott NJ (2004) Evidence for bulk flow of brain interstitial fluid: significance for physiology and pathology. Neurochem Int 45:545–552

Blumenfeld H (2002) Neuroanatomy through clinical cases. Sinauer, Sunderland, MA

Brozici M, van der Zwan A, Hillen B (2003) Anatomy and functionality of leptomeningeal anastomoses: a review. Stroke 34:2750–2762

Cajal SRY (1909, 1911) Histologie due système nerveux de l'homme et des vertébrés. Maloine, Paris; English translation by Swanson N, Swanson L (1995) Oxford University Press, New York

Davson H, Segal MB (1996) Physiology of the CSF and blood-brain barriers. CRC Press, Boca Raton, FL

DeArmond SJ, Fusco MM, Dewey MM (1989) Structure of the human brain: a photographic atlas. Oxford University Press, New York
Gillilan LA (1974) Potential collateral circulation to the human cerebral cortex. Neurology 24:941–948
Haines DE (2012) Neuroanatomy: an atlas of structures, sections, and systems. Wolters Kluwer/Lippincott Williams & Wilkens, Philadelphia, PA
Hammarlund-Udenaes M, Friden M, Syvanen S, Gupta A (2008) On the rate and extent of drug delivery to the brain. Pharm Res 25:1737–1750
Jones HR (ed) (2005) Netter's neurology. Icon Learning Systems, Teterboro, NJ
Kandel ER, Schwartz JH, Jessel TM, Siegelbaum SA, Hudspeth AJ (2013) Principles of neural science, 5th edn. McGraw-Hill, New York
Martin JH (1996) Neuroanatomy: text and atlas. Appleton & Lange, Stamford, CT
Nolte J (2009) The human brain: an introduction to its functional anatomy, 6th edn. Mosby Elsevier, Philadelphia, PA
Nieuwenhuys R, ten Donkelaar HJ, Nicholson C (1998) The central nervous system of vertebrates. Springer, Berlin
Nieuwenhuys R, Voogd J, van Huijzen C (2008) The human central nervous system. Springer, Berlin
Oberheim NA, Wang X, Goldman S, Nedergaard M (2006) Astrocyte complexity distinguishes the human brain. Trends Neurosci 29:547–553
Purves MJ (1972) The physiology of the cerebral circulation. Cambridge University Press, Cambridge
Rapaport SI, Ohno K, Pettigrew KD (1979) Drug entry into the brain. Brain Res 172:354–359
Schuenke M, Schulte E, Schumacher U (2010) Atlas of anatomy: head and neuroanatomy. Thieme, Stuttgart
Somjen GG (2004) Ions in the brain: normal function, seizures and stroke. Oxford University Press, New York
Swanson LW (1995) Mapping the human brain: past, present, and future. Trends Neurosci 18:471–474
Swanson LW (2012) Brain architecture: understanding the basic plan. Oxford University Press, Oxford
Sundsten JW, Mulligan KA (1998) Neuroanatomy interactive syllabus. http://www9.biostr.washington.edu/da.html. Accessed 1 Aug 2012
Strazielle N, Ghersi-Egea JF (2013) Physiology of blood-brain interfaces in relation to brain disposition of small compounds and macromolecules. Mol Pharm 10:1473–1491
Sykova E, Nicholson C (2008) Diffusion in brain extracellular space. Physiol Rev 88:1277–1340
Thorne RG, Nicholson C (2006) In vivo diffusion analysis with quantum dots and dextrans predicts the width of brain extracellular space. Proc Natl Acad Sci U S A 103:5567–5572
Turner MH, Ullmann JFP, Kay AR (2012) A method for detecting molecular transport within the cerebral ventricles of live zebrafish (*Danio rerio*) larvae. J Physiol 590(10):2233–2240
van der Zwan A, Hillen B (1991) Review of the variability of the territories of the major cerebral arteries. Stroke 22:1078–1084
van der Zwan A, Hillen B, Tulleken CAF, Dujovny M, Dragovic L (1992) Variability of the territories of the major cerebral arteries. J Neurosurg 77:927–940
Watson C, Kirkcaldie M, Paxinos G (2010) The brain: an introduction to functional neuroanatomy. Elsevier, Amsterdam
Willis T (1664) Cerebri anatome: cui accessit nervorum descripto et usus; English translation by Samuel Pordage (1681) T. Dring, C. Harper, J. Leigh and S. Martin, London
Wolak DJ, Thorne RG (2013) Diffusion of macromolecules in the brain: implications for drug delivery. Mol Pharm 10:1492–1504
Zeman W, Innes JRM (1963) Craigie's neuroanatomy of the rat. Academic Press, New York
Zilles K, Amunts K (2010) Centenary of Brodmann's map—conception and fate. Nat Rev Neurosci 11:139–145

Index

A
AAV. *See* Adeno associated virus (AAV)
ABC. *See* ATP-binding cassette (ABC) transporter
Abelcet, 435
Abraxane, 435, 439–440
Absorption, distribution, metabolism, excretion (ADME)
  properties, 341, 349
  screens, 349, 360
Adeno associated virus (AAV), 415, 487–488, 493–495, 505, 506, 511, 513, 514, 552, 562
  serotypes, 491–492
  single-stranded DNA virus, 486
Adhesion molecule expression, 581
Adsorptive-mediated transcytosis (AMT)
  cationic molecules, brain delivery, 476
  nanoparticles coated, Tat (49-57) peptides, 475–476
  PAMAM, 475
  poly-arginines, 474–475
  SynB and PTDS-based vectors, 473–474
Agonist-occupied receptor (AR)
  description, 245
  3-dimensional interrelationship, 246, 247
  intrinsic activity and affinity, 246
  mathematical representation, transduction, 245–246
  PKPD relationships, 246–248
Albumin
  brain and coronal slices, 526, 527
  CNS delivery, 528
  contrast-enhanced computerised tomography (CT) scan, 526
  coronal slice, 527
  delivery ratio, 527, 528
  description, 526
  immunohistochemistry, 526
  nanoparticles
    Abraxane, 439
    brain uptake, AZT, 440
    drug delivery system, 439
    oximes, 440
  permeabilization, 527
Alfentanil, 248–249
ALS. *See* Amyotrophic lateral sclerosis (ALS)
Alzheimer's disease, 25, 35, 41, 48, 225, 417, 456–457, 511, 549, 550, 593, 608, 610
  aging brain, 597
  Aβ accumulation, 595–596
  insulin resistance, 596
  memory loss and confusion, 595
  pathological brain aging, 596
  transcytosis, 595
Amitriptyline, 36
Amoxapine, 36
Amphotericin B, 435
AMT. *See* Adsorptive-mediated transcytosis (AMT)
Amyotrophic lateral sclerosis (ALS), 456, 492, 494, 511, 549, 591, 597
Anatomy and physiology, 404–411, 704
  astrocytes and microglial cells, 522
  of BBB, 112–113
  BCSFB, 15–16
  brain endothelial tight junction, 8–10
  brain endothelium and neurovascular unit, 6–7
  implications, drug delivery, 16

M. Hammarlund-Udenaes et al. (eds.), *Drug Delivery to the Brain*, AAPS Advances in the Pharmaceutical Sciences Series 10, DOI 10.1007/978-1-4614-9105-7,

Anatomy and physiology (*cont.*)
induction, maintenance and heterogeneity, 12–13
ISF and CSF, 13–15
nasal (*see* Nasal anatomy and physiology)
nature and organisation, membranes, 7–8
neural signaling and CNS (*see* Central nervous system (CNS))
permeation, 11
SLCs, 10–11
techniques, 17
vesicular and transcytosis, 11
Angiopep-2, 434, 439
Anterior circulation, 697, 699
Anti-angiogenic therapy, 523, 675, 676
Antiarrhythmics, 36
Antibodies, 65, 74–77, 113, 225–227, 341, 387, 419, 460–462, 467, 524, 564, 646, 674–675
Antipyrine, 200
Aprotinin, 467, 473
Arachnoid epithelial cells, 5, 10, 185–186
Aricept, 595
Astrocytes, 12, 165, 470, 647Atenolol, 318
ATP-binding cassette (ABC) transporter, 10, 26, 36, 37, 49, 111, 351, 364, 522, 574, 610, 641, 647
Atrial natriuretic peptide (ANP), 42
Avonex, 577
Azelastin, 35
Azidothymidine (AZT), 440
AZT. *See* Azidothymidine (AZT)

B

Baclofen, 238, 599
Basal lamina, 608
Basic fibroblast growth factor (bFGF), 640, 645
BBB. *See* Blood–brain barrier (BBB)
BCRP. *See* Breast-cancer resistance protein (BCRP)
BCSFB. *See* Blood–CSF barrier (BCSFB)
BDDCS. *See* Biopharmaceutics Drug Disposition Classification System (BDDCS)
BDNF. *See* Brain derived neurotropic factor (BDNF)
Benzodiazepines, 238, 247
Betaseron, 577
Bevacizumab, 402, 523
bFGF. *See* Basic fibroblast growth factor (bFGF)
Binding potential (BP), drug administration, 219
bradykinin, 664
brain distribution, 228
central histamine, 362
dose-occupancy relationship, 217
endothelial glucocorticoid, 644
endothelin, 364
gp60 and SPARC, 439
human insulin, 434
IGF-I density, 418
insulin, 670
mediated transcytosis (*see* Receptor-mediated transcytosis)
neuronal and glial plasma membrane, 200
opioid μ-receptor, 344
oxytocin, 418
pharmacodynamic models, 205
remoxipride, 416
RMT, 176
transferrin, 434, 640, 645, 670
Biologics, 50, 68, 72, 75, 226–227, 249, 255, 393, 456, 459, 467, 477, 620, 670–671
Biomarkers, PKPD modeling
animal models, 251
classification, 250–251
description, 249–250
Biopharmaceutics Drug Disposition Classification System (BDDCS), 332
Blood–brain barrier (BBB)
anatomical and functional features, 106–107
anatomy and physiology (*see* Anatomy)
applications, PPx
developmental changes, 84–85
interindividual differences, 83–84
interspecies differences, 78–83
QTAP (*see* Quantitative targeted absolute proteomics (QTAP))
BCSFB, 402
brain endothelial cells, 402
CNS (*see* Central nervous system (CNS))
drug delivery (*see* Drug delivery)
drug exposure (*see* Drug exposure)
dysfunction
ABC transporters, 538
actin, 608
active efflux transporters, 610
adverse effects, 533–534
anatomical substrate, 607
anesthesia, 532–533
animal and human clinical data, 523
basal lamina, 608

brain angiogenesis, 609
brain bioavailability, 537
brain capillaries and reductions, 611
BTB permeability, 537–538
carboplatin and etoposide, 535
CBF, 611
chemotherapy agent, 534–535
claudin-5, 608
drug administration protocols, 539
drug treatment, brain tumors (*see* Brain tumors)
facilitative and active transport systems, 610
graphical sketch, 523, 524
human vascular cerebral system, 532
immune system, 611
intra-arterial carboplatin, 534–535
ketamine, 525
malignant astrocytomas, 534
metabolic enzymes, 609
MRI quantification, 528–530
multiple brain lesions, 535, 536
murine models, 525
neuronal influence, 608–609
neurovascular unit, 607–608
occludin, 608
oncology organizations, 537
operation theater/angiography suite, 531
osmotic opening, 531
ovarian adenocarcinoma, 535, 536
pericytes, 609
perivascular astrocytes, 608
pontine gliomas, 537
preclinical quantitative studies, 526–530
propofol, 526
radiological response, 537, 539
surgical setup, 525
tight junctions, 608
treatment modality, 535
endogenous mechanisms, 457–458
engineering technologies (*see* Engineering technologies, BBB)
homeostasis, CNS, 402
invasive approaches, 458
mannitol, 487
multiple species
astrocyte transduction, 489
distribution, preclinical studies, 491
motor neuron transduction, 488
neonatal and adult mice, 490
sympathetic preganglionic cells, 488
transgene expression, 488, 489
osmotic opening (*see* Brain tumors)
penetration, 85, 133, 274, 275, 419, 456, 552
permeability, 27, 32, 34, 35, 50, 116, 180, 183, 200, 201, 204, 242, 320, 361, 417, 528–530, 579, 581, 582, 608, 611, 647
pharmacological approaches, 458
phase I DME
BMVECs, 107
CYP activity and expression, 108
MAOs, 107
peripheral, 107
phase II reactions
COMT and TPMT, 110
GSTs, 109–110
SULTs, 110
UGT activity, 109
physiological approaches, 459
PKPD, transport
brain intracellular concentrations, 240
impacts, 243–244
microdialysis techniques, 241
P-glycoprotein efflux (P-gp), 239, 240
regulation, DME, 110–111
transport, 27, 28, 30, 35, 39, 43, 51, 83, 134, 135, 207, 225–226, 241, 274, 298, 304, 355, 551, 592
transporters, 27, 28, 45, 85, 94, 107, 176, 182, 286, 304, 355, 581, 648
Blood–CSF barrier (BCSFB), 4, 112, 116–117, 131, 658
BBB (*see* Blood–brain barrier (BBB))
complexities, 50
differences from BBB, 50–51
drug distribution, brain parenchyma and CSF, 25, 26
endogenous compounds and drugs distribution, 49–50
endogenous peptides
β-amyloid, 41–42
ANP, 42
ependyma
anatomical and functional features, 112–113
brain development, 117
choroid plexuses (*see* Choroid plexus)
pharmaco-toxicological significance and regulation, 116–117
expression, 27–28
in vivo characteristics, cationic drugs, 27–29

Blood–CSF barrier (BCSFB) (*cont.*)
in vivo transport function, 50
influx and efflux (*see* Transport systems)
manipulation, 50
models, 25, 27
neurotransmitters and organic anions, 43–44
organic anion transporters, 45
peptide drugs, 42–43
pharmacokinetic analysis, 25–26
pharmacoproteomics, 50–51
physiological interfaces, 26
rat brain, 50
systemic circulation, 416
transendothelial electrical resistance, 51
transporters, 26–27
transport, PKPD, 242–243
treatment, CNS disorders, 25
Blood supply, 405, 410, 411, 697, 703
arachnoid villi, 407
cribriform plate, 407
ethmoidal arteries branch, 406
intranasal administration, 406
localization, microfil, 407
nasal mucosa, 405–406
venous drainage, 406
Blood–tumor barrier (BTB), 521, 522, 524, 537, 540, 658, 659, 664, 669
B/P, brain-to-total plasma concentration ratio, 133
Bradykinin, 664
Brain
BBB (*see* Blood–brain barrier (BBB))
delivery, therapeutic compounds (*see* Delivery)
drug delivery (*see* Brain drug delivery)
IN drug delivery
CNS delivery, intranasal administration, 422–423
nasal epithelial barrier, 423
pathways and mechanisms, 423, 424
drug exposure (*see* Drug exposure)
endothelial cells
Bovine models, 175–176
human models, 176–177
Porcine models, 176
rat and mouse models, 174–175
microdialysis (*see* Microdialysis)
parenchyma, 506–507
pathology, 511
PET, drug delivery (*see* Positron emission tomography (PET))
tumors (*see* Brain tumors)
vascular correction, 206
Brain derived neurotropic factor (BDNF), 562, 564–566, 598, 606, 640
Brain distribution, 36–38, 44, 48, 49, 85, 92, 93, 143–146, 207, 222–223, 241, 592, 612, 614
calculation, 202
description, 201
drug discovery (*see* Drug discovery)
equilibrium, 202
influx, BBB PS, 201
parameters, 201
PET
CNS active drugs, 222
description, 222
microdosing, 222
P-gp substrate, 223
radioactivity, 222
radiotracer, 222
serum/plasma, 202
at steady and non-steady state, 202
Brain drug delivery, 562, 566, 582, 583
active efflux, 148–149
albumin nanoparticles, 439–440
antineoplastic agents, 523
BBB and BCSFB (*see* Blood-brain barrier (BBB) and CSF barrier (BCSFB))
BCSFB, 131
bioavailability, 138brain penetration, 135
chemotherapy, 534
concentration-time profile, 148
cooperation, P-gp and BCRP, 149
delivery technique, CED (see Convection-enhanced delivery (CED))
drug discovery (*see* Drug discovery)
FUS-facilitated BBB opening, 552
health and disease, 186
ICF, 131
IN (*see* Intranasal (IN) drug delivery)
IN administration (*see* Intranasal (IN) drug delivery)
$K_{p,uu,brain}$ value, 138
liposomes, 438–439
measurements, steady-state, 138
methods and relationships
$AUC_{u,brainISF}$, 139–140
CL_{in} and CL_{out}, 140–141
homogenate measurements, 139
$K_{p,uu,brain}$ values, 143
microdialysis, 139
rate and extent of equilibration, 142
steady-state drug concentrations, 138–139
micellar formulations and nanoemulsions, 442

neurodegenerative disease
drug delivery system, 550
trans-BBB transport/disruption, 550, 551
pharmacological agents, 550
treatment, 549
neurotoxicity, 526PAMAM approach, 441
permeability, 521
PET (*see* Positron emission tomography (PET))
pharmacokinetics (*see* Pharmacokinetics, brain drug delivery)
PKPD (*see* Pharmacokinetics-pharmacodynamics (PKPD))
polymeric nanoparticles, 440–441
QTAP-based reconstruction
in vitro data, 91
mdr1a efflux activity ($K_{p,brain}$ ratio), 91–93
pharmacological actions and toxic effects, CNS, 90
unbound concentration, 91
relationship, 154
SLNs, 441
species (*see* Species differences, drug transport)
strategies, 402, 434, 503, 550, 583
stroke and TBI (*see* Stroke)
theoretical effects, P-gp, 149
therapeutic compounds
AMT, 473–476
BBB, 457–460
biopharmaceutical agents, 477
brain parenchyma, 477, 478
brain technology, 456–457
lysosomal enzymes and antibodies, 477
physiological approaches, 459
receptor-mediated transcytosis, 460–473
small molecules, 455
transporter mediated, 459–460
topographic extent, 526
trade-off, 138
transport, 134
treatment, brain tumors (*see* Brain tumors)
unbound drug concentrations, 131, 148, 149
vincristine penetration, 521
$V_{u,brain}$ and $K_{p,uu,brain}$ values, 147, 148
Brain exposure assessment, 303–304
Brain homogenate method, 93, 132–134, 139, 143–145, 276–282, 289, 290, 293, 294, 343, 351, 445
bioanalysis, 280–281
ED techniques, 276
equilibration process, 280
evaluation, plasma protein binding, 276
neurotherapeutics, 276
preparation, 279
principles, 277–278
selection, dialysis membrane, 278–279
tissue binding, 276
unbound drug concentration, 276
Brain microdialysis, 144, 205–206, 344, 445, 603–604, 615
Brain microvessel endothelial cells (BMVECs), 107
Brain penetration, 39, 79, 132, 135, 149, 223, 298, 332, 340, 342, 352, 358–361, 368, 380, 537, 644
avoidance, strategies, 362–363
multiparameter optimisation (MPO) strategy, 361
PK properties, 360–361
$K_{p,uu,brain}$, 359
Brain/plasma ratio ($K_{p,brain}$), 86, 91, 133, 205, 343–345, 360, 364
drug–drug interactions (DDIs), 365
ISF, 360
$K_{p,uu,brain}$, 352–353
morphine-6-glucuronide, 344
P-gp substrates and non-substrates, 345
Brain slice method, $V_{u,brain}$
advantages, 281
bioanalysis, 286
establishment, 282–283
extracellular fluid and cassettes formation, 284
implementation, 282
measures, 281, 282
preparation and incubation, 284–286
principles, 283
unbound drug distribution, 281
Brain target exposure, 340, 359, 368
Brain target site drug delivery
CNS drug effects, 611
drug treatment, 611
pharmacological studies, 612
PKPD, 614–619
unbound plasma and brain pharmacokinetics, 612–615
Brain tissue binding assays
estimation, cerebral concentrations, 301
evolution, 301–302
relationship, rat and mouse brain slices, 303

Brain-to-blood efflux transport systems
ABC transporters, 36–37
BCRP functions, 37–39
CNS-active drugs, 37
drug distribution, 36, 37
Mrp4
azidothymidine, 39
β-lactam antibiotics, 41
localization, 39
organic anion transporter 3 (Oat3/Slc22a8), 39–40
oseltamivir, 39
prostaglandin E_2 (PGE_2) action, 40
MRP4 substrates, 37
PET-imaging, 37
P-gp, 37–38
Brain-to-blood influx transport systems
Cnt1/Slc28a1, 33
Crt/Slc6a8, 33
drug delivery, 29
nutrients
GLUT1/SLC2A1, 32
Lat1/Slc7a5, 29–32
Mct1/Slc16a1, 33
organic cations, 34–36
Brain-to-plasma concentration ratio ($K_{p,brain}$), 86, 91, 133, 205, 343–345, 360, 364
calculation, 88
CNS and non-CNS drugs, 93
definition, 91
description, 86
human, 93
in vitro transport experiments, 93
mdr1a function, 87–90
observation and reconstruction, 92, 93
predictions, 93
unbound fractions, 91
Brain tumors
anti-VEGF therapy, 675–676
bypassing, BBB, 523, 524
DNA alkylating agents, 658
drug penetration, 520
drug transport (*see* Drug transport)
local drug delivery
CED, 673–674
clinical impact, 671, 672
implanted polymers, 673
intracavitary delivery, 674–675
MRI, glioblastoma, 659–660
neoplasia (*see* Neoplasia, brain)
osmotic BBB disruption (*see* Blood–brain barrier (BBB))
P-gp, 520
requirements, drug therapy, 660–661
transvascular extravasation, contrast agent, 658–659
treatment, 520–521
Brain uptake index (BUI), 28, 29, 183
Breast-cancer resistance protein (BCRP), 8–11, 36–41, 49, 79, 149, 152, 185, 304, 355, 362, 366, 601
Bremazocine, 43
Bromocriptine, 601
BTB. *See* Blood–tumor barrier (BTB)
BUI. *See* Brain uptake index (BUI)
Bupropion, 301, 302

C
Caelyx, 435, 439, 448
Caffeine, 200, 638
Candidate evaluation/selection, 214, 215, 229, 274, 286, 304
Carbamazepine, 282, 604
Carboplatin, 535, 537, 539, 664
Catechol-O-methyl transferase (COMT), 110
CBF. *See* Cerebral blood flow (CBF)
CED. *See* Convection-enhanced delivery (CED)
Cefazolin, 40
Cefmetazole, 40
Cefotaxime, 40
Ceftriaxone, 40
Cell-based therapies, stroke and TBI, 648
Central nervous system (CNS)
antipsychotic and anti-depressive drugs, 214
barriers
BCSFB, 164
enzymes, transcytosis and immune responses, 172–173
microfluidics, 186–187
model development, standardization, refinement and innovation, 165–167
physiology and pathology, 164
tight junctions and physical barrier (*see* Tight junctions (TJ))
transcriptomics, proteomics and PKPD modelling, 187
BBB system, 200
behavioral effects, 447
brain lobes, 689
brains weight, 686
Brodmann's classification system, 692–694
cerebral hemisphere, 689, 690
challenges, 380–381
characteristics, 324, 325
classification, 320–321, 330–332

clinical development, phases, 379
commercial potential, 388–392
cranial nerves, 691, 692
IN delivery (*see* Intranasal delivery)
description, 392–393, 415–416
directional terms and planes, 687–688
disease models, 416
disorders
Alzheimer's disease, 575–576
epilepsy, 576
MS, 577–578
PD, 575
stroke, 576–577
distribution, 11, 17, 133, 345, 364, 368, 415, 418, 511, 512
drug candidate, 226
drug discovery (*see* Drug discovery)
drugs, 5, 11, 16, 37, 64, 79, 95, 134, 166, 200, 235, 240, 256, 257, 273, 320, 340, 364, 366–368
drug partitioning, 379–380
drug/reagent costs, 386–388
frontal lobe, 694
functional subdivisions, 690–691
funding, 377–378
gene therapy (*see* Gene therapy)
hypothalamus and thalamus, 692
indications, 435
motor (ventral) and sensory (dorsal) roots, 691
neoplasm treatment, 523
neural signalling and barrier layers
chemical and electrical, 4
location, barrier sites, 4–5
microenvironment, 4
molecular flux control, 3, 4
neuronal signaling, 200
neurons and glia, 686
occipital lobe, 696
parenchymal tissue, 203–204
parietal lobe, 694–695
penetration
avoiding, 362
improvement, 135, 300, 368, 450
methods, 132–133, 179, 298, 487, 488, 495, 665
preclinical studies, 415
pricing (*see* Drug pricing)
rodent model, clinical validation, 376, 377
safety and efficacy, 376–377
stage gates and costs, 378
spinal cord and brain, embryological development, 686–687
telencephalon and diencephalon, forebrain, 688–689
temporal lobe, 695
therapeutic compounds (*see* Delivery)
transport and availability, drug, 200
vasculature, 521
Cerebral arteries, 406, 532, 637, 638, 642, 698–702
Cerebral blood flow (CBF), 611
Cerebral edema, 532, 608, 644, 649, 664, 675
Cerebral hemorrhage, 646
Cerebral ischemia, 534, 636–639, 641, 642, 644, 646, 649
Cerebrospinal fluid (CSF), 112–117, 242, 243, 511–513
IN administration, 423
BCSFB (*see* Blood–CSF barrier (BCSFB))
brain ISF, 208
brain pathology, 511
cisterna magna, rat and mouse, 354
delivery, AAV9 vector, 513–514
3-D reconstruction, thalamic CED/RCD, 512
drug concentration, 445–446
drug ISF concentrations, 354–355
intracerebroventricular (ICV) delivery, 512
intraventricular catheters, 650
ISF, 13–15
levels, 47, 343, 344, 354–355, 362, 417
LSD models, 512
lumbar space, 208
mucopolysaccharidosis (MPS), 512
nanocarriers, 446
nasal lamina propria, 407
perivascular spaces, 520
P-gp/BCRP substrates, 355
protein content, 208
small molecules, 416
subarachnoid space, 413
thrombolytics, 650
transport, BCSFB (*see* Blood–CSF barrier (BCSFB))
unilateral ICV administration, 512, 513
ventricular system
arachnoid projections, 703, 704
buoyancy force, 702
extracellular spaces (ECS), 705–706
physiological parameters, 705
thalamus and hypothalamus, 703, 704
Cerebrovasculature
anterior and posterior circulations, 699
arterial supply, 702, 703
capillary abundance, 697

Cerebrovasculature (*cont.*)
carotid and vertebral arteries, blood supply, 697–698
cerebral arteries, 699–700
cerebral veins, 702
glucose and oxygen delivery, 697
neurons, 697
watershed/borderzone regions, 700, 701
Chemotherapy, 44, 447, 457, 520, 523, 524, 530, 533–539, 663–665, 675
Chitosan, 423
Choroid plexus, 4, 10, 11, 14, 17, 25, 45, 47–50, 105, 112–118, 151, 170, 184–185, 638, 703
antioxidant systems, 115–116
detoxification reactions, 113
functions, 112
location, 112
phase I metabolism
alcohol dehydrogenase, 114
CYP-dependent monooxygenase activities, 113–114
EH activity, 114
phase II metabolism
choroidal activity, UGT1A isoenzymes, 114
detoxification, SULT1A1, 115
immunoreactivity, GSTs, 115
phase III metabolism, 115
rat, 113
Choroid plexus epithelial (CPE) cells, 184–185
Ciprofloxin, 475
Circle of Willis, 699, 700
Cisplatin, 526, 663
Citalopram, 282
Clinical development, 357, 378, 379, 384–385, 387, 391, 393, 436, 448, 449, 469
drug delivery, neurodegenerative disease, 549–551
FUS-facilitated BBB opening, 552
neurodegenerative disease, 549
Clinical trials, 64, 301, 366–368, 377, 380, 385, 390, 418, 419, 435, 469, 477, 495, 507–510, 638, 644, 650, 658, 671, 673, 675
Clomipramine, 36
Clonazepam, 599
Clonidine, 28, 36
CNS. *See* Central nervous system (CNS)
Commercial potential, BBB delivery
CNS gene therapy, 392
intranasal delivery, 388–389
nanocarriers, 389–390
neurosurgical direct delivery approaches, 391–392
receptor-mediated approaches
transient disruption, 392
COMT. *See* Catechol-O-methyl transferase (COMT)
Convection-enhanced delivery (CED), 458, 502–511, 515, 524, 671, 673–674
biophysical properties, 503
brain parenchyma, 506–507
brain's perivascular spaces, 503
cannula placement guidelines, 507–508
CNS delivery technique, 503
fluid pressure gradient, 503
infusion catheter design, 506
infusion setup, 503, 504
MRI-guided placement, cannula, 508–510
real-time convective delivery, 503–505
simulation algorithm, RCD, 510–511
Convection enhanced drug delivery. *See* Convection-enhanced delivery (CED)
Copaxone, 577, 599
Cost of goods, 383, 384, 386–389, 391, 393, 437
CPE. *See* Choroid plexus epithelial (CPE) cells
Cranial nerves, 13, 403, 411, 691, 692
Cremophor, 439
CSF. *See* Cerebrospinal fluid (CSF)
CSF *vs.* brain ISF pharmacokinetics
correlation, human and rat, 151
drug selection, 150
$K_{p,uu,brain}$ and $K_{p,uu,CSF}$, rat, 150–151
location and expression, P-gp, 151
timing, dosage and sampling site, 151–152
unbound brain concentrations, 149–150
$C_{u,brain}$, 86, 91, 127, 140, 276, 282, 289, 304, 356, 358, 359, 362
Cyclophosphamide, 535
Cyclosporine, 152, 364, 665
Cyproheptadine, 35
Cytosolic-to-interstitial fluid unbound drug concentration ratio, 292

D

Dalargin, 473
Dalfampridine, 599
Dantrolene, 599
Dasatinib, 38
Daunorubicin, 435
Daunoxome, 435

DDI. *See* Drug-drug interactions (DDI)
Deferoxamine, 417
Definity®, 548, 553, 554
Delivery. *See* Brain drug delivery
Deltorphin II, 43
DepoCyt®, 435
Developmental change, 84–85
Dexamethasone, 87, 92, 104, 644
Dextran, 552, 556
Diaminobenzidine, 420–421
Diazepam, 87, 92, 147, 200, 599
Diclofenac, 47
Digoxin, 87, 92
Diphenhydramine, 35
Dizocilpine, 603
DMEs. *See* Drug metabolising enzymes (DMEs)
Donepezil, 29, 35, 575, 595
L-Dopa, 30, 31, 366, 460, 575, 600, 601, 609, 617–619, 648
Dopamine-D2 receptor inhibition, PKPD
  human brain, 252
  intravenous administration, rats development, 252–254
  prediction, human, 255–256
Doxil, 435, 439, 448
Doxorubicin, 391, 434, 435, 437, 439, 444, 449, 460, 464, 468, 471–473, 475, 552
Drug delivery. *See* Brain drug delivery
  treatment, brain tumors (*see* Brain tumors)
  vincristine penetration, 521
Drug discovery, 51, 65, 79, 93, 129, 138, 147, 150, 157, 200, 321, 658
  approaches, 276
  BBB and BCSFB (*see* Blood–CSF barrier (BCSFB))
  BDDCS class 1 drugs, 340, 345
  Big Pharma companies, 366
  brain homogenate (*see* Brain homogenate method)
  brain penetration (*see* Brain penetration)
  CNS drug delivery, 273–274
  complications, CNS drugs, 305
  correlations, brain levels, potency and efficacy, 343
  CSF levels, 354–355
  development and programs, 273, 274
  drug–transporter interactions, 363–366
  efflux and influx transporters, 305
  extent of BBB transport, 274–275
  fraction unbound, brain tissue, 351–352
  "free drug hypothesis", 344
  function and diseases, 340
  in vitro and *in vivo* testing, 341, 342
  ISF levels and microdialysis, 344
  $K_{p,brain}$, $K_{p,uu,brain}$ and $C_{u,brain}$, 352–354
  $K_{p,uu,brain}$ estimation (*see* $K_{p,uu,brain}$)
  "lipid escalator", 345
  MDCK-MDR1 cells, 341
    mode of action and efficacy, 340–341
    morphine-6-glucuronide, 344
  non-CNS projects (*see* Non-CNS projects)
  optimisation, 346–347
  permeability and susceptibility, drug efflux, 350–351
  permeability and transport rate, BBB, 274
  PKPD modeling, 305
  PET imaging, 368
  P-gp efflux pump, 343
  P-gp substrates and non-substrates, 345
  PKPD (*see* Pharmacokinetics-pharmacodynamics (PKPD))
  psychiatric disorders, 340
  reasons for failure, 340
  selection and optimization, compounds, 305
  slice method (*see* Brain slice method)
  translation, NCEs
    brain exposure assessment, 303–304
    brain tissue binding assays, 301–303
  unbound brain concentration, 344–345, 367
  unbound drug distribution, 275
Drug exposure, 200, 201, 676
  characteristics, CNS drugs, 324, 325
  classification approaches, 320–321
  CNS^+/CNS^- classification, 330–332
  compound selection, 321
  description, 334–335
  drug design strategies, 333–334
  experimental data, molecular descriptors, 322–323
  hydrogen bonding, 324
  hydrophilic beta-blocker atenolol, 318
  in silico modellers, 324–325
  $K_{p,uu,brain}$ (*see* $K_{p,uu,brain}$)
  logBB, 319–320
  molecular descriptors, 321–322
  octanol–water partitioning coefficient (LogP), 324
  permeability surface area product (PS), 320
  validation, 323

Drug infusion
CED, 503–511
CSF, 511–514
direct brain administration, therapeutics, 502
intravenous/intra-arterial approaches, 502
PD, 501
Drug interactions, 41, 152, 221, 292, 300, 341, 363
Drug metabolising enzymes (DMEs), 364
Drug metabolism, 73, 186, 349, 359, 360, 363, 364
BBB (*see* Blood–brain barrier (BBB))
BCSFB and ependyma (*see* Blood–CSF barrier (BCSFB))
cerebral
assessment, 117–118
brain, 104, 106
cell types and sites, parenchyma, 102, 105
multiphase process, 102
neurotoxicity, 117
pathways, 102, 103
xenobiotics, 101–102, 104
choroidal DME isoforms, 118
detoxification processes, 118
enzyme activities, 104, 117, 118
Drug pricing
clinical development, 384–385
clinical efficacy, 385–386
commercial potential, 382–384
companies and investors, 381
complexity, 388
dose amount and frequency, 386–387
manufacturing costs and economy of scale, 387
patients and society benefit, 381
preclinical safety, 385
safety and efficacy, 382
untreated illness, 382
Drugs
IN (*see* Intranasal (IN) drug delivery)
ABC transporters, 538
BBB kinetic analyses and microdialysis, 205–206
bio-distribution, 214
brain distribution (*see* Brain distribution)
CNS penetrability, 172
in vitro models, BBB (*see In vitro* models)
infusion (*see* Drug infusion)
macromolecular, 227
nanocarriers (*see* Nanocarriers)
NCEs, 164
neuro-oncology, 539
pharmacological agent, 168
steady-state approaches, 221
transport and availability, 200
tyrosine kinase inhibitors, 366
Drug targeting, 27, 50, 214, 215, 217, 223–224, 306, 340, 343, 346, 347, 367, 461, 539, 580, 582
Drug-target interactions
dose-receptor occupancy, 224
imaging tools, 223
PET radiotracers and probes, 223
receptor occupancy, 223
single-dose PET occupancy, 224
time and money, 224
Drug transport
active efflux transporters, 665, 668
biochemical disruption, 664
chemical modifications, 662
chemotherapeutic agents, 661
clinical impacts, 668, 669
CNS lymphoma, 668
high-dose chemotherapy (HD-CTx), 665, 666, 668
nanocarriers
“drug trafficking”, 669
exosomes, 670–671
nanoparticles, 669–670
requirements, 670
osmotic disruption, 663–664, 667
PKPD relationship
BBB (*see* Blood–brain barrier (BBB))
BCSFB, 242–243
doses, 238, 240
impacts, 243–244
intracerebral distribution (*see* Intracerebral distribution, PKPD)
multiple active transport mechanisms, 238, 239
pathologic conditions, 243
target interaction and signal transduction, 238, 239
plasma concentration, 662–663
ultrasound mediated disruption, 664–665, 667
Drug-transporter interactions (DTI), 15, 50, 80, 82, 115, 185, 332
DMEs and P-gp, 364
evaluation, 365
ITC White Paper on transporters, 365
liver and kidneys, 364–365
L-system amino acid, 366
NCE and co-medication, 363

E
ECF. *See* Extracellular fluid (ECF)
Efflux, 79, 82, 84, 85, 89, 93, 110, 117, 576
  clearance, 31, 134, 135, 140, 142, 147, 148
    Lat1/Slc7a5, 31
    PGE_2, 31
  in situ brain perfusion (*see In situ* brain perfusion)
  transporter (*see* Brain-to-blood efflux transport systems)
Elacridar, 665
EMA. *See* European Medicine Agency (EMA)
Emedastine, 35
Endocytosis, 640
Endogenous substrate, 29–32, 51, 110
Endothelial cells, BBB
  in vitro BBB models (*see In vitro* BBB models)
  ligands
    delivery vectors, 472–473
    receptors, 471
  LRP, 463–471
  sdAb, 471–472
Enfuvirtide, 388
Engineering technologies, BBB
  acoustic parameter dependence, 555–556
  brain drug delivery, 566
  clinical relevance, 549–552
  drug delivery, 552
  emission signal acquisition and analysis, 555
  FUS and microbubbles, 553–554
  large animals, 562
  microbubbles, contrast ultrasound and bioeffects, 548–549
  molecular delivery study, 556–558
  MRI, 554
  neuronal pathways, 566
  neurotrophic delivery, FUS-induced opening, 562, 564–565
  nonhuman primates and humans, 566
  opening, FUS and microbubbles, 547–548
  physiology, 546
  properties, 560–562
  safety and reversibility, 559–560
Enzyme replacement therapy (ERT), 466
Enzymes, 4, 9, 11–13, 15, 73, 76, 94, 102, 103, 106, 117, 168, 185, 287, 290, 359, 363, 434, 458, 462, 466–467, 511, 512, 574, 593, 595, 601, 604, 609, 642
Epilepsy, 11, 15, 25, 110, 177, 244, 361, 549–550, 575, 576, 606, 610, 612, 614
Equilibrium dialysis, 93, 135, 147, 205, 275, 276, 281
Erlotinib, 39, 79
ERT. *See* Enzyme replacement therapy (ERT)
Ethanol, 200
Etoposide, 468, 535
European Medicine Agency (EMA)
  drug formulation, 435
  FDA, 437
Evans Blue, 552
Exelon, 595
Exosome nanovesicles, 670–671
Exposure screen, 349
Expression drug metabolizing enzymes, 73, 107, 117, 118, 360
Extavia, 577
Extent of
  BBB transport, 240, 241, 244, 274, 354
  brain drug delivery, 550, 551, 562, 566, 582
  brain penetration, 132–133, 352, 367
Extracellular fluid (ECF)
  AUC ratios, 417
  brain, 240
  ISF (*see* Interstitial fluid (ISF))
  plasma area, 416–417
Extracellular space, 112, 287, 529, 646, 647, 649, 660–663, 705, 706

F
Felbamate, 604
Fentanyl, 29, 43, 248–249
Fibrates, 104
Flavopiridol, 39
Flecainine, 36
Fluoroquinolone, 241
Fluvoxamine, 36
Focused ultrasound (FUS), 392, 547–554, 556, 557, 559, 562–564, 566, 567
  microbubbles, 547–548
  neurotrophic delivery, FUS–induced opening, 562, 564–564
  therapeutic delivery, 562, 564–565
Fraction of unbound drug, 91–93, 225, 325, 344–345, 351–352
  in brain homogenat ($f_{u,brain}$), 93, 132, 133, 135, 139, 144, 275–281, 289, 293, 294, 301, 351, 352, 354
  in plasma ($f_{u,plasma}$), 86, 91, 93, 133, 135, 139, 143, 149, 206, 275, 280, 295, 298, 352, 359–360
Free drug hypothesis, 298, 320, 344
Frontal lobe, 406, 694

$f_{u,brain}$. *See* Fraction of unbound drug
Funding, 376–379, 384–385, 392
$f_{u,plasma}$. *See* Fraction of unbound drug
FUS. *See* Focused ultrasound (FUS)
Fuzeon, 388

G
Gabapentin, 30, 144, 243, 244, 295–297
Gadomer diffusion process, 529
Galantamine, 35, 595
Ganciclovir, 282
Gd-DTPA. *See* Graphic depicting the Magnevist (Gd-DTPA)
GDNF. *See* Glial cell line-derived neurotrophic factor (GDNF)
Gefitinib, 38, 79
Gene delivery, 469, 485–486, 491, 493–496
Gene therapy, 392, 402, 439, 485–496, 502, 505, 506, 508, 511, 513
  AAV9-hNAGLU, 493–494
  AAV serotypes, 487–488
  BBB, 487–491
  focal neurologic diseases, 486
  gene expression, 485
  mouse disease models, 496
  scAAV9-SMN, 493
  self-complementary AAV vectors, 486–487
  systemic intravascular delivery, 487
  system-wide diseases, 486
  transient disruption, blood-brain barrier, 487
  translational research, 495
  vector system, 495
  viruses and techniques, 491–492
Gene vectors, 404, 416, 421–422, 456
GFAP. *See* Glial fibrillary-associated protein (GFAP)
Gilenya, 577
Glial cell line-derived neurotrophic factor (GDNF), 512
Glial fibrillary-associated protein (GFAP), 467
Glioblastoma, 79, 402, 438, 463, 467, 469, 502, 535, 537, 659–661
Glioma, 79, 108, 422, 435, 477, 511, 521–522, 537, 539–540, 663, 665, 675, 676
  BBB permeability, 521
  BTB and CNS, 521–522
  drug delivery, 521
  fluorescein micro-angiograms, 522
  glial tumor, 521
Glucocorticoids, 644
Glutathione-S-transferases (GSTs), 103, 109–110
GSTs. *See* Glutathione-S-transferases (GSTs)

H
Herceptin, 552
hPSCs. *See* Human pluripotent stem cells (hPSCs)
Human
  brain concentrations, 223
  CNS (*see* Central nervous system (CNS))
  CSF, 650
  disease, 380
  drug candidates, 222
  drug concentrations, 320
  drug delivery systems, 441
  fluorescein micro-angiograms, 522
  in vivo imaging, 205
  immunodeficiency virus, 388
  intranasal administration, 649
  manufacturing and safety data, 378
  models, 176–177
  nasal cavity, 405
  oxytocin, 418
  PET scanner, 214
  PKPD (*see* Pharmacokinetic-pharmacodynamic (PKPD) modeling)
  pluripotent stem cells, 647
  positron emission tomography (PET), 331
  rats, 406
  rodent models, 209
  standard therapy-failure, 435
  vascular cerebral system, 532
Human pluripotent stem cells (hPSCs), 186
Huntington's disease (HD), 550, 591, 594, 597–598, 610, 692
Hypothermia, 645, 650

I
ICH. *See* Intracerebral hemorrhage (ICH)
Imaging
  brain tissue, 446
  cellular/organ physiology, 225
  drug infusion, 503–505
  in vivo, 205
  live cell, 186
  PET (*see* Positron emission tomography (PET))
  tracers, 166
Imagent, 548
Imatinib, 38, 79
Imipramine, 36
Implanted polymers, 673
Indinavir, 87, 92
Indomethacin, 47
IN drug delivery. *See* Intranasal (IN) drug delivery

Intranasal (IN) drug delivery
cell-based therapies to CNS, 422
gene vectors and oligonucleotides to CNS, 421–422
peptides/proteins to CNS, 417–421
small molecules, 416–417
Inflammatory disorders
ABC-transporter function, 574
BBB
ABC transporters, 581–582
adhesion molecule expression, 581
adsorptive-mediated endocytosis, 580
paracellular transport, 579
receptor-mediated endocytosis, 580
CNS disorders, 574–578
drug delivery strategies, 583
neuro-inflammatory conditions, 582
transport and receptor systems, 582
Influx clearance, 31, 131, 135, 138, 154, 218
Influx transporter, 29, 43, 50, 242, 304, 305, 647
Cat1/Slc7a2, 33
concentrative nucleoside transporter (Cnt1/Slc28a1), 33
Crt/Slc6a8, 33
drug delivery, 29
GLUT1/SLC2A1, 32
guanidinoacetate, 33
Lat1/Slc7a5, 29–32
Mct1/Slc16a1, 33
organic cations (see Organic cations)
In silico, 68–70, 75, 136, 181, 200, 295, 310, 321, 324, 326, 330, 332–334, 341, 347, 348, 361
In situ and *in vivo* animal models
BBB system, 200
brain drug distribution experiments (*see* Brain distribution)
brain perfusion and efflux index, 207–208
brain uptake and BBB PS, 206–207
brain vascular correction, 207
CSF, 208
drug transport, 200
free *vs.* total drug, 205–206
lipophilic solutes, 200
systemic administration method
brain tumor uptake, 203, 204
“gold standard” approach, 202
intravenous diagram, 203
primates/humans, 205
time course, drug concentration, 203, 204
vascular endothelium, 200
In situ brain perfusion, 132, 135–138, 141, 183, 184, 207–208, 445, 697
blood flow and drug concentration, 207
brain-to-plasma efflux, 207
in vivo analysis, 207
setup, 207, 208
transient nature, 207–208
Insulin receptor (IR), 461
Intellectual property, 381
Intercellular adhesion molecule 1 (ICAM-1), 605
Inter-individual difference, protein expression levels, 80–81, 83–84, 94
Interspecies differences, 65, 78–83, 247, 303
ASCT1 and ASCT2, 83
BCRP protein expression, 79
CNS, 82
drug development, humans and experimental animals, 78
EAATs, 83
endogenous compounds, 82
L-glutamic acid (L-Glu) and L-aspartic acid (L-Asp), 82–83
MDR1 expression, 79
MRP4 and OAT3, 79, 82
neurological abnormalities, 82
OATP, 82
protein expression levels, transporters and receptors, 79–81
Interstitial fluid (ISF)
CSF, 13–15, 200
diffusion rate, 352, 353
nonsteady-state conditions, 208
pharmacodynamic studies, 205
therapeutic concentrations, 200
Intra-brain distribution, 131, 132, 234, 235, 256–257, 351, 592, 604, 611, 619
brain homogenate, 144–145
brain slice, 145
interpretations and caveats, 145–146
measurement, 143
microdialysis, 143, 144
patterns, 143–146
Intracavitary drug delivery, 671, 674–675
Intracellular brain concentration, 612
Intracellular drug distribution
brain slice and homogenate data, 146–147
concentrations, 146
estimation, extent of cellular barrier transport, 288–290
intracerebral distribution, NCEs, 286–287
ligand-target interactions, 288
lipoproteins and phospholipids, 288

Intracellular drug distribution (*cont.*)
lysosomal trapping (*see* Lysosomotropism/lysosomal trapping)
neurocompartments, BBB transport, 286, 287
partition, nonspecific plasma membrane, 288
patterns, intracerebral unbound drug concentration ratio, 297
gabapentin, 295, 297
lysosomal trapping, 295
NCEs and side effects, 297
physicochemical properties, 295, 296
salicylic acid, 295
thioridazine, 295
Intracerebral distribution, PKPD, 241–242
Intracerebral hemorrhage (ICH), 637, 638, 643, 645
Intranasal (IN) drug delivery, 388–389
BBB and BCSFB, 402
to brain (*see* Brain)
calcitonin, 403
cell-based therapies to CNS, 422
chronic administration, 402
clinical application, 403
CNS targeting (*see* Central nervous system (CNS))
delivery technique, CED (*see* Convection-enhanced delivery (CED))
epithelial transporter, 403
gene vectors and oligonucleotides to CNS, 421–422
lipophilic molecules, 402
nasal anatomy and physiology, 404
nasal passages (*see* Nasal passages)
olfactory and trigeminal pathways, 402, 403
peptides/proteins to CNS, 417–421
small molecules, 416–417
TJ protein complexes, 402
Inverted terminal repeat (ITR) sequences, 486
Investment, 376–379, 381–387, 390, 391, 393
In vitro BBB models
drug permeability assay, 181–182
endothelial cell-astrocyte co-culture models, 164, 165
epithelial CNS barriers
arachnoid epithelial cells, 185–186
CPE cells, 184–185
hPSCs (*see* Human pluripotent stem cells (hPSCs))
immortalized brain endothelial cell lines
applications, 179–180
bovine and porcine cell lines, 177
human cell lines, 179
rat and mouse cell lines, 178–179
isolated brain capillaries, 173–174
isolated brain microvessels, 164
IVIVC (*see In vitro-in vivo* correlations (IVIVC))
primary and low passage brain endothelial cells, 174–177
protocols, 165
selection, 183–184
tri-culture, dynamic flow and 3-D models, 180–181
In vitro-in vivo correlations (IVIVC)
BUI/permeability data, 184
water layer, paracellular permeability and intrinsic permeability calculation, 184
ISF. *See* Interstitial fluid (ISF)
IVIVC. *See In vitro-in vivo* correlations (IVIVC)

K
Ketamine, 36
Ketoprofen, 30, 31, 40
Ketotifen, 35
$K_{p,brain}$
BBB PS, 203
brain distribution volume/partition coefficient, 201
equilibrium drug distribution, 202
$K_{p,uu,brain}$, distribution, 225, 326, 327
linear correlation coefficient, 326, 328
logBB, 132, 138, 274, 298, 319–320, 324–334, 336
measurement, 202
microdialysis, 320
PET nomenclature, 218
steady-state concentrations, 220
$K_{p,free}$, 133, 298
$K_{p,uu,brain}$, 349, 352–355, 357–363, 367
acidic drugs, 330
assessment, 299–300
atenolol *vs.* propranolol, 328
benefits, 301
CNS drug discovery screening programs, 297
compartments and relevant concentration relationships, 301, 302
complexity, 301
distribution, 326, 327
“free-drug hypothesis”, 298
hydrogen bonding, 329

identification and selection, drug candidates, 298
interactions, molecular modelling, 333
Kappa2 values, 327, 330
$K_{p,brain}$, 330, 331
linear correlation coefficient, molecular descriptors, 326, 328
microdialysis, 298
molecular properties, 334, 335observed *vs.* predicted rat, HBA, 326, 329
pH partitioning, 298–299
plasma protein binding, 300–301, 328–329
single-dose approach, industrial setting, 300
steady-state conditions, 297

L
Lamotrigine, 604, 612
Lapatinib, 38Lat1/Slc7a5
brain perfusion technique, rat, 30
effux transport and clearance, 31
features, 3D pharmacophore, 31
heterodimer forms, 29, 30
human and nonprimate BBB, 31–32
L-DOPA, 31
localization, 29–30
permeability, 30
pro-drug approach, 30–31
saturation, endogenous amino acids, 31
structures, 30
thyroid hormones, 30
LBD. *See* Ligand binding domains (LBD)
LC-MS/MS. *See* Liquid chromatography–tandem mass spectrometry (LC-MS/MS)
Levetiracetam, 604
Levitiracetam, 613
Lidocaine, 36, 417
Ligand binding domains (LBD), 463
Ligands, 9, 31, 38, 42, 65, 85–86, 111, 117, 223, 288, 390, 434, 437, 439–441, 446, 447, 450, 459, 460, 463–473, 477, 581, 583, 594, 597, 674
Liposomes, 390–391, 415, 435–439, 442, 443, 445, 446, 448, 460, 461, 463, 472, 503, 506, 669
blood–brain barrier, 438
choice, lipids, 438
description, 438
DNA/antisense gene therapy, 439
drug delivery strategies, 439
Liquid chromatography–tandem mass spectrometry (LC-MS/MS), 26, 65–68, 70, 71, 74–78, 83, 84, 93, 203, 280, 281, 286
antibody-based analysis
advantages, 76
database search, target peptide, 75–76
development, quantification method, 74–75
limitation, 76–77
phosphorylated proteins, 76
quantitative, 74, 75
single nucleotide polymorphism (SNP), 76
protein quantification, SRM/MRM
accurate, internal standard, 66–67
functional analysis, 66
high-resolution (HR-SRM/MRM), 77–78
internal standard peptide, 66–68
nonlabeled small-molecular compounds, 66
peptide target, triple Q MS, 66, 67
protease digestion, 66
radio-isotope methods, 66
transition analysis, 68
LogBB, 132, 138, 274, 298, 319–320, 332–334, 336
$K_{p,uu,brain}$
acidic drugs, 330
hydrogen bonding, 329
$K_{p,brain}$, 330, 331
plasma protein binding, 328–329
lipophilicity, 324
optimization, 325
permeability surface area product (PS), 320
pitfalls, 324–325
Log P octanol/water, 343, 345
Loperamide, 43, 87, 92, 140, 141, 145–147, 152, 364, 440
Loratadine, 87, 92
Losartan, 417
Low-density lipoprotein receptor-related protein (LRP)-1
Angiopep-coated nanoparticles, 469–471
Apo E-, B-and A-coated nanoparticles, 464
in-vitro barrier model, 464
LBD, 463
melanotransferrin (MTf) (*see* Melanotransferrin (MTf))
receptor-associated protein, 467
therapeutics, 467, 469
tPA, 463
transcytosis receptor, 463
LSD. *See* Lysosomal storage diseases (LSD)
Lymphatic drainage. *See* Blood supply
Lysosomal storage diseases (LSD), 511

Lysosomal trapping, 145, 281–282, 290–297
acidic compartment, 291–292
acidic hydrolases, 293
compartments, cells, 291
compensation, pH partitioning, 293–295
description, 290–291
drug-drug interactions, 292
lungs, liver and kidneys, 292–293
phospholipids, 292
physiological volume, 292
process, 291Lysosomes, 130, 131, 133, 147, 286, 288, 290–297, 301, 379, 461, 465–467, 472, 477, 598
Lysosomic-to-cytosolic unbound drug concentration ratio ($K_{p,uu,lyso}$), 292, 294, 297
Lysosomotropism/lysosomal trapping. *See* Lysosomal trapping

M
Madin–Darby canine kidney (MDCK) cells, 136, 165–166, 180–182, 341, 349, 359, 362, 364
Magnetic resonance imaging (MRI)
glioblastoma, 659–660
guided placement, cannula, 508–510
nanocarrier, 446
quantification
disrupted hemisphere and non-disrupted hemisphere, 529, 530
Gadomer diffusion process, 529
Gd-DTPA, 529–530
intra-arterial chemotherapy infusion, 530
molecular weight, 528
osmotic disruption, 530
T1 MRI signal drop, 529
tumor-bearing animals, 530
Wistar rat, 528, 529
structural and functional data, 227
Magnevist®, 552
MAOs. *See* Monoamine oxidases (MAOs)
Mannitol, 359
Marqibo, 435Mastermind research approach, 257, 258
Mathematical modeling, 235, 236, 249, 257–259, 285, 305, 529, 619, 621
MCT2. *See* Monocarboxylate transporter 2 (MCT2)
Mct1/Slc16a1, 33
MDCK cells. *See* Madin–Darby canine kidney (MDCK) cells
Mechanism, 324, 359, 362, 367, 380, 384, 388, 389, 393, 640, 648, 705
active efflux transporters, 665
brain-to-plasma efflux, 207
brain uptake, 439
chemotherapy failure, 523
CNS diseases, 225
drug action and permeation, 175
endogenous, BBB (*see* Blood–brain barrier (BBB))*in vitro* models, 444
nasal passages (*see* Nasal passages)
P-gp efflux pump, 524
protein binding, 222
transport regulation, 173
Melanotransferrin (MTf)
BBB drug delivery vehicles, 465
brain distribution, 467, 468–469
ERT, 466
human melanoma-associated antigen p97, 465
mucopolysaccharisosis I (MPS I), 467
p97, lysosomes, 466
Melatonin, 416
Melphalan, 366, 539
Memantine, 595
Meperidine, 43
Methadone, 43
Methotrexate (MTX), 38, 537, 662, 663–664
Metoclopramide, 282
Mexiletine, 36
Microbubble, 392, 644
Microdialysis, 320, 326, 344, 352
calcualtion, 205
DAMGO, 445
drug concentrations, 445
efflux transport, 205–206
f_u measurement, 205
regulatory tool, 445
semipermeable membrane, 445
striatum, 417
Microfluidics, 186–187
Mitoxantrone, 38, 39, 79
MK571, 604
MK-801, 603
MoA. *See* Mode-of-action (MoA)
Mode-of-action (MoA), 340–341, 346–347, 349, 355, 356, 402
Molecular descriptors, 321–323, 326, 328, 329, 333, 335
Monoamine oxidases (MAOs), 103, 107
Monocarboxylate transporter 2 (MCT2), 607
Monoclonal antibodies (mAbs)
IR, 461
TR, 461
use, receptors, 462–463

Morphine, 29, 36, 43, 140, 153, 241, 248, 249, 344
Morphine-6-glucuronide (M6G), 244
MPS. *See* Mucopolysaccharidosis (MPS)
MS. *See* Multiple sclerosis (MS)
Mucopolysaccharidosis (MPS), 512
Mucopolysaccharidosis IIIB, 493–494
Multiple sclerosis (MS)
  Alzheimer's disease, 177
  axonal degeneration, 599–600
  cognitive impairments, 599
  demyelination, 599–600
  endothelial barriers, 402
  focal lesions, 599
  glutamate release and transport, 600
  hypoxia, 179
  inflammation, mouse model, 422
  MRI, 599
  symptoms, 599
Multivariate data analysis, 535
Myocet, 435

N
Naloxone, 29
Naltrindole, 43
Namenda, 595
Nanocarrier brain delivery systems, 389–390
Nanocarriers
  brain-targeted delivery-based therapies, 434
  clinical practice, 436–437
  CNS drug delivery, 433
  delivery and efficacy, 448–449
  description, 433
  EMA, 435
  NL-CPT11, 435
  pegylated liposomal doxorubicin, 435
  pharmaceutical and biotechnology companies, 434
  preparation and characterization, 448
  regulatory approval
    pharmaceuticals, 442–444
    pharmacology, 444–446
    product quality and safety, 442
    safety, 446–447
  research, clinics, 449
  safety, brain-targeted nanocarriers, 449
  treatments, 436
Nasal anatomy and physiology
  blood supply and lymphatic drainage, 405–407
  human nasal cavity, 405
  monkeys and humans, 405
  nasopharynx, 404
  olfactory region, 407–409
  respiratory region, 409–411
  surface epithelia, nasal passage, 404
  systemic/mucosal immunity, 405
Nasal passages, 403–409, 412–415, 423
  olfactory region (*see* Olfactory region)
  respiratory region, 409–411
  transportation
    brain entry sites to CNS, 415
    nasal lamina propria to brain entry, 413–415
    olfactory and respiratory epithelial barriers, 412–413
Natalizumab, 578NCEs. *See* New chemical entities (NCEs)
Neoplasia, brain
  glioma, 521–522
  metastatic disease, 522–523
Neuroanatomy. *See* Central nervous system (CNS)
Neurodegeneration, 591–594, 596, 598, 599, 601, 605, 606, 619, 620
Neurodegenerative diseases
  ALS, 597
  Alzheimer's disease, 549, 595–597
  BBB dysfunction, 592
  brain diseases, 477
  brain target site drug delivery, 611–619
  cell death, 594
  diet and lifestyle changes, 591
  drug delivery, 549–551
  drug transport, 594
  drug treatment modalities, 619
  dysfunction, BBB, 607–611
  FUS-facilitated BBB opening, drug delivery, 552
  gene defects, 593
  Huntington's disease, 597–598
  MS, 599–600
  neurodegeneration, 592
  neuronal structure and function, 591
  oxidative stress, 593–594
  Parkinson's disease, 600–602
  pharmacoresistant epilepsy, 602–605
  protein misfolding and accumulation, 594
  research tools, 620
  strategies and treatment, 607
  TBI, 606–607
  treatment, 619
Neuroinflammation, 47, 600, 605, 619
Neurological disease, 340, 494–496, 552, 605
Neuro-oncology, 503, 519–520, 535, 537, 539, 540, 660

Neuropharmacokinetics (neuroPK), 273–274, 280, 297, 300, 304–306
Neuroprotection, 109, 118, 417, 532, 552, 602, 645
Neurosurgery, 503–504, 522, 602
Neurosurgical direct delivery approaches, 391–392
Neurotherapeutics, 109, 275, 276, 305, 546, 550
Neurovasculature, 200, 204–206, 416, 521, 578, 609, 697
New chemical entities (NCEs), 147, 164, 181, 187, 273, 276, 286, 297, 298, 300, 301, 340, 363–365
Nicotine, 28, 35, 36
Nimodipine, 644
Nitrosoureas, 661
  Non-CNS projects
  ADME screens, 349
  in vivo PD experiment, 349, 350
  low dose full PK in rat, 350
  non-rodent PK, 350
  physicochemical properties, 347, 348
  potency and selectivity, 349
  PXR, Cyp inhibition and hERG assays, 349
  rapid exposure screen, PD species, 349
  secondary and tertiary *in vitro* pharmacology assays, 349
Non-specific binding, 328–329, 332, 351, 354, 358, 367
Non-specific endocytosis, 11
Novantrone, 577, 599

O

Occipital lobe, 689, 696
Olfactory intranasal administration, 649, 692, 695–697
Olfactory region
  nasal passage
    axons, 407
    microvillar cells, 409
    nerve bundles, 407
    olfactory sensory neurons (OSN), 407
    organization and histology, 407, 408
    sustentacular cells, 409
  respiratory epithelial barrier transportation, 412–413
Omniscan®, 552, 554
Optison™, 547
Organic cations
  acetylcholine esterase inhibitors, 35
  characteristics, 28–29, 34
  clonidine, 36
  H1-antagonists, 35
  oxycodon, 36
  Pmat, 34–35
  structures, 34
  tertiary amines, 36
  tobacco alkaloid, 35–36
Oxcarbamazepine, 244
Oxcarbazepine, 604, 615, 617
Oxycodone, 29, 36, 152

P

Paclitaxel, 87, 92, 202, 204, 464, 467–468, 471, 477, 673–674
PAMAM. *See* Polyamidoamine dendrimers (PAMAM)
Parenchyma, 14, 15, 25, 26, 104, 105, 111, 115, 129, 130, 145, 148, 203, 206, 290, 402, 403, 462, 469, 473, 477, 478, 581, 613, 643, 649, 650, 705
Parietal lobe, 595, 690, 694, 695, 703
Parkinson's disease (PD), 25, 30, 32, 36, 214, 251, 379, 417, 456, 460, 502, 503, 509, 549, 575, 617
  alpha-synuclein, 600
  cytokine network, 602
  motor system disorders, 600
  peripheral inflammation, 601
  treatment, 600
  type 2 diabetes and lipid abnormalities, 602
Partitioning, 102, 133, 139, 205, 275, 288, 292, 294, 295, 297–300, 304, 351, 380, 389
Patent, 381–383
Pathology, 5, 11, 12, 16, 33, 37, 38, 164, 179, 183, 235, 243, 305, 367, 445, 511, 512, 549, 575
PD. *See* Parkinson's disease (PD)
Pentazocine, 29
Pentylenetetrazole, 236
Pericytes, 6, 7, 12, 106, 167, 180, 243, 444, 609, 610
Permeability, 136, 349
Permeation, 8, 10, 32, 132, 134, 166, 169, 171, 175, 177, 186, 274, 287, 289, 351
P-glycoprotein (P-gp), 8, 27, 37–38, 65, 73, 117, 174, 221, 238, 274, 328, 362, 403, 575, 596, 603, 641, 644, 665
P-gp. *See* P-glycoprotein (P-gp)
Pharmaceutical industry, 214, 226, 273, 274, 298

Pharmacodynamics, 147, 187, 205, 215, 237, 238, 252, 255, 282, 346, 349–351, 368, 422, 456, 502, 575, 614, 617
Pharmacoeconomics, 375–450
Pharmacokinetic-pharmacodynamic (PKPD) modeling, 175, 187, 238, 247, 248, 253, 254, 305, 347, 356, 368, 614–618
  biomarkers, 249–251
  challenges, 257–258
  CNS drugs and drug therapies, 234–235, 256–258
  D2 (*see* Dopamine-D2 receptor inhibition, PKPD)
  description, 235
  disease
    biophase compartment, 614
    brain distribution, 615
    distribution process, 614
    "flip-flop kinetics", 617
    multidrug transporter inhibitors, 615
    oxcarbazepine, 615
    pharmacodynamic markers, 617
    quinidine transport, 615
    status epilepticus (SE), 615
  distribution, complex target site, 248–249
  drug transport, blood and CNS (*see* Drug transport)*in vitro-in vivo* extrapolation, 187
  "Mastermind research" approach, 257, 258
  mathematical modeling techniques, 259
  prediction, CNS drugs
    concentration-response profiles, 236–237
    CSF concentrations, 235–236
    mathematical modeling techniques, 236
  quantitative translational systems, 249
  RO, 355–356
  rodents, larger animals and human
    concentration-time profile, 357
    $C_{u,brain}$, estimation, 356–357
    non-parallel c-t profile, 357–358
    side effects, 356
  target site interaction and signal transduction
    activation, 244
    added value, 243–244
    agonism, 245–248
    receptor, 244
  unbound brain, 614
Pharmacokinetics (PK)
  BBB PS, 201
  biodistribution, 444
  brain biodistribution studies, 219
  brain drug delivery (*see* Brain drug delivery)
  CSF *vs.* brain ISF, 149–152
  equilibration across BBB, 149
  extent, 138–143
  intra-brain distribution, 132, 143–146
  intracellular drug distribution, 146–147
  PET and pharmacokinetic expressions, 135
  prediction and measurements, CNS, 153
  rate *vs.* extent measurements, 153drug penetration and distribution, 202–203
  drug transport, 319
  efficacy, 448
  L-DOPA, 617, 618
  PET tracer, 215
  P-gp substrate, 615, 616
  unbound plasma and brain
    disease, 615–619
    intracellular concentration, 612
    in vivo microdialysis, 612–614
    levitiracetam, 613
Pharmacoproteomics (PPx), 50, 90, 304
  anticancer and CNS drugs, 64
  applications, BBB (*see* Blood–brain barrier (BBB))
  drug development, 64
  efficacy, toxicity and drug distribution, 64–65
  imaging technologies, 65
  protein expression levels, 65
  QTAP (*see* Quantitative targeted absolute proteomics (QTAP))
  transporters and receptors (*see* Transporters)
Pharmacoresistant epilepsy, 591, 603, 610, 613, 614, 617
  chronic neurological disorders, 602
  epileptogenic brain tissue, 603
  ICAM-1, 605
  kainate-induced seizures, 605
  medications, 602
  phenytoin and levetiracetam, 604
  temporal lobe epilepsy, 603
  transport restriction, 604
  types, seizures, 602
Phenobarbital, 104, 604
Phenytoin, 604, 615
pH partitioning model, 93, 139, 292, 294, 295, 297, 298, 351
Physiology, 107, 164, 179, 183, 217, 404
  anatomy, BBB (*see* Anatomy and physiology)
  nasal (*see* Nasal anatomy and physiology)

PK. *See* Pharmacokinetics (PK)
pK_a, 183, 247, 248, 293–295, 322
Plasma drug concentration, 662–663
Plasma protein binding, 79, 138, 139, 142, 144, 146, 226, 276, 288, 300, 301, 328, 359
PoC. *See* Proof-of-concept (PoC)
Polyamidoamine dendrimers (PAMAM)
  angiopep, 469
  dendrimers, 475
  gene carrier, 471
Polymeric nanoparticles, 437, 440, 441, 447
  CNS drug delivery, 441
  description, 440
  intravenous administration, 441
  nonbiodegradable polymers, 440
  PLGA, 440–441
  PubMed search, 440–441
Positron emission tomography (PET), 65, 79, 132, 205, 218, 220, 223, 226, 228, 229, 250, 280, 331, 356, 368, 604, 697
  antipsychotic and anti-depressive drugs, 214
  application, CNS drug development, 214, 215
  BBB transport, 225–226
  brain distribution studies, 222–223
  chemistry, 228–229
  concepts and nomenclature, 218–219
  decay, ^{11}C, 216
  description, 215
  drug effects, 225
  drug-target interactions, 223–224
  dynamic time-activity curve, 217
  [^{18}F]FDG PET, 214
  macromolecules and biologics, 226–227
  medical imaging technique, 214
  novel technologies, 227–228
  pharmacokinetics, 217
  radionuclides, 215
  radiotracer, 215
  single-tissue compartment model, 220
  study protocols, 220–221
  in vivo drug behaviour, 217
Posterior circulation, 698, 699
PPx. *See* Pharmacoproteomics (PPx)
Preclinical, 64, 78, 154, 209, 214, 222, 223, 226, 235, 251, 301, 304, 335, 340, 378, 384, 386, 387, 415, 436, 445, 449, 491, 539, 607, 645, 665
Prediction of drug distribution in brain, 50, 51, 93–95, 136, 150, 201–202, 247, 254, 290, 293, 304, 306, 350, 511, 618
Pregabalin, 614
Probenecid, 241, 242, 244, 604, 612
Proof-of-concept (PoC), 215, 257, 346, 350, 368, 384, 392, 671
Propranolol, 171, 318Protein expression level, 51, 65, 70, 73, 77, 78, 80, 81, 83, 84, 86, 89, 90, 95
Proteins, 376, 391
  active protein/enzyme, 434
  albumin, 527
  antibodies, 419, 439
  BBB mRNA, 174
  blood-CSF barrier function, 186
  breast cancer resistance, 207
  carrier-based drug delivery systems, 435
  cerebral vessels, 522
  CNS pharmacokinetic data, 417
  IN delivery (*see* Intranasal delivery)
  drug delivery, stroke and TBI, 645–646
  IFN-β1b, 420
  IgG, 421
  insulin, 418
  interferon-β1B (IFN-β1B), 419
  knockout animals, 207
  lipids, 205
  LRP, 463
  NAP, 419
  orexin-A, 418–419
  oxytocin, 418
  physiological approach, 477
  properties, cationic peptides, 476
  transporters, 477
Protein transduction domains (PTDS), 473–474
PTDS. *See* Protein transduction domains (PTDS)
Pyrilamine, 29, 35, 36

Q

QALY. *See* Quality-adjusted life year (QALY)
QSAR. *See* Quantitative structure-activity relationship (QSAR)
QTAP. *See* Quantitative targeted absolute proteomics (QTAP)
Quality-adjusted life year (QALY), 382
Quantitative targeted absolute proteomics (QTAP)
  advantages and limitations
    global proteomics, 72–73
    LC-MS/MS and antibody-based analysis, 74–77
    protein and mRNA analysis, 73–74
  cost, 71

description, 94
in silico selection, target peptide
criteria, 68, 69
time-consuming method, 68
tryptic peptides, HSA, 68–70
procedure, 70–71
reconstruction
drug distribution (*see* Brain drug delivery)*in vivo* transporter activity, BBB (*see* Transporters)
SRM/MRM, LC-MS/MS, 66–68
Quinidine, 29, 38, 87, 92, 152, 282, 364

R
Rate of brain drug delivery
measurements, 136
methods and relationships
in situ brain perfusion, 137–138
in vitro measurement, 136
permeation, 136
permeability, 136
physiological differences, 136
Razadyne, 595
Rebif, 577
Receptor
adsorptive-mediated endocytosis, 174
AR
description, 245
3-dimensional interrelationship, 246, 247
intrinsic activity and affinity, 246
mathematical representation, transduction, 245–246
PKPD relationships, 246–248
BP, drug administration, 219
bradykinin, 664
brain distribution, 228
central histamine, 362
dose-occupancy relationship, 217
endothelial glucocorticoid, 644
endothelin, 364
gp60 and SPARC, 439
human insulin, 434
IGF-I density, 418
insulin, 670
mediated transcytosis (*see* Receptor-mediated transcytosis)
neuronal and glial plasma membrane, 200
opioid μ-receptor, 344
oxytocin, 418
pharmacodynamic models, 205
remoxipride, 416
RMT, 176
transferrin, 434, 640, 645, 670
Receptor-mediated endocytosis, 234, 579, 580
Receptor-mediated transcytosis (RMT)
bispecific antibodies, lower affinities, 461–462
endothelial cells, BBB, 463–473
monoclonal antibodies
IR, 461
TR, 461
use, 462–463
Receptor occupancy (RO), 131, 132, 154, 218, 219, 223, 224, 228, 246, 255, 355–356, 368, 446
Remoxipride, 416–417
Ribavirin, 438
Riluzole, 597
Risk, 279, 322, 381, 383, 385, 389, 436, 447, 507, 549, 596, 606, 664
Risperidone, 87, 92, 282
Ritonavir, 476
Rivastigmine, 595
RMT. *See* Receptor-mediated transcytosis (RMT)
RO. *See* Receptor occupancy (RO)

S
SAH. *See* Subarachnoid hemorrhage (SAH)
Screening tree, 347–350
sdAb. *See* Single domain antibody (sdAb)
Simian virus 40 (SV40), 177, 492, 495
Single domain antibody (sdAb), 471–472
SLNs. *See* Solid lipid nanoparticles (SLNs)
SMA. *See* Spinal muscular atrophy (SMA)
Small molecules, 27, 274, 286, 305, 376, 387, 388, 390, 404, 423, 437, 455, 457, 477, 503, 539, 598, 612, 670, 675
IN administration, 416, 417
Alzheimer's disease, 417
description, 416
ECF, 416–417
melatonin, 416
olfactory/trigeminal nerve-associated pathways, 416
Small solute transport, BBB, 10–11
SNC121, 43
Solid lipid nanoparticles (SLNs), 441
Solute carrier (SLC) transporters, 10, 26, 27, 662
Sorafenib, 38
Sparfloxacin, 241
Species differences, 13, 31, 45, 78, 79, 114, 118, 135, 145, 152–153, 209, 223, 302, 304, 355, 363

Spinal muscular atrophy (SMA), 493, 511
Steady-state ratio of brain interstitial fluid to plasma unbound drug concentrations, 147, 202, 205, 274–275, 319
Stem cells, 376, 422, 552, 671
Stroke, 352, 361, 367
  blood supply, 638
  cell-based therapies, 648
  cell trafficking, 640–641
  cerebral ischemia and hemorrhage, 637
  CNS disease, 456
  distribution, Evan's blue, 637
  endocytosis/transcytosis, 640
  glucocorticoids, 644
  hypothermia, 645
  metabolic barrier, 642
  modifiers, 642–643
  nimodipine, 644
  nonvascular delivery strategies, 649–650
  proteins, 645–646
  reduction, blood flow, 636
  small molecular weight compounds, 647–648
  TBI, drug delivery (*see* Drug delivery, stroke and TBI)
  TJ, 638–640, 645, 647
  tPA, 643
  transport, 641–642
  ultrasound and mechanical thrombolysis, 643–644
Subarachnoid hemorrhage (SAH), 638, 644, 706
Sufentanil, 248–249
Sulfotransferases (SULTs), 103, 109, 110
SULTs. *See* Sulfotransferases (SULTs)
SV40 virus. *See* Simian virus 40 (SV40)

T

Target engagement, 275, 301, 304, 306, 340–341, 346, 368
Target site, 131, 217, 225, 235–238, 240, 244–250, 253, 259, 286, 302, 346, 425, 592, 611–619, 661
TBI. *See* Traumatic brain injury (TBI)
TEER. *See* Transendothelial electrical resistance (TEER)
Temozolomide, 79, 661, 662
Temporal lobe, 536, 595, 596, 603–605, 689, 695, 699
Tenascin, 675
Tetrabenazine, 598
Therapeutic index, 385, 436, 437, 447
Thiopental, 282
Thiopurine methyltransferase (TPMT), 110
Thioridazine, 295
Tight junctions (TJ), 4–6, 8–10, 13, 15, 16, 25, 50, 51, 94, 104, 105, 112, 117, 165–172, 179, 182, 183, 406, 521, 546, 547, 563, 597, 608, 638–640, 645, 647, 664, 697
  impedance spectroscopy systems, 170–171
  measurement methods, 168–169
  Ohm's Law, 170
  permeability and TEER, 171–172
  TJ proteins, 406
Tissue binding, 134, 202, 275, 278, 283, 289, 301–303, 346, 349, 358, 361
Tissue plasminogen activator (tPA), 463, 643, 644, 650
Tizanidine, 599
TJ. *See* Tight junctions (TJ)
Topiramate, 612
Topotecan, 38, 49, 79
Total brain to total plasma drug concentrations, 154, 274
tPA. *See* Tissue plasminogen activator (tPA)
TPMT. *See* Thiopurine methyltransferase (TPMT)
Transcytosis, 9, 11, 172–173, 182, 186, 412, 457, 459–473, 476, 580, 595, 640, 645–647
Transendothelial electrical resistance (TEER), 9–10
  barrier permeability, 168–169
  measurement, Ohm's law, 170
  vs. permeability, 171–172
  small ions, 164
Transferrin receptor (TR), 461
Translation, 151, 222, 226, 301–305, 333, 335, 356, 450, 494, 512, 671
Transporters, 390
  ABC, 540
  active efflux, 665, 668
  BBB, 207
  BCSFB, 49
  bio-distribution, labelled drugs, 214
  brain-to-bloodinflux (*see* Brain-to-bloodinflux transport systems)
  brain tumor vessels, 522
  chemical inhibition, 221
  CoMFA, 333
  DTI (*see* Drug-transporter interactions (DTI))
  efflux (*see* Brain-to-blood efflux transport systems)
  endothelial cells, 402
  enzymes, 168
  expression, drug, 402

fluorescent substrates, 168
guanido compounds, 47–48
organic anions, 44–47
organic cations, 45
peptides, 48
permeability surface area product (PS), 320
P-gp, 328
P-gp and BCRP, 209
QTAP-based reconstruction
differences, protein expression levels, 85, 86
drug distribution, 85
$K_{p,brain}$ ratio, 86, 90
mdr1 function, 86–90
monolayers, L-mdr1, 90
permeability clearances, 86–88
PET and SPECT, 85–86
P-gp efflux ratio, 89, 90
PS products, 86, 89
receptors, protein expression levels
developmental changes, 84–85
interindividual differences, 83–84
interspecies differences (*see* Interspecies differences)
standard physicochemical descriptors, 321–322
transcytosis and immune responses, 172–173
xenobiotics, 402
Transport systems, 25, 27, 29–51, 82–84, 208, 459, 463, 662
brain-to-bloodefflux (*see* Brain-to-bloodefflux transport systems)
influx (*see* Brain-to-bloodinflux transport systems)
influx and efflux, BCSFB
contribution, ABC, 49
guanidino compounds (GCs), 47–48
lipophilic compounds, 49
organic anions, 46–47
organic cations, 45
peptides, 48
transporters actions, 45
neurotransmitters and organic anions, 43–44
peptides
β-amyloid, 41–42
ANP, 42
drugs, 42–43
Trastuzumab, 457, 467–469
Traumatic brain injury (TBI), 574, 591, 592, 610, 636. *See also* Drug delivery, stroke and TBI
damage, brain, 606
MCT2, 607
pathophysiology, 606
proinflammatory mediators, 606
translational research, 606
Trigeminal, 402, 403, 406, 410–419, 423, 424, 649
Trypan Blue, 552
Tysabri, 578

U
U-69593, 43
Unbound brain-to-plasma concentration ratio ($K_{p,uu,brain}$), 90–91, 93
Unbound drug, 37, 130–135, 139–141, 143, 144, 147–150, 205, 234, 240, 274–278, 281, 283, 294, 297, 299, 303, 329, 367
in brain interstitial fluid, 225, 283, 344, 347, 353
brain partitioning coefficient, 205, 275, 299, 300
concentration, 132, 133, 140, 149, 239, 257, 259, 289, 292–294, 301, 347, 355, 592, 611, 612
Uridine diphosphoglucuronosyl transferases (UGTs), 103, 109, 114

V
Valproate, 604
Valspodar, 665
Valuation, 382, 393
Value proposition, 387, 389
VC. *See* Venture capital (VC)
Ventricular system and brain fluids. *See* Cerebrospinal fluid (CSF)
Venture capital (VC), 384
Verapamil, 29, 36–38, 85, 87, 92, 152, 221, 244, 364, 604, 612, 613, 665
Vinblastine, 38, 87, 92, 182
Volume of distribution of unbound drug in the brain, 275, 281, 289, 303

W
Woodchuck post response enhancing element (WPRE), 490
WPRE. *See* Woodchuck post response enhancing element (WPRE)

Z
Zosuquidar, 665